



Deliverable 4.2

Pilot description and assessment reports work package 4

Contribution partners:

GEUS, TNO, GTK, BRGM, BGR, ISPRA, GSI, GSS, IGME, SGU, BGS (UKRI)

This report is part of a project that has received funding by the European Union's Horizon 2020 research and innovation programme under grant agreement number 731166.



Deliverable Data	
Deliverable number	D4.2
Dissemination level	Public
Deliverable name	Pilot description and assessment reports
Work package	WP4
Lead WP	BRGM, BGS
Deliverable status	
Version	Version 1.1
Date	29/04/2021

[This page has intentionally been left blank]

TABLE OF CONTENTS

INTRODUCTION.....
ALTO GENIL BASIN (SPAIN)
CHALK AQUIFER (UNITED KINGDOM)
CONTINENTAL SPAIN (SPAIN)
DE RAAM (NETHERLANDS)
DEVONIAN AQUIFER (UNITED KINGDOM)
JURASSIC AQUIFER (UNITED KINGDOM)
KINDA AND BÖDA (SWEDEN)
LORCA (SPAIN)
MAGNESIAN AQUIFER (UNITED KINGDOM)
NATIONAL SCALE FINLAND (FINLAND)
NATIONAL SCALE FRANCE (FRANCE)
NORTH EAST PO PLAIN (VENETO PLAIN, ITALY)
POSAVINA (SERBIA)
SIERRA DE LAS NIEVES AQUIFER (SPAIN)
SOUTH EAST MIDLAND AQUIFERS (IRELAND)
TRIASSIC AQUIFER (UNITED KINGDOM).....

1 INTRODUCTION

The pilot description reports are compiled in this document (as a single D4.2 document) but are separate reports from the individual pilots. Reports can include more than one pilot from the same country and present work performed in other work packages (WPs) together with the work done in work package 4. Hence, there is only one pilot report for each pilot although the pilot appears in several TACTIC work packages.

The hereby presented document includes all the pilot assessments reports and results performed in WP4. Assessments in WP4 focuses on assessments of water resources through the assessment of infiltration recharge using multiple tools. The vulnerability of water resources to climate change impacts has been also investigated at different pilot scales. The pilot scale varies from borehole scale where lumped models are applied (e.g. North east Po Plain, Italy and Posavina, Serbia, south-east Ireland) to local and regional scale (e.g. De Raam, Netherland, Knda and Boda, Sweden, UK aquifers) to large country scale (e.g. France, Finland, and Ireland). WP4 employs a variety of different models from lumped models applied at borehole scale to statistical models for time series analysis, as well as distributed models for the calculation of diffuse recharge. WP4 also includes a task to calculate infiltration recharge at pan-European scale, which is reported in a different TACTIC deliverable. Despite the large variety of groundwater modelling concepts, when climate change impact is studied, all models use the TACTIC standard climate change scenarios, developed in WP3.

The pilot assessment reports are ordered alphabetically and organized into separate documents within D4.2 because the individual reports are used for documentation toward local stakeholders.



Deliverable 4.2

PILOT DESCRIPTION AND ASSESSMENT

Alto Genil Basin (Spain)

Authors and affiliation:

AJ. Collados-Lara, David Pulido-Velazquez, Leticia Baena-Ruiz, E. Pardo-Igúzquiza, Juan de Dios Gómez-Gómez.

Geological Survey of Spain (IGME)



This report is part of a project that has received funding by the European Union's Horizon 2020 research and innovation programme under grant agreement number 731166.



Deliverable Data	
Deliverable number	D4.2
Dissemination level	Public
Deliverable name	Pilots description and assessment report for Groundwater Recharge and vulnerability.
Work package	WP4
Lead WP	BGS & BRGM (WP4)
Deliverable status	
Version	Version 1
Date	14/01/2019

[This page has intentionally been left blank]

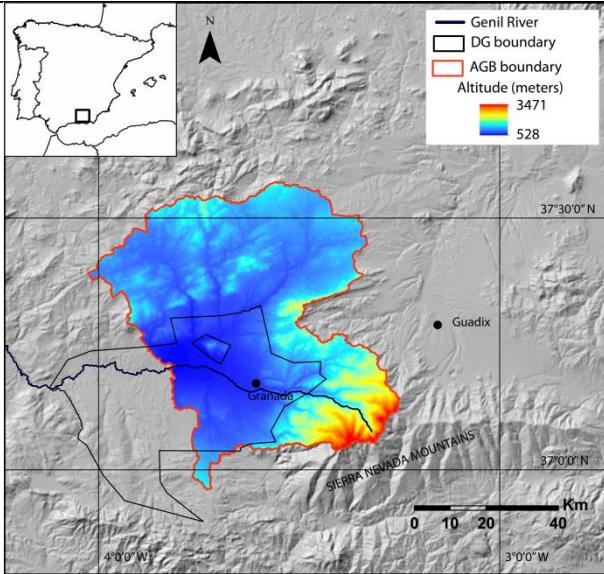
LIST OF ABBREVIATIONS & ACRONYMS

AG	Alto Genil
DG	Depression of Granada
VG	Vega de Granada

TABLE OF CONTENTS

LIST OF ABBREVIATIONS & ACRONYMS	4
1 EXECUTIVE SUMMARY	5
2 INTRODUCTION	7
3 PILOT AREA	9
3.1 Site description and data	9
3.1.1 Location and extension of the pilot area	9
3.1.2 Geology/Aquifer type	10
3.1.3 Topography and soil types	10
3.1.4 Surface water bodies	11
3.1.5 Hydraulic head evolution and subsidence	12
3.1.6 Climate	14
3.1.7 Land use	15
3.1.8 Abstractions/irrigation	16
3.1.9 Flow balance components	16
3.2 Climate change challenge	17
4 METHODOLOGY AND DATA	18
4.1 Data	18
4.1.1 Climate data	18
4.1.2 Hydrological data	18
4.1.3 Subsidence data	18
4.1.4 Material of piezometers data	18
4.2 Generation of Future Potential Scenarios	19
4.2.1 Generation of Future Individual Projections	19
4.2.2 Multi-Objective Analysis of the individual projections (Basic and Drought Statistics)	20
4.2.3 Ensembles of Predictions to Define More Representative Future Climate Scenarios	20
4.3 Potential Impacts of Future Climate Change Scenarios on Ground Subsidence	20
4.3.1 Hydrological Impacts of Climate Change on Groundwater Levels	21
4.3.2 Assessment of the subsidence from satellite data	22
4.3.3 Propagation of Hydrological Impacts to Subsidence	23
5 RESULTS AND CONCLUSIONS	24
5.1 Influence of the fine-grained material in the aquifer subsidence	24
5.2 Impacts of climate change on precipitation, temperature, and droughts	25
5.3 Impacts of climate change on hydraulic head and subsidence	26
6 REFERENCES	29

1 EXECUTIVE SUMMARY

Pilot name	ALTO GENIL BASIN	 <p><i>Modified from Collados-Lara et al., 2018a</i></p>
Country	Spain	
EU-region	Mediterranean region	
Area (km ²)	2596 km ²	
Aquifer geology and type classification	AG basin (detrital, shale, limestone and conglomerate); DG (detrital)	
Primary water usage	Irrigation / Drinking water / Industry	
Main climate change issues	The Alto Genil (AG) basin is located in a Mediterranean region where the latest studies on climate change forecast important increases in temperature and a decreases in precipitation, which will cause a decrease in water resources linked considerable increases in length, magnitude and intensity of droughts. The main contributions to the basin come from Sierra Nevada Mountains in the melt season through the Genil river. The alpine systems where the majority of precipitation is solid (snow) could be very sensitive to climate change too. On the other hand the DG (depresión de Granada) aquifer, located in the AG basin, is one of the largest groundwater bodies in Andalusia and it is considered as strategic for the economy of this semi-arid region. Decreases in water resources can provoke also important subsidence issues in this detrital aquifers.	
Models and methods used	Generation of local future climate change scenarios to analyse droughts following the method proposed in the framework of this project (Collados-Lara et al., 2018a). Analysis of the influence of the fine-grained material in the aquifer subsidence and assessment of the impact of climate change scenarios on land subsidence related to groundwater level depletion in the detrital aquifer..	
Key stakeholders	Genil River Basin Authority, water supply companies, Environmental Conservation Groups.	
Contact person	AJ Collados-Lara, D. Pulido, L. Baena, E. Pardo; JD Gómez. IGME (Spain), aj.collados@igme.es; d.pulido@igme.es; l.baena@igme.es; j.dedios@igme.es;	

The AG basin has an area of 2596 km², and it is situated in the Mediterranean region of EU (south of Spain) which is very vulnerable to climate change. The basin varies substantially in elevation,



from 528 to 3471 m.a.s.l. The main river of the basin is the Genil river, which is the most important in the province of Granada, and one of the most important in Andalusia. The main contributions to the river come from Sierra Nevada Mountains in the melt season. The main groundwater body related to the AG basin is the DG which cover an extension of around 1350 km². The aquifer is mainly detrital although there are some karstic horizons. Two subunits can be differentiated within the groundwater body, the VG aquifer and a Mioplioceno Subunit.

In the AG basin different correction approaches and climate models were used to generate local future climate change scenarios of precipitation and temperature to analyse droughts. We considered different correction techniques (first moment correction, first and second moment correction, regression and quantile mapping) under the bias correction and delta change approaches. Two ensemble scenarios were defined by combining as equiflexible members all the future projections for the two correction approaches. Two other options were defined by combining only the not eliminated projections in a multi-objective analysis that takes into account basic and droughts statistics.

The average changes predicted using the four ensembles of scenarios for the period 2071-2100 and the scenario RCP 8.5 are around -27 % in precipitation and + 32 % in temperature and all four ensembles predict considerable increases in length, magnitude and intensity of droughts. The uncertainty related to the correction approaches is lower than the related to RCMs.

In the VG aquifer we analysed the influence of the fine-grained material in the aquifer subsidence and assessed the impact of climate change scenarios on the land subsidence related to groundwater level depletion. An equiflexible ensemble of the generated projections from different climatic models is also proposed. A simple water balance approach is applied to assess climate change impacts on lumped global drawdowns. Climate change impacts are propagated to drawdowns within piezometers by applying the global delta change observed with the lumped assessment. Regression models are employed to estimate the impacts of these drawdowns in terms of land-subsidence, as well as to analyze the influence of the fine-grained material in the aquifer.

The impacts of climate change on the subsidence would be very significant for the case study. The mean increment of the maximum subsidence rates in the considered wells for the future horizon (2016-2045) and the scenario RCP 8.5 is 54%. In order to avoid undesirable consequences/risks some adaptation strategies should be applied to control and minimize land subsidence caused by groundwater withdrawals.

2 INTRODUCTION

Climate change (CC) already have widespread and significant impacts on Europe's hydrological systems including groundwater bodies, which is expected to intensify in the future. Groundwater plays a vital role for the land phase of the freshwater cycle and has the capability of buffering or enhancing the impact from extreme climate events causing droughts or floods, depending on the subsurface properties and the status of the system (dry/wet) prior to the climate event. Understanding and taking the hydrogeology into account is therefore essential in the assessment of climate change impacts. Providing harmonised results and products across Europe is further vital for supporting stakeholders, decision makers and EU policies makers.

The Geological Survey Organisations (GSOs) in Europe compile the necessary data and knowledge of the groundwater systems across Europe. To enhance the utilisation of these data and knowledge of the subsurface system in CC impact assessments, the GSOs, in the framework of GeoERA, has established the project "Tools for Assessment of Climate change Impact on Groundwater and Adaptation Strategies – TACTIC". By collaboration among the involved partners, TACTIC aims to enhance and harmonise CC impact assessments and identification and analyses of potential adaptation strategies.

TACTIC is centred around 40 pilot studies covering a variety of CC challenges as well as different hydrogeological settings and different management systems found in Europe. Knowledge and experiences from the pilots will be synthesised and provide a basis for the development of an infrastructure on CC impact assessments and adaptation strategies. The final projects results will be made available through the common GeoERA Information Platform (<http://www.europe-geology.eu>).

The specific TACTIC activities focus on the following research questions:

- What are the challenges related to groundwater- surface water interaction under future climate projections (TACTIC WP3).
- Estimation of renewable resources (groundwater recharge) and the assessment of their vulnerability to future climate variations (TACTIC WP4).
- Study the impact of overexploitation of the groundwater resources and the risks of saline intrusion under current and future climates (TACTIC WP5).
- Analyse the effectiveness of selected adaptation strategies to mitigate the impacts of climate change (TACTIC WP6).

This report describes the work undertaken by the Spanish Geological Survey (IGME) as a part of TACTIC WP4 to assess impacts of climate change on water resources at the AG basin. It also analyzes the influence of fine-grained material in the aquifer subsidence and assess impacts of climate change on subsidence in the VG detrital aquifer.

The work presented here aims to perform an analysis of several statistical approaches and RCMs, to generate future potential scenarios at a monthly scale, which is the usual timescale for the analysis of water resource management problems. We assessed different solutions, taking into account basic and drought statistics of the historical series and the climatic model simulations. A multi-objective analysis is proposed to identify the inferior approaches which



would also help to reduce the uncertainties associated. The proposed methodology is applied to the AG basin (south Spain). It also aims to perform a first assessment of potential climate change impacts on land subsidence related to groundwater-level depletion in the VG detrital aquifer and to analyse the influence of the fine-grained material in the aquifer subsidence.

3 PILOT AREA

This pilot area is very sensitive to climate change because it is located in a mediterranean alpine region where the latest studies forecast important increase in temperature and a decrease in precipitation. For the propagation of climate change impacts we will employ Hydrological lumped model approach integrating variables deduced from remote sensing earth observation (eg. Snow). Special attention will be paid to the analysis of droughts and subsidence that will be exacerbated in future due to climate change. We also intend to define methodological guidelines to assess potential future climate scenarios at river basin and aquifer scale. Different ensemble and downscaling techniques will be employed to define potential future global change scenarios for the study area based on the data coming from simulations with different Regional Circulation Models (RCMs). In this project we intent to propagate climate change scenarios considering future potential impacts of global change scenarios in droughts in the AG basin and groundwater subsidence in the DG (Depresión de Granada) groundwater body.

3.1 Site description and data

3.1.1 Location and extension of the pilot area

The study basin has an area of 2596 km², and it is situated in the Mediterranean region of EU (south of Spain) (see Fig. 1). The basin varies substantially in elevation, from 528 to 3471 m.a.s.l. The main river of the basin is the Genil river, which is the most important in the province of Granada, and one of the most important in Andalusia. The main contributions to the river (e.g. Dílar, Monachil or Cubillas rivers) come from Sierra Nevada Mountains in the melt season (Collados-Lara et al., 2018a). The main groundwater body related to the AG basin is the DG which cover an extension of around 1350 km² (see Fig. 1).

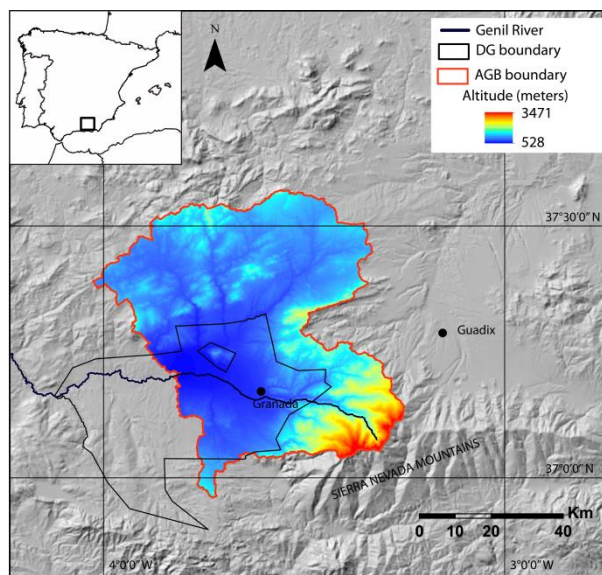


Fig. 1. Location of the pilot area (modified from Collados-Lara et al., 2018a).

3.1.2 Geology/Aquifer type

The DG groundwater body (05.32) is located in a basin between the Betics Mountains. In this basin, Neogene and Quaternary materials were deposited with high thickness and strong lateral variations (see Fig. 2). The aquifer is mainly detrital although there are some karstic horizons. Two subunits can be differentiated within the groundwater body, VG aquifer and a Mioplioceno Subunit, but we will focus on the first due to the second is not well known and its relevance is limited. The VG Subunit defines an unconfined aquifer. Its surface is around 200 Km². Recharge mainly appears in the eastern sector through rainfall and runoff infiltration. The aquifer outputs are produced in the western side by natural drainage to rivers, irrigation canals and springs. The main drainage axis is the Genil River from the Puente de los Vados and the discharge to the Cubillas River is also important. There is also pumping to supply irrigation, urban and industrial demands.

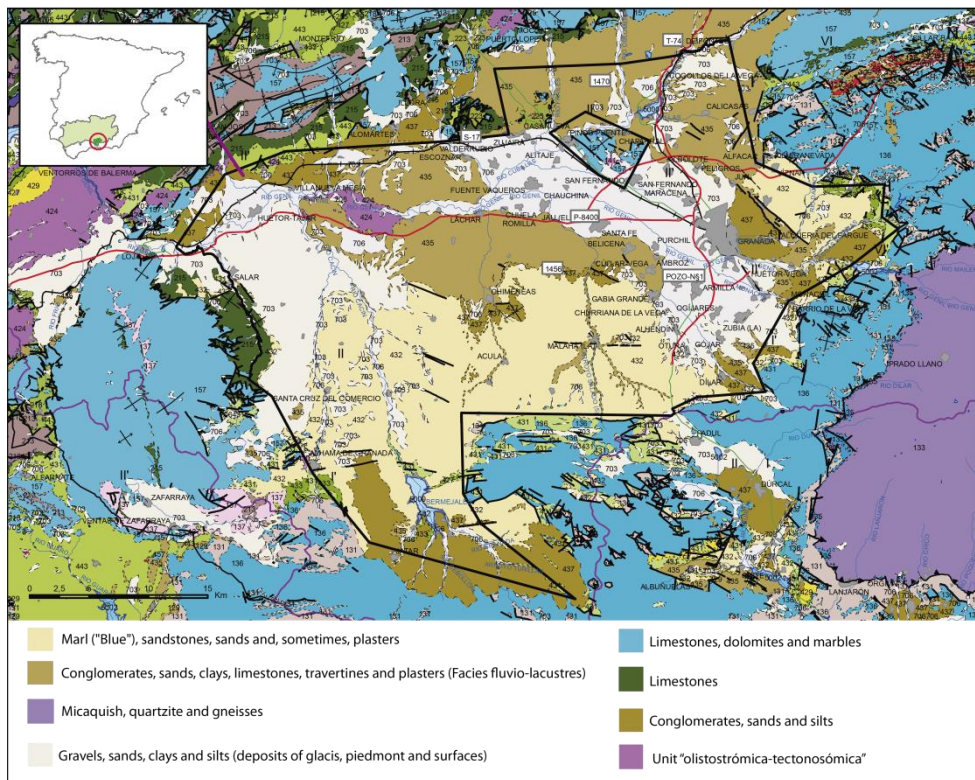


Fig. 2. Geological map of DG (modified from IGME-DGA (2009)).

3.1.3 Topography and soil types

Despite the variation in elevation in the AG basin is strong (from 528 to 3471 m.a.s.l.) (see Fig. 1), the DG groundwater body area is predominantly flat, with variation in elevation from 550 to 950 m.a.s.l. (see Fig. 3A). The soils in the groundwater body surface mainly belong to the cambisol group but it also can be found Regosol and others such as Litosol and Fluvisol in the area. Fig. 3B shows a soil map of DG groundwater body.



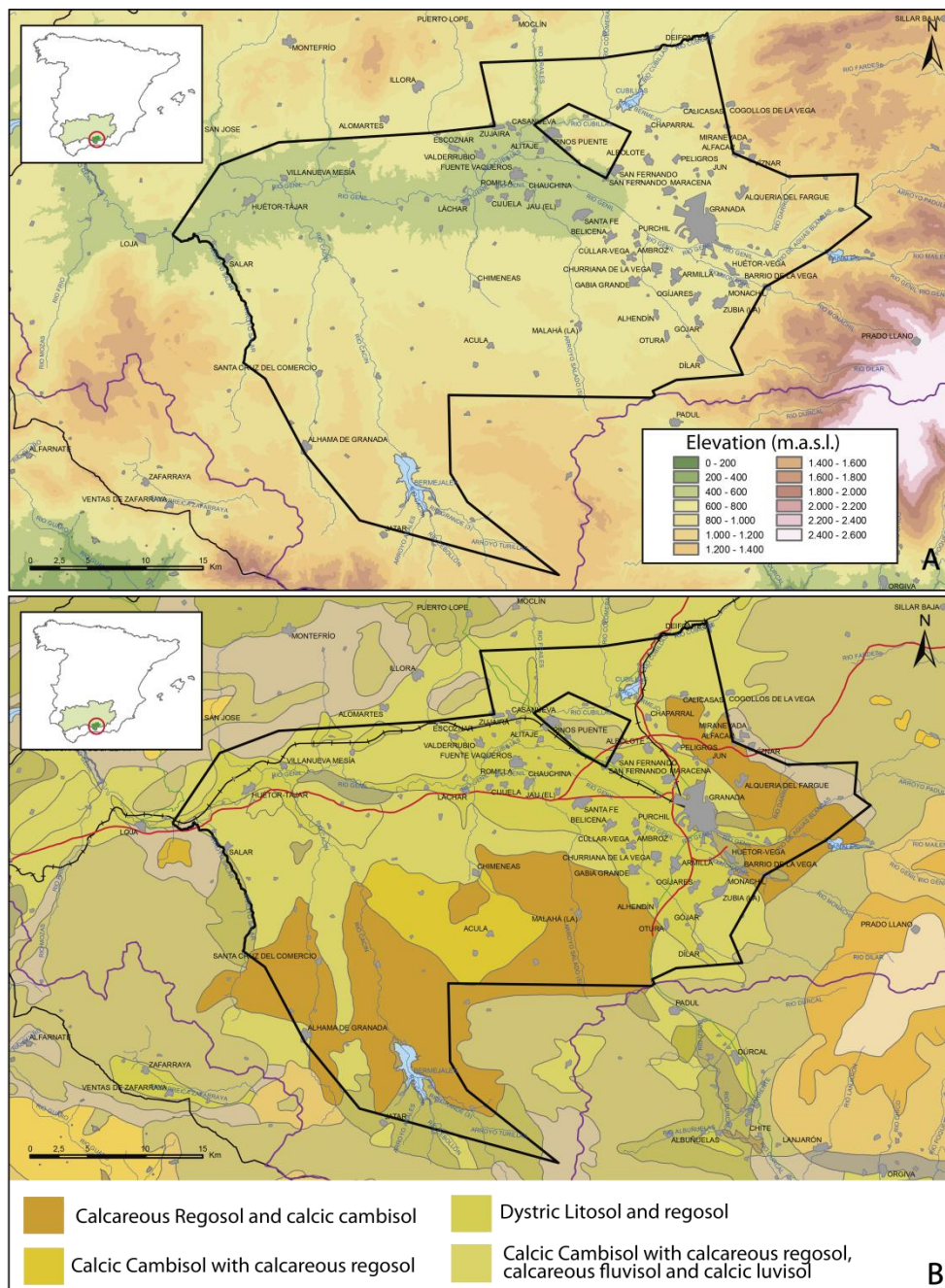


Fig. 3. A) Digital elevation map and B) soil map of DP ground water body (modified from IGME-DGA (2009)).

1.1.4 Surface water bodies

At the headwaters of the AG basin, streamflows are regulated by the reservoirs of Colomera, Cubillas, Bermejales, Quéntar and Canales. Fig. 4 shows the surface water system (rivers and reservoirs) of the AG basin. The quality of the surface water resources is higher in the high mountain reservoirs (Canales and Quéntar). Most of the surface resources comes from the Sierra



Table 1: Maximum and minimum volumes in the reservoirs (hm³) from 1970 to 2002 (modified from UPV (2004)).

		Maximum											
Reservoir	Minimum	October	November	December	January	February	March	April	May	June	July	August	September
Cubillas	5	19	19	15	15	15	19	19	19	19	19	19	19
Colomera	5	42	42	34	34	34	42	42	42	42	42	42	42
Quentar	1	14	14	11	10	10	10	14	14	14	14	14	14
Canales	1	71	71	58	58	58	58	71	71	71	71	71	71

As we have already pointed the main aquifer of the DG groundwater body is the VG detrital aquifer, which is one of the largest groundwater reservoirs in Andalusia and considered as strategic for the economy of this semi-arid region. Fig. 5 shows the historical evolution of the hydraulic head in three representative piezometers of the aquifer. A significant reduction trend in the piezometric levels is observed. These drawdowns are more important in the area of preferential recharge (piezometers A and B) (Castillo et al., 2010). On the other hand, in this aquifer, subsidence processes have been detected and related to groundwater level depletion (Mateos et al., 2017). Fig. 6 shows the evolution of hydraulic head and land displacements observed in six boreholes located in the Vega the Granada aquifer. All the subsiding areas detected by Mateos et al. (2017) are located in areas with higher clay composition.

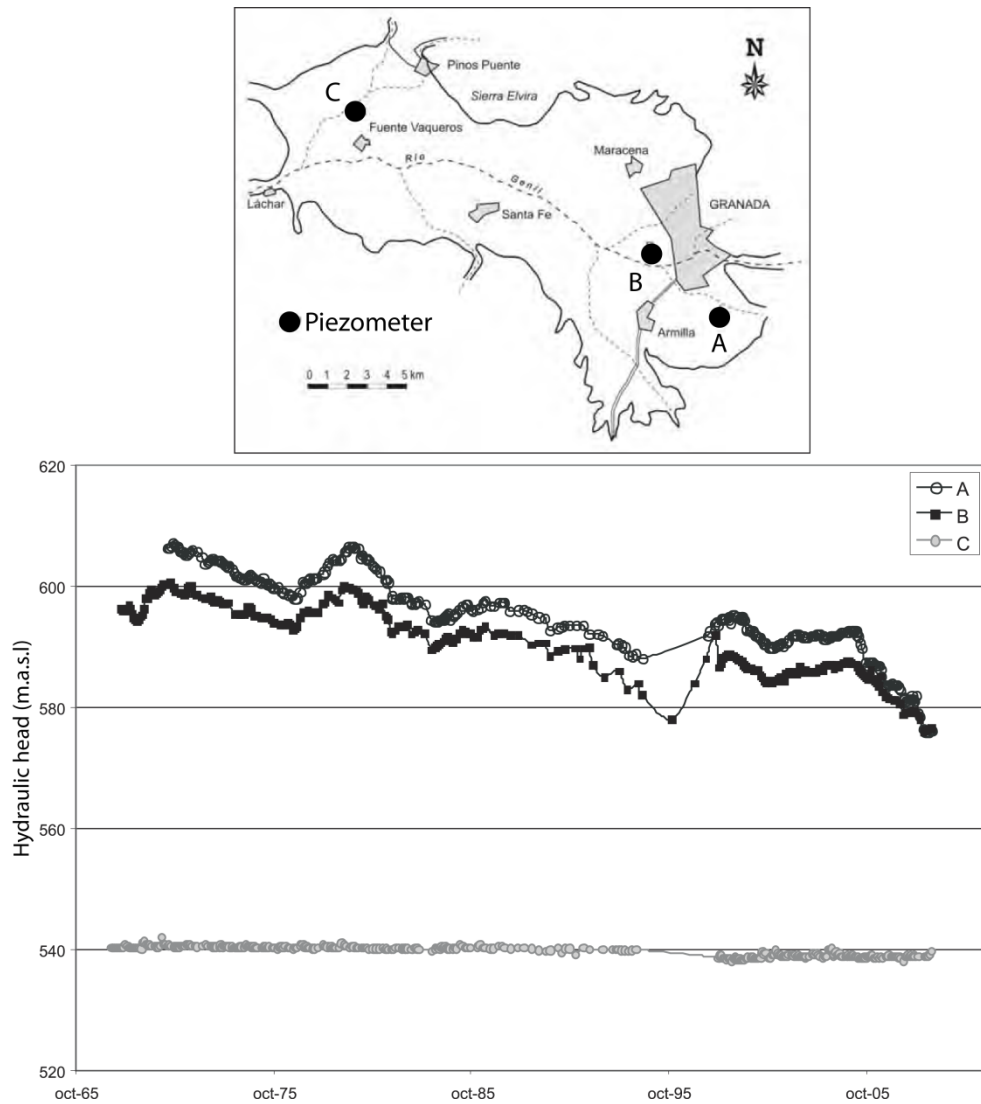


Fig. 5. Historical evolution of hydraulic head in three representative piezometers of the VG Aquifer (modified from Castillo et al., 2010).

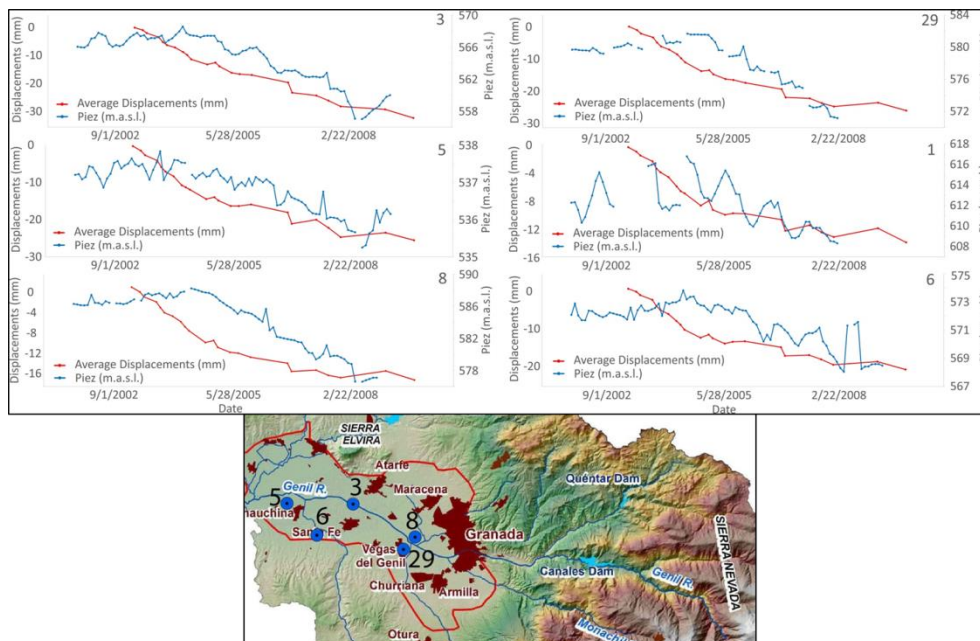


Fig. 6. Hydraulic head and displacements in the DG groundwater body from 2002 to 2008 (modified from Mateos et al., 2017).

3.1.6 Climate

The region has a Mediterranean climate very influenced by the proximity of Sierra Nevada Mountain. Summers are hot and dry and winters are cool and relatively damp, with most of the rainfall concentrated between November to January. The coldest months are December, January and February while the hottest months are July and August. The annual mean temperature and precipitation for the period 1971-2000 in the AG basin are respectively 14 °C and 525 mm/year. The mean values of temperature and precipitation for the different months are showed in Fig. 7. For the AG basin, Collados-Lara et al. (2018b) observed an inversion of the precipitation gradient (it become negative above a certain elevation) and a linear variation of temperature (see Fig. 8).

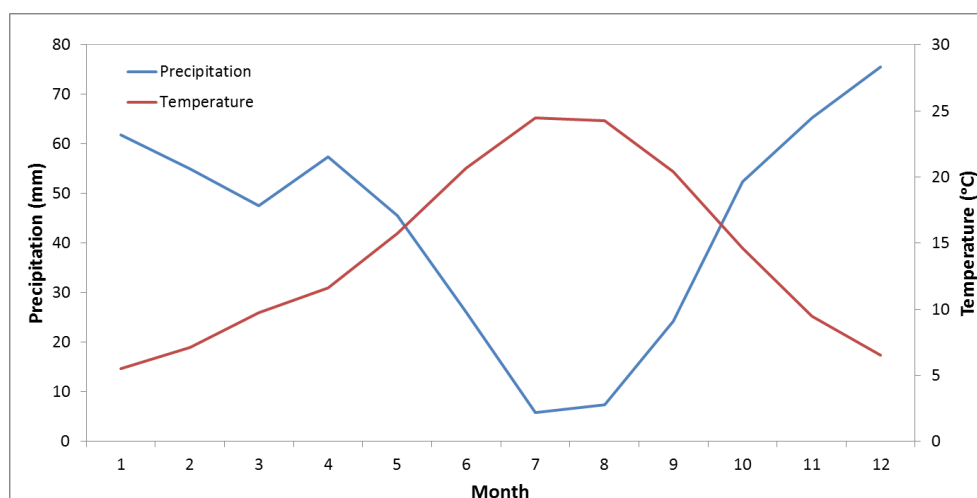


Fig. 7. Mean temperature and precipitation for the AG basin in the period 1971-2000 (Data from Spain02 v4 project (Herrera et al., 2016)).

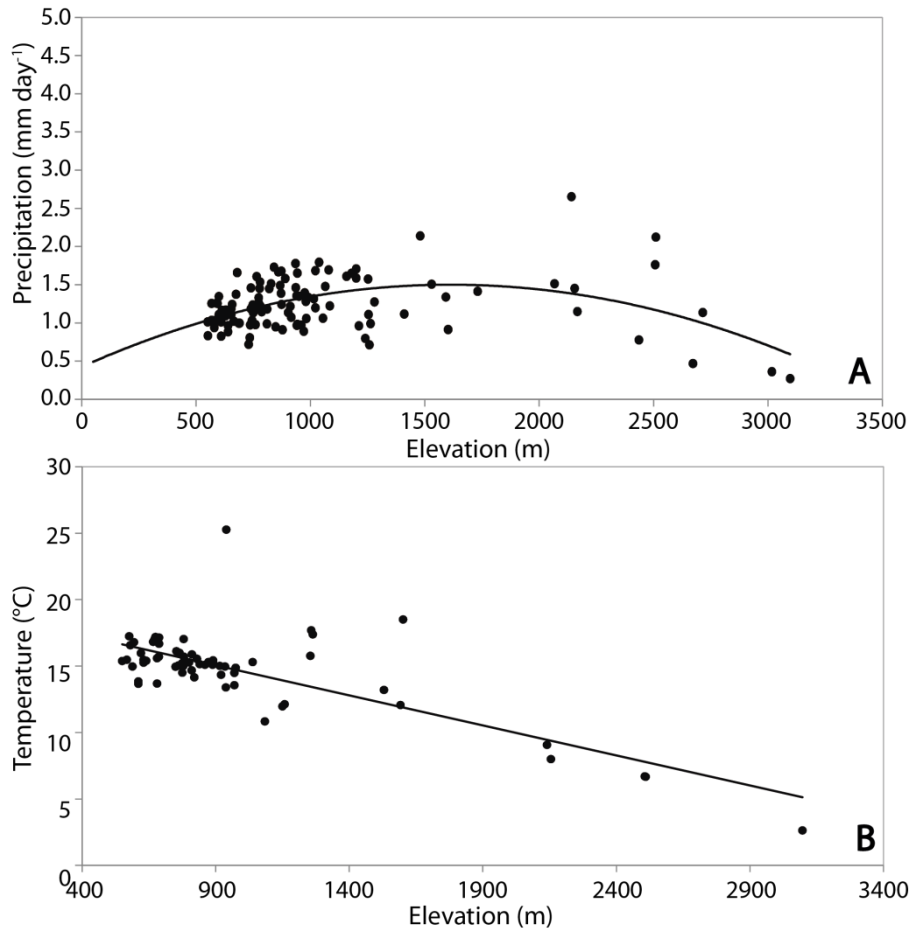


Fig. 8. (A) Mean daily precipitation data for different elevations. (B) Mean daily temperature data for different elevations. (modified from Collados-Lara et al., 2018b)).

3.1.7 Land use

The AG basin and especially the VG aquifer have suffered in the last decades significant territorial transformations (physical, demographic, socio-economic). Thus, a mainly agriculture sphere has become a complex and interrelated urban agglomeration (Fernández, 2010). The main land use in the Vega the Granada aquifer is irrigated agriculture and urban use while the non-irrigated agriculture is located in the Mioplioceno Subunit (see Fig. 9). In the DG groundwater body surface the preferential irrigated agriculture are herbaceous crops and the predominant non-irrigated agriculture are olive trees.

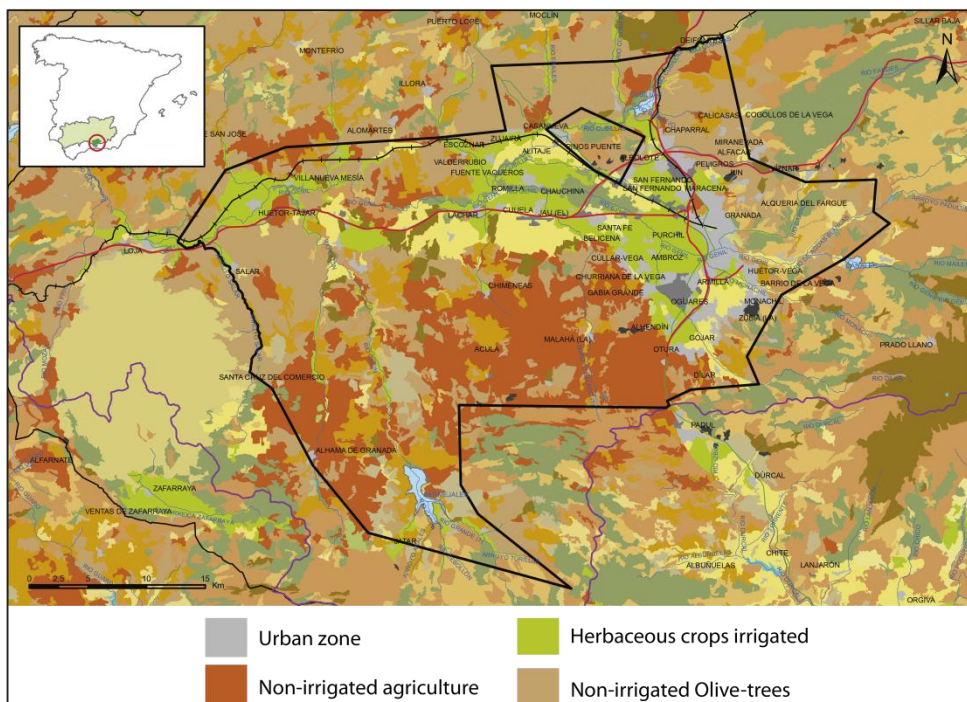


Fig. 9. Land use maps from CORINE (2000) (modified from IGME-DGA (2009)).

3.1.8 Abstractions/irrigation

The irrigated agriculture has been the economic engine of the region before 1960s. From the 1960s a transformation process began in favor of other economic activities. The crisis of the agriculture sector is understood as a change in the economic model. The causes of the crisis of the agriculture sector in the VG are the fragility of the agriculture structures and the pressure provoked by the urban-industrial growth (Fernández, 2010). As we pointed previously, nowadays the main water uses in the AG basin are due to irrigation, drinking water, and industry demands. For the DG groundwater body these activities represent 48, 46, and 6 % of water use respectively. Table 2 shows the groundwater amounts destined for the different activities in the year 2007.

Table 2. Groundwater pumping amounts (Hm^3) by activity (from IGME-DGA (2009)).

Year	Water supply population	Agriculture and Livestock	Industry	Total
2007	24.34	25.14	3.31	52.8

3.1.9 Flow balance components

The flow balance proposed by different authors in the Vega the Granada aquifer is summarized in Table 3. The main inputs to the aquifer are recharge from precipitation and irrigation and the main outputs are abstractions and gaining rivers.

Table 3. Water budget proposed by different authors for VG Aquifer (modified from Calvache et al., 2013).



Water budget (hm ³ /year)	FAO (1972)	Castillo (1986-2005)	AAA (2008)	Calvache et al. (2013)
Surface Recharge (Precipitation)	6	24	30	66
Surface Recharge (Irrigation)	62	141	155	
Rivers infiltrations	6	19	25	50
Lateral Transference	-	-	-	17
TOTAL INFLOWS	74	184	210	133
Pumping	10-60	32-50	40	43
Gaining in Rivers	40-60	100-110	160	54
West Border	—	—	4	40
Evapotranspiration	9-14	7	6	-
TOTAL OUTFLOWS	59-134	139-167	210	137

3.2 Climate change challenge

In accordance with the EEA map the main expected issues due to climate change in this case study are those described in the Figure 10 for the Mediterranean regions. Existing national estimates in Spain showing also a significant reduction (around a 19% for the RCP8.5 emission scenario in the horizon 2071-2100) of the aquifer recharge in the area (see Pulido-Velazquez et al., 2017). The main challenge is to assess potential impacts of future climate change scenarios on the resources of the basin and the subsidence in the VG aquifer.

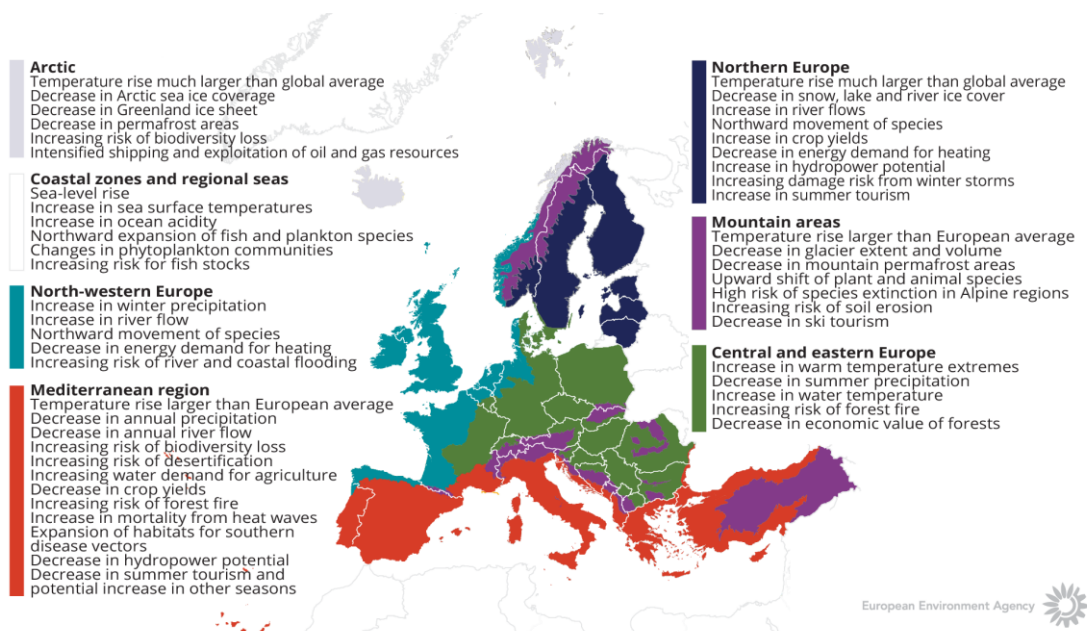


Fig. 10. How is climate expected to change in Europe. The European Environment Agency map.

4 METHODOLOGY AND DATA

4.1 Data

4.1.1 Climate data

The historical precipitation and temperature data have been taken from the project Spain02 v4 (Herrera et al. 2016) for the period 1971–2000 in the case of AG basin and 1986–2015 in the case of VG aquifer. Periods of 30 years are frequently employed in climate change impact studies. The Spain02 project provides an estimation of precipitation and temperature obtained using the original data from the Agencia Estatal de Meteorología (State Meteorological Agency—AEMET). The spatial resolution of the data is around 12.5 km and the spatial support is the same than the Euro-CORDEX project, from which the different RCMs were obtained. We used nine RCMs (see Table 4) nested to different GCMs under the most pessimistic scenario of the AR5 of the IPCC, the RCP 8.5, for the period 2071–2100 in the case of AG basin and 2016–2045 in the case of VG aquifer.

Table 4. RCMs and GCMs considered.

RCM \ GCM	CNRM-CM5	EC-EARTH	MPI-ESM-LR	IPSL-CM5A-MR
CCLM4-8-17	X	X	X	
RCA4	X	X	X	
HIRHAM5		X		
RACMO22E		X		
WRF331F				X

4.1.2 Hydrological data

We also employed some hydrological information. It includes hydraulic head evolution in different piezometers obtained from the Spanish official network for monitoring the quantitative state of groundwater (see their location in Figure 6) and the historical recharge and pumping rates within the aquifer, which were taken from the information included in the Guadalquivir River Basin Plan (2015–2021).

4.1.3 Subsidence data

For those wells we also have information about the land subsidence rates obtained by applying PInSAR techniques (Mateos et al., 2017). The average vertical displacement based on the time series was estimated by using buffer areas with a radius of 1000 m for each piezometer and considering all PSI (Persistent Scatterer Interferometry) data included in the area.

4.1.4 Material of piezometers data

The percentage of fine-grained material (clay and silt) for each piezometer was obtained by exploiting geological data recorded in 38 boreholes drilled in the area. They were interpreted (Mateos et al., 2017) providing isolines of fine-grained sediment percentage taking into account the clay and silt content in the first 50 m of the borehole, as the borehole depths are quite



variable (from 50 m to 122 m). Results showed higher clay content in the piezometers located in the northern and southern extremes of the aquifer as well as in its central part (see Table 5).

Table 5. Content of clay and silt in the considered piezometers (see Fig. 6).

Piezometer	Clay and silt content (%)
5	40
3	5
6	70
8	20
29	20

4.2 Generation of Future Potential Scenarios

The steps of the proposed methodology to generate potential monthly future climate scenarios (precipitation and temperature) are represented in Figure 11. It includes the analysis of data and generation of future individual projections, a multi-objective analysis to identify inferior models, and different ensembles of predictions.

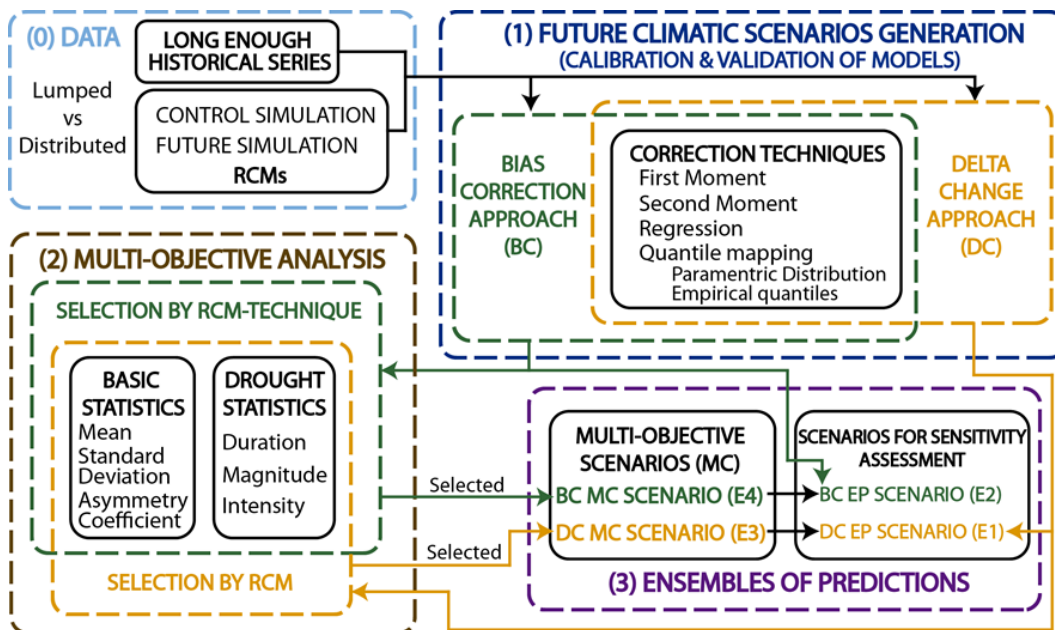


Fig. 11. Flow chart of the methodology to generate future potential scenarios (from Collados-Lara et al., 2018a)

4.2.1 Generation of Future Individual Projections

An analysis of historical data and RCMs simulations allows to identifying the necessity of applying statistical correction techniques to generate future scenarios. These techniques can be employed under two different approaches, bias correction and delta change. The first applies a transformation function to the control simulation series to force some of its statistics or quantile distribution to get closer to the historical ones. This transformation function is also applied to



the future simulation series to obtain the corrected future scenarios. It assumes that the bias between the statistics of historical data and the control simulation will remain invariant in the future. On the other hand, the delta change approach assumes that the relative changes between future simulation and control simulation from RCMs are accurate and applies these changes to the historical series to obtain the corrected future series.

For both conceptual approaches, we tested several statistical techniques with various degrees of complexity and accuracy that intend to preserve different statistics: correction of first- and second- order moments, regression approach (we used the GROUNDST tool developed by Collados-Lara et al. 2020) and quantile mapping (we used qmap package developed by Gudmundsson et al. 2002), which are described below.

- a) Correction of first moment: In the first-moment correction techniques the transformation function only intends to provide a good approximation to the mean values.
- b) Correction of first and second moment: It is focused on the approximation of the mean and standard deviation to define the transformation function.
- c) Regression: It defines the transformation function by adjusting a regression function. Usually, a linear function can provide reliable results in the adjustment.
- d) Quantile mapping: The transformation function is elaborated using the cumulative distribution function of the series.

4.2.2 Multi-Objective Analysis of the individual projections (Basic and Drought Statistics)

A multi-objective analysis based on the goodness-of-fit to some statistics is proposed to identify the approaches (RCMs in the case of delta change and combination of RCM – technique in the case of bias correction) that provide more reliable approximations to historical basic (mean, standard deviation and asymmetry coefficient) and drought statistics (duration, magnitude and intensity). An approach is inferior if any other approach provides approximations significantly better for all the cited statistics (basic and drought statistics).

4.2.3 Ensembles of Predictions to Define More Representative Future Climate Scenarios

Two ensemble scenarios were defined by combining as equifeasible members all the future series (that correspond to different RCMs simulations) generated by applying delta change (scenario E1) or bias correction (scenario E2) approaches. Note that, in the equifeasible ensembles, the number of members employed to define the future scenarios can be obtained by multiplying the number of RCMs and the number of techniques. Two other options were defined by combining only the not eliminated models (E3) (in delta change approach) or the not eliminated combinations of models and correction techniques (E4) (bias correction techniques), assuming that we do not trust the eliminated ones. Note that eliminate models are the identified as inferior in the multi-objective analysis.

4.3 Potential Impacts of Future Climate Change Scenarios on Ground Subsidence

A flowchart of the proposed method used to assess potential impacts of climate change on subsidence has been represented in Fig. 12.

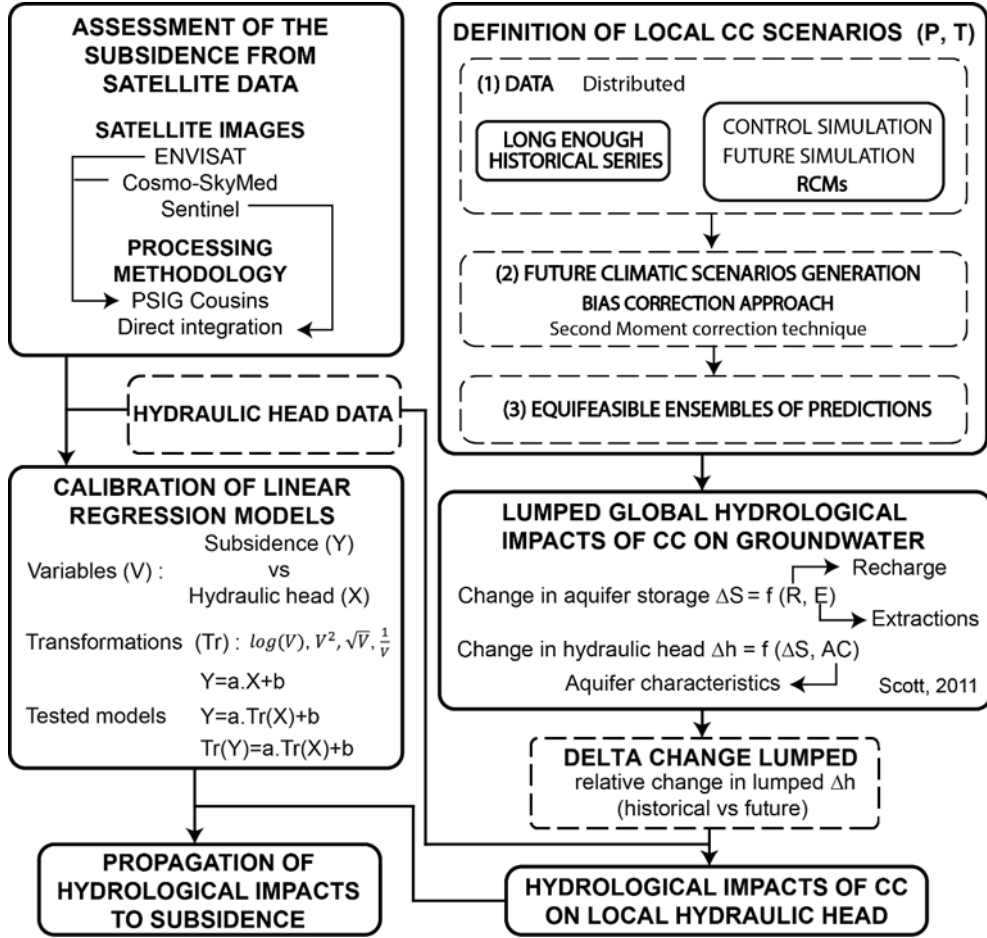


Fig. 12. Flow chart of the methodology to assess impacts of climate change on subsidence (from Collados-Lara et al., 2020)

4.3.1 Hydrological Impacts of Climate Change on Groundwater Levels

A simple approach proposed by Scott (2011) is applied to assess future CC impacts on global lumped drawdowns due to the future potential rainfall recharge and pumping. Following this approach, simple balance equations are applied in order to assess the global lumped change in hydraulic head (Δh_t) from aquifer storage (ΔS_t), which is calculated as follow:

$$\Delta S_t = R_t - E_t \quad (1)$$

where R_t is the aquifer rainfall recharge and E_t are the aquifer extractions which can be obtained from Eq. 2.

$$E_t = Eag_t - Enonag_t \quad (2)$$

where Eag_t represents the agricultural extractions and $Enonag_t$ the non-agricultural extractions. They have been calculated using Eq. 3 and 4 respectively.

$$Eag_t = Eag_{t-1} \left[1 + \frac{ET_t - ET_{t-1}}{ET_{t-1}} \right] \quad (3)$$



$$Enonag_t = Enonag_{t-1} \left[1 + \frac{Pop_t - Pop_{t-1}}{Pop_{t-1}} \right] \quad (4)$$

where ET is the evapotranspiration calculated using the Blaney-Criddle method ($ET = p(0.46T_{mean} + 8)$) on the basis of monthly temperature in °C (T_{mean}) and latitude-derived sunshine-hour fraction (p) and Pop is the population of the area.

Finally, the hydraulic head (Δh_t) is obtained using Eq. 5:

$$\Delta h_t = \frac{\Delta S_t}{A \cdot S_y} \quad (5)$$

where A is the aquifer area S_y the specific yield.

The initial conditions to simulate the recharge (R_{t-1}) and pumpings (agricultural or non-agricultural, Eag_{t-1} and $Enonag_{t-1}$) evolutions were taken from the information included in the Guadalquivir River Basin Plan (2015-2021).

The lumped approach proposed by Scott (2011) has been also applied to estimate the lumped hydraulic head drawdowns in the reference historical period (1986-2015). It allows to estimate the delta change (percentage of increment) in the lumped aquifer drawdowns, taking into account the relative difference between the maximum lumped drawdowns in the historical and the future period (2016-2045). These results are obtained assuming that a business as usual management scenario will be maintained in the future. The future potential hydraulic head in each piezometer will be obtained by applying a delta change correction, using the lumped change to modify the historical evolution (for the reference period) of this variable within the piezometer.

4.3.2 Assessment of the subsidence from satellite data

In the present study, spatial and temporal ground surface deformation assessment was obtained by exploiting 70 SAR images from 3 different satellites: ENVISAT (2003-2009, C band), Cosmo-SkyMed (2011-2014, X band) and Sentinel 1A (2015-2016, C band). The processing methodologies applied for each dataset were: (1) PSIG Cousins for ENVISAT and COSMO-Sky-Med datasets, and (2) Direct integration approach for Sentinel 1A dataset. More detailed specifications can be found in Mateos et al. (2017). This combination allows a thorough assessment of the ground deformation pattern in the aquifer and both temporal and spatial dimensions of the subsidence.

PSInSAR measurements were obtained in the VG aquifer, covering a large temporal span of 13 years (from 2003 to 2016). Along this time, a severe drought affected the area during the ENVISAT period (2003-2006), when greater groundwater withdrawals took place.

PSInSAR data were correlated (temporally and spatially) with hydraulic head changes in the aquifer along the monitoring period and with geological data (from boreholes) regarding the clay and silt content in the aquifer. Based on the borehole information, isolines of fine sediments percentage were obtained by Mateos et al. (2017). Clay and silt content is a key information which can explain spatial response of the aquifer-system to hydraulic head changes and the subsequent vertical land movements.



4.3.3 Propagation of Hydrological Impacts to Subsidence

Simple linear regression models have been defined in order to approximate subsidence as a function of hydraulic head drawdowns in the selected head observation wells. We have tested different transformation ($Tr(X)$) of the explanatory and target variables (logarithm, inverse, square, and square root mathematical transformations) in order to identify the one that provides better approximation to the empirical data for this problem (see Table 6).

*Table 6. Regression models and transformation of variables applied. The symbol * represents the tested combinations of model and transformation of variables.*

Model	$Tr(X)$				
	X^2	\sqrt{X}	$\log(X)$	$1/X$	
$Y=a.X+b$	*	-	-	-	-
$Y=a.Tr(X)+b$	-	*	*	*	*
$Tr(Y)=a.Tr(X)+b$	-	*	*	*	*

The models assume that there is a linear relation between both variables, the depending variable and the explanatory variable and its transformations, which is reasonable if the deformation is elastic. An analysis of the linear correlation depending on the percentage of clay and silt content in the ground is also proposed in order to identify and discuss when the linear regression provides better approaches.

5 RESULTS AND CONCLUSIONS

5.1 Influence of the fine-grained material in the aquifer subsidence

In the VG aquifer, we have analyzed the influence of the percentage of clay and silt (in the surrounding area of the piezometer) on the historical subsidence rate and the linear behaviour of the subsidence, assessed in term of the R^2 of the regression models.

Fig. 13a shows the relationship between the percentage of fine-grained material and the historical subsidence rate and Fig. 13b the coefficient of determination obtained for the best approach in each piezometer vs the percentage of clay and silt. In general, a higher percentage of fine-grained material is related to a lower subsidence rate but the correlation of this relationship is poor ($R^2=0.24$). On the other hand, higher coefficients of determination are related with a more linear behaviour between hydraulic heads and subsidence, which is observed for the cases with lower percentage of clay and silt. Note that, in general, the relationship between the percentage of fine-grained material and the coefficients of determination of the linear models has a good correlation (R^2 higher than 0.8).

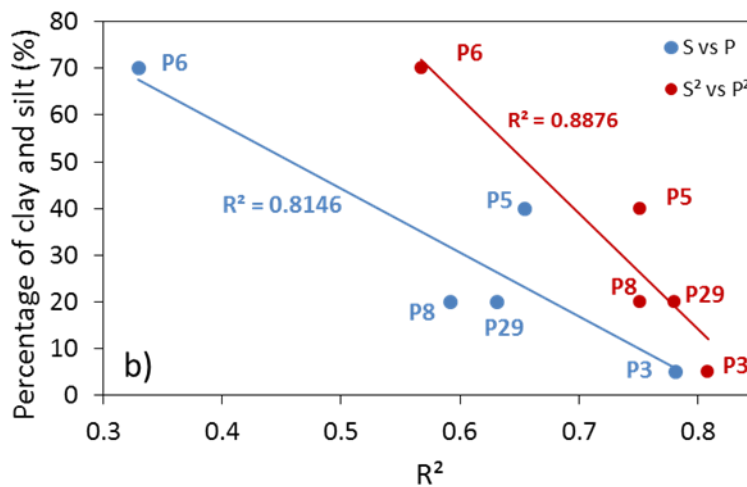
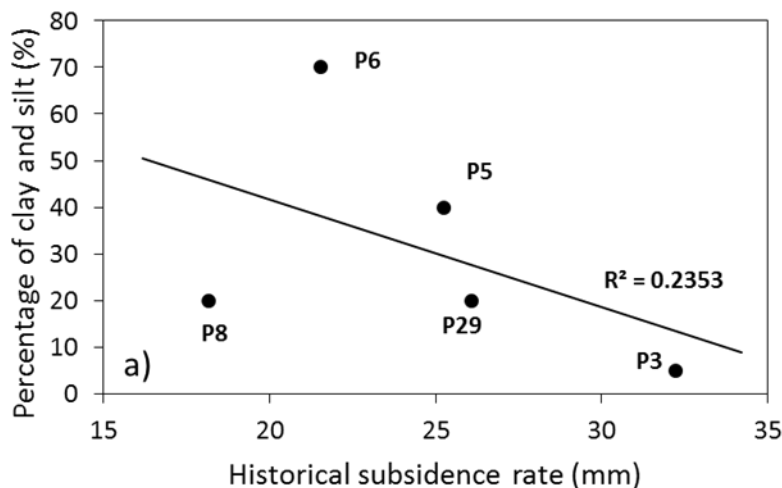


Fig. 13. Relationship between the percentage of clay and silt and the historical subsidence rate (a) and between the correlation coefficient obtained for the two best linear regression model [$S=a.P+b$; $S^2=a.P^2+b$] (b) (from Collados-Lara et al., 2020)

5.2 Impacts of climate change on precipitation, temperature, and droughts

We considered four options to define the most representative future scenarios by applying different ensembles of potential scenarios deduced from the available climate models in the AG basin (see section 4.2.3). In terms of future temperature statistics, the ensemble scenarios defined with the lumped approach (Fig. 14) show practically the same increment in monthly means. The standard deviation estimated using delta change approaches are quite similar to the historical, but both ensembles defined by applying bias correction show significantly lower values.

In terms of future precipitation statistics, almost the same reduction in future mean values are predicted by all the ensembles for every month (Fig. 14). The standard deviation of the future precipitation predicted using the delta change approaches are more similar to the historical (as for temperature variable) than those defined by applying bias correction, whose values are significantly lower. The scenarios under the same approach provide very similar statistics. The average changes predicted using the four ensembles of scenarios are around -27 % in precipitation and + 32 % in temperature.

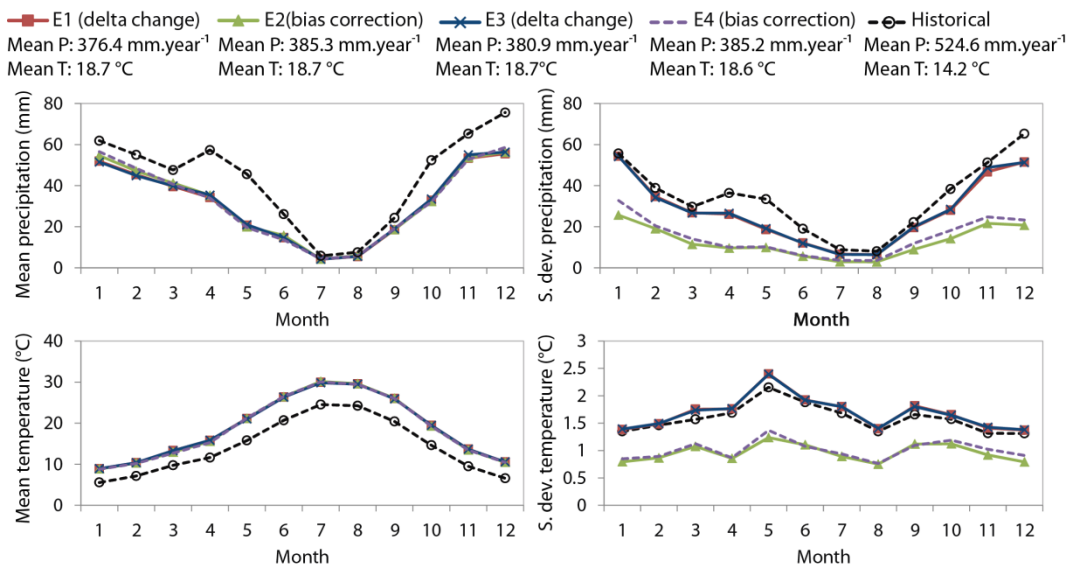


Fig. 14. Mean and standard deviation of future precipitation and temperature series obtained by the four ensemble options (E1, E2, E3, and E4) (from Collados-Lara et al., 2018a).

The future ensemble precipitation scenarios were also analysed in terms of drought statistics (Fig. 15). All four ensembles predict considerable increases in length, magnitude and intensity of droughts. The hypothesis assumed to define the ensembles (equifeasible or non-equifeasible) is higher in the bias correction approach.



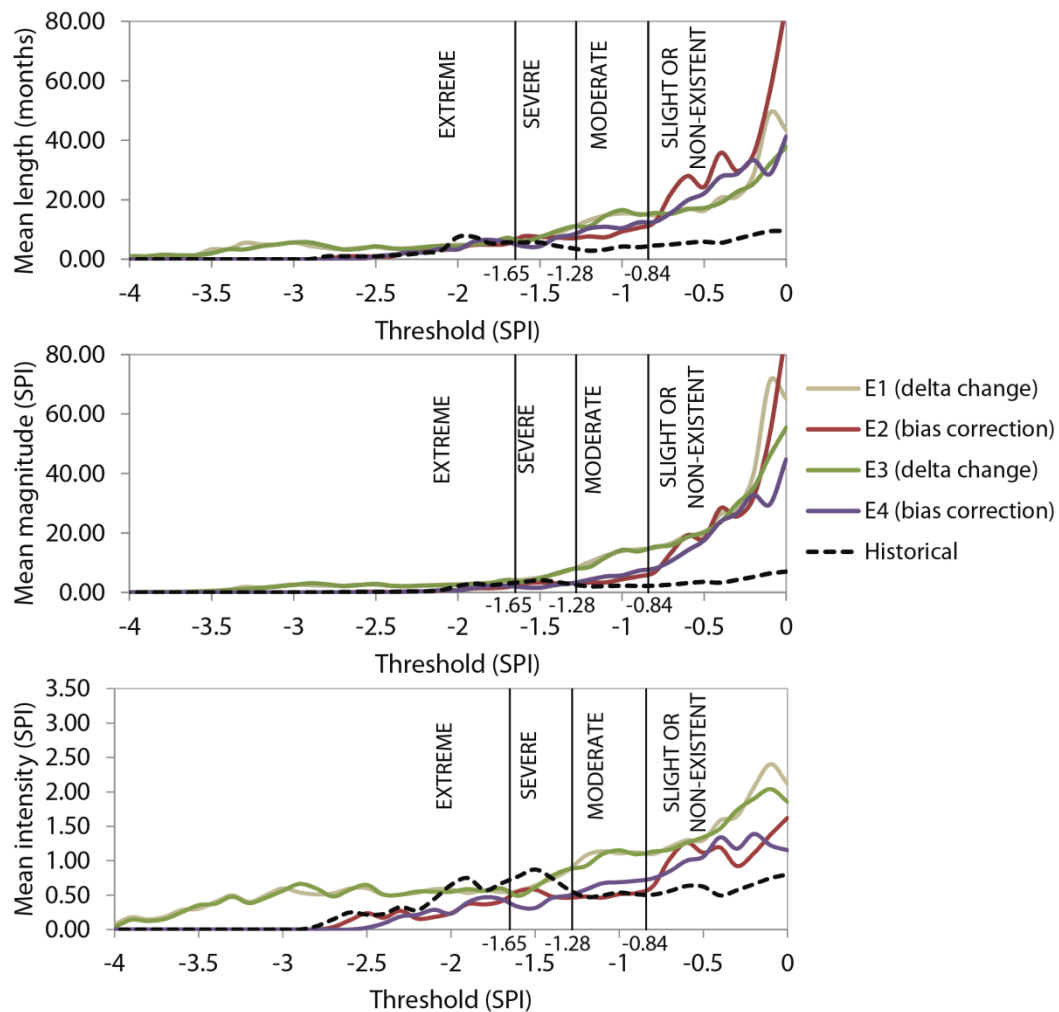


Fig. 15. Drought statistics of future precipitation series obtained by the four ensemble options (E1, E2, E3 and E4) (from Collados-Lara et al., 2018a).

5.3 Impacts of climate change on hydraulic head and subsidence

In the case of the VG aquifer we used an ensemble of different projections generated by using the bias correction approach, the first and second moment correction and the nine considered RCMs. Note that uncertainty related to correction approaches is low compared to the uncertainty related to RCMs. The global lumped hydraulic head drawdowns in the VG aquifer are obtained by applying the Scott approach (Scott, 2011). The maximum lumped drawdown obtained in the future is 3.3% greater than the one obtained in the historical period. This relative change is employed to apply a delta change to correct the historical drawdowns in the selected head observation wells (See Fig. 12) obtaining for the future period the values represented in Fig. 16.

The propagation of the impacts of the potential future CC scenario on subsidence (Fig. 16) shows important increment of the maximum subsidence (55,3 and 52,7% for the models $[S=a.P+b]$ and



[$S^2=a.P^2+b$] respectively) with respect to the historical maximum observed values. The higher increment of the maximum subsidence (68,3 and 65,7% for the models [$S=a.P+b$] and [$S^2=a.P^2+b$] respectively) with respect to the historical maximum observed values occurs in the piezometer 5, which is located in the western area where the percentage of clay is 40%.

In terms of mean subsidence (see Fig. 17) the mean increment of subsidence is 4,1 and 4,5 mm for the models [$S=a.P+b$] and [$S^2=a.P^2+b$] respectively. The piezometer with the higher increment of mean subsidence is the number 3 with 5,4 and 5,9 mm for the models [$S=a.P+b$] and [$S^2=a.P^2+b$] respectively. This piezometer shows the higher variability of subsidence in the historical and future period and has the lower content of clay and silt.

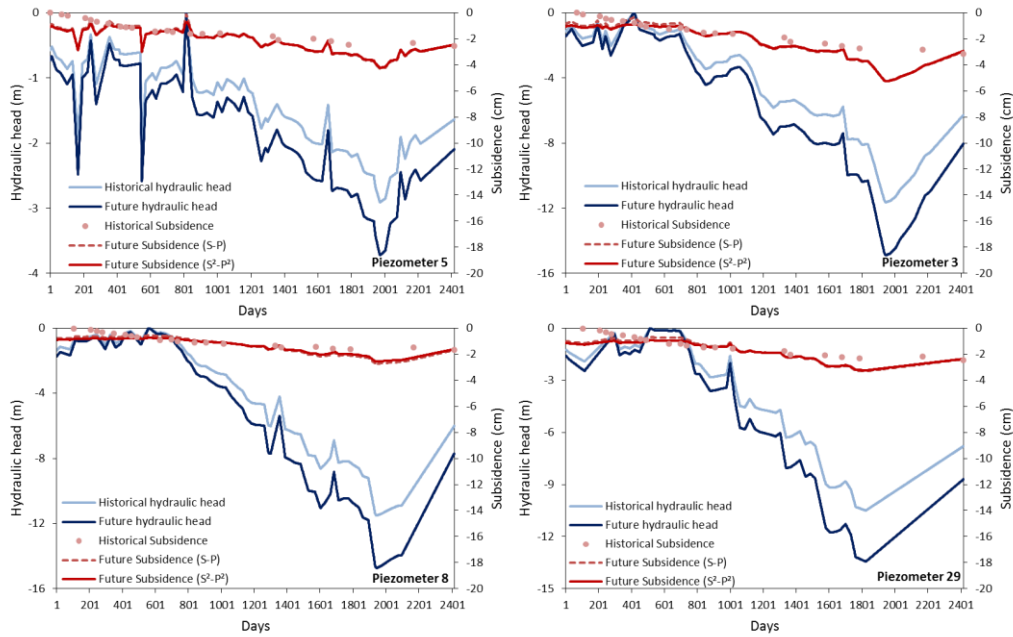


Fig. 16. Historical and future subsidence and hydraulic head for the two best linear regression model [$S=a.P+b$; $S^2=a.P^2+b$] (from Collados-Lara et al., 2020).

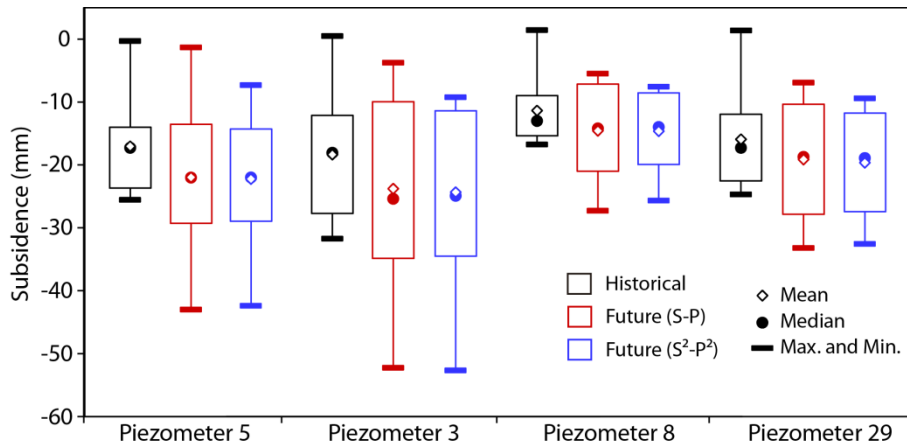


Fig. 17. Historical and future subsidence for the two best linear regression model [$S=a.P+b$; $S^2=a.P^2+b$] (from Collados-Lara et al., 2020).



The analyses of results show that, assuming a business as usual management scenario, the impacts of CC on the subsidence would be very significant for the case study. The mean increment of the maximum subsidence rates in the considered wells for the future horizon (2016-2045) and the scenario RCP 8.5 is 54%. In order to avoid undesirable consequences/risks some adaptation strategies should be applied to control and minimize land subsidence caused by groundwater withdrawals.

6 REFERENCES

Calvache, M.L.; Gómez Fontalva, J.M.; Duque, C. (2013). New data about the water budget generated with a flow model in the aquifer of Vega de Granada. *GEOGACETA*, 54, 127-130.

Castillo, A.; Robles-Arenas, V.; Sánchez-Díaz, I.; Martín-Rosales, W. (2010). Evolución hidrogeológica del acuífero de la Vega de Granada (Andalucía, España), como base de la gestión de los recursos hídricos subterráneos. In: *Estudios hidrológicos, hidrogeológicos y ambientales, como base de la gestión de los recursos hídricos*. Ed. Asociación Internacional de Hidrogeólogos-Grupo Argentino.

CHG (1995). River Basin Plan of Guadalquivir. Confederación hidrográfica del Guadalquivir.

Collados-Lara, A.J.; Pulido-Velazquez, D.; Pardo-Igúzquiza, E. (2018a). An Integrated Statistical Method to Generate Potential Future Climate Scenarios to Analyse Droughts. *Water*, 10, 1224. doi:10.3390/w10091224.

Collados-Lara, A.J.; Pulido-Velazquez, D.; Pardo-Igúzquiza, E. (2018b). Precipitation fields in an alpine Mediterranean catchment. Inversion of precipitation gradient with elevation or undercatch of snowfall? *International Journal of Climatology* 38, 3565–3578. doi: 10.1002/joc.5517.

Collados-Lara, A. J., Pulido-Velazquez, D., Mateos, R. M., & Ezquerro, P. (2020). Potential impacts of future climate change scenarios on ground subsidence. *Water (Switzerland)*. <https://doi.org/10.3390/w12010219>

Fernández, C. (2010). Usos agrícolas en la Vega de Granada. La historia de los intentos de protección frente la presión urbana con débiles resultados. In: *Ciudades para un Futuro más Sostenible*. Ed. Universidad Politécnica de Madrid.

Gudmundsson, L., Bremnes, J. B., Haugen, J. E., & Engen-Skaugen, T. (2012). Technical Note: Downscaling RCM precipitation to the station scale using statistical transformations & A comparison of methods. *Hydrology and Earth System Sciences*. <https://doi.org/10.5194/hess-16-3383-2012>

Herrera, S., Fernández, J., Gutiérrez, J.M., 2016. Update of the Spain02 Gridded Observational Dataset for Euro-CORDEX evaluation: Assessing the Effect of the Interpolation Methodology. *International Journal of Climatology* 36, 900–908.

IGME-DGA (2009). Apoyo a la caracterización adicional de las masas de agua subterránea en riesgo de no cumplir los objetivos medioambientales en 2015. Demarcación Hidrográfica del Guadalquivir. Encomienda de gestión de la Dirección General del Agua (MARM) al IGME (MCIN) para la realización de trabajos científico-técnicos de apoyo a la sostenibilidad y protección de las aguas subterráneas.

Mateos, R.M., Ezquerro, P., Luque-Espinar, J.A., Béjar-Pizarro, M., Notti, D., Azañón, J.M., Montserrat, O., Herrera, G., Fernández-Chacón, F., Peinado, T., Pedro, Galve J., Pérez-Peña, V., Fernández-Merodo, J.A., Jiménez, J., 2017. Multiband PSInSAR and long-period monitoring of land subsidence in a strategic detrital aquifer (Vega de Granada, SE Spain): an approach to support management decisions. *J. Hydrol.* 553, 71–87.

Pulido-Velazquez, D.; Collados-Lara, A.-J.; Alcalá, F.J. (2017). Assessing impacts of future potential climate change scenarios on aquifer recharge in continental Spain. *J. Hydrol.* doi:10.1016/j.jhydrol.2017.10.077.

Scott, C. A. (2011). The water-energy-climate nexus: Resources and policy outlook for aquifers in Mexico. *Water Resources Research*. <https://doi.org/10.1029/2011WR010805>

UPV (2004). Gestión integral del agua en la Vega de Granada. Modelo de simulación y gestión de los recursos hídricos. Instituto de Ingeniería Hidráulica y Medio Ambiente (I.I.A.M.A) de la Universidad Politécnica de Valencia (U.P.V.).



Deliverable 4.2

PILOT DESCRIPTION AND ASSESSMENT

Chalk aquifer (United Kingdom)

Authors and affiliation:

**Majdi Mansour, Vasileios
Christelis**

British Geological Survey (BGS)

This report is part of a project that has received funding by the European Union's Horizon 2020 research and innovation programme under grant agreement number 731166.



Deliverable Data	
Deliverable number	D4.2
Dissemination level	Public
Deliverable name	Pilots description and assessment report for recharge and groundwater vulnerability
Work package	WP4
Lead WP	BRGM, BGS
Deliverable status	
Version	Version 3
Date	23/3/2021

[This page has intentionally been left blank]

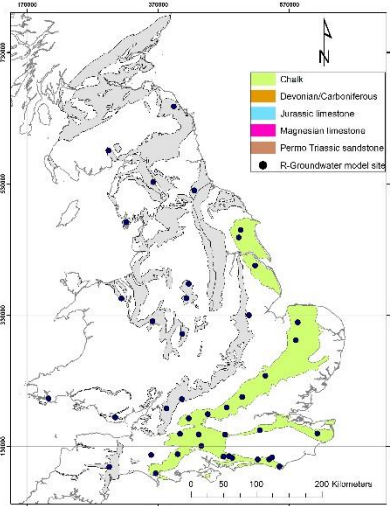
LIST OF ABBREVIATIONS & ACRONYMS

BGS	British Geological Survey
CC	Climate Change
EU	European Union
FAO	Food and Agriculture Organization
GCM	Global Circulation Models
GSO	Geological Survey Organization
ISIMIP	Inter Sectoral Impact Model Inter-comparison Project
NSE	Nash-Sutcliffe Efficiency
PET	Potential Evapo-Transpiration
R	Regression coefficient error
WP	Work Package

TABLE OF CONTENTS

LIST OF ABBREVIATIONS & ACRONYMS	5
1 EXECUTIVE SUMMARY	5
2 INTRODUCTION	7
3 PILOT AREA	9
3.1 Site description and data	9
3.1.1 Index boreholes in the Chalk aquifer in the UK	9
3.1.2 Topography	12
3.1.3 Land use and climate	13
3.1.4 Rainfall	14
3.1.5 Potential evaporation	16
3.1.6 Hydrogeology	17
3.1.7 Groundwater levels	18
3.2 Climate change challenge	18
4 METHODOLOGY	20
4.1 Methodology and climate data	20
4.1.1 AquiMod	20
4.1.2 Metran	21
4.1.3 The distributed recharge model ZOODRM applied at the UK scale	22
4.1.4 Climate data	23
4.2 Model set-up	24
4.2.1 AquiMod	24
4.2.2 Metran	27
4.2.3 National scale model (ZOODRM)	28
4.3 Model calibration	29
4.3.1 Calibration of AquiMod models	29
4.3.2 Calibration of Metran models	32
4.3.3 Calibration of the UK national scale model using ZOODRM	33
5 RESULTS AND CONCLUSIONS	34
5.1 Historical recharge values	34
5.2 Projected recharge values	38
REFERENCES	45
APPENDICES	47
Appendix A: AquiMod methodology	47
The soil moisture module	48
The unsaturated zone module	49
The saturated zone module	49
Limitations of the model	51
Model input and output	51
Appendix B: Metran methodology	53
Limitations	54
Time step	54
Model output	54
Model quality	55
Recharge	55

1 EXECUTIVE SUMMARY

Pilot name	Chalk aquifer	
Country	United Kingdom	
EU-region	North-western Europe	
Area (km ²)	21 500 km ²	
Aquifer geology and type classification	A soft, white limestone traversed by layers of flint. A dual porosity medium with groundwater flow occurring within both the matrix and through fractures. Yield is typically of the order of 150 l/sec.	
Primary water usage	Irrigation / Drinking water / Industry	
Main climate change issues	Risk of high precipitation causing groundwater flooding. Risk of drought during dry weather periods.	
Models and methods used	Lumped groundwater modelling (AquiMOD)	
Key stakeholders	Government. Research institutes. Water companies.	
Contact person	British Geological Survey. Andrew McKenzie	

This report describes the work undertaken by the British Geological Survey (BGS/UKRI) as a part of TACTIC WP4 to calculate historical and future groundwater recharge across the outcrop of the Chalk aquifer and at selected observation boreholes within the chalk. Multiple tools, selected from the TACTIC toolbox that is developed under WP2 of the TACTIC project, have been used for this purpose.

The Chalk aquifer is a major aquifer in England providing more than 70% of the public water supply in southern England (Foster and Sage, 2017). It is a microporous white limestone with low matrix permeability but with well-developed interconnected network of fractures and solution enhancement fractures. The Chalk outcrop is characterised by smooth rolling hills with a land use that includes enclosed fields, woodland, open land, and built-up areas. The central part of the aquifer is overlain by deposits of Palaeogene age and where the groundwater becomes under confined conditions. Groundwater within the outcrop is mostly under unconfined conditions, albeit the presence of patches of Clay and flints.

Three tools have been used to estimate the recharge values. These are the lumped parameter computer model *AquiMod* (Mackay et al., 2014a), the transfer function-noise model *Metran* (Zaadnoordijk et al., 2019), and the distributed recharge model *ZOONDRM* (Mansour and Hughes, 2004). Future climate scenarios are developed based on the ISIMIP (Inter Sectoral Impact Model Inter-comparison Project (www.isimip.org) datasets. The resolution of the data is 0.5°x0.5° global grid and at daily time steps. As part of ISIMIP, much effort has been made to standardise the climate data (e.g. undertake bias correction).

The estimation of the recharge model using the lumped model *AquiMod* is achieved by running the model in Monte Carlo mode. This produces many runs that are equally acceptable and consequently the uncertainty in the estimated recharge values can be assessed. The application of additional tools provides an additional mean to assess this uncertainty. Generally speaking, the differences between the 75th and 25th percentile recharge values are not significant when compared to the absolute recharge values calculated at the selected boreholes. In addition, the recharge values estimated using the distributed recharge model at these boreholes are very close to those obtained from the lumped model. This was expected as the two models use the same recharge calculation method; however, the former calculates potential recharge and the latter calculates actual recharge. The absolute recharge values calculated by the transfer function-noise model *Metran* are different from those calculated by the lumped model, but the pattern of spatial distribution is maintained.

Future recharge values have been calculated using the projected rainfall and potential evaporation values are 5 to 20% different from historical values on average. The 3° Max scenario, the wettest used in this work, produces values that are very different from the historical ones. This is observed in the output of both the lumped and the distributed models. Finally, future estimates are discussed in this report using long term average recharge values. It is recommended to carry out further analysis to these output in order to understand the temporal changes in recharge values in future, especially over the different seasons. In addition, it is recommended that the values and conclusion produced from this work should be compared to those obtained from different studies that applies future climate data obtained from different climate models.

2 INTRODUCTION

Climate change (CC) already has widespread and significant impacts on Europe's hydrological systems including groundwater bodies, which is expected to intensify in the future. Groundwater plays a vital role for the land phase of the freshwater cycle and has the capability of buffering or enhancing the impact from extreme climate events causing droughts or floods, depending on the subsurface properties and the status of the system (dry/wet) prior to the climate event. Understanding the hydrogeology is therefore essential in the assessment of climate change impacts. Providing harmonised results and products across Europe is further vital for supporting stakeholders, decision makers and EU policies makers.

The Geological Survey Organisations (GSOs) in Europe compile the necessary data and knowledge of the groundwater systems across Europe. To enhance the utilisation of these data and knowledge of the subsurface system in CC impact assessments, the GSOs, in the framework of GeoERA, has established the project "Tools for Assessment of Climate change Impact on Groundwater and Adaptation Strategies – TACTIC". By collaboration among the involved partners, TACTIC aims to enhance and harmonise CC impact assessments and identification and analyses of potential adaptation strategies.

TACTIC is centred around 40 pilot studies covering a variety of CC challenges as well as different hydrogeological settings and different management systems found in Europe. Knowledge and experiences from the pilots will be synthesised and provide a basis for the development of an infrastructure on CC impact assessments and adaptation strategies. The final projects results will be made available through the common GeoERA Information Platform (<http://www.europe-geology.eu>).

The specific TACTIC activities focus on the following research questions:

- What are the challenges related to groundwater- surface water interaction under future climate projections (TACTIC WP3)?
- Estimation of renewable resources (groundwater recharge) and the assessment of their vulnerability to future climate variations (TACTIC WP4).
- Study the impact of overexploitation of the groundwater resources and the risks of saline intrusion under current and future climates (TACTIC WP5).
- Analyse the effectiveness of selected adaptation strategies to mitigate the impacts of climate change (TACTIC WP6).

This report describes the work undertaken by the British Geological Survey (BGS/UKRI) as a part of TACTIC WP4 to calculate groundwater recharge at selected locations within the Chalk aquifer. WP4 is divided into seven tasks that cover the following activities: Review of tools and methods and identification of data requirements (Task 4.1), identification of principal aquifers and their characteristics aided by satellite data (Task 4.2), recharge estimation and its evolution under climate change scenarios in the principal aquifers (Task 4.3), analysis of long-term piezometric time series to evaluate aquifer vulnerability to climate change (Task 4.4), assessment of subsidence in aquifer systems using DInSAR satellite data (Task 4.5), development of a satellite based net precipitation and recharge map at the pan-European scale (Task 4.6), and tool descriptions and guidelines (Task 4.7).

The work presented here is related to Task 4.3 that aims at the estimation of recharge under current and future climates. This is undertaken using multiple tools selected from the TACTIC toolbox that has been developed under WP2 of the TACTIC project. The toolbox is a collection of groundwater models, scripts, spreadsheets that serves all the activities identified in TACTIC workpackages. Here we use the lumped groundwater model *AquiMod* (Mackay et al., 2014a and Mackay et al., 2014b) and the Transfer Function-Noise Model *Metran* (Zaadnoordijk et al., 2019) with main challenge to calibrate these models to reproduce the behaviour of the observed groundwater level time series. The calibrated models are then used to calculate historical and future recharge values. In addition to these two models, we apply the UK national scale recharge model (Mansour et al., 2018) to validate the calculated recharge values and also to address the uncertainty associated with the calculation of these values.

3 PILOT AREA

3.1 Site description and data

3.1.1 *Index boreholes in the Chalk aquifer in the UK*

The Chalk aquifer is a major aquifer in England providing more than 70% of the public water supply in southern England. It is a microporous white limestone with low matrix permeability. It is an aquifer due to its well-developed interconnected network of fractures and because of solution enhancement of the fractures. The chalk stretches from the south coast of England including the Isle of Wight to the southeast of Yorkshire in the North and has a large outcrop area of over 21 500 km² (Figure 1).

The chalk has been subject to several historical drought events but groundwater has played an important role dampening the impact of these events on public water supply. Groundwater flooding, on the other hand, has caused significant disruptions during many wet winters and caused infrastructure damage.

Extensive hydrogeological works including numerical modelling have been undertaken to conceptualise and simulate recharge and groundwater flow in the Chalk (Cross et al., 1995, Ragab et al., 1997, Jackson et al, 2001, Bradford et al., 2002, Hutchinson, et al., 2012, ESI, 2015, etc.). These studies calculate infiltration recharge into the chalk outcrop. However, the study area is rich with observed groundwater level data obtained from the large number of boreholes that have been drilled over the past century. In addition to the important role these groundwater level data can play in the calibration of the developed numerical models, they can be also used to undertake statistical analysis and apply lumped models. This allows better understanding of the hydrogeological behaviour of the chalk, the reconstruction of past groundwater levels to study past drought and flooding events, making short-term groundwater level predictions, and studying the impact of climate change. Figure 1 shows a number of observation boreholes within the Chalk aquifer and that are selected to estimate the recharge values, and to study the variation of the recharge under the conditions of future climate.

Table 1 shows the locations of the observation boreholes across the Chalk. The locations of these boreholes are intentionally selected to give a good spatial coverage of the Chalk and consequently to include a range of aquifer characteristics in the analysis. Lumped groundwater models are built to estimate the recharge values.

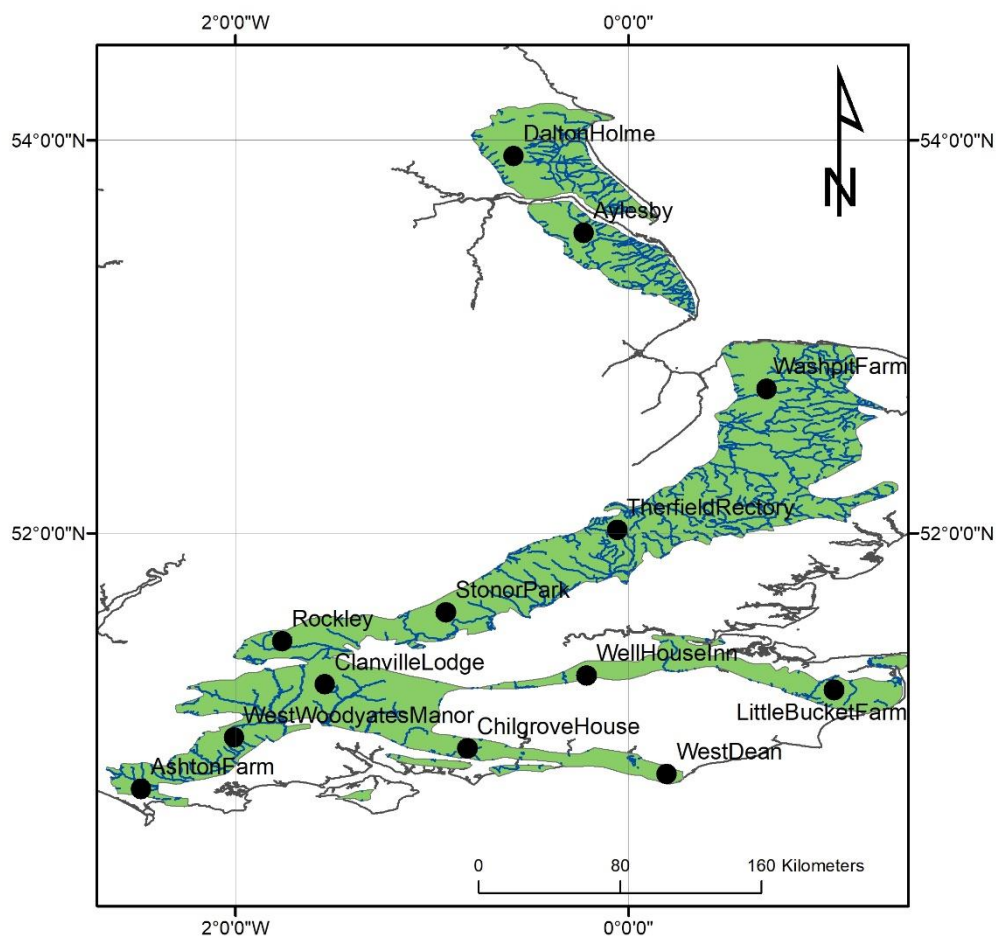


Figure 1. Extent of the Chalk aquifer outcrop with borehole locations.

Table 1. Description of observation boreholes

Borehole name	Location	GWls record	Hydrogeological response
Ashton Farm	South of England	1974-current	Sinusoidal annual hydrograph signal. Rapid response to recharge.
Aylesby	Northeast of England	1978-current	Minor direct response to winter rainfall. Possible impact of abstraction.
Chilgrove House	South of England	1836-current	Rapid response to recharge. The borehole occasionally overflows.
Clanville Lodge Gate	South of England	1996-current	Relatively slower response with additional peaks in some years.
Dalton Holme	Northeast of England	1889-current	Respond relatively slowly to rainfall, perhaps influenced by the drift cover.
Little Bucket Farm	Southeast of England	1971-current	Rapid response to recharge. Water approaching ground surface in wet years and borehole drying up in driest years.
Rockley	Southwest of England	1932-current	Hydrograph has an annual sinusoidal response with low levels controlled by a marl band.
Stonor Park	South of England	1961-current	Damped response to recharge but with possible hydrogeological constraint on low levels.
Therfield Rectory	Southeast of England	1883-current	Large unsaturated zone thickness causing significant delay of groundwater level response to recharge.
Washpit Farm	East of Anglia	1950-current	Typical unconfined Chalk groundwater level fluctuation behaviour.
Well House Inn	Southeast of England	1999-current	Relatively stable maxima observed possibly due to some degree of structural control.
Westdean No.3	Southeast of England	1940-current	The hydrograph exhibits a relatively flashy response possibly due to the relatively small size of the associated chalk blocks.
West Woodyates Manor	South of England	1942-current	Relatively rapid and flashy response for a Chalk well.

3.1.2 Topography

The topography of the Chalk outcrop is characterised by smooth rolling hills with ground surface elevations ranging from zero to approximately 207 m AOD (Figure 2). The Chalk has a great resistance to weathering thus forms steep cliffs at the sea. Scarp slopes, where the chalk meets the surface at an angle, define the Chalk outcrop and include issuing springs that discharge chalk groundwater into rivers that run away from the Chalk.

Because of the permeable nature of the Chalk, rivers are sustained by groundwater input (baseflow), which typically provide between 85 to 95% of the total flow.

Topographical data can be extracted at the selected boreholes to study the occurrences flooding events under future climate conditions.

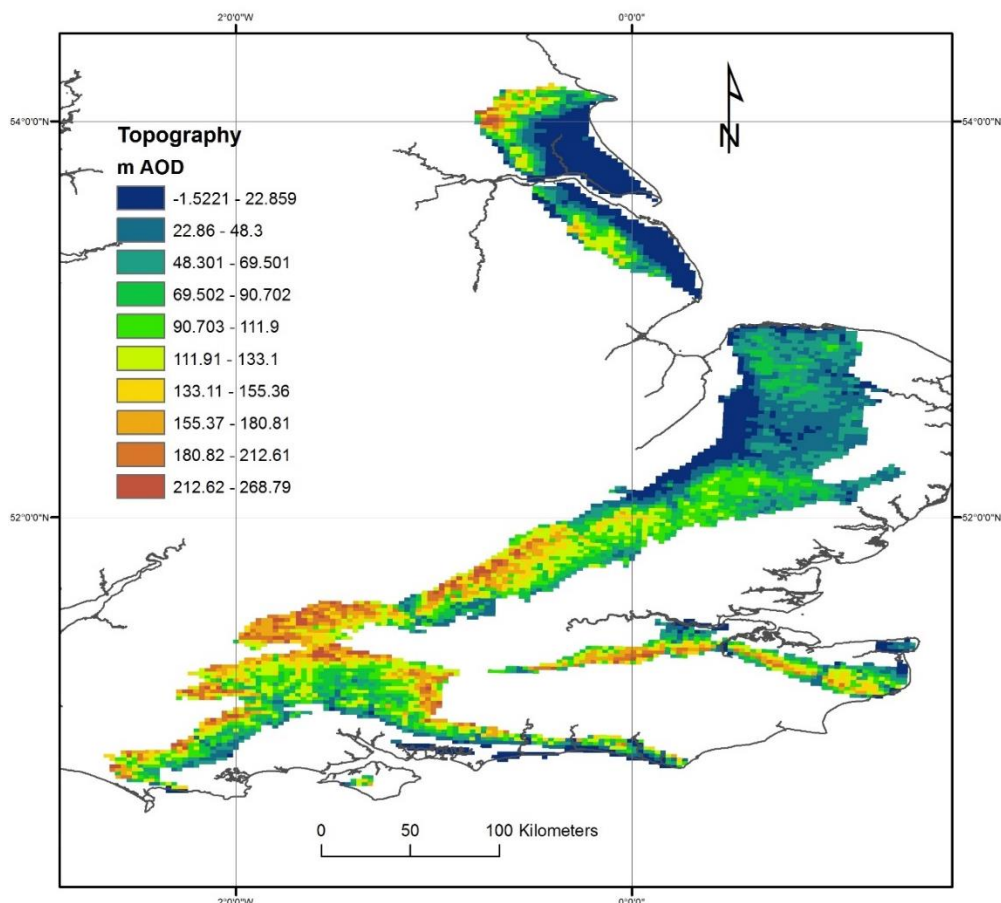


Figure 2. Topography map over the Chalk formation

3.1.3 Land use and climate

Land use includes enclosed fields, woodland, open land, and built-up areas (Figure 3). Most parts of the land over the Chalk are used for agriculture while smaller parts are covered with residential or commercial developments. Figure 3 shows the spatial distribution of landuse classes over the Chalk outcrop (Bibby, 2009). This figure clearly shows that arable is spread across the Chalk outcrop with patches of woodland and semi-natural grassland.

Landuse data can be extracted from this map at the selected boreholes to specify the model parameters that control evapo-transpiration, which is an important component of the total water balance produced by the applied models. Specific information about the landuse types at the selected boreholes are listed in Table 2.

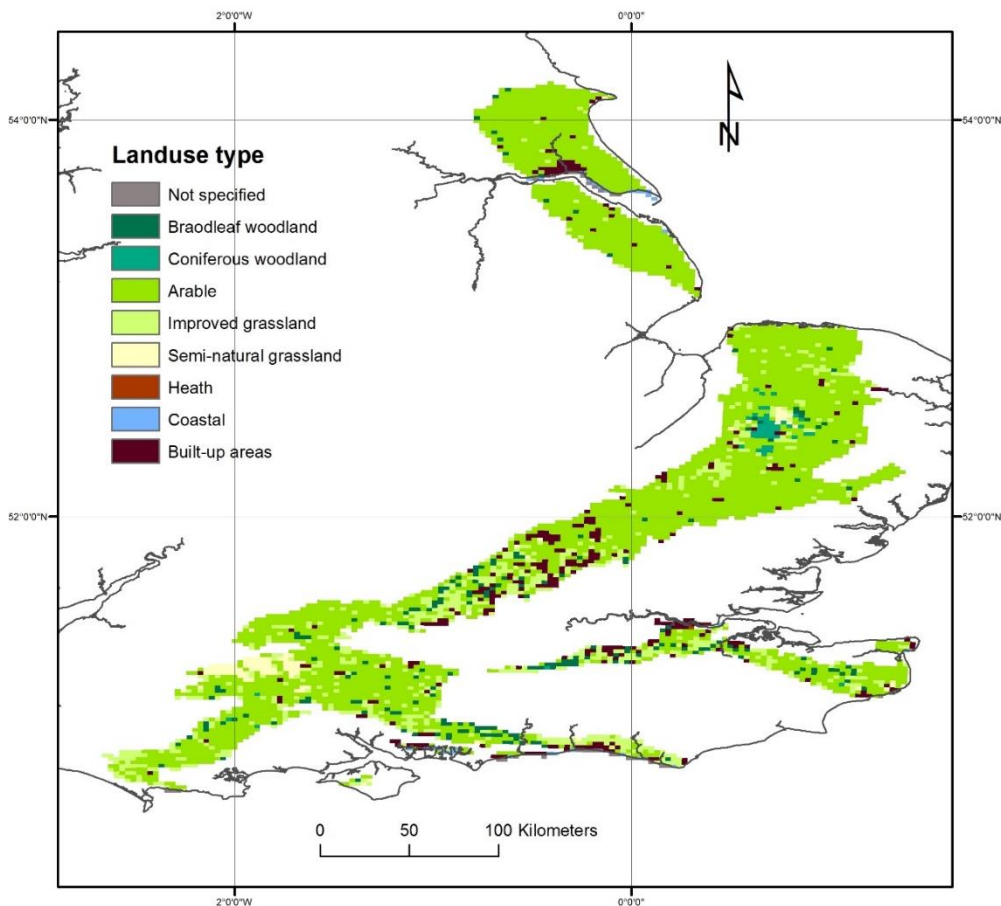


Figure 3. Map of land use over the Chalk formation

3.1.4 Rainfall

Daily rainfall raster data (1×1 km) were obtained from the Centre for Ecology and Hydrology (CEH) and were used to retrieve the daily rainfall values at the grid nodes pertaining to the Chalk. The long-term average (LTA) rainfall across the outcrop is approximately 720 mm year^{-1} (1.97 mm day^{-1}) with lowest rainfall values approximately 550 mm year^{-1} (1.5 mm day^{-1}) observed in east midlands and highest of approximately $1000 \text{ mm year}^{-1}$ (2.74 mm day^{-1}) in the south west of the chalk outcrop (Figure 4).

Spatially distributed rainfall data are available at daily time steps starting from 1961 to 2016 (CEH). While the size of this time step is too coarse to represent storm events for hydrological analysis, it is fine enough to calculate recharge values to drive groundwater models. These data are, therefore, used to drive the lumped models. Table 2 presents specific information about the rainfall values at the selected Chalk boreholes.

Projected (future) values of rainfall data are also available by the work of UKCP09 (Prudhomme et al., 2012; Murphy et al, 2007; Jenkins et al., 2009; Murphy et al, 2009), which provides projections of climate change in the UK. The probabilistic climate projections provided by UKCP09 are not fully spatially coherent; however, (IPCC, 2000) produced 11 physically plausible simulations, generated under the medium emissions scenario known as A1B SRES emission scenario, that overcome this problem. These data can be used for the estimation of projected (future) recharge values.

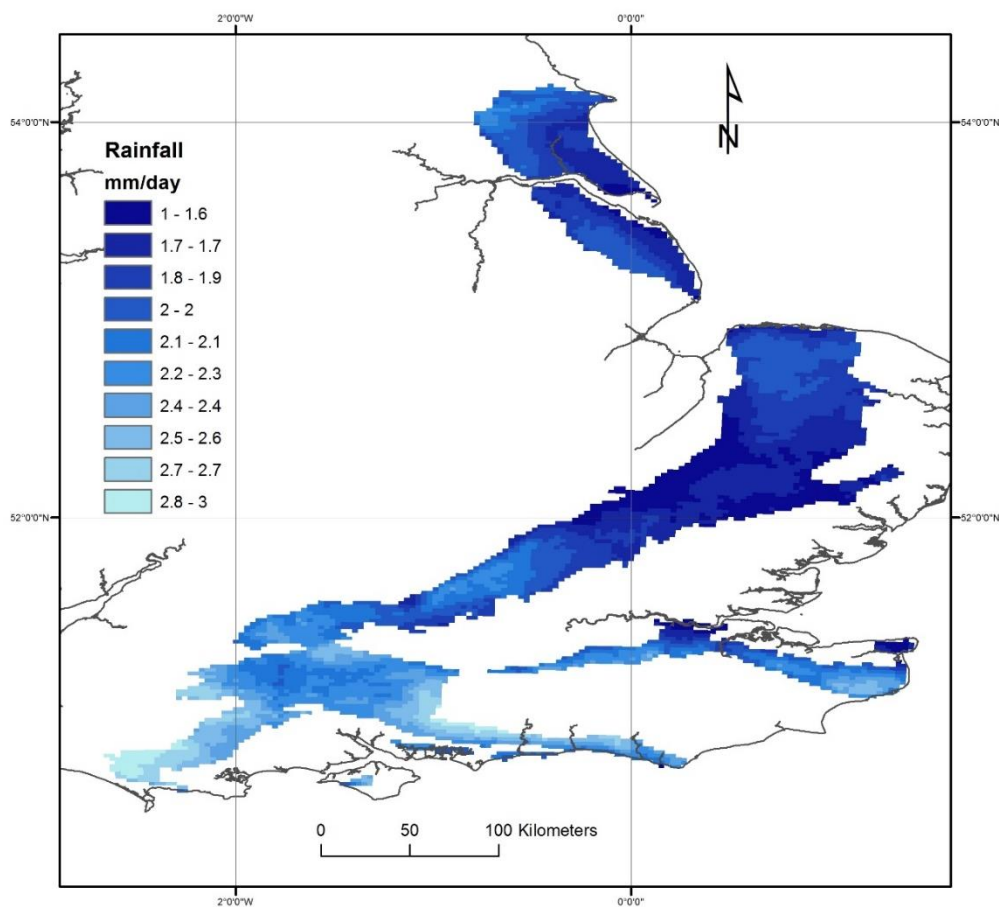


Figure 4. Spatial distribution of rainfall over the Chalk outcrop

3.1.5 Potential evaporation

The monthly potential evapotranspiration (PE) raster datasets (40×40 km) were gathered from a Met Office Rainfall and Evaporation Calculation System (MORECS) in the Met Office of the UK (Hough and Jones, 1997). Figure 5 shows the distributed long-term average potential evaporation data. Highest potential evaporation rates of approximately 670 mm year^{-1} (1.83 mm day^{-1}) are observed to the east of the Chalk as well as in the middle of the central formation. Lowest potential evaporation rates of approximately 540 mm year^{-1} (1.48 mm day^{-1}) are observed to the west and the north of the Chalk outcrop (Figure 5). Table 2 presents specific information about the PE records at the selected boreholes in the Chalk.

Similar to rainfall data, UKCP09 potential evaporation data can be used to run simulations to calculate future recharge values.

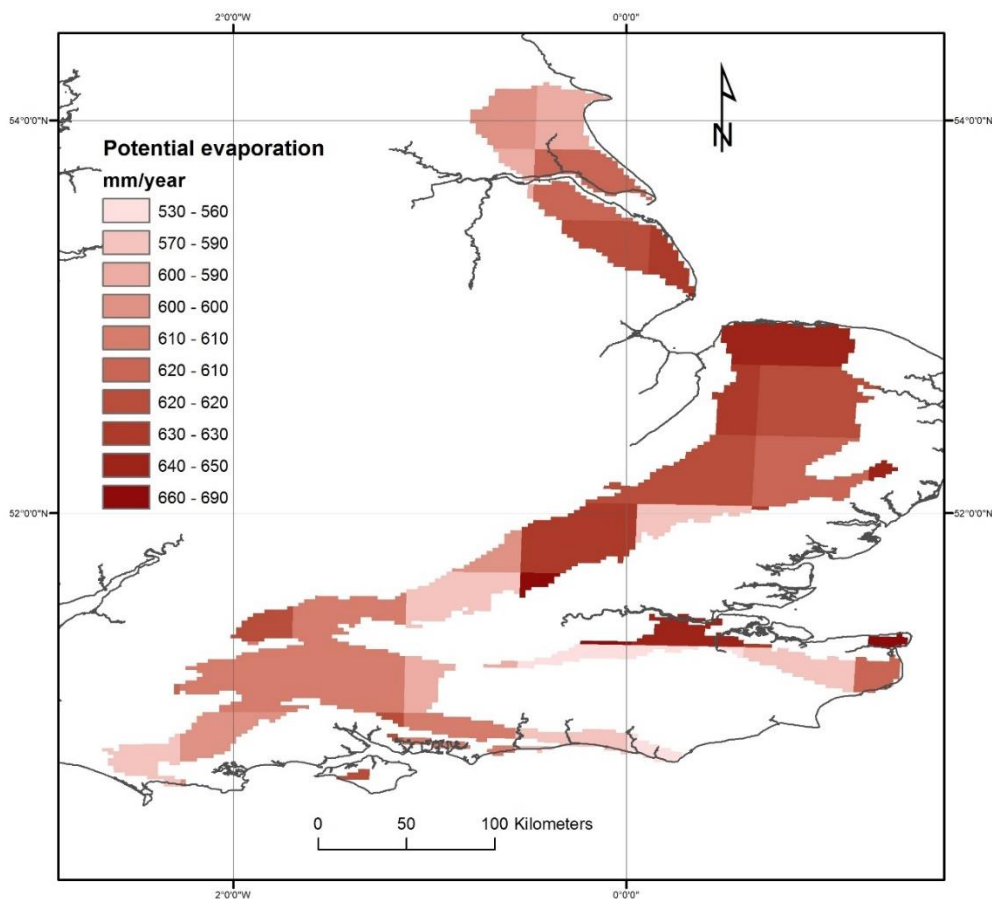


Figure 5. Spatial distribution of potential evaporation in the Chalk

Table 2. Landuse, rainfall and evapotranspiration information for the Chalk

Borehole name	Dominant landuse	Av. Rainfall (mm/day)	Rainfall record	Av. PE (mm/day)	PE record
Ashton Farm	Improved grassland	2.73	1961-current	1.60	1961-current
Aylesby	Arable	1.8	1961-current	1.66	1961-current
Chilgrove House	Arable	2.51	1961-current	1.65	1961-current
Clanville Lodge Gate	Arable	2.1	1961-current	1.66	1961-current
Dalton Holme	Arable	0.53	1961-current	1.61	1961-current
Little Bucket Farm	Arable	2.2	1961-current	1.53	1961-current
Rockley	Improved grassland	2.2	1961-current	1.67	1961-current
Stonor Park	Coniferous woodland	2.13	1961-current	1.60	1961-current
Therfield Rectory	Arable	1.69	1961-current	1.71	1961-current
Washpit Farm	Arable	1.97	1961-current	1.70	1961-current
Well House Inn	Improved grassland	2.25	1961-current	1.50	1961-current
Westdean No.3	Broadleaf woodland	2.24	1961-current	1.52	1961-current
West Woodyates Manor	Arable	2.4	1961-current	1.63	1961-current

3.1.6 Hydrogeology

The Chalk, which is the most important aquifer within the UK (Allen et al., 1996), is a highly permeable aquifer with fractures and solution enhancement leading to karstic features. In the central part of the basin, the Chalk is overlain by deposits of Palaeogene age, consisting of inter-bedded sands and clays underlying thick confining clays. Groundwater within the outcrop part of the Chalk is mostly unconfined, albeit the presence of patches of Clay and flints; however, the water table can be found at large depths from the ground surface, indicating the presence of a thick unsaturated zone.

Palaeogene deposits cover large part of the Chalk in the central part of the south of England, mainly in the Thames Basin. London Clay confines the aquifer groundwater system in this region. behaviour of the groundwater system and the infiltration of recharge.



The Chalk hydraulic characteristics vary spatially. A general observation is that aquifer transmissivity and storage coefficient appear to have a close linkage with topography (Figure 2). The aquifer has high transmissivity and storage characteristics within the valleys but these reduce in the interfluvies. Periglaciation could have contributed to the enhancement of permeability in the valleys. However, lithology, structure and the glacial and Palaeogene cover also have important effects on the hydraulic characteristics of the aquifer (Allen et al., 2005).

Recharge can reach the saturated zone very rapidly through fractures or slowly within the matrix.

3.1.7 Groundwater levels

The unconfined part of the Chalk aquifer is characterised by the presence of a deep unsaturated zone especially in the interfluvies. However, the water table approaches the ground surface in the proximity of rivers and areas of the Chalk have suffered from historical groundwater flooding. The majority of the observation boreholes has been installed in unconfined aquifers of the Chalk formation. The time series of groundwater levels recorded in these boreholes (

Table 1) reflect the different hydrogeological characteristics of this aquifer. There is a long groundwater level (GWL) records available at these boreholes on either a daily or monthly basis with the longest being at the Chilgrove House observation borehole. The groundwater level data at this borehole spans over a period of 180 years.

These time series are used in this study to characterise the aquifer properties and to estimate the infiltration recharge values for water resources management.

While the boreholes are selected so that they are not significantly impacted by the presence of nearby surface features, the records show that some boreholes are affected by nearby pumping. Pumping data are available on a daily basis and these can be included in the simulations if necessary.

3.2 Climate change challenge

The British Geological Survey (BGS) with the support of the Environment Agency (EA) have undertaken a study to investigate the impact of climate change on groundwater resources using the distributed recharge model ZOODRM (Mansour and Hughes, 2018). Potential recharge values for Great Britain (England, Scotland and Wales) are produced using rainfall and potential evaporation data from the Future Flows Climate datasets (11 ensembles of the HadCM3 Regional Climate Model or RCM). This study has shown that generally the recharge season appears to be forecast to become shorter, but with greater amount of recharge “squeezed” into fewer months. This conclusion is aligned with the European Environment Agency map that describes the expected climate change across the different areas in Europe as shown in Figure 6.

The shortening of recharge season indicates that aquifers may become more vulnerable to droughts if rainfall fails in one or two months rather than a prolonged dry winter as can occur

now. At the very least, water management measures have to be put in place to account for periods when recharge volumes reduce. On the other hand, the increased recharge signal could result in flashier groundwater level response and potentially leading to more flooding.

The main climate challenge for water resources managers and stakeholders is to assess the risk of future flooding and drought events. This requires detailed assessment of the variation of resources at regional and local scales rather than national or continental scales.

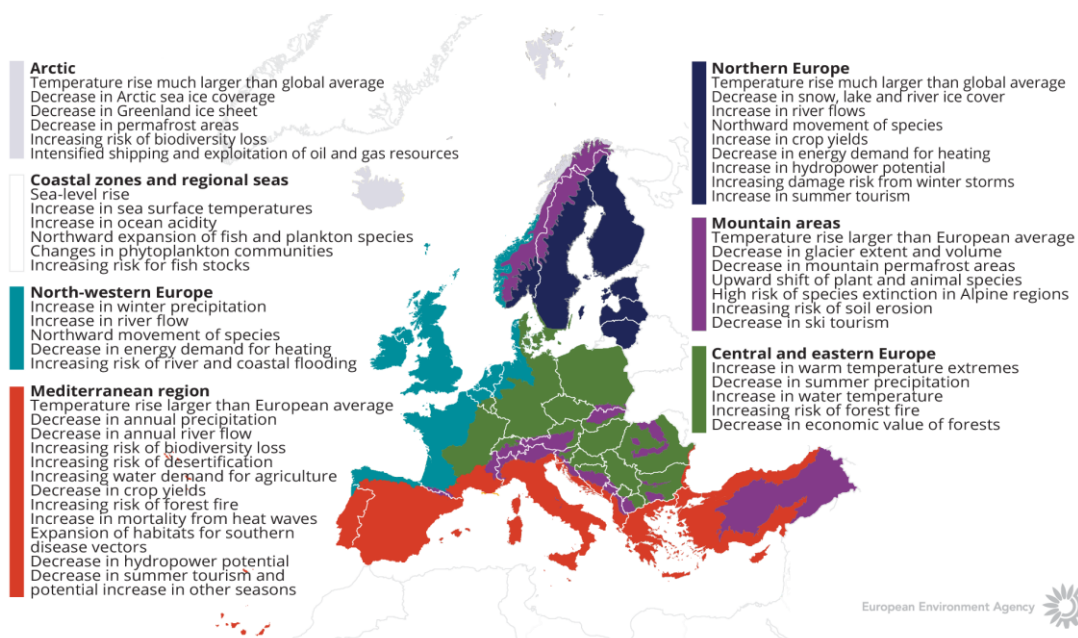


Figure 6. How is climate expected to change in Europe. The European Environment Agency map

4 METHODOLOGY

4.1 Methodology and climate data

4.1.1 *AquiMod*

AquiMod is a lumped parameter computer model that has been developed to simulate groundwater level time series at observational boreholes (Mackay et al., 2014a). It is based on hydrological algorithms that simulate the movement of groundwater within the soil zone, the unsaturated zone, and the saturated zone. The lumped models neglect complexities included in distributed groundwater models but maintain some of the fundamental physical principles that can be related to the conceptual understanding of the groundwater system (Mackay et al., 2014b).

The primary aim of AquiMod is to capture the behaviour of a groundwater system through the analysis of the available groundwater level time series. Once calibrated the model can be run in predictive mode and be used to fill in gaps in historical groundwater level time series and to calculate future groundwater levels. In addition to groundwater levels, it also provides predictions of historical and future recharge values and groundwater discharges.

The mathematical equations that are used to simulate the movement of groundwater flows within the three modules are detailed in Appendix A. The model uses rainfall and potential evaporation time series as forcing data. These are interpreted by the soil module representing the soil zone. The soil module calculates the rainfall infiltration and pass it to the unsaturated zone module. This module delays the arrival of the infiltrating water to the saturated zone module. The latter calculates the variations of groundwater heads and flows accordingly.

The model is calibrated using a Monte Carlo approach. It compares the simulated and observed groundwater level fluctuations and calculates a goodness of fit. The AquiMod version used in this work employs the Root Square Mean Error (RMSE) or the Nash Sutcliffe (NSE) performance measures to assess the performance of the model. The user sets a threshold value to accept all the models that perform better than the specified threshold. The possibility of producing many models that are all equally acceptable, allows the user to interpret the results from all these models and calculate uncertainty.

The recharge values calculated from AquiMod are those that reach the aquifer system and drive the groundwater levels. Thus, it is assumed that these are the actual recharge values as defined by the guidance report prepared by TACTIC project.

4.1.2 Metran

Metran applies a transfer function-noise model to simulate the fluctuation of groundwater heads with precipitation and evaporation as independent variables (Zaadnoordijk et al., 2019). The modelling approach consists mainly of two impulse functions and a noise model. The first impulse function is used for convolution with the precipitation to yield the precipitation contribution to the piezometric head. The second is for evaporation which is either a separately estimated function, or a factor times the function used for precipitation. The noise model is a stochastic noise process described by a first-order autoregressive model with one parameter and zero mean white noise. Further information about the model is given in Appendix B with the model setup shown in the Figure B1.

Metran allows the addition of other processes affecting the behaviour of the groundwater heads, for example pumping or the presence of surface features such as rivers. The contributions from these processes are added to the deterministic part of the model.

Metran has been designed to work with explanatory series that have a daily time step. However, it has been adapted so that other time step lengths can be applied. However, the explanatory variables must still have a constant frequency.

The model is calibrated automatically; however, the model uses two binary parameters, Regimeok and Modok, to judge a resulting time series model. Regimeok cross-examines the explained variance R^2 (> 0.3), the absolute correlation between deterministic component and residuals (< 0.2), and the null hypothesis of non-correlated innovations (p value > 0.01). If all these criteria are satisfied, Regimeok returns a value of 1 indicating highest quality. Modok also cross-examines the explained variance R^2 (> 0.1) and the absolute correlation between deterministic component and residuals (< 0.3) as well as the decay rate parameter (> 0.002) and if all these criteria are satisfied, it is given a value of 1. If Modok = 1 and Regimeok = 0, the model is still considered acceptable. If both these parameters are 0, the model quality is insufficient and the model is rejected.

Metran's time series model is linear and the model creation fails when the system is strongly nonlinear. It is also limited to the response function being appropriate for the simulated groundwater system. Metran uses a gradient search method in the parameter space, so it can be sensitive to initial parameter values in finding an optimal solution.

The model calculates an evaporation factor f that gives the importance of evapotranspiration compared to precipitation. It is possible to use this factor to calculate the recharge values as shown by Equation B2 in appendix B. However, it must be noted that the use of Equation B2 is based on too many assumptions that are easily violated. Because of this, the equations should be applied only to long-term averages using only models of the highest quality.

Following the definitions used in the TACTIC project (See the guidance report) this recharge quantity corresponds to the effective precipitation. It is equal to the potential recharge when the surface runoff is negligible. This in turn is equal to the actual recharge at the groundwater table if there is also no storage change or interflow.

4.1.3 *The distributed recharge model ZOODRM applied at the UK scale*

A distributed recharge model, ZOODRM, has been developed by the British Geological Survey to calculate recharge values required to drive groundwater flow simulators. This recharge model allows grid nesting to increase the resolution over selected area and is called therefore the zooming object-oriented distributed recharge model (ZOODRM) ((Mansour and Hughes, 2004). The model can implement a number of recharge calculation methods that are suitable for temperate climates, semi-arid climates, or for urban areas. One of the methods that is implemented is the recharge calculation method used by Aquimod and detailed in Appendix A1.

ZOODRM uses a Cartesian grid to discretise the study area. It reads daily rainfall and potential evaporation data in time series or gridded format and calculates the recharge and overland flow at a grid node using a runoff coefficient as detailed in appendix A1. However, since this is a spatially distributed model, it reads a digital terrain model and calculates the topographical gradients between the grid nodes. It then uses the steepest gradient to route the calculated surface water downstream until a surface feature, such as a river or a pond, is reached. While the connections between the grid nodes based on the topographical gradients define the water paths along which surface water moves, major rivers are also user-defined in the model. This allows the simulation of river water accretion on a daily basis and the production of surface flow hydrograph. The model is then calibrated by matching the simulated river flows at selected gauging stations to the observed flows, by varying the values of the runoff coefficients.

The procedure used to calibrate the model involves dividing the study area into a number of zones and then to specify runoff values for each one. It is possible to vary the runoff coefficient values on a seasonal basis by using different runoff values for the different months of the year.

The recharge model ZOODRM calculates rainfall infiltration after accounting for evapo-transpiration and soil storage. The simulated infiltration may not reach the aquifer system as it may travel laterally within the soil and discharge into surface water features away from the infiltration location. The simulated infiltration is therefore considered, as potential recharge according to the definitions of recharge processes provided by the guidance report prepared by TACTIC project.

4.1.4 Climate data

The TACTIC standard scenarios are developed based on the ISIMIP (Inter Sectoral Impact Model Inter-comparison Project, see www.isimip.org) datasets. The resolution of the data is 0.5°x0.5° global grid and at daily time steps. As part of ISIMIP, much effort has been made to standardise the climate data (e.g. bias correction). Data selection and preparation included the following steps:

1. Fifteen combinations of RCPs and GCMs from the ISIMIP data set were selected. RCPs are the Representative Concentration Pathways determining the development in greenhouse gas concentrations, while GCMs are the Global Circulation Models used to simulate the future climate at the global scale. Three RCPs (RCP4.5, RCP6.0, RCP8.5) were combined with five GCMs (noresm1-m, miroc-esm-chem, ipsl-cm5a-lr, hadgem2-es, gfdl-esm2m).
2. A reference period was selected between 1981 – 2010 and an annual mean temperature was calculated for the reference period.
3. For each combination of RCP-GCM, 30-years moving average of the annual mean temperature were calculated and two time slices identified in which the global annual mean temperature had increased by +1 and +3 degree compared to the reference period, respectively. Hence, the selection of the future periods was made to honour a specific temperature increase instead of using a fixed time-slice. This means that the temperature changes are the same for all scenarios, while the period in which this occur varies between the scenarios.
4. To represent conditions of low/high precipitation, the RCP-GCM combinations with the second lowest and second highest precipitation were selected among the 15 combinations for the +1 and +3 degree scenario. This selection was made on a pilot-by-pilot basis to accommodate that the different scenarios have different impact on the various parts of Europe. The scenarios showing the lowest/highest precipitation were avoided, as these endmembers often reflects outliers.
5. Delta change values were calculated on a monthly basis for the four selected scenarios, based on the climate data from the reference period and the selected future period. The delta change values express the changes between the current and future climates, either as a relative factor (precipitation and evapotranspiration) or by an additive factor (temperature).
6. Delta change factors were applied to local climate data by which the local particularities are reflected also for future conditions. These monthly values (one set of rainfall and PE for each warming scenario) are used to drive the groundwater models presented in this report.

For the analysis in the present pilot the following RCP-GCM combinations were employed:

Table 3. Combinations of RCPs-GCMs used to assess future climate

		RCP	GCM
1-degree	"Dry"	rcp6p0	noresm1-m
	"Wet"	rcp4p5	miroc-esm-chem
3-degree	"Dry"	rcp4p5	hadgem2-es
	"Wet"	rcp8p5	miroc-esm-chem

4.2 Model set-up

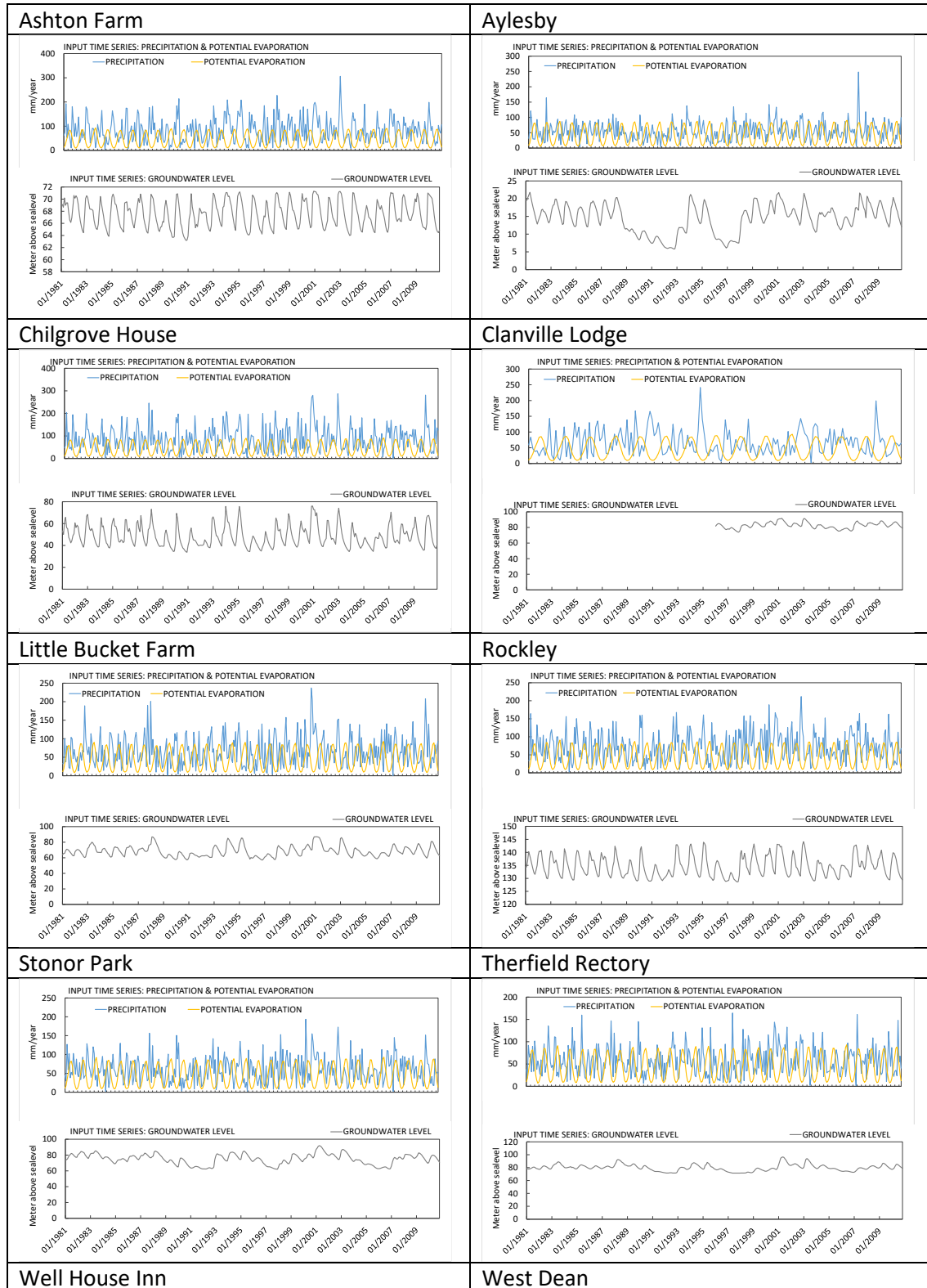
4.2.1 *AquiMod*

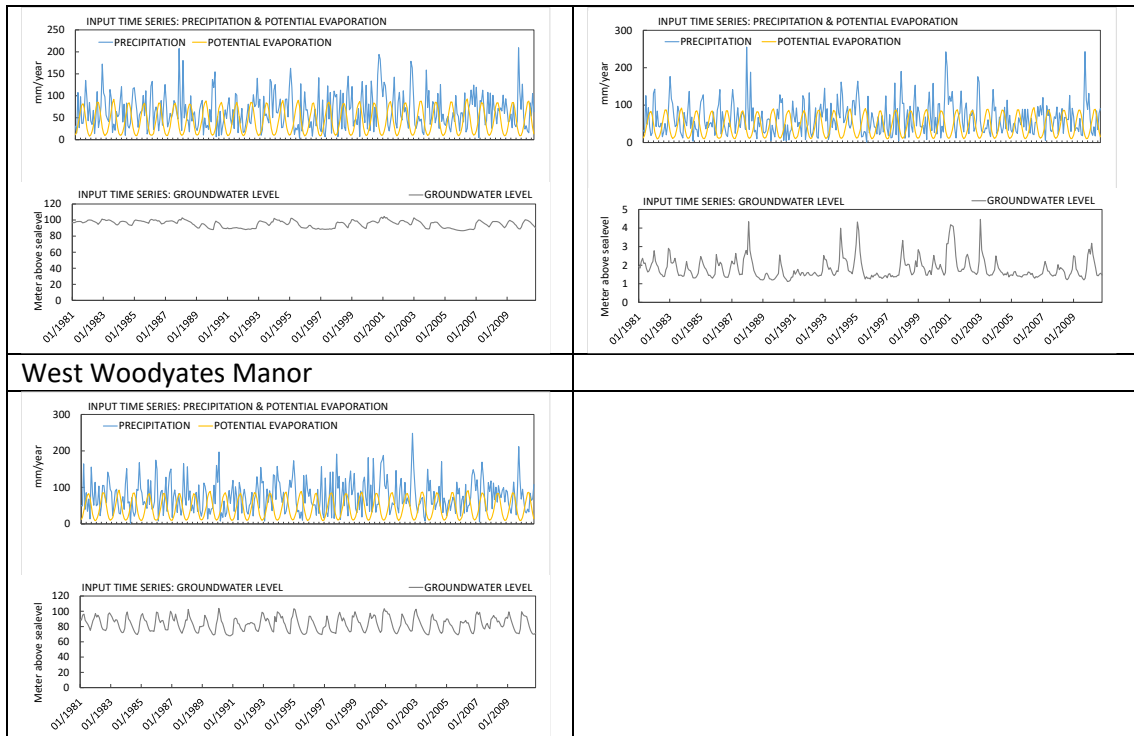
The Chalk boreholes addressed in this study are listed in Table 1. Aquimod model setup relies mainly on two input files. The first input file "Input.txt" is a control file where the module types and model structure are defined. Aquimod is executed first under a calibration mode where a range of parameter values of the different selected modules are given in corresponding text files and a Monte Carlo approach is used to select the parameter values that yield best model performance. "Input.txt" also controls the mode under which Aquimod is executed, the number of Monte Carlo runs to perform, the number of models to keep with an acceptable performance, and the number of runs to execute in evaluation mode.

The second file Aquimod uses is called "observations.dat". This file holds the forcing data mainly the potential evaporation and rainfall. However, it is also possible to include the anthropogenic impact on groundwater levels by including a time series of pumping data in this file. None of the boreholes studied here includes pumping data. The observed groundwater levels that are used for model calibration are also given in this file. The data are provided to the model on a daily basis, and this forces Aquimod to run using a time step length of one day. Table 4 shows daily time series of rainfall and potential evaporation values (mm/month) as well as the fluctuations of water table at the different boreholes.

All Aquimod models built for the boreholes in Table 1 use the FAO Drainage and Irrigation Paper 56 (FAO, 1988) method in the soil module, and employ the two-parameter Weibull probability density function to control the movement of infiltrated water in the unsaturated zone (Appendix A1). However, the groundwater module structures vary between the different boreholes. The best groundwater module structure is found by trial and error during the calibration process. The simplest structure, one layer with one discharge feature, is selected first and then the complexity of the module structure is increased gradually to see if the model performance improves. The structure with best model performance is selected to undertake the recharge calculations. The structures selected for these boreholes are mainly of one layer or three layered systems.

Table 4 Figures showing time series of daily rainfall and potential evaporation values (mm/month) as well as the fluctuations of water table at the different boreholes.





4.2.2 Metran

Metran applies transfer function noise modelling with daily precipitation and evaporation as input and of groundwater levels as output (Zaadnoordijk et al., 2019). The setup is shown in Figure 7. If time series of other influences on the groundwater head are available, these contributions can be added to the deterministic part of the model. An input file that holds the daily information of precipitation, potential evaporation and groundwater levels is prepared for each borehole in Table 1. Plots of these data are shown in Table 4. It must be noted that, while the groundwater levels used in AquiMod and shown in Table 4 have missing values, these have to be provided as complete time series to Metran. To achieve this, a linear interpolation procedure is used to fill in the missing values in the groundwater level time series. Once executed, it calculates the characteristics of the impulse functions and the corresponding parameters automatically.

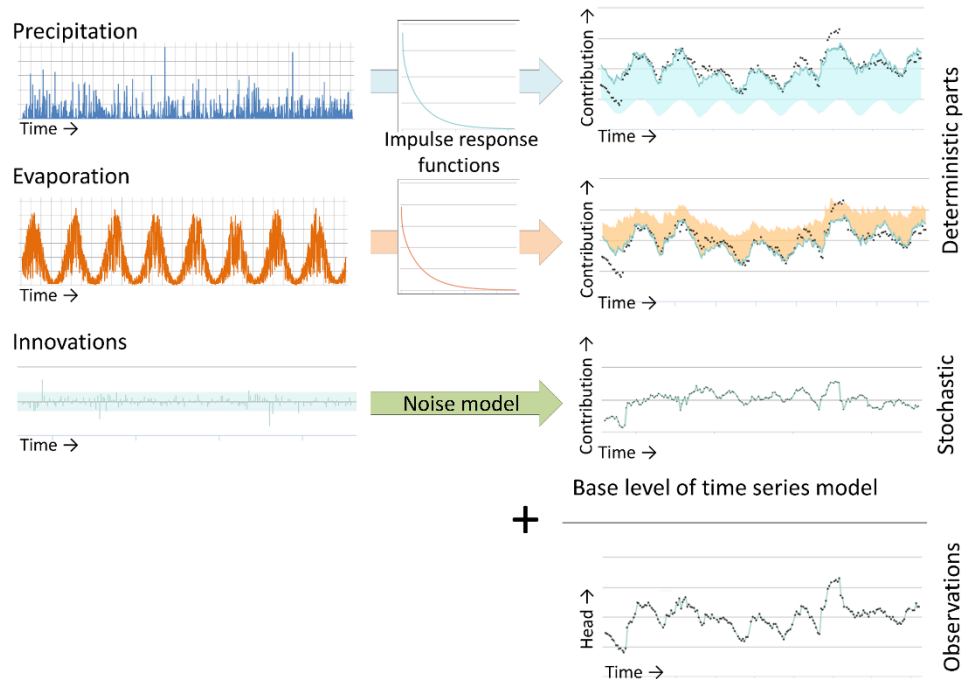


Figure 7 Illustration of METRAN setup

4.2.3 National scale model (ZOODRM)

The distributed recharge model (ZOODRM) is applied at national over the British Mainland (England, Scotland, and Wales) (Figure 8) using a Cartesian grid with 2 km square cells. The model reads a text file that defines the locations of the grid nodes as well as the connections between the nodes. This text file is prepared using a specific tool, called ZETUP (Jackson, 2004), where the extent of the study area is defined using the coordinates of the lower left and upper right corners of a rectangle that covers the modelled area. The spacing between the nodes and the information that dictate the boundary of the irregular shape of the area are also given in this file. This tool also uses a file that contains the locations of the nodes as obtained from a geographical information system tool (GIS) and converts this information into a text file that describes the river extents and characteristics.

The map defining the runoff zones is based on the hydrogeology of the study area. It is produced in gridded *ascii* format using the hydrogeological map available for Great Britain. Additional text files, one for each runoff zone, are also prepared to define the monthly runoff values.

The topographical information is also provided in a gridded *ascii* format for the model to calculate the topographical gradients between the nodes. While a surface water routing procedure that accounts for indirect recharge and surface water storage is available in the model, this is not used in the current application. It is assumed that all the water originated at one grid nodes travel downstream and reaches a discharging feature in one day, which is equal to the length of the time step used.

Landuse data (Section 3.1.3) and soil data that are required to calculate the water capacity at every grid node are also provided to the model using maps in gridded *ascii* format. A set of ten gridded landuse maps are used to give the percentage of landuse type at any given location. The gridded soil map gives the soil type at a selected location. The landuse type and soil type ids are linked to text files that hold the corresponding information such as the soil moisture at saturation, the soil moisture at wilting and the root constants can be obtained.

The driving data are provided to the model as daily gridded rainfall data (Sections 3.1.4) and time series of monthly potential evaporation values as described in (Section 3.1.5). Mansour et al. (2018) provide a full description of the construction of this model together with a more detailed description of the data used. The calculated recharge values are also provided in the published work; however, it must be noted that the historical recharge values shown in this work are simulated over the period from 1981 to 2010 in order to be consistent and comparable with the recharge values calculated by Aquimod and Metran. In addition, in this study, the model has been re-run using the climate change data specifically provided by the TACTIC project to calculate the projected distributed recharge values.

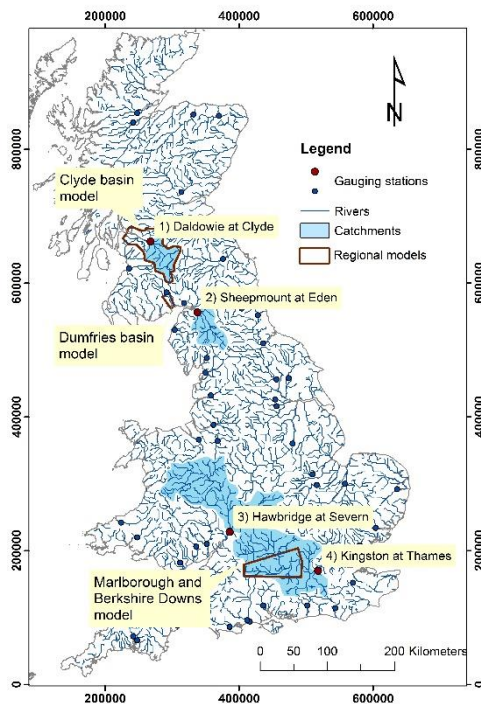


Figure 8. Extent of the UK national scale recharge model in UK national grid reference after Mansour et al. (2018). Figure also shows the locations of the gauging stations downstream of the major rivers used for model calibration.

4.3 Model calibration

4.3.1 Calibration of *AquiMod* models

The calibration of *AquiMod* is performed automatically using the Monte Carlo approach. The user populates the files of the selected modules with minimum and maximum parameter values and then the model randomly selects a value from the specified range for any given run. The selection of the minimum and maximum values is physically based depending on the characteristics of the study area. For example, the minimum and maximum values of the root depth in the soil module are set to 15 cm and 60 cm respectively for a study area covered with grass, while these values are set to 120 cm and 200 cm for a woodland area. The storage coefficients bounds of a groundwater module are set to much lower values in a confined aquifer compared to those used for an aquifer under unconfined conditions.

A conceptual hydrogeological understanding must be available before the use of *AquiMod*, since this is necessary to set the limits of the parameter values for the calibration process. In some cases, it is not possible to obtain a good performing model with the selected values and that necessitates the relaxation of these parameters beyond the limits informed by the conceptual understanding. In such cases, the parameter values must feed back into the conceptual understanding if better performing models are obtained.



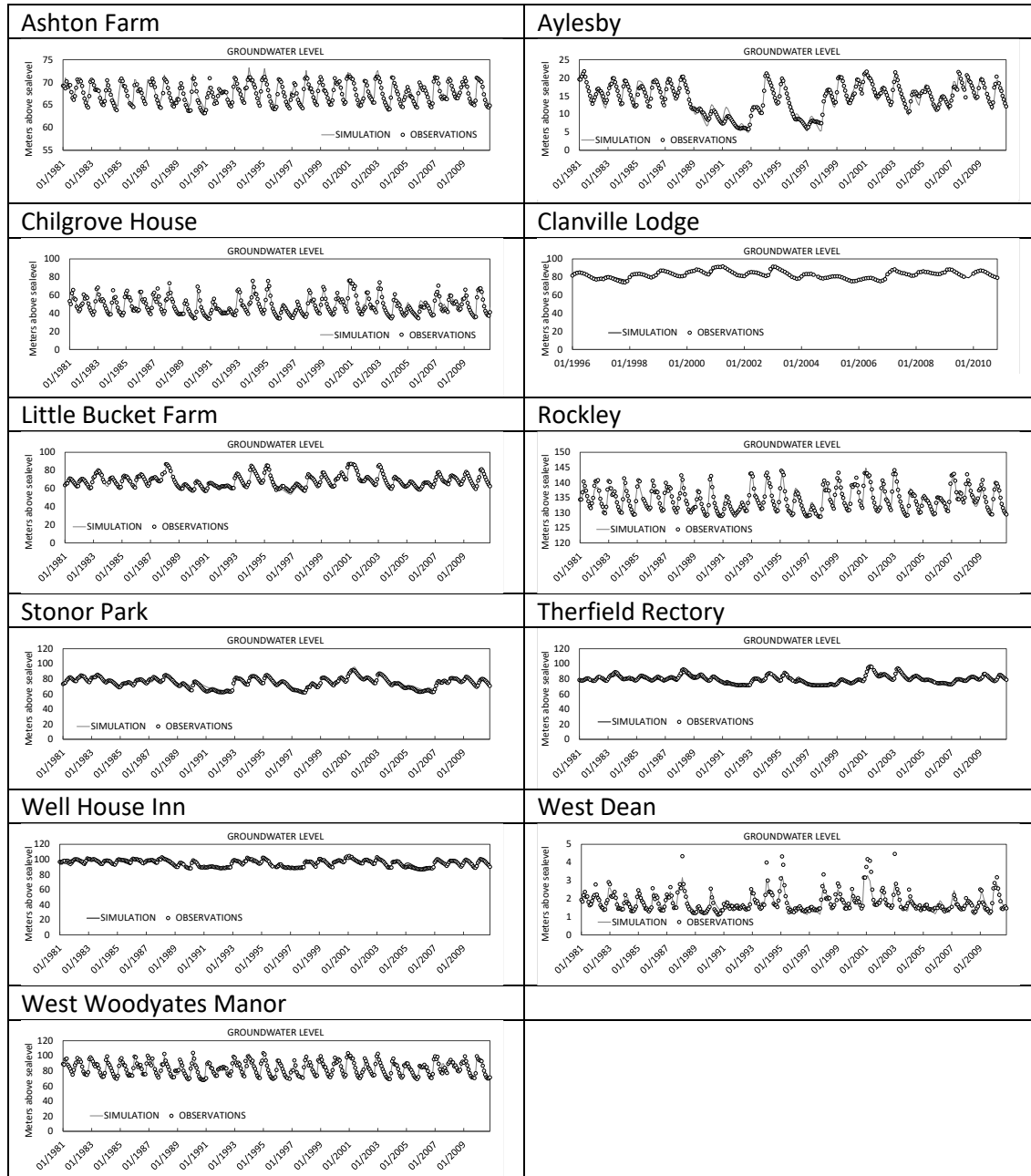
AquiMod execution time is relatively small, which allows the calibration of the model using hundreds of thousands of runs in couple of hours. The performance measure used to assess the quality of the simulation is the Nash Sutcliffe Error (Appendix A) that takes a maximum value of unity for a perfect match between the simulated and observed data. The threshold at which models are accepted is set to a value of 0.6. All the models that achieve an NSE higher than 0.6 are included in the analysis but a maximum number of 1000 runs are used if the number of acceptable models is greater than 1000.

Table 5 shows the best NSE values obtained for the models calibrated at the Chalk boreholes listed in Table 1. It is clear that a good match was achieved between the simulated and observed groundwater levels as illustrated in the plots shown in Table 6. The best performing model is the AquiMod model built at Clanville Lodge borehole with an NSE value of 0.97. The least performing AquiMod model is that built for Therfield Rectory borehole with an NSE value of 0.66.

Table 5 Nash Sutcliff Error measure at the Chalk boreholes

Borehole name	NSE
Ashton Farm	0.89
Aylesby	0.95
Chilgrove House	0.90
Clanville Lodge	0.97
Little Bucket Farm	0.95
Rockley	0.87
Stonor Park	0.88
Therfield Rectory	0.66
Well House Inn	0.81
West Dean	0.81
West Woodyates Manor	0.91

Table 6 Comparison between the simulated and observed groundwater levels at the Chalk observation boreholes.



4.3.2 Calibration of Metran models

For the standard setup with precipitation and evaporation, there are five parameters that have to be determined during the calibration of the model. Three parameters are related to the precipitation response, the evaporation factor, and the noise model parameter (Appendix B). There are three extra parameters for each additional input series, such as pumping. The parameter optimization of Metran uses a gradient search method in the parameter space to reach a global minimum. As explained in Appendix B, two parameters indicate if Metran succeeded with producing a match between the simulated and observed data. These are called the Regimeok and Modok. When Regimeok is equal to one, the calibration is of highest quality. If Modok is equal to one and Regimeok is equal to zero, the calibration is of acceptable quality. Finally, if both parameters are equal to zero, the calibration quality is insufficient.

Table 7 shows the performance of Metran across the Chalk boreholes considered in this study. It is clear that according to criteria set above, Metran fails to produce a model at four boreholes but succeeds at the seven other boreholes with the model output showing highest quality at four of these boreholes (with highest value of R^2).

Table 7 Performance of Metran across the selected Chalk boreholes.

Borehole name	Metran performance parameter Regimeok	Metran performance parameter Modok	Overall quality	R2	RMSE
Ashton Farm	1	1	Highest	0.81	0.96
Aylesby	0	0	Insufficient	0.87	1.87
Chilgrove House	1	0	Acceptable	0.75	4.97
Clanville Lodge	0	0	Insufficient	0	3.88
Little Bucket Farm	1	1	Highest	0.82	2.88
Rockley	1	1	Highest	0.81	1.75
Stonor Park	0	0	Insufficient	0	6.56
Therfield Rectory	0	0	Insufficient	0	4.99
Well House Inn	1	0	Acceptable	0.63	2.52
West Dean	1	0	Acceptable	0.64	0.35
West Woodyates Manor	1	1	Highest	0.82	3.89

4.3.3 Calibration of the UK national scale model using ZOODRM

Model calibration of the national scale recharge model was based on the comparison of the simulated long-term average overland flows to the observed ones (Mansour et al., 2018) recorded at gauging stations of selected major rivers (Figure 8). However, additional checks were also undertaken to assess the performance of the model. These include checking the match between the seasonal overland flow volumes at four gauging stations, shown in red in Figure 8, checking the calculated recharge volumes with those calculated by other tools over selected catchment areas, and checking the temporal fluctuations of soil moisture deficit with those calculated by other tools. Figure 9 shows a Q plot for the simulated vs observed long term average runoff values at the 56 gauging stations shown in Figure 8. The solid line shows the one to one match and the dotted line shows the linear relationship between the two datasets.

It must be noted that while this model uses the same recharge calculation methods used by AquiMod, these two models are calibrated using different datasets, with AquiMod using the groundwater levels and the distributed recharge model using the overland flows.

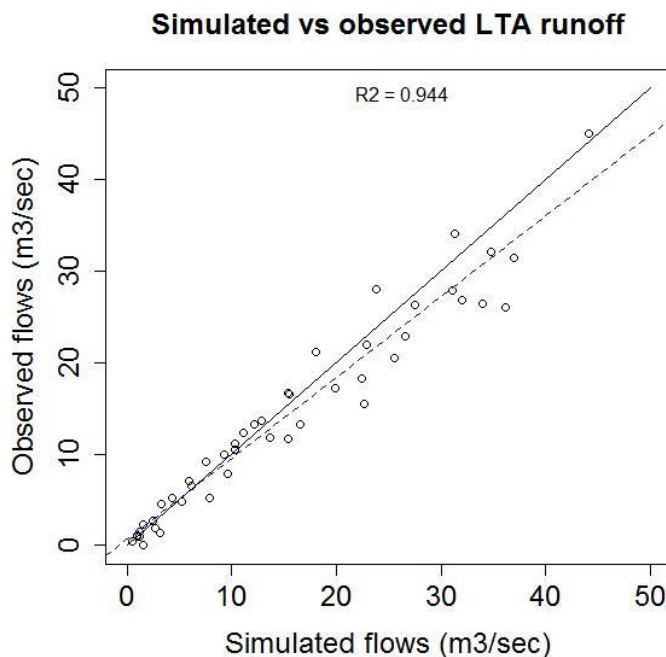


Figure 9 Q plot for the simulated vs observed long term average runoff values at the 56 gauging stations shown in Figure 8 after Mansour et al. (2018)

5 RESULTS AND CONCLUSIONS

5.1 Historical recharge values

Table 8 shows the time series of the historical recharge values calculated using the Aquimod model at the Chalk boreholes listed in Table 1. The plots in this table also show the 10th percentile, the mean, and the 90th percentile of recharge values calculated from the time series.

As mentioned Appendix B, the formulas used by Metran are based on assumptions that can be violated and it is better to use the infiltration coefficient f_c with the long-term average values of rainfall and potential evaporation to calculate long-term average values of recharge and using only models of the highest quality. Time series of recharge values are not therefore produced, from the analysis undertaken using Metran. The long-term average recharge values calculated using Metran are shown in Table 9.

One of the benefits of running Aquimod in Monte Carlo mode is the possibility of producing many models with acceptable performance. Consequently, the recharge values estimated from these models are all equally likely. This provides us with a range of recharge values at each borehole that reflects the uncertainty of the optimised hydraulic parameter values. In the current study, the long-term average recharge values are calculated from up to 1000 acceptable models if they exist at each borehole; otherwise, all the acceptable models are used. The mean, 25th and 75th percentiles are then calculated from these long-term recharge values and displayed in Figure 10. It is clear that the differences between the 75th and 25th percentile values is negligible at almost all the boreholes; however, there is approximately 5 mm/month between the 25th and 75th percentile values at Ashton Farm borehole (~14% difference) and West Woodyates Manor borehole (~17% difference).

In addition to the recharge values calculated using Aquimod, Figure 10 shows the recharge values calculated using Metran and the distributed national scale model at these boreholes. It is clear that there is a good agreement between the Aquimod calculated recharge values and those calculated using the distributed national scale model. This is expected as they both use the same recharge calculation method; however, since they are calibrated using different target functions, the match was not guaranteed. It must be noted that the recharge values calculated by these two models are of different types. The distributed recharge model calculates potential recharge and Aquimod calculates actual recharge. However, previous experience with the Chalk aquifer indicates that the infiltration recharge occurring at the ground surface is more likely to reach the groundwater system below. Then, the recharge calculated using the distributed recharge model at these boreholes is considered as actual recharge.

The pattern of the recharge values calculated using Metran at the selected boreholes match that of the recharge values calculated by the other two models. In addition, Metran succeeds to produce long-term recharge values that match those of the other models at four boreholes (Ashton Farm, Aylesby, Little Bucket Farm, West Woodyates Manor). However, it overestimates the recharge values at the remaining four boreholes by approximately twice the amount of recharge (Chilgrove House, Rockley, Well House Inn, West Dean).

Metran estimates an upper and a lower value for the infiltration coefficient, f_c . This can be used as an indication of uncertainty associated with the calculated f_c value. These bounds are also shown in Table 9. The upper and lower bound values at Chilgrove House and West Dean are greater than the estimated f_c value. It is not possible to use these bound values to correct the recharge estimated by Metran. However, for Rockley borehole, Metran produces a recharge value that matches those calculated by AquiMod and the distributed recharge model if the lower bound f_c value is used. At Well House Inn boreholes, the recharge values calculated by AquiMod and the distributed recharge model fall within the bounds estimated by Metran.

Table 8 Time series of recharge values obtained from the best performing AquiMod models at the Chalk boreholes



Table 9 Recharge values calculated using the recharge factors estimated by Metran

Borehole name	Average precipitation (mm/month)	Average potential evaporation (mm/month)	Recharge factor	Recharge (mm/month)
Ashton Farm	82.80	44.64	1.05 ± 1.18	34.21
Aylesby	55.04	41.90	0.89 ± 0.69	
Chilgrove House	87.20	43.96	0.67 ± 1.18	57.96
Clanville Lodge	66.17	44.29	0.04 ± 0.25	---
Little Bucket Farm	66.30	44.15	0.83 ± 0.36	29.88
Rockley	71.25	42.61	0.74 ± 0.38	39.80
Stonor Park	60.06	43.45	0.17 ± 2.91	---
Therfield Rectory	56.96	43.01	1.35 ± 0.25	---
Well House Inn	65.78	43.55	0.58 ± 0.58	40.61
West Dean	64.83	45.33	0.66 ± 3.52	34.87
West Woodyates Manor	76.28	43.94	1.11 ± 0.22	24.85

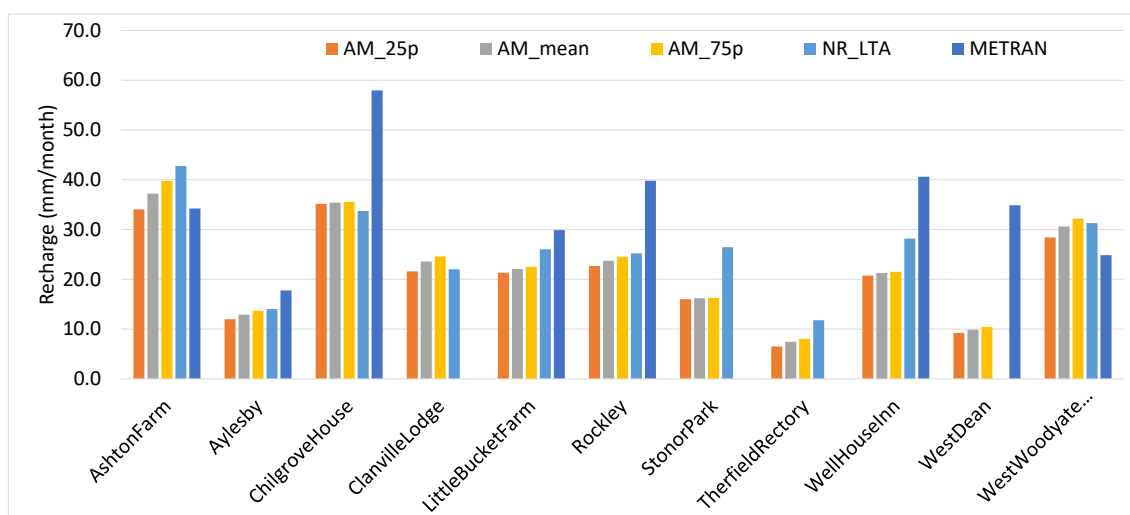


Figure 10 Historical recharge values calculated by AquiMod, Metran, and the national scale recharge model.

5.2 Projected recharge values

The forcing data, rainfall and potential evaporation, are altered using the change factors of the climate models (see Section 4.1.4). For the United Kingdom, there are two sets of monthly change factors, one used with the data driving Aquimod and Metran (Table 10A), and the other used to calculate the spatially distributed recharge (Table 10B). These change factors are used as multipliers to both the historical rainfall and potential evaporation values.

For the application involving Aquimod, these factors are used to alter the time series of historical rainfall and potential evaporation values used to drive the model.

When using Metran, the historical time series are altered using these factors first and then the long-term average rainfall and potential evaporation values are calculated. The recharge coefficient f_c values of the different boreholes, as calculated from the calibration of Metran model using the historical data, are then applied to calculate the projected long-term average recharge values.

The distributed recharge model ZOODRM includes the functionality of using these change factors to modify the historical gridded rainfall and potential evaporation data before using them as input to calculate the recharge. In this case, and for any simulation date, the rainfall and potential evaporation change factors for the month corresponding to the date, are used to modify all the spatially distributed historical rainfall and potential evaporation values respectively.

Table 10A Monthly change factors as multipliers used for the borehole data

	Scenario	Jan	Feb	Mar	Apr	May	Jun	Jul	Aug	Sep	Oct	Nov	Dec
Rainfall	1° Min	1.087	0.956	0.994	1.072	0.888	0.909	0.836	0.988	1.017	1.106	0.962	1.031
	1° Max	1.140	1.012	1.033	1.045	1.022	0.863	1.086	0.953	0.995	1.067	1.148	1.053
	3° Min	0.936	1.056	0.994	1.153	1.063	0.900	0.846	0.721	0.854	0.970	1.047	1.116
	3° Max	1.191	1.177	0.989	1.014	0.949	0.986	1.473	1.145	1.173	1.074	1.152	1.112
PE	1° Min	1.082	1.082	1.062	1.089	1.091	1.061	1.078	1.083	1.082	1.063	1.049	1.076
	1° Max	1.049	0.993	1.014	1.007	1.019	1.013	1.021	1.015	1.029	1.028	1.020	1.026
	3° Min	1.034	1.057	1.039	1.056	1.060	1.086	1.085	1.091	1.109	1.097	1.064	1.066
	3° Max	1.072	1.070	1.055	1.071	1.105	1.106	1.072	1.083	1.082	1.076	1.072	1.060

Table 11B Monthly change factors as multipliers used for the distributed recharge model

	Scenario	Jan	Feb	Mar	Apr	May	Jun	Jul	Aug	Sep	Oct	Nov	Dec
Rainfall	1° Min	1.086	0.953	0.975	1.064	0.918	0.914	0.856	0.973	1.008	1.103	0.976	1.038
	1° Max	1.132	1.090	1.008	0.899	1.034	1.087	1.310	0.983	1.020	1.006	1.012	1.025
	3° Min	1.156	1.118	1.033	1.011	0.914	0.821	0.908	0.656	0.821	0.986	0.980	1.181
	3° Max	1.192	1.131	0.960	0.990	0.899	0.957	1.437	1.109	1.134	1.068	1.139	1.106
PE	1° Min	1.081	1.081	1.059	1.089	1.091	1.061	1.078	1.083	1.085	1.063	1.049	1.076
	1° Max	1.051	1.036	1.020	1.039	1.051	1.049	1.031	1.043	1.054	1.039	1.044	1.034
	3° Min	1.016	1.031	1.021	1.029	1.038	1.029	1.047	1.057	1.059	1.059	1.040	1.045
	3° Max	1.070	1.066	1.051	1.071	1.105	1.106	1.072	1.083	1.083	1.076	1.072	1.060

Figure 11 shows the historical and future long-term average recharge values calculated using the best performing Aquimod model. It is clear that the highest reduction in recharge values are observed when the 3° Min rainfall and evaporation data are used, while the highest increase in recharge values are observed when the 3° Max rainfall and potential evaporation data are used.

When the 1° Min scenario data are used, all the boreholes show reduction in recharge values with the smallest reduction observed at West Woodyates Manor borehole (5.2%) and the highest reduction observed at Stonor Park borehole (14.8%). When the 1° Max scenario data are used, all the boreholes show increase in recharge values with the smallest increase observed at Chilgrove House borehole (7.4%) and the highest increase observed at West Dean borehole (10.8%).

When the 3° Min scenario data are used, all the boreholes show reduction in recharge values with the smallest reduction observed at West Woodyates Manor borehole (4.9%) and the highest reduction observed at Well house Inn borehole (16.7%). When the 3° Max scenario data are used, all the boreholes show increase in recharge values with the smallest increase observed at Chilgrove House borehole (15.9%) and the highest increase observed at Aylsby borehole (21.9%).

Recharge values calculated by Metran and using the future climate data are shown in Figure 12. Table 12 shows the monthly historical and future recharge values calculated at the different boreholes. It is clear that in almost all the cases, the recharge values become lower than the



historical values when the 1° Min and 3° Min data are used and they become higher than the historical values when the 1° Max and 3° Max are used. The exceptions of this observation are due to the complex effect of the use of the change factors, which may reduce both the rainfall and potential evaporation at the same period but at different rates. The reduction in potential evaporation volume in one month may yield increased recharge volume even if the rainfall volume is reduced for that month.

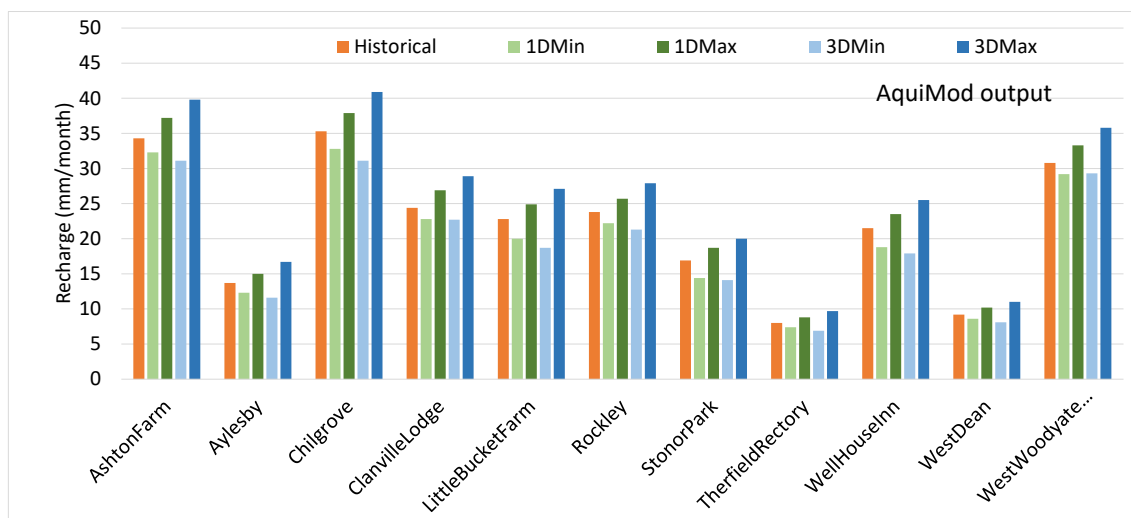


Figure 11 Historical (orange) and future recharge values (blue and green) as produced by the best performing Aquimod model.

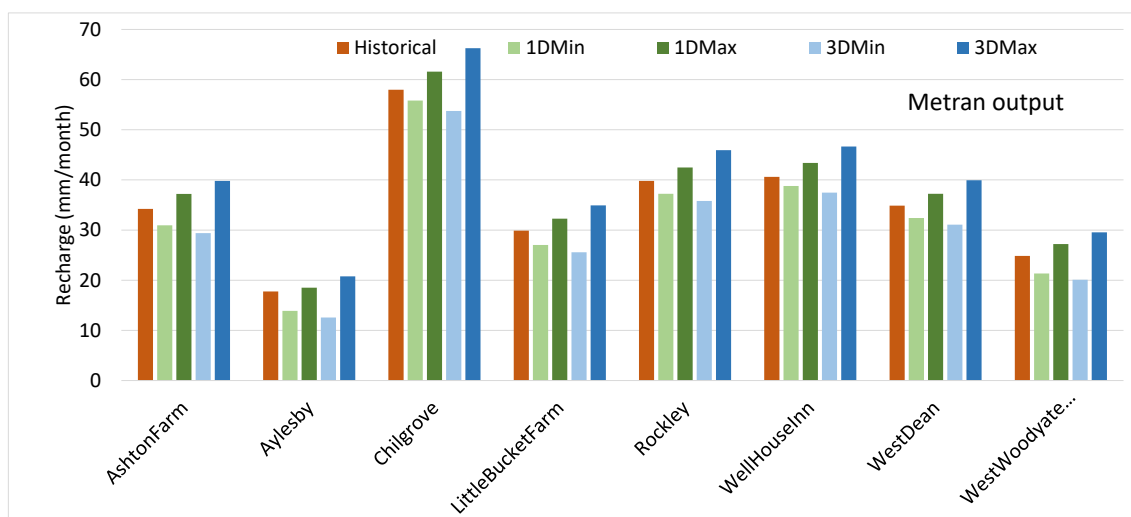


Figure 12 Historical (orange) and future recharge values (blue and green) produced by Metran.

Table 12 Monthly recharge values estimated using the historical and the projected forcing data. Dotted line is the monthly historical recharge values. Green shaded area shows the 1^o Min and Max monthly recharge values and the blue shaded area shows the 3^o Min and Max monthly recharge values

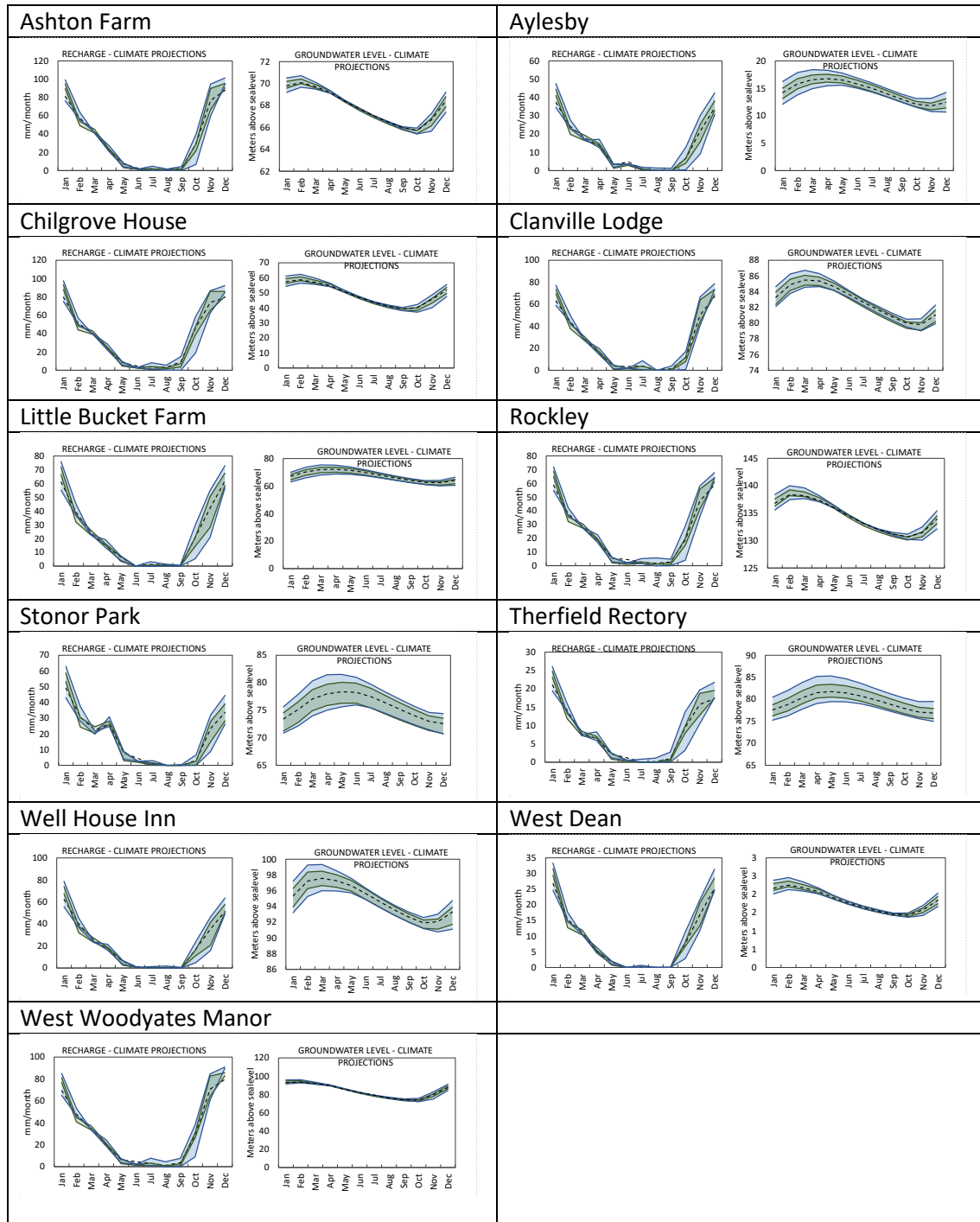


Table 13 shows maps of the spatially distributed recharge values calculated over the Chalk aquifer. The plots are for the historical potential recharge values as well as those calculated using the distributed recharge model but with rainfall potential evaporation data altered using the 1° Min, 1° Max, 3° Min, and 3° Max UK change factors. While the differences in the maps are not clear, it can be still easily observed that with the 1° Min and 3° Min data, the produced maps show drier pattern of recharge across the Chalk outcrop and conversely, with the 1° Max and 3° Max data, the produced maps show wetter pattern of recharge across the Chalk outcrop.

The differences between the simulated future recharge values and the historical ones are shown in the plots in Table 14. While the differences between the future and historical recharge values is mainly between -5% and 5%, when the rainfall and potential evaporation data are altered using the 1° Min, 1° Max, and 3° Min change factors, the differences are much more noticeable when the 3° Max change factors are used. In the latter case, the recharge increase is greater than 15% indicating that this is a very wet scenario. However, it must be also noted that on a long term average basis, the 1° Min scenario is looking to be drier than the 3° Min scenario as illustrated by the first and third plots in Table 14.

Table 15 shows the average, maximum, and the standard deviation values calculated using the pixel values of the maps shown in Table 13. Looking at the average values, it is clear that there is reduction in recharge when the 1° Min data are used compared to the historical recharge; however, this is not the case when the 3° Min data are used. In this case, the average recharge value is slightly higher than the historical recharge value indicating that over half of the Chalk area, the recharge values increased which is opposite to what was expected. This can be confirmed by checking the maximum recharge values, where the maximum value in the 1° Min recharge map is lower than the maximum recharge value in the historical recharge map, while the maximum recharge value in the 3° Min recharge map is higher than that in the historical map. The average recharge values of the pixel values of the 1° Max and 3° Max maps are both higher than the average from the historical map as expected. The maximum value from these two maps are also higher than the maximum obtained from the historical as also expected. Finally, there is little difference in the standard deviation values shown in Table 15 indicating that the spatial distribution of recharge values is not notably different between the different scenarios.

Table 13 Spatially distributed historical and projected recharge values

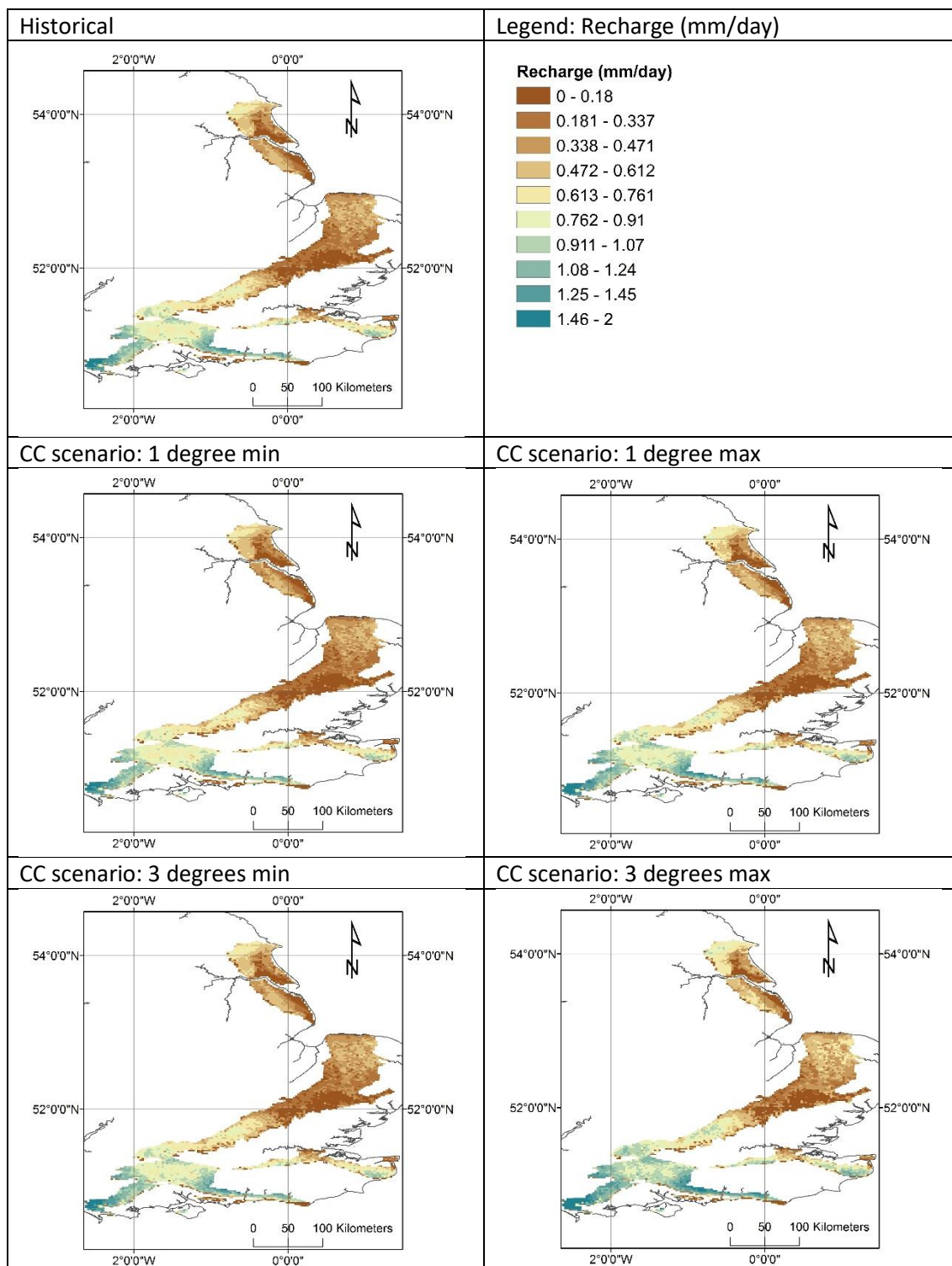


Table 14 Differences between the projected and historical recharge values calculated as projected values minus historical values

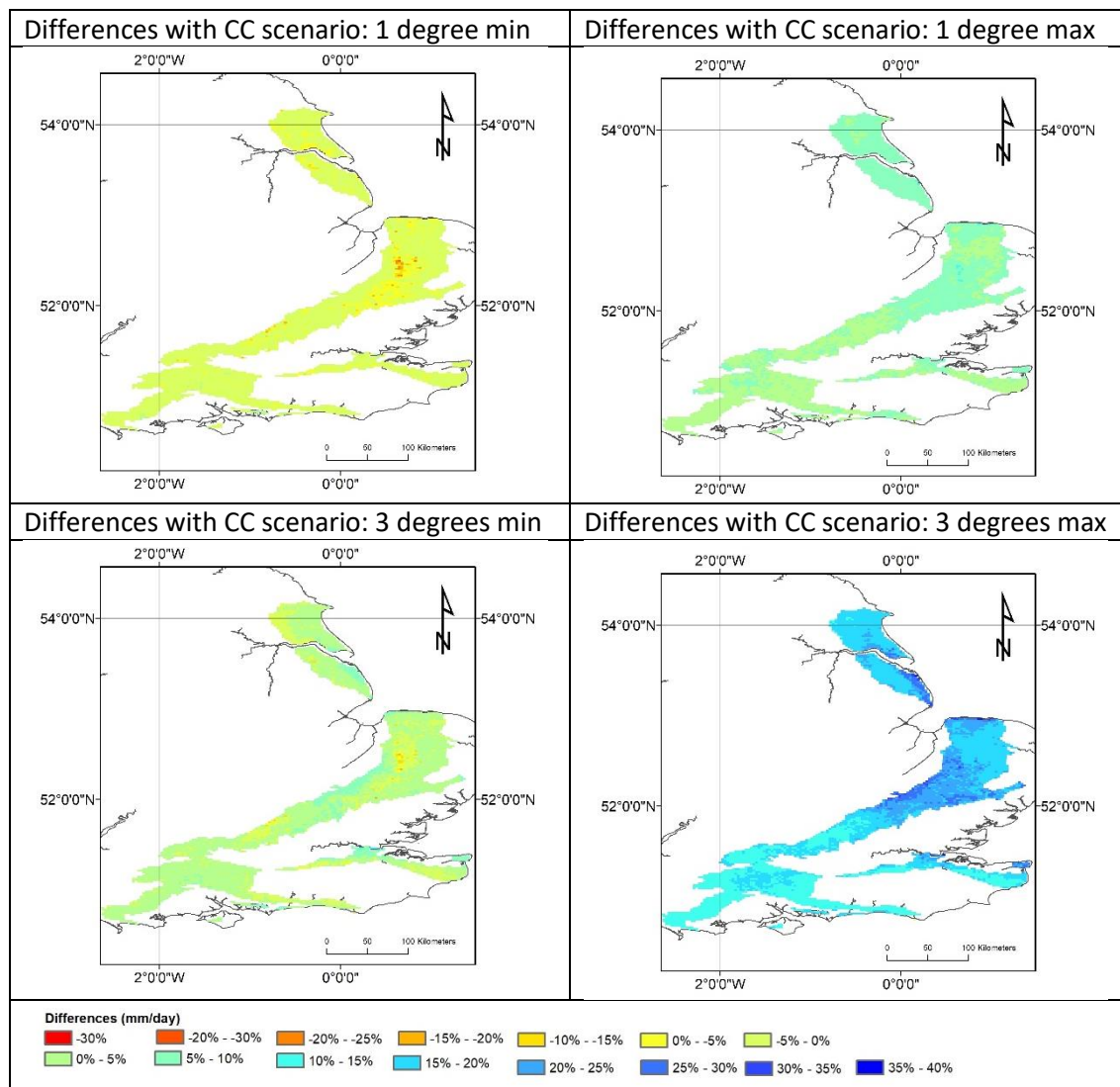


Table 15 Statistical information about the maps shown in Table 13

Map	Average recharge (mm/day)	Maximum recharge (mm/day)	Standard deviation (mm/day)
Historical	0.548	1.715	0.337
CC scenario: 1 degree min	0.533	1.69	0.332
CC scenario: 1 degree max	0.576	1.796	0.352
CC scenario: 3 degrees min	0.555	1.721	0.34
CC scenario: 3 degrees max	0.636	1.923	0.378

REFERENCES

- Allen, D. J., L. J. Brewerton, L. M. Coleby, B. R. Gibbs, M. A. Lewis, A. M. MacDonald, S. J. Wagstaff, A. T. Williams. 1997. 'The Physical Properties of Major Aquifers in England and Wales'.
- Besbes, M. & de Marsily, G. (1984) From infiltration to recharge: use of a parametric transfer function. *Journal of Hydrology*, 74, p. 271-293.
- Bradford, R. B., Ragab, R., Crooks, S. M., Bouraoui, F. & Peters, E. 2002. Simplicity versus complexity in modelling groundwater recharge in Chalk catchments. *Hydrology and Earth Systems Sciences*, 6, 927–937. Bibby, P. 2009. Land use change in Britain. *Land Use Policy*, 26, S2–S13. <https://doi.org/10.1016/j.landusepol.2009.09.019>.
- Cross, G. A., Rushton, K. R. & Tomlinson, L. M. 1995. The East Kent Chalk aquifer during the 1988–92 drought. *Journal of the Institute of Water and Environmental Management*, 9, 37–48.
- ESI 2015. East Yorkshire Chalk Aquifer Investigation: Model Update and Recalibration. Report reference: 62986 R2. Prepared for the Environment Agency.
- Foster, S. & Sage, R. 2017. Groundwater science in water-utility operations: global reflections on current status and future needs. *Hydrogeology Journal* 25: 1233-1236. DOI 10.1007/s10040-017-1602-4
- Hough, M. N. & Jones, R. J. A. 1997. The United Kingdom Meteorological Office rainfall and evaporation calculation system: MORECS version 2.0 – an overview. *Hydrology and Earth System Sciences*, 1, 227–239.
- Hutchinson, M. J., Ingram, R. G. S., Grout, M. W. & Hayes, P. J. 2012. A successful model: 30 years of the Lincolnshire Chalk model. In: Shepley, M. G. (ed.) *Groundwater Resources Modelling: A Case Study from the UK*. Geological Society, London, Special Publications, 364, 85–98, <https://doi.org/10.1144/SP364.12>
- IPCC: 2000, Special report on emissions scenarios (SRES): A special report of Working Group III of the Intergovernmental Panel on Climate Change, Cambridge University Press, Cambridge, p. 599
- Jackson, C. R.; Meister, R., Prudhomme, C. 2011. Modelling the effects of climate change and its uncertainty on UK Chalk groundwater resources from an ensemble of global climate model projections. *Journal of Hydrology*, 399 (1-2). 12-28. <https://doi.org/10.1016/j.jhydrol.2010.12.028>
- Ragab, R., Finch, J. W. & Harding, R. J. 1997. Estimation of groundwater recharge to Chalk and sandstone aquifers using simple soil models. *Journal of Hydrology*, 190, 19–41.
- Jenkins, G.J., Murphy, J.M., Sexton, D.S., Lowe, J.A., Jones, P. and Kilsby, C.G. 2009, UK Climate Projections: Briefing report, Met Office Hadley Centre, Exeter, UK.

- Mackay, J. D., Jackson, C. R., Wang, L. 2014. A lumped conceptual model to simulate groundwater level time-series. *Environmental Modelling and Software*, 61. 229-245. <https://doi.org/10.1016/j.envsoft.2014.06.003>
- Mackay, J. D., Jackson, C. R., Wang, L. 2014. *AquiMod user manual (v1.0)*. Nottingham, UK, British Geological Survey, 34pp. (OR/14/007) (Unpublished)
- Mansour, M. M. and Hughes, A. G. 2018. Summary of results for national scale recharge modelling under conditions of predicted climate change. British Geological Survey Internal report. Commissioned Report OR/17/026.
- Mansour, M. M., Wang, L., Whiteman, Mark, Hughes, A. G. 2018. Estimation of spatially distributed groundwater potential recharge for the United Kingdom. *Quarterly Journal of Engineering Geology and Hydrogeology*, 51 (2). 247-263. <https://doi.org/10.1144/qjengh2017-051>
- Murphy, J.M., Booth, B.B.B., Collins, M., Harris, G.R., Sexton, D.M.H., and Webb, M.J. 2007. A methodology for probabilistic predictions of regional climate change from perturbed physics ensembles. *Phil. Trans. R. Soc. A* 365, 1993–2028.
- Murphy, J.M., Sexton, D.M.H., Jenkins, G.J., Boorman, P.M., Booth, B.B.B., Brown, C.C., Clark, R.T., Collins, M., Harris, G.R., Kendon, E.J., Betts, R.A., Brown, S.J., Howard, T. P., Humphrey, K. A., McCarthy, M. P., McDonald, R. E., Stephens, A., Wallace, C., Warren, R., Wilby, R., and Wood, R. A. 2009, 'UK Climate Projections' Science Report: Climate change projections. Met Office Hadley Centre, Exeter.
- Obergfell, C., Bakker, M., & Maas, K. (2019). Estimation of average diffuse aquifer recharge using time series modeling of groundwater heads. *Water Resources Research*, 55. <https://doi.org/10.1029/2018WR024235>
- Prudhomme, C., Dadson, S., Morris, D., Williamson, J., Goodsell, G., Crooks, S., Boelee, L., Davies, H., Buys, G., Lafon, T. and Watts, G., 2012. Future Flows Climate: an ensemble of 1-km climate change projections for hydrological application in Great Britain. *Earth System Science Data*, 4(1), pp.143-148.
- Zaadnoordijk, W.J., Bus, S.A.R., Lourens, A., Berendrecht, W.L. (2019) Automated Time Series Modeling for Piezometers in the National Database of the Netherlands. *Groundwater*, 57, no. 6, p. 834-843. <https://onlinelibrary.wiley.com/doi/epdf/10.1111/gwat.12819>

APPENDICES

Appendix A: AquiMod methodology

AquiMod is a lumped parameter computer model that has been developed to simulate groundwater level time series at observational boreholes (Mackay et al., 2014a). It is based on hydrological algorithms that simulates the movement of groundwater within the soil zone, the unsaturated zone, and the saturated zone. The lumped models neglect complexities included in distributed groundwater models but maintains some of the fundamental physical principles that can be related to the conceptual understanding of the groundwater system (Mackay et al., 2014b).

While AquiMod was originally designed to capture the behaviour of a groundwater system through the analysis of groundwater level time series, it can produce the infiltration recharge values and groundwater discharges from the aquifer as a by-product. AquiMod is driven by complete time series of forcing data for either historical or predicted future conditions. Running AquiMod in predictive mode can be used to fill in gaps in historical groundwater level time series, or calculate future groundwater levels. In addition to groundwater levels, it also provides predictions of historical and future recharge values and groundwater discharges. In the current application we use calibrated AquiMod models to estimate the recharge values at selected boreholes.

AquiMod consists of three modules (Figure A1). The first is a soil water balance module that calculates the amount of water that infiltrates the soil as well as the soil storage. The second module controls the movement of water in the unsaturated zone, mainly it delays the arrival of infiltrating water to the saturated zone. The third module calculates the variations in groundwater levels and discharges. The model executes the modules separately following the order listed above.

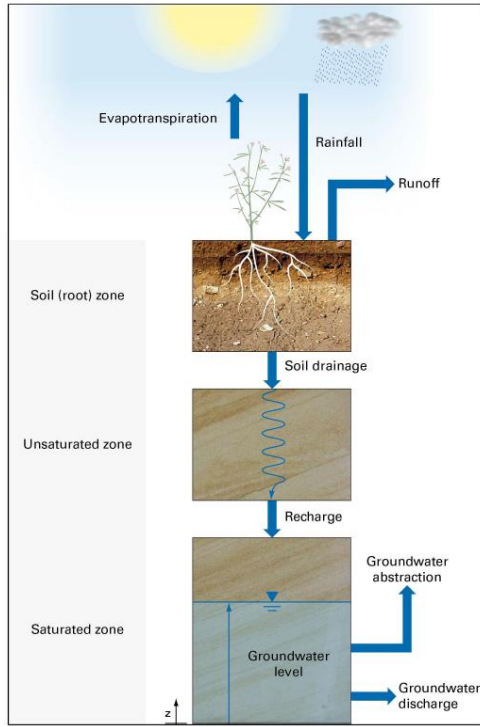


Figure A1 Generalised structure of Aquimod (after Mackay et al., 2014a)

The soil moisture module

There are several methods available in Aquimod that can be used to calculate the rainfall infiltration into the soil zone. In this study we use the FAO Drainage and Irrigation Paper 56 (FAO, 1988) approach. In this method, the capacity of the soil zone, from which plants draw water to evapo-transpire, is calculated first using the plants and soil characteristics. Evapo-transpiration is calculated according to the soil moisture deficit level compared to two parameters: Readily Available Water (RAW) and Total Available Water (TAW). These are a function of the root depth and the depletion factor of the plant in addition to the soil moisture content at field capacity and wilting point as shown in Equations A1 and A2.

$$TAW = Z_r(\theta_{fc} - \theta_{wp})$$

Equation A1

$$RAW = p \cdot TAW$$

Equation A2

Where Z_r [L] and p [-] are the root depth and depletion factor of a plant respectively, θ_{fc} [$L^3 L^{-3}$] and θ_{wp} [$L^3 L^{-3}$] are the moisture content at field capacity and wilting point respectively.

The FAO method is simplified by Griffiths et al. (2006) who developed a modified EA-FAO method. In this method the evapotranspiration rates are calculated as a function of the potential evaporation and an intermediate soil moisture deficit as:

$$\begin{aligned} e_s &= e_p \left[\frac{s_s^*}{TAW - RAW} \right]^{0.2} & s_s^* > RAW \\ e_s &= e_p & s_s^* \leq RAW \\ e_s &= 0 & s_s^* \geq TAW \end{aligned}$$

Equation A3



Where e_s [L] is the evapo-transpiration rate, e_p [L] is the potential evaporation rate and s_s^* [L] is the intermediate soil moisture deficit given by

$$s_s^* = s_s^{t-1} - r + e_p \quad \text{Equation A4}$$

Where r [L] is the rainfall at the current time step and s_s^{t-1} [L] is the soil moisture deficit calculated at the previous time step.

The new soil moisture deficit is then calculated from:

$$s_s = s_s^{t-1} - r + e_s \quad \text{Equation A5}$$

Griffiths et al. (2006) proposed that the recharge and overland flow are only generated when the calculated soil moisture deficit becomes zero. The remaining volume of water, the excess water, is then split into recharge and overland flow using a runoff coefficient. In Aquimod a baseflow coefficient is used to reflect the fact that a groundwater discharge is calculated rather than overland water. In this application, the baseflow coefficient is one minus the runoff coefficient.

The unsaturated zone module

The Aquimod version used in this study to simulate the movement of groundwater flow within the unsaturated zone is based on a statistical approach rather than a process-based approach. This method distributes the amount of rainfall recharge over several time steps where the soil drainage for each time step is calculated using a two-parameter Weibull probability density function. The Weibull function can represent exponentially increasing, exponentially decreasing, and positively and negatively skewed distributions. This can be used to focus the soil drainage over earlier or later time steps or to spread it over a number of time steps after the infiltration occurs. The shape of the Weibull function is controlled by two parameters, k and λ as shown in Equation A6.

$$f(t, k, \lambda) = \begin{cases} \frac{k}{\lambda} \left(\frac{t}{\lambda}\right)^{k-1} e^{-(t/\lambda)^k} & t > 0 \\ 0 & t \leq 0 \end{cases} \quad \text{Equation A6}$$

Where k and λ are two parameters the values of which are calculated during the calibration of the model and t is the time step.

The saturated zone module

Aquimod considers the saturated zone as a rectangular block of porous medium with dimensions L and B as its length and width [L] respectively. This block is divided into a number of layers, each has a defined hydraulic conductivity value, a storage coefficient value, and a discharging feature. The number of layers define the structure of the saturated module used in the study.

The mass balance equation that gives the variation of hydraulic head with time is given by:

$$SLB \frac{dh}{dt} = RLB - Q - A \quad \text{Equation A7}$$

Where:

S is the storage coefficient of the porous medium [-]

h is the groundwater head [L]

t is the time [T]

R is the infiltration recharge [L T⁻¹]

Q is the discharge out of the aquifer [L T⁻¹]



A is the abstraction rate [$L T^{-1}$]

It must be noted that in a multi-layered groundwater system as shown in Figure A2, we calculate one groundwater head (h) for the whole system. The discharges (Q) from Outlet 1, 2, etc. are calculated using the Darcy law. The total discharges can be summarised using the following equation:

$$Q = \sum_{i=1}^m \frac{T_i B}{0.5 L} \Delta h_i \quad \text{Equation A8}$$

Where:

m is the number of layers in the groundwater system [-]

T_i is the transmissivity of the layer i [$L T^{-2}$]

Δh_i is the difference between the groundwater head h and z_i , the elevation of the base of layer i

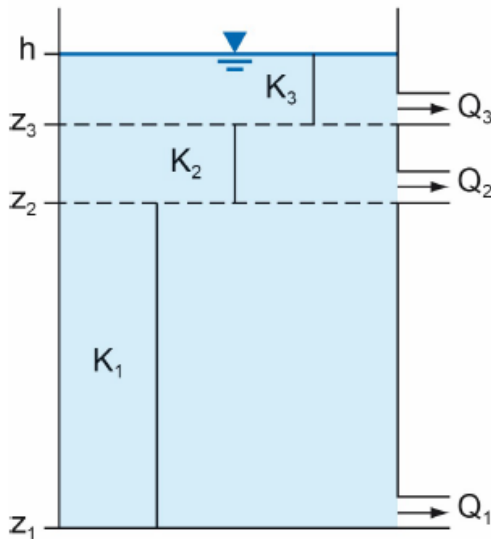


Figure A2 Representation of the saturated zone using a multi-layered groundwater system

Substituting Equation A8 into Equation A7 yields a numerical equation in the form:

$$S \frac{(h-h^*)}{\Delta t} = R - \sum_{i=1}^m \frac{T_i}{0.5 L^2} \Delta h_i - \frac{A}{LB} \quad \text{Equation A9}$$

Equation A9 is an explicit numerical equation that allows the calculation of the groundwater head h [L] at any time and using time steps of Δt [T]. In this equation h^* [L] is the groundwater head calculated at the previous time step and the term Δh_i [L] is calculated as $(h^* - z_i)$.

The terms S , T_i , and L are optimised during the calibration of the model. A groundwater system can be specified with one storage coefficient as shown in the equations above or with different storage coefficient values for the different layers. Several saturated modules are included in AquiMod to provide this flexibility and the model user can select the model structure that represent the conceptual understanding best.



Limitations of the model

AquiMod is a lumped groundwater model that aims at reproducing the behaviour of the observed groundwater levels. It tries to encapsulate the conceptual understanding of a groundwater system in a simple numerical representation. The model results have to be therefore discussed, taking this into consideration. For example, the model represents the groundwater system as a closed homogeneous medium, with no impact from any outer boundary or feature, whether physical or hydrological, such as the presence of rising and falling river stage.

Vertical heterogeneity can be accounted for by using multi-layered groundwater module structure. However, this model setting does not provide any information about the vertical connections between the layers as the discharge from all the layers is calculated using one representative groundwater head value. In other words, it is assumed that all layers are in perfect hydraulic connection.

As mentioned before, the model is designed to simulate the groundwater levels. However, it produces the recharge values and groundwater discharges as by products. In this application we use the calibrated model to calculate recharge. The mass balance equation (Equation A7) shows that recharge is a function of transmissivity and storage coefficient values, which are estimated during the calibration process of the model, i.e. they are not parameters with fixed values provided by the user. The inter-connections between these parameters leads to uncertainties in the estimated recharge values as a high storage coefficient value can produce a high recharge estimate and vice versa. To overcome this problem, it is suggested that the recharge values estimated by AquiMod are always presented as a range of possibilities rather than an absolute value. This can be achieved by estimating the recharge values from all the models that have a performance measure above than a threshold that is deemed acceptable by the user. The recharge estimates can then be presented as an average of all estimates and values corresponding to selected percentiles.

Model input and output

AquiMod includes a number of methods that calculates rainfall recharge as well as a number of model structure from which the user can select what better suits the case study.

Model input consists time series of forcing data including rainfall and potential evaporation, time series of anthropogenic impact mainly groundwater abstraction and time series of groundwater levels that will be used to calibrate the model. These time series must be complete, i.e. a value is available at every time step except the groundwater level time series, which can include missing data. The time step can be one day or multiple of days, and the model automatically calculate the size of the time step based on the input data time series.

The model is run first in calibration mode where a range of parameter values are specified for the different parameters included in the three model modules. A Monte Carlo approach is used to select the best parameter values. The performance of the model is measured by comparing the simulated groundwater levels to the observed ones using the Nash Sutcliffe Efficient (NSE) or the Root Mean Squared Error (RMSE) performance measures. The parameter set that produces the best model performance is selected to run the model in evaluation mode.

When the model is run in evaluation mode, it produces output files that give recharge values, groundwater levels and groundwater discharges time series with time as specified in the input file. The number of output files is equal to the number of acceptable models set by the user.

Appendix B: Metran methodology

Metran applies transfer function noise modelling of (groundwater head) time series with usually daily precipitation and evaporation as input (Zaadnoordijk et al., 2019). The setup is shown in the Figure B1. If time series of other influences on the groundwater head are available, these contributions can be added to the deterministic part of the model. The stochastic part is the difference between the total deterministic part and the observations (the residuals). The corresponding input of the noise model should have the character of white noise.

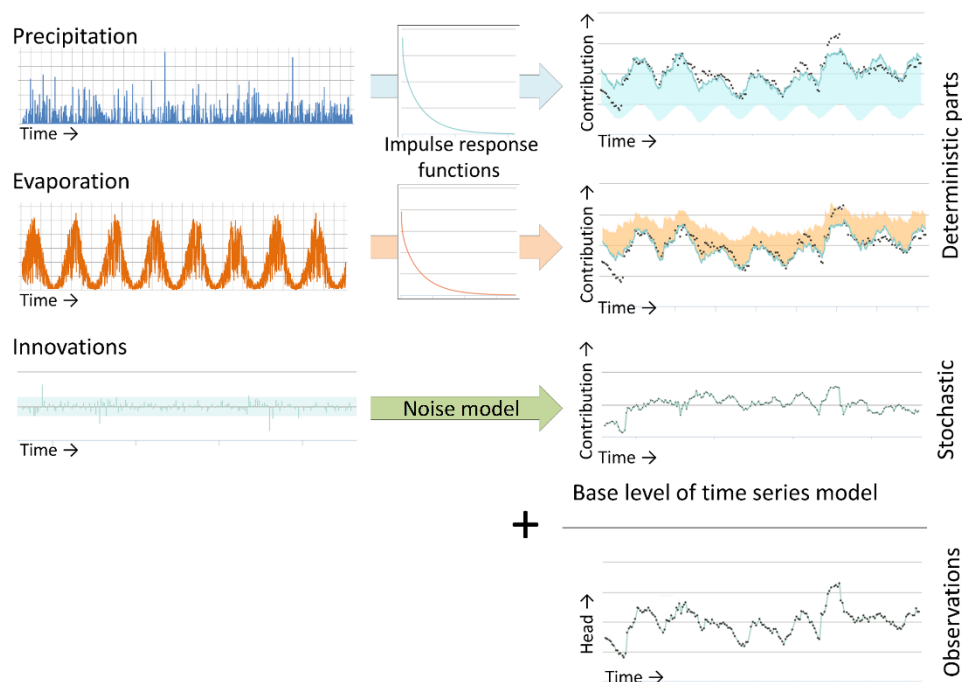


Figure B1 Illustration of METRAN setup

The stochastic part is needed because of the time correlation of the residuals, which does not allow a regular regression to obtain the parameter values of the transfer functions.

The incomplete gamma function is used as transfer function. This is a uni-modal function with only three parameters that has a quite flexible shape and has some physical background (Besbes & de Marsily, 1984). The evaporation response is set equal to the precipitation response except for a factor (f_c). The noise model has one parameter that determines an exponential decay. Thus, for the standard setup with precipitation and evaporation, there are five parameters that have to be determined from the comparison with the observations. Three parameters regarding the precipitation response, the evaporation factor, and the noise model parameter (actually, the time series model has a fifth parameter, the base level, but this is determined from the assumption that the average of the calculated heads is equal to the average of the observations). There are three extra parameters for each additional input series, such as pumping.



Limitations

Metran's time series model is linear. So, the model creation breaks down when the system is strongly nonlinear. This can occur e.g. when drainage occurs for high groundwater levels, when the ratio between the actual evapotranspiration and the inputted reference evaporation varies strongly, or when the groundwater system changed during the simulated period.

Metran is not able to find a decent time series model when the response function is not appropriate for the groundwater system. An example of this is a system with a separate fast and slow response as was found for a French piezometer in the Avre region, as is illustrated in Figure B2.

Finally, the parameter optimization of Metran uses a gradient search method in the parameter space, so it can be sensitive to initial parameter values in finding an optimal solution.

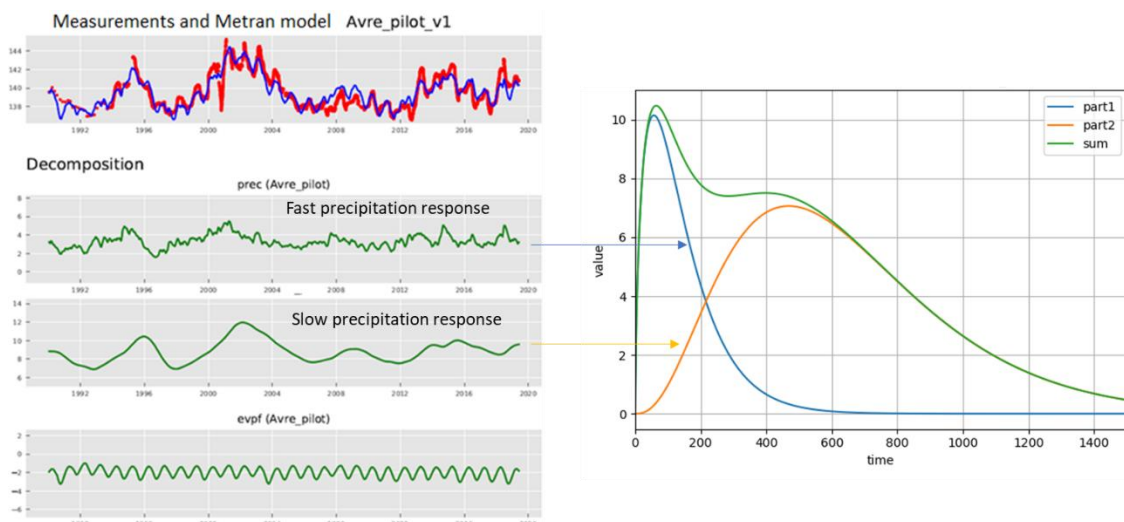


Figure B2. An example where the response function implemented in METRAN is not suitable for the groundwater system

Time step

Metran has been designed to work with explanatory series that have a daily time step. However, it has been adapted so that other time step lengths can be applied; although Metran still has the limitation that the explanatory variables have a constant frequency. For the TACTIC simulations of series with monthly or decadal meteorological input series, the time step has been set to 30 and 10 days, respectively. This time step has been applied from the end date backward.

Note that the heads may be irregular in time as long as the frequency is not greater than the frequency of the explanatory series.

Model output

The evaporation factor f_c gives the importance of evapotranspiration compared to precipitation. The parameter M_0 gives the total precipitation response, which is equal to the area below the impulse response function and the final value of the step response function.



The average response time is another characteristic of the precipitation response. The influence is illustrated in Figure B3 with the impulse response functions and head time series for two models with very different response times for time series of SGU in Sweden.

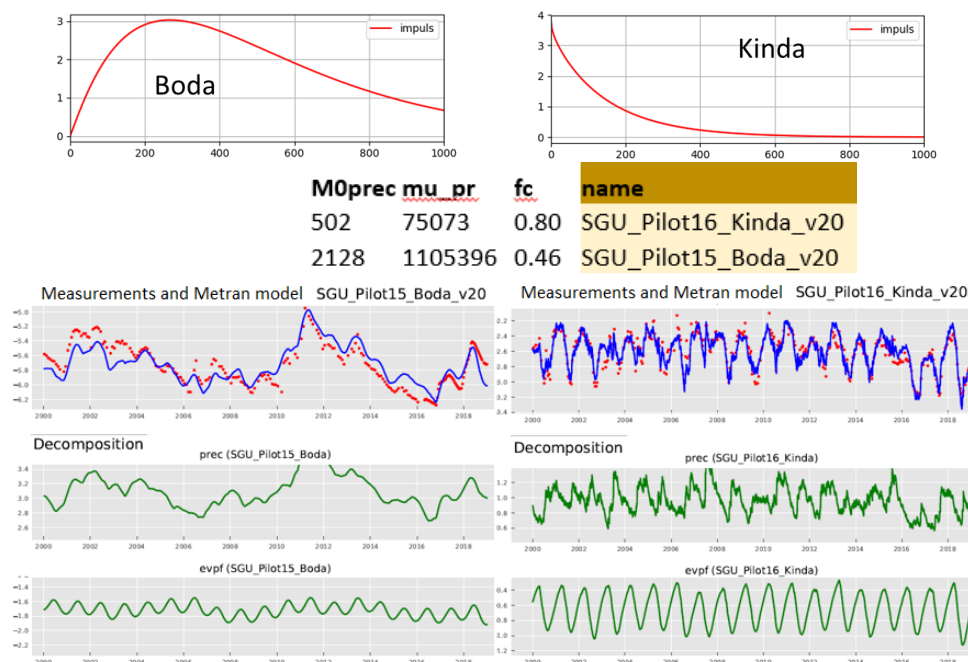


Figure B3 Illustration of Metran output for two case studies in Sweden with different response times.

Model quality

Metran judges a resulting time series model according to a number of criteria and summarizes the quality using two binary parameters Regimeok, Modok (see Zaadnoordijk et al., 2019):

- Regimeok =1 : highest quality
- Modok = 1 (and Regimeok = 0) : ok
- Both zero = model quality insufficient

More detailed information on the model quality is given in the form of scores for two information criteria (AIC and BIC), a log likelihood, R2, RMSE, and the standard deviations and correlations of the parameters.

Recharge

Although the transfer-noise modelling of Metran determines statistical relations between groundwater heads and explanatory variables, we like to think of the results in physical terms. It is tempting to interpret the evaporation factor, as the factor translating the reference into the actual evapotranspiration. Then, we can calculate a recharge as

$$R = P - fE$$

Equation B1



where R is recharge, P precipitation, E evapotranspiration, and f the evaporation factor.

Following the definitions used in the TACTIC project, this recharge R actually is the effective precipitation. It is equal to the potential recharge when the surface runoff is negligible. This in turn is equal to the actual recharge at the groundwater table if there also is no storage change or interflow. In such cases it may be expected that this formula indeed corresponds to the meteorological forcing of the groundwater head in a piezometer, so that it gives a reasonable estimate of the recharge. Obergfell et al. (2019) showed this for an area on an ice pushed ridge in the Netherlands. However, this assumes that all precipitation recharges the groundwater, which cannot be done in many places.

In Dutch polders with shallow water tables and intense drainage networks, it is reasonable to assume that the actual evapotranspiration is equal to the reference value. In that case, the factor f becomes larger than 1 because 1 mm of evaporation has less effect than 1 mm of precipitation (because part of the evaporation does not enter the ground but is immediately drained to the surface water system). In that case, we can calculate recharge as:

$$\begin{aligned} R &= P - fE & f &\leq 1 \\ R &= P/f - E & f &> 1 \end{aligned} \quad \text{Equation B2}$$

These simple formulas can be applied easily for the situations currently modelled in Metran and for the simulations that are driven by future climate data using the delta-change climate factors. However, it is noted that it is a crude estimate using assumptions that are easily violated. Because of this, the equations should be applied only to long term averages using only models of the highest quality.



Deliverable 4.2

PILOT DESCRIPTION AND ASSESSMENT

Continental Spain (Spain)

Authors and affiliation:

David Pulido-Velazquez, Francisco Javier Alcalá; AJ. Collados-Lara, L. Baena Ruiz.

Geological Survey of Spain (IGME)



This report is part of a project that has received funding by the European Union's Horizon 2020 research and innovation programme under grant agreement number 731166.



Deliverable Data	
Deliverable number	D4.2
Dissemination level	Public
Deliverable name	Pilots description and assessment report for groundwater recharge and vulnerability
Work package	WP4
Lead WP	GEUS (WP4)
Deliverable status	
Version	Version 1
Date	14/01/2019

[This page has intentionally been left blank]

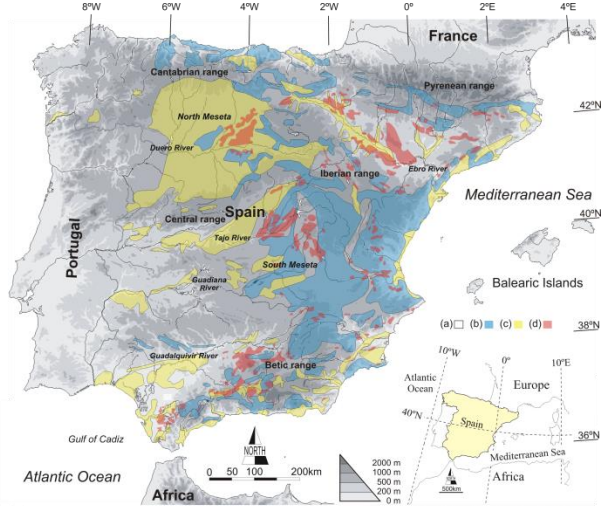
LIST OF ABBREVIATIONS & ACRONYMS

R	Net aquifer recharge
RCM	Regional climate model
GCM	General circulation model
CC	Climate change
GWB	Groundwater body
AET	Actual evapotranspiration
CMB	Chloride mass balance method

TABLE OF CONTENTS

	LIST OF ABBREVIATIONS & ACRONYMS	5
1	EXECUTIVE SUMMARY	5
2	INTRODUCTION	8
3	PILOT AREA	10
	3.1 Site description and data	10
	3.1.1 Location and extension of the pilot area	10
	3.1.2 Geology/Aquifer type	10
	3.1.3 Topography and soil types	12
	3.1.4 Surface water bodies	13
	3.1.5 Hydraulic head evolution	13
	3.1.6 Climate	14
	3.1.7 Land use	16
	3.1.8 Abstractions/irrigation	16
	3.1.9 Flow balance components	17
	3.2. Climate change challenge	19
4	METHODOLOGY	20
	4.1 Methodology and future scenarios	20
	4.1.3 Generation of local climate scenarios	21
	4.1.4. Propagation of impacts on Net GW Recharge: Historical and Future Scenarios	21
	4.1.5. Identification of Potential Strategic Groundwater Resources to Manage Droughts within Continental Spain	22
	4.2 Tool(s) / Model set-up /calibration	24
	4.3. Uncertainty	27
5	RESULTS AND CONCLUSIONS	28
	5.1 Future local climatic scenarios	28
	5.2 Impacts on Net Aquifer Recharge	29
	5.3 The T Index in Continental Spain: Historical and Future Scenarios	30
6	REFERENCES	34

1 EXECUTIVE SUMMARY

Pilot name	CONTINENTAL SPAIN	 <p>(a) Low-permeability pre-Triassic crystalline bedrock and Triassic to Miocene marly sedimentary formations; (b) moderate-to-high permeability Palaeozoic to Tertiary carbonates; (c) moderate-to-high permeability Plio-Quaternary detritic materials; and (d) Triassic to Miocene evaporitic outcrops.</p> <p>Modified from Alcalá and Custodio (2014)</p>
Country	Spain	
EU-region	Mediterranean region and south-western Europe	
Area (km ²)	493519 km ²	
Aquifer geology and type classification	Varied geology, the most important aquifers being Plio-Quaternary sedimentary formations and Triassic to Tertiary carbonate massifs.	
Primary water usage	Irrigation / Drinking water / Industry	
Main climate change issues	<p>The last climate change prediction for the mediterranean area are very significant and will increse drought and scarsity issues (Tramblay et al, 2020). Groundwater resources will play a significant role in the definition of sustainable adaptation strategies (Pulido-Velazquez et al., 2020). Therefore, an apropiate assessment of climate change impacts on grondwater recharge in continental Spain is required. We are also interested in the vulnerability to pumping in order to Identify Potential Strategic Groundwater Resources to Manage Droughts within Continental Spain.</p>	
Models and methods used	<p>The method for impacts of future potential CC scenarios on distributed net AR (R) from precipitation, which is proposed by Pulido-Velázquez et al. (2018) (1) generates future time series of climatic variables (precipitation, temperature) spatially distributed over Continental Spain for potential Aquifer Recharge, and (2) simulates them within previously calibrated empirocal spatial R models from the available historical information to provide distributed R time series. It employs historical climatic data comes from the Spain02 project (Herrera et al., 2016), historical spatial R from Alcalá and Custodio (2014, 2015), and Regional Climate models (RCMs) simulations for future CC scenarios from the CORDEX EU project (2013). The combination of RCMs and Circulation models (GCMs) shows a wide spentrum of variability.</p> <p>Assuming that the long term natural mean reserves were maintained, a preliminary assessment of GW vulnerability to pumping can be obtained by using the natural turnover time index (total storage divided by the R) as approximation of the mean groundwater residence time.</p>	
Key stakeholders	<p>Spanish River Basin Authorities; Spanish Groundwater Users Association; Spanish Water-Supply Companies Group.</p>	



Contact person	F.J. Alcalá, AJ Collados-Lara, D. Pulido, L. Baena,. IGME (Spain), fj.alcala@igme.es, aj.collados@igme.es; d.pulido@igme.es, l.baena@igme.es, j.dedios@igme.es;
----------------	---

In Continental Spain we find a very varied Geology. The most important aquifers are Plio-Quaternary sedimentary formations and Triassic to Tertiary carbonate massifs. Groundwater resources play a key role in the supply of water demands within the territory. On the other hand, the latest studies on climate change (CC) expect significant decreases in water resources in Continental Spain river catchments, with significant environmental, economic and social impacts. In most of these areas, the problem will be exacerbated in the future due to CC, which is associated with an increment in the occurrence of extreme events as droughts. Desertification will also increase into the current framework of land and water degradation; nowadays 20% of the territory is degraded and an additional 1% is actively degrading (Martínez-Valderrama et al., 2016). The objective of this study is to assess and summarise impacts of potential future CC scenarios (for the horizon 2016-2045 under the most pessimistic emission scenario included in the AR5 IPCC report) on recharge in Continental Spain. We also intend to assess groundwater vulnerability to pumping, in order to Identify Potential Strategic Groundwater Resources to Manage Droughts.

The assessment of climate change impacts on the recharge in continental Spain (Pulido-Velazquez et al. 2018) has been performed following the next steps: 1) Definition of local climate scenarios by correcting the climatic model simulations in accordance with the historical data; 2) Propagation of potential climate change scenarios to assess impacts on aquifer recharge by applying a previously calibrated empirical recharge model. This model defines the relationship between the main climatic variables (precipitation and temperature) and the groundwater recharge, relationship that is assumed to be invariant also in the future to propagate the impacts. Assuming that long term natural mean reserves were maintained, a preliminary assessment of GW vulnerability can be also obtained by using the natural turnover time (T) index, defined in each GW body as the storage capacity (S) divided by the recharge (R). Aquifers where R is close to S are extremely vulnerable to exploitation.

The results show a mean lumped reduction of the rainfall recharge equal to 12%. The distribution of the impacts is quite heterogeneous. The largest reduction in mean R appears in the centre and south-east of the territory, dropping 28% in some areas. Only 6.6% of continental Spain corresponds to reductions of more than 20% in mean R. Nevertheless, 52.3% of the territory would suffer mean R reductions between 10% and 20%, while the reduction would be between 0% and 10% over 40.9% of the territory. In the case of the standard deviation on mean R, an increment of 41% on average is expected over 71.5% of the territory, being particularly marked in localized southern areas, with 36.7% of this area showing more than 50% increase. There would also be a significant reduction in the standard deviation in northern areas, with 6.9% of this area showing reductions greater than 30%.

The natural turnover time (T) analyses will be applied in the 146 Spanish GW bodies at risk of not achieving the Water Framework Directive (WFD) objectives to maintain a good



quantitative status. The analyses will be focused on the impacts of the climate drivers on the mean T value for historical and potential future scenarios, assuming that, the Land Use and Land Cover (LULC) changes, and the management strategies will allow to maintain the long term mean natural GW body reserves. Around 26.9% of those GW bodies show low vulnerability to pumping, with historical T values above 100 years, growing this percentage to 33.1% in the near future horizon values (until 2045). The results show a significant heterogeneity. The range of variability for the historical T values is around 3700 years, which is also increased in the near future to 4200 years. Those T indices will change in future horizons, and, therefore, the potential of those GW resources to define sustainable strategies to adapt to climate change will also change accordingly, making it necessary to apply adaptive management strategies.

2 INTRODUCTION

Climate change (CC) already have widespread and significant impacts on Europe's hydrological systems including groundwater bodies, which is expected to intensify in the future. Groundwater plays a vital role for the land phase of the freshwater cycle and has the capability of buffering or enhancing the impact from extreme climate events causing droughts or floods, depending on the subsurface properties and the status of the system (dry/wet) prior to the climate event. Understanding and taking the hydrogeology into account is therefore essential in the assessment of climate change impacts. Providing harmonised results and products across Europe is further vital for supporting stakeholders, decision makers and EU policies makers.

The Geological Survey Organisations (GSOs) in Europe compile the necessary data and knowledge of the groundwater systems across Europe. To enhance the utilisation of these data and knowledge of the subsurface system in CC impact assessments, the GSOs, in the framework of GeoERA, has established the project "Tools for Assessment of Climate change Impact on Groundwater and Adaptation Strategies – TACTIC". By collaboration among the involved partners, TACTIC aims to enhance and harmonise CC impact assessments and identification and analyses of potential adaptation strategies.

TACTIC is centred around 40 pilot studies covering a variety of CC challenges as well as different hydrogeological settings and different management systems found in Europe. Knowledge and experiences from the pilots will be synthesised and provide a basis for the development of an infrastructure on CC impact assessments and adaptation strategies. The final projects results will be made available through the common GeoERA Information Platform (<http://www.europe-geology.eu>).

The specific TACTIC activities focus on the following research questions:

- What are the challenges related to groundwater- surface water interaction under future climate projections (TACTIC WP3).
- Estimation of renewable resources (groundwater recharge) and the assessment of their vulnerability to future climate variations (TACTIC WP4).
- Study the impact of overexploitation of the groundwater resources and the risks of saline intrusion under current and future climates (TACTIC WP5).
- Analyse the effectiveness of selected adaptation strategies to mitigate the impacts of climate change (TACTIC WP6).

The present document reports the TACTIC activities in the pilot Continental Spain within the framework of WP4.

In Continental Spain we find a very varied Geology. The most important aquifers are Plio-Quaternary sedimentary formations and Triassic to Tertiary carbonate massifs. Groundwater resources play a key roles in the supply of water demands within the territory. On the other hand, The latest studies on climate change (CC) expect significant decreases in water resources in Continental Spain river catchments, with significant environmental, economic and social



impacts. In most of these areas, the problem will be exacerbated in the future due to CC, which is associated with an increment in the occurrence of extreme events as droughts. Desertification increases into the current framework of land and water degradation; nowadays 20% of the territory is degraded and an additional 1% is actively degrading (Martínez-Valderrama et al., 2016). New non-conventional sources of water, preferably reuse and desalinitacion for irrigation and domestic use will be needed (Sabater and Barceló, 2010). The objective of this study is to assess and summarise impacts of potential future CC on recharge in Continental Spain. We also intend to identify potential strategic Groundwater Resources to manage droughts by assessing the vulnerability of groundwater bodies to pumping.

3 PILOT AREA

3.1 Site description and data

3.1.1 Location and extension of the pilot area

Continental Spain, between latitudes 36° and 44°N (Figure 1), occupies a large portion of the Iberian Peninsula, the rest being continental Portugal and a part of southern France. The surface area of Continental Spain is 493,519 km².

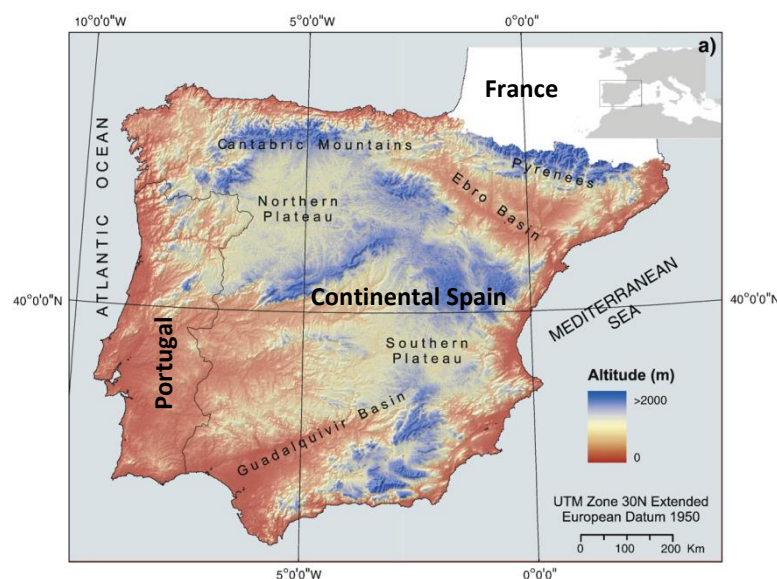


Figure 1. Location of the Iberian Peninsula, showing the elevation, and main mountain ranges and river basins; modified from Del Barrio et al. (2010).

3.1.2 Geology/Aquifer type

The varied geology of Continental Spain determines relatively small, high-yielding aquifers widely distributed throughout its area. The most important aquifers are located in Plio-Quaternary sedimentary formations and Triassic to Tertiary carbonate massifs (Figure 2). The former consist of inland groundwater bodies (GWBs) surrounded by mountain ranges, small alluvial and piedmont units, and deltaic formations on infilled estuaries in coastal areas. Carbonate massifs are common in quite extensive but compartmentalized areas along the northern, eastern, and southern ranges (IGME, 1993). To a minor extent, the weathered and fissured granite and Palaeozoic shale formations in northern, southern, and north-eastern ranges contain small aquifers of local significance.



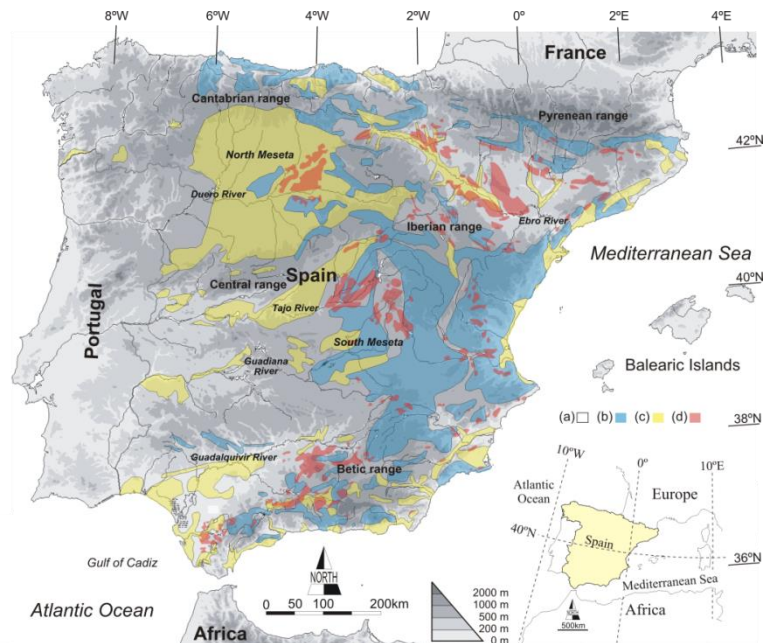


Figure 2. Lithology of continental Spain, synthesized from Alcalá and Custodio (2014), shows the hydrogeological behaviour of materials after permeability type: (a) low-permeability pre-Triassic metamorphic rocks, granitic outcrops, and Triassic to Miocene marly sedimentary formations; (b) Palaeozoic to Tertiary permeable carbonates; (c) Plio-Quaternary permeable detritic materials; and (d) Triassic to Miocene evaporitic outcrops

In Continental Spain, the number of administrative hydrogeological areas designated for groundwater management has varied over time. In the 1990s, most of the regional water formations were integrated into 370 hydrogeological units covering 252.205 km² (51% of Continental Spain), of which 165.503 km² (34% of Continental Spain) were high-permeability formations. For the implementation of the European Water Framework Directive (WFD, 2000) in Spain, 699 GWBs covering nearly 70% of the territory were defined (Figure 3). This classification included former geological formations cataloged as UH and new areas in low-permeability regions where shallow weathering and fissuration of the bedrock favours the development of shallow aquifers of local significance. The current area covered by high-permeability formations is 177.515 km² (36% of Continental Spain).

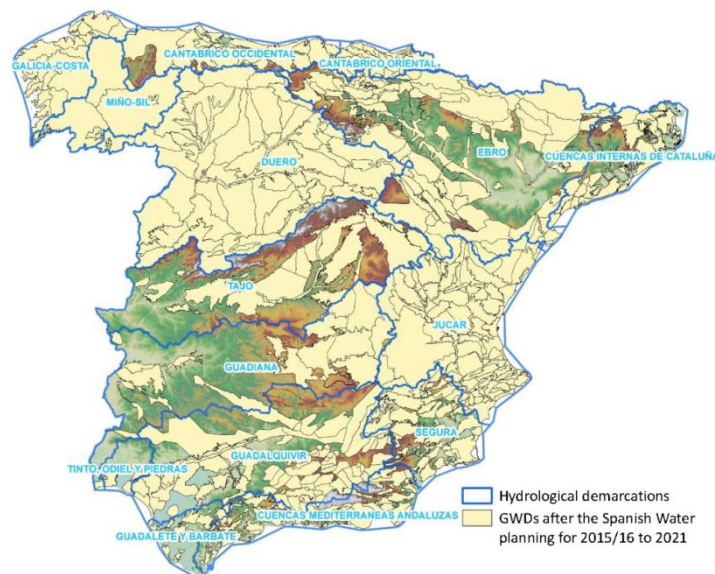


Figure 3. GWDs defined for the implementation of the European Water Framework Directive (WFD, 2000) in Spain.

3.1.3 Topography and soil types

Relatively high-altitude highlands (*mesetas*), about 900 m a.s.l. in the northern half and about 700 m a.s.l. in the southern half, constitute a large part of the country (Figure 1; Figure 2). The *meseta*, which bisected by the Central Cordillera, is surrounded by mountain ranges that may exceed 2500 m of altitude, such as the Cantabrian and Iberian ranges to the north and east and Sierra Morena to the south. This isolated configuration and elevation determines its continental climate (MIMAM, 2000). The Ebro and the Guadalquivir River basins are located outside the *meseta*. Peak elevations exceed 3000 m a.s.l. in the Pyrenean and Betic ranges. The *meseta* is sloping gently from east to west, thus determining the flow direction of the main rivers of the Iberian Peninsula to the Atlantic Ocean, except for the Ebro River (Figure 1; Figure 3).

The abrupt topography and the predominant continental-to-semiarid climatic condition induce thin soils with low organic-matter content in most of Continental Spain. Large areas are dominated by lithosols and regosols in semiarid southern regions, by poorly drained, clay-rich soils over low-permeability marly formations in the large river valleys, and by large bare areas in most carbonate landscapes (EEA, 2007). Figure 4 shows the basic soil-type distribution.



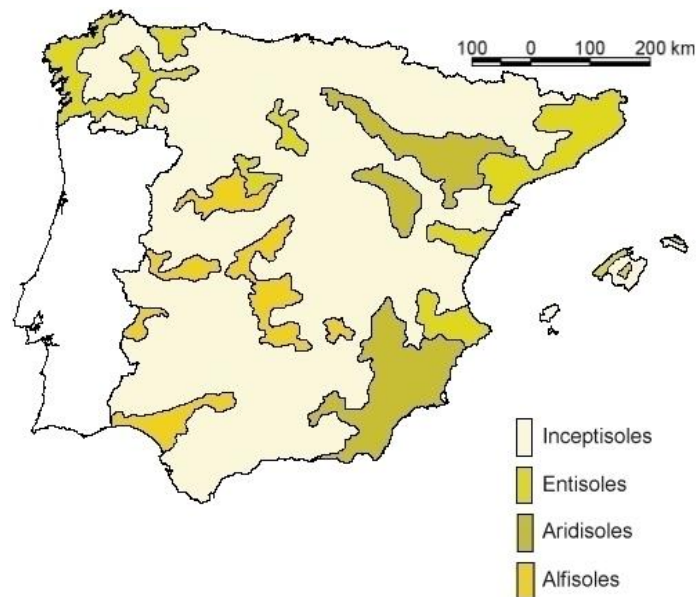


Figure 4. Basic soil-type distribution in continental Spain.

3.1.4 Surface water bodies

In countries and regions that suffer a chronic water resources shortages, as is the case of Spain, there is a necessity to adapt to the environment using a water resources system based on both, groundwater and surface water. Table 1 shows a summary of the natural surface water bodies in Spain. Rivers are the most abundant natural water bodies. Lakes and wetlands are less significant water bodies but they have a great ecological and socioeconomic importance (e.g. Daimiel and Doñana wetlands) (Willaarts et al., 2014). However, the natural surface water bodies are not enough for Spain necessities and there are many reservoirs. Spain has around 1000 large reservoirs with a surface area exceeding 8 km². In Spain there are more than 350 reservoirs with a storage capacity around 54000 cubic hectometres of water, which represents around 50% of the river's flow in the territory.

Table 1. Natural surface water bodies in Spain (information from Willaarts et al., 2014)

Surface water bodies	Total
Rivers (km)	70648
Lakes (km ²)	1010

3.1.5 Hydraulic head evolution

Because the local conditions of climate and water resources needs widely vary throughout the territory, several hydraulic head evolutions can be identified among GWBs. In northern regions, groundwater abstraction is low to moderate and the hydraulic head evolutions coarsely follows the climatic pattern. In southern, south-eastern, and eastern regions, different degrees of exploitation occur, with cases of groundwater mining in some GWBs in which groundwater reserves are being consumed (Custodio et al., 2016). In general, during the last 5



decades, piezometric levels had show a general decreasing trend in some GWBs located in the northern and southern *mesetas* and in the Mediterranean coastal fringe. Hydraulic gradient inversion between low-quality, low-exploitated shallow unconfined aquifers and heavily-exploited confined aquifers with better groundwater quality has been described in some mediterranean GWBs. The cases of overexploitation with negative consequences on groundwater quantity and quality are increasing. Figure 5 shows GWBs in quantitative risk in Continental Spain.

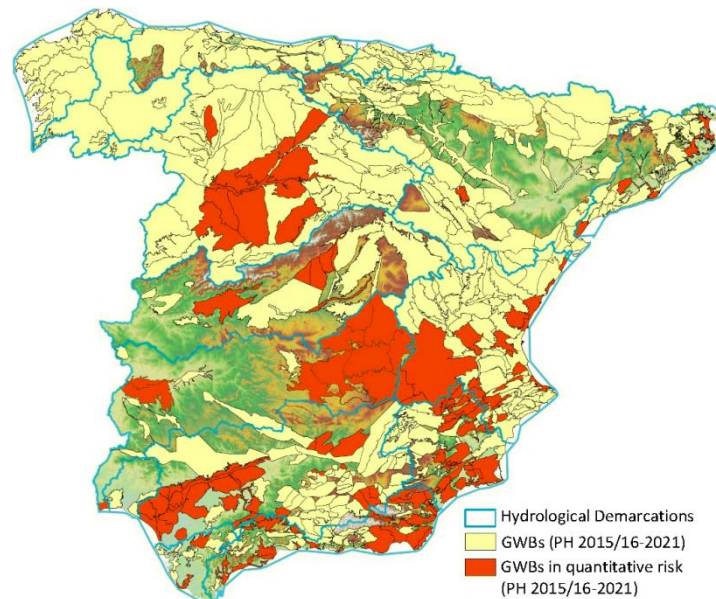


Figure 5. Groundwater bodies in quantitative risk in continental Spain.

3.1.6 Climate

Inland areas of Continental Spain constitute a large part of the country characterized by continental climate. This means hot, dry summers, and cold, relatively wet winter-spring seasons. There are recurrent dry spells lasting 2 to 5 years with variable influence of the wet and dry periods over the Atlantic and the Mediterranean areas. Other climates are semiarid in large areas of the territory, subhumid dry and wet, and humid in northern areas and high mountains (MIMAM, 2000).

The average precipitation in continental Spain ranges from 2000 mm year⁻¹ in the western and northern coastal mountain areas, to about 500-600 mm year⁻¹ over the northern *meseta*, and 380-500 mm year⁻¹ in the southern *meseta*. In the semiarid south-eastern coastal areas and north-eastern inland areas, precipitation averages around 300 mm year⁻¹ or less, reaching as low as 180 mm year⁻¹ (Figure 6a). Precipitation occurs predominantly in late autumn and winter, associated with the circulation of cold air masses from the North Atlantic Ocean and deep pressure lows, initially located over the Gulf of Cádiz, which travel eastwards and generate the inflow of air masses from the Subtropical Atlantic Ocean (Trigo *et al.*, 2004). At the same time, the eastern coast of Spain may receive precipitation from humid air masses

over the West Mediterranean Sea, which generally do not penetrate far from the coastal fringe and may be accompanied by heavy storms from convective rains, especially in late summer and autumn (Martín-Vide and López-Bustins, 2006). Although these storms may represent less than 15% of annual precipitation in these areas, they can cause flooding and are significant for aquifer recharge after the soil-water deficit is satisfied. Coefficient of variation of average yearly precipitation is irregularly distributed in the 0.2-0.5 range (MIMAM, 2000).

The annual mean temperature (T) varies from 4.6 to 21.1 °C (Figure 6b) with minimums in January and maximums in August; the daily T amplitude on a year may be as high as 50 °C in the southern meseta and river valleys. There is a pronounced gradient of T with elevation in mountain areas, thus favouring the seasonal snow-melting contribution to surface and groundwater bodies (MIMAM, 2000). The mean annual T is around 8 °C in northern areas and more than 18 °C in lowlying areas of southern and eastern regions. The average mean potential evapotranspiration is in the 600-800 mm/year range in most of the territory, with extreme values that vary from 400 mm/year in northern high mountains to 1200 mm/year in semiarid inland areas of the Ebro River (MIMAM (2000).

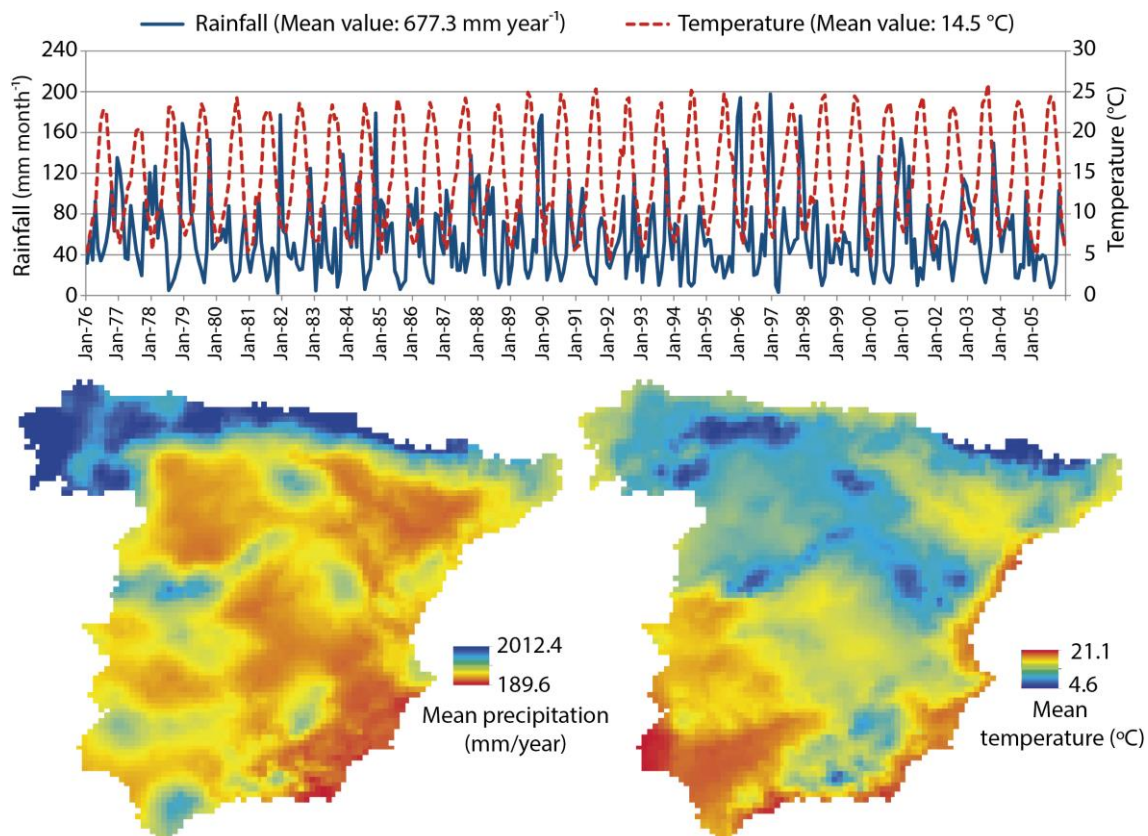


Figure 6. Spatio-temporal distribution of historical mean (a) precipitation (mm/year) and (b) temperature (°C) in continental Spain during the period 1976-2005; modified from Pulido-Velazquez et al. (2018).

3.1.7 Land use

The northern and north-western high-rainfall zones have densely vegetated areas with stable and well-drained organic-matter-rich soils (Figure 7). Natural and semi-natural vegetation cover 47% of the territory, mostly sparse scrublands. In the valleys and flat highlands, traditional rain-fed agriculture combines with newly developed irrigated agriculture to cover 49% of the territory. The rest are urbanized areas and other land uses (Del Barrio et al., 2010).

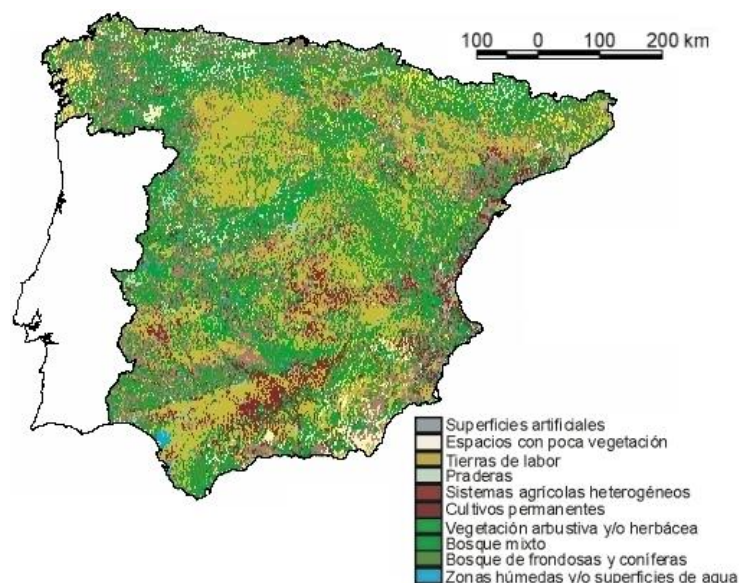


Figure 7. Land-use conditon in continental Spain from CORINE (1990 and 2012).

3.1.8 Abstractions/irrigation

Groundwater exploitation has increased more than 3-fold in the last 50 years (Garrido and Llamas, 2009). The current use of groundwater is estimated at about 6.5 km³ year⁻¹, about 75% for crop irrigation. Much of the groundwater exploitation is concentrated in the Mediterranean area for different uses. Irrigation areas are widely dispersed over the territory, surface-water developed in the main river valleys and mostly groundwater developed in the southern *meseta* and in the southern and south-eastern coastal fringes (Figure 8).

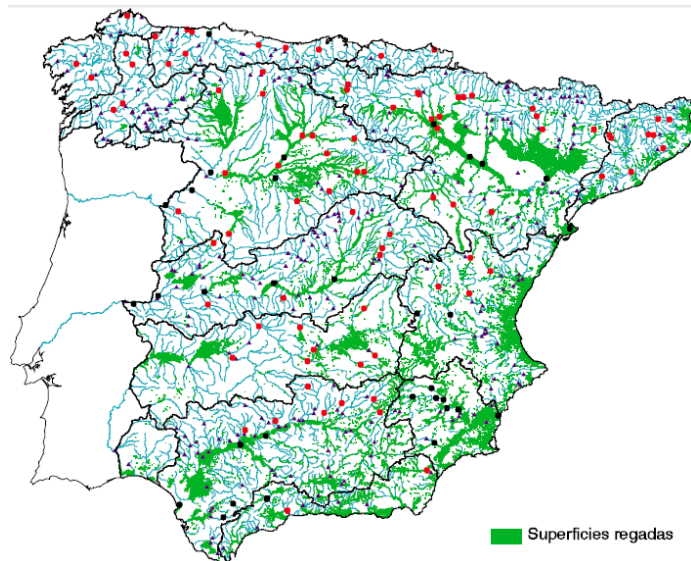


Figure 8. Irrigated areas in continental Spain, after satellite-based land-use condition in continental Spain from CORINE (1990 and 2012).

3.1.9 Flow balance components

This section refers exclusively to the component R from precipitation. In Continental Spain, the wide lithological, orographic, pedological, and climatic diversity of Continental Spain produces a large number of different conditions for R. At the Continental Spain scale, R was estimated from the second half of the 20th century through different distributed techniques (Alcalá and Custodio, 2012), but its uncertainty was not explicitly indicated. Only the permeable formations were traditionally considered in Water Planning. Recently, Alcalá and Custodio (2014, 2015) used the atmospheric chloride mass balance (CMB) method to estimate R at the same 4976 nodes of a 10 km x 10 km grid covering the whole territory. Average nodal R values vary from 17 to 715 mm/year, with 90% of results between 30 and 300 mm/year (Figure 9a). Mapped results are considered potential estimates in low permeability areas and net estimates over permeable formations. The potential estimation is around 66 km³/year over Continental Spain; the remaining 32 km³/year is for permeable outcrops. The fraction of precipitation (Figure 9b) that transforms into R vary between 0.03 and 0.65; the lower values are in low-permeability sedimentary formations in the large river valleys, crystalline outcrops, and semiarid southern regions, and the higher values in carbonate formations (Figure 9c). Two main sources of uncertainty affecting the average R estimates (given by the coefficient of variation, CV) were segregated, that induced by the inherent natural variability of the CMB variables, CV_R , and that produced when mapping the CMB variables, CV_K . The average CV_R is 0.29 (Figure 9d) and the average CV_K is 0.09 (Figure 9e). Average R varies from 23 to 41 km³/year over permeable formations when only CV_R is taken into account. Results were compared with other regional R estimates, such as provided by MIMAM (2000); the CMB estimates being 4% higher (Figure 9f). The differences were explained by the different data coverage and the different hydrological meaning of R estimates that each technique provides, as explained by Alcalá and Custodio (2014, 2015).



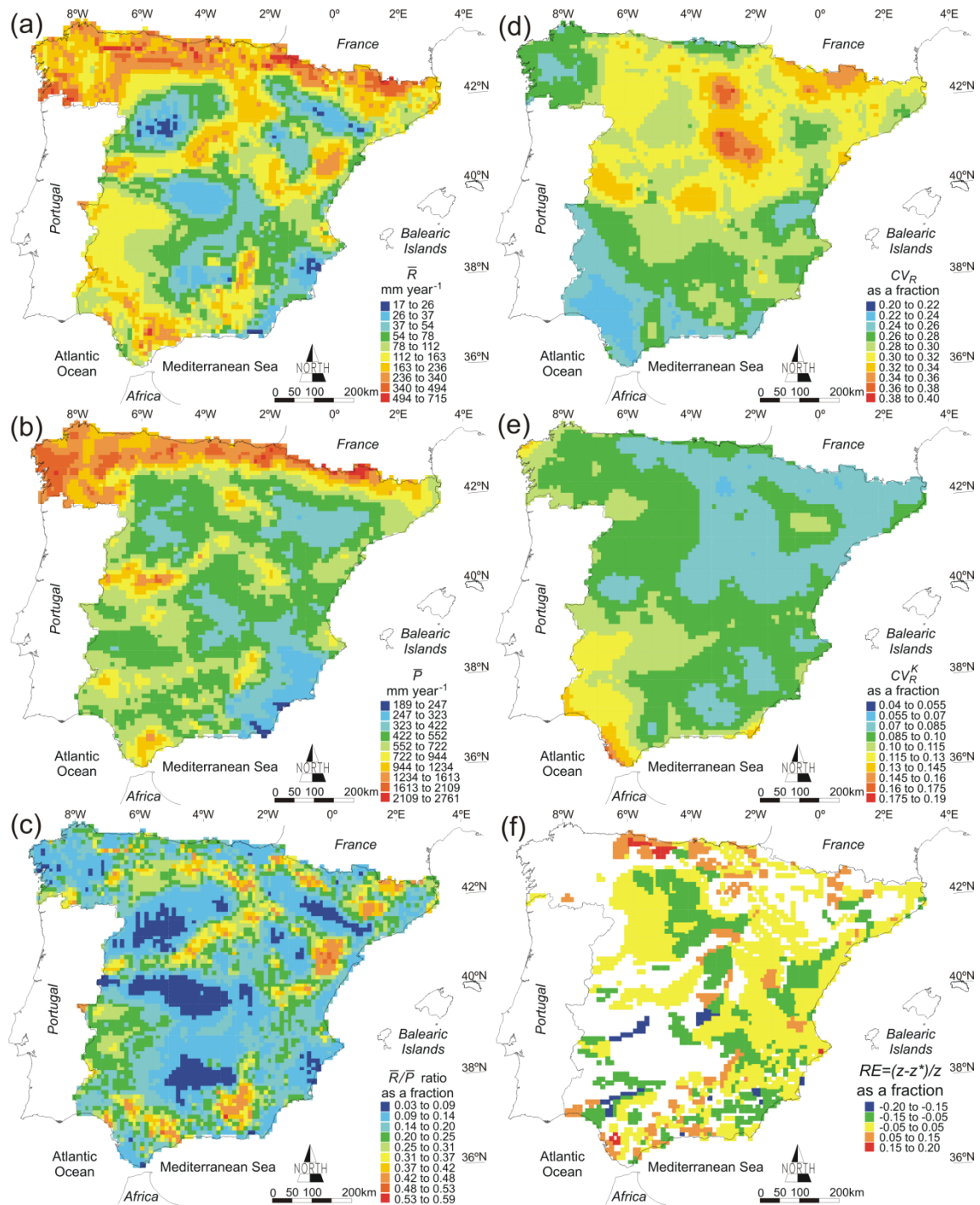


Figure 9. Mapping of R in Continental Spain: (a) average yearly R (mm/year); (b) average yearly precipitation (mm/year) from MIMAM (2000); (c) dimensionless R /precipitation ratio; (d) dimensionless natural uncertainty of R , CV_R ; (e) dimensionless mapping uncertainty of R , CV_K ; and (f) comparison of Alcalá and Custodio (2014, 2015) (z^*) and MIMAM (2000) (z) R estimates for coincident areas: the outcropping of the former Hydrological Units, where $RE=(z-z^*)/z$ is the dimensionless relative difference. Data are discretized in 10 km x 10 km cells.

3.2. Climate change challenge

In accordance with the EEA map the main expected issues due to CC in Continental Spain are those described in the Figure 10 for the Atlantic and Mediterranean regions. Existing national estimates show also a significant reduction (around a 20% for the RCP8.5 emission scenario in the horizon 2071-2100) of the R in the territory (Pulido-Velázquez et al., 2018).

The main challenge is to find adaptation measures to maintain a sustainable use of the GWBs with a positive balance between supply water demands (different uses) under future CC conditions and maintaining a good status in the related ecosystem. Additional measures for non-conventional water resources will include reuse and desalination.

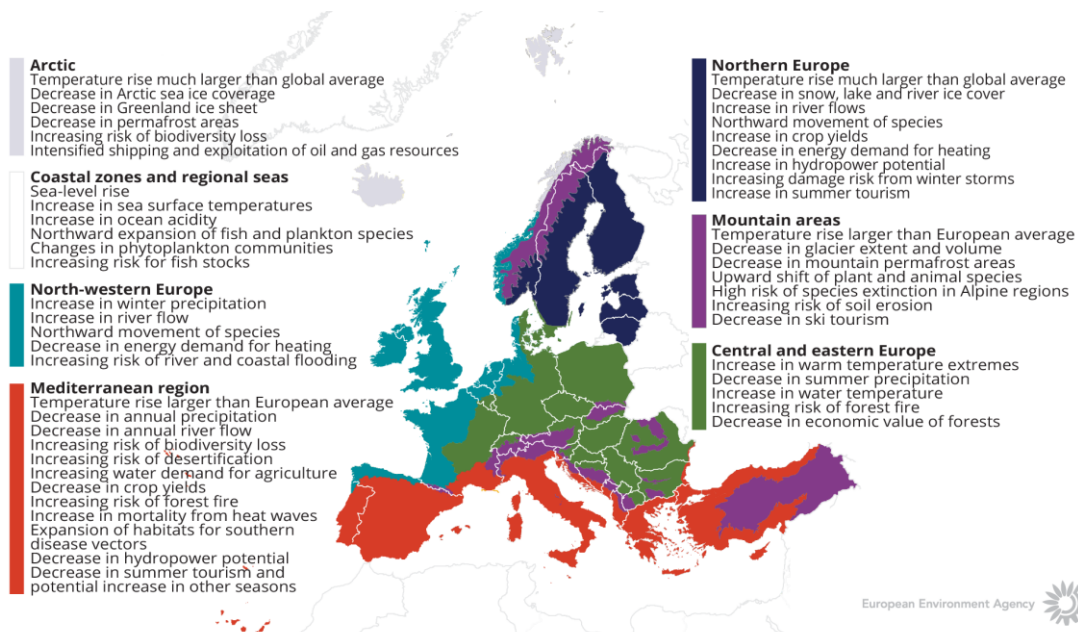


Figure 10. How is climate expected to change in Europe. The European Environment Agency map.

4 METHODOLOGY

4.1 Methodology and future scenarios

4.1.1 Tools/ model description

An impact and adaptation assessment has been performed for historical and some future potential GC scenarios. We have defined potential local climatic scenarios from RCM simulations within the horizon 2016-2045 assuming the most pessimistic emission scenarios, the Representative Concentration Pathways 8.5 (RCP8.5). The GROUNDS tool (Collados-Lara et al., 2020) was applied to generate those local future climatic series. Ensemble of all the projections derived from the RCMs simulations were defined under the hypothesis that they are equi-feasible. An empirical net aquifer recharge (R) model was calibrated from the historical climatic observations and the historical R values previously derived by chloride mass balance Alcalá and Custodio (2014). Assuming that the relationship between effective precipitation and net aquifer recharge remain invariant also in the future, the empirical model is used to propagate the generated future potential scenarios to assess climate change impacts on future net recharge in continental Spain.

4.1.2 Future scenarios. Climate data

In order to generate future local scenarios, the historical climatic data (precipitation and temperature series) in the reference period (1976-2005) were combined with the Climatic model simulations for the Control period (1976-2005) and future scenarios (2016-2045). It includes various climatic model simulations undertaken by the CORDEX EU project for the most pessimistic IPCC emission scenario, the Representative Concentration Pathways 8.5 (RCP8.5). Selected simulations consist of results from five Regional Climate Models (RCMs) (CCLM4-8-17, RCA4, HIRHAM5, RACMO22E, and WRF331F) nested within four distinctive General Circulation Models. An equi-feasible ensemble of all RCMs simulations was performed using 1976-2005 as the control/historical reference period, and fixing the future horizon scenario as 2016-2045.

The RCPs are greenhouse gas concentration trajectory adopted by the IPCC. They are named according the radiative forcing that represent. Radiative forcing is the change in the net, downward minus upward, radiative flux at the troposphere or top of atmosphere due to a change in an external driver of climate change. The RCP8.5 is the most pessimistic pathway for which radiative forcing reaches values greater than 8.5 W m^{-2} by 2100. The selected RCMs projections were performed using the simulations of the RCP8.5 trajectories to generate potential future series of precipitation and temperature. In this work, we corrected these series to generate local scenarios and to propagate their impacts on R.

The RCM climate modelling simulates climate conditions defined with some initial conditions, time-dependent lateral meteorological conditions and surface boundary conditions to drive high-resolution models. These conditions are typically wind components, temperature, water



vapor, and surface pressure. The driving data are derived from GCMs that simulates with a coarse resolution. Table 1 shows the GCMs used by the RCMs employed in this work. The World Climate Research Programme (WCRP) through the CORDEX project guarantees the quality of the RCMs collected by them. However, the uncertainties related to RCMs can be important and they must be adapted to the study area.

Table 1. Regional Climatic Models (RCMs) and General Circulation Models (GCMs) considered to define the climatic scenarios.

RCMs \ GCMs	CNRM-CM5	EC-EARTH	MPI-ESM-LR	IPSL-CM5A-MR
CCLM4-8-17	X	X	X	
RCA4	X	X	X	
HIRHAM5		X		
RACMO22E		X		
WRF331F				X

4.1.3 Generation of local climate scenarios

The GROUNDSD tool (Collados-Lara et al., 2020) allows us to generate local potential scenarios climatic variables. The monthly bias of the model within the reference period (1976-2005) was estimated as the mean relative differences between the control simulation and the historical precipitation and temperature time series calculated for each month of an average year. It was used to generate the future series by applying a bias correction technique (scenario E1). The monthly delta changes between control and future precipitation (2016-2045) was also estimated to generate series by applying a delta change approach (scenario E2).

4.1.4. Propagation of impacts on Net GW Recharge: Historical and Future Scenarios

An empirical precipitation-R model was employed to estimate the historical R within the reference period and the impacts of potential future climatic scenarios on R (Pulido-Velazquez et al., 2018). It is defined as follow:

$$R = C(P - E) \quad (1)$$

where R, P (precipitation), and E in mm year⁻¹, and dimensionless C. For estimating E, we used the non-global Turc formulation:

$$E = \frac{P}{\sqrt{0.9 + \frac{P^2}{L^2}}} \quad (2)$$

where $L = 300 + 25Ta + 0.05Ta^3$ is a dimensionless form parameter of annual temperature.

This model has been used to propagate the impacts of local historical and future climatic fields in continental Spain



4.1.5. Identification of Potential Strategic Groundwater Resources to Manage Droughts within Continental Spain.

This method intends to perform a preliminary analysis of GW vulnerability to intensive pumping during drought periods through the renewal time of their resources (GW age) approached by the T index as the S/R ratio. Assuming that the long term natural mean reserves is kept invariant and the actual recharge is the main inflow of groundwater resources, the GW bodies with high renewal time, will be less vulnerable to pumping than those with low values, even in periods in which pumping is smaller than mean R. It can be especially relevant in Basins or Water Resources systems with scarce reserves where long and intensive droughts appear and will be even exacerbated in the future due to climate change. The methodology is summarized in Figure 11.

VULNERABILITY TO PUMPING ► MEAN GROUNDWATER TURNOVER TIME (T) INDEX

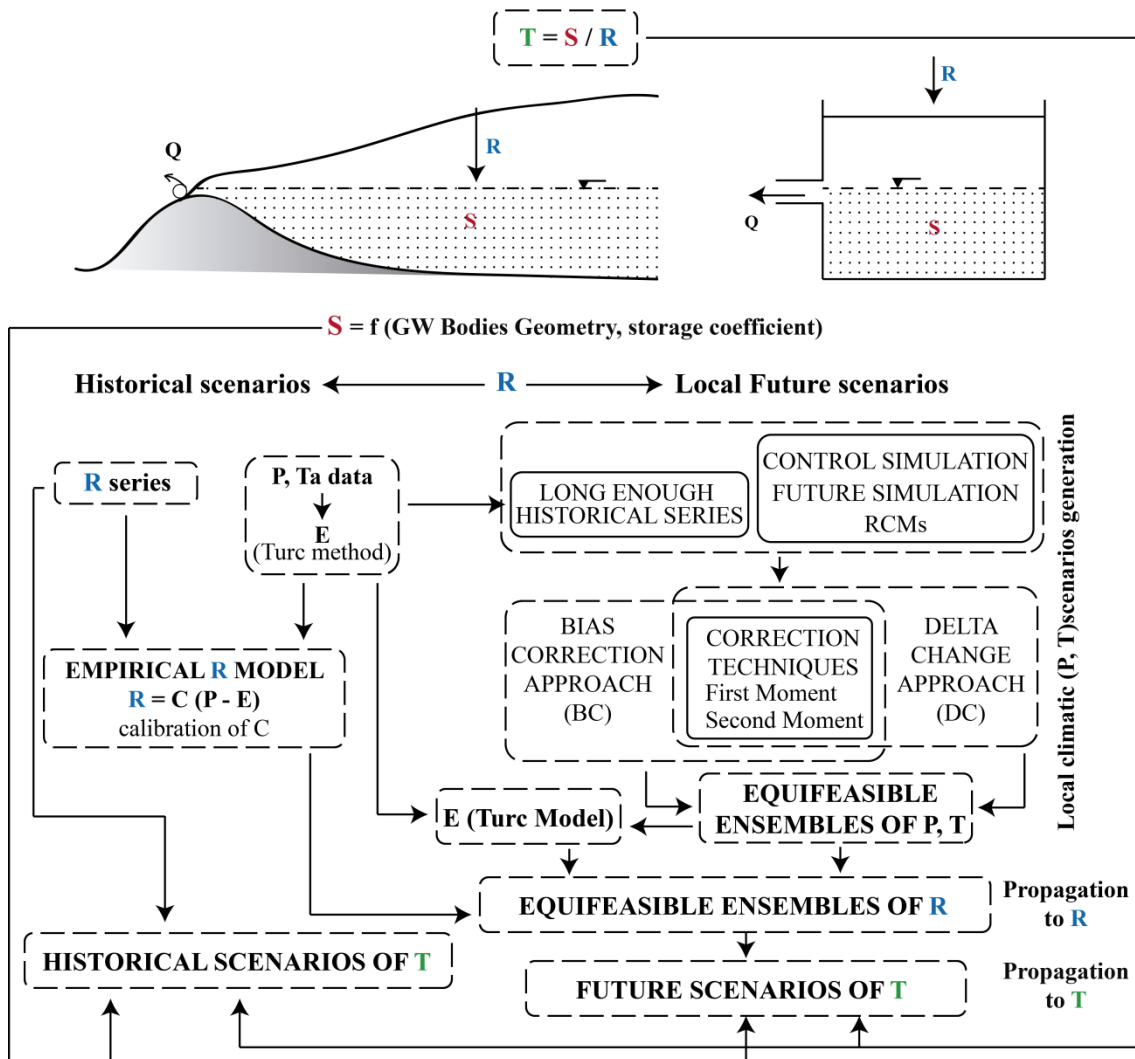


Figure 11. Flowchart of the methodology developed to assess GW Bodies vulnerability to pumping. Notation and units for variables used: P, E, R, and Q are respectively precipitation, actual evapotranspiration, net GW recharge from P, and net GW discharge in mm year⁻¹; Ta is temperature in °C; C and S are respectively a dimensionless effective recharge coefficient (-) and a GW storage (Mm³); and T is the natural turnover time index in years. (Pulido-Velazquez et al., 2020)

Making a parallelism between unconfined aquifers and reservoirs, the GW discharge (Q) will start when the potential aquifer storage reaches the threshold level of the surface connection (See Figure 11). Assuming that there is not any pumping, a preliminary assessment of the natural mean age of the groundwater leaving the GB body through the connection with the surface system (springs and or stream-aquifer interaction boundary conditions), can be obtained through the natural mean T index, defined as:

$$T = S/R \quad (3)$$

where T, S, and R are defined in Figure 11 caption.

In each GW body, S can be obtained by combining information about the geometry and the storage coefficients, which can be derived from different sources of information (eg. field works, models and/or research papers and official reports, as well as the River Basin Plans published by the different River Basin authorities). The historical R can be estimated through field work or previously calibrated models. The historical mean T value can be estimated by combining the mean historical R values with S in accordance with Equation 3.

The impacts of future potential climatic scenarios on GW bodies R, and, therefore, on their T index, requires climatic scenarios to be downscaled and propagated with the previous calibrated recharge model. The impacts of the generated potential local scenarios on the mean T will require future mean R to be estimated, which will be assessed by propagating/simulating the generated climatic scenarios with previously calibrated recharge models.

For each of the selected GW bodies, we have taken the available information about the potential GW storage under the surface connection. They were collected from the last River Basin Plans (2015-2021) published by the different River Basin authorities. It summarizes geological and topographical information to define the GW body geometry, that combined with the storage coefficients provide the S (Mm³) value for these GW bodies.

This preliminary method has been applied only in the 146 Spanish GW bodies at risk of not fulfilling the WFD (2000) quantitative objectives (see Figure 12). After the WFD went into effect, the European Environment Agency established the guidelines for declaring those GW bodies at risk of not fulfil a good quantitative and qualitative level in the 2020 horizon, as well as some general measures to mitigate negative impacts.



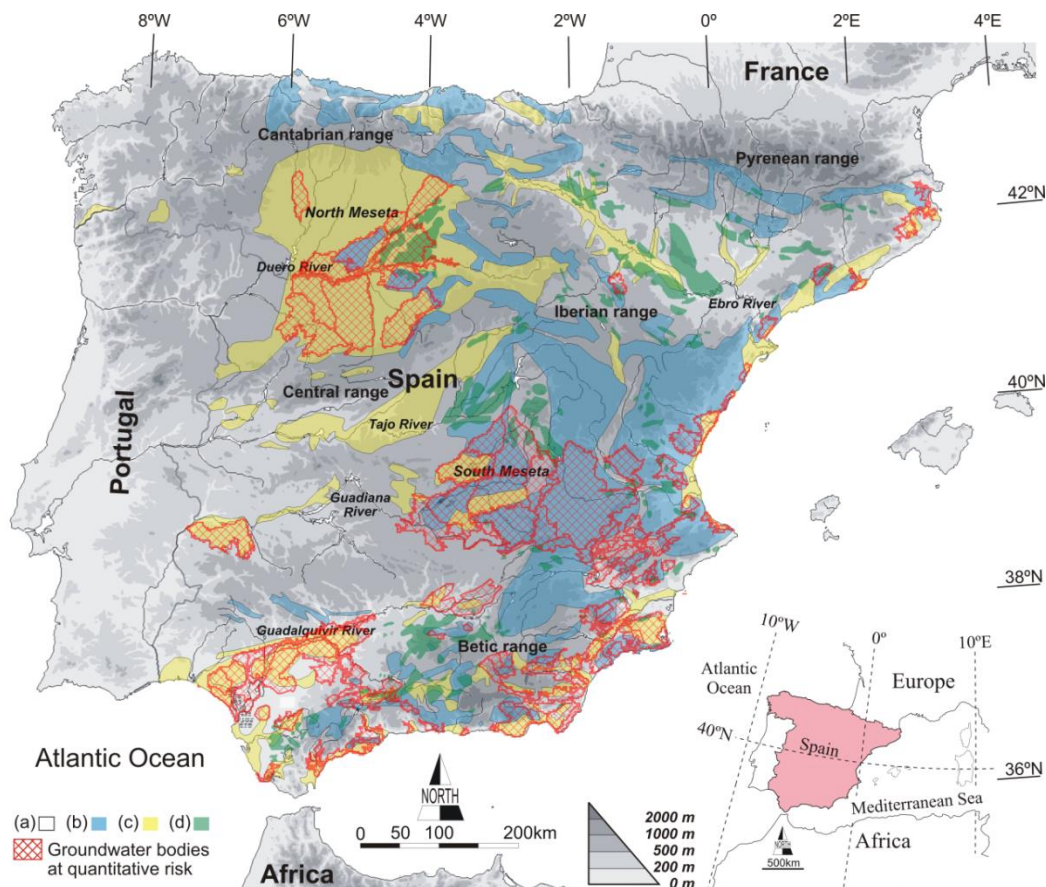


Figure 12. Map of continental Spain, showing the 146 Spanish GW bodies at quantitative risk of not fulfilling the WFD (2000) objectives (red shadowed areas), the main mountain ranges and hydrographic basins, and the hydrogeological behavior of geological materials forming the GW bodies according to permeability type as: (a) low to moderate permeability pre-Triassic metamorphic rocks, granitic outcrops, and Triassic to Miocene marly sedimentary formations; (b) moderate to high permeability Palaeozoic to Tertiary; (c) moderate to high permeability Plio-Quaternary detritic; and (d) Triassic to Miocene evaporitic outcrops.

4.2 Tool(s) / Model set-up /calibration

4.2.1. Generation of local climate change scenarios. GROUNDSD tool (Collados-Lara et al., 2020)

The differences between the control simulations and the historical data are employed to calibrate the downscaling approach to be applied. Figure 13 summarize these differences in mean monthly precipitation.



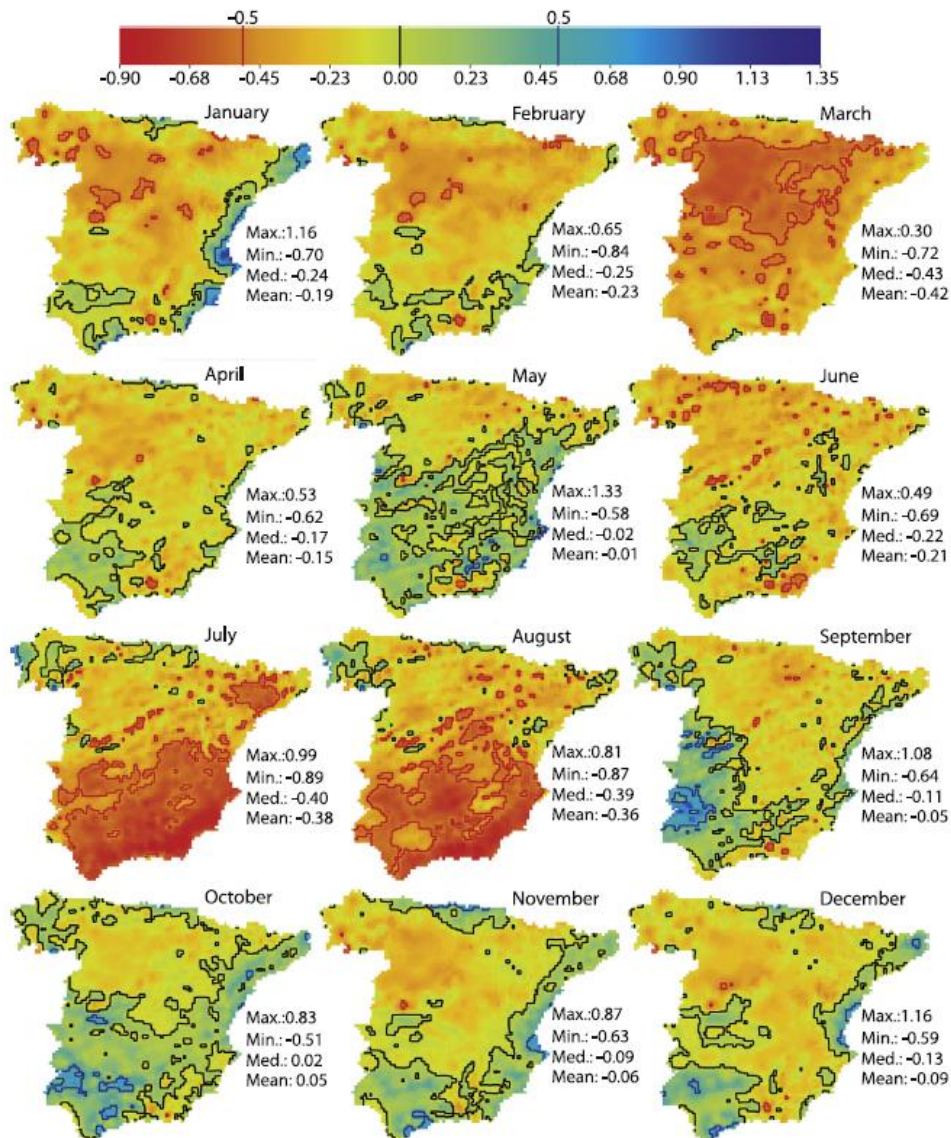


Figure 13. Dimensionless spatial monthly mean relative differences between the control simulation and the historical precipitation time series for an average year in the reference period (1976–2005). The ± 0.5 range is indicated.

The transformation functions to correct the historical series also need information about the differences between future and control simulations (showed in Figure 14).

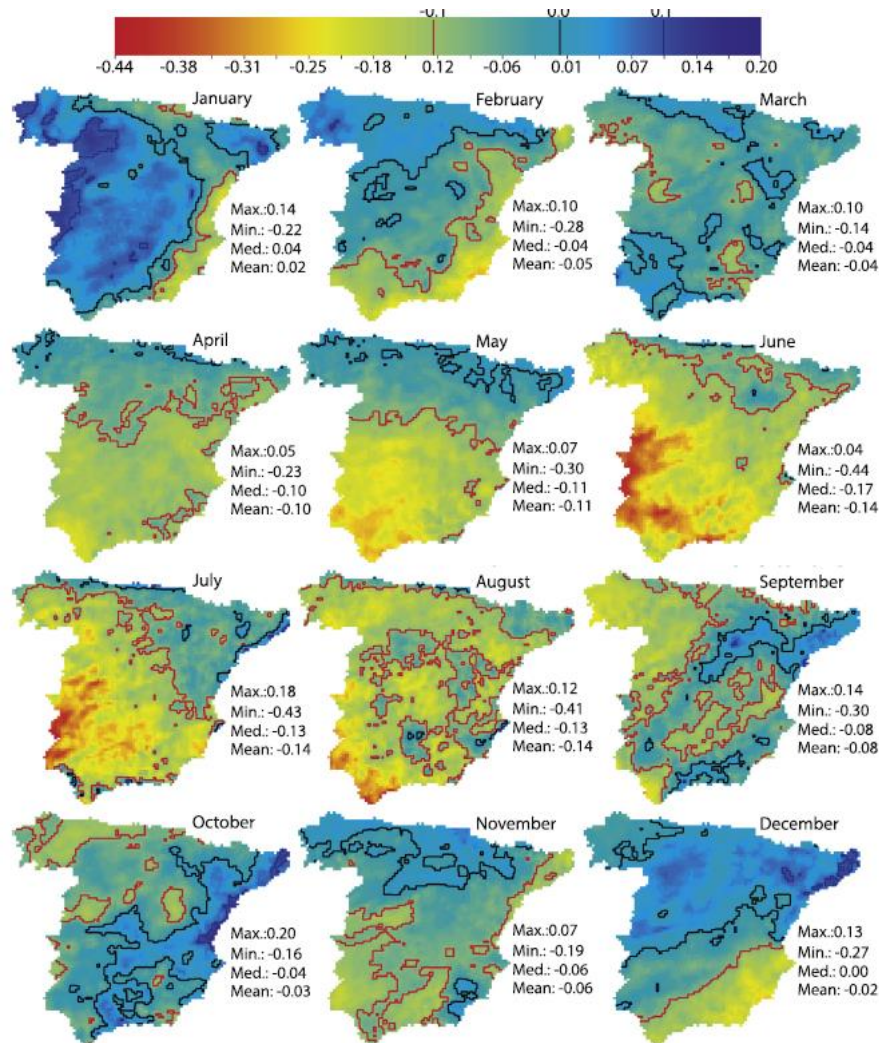


Figure 14. Dimensionless spatial monthly mean relative differences between future (2016–2045) and control (1976–2005) precipitation time series. The ± 0.1 range is indicated.

4.2.2. Definition of a R model

The R model was calibrated using precipitation recharge time series from historical climatic data and historical R data from the CMB method for the period 1996–2005. We assume that the statistics (mean and standard deviation) of R time series from the CMB method for the period 1996–2005 and R time series generated from a longer historical period 1976–2005 do not differ substantially, and can be considered identical. This assumption is supported by assuming steady-state conditions of the mean and standard deviation of the balance variables determining the historical recharge when simulating the period 1976–2005. The distributed mean annual recharge was 139 mm and 144.4 mm, respectively, thus the relative difference was less than 4% on average. The mean estimated recharge in the period 1976–2005 is represented in Figure 15.



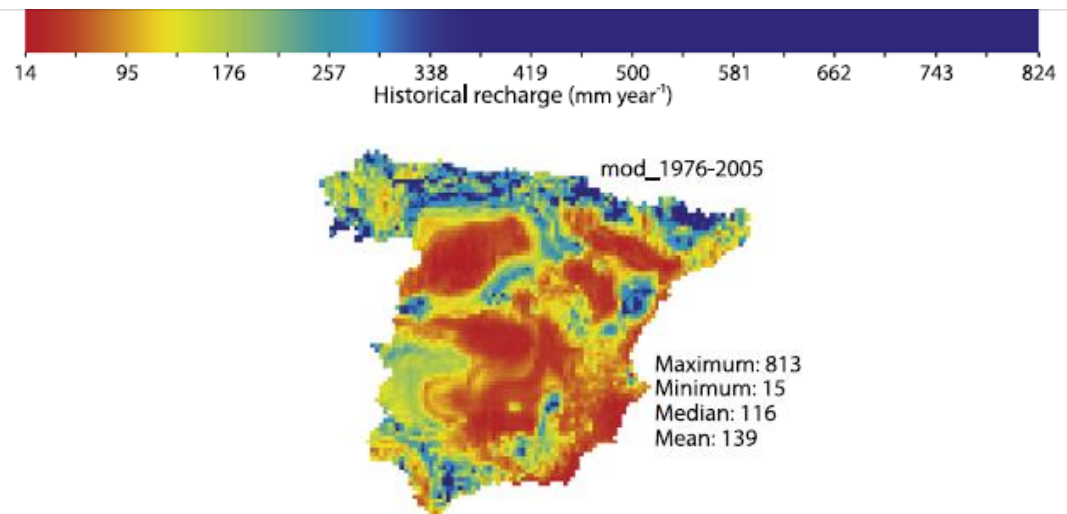


Figure 15. Mean net aquifer recharge (mm year₋₁) for the period 1976–2005

4.3. Uncertainty

In this study the dominating source of uncertainty is related to RCMs future simulation. In general, there is a large degree of uncertainty in climate change impacts assessments. There are different climate models (both RCMs and GCMs) that can be used to make future climate projections. Every climate model includes its own model for the atmosphere, the ocean, the Earth's surface, and ice sheets as well, as different parameterizations of the physical processes that must be considered within each of these models. The correction approaches are another source of uncertainty but its importance in climate change impacts assessments is lower (Collados-Lara et al., 2018).

In this study we considered different combinations of RCMs nested to GCM (nine) and two correction approaches to take into account uncertainty. Note that the impacts on recharge was assessed by considering 18 future projections. It allows us to calculate mean changes and the ranges of variability of these changes. Nevertheless, this study is focused on the mean assessment, and for this reason two equi-feasible ensembles of projections (one for the bias (E1) approach and another for delta (E2) approach) have been employed to define the scenarios to be propagated within the recharge model to assess future impacts.

5 RESULTS AND CONCLUSIONS

5.1 Future local climatic scenarios

Despite the temporal series being different, the two equifeasible ensembles E1 (applying bias correction techniques) and E2 (applying delta change techniques) produced identical future mean temperature maps (Figure 16).

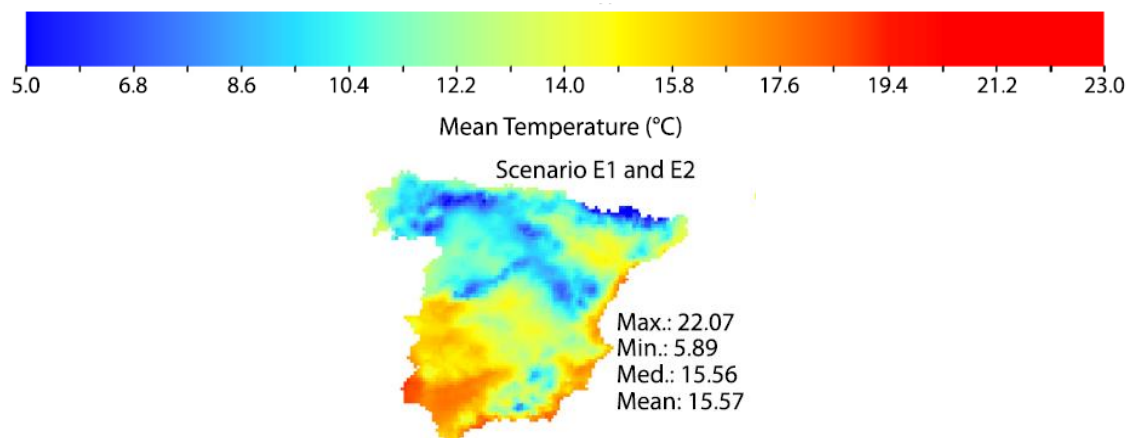


Figure 16. Potential future mean temperature (°C) scenarios obtained with the two ensemble options (E1, E2)

In terms of precipitation, there are very small differences between the two equi-feasible ensembles E1 and E2 due to a reduced number of negative values appearing in some cells when correcting using the second moment approach (Figure 17).

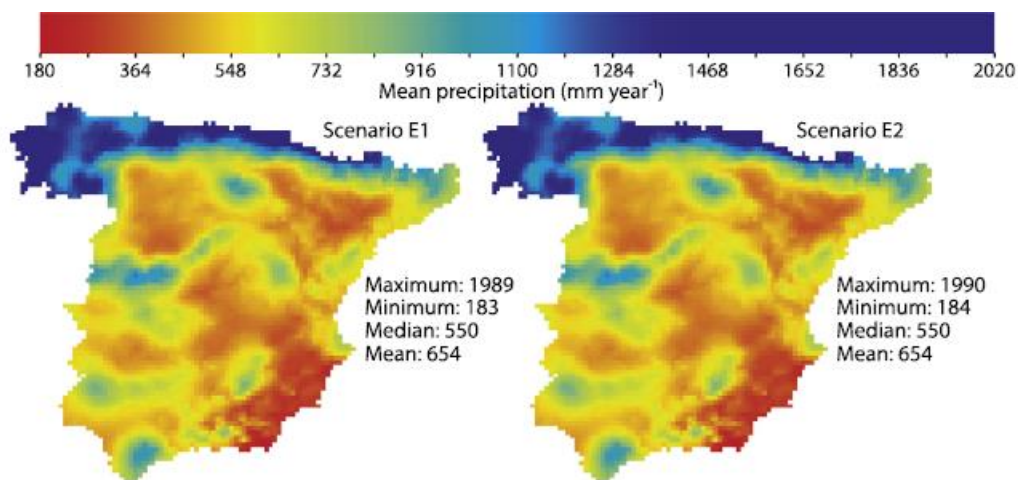


Figure 17. Potential future mean precipitation (mm.year⁻¹) scenarios obtained with the two ensemble options (E1, E2)

5.2 Impacts on Net Aquifer Recharge

Figure 18 shows that, although a small reduction in mean R is expected over 99.8% of continental Spain, there are two small north-eastern (600 km²) and eastern (100 km²) areas of the territory where a small increase is expected. A largest reduction in mean R in the centre and south-east of the territory is expected, dropping 28% in some areas. Only 6.6% of continental Spain corresponds to reductions of more than 20% in mean R. Nevertheless, 52.3% of the territory would suffer mean R reductions between 10% and 20%, while the reduction would be between 0% and 10% over 40.9% of the territory. In the case of the standard deviation on mean R, an increment of 41% on average is expected over 71.5% of the territory, being particularly marked in localized southern areas, with 36.7% of this area showing more than 50% increase. There would also be a significant reduction in the standard deviation in northern areas, with 6.9% of this area showing reductions greater than 30%.

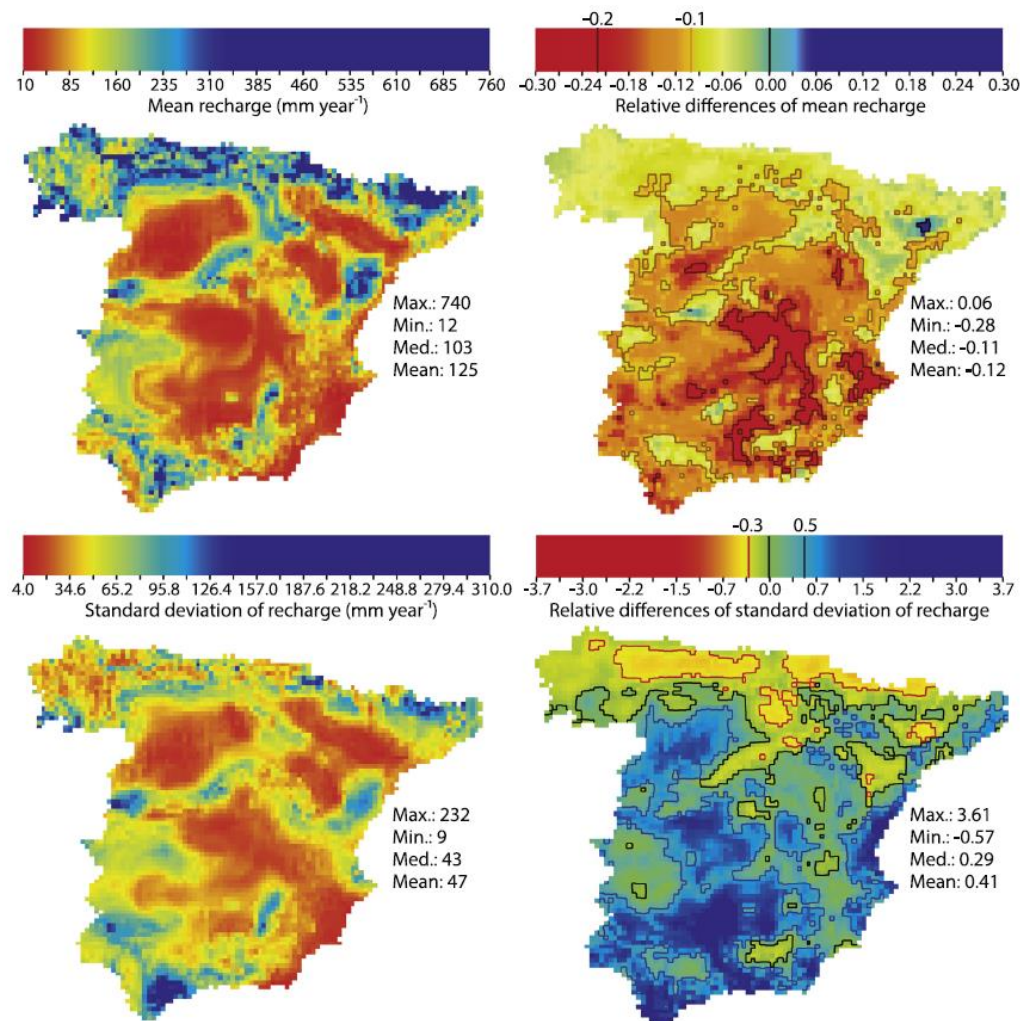


Figure 18. Potential future mean net aquifer recharge (R) (mm year⁻¹), standard deviation of future mean R (mm year⁻¹), and dimensionless relative differences between historical and future scenarios (equi-feasible ensemble of all the scenarios).

5.3 The T Index in Continental Spain: Historical and Future Scenarios

The information previously summarized was used to assess the natural T for the historical period (reference period 1976-2005) and future potential scenarios in the horizon 2016-2045 that correspond to the RCP 8.5 emission scenario. Two different local climatic scenarios have been considered to assess the potential impacts on T values, one generated by an ensemble of bias correction approaches (E1=EB) and another by an ensemble of delta change approaches (E2=ED). The methodology and the series generated for those scenarios were described in section 4.1.3. Figure 19 shows a heterogeneous distribution of T values within the 146 selected GW bodies as case studies. The box whiskers plot also reflects this wide range of T values moving from a minimum of 0.25 to a maximum of 3693 years in the historical period. The minimum and maximum values in the future scenarios are 0.32 and 4176 years for EB, and



0.28 and 3953 years for ED. In order to understand the variability of this value, we should take into account the formulation applied to estimate T (Equation 3) in each GW body, defined as S divided by R , where S depends on the geometry ("the size" of the GW body) and the storage coefficients (hydrodynamic parameter depending on the geology and hydraulic behavior of the aquifer). Therefore, this variability in T values is logical taking into account the varied geology, size and hydraulic behavior of the considered GW bodies.

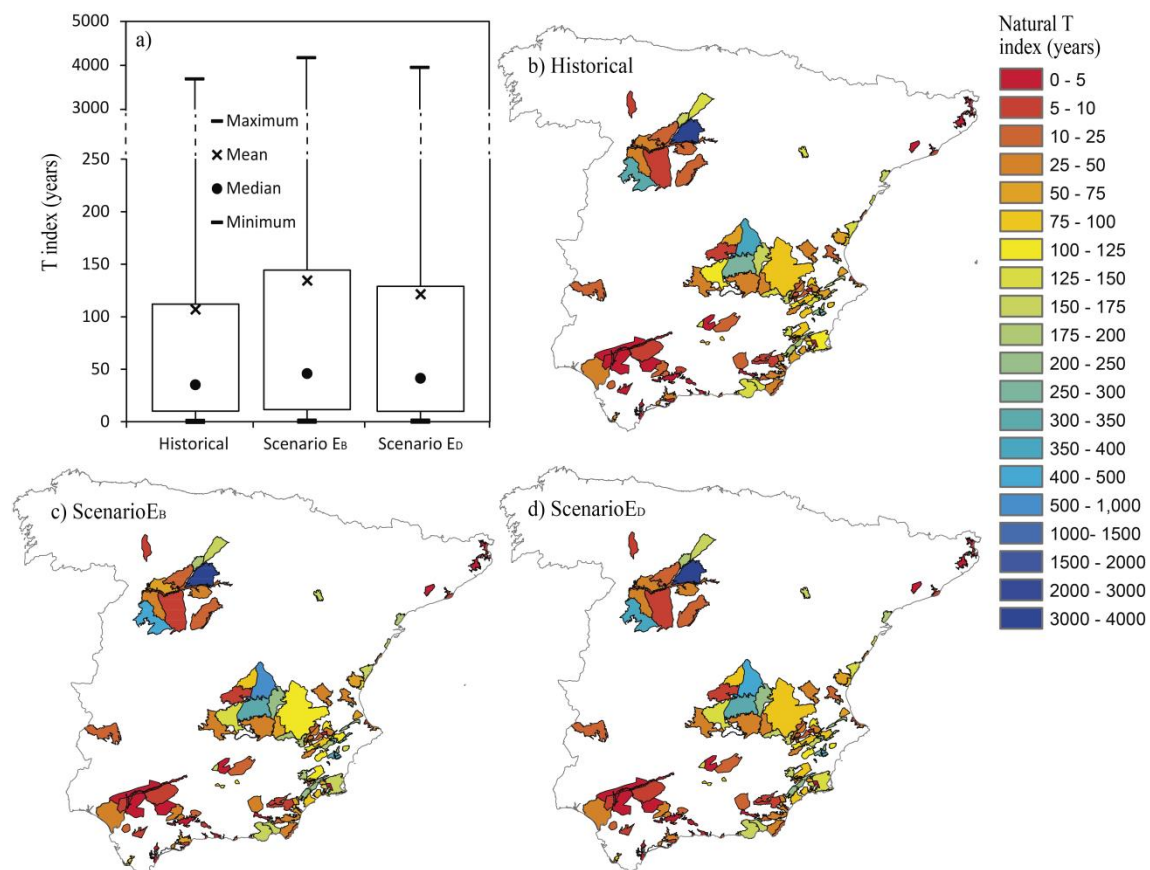


Figure 19. Box-whiskers (a) and maps of the T index in the 146 Spanish GW bodies at risk. Historical (b) values and future potential scenarios (EB (c) and ED (d)) in the horizon 2011-2045. The differences between the future scenarios (EB and ED) in terms of impacts on the T index are small, due to the differences between the impacts on mean R are also small (see maps of Figure 6). The mean values of R for both scenarios are very similar, although the monthly series are different.

Low T values means that R is close to S , and therefore, they are extremely vulnerable to exploitation, even in periods when pumping is smaller than the average R . It can be especially relevant in areas with scarce resources where long and intensive drought appear and will be even exacerbated in the future due to climate change. If we assume that the long term management of the Water Resources Systems allows to maintain the natural mean reserves (the mean S) of the GW bodies, the highest values of T correspond to GW bodies that can be very useful due to their buffer values role to manage drought periods. Around 26.9% of the



studied GW bodies show low pumping vulnerability with historical T values above 100 years, with this percentage increasing to 33.1% in the near future horizon values (until 2045).

Taking into account the formulation employed to assess T as S divided by R (see Equation 1), the impacts of the future scenarios on T are explained by the change in R, which is the only variable that depends on the climatic conditions. The T values will increase in the future in most of the GW bodies (Figure 20) due to the recharge (R) being reduced, meanwhile the total potential storage under the surface connection (S) will stay invariant. The impacts of potential future scenarios on T values will be heterogeneous (see maps of Figure 20). The box whiskers plot also reflects a wide range of T value changes with respect to the historical values moving from a reduction of 2.8 years to an increment of 483 years, which is due to the variability observed also for the recharge, where we estimate changes with respect to the historical between a reduction $47.0 \text{ mm} \cdot \text{year}^{-1}$ to an increment of $2.7 \text{ mm} \cdot \text{year}^{-1}$.

The increments in T values will force to apply more restrictive long-term management strategies within the systems to maintain the natural mean reserves, but if this long term constraint is fulfilled, the potentiality of those GW bodies to be used playing a buffer role to manage drought periods, will be even in many cases higher than in the historical period (Figure 19a).

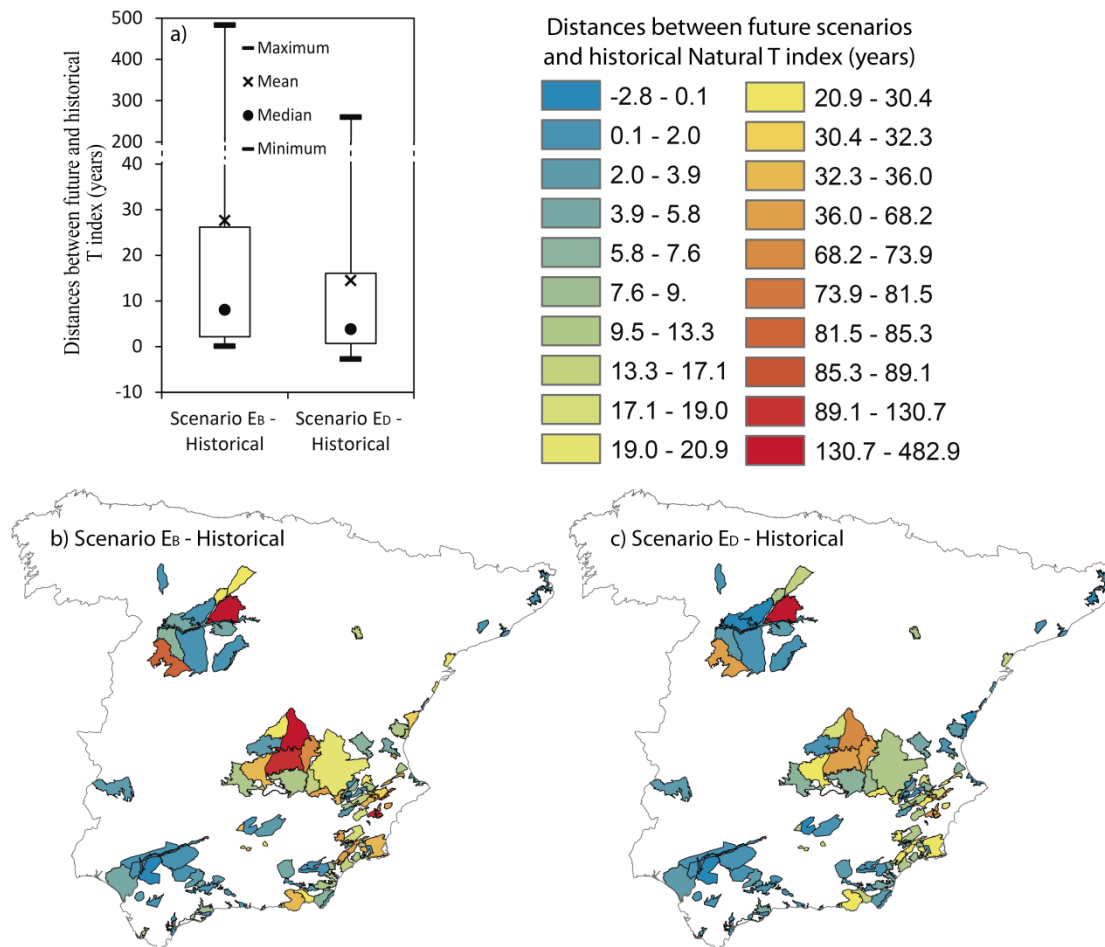


Figure 20. Box-Whiskers (a) and maps (b and c) of the distances between historical Natural T and future potential values in horizon 2011-2045.

6 REFERENCES

AEMET (2009). Generación de escenarios regionalizados de cambio climático para España, Agencia Estatal de Meteorología, Mto, Medio Ambiente, Medio Rural y Marino.

Alcalá, F.J., Custodio, E. (2012). Evaluación de la recarga a los acuíferos mediante balance de masa de cloruro atmosférico y su incertidumbre en el territorio continental español. J. Zurutuza (Ed.) In VII Asamblea Hispano Portuguesa de Geodesia y Geofísica, 1, 549-554. San Sebastián, Spain.

Alcalá, F.J., Custodio, E. (2014). Spatial average aquifer recharge through atmospheric chloride mass balance and its uncertainty in continental Spain. *Hydrological Processes*. 28, 218-236.

Alcalá, F.J., Custodio, E. (2015). Natural uncertainty of spatial average aquifer recharge through atmospheric chloride mass balance in continental Spain. *Journal of Hydrology*. 524, 642-661.

Christensen, N.S., Lettenmaier, D. precipitation. (2007). A multimodel ensemble approach to assessment of climate change impacts on the hydrology and water resources of the Colorado River Basin. *Hydrol. Earth Sys. Sci.*, 11, 1417-1434.

Collados-Lara, A.J., Pulido-Velazquez, D., Pardo-Igúzquiza, E. (2018). An Integrated Statistical Method to Generate Potential Future Climate Scenarios to Analyse Droughts. *Water*, 10, 1224. doi:10.3390/w10091224.

CORDEX EU Project (2013). The Coordinated Regional Climate Downscaling Experiment CORDEX. Program sponsored by World Climate Research Program (WCRP). Available at: <http://wcrp-cordex.ipsl.jussieu.fr/>.

Custodio, E., Andreu-Rodes, J., Aragón, R., Estrela, T., Ferrer, J., García-Aróstegui, J.L., Manzano, M., Rodríguez-Hernández, L., Sahuquillo, A., del Villar, A. (2016). Groundwater intensive use and mining in south-eastern peninsular Spain: Hydrogeological, economic and social aspects. *Science of the Total Environment*, 559, 302-316.

Del Barrio, G., Puigdefabregas, J., Sanjuan, M.E., Stellmes, M., Ruiz, A. (2010). Assessment and monitoring of land condition in the Iberian Peninsula, 1989-2000. *Remote Sensing of Environment*, 114, 1817-1832.

Earman, S., Campbell, A.R., Newman, B.D., Phillips, F.M. (2006). Isotopic exchange between snow and atmospheric water vapor: Estimation of the snowmelt component of groundwater recharge in the southwestern United States. *J. Geophys. Res.*, 111, D09302.

EEA. 2007. Corine land cover 2000 (CLC2000) seamless vector database. European Environment Agency: Copenhagen. (<http://www.eea.europa.eu/data-and-maps/data/corine-land-cover-2000-clc2000-seamless-vectordatabase>).

Escriva-Bou, A., Pulido-Velazquez, M., Pulido-Velazquez, D. (2017). The economic value of adaptive strategies to global change for water management in Spain's Jucar basin. *J. Water Resour. Plann. Manage.* [https://doi.org/10.1061/\(ASCE\)WR.1943-5452.0000735](https://doi.org/10.1061/(ASCE)WR.1943-5452.0000735).

España, S., Alcalá, F.J., Vallejos, A., Pulido-Bosch, A. (2013). A GIS tool for modelling annual diffuse infiltration on a plot scale. *Comput. Geosci.*, 54, 318-325.

Garrido, A., Llamas, M.R. (2009). *Water policy in Spain*. John Wiley & Sons, Boca Raton, FL; 254 pp.

Herrera, S., Fernández, J., Gutiérrez, J.M. (2016). Update of the Spain02 gridded observational dataset for Euro-CORDEX evaluation: assessing the effect of the interpolation methodology. *Int. J. Climatol.*, 36, 900-908.

Hurrell, J.W. (1995). Decadal trends in the North Atlantic Oscillation, regional temperatures and precipitation. *Nature*, 269, 676-679.

IGME (1993). *Groundwater in Spain: synthetic study*, Technical Report. Ministry of Industry and Energy of Spain: Madrid; 591 pp. [in Spanish]. (<http://aguas.igme.es/igme/publica/libro20/lib20.htm>).

Martínez-Valderrama, J., Ibáñez, J., Del Barrio, G., Sanjuán, M.E., Alcalá, F.J., Martínez-Vicente, S., Ruiz, A., Puigdefábregas, J. (2016). Present and future of desertification in Spain: implementation of a surveillance system to prevent land degradation. *Science of the Total Environment*. 563-564, 169-178.

Martín-Vide, J., López-Bustins, J.A. (2006). The Western Mediterranean Oscillation and Rainfall in the Iberian Peninsula. *International Journal of Climatology*, 26, 1455-1475.

MIMAM (2000). *White book of water in Spain*. Ministry of the Environment, State Secretary of Waters and Coast, General Directorate of Hydraulic Works and Water Quality: Madrid; 637 pp. [in Spanish]. (http://hercules.cedex.es/Informes/Planificacion/2000-Libro_Blanco_del_Agua_en_Espana/).

Pardo-Iguzquiza, E., Collados-Lara, A.J., Pulido-Velazquez, D. (2017). Estimation of the spatiotemporal dynamics of snow covered area by using cellular automata models. *J. Hydrol.*, 550, 230-238.

Pulido-Velazquez, D., Romero, J., Collados-Lara, AJ, Alcalá, Francisco FJ, Fernández-Chacón, F. and L. Baena-Ruiz, (2020). Using the Turnover Time Index to Identify Potential Strategic Groundwater Resources to Manage Droughts within Continental Spain. *Water* 2020, 12(11), 3281; <https://doi.org/10.3390/w12113281> (registering DOI)

Pulido-Velazquez, D., Garrote, L., Andreu, J., Martín-Carrasco, F.J., Iglesias, A. (2011). A methodology to diagnose the effect of climate change and to identify adaptive strategies to



reduce its impacts in conjunctive-use systems at basin scale. *Journal of Hydrology*, 405, 110-122.

Pulido-Velazquez, D., García-Aróstegui, J.L., Molina, J.L., Pulido-Velazquez, M. (2015). Assessment of future groundwater recharge in semi-arid regions under climate change scenarios (Serral-Salinas aquifer, SE Spain). Could increased rainfall variability increase the recharge rate? *Hydrological Processes*, 29, 828-844.

Pulido-Velázquez, D., Collados-Lara, A.J., Baena-Ruiz, L., Fernández-Chacón, F., Alcalá, F.J. (2017). Assessment of present and future vulnerability to pumping in Spanish GW bodies using a natural turnover time index. In 44th Annual Congress of the International Association of Hydrogeologists: Groundwater Heritage and Sustainability (IAH, Ed.). e-Poster. Session T2.5. Abstract T2.5.24. Dubrovnik. ISBN: 978-953-6907-61-8.

Pulido-Velázquez, D., Collados-Lara, A.J., Alcalá, F.J. (2018). Assessing impacts of future potential climate change scenarios on aquifer recharge in continental Spain. *Journal of Hydrology*. 567, 803-819.

Quintana-Seguí, precipitation., Turco, M., Herrera, S., Miguez-Macho, G. (2017). Validation of a new SAFRAN-based gridded precipitation product for Spain and comparisons to Spain02 and ERA-Interim. *Hydrol. Earth Syst. Sci.*, 21, 2187-2201.

Räisänen, J., Räty, O. (2012). Projections of daily mean temperature variability in the future: cross-validation tests with ENSEMBLES regional climate simulations. *Clim. Dyn.*, 41, 1553-1568.

Sabater, S., Barceló, D. (2010). *Water Scarcity in the Mediterranean. Perspectives Under Global Change*. Springer-Verlag Berlin Heidelberg. 234 pp. doi:10.1007/978-3-642-03971-3.

Trigo, R.M., Pozo-Vazquez, D., Osborn, T.J., Castro-Diez, Y., Gamiz-Fortis, S., Esteban-Parra, M.J. (2004). North Atlantic Oscillation influence on precipitation, river flow and water resources in the Iberian Peninsula. *International Journal of Climatology*. 24, 925-944.

WFD (2000). Water Framework Directive Directive 2000/60/EC of the European Parliament and of the Council, of 23 October 2000, establishing a framework for Community action in the field of water policy, *Official Journal of the European Union* L 327/1, 22.12.2000 (http://europa.eu.int/comm/environment/water/water-framework/index_en.html).

Willaarts, B.A., Ballesteros, M., Hernández-Mora, N. (2014) Ten years of the Water Framework Directive in Spain: An overview of the ecological and chemical status of surface water bodies. *Integrated Water Resources Management in the 21st Century: Revisiting the Paradigm*, 99.

Winograd, I.J., Riggs, A.C., Coplen, T.B. (1998). The relative contributions of summer and cool-season precipitation to groundwater recharge, Spring Mountains, Nevada, USA. *Hydrogeol. J.*, 6, 7793.





Deliverable 3.2 + 4.2

PILOT DESCRIPTION AND ASSESSMENT

The Netherlands
&
De Raam, Netherlands

Authors and affiliation:

Willem J. Zaadnoordijk (TNO-GSN)
Timo Kroon (Deltares)
Eva Schoonderwoerd (Deltares)
Janneke Pouwels (Deltares)

This report is part of a project that has received funding by the European Union's Horizon 2020 research and innovation programme under grant agreement number 731166.



Deliverable Data

Deliverable number	D3.2, D4.2
Dissemination level	Public
Deliverable name	Pilot description and assessment
Work package	WP3, WP4
Lead WP/Deliverable beneficiary	GEUS

Deliverable status

Version	3
Date	26/03/2021

LIST OF ABBREVIATIONS & ACRONYMS

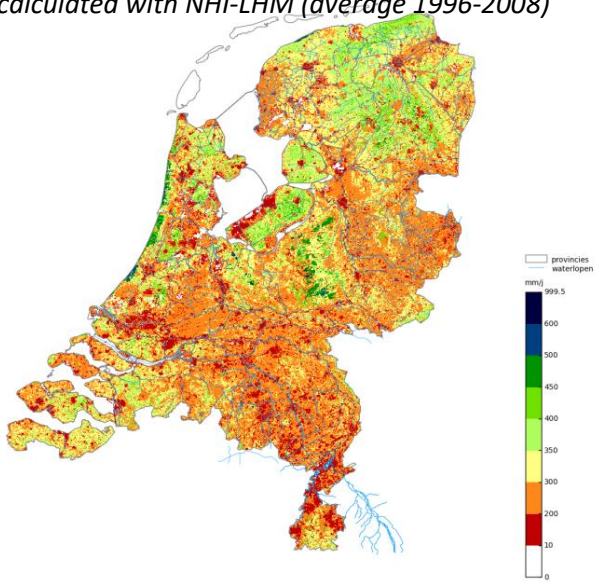
AHN	Open Source Data set with Actual Elevation Levels for the Netherlands (in Dutch “Actueel Hoogtebestand Nederland”)
BIS	Data base with Dutch soil characteristics (in Dutch: “Bodemkundig Informatie Systeem”).
Deltares	Dutch research institute.
iMOD	Open Source modelling software of Deltares, based on the MODFLOW model (USGS), adapted to apply for large datasets, and including a user interface.
LGN	Data set with land use for the Netherlands (in Dutch: “Landelijk Grondgebruik Nederland”)
Metran	Tool for transfer noise modelling and dynamic factor analysis of groundwater head time series.
NAP	National Dutch Datum (equal to mean sea level; in Dutch: “Normaal Amsterdams Peil”)
NHI	Netherlands Hydrological Instrument (integrated hydrological model based on iMOD).
NHI-LHM	National Hydrological Model of the NHI (in Dutch: “Landelijk Hydrologisch Model”).
TNO-GSN	TNO Geological Survey of the Netherlands.

TABLE OF CONTENTS

LIST OF ABBREVIATIONS & ACRONYMS	5
1 EXECUTIVE SUMMARY	5
2 INTRODUCTION	8
3 PILOT AREAS	11
3.1 Site description and data	11
3.1.1 Meteorological data	11
3.1.2 Topography	13
3.1.3 Geology/Aquifer type	14
3.1.4 Soil types	15
3.1.5 Surface water bodies	16
3.1.6 Land use	17
3.1.7 Abstractions/irrigation	19
3.2 Climate change challenge	20
3.2.1 How is the climate expected to change in the Netherlands	20
3.2.2 What are the challenges related to the expected climate change?	21
4 METHODOLOGY	22
4.1 National Hydrological Model NHI-LHM	22
4.1.1 NHI components and coupling	23
4.1.2 NHI-LHM version and calibration	24
4.2 Regional groundwater model used in de pilot Raam	24
4.3 Metran	25
4.4 Climate change scenarios	26
4.4.1 TACTIC standard Climate Change scenarios	27
5 RESULTS	29
5.1 National pilot	29
5.1.1 Reference period results	29
5.1.2 Climate change scenario results	38
5.2 De Raam	50
5.2.1 Reference period results	50
5.2.2 Climate change scenario results	56
6 DISCUSSION	57
6.1 NHI-LHM	57
6.2 De Raam	58
6.3 Metran	59
6.4 Comparison between models	62
6.4.1 Regional and national physically based distributed models	62
6.4.2 Physically based distributed models and time series models	65
7 CONCLUDING REMARKS	70
8 REFERENCES	71

1 EXECUTIVE SUMMARY


TNO Geological Survey of the Netherlands (TNO-GSN) and Deltares together contribute two pilots to the TACTIC project: a national pilot “Netherlands” and a regional pilot “de Raam”.

Pilot name	Netherlands	<p><i>Example of groundwater recharge (mm/year) calculated with NHI-LHM (average 1996-2008)</i></p> 
Country	Netherlands	
EU-region	North-western Europe	
Area (km ²)	40 500	
Aquifer geology and type classification	Sand and gravel – Porous; Chalk – Fissured	
Primary water usage	Drinking water / Irrigation / Industry / Ecology	
Main climate change issues	Climate change (change of precipitation, evaporation, incoming river discharges and sea level rise), combined with socio-economic developments	
Models and methods used	Integrated Hydrological model (national application of the Netherlands Hydrological Instrument; NHI-LHM), Time series analysis (using Metran)	
Key stakeholders	Rijkswaterstaat, Ministry of Infrastructure and Water (including Delta Programme), Ministry of Economic Affairs and Climate policy. Further the waterboards, provinces and drinking water companies are involved in development and application of the hydrologic instrument.	
Contact persons	Timo Kroon, Deltares, timo.kroon@deltares.nl Willem Jan Zaadnoordijk, TNO, willem_jan.zaadnoordijk@tno.nl	

This pilot considers the groundwater and interaction with the surface water system at a national scale with the national hydrologic model for the Netherlands (NHI-LHM). Usually this integrated model for simulations in the subsurface and surface water in the Netherlands is applied for national water management and national policy making (quantity and water quality). Water management on a national level with the model relates to national water supply and measures for drought prevention, such as setting of the weirs in the main water system in the (branches of) the Meuse and Rhine, and the management of the storage in lake IJsselmeer, which serves during drought as the largest fresh water reservoir in the Netherlands.



Within TACTIC simulations with the national model are presented for the current climate and for four climate change scenarios. The calculated heads are compared at a few locations with simulations from linear transfer noise models (created using Metran, the groundwater dynamics tool of <http://www.grondwatertools.nl>).

Pilot name	De Raam	
Country	Netherlands	
EU-region	North-western Europe	
Area (km ²)	224	
Aquifer geology and type classification	Sand and gravel – Porous	
Primary water usage	Irrigation / Ecology / Drinking water	
Main climate change issues	climate change (change of precipitation, evaporation, incoming river discharges and sea level rise), combined with socio-economic developments	
Models and methods used	Integrated Hydrological model (regional model, based on iMOD), Time series analysis (using Metran)	
Key stakeholders	Waterboard Aa en Maas, province of Noord-Brabant and drinking water company Brabant Water	
Contact person	Timo Kroon, Deltares, timo.kroon@deltares.nl Willem Jan Zaadnoordijk, TNO, willem_jan.zaadnoordijk@tno.nl	

For the regional pilot in the Netherlands, 'de Raam' a regional model is applied. This model has been developed for regional management of groundwater and surface water and is a refined version of the national instrument (NHI). It is used by the waterboard, province and drinking water company to investigate the effects of regional and local measures in the current and future (climate change) situation.

Within TACTIC the regional groundwater model has been used to simulate the current climate and for the TACTIC climate change scenarios. A comparison between the results from the regional and the national integrated hydrological model is presented.

At the location of a few monitoring wells, the calculated heads are compared with simulations from linear transfer noise models from Metran. Also time series modelling has been carried out for a few piezometers influenced by an accident on the river Meuse during which the river level was 3 meters lower than normal.



The transfer noise modelling of monitoring of measured groundwater heads reproduces the measured heads better than a distributed physically based model at the location of the piezometer. However, a physically based model is better suited for scenario calculations, even if the scenarios only involve changes in the explaining variables of the transfer noise model. The reason for this, is the non-linearity of the groundwater system or change of system behaviour when the situation differs from the calibration period. The simulations of time series near the river Meuse illustrated this with different responses to the river level for the normal situation and during an accident with much lower water levels.

The transfer noise models using only groundwater heads as calibration variables do not provide a useful estimate of groundwater recharge. Moreover, transfer noise modelling of time series itself does not provide information in between piezometers – for the best spatial estimation of historic groundwater heads a combination of time series and a physically based distributed model provides the best results.

Lastly, a comparison of a fine resolution regional model and a coarse resolution national model indicates that the fine resolution is necessary to study local variations. This also corresponds to the different purposes of these models. The national model is used for the management of the main rivers and for national policy development. The model for De Raam is intended for improving the regional water management, e.g. by evaluating concrete local measures.

2 INTRODUCTION

The Netherlands is bordered by Belgium, Germany and the North Sea. The land area is 40 500 km². The surface topography is relatively flat ranging from below sea level in polders in the Western and Northern parts to 300 meters above in the South-eastern corner.

The large scale differences in the elevation of the phreatic groundwater level are related to the net groundwater replenishment from precipitation areas with relatively little drainage and surface water in the higher mostly Pleistocene inland part of the country and the drainage in polders and other lower areas mostly with a Holocene cover. The drainage is strongly influenced by anthropogenic surface waters.

The fresh groundwater of meteoric origin in this system in the Netherlands reaches its largest depths in the Holocene coastal dunes (tens of metres depth), the Pleistocene ice-pushed hills (Veluwe and Utrechtse Heuvelrug) in the central and Eastern part of the country (up to few hundred metres depth), and in the supra-regional groundwater flow system in the South-eastern part of the country (≥ 600 m). These fresh parts of the groundwater flow systems occur in unconsolidated sedimentary sequences of dominantly Holocene and Pleistocene to Neogene age.

The availability of groundwater in the Netherlands is influenced by the surface waters. Surface water is mainly supplied from the catchment areas of the Rhine and the Meuse (see figure 2.1).

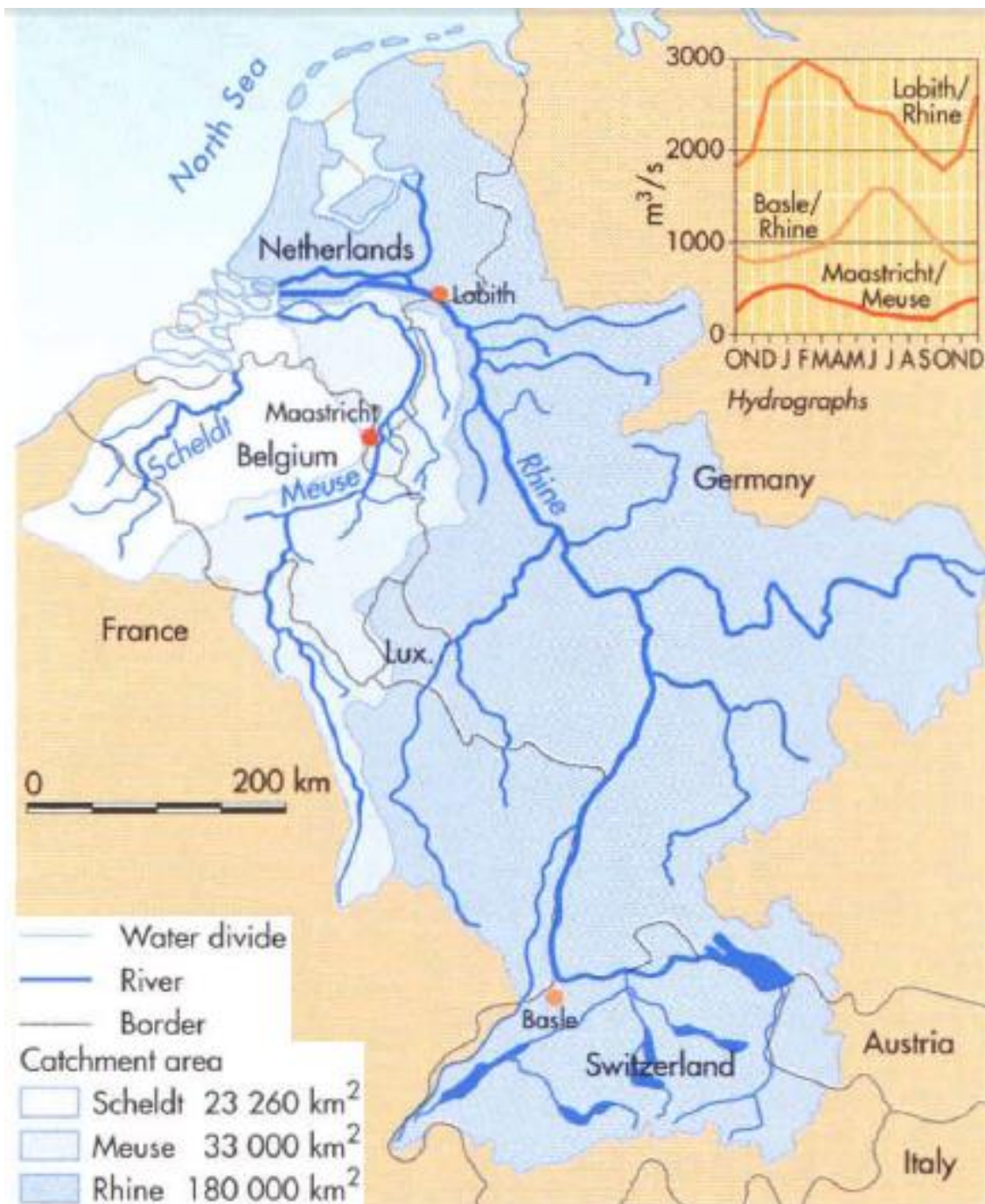


Figure 2.1 The Netherlands situated in the catchment of the river Rhine and Meuse

Deltares and TNO Geological Survey of the Netherlands contribute two pilots to the TACTIC project: a national and a regional pilot. For both pilots, two types of models are applied:

- Integrated hydrological model;
- Time series model.

The integrated models are based on the Netherlands Hydrological Instrument, NHI (de Lange et al., 2014). The time series models have been created using Metran (Berendrecht & van Geer, 2016).

The Netherlands Hydrological Instrument (NHI) (<https://www.nhi.nu>) is used for integrated hydrological modelling. It contains data and software for both the surface water and groundwater, based on iMOD (Vermeulen et al, 2020). The nationwide modelling is carried out with the LHM (National Hydrological Model) (Janssen et al., 2020), but the NHI also contains several regional models.

Metran is a tool for transfer noise modelling of groundwater head time series (Berendrecht & van Geer, 2016). It is applied to the groundwater head time series in the Dutch national subsurface database (<https://www.dinoloket.nl/en/subsurface-data>) on the groundwater tools website <http://www.grondwaterstandeninbeeld.nl> (Zaadnoordijk et al., 2019).

The National pilot of the Netherlands focusses on the groundwater simulations and interaction with the surface water at a national scale, based on 250 m grid cell calculations. On this scale the national hydrologic model (NHI-LHM) is typically applied in national policy studies in the Netherlands, for example to explore the effects of measures and climate change on the water quantity or water quality (salinity or nutrients). On this scale the model is also applied for national water management during drought, to decide on possible measure, for example concerning the weirs in the main water system in the (branches of) the Meuse and Rhine, and the management of the storage in lake IJsselmeer, which serves during drought as large fresh water reservoir in the Netherlands.

The regional pilot in the Netherlands, 'de Raam', uses a regional model of NHI (the GROUNDwater model of waterboard Aa en Maas, 'GRAM', Deltares & Aa en Maas, 2020), which has been developed for regional water management. The concepts and data are based on the same instrument (NHI) as the national model, but the model is applied with extra and more detailed information and on a higher resolution, typically on 25 m grid cell basis. This model is used in several projects for regional water management, for example to decide on measures in the regional water system, to explore the effects of land use (mostly agricultural and natural) and the regional effects of climate change on the regional groundwater and surface water system.

3 PILOT AREAS

3.1 Site description and data

Two pilot areas will be explained in this chapter: The Netherlands and The Raam. The Raam is a catchment area of the stream with the same name, situated in the province of Noord-Brabant. Figure 3.1 shows the location of The Raam within the Netherlands.



Figure 3.1 The location of pilot area The Raam within the Netherlands.

Data needed for physically-based distributed groundwater modelling are available as open data via the NHI data portal (<https://data.nhi.nu/>) and additional data sources within the Netherlands:

- Meteorological data is available from the Royal Dutch Meteorological Institute KNMI (<http://www.knmi.nl/nederland-nu/klimatologie-metingen-en-waarnemingen>),
- Data about the large surface waters from Rijkswaterstaat (<http://waterinfo.rws.nl>)
- Subsurface data including groundwater head measurements are available via TNO Geological Survey of the Netherlands (<https://www.DINOloket.nl>).
- Soil data: <http://www.bodemdata.nl/>

3.1.1 Meteorological data

According to the Köppen system, the Netherlands has a temperate maritime climate (type Cfb) with relatively mild winters, mild summers and rainfall throughout the year. The precipitation of 890 mm per year (climate period 1981-2010) is quite evenly distributed throughout the year, see table 3.1. The evaporation is on average 540 mm per year.



Figure 3.2 shows the spatial distribution of the precipitation and evaporation in the Netherlands. Higher precipitation can be found in some Eastern parts in the North, middle and South of the country, as well as some polder areas in the Western part of the country. The Southwest of the Netherlands has the highest evaporation, with a decrease in evaporation in the North-eastern direction.

Meteorological time series are available from 35 weather stations (hourly and daily precipitation and evaporation) and about 300 precipitation stations (daily precipitation) in the Netherlands. Those data are used in the ground water modelling.

Table 3-1 Monthly precipitation in the Netherlands, averaged over 1981 – 2010 (Bot, 2016).

Month	Average precipitation [mm]
January	75
February	59
March	74
April	45
May	65
June	68
July	84
August	77
September	81
October	89
November	96
December	84

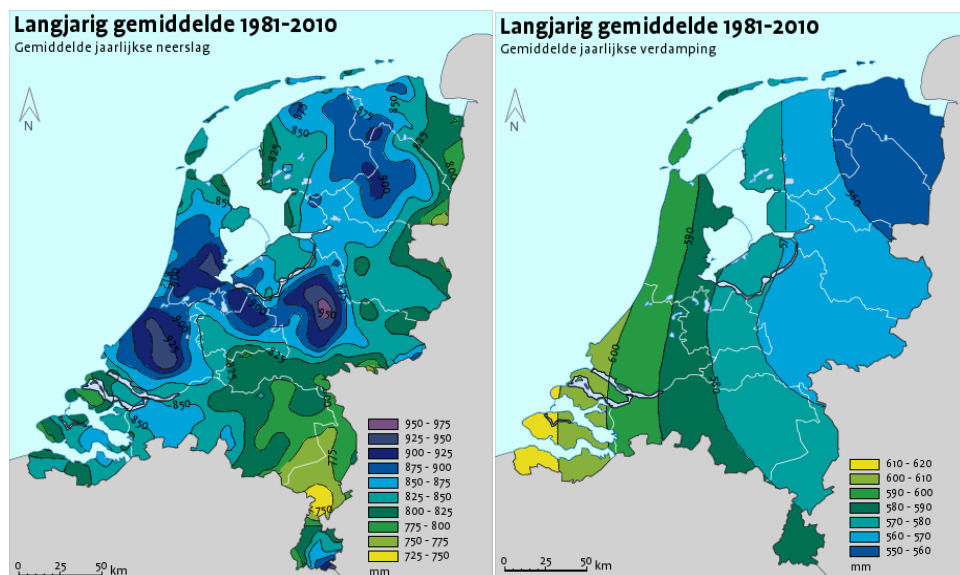


Figure 3.2 The average precipitation (left) and evaporation (right) for the period 1981 – 2010 in the Netherlands (KNMI, 2011).

3.1.2 Topography

Figure 3.3 shows the surface elevation of the Netherlands, based on public data for the Netherlands (AHN). Part of the Netherlands is below sea level; the lowest level is 6.7 m below mean sea level. In the South and East, the height of the landscape is relatively high. The maximum elevation in the central area of the Netherlands is about 100 meters above mean sea level; in the Southeast the highest elevation is 322 meters above mean sea level.

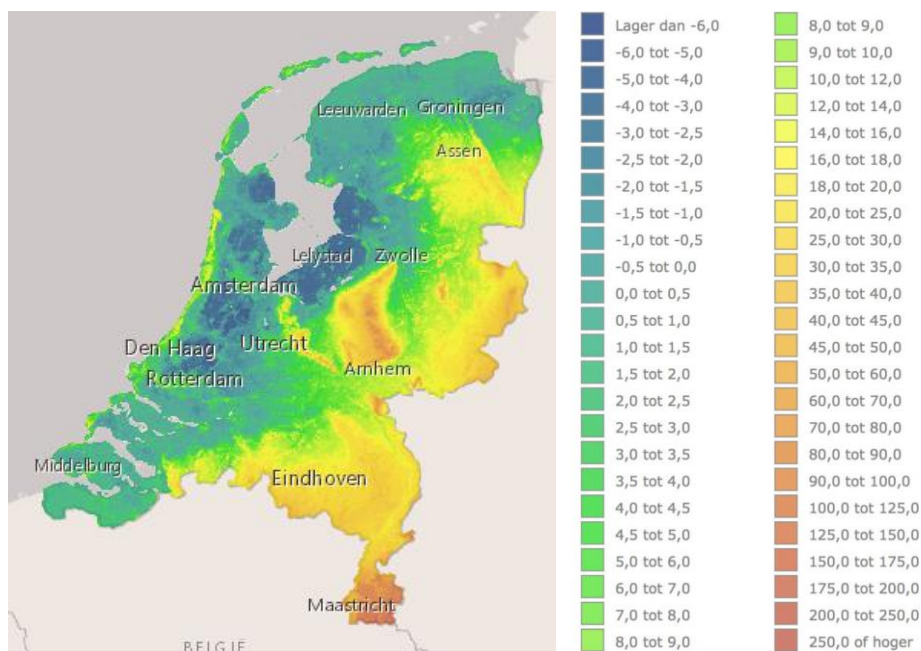


Figure 3.3 Surface elevation of the Netherlands, in meter above mean sea level (m+ NAP).
Source: <https://www.ahn.nl>.

Figure 3.4 shows the surface elevation in the pilot area of De Raam (located between the cities of Arnhem and Eindhoven shown in Figure 3.3).

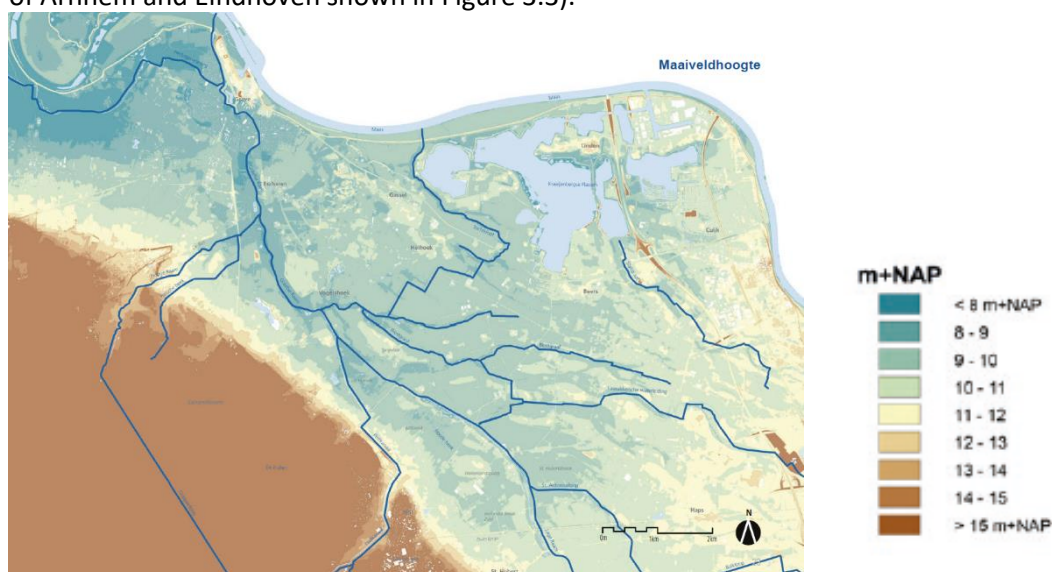


Figure 3.4 Surface elevation (m+NAP) of the area “De Raam” (Besselink, 2018).

3.1.3 Geology/Aquifer type

The Netherlands is located in the North Sea basin. Groundwater resources are limited primarily mainly to deposits of Quaternary age, which are the result of the interplay of rivers (Rhine, Meuse, Scheldt, and the previous Baltic river system Eridanos) and the North Sea.

Figure 3.5 gives a hydrogeological section across the country. It shows the Holocene confining layer, which is present in the Western and Northern parts of the country, the ice pushed ridges in the centre, and the clayey units of the marine Formations of Maassluis (MSk), Oosterhout (Ook), and Breda (BRk) which usually act as hydrological base depending on the location and context.

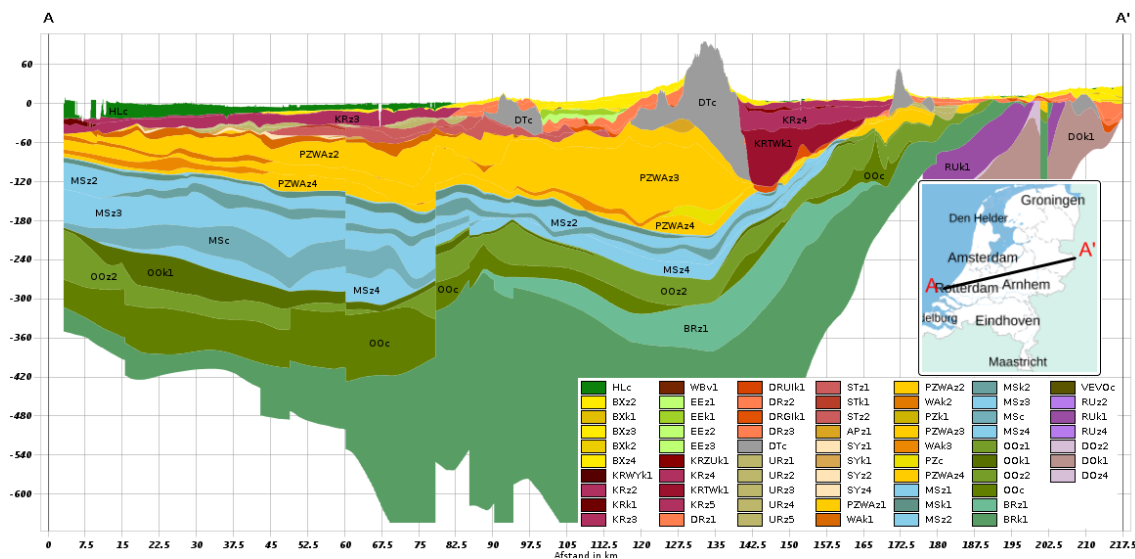


Figure 3.5 Hydrogeological units of the regional hydrogeological model REGIS II (see <https://www.dinoloket.nl/en/subsurface-models>) with the last two characters indicating sandy (z), clayey (k), or complex (c) units within the geological units.

The sandy units of the Formations of Kreftenheye and Peize & Waalre are important aquifers. Background information on the geological units can be found in the online stratigraphic nomenclator: <https://www.dinoloket.nl/en/stratigraphic-nomenclature>.

The South-eastern corner of the Netherlands has the highest elevations and also the subsurface is different from the rest of the country (Figure 3.6 and figure 3.3). There is a cover of loss and older geologic units come close to the surface, notably the chalk aquifers of the Formations of Gulpen (GUq), Maastricht (MTq), and Houthem (HOq).



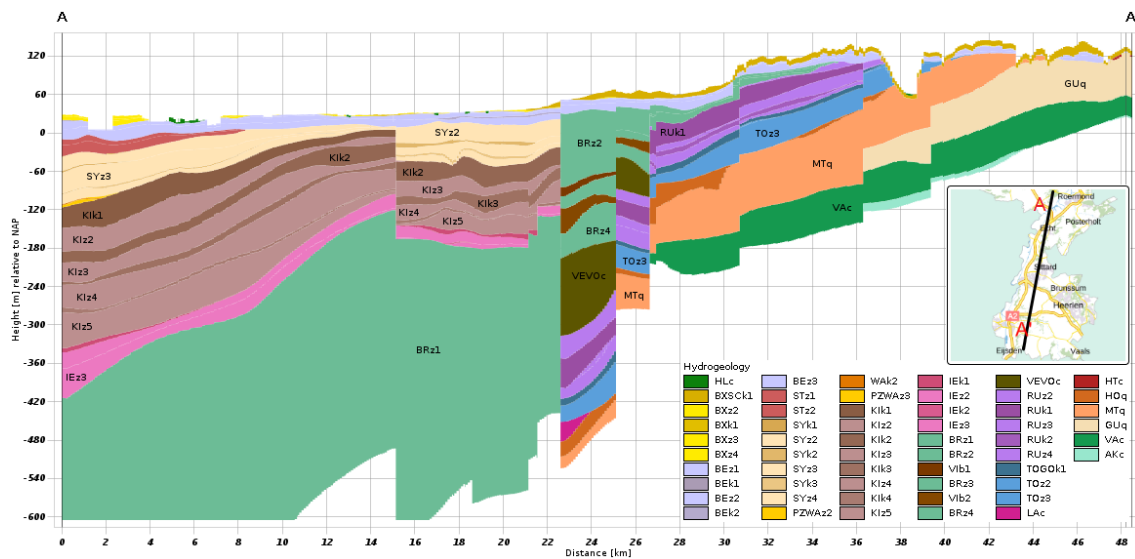


Figure 3.6 REGIS II section in South-eastern corner of the Netherlands with the highest elevation and the oldest deposits of the Netherlands.

3.1.4 Soil types

Figure 3.7 shows a soil map of the Netherlands, based on BIS (the Dutch Soil Database). The sandy soils occur in the South and East of the country. Along the main rivers, in the Southwest and in the North of the Netherlands, clayey soils can be found. The purple areas have peat soils and in the South-eastern corner, loamy soils occur. In the Raam area clayey soils can be found near the river Meuse in the North, and sandy soils in the South.

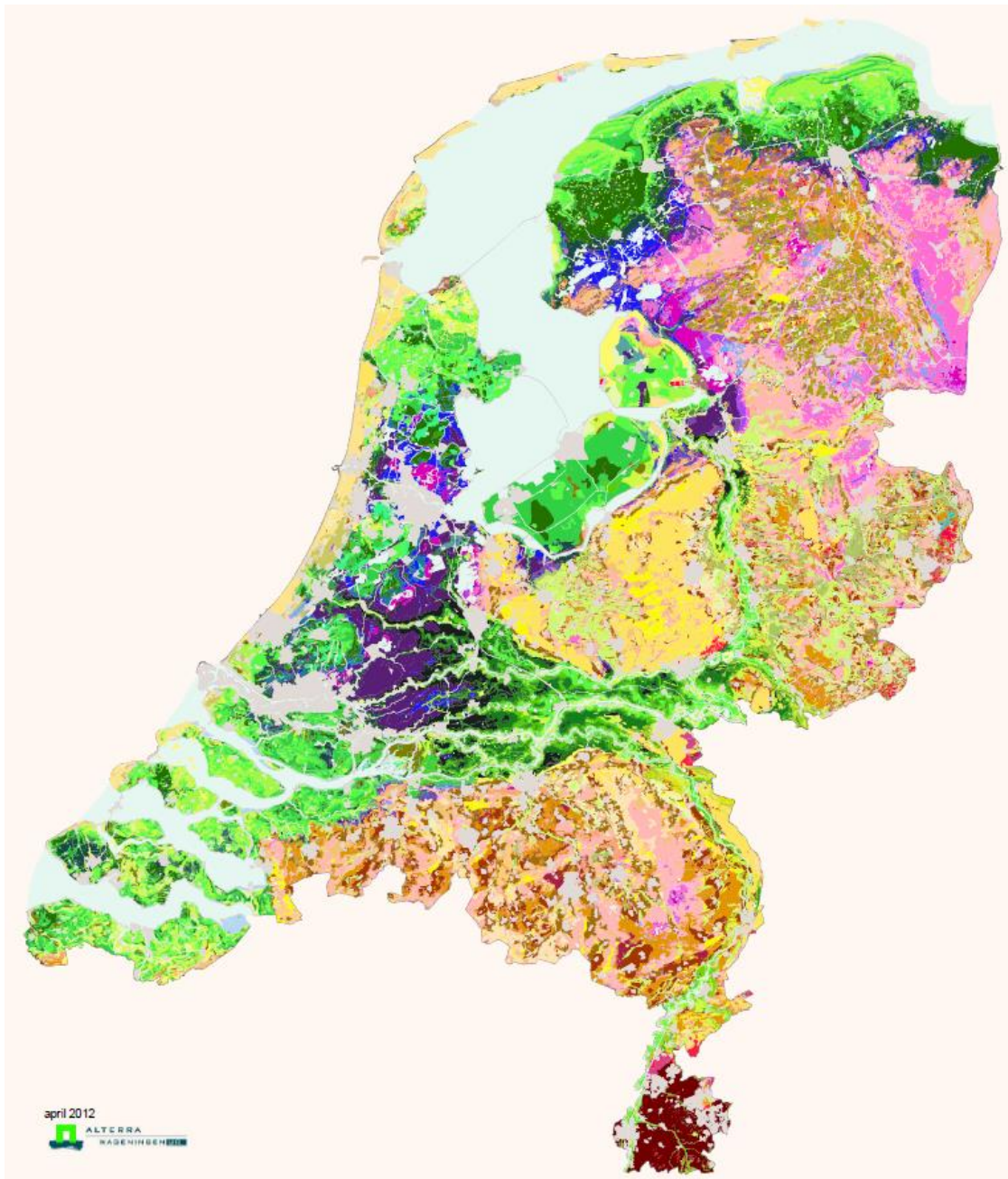


Figure 3.7 Soil types of the Netherlands (Wosten et al., 2012). The purple/blue colours are peat soils, the yellow/brown colours are sandy soils and green colours are clay soils. The dark brown colour in the South-eastern corner are loamy soils.

3.1.5 Surface water bodies

Figure 3.8 shows the largest surface water bodies in the Netherlands, including the larger river systems coming in from the East (Rhine) and Southeast (Meuse) (see also figure 2.1). The Scheldt flows from Belgium into an estuary in the Southwest. In the central West and North of the Netherlands lakes can be found, which are the result of peat extractions in the past. A larger zone in the North and the West of the country have many smaller water courses and ditches,



mainly in the lower areas (see *Figure 3.3*) with clay and peat soils (see *Figure 3.7*). These water bodies have a controlled surface water level and strongly influence the phreatic groundwater level, often in combination with tube drainage. This way inundation is prevented in winter and for the polders with large upward seepage also in summer. The surface water system serves as a water supply system in times of drought. In the sandy areas in the East and the South, less water bodies are present and these do not provide water in times of drought. These regions are more dependent on precipitation and irrigation from groundwater.



Figure 3.8 Surface water bodies (Topografische Dienst Kadaster, 2019)

3.1.6 Land use

Figure 3.9 shows the different types of land use in the Netherlands. A large part of the area in the Netherlands is used for agriculture. Urban area is most concentrated in the central Western part, whereas in the Eastern part larger areas with forest and dry nature occur.



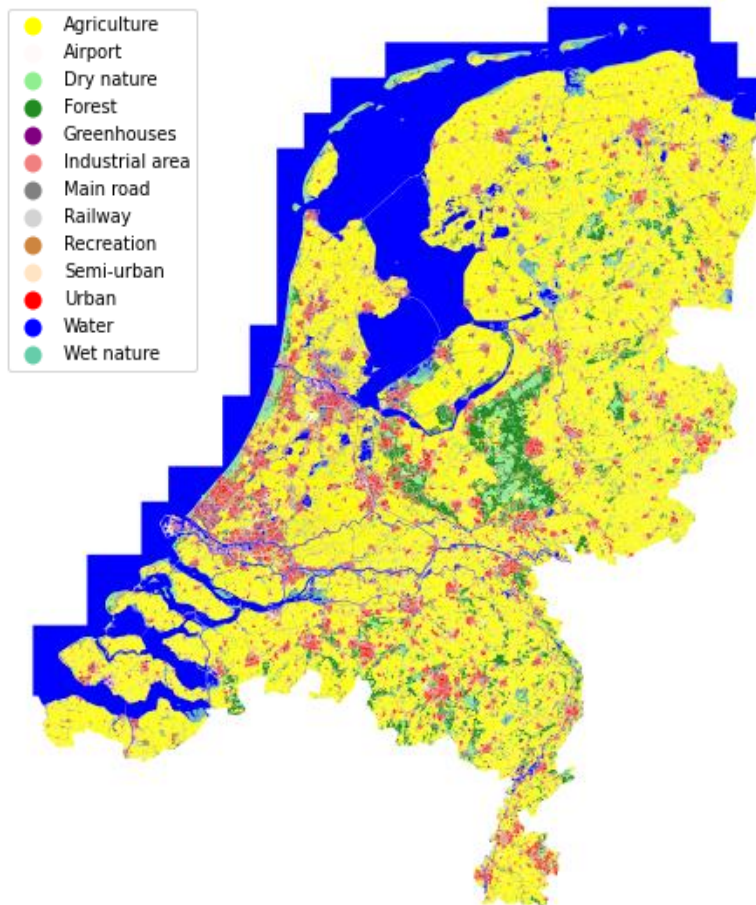


Figure 3.9. Land use types in the Netherlands (source: Dutch Statistical Bureau, CBS).

Figure 3.10 shows the different types of land use in De Raam, where mostly agricultural land can be found. Also, some urban areas and forests occur. The lakes in the Northeast are connected to the river Meuse, which is the North-eastern boundary of the area of De Raam.

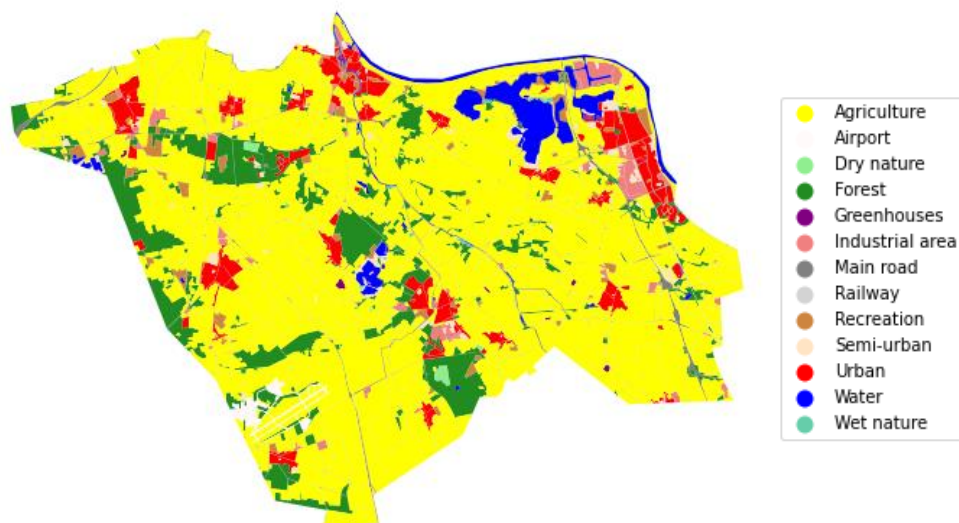


Figure 3.10 Land use types in the pilot De Raam

3.1.7 Abstractions/irrigation

Groundwater abstraction occurs in the Netherlands for drinking water production, industry and agriculture (for livestock and (overhead) irrigation). Figure 3.11 shows the wells fields used for drinking water production. They are located in areas with fresh water aquifers, which mostly coincide with higher surface elevations (cf. Figure 3.3).

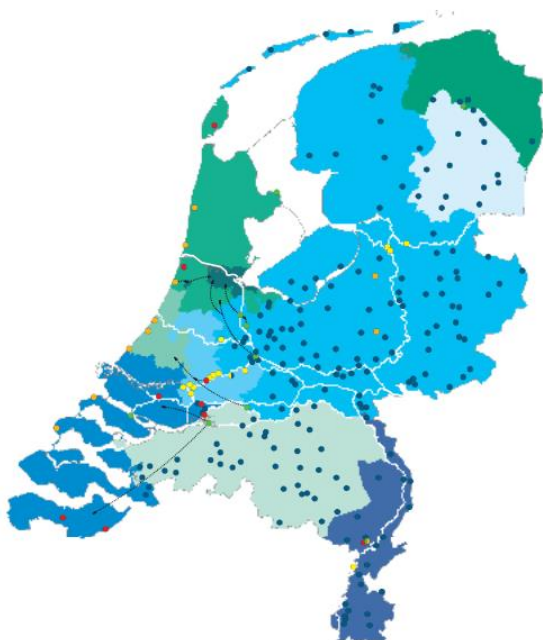


Figure 3.11: Blue dots indicate well fields for drinking water supply, yellow is groundwater extraction at the riverbank, orange are water infiltration locations, green is drinking water supply from surface water and red are emergency wells. The different areas indicate the regions of the drinking water supply companies (Vewin, 2017).

Figure 3.12 shows the locations of irrigation wells together with the locations where surface water is used for irrigation.

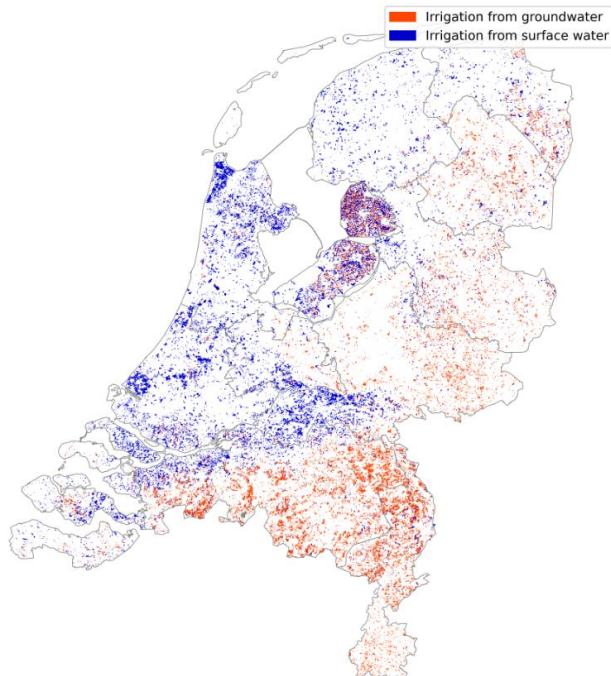


Figure 3.12: Locations of irrigation wells and irrigation from surface water (data available at <https://www.nhi.nu>).

3.2 Climate change challenge

3.2.1 How is the climate expected to change in the Netherlands

The Royal Dutch Meteorological Institute prepares climate change scenarios for the Netherlands. According to the most recent scenarios, climate change is expected to cause the following effects in the Netherlands (KNMI, 2015):

- Temperature will rise;
- Mild winters and hot summers will occur more often;
- Precipitation and extreme precipitation in the winter will increase;
- The intensity of extreme summer precipitation will increase;
- Hail and thunder will become more intense;
- Changes in wind speed are small;
- The amount of foggy days will decrease.

These predicted effects are aligned with the European Environment Agency map that describes the expected climate change across the different areas in Europe as shown in *Figure 3.13*. Scenarios for future climate change in the Netherlands are described by KNMI (KleinTank et al., 2015). In those scenarios the most likely changes in the Netherlands are described according to the latest insights.



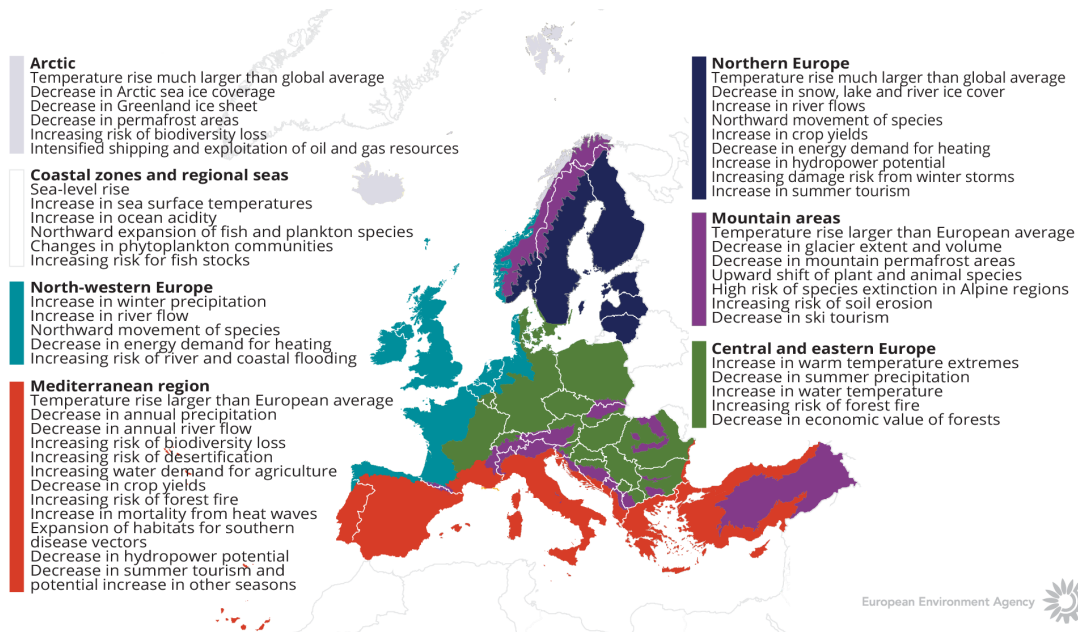


Figure 3.13. How is climate expected to change in Europe. The European Environment Agency map

3.2.2 What are the challenges related to the expected climate change?

Water shortage is one of the challenges from the extended droughts expected to result from climate change. This impacts many sectors, such as agriculture, ecology, and drinking water production, industrial water use, electricity production (because of restriction for cooling water), and transport (because of reduced depth of the rivers which are main waterways for shipping). Degradation of peat and emission of greenhouse gases threatens the peat areas (see Figure 3.7). In the Netherlands, lowering of the groundwater table in historical cities poses a special risk, because of wooden foundations of buildings that decay when they are no longer below the groundwater table.

Another major challenge is extreme precipitation, which can cause flooding. The threat from flooding is most severe in urban areas, where it is likely to be caused directly by precipitation. Streets can be covered by water, the ground floor of buildings may be flooded, and water can flow into basements. In addition, the sewer system may be overloaded, leading to sewage spilling into the surface water and causing water quality problems.

Sea level rise makes the coastal area more vulnerable for floods, and rivers more vulnerable for sea water intrusion.

4 METHODOLOGY

4.1 National Hydrological Model NHI-LHM

In 2005, Dutch national research institutes and the water authorities (both national and regional) started to combine their water expertise and financial means to construct a national water model: the Netherlands Hydrological Instrument NHI (<https://www.nhi.nu>). This had to replace various separated, partially parallel modelling efforts, such as the national models NAGROM (de Lange, 1991) and LGM (Lieste et al., 1993), and the regional model GMN (Iwaco, 1992). It started by bringing together the available data and technologies, resulting in a first version of the national model in 2008. In 2013, a next main version of NHI was achieved, based on the consensus of all national and regional water management organizations. An extensive description of the NHI can be found in De Lange et al. (2014).

The nationwide modelling is carried out with the LHM (National Hydrological Model), but the NHI also contains several regional models. The NHI contains a coupling of four sub-models, which together can simulate the groundwater, surface water and the vadose zone (see *Figure 4.1*). The groundwater is modelled with the use of iMOD (Vermeulen et al., 2020), which includes a Graphical User Interface developed by Deltares and an adapted version of MODFLOW 2005, to enable fast calculations in large domains. The surface water is divided into the regional surface water, modelled with the use of Mozart, and national surface water, which uses DM (Distribution Model) (De Lange et al, 2014). The vadose zone is modelled with the use of MetaSWAP (van Walsum et al., 2017). The grid cell size that is used in the NHI-LHM model is 250x250 m.

An important aim of the NHI is computing the water demand and allocation for different water users in periods of water scarcity. Therefore, the LHM is used within the National Water Model, a constellation of different models including water quality and effect modules for agriculture, terrestrial nature and other sectors. Besides, a special version of NHI is available for modelling salinity transport in the subsurface (Delsman et al, in prep 2021).

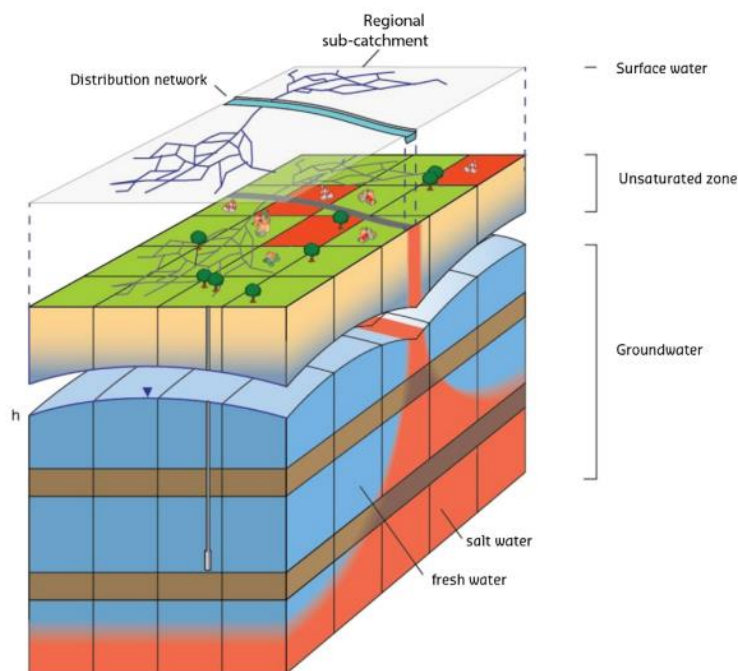


Figure 4.1 The hydrological components of the Netherlands Hydrological Instrument (NHI)

4.1.1 NHI components and coupling

The surface water is modelled on a large, national, scale with the Distribution Model (DM) and on local scale with Mozart. DM allocates water to various water users by optimizing the water demands. The allocation of water is calculated with water distribution rules, based on water management practice. This includes a prioritizing scheme for water scarcity, where first water is allocated to the most important category and then to the categories with lower priorities. These categories are as follows: 1: water safety (like dikes) or irreversible damage to nature areas. 2: public utilities (drinking water & energy). 3 & 4: for example agriculture, industry and recreation. MOZART is a lumped model, which calculates a balance for the surface water by accounting for withdrawals and discharges. MOZART is applied to every small catchment, resulting in a calculated surface water level that is coupled with the surface water levels in the corresponding MODFLOW cells.

The unsaturated zone is modelled with the use of MetaSWAP. This model computes the transfer of water between the saturated zone and the atmosphere, while also incorporating the root zone and vegetation. The coupling procedure is described by Van Walsum and Veldhuizen (2011). Recently the coupling procedure within NHI is improved by a BMI-coupling procedure, which is implemented in the original MODFLOW 6 code (Hughes et al., 2021, in prep.).

The groundwater, modelled with MODFLOW, interacts (drainage or infiltration) with the surface waters in MOZART. Other top system components in MODFLOW, the phreatic storage coefficient, phreatic head and the flux to and from the unsaturated zone, are based on information of MetaSWAP. Furthermore, the irrigation demand is calculated by MetaSWAP which results in a water demand for surface water in MOZART or groundwater in MODFLOW.



Recently, the national model has been extended with the crop growth model WOFOST (Hunink et al., 2019). This detailed crop model is coupled to MetaSWAP. By using WOFOST, the crop growth is not fixed input for the groundwater model, but calculated dynamically, depending on the condition in the soil and the atmosphere. This enables improved calculations of evapotranspiration, also for climate changes, because effect of changing temperatures and higher CO₂ concentrations on the crop growth can be taken into account.

The calculation of actual evapotranspiration of the crops within the combination MetaSWAP-WOFOST is based on Penman-Monteith, which is not directly compatible with the TACTIC climate scenarios with the delta change factors. Also, these scenarios do not contain carbon dioxide concentrations. This means that within the climate scenarios for TACTIC, the WOFOST option is not used.

4.1.2 NHI-LHM version and calibration

The national modelling is carried out with LHM version 4.1 (Janssen et al., 2020). The geohydrological schematization is represented by 8 model layers within NHI-LHM, based on geohydrological models of the Netherlands: REGIS II V2.2 (TNO-GSN, 2021a) and GeoTOP (TNO-GSN, 2020b).

NHI-LHM (version 4.1) has been calibrated in steady state mode using the average groundwater heads for the period 2011-2018 of piezometers available in the national subsurface database (<https://www.dinoloket.nl/en/subsurface-data>). The calibration was carried out by using the iPEST software, which is an implementation in iMOD (Vermeulen et al., 2020) of the parameter estimation package PEST (Doherty, 2015). The calibrated parameters were the aquifer transmissivities, aquitard resistances, drainage conductances, and the conductances of the groundwater-surface water exchange.

To evaluate the reliability of the model, NHI currently is extensively validated, in close collaboration with a broad group of stakeholders (Rijkswaterstaat, provinces, water boards and drinking water companies) covering the entire country, each bringing in their system knowledge and validation field data (Klopstra et al., 2021 in prep, Janssen et al., 2021 in prep). Recommendations for model improvement resulting from this validation will be implemented in the next version of the national model.

4.2 Regional groundwater model used in de pilot Raam

The regional NHI model of De Raam is developed by Waterboard Aa en Maas, based on the same software and data as in NHI-LHM 4.1. However, the spatial discretization is more refined and more detailed information is used. Therefore, the model is better equipped for regional analysis than the national model. The most important differences with the national model are:

- The grid size is 25x25 m (instead of 250 m);
- The subsurface is divided into 19 layers (instead of 8 layers);



- The meteorology is based on data from Meteobase (<http://www.meteobase.nl>), which includes extra radar data (instead of data from weather and precipitation stations of the Royal Dutch Meteorological Institute KNMI);
- The surface water levels in the smallest water bodies (the small ditches) are derived from a detailed Digital Elevation Model (DEM: the surface elevation along the ditch). This yields more detailed information for the surface water levels compared to the database of the waterboards used in the national model;
- The regional modules for the unsaturated zone (MetaSWAP) and for groundwater (MODFLOW) can be coupled to a hydraulic model for the surface water (instead of using only surface water routing through MOZART and the Distribution Model DM). Note that this has not been applied for the analysis of the TACTIC climate change in this report.

The groundwater model has been calibrated, based on measurements of groundwater heads in the period 2007 - 2016 (Bos-Burgering and Hunink, 2020).

4.3 Metran

The software Metran (Berendrecht & van Geer, 2016) is used for the time series modelling (Zaadnoordijk et al., 2019). The groundwater level time series is split into a deterministic part and a stochastic part (*Figure 4.2*). The deterministic part represents the variation due to the specified explanatory variables. For the models on the 'groundwatertools' website (<http://www.grondwaterstandeninbeeld.nl>), these are precipitation and potential evapotranspiration. It is possible to include additional influences, like surface water levels or a general trend. The difference between the deterministic part and the measurements is called the model residual.

A noise model is used for the stochastic part. The purpose is to remove the autocorrelation in the residuals. The smaller the time steps between the measurements, the larger the autocorrelation. The existence of autocorrelation decreases the reliability of the model. We use a noise model with an exponential decay. The inverse of the noise model is applied to the residuals to obtain so-called "innovations".

The explanatory variables are convoluted with an impulse response function (see e.g. Kreyszig, 2012): the value of each day is multiplied by the response function and the results are summed. An incomplete gamma distribution is used for the impulse response function (Berendrecht & Van Geer, 2016). It has three parameters, a multiplication factor A^* and two shape parameters a and n (Besbes & de Marsily, 1984). For the groundwatertools website, the same function is used for precipitation and potential evapotranspiration except for a factor. This leads to five parameters to be optimized: three of the precipitation response, one evaporation factor, and one noise model parameter. The parameters are determined by a minimization procedure for the innovations.

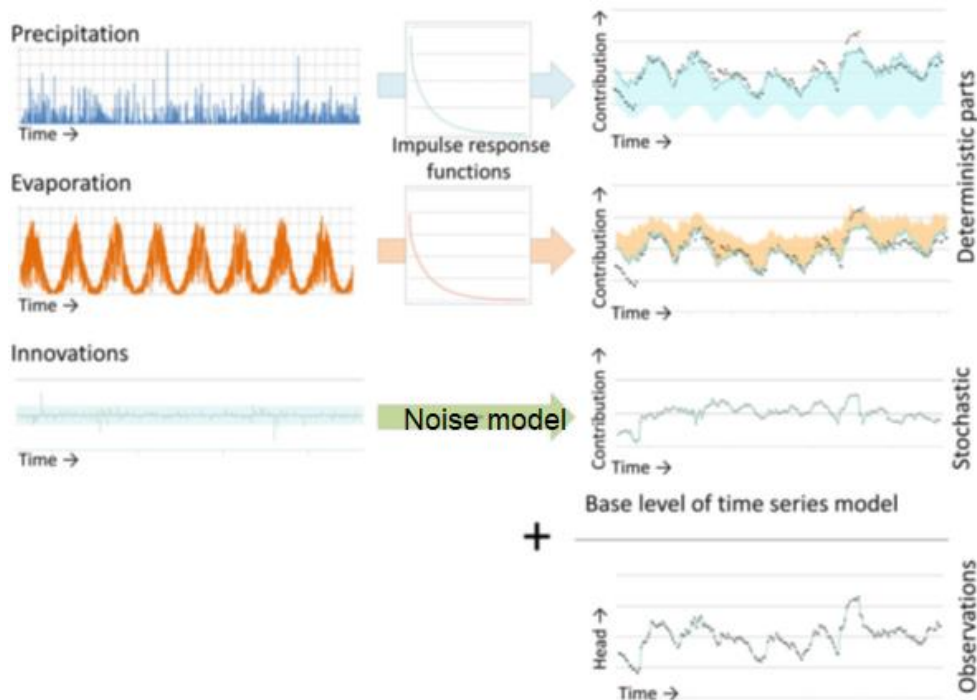


Figure 4.2 Setup of transfer function-noise model used for modelling head time series in Metran

The resulting time series models are evaluated using model evaluation criteria among which the explained fraction of the groundwater variation (Zaadnoordijk et al., 2019). Three classes are distinguished: bad models, reasonable models, and good models. The bad models are not shown on the website. The analysis in this report uses only the good models.

4.4 Climate change scenarios

In order to arrive at results that are inter-comparable for all of Europe a new procedure for selection of climate change scenarios has been developed within TACTIC.

The climate change scenarios have been based on climate data from the Inter-Sectoral Impact Model Inter-comparison Project (ISIMIP). These data consist of ensembles of 15 models: three Representative Concentration pathways (RCP) applied to five Global Climate Models. The spatial resolution is 0.5° and the temporal resolution 1 day. Two criteria were used to select an ensemble member (Sperna Weiland et al., 2021, in prep.):

- a global warming level of +3 degrees and +1 degrees, relative to a reference period (1980-2010);
- the 2nd highest and 2nd lowest scenario are selected, using the following indicators for regional climate change response: European mean temperature change, regional (case specific) precipitation change, regional net precipitation change and regional temperature change.



4.4.1 TACTIC standard Climate Change scenarios

The TACTIC standard scenarios are developed based on the ISIMIP (Inter Sectoral Impact Model Inter-comparison Project, see www.isimip.org) datasets. The resolution of the data is 0.5°x0.5° global grid and at daily time steps. As part of ISIMIP, much effort has been made to standardise the climate data (a.o. bias correction). Data selection and preparation included the following steps:

1. Fifteen combinations of RCPs and GCMs from the ISIMIP data set were selected. RCPs are the Representative Concentration Pathways determining the development in greenhouse gas concentrations, while GCMs are the Global Circulation Models used to simulate the future climate at the global scale. Three RCPs (RCP4.5, RCP6.0, RCP8.5) were combined with five GCMs (noresm1-m, miroc-esm-chem, ipsl-cm5a-lr, hadgem2-es, gfdl-esm2m).
2. A reference period was selected as 1981 – 2010 and an annual mean temperature was calculated for the reference period.
3. For each combination of RCP-GCM, 30-years moving average of the annual mean temperature were calculated and two time slices identified in which the global annual mean temperature had increased by +1 and +3 degree compared to the reference period, respectively. Hence, the selection of the future periods was made to honour a specific temperature increase instead of using a fixed time-slice. This means that the temperature changes are the same for all scenarios, while the period in which this occur varies between the scenarios.
4. To represent conditions of low/high precipitation, the RCP-GCM combinations with the second lowest and second highest precipitation were selected among the 15 combinations for the +1 and +3 degree scenario. This selection was made on a pilot-by-pilot basis to accommodate that the different scenarios have different impact in the various parts of Europe. The scenarios showing the lowest/highest precipitation were avoided, as these endmembers often reflects outliers.
5. Delta change values were calculated on a monthly basis for the four selected scenarios, based on the climate data from the reference period and the selected future period. The delta change values express the changes between the current and future climates, either as a relative factor (precipitation and evapotranspiration) or by an additive factor (temperature).
6. Delta change factors were applied to local climate data by which the local particularities are reflected also for future conditions.

Table 4-1 shows the RCP-GCM combinations employed for the analysis of the Dutch pilots in the TACTIC project. The average delta change factors for precipitation and evaporation for the national pilot and the pilot De Raam are shown in Table 4-2 and Table 4-3, respectively.

Table 4-1. Combinations of RCPs-GCMs used to assess future climate

		RCP	GCM
1-degree	"Dry"	4.5	noresm1-m
	"Wet"	6.0	miroc-esm-chem
3-degree	"Dry"	6.0	hadgem2-es



	"Wet"	8.5	miroc-esm-chem
--	-------	-----	----------------

Table 4-2. Average delta change factors per climate change scenarios for the national pilot.

Netherlands	P	PET
1°C min	0.986	1.087
1°C max	1.056	1.086
3°C min	0.969	1.082
3°C max	1.139	1.087

Table 4-3. Average delta change factors per climate change scenarios for pilot De Raam

Pilot area: Raam	P	PET
1°C min	0.985	1.089
1°C max	1.051	1.093
3°C min	0.973	1.081
3°C max	1.146	1.094

The yearly averaged factors in *Table 4-2* and *Table 4-3* show only small differences for the national pilot and the regional pilot De Raam. The monthly factors show some more variation as can be seen in *Figure 4.3*. This illustrates the deviations that may be expected when applying a single set of change factors for an area as large as the Netherlands.

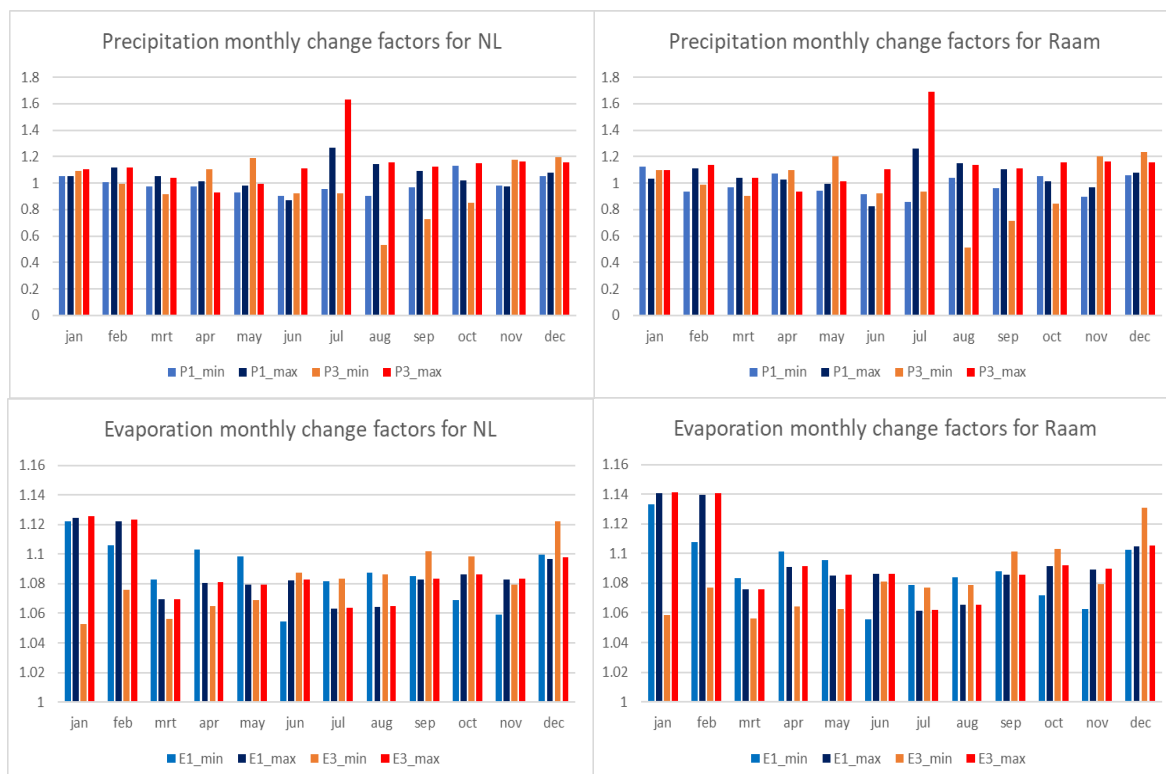


Figure 4.3. Delta change factors per month for the Netherlands (left) and De Raam (right).

5 RESULTS

This chapter presents the results for the national pilot and the pilot De Raam in separate sections (Section 5.1 and 5.2). Within these sections, results are presented for the reference period and the climate scenarios. Within these subsections the Integrated hydrological modelling (NHI) and the time series modelling are discussed independently.

Comparisons between the results in the various subsections are presented in the Discussion chapter (Chapter 6).

5.1 National pilot

The national pilot covers the entire country of Netherlands.

5.1.1 Reference period results

5.1.1.1 Integrated hydrological model

This subsection gives the results of the integrated model (NHI-LHM, see Section 4.1) of the national pilot. The model simulations have been carried out with LHM version 4.1. Although larger time series have been calculated with the model for the reference period, from 1980 - 2020, the following analysis focusses on the results in the period 2011 – 2018. This period is used more often for analyses of results of the national model, because extensive measurement sets are also available for this period, which allows extended validation of the model results. Besides, for this period also results are available for the regional pilot, which makes it easier to compare the national and regional approach.

In *Figure 5.1*, the phreatic head distribution and the deep groundwater heads are shown, averaged over the simulation period 2011 – 2018. The deep groundwater heads are the heads in Layer 4 of the model. Layer 4 is chosen, because this layer contains most of the groundwater abstraction wells in the Netherlands. In *Figure 5.2*, the typical winter and summer phreatic head are shown. The left picture is the typical winter head, which can be considered as the highest mean. This is a typical Dutch statistic of the water table depth. It is calculated as the yearly mean of the three highest phreatic heads calculated on every 14th and 28th day in a month, which is then averaged over the simulation period (in this analysis: 2011-2018). Similarly, the typical summer head (figure on the right), is calculated as the mean of the three lowest phreatic heads within a year, which is subsequently averaged over the same simulation period.

The average phreatic head illustrates the differences between the low-lying and higher parts of the Netherlands. In the reclaimed parts of the Netherlands (some typical polder areas mainly in the central and Western part of the Netherlands), the phreatic groundwater table is close to the ground surface. In the sandy ridges, the water table is at a higher depth below the surface area. A clear example is the Veluwe in the middle of the country, with phreatic heads at a depth of over 10 meter below ground level. In those typical infiltration areas with deep ground water levels, also higher model errors (> 1 m) might be found, when validation the model with measurements (figure 5.3). The typical winter and summer phreatic heads show the dynamics of the groundwater levels during a year. In the winter, the ground water level is almost at surface level in the Western and Northern parts of the Netherlands. In the driest period in the summer, the water table in these regions is about 1 meter lower compared to the winter situation.



Figure 5.1 shows that the deep groundwater heads in the regions with a low elevation are very high, often above surface level. This indicates that there is an upwards seepage flux in these areas.

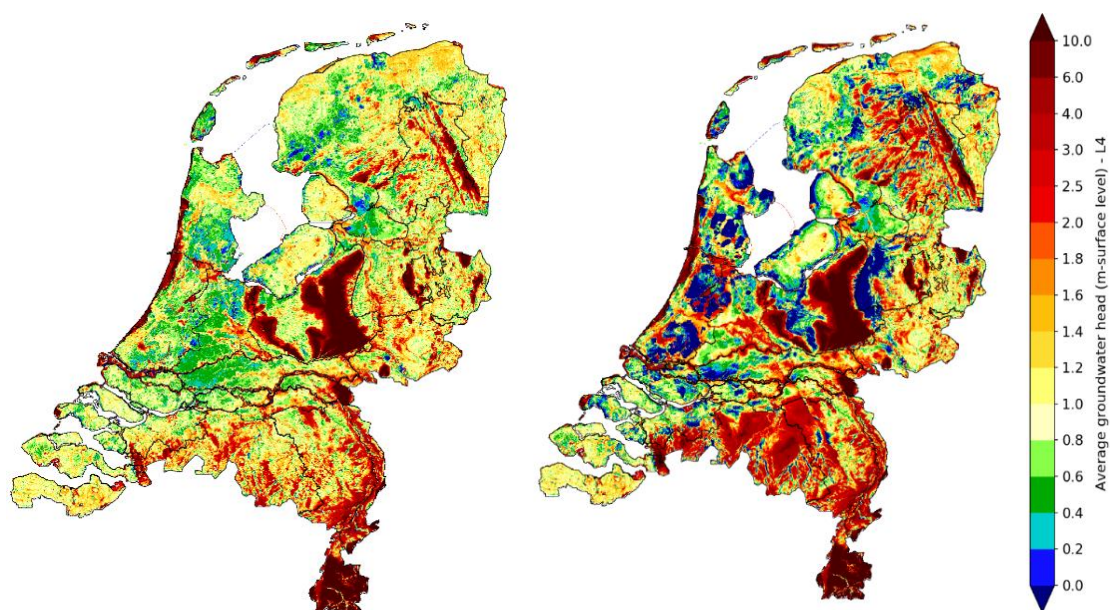


Figure 5.1. Average phreatic head (left) and deep groundwater head (model layer 4) in m below surface level.

Due to the seasonal variation mostly of evaporation and water use, the groundwater heads have a seasonal dynamic. This is illustrated by the high and low groundwater levels in Figure 5.2. These are the depth below the surface of approximately the 87.5th and 12.5th percentile of the groundwater table.

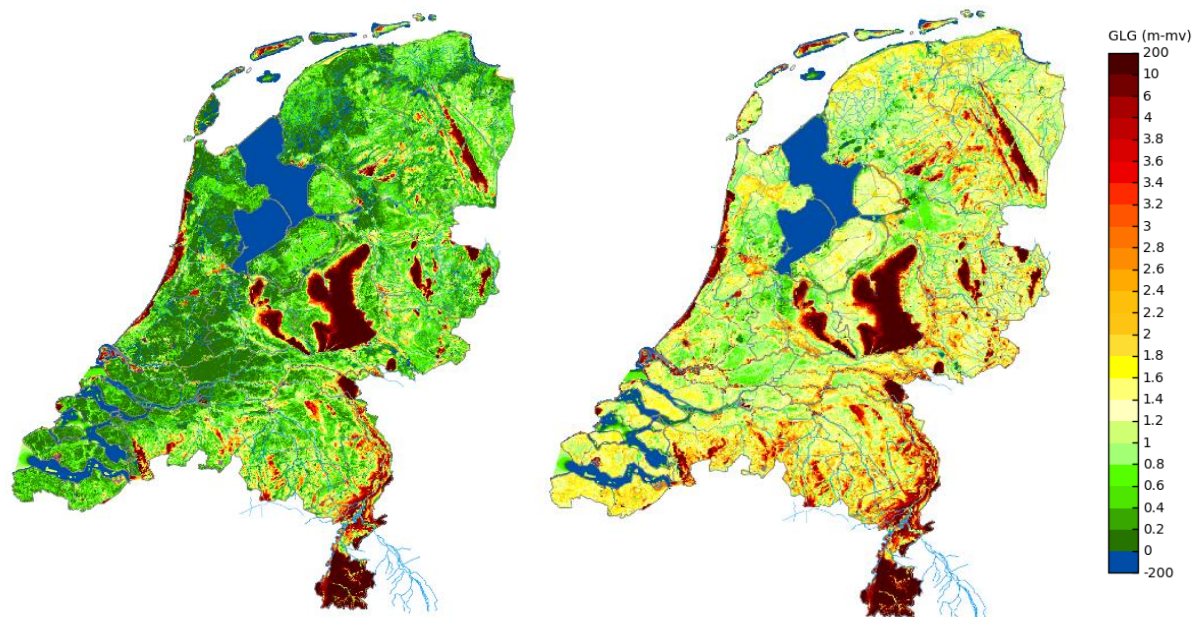


Figure 5.2. Average high (left) and low (right) groundwater levels in m below the surface level (approximately the 87.5th and 12.5th percentile).

The average high (GHG) and low (GLG) groundwater table is used for validation. *Figure 5.3* gives an example of the comparison of calculated and measured values for NHI-LHM version 4.1 for GHG, GLG and the difference between these (yearly dynamic).

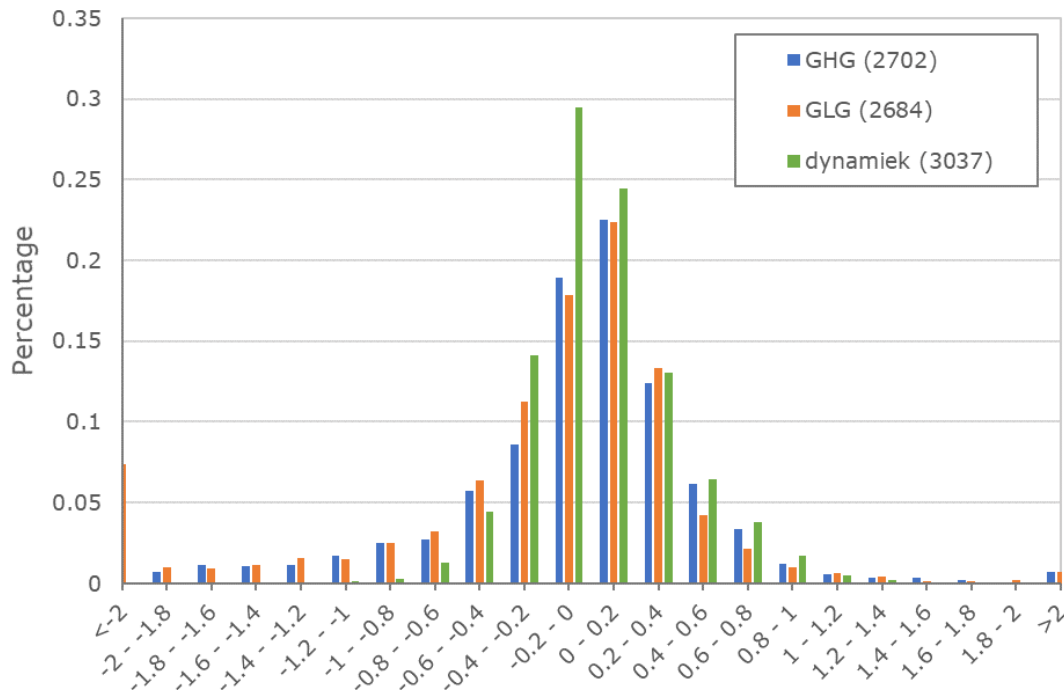


Figure 5.3. Example of validation of the calculated groundwater levels in LHM 4.1: the distribution (percentage on vertical axis) of prediction errors of calculated phreatic heads expressed in average high levels (GHG, approximately 87.5th percentile), average low (GLG, approximately 12.5th percentile), and the difference between GHG and GLG (yearly dynamics: “dynamiek”). Source: Berendrecht (2021).

NHI-LHM does not only calculate heads, but also fluxes. Due to the amount of detail in the schematization of the top system, groundwater recharge can be determined according to various definitions. Figure 5.4 gives two examples: the effective precipitation and the recharge at the groundwater table.

The yearly effective precipitation is calculated as the difference between the yearly precipitation and the yearly potential evaporation. The left picture in Figure 5.4 shows the average effective precipitation according to the national model (LHM) in the period 2011-2018. The reference situation shows that on a yearly basis, the Western and Northern part of the Netherlands are the areas that receive most precipitation. In these regions, the yearly average of the effective precipitation is positive. The South and East are dryer, where a small region stands out with negative effective precipitation (the higher potential evaporation is higher than the precipitation).

The groundwater recharge is calculated as the difference between the precipitation and the evapotranspiration and surface runoff, as calculated within the coupled models MetaSWAP and MODFLOW. This groundwater recharge which enters the upper boundary of the MODFLOW model is shown in the right picture of Figure 5.4. The reference situation shows that the calculated recharge is slightly higher in the lower part of the Netherlands: the Western and Northern areas. In the higher, sandy parts of the Netherlands, the recharge is slightly lower. These spatial differences are similar to the distribution of a high and low effective precipitation.



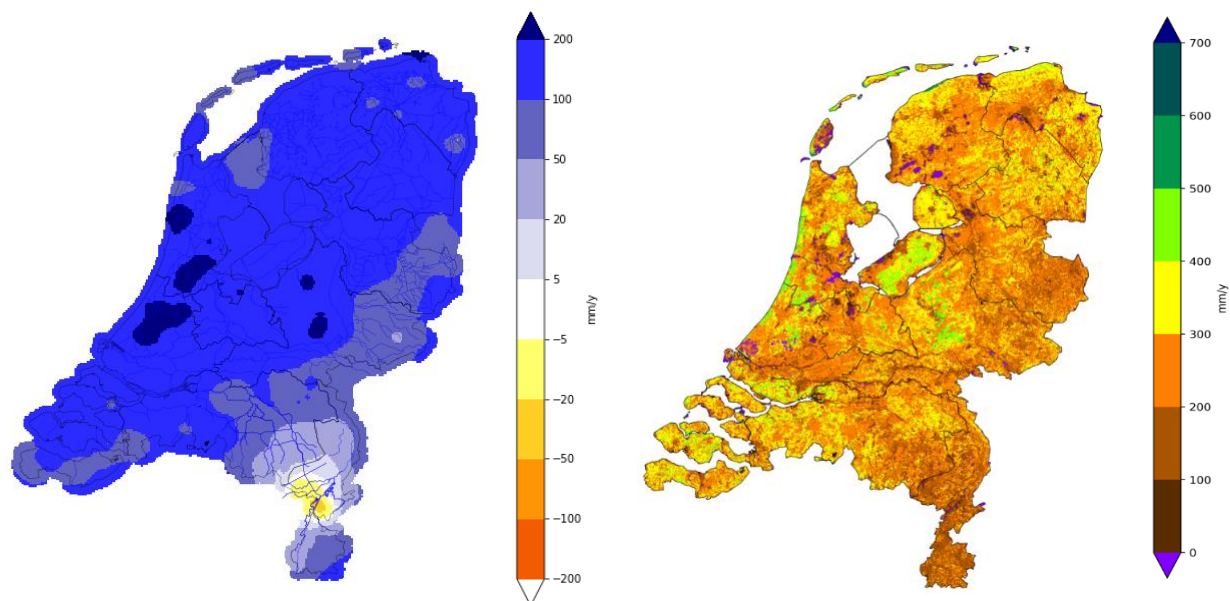


Figure 5.4. The average yearly effective precipitation in mm/year for the LHM (left) and average groundwater recharge in mm/year for the LHM (right)

Figure 5.4 illustrates that the recharge differs significantly from the net precipitation surplus, which mainly indicates large differences between reference evaporation (meteorological input for the model) and actual evapotranspiration (hydrological output of the model).

The surface water discharges, which are shown in Figure 5.5, contain the fluxes for all surface water systems as calculated by MODFLOW (DRN and RIV systems). The direction of these fluxes are relative to the groundwater system. This means that a negative flux describes water that is abstracted from the groundwater, whereas a positive flux is water that infiltrates the groundwater system. The discharge flux is generally negative, meaning the surface water bodies gain water from the groundwater. The West and North of the country have a very high density of surface water bodies, whereas the East and South show larger areas without surface water discharge.

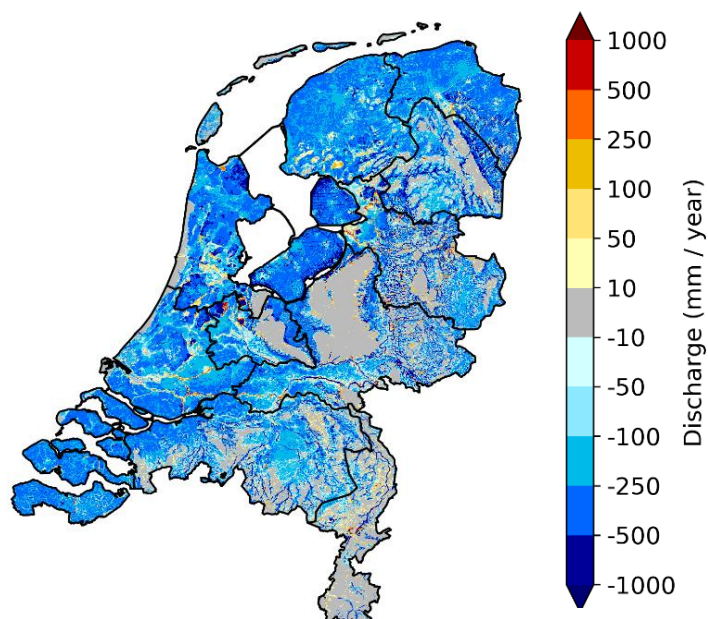


Figure 5.5. Average discharge of all surface water systems in mm/year

5.1.1.2 Time series models

The ground water tools website <http://www.grondwaterstandeninbeeld.nl> provides time series models for all groundwater head time series of the piezometers in the national database with subsurface data <https://www.DINOloket.nl/en/subsurface-data>. The time series models have been created by Metran (see Section 4.3). The precipitation response is related to the properties of the groundwater system (Zaadnoordijk & Lourens, 2019). The response can be characterized by the total response (or unit step response, i.e. the final value of the groundwater head change due to unit step change of the precipitation) and the median response time. These values usually are reliable for the models of good quality (Zaadnoordijk, 2018). See Section 4.3 and Zaadnoordijk et al., 2019 for the quality assessment of the time series models.

Figure 5.6 shows the total response from the piezometers in the upper regional aquifer of NHI-LHM with a good time series model.



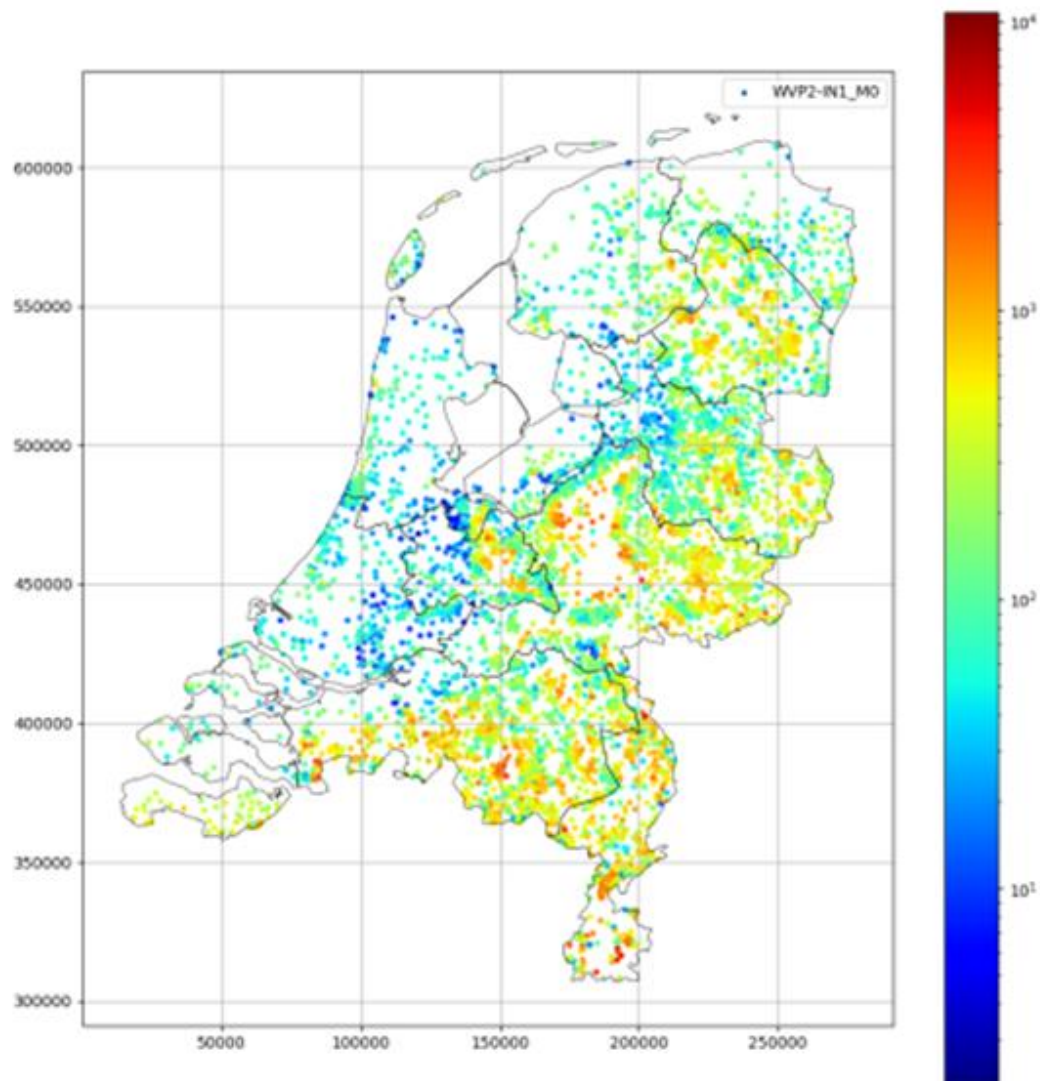


Figure 5.6 Total precipitation response (M0 or unit step response [100 day] groundwater head in cm over precipitation in meters per day) in the transfer-noise models for the upper regional aquifer (NHI-LHM code WVP2). Source: Zaadnoordijk & Lourens, 2019).

The pattern of the median precipitation response time in *Figure 5.7* is similar to that of the total response (*Figure 5.6*) with higher values in the East and South.

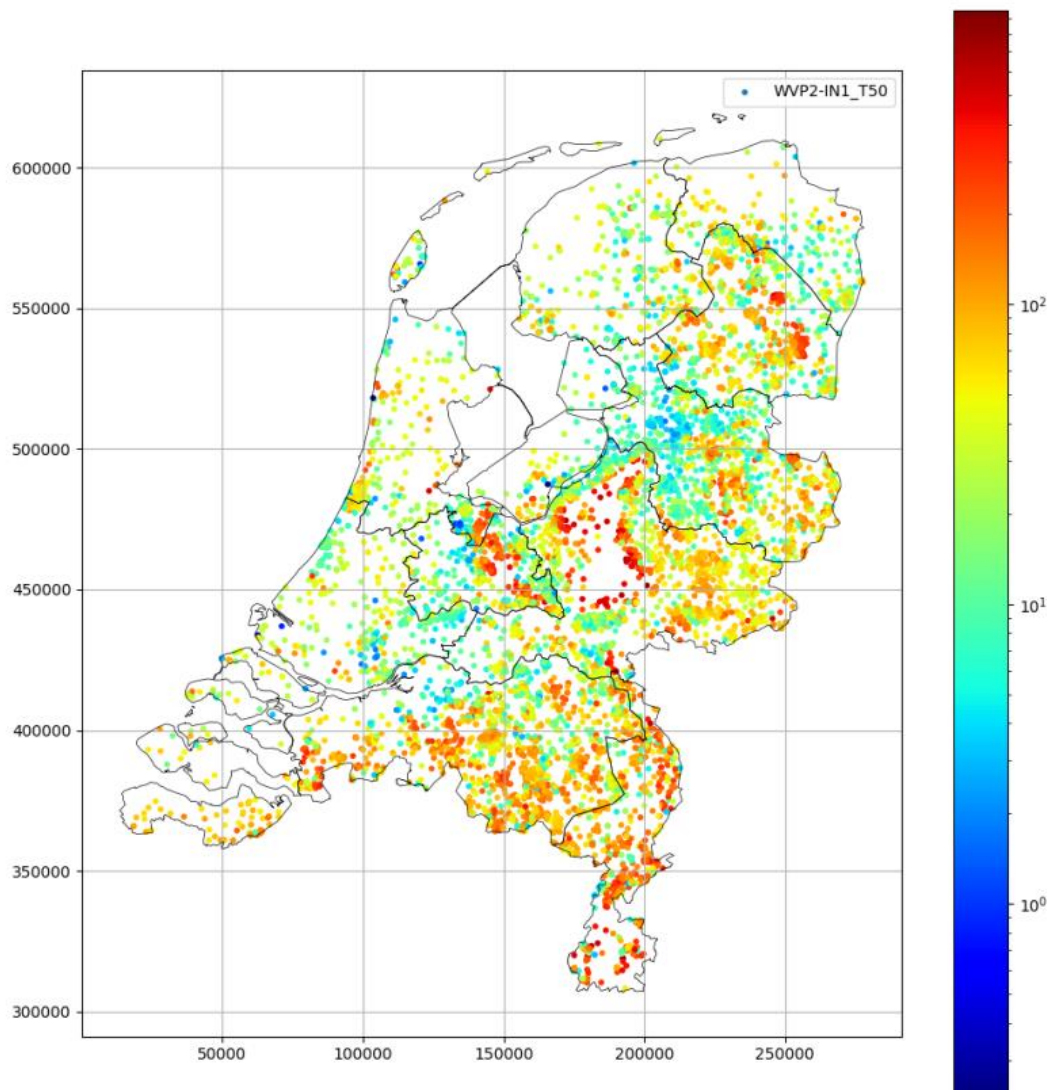


Figure 5.7 Precipitation response time (t_{50} [days]) in the transfer-noise models for the upper regional aquifer (NHI-LHM code: WVP2). Source: Zaadnoordijk & Lourens, 2019.

Under various assumptions, the evaporation coefficient of the Metran models can be used to determine a crude estimate of the long term average recharge (Oberghell et al., 2019). *Figure 5.8* and *Figure 5.9* show the values on a map for the piezometers located in the two upper model aquifers of NHI-LHM. The maps do not show an apparent spatial pattern. Comparisons of the Metran estimates with the groundwater recharge calculated by NHI-LHM are given in Sub-subsection 6.4.2.1 .

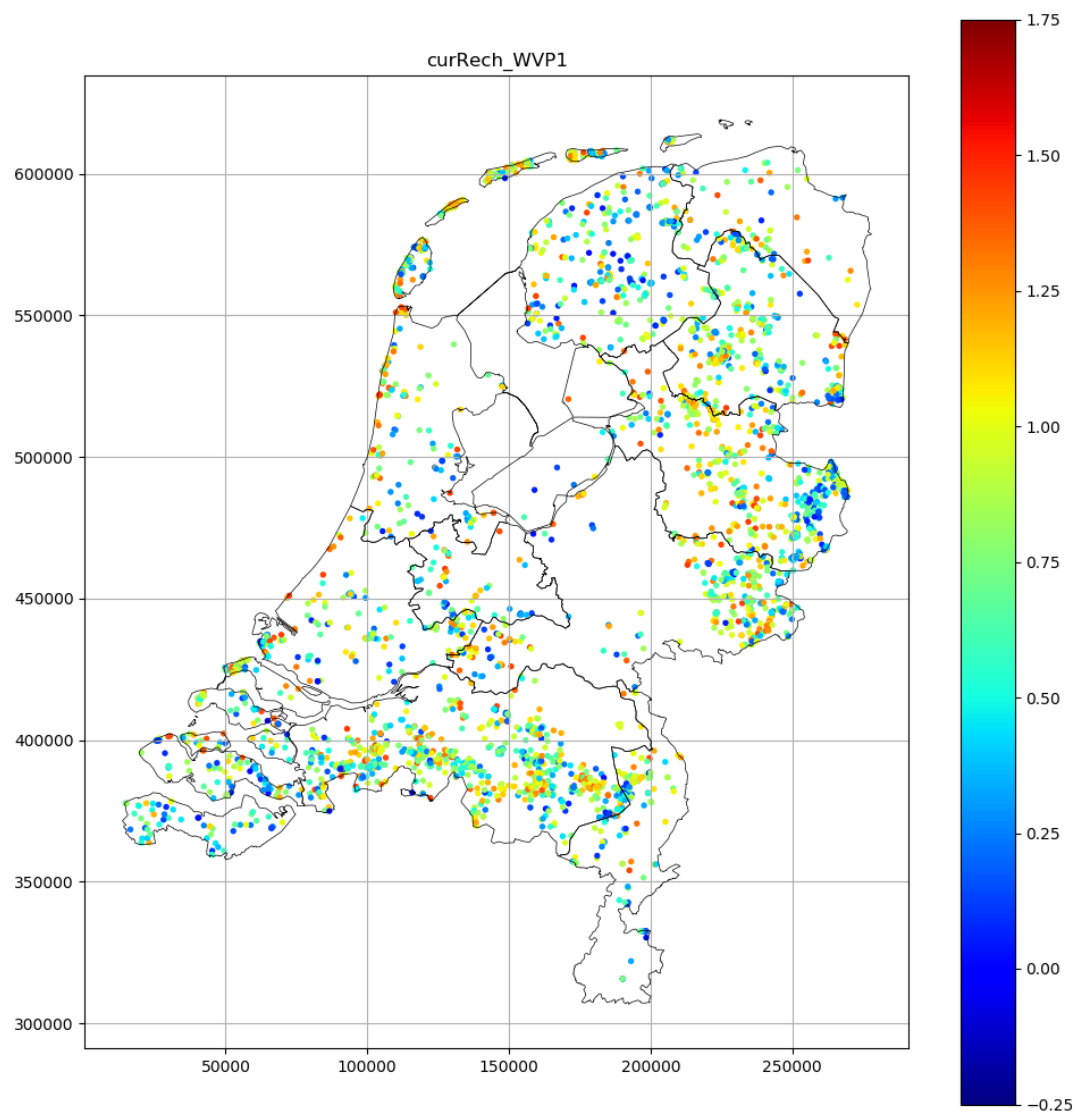


Figure 5.8 Crude estimate of groundwater recharge [mm/day] from evaporation factor in Metran models of piezometers in NHI-LHM model aquifer 1 (phreatic water table aquifer).

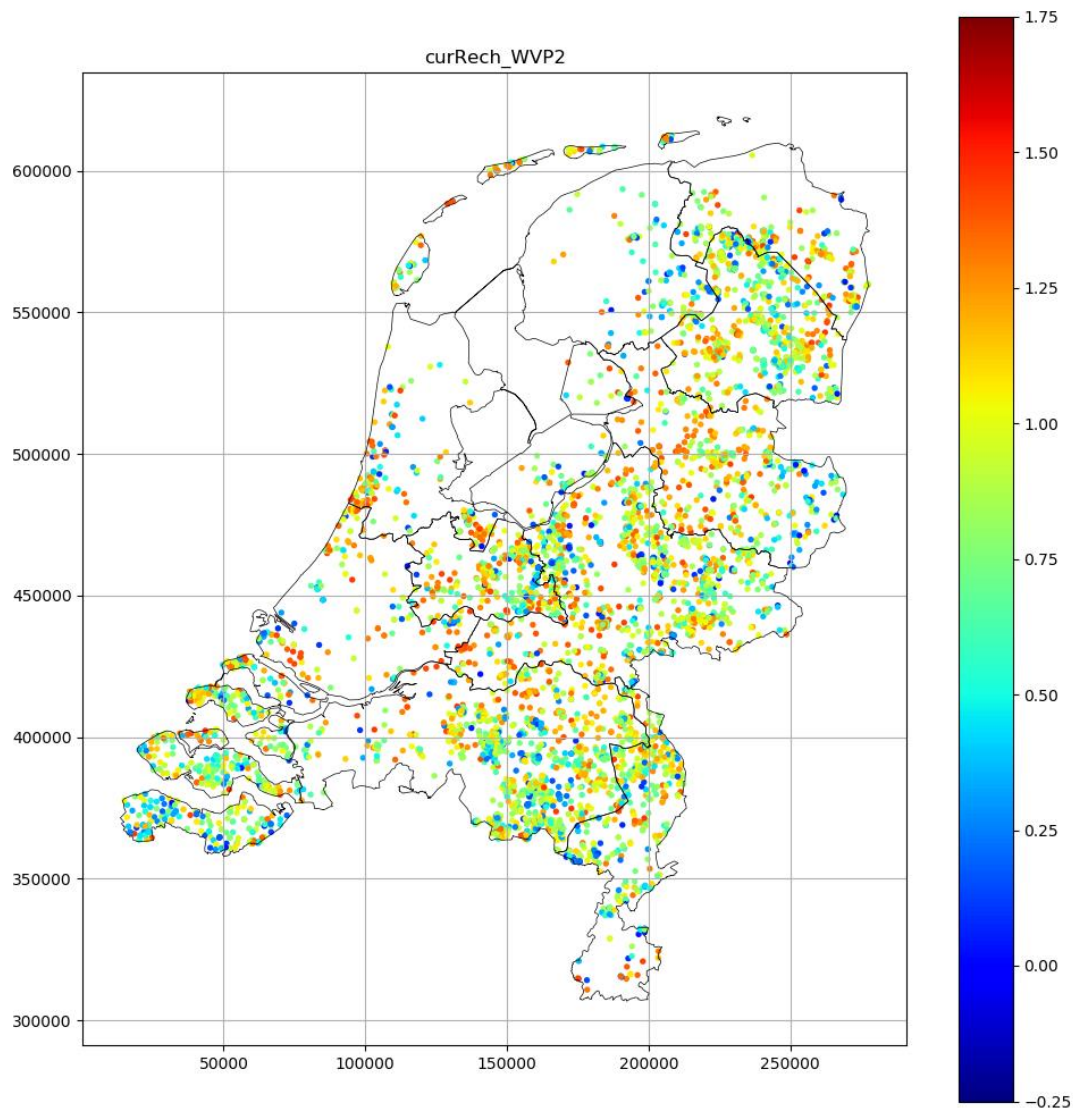


Figure 5.9 Crude estimate of groundwater recharge [mm/day] from evaporation factor in Metran models of piezometers in NHI-LHM model aquifer 2 (the upper regional aquifer)

5.1.2 Climate change scenario results

This subsection contains results for the climate change scenarios described in section 4.4.

5.1.2.1 Integrated hydrological model

The effective precipitation in the reference situation and under the different climate scenarios is shown in Figure 5.10. The climate scenarios have a different impact on the effective precipitation. The regional differences that are visible in the reference situation remain the



same: the North and West have a higher effective precipitation compared to the South and East of the Netherlands. The 'dry' scenarios of both temperature rise scenarios (1° min and 3° min) reduce the effective precipitation. In the 3° min scenario, almost the whole South-eastern half of the country will have on average a negative effective precipitation. The 'wet' scenarios (1° max and 3° max) increase the effective precipitation. The national variation of the effective precipitation in the 1° max scenario is comparable to the reference situation, but the whole country has a positive effective precipitation. In the 3° max scenario, the effective precipitation is over 200 mm/year for a large part of the country. The differences between the minimum and maximum variants of the climate scenarios are mainly caused by a strongly varying precipitation flux for the different variants.

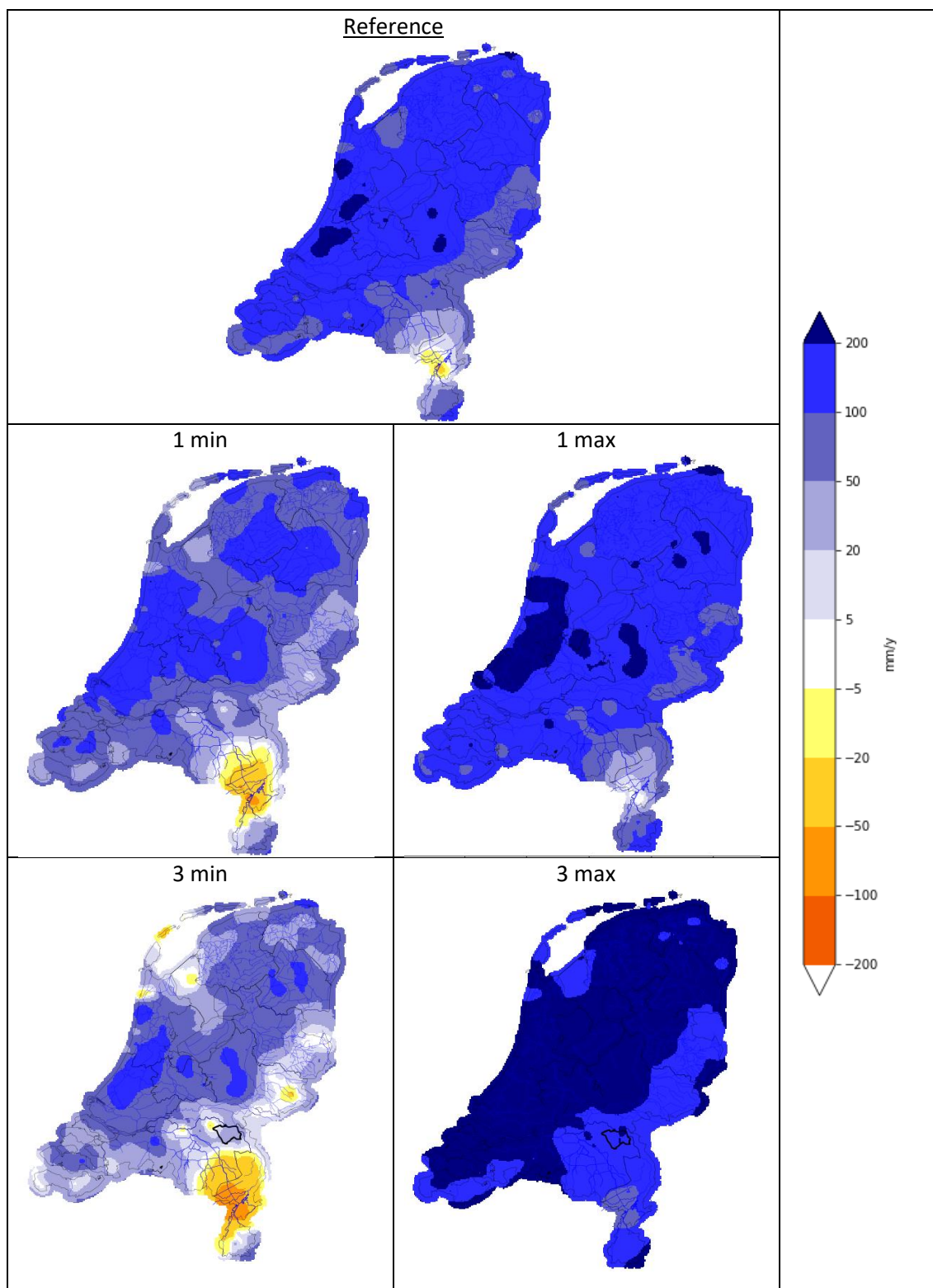


Figure 5.10. Average yearly effective precipitation (mm/year) for the reference situation (top) and the effect of the different climate scenarios (middle and bottom)

Figure 5.11 illustrates the effect of the climate scenarios on the phreatic groundwater head and *Figure 5.12* shows deeper groundwater heads. Generally, the ‘dry’ variants of the climate scenarios result in a decrease in the groundwater head, which means that the water table level decreases. On the contrary, the ‘wet’ scenarios result in an increase of the groundwater head and therefore increases the level of the water table.

The differences in heads due to climate change are larger in the South and East of the country compared to the low-lying areas in the North and West. The hydraulic head in these low-lying areas is generally very little affected in the 1° min scenario. In this scenario, only the regions with high surface elevations (the Veluwe and the South-eastern corner of the country) experience a decrease in phreatic head of about 0.5 – 1.0 m. For the ‘dry’ variant of 3 degrees temperature increase (3° min), the phreatic head is influenced in almost the whole country. This means that the phreatic head is lowered with at least 5 cm and locally up to 2 meters. The locations with the largest decrease in head in the 3° min scenario, are also the locations with the largest increase in phreatic head in the 3° max scenario. These sandy locations (the Veluwe for example) function as typical infiltration areas, where (change in) effective recharge directly leads to change in heights because the absence of surface waters. The increment in the phreatic head may locally exceed 2 m. In contrary, in the West of the Netherlands the changes are damped by the abundance of surface waters.

The 3° max scenario hardly leads to changes in ground water heads, because the surplus of water is easily drained by the intensive drainage systems. The lower net precipitation in the 3° min scenario does have effect the ground water heads in the Western part of the Netherlands, because the lower net precipitation can’t sufficiently be compensated by a surface water supply, while this can still be compensated in the 1° min scenario. This stresses the importance to have combined calculations for groundwater and availability of surface water for the Netherlands.

The 1° max scenario stands out from the other scenarios in the sense that there are regions that show an increase in head, as well as regions with a decreasing hydraulic head. The areas react differently in this scenario due to a difference in net precipitation, land use and geohydrological properties.

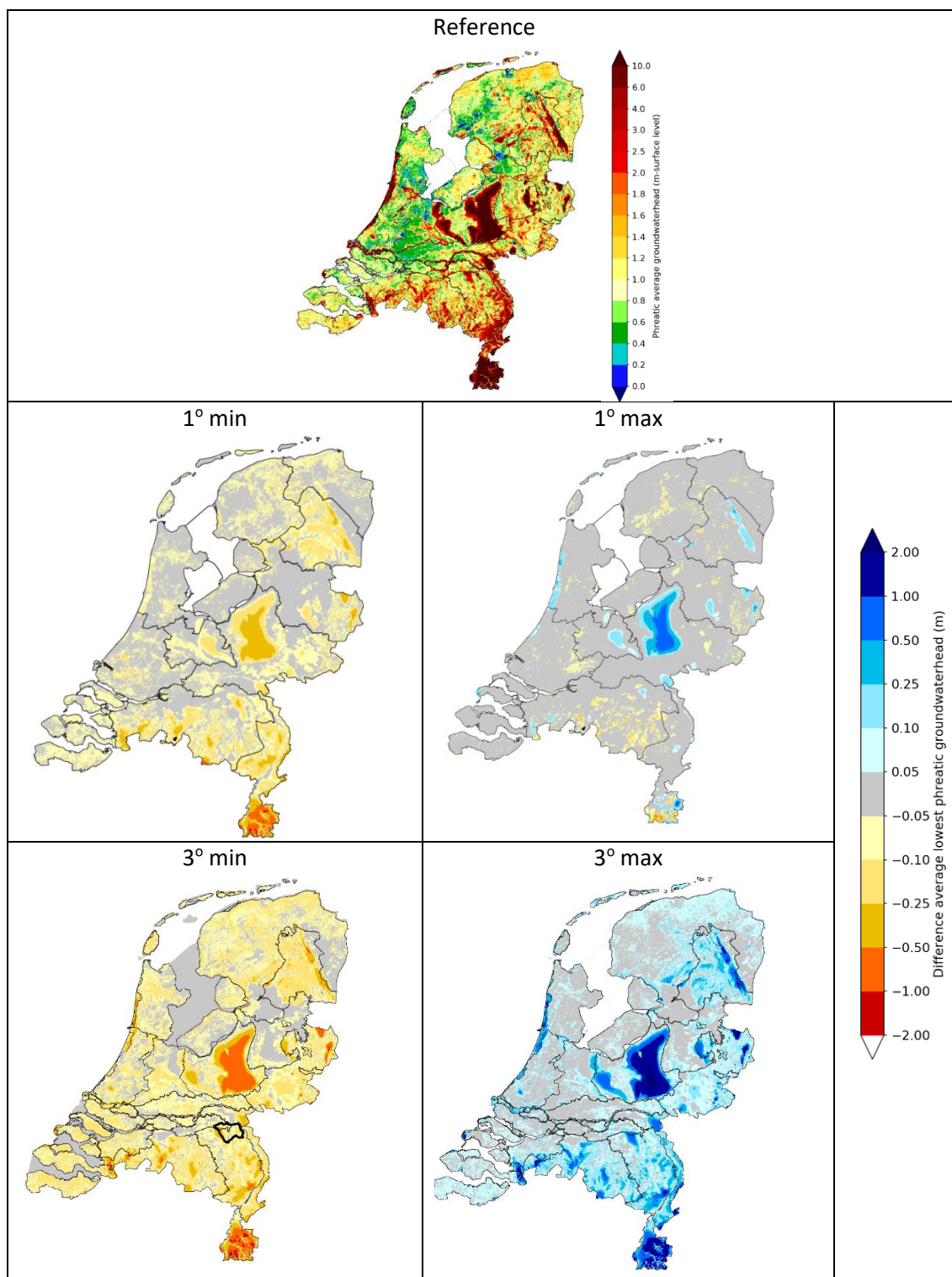


Figure 5.11. Average mean phreatic groundwater head in m below surface level (top) and the differences in mean phreatic groundwater head for all climate scenarios compared to the reference situation

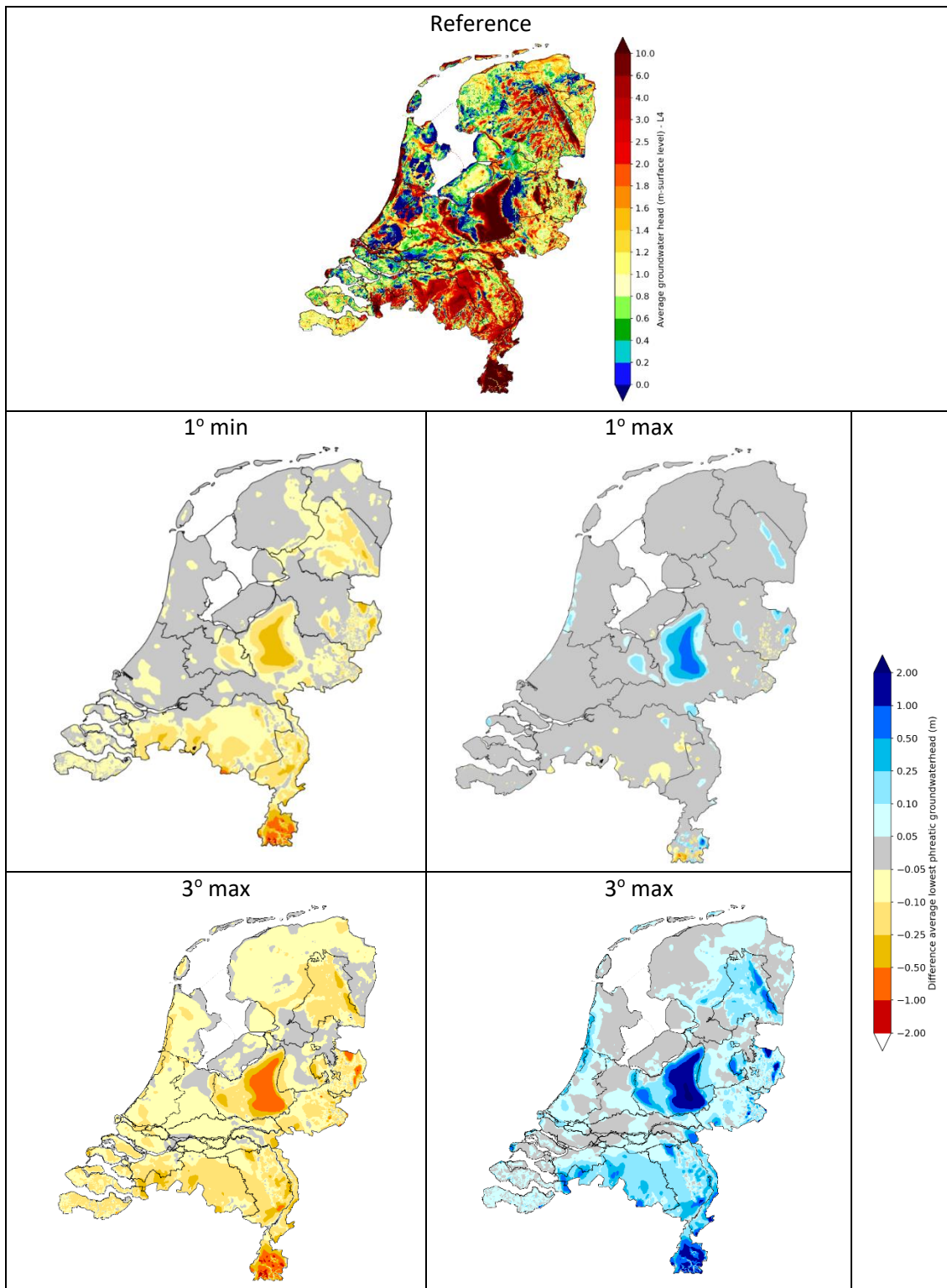


Figure 5.12. Average mean deep groundwater head (model layer 4) in m below surface level (top) and the differences in mean deep groundwater head for all climate scenarios compared to the reference situation.

The average groundwater recharge for the climate scenarios is shown in *Figure 5.13*. In the 1° min scenario, the recharge slightly decreases, mainly in the North-eastern part of the country. The 1° max scenario shows both an increase as a decrease in recharge, which is similar to the effect as shown for the heads. The regions where the hydraulic head increases, are also the regions with an increasing groundwater recharge. The 3° min scenario shows a decrease in recharge in almost the whole country, although this decrease is almost negligible in the very South. The 'wet' scenario (3° max) illustrates an increase in groundwater recharge, which is highest in the Northeast.

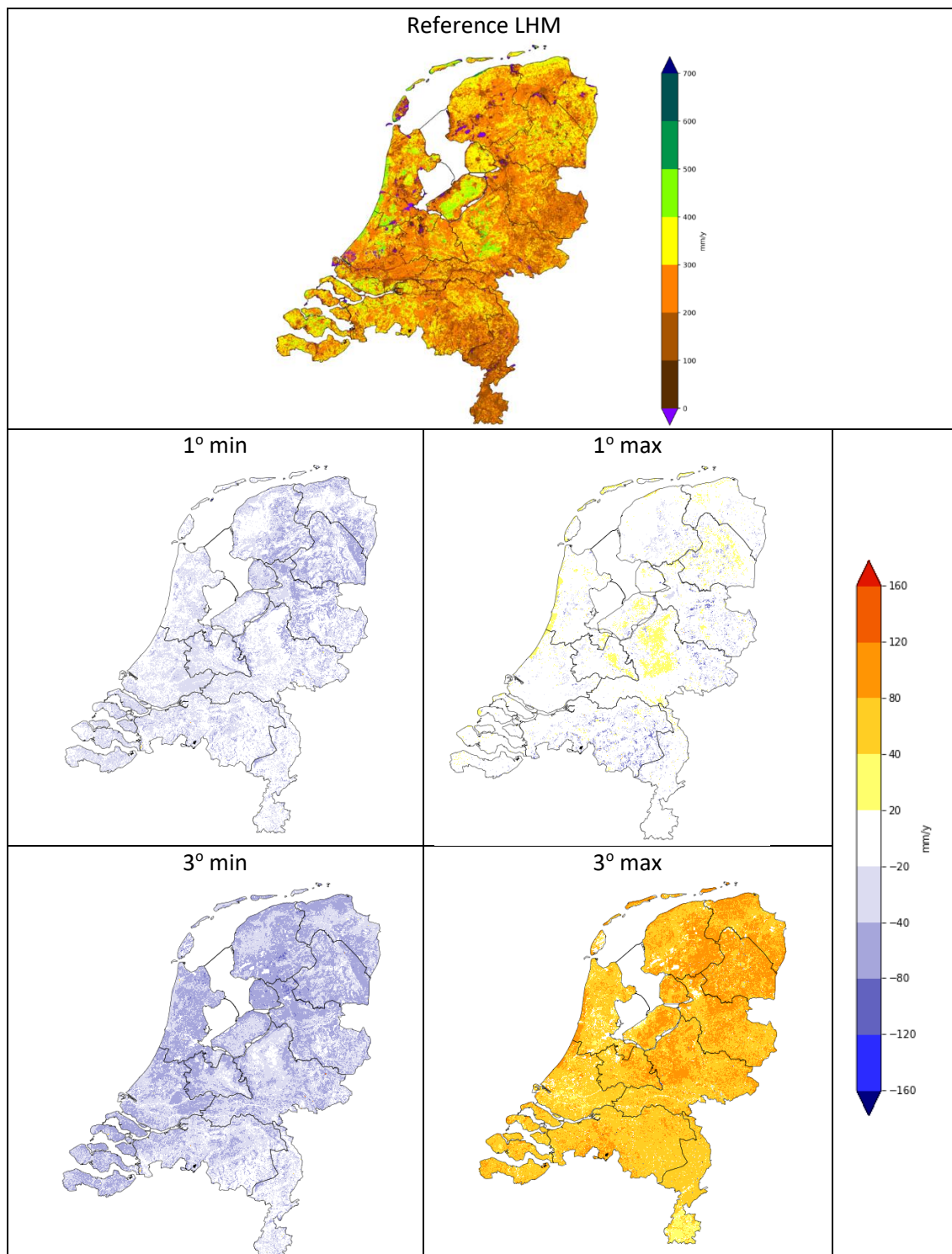


Figure 5.13. Average groundwater recharge in mm/year in 2011-2018. Top: groundwater recharge (mm/year) in the reference situation. Middle and bottom: difference in average groundwater recharge (mm/year) for the different climate scenarios compared to the reference situation.

In *Figure 5.14* the average nationwide recharge is plotted. The top left picture shows the average for every month in the whole simulation period, and compares the climate scenarios. Clearly, the biggest differences occur in the summer period (April – September). The 1° min and 3° min scenario have a lower recharge every month except for November and December, when the 3° min recharge exceeds the reference recharge. The 3° max scenario is clearly the wettest scenario, with a positive value in all months except April, May and June. The 1° max scenario shows an interesting pattern: it has the highest negative recharge in April, May and June, but abruptly switches to a slightly positive value in July.

The other graphs in *Figure 5.14* show the differences in recharge over the different years. To derive these graphs, the average recharge per month is calculated for every simulation year between 2011 and 2018. The lowest and highest value that is found for every month is shown as respectively the minimum and maximum value in *Figure 5.14*. These graphs show that the variation in recharge between years can be substantial. For example, the recharge in August was almost -0.5 mm/day in 2003, but more than +0.5 mm/day in 2004. In general, the ‘dry’ climate scenarios (1° min & 3° min) decrease this variability between years, whereas the ‘wet’ climate scenarios show an increased variability. To compare: the difference in the minimum average and maximum average recharge in August is in the reference situation about 1 mm/d, in the 3° min scenario about 0.5 mm/d and in the 3° max scenario about 1.25 mm/d.

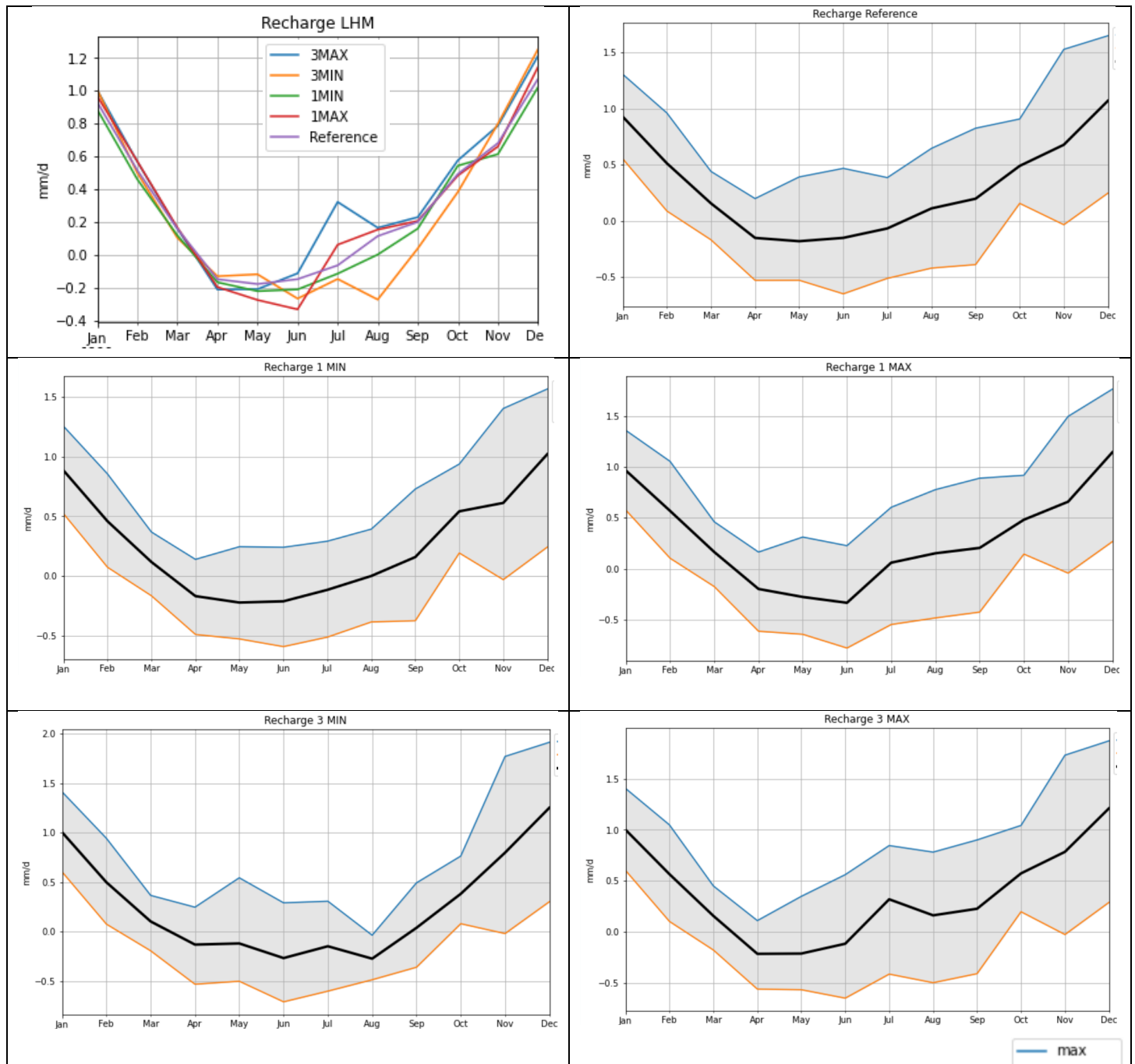


Figure 5.14. Top left: Average groundwater recharge in the Netherlands per month (mm/d) in the period 2011-2018 for the reference situation and all climate scenarios. Top right, middle and bottom row: average groundwater recharge per month and the maximum and minimum average groundwater recharge per month in the reference situation (top right) and the climate scenarios (middle and bottom row).

The effect of climate change on the discharges is relatively minor for the scenarios based on one degree temperature change, but may be significant for 3 degree temperature change (see *Figure 5.15*). In the latter case, differences in discharge reach up to 50 mm/year in many areas due to climate change, which is significant compared the total discharge of about 250 – 500 mm/year. The dry climate variants (the min scenarios) show a positive increase in the discharge flux. This means that the flux becomes less negative and the total discharge decreases. In the 1 degrees scenario, only the discharges in a limited amount of water bodies are affected; in the Western part of the Netherlands the effect is limited by the damping effect of the surface water systems. In the 3° min scenario, all surface water bodies are affected.

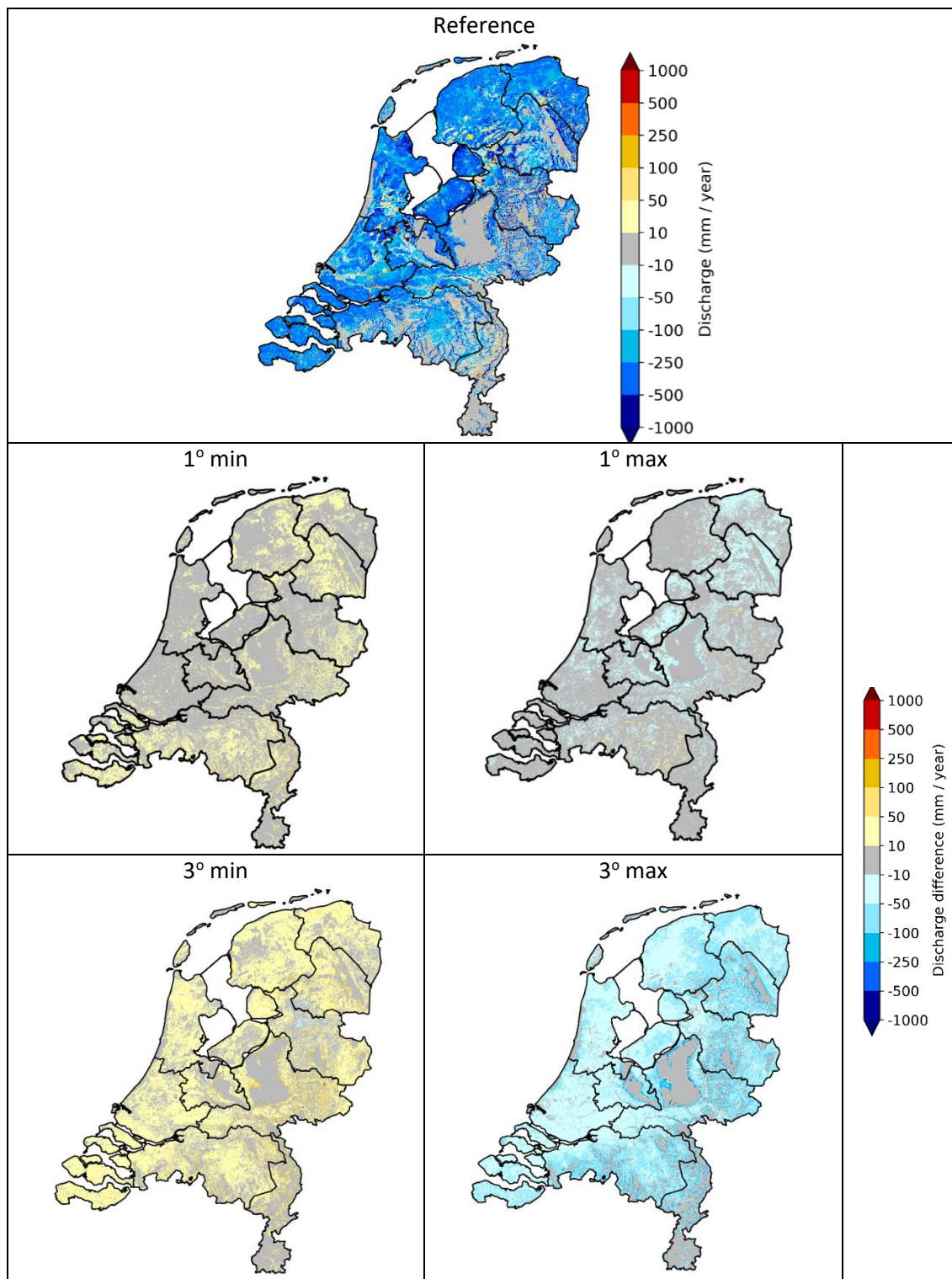


Figure 5.15. Average discharge of all surface water systems in mm/year in the reference situation (top) and the differences in discharge for all climate scenarios compared to the reference situation

5.1.2.2 Time series models

The piezometers selected for the regional pilot (subsection 5.2.1.2) have been simulated with the national climate change factors (in addition to the regional factors – see subparagraph 5.2.2.2) and compared to the results of the national integrated model NHI-LHM. The results are inter-compared in section 6.3.

Furthermore, long term average recharges have been calculated for the climate scenarios. The results offer only an indication of the change, with little spatial variation, due to the crude calculating and the usage of uniform meteorological data for the entire country (*Figure 5.16*).

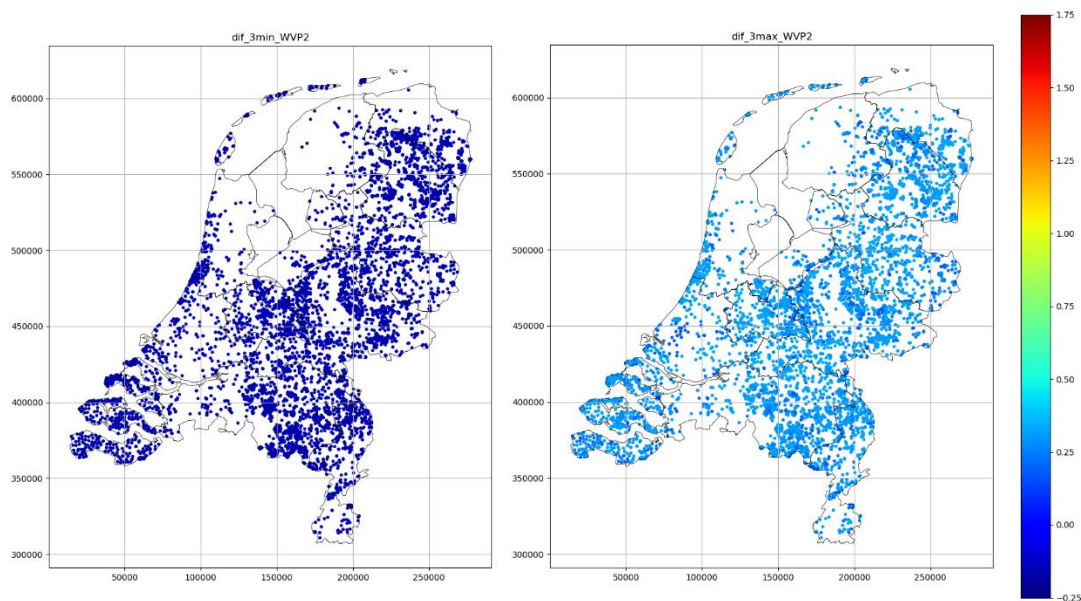


Figure 5.16 Change of the crude estimate of groundwater recharge from Metran models of piezometers in NHI-LHM model aquifer 2 for climate change scenario 3° min (left) and 3° max (right).

5.2 De Raam

5.2.1 Reference period results

5.2.1.1 Integrated hydrological model

The phreatic head distribution in pilot area 'De Raam' is shown in *Figure 5.17*. The Western part of the area has phreatic heads that are relatively far below the surface level. This is due to the fact that the surface elevation sharply increases towards this region: the elevation difference is about 8 m. Furthermore, the phreatic heads near the river Meuse are also relatively deep (far below surface level).

The groundwater recharge is shown in *Figure 5.18*. This picture shows that the groundwater recharge is quite uniform across the whole area. In the areas with land use type 'urban area' and 'forest' have the lowest groundwater recharges.



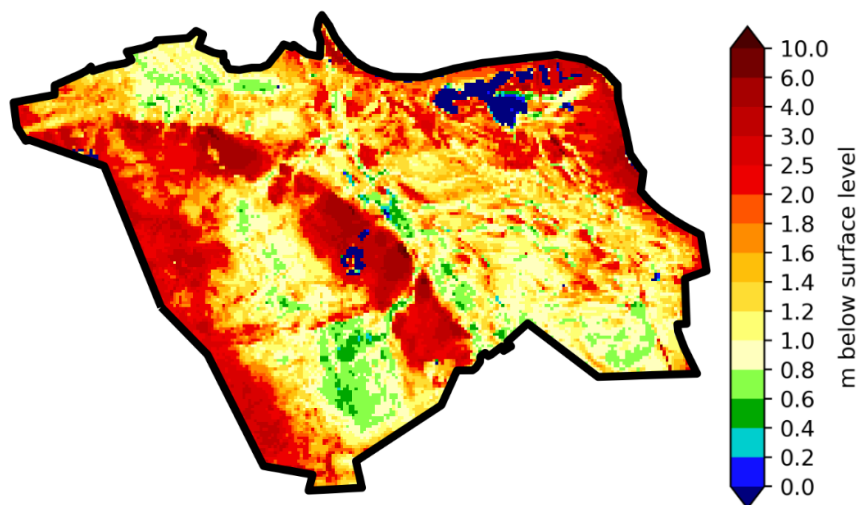


Figure 5.17. Average phreatic head in pilot area 'De Raam' in m below surface level.

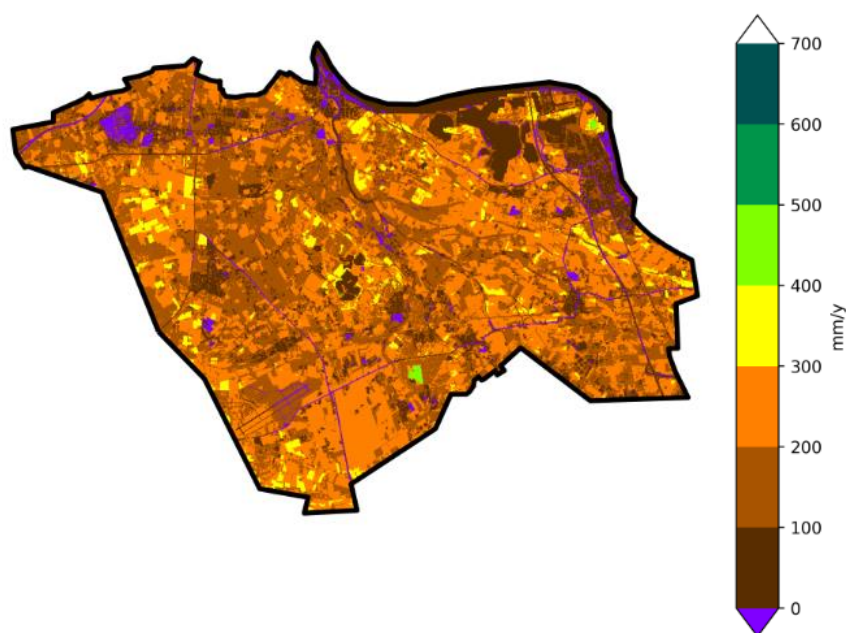


Figure 5.18. Average groundwater recharge in pilot area De Raam (mm/year) in period 2011-2018

5.2.1.2 Time series models

Metran (see section 4.3) has been used to create time series models for selected time series using precipitation and evaporation as explanatory variables to determine the precipitation response and to perform simulations for the climate scenarios (see subsection 5.2.2.2).

Also some time series along the river Meuse have been modelled with the river water level as a third explanatory variable in order to investigate the linearity of the river response under different circumstances.

Three monitoring wells have been selected to create time series models (see *Figure 5.19*). The wells have multiple piezometers at various depths.

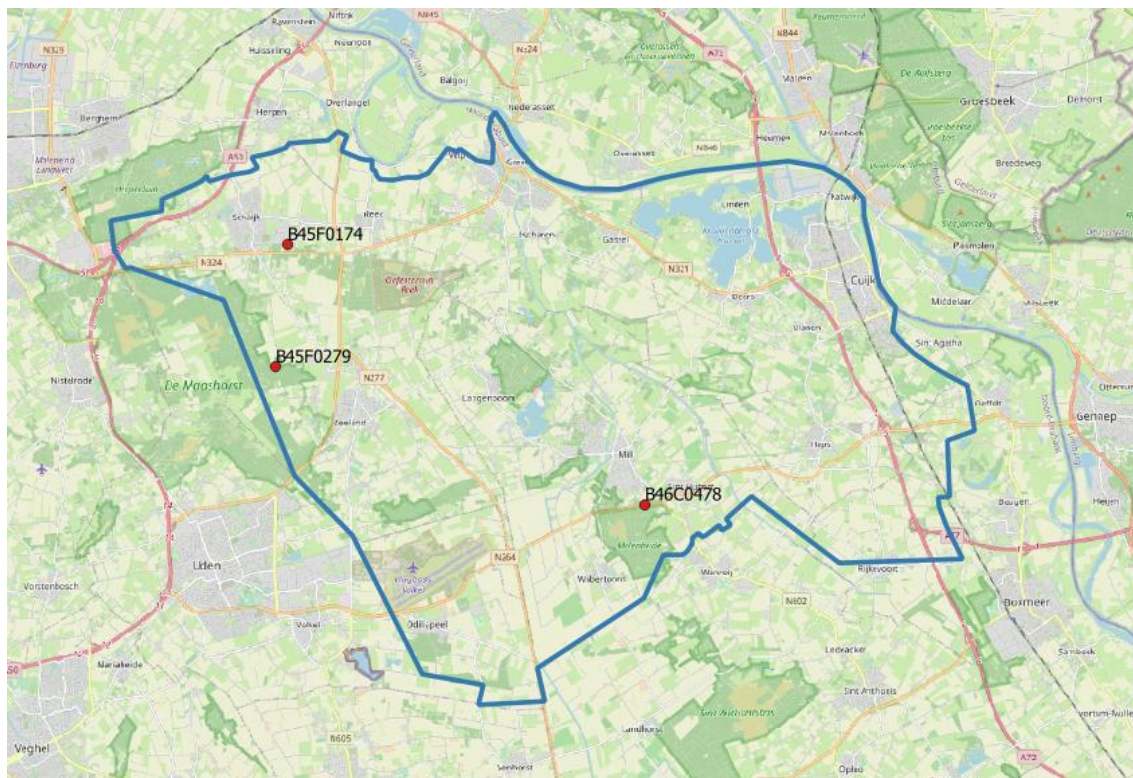


Figure 5.19 selected multi-piezometer monitoring wells for pilot de Raam.

Figure 5.20 and *Figure 5.21* show the median precipitation response time and the total precipitation response from the Metran models, respectively. The results show that these characteristics of the precipitation response are quite similar for all piezometers. They vary more in lateral direction compared to the vertical direction. This is due to the lack of aquitards with a high resistance and differences in conditions at the locations of piezometers.

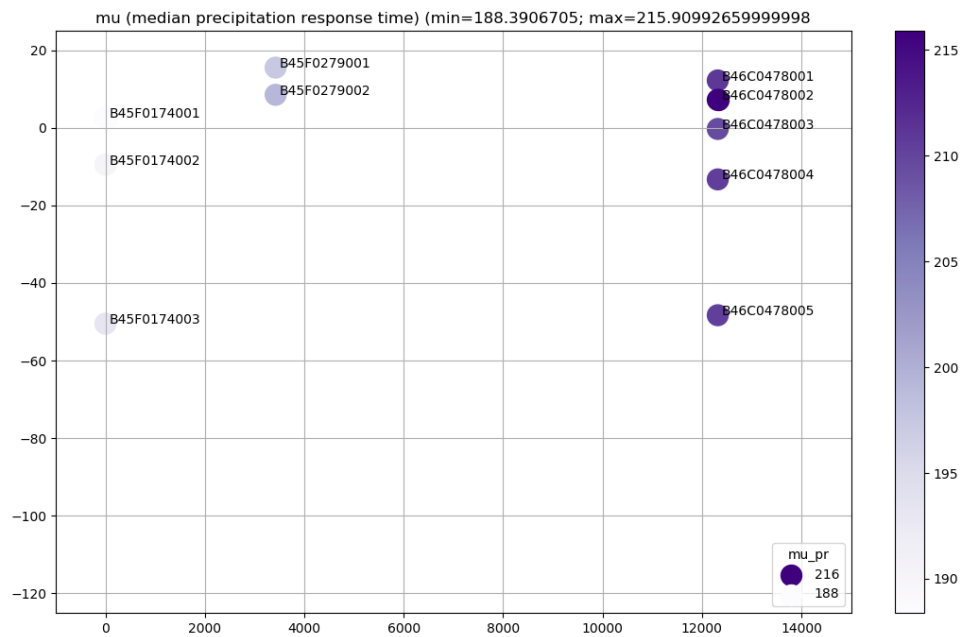


Figure 5.20 median precipitation response time [days] from Metran models of groundwater head time series with vertical coordinates in meters.

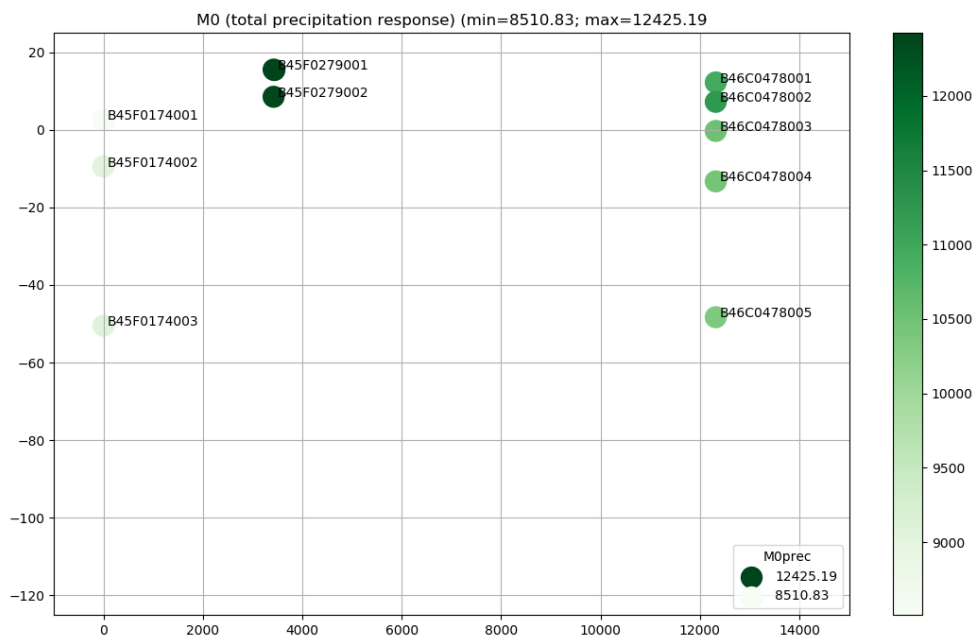


Figure 5.21 Total precipitation response $[0.1 \text{ d}] = [\text{mm}/(\text{cm}/\text{d})]$ from Metran models of groundwater head time series with vertical coordinates in meters.

Time series modelling of groundwater response to river water levels

A shipping accident on the river Meuse in December 2016 offered an opportunity to look at the performance of Metran under unusual consequences. A ship rammed the weir in the river Meuse at the Western boundary of the pilot area of de Raam (downstream). This caused a drop of the Meuse water level of 3 meters (Figure 5.22), while the normal fluctuation is much smaller (and mostly upward during high discharge events).

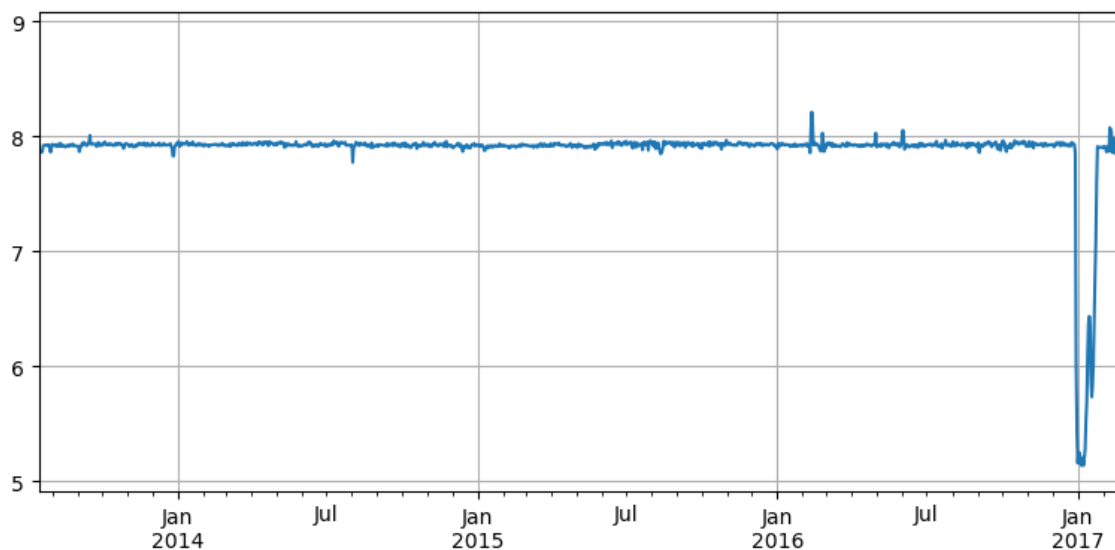


Figure 5.22 Meuse river level in meters above NAP

The groundwater in piezometer B46A1559001 at 160 meters from the Meuse reacts very quickly to the river level. Metran can match the slower response to precipitation and evaporation much better, but the timing and direction of the river response can be represented (*Figure 5.23*).

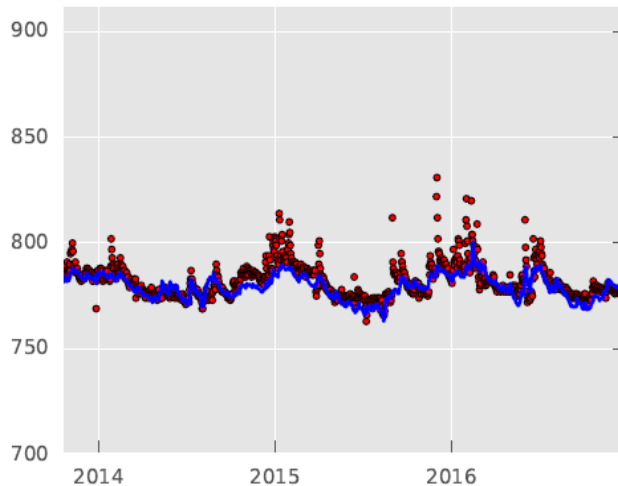


Figure 5.23 Calibration of Metran model for piezometer B46A1559001 during normal Meuse water levels.

This Metran model has been used to simulate the groundwater levels after the accident using the same explanatory variables: precipitation, evaporation, and Meuse water level (*Figure 5.24*).

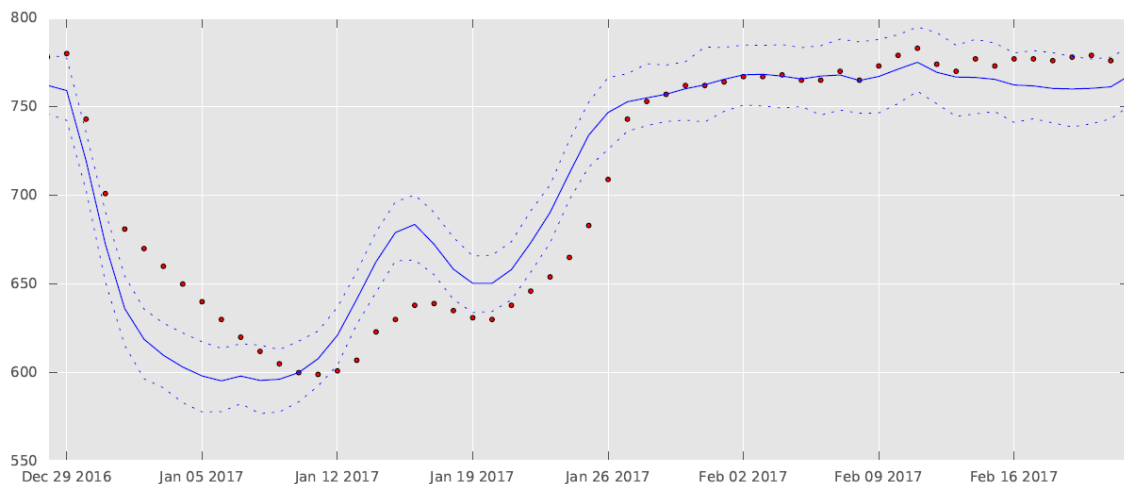


Figure 5.24 Simulation of Metran model (in blue; with 10- and 90-percentile as dotted lines) for piezometer B46A1559001 during unusual change of Meuse water levels (measurements in brown dots).

For this situation, Metran does not simulate the proper timing of the decline and the shape of the recovery also differs ostentatiously. One cause of these deviations is the fact that the



situation is outside the range of groundwater heads and river levels in the calibration period. Another reason is that the response to these extreme river levels is different from the normal response. This may be due to non-linearities and hysteresis in the groundwater system. This deficiency of the model is illustrated by the fact that the measurements (brown dots in *Figure 5.24*) lie outside the confidence interval created by the stochastic part of the model (the dotted blue lines in *Figure 5.24* represent the 10- and 90-percentile of the simulation).

5.2.2 Climate change scenario results

5.2.2.1 Integrated hydrological model

The effect of the climate scenarios on the groundwater recharge as calculated by the regional model of pilot area De Raam is shown in *Figure 5.25*. No further results are presented in this Subsubsection, but comparisons of De Raam with NHI-LHM are discussed in subsection 6.4.1.

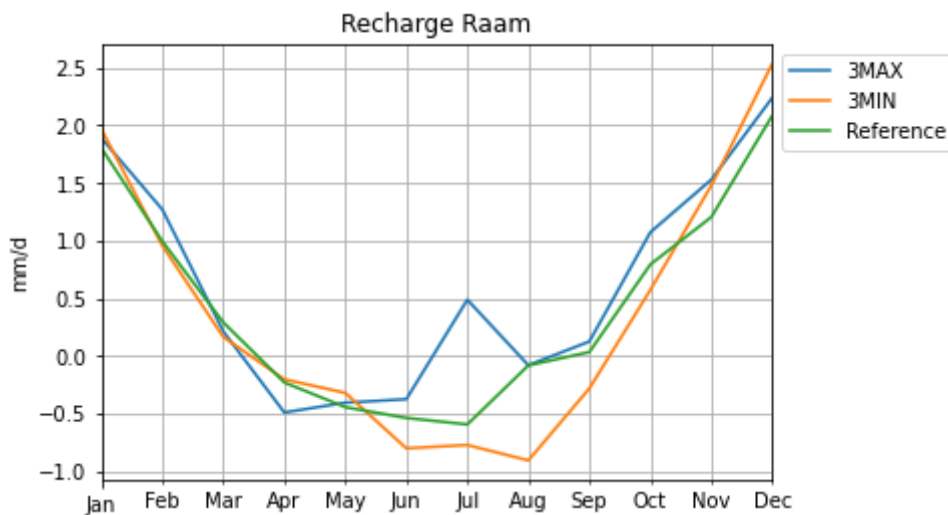


Figure 5.25. Average groundwater recharge as calculated by the regional model of De Raam per month (mm/d) in the period 2011-2018 for the reference situation and the 3 min and 3 max climate scenarios

5.2.2.2 Time series models

The Metran models for the selected piezometers from subsection 5.2.1.2 have been used for simulations of the climate change scenarios. The precipitation and evaporation series of the Volkel weather station of the Royal Dutch Meteorological Institute KNMI have been changed using the local change factors for the area of de Raam (see section 4.4).



6 DISCUSSION

6.1 NHI-LHM

The average effective precipitation and average groundwater recharge per month is shown in *Figure 6.1*. These graphs show the average value of the whole country, as an average for every month in the period 2011-2018. Clearly, there is a difference between the effective precipitation and the actual groundwater recharge. The effective precipitation has a much stronger variation throughout the year compared to the groundwater recharge. These differences can be explained by the fact that the actual evaporation is often lower than the potential evaporation and because a part of the precipitation will flow away as surface runoff.

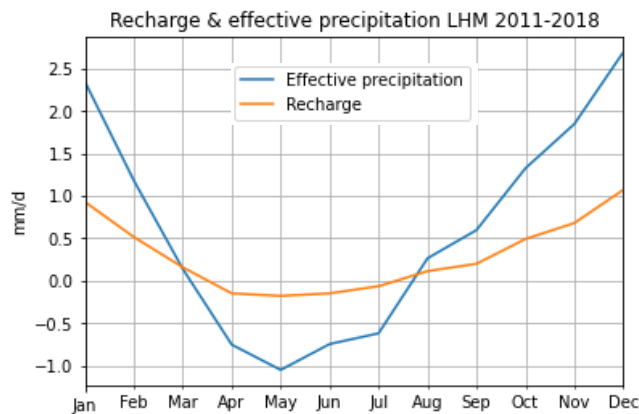


Figure 6.1. Monthly average of effective precipitation and recharge in mm/d

Including an atmosphere-plant model like WOFOST in an integrated model improves the estimation of the actual evapotranspiration. Moreover, the effect of higher CO₂ concentrations on the crop growth can be taken into account, in addition to the change in temperature. Depending on the schematization of the atmosphere-plant model, additional meteorological (and crop) information is needed as input, e.g. WOFOST is based on Penman-Monteith needing daily mean temperature, wind speed, relative humidity, and solar radiation as meteorological input. Because these were not available for the TACTIC climate scenarios, these were simulated without WOFOST.

The use of WOFOST can have a large impact on the model results. For example, a comparison of evapotranspiration in 2003 as modelled with or without WOFOST can result in a change up to 50 mm/year. This influences the calculated groundwater heads; in a relatively dry year they might increase up to 0.25 m compared to a run without WOFOST (Hunink et al., 2019).

The groundwater recharge in urban areas is not well known (Witte et al., 2019). The presence of buildings and pavement has a strong influence on the routing and infiltration of precipitation, with often a large portion going directly into storm sewers or surface water. Also, leaking sewers and drinking water infrastructure can have a large influence (e.g. Foster et al., 1998). In the Netherlands, urbanisation generally leads to a reduction of groundwater recharge because of



the implementation of drainage and the fact that in most urban areas, sewers start to act as drains when they age (Witte et al., 2019). The change of groundwater levels in urban areas may have high financial risks due to flooding, moisture problems (also a health risk), subsidence and deterioration of foundations.

6.2 De Raam

The model for De Raam has been created specifically to support the waterboard in their regional water management. This includes evaluation of local measures to improve the water availability during dry periods. Therefore, a resolution was used that allows for modelling at the parcel scale.

So far, changes in extreme precipitation have not been taken into account in the analysis of climate scenarios for GeoERA. If precipitation intensity changes due to the climate scenarios, an extension of the rapid discharge components might become important, as demonstrated within the Raam pilot.

Within the Lumbricus program in the Netherlands, the software of the regional groundwater model of De Raam has been coupled to a detailed hydraulic surface water model, D-FLOW FM (1D and 2D), through which fluxes between the various model components are dynamically exchanged on an hourly time step basis. This allows the calculation of refined interaction between groundwater and regional surface waters, which especially might be important for extreme rainfall events. The developments with this coupled software will be continued in 2021, especially the tuning of the different model parameters so that the linked models better match the measurements for groundwater and surface waters.

The interim results of the pilot De Raam (for the small river de Hooge Raam) demonstrates that inclusion of detailed processes of surface runoff (encountered in the 2D model, see *Figure 6.2*) and detailed hydraulic 1D calculations (*Figure 6.3*) affects the calculation results of the groundwater calculations. This development might be important for analyzing the effect of climate change on groundwater, if precipitation intensity might increase in the future.

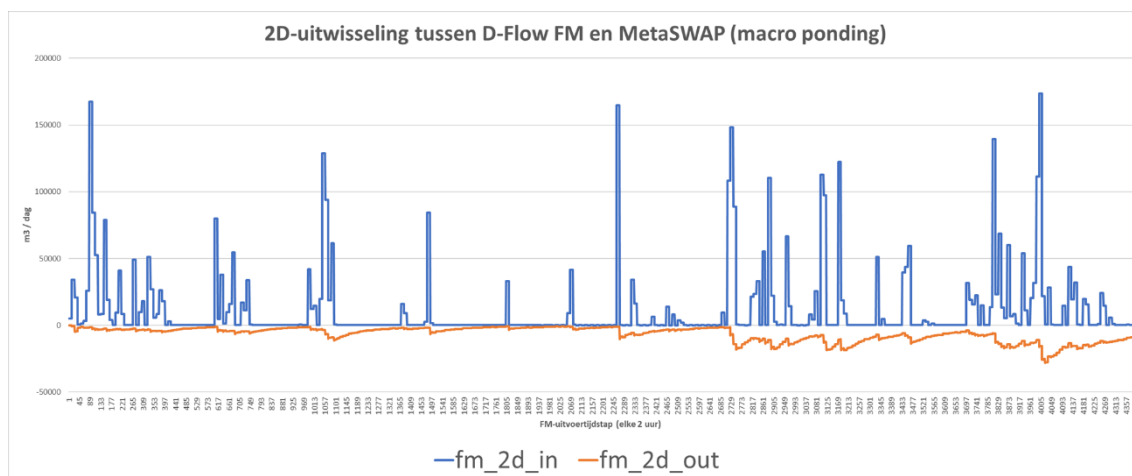


Figure 6.2 Example of exchanges of fluxes between the detailed 2D overland flow (in D-FLOW FM) and the coupled model for the unsaturated zone (MetaSWAP-MODFLOW). Blue: inflow D-FLOW FM, orange: outflow D-FLOW FM.

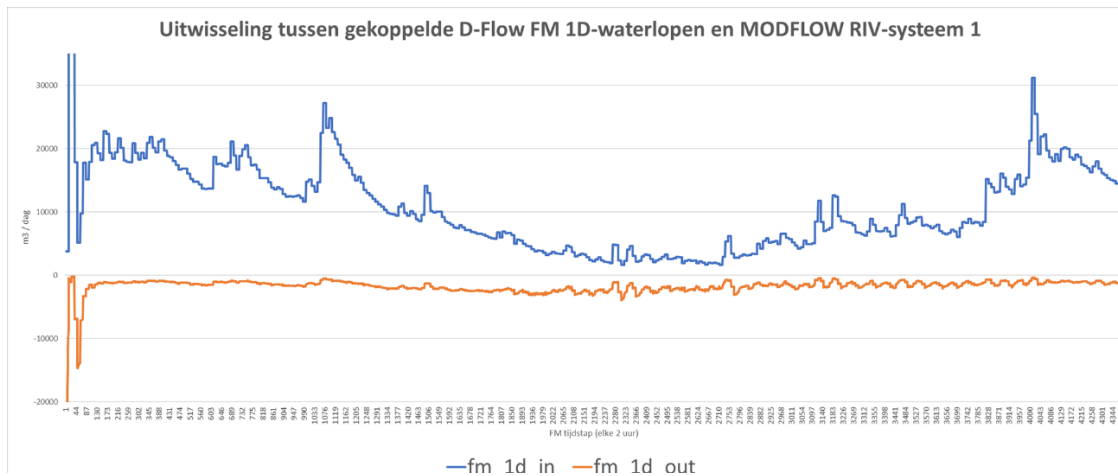


Figure 6.3 Example of exchanges of fluxes between the 1D hydraulic model (D-FLOW FM) and the river systems in the MODFLOW, as a result of the coupled software applied for the Raam region. In blue: inflow D-FLOW FM, orange: outflow MODFLOW.

The accident at the weir of Grave in December 2016 leading to exceptionally low water levels in the River Meuse for the first weeks of 2017 may provide a good opportunity to test the physically based model outside the normal situation it has been calibrated. Although the direct practical purpose may seem limited, it would provide insight into the performance outside of the calibration range. A potentially important aspect would be the release of water from storage and the subsequent refilling of the storage and the hysteresis that may be expected. The accident might provide a future test case for the coupled models of surface water and groundwater.

6.3 Metran

The physical basis of the transfer-noise modelling of time series is limited. The main aspects are the choice of explanatory variables and the shape of the response function. Metran uses an incomplete gamma function, which is connected to a physical schematization (Besbes & de Marsily, 1984).

Also, the output can illuminate physical patterns. The median response time of the groundwater head to precipitation has a similar pattern as the distance between surface waters and surface elevation (Figure 6.4).



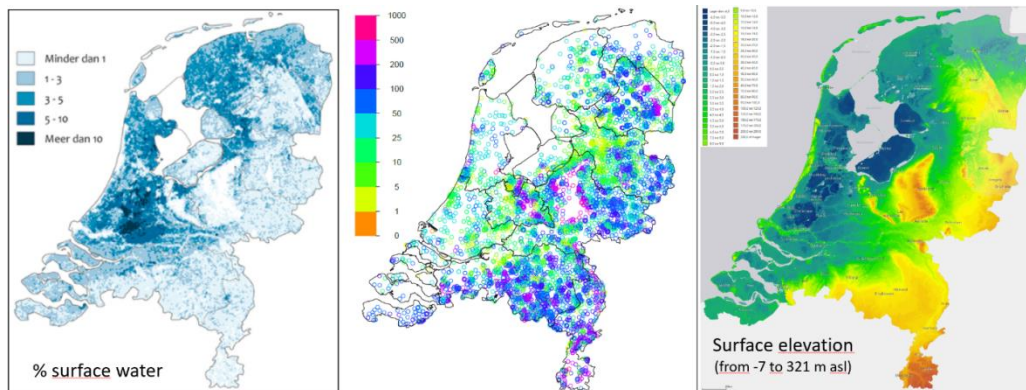


Figure 6.4 Precipitation response time [days] (centre, Figure 5.7), surface percentage of surface water (left) and surface elevation (right)

Comparison of Figure 5.6 with Figure 6.4 or Figure 5.7 shows that the total response also has a similar pattern. However, the correlation between both quantities decreases for larger values (Figure 6.5).

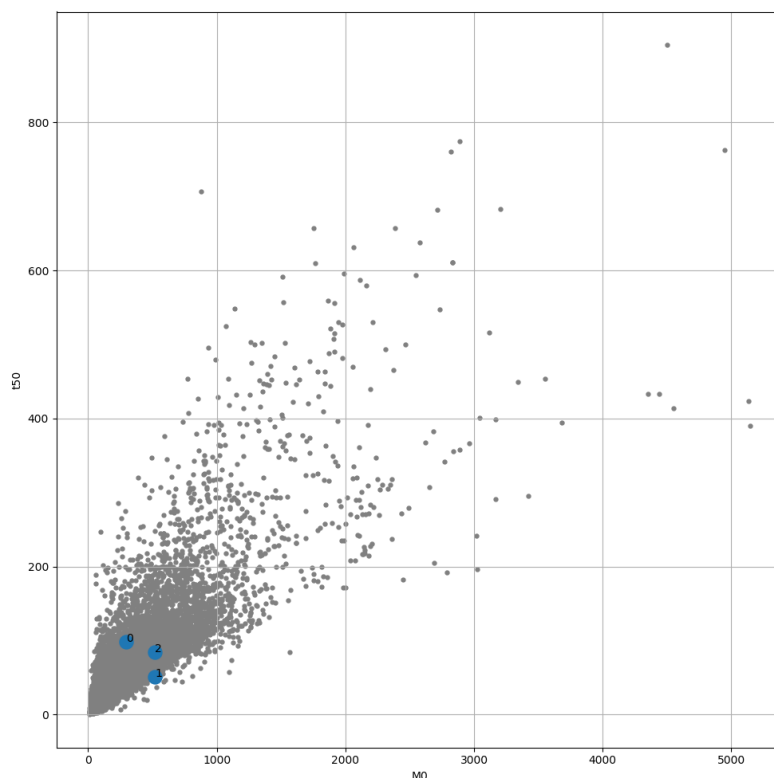


Figure 6.5 Mean precipitation response time t_{50} [days] as function of the total precipitation response MO [cm per m/d] for all good time series models together with K-means cluster centers for the upper regional aquifer (WVP2 in NHI-LHM).

The connection between these characteristics of the precipitation response and the physical properties of the groundwater system is not well known and is topic of research (e.g. Haaf et al., 2020). Here, K-means clustering (Pedregosa et al., 2011) has been used to obtain insight in the variation of ratio between the total precipitation response $M0$ and the mean precipitation response time $t50$ in Figure 6.5. The time series models of Cluster 2 have an average ratio of $M0$ and $t50$. The response time is relatively high in cluster 0 and relatively low in cluster 1.

The map in Figure 6.6 shows the clusters for piezometers in the upper regional aquifer. The Western part of the Netherlands contains mostly cluster 0. This mainly is relatively low lying polder area where the upper regional aquifer is covered by a Holocene confining layer. In the higher areas without a confining layer, the clusters 1 and 2 are interspersed.

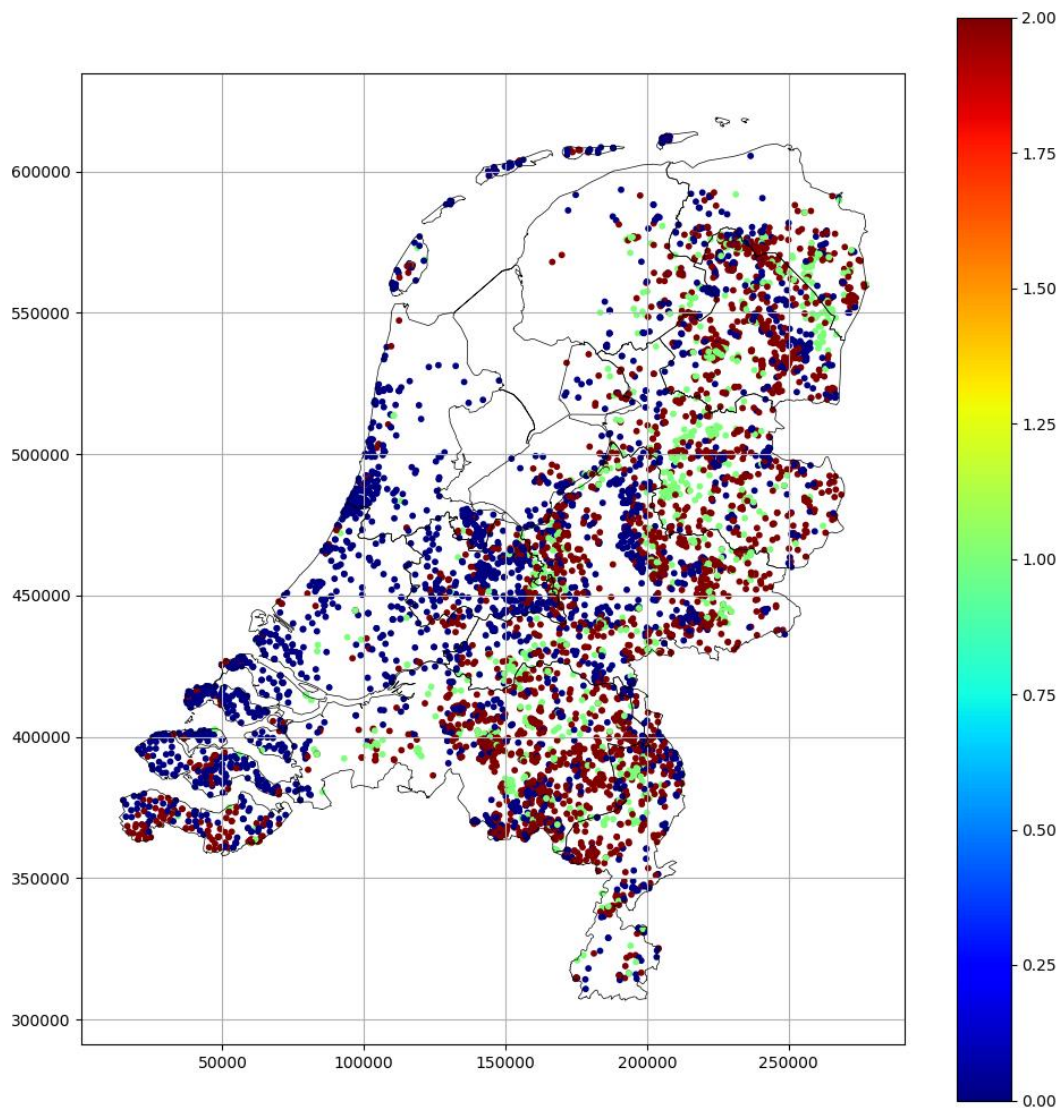


Figure 6.6 K-means clusters for the total precipitation response $M0$ (relative to the average $M0$) and ratio of $M0$ over the median response time $t50$ for the upper regional aquifer (WVP2 in NHI-LHM).

The piezometers selected for the regional pilot (subsubsection 5.2.1.2) have been simulated with Metran and the results are compared with heads from the national model NHI-LHM in section 6.3.

6.4 Comparison between models

6.4.1 Regional and national physically based distributed models

Figure 6.7 shows the difference between the effective precipitation for the national model and regional model. This figure illustrates that there are differences following from the way the meteorology has been created, using only data from weather and precipitation stations for the national model, but also radar information for De Raam. Also, the discretisation was different. The differences are small. The effective precipitation for the Raam model is about 3.5 mm/year higher than the effective precipitation of the national model, which is about 100 mm/year.

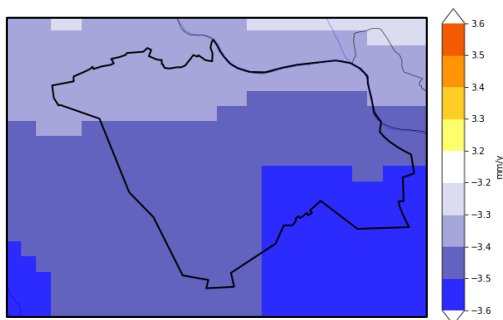


Figure 6.7. The difference between the effective precipitation of the LHM and De Raam model (mm/year). Calculated as LHM minus De Raam.

Figure 6.8 shows the depth of the phreatic groundwater table below the surface for both model for the three degrees climate scenarios.

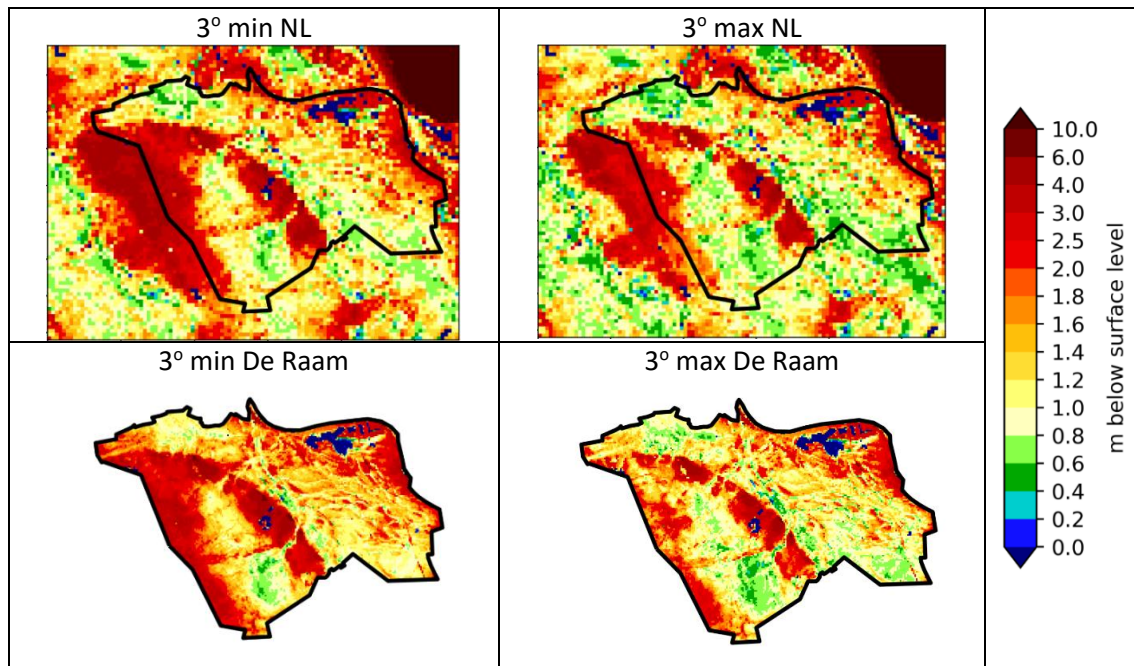


Figure 6.8. Phreatic head in m below surface level for the 3 min (left) and 3 max scenario (right). The top row are the results from the national model, the bottom row are the results of the local model of De Raam.

The phreatic head distribution of both models (see Figure 6.8) are similar, although there are some differences. The phreatic heads according to the regional model of De Raam are slightly lower compared to the national model, meaning that they are further below surface level. Moreover, due to the fine grid size of the regional model, a much more detailed head distribution can be distinguished.

The average groundwater recharge as computed by the national and regional model is spatially compared in Figure 6.10. In Figure 6.9 the average groundwater recharge in the whole area for every month is plotted. Both figures clearly indicate that the groundwater recharge according to the regional model is lower, at some points up to 200 mm/year. This corresponds to the differences that were seen in the results of the phreatic head, where it was shown that the phreatic heads according to the regional model are lower. This shows that the coarse resolution of the national model attenuates the effect of climate change.

In Figure 6.11, the recharge of the simulations with the 3° min and 3° max scenarios for the regional model and national model are compared to their reference situations. These figures show that the effect of the climate scenarios is slightly different for both models. Especially for the 3° max scenario: some regions that have a relatively large increase in recharge (at the west boundary) according to the national model, have a relatively low increase according to the regional model.

The variation of the groundwater recharge during the year as calculated by the regional model (see Figure 5.25) and for the national model (see Figure 5.14) also compare quite well. Spatially the differences are more distinct, as can be seen in Figure 6.10 and Figure 6.11.

In general, it can be concluded that the finer grid size for the regional model results in a much more detailed image of the effect of climate change in the pilot area. The national model results are only useful to describe a general effect of climate change in the area. Due to the fine grid size of the regional model, also the regional differences within the pilot area become known.

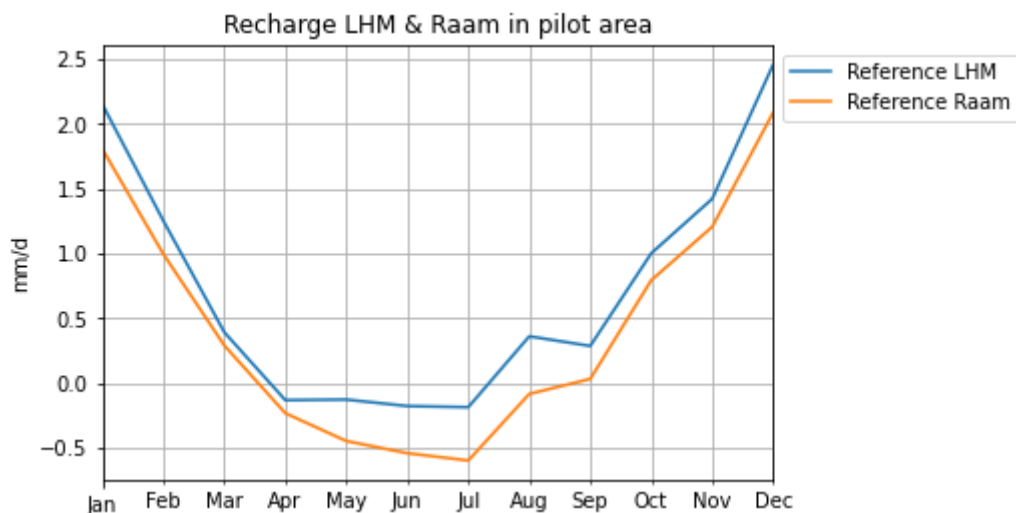


Figure 6.9. Average monthly recharge in the period 2011-2018 in pilot area De Raam as calculated by the national model (LHM, blue) and regional model (Raam, orange)

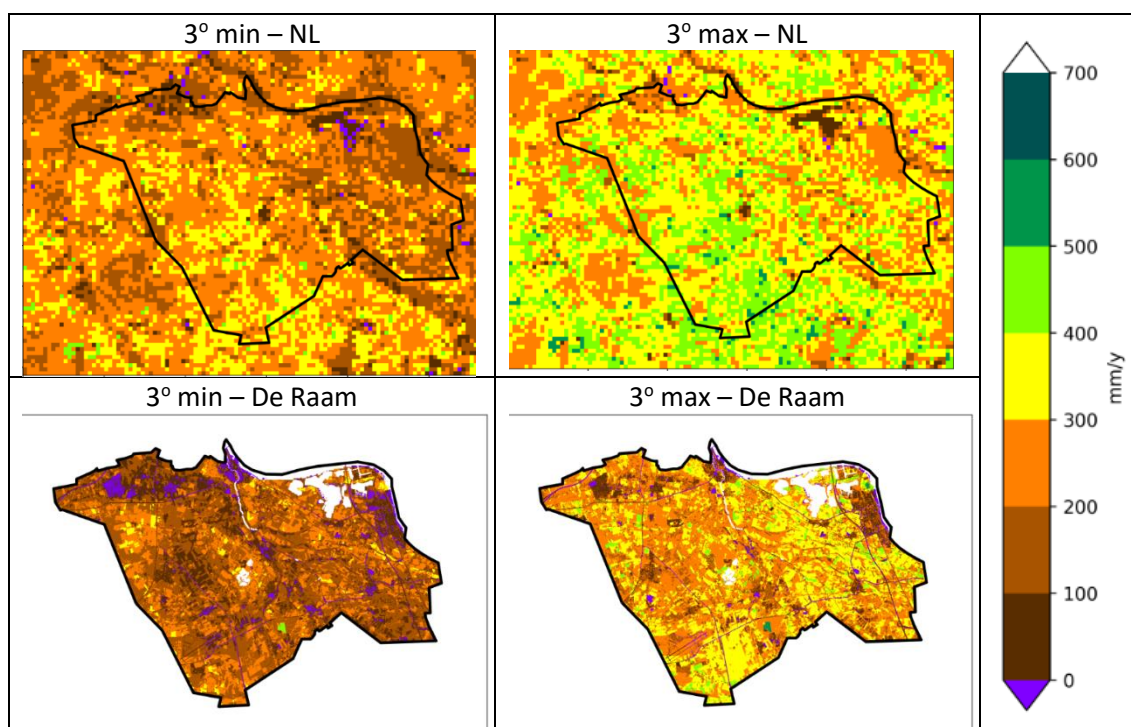


Figure 6.10. Groundwater recharge in mm/year for the 3° min scenario (left) and 3° max scenario (right). The top row are the results from the national model, the bottom row are the results of the regional model of De Raam

3° min – NL	3° max – NL	
-------------	-------------	--



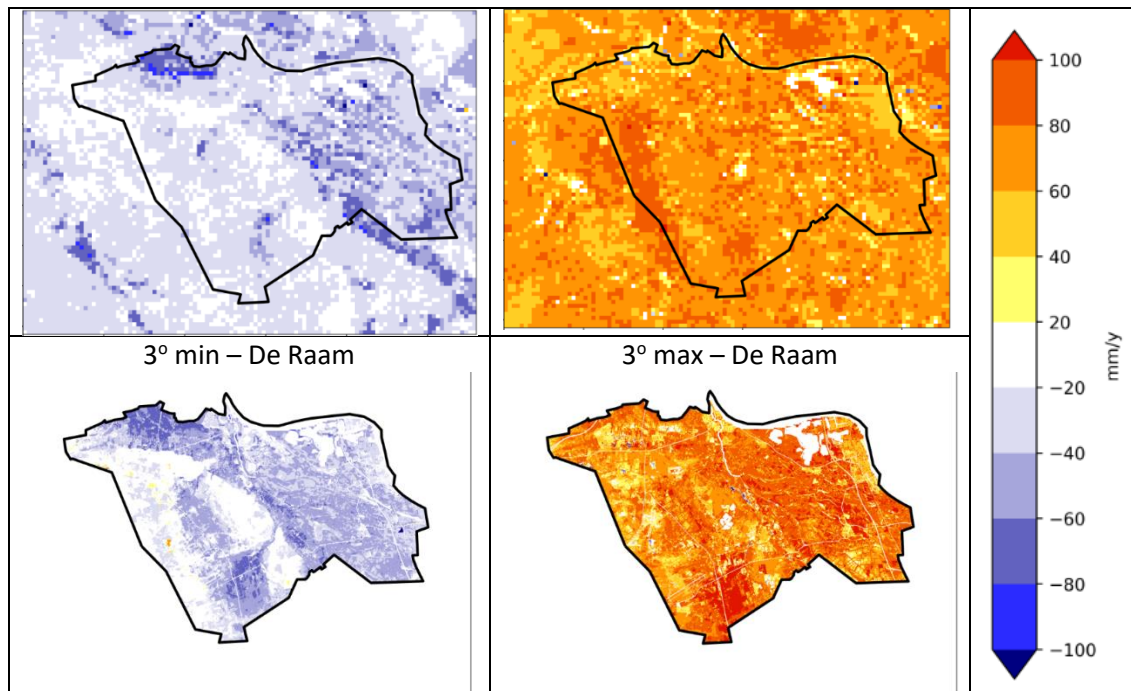


Figure 6.11. Groundwater recharge change in mm/year compared to the reference situation of the national model (top) and regional model (bottom) for the 3° min (left) and 3° max (right) scenario.

6.4.2 Physically based distributed models and time series models

The physically based distributed models NHI-LHM and de Raam have been built up from a conceptual model of the hydrology and the subsurface together with a parametrization derived from the knowledge of this physical system. The Metran models have a very limited physical base: the use of the incomplete gamma function as transfer function (Besbes & de Marsily, 1984) and the selection of explaining variables. This leads to differences in the results.

6.4.2.1 Reference situation

Figure 6.12 shows the measurements of the first piezometer of monitoring well B45B0174, which is located about 10 meters below the surface of 13.62 meters (from 3.51 to 1.5 m NAP).

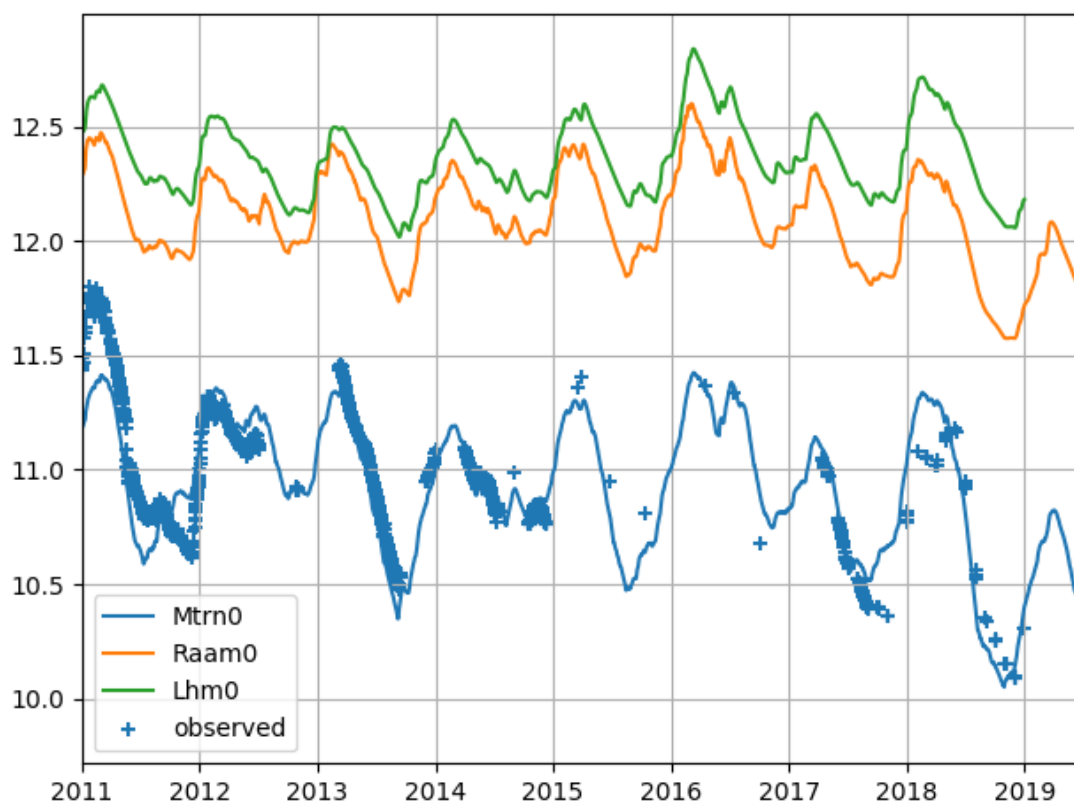


Figure 6.12 Measured groundwater heads for B45F0174001 together with simulated values from Metran (Mtrn0), de Raam model (Raam0), and NHI-LHM (Lhm0).

The main difference between the modelled heads in Figure 6.12 is the average level. That of the Metran model corresponds well with the measurements. A deviation is to be expected for the distributed models because of the spatial discretization, which leads to representative values of cells of 250 m x 250 m and 25 m x 25 m for the national and the regional model respectively. In these models the recharge processes depend on the depth of the groundwater below the surface. The difference between the actual surface elevation and the model value is 1.35 meter for the national model and 0.23 m for the regional model (see Table 6-1). This corresponds to the difference in averages of the model heads in Figure 6.12 for the National model. So, the surface processes may be simulated adequately, despite the deviation from the heads measured at this specific point.

Table 6-1 surface elevation from metadata of piezometer and models (m NAP).

Location	surface	NHI-LHM	De Raam
B45F0174	13.62	14.97	13.85
B45F0279	20.51	20.77	20.83
B46C0478	17.16	17.53	17.71

The fluctuation of all three models is less than the measured fluctuation of the groundwater heads in *Figure 6.12*, especially in the first three years of the graph. The drop of the head in the dry summer of 2018 is simulated better by Metran than the distributed models.

Figure 6.13 shows a similar graph for the upper piezometer of monitoring well B46C0478. The piezometer is perforated between 13.19 and 11.19 m NAP, while the surface elevation here is 17.16 m NAP.

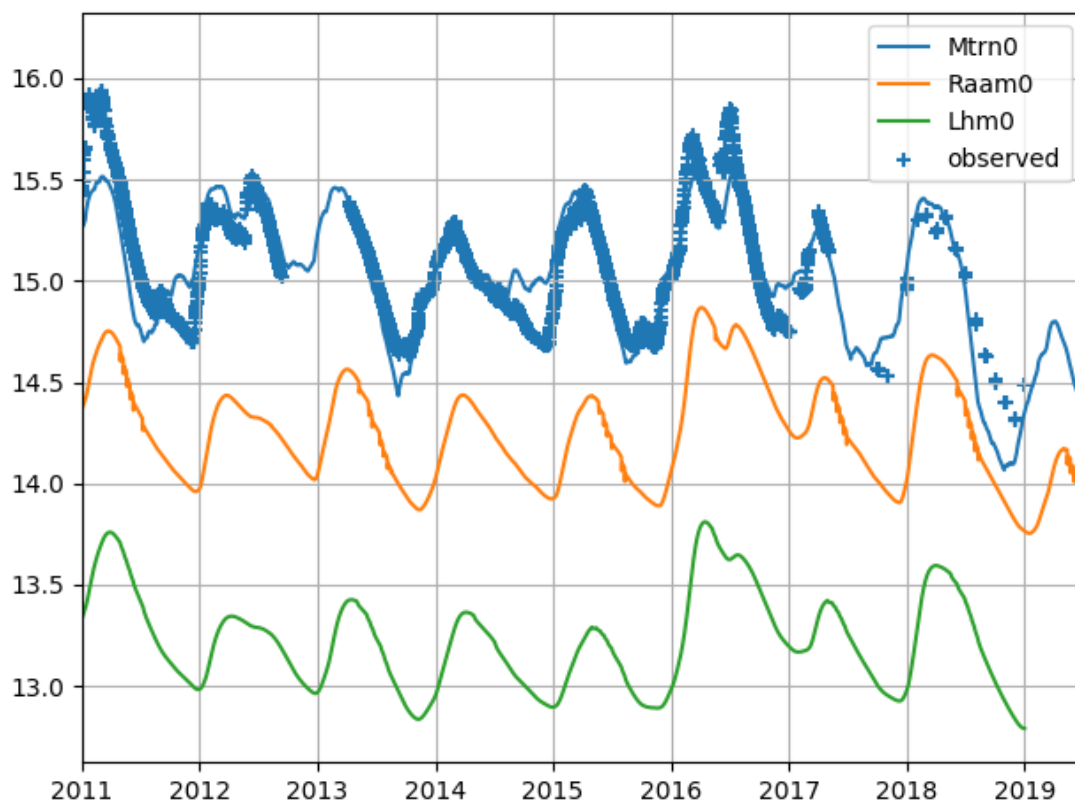


Figure 6.13 Measured groundwater heads for B46C0478001 together with simulated values from Metran, de Raam model, and NHI-LHM.

Figure 6.13 also shows a systematic difference between the models. Now the heads from the distributed models are lower, while the surface elevation is again higher (see Table 6-1). The regional model de Raam matches the measured heads much better than the national model. The distributed models simulated the fluctuation of the heads better for the year 2011. Metran overestimates the drop of the heads in 2018 and the minimum is off in timing. The distributed models underestimate the drop slightly, and model the timing better than Metran. This could be due to non-linear behaviour that the physically based models can reproduce, while the Metran model is linear.

6.4.2.2 Climate change scenarios

Figure 6.14 and Figure 6.15 show comparisons for integrated model results with time series models simulations for climate change scenarios in the upper piezometer of two monitoring wells.

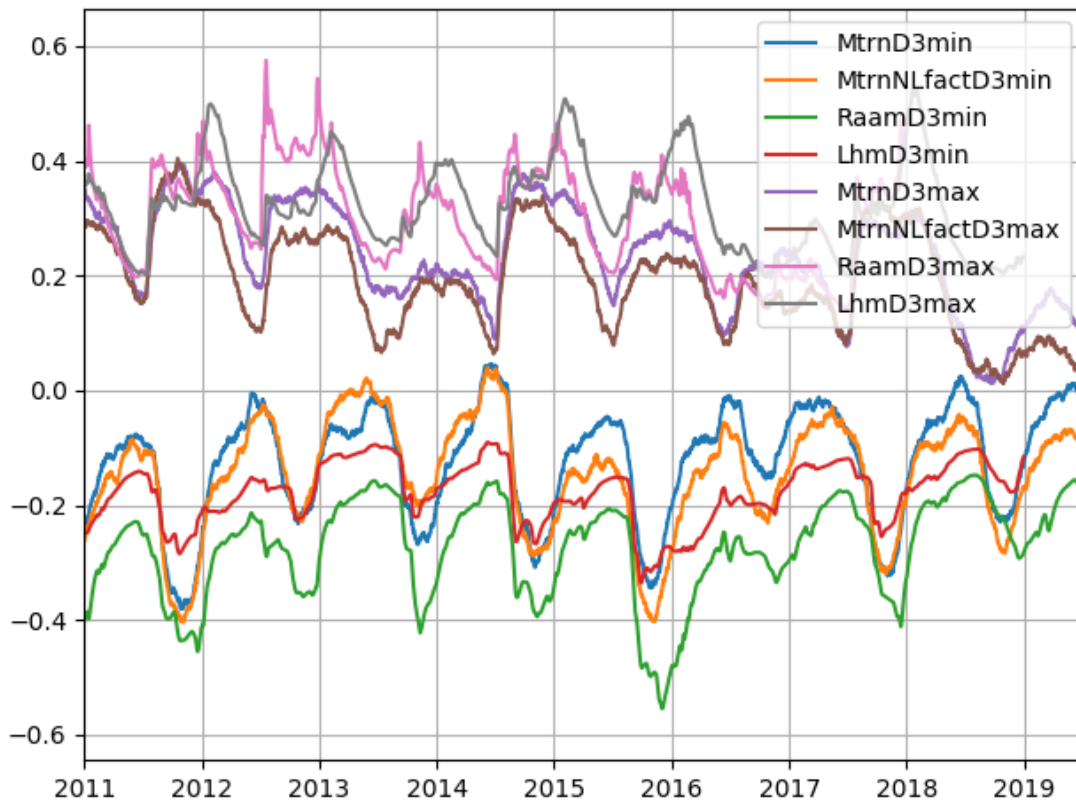


Figure 6.14 Calculated changes for the 3min and 3max climate change scenarios with respect to the reference simulation for piezometer B45F0174001.

There is some impact of the change factors visible in the two Metran simulations (Mtrn with De Raam factors, and MtrnNLfact with national factors). The difference in change factors is also contained in the integrated models. Moreover, the simulations for De Raam seem to benefit from the more detailed regional model.

The physical relations in the integrated models create different dynamics of the groundwater table than the relatively simple extrapolation of the current situation in the time series models. Because of this the changes from the integrated models are probably more reliable than from the time series models. However, given the larger deviation from the measurements for the current situation, the absolute values should be used with care.

This probably can be improved by constructing more accurate maps of the reference groundwater head by combining the measurements or time series models together with the integrated model results. This can be done by kriging with model output as a trend surface (e.g. Zaadnoordijk et al., 2021). The changes simulated by the integrated model are subsequently superimposed on this reference head map.



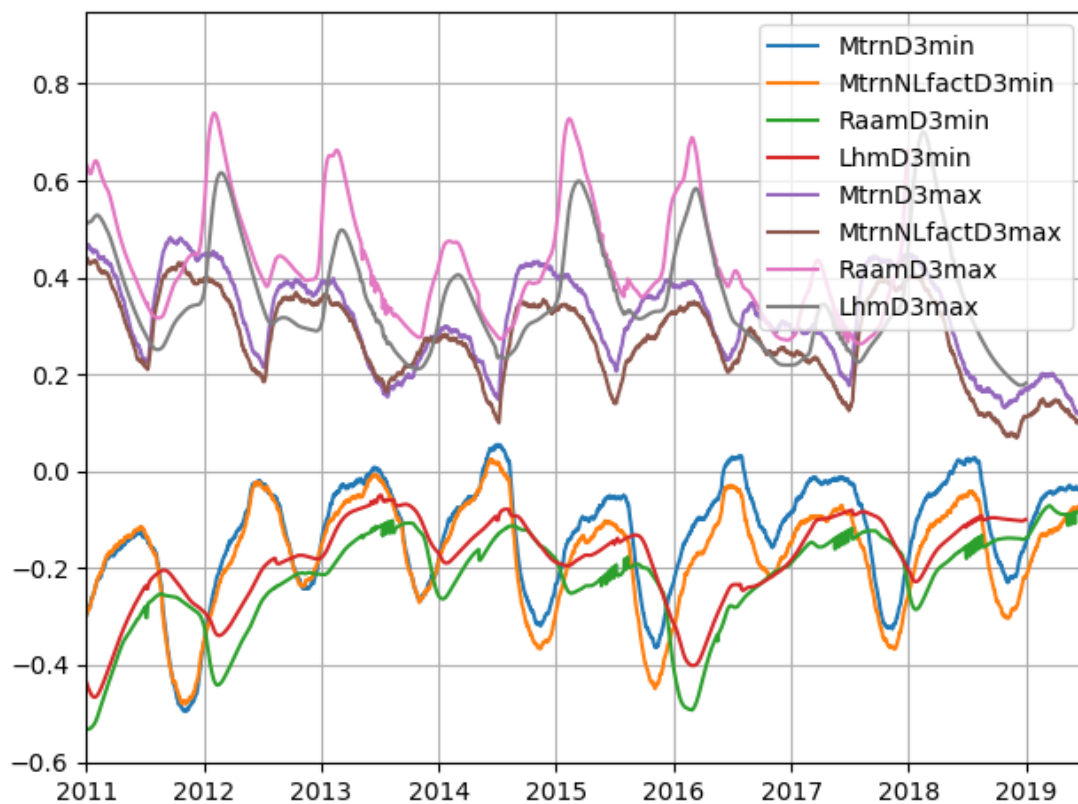


Figure 6.15 Calculated changes for the 3min and 3max climate change scenarios with respect to the reference simulation for B46C0478001.

The fact that simulations with time series models assume that the groundwater system does not change (and in case of the Metran simulations presented also assumes a linear behaviour) does limit their usefulness for propagation of climate change in the groundwater system, compared to the integrated models. On the other hand, making separate time series models for different periods is an easier way to detect whether the groundwater system has changed or temporarily behaves differently.

7 CONCLUDING REMARKS

Two pilots in the Netherlands have been investigated using integrated physically-based distributed hydrological modelling and transfer-noise time series modelling. The national pilot and the regional pilot De Raam have a large difference in resolution (250 m x 250 m and 25 m x 25 m, respectively), related to the different purposes. The national model is used for the management of the main rivers and for national policy development. The model for De Raam is intended for improving the regional water management, e.g. by evaluating concrete local measures.

A comparison of the results of the national and regional pilot has indicated that the finer resolution is necessary to study local variations within the pilot area. The national model is only able to roughly describe the effect of climate change in the pilot area. Moreover, the effect of climate change according to a regional model is also slightly more profound compared to the national model.

The time series modelling provides information only at locations of monitoring wells, although it is possible to create spatial images of various outputs.

The time series models provide more accurate history matching at the well locations, while the integrated models are better predictors for future scenarios.

The recharge calculated by the integrated models is more reliable than that of time series models calibrated only on groundwater heads. The time series model allows for an estimation of the correlation of the groundwater levels with surface water levels, which provides a limited insight in the groundwater-surface water interaction compared to the integrated models.

Both types of models can simulate climate change scenarios, albeit results of the integrated models are much more trustworthy, provided the important processes are included with an adequate parametrisation. It can be useful for climate analysis to further detail the processes within the integrated models, for example coupling with detailed crop models if crop evaporation might change in the future situation, or with detailed surface water models if the intensity of precipitation changes significantly.

The effort to setup and maintain the integrated model is much larger than for time series modelling. Combined use provides extra benefits e.g. improved spatial continuous history matching, determining important processes to include in the integrated model by time series modelling with known influences, and selection (and weighing) of piezometers to use for calibration.

8 REFERENCES

AHN2 (2013) accessed at 11-01-2019 through <http://www.ahn.nl/>

Berendrecht, W.L., F.C. van Geer (2016) A dynamic factor modeling framework for analyzing multiple groundwater head series simultaneously, *Journal of Hydrology*, volume 536, pages 50-60, <http://dx.doi.org/10.1016/j.jhydrol.2016.02.028>

Berendrecht, W.L. (2021, in prep.). Validatie en toetsing LHM 4.1. Deelrapport 1: grondwater, Berendrecht Consultancy, Harderwijk, Netherlands.

Besbes, M, G. de Marsily (1984) From Infiltration to Recharge: use of a parametric transfer function, *Journal of Hydrology*, volume 74, pages 271-293.

Besselink, D. (2018) Integrated plan development De Raam (in Dutch: Gebiedsplan Raam). Arcadis report C03091.000256.0220, Arcadis, Arnhem, Netherlands.
https://www.aaenmaas.nl/publish/pages/734/gebiedsplan_raam_-_september_2018.pdf

Bos-Burgering, L. & J. Hunink (2020) Optimalisatie grondwatermodel instrumentarium Waterschap Aa en Maas (Optimizing the groundwater modelling instrument of water board Aa and Maas; in Dutch). Deltares report 1220765-020, Delft

Bot, B. (2016) Grondwaterzakboekje GWZ2016. Bot Raadgevend Ingenieur, Rotterdam, Netherlands.

Delsman, J.R., G.H.P., S. Huizer (2021, in prep) Salinity modeling in the national groundwater model of the Netherlands Hydrological Instrument, Deltares, Utrecht, the Netherlands.

De Lange, W.J. (1991) NAGROM, een landsdekkend instrument voor grondwaterbeleid en -beheer (NAGROM a nationwide instrument for groundwater policy and management; in Dutch), *H2O*, volume 24, no. 16, pages 450-455.

De Lange, W.J., G.F. Prinsen, J.C. Hoogewoud, A.A. Veldhuizen, J. Verkaik, G.H.P. Oude Essink, P.E.V. van Walsum, J.R. Delsman, J.C. Hunink, H.Th.L. Massop, T. Kroon (2014) An operational, multi-scale, multi-model system for consensus-based, integrated water management and policy analysis: The Netherlands Hydrological Instrument, *Environmental Modelling & Software* (59), 98-108, <http://dx.doi.org/10.1016/j.envsoft.2014.05.009>.

Doherty, J., 2015. Calibration and Uncertainty Analysis for Complex Environmental Models. Watermark Numerical Computing, Brisbane, Australia. ISBN: 978-0-9943786-0-6 (see <https://pesthompage.org/>).

Foster, S.S.D., A. Lawrence, B. Morris (1998) Groundwater in urban development: assessing management needs and formulating policy strategies, World Bank Technical Paper; no. WTP 390, Washington DC, USA.
<http://documents.worldbank.org/curated/en/380261468765030397/Groundwater-in-urban-development-assessing-management-needs-and-formulating-policy-strategies390>.



Haaf, E., M. Giese, B. Heudorfer, K. Stahl, R. Barthel (2020) Physiographic and climatic controls on regional groundwater dynamics. Water Resources Research, volume 56, e2019WR026545. <https://doi.org/10.1029/2019WR026545>.

Hughes, J.D., M.J. Russcher, C.D. Langevin, R. R. McDonald, & E. D. Morway (2021, in prep) The MODFLOW 6 Application Programming Interface for simulation control and software interoperability. USGS report

Iwaco (1992) Onderzoek grondwaterbeheer Midden Nederland (GMN): Modelling watersysteem (Investigation groundwater management Central Netherlands (GMN): modelling watersysteem; in Dutch). Iwaco consultants for water and environment, Rotterdam, the Netherlands, Juli 1992.

Janssen, G., J. Hunink, T. Kroon, J. Pouwels, I. America, J. Verkaik, G. Prinsen, E. Schoonderwoerd P. van Walsum and A. Veldhuizen (2021, in prep) A Nationwide Integrated Hydrological Model for National Policy Support

Klopstra, D., W. Berendrecht, M. Pezij, V. van der Vliet, A. van Doorn en J. Velstra (2021, in prep) Validatie LHM, samenvattend hoofdrapport (Validation LHM, summary main report; in Dutch). HKV report

Kroes, J.G., J.C. van Dam, R.P. Bartholomeus, P. Groenendijk, M. Heinen, R.F.A. Hendriks, H.M. Mulder, I. Supit, P.E.V. van Walsum (2017) SWAP version 4; Theory description and user manual. Wageningen, Wageningen Environmental Research, Report 2780.

Hunink, J.C., P.E.V. van Walsum, P.T.M. Vermeulen, J.R. Pouwels, H.P. Bootsma, G.M.C.M. Janssen, W. Swierstra, G.F. Prinsen, A. Meshgi, A.A. Veldhuizen, W.J. de Lange, J. Hummelman, L.M.T. Bos-Burgering en T. Kroon (2019) Veranderingsrapportage LHM 4.0; Actualisatie van het lagenmodel, het topsysteem en de bodem-plant relaties (Change report LHM 4.0; Actualisation of the subsurface schematisation, the topsysteem and soil-plant relations; in Dutch), Deltares report 11203718-000-BGS-0001

Janssen, G.M.C.M., P.E.V. van Walsum, I. America, J.R. Pouwels, J.C. Hunink, P.T.M. Vermeulen, A. Meshgi, G.F. Prinsen, N. Mulder, M. Visser en T. Kroon. Veranderingsrapportage LHM 4.1; Actualisatie van het lagenmodel, het topsysteem en de bodemplant relaties. Deltares rapport 11205261-000-BGS-0001, 2020

Klein Tank, A., J. Beersma, J. Bessembinder, B. Van den Hurk, G. Lenderink, G. (2014). KNMI'14: Climate Change scenarios for the 21st Century—A Netherlands perspective. Report, KNMI, de Bilt, Netherlands. <http://www.climatescenarios.nl>

KNMI (2011) Klimaatatlas, accessed at 10-01-2019 through <http://www.klimaatatlas.nl/>.

Kroon, T., A.A. Veldhuizen, L.M.T. Burgering, P.E.V. van Walsum, G. Janssen, F.J.E. van der Bolt, J. Verkaik (2017) Improvements National Hydrological Model NHI-LHM: preparation for water



quality simulation (in Dutch: Veranderingsrapportage LHM 3.3.0; ontwikkelingen ten behoeve van de waterkwaliteit. Deltares report 11200573-000-BGS-0001, Deltares, Utrecht, Netherlands.

Lieste, R., K. Kovar, J.G.W. Verlouw, J.B.S. Gan (1993) Development of the GIS-based "RIVM National Groundwater Model for The Netherlands (LGM)" In: Application of Geographic Information Systems in Hydrology and Water Resources (ed. by K. Kovar & H. P. Nachtnebel) (Proc. Int. Conf. HydroGIS'93, Vienna, April 1993), IAHS Publication No. 211, pages 641-651.

NHI dataportal (2019) Water distribution network of the national hydrological model, accessed at 11-01-2019 through <https://data.nhi.nu/>.

Obergfell, C., M. Bakker, K. Maas (2019). Estimation of average diffuse aquifer recharge using time series modeling of groundwater heads. Water Resources Research, Volume 55. <https://doi.org/10.1029/2018WR024235>.

Prinsen, G., F. Sperna Weiland and E. Ruijgh (2015). The Delta Model for Fresh Water Policy Analysis in the Netherlands. Water Resour Manage 29:645–661.

Sperna Weiland, F., B. van der Hurk, T. Kroon, E. Schoonderwoerd (2021, in prep.) Consistent projections of European scale future hydrological change for 1 and 3 degrees warming scenarios, to be submitted.

TNO-GSN (2021a) REGIS II: the hydrogeological model, TNO Geological Survey of the Netherlands, Utrecht, <https://www.dinoloket.nl/en/regis-ii-hydrogeological-model>.

TNO-GSN (2021b) Detailing the upper layers with GeoTOP, TNO Geological Survey of the Netherlands, Utrecht, <https://www.dinoloket.nl/en/detailing-the-upper-layers-with-geotop>.

Topografische Dienst Kadaster (2019) Surface water in the Netherlands (in Dutch), accessed at 11-01-2019 through <https://www.clo.nl/indicatoren/nl1401-oppervlaktewater-in-nederland>.

Van der Gaast, J.W.J., P.J.T. Van Bakel (1997) Differentiation of water courses for pesticides (in Dutch: Differentiatie van waterlopen ten behoeve van bestrijdingsmiddelen in Nederland). Rapport 526, SC-DLO. Wageningen, Netherlands.

Vermeulen, P.T.M, F.J. Roelofsen, J. Hunink, G.M.C.M. Janssen, B. Romero Verastegui, J. van Engelen & M. Russcher (2020) iMOD 5.1 User Manual. Deltares rapport.

Vewin (2017) Drinkwaterstatistieken 2017. Van bron tot kraan (Drinkwater statistics, from source to tap; in Dutch)

Van Walsum, P. E. V., (2017) SIMGRO V7.3.3.2, Users Guide. Tech. Rep. Alterra-Report 913.2, Alterra, Wageningen. 111 pp.

Van Walsum, P.E.V., and A.A. Veldhuizen (2011). Integration of models using shared state variables: Implementation in the regional hydrologic modelling system SIMGRO. Journal of Hydrology 409 (2011) 363–370.



Witte, J.P.M., W.J. Zaadnoordijk, J.J. Buyse (2019) Forensic Hydrology Reveals Why Groundwater Tables in The Province of Noord Brabant (The Netherlands) Dropped More Than Expected, Water, Volume 11, No. 478, doi:10.3390/w11030478.

Wosten, H, F.de Vries, T. Hoogland, H. Massop, A. Veldhuizen, H. Vroon, J. Wesseling, J. Heijkers, A. Bolman (2012) Bofek2012, new soil physical schematization of the Netherlands (in Dutch: de nieuwe bodemfysische schematisatie van Nederland) Alterra rapport 2387, Alterra, Wageningen, Netherlands. <http://edepot.wur.nl/247678>

Zaadnoordijk, W.J. (2018) Time series modeling of piezometric heads – determination of precipitation response in the presence of other stresses and hydrogeological heterogeneity, AGU Fall Meeting 2018 - poster H23O-2160, Washington DC, USA, 10-14 December 2018, <https://www.essoar.org/doi/abs/10.1002/essoar.10500086.1>.

Zaadnoordijk, W.J., A. Lourens (2019) Groundwater dynamics in the aquifers of the Netherlands, TNO report TNO 2019 R12031, TNO Geological Survey of the Netherlands, Utrecht, Netherlands.

Zaadnoordijk, W.J., S.A.R. Bus, A. Lourens, W.L. Berendrecht (2019) Automated Time Series Modeling for Piezometers in the National Database of the Netherlands, Groundwater, volume 57, no. 6, pages 834-843, <https://onlinelibrary.wiley.com/doi/epdf/10.1111/gwat.12819>, open access.

Zaadnoordijk, W.J., A. Lourens, J.M.M. Hettelaar (2021) Kaarten met grondwaterisohypsen in de provincie Utrecht 2009-2020 (maps with groundwater head contours in the province of Utrecht; in Dutch), commissioned by the Province of Utrecht, report TNO 2021 R10281, TNO-GSN, Utrecht, the Netherlands.



Deliverable 4.2

PILOT DESCRIPTION AND ASSESSMENT

Permo-Triassic aquifer (United Kingdom)

Authors and affiliation:

**Majdi Mansour, Vasileios
Christelis**

British Geological Survey (BGS)

This report is part of a project that has received funding by the European Union's Horizon 2020 research and innovation programme under grant agreement number 731166.



Deliverable Data	
Deliverable number	D4.2
Dissemination level	Public
Deliverable name	Pilots description and assessment report for recharge and groundwater vulnerability
Work package	WP4
Lead WP	BRGM, BGS
Deliverable status	
Version	Version 3
Date	23/3/2021

[This page has intentionally been left blank]

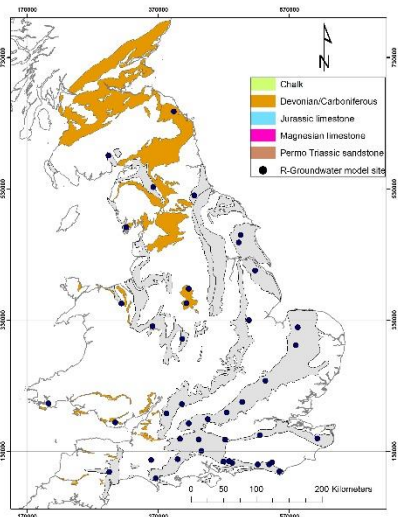
LIST OF ABBREVIATIONS & ACRONYMS

BGS	British Geological Survey
CC	Climate Change
EU	European Union
FAO	Food and Agriculture Organization
GCM	Global Circulation Models
GSO	Geological Survey Organization
ISIMIP	Inter Sectoral Impact Model Inter-comparison Project
NSE	Nash-Sutcliffe Efficiency
PET	Potential Evapo-Transpiration
R	Regression coefficient error
WP	Work Package

TABLE OF CONTENTS

LIST OF ABBREVIATIONS & ACRONYMS	5
1 EXECUTIVE SUMMARY	5
2 INTRODUCTION	7
3 PILOT AREA	9
3.1 Site description and data	9
3.1.1 Index boreholes in the Carboniferous Limestone and Devonian sandstone aquifers in the UK	9
3.1.2 Topography	11
3.1.3 Land use	12
3.1.4 Rainfall	13
3.1.5 Potential evaporation	14
3.1.6 Hydrogeology	15
3.1.7 Groundwater levels	16
3.2 Climate change challenge	16
4 METHODOLOGY	18
4.1 Methodology and climate data	18
4.1.1 AquiMod	18
4.1.2 Metran	18
4.1.3 The distributed recharge model ZOODRM applied at the UK scale	19
Climate data	20
4.2 Model set-up	21
4.2.1 AquiMod	21
4.2.2 Metran	24
4.2.3 National scale model (ZOODRM)	25
4.3 Model calibration	27
4.3.1 Calibration of AquiMod models	27
4.3.2 Calibration of Metran models	29
4.3.3 Calibration of the UK national scale model using ZOODRM	29
5 RESULTS AND CONCLUSIONS	31
5.1 Historical recharge values	31
5.2 Projected recharge values	33
REFERENCES	41
APPENDICES	43
Appendix A: AquiMod methodology	43
The soil moisture module	44
The unsaturated zone module	45
The saturated zone module	45
Limitations of the model	47
Model input and output	47
Appendix B: Metran methodology	49
Limitations	50
Time step	50
Model output	50
Model quality	51
Recharge	51

1 EXECUTIVE SUMMARY

Pilot name	Boreholes in the Devonian / Carboniferous Limestone aquifer	
Country	United Kingdom	
EU-region	North-western Europe	
Area (km ²)	NA	
Aquifer geology and type classification	Consists of Monitoring boreholes for water resources management up to 600 m thick. A possible yield up to 125 l/sec of good quality hard to moderately hard water from the upper parts of the aquifer.	
Primary water usage	Irrigation / Drinking water / Industry	
Main climate change issues	Risk of high precipitation causing increased river flows and flooding. Risk of drought.	
Models and methods used	Lumped groundwater modelling (AquiMOD). Transfer Function-Noise Model (Metran)	
Key stakeholders	Government. Research institutes. Water companies.	
Contact person	British Geological Survey. Andrew McKenzie	

This report describes the work undertaken by the British Geological Survey (BGS/UKRI) as a part of TACTIC WP4 to calculate historical and future groundwater recharge across the outcrop of Devonian / Carboniferous Limestone aquifer and at selected observation boreholes within these aquifers. Multiple tools, selected from the TACTIC toolbox that is developed under WP2 of the TACTIC project, have been used for this purpose.

The Carboniferous Limestone aquifer in England and Wales include a wide variety of rock types that are fractured and well developed as aquifers in some areas. Where it is a major aquifer, the Carboniferous Limestone aquifer exhibit 'karstic' hydrogeological behaviour. The Devonian sediments of south Wales and the Welsh borderlands are continental deposits known as the Old Red Sandstone facies. In Scotland, the Devonian sandstones in Fife and eastern Scotland are one of the most productive bedrock aquifers in Scotland (Macdonald et al., 2005).

Three tools have been used to estimate the recharge values. These are the lumped parameter computer model Aquimod (Mackay et al., 2014a), the transfer function-noise model Metran (Zaadnoordijk et al., 2019), and the distributed recharge model is developed ZOODRM (Mansour and Hughes, 2004). Future climate scenarios are developed based on the ISIMIP (Inter Sectoral Impact Model Inter-comparison Project (www.isimip.org) datasets. The resolution of the data is 0.5°x0.5° global grid and at daily time steps. As part of ISIMIP, much effort has been made to standardise the climate data (e.g. bias correction).

The estimation of the recharge model using the lumped model Aquimod is achieved by running the model in Monte Carlo mode. This produces many runs that are equally acceptable and consequently the uncertainty in the estimated recharge values can be assessed. The application of additional tools provides an additional mean to assess this uncertainty. Groundwater data at three boreholes are used in this model. The differences between the 75th and 25th percentile recharge values are found to be between 15% and 26%, which indicates a relatively high degree of uncertainty. In addition, the recharge values estimated using the distributed recharge model are found to be significantly higher than those estimated using the lumped model. It must be noted that the distributed recharge model calculates potential recharge while the lumped model calculates actual recharge. The absolute recharge values calculated by the transfer function-noise model Metran are also different from those calculated by the lumped model. The transfer function model estimates lower values at two boreholes and higher values at the third borehole.

Future recharge values calculated using the projected rainfall and potential evaporation values are -3.5 to 12.5% different from historical values on average. The 3o Max scenario, the wettest used in this work, produces values that are very different from the historical ones. This is observed in the output of both the lumped and the distributed models. Finally, future estimates are discussed in this report using long term average recharge values. It is recommended to carry out further analysis to these output in order to understand the temporal changes in recharge values in future, especially over the different seasons. In addition, it is recommended that the values and conclusion produced from this work should be compared to those obtained from different studies that applies future climate data obtained from different climate models.

2 INTRODUCTION

Climate change (CC) already has widespread and significant impacts on Europe's hydrological systems including groundwater bodies, which is expected to intensify in the future. Groundwater plays a vital role for the land phase of the freshwater cycle and has the capability of buffering or enhancing the impact from extreme climate events causing droughts or floods, depending on the subsurface properties and the status of the system (dry/wet) prior to the climate event. Understanding the hydrogeology is therefore essential in the assessment of climate change impacts. Providing harmonised results and products across Europe is further vital for supporting stakeholders, decision makers and EU policies makers.

The Geological Survey Organisations (GSOs) in Europe compile the necessary data and knowledge of the groundwater systems across Europe. To enhance the utilisation of these data and knowledge of the subsurface system in CC impact assessments, the GSOs, in the framework of GeoERA, has established the project "Tools for Assessment of Climate change Impact on Groundwater and Adaptation Strategies – TACTIC". By collaboration among the involved partners, TACTIC aims to enhance and harmonise CC impact assessments and identification and analyses of potential adaptation strategies.

TACTIC is centred around 40 pilot studies covering a variety of CC challenges as well as different hydrogeological settings and different management systems found in Europe. Knowledge and experiences from the pilots will be synthesised and provide a basis for the development of an infrastructure on CC impact assessments and adaptation strategies. The final projects results will be made available through the common GeoERA Information Platform (<http://www.europe-geology.eu>).

The specific TACTIC activities focus on the following research questions:

- What are the challenges related to groundwater- surface water interaction under future climate projections (TACTIC WP3).
- Estimation of renewable resources (groundwater recharge) and the assessment of their vulnerability to future climate variations (TACTIC WP4).
- Study the impact of overexploitation of the groundwater resources and the risks of saline intrusion under current and future climates (TACTIC WP5).
- Analyse the effectiveness of selected adaptation strategies to mitigate the impacts of climate change (TACTIC WP6).

This report describes the work undertaken by the British Geological Survey (BGS/UKRI) as a part of TACTIC WP4 to calculate groundwater recharge at selected locations within the Permo-Triassic sandstone aquifer. WP4 is divided into seven tasks that cover the following activities: Review of tools and methods and identification of data requirements (Task 4.1), identification of principal aquifers and their characteristics aided by satellite data (Task 4.2), recharge estimation and its evolution under climate change scenarios in the principal aquifers (Task 4.3), analysis of long-term piezometric time series to evaluate aquifer vulnerability to climate change (Task 4.4), assessment of subsidence in aquifer systems using DInSAR satellite data (Task 4.5),

development of a satellite based net precipitation and recharge map at the pan-European scale (Task 4.6), and tool descriptions and guidelines (Task 4.7).

The work presented here is related to Task 4.3 that aims at the estimation of recharge under current and future climates. This is undertaken using multiple tools selected from the TACTIC toolbox that has been developed under WP2 of the TACTIC project. The toolbox is a collection of groundwater models, scripts, spreadsheets that serves all the activities identified in TACTIC workpackages. Here we use the lumped groundwater model *AquiMod* (Mackay et al., 2014a and Mackay et al., 2014b) and the Transfer Function-Noise Model *Metran* (Zaadnoordijk et al., 2019) with main challenge to calibrate these models to reproduce the behaviour of the observed groundwater level time series. The calibrated models are then used to calculate historical and future recharge values. In addition to these two models, we apply the UK national scale recharge model (Mansour et al., 2018) to validate the calculated recharge values and also to address the uncertainty associated with the calculation of these values.

3 PILOT AREA

3.1 Site description and data

3.1.1 *Index boreholes in the Carboniferous Limestone and Devonian sandstone aquifers in the UK*

The Carboniferous Limestone aquifer in England and Wales include a wide variety of rock types, such as mudstones, siltstones and sandstones in addition to the limestones. The latter are fractured and well developed as aquifers in the Peak District of Derbyshire, the Mendip Hills, North and South Wales, and northwest Yorkshire (Allen et al., 1997). Where it is a major aquifer, the Carboniferous Limestone aquifer exhibit 'karstic' hydrogeological behaviour.

The Devonian sediments of south Wales and the Welsh borderlands are continental deposits known as the Old Red Sandstone facies (Robins and Davis, 2015). The sediments are divided into the Lower Old Red Sandstone and Upper Old Red Sandstone and there is a major unconformity between them.

In Scotland, the Devonian sandstones in Fife and eastern Scotland are one of the most productive bedrock aquifers in Scotland (Macdonald et al., 2005). The Carboniferous sedimentary rocks have been extensively mined for coal and are largely found in the Midland Valley, with minor outcrops in southern Scotland (O Dochartaigh et al., 2015).

Table 1 shows a list of boreholes located in the Carboniferous Limestone aquifer and to lumped groundwater models are built. These models are used to estimate the historical and future recharge values at these boreholes.

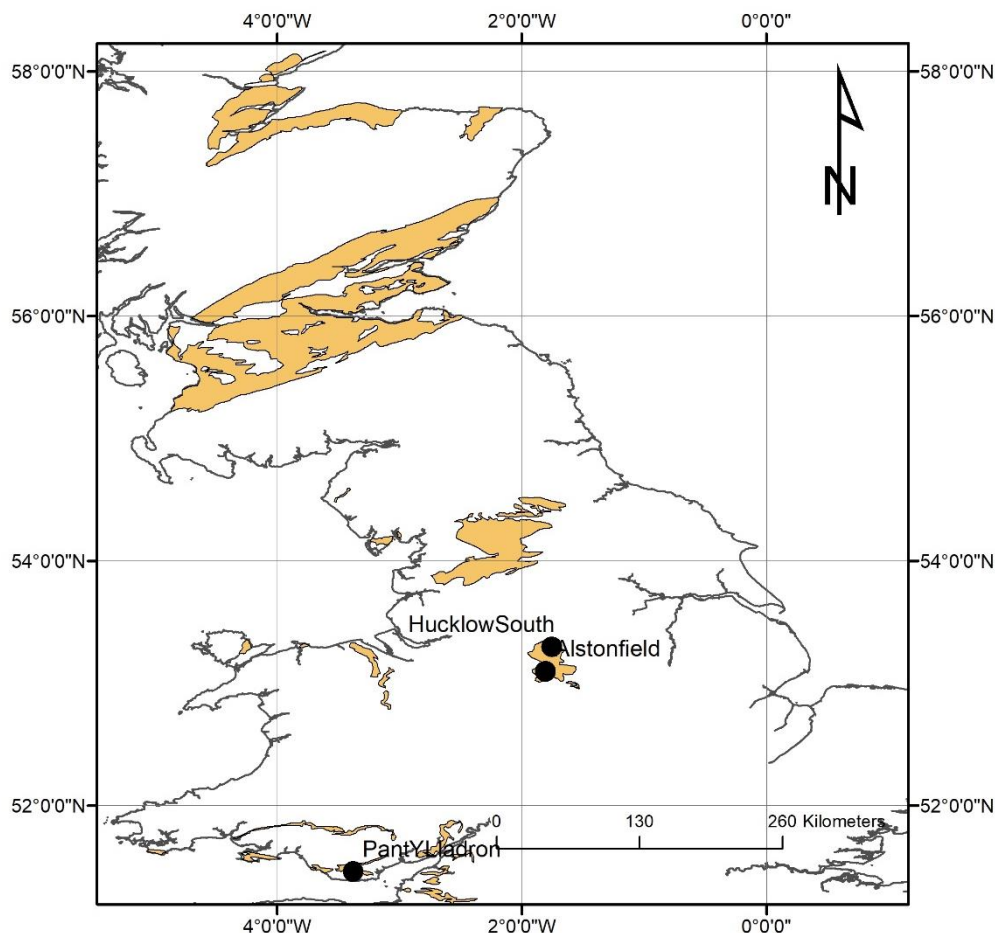


Figure 1. Extent of the Devonian sandstone / Carboniferous Limestone aquifer and borehole locations.

Table 1. Description of observation boreholes

Borehole name	Location	GWs record	Hydrogeological response
Hucklow South	North of England	1969-2012	The hydrograph has more than one peak in a year due to response to rainfall events.
Alstonefield	Northwest of England	1974-current	The hydrograph is very responsive to seasonal recharge. It has a rapid and peaky response to individual rainfall events through the winter.
Pant Y Lladron	South of Wales	1996-current	The hydrograph shows an annual sinusoidal pattern with significant yearly fluctuations of approximately 20 metres.



3.1.2 Topography

The Devonian/ Carboniferous Limestone aquifers discussed in this report cover different parts across the United Kingdom. Figure 2 shows the ground elevations as obtained from a digital terrain map (Nextmap, 2000). It is clear that the outcrops of the aquifers cover lowlands as well as hills reaching approximately 600 m above sea level. Infiltration recharge drives the groundwater to discharge areas where it appears in the form of springs at the periphery of the hills. Significant quantities of spring flows are used for public water supplies.

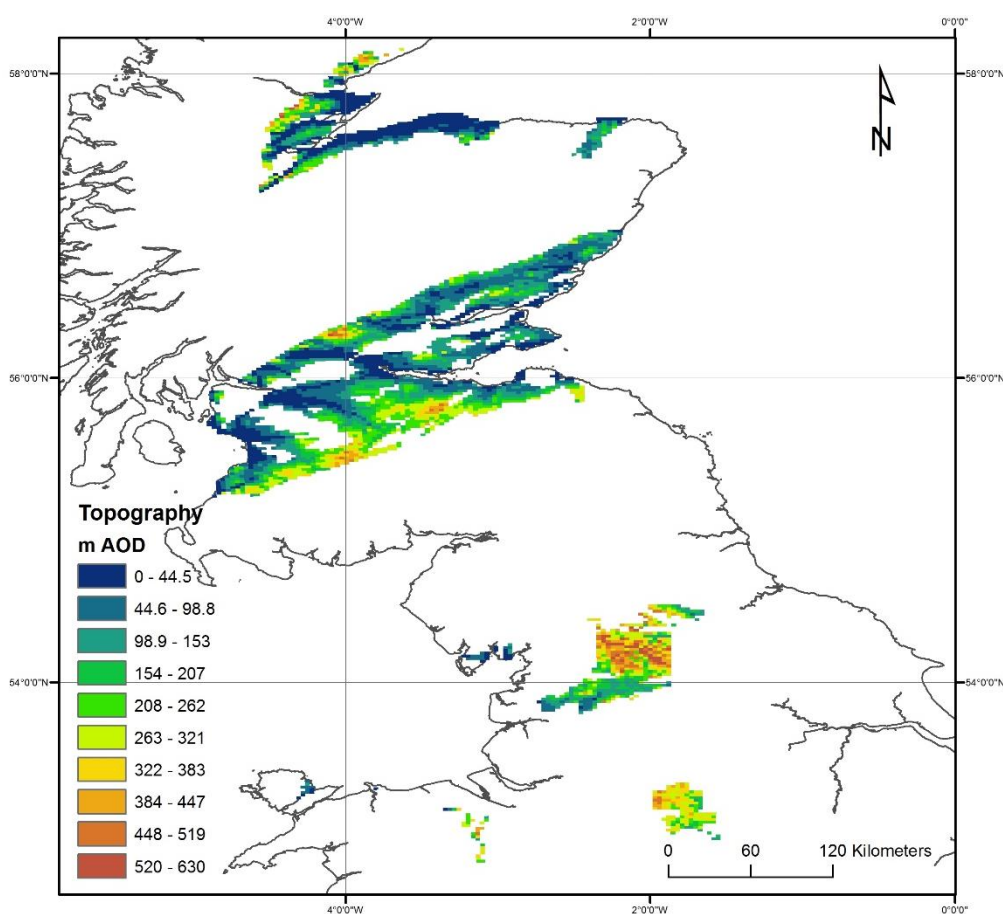


Figure 2. Topography map over the Devonian sandstone / Carboniferous Limestone formation

3.1.3 Land use

The dominant landuse over the aquifer outcrop is mainly arable and improved grassland; however, heath is the majority landuse over the hills especially in north of England. The outcrop incorporates a number of urban and industrial areas including Glasgow (Figure 3). Figure 3 shows the spatial distribution of landuse classes over the Permo-Triassic outcrop (Bibby, 2009).

Landuse data can be extracted from this map at the selected boreholes to specify the model parameters that control evapo-transpiration, which is an important component of the total water balance produced by the applied models. Specific information about the landuse types at the selected boreholes are listed in Table 2.

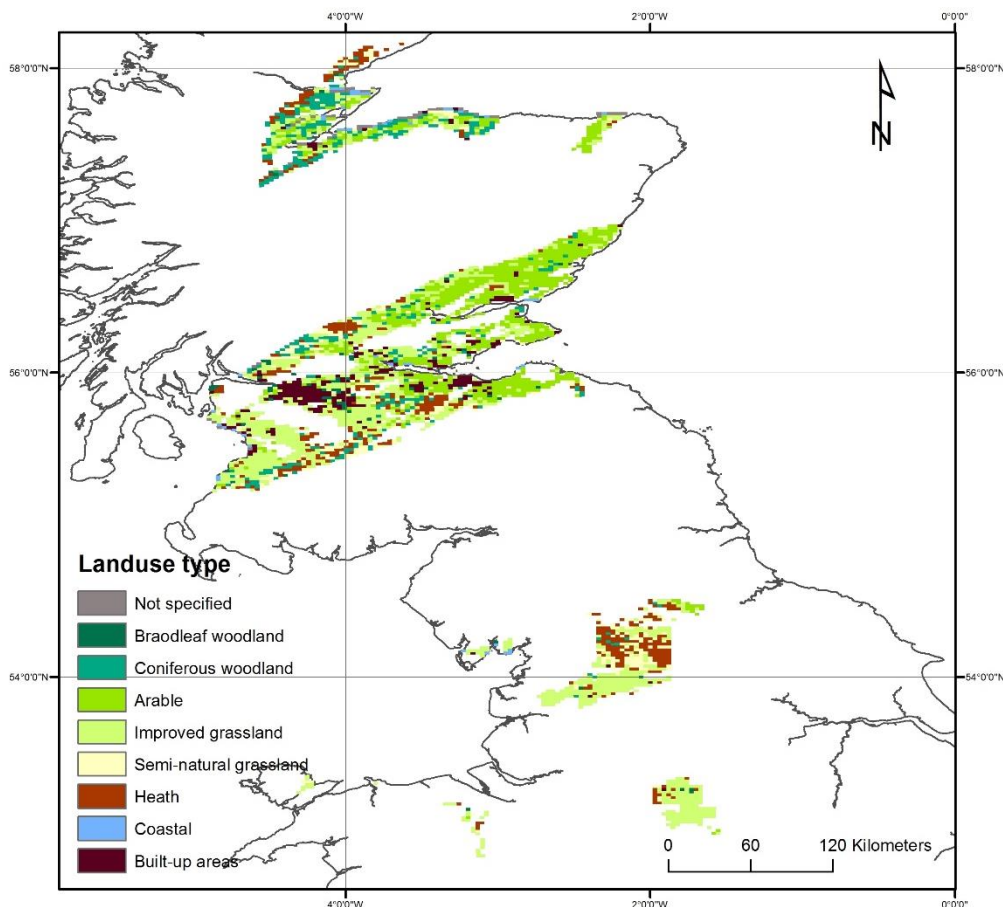


Figure 3. Map of land use over the Devonian sandstone / Carboniferous Limestone formation

3.1.4 Rainfall

Daily rainfall raster data (1×1 km) were obtained from the Centre for Ecology and Hydrology (CEH) and were used to retrieve the daily rainfall values at the grid nodes pertain to the Devonian and Carboniferous Limestone aquifers. The long-term average (LTA) rainfall across the outcrop of these aquifers is approximately $1050 \text{ mm year}^{-1}$ (2.87 mm day^{-1}); however, high rainfall values more than above $1825 \text{ mm year}^{-1}$ (5 mm day^{-1}) are observed in the areas in both north of England and Scotland (Figure 4).

Spatially distributed rainfall data are available at daily time steps starting from 1961 to 2016 (CEH). While the size of this time step is coarse to represent storm events for hydrological analysis, it is fine enough to calculate recharge values to drive groundwater models. These data are, therefore, used to drive the lumped models. Table 2 presents specific information about the rainfall values at the selected Carboniferous Limestone boreholes.

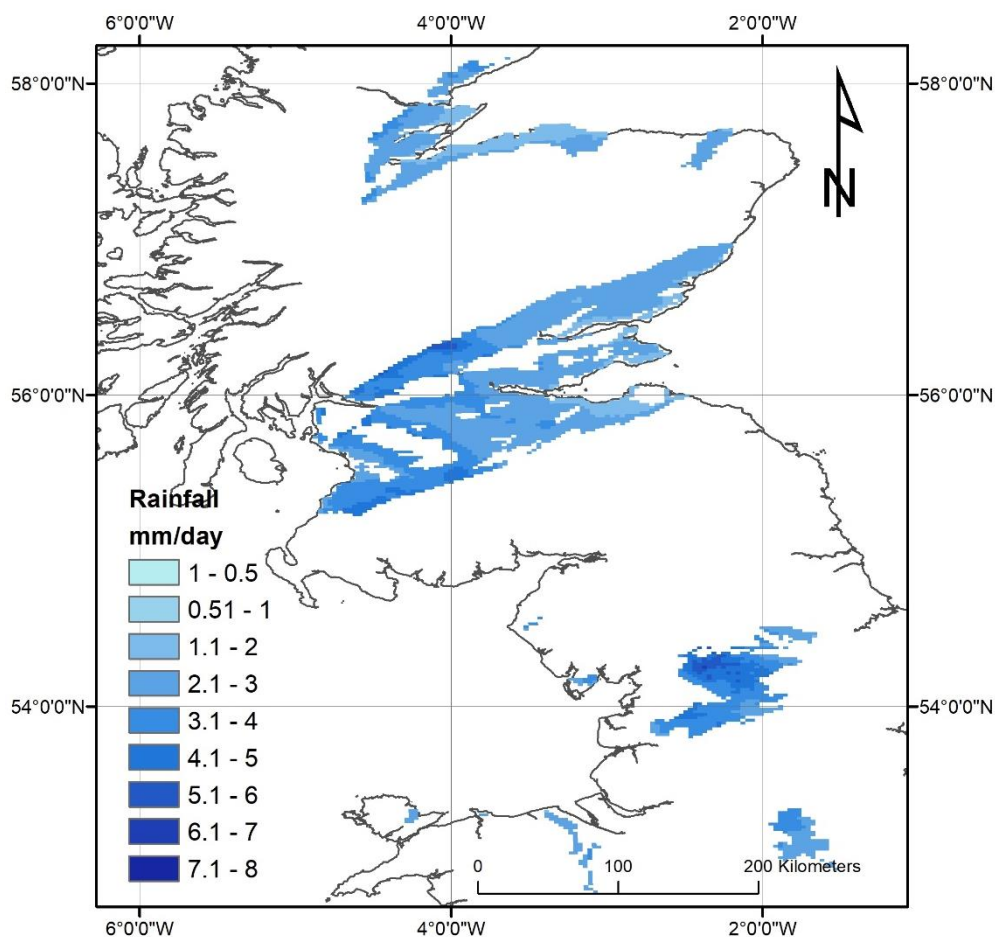


Figure 4. Spatial distribution of rainfall in the Devonian sandstone / Carboniferous Limestone

3.1.5 Potential evaporation

The monthly potential evapotranspiration (PE) raster datasets (40×40 km) were gathered from a Met Office Rainfall and Evaporation Calculation System (MORECS) in the Met Office of the UK (Hough and Jones 1997). Figure 5 shows the distributed long-term average potential evaporation data. Highest potential evaporation rates of approximately 686 mm year^{-1} (1.88 mm day^{-1}) are observed to the west of the aquifer outcrop. Lowest potential evaporation rates of approximately 430 mm year^{-1} (1.18 mm day^{-1}) are observed to the north of the aquifer (Figure 5). The average potential evaporation rates over the whole of the Devonian and Carboniferous aquifers is approximately 528 mm year^{-1} (1.45 mm day^{-1}). Table 2 presents specific information about the PE records at the selected boreholes in these aquifers.

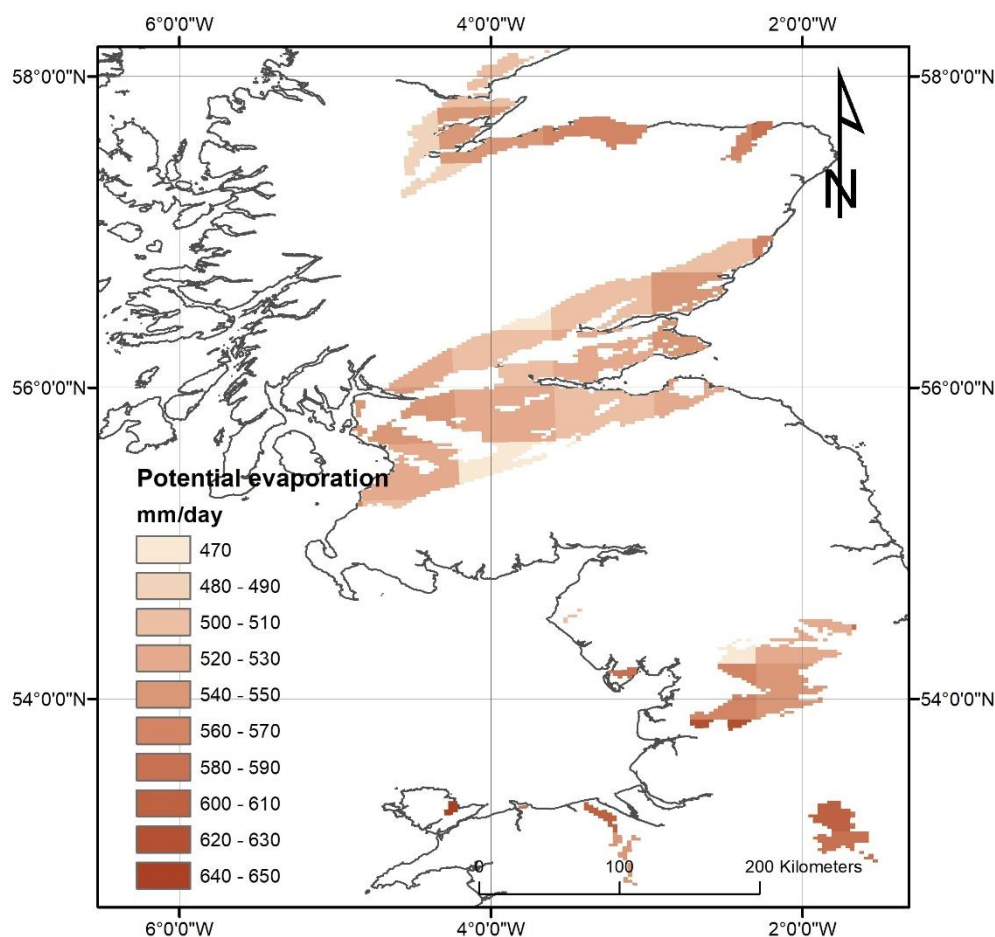


Figure 5. Spatial distribution of potential evaporation in the Devonian sandstone / Carboniferous Limestone

Table 2. Landuse, rainfall and evapotranspiration information for the Permo-Triassic

Borehole name	Dominant landuse	Av. Rainfall (mm/day)	Rainfall record	Av. PE (mm/day)	PE record
Hucklow South	Improved grassland	2.64	1961-current	1.31	1961-current
Alstonefield	Improved grassland	2.84	1961-current	1.61	1961-current
Pant Y Lladron	Improved grassland	3.12	1961-current	1.78	1961-current

3.1.6 Hydrogeology

The Carboniferous Limestone has very low values of porosity and permeability. Analysis on core from north-east England shows porosity values of 0.2% to 5.9% and a median hydraulic conductivity value of 3×10^{-6} m/d (Nirex, 1993). Secondary network of solution-enlarged fractures (commonly termed conduits) is the main contributor to the aquifer permeability. An important observation in this aquifer is that the conduit networks are continuously changing, which makes the karst systems a dynamic one. In general, karst systems will tend to evolve downwards, with newly developed lower conduit networks and drying up the upper networks.

In the Devonian sandstones in Fife and eastern Scotland, there is considerable variation in porosity and hydraulic conductivity with depth in the aquifer. Geophysical logging shows that fracture flow is dominant even where porosity high porosity exists. Mean porosity from four formations is approximately 20% and analysis of pumping tests from five boreholes show transmissivity values varying between 200 and 800 m² day⁻¹ (Macdonald et al., 2005). No lumped models are discussed in this study for boreholes located in this aquifer.

The productivity of Carboniferous sedimentary rocks in Scotland which depends on the nature of natural fracturing as well as on the extent and nature of mining impacts. Mine voids can artificially and greatly increase aquifer transmissivity. Aquifer storage can also be locally increased. The productivity of Carboniferous aquifers subject to extensive coal mining is reflected by the higher yield of boreholes drilled through these mines.

The Old Red Sandstone in Wales is approximately 2 km thick in places, but has no significant groundwater storage and transport; however, this aquifer is still arguably the most important aquifer in Wales. The principal controls on permeability and transmissivity arise from lithology changes, degree of induration/cementation, and extent/depth of fracturing along bedding planes. Transmissivity values obtained from pumping test analysis reach 350 m² day⁻¹, with a mean of 51 m² day⁻¹.

3.1.7 Groundwater levels

Depending on the investigated location, the aquifer can be under confined or unconfined conditions. At Huclow South, no superficial deposits are mapped on the ground surface, but clay and stones were encountered when drilling. The water is unconfined with a large seasonal range of about 25 m. At Alstonefield the water level hydrograph represents an open groundwater system. The water level in the borehole is relatively deep and reflects a regional water level controlled by drainage in the incised valley of the River Dove to the south of the borehole.

These time series of groundwater levels are used in this study to characterise the aquifer properties and to estimate the infiltration recharge values for water resources management. The boreholes are selected so that they are not significantly impacted by the presence of nearby surface features.

3.2 Climate change challenge

The British Geological Survey (BGS) with the support of the Environment Agency (EA) have undertaken a study to investigate the impact of climate change on groundwater resources using the distributed recharge model ZOODRM (Mansour and Hughes, 2018). Potential recharge values for Great Britain (England, Scotland and Wales) are produced using rainfall and potential evaporation data from the Future Flows Climate datasets (11 ensembles of the HadCM3 Regional Climate Model or RCM). This study has shown that generally the recharge season appears to be forecast to become shorter, but with greater amount of recharge “squeezed” into fewer months. This conclusion is aligned with the European Environment Agency map that describes the expected climate change across the different areas in Europe as shown in Figure 6.

The shortening of recharge season indicates that aquifers may become more vulnerable to droughts if rainfall fails in one or two months rather than a prolonged dry winter as can occur now. At the very least, water management measures have to be put in place to account for periods when recharge volumes reduce. On the other hand, the increased recharge signal could result in flashier groundwater level response and potentially leading to more flooding.

The main climate challenge for water resources managers and stakeholders is to assess the risk of future flooding and drought events. This requires detailed assessment of the variation of resources at regional and local scales rather than national or continental scales.

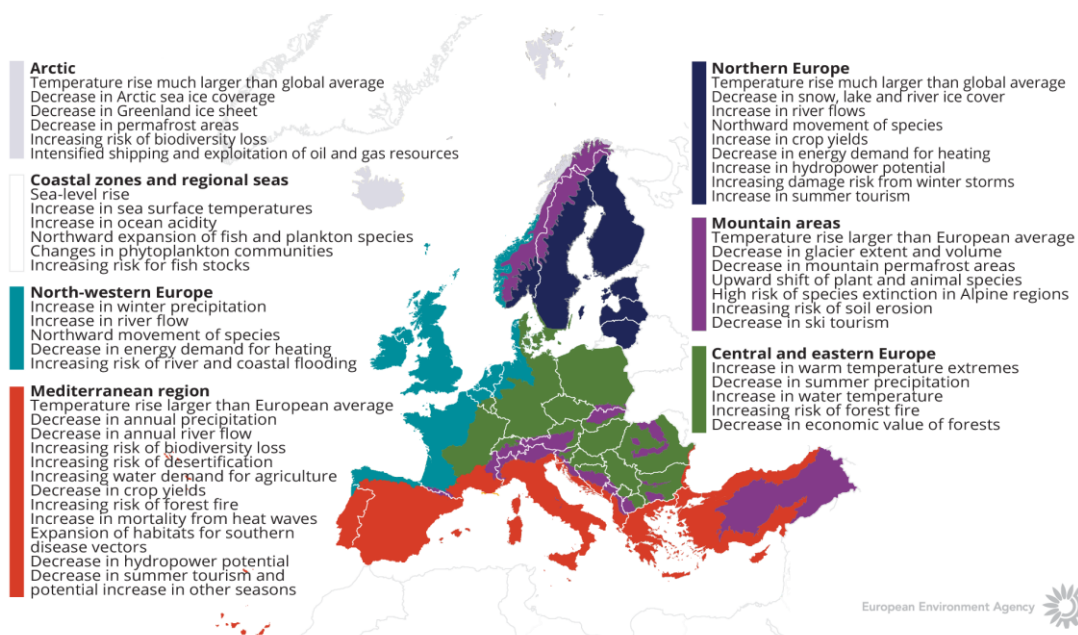


Figure 6. How is climate expected to change in Europe. The European Environment Agency map

4 METHODOLOGY

4.1 Methodology and climate data

4.1.1 *AquiMod*

AquiMod is a lumped parameter computer model that has been developed to simulate groundwater level time series at observational boreholes (Mackay et al., 2014a). It is based on hydrological algorithms that simulate the movement of groundwater within the soil zone, the unsaturated zone, and the saturated zone. The lumped models neglect complexities included in distributed groundwater models but maintain some of the fundamental physical principles that can be related to the conceptual understanding of the groundwater system (Mackay et al., 2014b).

The primary aim of AquiMod is to capture the behaviour of a groundwater system through the analysis of the available groundwater level time series. Once calibrated the model can be run in predictive mode and be used to fill in gaps in historical groundwater level time series and to calculate future groundwater levels. In addition to groundwater levels, it also provides predictions of historical and future recharge values and groundwater discharges.

The mathematical equations that are used to simulate the movement of groundwater flows within the three modules are detailed in Appendix A. The model uses rainfall and potential evaporation time series as forcing data. These are interpreted by the soil module representing the soil zone. The soil module calculates the rainfall infiltration and pass it to the unsaturated zone module. This module delays the arrival of the infiltrating water to the saturated zone module. The latter calculates the variations of groundwater heads and flows accordingly.

The model is calibrated using a Monte Carlo approach. It compares the simulated and observed groundwater level fluctuations and calculates a goodness of fit. The AquiMod version used in this work employs the Root Square Mean Error (RMSE) or the Nash Sutcliffe (NSE) performance measures to assess the performance of the model. The user sets a threshold value to accept all the models that perform better than the specified threshold. The possibility of producing many models that are all equally acceptable, allows the user to interpret the results from all these models and calculate uncertainty.

The recharge values calculated from AquiMod are those that reach the aquifer system and drive the groundwater levels. Thus, it is assumed that these are the actual recharge values as defined by the guidance report prepared by TACTIC project

4.1.2 *Metran*

Metran applies a transfer function-noise model to simulate the fluctuation of groundwater heads with precipitation and evaporation as independent variables (Zaadnoordijk et al., 2019). The modelling approach consists mainly of two impulse functions and a noise model. The first impulse function is used for convolution with the precipitation to yield the precipitation contribution to the piezometric head. The second is for evaporation which is either a separately estimated function, or a factor times the function used for precipitation. The noise model is a

stochastic noise process described by a first-order autoregressive model with one parameter and zero mean white noise. Further information about the model is given in Appendix B with the model setup shown in the Figure B1.

Metran allows the addition of other processes affecting the behaviour of the groundwater heads, for example pumping or the presence of surface features such as rivers. The contributions from these processes are added to the deterministic part of the model.

Metran has been designed to work with explanatory series that have a daily time step. However, it has been adapted so that other time step lengths can be applied. However, the explanatory variables must still have a constant frequency.

The model is calibrated automatically; however, the model uses two binary parameters, Regimeok and Modok, to judge a resulting time series model. Regimeok cross-examines the explained variance R^2 (> 0.3), the absolute correlation between deterministic component and residuals (< 0.2), and the null hypothesis of non-correlated innovations (p value > 0.01). If all these criteria are satisfied, Regimeok returns a value of 1 indicating highest quality. Modok also cross-examines the explained variance R^2 (> 0.1) and the absolute correlation between deterministic component and residuals (< 0.3) as well as the decay rate parameter (> 0.002) and if all these criteria are satisfied, it is given a value of 1. If Modok = 1 and Regimeok = 0, the model is still considered acceptable. If both these parameters are 0, the model quality is insufficient and the model is rejected.

Metran's time series model is linear and the model creation fails when the system is strongly nonlinear. It is also limited to the response function being appropriate for the simulated groundwater system. Metran uses a gradient search method in the parameter space, so it can be sensitive to initial parameter values in finding an optimal solution.

The model calculates an evaporation factor f that gives the importance of evapotranspiration compared to precipitation. It is possible to use this factor to calculate the recharge values as shown by Equation B2 in appendix B. However, it must be noted that the use of Equation B2 is based on too many assumptions that are easily violated. Because of this, the equations should be applied only to long-term averages using only models of the highest quality.

Following the definitions used in the TACTIC project, this recharge quantity corresponds to the effective precipitation. It is equal to the potential recharge when the surface runoff is negligible. This in turn is equal to the actual recharge at the groundwater table if there is also no storage change or interflow.

4.1.3 The distributed recharge model ZOODRM applied at the UK scale

A distributed recharge model, ZOODRM, has been developed by the British Geological Survey to calculate recharge values required to drive groundwater flow simulators. This recharge model allows grid nesting to increase the resolution over selected area and is called therefore the zooming object-oriented distributed recharge model (ZOODRM) (Mansour and Hughes, 2004). The model can implement a number of recharge calculation methods that are suitable for



temperate climates, semi-arid climates, or for urban areas. One of the methods that is implemented is the recharge calculation method used by Aquimod and detailed in Appendix A1.

ZOODRM uses a Cartesian grid to discretise the study area. It reads daily rainfall and potential evaporation data in time series or gridded format and calculates the recharge and overland flow at a grid node using a runoff coefficient as detailed in appendix A1. However, since this is a spatially distributed model, it reads a digital terrain model and calculates the topographical gradients between the grid nodes. It then uses the steepest gradient to route the calculated surface water downstream until a surface feature, such as a river or a pond, is reached. While the connections between the grid nodes based on the topographical gradients define the water paths along which surface water moves, major rivers are also user-defined in the model. This allows the simulation of river water accretion on a daily basis and the production of surface flow hydrograph. The model is then calibrated by matching the simulated river flows at selected gauging stations to the observed flows, by varying the values of the runoff coefficients.

The procedure used to calibrate the model involves dividing the study area into a number of zones and then to specify runoff values for each one. It is possible to vary the runoff coefficient values on a seasonal basis by using different runoff values for the different months of the year.

The recharge model ZOODRM calculates rainfall infiltration after accounting for evapotranspiration and soil storage. The simulated infiltration may not reach the aquifer system as it may travel laterally within the soil and discharge into surface water features away from the infiltration location. The simulated infiltration is therefore considered, as potential recharge according to the definitions of recharge processes provided by the guidance report prepared by TACTIC project.

Climate data

The TACTIC standard scenarios are developed based on the ISIMIP (Inter Sectoral Impact Model Intercomparison Project, see www.isimip.org) datasets. The resolution of the data is 0.5°x0.5°C global grid and at daily time steps. As part of ISIMIP, much effort has been made to standardise the climate data (e.g. bias correction). Data selection and preparation included the following steps:

1. Fifteen combinations of RCPs and GCMs from the ISIMIP data set were selected. RCPs are the Representative Concentration Pathways determining the development in greenhouse gas concentrations, while GCMs are the Global Circulation Models used to simulate the future climate at the global scale. Three RCPs (RCP4.5, RCP6.0, RCP8.5) were combined with five GCMs (noresm1-m, miroc-esm-chem, ipsl-cm5a-lr, hadgem2-es, gfdl-esm2m).
2. A reference period was selected between 1981 – 2010 and an annual mean temperature was calculated for the reference period.
3. For each combination of RCP-GCM, 30-years moving average of the annual mean temperature were calculated and two time slices identified in which the global annual mean temperature had increased by +1 and +3 degree compared to the reference period, respectively. Hence, the selection of the future periods was made to honour a



- specific temperature increase instead of using a fixed time-slice. This means that the temperature changes are the same for all scenarios, while the period in which this occurs varies between the scenarios.
4. To represent conditions of low/high precipitation, the RCP-GCM combinations with the second lowest and second highest precipitation were selected among the 15 combinations for the +1 and +3 degree scenario. This selection was made on a pilot-by-pilot basis to accommodate that the different scenarios have different impact on the various parts of Europe. The scenarios showing the lowest/highest precipitation were avoided, as these endmembers often reflect outliers.
 5. Delta change values were calculated on a monthly basis for the four selected scenarios, based on the climate data from the reference period and the selected future period. The delta change values express the changes between the current and future climates, either as a relative factor (precipitation and evapotranspiration) or by an additive factor (temperature).
 6. Delta change factors were applied to local climate data by which the local particularities are reflected also for future conditions. These monthly values (one set of rainfall and PE for each warming scenario) are used to drive the groundwater models presented in this report.

For the analysis in the present pilot the following RCP-GCM combinations were employed:

Table 3. Combinations of RCPs-GCMs used to assess future climate

		RCP	GCM
1-degree	"Dry"	rcp6p0	noresm1-m
	"Wet"	rcp4p5	miroc-esm-chem
3-degree	"Dry"	rcp4p5	hadm2-es
	"Wet"	rcp8p5	miroc-esm-chem

4.2 Model set-up

4.2.1 *AquiMod*

The boreholes located in the Carboniferous Limestone aquifer are listed in Table 1. *AquiMod* model setup relies mainly on two input files. The first input file "Input.txt" is a control file where the module types and model structure are defined. *AquiMod* is executed first under a calibration mode where a range of parameter values of the different selected modules are given in corresponding text files and a Monte Carlo approach is used to select the parameter values that yield best model performance. "Input.txt" also controls the mode under which *AquiMod* is executed, the number of Monte Carlo runs to perform, the number of models to keep with an acceptable performance, and the number of runs to execute in evaluation mode.

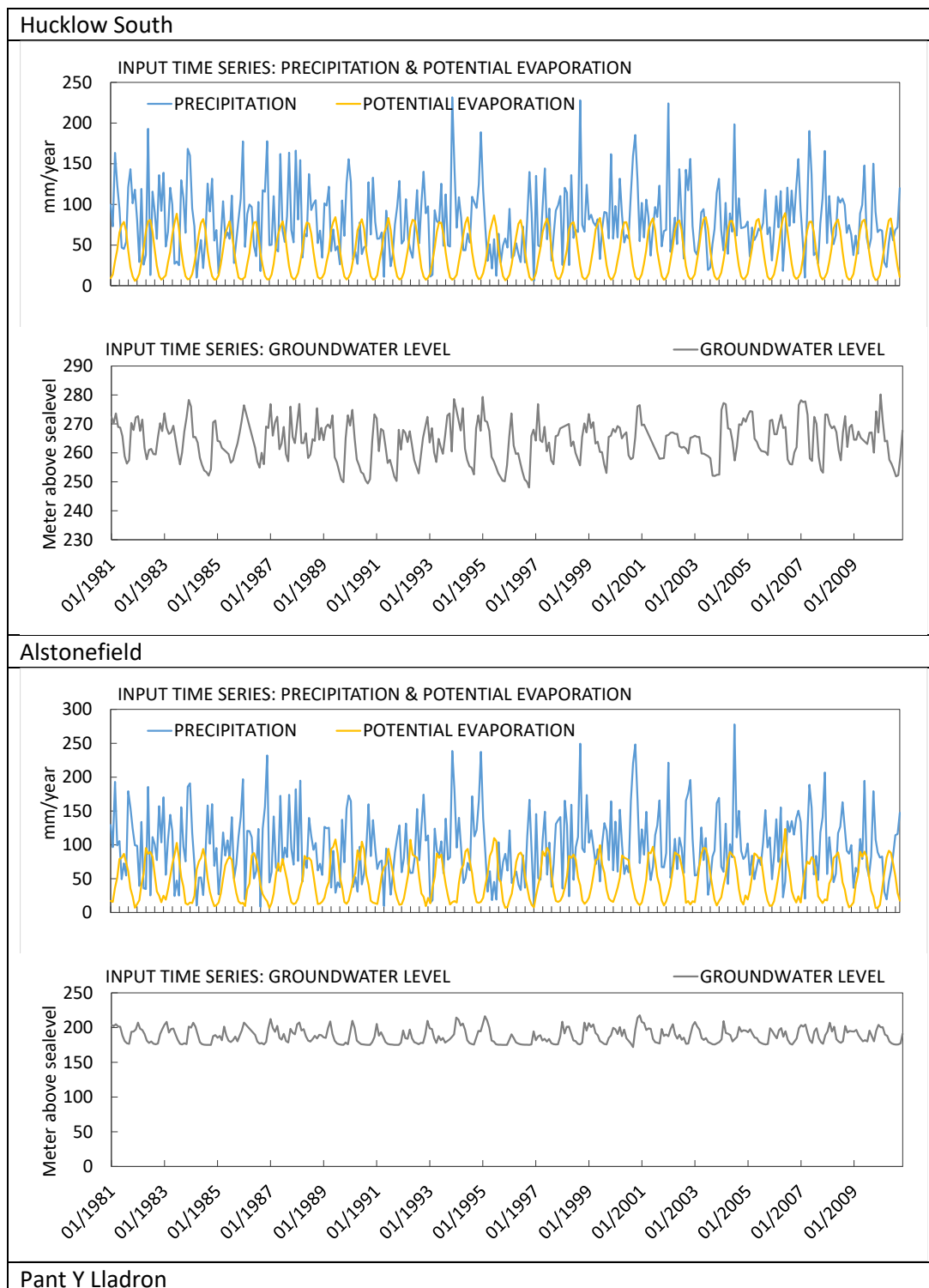
The second file *AquiMod* uses is called "observations.dat". This file holds the forcing data mainly the potential evaporation and rainfall. However, it is also possible to include the anthropogenic impact on groundwater levels by including a time series of pumping data in this file. None of the boreholes studied here includes pumping data. The observed groundwater levels that are used

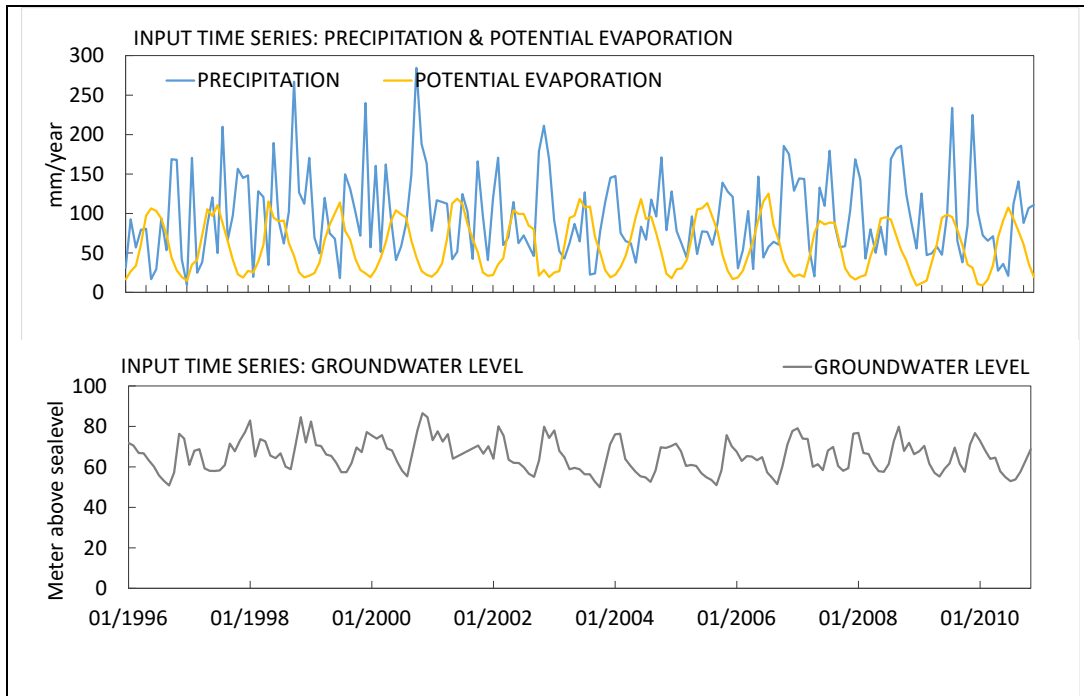


for model calibration are also given in this file. The data are provided to the model on a daily basis, and this forces AquiMod to run using a time step length of one day. Table 4 shows daily time series of rainfall and potential evaporation values (mm/month) as well as the fluctuations of water table at the different boreholes.

All AquiMod models built for the boreholes in Table 1 use the FAO Drainage and Irrigation Paper 56 (FAO, 1988) method in the soil module, and employ the two-parameter Weibull probability density function to control the movement of infiltrated water in the unsaturated zone (Appendix A1). However, the groundwater module structures vary between the different boreholes. The best groundwater module structure is found by trial and error during the calibration process. The simplest structure, one layer with one discharge feature, is selected first and then the complexity of the module structure is increased gradually to see if the model performance improves. The structure with best model performance is selected to undertake the recharge calculations. The structures selected for these boreholes are mainly of one layer or three-layered systems.

Table 4 Figures showing time series of daily rainfall and potential evaporation values (mm/month) as well as the fluctuations of water table at the different boreholes.





4.2.2 Metran

Metran applies transfer function noise modelling with daily precipitation and evaporation as input and of groundwater levels as output (Zaadnoordijk et al., 2019). The setup is shown in Figure 7. If time series of other influences on the groundwater head are available, these contributions can be added to the deterministic part of the model. An input file that holds the daily information of precipitation, potential evaporation and groundwater levels is prepared for each borehole in Table 1. Plots of these data are shown in Table 4. It must be noted that, while the groundwater levels used in Aquimod and shown in Table 4 have missing values, these have to be provided as complete time series to Metran. To achieve this, a linear interpolation procedure is used to fill in the missing values in the groundwater level time series.. Once executed, it calculates the characteristics of the impulse functions and the corresponding parameters automatically.

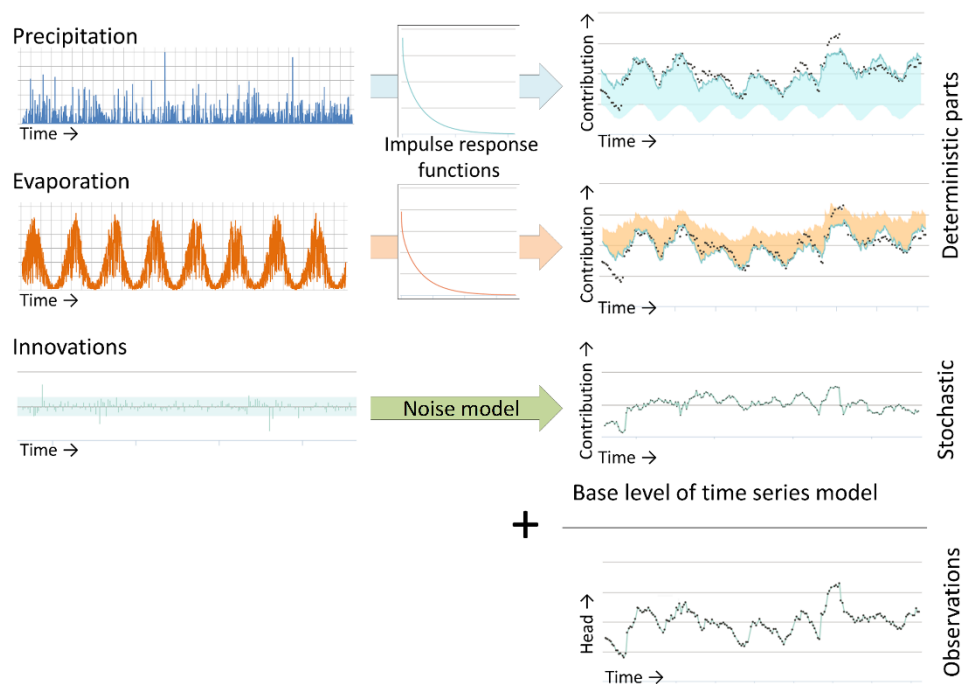


Figure 7 Illustration of METRAN setup

4.2.3 National scale model (ZOODRM)

The distributed recharge model (ZOODRM) is applied at national over the British Mainland (England, Scotland, and Wales) (Figure 8) using a Cartesian grid with 2 km square cells. The model reads a text file that defines the locations of the grid nodes as well as the connections between the nodes. This text file is prepared using a specific tool, called ZETUP (Jackson, 2004), where the extent of the study area is defined using the coordinates of the lower left and upper right corners of a rectangle that covers the modelled area. The spacing between the nodes and the information that dictate the boundary of the irregular shape of the area are also given in this file. This tool also uses a file that contains the locations of the nodes as obtained from a geographical information system tool (GIS) and converts this information into a text file that describes the river extents and characteristics.

The map defining the runoff zones is based on the hydrogeology of the study area. It is produced in gridded *ascii* format using the hydrogeological map available for Great Britain. Additional text files, one for each runoff zone, are also prepared to define the monthly runoff values.

The topographical information is also provided in a gridded *ascii* format for the model to calculate the topographical gradients between the nodes. While a surface water routing procedure that accounts for indirect recharge and surface water storage is available in the model, this is not used in the current application. It is assumed that all the water originated at one grid nodes travel downstream and reaches a discharging feature in one day, which is equal to the length of the time step used.



Landuse data (Section **Error! Reference source not found.**) and soil data that are required to calculate the water capacity at every grid node are also provided to the model using maps in gridded *ascii* format. A set of ten gridded landuse maps are used to give the percentage of landuse type at any given location. The gridded soil map gives the soil type at a selected location. The landuse type and soil type ids are linked to text files that hold the corresponding information such as the soil moisture at saturation, the soil moisture at wilting and the root constants can be obtained.

The driving data are provided to the model as daily gridded rainfall data (Sections **Error! Reference source not found.**) and time series of monthly potential evaporation values as described in (Section **Error! Reference source not found.**). Mansour et al. (2018) provide a full description of the construction of this model together with a more detailed description of the data used. The calculated recharge values are also provided in the published work; however, it must be noted that the historical recharge values shown in this work are simulated over the period from 1981 to 2010 in order to be consistent and comparable with the recharge values calculated by AquiMod and Metran. In addition, in this study, the model has been rerun using the climate change data specifically provided by the TACTIC project to calculate the projected distributed recharge values.

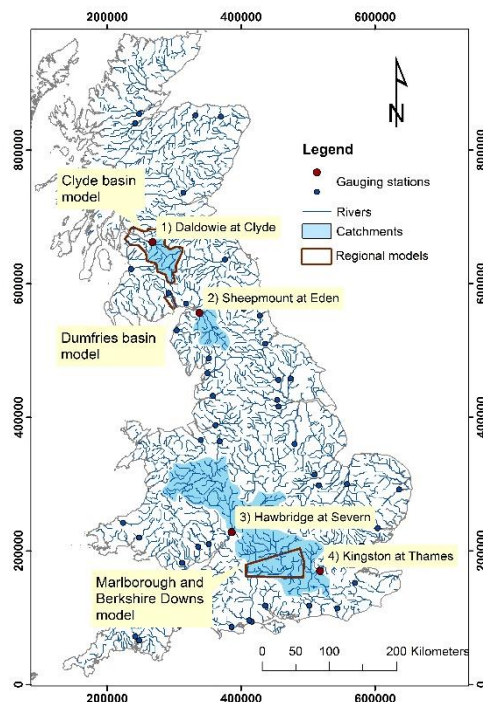


Figure 8. Extent of the UK national scale recharge model in UK national grid reference after Mansour et al. (2018). Figure also shows the locations of the gauging stations downstream of the major rivers used for model calibration.



4.3 Model calibration

4.3.1 Calibration of *AquiMod* models

The calibration of *AquiMod* is performed automatically using the Monte Carlo approach. The user populates the files of the selected modules with minimum and maximum parameter values and then the model randomly selects a value from the specified range for any given run. The selection of the minimum and maximum values is physically based depending on the characteristics of the study area. For example, the minimum and maximum values of the root depth in the soil module are set to 15 cm and 60 cm respectively for a study area covered with grass, while these values are set to 120 cm and 200 cm for a woodland area. The storage coefficients bounds of a groundwater module are set to much lower values in a confined aquifer compared to those used for an aquifer under unconfined conditions.

A conceptual hydrogeological understanding must be available before the use of *AquiMod*, since this is necessary to set the limits of the parameter values for the calibration process. In some cases, it is not possible to obtain a good performing model with the selected values and that necessitates the relaxation of these parameters beyond the limits informed by the conceptual understanding. In such cases, the parameter values must feed back into the conceptual understanding if better performing models are obtained.

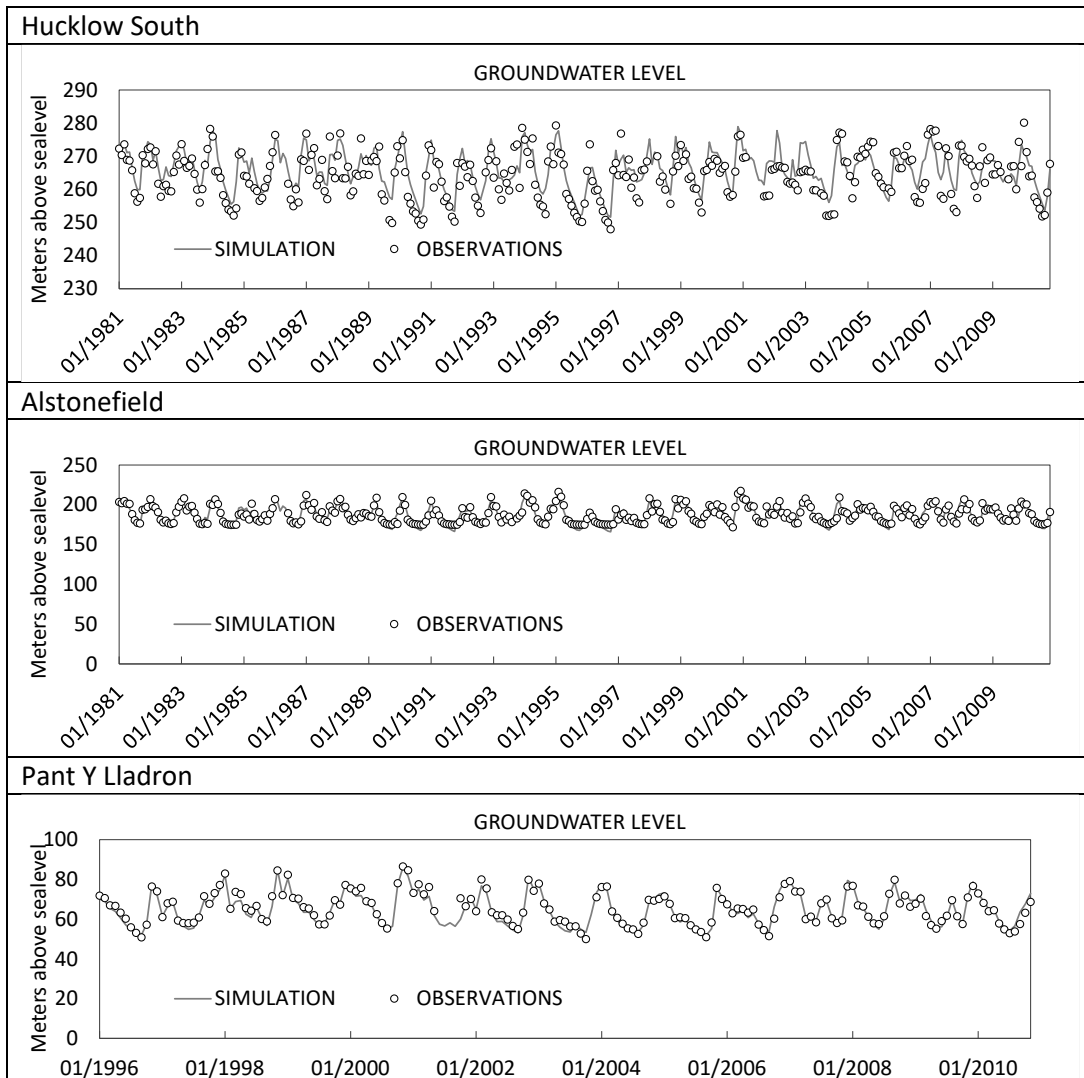
AquiMod execution time is relatively small, which allows the calibration of the model using hundreds of thousands of runs in couple of hours. The performance measure used to assess the quality of the simulation is the Nash Sutcliffe Error (Appendix A) that takes a maximum value of unity for a perfect match between the simulated and observed data. The threshold at which models are accepted is set to a value of 0.6. All the models that achieve an NSE higher than 0.6 are included in the analysis but a maximum number of 1000 runs are used if the number of acceptable models is greater than 1000.

Table 5 shows the best NSE values obtained for the models calibrated at the Devonian sandstone / Carboniferous Limestone boreholes listed in Table 1. It is clear that a good match was achieved between the simulated and observed groundwater levels as illustrated in the plots shown in Table 6. The best performing model is the *AquiMod* model built at PantYLLadron borehole with an NSE value of 0.92. The least performing *AquiMod* model is that built for Hucklow South borehole with an NSE value of 0.75.

Table 5 Nash Sutcliff Error measure at the Devonian sandstone / Carboniferous Limestone boreholes

Borehole name	NSE
Hucklow South	0.75
Alstonefield	0.89
Pant Y Lladron	0.92

Table 6 Comparison between the simulated and observed groundwater levels at the Devonian sandstone / Carboniferous Limestone observation boreholes.



4.3.2 Calibration of Metran models

For the standard setup with precipitation and evaporation, there are five parameters that have to be determined during the calibration of the model. Three parameters are related to the precipitation response, the evaporation factor, and the noise model parameter (Appendix B). There are three extra parameters for each additional input series, such as pumping. The parameter optimization of Metran uses a gradient search method in the parameter space to reach a global minimum. As explained in Appendix B, two parameters indicate if Metran succeeded with producing a match between the simulated and observed data. These are called the Regimeok and Modok. When Regimeok is equal to one, the calibration is of highest quality. If Modok is equal to one and Regimeok is equal to zero, the calibration is of acceptable quality. Finally, if both parameters are equal to zero, the calibration quality is insufficient.

Time series of rainfall, potential evaporation and groundwater levels are provided to Metran on a monthly basis. Metran input data must be complete dataset, i.e. without missing data. To overcome this problem that may exist in the groundwater level time series, these data are aggregated to monthly values first and then missing values were filled using linear interpolation. Table 7 shows the performance of Metran across the Carboniferous Limestone boreholes considered in this study. It is clear that according to criteria set above, Metran fails to produce a model at four boreholes but succeeds at the Hucklow South borehole; however, Metran produces acceptably performing models at Alestonefield and Pant_Y_Lladron with the model output showing highest quality is the one found for Alestonefield with R^2 value of 0.81.

Table 7 Performance of Metran across the selected Devonian sandstone / Carboniferous Limestone boreholes.

Borehole name	Metran performance parameter Modok	Metran performance parameter Regimeok	Overall quality	R2	RMSE
Hucklow South	0	0	Insufficient	0.55	4.34
Alestonefield	1	0	Acceptable	0.81	4.39
Pant Y Lladron	1	0	Acceptable	0.66	5.14

4.3.3 Calibration of the UK national scale model using ZOODRM

Model calibration of the national scale recharge model was based on the comparison of the simulated long-term average overland flows to the observed ones (Mansour et al., 2018) recorded at gauging stations of selected major rivers (Figure 8). However, additional checks were also undertaken to assess the performance of the model. These include checking the match between the seasonal overland flow volumes at four boreholes, shown in red in Figure 8, checking the calculated recharge volumes with those calculated by other tools over selected catchment areas, and checking the temporal fluctuations of soil moisture deficit with those



calculated by other tools. Figure 9 shows a Q plot for the simulated vs observed long term average runoff values at the 56 gauging stations shown in Figure 8. The solid line shows the one to one match and the dotted line shows the linear relationship between the two datasets.

It must be noted that while this model uses the same recharge calculation methods used by Aquimod, these two models are calibrated using different datasets, with Aquimod using the groundwater levels and the distributed recharge model using the overland flows.

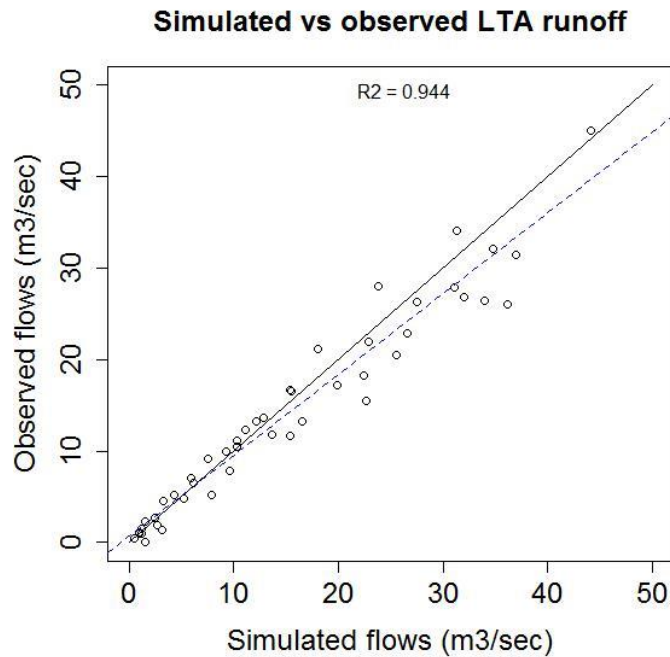


Figure 9 Q plot for the simulated vs observed long term average runoff values at the 56 gauging stations shown in Figure 8 after Mansour et al. (2018)

5 RESULTS AND CONCLUSIONS

5.1 Historical recharge values

Table 8 shows the time series of the historical recharge values calculated using the Aquimod model at the Carboniferous Limestone boreholes listed in Table 1. The plots in this table also show the 10th percentile, the mean, and the 90th percentile of recharge values calculated from the time series.

As mentioned in Appendix B, the formulas used by Metran are based on assumptions that can be violated and it is better to use the infiltration coefficient f_c with the long-term average values of rainfall and potential evaporation to calculate long-term average values of recharge and using only models of the highest quality. Time series of recharge values are not therefore produced, from the analysis undertaken using Metran. The long-term average recharge values calculated using Metran are shown in Table 9.

One of the benefits of running Aquimod in Monte Carlo mode is the possibility of producing many models with acceptable performance. Consequently, the recharge values estimated from these models are all equally likely. This provides us with a range of recharge values at each borehole that reflects the uncertainty of the optimised hydraulic parameter values. In the current study, the long-term average recharge values are calculated from up to 1000 acceptable models if they exist at each borehole; otherwise, all the acceptable models are used. The mean, 25th and 75th percentiles are then calculated from these long-term recharge values and displayed in Figure 10. It is clear that the differences between the 75th and 25th percentile values is negligible at Hucklow South borehole but more noticeable at the other two boreholes. At PantYlladron, the difference between the 25th and the 75th percentile values is approximately 8 mm/month (27%) and at Alestonefield the difference is approximately 5.7 mm/month (18.5%).

In addition to the recharge values calculated using Aquimod, Figure 10 shows the recharge values calculated using Metran and the distributed national scale model at these boreholes. It is clear that there is a good agreement between the Aquimod calculated recharge values and those calculated using the distributed national scale model at PantYlladron; however, there are significant differences at Hucklow South and Alestonefield with the national scale model producing significantly higher values at these boreholes. It must be noted that the recharge values calculated by these two models are of different types. The distributed recharge model calculates potential recharge and Aquimod calculates actual recharge.

Metran produces significantly different values from Aquimod at all three boreholes. While the recharge value produced by Metran at Hucklow South is shown in Figure 10, it must be treated with caution as Metran reported badly performing model at this borehole. Metran estimates an upper and a lower value for the infiltration coefficient f_c . This can be used as an indication of uncertainty associated with the calculated f_c value. These bounds are also shown in Table 9.

Table 8 Time series of recharge values obtained from the best performing AquiMod models at the Devonian sandstone / Carboniferous Limestone boreholes

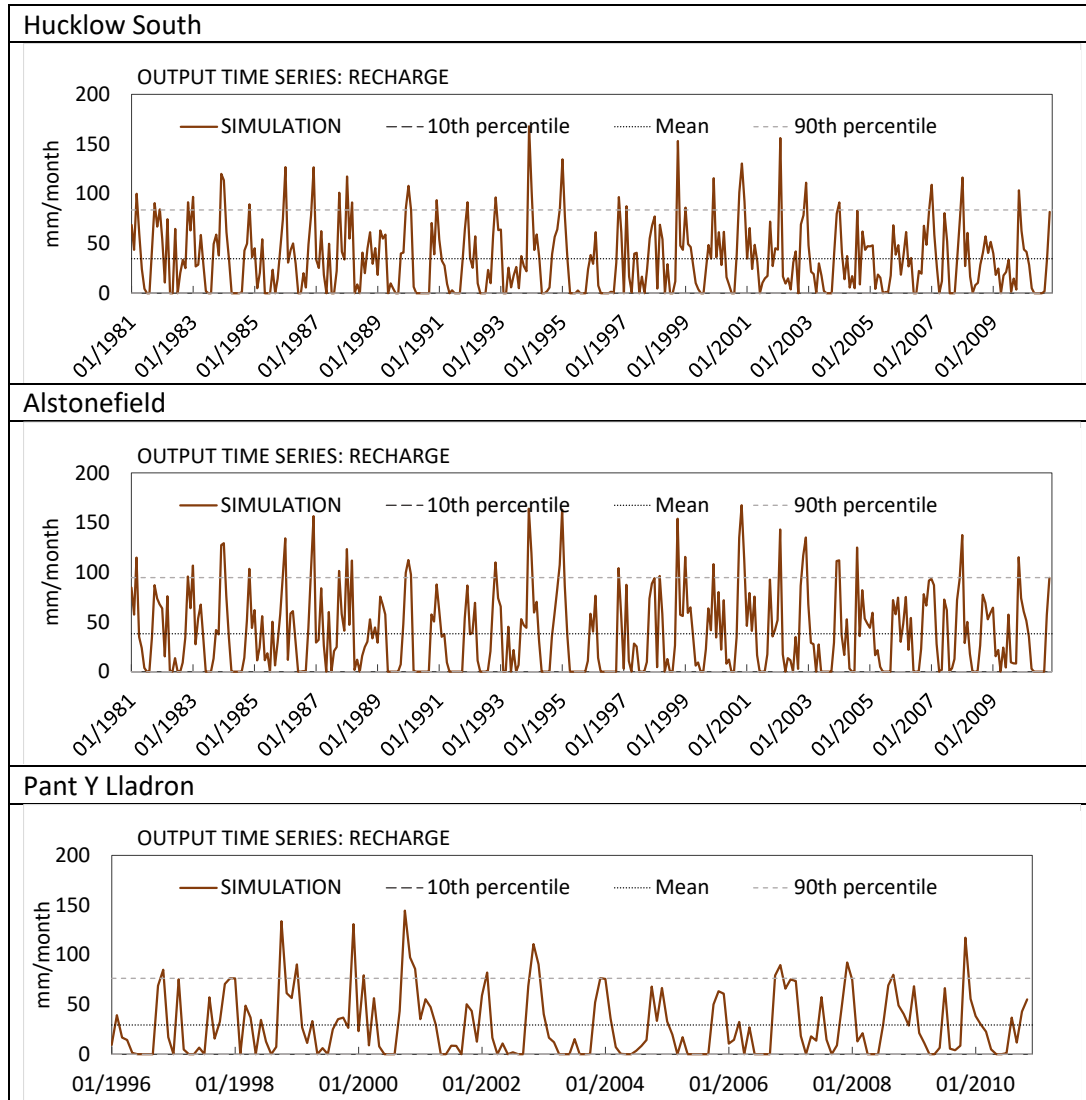


Table 9 Recharge values calculated using the recharge factors estimated by Metran

Borehole name	Average precipitation (mm/month)	Average potential evaporation (mm/month)	Recharge factor	Recharge (mm/month)
Hucklow South	80.63	39.95	1.49 +- 0.56	14.17
Alstonefield	86.47	48.98	1.24 +- 0.24	20.54
Pant Y Lladron	95.12	54.34	0.66 +- 0.203	59.42



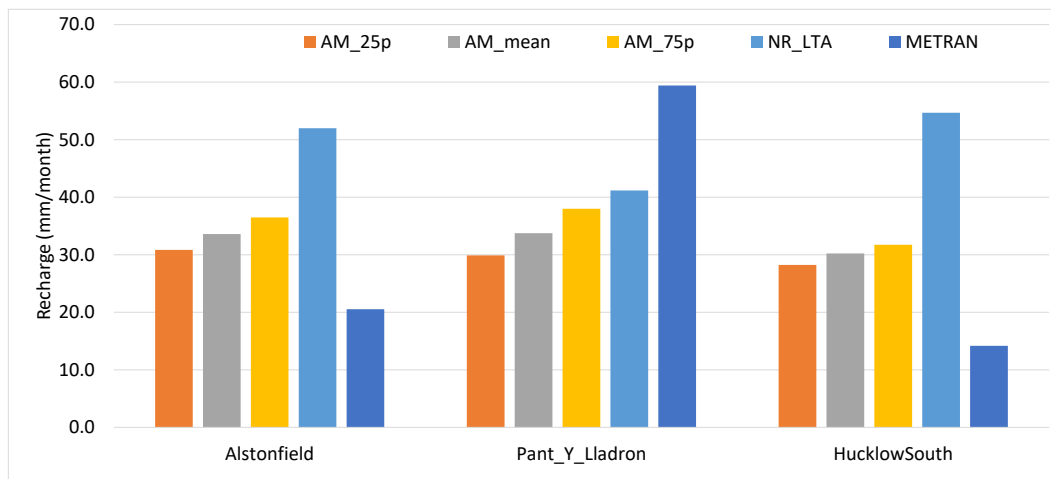


Figure 10 Historical recharge values calculated by AquiMod, Metran, and the national scale recharge model.

5.2 Projected recharge values

The forcing data, rainfall and potential evaporation, are altered using the change factors of the climate models (see Section **Error! Reference source not found.**). For the United Kingdom, there are two sets of monthly change factors, one used with the data driving AquiMod and Metran (Table 10), and the other used to calculate the spatially distributed recharge (Table 11). These change factors are used as multipliers to both the historical rainfall and potential evaporation values.

For the application involving AquiMod, these factors are used to alter the time series of historical rainfall and potential evaporation values used to drive the model.

When using Metran, the historical time series are altered using these factors first and then the long-term average rainfall and potential evaporation values are calculated. The recharge coefficient f_c values of the different boreholes, as calculated from the calibration of Metran model using the historical data, are then applied to calculate the projected long-term average recharge values.

The distributed recharge model ZOODRM includes the functionality of using these change factors to modify the historical gridded rainfall and potential evaporation data before using them as input to calculate the recharge. In this case, and for any simulation date, the rainfall and potential evaporation change factors for the month corresponding to the date, are used to

modify all the spatially distributed historical rainfall and potential evaporation values respectively.

Table 10 Monthly change factors as multipliers used for the borehole data

	Scenario	Jan	Feb	Mar	Apr	May	Jun	Jul	Aug	Sep	Oct	Nov	Dec
Rainfall	1° Min	1.087	0.956	0.994	1.072	0.888	0.909	0.836	0.988	1.017	1.106	0.962	1.031
	1° Max	1.140	1.012	1.033	1.045	1.022	0.863	1.086	0.953	0.995	1.067	1.148	1.053
	3° Min	0.936	1.056	0.994	1.153	1.063	0.900	0.846	0.721	0.854	0.970	1.047	1.116
	3° Max	1.191	1.177	0.989	1.014	0.949	0.986	1.473	1.145	1.173	1.074	1.152	1.112
PE	1° Min	1.082	1.082	1.062	1.089	1.091	1.061	1.078	1.083	1.082	1.063	1.049	1.076
	1° Max	1.049	0.993	1.014	1.007	1.019	1.013	1.021	1.015	1.029	1.028	1.020	1.026
	3° Min	1.034	1.057	1.039	1.056	1.060	1.086	1.085	1.091	1.109	1.097	1.064	1.066
	3° Max	1.072	1.070	1.055	1.071	1.105	1.106	1.072	1.083	1.082	1.076	1.072	1.060

Table 11 Monthly change factors as multipliers used for the distributed recharge model

	Scenario	Jan	Feb	Mar	Apr	May	Jun	Jul	Aug	Sep	Oct	Nov	Dec
Rainfall	1° Min	1.086	0.953	0.975	1.064	0.918	0.914	0.856	0.973	1.008	1.103	0.976	1.038
	1° Max	1.132	1.090	1.008	0.899	1.034	1.087	1.310	0.983	1.020	1.006	1.012	1.025
	3° Min	1.156	1.118	1.033	1.011	0.914	0.821	0.908	0.656	0.821	0.986	0.980	1.181
	3° Max	1.192	1.131	0.960	0.990	0.899	0.957	1.437	1.109	1.134	1.068	1.139	1.106
PE	1° Min	1.081	1.081	1.059	1.089	1.091	1.061	1.078	1.083	1.085	1.063	1.049	1.076
	1° Max	1.051	1.036	1.020	1.039	1.051	1.049	1.031	1.043	1.054	1.039	1.044	1.034
	3° Min	1.016	1.031	1.021	1.029	1.038	1.029	1.047	1.057	1.059	1.059	1.040	1.045
	3° Max	1.070	1.066	1.051	1.071	1.105	1.106	1.072	1.083	1.083	1.076	1.072	1.060

Figure 11 shows the historical and future long-term average recharge values calculated using the best performing AquMod model. It is clear that the highest reduction in recharge values are observed when the 3° Min rainfall and evaporation data are used, while the highest increase in recharge values are observed when the 3° Max rainfall and potential evaporation data are used.

When the 1° Min scenario data are used, all the boreholes show reduction in recharge values with the highest reduction observed at Alestonefield borehole (-4%) and then at Pant Y Lladron borehole (-3.3%) and the smallest reduction is observed at Hucklow South borehole (-2%). When the 1° Max scenario data are used, all the boreholes show increase in recharge values with the smallest increase observed at Hucklow South borehole (6.3%) and then at Alestonefield borehole (6.5%) and the highest increase is observed at Pant Y Lladron borehole (7.4%).

When the 3° Min scenario data are used, all the boreholes show reduction in recharge values with the highest reduction observed at Alestonefield borehole (-7.3%) and then at Pant Y Lladron borehole (-6.8%) and the smallest reduction is observed at Hucklow South borehole (-4%). When



the 3° Max scenario data are used, all the boreholes show increase in recharge values with the smallest increase observed at Pant Y Lladron borehole (18.3%) and Hucklow South and Alestonefield boreholes both showing an increase of 15.2%.

Projected recharge values calculated by Metran at Pant Y Lladron and Alestonefield boreholes are shown in Figure 12. The maximum reduction in recharge values as calculated by Metran at Pant Y Lladron borehole is -11.26 % while the maximum increase in recharge values at this borehole is as 13.8 %. Projected recharge values estimated at Alestonefield, however, shows unexpected increase compared to the historical recharge values using the data from all four scenarios. The maximum increase in recharge values of approximately 73% is produced using the rainfall and potential evaporation change factors of the 3° Max scenario.

Table 12 shows the monthly historical and future recharge values calculated at the different boreholes calculated by AquiMod. It is clear that in almost all the cases, the recharge values become lower than the historical values when the 1° Min and 3° Min data are used and they become higher than the historical values when the 1° Max and 3° Max are used. The exceptions of this observation are due to the complex effect of the use of the change factors, which may reduce both the rainfall and potential evaporation at the same period but at different rates. The reduction in potential evaporation volume in one month may yield increased recharge volume even if the rainfall volume is reduced for that month.

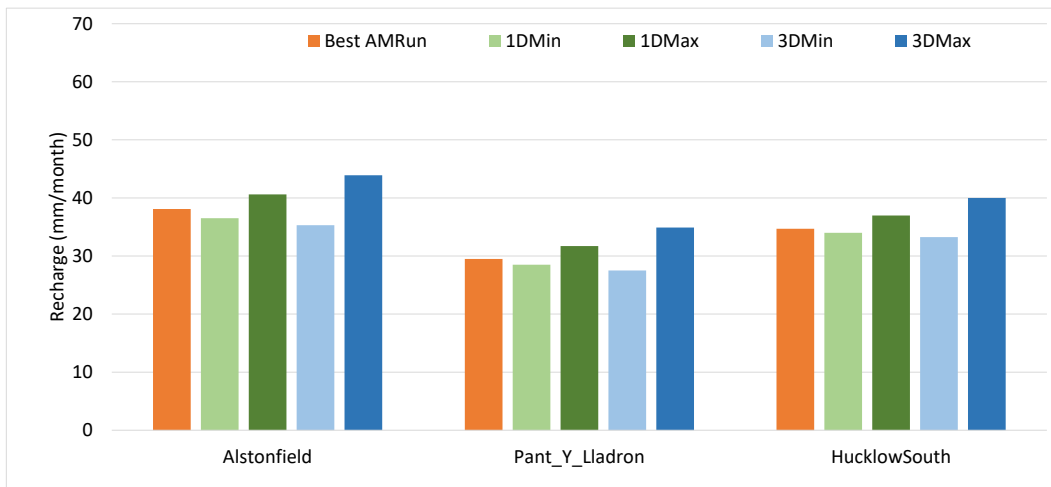


Figure 11 Historical (orange) and future recharge values (blue and green) as produced by the best performing AquiMod model.

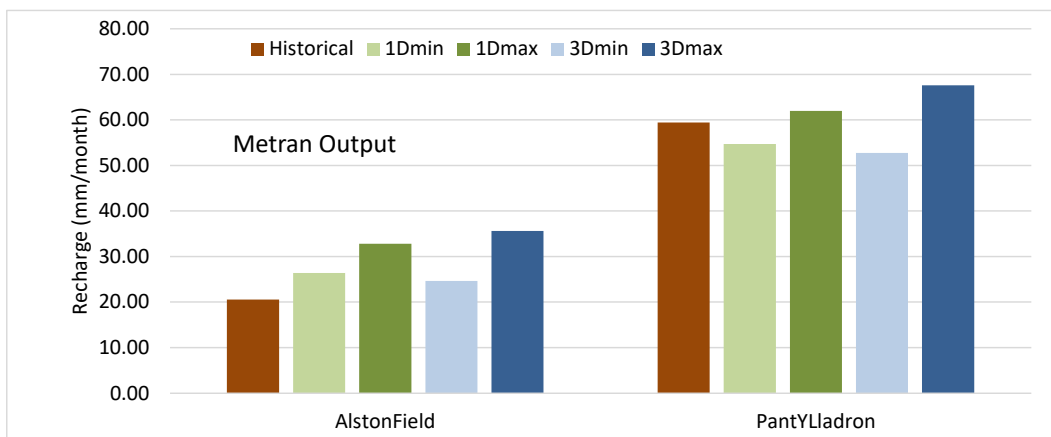


Figure 12 Historical (orange) and future recharge values (blue and green) produced by Metran.

Table 12 Monthly recharge values estimated using the historical and the projected forcing data.
Dotted line is the monthly historical recharge values. Green shaded area shows the 1° Min and Max monthly recharge values and the blue shaded area shows the 3° Min and Max monthly recharge values

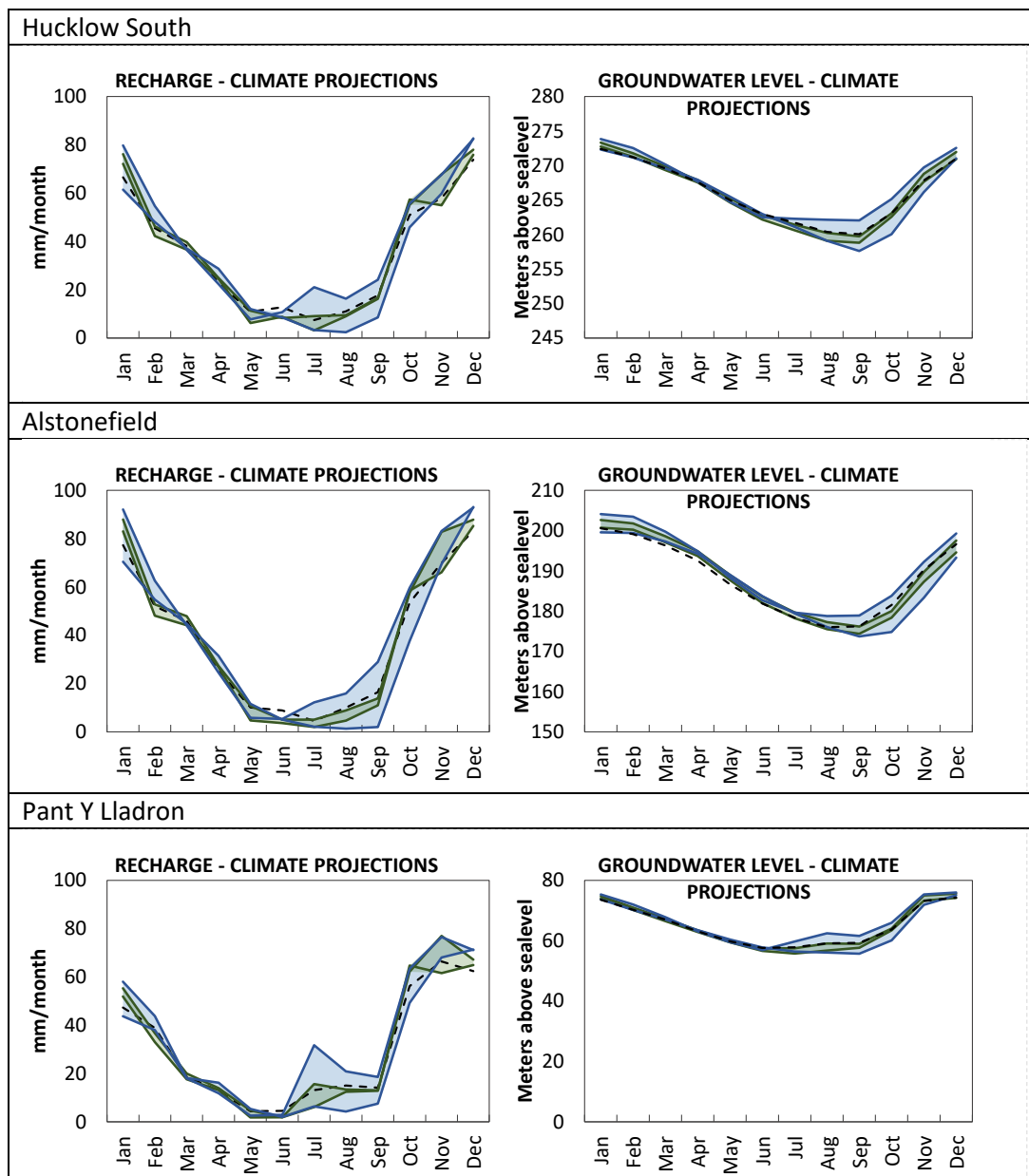


Table 13 shows maps of the spatially distributed recharge values calculated over the Devonian sandstone / Carboniferous Limestone aquifer. The plots are for the historical potential recharge values as well as those calculated using the distributed recharge model but with rainfall potential evaporation data altered using the 1° Min, 1° Max, 3° Min, and 3° Max UK change factors. The differences in the maps are not clear, however, the 1° Min and 3° Min data produce drier recharge maps and the 1° Max and 3° Max data produce wetter recharge maps as confirmed with the difference maps listed in Table 14.

Table 15 shows the average, maximum, and the standard deviation values calculated using the pixel values of the maps shown in Table 13. Looking at the average values, it is clear that there is reduction in recharge when the 1° Min or the 3° Min data are used compared to the historical recharge. The maximum of the pixel values of the 1° Min map is higher than the maximum of the pixel values of the 3° Min map as expected. The average recharge values of the pixel values of the 1° Max and 3° Max maps are both higher than the average from the historical map as expected. The maximum value from these two maps are also higher than the maximum obtained from the historical. Finally, there is little difference in the standard deviation values shown in Table 15 indicating that the spatial distribution of recharge values is not notably different between the different scenarios.

Table 13 Spatially distributed historical and projected recharge values

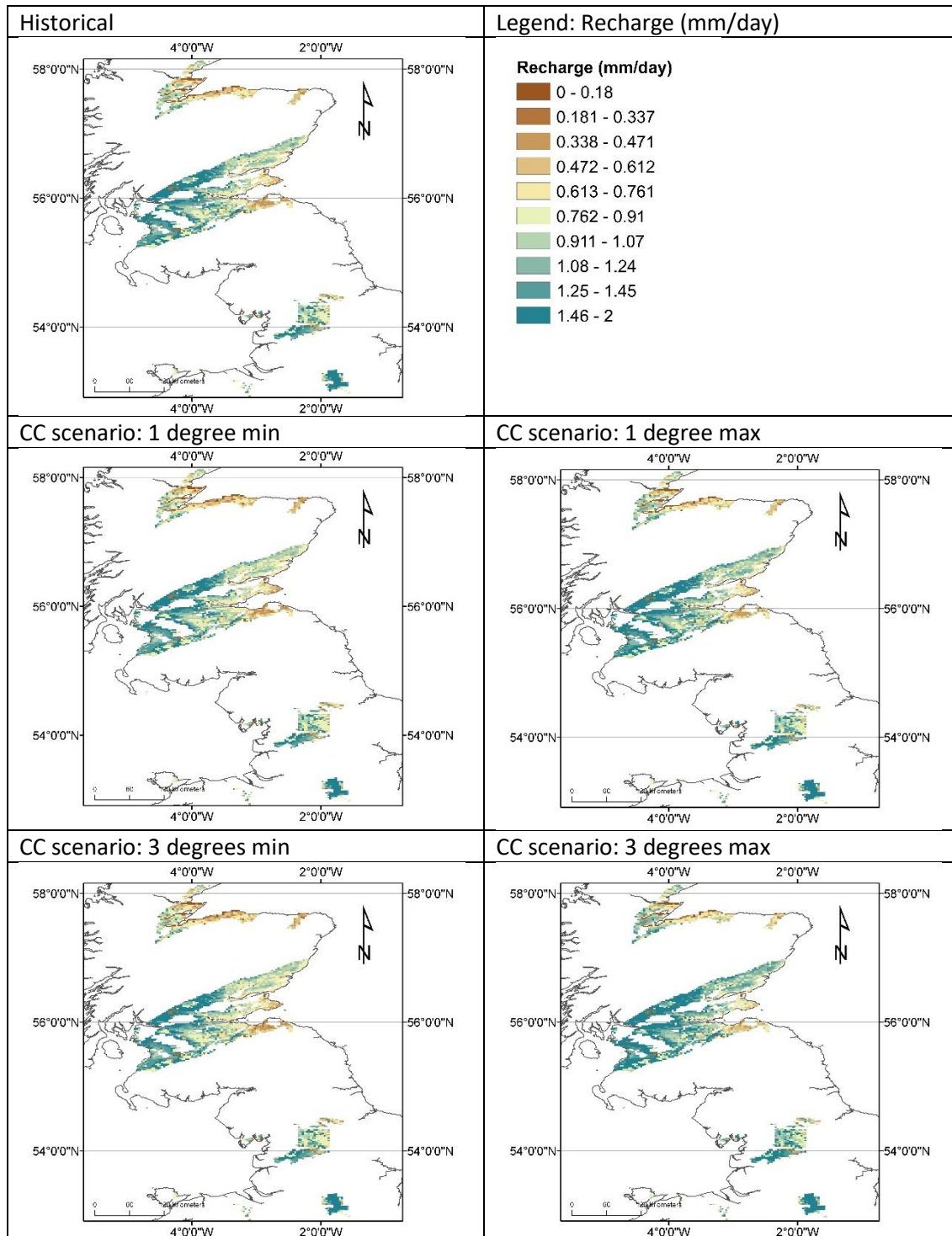


Table 14 Differences between the projected and historical recharge values calculated as projected values minus historical values

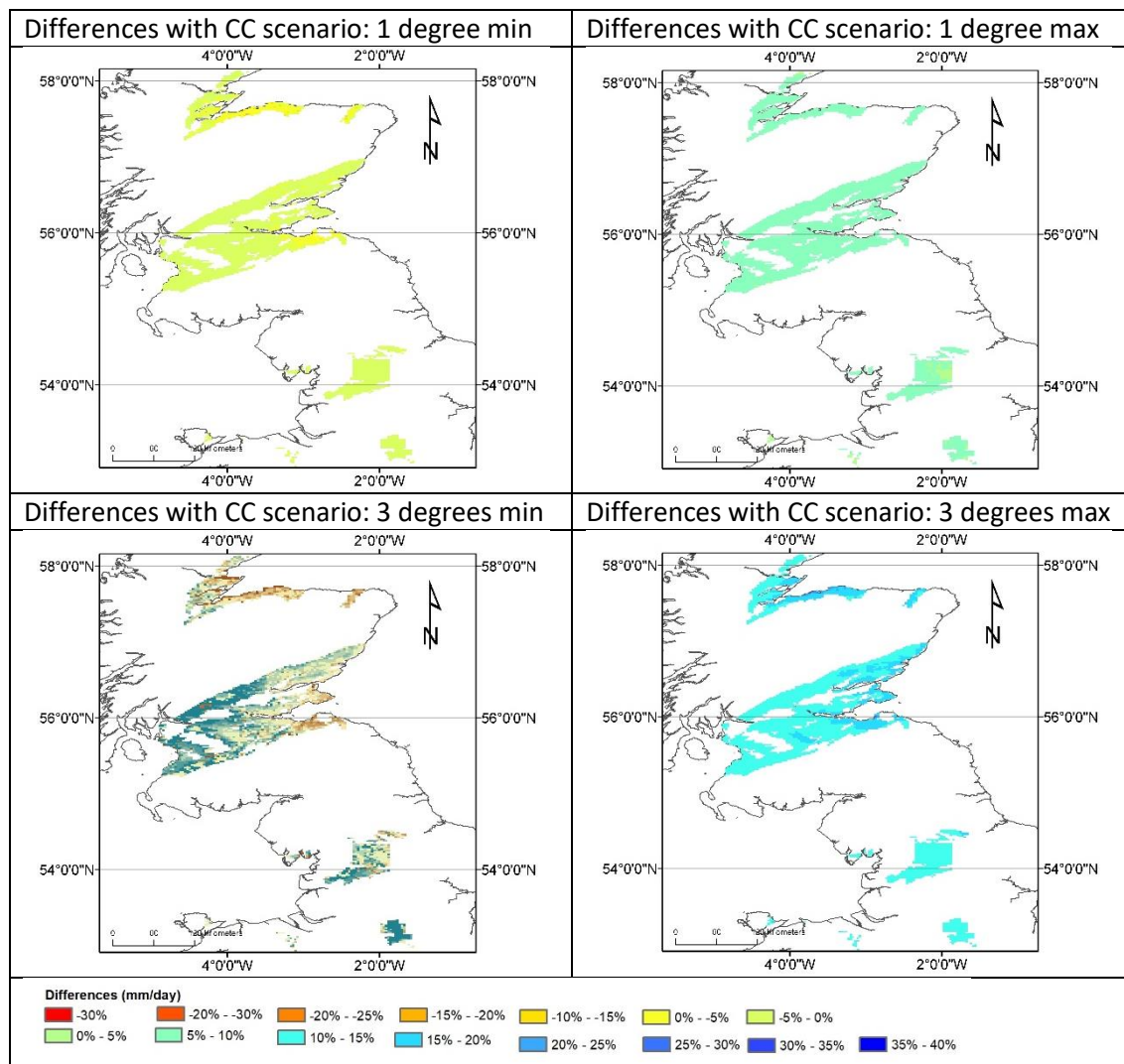


Table 15 Statistical information about the maps shown in Table 13

Map	Average recharge (mm/day)	Maximum recharge (mm/day)	Standard deviation (mm/day)
Historical	1.12	4.73	0.57
CC scenario: 1 degree min	1.087	4.71	0.567
CC scenario: 1 degree max	1.178	4.964	0.601
CC scenario: 3 degrees min	1.081	4.667	0.561
CC scenario: 3 degrees max	1.260	5.227	0.6334

REFERENCES

- Allen, D. J., L. J. Brewerton, L. M. Coleby, B. R. Gibbs, M. A. Lewis, A. M. MacDonald, S. J. Wagstaff, A. T. Williams. 1997. 'The Physical Properties of Major Aquifers in England and Wales'.
- Besbes, M. & de Marsily, G. (1984) From infiltration to recharge: use of a parametric transfer function. *Journal of Hydrology*, 74, p. 271-293.
- Hough, M. N. & Jones, R. J. A. 1997. The United Kingdom Meteorological Office rainfall and evaporation calculation system: MORECS version 2.0 – an overview. *Hydrology and Earth System Sciences*, 1, 227–239.
- IPCC: 2000, Special report on emissions scenarios (SRES): A special report of Working Group III of the Intergovernmental Panel on Climate Change, Cambridge University Press, Cambridge, p. 599
- Jenkins, G.J., Murphy, J.M., Sexton, D.S., Lowe, J.A., Jones, P. and Kilsby, C.G. 2009, UK Climate Projections: Briefing report, Met Office Hadley Centre, Exeter, UK.
- Mackay, J. D., Jackson, C. R., Wang, L. 2014. A lumped conceptual model to simulate groundwater level time-series. *Environmental Modelling and Software*, 61. 229-245. <https://doi.org/10.1016/j.envsoft.2014.06.003>
- Mackay, J. D., Jackson, C. R., Wang, L. 2014. *AquiMod user manual (v1.0)*. Nottingham, UK, British Geological Survey, 34pp. (OR/14/007) (Unpublished)
- Mansour, M. M. and Hughes, A. G. 2018. Summary of results for national scale recharge modelling under conditions of predicted climate change. British Geological Survey Internal report. Commissioned Report OR/17/026.
- Mansour, M. M., Wang, L., Whiteman, Mark, Hughes, A. G. 2018. Estimation of spatially distributed groundwater potential recharge for the United Kingdom. *Quarterly Journal of Engineering Geology and Hydrogeology*, 51 (2). 247-263. <https://doi.org/10.1144/qjegh2017-051>
- Murphy, J.M., Booth, B.B.B., Collins, M., Harris, G.R., Sexton, D.M.H., and Webb, M.J. 2007. A methodology for probabilistic predictions of regional climate change from perturbed physics ensembles. *Phil. Trans. R. Soc. A* 365, 1993–2028.
- Murphy, J.M., Sexton, D.M.H., Jenkins, G.J., Boorman, P.M., Booth, B.B.B., Brown, C.C., Clark, R.T., Collins, M., Harris, G.R., Kendon, E.J., Betts, R.A., Brown, S.J., Howard, T. P., Humphrey, K. A., McCarthy, M. P., McDonald, R. E., Stephens, A., Wallace, C., Warren, R., Wilby, R., and Wood, R. A. 2009, 'UK Climate Projections' Science Report: Climate change projections. Met Office Hadley Centre, Exeter.

Obergfell, C., Bakker, M., & Maas, K. (2019). Estimation of average diffuse aquifer recharge using time series modeling of groundwater heads. *Water Resources Research*, 55. <https://doi.org/10.1029/2018WR024235>

Prudhomme, C., Dadson, S., Morris, D., Williamson, J., Goodsell, G., Crooks, S., Boelee, L., Davies, H., Buys, G., Lafon, T. and Watts, G., 2012. Future Flows Climate: an ensemble of 1-km climate change projections for hydrological application in Great Britain. *Earth System Science Data*, 4(1), pp.143-148.

Zaadnoordijk, W.J., Bus, S.A.R., Lourens, A., Berendrecht, W.L. (2019) Automated Time Series Modeling for Piezometers in the National Database of the Netherlands. *Groundwater*, 57, no. 6, p. 834-843. <https://onlinelibrary.wiley.com/doi/epdf/10.1111/gwat.12819>

APPENDICES

Appendix A: AquiMod methodology

AquiMod is a lumped parameter computer model that has been developed to simulate groundwater level time series at observational boreholes (Mackay et al., 2014a). It is based on hydrological algorithms that simulates the movement of groundwater within the soil zone, the unsaturated zone, and the saturated zone. The lumped models neglect complexities included in distributed groundwater models but maintains some of the fundamental physical principles that can be related to the conceptual understanding of the groundwater system (Mackay et al., 2014b).

While AquiMod was originally designed to capture the behaviour of a groundwater system through the analysis of groundwater level time series, it can produce the infiltration recharge values and groundwater discharges from the aquifer as a by-product. AquiMod is driven by complete time series of forcing data for either historical or predicted future conditions. Running AquiMod in predictive mode can be used to fill in gaps in historical groundwater level time series, or calculate future groundwater levels. In addition to groundwater levels, it also provides predictions of historical and future recharge values and groundwater discharges. In the current application we use calibrated AquiMod models to estimate the recharge values at selected boreholes.

AquiMod consists of three modules (Figure A1). The first is a soil water balance module that calculates the amount of water that infiltrates the soil as well as the soil storage. The second module controls the movement of water in the unsaturated zone, mainly it delays the arrival of infiltrating water to the saturated zone. The third module calculates the variations in groundwater levels and discharges. The model executes the modules separately following the order listed above.

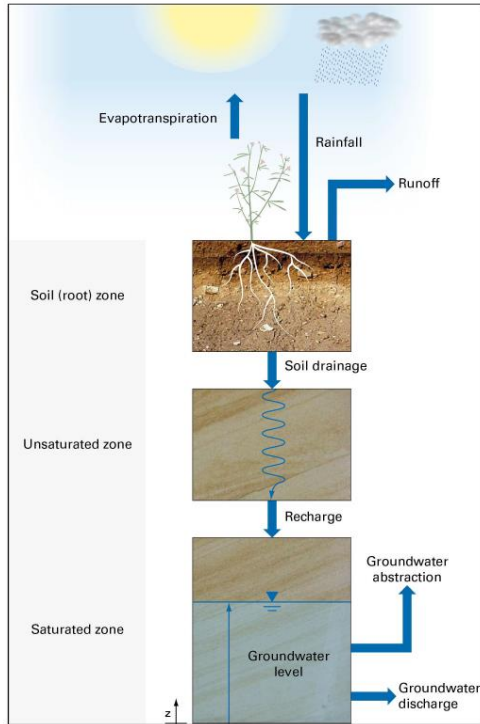


Figure A1 Generalised structure of Aquimod (after Mackay et al., 2014a)

The soil moisture module

There are several methods available in Aquimod that can be used to calculate the rainfall infiltration into the soil zone. In this study we use the FAO Drainage and Irrigation Paper 56 (FAO, 1988) approach. In this method, the capacity of the soil zone, from which plants draw water to evapo-transpire, is calculated first using the plants and soil characteristics. Evapo-transpiration is calculated according to the soil moisture deficit level compared to two parameters: Readily Available Water (RAW) and Total Available Water (TAW). These are a function of the root depth and the depletion factor of the plant in addition to the soil moisture content at field capacity and wilting point as shown in Equations A1 and A2.

$$TAW = Z_r(\theta_{fc} - \theta_{wp})$$

Equation A1

$$RAW = p \cdot TAW$$

Equation A2

Where Z_r [L] and p [-] are the root depth and depletion factor of a plant respectively, θ_{fc} [$L^3 L^{-3}$] and θ_{wp} [$L^3 L^{-3}$] are the moisture content at field capacity and wilting point respectively.

The FAO method is simplified by Griffiths et al. (2006) who developed a modified EA-FAO method. In this method the evapotranspiration rates are calculated as a function of the potential evaporation and an intermediate soil moisture deficit as:

$$\begin{aligned} e_s &= e_p \left[\frac{s_s^*}{TAW - RAW} \right]^{0.2} & s_s^* > RAW \\ e_s &= e_p & s_s^* \leq RAW \\ e_s &= 0 & s_s^* \geq TAW \end{aligned}$$

Equation A3



Where e_s [L] is the evapo-transpiration rate, e_p [L] is the potential evaporation rate and s_s^* [L] is the intermediate soil moisture deficit given by

$$s_s^* = s_s^{t-1} - r + e_p \quad \text{Equation A4}$$

Where r [L] is the rainfall at the current time step and s_s^{t-1} [L] is the soil moisture deficit calculated at the previous time step.

The new soil moisture deficit is then calculated from:

$$s_s = s_s^{t-1} - r + e_s \quad \text{Equation A5}$$

Griffiths et al. (2006) proposed that the recharge and overland flow are only generated when the calculated soil moisture deficit becomes zero. The remaining volume of water, the excess water, is then split into recharge and overland flow using a runoff coefficient. In Aquimod a baseflow coefficient is used to reflect the fact that a groundwater discharge is calculated rather than overland water. In this application, the baseflow coefficient is one minus the runoff coefficient.

The unsaturated zone module

The Aquimod version used in this study to simulate the movement of groundwater flow within the unsaturated zone is based on a statistical approach rather than a process-based approach. This method distributes the amount of rainfall recharge over several time steps where the soil drainage for each time step is calculated using a two-parameter Weibull probability density function. The Weibull function can represent exponentially increasing, exponentially decreasing, and positively and negatively skewed distributions. This can be used to focus the soil drainage over earlier or later time steps or to spread it over a number of time steps after the infiltration occurs. The shape of the Weibull function is controlled by two parameters, k and λ as shown in Equation A6.

$$f(t, k, \lambda) = \begin{cases} \frac{k}{\lambda} \left(\frac{t}{\lambda}\right)^{k-1} e^{-(t/\lambda)^k} & t > 0 \\ 0 & t \leq 0 \end{cases} \quad \text{Equation A6}$$

Where k and λ are two parameters the values of which are calculated during the calibration of the model and t is the time step.

The saturated zone module

Aquimod considers the saturated zone as a rectangular block of porous medium with dimensions L and B as its length and width [L] respectively. This block is divided into a number of layers, each has a defined hydraulic conductivity value, a storage coefficient value, and a discharging feature. The number of layers define the structure of the saturated module used in the study.

The mass balance equation that gives the variation of hydraulic head with time is given by:

$$SLB \frac{dh}{dt} = RLB - Q - A \quad \text{Equation A7}$$

Where:

S is the storage coefficient of the porous medium [-]

h is the groundwater head [L]

t is the time [T]

R is the infiltration recharge [L T⁻¹]



Q is the discharge out of the aquifer [$L T^{-1}$]
 A is the abstraction rate [$L T^{-1}$]

It must be noted that in a multi-layered groundwater system as shown in Figure A2, we calculate one groundwater head (h) for the whole system. The discharges (Q) from Outlet 1, 2, etc. are calculated using the Darcy law. The total discharges can be summarised using the following equation:

$$Q = \sum_{i=1}^m \frac{T_i B}{0.5 L} \Delta h_i \quad \text{Equation A8}$$

Where:

m is the number of layers in the groundwater system [-]

T_i is the transmissivity of the layer i [$L T^{-2}$]

Δh_i is the difference between the groundwater head h and z_i , the elevation of the base of layer i

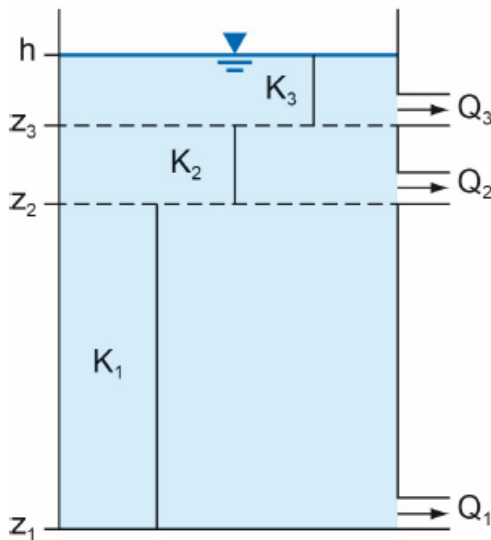


Figure A2 Representation of the saturated zone using a multi-layered groundwater system

Substituting Equation A8 into Equation A7 yields a numerical equation in the form:

$$S \frac{(h-h^*)}{\Delta t} = R - \sum_{i=1}^m \frac{T_i}{0.5 L^2} \Delta h_i - \frac{A}{LB} \quad \text{Equation A9}$$

Equation A9 is an explicit numerical equation that allows the calculation of the groundwater head h [L] at any time and using time steps of Δt [T]. In this equation h^* [L] is the groundwater head calculated at the previous time step and the term Δh_i [L] is calculated as $(h^* - z_i)$.

The terms S , T_i , and L are optimised during the calibration of the model. A groundwater system can be specified with one storage coefficient as shown in the equations above or with different storage coefficient values for the different layers. Several saturated modules are included in Aquimod to provide this flexibility and the model user can select the model structure that represent the conceptual understanding best.



Limitations of the model

AquiMod is a lumped groundwater model that aims at reproducing the behaviour of the observed groundwater levels. It tries to encapsulate the conceptual understanding of a groundwater system in a simple numerical representation. The model results have to be therefore discussed, taking this into consideration. For example, the model represents the groundwater system as a closed homogeneous medium, with no impact from any outer boundary or feature, whether physical or hydrological, such as the presence of rising and falling river stage.

Vertical heterogeneity can be accounted for by using multi-layered groundwater module structure. However, this model setting does not provide any information about the vertical connections between the layers as the discharge from all the layers is calculated using one representative groundwater head value. In other words, it is assumed that all layers are in perfect hydraulic connection.

As mentioned before, the model is designed to simulate the groundwater levels. However, it produces the recharge values and groundwater discharges as by products. In this application we use the calibrated model to calculate recharge. The mass balance equation (Equation A7) shows that recharge is a function of transmissivity and storage coefficient values, which are estimated during the calibration process of the model, i.e. they are not parameters with fixed values provided by the user. The inter-connections between these parameters leads to uncertainties in the estimated recharge values as a high storage coefficient value can produce a high recharge estimate and vice versa. To overcome this problem, it is suggested that the recharge values estimated by AquiMod are always presented as a range of possibilities rather than an absolute value. This can be achieved by estimating the recharge values from all the models that have a performance measure above than a threshold that is deemed acceptable by the user. The recharge estimates can then be presented as an average of all estimates and values corresponding to selected percentiles.

Model input and output

AquiMod includes a number of methods that calculates rainfall recharge as well as a number of model structure from which the user can select what better suits the case study.

Model input consists time series of forcing data including rainfall and potential evaporation, time series of anthropogenic impact mainly groundwater abstraction and time series of groundwater levels that will be used to calibrate the model. These time series must be complete, i.e. a value is available at every time step except the groundwater level time series, which can include missing data. The time step can be one day or multiple of days, and the model automatically calculate the size of the time step based on the input data time series.

The model is run first in calibration mode where a range of parameter values are specified for the different parameters included in the three model modules. A Monte Carlo approach is used to select the best parameter values. The performance of the model is measured by comparing the simulated groundwater levels to the observed ones using the Nash Sutcliffe Efficient (NSE) or



the Root Mean Squared Error (RMSE) performance measures. The parameter set that produces the best model performance is selected to run the model in evaluation mode.

When the model is run in evaluation mode, it produces output files that give recharge values, groundwater levels and groundwater discharges time series with time as specified in the input file. The number of output files is equal to the number of acceptable models set by the user.

Appendix B: Metran methodology

Metran applies transfer function noise modelling of (groundwater head) time series with usually daily precipitation and evaporation as input (Zaadnoordijk et al., 2019). The setup is shown in the Figure B1. If time series of other influences on the groundwater head are available, these contributions can be added to the deterministic part of the model. The stochastic part is the difference between the total deterministic part and the observations (the residuals). The corresponding input of the noise model should have the character of white noise.

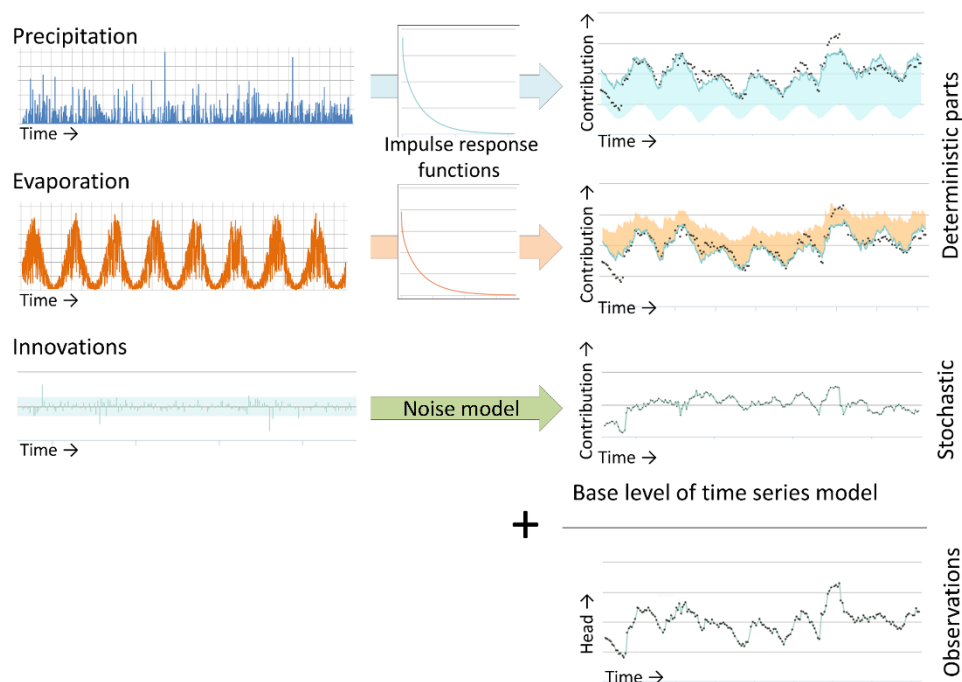


Figure B1 Illustration of METRAN setup

The stochastic part is needed because of the time correlation of the residuals, which does not allow a regular regression to obtain the parameter values of the transfer functions.

The incomplete gamma function is used as transfer function. This is a uni-modal function with only three parameters that has a quite flexible shape and has some physical background (Besbes & de Marsily, 1984). The evaporation response is set equal to the precipitation response except for a factor (f_c). The noise model has one parameter that determines an exponential decay. Thus, for the standard setup with precipitation and evaporation, there are five parameters that have to be determined from the comparison with the observations. Three parameters regarding the precipitation response, the evaporation factor, and the noise model parameter (actually, the time series model has a fifth parameter, the base level, but this is determined from the assumption that the average of the calculated heads is equal to the average of the observations). There are three extra parameters for each additional input series, such as pumping.



Limitations

Metran's time series model is linear. So, the model creation breaks down when the system is strongly nonlinear. This can occur e.g. when drainage occurs for high groundwater levels, when the ratio between the actual evapotranspiration and the inputted reference evaporation varies strongly, or when the groundwater system changed during the simulated period.

Metran is not able to find a decent time series model when the response function is not appropriate for the groundwater system. An example of this is a system with a separate fast and slow response as was found for a French piezometer in the Avre region, as is illustrated in Figure B2.

Finally, the parameter optimization of Metran uses a gradient search method in the parameter space, so it can be sensitive to initial parameter values in finding an optimal solution.

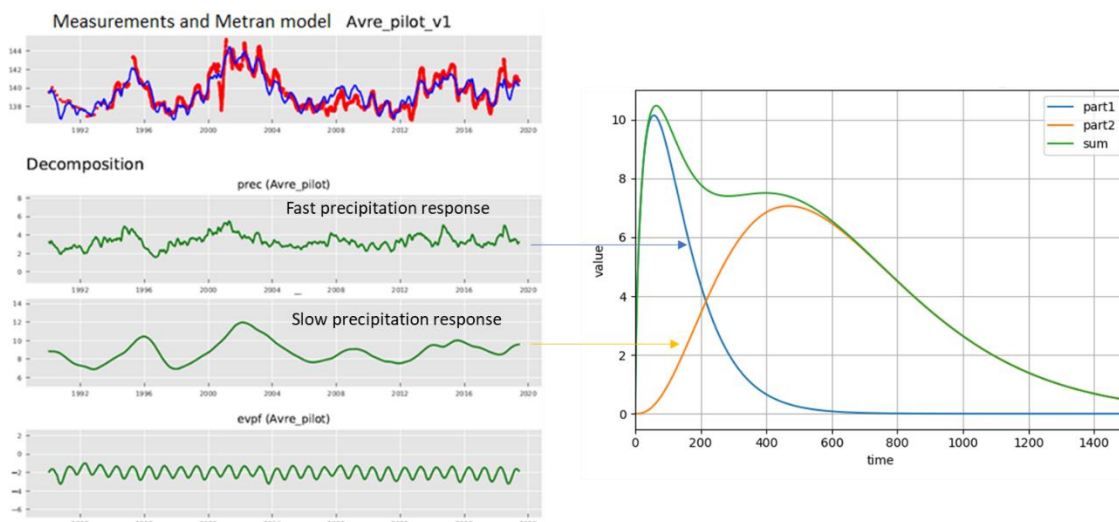


Figure B2. An example where the response function implemented in METRAN is not suitable for the groundwater system

Time step

Metran has been designed to work with explanatory series that have a daily time step. However, it has been adapted so that other time step lengths can be applied; although Metran still has the limitation that the explanatory variables have a constant frequency. For the TACTIC simulations of series with monthly or decadal meteorological input series, the time step has been set to 30 and 10 days, respectively. This time step has been applied from the end date backward.

Note that the heads may be irregular in time as long as the frequency is not greater than the frequency of the explanatory series.

Model output

The evaporation factor f_c gives the importance of evapotranspiration compared to precipitation. The parameter M_0 gives the total precipitation response, which is equal to the area below the impulse response function and the final value of the step response function.



The average response time is another characteristic of the precipitation response. The influence is illustrated in Figure B3 with the impulse response functions and head time series for two models with very different response times for time series of SGU in Sweden.

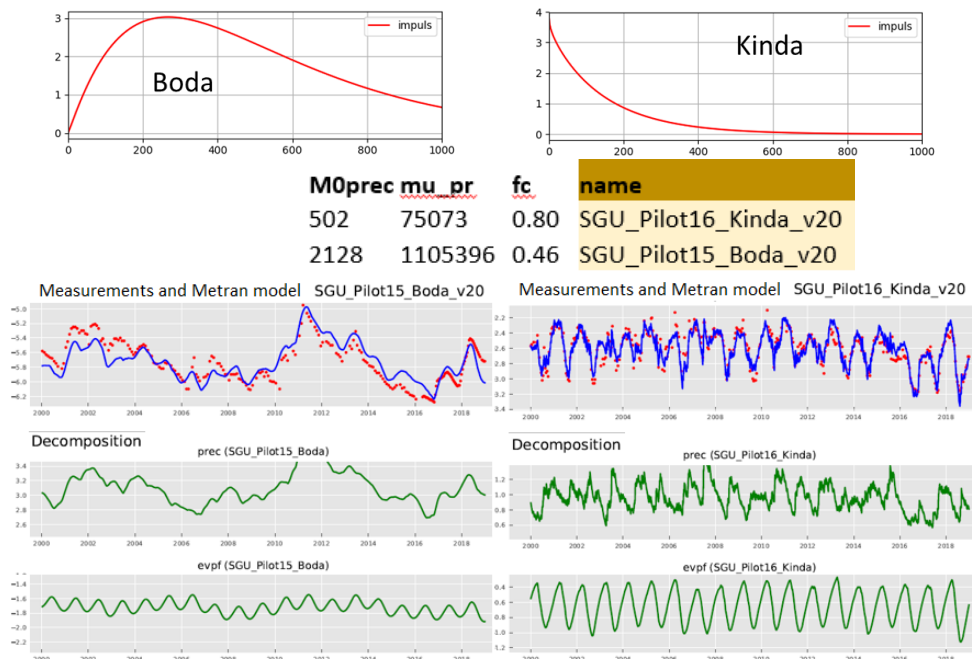


Figure B3 Illustration of Metran output for two case studies in Sweden with different response times.

Model quality

Metran judges a resulting time series model according to a number of criteria and summarizes the quality using two binary parameters Regimeok, Modok (see Zaadnoordijk et al., 2019):

- Regimeok = 1 : highest quality
- Modok = 1 (and Regimeok = 0) : ok
- Both zero = model quality insufficient

More detailed information on the model quality is given in the form of scores for two information criteria (AIC and BIC), a log likelihood, R², RMSE, and the standard deviations and correlations of the parameters.

Recharge

Although the transfer-noise modelling of Metran determines statistical relations between groundwater heads and explanatory variables, we like to think of the results in physical terms. It is tempting to interpret the evaporation factor, as the factor translating the reference into the actual evapotranspiration. Then, we can calculate a recharge as



$$R = P - fE$$

Equation B1

where R is recharge, P precipitation, E evapotranspiration, and f the evaporation factor.

Following the definitions used in the TACTIC project, this recharge R actually is the effective precipitation. It is equal to the potential recharge when the surface runoff is negligible. This in turn is equal to the actual recharge at the groundwater table if there also is no storage change or interflow. In such cases it may be expected that this formula indeed corresponds to the meteorological forcing of the groundwater head in a piezometer, so that it gives a reasonable estimate of the recharge. Obergfell et al. (2019) showed this for an area on an ice pushed ridge in the Netherlands. However, this assumes that all precipitation recharges the groundwater, which cannot be done in many places.

In Dutch polders with shallow water tables and intense drainage networks, it is reasonable to assume that the actual evapotranspiration is equal to the reference value. In that case, the factor f becomes larger than 1 because 1 mm of evaporation has less effect than 1 mm of precipitation (because part of the evaporation does not enter the ground but is immediately drained to the surface water system). In that case, we can calculate recharge as:

$$\begin{aligned} R &= P - fE & f &\leq 1 \\ R &= P/f - E & f &> 1 \end{aligned}$$

Equation B2

These simple formulas can be applied easily for the situations currently modelled in Metran and for the simulations that are driven by future climate data using the delta-change climate factors. However, it is noted that it is a crude estimate using assumptions that are easily violated. Because of this, the equations should be applied only to long term averages using only models of the highest quality.



Deliverable 4.2

PILOT DESCRIPTION AND ASSESSMENT

Jurassic aquifer (United Kingdom)

Authors and affiliation:

**Majdi Mansour, Vasileios
Christelis**

British Geological Survey (BGS)

This report is part of a project that has received funding by the European Union's Horizon 2020 research and innovation programme under grant agreement number 731166.



Deliverable Data	
Deliverable number	D4.2
Dissemination level	Public
Deliverable name	Pilots description and assessment report for recharge and groundwater vulnerability
Work package	WP4
Lead WP	BRGM, BGS
Deliverable status	
Version	Version 3
Date	23/3/2021

[This page has intentionally been left blank]

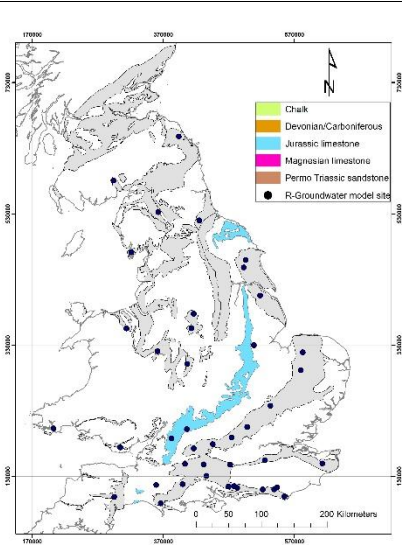
LIST OF ABBREVIATIONS & ACRONYMS

BGS	British Geological Survey
CC	Climate Change
EU	European Union
FAO	Food and Agriculture Organization
GCM	Global Circulation Models
GSO	Geological Survey Organization
ISIMIP	Inter Sectoral Impact Model Inter-comparison Project
NSE	Nash-Sutcliffe Efficiency
PET	Potential Evapo-Transpiration
R	Regression coefficient error
WP	Work Package

TABLE OF CONTENTS

LIST OF ABBREVIATIONS & ACRONYMS	5
1 EXECUTIVE SUMMARY	5
2 INTRODUCTION	7
3 PILOT AREA	9
3.1 Site description and data	9
3.1.1 Index boreholes in the Jurassic limestones aquifer in the UK	9
3.1.2 Topography	11
3.1.3 Land use	12
3.1.4 Rainfall	13
3.1.5 Potential evaporation	14
3.1.6 Hydrogeology	16
3.1.7 Groundwater levels	16
3.2 Climate change challenge	17
4 METHODOLOGY	18
4.1 Methodology and climate data	18
4.1.1 AquiMod	18
4.1.2 Metran	18
4.1.3 The distributed recharge model ZOODRM applied at the UK scale	19
Climate data	20
4.2 Model set-up	21
4.2.1 AquiMod	21
4.2.2 Metran	24
4.2.3 National scale model (ZOODRM)	25
4.3 Model calibration	27
4.3.1 Calibration of AquiMod models	27
4.3.2 Calibration of Metran models	29
4.3.3 Calibration of the UK national scale model using ZOODRM	30
5 RESULTS AND CONCLUSIONS	31
5.1 Historical recharge values	31
5.2 Projected recharge values	33
REFERENCES	41
APPENDICES	43
Appendix A: AquiMod methodology	43
The soil moisture module	44
The unsaturated zone module	45
The saturated zone module	45
Limitations of the model	47
Model input and output	47
Appendix B: Metran methodology	49
Limitations	50
Time step	50
Model output	50
Model quality	51
Recharge	51

1 EXECUTIVE SUMMARY

Pilot name	Jurassic aquifer	
Country	United Kingdom	
EU-region	North-western Europe	
Area (km ²)	NA	
Aquifer geology and type classification	Consists of a variable group of limestones, sands and clays up to 150 m thick. Yields are typically in the range 5 to 15 l/sec	
Primary water usage	Irrigation / Drinking water / Industry	
Main climate change issues	Risk of high precipitation causing groundwater flooding. Risk of drought.	
Models and methods used	Lumped groundwater modelling (AquiMOD)	
Key stakeholders	Government. Research institutes. Water companies.	
Contact person	British Geological Survey. Andrew McKenzie	

This report describes the work undertaken by the British Geological Survey (BGS/UKRI) as a part of TACTIC WP4 to calculate historical and future groundwater recharge across the outcrop of Jurassic aquifer and at selected observation boreholes within this aquifer. Multiple tools, selected from the TACTIC toolbox that is developed under WP2 of the TACTIC project, have been used for this purpose.

The Jurassic limestones are prominent aquifers in the Cotswold Hills, in eastern England and the North Yorkshire moors. They are relatively hard limestones with low specific yields but high permeability characteristics due to extensive fracture network and enlarged by solution. The topography of the Jurassic outcrop is characterised by vales and escarpments with arable being the dominant land use. While groundwater may remain under confined conditions during the year at some location, aquifer conditions switch between confined and unconfined at some other areas depending on the season of the year.

Three tools have been used to estimate the recharge values. These are the lumped parameter computer model *AquiMod* (Mackay et al., 2014a), the transfer function-noise model *Metran* (Zaadnoordijk et al., 2019), and the distributed recharge model *ZOODRM* (Mansour and Hughes, 2004). Future climate scenarios are developed based on the ISIMIP (Inter Sectoral Impact Model Inter-comparison Project (www.isimip.org) datasets. The resolution of the data is 0.5°x0.5° global grid and at daily time steps. As part of ISIMIP, much effort has been made to standardise the climate data (e.g. undertake bias correction).

The estimation of the recharge model using the lumped model *AquiMod* is achieved by running the model in Monte Carlo mode. This produces many runs that are equally acceptable and consequently the uncertainty in the estimated recharge values can be assessed. The application of additional tools provides an additional mean to assess this uncertainty. Groundwater data at three boreholes are used in this model. The differences between the 75th and 25th percentile recharge values are found to be between 26% and 33%, which indicates a relatively high degree of uncertainty. Three recharge values estimated using the distributed recharge model are found to be close to those estimated using the lumped model noting that these models calculate potential recharge and actual recharge values respectively. The absolute recharge values calculated by the transfer function-noise model *Metran* are also different from those calculated by the lumped model with no consistent pattern that can be reported.

Future recharge values have been calculated using the projected rainfall and potential evaporation values are -4.4 to 15.8% different from historical values on average. The 3^o Max scenario, the wettest used in this work, produces values that are very different from the historical ones. This is observed in the output of both the lumped and the distributed models. Finally, future estimates are discussed in this report using long term average recharge values. It is recommended to carry out further analysis to these output in order to understand the temporal changes in recharge values in future, especially over the different seasons. In addition, it is recommended that the values and conclusion produced from this work should be compared to those obtained from different studies that applies future climate data obtained from different climate models.

2 INTRODUCTION

Climate change (CC) already has widespread and significant impacts on Europe's hydrological systems including groundwater bodies, which is expected to intensify in the future. Groundwater plays a vital role for the land phase of the freshwater cycle and has the capability of buffering or enhancing the impact from extreme climate events causing droughts or floods, depending on the subsurface properties and the status of the system (dry/wet) prior to the climate event. Understanding the hydrogeology is therefore essential in the assessment of climate change impacts. Providing harmonised results and products across Europe is further vital for supporting stakeholders, decision makers and EU policies makers.

The Geological Survey Organisations (GSOs) in Europe compile the necessary data and knowledge of the groundwater systems across Europe. To enhance the utilisation of these data and knowledge of the subsurface system in CC impact assessments, the GSOs, in the framework of GeoERA, has established the project "Tools for Assessment of Climate change Impact on Groundwater and Adaptation Strategies – TACTIC". By collaboration among the involved partners, TACTIC aims to enhance and harmonise CC impact assessments and identification and analyses of potential adaptation strategies.

TACTIC is centred around 40 pilot studies covering a variety of CC challenges as well as different hydrogeological settings and different management systems found in Europe. Knowledge and experiences from the pilots will be synthesised and provide a basis for the development of an infrastructure on CC impact assessments and adaptation strategies. The final projects results will be made available through the common GeoERA Information Platform (<http://www.europe-geology.eu>).

The specific TACTIC activities focus on the following research questions:

- What are the challenges related to groundwater- surface water interaction under future climate projections (TACTIC WP3)?
- Estimation of renewable resources (groundwater recharge) and the assessment of their vulnerability to future climate variations (TACTIC WP4).
- Study the impact of overexploitation of the groundwater resources and the risks of saline intrusion under current and future climates (TACTIC WP5).
- Analyse the effectiveness of selected adaptation strategies to mitigate the impacts of climate change (TACTIC WP6).

This report describes the work undertaken by the British Geological Survey (BGS/UKRI) as a part of TACTIC WP4 to calculate groundwater recharge at selected locations within the Jurassic aquifer. WP4 is divided into seven tasks that cover the following activities: Review of tools and methods and identification of data requirements (Task 4.1), identification of principal aquifers and their characteristics aided by satellite data (Task 4.2), recharge estimation and its evolution under climate change scenarios in the principal aquifers (Task 4.3), analysis of long-term piezometric time series to evaluate aquifer vulnerability to climate change (Task 4.4), assessment of subsidence in aquifer systems using DInSAR satellite data (Task 4.5), development of a satellite based net precipitation and recharge map at the pan-European scale (Task 4.6), and tool descriptions and guidelines (Task 4.7).

The work presented here is related to Task 4.3 that aims at the estimation of recharge under current and future climates. This is undertaken using multiple tools selected from the TACTIC toolbox that has been developed under WP2 of the TACTIC project. The toolbox is a collection of groundwater models, scripts, spreadsheets that serves all the activities identified in TACTIC workpackages. Here we use the lumped groundwater model *AquiMod* (Mackay et al., 2014a and Mackay et al., 2014b) and the Transfer Function-Noise Model *Metran* (Zaadnoordijk et al., 2019) with main challenge to calibrate these models to reproduce the behaviour of the observed groundwater level time series. The calibrated models are then used to calculate historical and future recharge values. In addition to these two models, we apply the UK national scale recharge model (Mansour et al., 2018) to validate the calculated recharge values and also to address the uncertainty associated with the calculation of these values.

3 PILOT AREA

3.1 Site description and data

3.1.1 *Index boreholes in the Jurassic limestones aquifer in the UK*

The Jurassic limestones are prominent aquifers in the Cotswold Hills, in eastern England and the North Yorkshire moors (Figure 1). They consist of the Great and Inferior Oolites, the Lincolnshire Limestone and the Corallian limestones. They are relatively hard limestones with low specific yields but there is an extensive fracture network, enlarged by solution, which gives its high permeability characteristics. The largest yields from individual wells in the UK are provided by the Lincolnshire Limestone; the initial natural artesian overflow from one borehole was more than 30 Ml/d. (Source: UK Groundwater forum).

Throughout England, the Jurassic sedimentation was affected by a series of marine transgressions and regressions. The first transgression was in early Jurassic times with a predominantly clay sequence overstepping rocks varying in age from latest Triassic to Palaeozoic. A regression followed in the early Mid-Jurassic and characterised by the replacement of marine sediments by non-marine deltaic sediments in northern and some of central England. This was followed by large-scale limestone deposition everywhere with the exception being the Cleveland Basin. A second transgression was followed by a long period of clay deposition. A final major regression occurred at the end of the Jurassic, with the sequence shallowing. The majority of the sequence comprises shales and clays, with limestones and sandstones forming a relatively small part of the total thickness. The complex facies variation of the Jurassic, make it ideal as an aquifer in many places, mainly due to the presence of limestones and the alternation of permeable and impermeable strata.

The principle Jurassic aquifers, the Inferior Oolite and Great Oolite limestones, have an outcrop area of approximately 600 km² in the Upper Cotswolds.

Table 1 shows the location of the three observation boreholes in the Jurassic aquifer that are currently included in the analysis. A lumped groundwater model is built to estimate the recharge values at these boreholes.

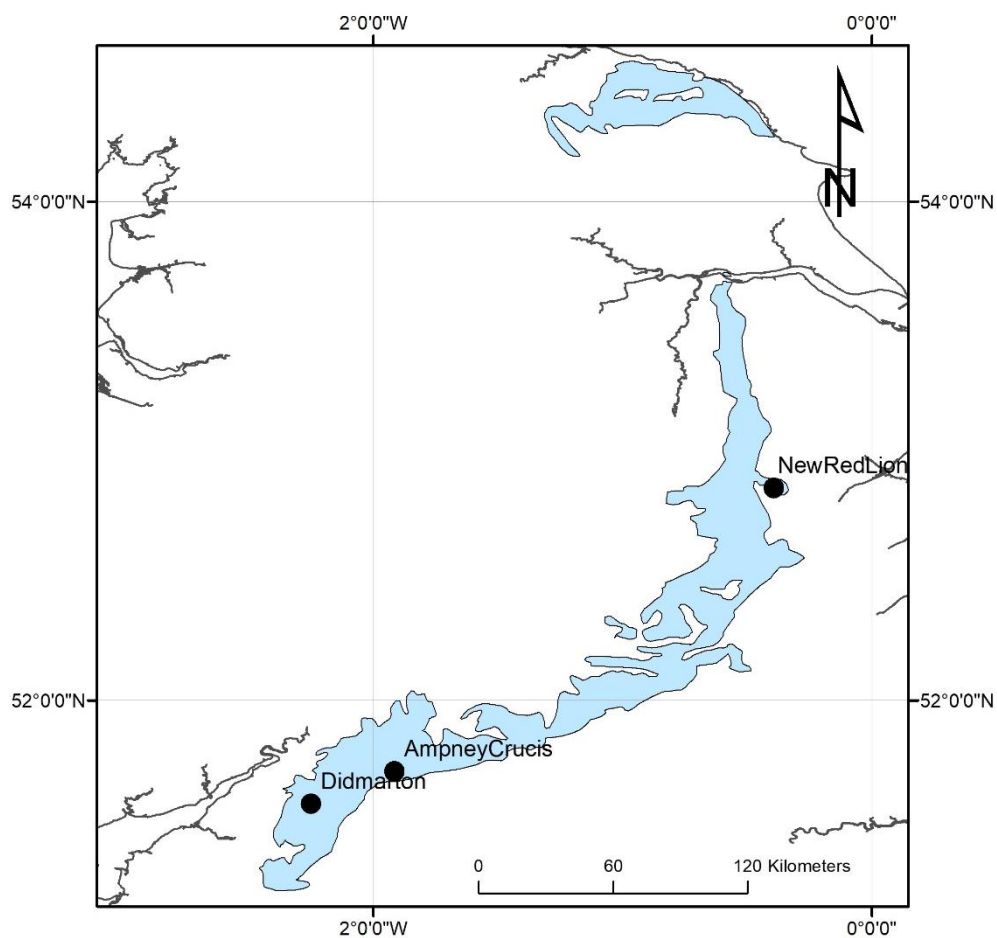


Figure 1. Extent of the Jurassic aquifer and borehole locations.

Table 1. Description of observation boreholes

Borehole name	Location	GWs record	Hydrogeological response
Didmarton	South of England	1977-current	The hydrograph shows a smooth sinusoidal pattern but with large seasonal fluctuations. The maximum water level appears to be constrained.
New Red lion	East of England	1964-current	The hydrograph has an annual sinusoidal appearance with up to 20 metres inter-annual variation.
Ampney Crucis	South of England	1959 - current	The hydrograph has multiple peaks in response to rainfall events. It shows its maxima in late spring. Fluctuations are normally around three metres with a ceiling at around 103 m AOD that is linked to the presence of springs.

3.1.2 Topography

The topography of the Jurassic outcrop is characterised by vales and escarpments with ground surface elevations ranging from zero to approximately 450 m AOD (Figure 2). Many of the steeper slopes are wooded and there are sea cliffs along the coasts in Yorkshire, south wales and Dorset.

Spring lines are well-developed at the boundary of geological contacts and provide significant baseflow to rivers. Spring discharge in the Cotswolds is considerable and is estimated to exceed pumped abstraction.

Topographical data can be extracted at the selected boreholes to study the occurrences flooding events under future climate conditions.

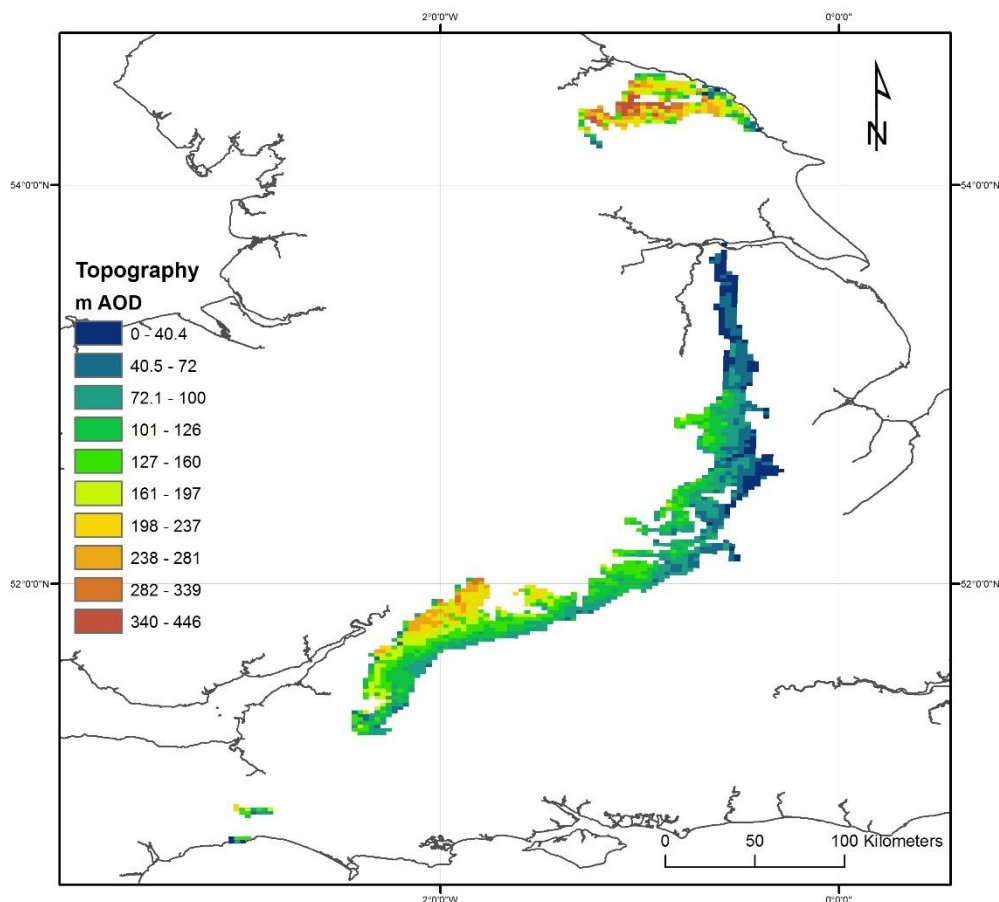


Figure 2. Topography map over the Jurassic formation

3.1.3 Land use

The dominant land use over the Jurassic aquifer outcrop is arable but managed grassland and forestry/woodland exists but over a relatively small proportion of the total area. There are several urban areas indicated by the dark red pixels in Figure 3.

Figure 3 shows the spatial distribution of landuse classes over the Jurassic outcrop (Bibby, 2009). Landuse data can be extracted from this map at the selected boreholes to specify the model parameters that control evapo-transpiration, which is an important component of the total water balance produced by the applied models. Specific information about the landuse types at the boreholes within this aquifer are listed in Table 2.

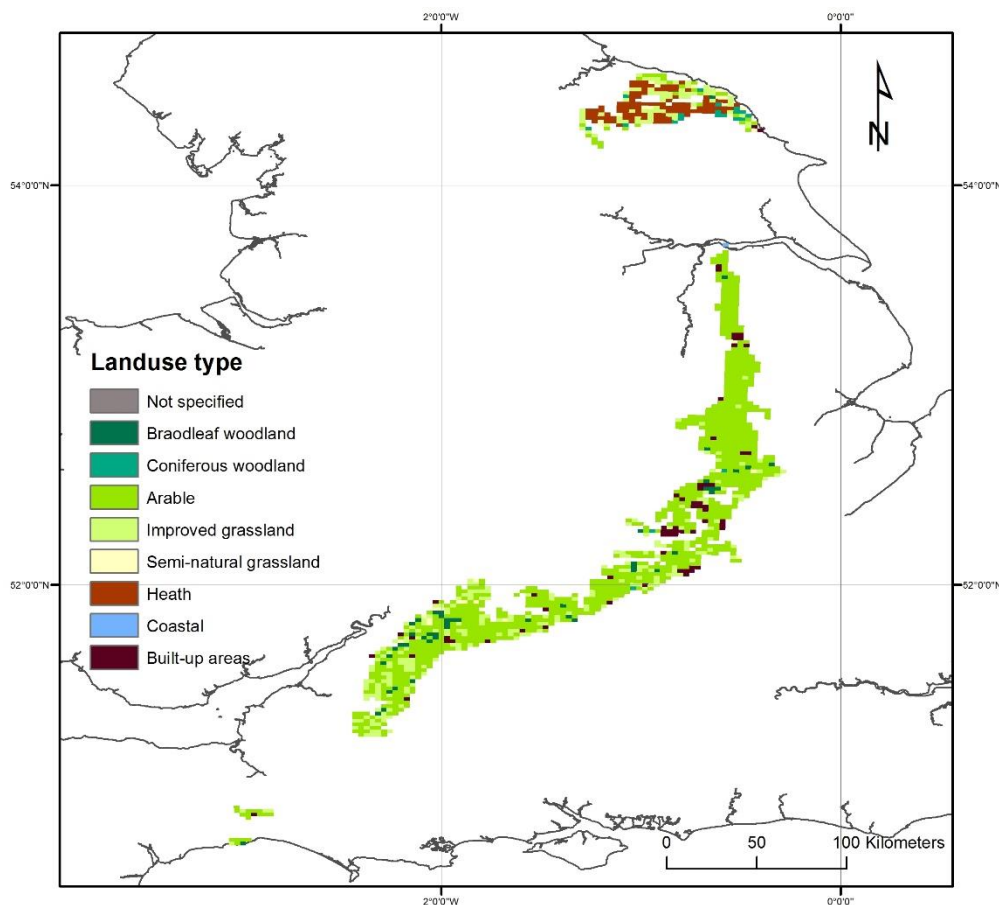


Figure 3. Map of land use over the Jurassic formation

3.1.4 Rainfall

Daily rainfall raster data (1×1 km) were obtained from the Centre for Ecology and Hydrology (CEH) and were used to retrieve the daily rainfall values at the grid nodes pertain to the Jurassic aquifer. The long-term average (LTA) rainfall across the outcrop is approximately 730 mm year^{-1} (2.0 mm day^{-1}) with lowest rainfall values approximately 365 mm year^{-1} (1.0 mm day^{-1}) observed to the east side of the outcrop and highest of approximately $1100 \text{ mm year}^{-1}$ (3.0 mm day^{-1}) in the south and the north of the Jurassic aquifer outcrop (Figure 4).

Spatially distributed rainfall data are available at daily time steps starting from 1961 to 2016 (CEH). While the size of this time step is coarse to represent storm events for hydrological analysis, it is fine enough to calculate recharge values to drive groundwater models. These data are, therefore, used to drive the lumped models. Table 2 presents specific information about the rainfall values at the selected Jurassic boreholes.

Projected (future) values of rainfall data are also available by the work of UKCP09 (Prudhomme et al., 2012; Murphy et al, 2007; Jenkins et al., 2009; Murphy et al, 2009), which provides projections of climate change in the UK. The probabilistic climate projections provided by



UKCP09 are not fully spatially coherent; however, (IPCC, 2000) produced 11 physically plausible simulations, generated under the medium emissions scenario known as A1B SRES emission scenario, that overcome this problem. These data can be used for the estimation of projected (future) recharge values.

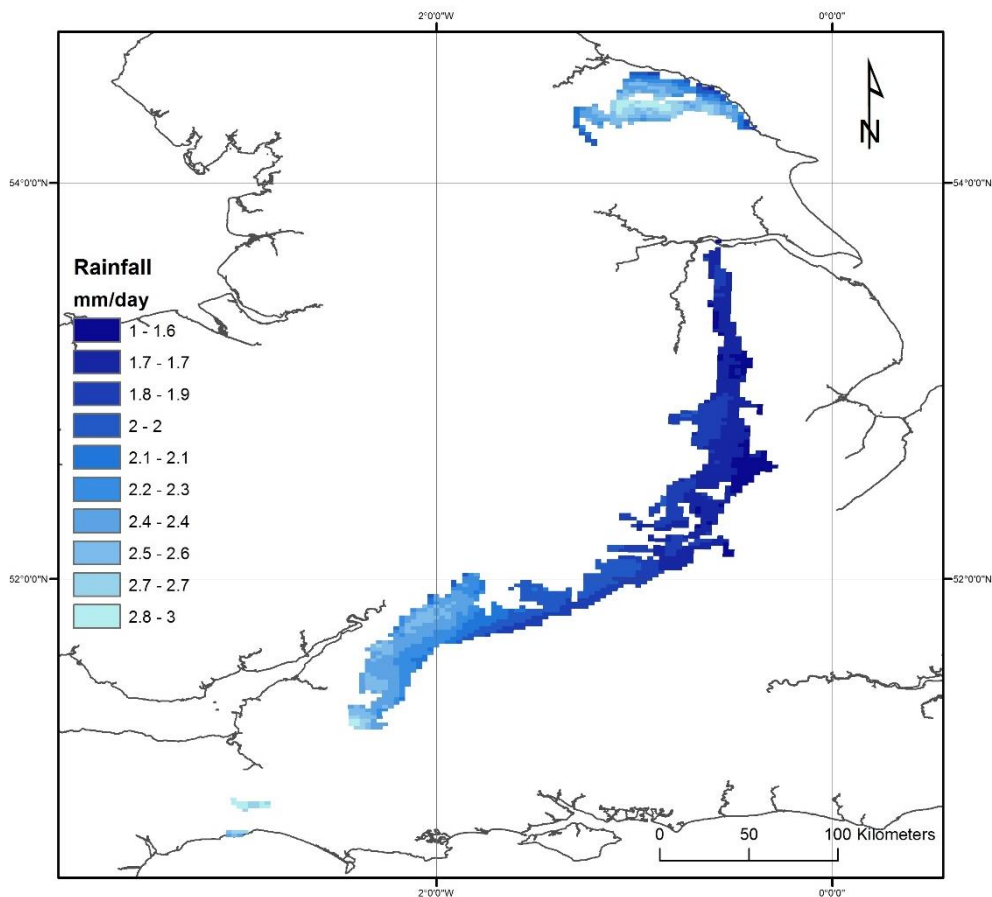


Figure 4. Spatial distribution of rainfall in the Jurassic aquifer

3.1.5 Potential evaporation

The monthly potential evapotranspiration (PE) raster datasets (40×40 km) were gathered from a Met Office Rainfall and Evaporation Calculation System (MORECS) in the Met Office of the UK (Hough and Jones 1997). Figure 5 shows the distributed long-term average potential evaporation data. The highest potential evaporation rates of approximately 685 mm year^{-1} (1.87 mm day^{-1}) are observed to the east and to the west of the Jurassic aquifer outcrop. The lowest potential evaporation rates of approximately 530 mm year^{-1} (1.45 mm day^{-1}) are observed to the north of the aquifer outcrop (Figure 5). Table 2 presents specific information about the PE records at the selected boreholes in the Jurassic aquifer.

Similar to rainfall data, UKCP09 potential evaporation data can be used to run simulations to calculate future recharge values.



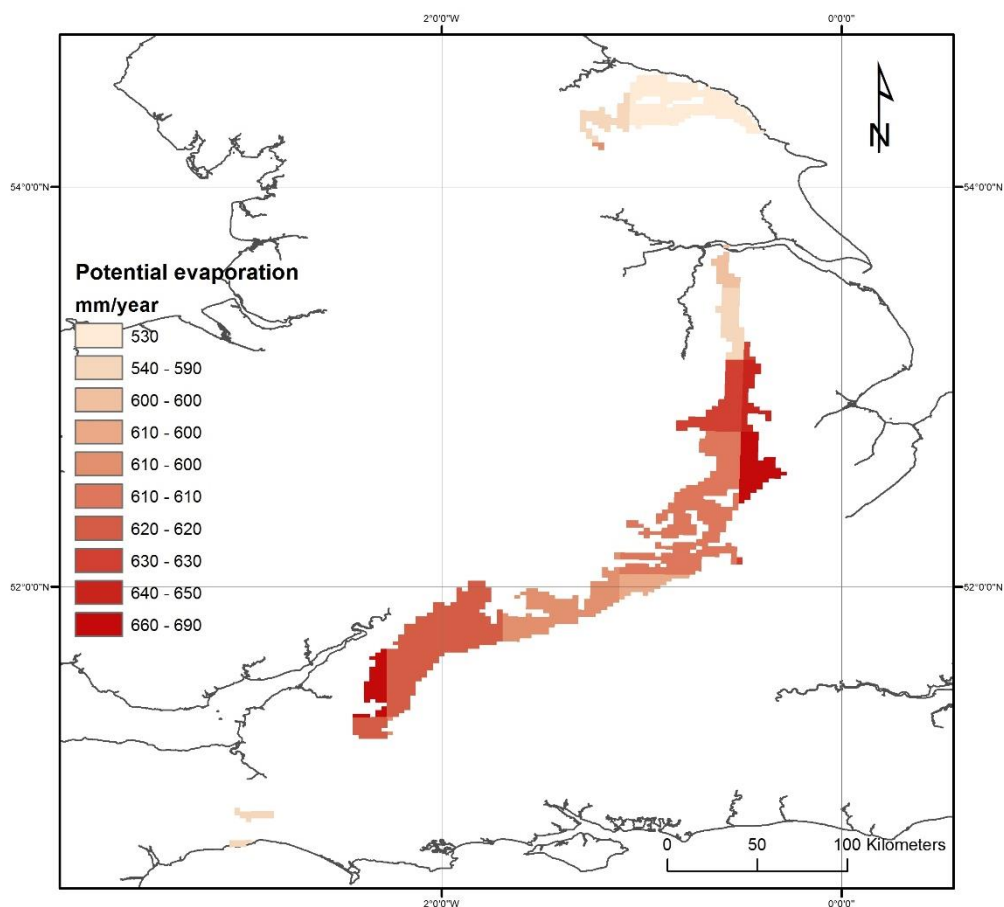


Figure 5. Spatial distribution of potential evaporation in the Jurassic aquifer

Table 2. Landuse, rainfall and evapotranspiration information for the Jurassic aquifer

Borehole name	Dominant landuse	Av. Rainfall (mm/day)	Rainfall record	Av. PE (mm/day)	PE record
Didmarton	Arable	2.32	1961-current	1.72	1961-current
New Red lion	Improved grassland	1.65	1961-current	1.67	1961-current
Ampney Crucis	Arable	2.13	1961-current	1.68	1961-current

3.1.6 Hydrogeology

The major aquifers in the Jurassic are the limestones. They are characterised by sequences of relatively thin beds, which rarely extend over large areas. In addition as the aquifer units are relatively thin, quite small throws on faults can split the aquifer into separate compartments, which may be hydraulically isolated. Further, since the over- and underlying strata are generally clays small throws can make the limestone a low permeability formations. In the unconfined parts of the aquifer, the unsaturated zone is often thick.

The Jurassic limestone aquifers are characterised by high transmissivities and low storage coefficients. Intergranular permeabilities are very low and water movement takes place through fractures. Fractures are irregularly distributed vertically and horizontally but can extend for considerable distances and borehole yields are highly dependent on whether the boreholes intersect them. Horizontal permeabilities are generally higher than vertical ones due to the presence of clay-rich layers within the limestones but locally, karstic features have been noted. The quality of water from the Jurassic limestones is generally good, but hard with calcium and bicarbonate ions predominating.

3.1.7 Groundwater levels

At Didmarton 1 observation boreholes, the aquifer is under confined conditions. The fluctuations of the time series of groundwater levels recorded at this boreholes show that the aquifer remains under these conditions all year round (

Table 1). The piezometric head, however, does not reach the ground surface and no artesian conditions are observed.

The fluctuations of the piezometric heads recorded at the New Red Lion switches the aquifer conditions at this location between confined and unconfined depending on the season of the year. However, and similar to the Didmarton borehole, the maximum piezometric head elevation is always below the ground surface.

The fluctuations at the Ampney Crucis borehole are normally around three metres per annum. They have multiple peaks in response to rainfall events. A ceiling at just over 103 m AOD may be linked to the presence of local springs.

The time series recorded at these three observation boreholes are used in this study to characterise the aquifer properties and to estimate the infiltration recharge values for water resources management.

While the boreholes are selected so that they are not significantly impacted by the presence of nearby surface features, the records show that some boreholes are affected by nearby pumping. Pumping data are available on a daily basis and these can be included in the simulations if necessary.

3.2 Climate change challenge

The British Geological Survey (BGS) with the support of the Environment Agency (EA) have undertaken a study to investigate the impact of climate change on groundwater resources using the distributed recharge model ZODRM (Mansour and Hughes, 2018). Potential recharge values for Great Britain (England, Scotland and Wales) are produced using rainfall and potential evaporation data from the Future Flows Climate datasets (11 ensembles of the HadCM3 Regional Climate Model or RCM). This study has shown that generally the recharge season appears to be forecast to become shorter, but with greater amount of recharge “squeezed” into fewer months. This conclusion is aligned with the European Environment Agency map that describes the expected climate change across the different areas in Europe as shown in Figure 6.

The shortening of recharge season indicates that aquifers may become more vulnerable to droughts if rainfall fails in one or two months rather than a prolonged dry winter as can occur now. At the very least, water management measures have to be put in place to account for periods when recharge volumes reduce. On the other hand, the increased recharge signal could result in flashier groundwater level response and potentially leading to more flooding.

The main climate challenge for water resources managers and stakeholders is to assess the risk of future flooding and drought events. This requires detailed assessment of the variation of resources at regional and local scales rather than national or continental scales.

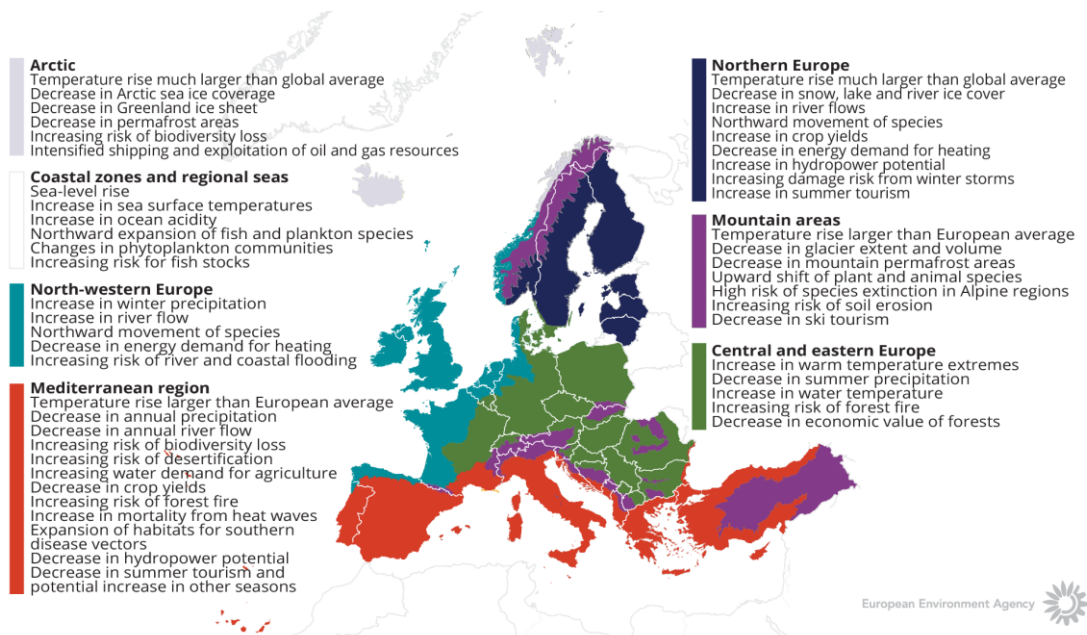


Figure 6. How is climate expected to change in Europe. The European Environment Agency map



4 METHODOLOGY

4.1 Methodology and climate data

4.1.1 *AquiMod*

AquiMod is a lumped parameter computer model that has been developed to simulate groundwater level time series at observational boreholes (Mackay et al., 2014a). It is based on hydrological algorithms that simulate the movement of groundwater within the soil zone, the unsaturated zone, and the saturated zone. The lumped models neglect complexities included in distributed groundwater models but maintain some of the fundamental physical principles that can be related to the conceptual understanding of the groundwater system (Mackay et al., 2014b).

The primary aim of AquiMod is to capture the behaviour of a groundwater system through the analysis of the available groundwater level time series. Once calibrated the model can be run in predictive mode and be used to fill in gaps in historical groundwater level time series and to calculate future groundwater levels. In addition to groundwater levels, it also provides predictions of historical and future recharge values and groundwater discharges.

The mathematical equations that are used to simulate the movement of groundwater flows within the three modules are detailed in Appendix A. The model uses rainfall and potential evaporation time series as forcing data. These are interpreted by the soil module representing the soil zone. The soil module calculates the rainfall infiltration and pass it to the unsaturated zone module. This module delays the arrival of the infiltrating water to the saturated zone module. The latter calculates the variations of groundwater heads and flows accordingly.

The model is calibrated using a Monte Carlo approach. It compares the simulated and observed groundwater level fluctuations and calculates a goodness of fit. The AquiMod version used in this work employs the Root Square Mean Error (RMSE) or the Nash Sutcliffe (NSE) performance measures to assess the performance of the model. The user sets a threshold value to accept all the models that perform better than the specified threshold. The possibility of producing many models that are all equally acceptable, allows the user to interpret the results from all these models and calculate uncertainty.

The recharge values calculated from AquiMod are those that reach the aquifer system and drive the groundwater levels. Thus, it is assumed that these are the actual recharge values as defined in the guidance report prepared by TACTIC project.

4.1.2 *Metran*

Metran applies a transfer function-noise model to simulate the fluctuation of groundwater heads with precipitation and evaporation as independent variables (Zaadnoordijk et al., 2019). The modelling approach consists mainly of two impulse functions and a noise model. The first impulse function is used for convolution with the precipitation to yield the precipitation contribution to the piezometric head. The second is for evaporation which is either a separately estimated function, or a factor times the function used for precipitation. The noise model is a

stochastic noise process described by a first-order autoregressive model with one parameter and zero mean white noise. Further information about the model is given in Appendix B with the model setup shown in the Figure B1.

Metran allows the addition of other processes affecting the behaviour of the groundwater heads, for example pumping or the presence of surface features such as rivers. The contributions from these processes are added to the deterministic part of the model.

Metran has been designed to work with explanatory series that have a daily time step. However, it has been adapted so that other time step lengths can be applied. However, the explanatory variables must still have a constant frequency.

The model is calibrated automatically; however, the model uses two binary parameters, Regimeok and Modok, to judge a resulting time series model. Regimeok cross-examines the explained variance R^2 (> 0.3), the absolute correlation between deterministic component and residuals (< 0.2), and the null hypothesis of non-correlated innovations (p value > 0.01). If all these criteria are satisfied, Regimeok returns a value of 1 indicating highest quality. Modok also cross-examines the explained variance R^2 (> 0.1) and the absolute correlation between deterministic component and residuals (< 0.3) as well as the decay rate parameter (> 0.002) and if all these criteria are satisfied, it is given a value of 1. If Modok = 1 and Regimeok = 0, the model is still considered acceptable. If both these parameters are 0, the model quality is insufficient and the model is rejected.

Metran's time series model is linear and the model creation fails when the system is strongly nonlinear. It is also limited to the response function being appropriate for the simulated groundwater system. Metran uses a gradient search method in the parameter space, so it can be sensitive to initial parameter values in finding an optimal solution.

The model calculates an evaporation factor f that gives the importance of evapotranspiration compared to precipitation. It is possible to use this factor to calculate the recharge values as shown by Equation B2 in appendix B. However, it must be noted that the use of Equation B2 is based on too many assumptions that are easily violated. Because of this, the equations should be applied only to long-term averages using only models of the highest quality.

Following the definitions used in the TACTIC project (See the guidance report), this recharge quantity corresponds to the effective precipitation. It is equal to the potential recharge when the surface runoff is negligible. This in turn is equal to the actual recharge at the groundwater table if there is also no storage change or interflow.

4.1.3 The distributed recharge model ZOODRM applied at the UK scale

A distributed recharge model, ZOODRM, has been developed by the British Geological Survey to calculate recharge values required to drive groundwater flow simulators. This recharge model allows grid nesting to increase the resolution over selected area and is called therefore the zooming object-oriented distributed recharge model (ZOODRM) ((Mansour and Hughes, 2004). The model can implement a number of recharge calculation methods that are suitable for

temperate climates, semi-arid climates, or for urban areas. One of the methods that is implemented is the recharge calculation method used by Aquimod and detailed in Appendix A1.

ZOODRM uses a Cartesian grid to discretise the study area. It reads daily rainfall and potential evaporation data in time series or gridded format and calculates the recharge and overland flow at a grid node using a runoff coefficient as detailed in appendix A1. However, since this is a spatially distributed model, it reads a digital terrain model and calculates the topographical gradients between the grid nodes. It then uses the steepest gradient to route the calculated surface water downstream until a surface feature, such as a river or a pond, is reached. While the connections between the grid nodes based on the topographical gradients define the water paths along which surface water moves, major rivers are also user-defined in the model. This allows the simulation of river water accretion on a daily basis and the production of surface flow hydrograph. The model is then calibrated by matching the simulated river flows at selected gauging stations to the observed flows, by varying the values of the runoff coefficients.

The procedure used to calibrate the model involves dividing the study area into a number of zones and then to specify runoff values for each one. It is possible to vary the runoff coefficient values on a seasonal basis by using different runoff values for the different months of the year.

The recharge model ZOODRM calculates rainfall infiltration after accounting for evapotranspiration and soil storage. The simulated infiltration may not reach the aquifer system as it may travel laterally within the soil and discharge into surface water features away from the infiltration location. The simulated infiltration is therefore considered, as potential recharge according to the definitions of recharge processes provided by the guidance report prepared by TACTIC project.

Climate data

The TACTIC standard scenarios are developed based on the ISIMIP (Inter Sectoral Impact Model Inter-comparison Project, see www.isimip.org) datasets. The resolution of the data is 0.5°x0.5° global grid and at daily time steps. As part of ISIMIP, much effort has been made to standardise the climate data (e.g. bias correction). Data selection and preparation included the following steps:

1. Fifteen combinations of RCPs and GCMs from the ISIMIP data set were selected. RCPs are the Representative Concentration Pathways determining the development in greenhouse gas concentrations, while GCMs are the Global Circulation Models used to simulate the future climate at the global scale. Three RCPs (RCP4.5, RCP6.0, RCP8.5) were combined with five GCMs (noresm1-m, miroc-esm-chem, ipsl-cm5a-lr, hadgem2-es, gfdl-esm2m).
2. A reference period was selected between 1981 – 2010 and an annual mean temperature was calculated for the reference period.
3. For each combination of RCP-GCM, 30-years moving average of the annual mean temperature were calculated and two time slices identified in which the global annual mean temperature had increased by +1 and +3 degree compared to the reference period, respectively. Hence, the selection of the future periods was made to honour a specific temperature increase instead of using a fixed time-slice. This means that the

- temperature changes are the same for all scenarios, while the period in which this occurs varies between the scenarios.
4. To represent conditions of low/high precipitation, the RCP-GCM combinations with the second lowest and second highest precipitation were selected among the 15 combinations for the +1 and +3 degree scenario. This selection was made on a pilot-by-pilot basis to accommodate that the different scenarios have different impact on the various parts of Europe. The scenarios showing the lowest/highest precipitation were avoided, as these endmembers often reflect outliers.
 5. Delta change values were calculated on a monthly basis for the four selected scenarios, based on the climate data from the reference period and the selected future period. The delta change values express the changes between the current and future climates, either as a relative factor (precipitation and evapotranspiration) or by an additive factor (temperature).
 6. Delta change factors were applied to local climate data by which the local particularities are reflected also for future conditions. These monthly values (one set of rainfall and PE for each warming scenario) are used to drive the groundwater models presented in this report.

For the analysis in the present pilot the following RCP-GCM combinations were employed:

Table 3. Combinations of RCPs-GCMs used to assess future climate

		RCP	GCM
1-degree	"Dry"	rcp6p0	noresm1-m
	"Wet"	rcp4p5	miroc-esm-chem
3-degree	"Dry"	rcp4p5	hadgem2-es
	"Wet"	rcp8p5	miroc-esm-chem

4.2 Model set-up

4.2.1 *AquiMod*

The boreholes located in the Jurassic limestone are listed in Table 1. *AquiMod* model setup relies mainly on two input files. The first input file "Input.txt" is a control file where the module types and model structure are defined. *AquiMod* is executed first under a calibration mode where a range of parameter values of the different selected modules are given in corresponding text files and a Monte Carlo approach is used to select the parameter values that yield best model performance. "Input.txt" also controls the mode under which *AquiMod* is executed, the number of Monte Carlo runs to perform, the number of models to keep with an acceptable performance, and the number of runs to execute in evaluation mode.

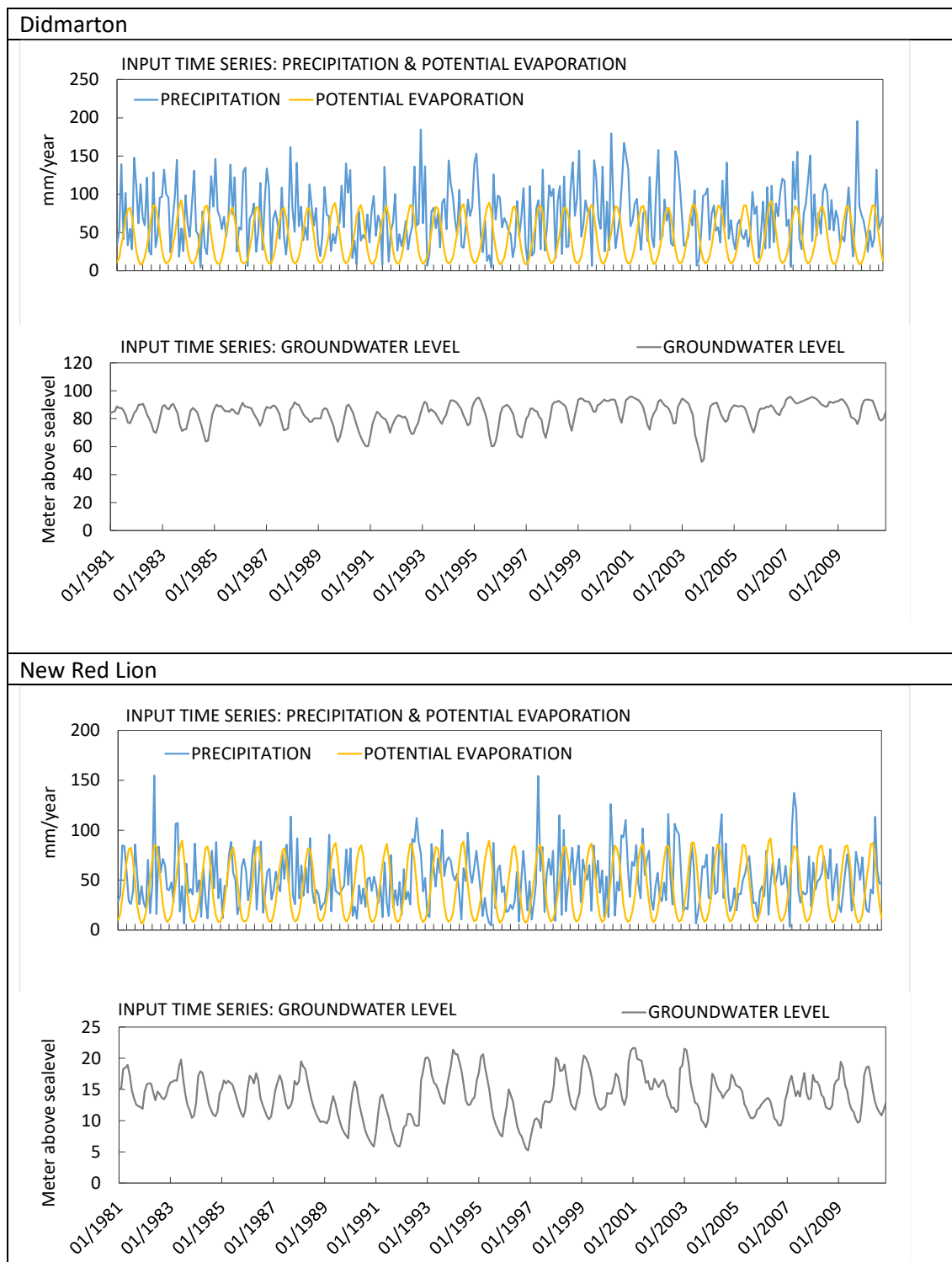
The second file *AquiMod* uses is called "observations.dat". This file holds the forcing data mainly the potential evaporation and rainfall. However, it is also possible to include the anthropogenic impact on groundwater levels by including a time series of pumping data in this file. None of the boreholes studied here includes pumping data. The observed groundwater levels that are used for model calibration are also given in this file. The data are provided to the model on a daily basis, and this forces *AquiMod* to run using a time step length of one day. Table 4 shows daily



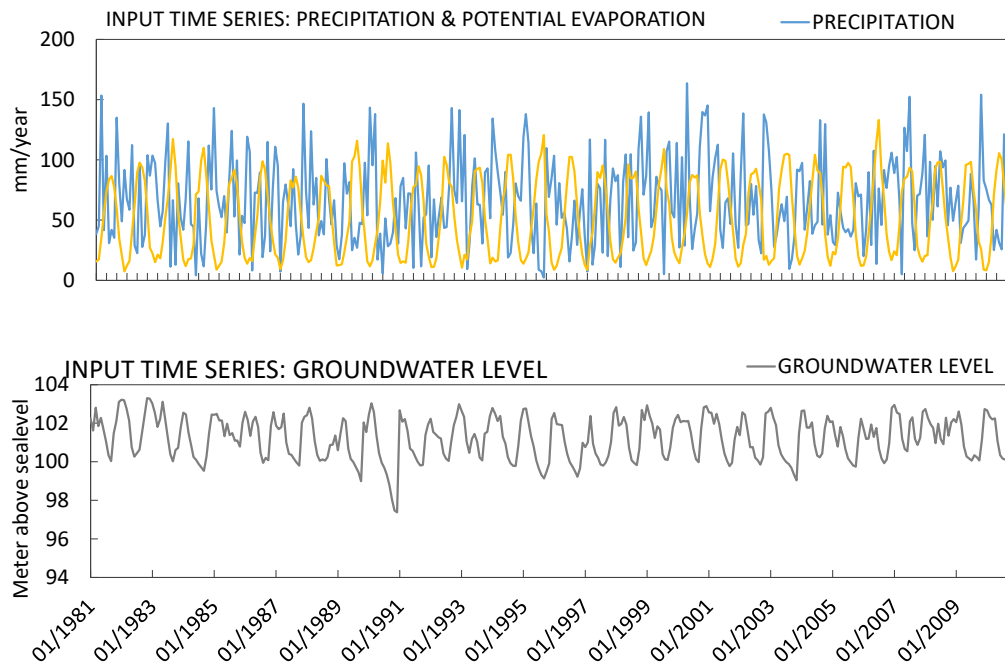
time series of rainfall and potential evaporation values (mm/month) as well as the fluctuations of water table at the different boreholes.

All AquiMod models built for the boreholes in Table 1 use the FAO Drainage and Irrigation Paper 56 (FAO, 1988) method in the soil module, and employ the two-parameter Weibull probability density function to control the movement of infiltrated water in the unsaturated zone (Appendix A1). However, the groundwater module structures vary between the different boreholes. The best groundwater module structure is found by trial and error during the calibration process. The simplest structure, one layer with one discharge feature, is selected first and then the complexity of the module structure is increased gradually to see if the model performance improves. The structure with best model performance is selected to undertake the recharge calculations. The structures selected for these boreholes are mainly of one layer or three layered systems.

Table 4 Figures showing time series of daily rainfall and potential evaporation values (mm/month) as well as the fluctuations of water table at the different boreholes.



Ampney Crucis



4.2.2 Metran

Metran applies transfer function noise modelling with daily precipitation and evaporation as input and of groundwater levels as output (Zaadnoordijk et al., 2019). The setup is shown in Figure 7. If time series of other influences on the groundwater head are available, these contributions can be added to the deterministic part of the model. An input file that holds the daily information of precipitation, potential evaporation and groundwater levels is prepared for each borehole in Table 1. Plots of these data are shown in Table 4. It must be noted that, while the groundwater levels used in AquMod and shown in Table 4 have missing values, these have to be provided as complete time series to Metran. To achieve this, a linear interpolation procedure is used to fill in the missing values in the groundwater level time series. Once executed, it calculates the characteristics of the impulse functions and the corresponding parameters automatically.

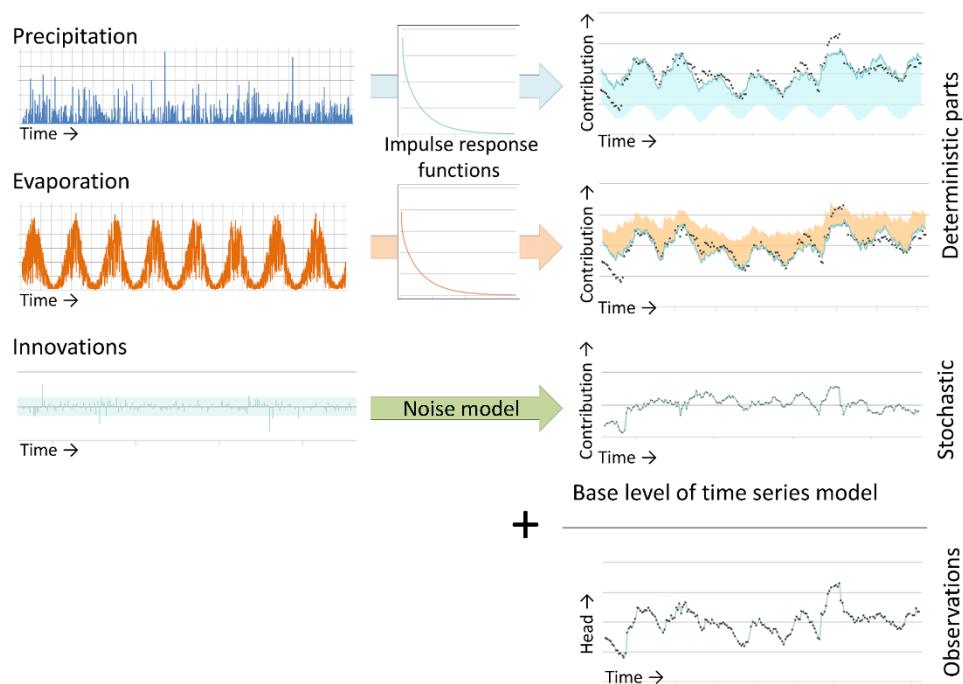


Figure 7 Illustration of METRAN setup

4.2.3 National scale model (ZOODRM)

The distributed recharge model (ZOODRM) is applied at national over the British Mainland (England, Scotland, and Wales) (Figure 8) using a Cartesian grid with 2 km square cells. The model reads a text file that defines the locations of the grid nodes as well as the connections between the nodes. This text file is prepared using a specific tool, called ZETUP (Jackson, 2004), where the extent of the study area is defined using the coordinates of the lower left and upper right corners of a rectangle that covers the modelled area. The spacing between the nodes and the information that dictate the boundary of the irregular shape of the area are also given in this file. This tool also uses a file that contains the locations of the nodes as obtained from a geographical information system tool (GIS) and converts this information into a text file that describes the river extents and characteristics.

The map defining the runoff zones is based on the hydrogeology of the study area. It is produced in gridded ascii format using the hydrogeological map available for Great Britain. Additional text files, one for each runoff zone, are also prepared to define the monthly runoff values.

The topographical information is also provided in a gridded ascii format for the model to calculate the topographical gradients between the nodes. While a surface water routing procedure that accounts for indirect recharge and surface water storage is available in the model, this is not used in the current application. It is assumed that all the water originated at one grid nodes travel downstream and reaches a discharging feature in one day, which is equal to the length of the time step used.



Landuse data (Section **Error! Reference source not found.**) and soil data that are required to calculate the water capacity at every grid node are also provided to the model using maps in gridded ascii format. A set of landuse gridded maps, a total of ten, are used to give the percentage of landuse type at any given location. The gridded soil map gives the soil type at a selected location. The landuse type and soil type ids are linked to text files that hold the corresponding information such as the soil moisture at saturation, the soil moisture at wilting and the root constants can be obtained.

The driving data are provided to the model as daily gridded rainfall data (Sections **Error! Reference source not found.**) and time series of monthly potential evaporation values as described in (Section **Error! Reference source not found.**). Mansour et al. (2018) provide a full description of the construction of this model together with a more detailed description of the data used. The calculated recharge values are also provided in the published work; however, it must be noted that the historical recharge values shown in this work are simulated over the period from 1981 to 2010 in order to be consistent and comparable with the recharge values calculated by AquiMod and Metran. In addition, in this study, the model is rerun using the climate change data specifically provided by the TACTIC project to calculate the projected distributed recharge values.

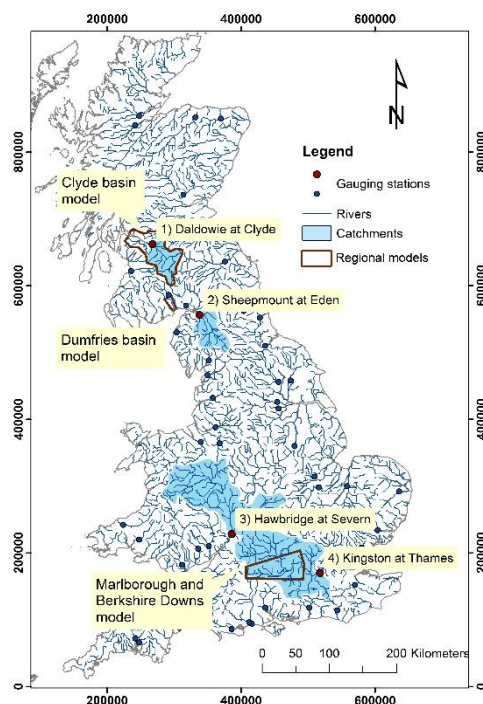


Figure 8. Extent of the UK national scale recharge model in UK national grid reference after Mansour et al. (2018). Figure also shows the locations of the gauging stations downstream of the major rivers used for model calibration.

4.3 Model calibration

4.3.1 Calibration of *AquiMod* models

The calibration of *AquiMod* is performed automatically using the Monte Carlo approach. The user populates the files of the selected modules with minimum and maximum parameter values and then the model randomly selects a value from the specified range for any given run. The selection of the minimum and maximum values is physically based depending on the characteristics of the study area. For example, the minimum and maximum values of the root depth in the soil module are set to 15 cm and 60 cm respectively for a study area covered with grass, while these values are set to 120 cm and 200 cm for a woodland area. The storage coefficients bounds of a groundwater module are set to much lower values in a confined aquifer compared to those used for an aquifer under unconfined conditions.

A conceptual hydrogeological understanding must be available before the use of *AquiMod*, since this is necessary to set the limits of the parameter values for the calibration process. In some cases, it is not possible to obtain a good performing model with the selected values and that necessitates the relaxation of these parameters beyond the limits informed by the conceptual understanding. In such cases, the parameter values must feed back into the conceptual understanding if better performing models are obtained.

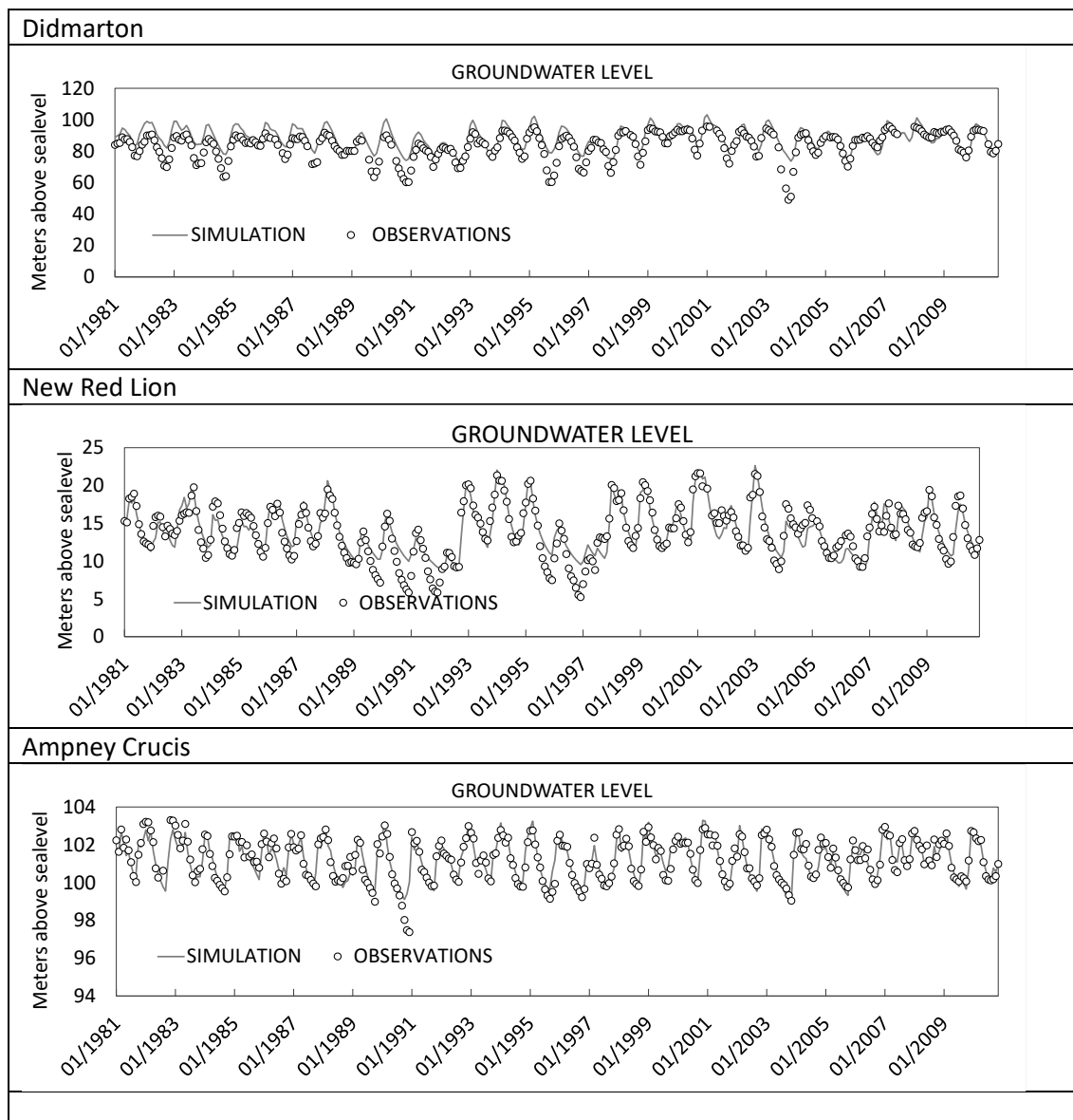
AquiMod execution time is relatively small, which allows the calibration of the model using hundreds of thousands of runs in couple of hours. The performance measure used to assess the quality of the simulation is the Nash Sutcliffe Error (Appendix A) that takes a maximum value of unity for a perfect match between the simulated and observed data. The threshold at which models are accepted is set to a value of 0.6. All the models that achieve an NSE higher than 0.6 are included in the analysis but a maximum number of 1000 runs are used if the number of acceptable models is greater than 1000.

Table 5 shows the best NSE values obtained for the models calibrated at the Jurassic limestones boreholes listed in Table 1. It is clear that a good match was achieved between the simulated and observed groundwater levels as illustrated in the plots shown in Table 6. The best performing model is the *AquiMod* model built at New Red Lion borehole with an NSE value of 0.82. The least performing *AquiMod* model is that built for Ampney Crucis borehole with an NSE value of 0.6.

Table 5 Nash Sutcliffe Error measure at the boreholes located in the Jurassic limestone

Borehole name	NSE
Didmarton	0.72
New Red Lion	0.82
Ampney Crucis	0.6

Table 6 Comparison between the simulated and observed groundwater levels at the boreholes located within the Jurassic limestones.



4.3.2 Calibration of Metran models

For the standard setup with precipitation and evaporation, there are five parameters that have to be determined during the calibration of the model. Three parameters are related to the precipitation response, the evaporation factor, and the noise model parameter (Appendix B). There are three extra parameters for each additional input series, such as pumping. The parameter optimization of Metran uses a gradient search method in the parameter space to reach a global minimum. As explained in Appendix B, two parameters indicate if Metran succeeded with producing a match between the simulated and observed data. These are called the Regimeok and Modok. When Regimeok is equal to one, the calibration is of highest quality. If Modok is equal to one and Regimeok is equal to zero, the calibration is of acceptable quality. Finally, if both parameters are equal to zero, the calibration quality is insufficient.

Time series of rainfall, potential evaporation and groundwater levels are provided to Metran on a monthly basis. Metran input data must be also a complete dataset and this cannot be guaranteed for the observed groundwater levels at all the boreholes. To overcome this problem, groundwater level data are aggregated to monthly values first and then missing values were filled using linear interpolation. Table 7 shows the performance of Metran across the Jurassic limestones boreholes considered in this study. It is clear that according to criteria set above, Metran fails to produce a model for Didmarton but finds acceptable models for New Red Lion and Ampney Crucis boreholes.

Table 7 Performance of Metran across the selected Jurassic boreholes.

Borehole name	Metran performance parameter Modok	Metran performance parameter Regimeok	Overall quality	R2	RMSE
Didmarton	0	0	Insufficient	0.0	8.36
New Red Lion	1	0	Acceptable	0.82	1.45
Ampney Crucis	1	0	Acceptable	0.76	0.53

4.3.3 Calibration of the UK national scale model using ZOODRM

Model calibration of the national scale recharge model was based on the comparison of the simulated long-term average overland flows to the observed ones (Mansour et al., 2018) recorded at gauging stations of selected major rivers (Figure 8). However, additional checks were also undertaken to assess the performance of the model. These include checking the match between the seasonal overland flow volumes at four boreholes, shown in red in Figure 8, checking the calculated recharge volumes with those calculated by other tools over selected catchment areas, and checking the temporal fluctuations of soil moisture deficit with those calculated by other tools. Figure 9 shows a Q plot for the simulated vs observed long term average runoff values at the 56 gauging stations shown in Figure 8. The solid line shows the one to one match and the dotted line shows the linear relationship between the two datasets.

It must be noted that while this model uses the same recharge calculation methods used by AquiMod, these two models are calibrated using different datasets, with AquiMod using the groundwater levels and the distributed recharge model using the overland flows.

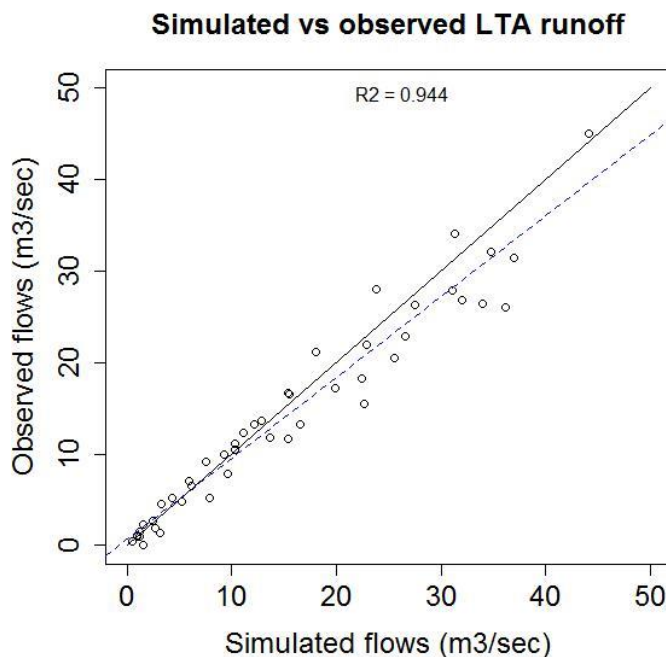


Figure 9 Q plot for the simulated vs observed long term average runoff values at the 56 gauging stations shown in Figure 8 after Mansour et al. (2018)

5 RESULTS AND CONCLUSIONS

5.1 Historical recharge values

Table 8 shows the time series of the historical recharge values calculated using the Aquimod model at the Jurassic boreholes listed in Table 1. The plots in this table also show the 10th percentile, the mean, and the 90th percentile of recharge values calculated from the time series.

As mentioned Appendix B, the formulas used by Metran are based on assumptions that can be violated and it is better to use the infiltration coefficient f_c with the long-term average values of rainfall and potential evaporation to calculate long-term average values of recharge and using only models of the highest quality. Time series of recharge values are not therefore produced, from the analysis undertaken using Metran. The long-term average recharge values calculated using Metran are shown in Table 9.

One of the benefits of running Aquimod in Monte Carlo mode is the possibility of producing many models with acceptable performance. Consequently, the recharge values estimated from these models are all equally likely. This provides us with a range of recharge values at each borehole that reflects the uncertainty of the optimised hydraulic parameter values. In the current study, the long-term average recharge values are calculated from up to 1000 acceptable models if they exist at each borehole; otherwise, all the acceptable models are used. The mean, 25th and 75th percentiles are then calculated from these long-term recharge values and displayed in Figure 10. The differences between the 75th and 25th at the three boreholes interpreted in this study vary between 10 and 15 mm /month.

In addition to the recharge values calculated using Aquimod, Figure 10 shows the recharge values calculated using Metran and the distributed national scale model at these boreholes. It is clear that there is a good agreement between the Aquimod calculated recharge values and those calculated using the distributed national scale model. This is expected as they both use the same recharge calculation method; however, since they are calibrated using different target functions, the match was not guaranteed. It must be noted that the recharge values calculated by these two models are of different types. The distributed recharge model calculates potential recharge and Aquimod calculates actual recharge.

Metran estimates an upper and a lower value for the infiltration coefficient f_c . This can be used as an indication of uncertainty associated with the calculated f_c value. These bounds are also shown in Table 9. The upper and lower bound values of f_c at New Red Lion are above 40% of the estimated f_c value, while those at Ampney Crucis are greater than the estimated f_c Chilgrove House and West Dean are greater than the estimated f_c value. It is not possible to use and that illustrates the degree of uncertainty associated with the estimated recharge values. At both boreholes, recharge values estimated by Metran are not comparable with those calculated by Aquimod. The Metran recharge values at the New Red Lion are approximately three times larger than those calculated by Aquimod, while at Ampney Crucis, the Metran recharge values are approximately half those calculated by Aquimod (Figure 10).



Table 8 Time series of recharge values obtained from the best performing AquiMod models at the Jurassic boreholes

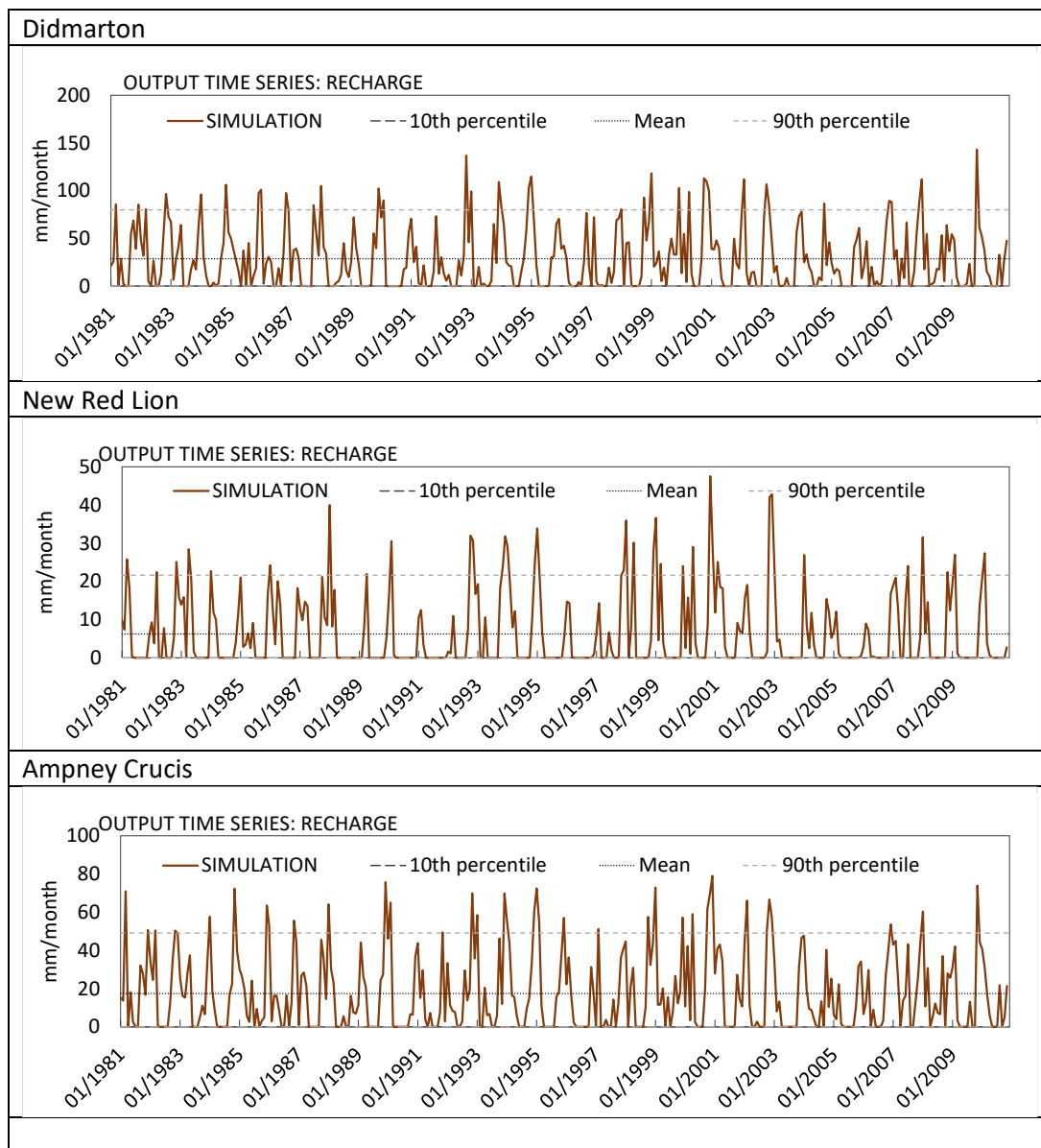


Table 9 Recharge values calculated using the recharge factors estimated by Metran

Borehole name	Average precipitation (mm/month)	Average potential evaporation (mm/month)	Recharge factor	Recharge (mm/month)
New Red Lion	51.06	42.61	0.685 +- 0.292	21.87
Ampney Crucis	65.19	51.31	1.041 +- 1.488	11.34

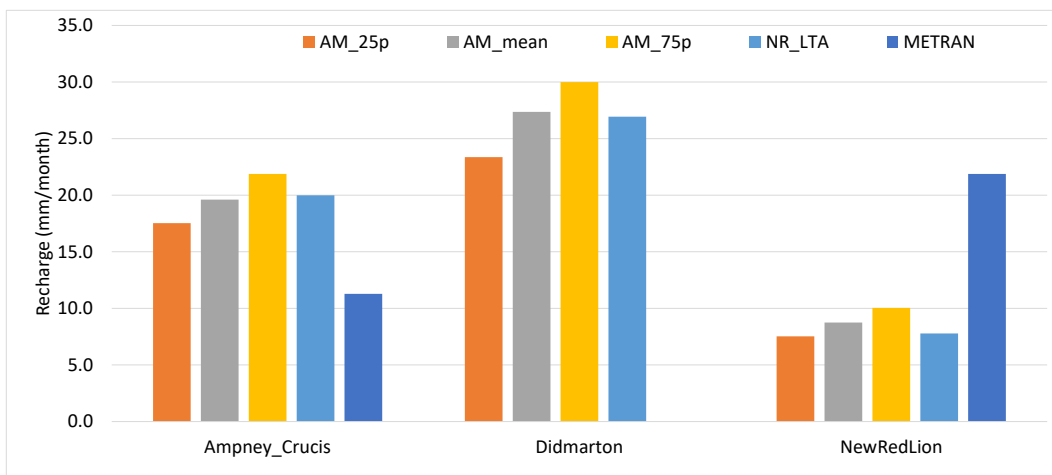


Figure 10 Historical recharge values calculated by AquiMod, Metran, and the national scale recharge model.

5.2 Projected recharge values

The forcing data, rainfall and potential evaporation, are altered using the change factors of the climate models (see Section **Error! Reference source not found.**). For the United Kingdom, there are two sets of monthly change factors, one used with the data driving AquiMod and Metran (Table 10), and the other used to calculate the spatially distributed recharge (Table 11). These change factors are used as multipliers to both the historical rainfall and potential evaporation values.

For the application involving AquiMod, these factors are used to alter the time series of historical rainfall and potential evaporation values used to drive the model.

When using Metran, the historical time series are altered using these factors first and then the long-term average rainfall and potential evaporation values are calculated. The recharge coefficient f_c values of the different boreholes, as calculated from the calibration of Metran model using the historical data, are then applied to calculate the projected long-term average recharge values.

The distributed recharge model ZOODRM includes the functionality of using these change factors to modify the historical gridded rainfall and potential evaporation data before using them as input to calculate the recharge. In this case, and for any simulation date, the rainfall and potential evaporation change factors for the month corresponding to the date, are used to modify all the spatially distributed historical rainfall and potential evaporation values respectively.

Table 10 Monthly change factors as multipliers used for the borehole data

	Scenario	Jan	Feb	Mar	Apr	May	Jun	Jul	Aug	Sep	Oct	Nov	Dec
Rainfall	1° Min	1.087	0.956	0.994	1.072	0.888	0.909	0.836	0.988	1.017	1.106	0.962	1.031
	1° Max	1.140	1.012	1.033	1.045	1.022	0.863	1.086	0.953	0.995	1.067	1.148	1.053
	3° Min	0.936	1.056	0.994	1.153	1.063	0.900	0.846	0.721	0.854	0.970	1.047	1.116
	3° Max	1.191	1.177	0.989	1.014	0.949	0.986	1.473	1.145	1.173	1.074	1.152	1.112
PE	1° Min	1.082	1.082	1.062	1.089	1.091	1.061	1.078	1.083	1.082	1.063	1.049	1.076
	1° Max	1.049	0.993	1.014	1.007	1.019	1.013	1.021	1.015	1.029	1.028	1.020	1.026
	3° Min	1.034	1.057	1.039	1.056	1.060	1.086	1.085	1.091	1.109	1.097	1.064	1.066
	3° Max	1.072	1.070	1.055	1.071	1.105	1.106	1.072	1.083	1.082	1.076	1.072	1.060

Table 11 Monthly change factors as multipliers used for the distributed recharge model

	Scenario	Jan	Feb	Mar	Apr	May	Jun	Jul	Aug	Sep	Oct	Nov	Dec
Rainfall	1° Min	1.086	0.953	0.975	1.064	0.918	0.914	0.856	0.973	1.008	1.103	0.976	1.038
	1° Max	1.132	1.090	1.008	0.899	1.034	1.087	1.310	0.983	1.020	1.006	1.012	1.025
	3° Min	1.156	1.118	1.033	1.011	0.914	0.821	0.908	0.656	0.821	0.986	0.980	1.181
	3° Max	1.192	1.131	0.960	0.990	0.899	0.957	1.437	1.109	1.134	1.068	1.139	1.106
PE	1° Min	1.081	1.081	1.059	1.089	1.091	1.061	1.078	1.083	1.085	1.063	1.049	1.076
	1° Max	1.051	1.036	1.020	1.039	1.051	1.049	1.031	1.043	1.054	1.039	1.044	1.034
	3° Min	1.016	1.031	1.021	1.029	1.038	1.029	1.047	1.057	1.059	1.059	1.040	1.045
	3° Max	1.070	1.066	1.051	1.071	1.105	1.106	1.072	1.083	1.083	1.076	1.072	1.060

Figure 11 shows the historical and future long-term average recharge values calculated using the best performing AquiMod model. It is clear that the highest reduction in recharge values are observed when the 3° Min rainfall and evaporation data are used, while the highest increase in recharge values are observed when the 3° Max rainfall and potential evaporation data are used.



When the 1° Min scenario data are used, all the boreholes show reduction in recharge values with the smallest reduction observed at Didmarton borehole (-2%) and the highest reduction observed at New Red Lion borehole (-13%). When the 1° Max scenario data are used, all the boreholes show increase in recharge values with the smallest increase observed at both Ampney Crucis and Didmarton boreholes (8%) and the highest increase observed at West Dean borehole (10%).

When the 3° Min scenario data are used, all the boreholes show reduction in recharge values with the smallest reduction observed at both Ampney Crucis and Didmarton boreholes (-4.6%) and the highest reduction observed at New Red Lion borehole (19%). When the 3° Max scenario data are used, all the boreholes show increase in recharge values with the smallest increase observed at both Ampney Crucis and Didmarton boreholes (15 and 15.7% respectively) and the highest increase observed at New Red Lion borehole (25.5%).

Table 12 shows the monthly historical and future recharge values calculated at the different boreholes. It is clear that in almost all the cases, the recharge values become lower than the historical values when the 1° Min and 3° Min data are used and they become higher than the historical values when the 1° Max and 3° Max are used. The exceptions of this observation are due to the complex effect of the use of the change factors, which may reduce both the rainfall and potential evaporation at the same period but at different rates. The reduction in potential evaporation volume in one month may yield increased recharge volume even if the rainfall volume is reduced for that month.

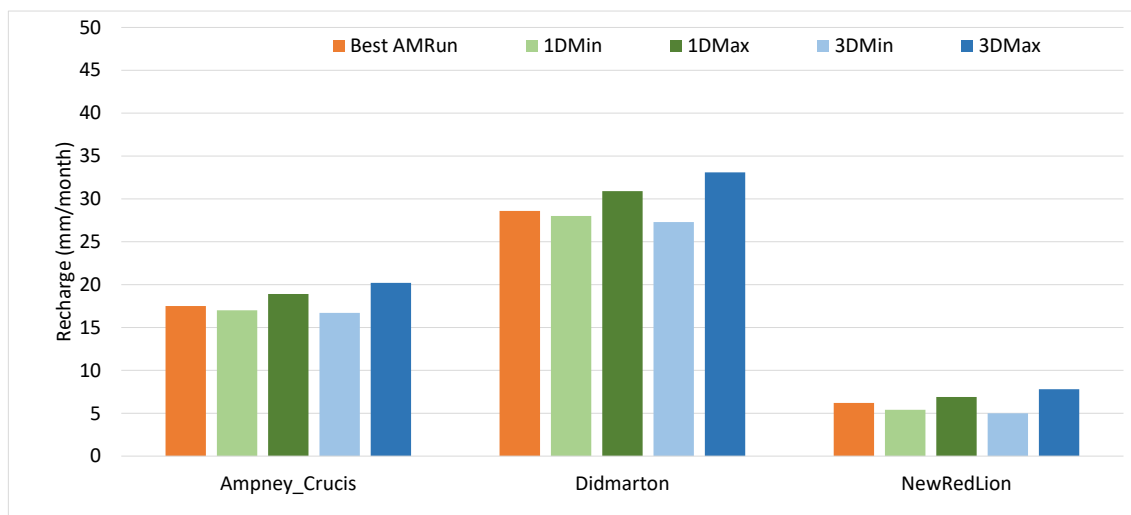


Figure 11 Historical (orange) and future recharge values (blue and green) as produced by the best performing AquiMod model.

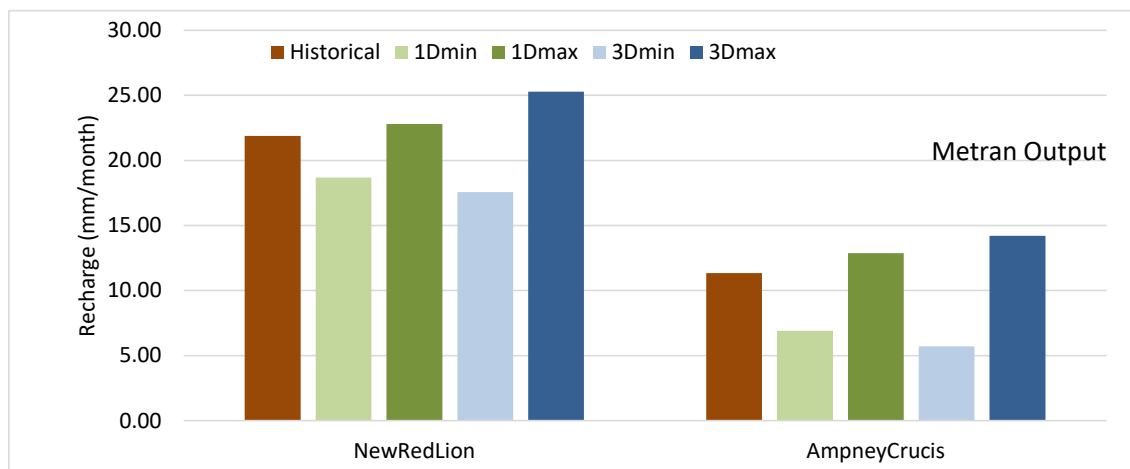


Figure 12 Historical (orange) and future recharge values (blue and green) produced by Metran.

Table 12 Monthly recharge values estimated using the historical and the projected forcing data.
Dotted line is the monthly historical recharge values. Green shaded area shows the 1° Min and Max monthly recharge values and the blue shaded area shows the 3° Min and Max monthly recharge values

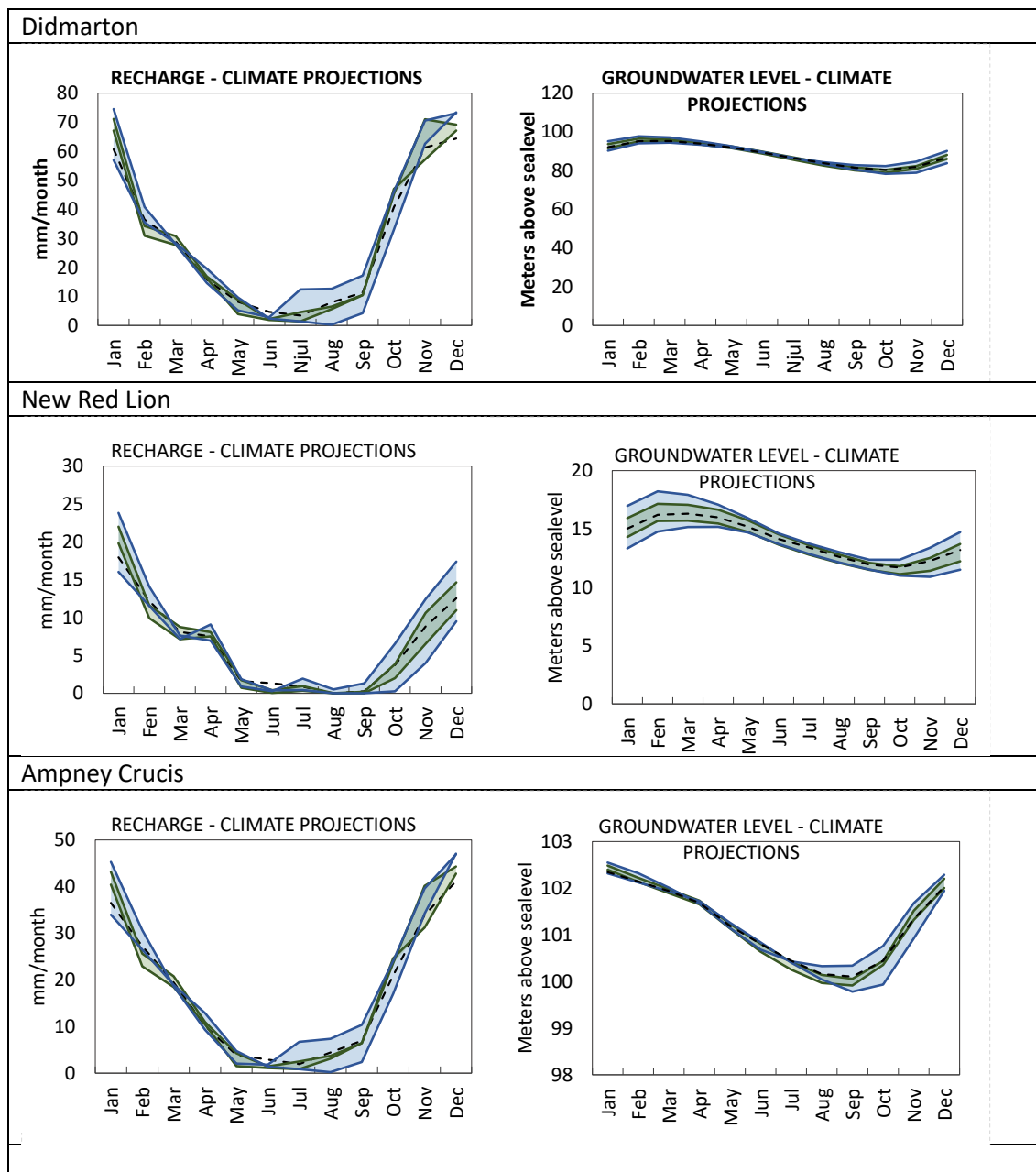


Table 13 shows maps of the spatially distributed recharge values calculated over the Jurassic limestones aquifer. The plots are for the historical potential recharge values as well as those calculated using the distributed recharge model but with rainfall and potential evaporation data that are altered using the 1° Min, 1° Max, 3° Min, and 3° Max UK change factors. While the differences in the maps are not clear, it can be easily observed that with the 1° Min and 3° Min data, the produced maps show drier pattern of recharge across the Jurassic limestones aquifer outcrop. Conversely, with the 1° Max and 3° Max data, the produced maps show wetter pattern of recharge across the Jurassic limestones aquifer outcrop.

The differences between the simulated future recharge values and the historical ones are shown in the plots in Table 14. While the differences between the future and historical recharge values is mainly between -4% and 6%, when the rainfall and potential evaporation data are altered using the 1° Min, 1° Max, and 3° Min change factors, the differences are much more noticeable when the 3° Max change factors are used. In the latter case, the recharge increase is greater than 15% indicating that this is a very wet scenario. However, it must be also noted that on a long term average basis, the 1° Min scenario is looking to be drier than the 3° Min scenario as illustrated by the first and third plots in Table 14.

Table 15 shows the average, maximum, and the standard deviation values calculated using the pixel values of the maps shown in Table 13. It can be noticed that, the average recharge value produced using the 1° Min data is smaller than that produced using the 3° Min data. This does not apply for the maximum recharge values where the value estimated using the 1° Min data is higher than that estimated using the 3° Min data. Finally, there is little difference in the standard deviation values shown in Table 15 indicating that the spatial distribution of recharge values is not notably different between the different scenarios.

Table 13 Spatially distributed historical and projected recharge values

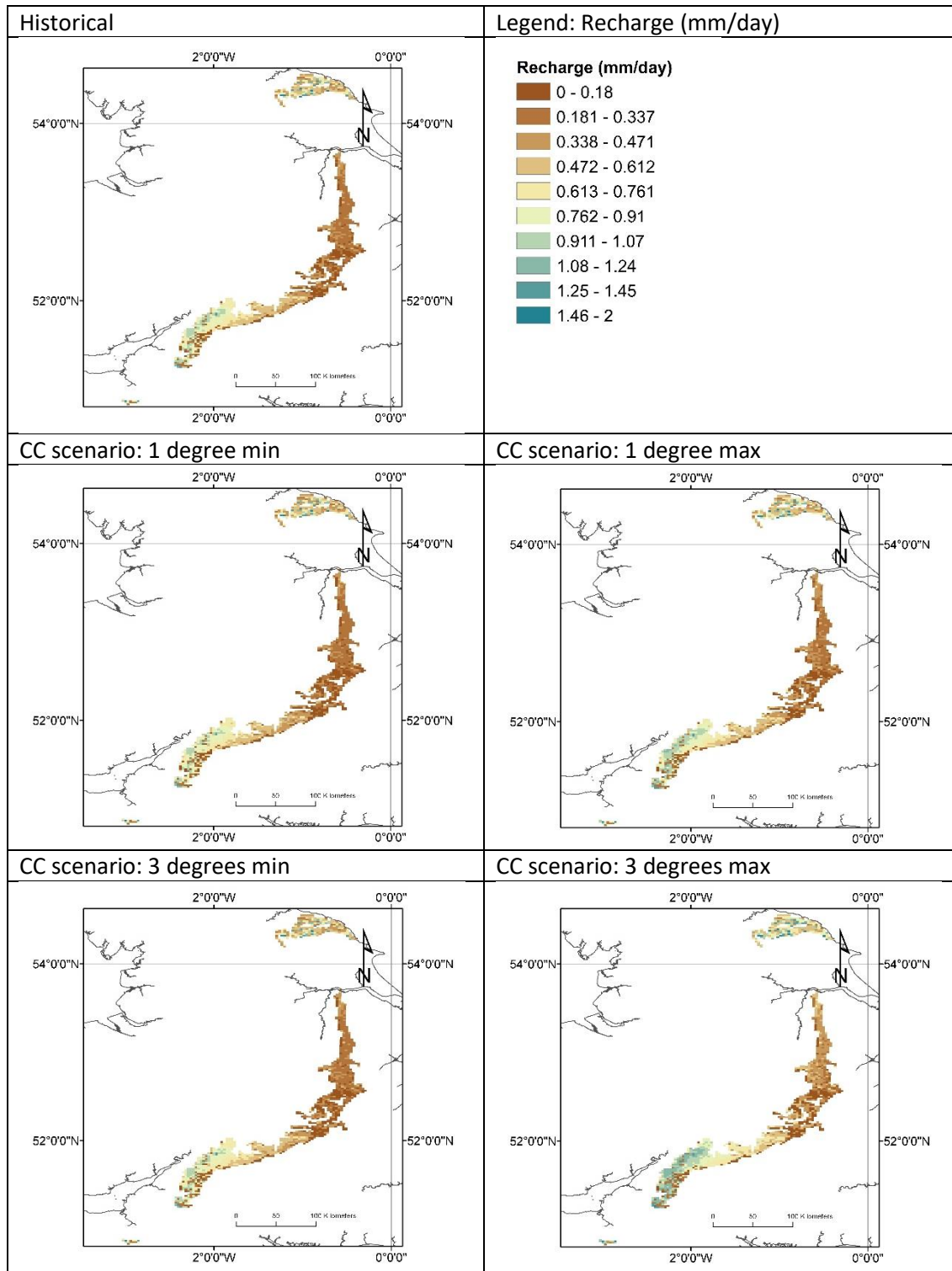


Table 14 Differences between the projected and historical recharge values calculated as projected values minus historical values

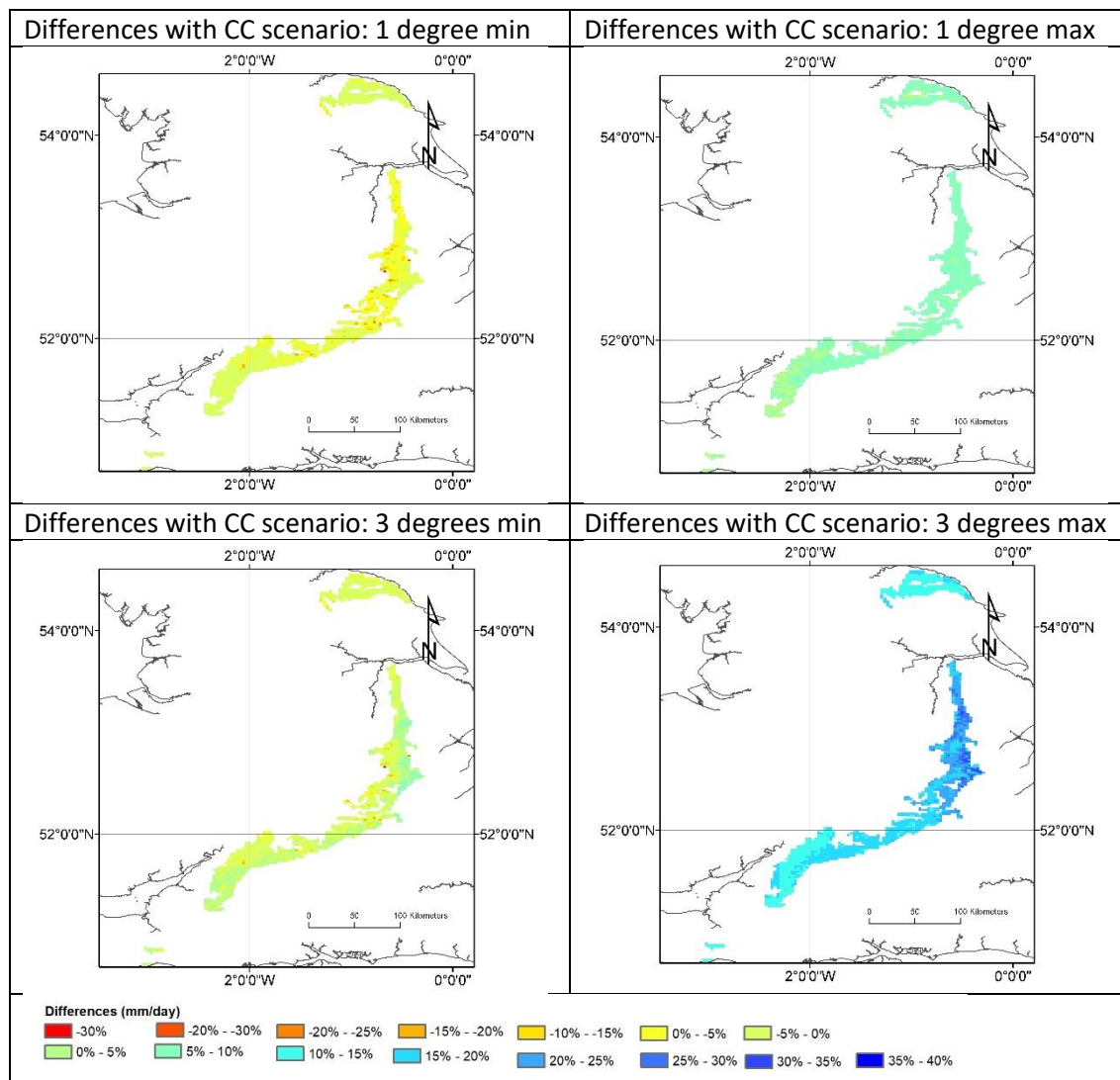


Table 15 Statistical information about the maps shown in Table 13

Map	Average recharge (mm/day)	Maximum recharge (mm/day)	Standard deviation (mm/day)
Historical	0.475	1.819	0.296
CC scenario: 1 degree min	0.454	1.793	0.288
CC scenario: 1 degree max	0.502	1.911	0.31
CC scenario: 3 degrees min	0.467	1.75	0.29
CC scenario: 3 degrees max	0.55	2.02	0.331

REFERENCES

- Allen, D. J., L. J. Brewerton, L. M. Coleby, B. R. Gibbs, M. A. Lewis, A. M. MacDonald, S. J. Wagstaff, A. T. Williams. 1997. 'The Physical Properties of Major Aquifers in England and Wales'.
- Besbes, M. & de Marsily, G. (1984) From infiltration to recharge: use of a parametric transfer function. *Journal of Hydrology*, 74, p. 271-293.
- Hough, M. N. & Jones, R. J. A. 1997. The United Kingdom Meteorological Office rainfall and evaporation calculation system: MORECS version 2.0 – an overview. *Hydrology and Earth System Sciences*, 1, 227–239.
- IPCC: 2000, Special report on emissions scenarios (SRES): A special report of Working Group III of the Intergovernmental Panel on Climate Change, Cambridge University Press, Cambridge, p. 599
- Jenkins, G.J., Murphy, J.M., Sexton, D.S., Lowe, J.A., Jones, P. and Kilsby, C.G. 2009, UK Climate Projections: Briefing report, Met Office Hadley Centre, Exeter, UK.
- Mackay, J. D., Jackson, C. R., Wang, L. 2014. A lumped conceptual model to simulate groundwater level time-series. *Environmental Modelling and Software*, 61. 229-245. <https://doi.org/10.1016/j.envsoft.2014.06.003>
- Mackay, J. D., Jackson, C. R., Wang, L. 2014. *AquiMod user manual (v1.0)*. Nottingham, UK, British Geological Survey, 34pp. (OR/14/007) (Unpublished)
- Mansour, M. M. and Hughes, A. G. 2018. Summary of results for national scale recharge modelling under conditions of predicted climate change. British Geological Survey Internal report. Commissioned Report OR/17/026.
- Mansour, M. M., Wang, L., Whiteman, Mark, Hughes, A. G. 2018. Estimation of spatially distributed groundwater potential recharge for the United Kingdom. *Quarterly Journal of Engineering Geology and Hydrogeology*, 51 (2). 247-263. <https://doi.org/10.1144/qjegh2017-051>
- Murphy, J.M., Booth, B.B.B., Collins, M., Harris, G.R., Sexton, D.M.H., and Webb, M.J. 2007. A methodology for probabilistic predictions of regional climate change from perturbed physics ensembles. *Phil. Trans. R. Soc. A* 365, 1993–2028.
- Murphy, J.M., Sexton, D.M.H., Jenkins, G.J., Boorman, P.M., Booth, B.B.B., Brown, C.C., Clark, R.T., Collins, M., Harris, G.R., Kendon, E.J., Betts, R.A., Brown, S.J., Howard, T. P., Humphrey, K. A., McCarthy, M. P., McDonald, R. E., Stephens, A., Wallace, C., Warren, R., Wilby, R., and Wood, R. A. 2009, 'UK Climate Projections' Science Report: Climate change projections. Met Office Hadley Centre, Exeter.

Obergfell, C., Bakker, M., & Maas, K. (2019). Estimation of average diffuse aquifer recharge using time series modeling of groundwater heads. *Water Resources Research*, 55. <https://doi.org/10.1029/2018WR024235>

Prudhomme, C., Dadson, S., Morris, D., Williamson, J., Goodsell, G., Crooks, S., Boelee, L., Davies, H., Buys, G., Lafon, T. and Watts, G., 2012. Future Flows Climate: an ensemble of 1-km climate change projections for hydrological application in Great Britain. *Earth System Science Data*, 4(1), pp.143-148.

Zaadnoordijk, W.J., Bus, S.A.R., Lourens, A., Berendrecht, W.L. (2019) Automated Time Series Modeling for Piezometers in the National Database of the Netherlands. *Groundwater*, 57, no. 6, p. 834-843. <https://onlinelibrary.wiley.com/doi/epdf/10.1111/gwat.12819>

APPENDICES

Appendix A: AquiMod methodology

AquiMod is a lumped parameter computer model that has been developed to simulate groundwater level time series at observational boreholes (Mackay et al., 2014a). It is based on hydrological algorithms that simulates the movement of groundwater within the soil zone, the unsaturated zone, and the saturated zone. The lumped models neglect complexities included in distributed groundwater models but maintains some of the fundamental physical principles that can be related to the conceptual understanding of the groundwater system (Mackay et al., 2014b).

While AquiMod was originally designed to capture the behaviour of a groundwater system through the analysis of groundwater level time series, it can produce the infiltration recharge values and groundwater discharges from the aquifer as a by-product. AquiMod is driven by complete time series of forcing data for either historical or predicted future conditions. Running AquiMod in predictive mode can be used to fill in gaps in historical groundwater level time series, or calculate future groundwater levels. In addition to groundwater levels, it also provides predictions of historical and future recharge values and groundwater discharges. In the current application we use calibrated AquiMod models to estimate the recharge values at selected boreholes.

AquiMod consists of three modules (Figure A1). The first is a soil water balance module that calculates the amount of water that infiltrates the soil as well as the soil storage. The second module controls the movement of water in the unsaturated zone, mainly it delays the arrival of infiltrating water to the saturated zone. The third module calculates the variations in groundwater levels and discharges. The model executes the modules separately following the order listed above.

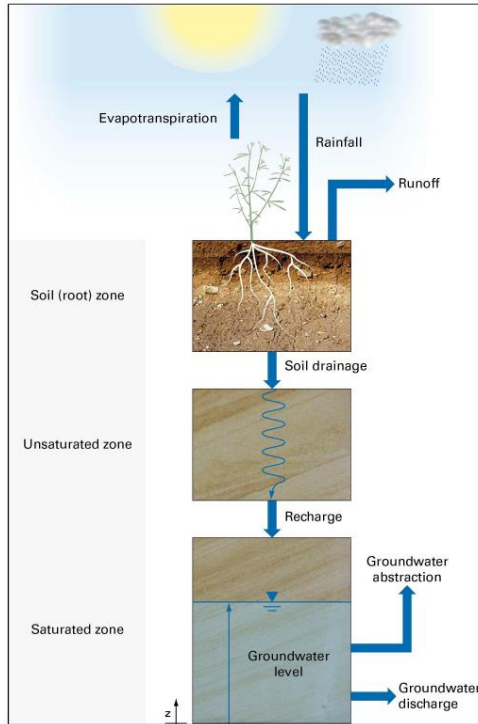


Figure A1 Generalised structure of Aquimod (after Mackay et al., 2014a)

The soil moisture module

There are several methods available in Aquimod that can be used to calculate the rainfall infiltration into the soil zone. In this study we use the FAO Drainage and Irrigation Paper 56 (FAO, 1988) approach. In this method, the capacity of the soil zone, from which plants draw water to evapo-transpire, is calculated first using the plants and soil characteristics. Evapo-transpiration is calculated according to the soil moisture deficit level compared to two parameters: Readily Available Water (RAW) and Total Available Water (TAW). These are a function of the root depth and the depletion factor of the plant in addition to the soil moisture content at field capacity and wilting point as shown in Equations A1 and A2.

$$TAW = Z_r(\theta_{fc} - \theta_{wp})$$

Equation A1

$$RAW = p \cdot TAW$$

Equation A2

Where Z_r [L] and p [-] are the root depth and depletion factor of a plant respectively, θ_{fc} [L³ L⁻³] and θ_{wp} [L³ L⁻³] are the moisture content at field capacity and wilting point respectively.

The FAO method is simplified by Griffiths et al. (2006) who developed a modified EA-FAO method. In this method the evapotranspiration rates are calculated as a function of the potential evaporation and an intermediate soil moisture deficit as:

$$\begin{aligned} e_s &= e_p \left[\frac{s_s^*}{TAW - RAW} \right]^{0.2} & s_s^* > RAW \\ e_s &= e_p & s_s^* \leq RAW \\ e_s &= 0 & s_s^* \geq TAW \end{aligned}$$

Equation A3



Where e_s [L] is the evapo-transpiration rate, e_p [L] is the potential evaporation rate and s_s^* [L] is the intermediate soil moisture deficit given by

$$s_s^* = s_s^{t-1} - r + e_p \quad \text{Equation A4}$$

Where r [L] is the rainfall at the current time step and s_s^{t-1} [L] is the soil moisture deficit calculated at the previous time step.

The new soil moisture deficit is then calculated from:

$$s_s = s_s^{t-1} - r + e_s \quad \text{Equation A5}$$

Griffiths et al. (2006) proposed that the recharge and overland flow are only generated when the calculated soil moisture deficit becomes zero. The remaining volume of water, the excess water, is then split into recharge and overland flow using a runoff coefficient. In Aquimod a baseflow coefficient is used to reflect the fact that a groundwater discharge is calculated rather than overland water. In this application, the baseflow coefficient is one minus the runoff coefficient.

The unsaturated zone module

The Aquimod version used in this study to simulate the movement of groundwater flow within the unsaturated zone is based on a statistical approach rather than a process-based approach. This method distributes the amount of rainfall recharge over several time steps where the soil drainage for each time step is calculated using a two-parameter Weibull probability density function. The Weibull function can represent exponentially increasing, exponentially decreasing, and positively and negatively skewed distributions. This can be used to focus the soil drainage over earlier or later time steps or to spread it over a number of time steps after the infiltration occurs. The shape of the Weibull function is controlled by two parameters, k and λ as shown in Equation A6.

$$f(t, k, \lambda) = \begin{cases} \frac{k}{\lambda} \left(\frac{t}{\lambda}\right)^{k-1} e^{-(t/\lambda)^k} & t > 0 \\ 0 & t \leq 0 \end{cases} \quad \text{Equation A6}$$

Where k and λ are two parameters the values of which are calculated during the calibration of the model and t is the time step.

The saturated zone module

Aquimod considers the saturated zone as a rectangular block of porous medium with dimensions L and B as its length and width [L] respectively. This block is divided into a number of layers, each has a defined hydraulic conductivity value, a storage coefficient value, and a discharging feature. The number of layers define the structure of the saturated module used in the study.

The mass balance equation that gives the variation of hydraulic head with time is given by:

$$SLB \frac{dh}{dt} = RLB - Q - A \quad \text{Equation A7}$$

Where:

S is the storage coefficient of the porous medium [-]

h is the groundwater head [L]

t is the time [T]

R is the infiltration recharge [L T⁻¹]

Q is the discharge out of the aquifer [L T⁻¹]



A is the abstraction rate [$L T^{-1}$]

It must be noted that in a multi-layered groundwater system as shown in Figure A2, we calculate one groundwater head (h) for the whole system. The discharges (Q) from Outlet 1, 2, etc. are calculated using the Darcy law. The total discharges can be summarised using the following equation:

$$Q = \sum_{i=1}^m \frac{T_i B}{0.5 L} \Delta h_i \quad \text{Equation A8}$$

Where:

m is the number of layers in the groundwater system [-]

T_i is the transmissivity of the layer i [$L T^{-2}$]

Δh_i is the difference between the groundwater head h and z_i , the elevation of the base of layer i

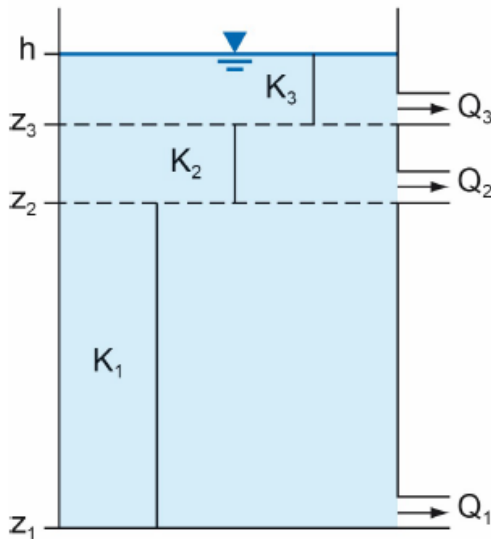


Figure A2 Representation of the saturated zone using a multi-layered groundwater system

Substituting Equation A8 into Equation A7 yields a numerical equation in the form:

$$S \frac{(h-h^*)}{\Delta t} = R - \sum_{i=1}^m \frac{T_i}{0.5 L^2} \Delta h_i - \frac{A}{LB} \quad \text{Equation A9}$$

Equation A9 is an explicit numerical equation that allows the calculation of the groundwater head h [L] at any time and using time steps of Δt [T]. In this equation h^* [L] is the groundwater head calculated at the previous time step and the term Δh_i [L] is calculated as $(h^* - z_i)$.

The terms S , T_i , and L are optimised during the calibration of the model. A groundwater system can be specified with one storage coefficient as shown in the equations above or with different storage coefficient values for the different layers. Several saturated modules are included in AquiMod to provide this flexibility and the model user can select the model structure that represent the conceptual understanding best.



Limitations of the model

AquiMod is a lumped groundwater model that aims at reproducing the behaviour of the observed groundwater levels. It tries to encapsulate the conceptual understanding of a groundwater system in a simple numerical representation. The model results have to be therefore discussed, taking this into consideration. For example, the model represents the groundwater system as a closed homogeneous medium, with no impact from any outer boundary or feature, whether physical or hydrological, such as the presence of rising and falling river stage.

Vertical heterogeneity can be accounted for by using multi-layered groundwater module structure. However, this model setting does not provide any information about the vertical connections between the layers as the discharge from all the layers is calculated using one representative groundwater head value. In other words, it is assumed that all layers are in perfect hydraulic connection.

As mentioned before, the model is designed to simulate the groundwater levels. However, it produces the recharge values and groundwater discharges as by products. In this application we use the calibrated model to calculate recharge. The mass balance equation (Equation A7) shows that recharge is a function of transmissivity and storage coefficient values, which are estimated during the calibration process of the model, i.e. they are not parameters with fixed values provided by the user. The inter-connections between these parameters leads to uncertainties in the estimated recharge values as a high storage coefficient value can produce a high recharge estimate and vice versa. To overcome this problem, it is suggested that the recharge values estimated by AquiMod are always presented as a range of possibilities rather than an absolute value. This can be achieved by estimating the recharge values from all the models that have a performance measure above than a threshold that is deemed acceptable by the user. The recharge estimates can then be presented as an average of all estimates and values corresponding to selected percentiles.

Model input and output

AquiMod includes a number of methods that calculates rainfall recharge as well as a number of model structure from which the user can select what better suits the case study.

Model input consists time series of forcing data including rainfall and potential evaporation, time series of anthropogenic impact mainly groundwater abstraction and time series of groundwater levels that will be used to calibrate the model. These time series must be complete, i.e. a value is available at every time step except the groundwater level time series, which can include missing data. The time step can be one day or multiple of days, and the model automatically calculate the size of the time step based on the input data time series.

The model is run first in calibration mode where a range of parameter values are specified for the different parameters included in the three model modules. A Monte Carlo approach is used to select the best parameter values. The performance of the model is measured by comparing the simulated groundwater levels to the observed ones using the Nash Sutcliffe Efficient (NSE) or the Root Mean Squared Error (RMSE) performance measures. The parameter set that produces the best model performance is selected to run the model in evaluation mode.

When the model is run in evaluation mode, it produces output files that give recharge values, groundwater levels and groundwater discharges time series with time as specified in the input file. The number of output files is equal to the number of acceptable models set by the user.

Appendix B: Metran methodology

Metran applies transfer function noise modelling of (groundwater head) time series with usually daily precipitation and evaporation as input (Zaadnoordijk et al., 2019). The setup is shown in the Figure B1. If time series of other influences on the groundwater head are available, these contributions can be added to the deterministic part of the model. The stochastic part is the difference between the total deterministic part and the observations (the residuals). The corresponding input of the noise model should have the character of white noise.

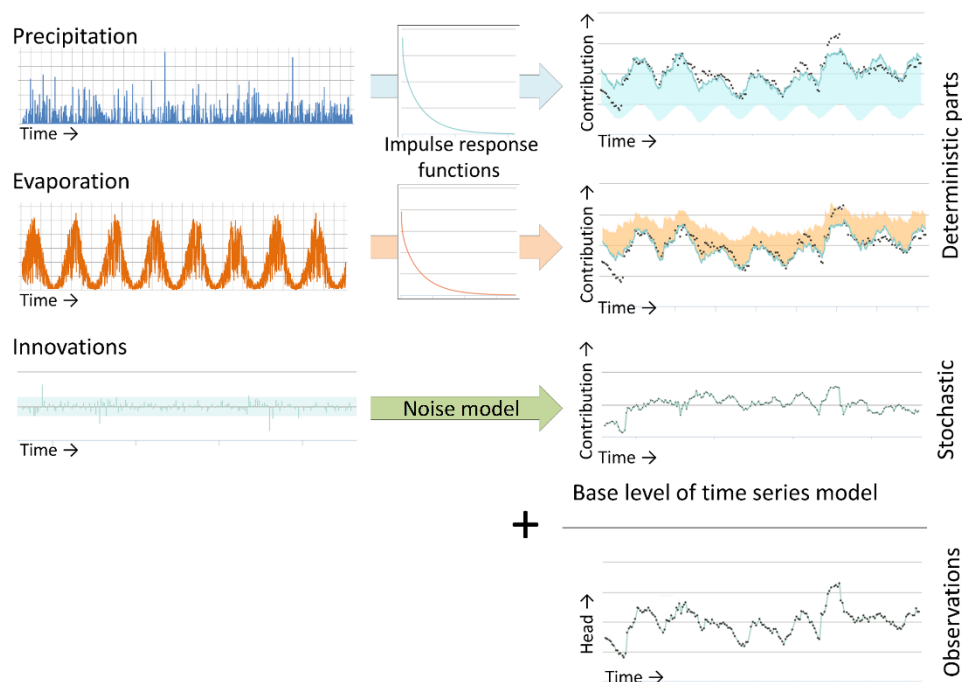


Figure B1 Illustration of METRAN setup

The stochastic part is needed because of the time correlation of the residuals, which does not allow a regular regression to obtain the parameter values of the transfer functions.

The incomplete gamma function is used as transfer function. This is a uni-modal function with only three parameters that has a quite flexible shape and has some physical background (Besbes & de Marsily, 1984). The evaporation response is set equal to the precipitation response except for a factor (f_c). The noise model has one parameter that determines an exponential decay. Thus, for the standard setup with precipitation and evaporation, there are five parameters that have to be determined from the comparison with the observations. Three parameters regarding the precipitation response, the evaporation factor, and the noise model parameter (actually, the time series model has a fifth parameter, the base level, but this is determined from the assumption that the average of the calculated heads is equal to the average of the observations). There are three extra parameters for each additional input series, such as pumping.



Limitations

Metran's time series model is linear. So, the model creation breaks down when the system is strongly nonlinear. This can occur e.g. when drainage occurs for high groundwater levels, when the ratio between the actual evapotranspiration and the inputted reference evaporation varies strongly, or when the groundwater system changed during the simulated period.

Metran is not able to find a decent time series model when the response function is not appropriate for the groundwater system. An example of this is a system with a separate fast and slow response as was found for a French piezometer in the Avre region, as is illustrated in Figure B2.

Finally, the parameter optimization of Metran uses a gradient search method in the parameter space, so it can be sensitive to initial parameter values in finding an optimal solution.

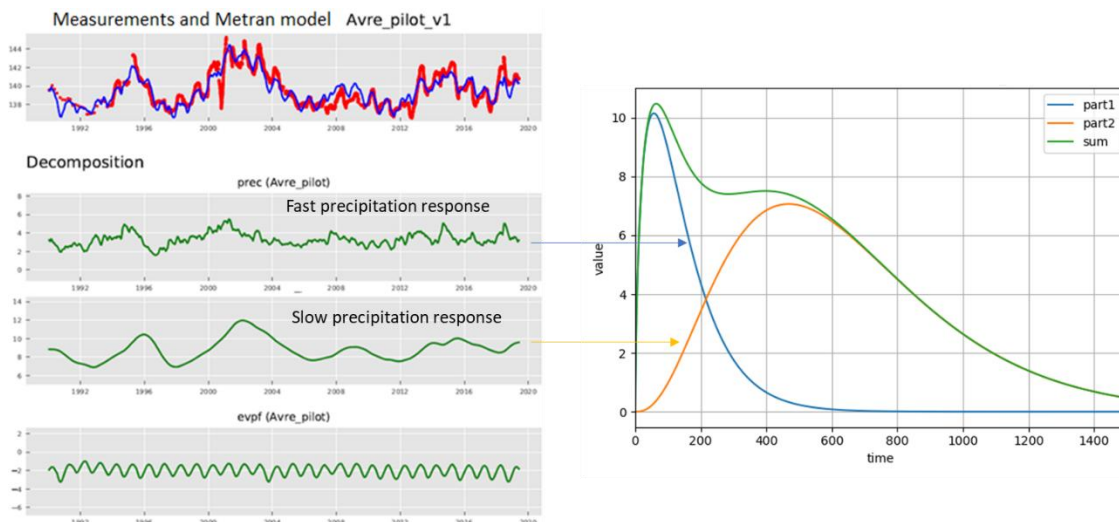


Figure B2. An example where the response function implemented in METRAN is not suitable for the groundwater system

Time step

Metran has been designed to work with explanatory series that have a daily time step. However, it has been adapted so that other time step lengths can be applied; although Metran still has the limitation that the explanatory variables have a constant frequency. For the TACTIC simulations of series with monthly or decadal meteorological input series, the time step has been set to 30 and 10 days, respectively. This time step has been applied from the end date backward.

Note that the heads may be irregular in time as long as the frequency is not greater than the frequency of the explanatory series.

Model output

The evaporation factor f_c gives the importance of evapotranspiration compared to precipitation. The parameter M_0 gives the total precipitation response, which is equal to the area below the impulse response function and the final value of the step response function.



The average response time is another characteristic of the precipitation response. The influence is illustrated in Figure B3 with the impulse response functions and head time series for two models with very different response times for time series of SGU in Sweden.

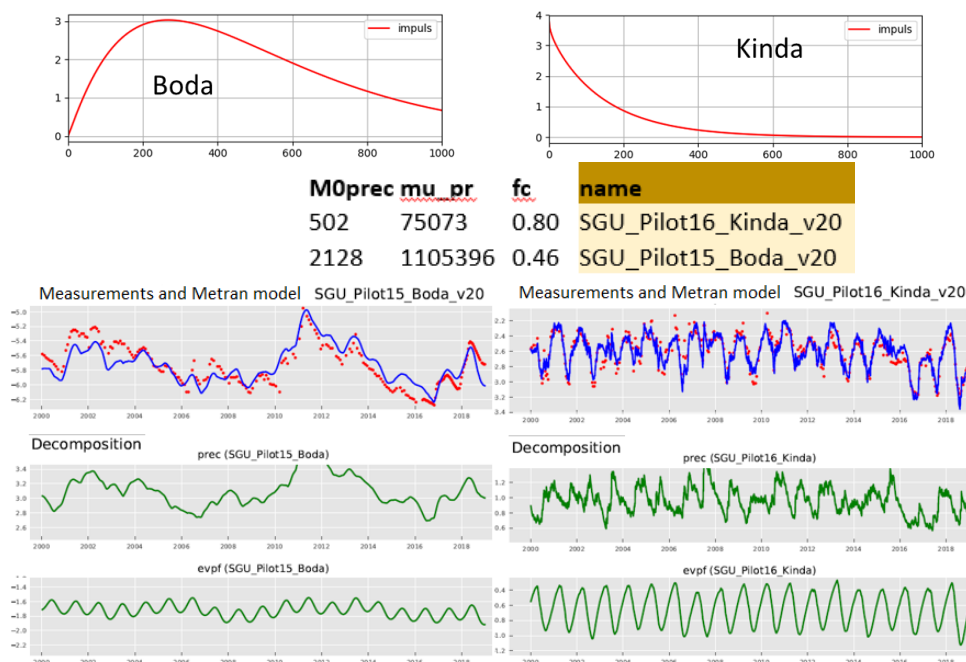


Figure B3 Illustration of Metran output for two case studies in Sweden with different response times.

Model quality

Metran judges a resulting time series model according to a number of criteria and summarizes the quality using two binary parameters Regimeok, Modok (see Zaadnoordijk et al., 2019):

- Regimeok = 1 : highest quality
- Modok = 1 (and Regimeok = 0) : ok
- Both zero = model quality insufficient

More detailed information on the model quality is given in the form of scores for two information criteria (AIC and BIC), a log likelihood, R2, RMSE, and the standard deviations and correlations of the parameters.

Recharge

Although the transfer-noise modelling of Metran determines statistical relations between groundwater heads and explanatory variables, we like to think of the results in physical terms. It is tempting to interpret the evaporation factor, as the factor translating the reference into the actual evapotranspiration. Then, we can calculate a recharge as

$$R = P - fE$$

Equation B1



where R is recharge, P precipitation, E evapotranspiration, and f the evaporation factor.

Following the definitions used in the TACTIC project, this recharge R actually is the effective precipitation. It is equal to the potential recharge when the surface runoff is negligible. This in turn is equal to the actual recharge at the groundwater table if there also is no storage change or interflow. In such cases it may be expected that this formula indeed corresponds to the meteorological forcing of the groundwater head in a piezometer, so that it gives a reasonable estimate of the recharge. Obergfell et al. (2019) showed this for an area on an ice pushed ridge in the Netherlands. However, this assumes that all precipitation recharges the groundwater, which cannot be done in many places.

In Dutch polders with shallow water tables and intense drainage networks, it is reasonable to assume that the actual evapotranspiration is equal to the reference value. In that case, the factor f becomes larger than 1 because 1 mm of evaporation has less effect than 1 mm of precipitation (because part of the evaporation does not enter the ground but is immediately drained to the surface water system). In that case, we can calculate recharge as:

$$\begin{aligned} R &= P - fE & f &\leq 1 \\ R &= P/f - E & f &> 1 \end{aligned} \quad \text{Equation B2}$$

These simple formulas can be applied easily for the situations currently modelled in Metran and for the simulations that are driven by future climate data using the delta-change climate factors. However, it is noted that it is a crude estimate using assumptions that are easily violated. Because of this, the equations should be applied only to long term averages using only models of the highest quality.



Deliverable x.2

PILOT DESCRIPTION AND ASSESSMENT

Kinda and Böda, Sweden

Authors and affiliation:

**Emil Fagerström, Johan Öhman,
Mattias Gustafsson, Ellen Walger**

Geological survey of Sweden

This report is part of a project that has received funding by the European Union's Horizon 2020 research and innovation programme under grant agreement number 731166.



Deliverable Data	
Deliverable number	D2.4
Dissemination level	Public
Deliverable name	<i>Pilot description and assessment report for recharge and groundwater vulnerability</i>
Work package	WP4
Lead WP/Deliverable beneficiary	BRGM, BGS
Deliverable status	
Version	<i>Version 2</i>
Date	28/02/21

[This page has intentionally been left blank]

LIST OF ABBREVIATIONS & ACRONYMS

CC	Climate Change
GSOs	Geological Survey Organisations
TACTIC	Tools for Assessment of Climate change Impact on Groundwater and Adaptation Strategies
HYPE	Hydrological Predictions for the Environment
SGU	The Geological Survey of Sweden
ET	evapotranspiration
NSE	Nash Sutcliffe Efficiency coefficient
ISIMIP	Inter Sectoral Impact Model Intercomparison Project
RCPs	Representative Concentration Pathways (development in greenhouse gas concentrations)
GCMs	Global Circulation Models
SMHI	the Swedish Meteorological and Hydrological Institute
TNO	Netherlands Organisation for Applied Scientific Research

TABLE OF CONTENTS

LIST OF ABBREVIATIONS & ACRONYMS	5
1 EXECUTIVE SUMMARY	5
2 INTRODUCTION	8
2.1 Background on TACTIC	8
2.2 Introduction to the pilot areas	9
3 PILOT AREAS	11
3.1 Site description and data for pilot Kinda	12
3.2 Site description and data for pilot Böda	13
3.3 Climate change challenge	16
4 METHODOLOGY	19
4.1 Methodology and climate data	19
4.1.1 HYPE	19
4.1.2 AquiMod	20
4.1.3 Metran	21
4.1.4 Climate data	22
4.2 Model set-up	25
4.2.1 Observation data	25
4.3 Model calibration	27
4.4 Uncertainty	29
5 RESULTS AND CONCLUSIONS	30
5.1 Historical recharge	30
5.2 Climate projections on recharge	32
6 REFERENCES	36
7 APPENDICES	38
Appendix A: AquiMod methodology	38
The soil moisture module	39
The unsaturated zone module	40
The saturated zone module	40
Limitations of the model	42
Model input and output	42
Appendix B: Metran methodology	43
Limitations	44
Time step	44
Model output	45
Model quality	45
Recharge	46

1 EXECUTIVE SUMMARY

As a partner of TACTIC WP4, the Geological Survey of Sweden (SGU) has studied groundwater-related effects from climate change in two pilot areas, Kinda and Böda (Table 1 and Table 2). The primary challenge regarding the future groundwater situation in these areas is the supply of drinking water. A specific challenge for Böda concerns peak consumption, related to tourism, which coincides with minimum groundwater storage at the end of the drought period. As such, model results were analysed from a drinking-water supply context, focusing on the delicate balance between recharge and drought periods that essentially determines if the groundwater, stored during winter recharge, is sufficient to last during the subsequent drought period.

Typically, groundwater resources in Sweden are found in the overburden regolith (soil thickness in the pilot areas: 0 to 10 m). Swedish groundwater resources are, depending on geology, divided into two groups: major and minor resources (Figure 1). Here the pilot Böda represents a major resource, while Kinda is taken to represent a minor resource. Effectively, the groundwater regime at Kinda exhibits strong seasonality, with snowmelt as a key component in recharge, compared to Böda, where, owing to its larger storage capacity, the regime is dominated by interannual variation.

Table 1. Summarized description of the Kinda pilot area

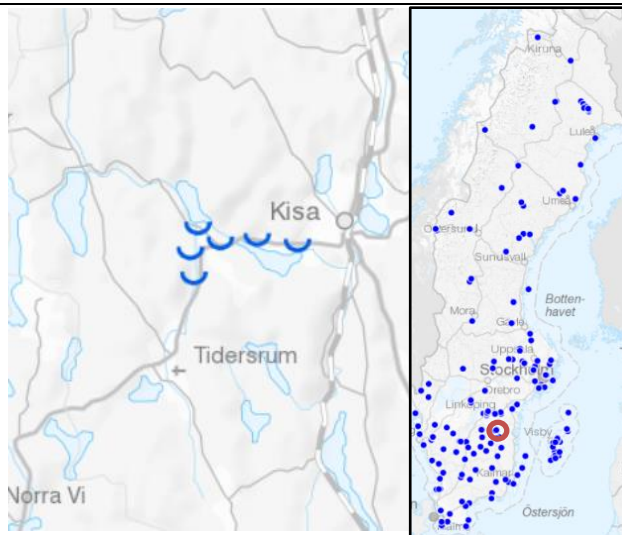
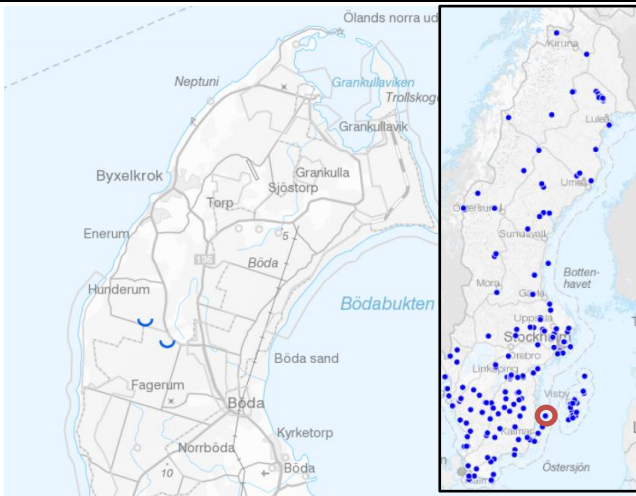
Pilot name	Kinda	
Country	Sweden	
EU-region	Northern europe	
Area (km ²)	2/40 km ² (area of groundwater body/catchment)	
Aquifer geology and type classification	Glacial sand and gravel deposits and till, Porous	
Primary water usage	Drinking water	
Main climate change issues	Future challenges with precipitation in the form of rain during winter (less snow) and longer summer periods with less recharge	
Models and methods used	Lumped-catchment modelling of time series (HYPE, Aquimod, Metran)	
Key stakeholders	SGU, municipality of Kisa, Region of Östergötland	
Contact person	Mattias Gustafsson, SGU, Mattias.gustafsson@sgu.se	

Table 2. Summarized description of the Böda pilot area

Pilot name	Böda	
Country	Sweden	
EU-region	Central and Eastern Europe	
Area (km ²)	26 km ²	
Aquifer geology and type classification	Glacial sand and gravel deposits, Porous	
Primary water usage	Drinking water	
Main climate change issues	Future challenges with more precipitation in winter (less snow) and longer summer periods with less recharge. The island of Öland has busy tourism during summertime, and the precipitation is low.	
Models and methods used	Lumped-catchment modelling of time series (HYPE, Aquimod, Metran)	
Key stakeholders	SGU, municipality of Borgholm, Region of Kalmar	
Contact person	Mattias Gustafsson, SGU, Mattias.gustafsson@sgu.se	

Three lumped precipitation-runoff models, HYPE, Aquimod, and Metran, were used to evaluate groundwater recharge in the two pilot areas. The models were first calibrated for a historic period, 1980 to 2010. Next, a selection of future climate scenarios (i.e., forcing data subject to climate change: P, T, and PET) was applied for the calibrated models, to project expected climate-change effects on the groundwater regime for the two pilot areas.

The TACTIC project employs four standard climate scenarios based on the Inter Sectoral Impact Model Inter-comparison Project (ISIMIP) that represent two stages of global annual mean warming (+1°C and +3°C), combined with two cases to cover the range of likely precipitation: Wet and Dry cases.

Although all three models could be reasonably well calibrated to the historic time period, Aquimod and Metran were suspected to fit for the wrong reasons (as they lack snow storage), and hence their climate-change projections were considered to be less reliable. Confidence in HYPE was, on the other hand, well-supported by field data, not only by standard performance measures as NSE, but also by: 1) a close resemblance in seasonal patterns and 2) an ongoing, climate-related, transition in groundwater regime (a widespread phenomenon in SGU's monitoring programme). Hence, the HYPE simulations are considered sufficiently reliable for assessing the current recharge situation, as well as future changes in groundwater regime, which is associated to stress for the drinking-water supply.



For the present-day situation, the simulated recharge agrees reasonably well with earlier estimates for both pilot areas. For climate-change projections, simulations re-produce a concerning pattern (consistent with both observed trends in field data and in earlier modelling), where the groundwater regime is shifting towards: 1) increased winter recharge, 2) retreating snowmelt, resulting in 3) an earlier and prolonged drought period. In turn, the prolonged drought period increases the stress on water resources, particularly during late summer when consumption peaks due to tourism.

Taken as an average of the Dry and Wet cases, the reduction in recharge is estimated to -15% for Kinda and -30% for Böda (results apply to both +1°C and +3°C warming). This study is consistent with earlier work and underpins the current understanding of future challenges for drinking-water supply, particularly along the south-eastern coast of Sweden (here exemplified by the Böda pilot area on Öland).

2 INTRODUCTION

2.1 Background on TACTIC

Climate change (CC) already have widespread and significant impacts on Europe's hydrological systems including groundwater bodies, which is expected to intensify in the future. Groundwater plays a vital role for the land phase of the freshwater cycle and has the capability of buffering or enhancing the impact from extreme climate events causing droughts or floods, depending on the subsurface properties and the status of the system (dry/wet) prior to the climate event. Understanding and taking the hydrogeology into account is therefore essential in the assessment of climate change impacts. Providing harmonised results and products across Europe is further vital for supporting stakeholders, decision makers and EU policies makers.

The Geological Survey Organisations (GSOs) in Europe compile the necessary data and knowledge of the groundwater systems across Europe. To enhance the utilisation of these data and knowledge of the subsurface system in CC impact assessments, the GSOs, in the framework of GeoERA, has established the project "Tools for Assessment of Climate change Impact on Groundwater and Adaptation Strategies – TACTIC". By collaboration among the involved partners, TACTIC aims to enhance and harmonise CC impact assessments and identification and analyses of potential adaptation strategies.

TACTIC is centred around 40 pilot studies covering a variety of CC challenges as well as different hydrogeological settings and different management systems found in Europe. Knowledge and experiences from the pilots will be synthesised and provide a basis for the development of an infrastructure on CC impact assessments and adaptation strategies. The final projects results will be made available through the common GeoERA Information Platform (<http://www.europe-geology.eu>).

The following TACTIC activities have been defined to focus on specific research questions:

- What are the challenges related to groundwater- surface water interaction under future climate projections (TACTIC WP3).
- Estimation of renewable resources (groundwater recharge) and the assessment of their vulnerability to future climate variations (TACTIC WP4).
- Study the impact of overexploitation of the groundwater resources and the risks of saline intrusion under current and future climates (TACTIC WP5).
- Analyse the effectiveness of selected adaptation strategies to mitigate the impacts of climate change (TACTIC WP6).

WP4 is divided into seven tasks that cover the following activities: Review of tools and methods and identification of data requirements (Task 4.1), identification of principal aquifers and their characteristics aided by satellite data (Task 4.2), recharge estimation and its evolution under climate change scenarios in the principal aquifers (Task 4.3), analysis of long-term piezometric time series to evaluate aquifer vulnerability to climate change (Task 4.4), assessment of subsidence in aquifer systems using DInSAR satellite data (Task 4.5), development of a satellite based net precipitation and recharge map at the pan-European scale (Task 4.6), and tool descriptions and guidelines (Task 4.7).

2.2 Introduction to the pilot areas

This report describes the work undertaken by the Swedish Geological Survey (SGU) as a part of TACTIC WP4 to calculate groundwater recharge at two locations, Kinda and Böda. The two pilots have been selected to represent two different types groundwater resources, which are typical for the supply of drinking water in Sweden. Sweden is dominated by crystalline bedrock where the porosity is considerably lower than it is in sedimentary rock. As the bedrock does not serve as drinking water aquifers (at least, in general), the groundwater resources are mainly found the regolith (overlying loose soil deposits). These groundwater resources are divided into two main types (Figure 1):

- **Major groundwater resources (Böda pilot area):** found in glaciofluvial eskers, typically abstracted via groundwater wells to supply municipal water works. The groundwater dynamics is dominated by interannual variation, with periodicity ranging from years to decades.
- **Minor groundwater resources (Kinda pilot area):** typically thin (few meters) till layer, typically abstracted via bedrock boreholes to supply private households in rural areas. The groundwater dynamics is dominated by flashy, intra-annual variation (strong seasonal pattern).

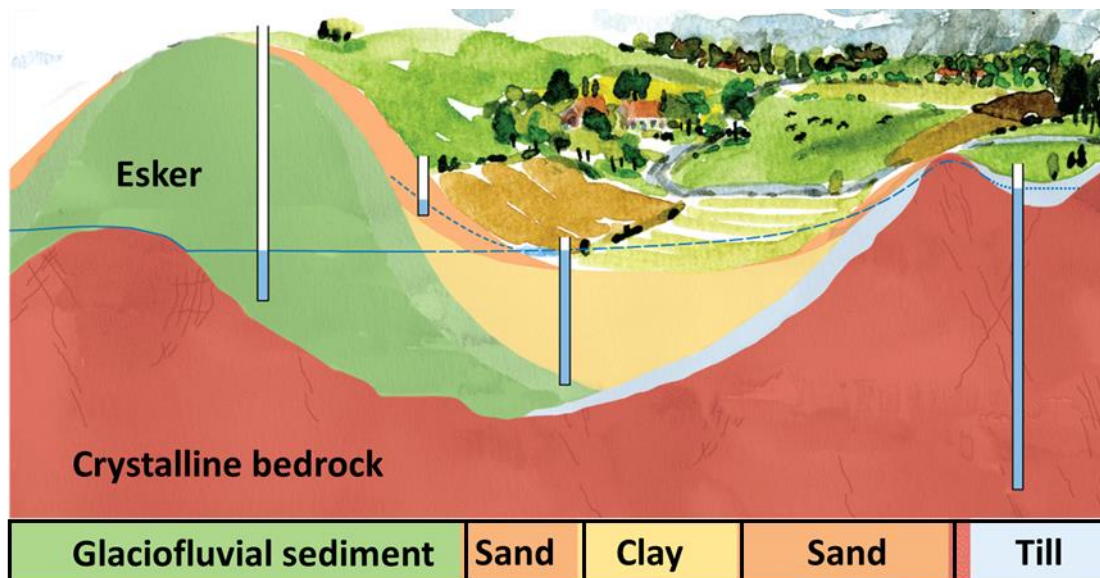


Figure 1. Conceptual figure illustrating the classification of Swedish groundwater resources: Major resources, illustrated by well in glaciofluvial esker (left, here represented by pilot Böda) and Minor resources, illustrated by drilled borehole dewatering thin layers of overlying till, sand or silt (right, here represented by pilot Kinda).

The work presented here is related to Task 4.3 with the aim to estimate of recharge under current and future climates. This is undertaken using multiple tools selected from the TACTIC toolbox (developed under WP2 of TACTIC). The toolbox is a collection of hydrogeological models, scripts, spreadsheets that serves all the activities identified in TACTIC workpackages.

Here, we use three lumped groundwater models: HYPE (Lindström et al., 2010), Aquimod (Mackay et al., 2014a and Mackay et al., 2014b), and the Transfer Function-Noise Model Metran (Zaadnoordijk et al., 2019). The modelling is undertaken in two steps. In the first step, the models are calibrated to reproduce the behaviour of the observed groundwater level time series, during the period 1980-2010. In the second step, the calibrated models are used to study future recharge by means of a simplified sensitivity analysis.

3 PILOT AREAS

Two pilot areas have been selected for the WP4 TACTIC project: Kinda and Böda. These pilot areas were selected to cover two aspects, which are considered key to understanding recharge under present and future climate conditions. The pilots are to represent:

- both the Swedish groundwater-resource types (Figure 1)
- the most critical climate challenges (Figure 8); as categorised by the Northern Europe and the Central-and-eastern Europe regions.

Furthermore, the pilot areas were also selected on the basis of modelling data quality and previous modelling experience on groundwater dynamics at the sites (using several lumped-catchment precipitation-runoff models, including Coup, HBV and HYPE).

Here, the Kinda pilot area is taken to represent a *minor groundwater resource* in the *Northern Europe region* (the dominant type of recharge area in Sweden, both under present and future conditions). It should be noted that, strictly speaking, the selected observation well at Kinda, ID 66_5, is classified as an *intermediate* groundwater resource; however, in comparison to the other Swedish pilot, Böda, it may well be taken to represent a minor groundwater resource.

The Böda pilot area is – on the other hand – taken to represent a contrasting situation: a *major groundwater resource* of the *Central-and-eastern Europe region* (the most important groundwater-resource type for municipal waterworks in Sweden, being stressed under present conditions). The area has busy tourism during summer, when the recharge is at its minimum.

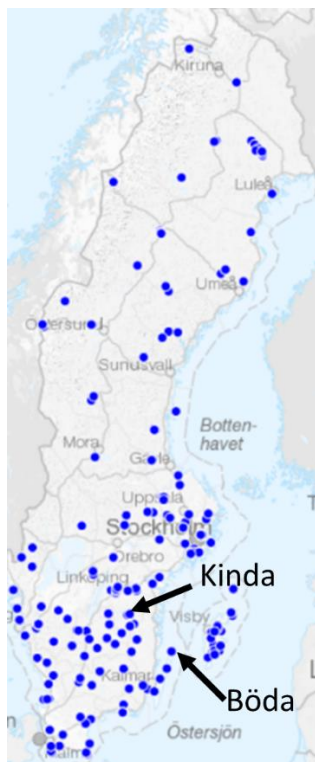


Figure 2. The location of the pilot areas Kinda and Böda in Sweden (blue dots marking SGU monitoring wells).



3.1 Site description and data for pilot Kinda

The Kinda pilot is an inland area located in the south of Sweden (Figure 2). The basin has an approximate area of 40 km² (Figure 3, left). There are several lakes and creeks in the area and they are surrounded with small soft surging hills and ridges of about 100 meters height. The area is located approx. 5 km west of a small town called Kisa, regional centre in the Municipality of Kinda, and the land use of the area is mainly forest and agricultural (Figure 3, right).

The groundwater resources for private wells in the area are formed by a patchwork of soil deposits (Figure 4; left), ranging from thin till layers to thicker glaciofluvial sand- and gravel deposits. The soil coverage (Figure 4; left) is characterised by a mosaic pattern, which is dominated by uncovered bedrock (red) and scattered areas of thin till layers (blue), which are interlaced with thicker esker-type sand and gravel deposits (green). The underlying bedrock (Figure 4; right) is of crystalline origin with limited storage capacity, which is why the overburden soil has such a prominent role for drinking-water supply.

The climate of the Kinda pilot area is of Boreal Northern European type, with a precipitation of approximately 700 mm/year and a potential evapotranspiration of 560 mm/year (P-PET = 140 mm/year). The groundwater recharge is largely limited by storage capacity in the soil deposits and has been estimated to 260 mm/year (Rodhe et al., 2006; Figure 7). The recharge is limited by low storage capacity in areas of uncovered bedrock and thin soil coverage (generally 0-5 m). The main water storages are found in sand and gravel deposits where the soil depth is up to about 20 m.

Precipitation and temperature data are available on daily basis since 1961-01-01 (provided via the Swedish Meteorological and Hydrological Institute, SMHI's PTHBV-raster at a resolution of 4 km). Forcing data for modelling can be downloaded from SMHI's webpage (<https://www.smhi.se/data/meteorologi/>). Potential evapotranspiration, PET, is calculated from temperature, based on an empirical relationship (Rodhe et al., 2006).

The groundwater level in the area is monitored in six wells, of which two are located in sand and gravel deposits and the remaining four are located in till. In this study, groundwater well 66_5 was used for modelling historic and future change in groundwater recharge. This particular well is located in a 4.5 m thick sand deposit, which is classified as an *intermediate* groundwater resource (i.e., falling between the two end points illustrated in Figure 1). The groundwater level has been measured manually twice a month since 1975-08-28, and daily since the installation of an automatic logger system in 2017-12-12. The groundwater time series can be downloaded from SGU's web page (<https://www.sgu.se/grundvatten/grundvattennivaer/matstationer/>).

There are no streamflow data available for the pilot area.

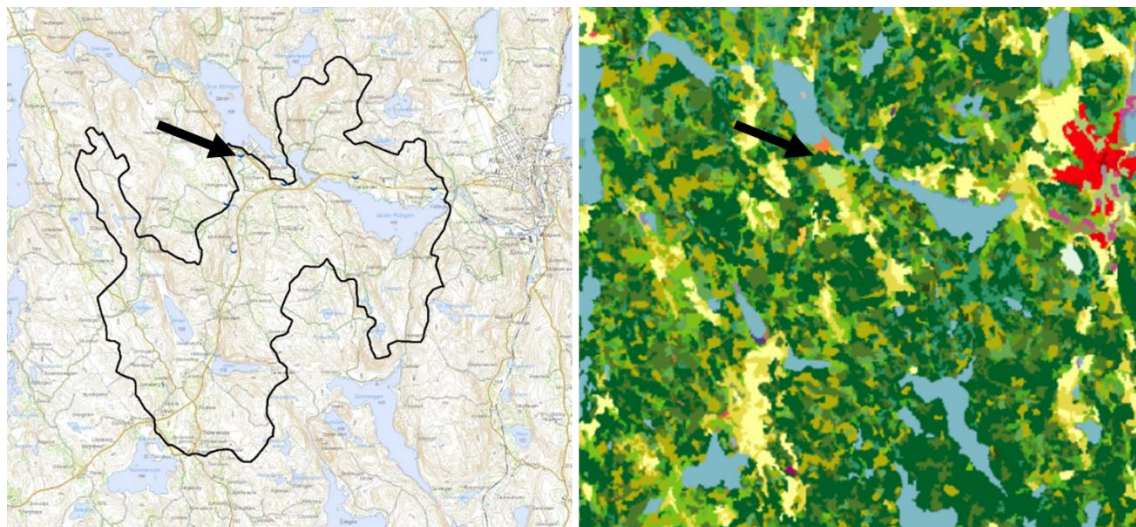


Figure 3. Catchment of the Kinda pilot area and land use (mainly forest and agricultural). Arrow marks the location of well 66_5.

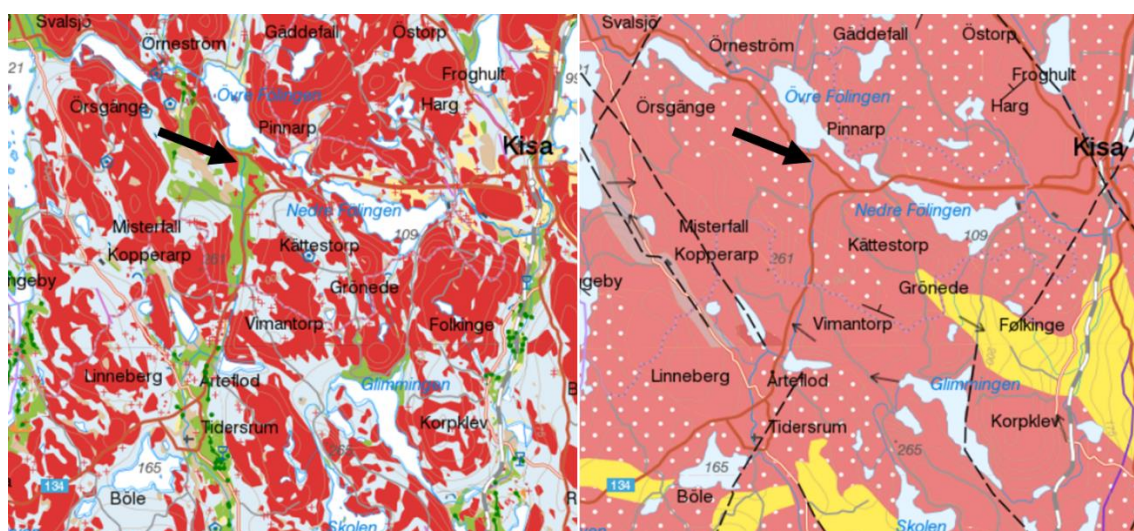


Figure 4. The soil coverage in the Kinda area (left) is a mosaic pattern of: till (blue), sand and gravel deposits (green), and clay (yellow), but soil layers are thin and the area is dominated by uncovered bedrock (red). The underlying bedrock (right) is dominated by granite (pink) and rhyolite (yellow).

3.2 Site description and data for pilot Böda

The Böda pilot is located on the island of Öland in the Baltic Sea, about 10 km east of the mainland of south-eastern Sweden (Figure 2). The climate is of Baltic-island Central and Eastern European type. The island extends c. 140 km in the north-south and 15 km in the east-western direction. The catchment area (coast to coast) is 26 km² and is characterised by a very flat topography, ranging from zero to about 20 meters above sea level, and a few small creeks. The pilot area is mainly covered by forest, with visible drainage trenches (Figure 5, left), but also some areas are also agricultural (Figure 5, right).



The soil coverage in the area is up to 10 m and is dominated by sand and gravel deposits (Figure 6, left), including a few isolated patches of till. The underlying bedrock is Ordovician limestone (Figure 6, right), and has been investigated with a large-scale geophysical airborne survey (SKY-TEM; Dahlqvist et al., 2018). As such, the constraining factor for recharge at Böda is quite different from that of Kinda; the recharge at Böda is not limited by the storage capacity of soil (as is the case for Kinda; Figure 7), but instead by its significantly lower precipitation (i.e., $PET > P$).

The precipitation is approximately 500 mm/year and the potential evapotranspiration is c. 600 mm/year. The groundwater recharge is approximately 150 mm/year (Rodhe et al., 2006; Figure 7). Precipitation is low during summer resulting in negligible recharge during the vegetation period. Moreover, the water balance is stressed during summer by the water consumption from tourism, which peaks during the dry period. Precipitation and temperature data are available on daily basis since 1961-01-01 (provided via the Swedish Meteorological and Hydrological Institute, SMHI's PTHBV-raster at a resolution of 4 km). Forcing data for modelling can be downloaded from SMHI's webpage (<https://www.smhi.se/data/meteorologi/>). Potential evapotranspiration, PET, is calculated from temperature, based on an empirical relationship established by Rodhe et al. (2006).

The groundwater level in the area is monitored in two active wells located in sand and gravel deposits (there are 14 more groundwater wells with data from 1968 to 1980). In this study, groundwater well 7_9 was used for modelling historic and future change in groundwater recharge. This particular well is located in a 10 m thick sand deposit, which is classified as a *major* groundwater resource (Figure 1). The groundwater level has been measured manually twice a month from 1968-05-28, and daily since the installation of an automatic logger system in 2016-04-26. The groundwater time series can be downloaded from SGU's web page (<https://www.sgu.se/grundvatten/grundvattennivaer/matstationer/>).

There are no streamflow data available for the pilot area.

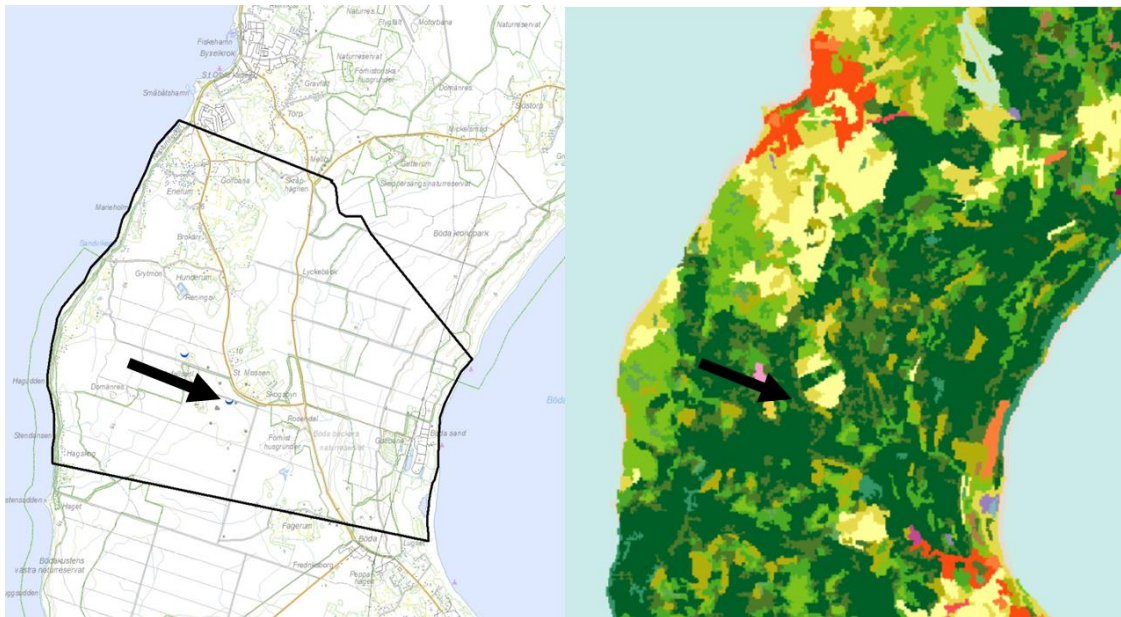


Figure 5. Catchment of the Boda pilot area, c. 6 km wide coast to coast (left), and land use (right), mainly forest (dark green), but also agricultural (yellow). Arrow marks the location of well 7_9.

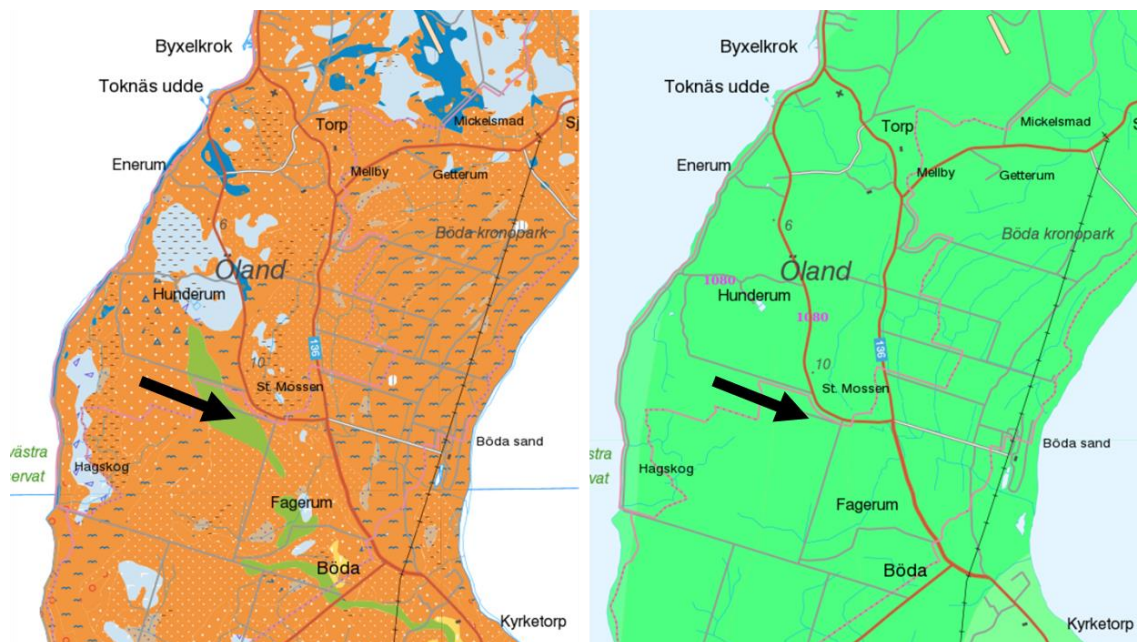


Figure 6. The dominant soil type in the Boda area (left) is sand (orange) with streaks of glacial sand- and gravel deposits (green), and patches of till (light blue). The underlying bedrock (right) is Ordovician limestone (green). Arrow marks the location of well 7_9.

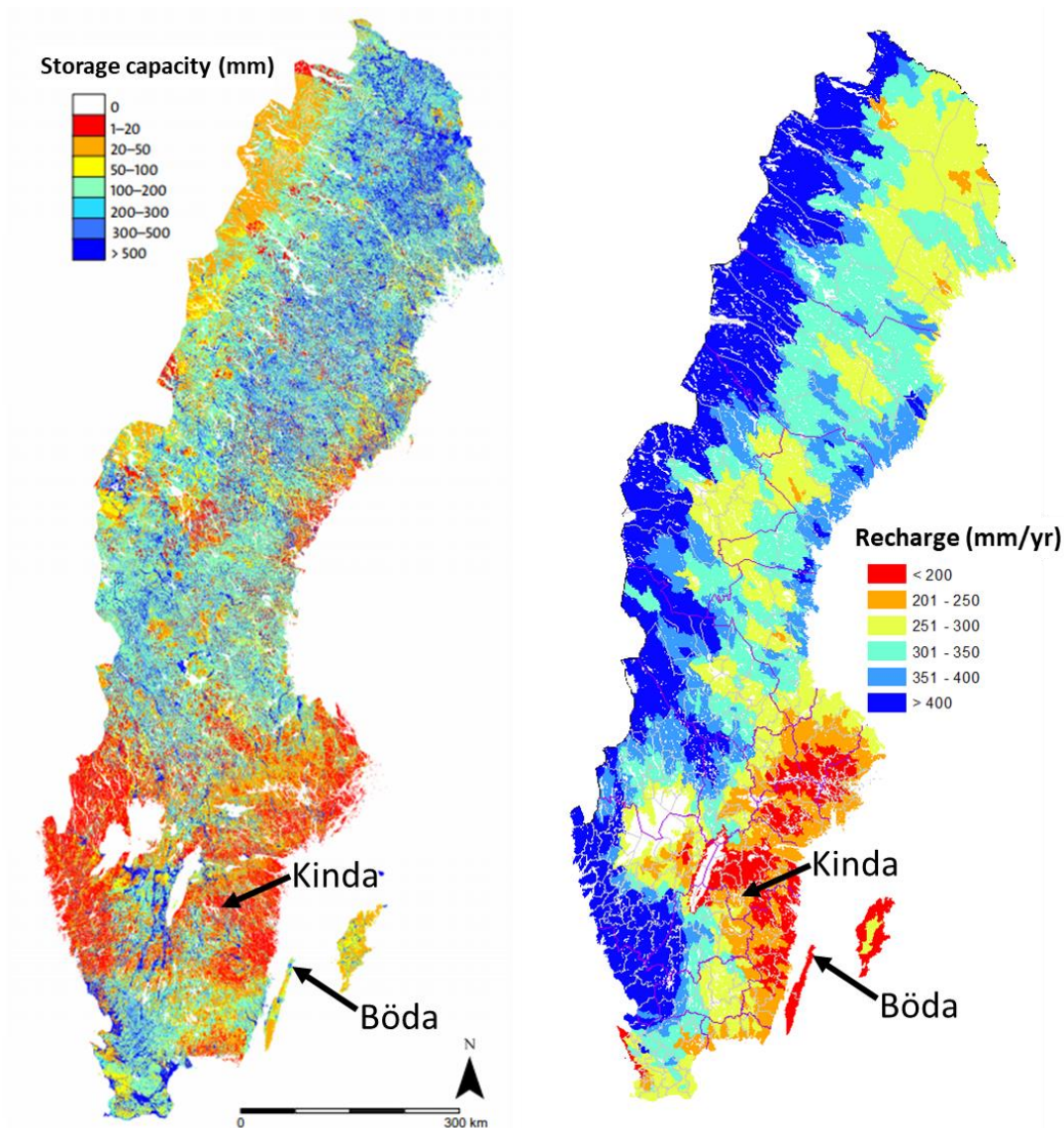


Figure 7. National maps of storage capacity (left) and recharge (right) available for Sweden. The glacialfluvial deposits at Böda has high storage capacity (c. 400 mm) compared to the thin soil cover at Kinda (c. 20 – 100 mm).

3.3 Climate change challenge

The expected consequences that climate change (CC) has on society depends, among other factors, on geographical location. The geographical diversity in expected CC challenges is illustrated in a generalised map over EU (Figure 8). The two Swedish pilot areas fall into different regions, indicating that somewhat different CC challenges are to be expected in future; Kinda belongs to the Northern-Europe region, while Böda belongs to the Central and eastern Europe region (Figure 8).



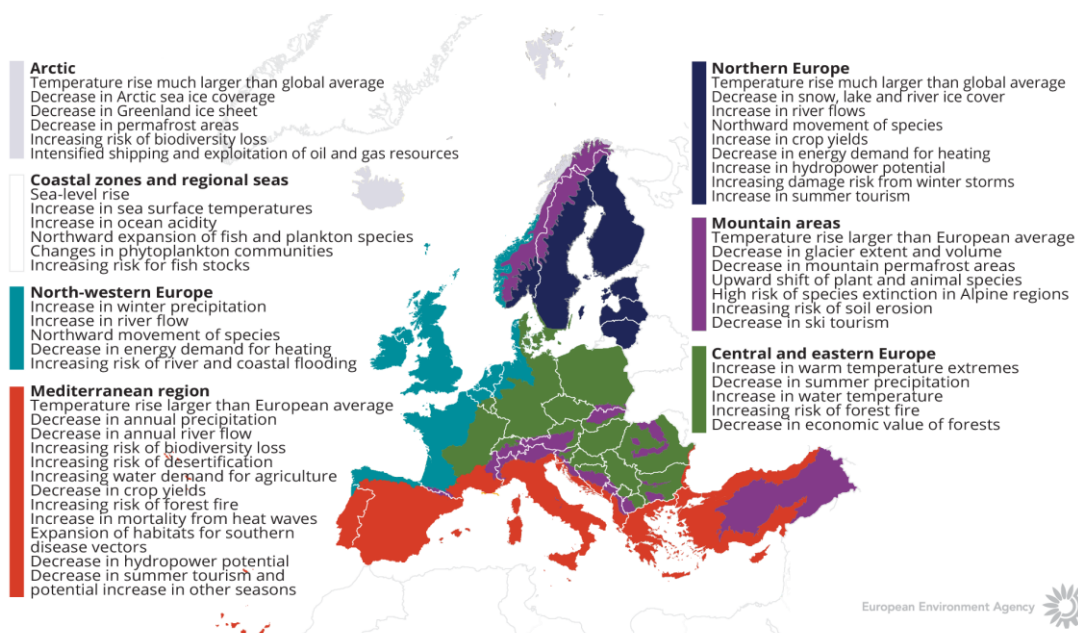


Figure 8. General expected climate challenges in different EU-regions.

As such, the main future CC changes, relevant to drinking-water supply, are:

- **Warmer winters:** precipitation falling as rain (less snow storage, causing less groundwater recharge during spring, and in turn less significance of maximum infiltration rate during snowmelt)
- **Longer summer period** (or vegetation period, during which recharge is negligible): longer drought, or at least longer groundwater recession period, with additional stress on storage capacity to last longer period.
- **Less summer precipitation:** may increase the need of irrigation, additionally stressing storage capacity during summer
- **Increased tourism:** increased water consumption, additionally stressing storage capacity during summer

In particular for Böda, groundwater resources are already under strain during the summer, due to limited recharge and storage capacity combined with peaking consumption (tourism). Expected consequences are longer periods of shortage in water supply, resulting in salt-water intrusion into drinking-water wells from the Baltic Sea.

The recharge for pilot areas Böda and Kinda is expected to follow the typical pattern for south-eastern Sweden. In effect, the recharge is expected to decline c. -10% to -15% at Böda and Kinda, respectively (Figure 9), which might cause shortage of drinking water and saltwater intrusion (i.e., at least for borehole wells).

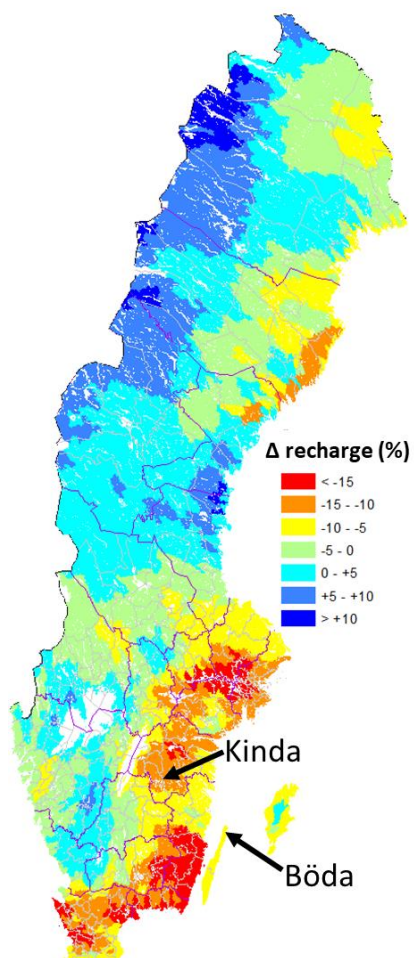


Figure 9. Existing modelling indicates decreasing groundwater recharge at Kinda and Böda, ranging from -5% to -15% (scenario SRES A1b, corresponding to RCP4.5; modified from Rodhe et al., 2009).

4 METHODOLOGY

Climate change impacts on recharge is assessed for the two Swedish pilot areas, based on the TACTIC standard climate change scenarios and two lumped models: HYPE and AQUIMOD. The transfer noise model, METRAN, is also calibrated to measured groundwater data for the two pilots.

4.1 Methodology and climate data

4.1.1 HYPE

In essence, the Hydrological Predictions for the Environment model (HYPE) originates from the lumped-model concept, describing precipitation and runoff at catchment scale, e.g., the classical HBV model (Bergström et al., 1976). However, one of the many strengths of HYPE is its wide flexibility in setup, offering complex semi-distributed setups; for example, national-scale simulation of surface water flow and nutrient fluxes, from precipitation and via various storage compartments on its way towards the sea (Lindström et al., 2010). The model code is open source and offers a range of descriptions to hydrological processes in interconnected sub-basins. An implication of the lumped concept is that its algorithms are not strictly based on physical laws but are instead formulated on a more conceptual basis. The model can be set up in a multi-basin manner to simulate flow paths in the landscape at a high spatial resolution. Moreover, the model can be calibrated or evaluated against various types of measurements, e.g., river flow or groundwater levels. The model was initiated in 2003, applied on national scale for Sweden in 2008, and finally for the entire globe (e.g., Arheimer et al., 2019).

This study employs HYPE in its most basic setup (details at: <http://www.smhi.net/hype/wiki/>), namely groundwater level modelling as a standalone point-observation. In terms of modelled groundwater levels, the Böda model is representative of the glaciofluvial deposits in the area, whereas the Kinda model representativeness is limited to the immediate surroundings of the observation well. The modelled CC effects, on the other hand, are assumed to be representative of Major and Minor groundwater resources at wider geographical area (as expressed in relative terms of change). The model uses precipitation, P mm/day, and temperature, T °C, as forcing data and is run at a daily time step. Potential evapotranspiration, PET mm/day, is not treated as forcing data (i.e., not used as model input), but is instead calculated from temperature and season (based on a set of pre-determined model parameters that have been calibrated on national scale for the water balance for > 100 large catchments).

The many model options offered combined with the open-source code, leads to branching of purpose-specific HYPE versions; the version in this study was developed by SGU to address specific processes relevant to groundwater modelling (such as delayed percolation, capillary rise, and recharge calculation). Like most precipitation-runoff models the soil horizon in HYPE is typically divided into three conceptual soil boxes holding and exchanging soil water. Depending on seasonal variation in water content, the groundwater table is allowed to vary freely between these three boxes (however, underlying soil boxes must be fully saturated). Recharge is calculated as percolation (mm/day) reaching the soil box that currently holds the groundwater table (i.e., percolating soil water that adds to the groundwater table).



Two main differences against Aquimod can be noted: 1) HYPE allows snow-cover storage during wintertime and 2) HYPE allows the groundwater level to reach ground surface (i.e., does not assume an unsaturated zone, for example during snow melt). HYPE offers a range of calibration methods and performance measures; in this study we calibrated the model to observed groundwater data in a Monte Carlo approach to maximise the Nash Sutcliffe Efficiency (NSE) performance measure.

4.1.2 *AquiMod*

AquiMod is a lumped parameter computer model that has been developed to simulate groundwater level time series at observational boreholes (Mackay et al., 2014a). It is based on hydrological algorithms that simulate the movement of groundwater within the soil zone, the unsaturated zone, and the saturated zone. The lumped models neglect complexities included in distributed groundwater models but maintain some of the fundamental physical principles that can be related to the conceptual understanding of the groundwater system (Mackay et al., 2014b).

The primary aim of AquiMod is to capture the behaviour of a groundwater system through the analysis of the available groundwater level time series. Once calibrated the model can be run in predictive mode and be used to fill in gaps in historical groundwater level time series and to calculate future groundwater levels. In addition to groundwater levels, it also provides predictions of historical and future recharge values and groundwater discharges.

The mathematical equations that are used to simulate the movement of groundwater flows within the three modules are detailed in Appendix A. The model uses rainfall, P mm/day, and potential evapotranspiration, PET mm/day, as forcing data. In this study, PET was precalculated based on the empirical relationship defined for HYPE. These are interpreted by the soil module representing the soil zone. The soil module calculates the rainfall infiltration and pass it to the unsaturated zone module. This module delays the arrival of the infiltrating water to the saturated zone module. The latter calculates the variations of groundwater heads and flows accordingly.

The model is calibrated using a Monte Carlo approach. It compares the simulated and observed groundwater level fluctuations and calculates a goodness of fit. The AquiMod version used in this work employs the Root Square Mean Error (RMSE) or the Nash Sutcliffe (NSE) performance measures to assess the performance of the model. The user sets a threshold value to accept all the models that perform better than the specified threshold. The possibility of producing many models that are all equally acceptable, allows the user to interpret the results from all these models and calculate uncertainty.

The recharge values calculated from AquiMod are those that reach the aquifer system and drive the groundwater levels.



4.1.3 Metran

Metran applies a transfer function-noise model to simulate the fluctuation of groundwater heads with precipitation and evaporation as independent variables (Zaadnoordijk et al., 2019). The modelling approach consists mainly of two impulse functions and a noise model. The first impulse function is used for convolution with the precipitation to yield the precipitation contribution to the piezometric head. The second is for evaporation which is either a separately estimated function, or a factor times the function used for precipitation. The noise model is a stochastic noise process described by a first-order autoregressive model with one parameter and zero mean white noise. Further information about the model is given in Appendix B with the model setup shown in the Figure B1.

Metran allows the addition of other processes affecting the behaviour of the groundwater heads, for example pumping or the presence of surface features such as rivers. The contributions from these processes are added to the deterministic part of the model.

Metran has been designed to work with explanatory series that have a daily time step. However, it has been adapted so that other time step lengths can be applied. However, the explanatory variables must still have a constant frequency.

The model is calibrated automatically; however, the model uses two binary parameters, Regimeok and Modok, to judge a resulting time series model. Regimeok cross-examines the explained variance R^2 (> 0.3), the absolute correlation between deterministic component and residuals (< 0.2), and the null hypothesis of non-correlated innovations (p value > 0.01). If all these criteria are satisfied, Regimeok returns a value of 1 indicating highest quality. Modok also cross-examines the explained variance R^2 (> 0.1) and the absolute correlation between deterministic component and residuals (< 0.3) as well as the decay rate parameter (> 0.002) and if all these criteria are satisfied, it is given a value of 1. If Modok = 1 and Regimeok = 0, the model is still considered acceptable. If both these parameters are 0, the model quality is insufficient, and the model is rejected.

Metran's time series model is linear and the model creation fails when the system is strongly nonlinear. It is also limited to the response function being appropriate for the simulated groundwater system. Metran uses a gradient search method in the parameter space, so it can be sensitive to initial parameter values in finding an optimal solution.

The model calculates an evaporation factor f that gives the importance of evapotranspiration compared to precipitation. It is possible to use this factor to calculate the recharge values as shown by Equation B2 in appendix B. However, it must be noted that the use of Equation B2 is based on too many assumptions that are easily violated. Because of this, the equations should be applied only to long-term averages using only models of the highest quality.

Following the definitions used in the TACTIC project, this recharge quantity corresponds to the effective precipitation. It is equal to the potential recharge when the surface runoff is negligible. This in turn is equal to the actual recharge at the groundwater table if there is also no storage change or interflow.

4.1.4 Climate data

The TACTIC standard scenarios are developed based on the ISIMIP (Inter Sectoral Impact Model Intercomparison Project, see www.isimip.org) datasets. The resolution of the data is 0.5°x0.5°C global grid and at daily time steps. As part of ISIMIP, much effort has been made to standardise the climate data (e.g. bias correction). Data selection and preparation included the following steps:

1. Fifteen combinations of RCPs and GCMs from the ISIMIP data set were selected. RCPs are the Representative Concentration Pathways determining the development in greenhouse gas concentrations, while GCMs are the Global Circulation Models used to simulate the future climate at the global scale. Three RCPs (RCP4.5, RCP6.0, RCP8.5) were combined with five GCMs (noresm1-m, miroc-esm-chem, ipsl-cm5a-lr, hadgem2-es, gfdl-esm2m).
2. A reference period was selected between 1981 – 2010 and an annual mean temperature was calculated for the reference period.
3. For each combination of RCP-GCM, 30-years moving average of the annual mean temperature were calculated and two time slices identified in which the global annual mean temperature had increased by +1 and +3 degree compared to the reference period, respectively. Hence, the selection of the future periods was made to honour a specific temperature increase instead of using a fixed time-slice. This means that the temperature changes are the same for all scenarios, while the period in which this occur varies between the scenarios.
4. To represent conditions of low/high precipitation (referred to as Dry and Wet), the RCP-GCM combinations with the second lowest and second highest precipitation were selected among the 15 combinations for the +1 and +3 degree scenario. This selection was made on a pilot-by-pilot basis to accommodate that the different scenarios have different impact on the various parts of Europe (Table 3). The scenarios showing the lowest/highest precipitation were avoided, as these endmembers often reflects outliers.
5. Delta change values were calculated on a monthly basis for the four selected scenarios, based on the climate data from the reference period and the selected future period. The delta change values express the changes between the current and future climates, either as a relative factor ($\times\Delta P$ and $\times\Delta PET$) or by an additive factor ($+\Delta T$).
6. Delta change factors were applied to local climate data by which the local particularities are reflected also for future conditions.

Table 3. RCP-GCM combinations to assess future climate in the Kinda and Böda pilot areas

Scenario		RCP	GCM
+1 °C	“Dry”	noresm1-m	rcp4p5
	“Wet”	gfdl-esm2m	rcp4p5
+3 °C	“Dry”	hadgem2-es	rcp6p0
	“Wet”	miroc-esm-chem	rcp8p5

The “Dry” and “Wet” cases are selected to cover the likely span of precipitation on annual basis; thus, no consideration is taken to if the precipitation falls under typical recharge seasons, or



not). In fact, the largest differences between the Wet and Dry cases occur during summer months (Figure 10), a period during which most precipitation is lost as evapotranspiration without contribution to groundwater recharge. This implies that precipitation range spanned by Dry and Wet cases, *defined on annual basis*, does not necessarily cover the full uncertainty range for recharge. In particular, it can be noted that the precipitation in the “+1 °C Wet” scenario falls below its current value (i.e., $\times\Delta P < 1$) during three “typical recharge months”: March, September and October (Table 4). Note also that, for individual months, the relation between Dry and Wet cases may in fact be reversed; for example, the October precipitation in the “+1 °C, Dry” case exceeds the “Wet” case by some +15%. Note also that the “Dry” cases have only 3% lower precipitation, while the “Wet” cases have 9% and 21% higher precipitation for the +1°C and +3°C cases, respectively.

The provided correction factor for PET was not used in modelling of the Swedish pilots. The reason for this is that the temperature increase in CC scenarios (+ ΔT) reduces the number of days below freezing in wintertime (i.e., when $PET = 0$), which is not well-represented by a multiplication factor for PET. Instead, PET was re-calculated based on the future temperature (+ ΔT) and the established empirical Swedish relationship between T and PET . This way, increasing evaporation wintertime, during periods which are currently below freezing, could be accounted for (Figure 10). Moreover, the cases +1 °C Wet and +3 °C Wet have average temperature increases of 2.5°C and 3.4°C during winter, which is expected to have a drastic impact on the groundwater regime (snowmelt-induced recharge).

Table 4. Temperature and precipitation* correction factors in CC scenarios for Kinda and Böda

scenario	Temperature additive factor + ΔT				Precipitation multiplication factor $\times\Delta P$			
	+1 °C		+3 °C		+1 °C		+3 °C	
	Dry	Wet	Dry	Wet	Dry	Wet	Dry	Wet
Jan	0.56	3.44	2.38	3.35	1	1.18	1.25	1.31
Feb	1.01	2.13	2.02	3.77	1	1.07	0.98	1.33
Mar	1.41	1.6	2.01	3.09	0.87	0.92	1.03	1.04
Apr	1.5	1.39	2.94	3.38	0.98	1.15	0.99	0.92
May	1.53	1.29	3.14	3.2	0.98	1.14	0.7	1
Jun	1.06	0.97	3.35	3.24	0.98	1.1	0.79	1.08
Jul	1.77	1.06	2.73	3	0.87	1.12	0.96	1.45
Aug	1.11	1.28	2.86	3.07	0.81	1.18	0.75	1.33
Sep	1.2	1.12	2.79	2.97	1.01	0.98	0.86	1.27
Oct	0.54	1.42	3.07	2.37	1.14	0.99	0.98	1.3
Nov	0.6	1.73	1.73	3.2	1.02	1.08	1.2	1.25
Dec	1.17	1.99	2.75	3.03	0.99	1.11	1.17	1.22

* Precipitation change pronounced by colouring: blue indicates lower than the current situation and red indicates future increase.

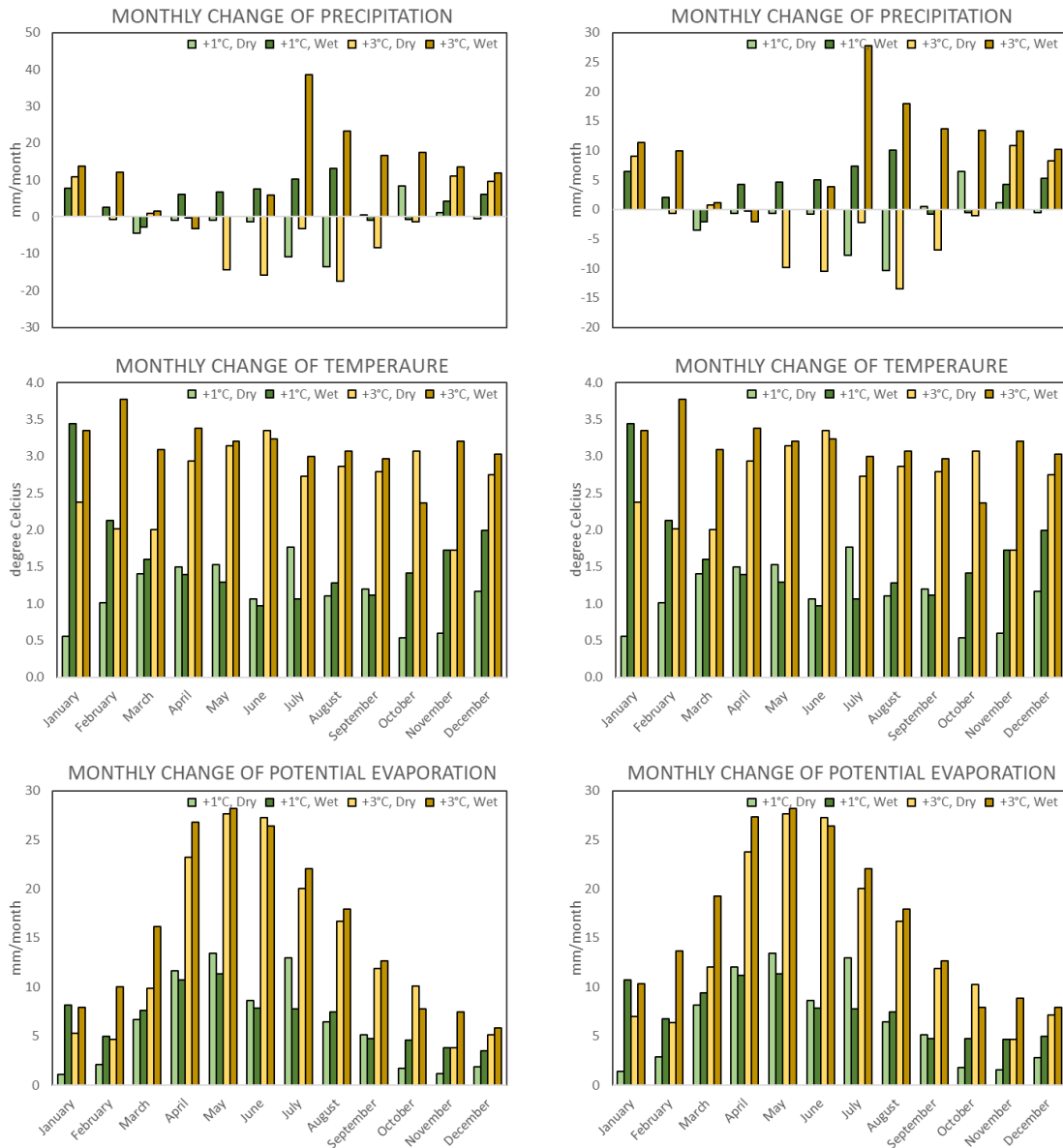


Figure 10. Climate effect on forcing data for TACTIC standard scenarios. Kinda (left) and Böda (right). Note that monthly change in PET does not reflect the provided multiplication factor ($\times \Delta \text{PET}$), but re-calculated values using the established empirical relationship for $(T + \Delta T)$. Note that, although the CC effects on P and PET differ somewhat between the pilots, the change in T is identical.

4.2 Model set-up

The three models HYPE, Aquimod, and Metran were setup as independent point models for the wells 66_5, at Kinda, and 7_9, at Böda (i.e., without claiming to represent the entire pilot area). The Metran modelling was undertaken by the Dutch TACTIC partner TNO, and hence not described here.

HYPE and Aquimod were calibrated in a Monte-Carlo approach to find the best set of parameters that can reproduce groundwater observations based on local time series of forcing data at a daily time step (i.e., precipitation, temperature, and/or potential evapotranspiration). Due to the lack of streamflow data for the two pilots, the model calibration is constrained by groundwater-level data, alone. This implies that water balance at catchment scale is neglected, and in turn, that the magnitude in simulated recharge is unconstrained. However, this difficulty is partly circumvented by relying on an established empirical relationship for calculating PET based on T (determined by Rodhe et al., 2006). The authors established this relationship in a national-scale calibration, involving the water balance for a large number of catchments (several hundreds). Thus, the use of the empirical relationship is assumed to compensate the lack of site-specific constraining streamflow data and to provide realistic magnitudes of recharge.

HYPE allows several inbuilt model options for the calculation of PET, of which one possibility is the aforementioned empirical PET relationship. Both Aquimod and Metran use PET as forcing data (PET is not available as measured observations); thus, to enhance consistent input data between the models, PET for Aquimod and Metran was calculated as daily forcing data using the same empirical relationship as used in HYPE (Rodhe et al., 2006).

4.2.1 Observation data

The forcing data (precipitation and potential evapotranspiration) and calibration targets (groundwater levels) are presented in Figure 11 and Figure 12, for Kinda and Böda, respectively.

The models were run from the starting point of forcing data, 1961-01-01 (i.e., allowing 20 years of warm up period). The calibration applied the full period of available groundwater data, 1975-2018 and 1968-2018, respectively (Sections 3.1 and 3.2); however, for consistency in the TACTIC project, model performance is presented only for the period 1980 – 2010 (e.g., Table 5). To avoid calibration bias to periods of high data measurement frequency (i.e., overwhelming amounts of conditional data during the period of logger recording), the excessive data during the logger-measuring period was reduced for application in Aquimod (to compensate for inbuilt feature in HYPE).

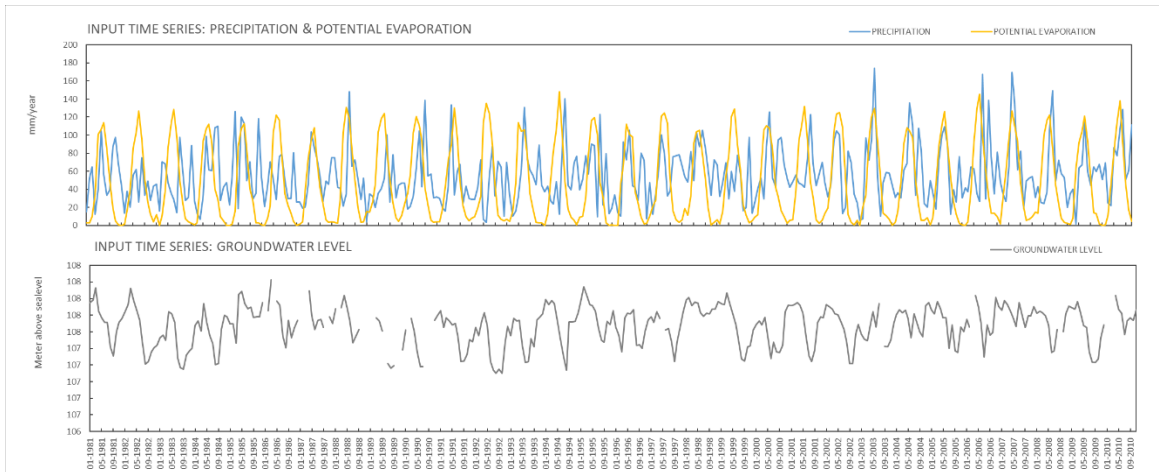


Figure 11. Daily time series of forcing data, P and PET (mm/year), as well as the calibration target groundwater table fluctuation at Kinda (time period 1980 to 2010).

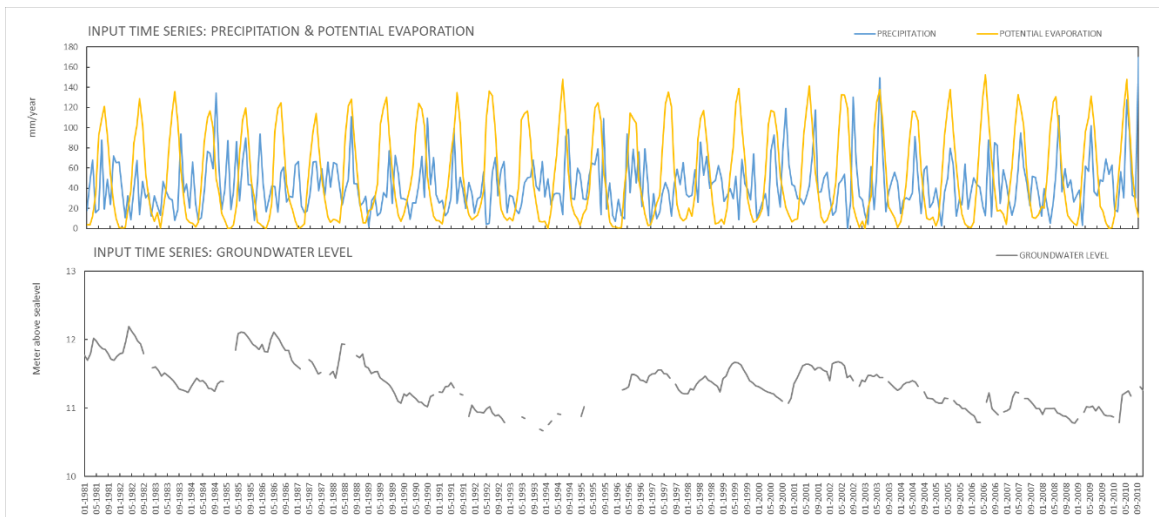


Figure 12. Daily time series of forcing data, P and PET (mm/year), as well as the calibration target groundwater table fluctuation at Böda (time period 1980 to 2010).

For both pilots, the key recharge periods occur in spring and autumn, when temperature is sufficiently low to hamper evapotranspiration, but still above freezing, to allow percolation from rain or melting snow. The two recharge periods can be described as (Figure 13):

- March/April: snowmelt with low evapotranspiration (just before the vegetation period)
- September/October: falling evapotranspiration, precipitation still in form of rain (just after the vegetation period)

As described earlier, the snow-melt induced recharge at Kinda is limited by storage capacity and infiltration rate, whereas the recharge at Böda is more limited by the low net precipitation. Aquimod does not feature snow-cover storage, and hence does not reproduce the recharge peak associated to snowmelt; this is a limitation in describing recharge for Swedish conditions.



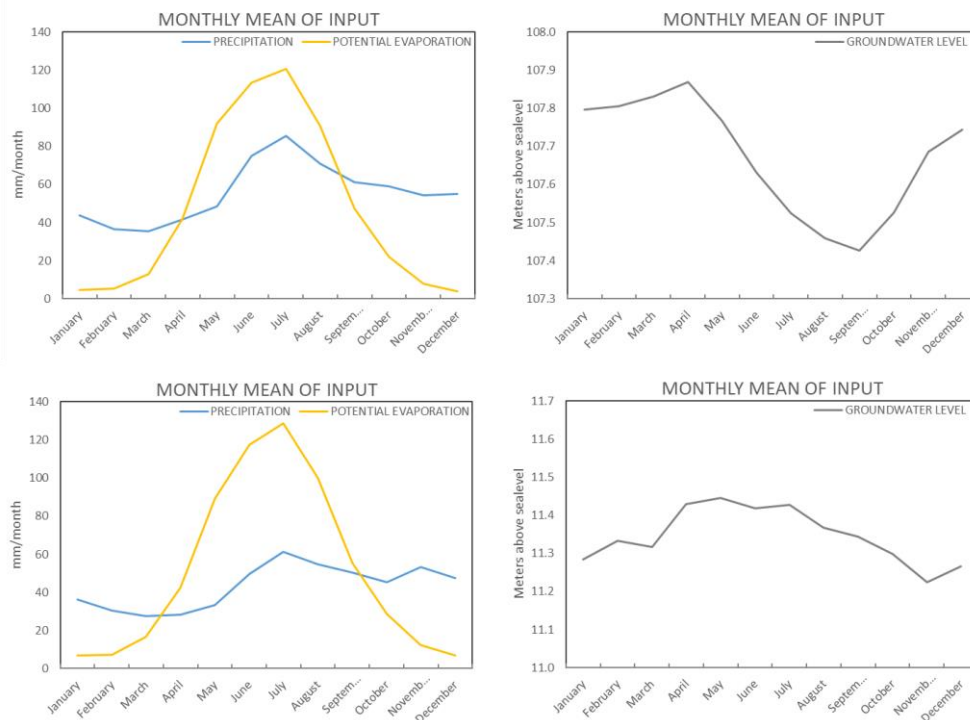


Figure 13. Seasonal patterns in forcing data, P and PET, as well as groundwater regime (time period 1980 to 2010). Kinda (above) has a strong seasonal pattern, with groundwater levels peaking at snowmelt, whereas the seasonality pattern is weak at Böda (below), whereas long-term periodicity spans over decades (Figure 12).

4.3 Model calibration

All three models are reasonably well calibrated to the groundwater data (Table 5). As the exception, Aquimod provides a notably poorer calibration for Kinda, NSE = 0.59. This poorer fit is associated to the significant role that snowmelt has for the seasonal patterns at Kinda (Figure 15, left), as the snowmelt phenomenon is not featured in Aquimod. The snowmelt peak is less pronounced at Böda, and consequently, all three models perform more or less equally well. In fact, HYPE even overestimates the recharge somewhat during the snowmelt period; however, it is unclear if this implies overestimation of the snowmelt phenomenon, or if the percolation delay is underestimated (Figure 15, right). Moreover, parts of the long-term periodicity at Böda can be captured, whereas the period 1996-2000 is poorly captured by both models (Figure 14). This period could be fitted in Metran, but at the expense of a poor fit during the 1980's. This signifies that a component of this long-term periodicity cannot be captured by our lumped model concepts or the forcing data used. For example, it may reflect some type of external disturbance, such as change in land use (clearcutting a forest, maintenance restoration of drainage trenches) or periods of groundwater abstraction.

Table 5. Model performances for the historic period 1980-2010

		Kinda			Böda		
		HYPE	Aquimod	Metran	HYPE	Aquimod	Metran
Nash Sutcliffe efficiency	NSE	0.81	0.59	0.83	0.67	0.61	0.62
Root mean square error	RMSE	0.1	0.16	0.1	0.19	0.21	0.2
Mean error	ME	0.04	0.02		0.10	0.09	

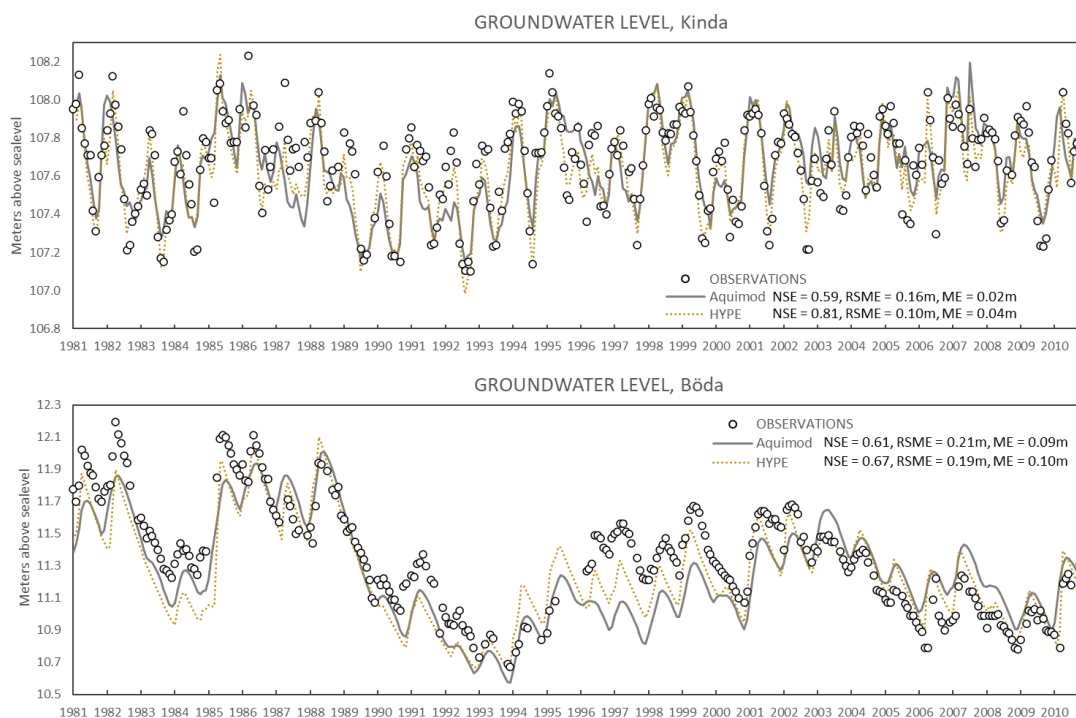


Figure 14. Model calibration for the historical time period 1980 to 2010; Kinda (upper) and Böda (lower). Aquimod (solid lines) compared to HYPE (dashed lines).

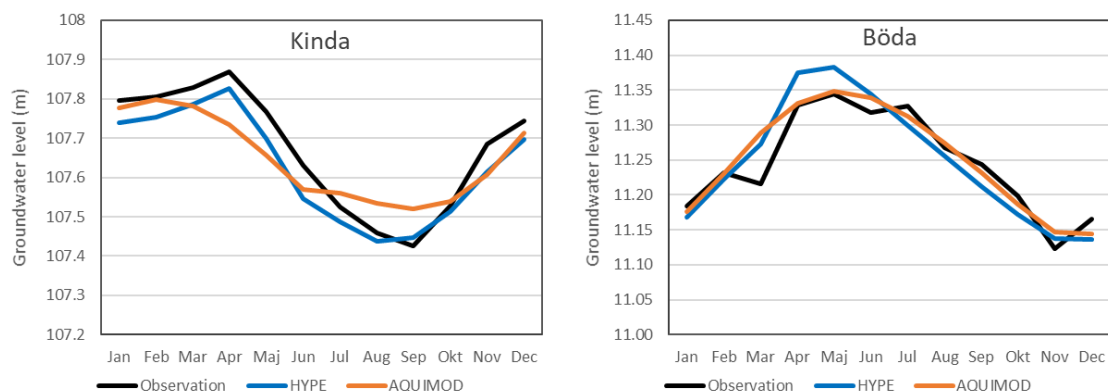


Figure 15. Simulated groundwater seasonality during historical time period, 1980 to 2010.

4.4 Uncertainty

The dominating uncertainty in the calibrated models is the lacking constraint on water balance on catchment scale (Section 4.2). At least for Böda, a substantial amount of discharge may also occur as underground groundwater flow into the Baltic sea.

A typical problem in lumped models is that of equifinality due to linearly dependent parameters. The impact of uncertainty in model parameterisation in predictive modelling can be quantified in a stochastic onset (e.g., evaluating the range of predictions arising from an ensemble of equally likely parameterisation combinations). Both HYPE and Aquimod offers the possibility to quantify the uncertainty in model parameterisation in simulations. That is: during the calibration phase, all parameterisation combinations that reproduce the calibration target (groundwater time series) sufficiently well (meet a defined by e.g., NSE-criterion), are stored to define the span of parameterisation uncertainty. In the second phase, all the members in the ensemble of equally likely parameter combinations are used in predictive simulation, to evaluate the effect that model uncertainty has in simulated results. A drawback of this stochastic approach is that it requires management of results from multiple realisations, which may complicate the sensitivity analysis of CC projections. It was therefore decided not to evaluate this model uncertainty, and instead focus on the best-fitted model in CC projections.

5 RESULTS AND CONCLUSIONS

5.1 Historical recharge

The recharge, as estimated with the three models, is compared against the established national estimates for Sweden (Figure 7, right). The HYPE results agree well with the existing estimates by Rodhe et al., 2006 (Table 6 and Figure 16); however, this agreement partly rests on circular evidence, as both values are intimately related to the established PET relationship (Rodhe et al., 2006). Bearing in mind Aquimod's lower NSE for Kinda, which has been associated to its lack of snowmelt model (Table 5), its discrepancy in simulated recharge is to be expected (Table 6). It can also be noted that the simulated recharge for Kinda (and consequently also runoff) is systematically higher in Aquimod (Figure 18). This suggests a higher percolation in Aquimod, with a lesser fraction of the PET (provided as forcing data) actually lost as ET from the root zone, compared to HYPE. Again, this highlights that the assumed water balance, associated to the empirical PET relationship, is probably more valid for HYPE, than it is for Aquimod. It is somewhat surprising that Metran provides the lowest estimate for Kinda, as the reported value refers to potential recharge (i.e., an upper estimate for actual recharge).

HYPE and Aquimod provides fairly similar recharge estimates for Böda, which are somewhat below the existing estimate, whereas Metran stands out with a significantly higher estimate. A clear difference can be observed between the simulated recharge patterns at Böda, with spiky peaks in HYPE compared to the dampened pulses in Aquimod (Figure 17).

The concern, whether this suggests an overestimation of the snowmelt phenomenon at Böda, or if its percolation delay is underestimated in HYPE was raised in Section 4.3 (Figure 15, right). It should be noted that this type of delayed percolation pulses can also be simulated with HYPE, although such a model parameterisation was not optimised in the Monte Carlo simulations. This suggests linear dependency in parameters, which may cause optimization to be trapped in local performance maxima. There are numerical schemes to escape such local optima (e.g., simulated annealing), or the optimization can simply be manually restarted with other initial settings.

In hindsight, this demonstrates the benefit of addressing model uncertainty by means of a stochastic onset in model parameterisation (Section 4.4).

Table 6. Estimated recharge (mm/year), period 1980-2010 (compared to Rodhe et al., 2006)

Kinda				Böda			
Existing estimate ²⁾	HYPE ²⁾	Aquimod ³⁾	Metran ¹⁾	Existing estimate ²⁾	HYPE ²⁾	Aquimod ³⁾	Metran ¹⁾
260	239	344	217	150	119	105	237

1) Potential recharge: Water that leaves the root zone

2) Actual recharge GWT: Water reaching the phreatic groundwater table

3) Actual recharge GWA: Water reaching a groundwater aquifer (non-phreatic)



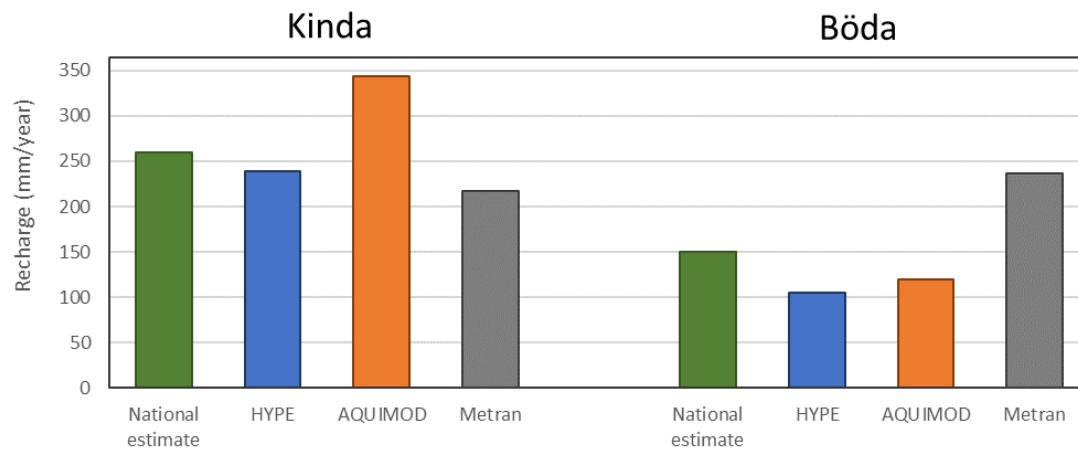


Figure 16. Simulated recharge during historical time period, 1980 to 2010, compared to existing estimates by Rodhe et al. (2006; Figure 7).

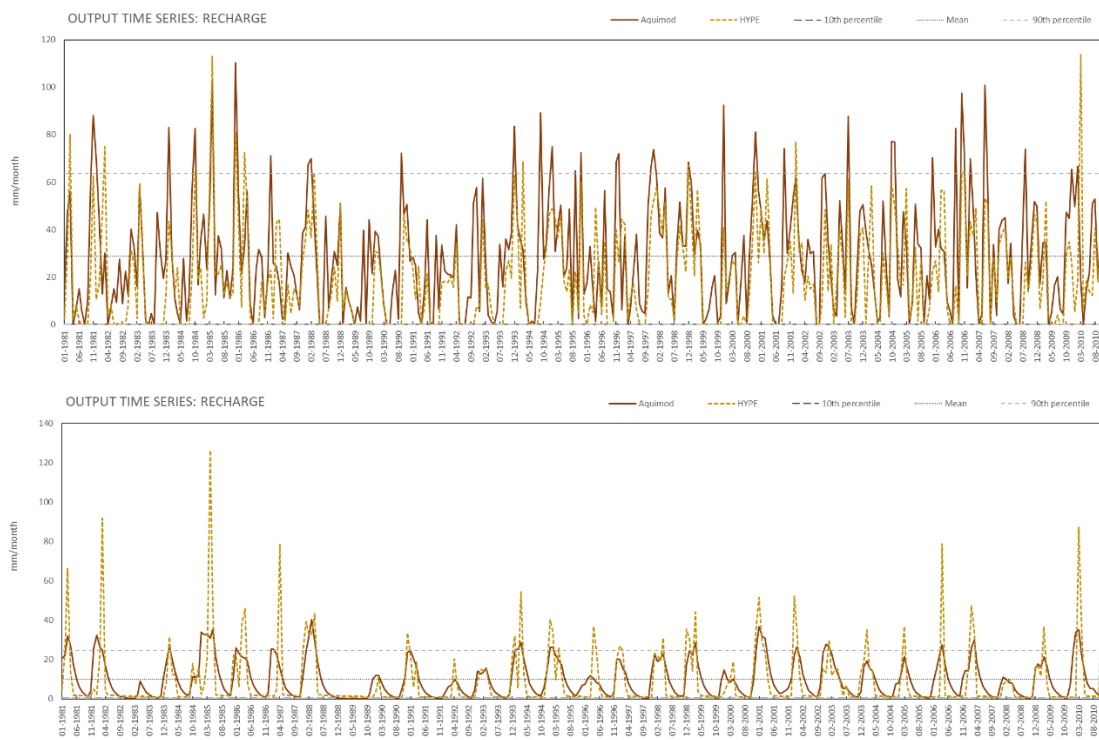


Figure 17. Simulated recharge during historical time period, 1980 to 2010, for Kinda (upper) and Böda (lower). Aquimod (solid lines) compared to HYPE (dashed lines).

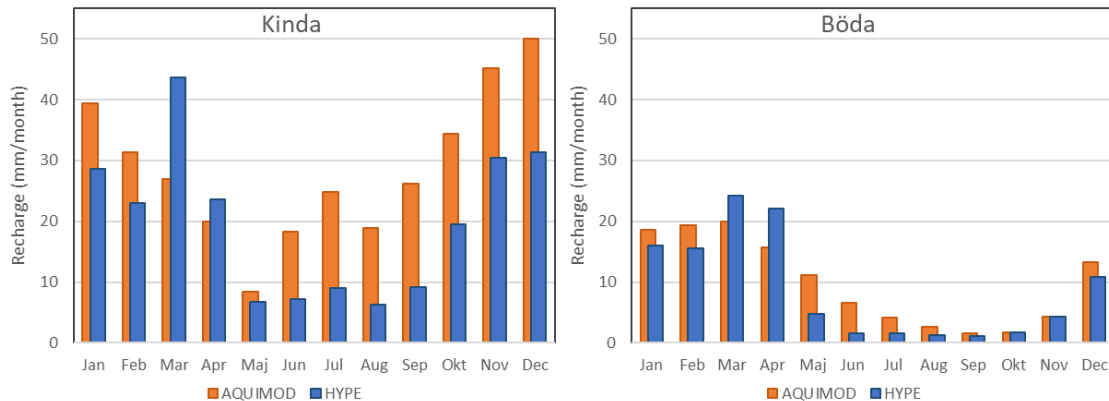


Figure 18. Seasonal patterns in simulated recharge during historical time period, 1980 to 2010.

5.2 Climate projections on recharge

The climate-change effects on groundwater regimes at Kinda and Böda are projected as a sensitivity analysis of modified forcing data (Table 4); here, the analysed cases are temperature scenarios +1°C and +3°C, combined with Dry and Wet cases (i.e., minimum/maximum precipitation, as explained in Section 4.1.4). The modelled CC projections are analysed separately for the pilots Kinda and Böda, based on the outcome of both HYPE and Aquimod.

The main climate-change effect projected for Kinda is associated to the gradual retreat of snowmelt (Figure 19). The projected outcome is in accordance with expectations (Section 3.3): mild winters imply an increasing number of winter days with temperature above freezing, which allows percolation, either from precipitation in the form of rain, or from temporarily melting snow cover. This increasing recharge during winter months occurs at the expense of less snow accumulation, and in turn less snowmelt-induced recharge in spring. In effect, mild winters shifts the seasonal pattern in recharge from a spring peak to a gradual increase wintertime.

Now, the role of snowmelt for the groundwater regime at Kinda pinpoints the need to capture the dominant system processes for obtaining realistic future projections (i.e., here: snow accumulation). In this situation, HYPE is evidently the better-suited tool. In visual comparison between the two models (Figure 19), HYPE clearly provides a more coherent outcome of the analysed cases. The impact of warmer winters on the groundwater regime (i.e., seasonal pattern) is systematic and independent of change in precipitation, ΔP (i.e., both Dry and Wet cases demonstrate the same change).

The projected change in groundwater regime, with more winter recharge (November through February) followed by less spring/summer recharge (March to June), implies an earlier onset of the drought period (period of falling groundwater levels), which – in effect – prolongs the duration of the drought period and hence resulting in deeper groundwater levels during summer/autumn. This model result is consistent both with field observations and previously modelling of altered groundwater regimes (Vikberg et al., 2015).

Albeit a bit more erratic in appearance, the Aquimod simulations do support the observations made for the HYPE climate-change projections: the projected recharge is clearly lower in the



spring/summer period (March to May), which advances the onset of the drought period to an earlier date. However, in Aquimod simulations the prolonged drought period does not automatically lead to deeper groundwater levels (i.e., within the precipitation uncertainty spanned by the Wet and Dry cases). The reason for this is that the summer recharge is notably higher in Aquimod, which can be disregarded as less realistic.

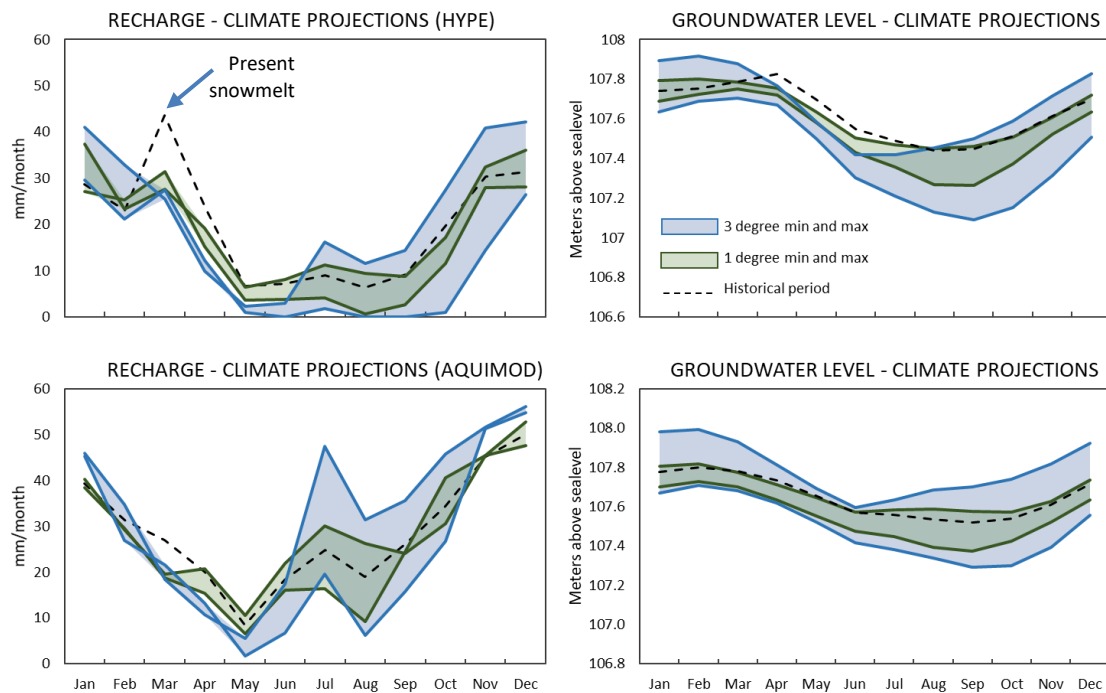


Figure 19. Climate projections on recharge and groundwater levels for Kinda, as simulated with HYPE (upper) and Aquimod (lower).

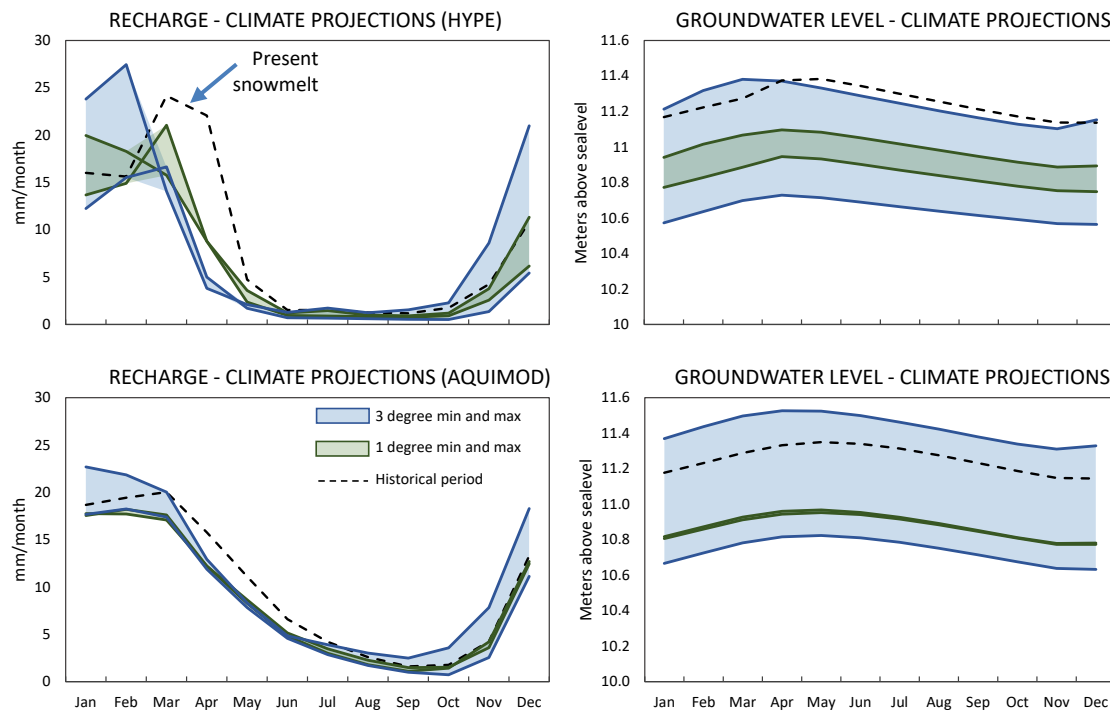


Figure 20. Climate projections on recharge and groundwater levels for Böda, as simulated with HYPE (upper) and Aquimod (lower).

The HYPE simulations provide very similar findings for Böda; also here, the retreating snowmelt is the dominant driver for future changes to the groundwater regime (Figure 20). The results again demonstrate falling spring recharge that goes hand-in-hand with boosted winter recharge, resulting in an earlier start of the drought period (virtually no recharge May to October), and the net effect of the prolonged drought is lower groundwater levels (again, more or less independent of precipitation case Dry/Wet).

Although the results of Aquimod cannot be inferred in terms of changing snowmelt, its outcome is in line with those from HYPE (Figure 20). Also the Aquimod results indicate an overall drop in recharge, particularly during spring, leading to falling groundwater levels, of similar magnitude as that modelled in HYPE. Only the +3°C Wet scenario (maximum precipitation) leads to somewhat higher projected groundwater levels.

In summary, HYPE CC projections re-produce a concerning pattern that has been observed both in trends of measured groundwater levels (Lagergren, 2015) and in earlier modelling (Vikberg et al., 2015), where the groundwater regime is shifting towards: 1) boosted winter recharge, 2) retreating snowmelt, resulting in 3) an earlier and prolonged drought period. The prolonged drought period in turn increases the stress on resources, particularly during late summer when consumption peaks due to tourism. Taken as an average of the Dry and Wet cases the reduction in recharge is estimated to be by -15% for Kinda (for both +1°C and +3°C) and -30% for Böda (Figure 21).



This study is consistent with earlier work and supports the prevailing understanding of future challenges for drinking-water supply, particularly along the south-eastern coast of Sweden (here exemplified by the Böda pilot area on Öland).

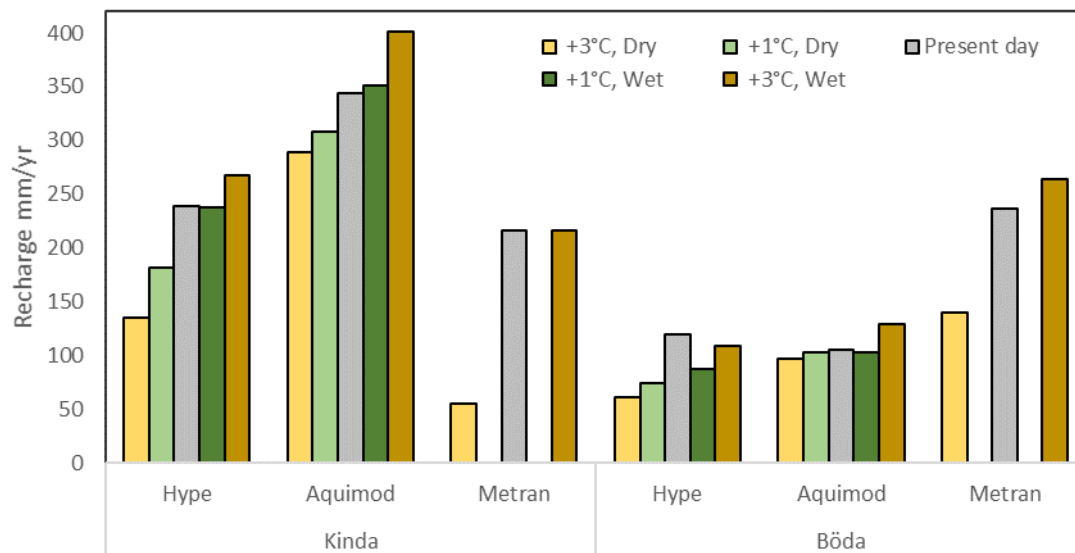


Figure 21. Climate projections on annual recharge.

6 REFERENCES

Arheimer, B., Pimentel, R., Isberg, K., Crochemore, L., Andersson, J. C. M., Hasan, A., and Pineda, L. (accepted). Global catchment modelling using World-Wide HYPE (WWH), open data and stepwise parameter estimation, Hydrol. Earth Syst. Sci, <https://doi.org/10.5194/hess-2019-111>, 2019.

Bergström, S. (1976). Development and application of a conceptual runoff model for Scandinavian catchments. SMHI, Reports RHO, No. 7, Norrköping.

Besbes, M. & de Marsily, G. (1984) From infiltration to recharge: use of a parametric transfer function. Journal of Hydrology, 74, p. 271-293.

Dahlqvist, P., Bastani, M., Triumf, C-A., Erlström, M., Gustafsson, M., Persson, L. 2018: SkyTEM-undersökningar på Öland – Geologiska tolkningar och hydrogeologisk tillämpning. SGU Rapporter och Meddelanden 145.

Lagergren H, 2015, Grundvattennivåns tidsmässiga variationer i morän och jämförelser med klimatscenarier. SGU-rapport 2015:20.

Lindström, G., Pers, C., Rosberg, J., Strömqvist, J. & Arheimer, B. (2010). Development and testing of the HYPE (Hydrological Predictions for the Environment) water quality model for different spatial scales. Hydrology Research 41.3–4, 295-319.

Mackay, J. D., Jackson, C. R., Wang, L. 2014a. A lumped conceptual model to simulate groundwater level time-series. Environmental Modelling and Software, 61. 229-245. <https://doi.org/10.1016/j.envsoft.2014.06.003>.

Mackay, J. D., Jackson, C. R., Wang, L. 2014b. Aquimod user manual (v1.0). Nottingham, UK, British Geological Survey, 34pp. (OR/14/007) (Unpublished)

Obergfell, C., Bakker, M., & Maas, K. (2019). Estimation of average diffuse aquifer recharge using time series modeling of groundwater heads. Water Resources Research, 55. <https://doi.org/10.1029/2018WR024235>

Rodhe, A., Lindström, G., Rosberg, J. & Pers, C., 2006: Grundvattenbildning i svenska typjordar – översiktlig beräkning med en vattenbalansmodell. Uppsala universitet, Institutionen för geovetenskaper, Report Series A No. 66, 20 s.

Rodhe, A., Lindström, G. & Dahné, J., 2009: Grundvattennivåer i ett förändrat klimat. Slutrapport från SGU-projektet "Grundvattenbildning i ett förändrat klimat", SGUs diarienummer 60-1642/2007. Institutionen för Geovetenskaper, Uppsala universitet och Sveriges meteorologiska och hydrologiska institut. 44s.

Vikberg, E., Thunholm, B., Thorsbrink M., Dahné J. 2015: Grundvattennivåer i ett förändrat klimat – nya klimatscenarier. SGU-rapport 2015:19



Zaadnoordijk, W.J., Bus, S.A.R., Lourens, A., Berendrecht, W.L. (2019) Automated Time Series Modeling for Piezometers in the National Database of the Netherlands. *Groundwater*, 57, no. 6, p. 834-843. <https://onlinelibrary.wiley.com/doi/epdf/10.1111/gwat.12819>

7 APPENDICES

Appendix A: AquiMod methodology

AquiMod is a lumped parameter computer model that has been developed to simulate groundwater level time series at observational boreholes (Mackay et al., 2014a). It is based on hydrological algorithms that simulates the movement of groundwater within the soil zone, the unsaturated zone, and the saturated zone. The lumped models neglect complexities included in distributed groundwater models but maintains some of the fundamental physical principles that can be related to the conceptual understanding of the groundwater system (Mackay et al., 2014b).

While AquiMod was originally designed to capture the behaviour of a groundwater system through the analysis of groundwater level time series, it can produce the infiltration recharge values and groundwater discharges from the aquifer as a by-product. AquiMod is driven by complete time series of forcing data for either historical or predicted future conditions. Running AquiMod in predictive mode can be used to fill in gaps in historical groundwater level time series, or calculate future groundwater levels. In addition to groundwater levels, it also provides predictions of historical and future recharge values and groundwater discharges. In the current application we use calibrated AquiMod models to estimate the recharge values at selected boreholes.

AquiMod consists of three modules (Figure A1). The first is a soil water balance module that calculates the amount of water that infiltrates the soil as well as the soil storage. The second module controls the movement of water in the unsaturated zone, mainly it delays the arrival of infiltrating water to the saturated zone. The third module calculates the variations in groundwater levels and discharges. The model executes the modules separately following the order listed above.

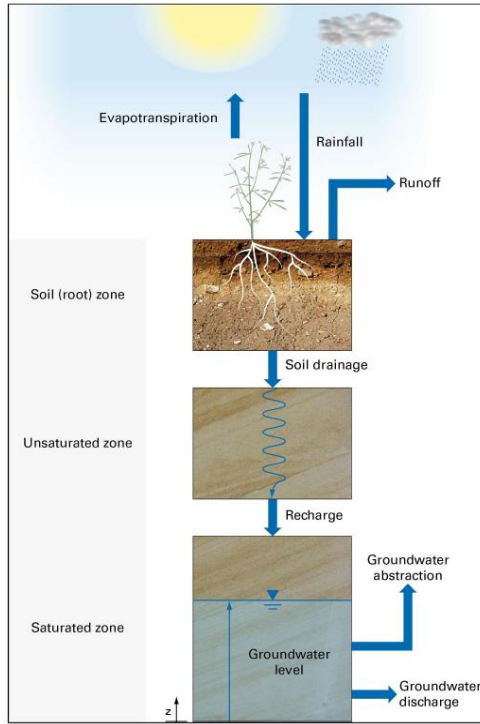


Figure A1 Generalised structure of Aquimod (after Mackay et al., 2014a)

The soil moisture module

There are several methods available in Aquimod that can be used to calculate the rainfall infiltration into the soil zone. In this study we use the FAO Drainage and Irrigation Paper 56 (FAO, 1988) approach. In this method, the capacity of the soil zone, from which plants draw water to evapotranspire, is calculated first using the plants and soil characteristics. Evapotranspiration is calculated according to the soil moisture deficit level compared to two parameters: Readily Available Water (RAW) and Total Available Water (TAW). These are a function of the root depth and the depletion factor of the plant in addition to the soil moisture content at field capacity and wilting point as shown in Equations A1 and A2.

$$TAW = Z_r(\theta_{fc} - \theta_{wp})$$

Equation A1

$$RAW = p \cdot TAW$$

Equation A2

Where Z_r [L] and p [-] are the root depth and depletion factor of a plant respectively, θ_{fc} [L³ L⁻³] and θ_{wp} [L³ L⁻³] are the moisture content at field capacity and wilting point respectively.

The FAO method is simplified by Griffiths et al. (2006) who developed a modified EA-FAO method. In this method the evapotranspiration rates are calculated as a function of the potential evaporation and an intermediate soil moisture deficit as:

$$\begin{aligned} e_s &= e_p \left[\frac{s_s^*}{TAW - RAW} \right]^{0.2} & s_s^* > RAW \\ e_s &= e_p & s_s^* \leq RAW \\ e_s &= 0 & s_s^* \geq TAW \end{aligned}$$

Equation A3

Where e_s [L] is the evapo-transpiration rate, e_p [L] is the potential evaporation rate and s_s^* [L] is the intermediate soil moisture deficit given by

$$s_s^* = s_s^{t-1} - r + e_p \quad \text{Equation A4}$$

Where r [L] is the rainfall at the current time step and s_s^{t-1} [L] is the soil moisture deficit calculated at the previous time step.

The new soil moisture deficit is then calculated from:

$$s_s = s_s^{t-1} - r + e_s \quad \text{Equation A5}$$

Griffiths et al. (2006) proposed that the recharge and overland flow are only generated when the calculated soil moisture deficit becomes zero. The remaining volume of water, the excess water, is then split into recharge and overland flow using a runoff coefficient. In Aquimod a baseflow coefficient is used to reflect the fact that a groundwater discharge is calculated rather than overland water. In this application, the baseflow coefficient is one minus the runoff coefficient.

The unsaturated zone module

The Aquimod version used in this study to simulate the movement of groundwater flow within the unsaturated zone is based on a statistical approach rather than a process-based approach. This method distributes the amount of rainfall recharge over several time steps where the soil drainage for each time step is calculated using a two-parameter Weibull probability density function. The Weibull function can represent exponentially increasing, exponentially decreasing, and positively and negatively skewed distributions. This can be used to focus the soil drainage over earlier or later time steps or to spread it over a number of time steps after the infiltration occurs. The shape of the Weibull function is controlled by two parameters, k and λ as shown in Equation A6.

$$f(t, k, \lambda) = \begin{cases} \frac{k}{\lambda} \left(\frac{t}{\lambda}\right)^{k-1} e^{-(t/\lambda)^k} & t > 0 \\ 0 & t \leq 0 \end{cases} \quad \text{Equation A6}$$

Where k and λ are two parameters the values of which are calculated during the calibration of the model and t is the time step.

The saturated zone module

Aquimod considers the saturated zone as a rectangular block of porous medium with dimensions L and B as its length and width [L] respectively. This block is divided into a number of layers, each has a defined hydraulic conductivity value, a storage coefficient value, and a discharging feature. The number of layers define the structure of the saturated module used in the study.

The mass balance equation that gives the variation of hydraulic head with time is given by:

$$SLB \frac{dh}{dt} = RLB - Q - A \quad \text{Equation A7}$$

Where:

S is the storage coefficient of the porous medium [-]

h is the groundwater head [L]

t is the time [T]

R is the infiltration recharge [L T⁻¹]

Q is the discharge out of the aquifer [L T⁻¹]



A is the abstraction rate [$L T^{-1}$]

It must be noted that in a multi-layered groundwater system as shown in Figure A2, we calculate one groundwater head (h) for the whole system. The discharges (Q) from Outlet 1, 2, etc. are calculated using the Darcy law. The total discharges can be summarised using the following equation:

$$Q = \sum_{i=1}^m \frac{T_i B}{0.5 L} \Delta h_i \quad \text{Equation A8}$$

Where:

m is the number of layers in the groundwater system [-]

T_i is the transmissivity of the layer i [$L T^{-2}$]

Δh_i is the difference between the groundwater head h and z_i , the elevation of the base of layer i

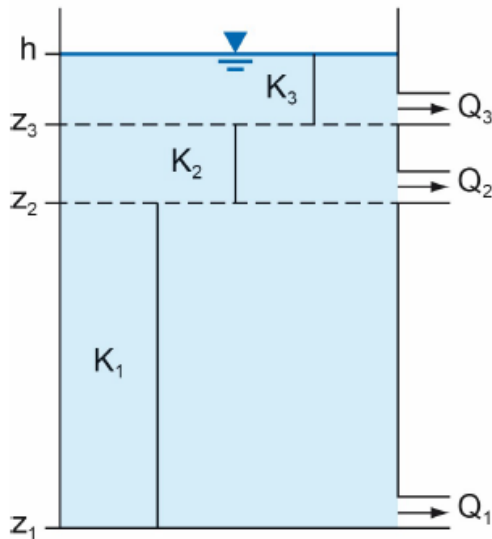


Figure A2 Representation of the saturated zone using a multi-layered groundwater system

Substituting Equation A8 into Equation A7 yields a numerical equation in the form:

$$S \frac{(h-h^*)}{\Delta t} = R - \sum_{i=1}^m \frac{T_i}{0.5 L^2} \Delta h_i - \frac{A}{LB} \quad \text{Equation A9}$$

Equation A9 is an explicit numerical equation that allows the calculation of the groundwater head h [L] at any time and using time steps of Δt [T]. In this equation h^* [L] is the groundwater head calculated at the previous time step and the term Δh_i [L] is calculated as $(h^* - z_i)$.

The terms S , T_i , and L are optimised during the calibration of the model. A groundwater system can be specified with one storage coefficient as shown in the equations above or with different storage coefficient values for the different layers. Several saturated modules are included in AquiMod to provide this flexibility and the model user can select the model structure that represent the conceptual understanding best.



Limitations of the model

AquiMod is a lumped groundwater model that aims at reproducing the behaviour of the observed groundwater levels. It tries to encapsulate the conceptual understanding of a groundwater system in a simple numerical representation. The model results have to be therefore discussed, taking this into consideration. For example, the model represents the groundwater system as a closed homogeneous medium, with no impact from any outer boundary or feature, whether physical or hydrological, such as the presence of rising and falling river stage.

Vertical heterogeneity can be accounted for by using multi-layered groundwater module structure. However, this model setting does not provide any information about the vertical connections between the layers as the discharge from all the layers is calculated using one representative groundwater head value. In other words, it is assumed that all layers are in perfect hydraulic connection.

As mentioned before, the model is designed to simulate the groundwater levels. However, it produces the recharge values and groundwater discharges as by products. In this application we use the calibrated model to calculate recharge. The mass balance equation (Equation A7) shows that recharge is a function of transmissivity and storage coefficient values, which are estimated during the calibration process of the model, i.e. they are not parameters with fixed values provided by the user. The inter-connections between these parameters leads to uncertainties in the estimated recharge values as a high storage coefficient value can produce a high recharge estimate and vice versa. To overcome this problem, it is suggested that the recharge values estimated by AquiMod are always presented as a range of possibilities rather than an absolute value. This can be achieved by estimating the recharge values from all the models that have a performance measure above than a threshold that is deemed acceptable by the user. The recharge estimates can then be presented as an average of all estimates and values corresponding to selected percentiles.

Model input and output

AquiMod includes a number of methods that calculates rainfall recharge as well as a number of model structure from which the user can select what better suits the case study.

Model input consists time series of forcing data including rainfall and potential evaporation, time series of anthropogenic impact mainly groundwater abstraction and time series of groundwater levels that will be used to calibrate the model. These time series must be complete, i.e. a value is available at every time step except the groundwater level time series, which can include missing data. The time step can be one day or multiple of days, and the model automatically calculate the size of the time step based on the input data time series.

The model is run first in calibration mode where a range of parameter values are specified for the different parameters included in the three model modules. A Monte Carlo approach is used to select the best parameter values. The performance of the model is measured by comparing the simulated groundwater levels to the observed ones using the Nash Sutcliff Efficient (NSE) or the Root Mean Squared Error (RMSE) performance measures. The parameter set that produces the best model performance is selected to run the model in evaluation mode.



When the model is run in evaluation mode, it produces output files that give recharge values, groundwater levels and groundwater discharges time series with time as specified in the input file. The number of output files is equal to the number of acceptable models set by the user.

Appendix B: Metran methodology

Metran applies transfer function noise modelling of (groundwater head) time series with usually daily precipitation and evaporation as input (Zaadnoordijk et al., 2019). The setup is shown in the Figure B1. If time series of other influences on the groundwater head are available, these contributions can be added to the deterministic part of the model. The stochastic part is the difference between the total deterministic part and the observations (the residuals). The corresponding input of the noise model should have the character of white noise.

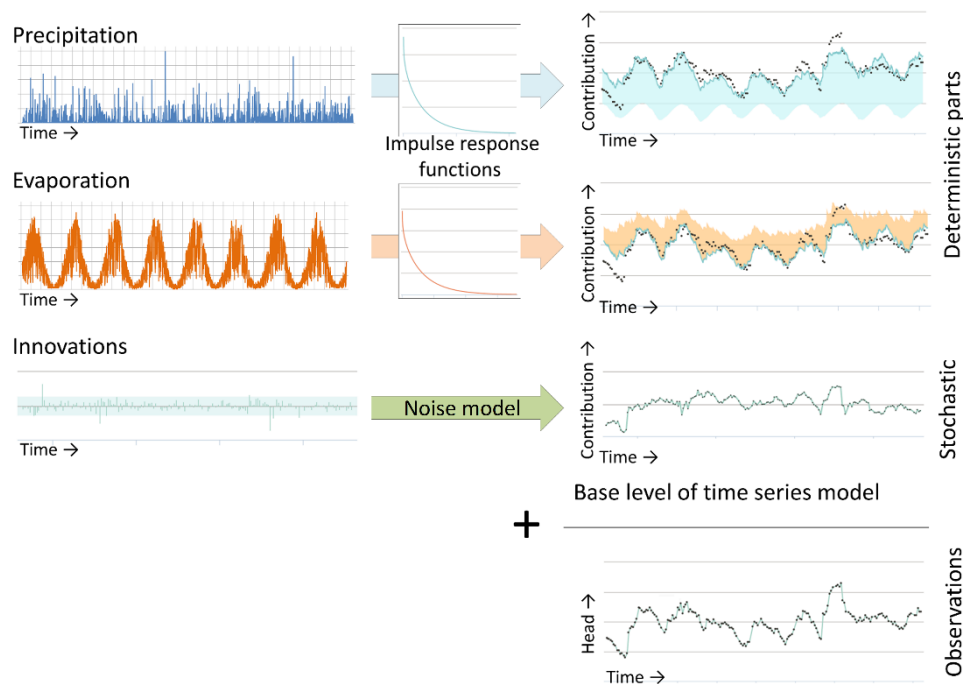


Figure B1 Illustration of METRAN setup

The stochastic part is needed because of the time correlation of the residuals, which does not allow a regular regression to obtain the parameter values of the transfer functions.

The incomplete gamma function is used as transfer function. This is a unimodal function with only three parameters that has a quite flexible shape and has some physical background (Besbes & de Marsily, 1984). The evaporation response is set equal to the precipitation response except for a factor (f_c). The noise model has one parameter that determines an exponential decay. Thus, for the standard setup with precipitation and evaporation, there are five parameters that have to be determined from the comparison with the observations. Three parameters regarding



the precipitation response, the evaporation factor, and the noise model parameter (actually, the time series model has a fifth parameter, the base level, but this is determined from the assumption that the average of the calculated heads is equal to the average of the observations). There are three extra parameters for each additional input series, such as pumping.

Limitations

Metran's time series model is linear. So, the model creation breaks down when the system is strongly nonlinear. This can occur e.g. when drainage occurs for high groundwater levels, when the ratio between the actual evapotranspiration and the inputted reference evaporation varies strongly, or when the groundwater system changed during the simulated period.

Metran is not able to find a decent time series model when the response function is not appropriate for the groundwater system. An example of this is a system with a separate fast and slow response as was found for a French piezometer in the Avre region, as is illustrated in Figure B2.

Finally, the parameter optimization of Metran uses a gradient search method in the parameter space, so it can be sensitive to initial parameter values in finding an optimal solution.

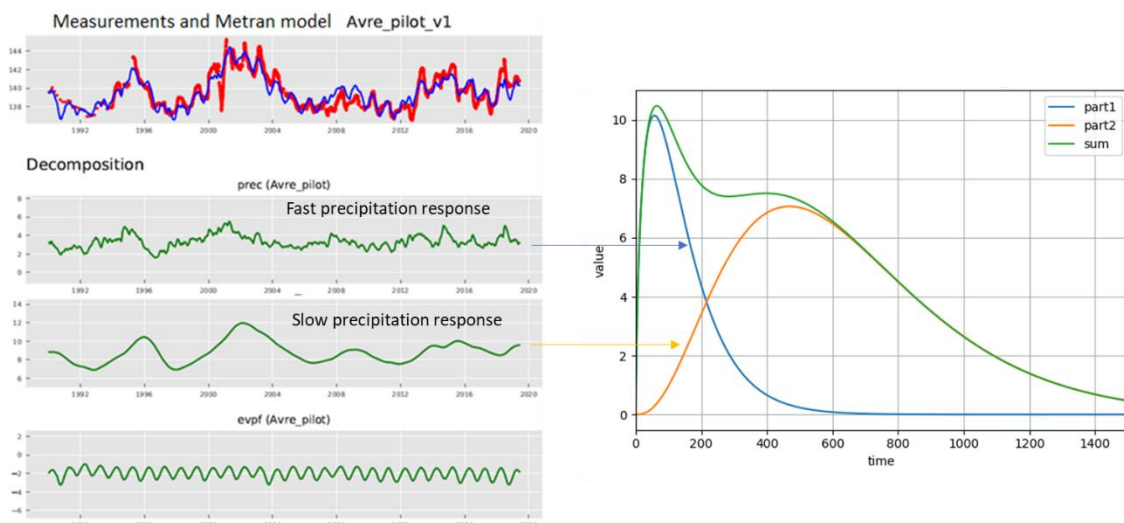


Figure B2. An example where the response function implemented in METRAN is not suitable for the groundwater system

Time step

Metran has been designed to work with explanatory series that have a daily time step. However, it has been adapted so that other time step lengths can be applied; although Metran still has the limitation that the explanatory variables have a constant frequency. For the TACTIC simulations of series with monthly or decadal meteorological input series, the time step has been set to 30 and 10 days, respectively. This time step has been applied from the end date backward. Note that the heads may be irregular in time as long as the frequency is not greater than the frequency of the explanatory series.



Model output

The evaporation factor fc gives the importance of evapotranspiration compared to precipitation. The parameter M_0 gives the total precipitation response, which is equal to the area below the impulse response function and the final value of the step response function.

The average response time is another characteristic of the precipitation response. The influence is illustrated in Figure B3 with the impulse response functions and head time series for two models with very different response times for time series of SGU in Sweden.

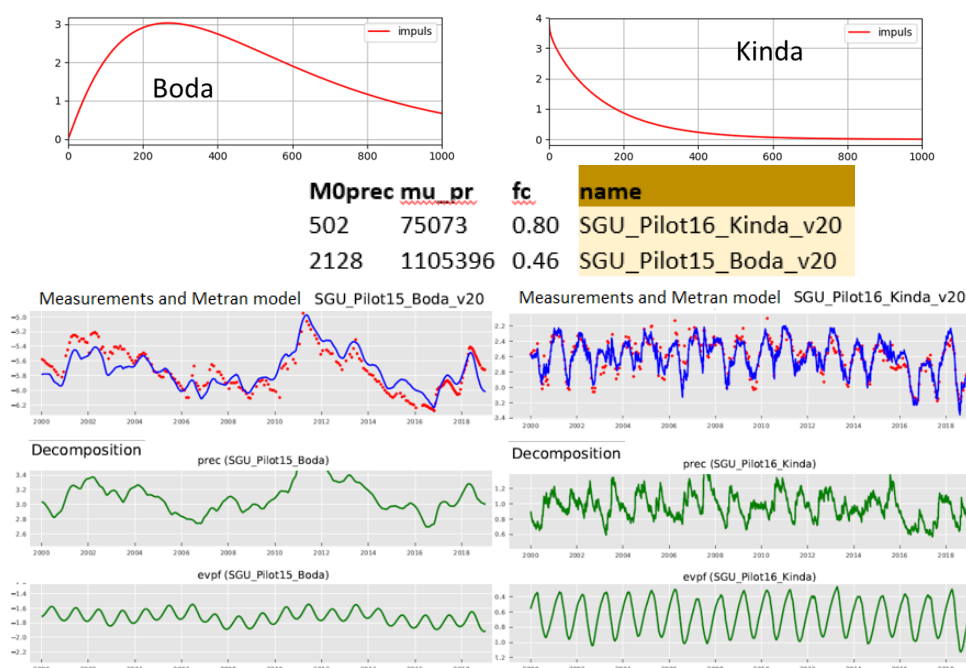


Figure B3 Illustration of Metran output for two case studies in Sweden with different response times.

Model quality

Metran judges a resulting time series model according to a number of criteria and summarizes the quality using two binary parameters Regimeok, Modok (see Zaadnoordijk et al., 2019):

- Regimeok = 1 : highest quality
- Modok = 1 (and Regimeok = 0) : ok
- Both zero = model quality insufficient

More detailed information on the model quality is given in the form of scores for two information criteria (AIC and BIC), a log likelihood, R^2 , RMSE, and the standard deviations and correlations of the parameters.



Recharge

Although the transfer-noise modelling of Metran determines statistical relations between groundwater heads and explanatory variables, we like to think of the results in physical terms. It is tempting to interpret the evaporation factor, as the factor translating the reference into the actual evapotranspiration. Then, we can calculate a recharge as

$$R = P - fE \quad \text{Equation B1}$$

where R is recharge, P precipitation, E evapotranspiration, and f the evaporation factor.

Following the definitions used in the TACTIC project, this recharge R actually is the effective precipitation. It is equal to the potential recharge when the surface runoff is negligible. This in turn is equal to the actual recharge at the groundwater table if there also is no storage change or interflow. In such cases it may be expected that this formula indeed corresponds to the meteorological forcing of the groundwater head in a piezometer, so that it gives a reasonable estimate of the recharge. Obergfell et al. (2019) showed this for an area on an ice pushed ridge in the Netherlands. However, this assumes that all precipitation recharges the groundwater, which cannot be done in many places.

In Dutch polders with shallow water tables and intense drainage networks, it is reasonable to assume that the actual evapotranspiration is equal to the reference value. In that case, the factor f becomes larger than 1 because 1 mm of evaporation has less effect than 1 mm of precipitation (because part of the evaporation does not enter the ground but is immediately drained to the surface water system). In that case, we can calculate recharge as:

$$\begin{aligned} R &= P - fE & f &\leq 1 \\ R &= P/f - E & f &> 1 \end{aligned} \quad \text{Equation B2}$$

These simple formulas can be applied easily for the situations currently modelled in Metran and for the simulations that are driven by future climate data using the delta-change climate factors. However, it is noted that it is a crude estimate using assumptions that are easily violated. Because of this, the equations should be applied only to long term averages using only models of the highest quality.



Deliverable 4.2

PILOT DESCRIPTION AND ASSESSMENT

**Lorca
(Spain)**

Authors and affiliation:

**Pablo Ezquerro, Guadalupe Bru,
Marta Béjar, Carolina Guardiola-
Albert, Gerardo Herrera.**

Geological Survey of Spain (IGME)



This report is part of a project that has received funding by the European Union's Horizon 2020 research and innovation programme under grant agreement number 731166.



Deliverable Data	
Deliverable number	D4.2
Dissemination level	Public
Deliverable name	Pilots description and assessment report for WP4
Work package	WP4
Lead WP	BRGM and NERC (WP4)
Deliverable status	
Version	Version 2
Date	3/3/2021

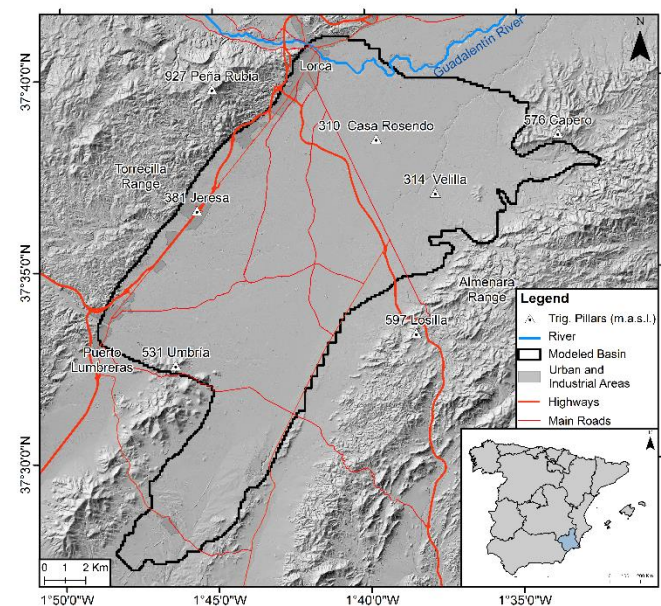
[This page has intentionally been left blank]

LIST OF ABBREVIATIONS & ACRONYMS

TABLE OF CONTENTS

	LIST OF ABBREVIATIONS & ACRONYMS	5
1	EXECUTIVE SUMMARY	5
2	INTRODUCTION	7
3	PILOT AREA	8
	Site description and data.....	8
	Location and extension of the pilot area.....	8
	Geology/Aquifer type	9
	Inflows	10
	Hydraulic head evolution.....	12
	Outflows	13
4	METHODOLOGY.....	14
	Sentinel-1 SAR Data	Error! Bookmark not defined.
	A-DinSAR processing	14
	Groundwater Numerical Model Development and Calibration.....	17
	Calibration data	18
	Deformation model and validation	18
5	RESULTS AND CONCLUSIONS	19
	A-DinSAR processing in Lorca.....	19
	Groundwater numerical model.....	19
	SAR deformation model	21
	Conclusions.....	23
	Acknowledgements	23
6	REFERENCES	24

1 EXECUTIVE SUMMARY

Pilot name	UPPER GUADALENTÍN BASIN	
Country	Spain	
EU-region	Mediterranean region	
Area (km ²)	250 km ²	
Aquifer geology and type classification	Detrital. Sedimentary	
Primary water usage	Irrigation / Drinking water	
Main climate change issues	<p>The Spanish Mediterranean arc is a drought vulnerable area that experienced three important dry periods between 1990 and 2012, where 68 aquifer systems have been declared partially overexploited and 10 as completely overexploited by national authorities. Agriculture, traditionally the most important economic activity in the area, is being progressively replaced by urban and touristic activities. These both activities still have an important impact over groundwater resources.</p> <p>Piezometric data from the Alto Guadalentín basin show a continuously descending piezometric level over the last 60 years; from a few meters below land surface in the 60's to approximately 200 m below land surface nowadays. This piezometric level drop has generated of the highest subsidence rates induced by groundwater extraction measured in Europe (>10 cm/yr).</p>	
Models and methods used	<p>Groundwater mathematical model that reproduces groundwater evolution during 52 years is developed. The geometry of the model was improved introducing data derived from InSAR deformation ad borehole data. The resulting aquifer system history of the piezometric level is compared with ENVISAT deformation data to calculate a first-order relationship between groundwater changes, soft soil thickness and surface deformation. This deformation is validated with displacement data from ERS and ComoSkyMed satellites. Future climate changes scenarios are used to generate recharge series, which are introduced in the model to evaluate future groundwater and deformations in the aquifer.</p>	
Key stakeholders	<p>Segura River Basin Authority, farmers associations (farmers are a highly heterogeneous group, whose interests often cannot be generalised; this implies a wide range between those associations working at institutional level and those working at political scale representation), water supply companies,</p>	



	Environmental Conservation Groups.
Contact person	M. Béjar, P. Ezquerro, C. Guardiola-Albert, G. Herrera (IGME): m.bejar@igme.es , p.ezquerro@igme.es , c.guardiola@igme.es , g.herrera@igme.es

Lorca pilot site is located over the Alto Guadalentín aquifer, which is situated in Murcia Region, Southeast Spain. The Guadalentín hydrographic system responds to a structural control: the main watercourses fit in the geological fracture system, partially controlled by the faults activity in the Guadalentín area. The hydrographic system provokes multiple deposits and geological features (gullies, badlands, alluvial fans, debris cones, glacis, alluvial terraces, ravines, etc. (Cerón and Pulido-Bosch, 1996). The main watercourse in the area is the Guadalentín River with very low flow non- permanent rates that only increase due to extreme flood events (Ezquerro et al., 2017), reaching up to 3000 m³/s (Cerón, 1995). Mediterranean areas such as the Southeast of Spain are affected by convective storms (commonly developed in Autumn) with very quick development, short duration and very high intensity constituting a permanent potential threat. For Guadalentín basin, these events resulted in numerous catastrophic floods (Ezquerro et al., 2017). The area presents a dry climate following the Koppen-Geiger Classification modified (AEMET-IM, 2011). This matches with severe drought periods, and consequently, water stress in the area has historically appeared with temporal effect causing water shortages. Agricultural development has led to the overexploitation of the aquifer system (CHS, 2007). This fact is reflected in a global descendent groundwater level trend until 2009. The aquifer has been also declared to not achieve a good quality status.

In order to increase the knowledge about the aquifer system behavior and ultimately improve its management, a numerical groundwater model was developed. This model simulates changes in groundwater flow, from the original steady state conditions in the aquifer system back in 1960 to 2012 conditions. The conceptual model was rigorously set up using available geological, geophysical and groundwater flow data, and included the delineation of the model geometry and the boundaries conditions. Earth Observation (EO) techniques, more precisely A-DInSAR, were also used to improve the conceptual and physical groundwater flow models. This method provides surface displacements time series caused by terrain motion such as land subsidence, and corroborated an important relationship between subsidence, piezometric levels changes and compressible thickness variations in the studied area. An empirical deformation model based on the groundwater numerical model results was adjusted.

Most of the work presented here was developed in the study by Ezquerro et al. (2017). Shortages in the TACTIC budget have not allowed further development of this methodology or its application in other pilot sites. For future works or projects, two are the main recommendations: (i) from the stakeholder perspective, the real use of the numerical groundwater model for water management purposes, and (ii) from a research view, further work should be done to numerically coupled flow and geomechanical models, that will allow a realistic estimation of water storage variations in the aquifer.

2 INTRODUCTION

Climate change (CC) already have widespread and significant impacts in Europe, which is expected to increase in the future. Groundwater plays a vital role for the land phase of the freshwater cycle and has the capability of buffering or enhancing the impact from extreme climate events causing droughts or floods, depending on the subsurface properties and the status of the system (dry/wet) prior to the climate event. Understanding and taking the hydrogeology into account is therefore essential in the assessment of climate change impacts. Providing harmonised results and products across Europe is further vital for supporting stakeholders, decision makers and EU policies makers.

The Geological Survey Organisations (GSOs) in Europe compile the necessary data and knowledge of the groundwater systems across Europe. In order to enhance the utilisation of these data and knowledge of the subsurface system in CC impact assessments the GSOs, in the framework of GeoERA, has established the project “Tools for Assessment of Climate change Impact on Groundwater and Adaptation Strategies – TACTIC”. By collaboration among the involved partners, TACTIC aims to enhance and harmonise CC impact assessments and identification and analyses of potential adaptation strategies.

TACTIC is centred around 40 pilot studies covering a variety of CC challenges as well as different hydrogeological settings and different management systems found in Europe. Knowledge and experiences from the pilots will be synthesised and provide a basis for the development of an infra structure on CC impact assessments and adaptation strategies. The final projects results will be made available through the common GeoERA Information Platform (<http://www.europe-geology.eu>).

The present document reports the TACTIC activities in the pilot site of Lorca, in Spain. More specifically, the results related with Task 4.5. of WP4. This task aims to assess subsidence in aquifer systems using DInSAR satellite data. Numerical groundwater flow models and synthetic aperture radar differential interferometry (DInSAR) that detects surface movements were used to understand subsidence related with groundwater withdrawal and calibrate hydrogeological and geomechanical models. SAR-derived deformation series were compared with piezometric change data and soft soils thickness data in order to evaluate a first relationship between them and improve the conceptual and physical hydrogeological model. The historical analysis of satellite SAR images since 1992 permitted to implement robust numerical models that can be used to understand the impact of global change into aquifer systems. The task is focus on Lorca pilot in Spain, but the same methodology could be applied elsewhere (aquifer having subsidence problems, enough piezometric data, and good response of InSAR).

3 PILOT AREA

The Guadalentín Basin, SE Spain, is one the driest regions of Europe. It is located in Murcia Province (Southeastern of Spain), where the Guadalentín River, tributary of the Segura River, flows. This fertile depression was drilled in 1960 in order to improve the area's productivity by exploiting the important underlying aquifer. Increasing groundwater extractions revitalized Guadalentín agriculture in the 1980s, but led to the declaration that the aquifer-system was temporally overexploited in 1987 (CHS, 2006). New regulations and water transferred from Tajo's basin produced a reduction of pumping and abandonment of some wells from 1988. Piezometric levels began to slowly stabilize in major areas but continued declining in areas close to the still numerous active wells.

Site description and data

Location and extension of the pilot area

The Alto Guadalentín basin (Figure 1) is an intramontane sedimentary NE-SW-oriented basin containing an aquifer system hydraulically connected to the Bajo Guadalentín aquifer-system. Altitudes in the basin range from 300 to 400 m a.s.l. while the surrounding mountains range from 500 to 950 m a.s.l. This basin is an alpine orogenic tectonic depression with a Paleozoic pre-orogenic metamorphic basement covering an area of approximately 250 km². Basement shows a horst and graben pattern with maximum depths of 1000 m below land surface (Cerón and Pulido-Bosch, 1996). The Guadalentín depression is bounded to the north by the active Alhama de Murcia fault (Martínez-Díaz et al., 2012).

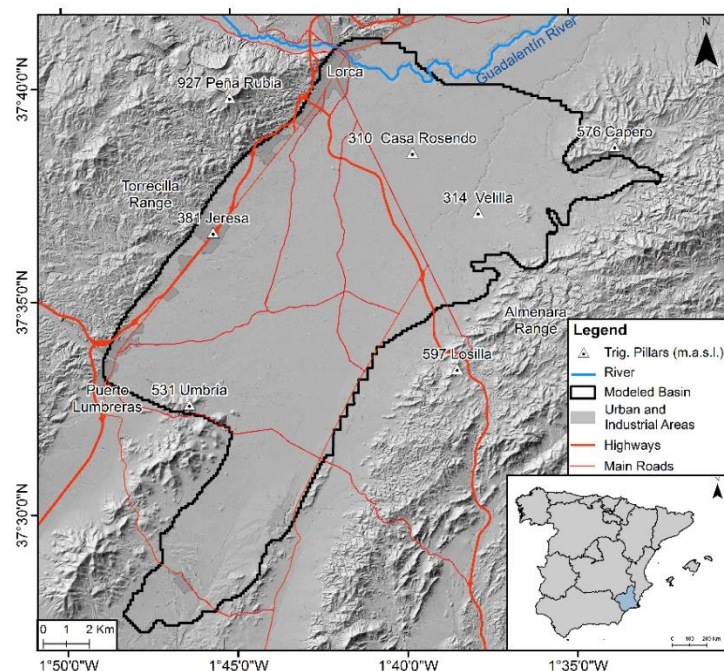


Figure 1. Location of the pilot area



The Segura Hydrographic Demarcation is the organism that manages both surface and ground water bodies in the area. Land uses in the study area comprise artificial (4.5%), agricultural (91.0%) and forest areas (4.5%). Among the agricultural areas (248 km²), 85% corresponds to irrigated surfaces. Related to the artificial land use, Lorca and Puerto Lumbreras (Figure 1) constitute the two principal urban areas. The population in the basin area reached 107,000 inhabitants in 2012, with a slow decreasing trend since then. The main population centre is Lorca city (nearly 94,500 inhabitants in 2019), which constitutes the third most populated urban area in the Murcia Region. The economy is based mainly on irrigated agriculture, although farming and industrial activities are also weakly developed.

Geology/Aquifer type

The aquifer system developed over the metamorphic basement is constituted by sedimentary materials accumulated during the basin formation (IGME, 1981). Taking into account the horst and graben pattern of the basement, its thickness has a remarkable variability oscillating from 300 to 900 m depending on the location (Cerón, 1995; IGME, 1985). The geometry of the aquifer is defined by limits in NW (permian-triassic materials), SE (triassic-miocene materials) and N. The northern limit is defined by the contact with the multilayer aquifer system of Bajo Guadalentín. The transition zone between the two aquifers is characterized by thick clay layers that lose lateral continuity towards the Alto Guadalentín. The southern border (open) is defined by the contact with the Sierra de Enmedio triassic loamy materials (CHS, 2015). The plio-quaternary sediments (gravels and sands) define the upper unconfined aquifer layer followed by a layer composed of miocene detrital materials with conglomerate and sand deposits. This layer constitutes a low permeable semiconfined level. The triassic materials represent the deepest impermeable limit.

Plio-Quaternary sediments compose the main and most productive layer of the aquifer system (Figure 2). This layer comprises sediments from near ranges alluvial fans generating sand and gravel lenses embedded in a clay and silt matrix. The upper part of the aquifer is unconfined, while deeper areas have a semiconfined behavior.

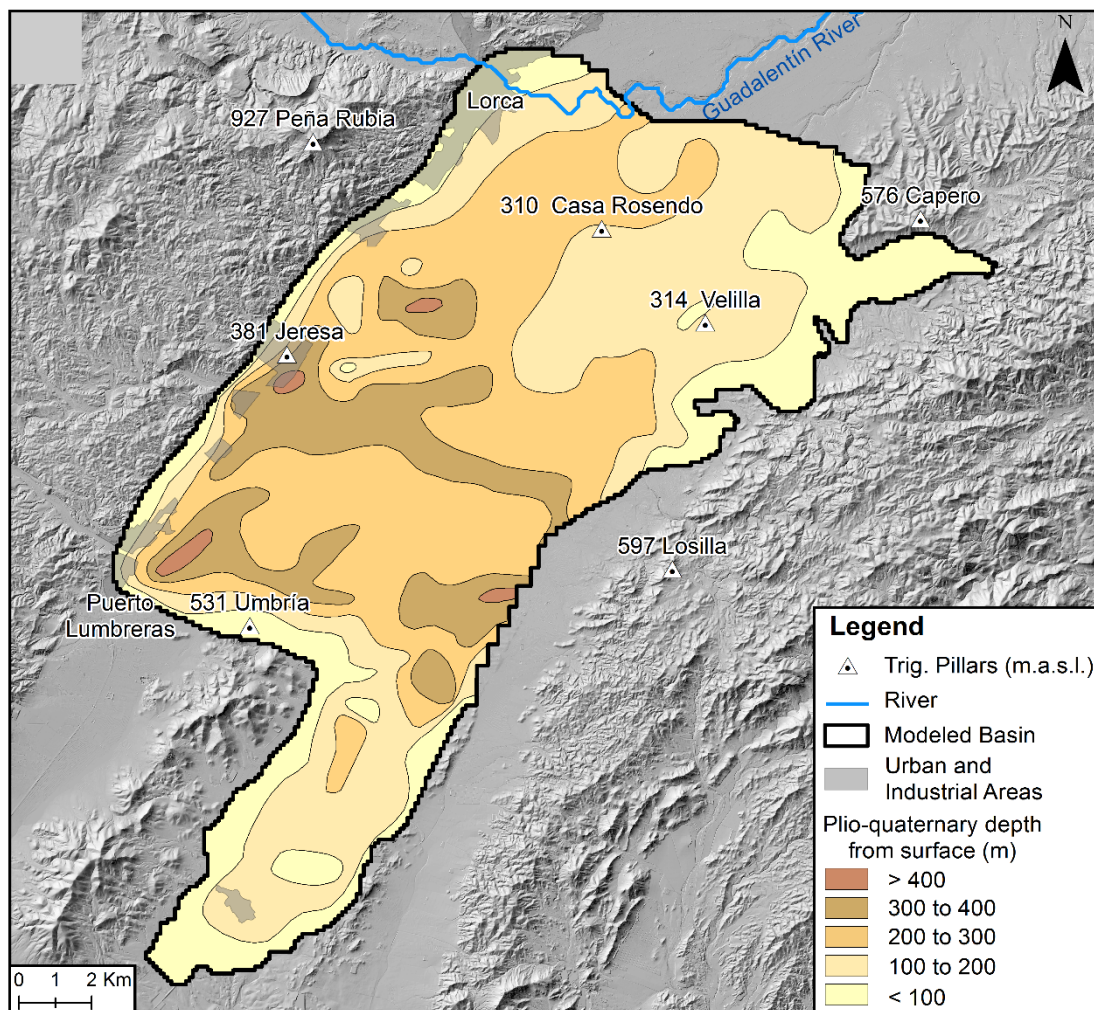


Figure 2. Main aquifer layer depth

Inflows

Table 1 resumes yearly water inflows estimated for the period 1960-2012 by Ezquerro et al. (2017). Aquifer-system recharge strongly depends on rainfall (8.80 hm³/year, CHS, 2005). There is an area in the northern part of the basin of 30 km² with low permeability materials outcropping at the surface which can be considered impervious and not susceptible to surface recharge. According to the rainfall series provided by the Spanish National Meteorological Agency (AEMET) average rainfall is around 250 mm/yr, usually concentrated in storm events from August to October (Figure 3). During the 52 studied years a rainfall declining trend can be observed with two severe droughts from 1994 to 1996 and from 2001 to 2003.

There are also inflows to the aquifer system infiltration and stream infiltration through Guadalentín River, Nogalte Rambla and other minor water courses along the eastern and western margins (Figure 4). Another important source of recharge is infiltration from the irrigation return flow (2.70 hm³/year, CHS, 2005).



Table 1. Yearly water inflows to the Alto Guadalentín River, estimated for the period 1960-2012 by Ezquerro et al. (2017)

Inflows	Average (hm ³)	Max (hm ³)	Min (hm ³)
Guadalentín River	1.04	2.60	0.20
Nogalte Rambla	1.04	2.60	0.20
W rambla	0.70	1.73	0.13
E rambla	1.39	3.47	0.27
Rainfall infiltration	7.0	26.74	2.23
Irrigation returns Lorca Irrigators Association	2.09	2.83	1.65
Irrigation returns Puerto Lumbreras Irrigators Association	1.55	3.09	0.12

Agricultural importance of this area is linked with water availability, supplied by different sources (Figure 4). This agricultural water demand is being met by water supplied from nearby reservoirs, groundwater extractions and, more recently, transference of water from other major basins (Tajo-Segura water transference, 1979). Agricultural development has affected the aquifer because of the extractions and the recharge from irrigation returns.

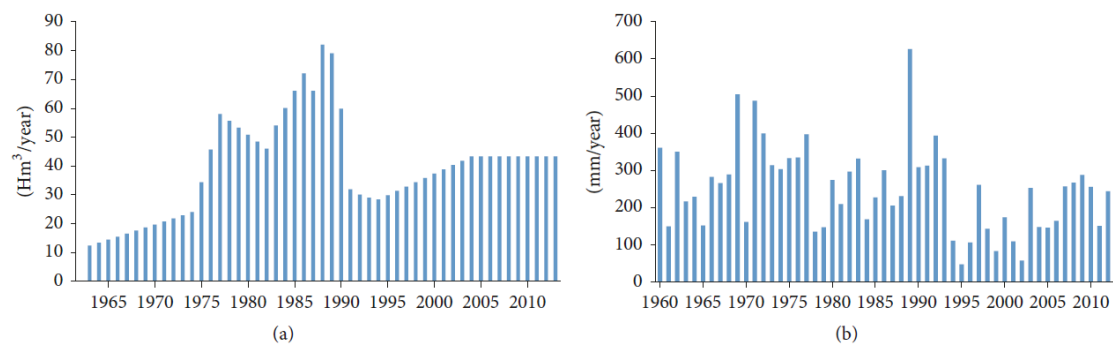


Figure 3. (a) Wells extraction rate. Maximum extractions of 80 hm³ reached in 1987 were drastically reduced after 1989 restrictions. (b) Rainfall series from Spanish Meteorological Survey. Two dry periods are clearly represented from 1994 to 2003

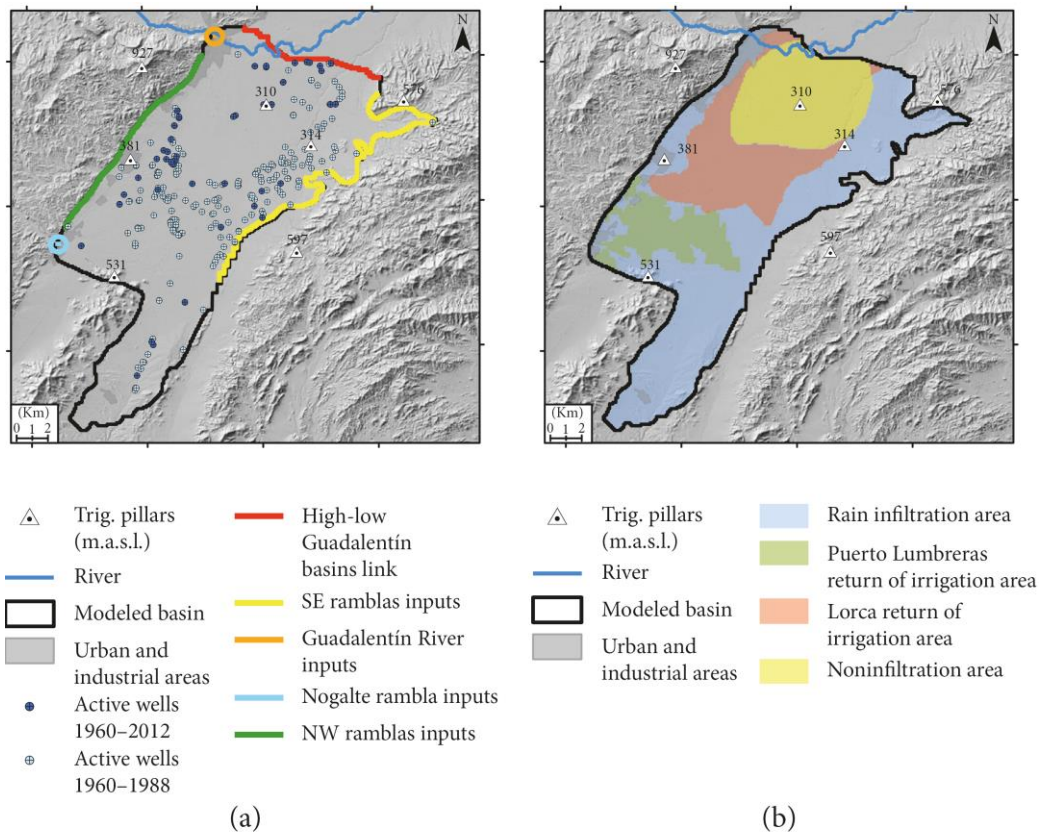


Figure 4. Basin inflows and outflows

Hydraulic head evolution

As previously commented, an intensive groundwater withdrawal has been depleting the aquifer-system since 1960 from a few meters below land surface to approximately 200 m below land surface nowadays (Ezquerro et al., 2017). The declaration of the aquifer as temporally overexploited in 1987 reduced the pressure of the aquifer-system produced a slight stabilization of the general piezometric level but continued declining near the still active wells.

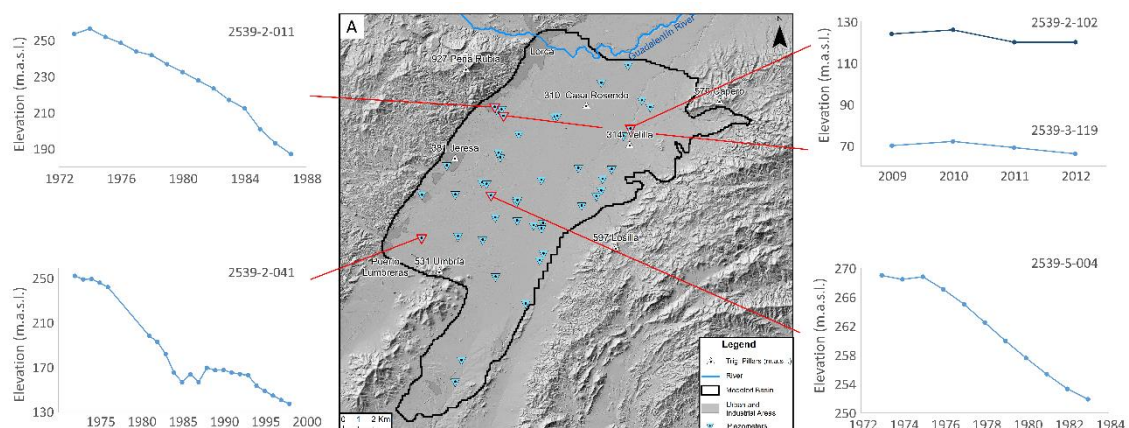


Figure 5. Location of hydraulic head observation points and piezometric evolution



Outflows

Discharge from the Alto Guadalentín aquifer occurs through the connection with the Bajo Guadalentín aquifer-system (Figure 4) and the numerous wells pumping its resources, which in occasions, take water from nearly 400 m depth. Extraction rates were governed by the increasing irrigation water demand and annual rainfall (Figure 3), reaching its maximum at the end of 1980s when 80 hm³/yr were pumped. After restrictions on groundwater pumping were imposed in 1989, the extraction rate dropped to less than 30 hm³/yr in the early 1990s. During the mid-to late 1990s, extractions increased slightly to compensate for a series of dry years. From 1960 to 1989 312 wells were registered and distributed throughout the basin. Two areas near the basin center (eastern center and western center) showed denser concentrations of wells. Since 1989 the number of wells has been reduced. Of the remaining 50 wells, the deepest and most productive are mainly concentrated in the western area. Nowadays, average value of pumping rates is quantified in around 34 hm³/year. Groundwater discharge to streams was not considered because the Guadalentín stream has a losing-disconnected relation with the Alto Guadalentín aquifer-system.

4 METHODOLOGY

In this section the different methods used to set up and adjust the aquifer groundwater mathematical model are described

A-DinSAR processing

A-DInSAR technique

Advanced Differential synthetic aperture radar interferometry (A-DInSAR) is a remote sensing technique for monitoring large-coverage deformation episodes of the earth surface. It uses Synthetic Aperture Radar (SAR) images that are collected by Earth-orbiting satellites. These spaceborne sensors acquire data regardless of the weather and operate day and night in a quasi-polar orbit, either ascending (south - north) or descending (north - south).

SAR sensors

Since the early 90s, several SAR satellites with ever-improving imaging characteristics have been launched by an international community of satellite providers, collectively ensuring continuous coverage of the Earth with SAR data (Flores-Anderson et al., 2019). The characteristic bands at which SAR satellites operates are L-band, C-band and X-band (Figure 6), with wavelengths of 23.6, 5.6 and 3.1 cm, respectively. With moderate to high-resolution capabilities and increased vegetation penetration, C-band data can be seen as a good compromise between X-band and the longer wavelength L-band sensor classes to monitor areas with low to moderate vegetation.

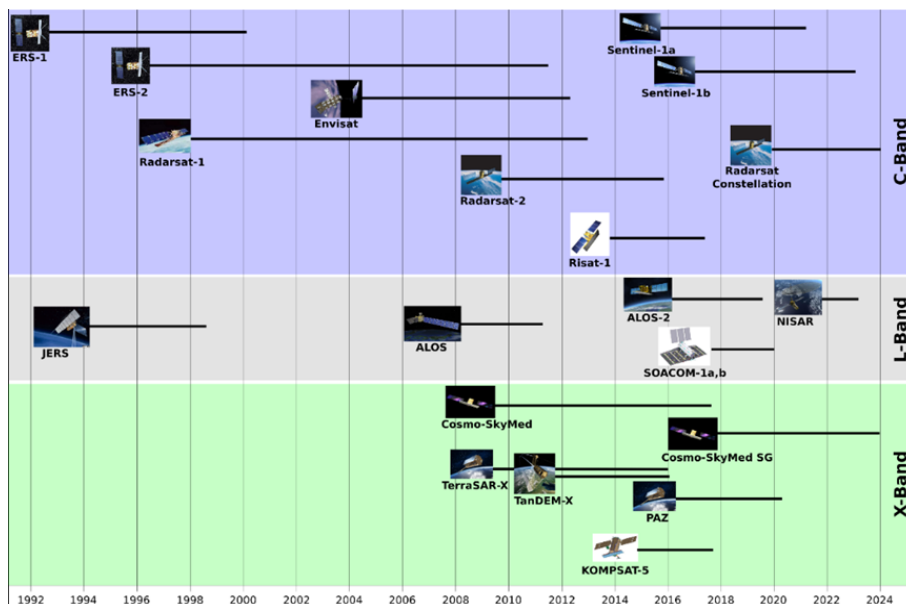


Figure 6. Chart of past, present and upcoming SAR satellite missions operating at L-band, C-band and X-band (UNAVCO, web).



The Alto Guadalentin aquifer groundwater model has been adjusted using various SAR satellite datasets, covering different time periods from 1992 to 2012. These are C-band ERS (1992–2000), ENVISAT (2003–2010), and X-band Cosmo-SkyMed (CSK) (2011–2012). Later studies of the basin have also used Sentinel 1 data, but this satellite was launched in 2014, so its out of the modelled period. The details of each sensor are summarized in Table 2 (Flores-Anderson et al., 2019).

Table 2 Properties of the spaceborne SAR sensor used to adjust the aquifer numerical model.

SENSOR	ERS-1	ERS-2	ENVISAT	CSK
LIFETIME	1991-2001	1995-2011	2002-2012	2007-
WAVELENGTH/ FREQUENCY	C-band $\lambda = 05.6\text{cm}$	C-band $\lambda = 05.6\text{cm}$	C-band $\lambda = 05.6\text{cm}$	X-band $\lambda = 03.5\text{cm}$
POLARIZATION	VV	VV	HH, VV, VV/HH, HH/HV, VV/VH	Single: HH, VV, HV, VH Dual: HH/HV, HH/VV, VV/VH
RESOLUTION	Az: 6-30m Rg: 26m	Az: 6-30m Rg: 26m	Az: 28m Rg: 28m	Spotlight: $\leq 1\text{m}$ Stripmap: 3-15m ScanSAR: 30-100m
FRAME SIZE	100km	100km	100km	Spotlight: 10x10km Stripmap: 40x40km ScanSAR: 100x100 - 200x200km
REPEAT CYCLE	35 days	35 days	35 days	Satellite: 16 days Constellation: ~hrs
ACCESS	Restrained	Restrained	Restrained	Commercial; limited proposalbased scientific

A-DinSAR processing

SAR images collected by the space borne sensors have amplitude and phase information in each pixel that compose them. The SAR interferometry technique uses two SAR images of the same area acquired at different times and "interferes" (differences) them, resulting in maps called interferograms that show ground-surface displacement (range change) between the two time periods. Thanks to the availability of large SAR data archives, a stack of independent interferograms can be created from various SAR images of the same illuminated area. This allows to reconstruct displacement time series from selected point scatterers (PS) or distributed scatterers (DS) that are above a phase stability threshold in all the interferograms, using the so-called multitemporal or Advanced Differential radar interferometry (A-DInSAR)



algorithms. Any A-DInSAR algorithm dealing with data stacks, requires a number of conceptual steps that have to be sequentially performed (Casu et al., 2014). These are the SAR image focusing (if raw data is used, not needed in SLC images), the SAR image co-registration using a Digital Elevation Model (DEM), the interferogram generation, the unwrapping of the computed phases and the retrieval of the final displacement time-series. A simplified block diagram of A-DInSAR algorithms is shown in Figure 8 (De Luca et al., 2015).

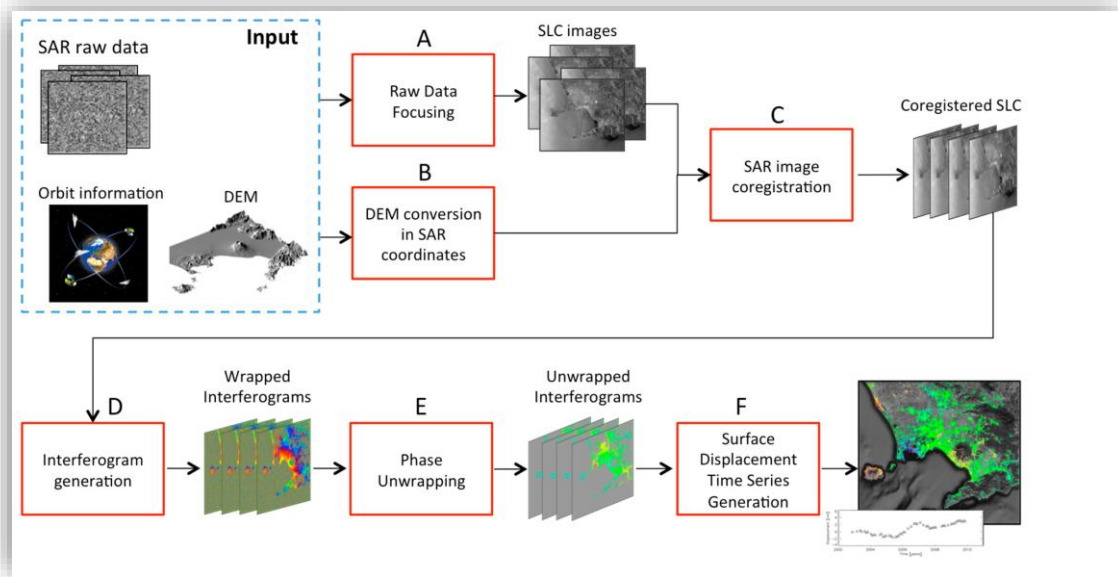


Figure 8. Simplified block diagram of A-DInSAR algorithm steps (De Luca et al., 2015).

Typically, a minimum of 15-20 images is needed to perform an A-DInSAR analysis with C-band (Crosetto et al., 2016), although it is possible to use shorter datasets with X-band due to the higher resolution and the shorter wavelength of this band (Bovenga et al., 2012). In any case, the larger the number of available scenes, the better the quality of the deformation velocity and time series estimation. There are two methods to create the stack of interferograms. The first one uses a single reference SAR image (Single master) so the number of interferograms will be $N-1$, where N is the number of SAR images. The second one uses a small baseline configuration, where a denser interferogram network is created linking multiple SAR images (Multi-master). The criterion to select the punctual targets in the interferograms can be simplified in amplitude and coherence methods. Amplitude selection methods work at full resolution and limit the interferometric processing only to those pixels that behave consistently over a long period of time (PS). Coherence based methods use distributed scatterers (DS), or in other words, areas whose scatter properties are not altered with time, which requires a multilook that lowers the resolution. A comparison of different A-DInSAR algorithms can be found in (Crosetto et al., 2016; Osmanoğlu et al., 2016) and (Minh et al., 2020). The algorithms used to compute the time series of surface displacements in the Alto Guadalentin aquifer are based on the Stanford Method for Persistent Scatterers (StaMPS) software and on

the Stable Point Network (SPN) software. Further details of SPN and StaMPS methods are summarized in Table 3.

Table 3 Comparison of A-DInSAR methods used in Alto Guadalentín aquifer model

METHOD	REFERENCE	SCATTER	PIXEL SELECTION CRITERION	NETWORK
StaMPS	(Hooper et al., 2004)	Point, distributed	Amplitude and phase criterion	Multi-master
SPN	(Crosetto et al., 2008; Duro et al., 2003)	Point, distributed	Amplitude dispersion, coherence, spectral coherence	Multi-master

Groundwater Numerical Model Development and Calibration

In order to develop a groundwater numerical flow model of the Alto Guadalentín aquifer, we have used MODFLOW-2005 with the ModelMuse interface, both developed by the USGS (Harbaugh, 2005; Winston, 2009). Modeling was carried out in two steps; first a steady-state simulation was performed using 1960 data, and second, a transient simulation for the period from 1961 to 2012 was performed using the steady-state simulation model as starting conditions. A model time step of one year was specified because the model input data such as water balance, recharge, and extraction were compiled annually.

The model is composed by three layers using square 100m grid cells over 243.5 km² across the basin. Flow between cells is controlled by Layer-Property Flow Package (LPF) due to its capability to allow later calibration of hydrogeological parameters. The first layer of the model comprises soft soils Plio-Quaternary materials, the second layer is formed by coarse-grained Plio-Quaternary sediments, and the third layer is formed by Miocene material. Due to the aquifer characteristics and the LPF available options all the layers are described as convertible layers.

Model calibration was performed using UCODE 2014 (Poeter et al., 2014) using the graphical interface Model Mate Banta (2011) developed by the IGWMC and USGS to minimize the root mean squared residual through adjustment of hydraulic conductivity and storage coefficients.

Initial hydrogeological parameters have been estimated using data from pumping tests and calibrated information from IGME IGME (1994) and CHS (1992) models. After the calibration phase is carried out over the presented model, hydraulic conductivity (K , cm/s) ranges from 2.5×10^{-3} to 9×10^{-6} depending on the layer. Coarse-grained Plio-Quaternary materials show higher hydraulic conductivity than Plio-Quaternary soft soils and Miocene layers. The calibrated storage coefficients vary from 1.5×10^{-1} to 1×10^{-3} with the highest values corresponding to the coarse-grained Plio-Quaternary layer.

Ideally, a transient groundwater flow model should begin from a steady-state condition. Because pumping from the Alto Guadalentín aquifer began more than 50 years ago, the search for information on steady-state conditions in the aquifer, used as initial condition of the



steady-state simulation step, has to go back to the information gathered by the early studies in 1960. That time was chosen because the system was not suffering significant stress. The piezometric level was between 260 and 320m a.s.l. as seen in Figure 5.

Calibration data

Model calibration has been implemented using 47 piezometric level measurement points spatially distributed with 189 annual piezometric measurements recorded (Figure 5) by IGME and CHS during consecutive measurement campaigns. Low measurement/measurement point ratio and long simulation time indicate that the available time series are not sufficiently long enough to adequately constrain the calibration. Only 4 measuring points have more than 10 years' data, with the longest one being 23 years. 14 of the remaining points present series from 4 to 10 years of piezometric levels. 29 have piezometric levels with less than 4 years, most of them with only one year. None of the 47 series covers the simulation period. The existing data is well distributed spatially but poorly in time. Additionally, near time records are even more limited, bringing to light the necessity of aquifer monitoring improvements. Piezometric level observations were implemented using the Head Observation Package (Hill et al., 2000). Piezometric series presented in Figure 5 show a continuously declining piezometric level from 1970 to more recent times with a slight recovery in some areas near the late 1980s, consistent with the aquifer history of extractions (Figure 3). Recent measured piezometric levels (2009–2012) revealed a nearly stable trend but with lower levels than older data (average decline of 90 m from 1990 to 2009), indicating a net loss of groundwater storage.

Deformation model and validation

Fusion of this groundwater model result with subsidence data resulting from SAR images processing provides the opportunity to analyse both phenomena together and establish relations between them (Ezquerro et al., 2017). Using surface deformation, piezometric level history, and soft soil thickness, we propose an empirical formulation, without geotechnical parameters and time independence, which allows the calculation of surface deformation from piezometric level changes. Parameter calibration was carried out using the ENVISAT results because its time centred position (2003–2010) permits the validation of the model fit for both earlier and later time periods using ERS (1992–2000) and CSK (2011–2012) results, respectively. Two independent variables were used to estimate deformation, piezometric level change, and soft soil thickness. Both linear and nonlinear regression models were considered. The quality of the models to replicate the observed data was assessed using coefficient of determination (r^2). Due to the importance of the soft soils layer the percentage of its thickness over complete Plio-Quaternary sediments thickness was calculated and used to distinguish areas with high percentages (>25%) where described analysis and relationships were done. The empirical deformation models were used to estimate deformation within the range of the simulated piezometric level variation. Accumulated deformation in 1992 and 2012 was estimated and validated with ERS and CSK SAR data by evaluating the ratio error/total displacement.

5 RESULTS AND CONCLUSIONS

A-DinSAR processing in Lorca

Three different sets of images were used from C-band ERS (1992–2000), ENVISAT (2003–2010), and X-band Cosmo-SkyMed (CSK) (2011–2012) satellites. InSAR-derived ground displacements covering the period 1992–2012 (Figure 9) were collected from previous studies (González and Fernández, 2011; Boni et al., 2015; Béjar et al., 2016). Deformation measurements from the ERS dataset are from Rigo et al. (2013). This dataset was processed using DORIS interferometric software (Kampes et al., 2003) to complete the coregistration and interferogram generation phases. Time series were computed using the SBAS approach (Berardino et al., 2002) through StaMPS software (Hooper, et al., 2007) (Figure 8). CSK dataset (from Boni et al., (2015)) was processed using DIAPASON for the interferometric stage and SPN software (Duro et al., 2004) during the final products calculation following the Persistent Scatterer approach.

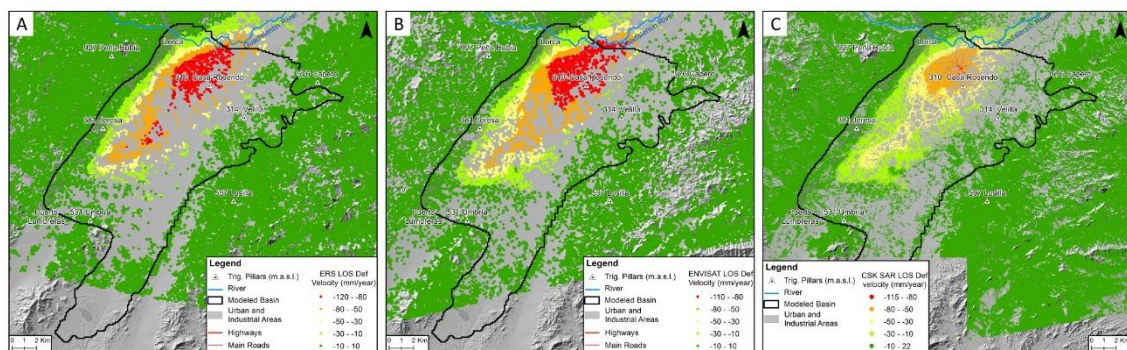


Figure 9. InSAR-derived deformation used in this study. LOS deformation velocities from (a) ERS data (C-band, 1992–2000), (b) ENVISAT data (C-band, 2003–2010), and (c) Cosmo-SkyMed data (X-band, 2011–2012). Figure modified from Boni et al. (2015) and Ezquerro et al. (2017)

Groundwater numerical model

Modeling results present the evolution of the piezometric levels throughout 52 years (1960–2012) across the Alto Guadalentín basin and how the actions on the aquifer have affected them. Figure 10 shows the results at specific and relevant dates. In 1972 during the early expansive phase of the agricultural water use and increased groundwater extractions, piezometric levels were declining slightly and uniformly, and piezometric level depressions began to form in the areas where the wells were concentrated. In 1989, at the end of the period of high, agricultural water use and groundwater extractions when the aquifer was declared partially overexploited, piezometric levels had declined between 100 and 160 m from their original position, creating two steep depressions surrounding the eastern and western well fields. After the measures adopted by the basin management authorities, a decrease in agricultural water use, and consecutive rainy years from 1989 to 1993 (Figure 3), model results in 1993 reflect a slight recovery in some areas of piezometric levels. The inactivity of the



extractive activity in the eastern well field produced the recovery of the piezometric levels over the surrounding area. This fact suggests the ability of the aquifer system to recover its piezometric levels after severe extractions were stopped. Progressive increases in extractions and a lower rainfall period with three severe droughts associated CHS (2015) led to declining piezometric levels by the end of the simulation period in 2012. The active western well field produced a water level decrement of 70m from 1993 and an overall decrement of 40 m throughout the basin.

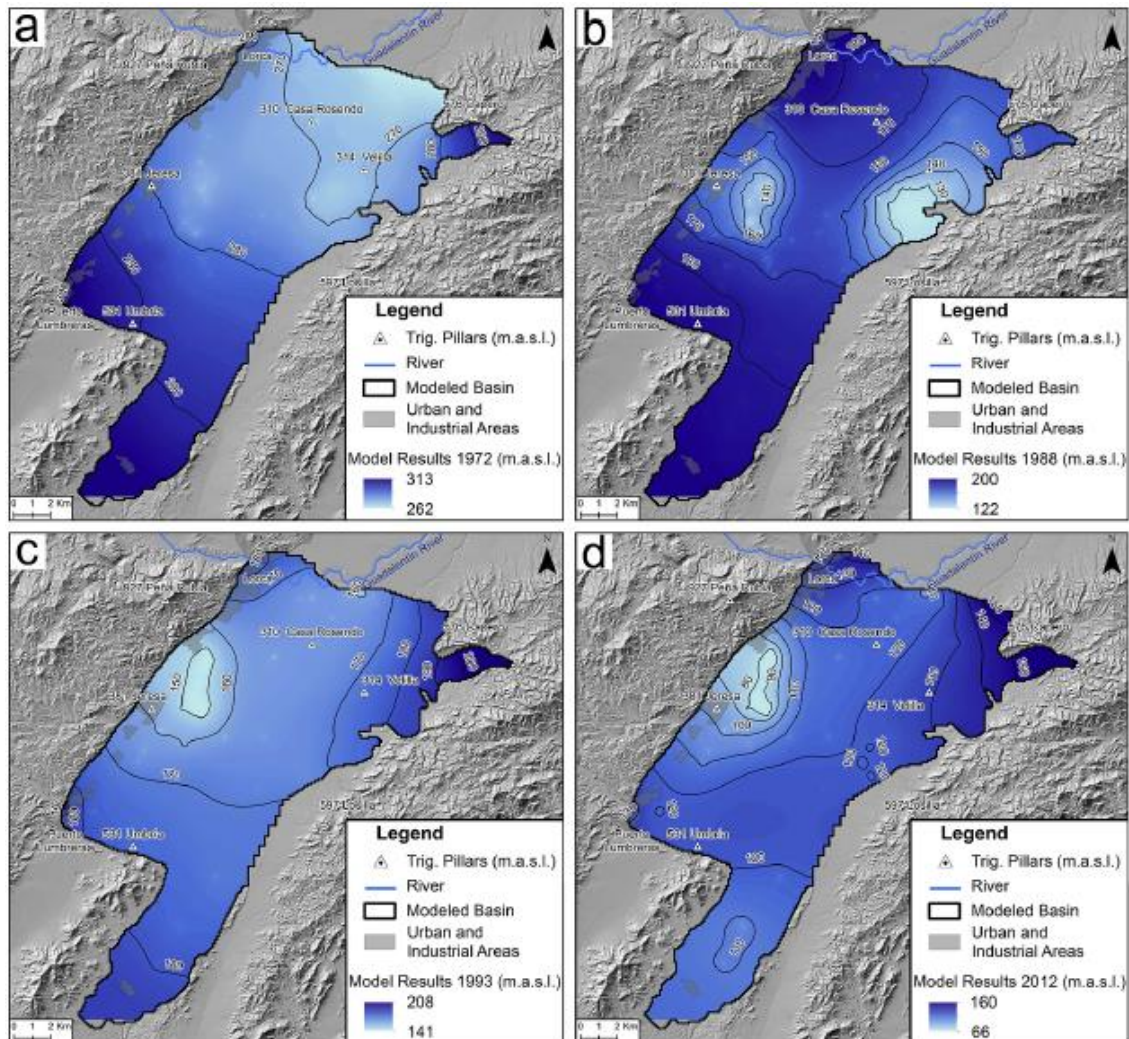


Figure 10. Groundwater model results in different years. Computed hydraulic head spatial distribution 1972 (a), 1988 (b), 1993 (c), and 2012 (d) (Ezquerro et al., 2017)

In order to evaluate the groundwater model results two important factors must be taken into account: its length, 52 years, and the piezometric level global change, between 170 and 210 m. Both of them can generate important differences between results and observations with slight changes in water contributions and uses (specially, pumping rates and watering). Despite these limitations the computed model levels fit well with the observations. Figure 11 shows the



simulated levels against the observed levels at the validation points. These values group around the $X = Y$ line with an RSME of 17.4 m. Average absolute difference between simulated and observed piezometric levels is 14.9 m. Assuming an average piezometric level drop of 190 m, both errors are under 10% of the total water displacement, an acceptable error for a long duration regional model.

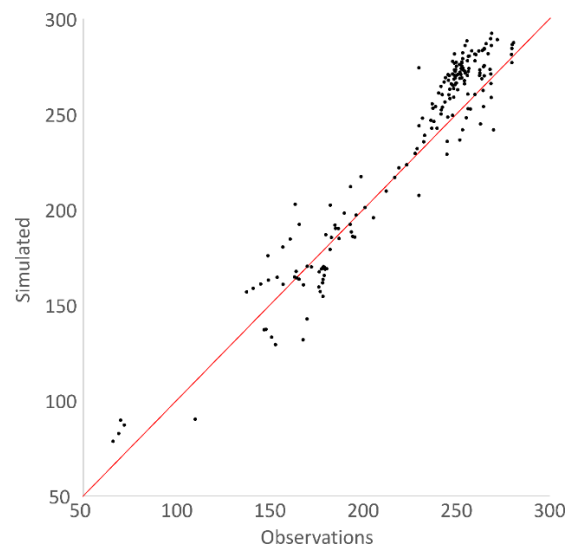


Figure 11. Groundwater model calibration diagram. Black points represent each water level datum observed and its simulated position. Red line is $X = Y$ line

An overall comparison of simulated piezometric data reflects a slight overestimation trend in the modeled level (piezometer 2539-1-001) converging both series towards the 1980s (piezometers 2539-2-043, 2539-6-024). From that date the model shows better results as can be seen in piezometer 2539-2-011. Piezometers related to the well fields (2539-2-011, 2539-2-043, 2539-3-066, or 2539-3-119) display some of the best fits between modeled and observed series, supporting a precise estimation of water extraction effects in the aquifer system dynamic. The northern area, with denser urbanization and specially affected by subsidence processes (Rigo et al., 2013; Boni et al., 2015), is located within the best fitting zone.

SAR deformation model

Statistical analysis of deformation and piezometric change series results in a low correlation between them ($r^2 < 0.05$). Despite the poor relationship observed, this study was able to reveal the presence of at least two data populations in the original data. Previous studies in the Alto Guadalentín basin have already probed the relationship between deformation and soft soil thickness (Boni et al., 2015; Béjar et al., 2016). Taking into account those works, the percentage of soft soils thickness over the complete Plio-Quaternary materials thickness has been computed. Using this parameter to identify the two observed populations, original SAR deformation data were divided into two samples of 1597 (percentage of soft soils over 25%) and 3393 (percentage under 25%) points each one. SAR deformation points with soft soils percentage over 25% show a stronger relationship ($r^2 = 0.61$) with piezometric changes and were selected to calibrate the deformation model.



Exponential term for thickness and linear term for piezometric level changes is disclosed as the best formulation to describe the relationship between water, thickness, and deformation. This correlation range of validity is for soft soils thickness over 10m and piezometric changes from 8.5m to 25 m. Calculated deformations out of the range are subjected to high error or incoherent results. Deformations are overestimated with low water changes while high piezometric variations generate underestimated deformations.

Deformation derived from CSK data (2011-2012) was added to the ENVISAT time series due to its short time span and the previously described problems with water changes out of the validity range. Model results for the period 2003–2012 (Figure 12) show differences between the simulated and measured spatial deformations patterns, but simulated maximum values are close to measured values (difference under 4%). Spatial discrepancy is mainly related to the influence of the soft soil thickness pattern in the model. The increasing error from present to past is caused by one of the most important limitations of this model, the temporal position of the calibration period in the deformation history. Material stress due to water withdraw began in 1960 and the calibrated relation calculated during ENVISAT period is related to an inelastic deformation period. Empirical relations calculated are related to inelastic deformations that need less water changes than elastic ones to generate the same deformation and overestimate ancient deformations.

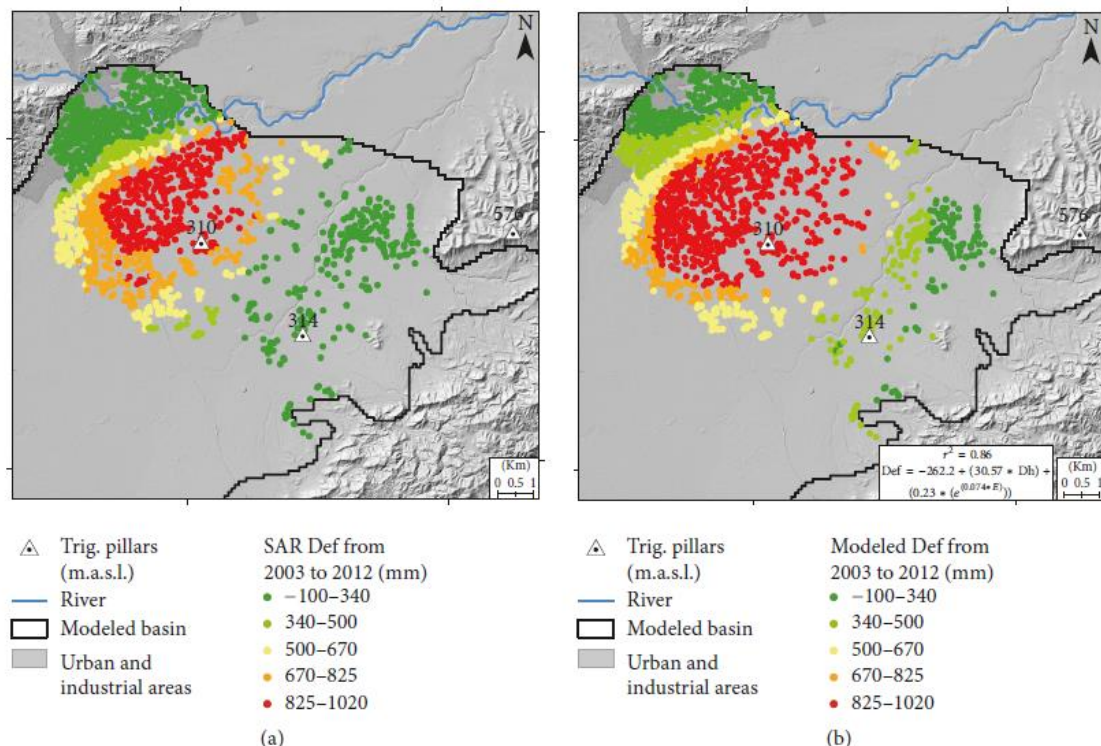


Figure 12. Results of the surface deformation modeled for the period 2003–2012 (ENVISAT + Cosmo-SkyMed). (a) SAR deformation measured from 2003 to 2012. (b) Calculated deformation using an exponential thickness model

Conclusions

It has been presented a hydrogeological model of an aquifer system that has experienced intensive pumping activities generating average piezometric level declines of about 150m during a period of 52 years (1960–2012). The model simulates changes in groundwater flow, from the original steady state conditions in the aquifer system to 2012 conditions, increasing our knowledge about the aquifer system behavior under stress in order to improve its management. The evolution of piezometry from this model is also a valuable constraint for geomechanical modeling aimed at characterizing the Alto Guadalentín basin that has one of the greatest subsidence rates in Europe (11 cm/yr).

The use of DInSAR has led to a better deformation monitoring due to exploitation of its spatial coverage and high-density measurements unattainable by traditional methods. The detailed characterization of the basin materials carried out by Bonì et al. (2015) through geological and SAR deformation data analysis has been used to refine the conceptual groundwater model. These geological updates constitute a first contribution of SAR data to improve water management.

Coupling groundwater flow and subsidence models can be used to refine the original groundwater model and better integrate the deformation data. Thanks to the European Space Agency (ESA) Sentinel-1 constellation, the monitoring of the study area continues today with enhanced characteristics of wide spatial coverage, great temporal resolution (six days' repeat cycle), and high spatial resolution. Future works combining these results with climatic change scenarios could facilitate the integration of piezometric level and deformation predictions into the management of the aquifer system, by assessing variability of water resources storage in the aquifer.

Acknowledgements

Data used in this work have used CSK® Products, © ASI (Italian Space Agency), delivered under an ASI licence to use: ASI Project Science Id 408 “Study of surface deformation due to groundwater exploitation in southern Spain”.

6 REFERENCES

AEMET-IM (2011) Iberian Climate Atlas. Air temperature and precipitation (1971- 2000) in Agencia Estatal de Metereologia (España), Instituto de Metereologia (Portugal) (Eds.) <http://www.aemet.es/es/conocermas/publicaciones/detalles/Atlas-climatologico>.

Banta, E. R. (2011) ModelMate—A Graphical User Interface for Model Analysis: U.S. Geological Survey Techniques and Methods, Book 6, Chap. E4, 31 p., 2011.

Béjar-Pizarro, M., Guardiola-Albert, C., García-Cárdenas, P. et al. (2016) Interpolation of GPS and Geological Data Using InSAR Deformation Maps: Method and Application to Land Subsidence in the Alto Guadalentín Aquifer (SE Spain),” Remote Sensing, vol. 8, no. 11, p. 965.

Berardino, P., Fornaro, G., Lanari, R., and Sansosti, E. (2002) A new algorithm for surface deformation monitoring based on small baseline differential SAR interferograms: Geoscience and Remote Sensing, IEEE Transactions on, v. 40, no. 11, p. 2375-2383.

Bonì, R., Herrera, G., Meisina, C., Notti, D., Béjar-Pizarro, M., Zucca, F., González, P. J., Palano, M., Tomás, R., and Fernández, J. (2015) Twenty-year advanced DInSAR analysis of severe land subsidence: The Alto Guadalentín Basin (Spain) case study: Engineering Geology, v. 198, p. 40-52.

Bovenga, F., Wasowski, J., Nitti, D., Nutricato, R., and Chiaradia, M. (2012) Using COSMO/SkyMed X-band and ENVISAT C-band SAR interferometry for landslides analysis: Remote Sensing of Environment, v. 119, p. 272-285.

Casu, F., Elefante, S., Imperatore, P., Zinno, I., Manunta, M., De Luca, C., and Lanari, R. (2014) SBAS-DInSAR parallel processing for deformation time-series computation: IEEE Journal of Selected Topics in Applied Earth Observations and Remote Sensing, v. 7, no. 8, p. 3285-3296.

Cerón, J.C. (1995) Estudio hidrogeoquímico del acuífero del Alto Guadalentín (Murcia) [Ph.D. thesis]: Granada, University of Granada, pp. 265.

Cerón, J.C., and Pulido-Bosch, A. (1996) Groundwater problems resulting from CO2 pollution and overexploitation in Alto Guadalentín aquifer (Murcia, Spain). Environmental Geology, 28 (4) 223–228. doi: 10.1007/s002540050096

CHS (1992) Estudio y redacción del plan de ordenación del acuífero alto Guadalentín, Tech. Rep.

CHS (2005) Estudio de cuantificación del volumen anual de sobreexplotación de los acuíferos de las unidades hidrogeológicas 07.28 Alto Guadalentín y 07.33 Águilas.

CHS (2006) Plan especial ante situaciones de alerta y eventual sequía en la cuenca del Segura: 238 Confederación hidrográfica del Segura, Tech. rep., 298 p., 239.

CHS (2007) Plan especial ante situaciones de alerta y eventual sequía en la cuenca del Segura. Confederación Hidrográfica del Segura.

CHS (2015) Plan Hidrológico de la Cuenca del Segura 2015/2021. Confederación hidrográfica del Segura.

Crosetto, M., Monserrat, O., Cuevas-González, M., Devanthéry, N., and Crippa, B. (2016) Persistent scatterer interferometry: A review: ISPRS Journal of Photogrammetry and Remote Sensing, v. 115, p. 78-89.

De Luca, C., Cuccu, R., Elefante, S., Zinno, I., Manunta, M., Casola, V., Rivolta, G., Lanari, R., and Casu, F. (2015) An on-demand web tool for the unsupervised retrieval of earth's surface deformation from SAR data: The P-SBAS service within the ESA G-POD environment: Remote Sensing, v. 7, no. 11, p. 15630-15650.

Duro, J., Inglada, J., Closa, J., Adam, N., and Arnaud, A. (2003) High resolution differential interferometry using time series of ERS and ENVISAT SAR data, Proceedings of FRINGE 2003 Workshop2003, p. 6.

Duro, J., Inglada, J., Closa, J., Adam, N., and Arnaud, A. (2004) High resolution differential interferometry using time series of ERS and ENVISAT SAR data, in Proceedings FRINGE 2004 workshop2004, Volume 550, p. 72.

Ezquerro, P., Guardiola-Albert, C., Herrera, G., Fernández-Merodo, J.A., Béjar-Pizarro, M., Boni, M. (2017) Groundwater and subsidence modelling combining geological and multi-satellite SAR data over the Alto Guadalentín aquifer (SE Spain). Geofluids, vol. 2017. <https://doi.org/10.1155/2017/1359325>.

Flores-Anderson, A. I., Herndon, K. E., Thapa, R. B., and Cherrington, E. (2019) The SAR Handbook: Comprehensive Methodologies for Forest Monitoring and Biomass Estimation.

González, P. J. and Fernández, J. (2011) Drought-driven transient aquifer compaction imaged using multitemporal satellite radar interferometry, Geology, vol. 39, no. 6, pp. 551–554.

Harbaugh, A. W. (2005) MODFLOW-2005, the U.S. Geological Survey modular ground-water model—the ground-water flow process,” U.S. Geological Survey Techniques and Methods 6-A16.

Hill, M. C. , Banta, E. R., Harbaugh, A. W. and Anderman, E. R. (2000) MODFLOW-2000, the U.S. Geological Survey modular ground-water model; user guide to the observation, sensitivity, and parameter-estimation processes and three post-processing programs,” Tech. Rep., U.S. Geological Survey, 2000, Open-File Report 00-184, p. 210.

Hooper, A., Zebker, H., Segall, P., and Kampes, B. (2004) A new method for measuring deformation on volcanoes and other natural terrains using InSAR persistent scatterers: Geophysical research letters, v. 31, no. 23.

Hooper, A., Segall, P., and Zebker, H. (2007) Persistent scatterer interferometric synthetic aperture radar for crustal deformation analysis, with application to Volcán Alcedo, Galápagos: Journal of Geophysical Research: Solid Earth, v. 112, no. B7.

IGME (1981) Mapa Geológico de España, 1:50.000, Sheet Lorca (953). Servicio de Publicaciones Ministerio de Industria, Madrid. Tech. rep.

IGME (1985) Mapa Hidrogeológico de España, 1:200.000, Sheet Murcia (79). Servicio de Publicaciones Ministerio de Industria, Madrid. Tech. rep.

IGME (1994) Estudio para la regulación y apoyo a la gestión de los recursos hídricos subterráneos del Alto Guadalentín (Murcia), Modelo matemático de flujo subterráneo. IGME internal report ref. 33237.

Kampes, B. M., Hanssen, R. F. and Perski, Z. (2003) Radar interferometry with public domain tools,” in Proceedings of the FRINGE, pp. 1–5, 2003

Martínez-Díaz, J. J., Béjar-Pizarro, M., Álvarez-Gómez, J. A., Mancilla, F. D. L., Stich, D., Herrera, G., Morales, J. (2012) Tectonic and seismic implications of an intersegment rupture: The damaging May 11th 2011 Mw 5.2 Lorca, Spain, earthquake. Tectonophysics 546, 28-37.

Minh, D. H. T., Hanssen, R., and Rocca, F. (2020) Radar Interferometry: 20 Years of Development in Time Series Techniques and Future Perspectives: Remote Sensing, v. 12, no. 9, p. 1364.

Osmanoğlu, B., Sunar, F., Wdowinski, S., and Cabral-Cano, E. (2016) Time series analysis of InSAR data: Methods and trends: ISPRS Journal of Photogrammetry and Remote Sensing, v. 115, p. 90-102.

Poeter, E. P. , Hill, M. C. , Lu, D. , Tiedeman, C. R. and Mehl, S. (2014) UCODE 2014, with new capabilities to define parameters unique to predictions , calculate weights using simulated values, estimate parameters with SVD, evaluate uncertainty with MCMC, and More: Integrated Groundwater Modeling Center Report Number: GWMI 2014-02,” GWMI.

Rigo, A., Béjar-Pizarro, M., and Martínez-Díaz, J. (2013) Monitoring of Guadalentín valley (southern Spain) through a fast SAR Interferometry method,” Journal of Applied Geophysics, vol. 91, pp. 39–48.

Winston, R. B. (2009) ModelMuse-A graphical user interface for MODFLOW-2005 and PHAST,” U.S. Geological Survey Techniques and Methods 6-A29, 52 pages.





Deliverable 4.2

PILOT DESCRIPTION AND ASSESSMENT

Magnesian aquifer (United Kingdom)

Authors and affiliation:

**Majdi Mansour, Vasileios
Christelis**

British Geological Survey (BGS)

This report is part of a project that has received funding by the European Union's Horizon 2020 research and innovation programme under grant agreement number 731166.



Deliverable Data	
Deliverable number	D4.2
Dissemination level	Public
Deliverable name	Pilots description and assessment report for recharge and groundwater vulnerability
Work package	WP4
Lead WP	BRGM, BGS
Deliverable status	
Version	Version 3
Date	23/3/2021

[This page has intentionally been left blank]

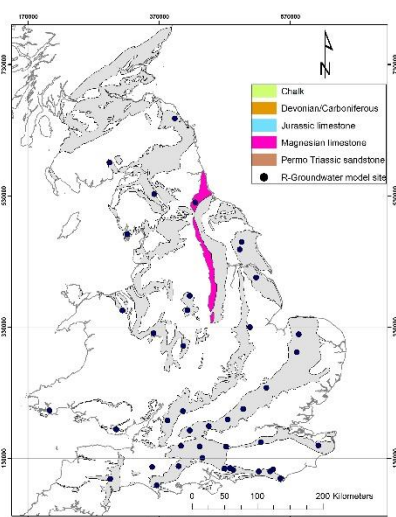
LIST OF ABBREVIATIONS & ACRONYMS

BGS	British Geological Survey
CC	Climate Change
EU	European Union
FAO	Food and Agriculture Organization
GCM	Global Circulation Models
GSO	Geological Survey Organization
ISIMIP	Inter Sectoral Impact Model Inter-comparison Project
NSE	Nash-Sutcliffe Efficiency
PET	Potential Evapo-Transpiration
R	Regression coefficient error
WP	Work Package

TABLE OF CONTENTS

LIST OF ABBREVIATIONS & ACRONYMS	5
1 EXECUTIVE SUMMARY	5
2 INTRODUCTION	7
3 PILOT AREA	9
3.1 Site description and data	9
3.1.1 Index boreholes in the Magnesian aquifer in the UK	9
3.1.2 Topography	11
3.1.3 Land use	12
3.1.4 Rainfall	13
3.1.5 Potential evaporation	14
3.1.6 Hydrogeology	15
3.1.7 Groundwater levels	16
3.2 Climate change challenge	16
4 METHODOLOGY	18
4.1 Methodology and climate data	18
4.1.1 AquiMod	18
4.1.2 Metran	18
4.1.3 The distributed recharge model ZOODRM applied at the UK scale	19
Climate data	20
4.2 Model set-up	21
4.2.1 AquiMod	21
4.2.2 Metran	23
4.2.3 National scale model (ZOODRM)	23
4.3 Model calibration	25
4.3.1 Calibration of AquiMod models	25
4.3.2 Calibration of Metran models	27
4.3.3 Calibration of the UK national scale model using ZOODRM	28
5 RESULTS AND CONCLUSIONS	29
5.1 Historical recharge values	29
5.2 Projected recharge values	31
REFERENCES	37
APPENDICES	39
Appendix A: AquiMod methodology	39
The soil moisture module	40
The unsaturated zone module	41
The saturated zone module	41
Limitations of the model	43
Model input and output	43
Appendix B: Metran methodology	45
Limitations	46
Time step	46
Model output	46
Model quality	47
Recharge	47

1 EXECUTIVE SUMMARY

Pilot name	Magnesian limestone aquifer	
Country	United Kingdom	
EU-region	North-western Europe	
Area (km ²)	NA	
Aquifer geology and type classification	Consists of massive dolomitic and reef limestones with marls, sandstones and breccias. It is up to 300 m thick. Typical yields up to 50 l/sec from the upper parts the water is typically very hard.	
Primary water usage	Irrigation / Drinking water / Industry	
Main climate change issues	Risk of high precipitation causing groundwater flooding. Risk of drought.	
Models and methods used	Lumped groundwater modelling (AquiMOD)	
Key stakeholders	Government. Research institutes. Water companies.	
Contact person	British Geological Survey. Andrew McKenzie	

This report describes the work undertaken by the British Geological Survey (BGS/UKRI) as a part of TACTIC WP4 to calculate historical and future groundwater recharge across the outcrop of Magnesian limestone aquifer including the analysis of groundwater levels at one borehole located within this aquifer. Multiple tools, selected from the TACTIC toolbox that is developed under WP2 of the TACTIC project, have been used for this purpose.

The Magnesian Limestone aquifer occupies a narrow north–south outcrop from Sunderland in the north to Nottingham to the south. The permeability of the aquifer is extremely variable due to fracturing. The Magnesian Limestone outcrop is relatively low lying but it presents an escarpment in some areas. The dominant land use is arable. At the observation borehole studied here, the aquifer is always under confined conditions. Generally the importance of the Limestone as an aquifer decreases southwards despite the existence of some abstractions

Three tools have been used to estimate the recharge values. These are the lumped parameter computer model *AquiMod* (Mackay et al., 2014a), the transfer function-noise model *Metran* (Zaadnoordijk et al., 2019), and the distributed recharge model is developed *ZOODRM* (Mansour and Hughes, 2004). Future climate scenarios are developed based on the ISIMIP (Inter Sectoral Impact Model Inter-comparison Project (www.isimip.org) datasets. The resolution of the data is 0.5°x0.5° global grid and at daily time steps. As part of ISIMIP, much effort has been made to standardise the climate data (e.g. bias correction).

The estimation of the recharge model using the lumped model *AquiMod* is achieved by running the model in Monte Carlo mode. This produces many runs that are equally acceptable and consequently the uncertainty in the estimated recharge values can be assessed. The application of additional tools provides an additional mean to assess this uncertainty. Model output at the borehole studied here show a difference between the 75th and 25th percentile recharge values of approximately 36%, which indicates a relatively high degree of uncertainty. The recharge value estimated using the distributed recharge model is approximately 1.5 higher than that estimated using the lumped model. It must be noted that the distributed recharge model calculates potential recharge while the lumped model calculates actual recharge. The absolute recharge value calculated by the transfer function-noise model *Metran* is found to be different, more than double, from that calculated by the lumped model.

Future recharge values calculated using the projected rainfall and potential evaporation values are -6.3 to 17.7% different from historical values on average. The 3° Max scenario, the wettest used in this work, produces values that are very different from the historical ones. This is observed in the output of both the lumped and the distributed models. Finally, future estimates are discussed in this report using long term average recharge values. It is recommended to carry out further analysis to these output in order to understand the temporal changes in recharge values in future, especially over the different seasons. In addition, it is recommended that the values and conclusion produced from this work should be compared to those obtained from different studies that applies future climate data obtained from different climate models.

2 INTRODUCTION

Climate change (CC) already has widespread and significant impacts on Europe's hydrological systems including groundwater bodies, which is expected to intensify in the future. Groundwater plays a vital role for the land phase of the freshwater cycle and has the capability of buffering or enhancing the impact from extreme climate events causing droughts or floods, depending on the subsurface properties and the status of the system (dry/wet) prior to the climate event. Understanding the hydrogeology is therefore essential in the assessment of climate change impacts. Providing harmonised results and products across Europe is further vital for supporting stakeholders, decision makers and EU policies makers.

The Geological Survey Organisations (GSOs) in Europe compile the necessary data and knowledge of the groundwater systems across Europe. To enhance the utilisation of these data and knowledge of the subsurface system in CC impact assessments, the GSOs, in the framework of GeoERA, has established the project "Tools for Assessment of Climate change Impact on Groundwater and Adaptation Strategies – TACTIC". By collaboration among the involved partners, TACTIC aims to enhance and harmonise CC impact assessments and identification and analyses of potential adaptation strategies.

TACTIC is centred around 40 pilot studies covering a variety of CC challenges as well as different hydrogeological settings and different management systems found in Europe. Knowledge and experiences from the pilots will be synthesised and provide a basis for the development of an infrastructure on CC impact assessments and adaptation strategies. The final projects results will be made available through the common GeoERA Information Platform (<http://www.europe-geology.eu>).

The specific TACTIC activities focus on the following research questions:

- What are the challenges related to groundwater- surface water interaction under future climate projections (TACTIC WP3)?
- Estimation of renewable resources (groundwater recharge) and the assessment of their vulnerability to future climate variations (TACTIC WP4).
- Study the impact of overexploitation of the groundwater resources and the risks of saline intrusion under current and future climates (TACTIC WP5).
- Analyse the effectiveness of selected adaptation strategies to mitigate the impacts of climate change (TACTIC WP6).

This report describes the work undertaken by the British Geological Survey (BGS/UKRI) as a part of TACTIC WP4 to calculate groundwater recharge at selected locations within the Magnesian aquifer. WP4 is divided into seven tasks that cover the following activities: Review of tools and methods and identification of data requirements (Task 4.1), identification of principal aquifers and their characteristics aided by satellite data (Task 4.2), recharge estimation and its evolution under climate change scenarios in the principal aquifers (Task 4.3), analysis of long-term piezometric time series to evaluate aquifer vulnerability to climate change (Task 4.4), assessment of subsidence in aquifer systems using DInSAR satellite data (Task 4.5), development

of a satellite based net precipitation and recharge map at the pan-European scale (Task 4.6), and tool descriptions and guidelines (Task 4.7).

The work presented here is related to Task 4.3 that aims at the estimation of recharge under current and future climates. This is undertaken using multiple tools selected from the TACTIC toolbox that has been developed under WP2 of the TACTIC project. The toolbox is a collection of groundwater models, scripts, spreadsheets that serves all the activities identified in TACTIC workpackages. Here we use the lumped groundwater model *AquiMod* (Mackay et al., 2014a and Mackay et al., 2014b) and the Transfer Function-Noise Model *Metran* (Zaadnoordijk et al., 2019) with main challenge to calibrate these models to reproduce the behaviour of the observed groundwater level time series. The calibrated models are then used to calculate historical and future recharge values. In addition to these two models, we apply the UK national scale recharge model (Mansour et al., 2018) to validate the calculated recharge values and also to address the uncertainty associated with the calculation of these values.

3 PILOT AREA

3.1 Site description and data

3.1.1 *Index boreholes in the Magnesian aquifer in the UK*

The Magnesian Limestone aquifer occupies a narrow north–south outcrop from Sunderland in the north to Nottingham to the south (Figure 1). To the north, the Magnesian Limestone aquifer is divided into three units. These are the Lower, Middle, and Upper Magnesian limestones. The lower and middle units are locally separated from the Upper Limestone by marls and siltstones. To the south it is divided into two units: the Upper and Lower Magnesian limestones, which are separated by marls and siltstones.

In Durham to the north, the Middle Magnesian Limestone is more porous than the Upper and Lower Magnesian Limestones; however, and due to fracturing, the permeability of the whole aquifer is extremely variable. Surface and groundwater flow are interconnected where drift is thin or absent (Allen et al., 1996).

Table 1 shows the location of the only observation borehole in the Magnesian aquifer that is currently included in the analysis. A lumped groundwater model is built to estimate the recharge values at this borehole.

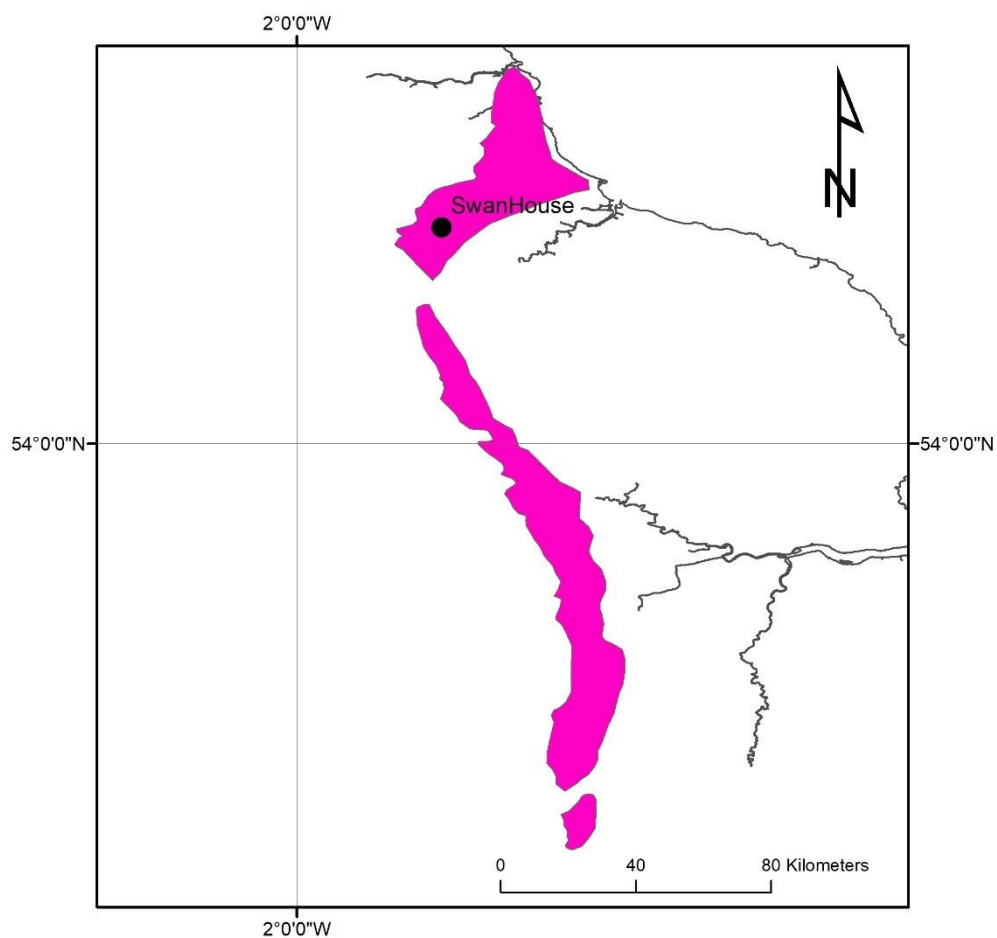


Figure 1. Extent of the Magnesian aquifer.

Table 1. Description of observation borehole

Borehole name	Location	GWs record	Hydrogeological response
Swan House	North of England	1969-current	Water levels are confined. The hydrograph has an annual sinusoidal pattern, fluctuating around 5 metres annually. There appears to be a clear response to major recharge events, with distinct peaks in wetter years

3.1.2 Topography

The Magnesian Limestone outcrop is relatively low lying and, along with the Triassic sandstones and mudstones, separates the upland areas of the Pennines from the North York Moors. In the Durham Province, the Magnesian Limestone presents an escarpment that rises from sea level in the east to approximately 180 m above sea level at its western extent. In the Yorkshire Province the outcrop is around 40 m above sea level. To the west of the Magnesian Limestone outcrop, the Carboniferous Coal Measures, Limestone and Millstone Grit rise to >800 m above sea level, forming the Pennines.

The main rivers in the area (Rivers Tyne, Wear and Tees) flow eastwards towards the sea from their sources in the Pennines. The other significant river in the area is the River Skerne. This rises in the Trimdon Hills and flows in a south-south-westerly direction until its confluence with the River Tees, which then flows eastwards to the sea. The River Skerne flows almost entirely over Magnesian Limestone strata and has a good hydraulic connection with the groundwater (Bearckock and Smedley, 2009).

Topographical data can be extracted at the selected boreholes to study the occurrences flooding events under future climate conditions.

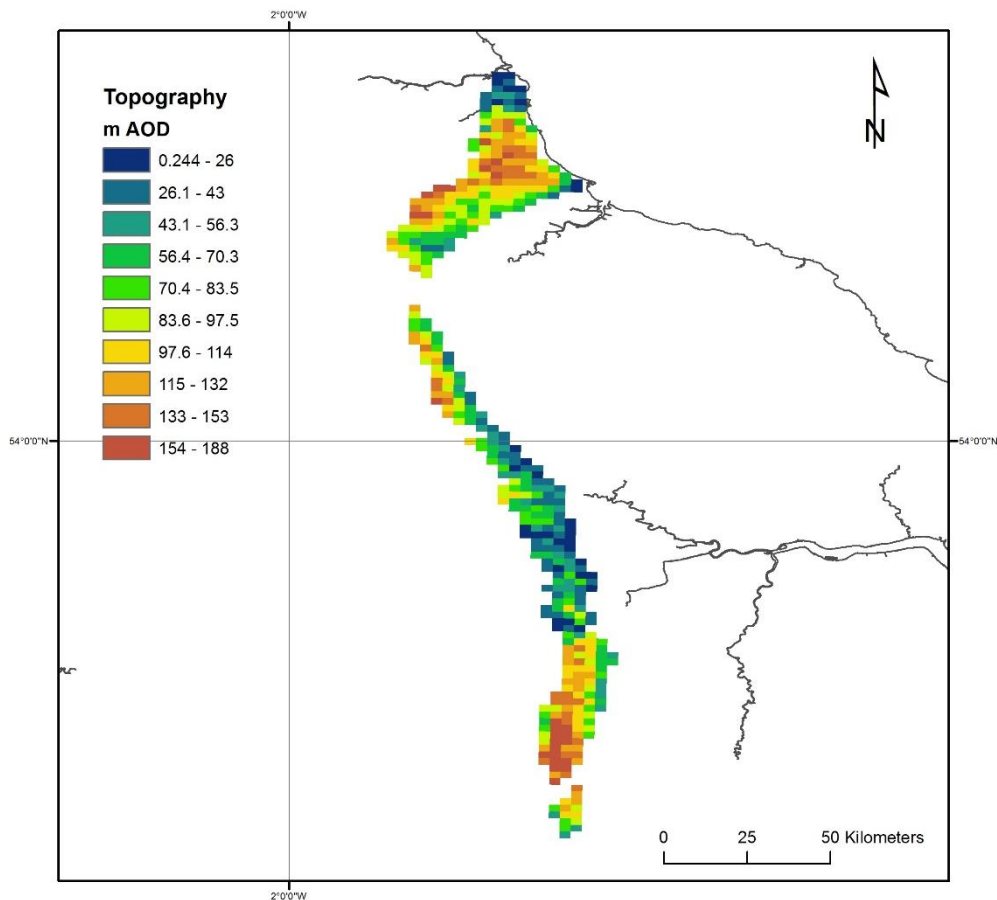


Figure 2. Topography map over the Magnesian formation

3.1.3 Land use

The dominant land use over the Magnesian aquifer outcrop is arable especially cereals. Non-arable vegetation is more abundant in the south than in the north. There exists patches of managed grassland. There are several urban areas indicated by the dark red pixels in Figure 3 but Middlesbrough and Newcastle urban areas dominate the part to the north of the outcrop.

Figure 3 shows the spatial distribution of landuse classes over the Magnesian outcrop (Bibby, 2009). Landuse data can be extracted from this map at the selected boreholes to specify the model parameters that control evapo-transpiration, which is an important component of the total water balance produced by the applied models. Specific information about the landuse types at the borehole within this aquifer are listed in Table 2.



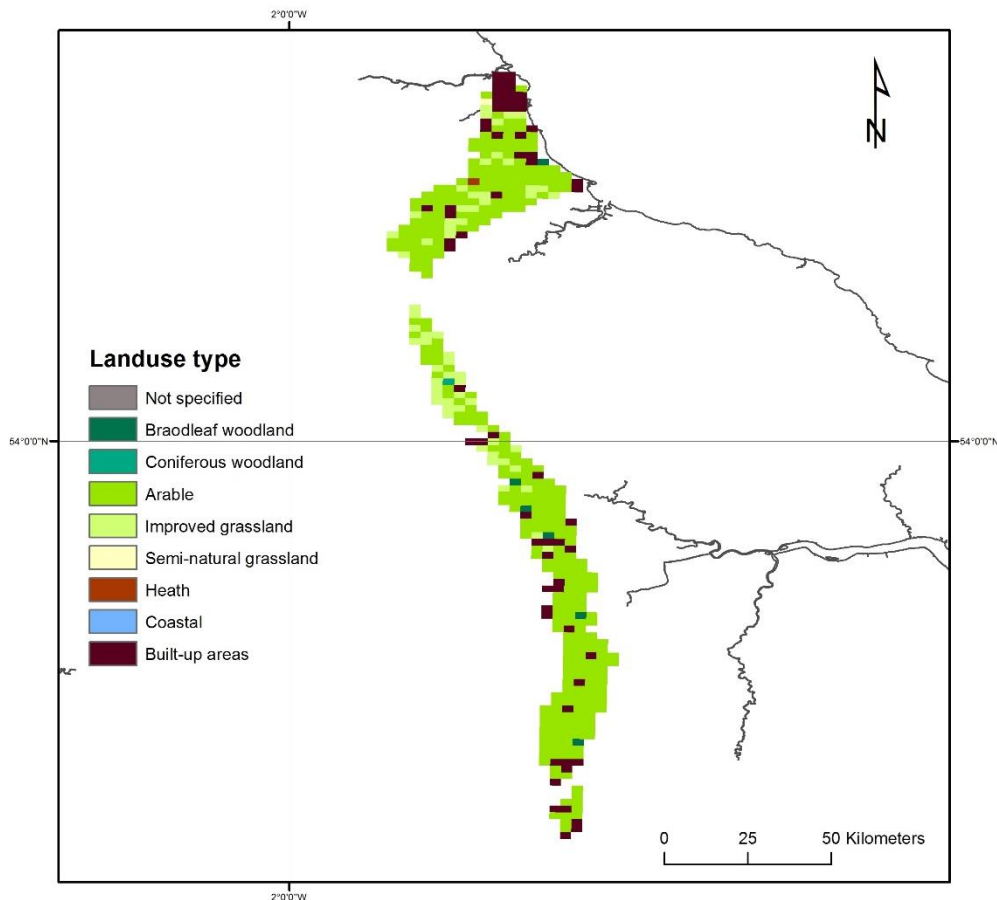


Figure 3. Map of land use over the Magnesian formation

3.1.4 Rainfall

Daily rainfall raster data (1×1 km) were obtained from the Centre for Ecology and Hydrology (CEH) and were used to retrieve the daily rainfall values at the grid nodes pertain to the Magnesian aquifer. The long-term average (LTA) rainfall across the outcrop is approximately 664 mm year^{-1} (1.82 mm day^{-1}) with lowest rainfall values approximately 591 mm year^{-1} (1.62 mm day^{-1}) observed at the centre of the outcrop and highest of approximately 840 mm year^{-1} (2.3 mm day^{-1}) in the north and south areas of the Magnesian aquifer outcrop (Figure 4).

Spatially distributed rainfall data are available at daily time steps starting from 1961 to 2016 (CEH). While the size of this time step is coarse to represent storm events for hydrological analysis, it is fine enough to calculate recharge values to drive groundwater models. These data are, therefore, used to drive the lumped models. Table 2 presents specific information about the rainfall values at the selected Magnesian boreholes.

Projected (future) values of rainfall data are also available by the work of UKCP09 (Prudhomme et al., 2012; Murphy et al, 2007; Jenkins et al., 2009; Murphy et al, 2009), which provides projections of climate change in the UK. The probabilistic climate projections provided by UKCP09 are not fully spatially coherent; however, (IPCC, 2000) produced 11 physically plausible



simulations, generated under the medium emissions scenario known as A1B SRES emission scenario, that overcome this problem. These data can be used for the estimation of projected (future) recharge values.

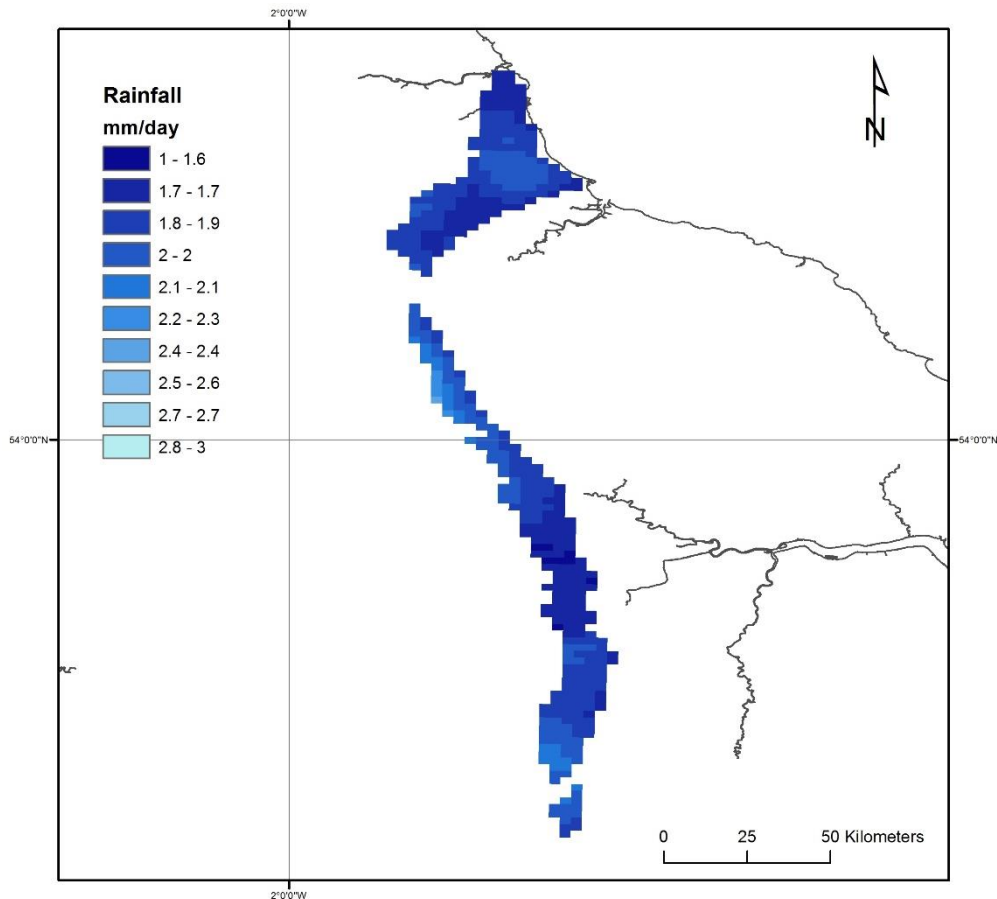


Figure 4. Spatial distribution of rainfall over the Magnesian aquifer outcrop

3.1.5 Potential evaporation

The monthly potential evapotranspiration (PE) raster datasets (40×40 km) were gathered from a Met Office Rainfall and Evaporation Calculation System (MORECS) in the Met Office of the UK (Hough and Jones 1997). Figure 5 shows the distributed long-term average potential evaporation data. The average potential evaporation recorded over the Magnesian aquifer outcrop is 530 mm year^{-1} (1.45 mm day^{-1}). Highest potential evaporation rates of approximately 686 mm year^{-1} (1.88 mm day^{-1}) are observed at the centre of the aquifer outcrop. Lowest potential evaporation rates of approximately 430 mm year^{-1} (1.18 mm day^{-1}) are observed to the north and the south of the outcrop (Figure 5). Table 2 presents specific information about the PE records at the selected boreholes in the Magnesian aquifer.

Similar to rainfall data, UKCP09 potential evaporation data can be used to run simulations to calculate future recharge values.



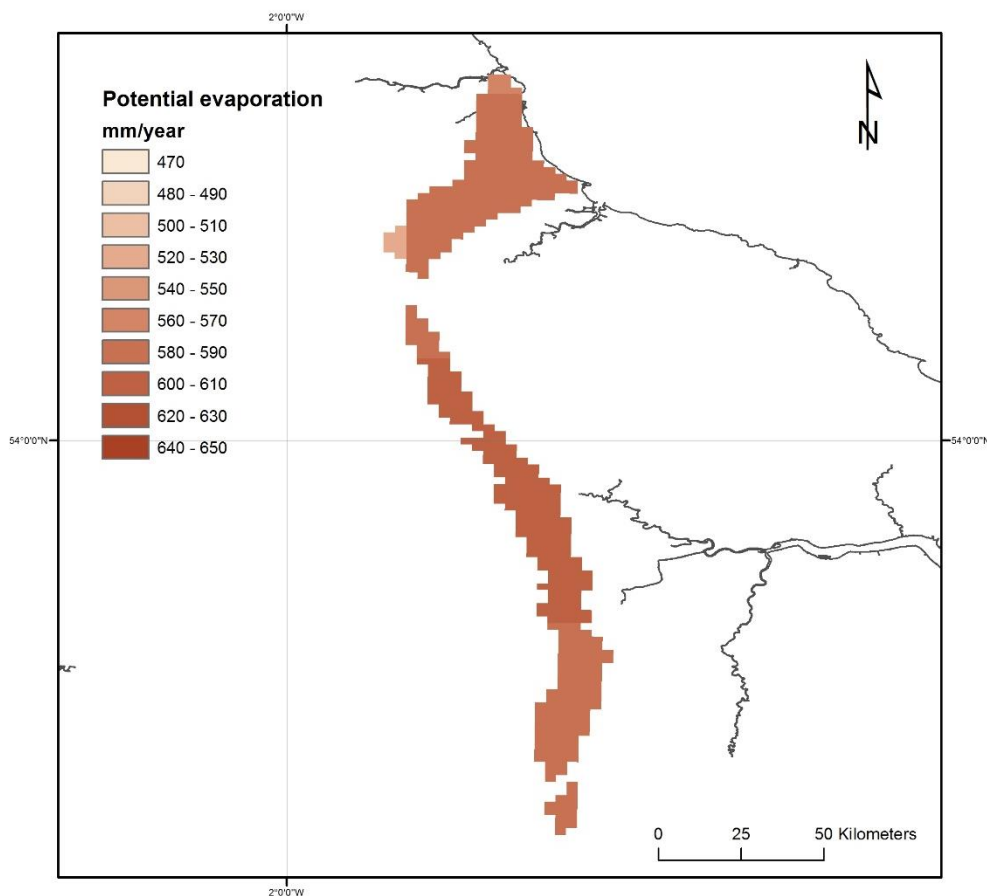


Figure 5. Spatial distribution of potential evaporation in the Magnesian aquifer

Table 2. Landuse, rainfall and evapotranspiration information for the Magnesian aquifer

Borehole name	Dominant landuse	Av. Rainfall (mm/day)	Rainfall record	Av. PE (mm/day)	PE record
Swan House	Arable	1.77	1961-current	1.58	1961-current

3.1.6 Hydrogeology

The hydrogeology of the Magnesian Limestone aquifer is controlled by lithology and structure. However, fracturing is the main control on the aquifer properties and as a consequence, aquifer properties are extremely unpredictable. While the transmissivity of the aquifer depends on fracturing, there is some intergranular storage.

The Middle Permian Marl functions as a 'leaky' aquitard and thus generally maintains a slight head difference between the Upper and Middle and/or Lower Magnesian limestones. The

Middle Magnesian Limestone to the north is generally thought to be the best prospect for groundwater development in the due to the presence of reef complexes, which are frequently permeable. In other places, the Lower and Upper Magnesian limestones may have substantial transmissivities where the fracture frequency is high. Small dry caves are recorded in the Lower Magnesian Limestone, which may locally influence the aquifer characteristics when they are phreatic.

The aquifer is developed for public supply in the north. Further south towards Nottingham there is a lateral facies variation. The Upper Magnesian Limestone wedges out and the Middle and Lower Permian Marls become more sandy and pass up into the Permo-Triassic sandstones. Generally the importance of the Limestone as an aquifer decreases southwards despite the existence of some abstractions.

3.1.7 Groundwater levels

At Swan House observation borehole, the aquifer is always under confined conditions. The piezometric head, however, reaches an elevation of approximately 90 m AOD, which is approximately 5 m below the ground surface (94.9 m AOD).

These time series recorded at this observation borehole are used in this study to characterise the aquifer properties and to estimate the infiltration recharge values for water resources management.

The groundwater level hydrograph at Swan House borehole shows a pattern that appear to be superimposed on longer term fluctuations possibly related to industrial abstraction. Pumping data are available on a daily basis and these can be included in the simulations if necessary.

3.2 Climate change challenge

The British Geological Survey (BGS) with the support of the Environment Agency (EA) have undertaken a study to investigate the impact of climate change on groundwater resources using the distributed recharge model ZODRM (Mansour and Hughes, 2018). Potential recharge values for Great Britain (England, Scotland and Wales) are produced using rainfall and potential evaporation data from the Future Flows Climate datasets (11 ensembles of the HadCM3 Regional Climate Model or RCM). This study has shown that generally the recharge season appears to be forecast to become shorter, but with greater amount of recharge “squeezed” into fewer months. This conclusion is aligned with the European Environment Agency map that describes the expected climate change across the different areas in Europe as shown in Figure 6.

The shortening of recharge season indicates that aquifers may become more vulnerable to droughts if rainfall fails in one or two months rather than a prolonged dry winter as can occur now. At the very least water management measures have to be put in place to account for

periods when recharge volumes reduce. On the other hand, the increased recharge signal could result in flashier groundwater level response and potentially leading to more flooding.

The main climate challenge for water resources managers and stakeholders is to assess the risk of future flooding and drought events. This requires detailed assessment of the variation of resources at regional and local scales rather than national or continental scales.

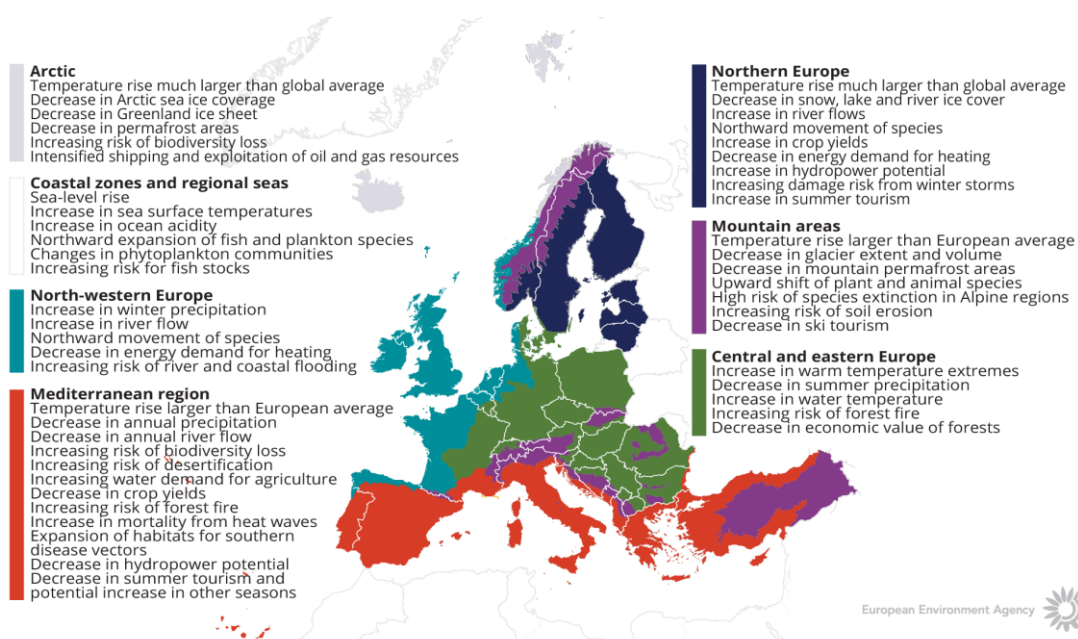


Figure 6. How is climate expected to change in Europe. The European Environment Agency map

4 METHODOLOGY

4.1 Methodology and climate data

4.1.1 *AquiMod*

AquiMod is a lumped parameter computer model that has been developed to simulate groundwater level time series at observational boreholes (Mackay et al., 2014a). It is based on hydrological algorithms that simulate the movement of groundwater within the soil zone, the unsaturated zone, and the saturated zone. The lumped models neglect complexities included in distributed groundwater models but maintain some of the fundamental physical principles that can be related to the conceptual understanding of the groundwater system (Mackay et al., 2014b).

The primary aim of AquiMod is to capture the behaviour of a groundwater system through the analysis of the available groundwater level time series. Once calibrated the model can be run in predictive mode and be used to fill in gaps in historical groundwater level time series and to calculate future groundwater levels. In addition to groundwater levels, it also provides predictions of historical and future recharge values and groundwater discharges.

The mathematical equations that are used to simulate the movement of groundwater flows within the three modules are detailed in Appendix A. The model uses rainfall and potential evaporation time series as forcing data. These are interpreted by the soil module representing the soil zone. The soil module calculates the rainfall infiltration and pass it to the unsaturated zone module. This module delays the arrival of the infiltrating water to the saturated zone module. The latter calculates the variations of groundwater heads and flows accordingly.

The model is calibrated using a Monte Carlo approach. It compares the simulated and observed groundwater level fluctuations and calculates a goodness of fit. The AquiMod version used in this work employs the Root Square Mean Error (RMSE) or the Nash Sutcliffe (NSE) performance measures to assess the performance of the model. The user sets a threshold value to accept all the models that perform better than the specified threshold. The possibility of producing many models that are all equally acceptable, allows the user to interpret the results from all these models and calculate uncertainty.

The recharge values calculated from AquiMod are those that reach the aquifer system and drive the groundwater levels. Thus, it is assumed that these are the actual recharge values as defined in the guidance report prepared by TACTIC project.

4.1.2 *Metran*

Metran applies a transfer function-noise model to simulate the fluctuation of groundwater heads with precipitation and evaporation as independent variables (Zaadnoordijk et al., 2019). The modelling approach consists mainly of two impulse functions and a noise model. The first impulse function is used for convolution with the precipitation to yield the precipitation contribution to the piezometric head. The second is for evaporation which is either a separately estimated function, or a factor times the function used for precipitation. The noise model is a

stochastic noise process described by a first-order autoregressive model with one parameter and zero mean white noise. Further information about the model is given in Appendix B with the model setup shown in the Figure B1.

Metran allows the addition of other processes affecting the behaviour of the groundwater heads, for example pumping or the presence of surface features such as rivers. The contributions from these processes are added to the deterministic part of the model.

Metran has been designed to work with explanatory series that have a daily time step. However, it has been adapted so that other time step lengths can be applied. However, the explanatory variables must still have a constant frequency.

The model is calibrated automatically; however, the model uses two binary parameters, Regimeok and Modok, to judge a resulting time series model. Regimeok cross-examines the explained variance R^2 (> 0.3), the absolute correlation between deterministic component and residuals (< 0.2), and the null hypothesis of non-correlated innovations (p value > 0.01). If all these criteria are satisfied, Regimeok returns a value of 1 indicating highest quality. Modok also cross-examines the explained variance R^2 (> 0.1) and the absolute correlation between deterministic component and residuals (< 0.3) as well as the decay rate parameter (> 0.002) and if all these criteria are satisfied, it is given a value of 1. If Modok = 1 and Regimeok = 0, the model is still considered acceptable. If both these parameters are 0, the model quality is insufficient and the model is rejected.

Metran's time series model is linear and the model creation fails when the system is strongly nonlinear. It is also limited to the response function being appropriate for the simulated groundwater system. Metran uses a gradient search method in the parameter space, so it can be sensitive to initial parameter values in finding an optimal solution.

The model calculates an evaporation factor f that gives the importance of evapotranspiration compared to precipitation. It is possible to use this factor to calculate the recharge values as shown by Equation B2 in appendix B. However, it must be noted that the use of Equation B2 is based on too many assumptions that are easily violated. Because of this, the equations should be applied only to long-term averages using only models of the highest quality.

Following the definitions used in the TACTIC project (See the guidance report), this recharge quantity corresponds to the effective precipitation. It is equal to the potential recharge when the surface runoff is negligible. This in turn is equal to the actual recharge at the groundwater table if there is also no storage change or interflow.

4.1.3 The distributed recharge model ZOODRM applied at the UK scale

A distributed recharge model, ZOODRM, has been developed by the British Geological Survey to calculate recharge values required to drive groundwater flow simulators. This recharge model allows grid nesting to increase the resolution over selected area and is called therefore the zooming object-oriented distributed recharge model (ZOODRM) ((Mansour and Hughes, 2004). The model can implement a number of recharge calculation methods that are suitable for



temperate climates, semi-arid climates, or for urban areas. One of the methods that is implemented is the recharge calculation method used by Aquimod and detailed in Appendix A1.

ZOODRM uses a Cartesian grid to discretise the study area. It reads daily rainfall and potential evaporation data in time series or gridded format and calculates the recharge and overland flow at a grid node using a runoff coefficient as detailed in appendix A1. However, since this is a spatially distributed model, it reads a digital terrain model and calculates the topographical gradients between the grid nodes. It then uses the steepest gradient to route the calculated surface water downstream until a surface feature, such as a river or a pond, is reached. While the connections between the grid nodes based on the topographical gradients define the water paths along which surface water moves, major rivers are also user-defined in the model. This allows the simulation of river water accretion on a daily basis and the production of surface flow hydrograph. The model is then calibrated by matching the simulated river flows at selected gauging stations to the observed flows, by varying the values of the runoff coefficients.

The procedure used to calibrate the model involves dividing the study area into a number of zones and then to specify runoff values for each one. It is possible to vary the runoff coefficient values on a seasonal basis by using different runoff values for the different months of the year.

The recharge model ZOODRM calculates rainfall infiltration after accounting for evapo-transpiration and soil storage. The simulated infiltration may not reach the aquifer system as it may travel laterally within the soil and discharge into surface water features away from the infiltration location. The simulated infiltration is therefore considered, as potential recharge according to the definitions of recharge processes provided by the guidance report prepared by TACTIC project.

Climate data

The TACTIC standard scenarios are developed based on the ISIMIP (Inter Sectoral Impact Model Intercomparison Project, see www.isimip.org) datasets. The resolution of the data is 0.5°x0.5° global grid and at daily time steps. As part of ISIMIP, much effort has been made to standardise the climate data (e.g. bias correction). Data selection and preparation included the following steps:

1. Fifteen combinations of RCPs and GCMs from the ISIMIP data set were selected. RCPs are the Representative Concentration Pathways determining the development in greenhouse gas concentrations, while GCMs are the Global Circulation Models used to simulate the future climate at the global scale. Three RCPs (RCP4.5, RCP6.0, RCP8.5) were combined with five GCMs (noresm1-m, miroc-esm-chem, ipsl-cm5a-lr, hadgem2-es, gfdl-esm2m).
2. A reference period was selected between 1981 – 2010 and an annual mean temperature was calculated for the reference period.
3. For each combination of RCP-GCM, 30-years moving average of the annual mean temperature were calculated and two time slices identified in which the global annual mean temperature had increased by +1 and +3 degree compared to the reference period, respectively. Hence, the selection of the future periods was made to honour a

- specific temperature increase instead of using a fixed time-slice. This means that the temperature changes are the same for all scenarios, while the period in which this occurs varies between the scenarios.
4. To represent conditions of low/high precipitation, the RCP-GCM combinations with the second lowest and second highest precipitation were selected among the 15 combinations for the +1 and +3 degree scenario. This selection was made on a pilot-by-pilot basis to accommodate that the different scenarios have different impact on the various parts of Europe. The scenarios showing the lowest/highest precipitation were avoided, as these endmembers often reflect outliers.
 5. Delta change values were calculated on a monthly basis for the four selected scenarios, based on the climate data from the reference period and the selected future period. The delta change values express the changes between the current and future climates, either as a relative factor (precipitation and evapotranspiration) or by an additive factor (temperature).
 6. Delta change factors were applied to local climate data by which the local particularities are reflected also for future conditions. These monthly values (one set of rainfall and PE for each warming scenario) are used to drive the groundwater models presented in this report.

For the analysis in the present pilot the following RCP-GCM combinations were employed:

Table 3. Combinations of RCPs-GCMs used to assess future climate

		RCP	GCM
1-degree	"Dry"	rcp6p0	noresm1-m
	"Wet"	rcp4p5	miroc-esm-chem
3-degree	"Dry"	rcp4p5	hadgem2-es
	"Wet"	rcp8p5	miroc-esm-chem

4.2 Model set-up

4.2.1 *AquiMod*

The boreholes located in the Magnesian aquifer are listed in Table 1. Aquimod model setup relies mainly on two input files. The first input file "Input.txt" is a control file where the module types and model structure are defined. Aquimod is executed first under a calibration mode where a range of parameter values of the different selected modules are given in corresponding text files and a Monte Carlo approach is used to select the parameter values that yield best model performance. "Input.txt" also controls the mode under which Aquimod is executed, the number of Monte Carlo runs to perform, the number of models to keep with an acceptable performance, and the number of runs to execute in evaluation mode.

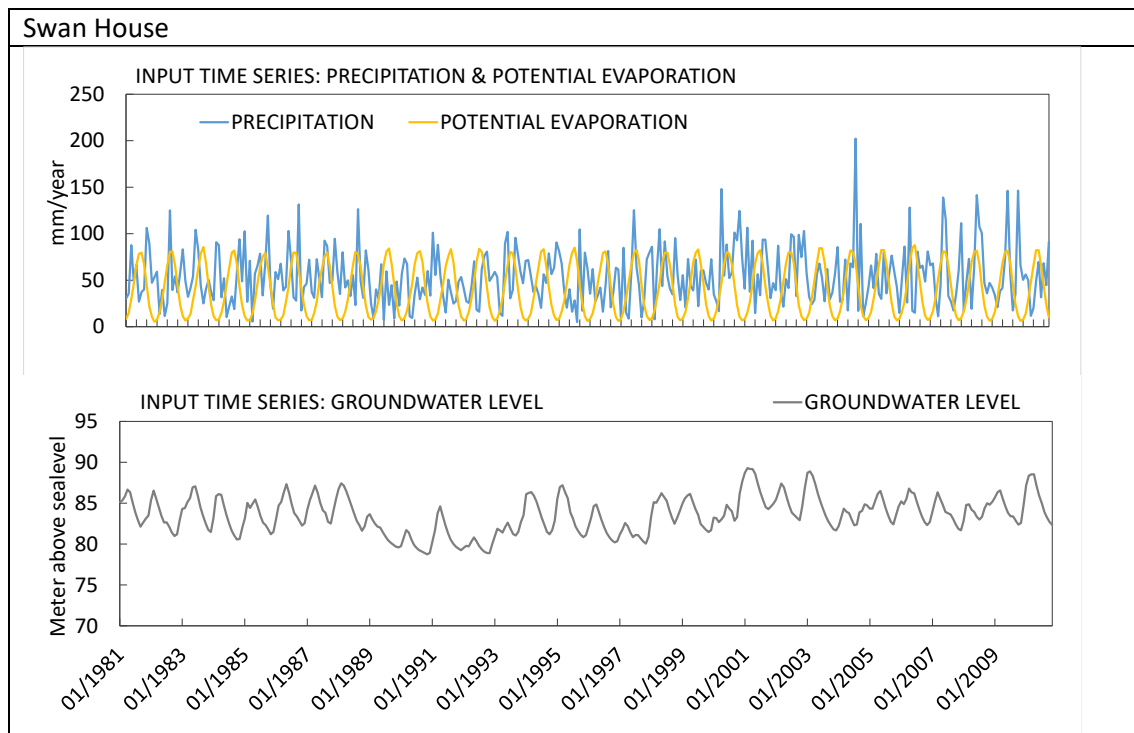
The second file Aquimod uses is called "observations.dat". This file holds the forcing data mainly the potential evaporation and rainfall. However, it is also possible to include the anthropogenic impact on groundwater levels by including a time series of pumping data in this file. None of the boreholes studied here includes pumping data. The observed groundwater levels that are used



for model calibration are also given in this file. The data are provided to the model on a daily basis, and this forces Aquimod to run using a time step length of one day. Table 4 shows daily time series of rainfall and potential evaporation values (mm/month) as well as the fluctuations of water table at the different boreholes.

All Aquimod models built for the boreholes in Table 1 use the FAO Drainage and Irrigation Paper 56 (FAO, 1988) method in the soil module, and employ the two-parameter Weibull probability density function to control the movement of infiltrated water in the unsaturated zone (Appendix A1). However, the groundwater module structures vary between the different boreholes. The best groundwater module structure is found by trial and error during the calibration process. The simplest structure, one layer with one discharge feature, is selected first and then the complexity of the module structure is increased gradually to see if the model performance improves. The structure with best model performance is selected to undertake the recharge calculations. The structures selected for these boreholes are mainly of one layer or three layered systems.

Table 4 Figures showing time series of daily rainfall and potential evaporation values (mm/month) as well as the fluctuations of water table at the different boreholes.



4.2.2 Metran

Metran applies transfer function noise modelling with daily precipitation and evaporation as input and of groundwater levels as output (Zaadnoordijk et al., 2019). The setup is shown in Figure 7. If time series of other influences on the groundwater head are available, these contributions can be added to the deterministic part of the model. An input file that holds the daily information of precipitation, potential evaporation and groundwater levels is prepared for each borehole in Table 1. Plots of these data are shown in Table 4. It must be noted that, while the groundwater levels used in AquiMod and shown in Table 4 have missing values, these have to be provided as complete time series to Metran. To achieve this, a linear interpolation procedure is used to fill in the missing values in the groundwater level time series. Once executed, it calculates the characteristics of the impulse functions and the corresponding parameters automatically.

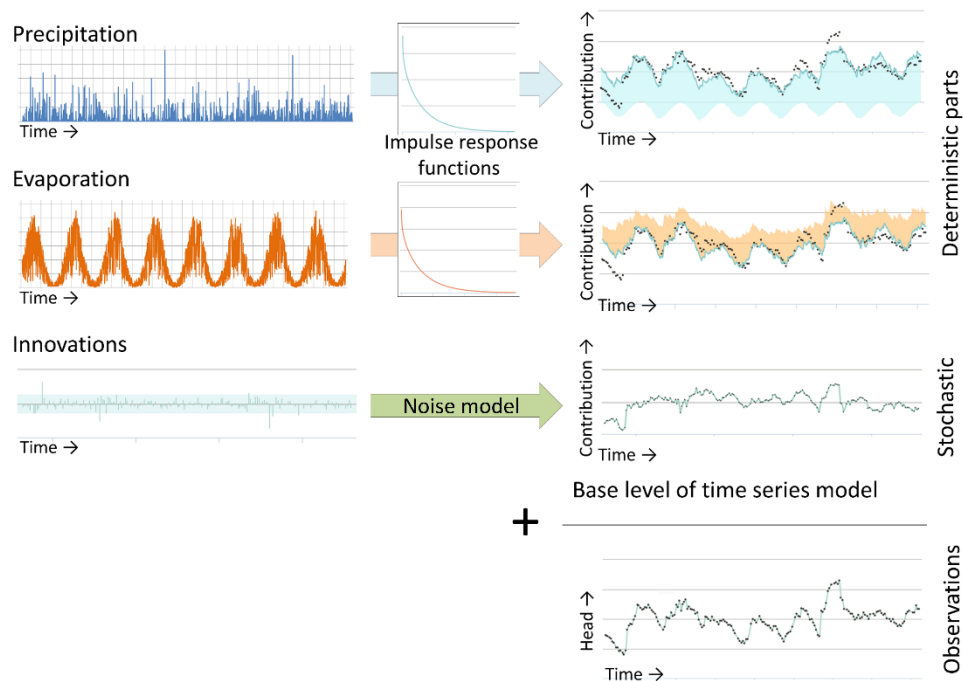


Figure 7 Illustration of METRAN setup

4.2.3 National scale model (ZOODRM)

The distributed recharge model (ZOODRM) is applied at national over the British Mainland (England, Scotland, and Wales) (Figure 8) using a Cartesian grid with 2 km square cells. The model reads a text file that defines the locations of the grid nodes as well as the connections between the nodes. This text file is prepared using a specific tool, called ZETUP (Jackson, 2004), where the extent of the study area is defined using the coordinates of the lower left and upper right corners of a rectangle that covers the modelled area. The spacing between the nodes and



the information that dictate the boundary of the irregular shape of the area are also given in this file. This tool also uses a file that contains the locations of the nodes as obtained from a geographical information system tool (GIS) and converts this information into a text file that describes the river extents and characteristics.

The map defining the runoff zones is based on the hydrogeology of the study area. It is produced in gridded ascii format using the hydrogeological map available for Great Britain. Additional text files, one for each runoff zone, are also prepared to define the monthly runoff values.

The topographical information is also provided in a gridded ascii format for the model to calculate the topographical gradients between the nodes. While a surface water routing procedure that accounts for indirect recharge and surface water storage is available in the model, this is not used in the current application. It is assumed that all the water originated at one grid nodes travel downstream and reaches a discharging feature in one day, which is equal to the length of the time step used.

Landuse data (Section **Error! Reference source not found.**) and soil data that are required to calculate the water capacity at every grid node are also provided to the model using maps in gridded ascii format. A set of landuse gridded maps, a total of ten, are used to give the percentage of landuse type at any given location. The gridded soil map gives the soil type at a selected location. The landuse type and soil type ids are linked to text files that hold the corresponding information such as the soil moisture at saturation, the soil moisture at wilting and the root constants can be obtained.

The driving data are provided to the model as daily gridded rainfall data (Sections **Error! Reference source not found.**) and time series of monthly potential evaporation values as described in (Section **Error! Reference source not found.**). Mansour et al. (2018) provide a full description of the construction of this model together with a more detailed description of the data used. The calculated recharge values are also provided in the published work; however, it must be noted that the historical recharge values shown in this work are simulated over the period from 1981 to 2010 in order to be consistent and comparable with the recharge values calculated by AquiMod and Metran. In addition, in this study, the model is rerun using the climate change data specifically provided by the TACTIC project to calculate the projected distributed recharge values.

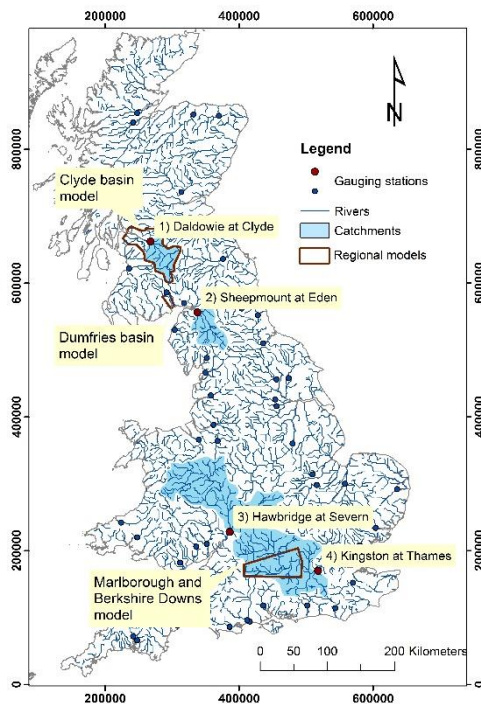


Figure 8. Extent of the UK national scale recharge model in UK national grid reference after Mansour et al. (2018). Figure also shows the locations of the gauging stations downstream of the major rivers used for model calibration.

4.3 Model calibration

4.3.1 Calibration of *AquiMod* models

The calibration of *AquiMod* is performed automatically using the Monte Carlo approach. The user populates the files of the selected modules with minimum and maximum parameter values and then the model randomly selects a value from the specified range for any given run. The selection of the minimum and maximum values is physically based depending on the characteristics of the study area. For example, the minimum and maximum values of the root depth in the soil module are set to 15 cm and 60 cm respectively for a study area covered with grass, while these values are set to 120 cm and 200 cm for a woodland area. The storage coefficients bounds of a groundwater module are set to much lower values in a confined aquifer compared to those used for an aquifer under unconfined conditions.

A conceptual hydrogeological understanding must be available before the use of *AquiMod*, since this is necessary to set the limits of the parameter values for the calibration process. In some cases, it is not possible to obtain a good performing model with the selected values and that necessitates the relaxation of these parameters beyond the limits informed by the conceptual



understanding. In such cases, the parameter values must feed back into the conceptual understanding if better performing models are obtained.

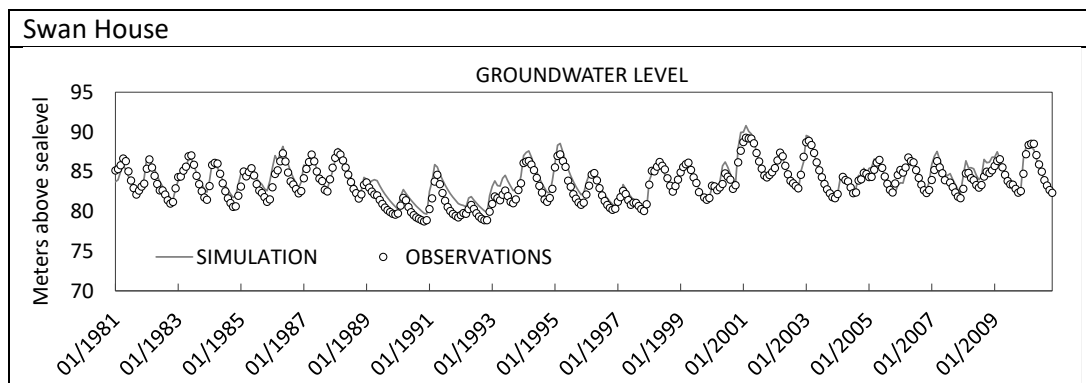
AquiMod execution time is relatively small, which allows the calibration of the model using hundreds of thousands of runs in couple of hours. The performance measure used to assess the quality of the simulation is the Nash Sutcliffe Error (Appendix A) that takes a maximum value of unity for a perfect match between the simulated and observed data. The threshold at which models are accepted is set to a value of 0.6. All the models that achieve an NSE higher than 0.6 are included in the analysis but a maximum number of 1000 runs are used if the number of acceptable models is greater than 1000.

Table 5 shows the best NSE values obtained for the Swan House borehole. It is clear that a good match was achieved between the simulated and observed groundwater levels as illustrated in the plots shown in Table 6. The best performing model is the AquiMod model achieved an NSE value of 0.83.

Table 5 Nash Sutcliff Error measure at the Magnesium Limestone boreholes

Borehole name	NSE
Swan House	0.83

Table 6 Comparison between the simulated and observed groundwater levels at the Magnesium Limestone observation boreholes.



4.3.2 Calibration of Metran models

For the standard setup with precipitation and evaporation, there are five parameters that have to be determined during the calibration of the model. Three parameters are related to the precipitation response, the evaporation factor, and the noise model parameter (Appendix B). There are three extra parameters for each additional input series, such as pumping. The parameter optimization of Metran uses a gradient search method in the parameter space to reach a global minimum. As explained in Appendix B, two parameters indicate if Metran succeeded with producing a match between the simulated and observed data. These are called the Regimeok and Modok. When Regimeok is equal to one, the calibration is of highest quality. If Modok is equal to one and Regimeok is equal to zero, the calibration is of acceptable quality. Finally, if both parameters are equal to zero, the calibration quality is insufficient.

Time series of rainfall, potential evaporation and groundwater levels are provided to Metran on a monthly basis. Metran input data must be complete dataset, i.e. without missing data. To overcome this problem that may exist in the groundwater level time series, these data are aggregated to monthly values first and then missing values were filled using linear interpolation. Table 7 shows the performance of Metran across the Magnesium Limestone boreholes considered in this study. It is clear that according to criteria set above, Metran fails to produce a model at four boreholes but succeeds at the seven other boreholes with the model output showing highest quality at four of these boreholes (with highest value of R^2).

Table 7 Performance of Metran across the selected Magnesium Limestone borehole.

Borehole name	Metran performance parameter Modok	Metran performance parameter Regimeok	Overall quality	R2	RMSE
Swan House	1	0	Acceptable	0.77	1.11

4.3.3 Calibration of the UK national scale model using ZOODRM

Model calibration of the national scale recharge model was based on the comparison of the simulated long-term average overland flows to the observed ones (Mansour et al., 2018) recorded at gauging stations of selected major rivers (Figure 8). However, additional checks were also undertaken to assess the performance of the model. These include checking the match between the seasonal overland flow volumes at four boreholes, shown in red in Figure 8, checking the calculated recharge volumes with those calculated by other tools over selected catchment areas, and checking the temporal fluctuations of soil moisture deficit with those calculated by other tools. Figure 9 shows a Q plot for the simulated versus observed long term average runoff values at the 56 gauging stations shown in Figure 8. The solid line shows the one to one match and the dotted line shows the linear relationship between the two datasets.

It must be noted that while this model uses the same recharge calculation methods used by AquiMod, these two models are calibrated using different datasets, with AquiMod using the groundwater levels and the distributed recharge model using the overland flows.

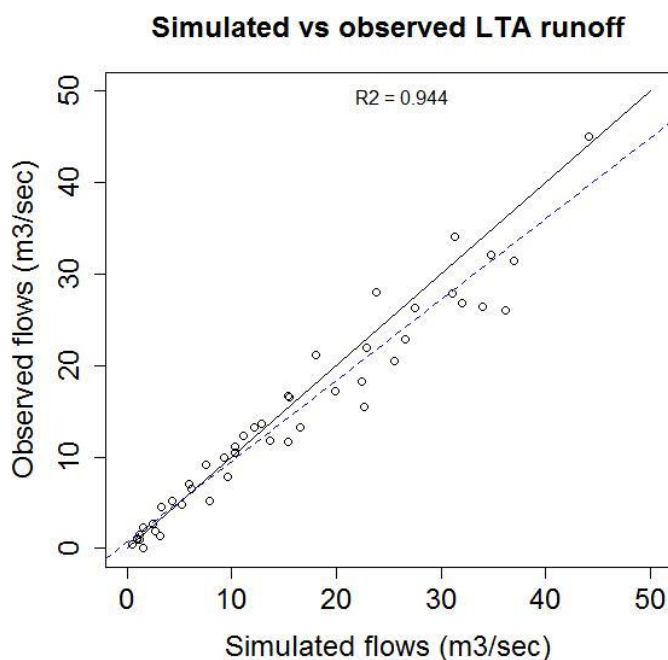


Figure 9 Q plot for the simulated vs observed long term average runoff values at the 56 gauging stations shown in Figure 8 after Mansour et al. (2018)

5 RESULTS AND CONCLUSIONS

5.1 Historical recharge values

Table 8 shows the time series of the historical recharge values calculated using the Aquimod model at the Swan House borehole in the Magnesian limestone aquifer. The plots in this table also show the 10th percentile, the mean, and the 90th percentile of recharge values calculated from the time series.

As mentioned Appendix B, the formulas used by Metran are based on assumptions that can be violated and it is better to use the infiltration coefficient f_c with the long-term average values of rainfall and potential evaporation to calculate long-term average values of recharge and using only models of the highest quality. Time series of recharge values are not produced, therefore, from the analysis undertaken using Metran. The long-term average recharge values calculated using Metran are shown in Table 9.

One of the benefits of running Aquimod in Monte Carlo mode is the possibility of producing many models with acceptable performance. Consequently, the recharge values estimated from these models are all equally likely. This provides us with a range of recharge values at each borehole that reflects the uncertainty of the optimised hydraulic parameter values. In the current study, the long-term average recharge values are calculated from up to 1000 acceptable models if they exist at each borehole; otherwise, all the acceptable models are used. The mean, 25th and 75th percentiles are then calculated from these long-term recharge values and displayed in Figure 10. It is clear that the differences between the 75th and 25th percentile values is approximately 2.5 mm/month, however, this is a considerable difference noting that the 25th and percentile recharge value is approximately 5 mm/month.

In addition to the recharge values calculated using Aquimod, Figure 10 shows the recharge values calculated using Metran and the distributed national scale model at these boreholes. In this particular case, Aquimod estimated average recharge value is smaller than that estimated using the distributed national scale model. It must be noted that the recharge values calculated by these two models are of different types. The distributed recharge model calculates potential recharge and Aquimod calculates actual recharge and this may explain the calculated difference. Metran estimated recharge value at Swan House is greater than both values calculated by the Aquimod and by the national scale recharge model Figure 10.

Metran estimates an upper and a lower value for the infiltration coefficient f_c . This can be used as an indication of uncertainty associated with the calculated f_c value. These bounds are also shown in Table 9. The estimated upper and lower bound values at Swan House are equal to 0.67, which is very close to the estimated f_c value of 0.87. This highlights a relatively large recharge value uncertainty bound and applying the lower bound for example, put the Metran estimated recharge value in the same range as those calculated by Aquimod.

Table 8 Time series of recharge values obtained from the best performing AquiMod models at the Magnesium Limestone boreholes

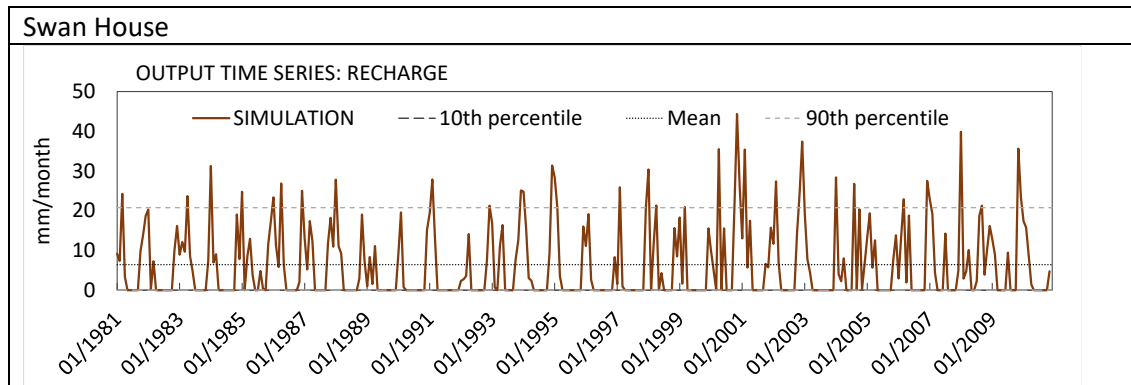


Table 9 Recharge values calculated using the recharge factors estimated by Metran

Borehole name	Average precipitation (mm/month)	Average potential evaporation (mm/month)	Recharge factor	Recharge (mm/month)
Swan House	53.72	40.22	0.87+- 0.67	18.73

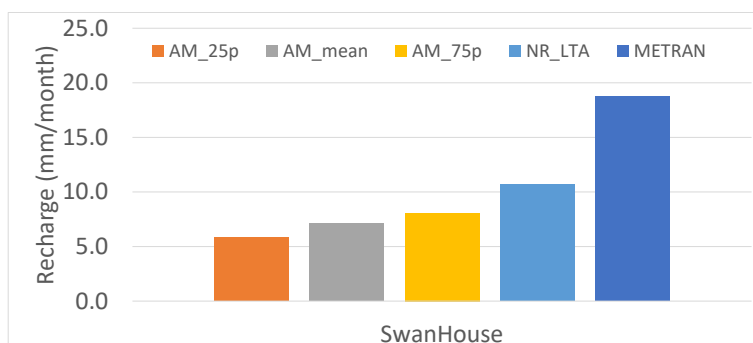


Figure 10 Historical recharge values calculated by AquiMod, Metran, and the national scale recharge model.

5.2 Projected recharge values

The forcing data, rainfall and potential evaporation, are altered using the change factors of the climate models (see Section **Error! Reference source not found.**). For the United Kingdom, there are two sets of monthly change factors, one used with the data driving Aquimod and Metran (Table 10), and the other used to calculate the spatially distributed recharge (Table 11). These change factors are used as multipliers to both the historical rainfall and potential evaporation values.

For the application involving Aquimod, these factors are used to alter the time series of historical rainfall and potential evaporation values used to drive the model.

When using Metran, the historical time series are altered using these factors first and then the long-term average rainfall and potential evaporation values are calculated. The recharge coefficient f_c values of the different boreholes, as calculated from the calibration of Metran model using the historical data, are then applied to calculate the projected long-term average recharge values.

The distributed recharge model ZODRM includes the functionality of using these change factors to modify the historical gridded rainfall and potential evaporation data before using them as input to calculate the recharge. In this case, and for any simulation date, the rainfall and potential evaporation change factors for the month corresponding to the date, are used to modify all the spatially distributed historical rainfall and potential evaporation values respectively.

Table 10 Monthly change factors as multipliers used for the borehole data

	Scenario	Jan	Feb	Mar	Apr	May	Jun	Jul	Aug	Sep	Oct	Nov	Dec
Rainfall	1° Min	1.087	0.956	0.994	1.072	0.888	0.909	0.836	0.988	1.017	1.106	0.962	1.031
	1° Max	1.140	1.012	1.033	1.045	1.022	0.863	1.086	0.953	0.995	1.067	1.148	1.053
	3° Min	0.936	1.056	0.994	1.153	1.063	0.900	0.846	0.721	0.854	0.970	1.047	1.116
	3° Max	1.191	1.177	0.989	1.014	0.949	0.986	1.473	1.145	1.173	1.074	1.152	1.112
PE	1° Min	1.082	1.082	1.062	1.089	1.091	1.061	1.078	1.083	1.082	1.063	1.049	1.076
	1° Max	1.049	0.993	1.014	1.007	1.019	1.013	1.021	1.015	1.029	1.028	1.020	1.026
	3° Min	1.034	1.057	1.039	1.056	1.060	1.086	1.085	1.091	1.109	1.097	1.064	1.066
	3° Max	1.072	1.070	1.055	1.071	1.105	1.106	1.072	1.083	1.082	1.076	1.072	1.060

Table 11 Monthly change factors as multipliers used for the distributed recharge model

	Scenario	Jan	Feb	Mar	Apr	May	Jun	Jul	Aug	Sep	Oct	Nov	Dec
Rainfall	1° Min	1.086	0.953	0.975	1.064	0.918	0.914	0.856	0.973	1.008	1.103	0.976	1.038
	1° Max	1.132	1.090	1.008	0.899	1.034	1.087	1.310	0.983	1.020	1.006	1.012	1.025
	3° Min	1.156	1.118	1.033	1.011	0.914	0.821	0.908	0.656	0.821	0.986	0.980	1.181
	3° Max	1.192	1.131	0.960	0.990	0.899	0.957	1.437	1.109	1.134	1.068	1.139	1.106
PE	1° Min	1.081	1.081	1.059	1.089	1.091	1.061	1.078	1.083	1.085	1.063	1.049	1.076
	1° Max	1.051	1.036	1.020	1.039	1.051	1.049	1.031	1.043	1.054	1.039	1.044	1.034
	3° Min	1.016	1.031	1.021	1.029	1.038	1.029	1.047	1.057	1.059	1.059	1.040	1.045
	3° Max	1.070	1.066	1.051	1.071	1.105	1.106	1.072	1.083	1.083	1.076	1.072	1.060

Figure 11 shows the historical and future long-term average recharge values calculated using the best performing AquMod model. It is clear that the highest reduction in recharge values are observed when the 3° Min rainfall and evaporation data are used, while the highest increase in recharge values are observed when the 3° Max rainfall and potential evaporation data are used. The use of the 1° Min scenario data yields a reduction in recharge values of -10.9%. The use of the 1° Max scenario data yields an increase in recharge values of 9.4%. Table 12 shows the historical and projected recharge values averaged over each month of the year.

Recharge values calculated by Metran and using the future climate data are shown in Figure 12. Similar to the recharge values estimated by AquMod and described above, the projected recharge values estimated by Metran are less than the historical value when the datasets of the 3° Min and the 1° Min data are used. They are larger than the historical values when the 1° Max and 3° Max datasets are used.



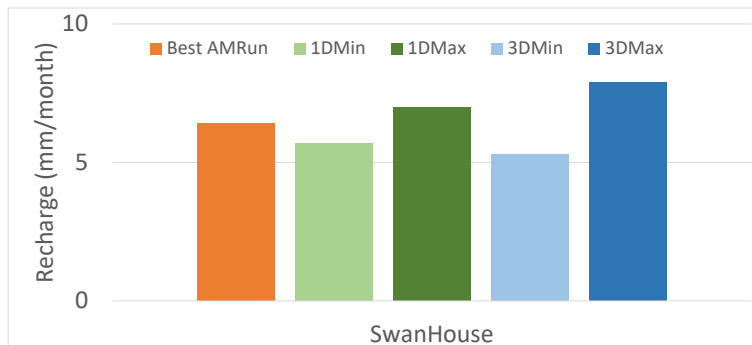


Figure 11 Historical (orange) and future recharge values (blue and green) as produced by the best performing AquiMod model.

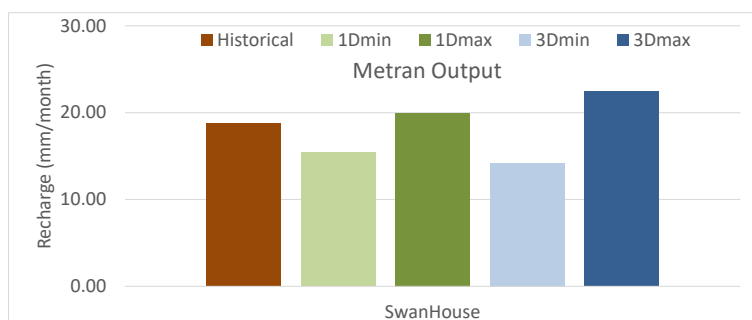


Figure 12 Historical (orange) and future recharge values (blue and green) produced by Metran.

Table 12 Monthly recharge values estimated using the historical and the projected forcing data. Dotted line is the monthly historical recharge values. Green shaded area shows the 1° Min and Max monthly recharge values and the blue shaded area shows the 3° Min and Max monthly recharge values

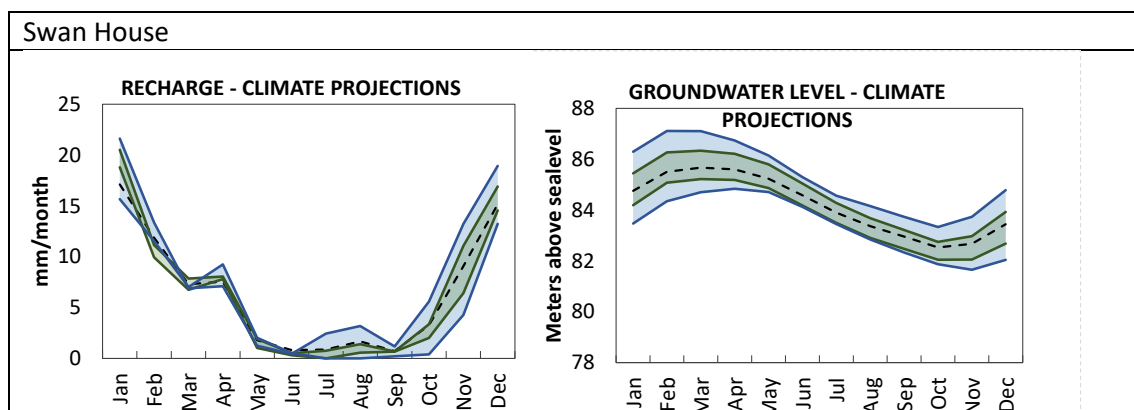


Table 13 shows maps of the spatially distributed recharge values calculated over the Magnesium Limestone aquifer. The plots are for the historical potential recharge values as well as those calculated using the distributed recharge model but with rainfall potential evaporation data altered using the 1° Min, 1° Max, 3° Min, and 3° Max UK change factors. While the differences in the maps are not clear, the maps show that with the 1° Min and 3° Min data, there is drier pattern of recharge across the Magnesian limestone outcrop especially to the north of the outcrop. Conversely, with the 1° Max and 3° Max data, the produced maps show increases in recharge especially at the north of the Magnesian limestone outcrop.

The differences between the simulated future recharge values and the historical ones are shown in the plots in Table 14. While the differences between the future and historical recharge values is between -6% and 6.2%, when the rainfall and potential evaporation data are altered using the 1° Min, 1° Max, and 3° Min change factors, the differences are much more noticeable when the 3° Max change factors are used. In the latter case, the recharge increase is greater than 17% indicating that this is a very wet scenario. However, it must be also noted that on a long term average basis, the 1° Min scenario is looking to be drier than the 3° Min scenario.

Table 15 shows the average, maximum, and the standard deviation values calculated using the pixel values of the maps shown in Table 13. Looking at the average values, it is clear that there is reduction in recharge when the 1° Min or the 3° Min data are used compared to the historical recharge. However, it must be noted that the average recharge value estimated using the 3° Min data used is higher than that estimated using the 1° Min data and this is opposite to what was expected. The maximum of the pixel values of the 1° Min map is higher than the maximum of the pixel values of the 3° Min map as expected. The average recharge values of the pixel values of the 1° Max and 3° Max maps are both higher than the average from the historical map as expected. The maximum value from these two maps are also higher than the maximum obtained from the historical. Finally, there is little difference in the standard deviation values shown in Table 15 indicating that the spatial distribution of recharge values is not notably different between the different scenarios.

Table 13 Spatially distributed historical and projected recharge values

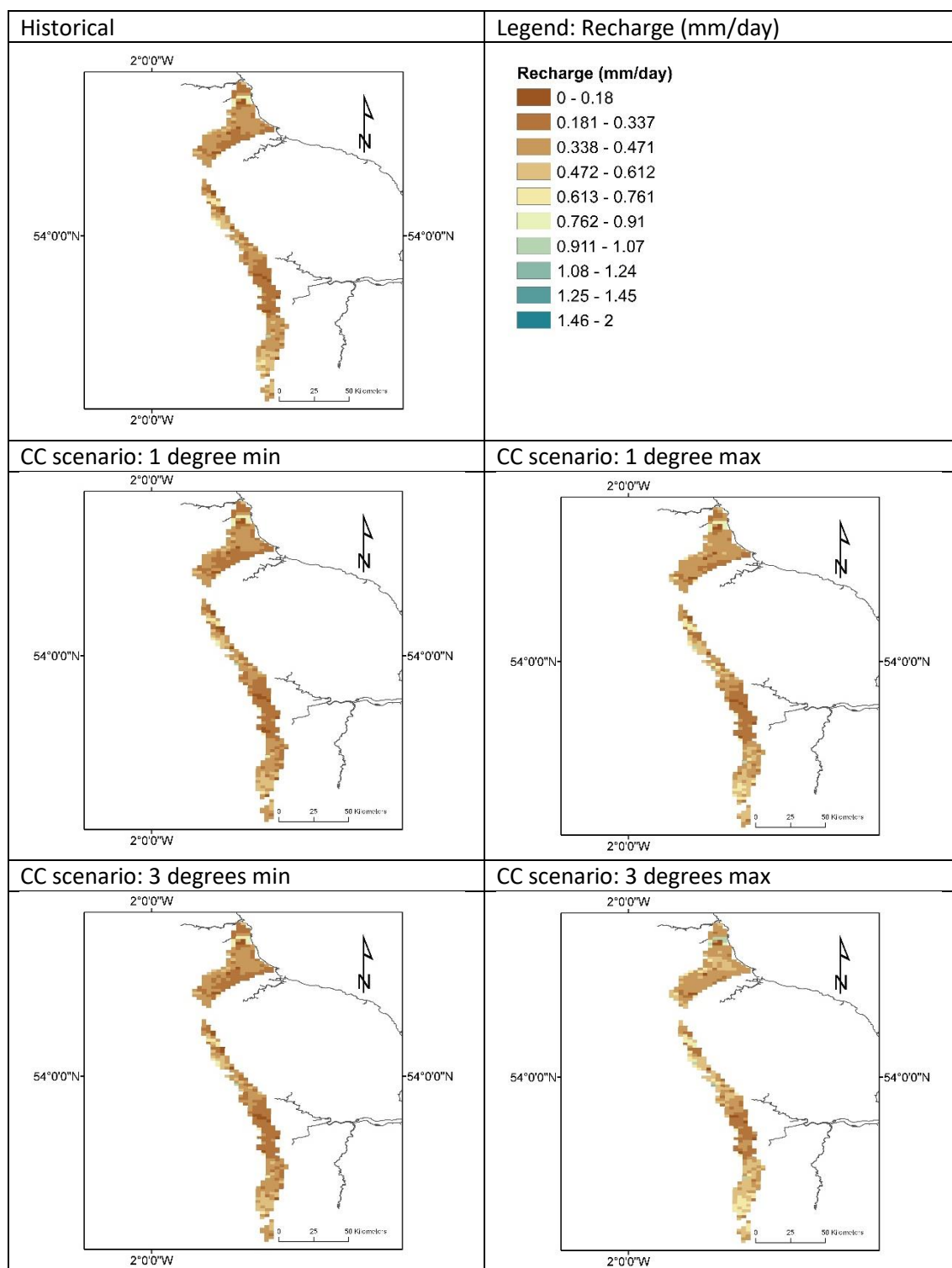


Table 14 Differences between the projected and historical recharge values calculated as projected values minus historical values

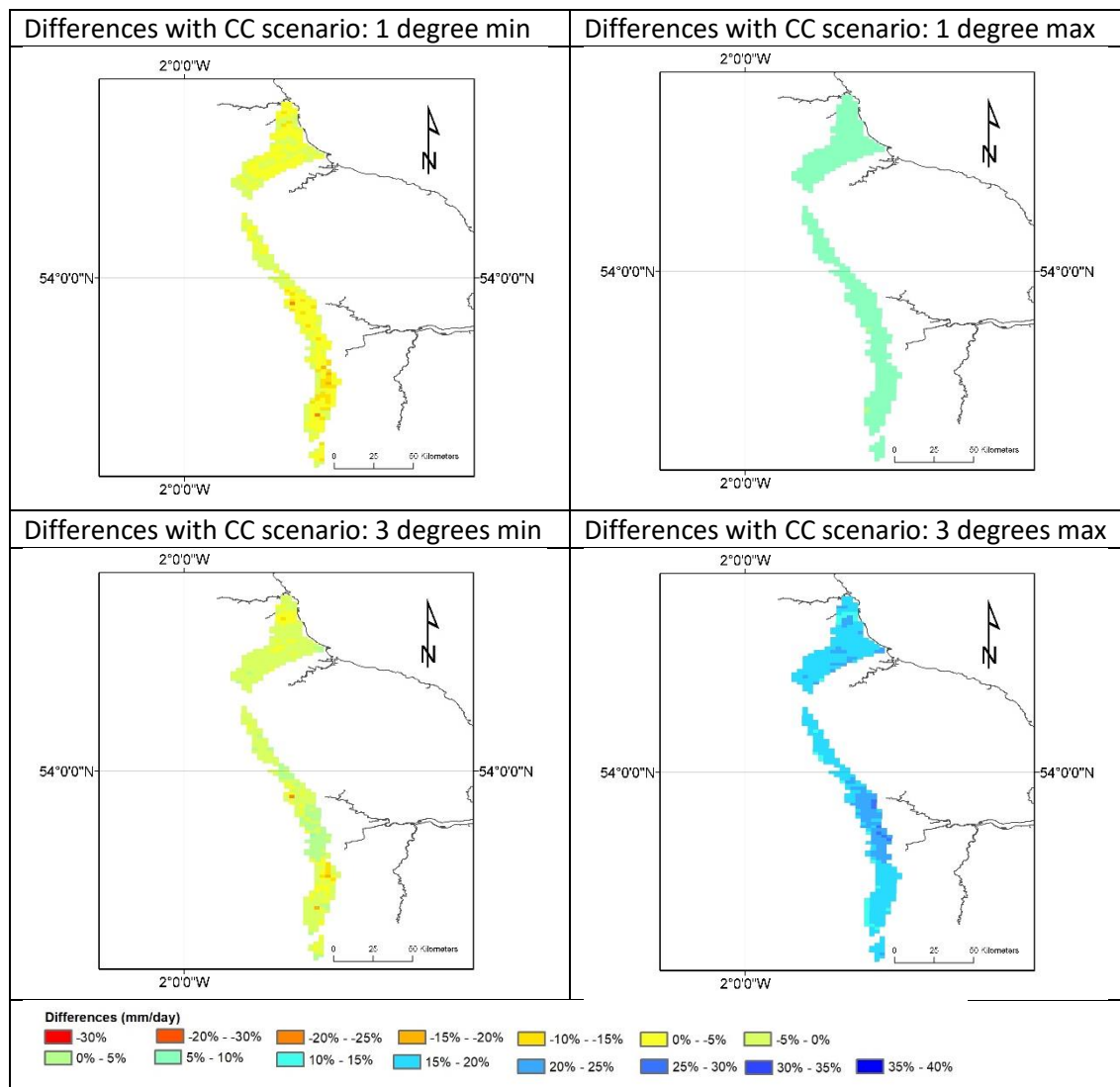


Table 15 Statistical information about the maps shown in Table 13

Map	Average recharge (mm/day)	Maximum recharge (mm/day)	Standard deviation (mm/day)
Historical	0.384	0.974	0.135
CC scenario: 1 degree min	0.361	0.953	0.132
CC scenario: 1 degree max	0.408	1.029	0.142
CC scenario: 3 degrees min	0.374	0.934	0.13
CC scenario: 3 degrees max	0.452	1.092	0.15



REFERENCES

- Allen, D. J., L. J. Brewerton, L. M. Coleby, B. R. Gibbs, M. A. Lewis, A. M. MacDonald, S. J. Wagstaff, A. T. Williams. 1997. 'The Physical Properties of Major Aquifers in England and Wales'.
- Besbes, M. & de Marsily, G. (1984) From infiltration to recharge: use of a parametric transfer function. *Journal of Hydrology*, 74, p. 271-293.
- Hough, M. N. & Jones, R. J. A. 1997. The United Kingdom Meteorological Office rainfall and evaporation calculation system: MORECS version 2.0 – an overview. *Hydrology and Earth System Sciences*, 1, 227–239.
- IPCC: 2000, Special report on emissions scenarios (SRES): A special report of Working Group III of the Intergovernmental Panel on Climate Change, Cambridge University Press, Cambridge, p. 599
- Jenkins, G.J., Murphy, J.M., Sexton, D.S., Lowe, J.A., Jones, P. and Kilsby, C.G. 2009, UK Climate Projections: Briefing report, Met Office Hadley Centre, Exeter, UK.
- Mackay, J. D., Jackson, C. R., Wang, L. 2014. A lumped conceptual model to simulate groundwater level time-series. *Environmental Modelling and Software*, 61. 229-245. <https://doi.org/10.1016/j.envsoft.2014.06.003>
- Mackay, J. D., Jackson, C. R., Wang, L. 2014. *AquiMod user manual (v1.0)*. Nottingham, UK, British Geological Survey, 34pp. (OR/14/007) (Unpublished)
- Mansour, M. M. and Hughes, A. G. 2018. Summary of results for national scale recharge modelling under conditions of predicted climate change. British Geological Survey Internal report. Commissioned Report OR/17/026.
- Mansour, M. M., Wang, L., Whiteman, Mark, Hughes, A. G. 2018. Estimation of spatially distributed groundwater potential recharge for the United Kingdom. *Quarterly Journal of Engineering Geology and Hydrogeology*, 51 (2). 247-263. <https://doi.org/10.1144/qjegh2017-051>
- Murphy, J.M., Booth, B.B.B., Collins, M., Harris, G.R., Sexton, D.M.H., and Webb, M.J. 2007. A methodology for probabilistic predictions of regional climate change from perturbed physics ensembles. *Phil. Trans. R. Soc. A* 365, 1993–2028.
- Murphy, J.M., Sexton, D.M.H., Jenkins, G.J., Boorman, P.M., Booth, B.B.B., Brown, C.C., Clark, R.T., Collins, M., Harris, G.R., Kendon, E.J., Betts, R.A., Brown, S.J., Howard, T. P., Humphrey, K. A., McCarthy, M. P., McDonald, R. E., Stephens, A., Wallace, C., Warren, R., Wilby, R., and Wood, R. A. 2009, 'UK Climate Projections' Science Report: Climate change projections. Met Office Hadley Centre, Exeter.

Obergfell, C., Bakker, M., & Maas, K. (2019). Estimation of average diffuse aquifer recharge using time series modeling of groundwater heads. *Water Resources Research*, 55. <https://doi.org/10.1029/2018WR024235>

Prudhomme, C., Dadson, S., Morris, D., Williamson, J., Goodsell, G., Crooks, S., Boelee, L., Davies, H., Buys, G., Lafon, T. and Watts, G., 2012. Future Flows Climate: an ensemble of 1-km climate change projections for hydrological application in Great Britain. *Earth System Science Data*, 4(1), pp.143-148.

Zaadnoordijk, W.J., Bus, S.A.R., Lourens, A., Berendrecht, W.L. (2019) Automated Time Series Modeling for Piezometers in the National Database of the Netherlands. *Groundwater*, 57, no. 6, p. 834-843. <https://onlinelibrary.wiley.com/doi/epdf/10.1111/gwat.12819>

APPENDICES

Appendix A: AquiMod methodology

AquiMod is a lumped parameter computer model that has been developed to simulate groundwater level time series at observational boreholes (Mackay et al., 2014a). It is based on hydrological algorithms that simulates the movement of groundwater within the soil zone, the unsaturated zone, and the saturated zone. The lumped models neglect complexities included in distributed groundwater models but maintains some of the fundamental physical principles that can be related to the conceptual understanding of the groundwater system (Mackay et al., 2014b).

While AquiMod was originally designed to capture the behaviour of a groundwater system through the analysis of groundwater level time series, it can produce the infiltration recharge values and groundwater discharges from the aquifer as a by-product. AquiMod is driven by complete time series of forcing data for either historical or predicted future conditions. Running AquiMod in predictive mode can be used to fill in gaps in historical groundwater level time series, or calculate future groundwater levels. In addition to groundwater levels, it also provides predictions of historical and future recharge values and groundwater discharges. In the current application we use calibrated AquiMod models to estimate the recharge values at selected boreholes.

AquiMod consists of three modules (Figure A1). The first is a soil water balance module that calculates the amount of water that infiltrates the soil as well as the soil storage. The second module controls the movement of water in the unsaturated zone, mainly it delays the arrival of infiltrating water to the saturated zone. The third module calculates the variations in groundwater levels and discharges. The model executes the modules separately following the order listed above.

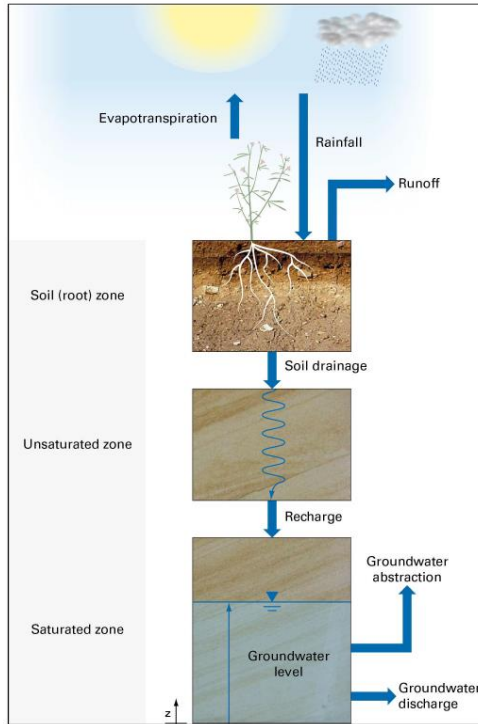


Figure A1 Generalised structure of Aquimod (after Mackay et al., 2014a)

The soil moisture module

There are several methods available in Aquimod that can be used to calculate the rainfall infiltration into the soil zone. In this study we use the FAO Drainage and Irrigation Paper 56 (FAO, 1988) approach. In this method, the capacity of the soil zone, from which plants draw water to evapo-transpire, is calculated first using the plants and soil characteristics. Evapo-transpiration is calculated according to the soil moisture deficit level compared to two parameters: Readily Available Water (RAW) and Total Available Water (TAW). These are a function of the root depth and the depletion factor of the plant in addition to the soil moisture content at field capacity and wilting point as shown in Equations A1 and A2.

$$TAW = Z_r(\theta_{fc} - \theta_{wp})$$

Equation A1

$$RAW = p \cdot TAW$$

Equation A2

Where Z_r [L] and p [-] are the root depth and depletion factor of a plant respectively, θ_{fc} [$L^3 L^{-3}$] and θ_{wp} [$L^3 L^{-3}$] are the moisture content at field capacity and wilting point respectively.

The FAO method is simplified by Griffiths et al. (2006) who developed a modified EA-FAO method. In this method the evapotranspiration rates are calculated as a function of the potential evaporation and an intermediate soil moisture deficit as:

$$\begin{aligned} e_s &= e_p \left[\frac{s_s^*}{TAW - RAW} \right]^{0.2} & s_s^* > RAW \\ e_s &= e_p & s_s^* \leq RAW \\ e_s &= 0 & s_s^* \geq TAW \end{aligned}$$

Equation A3



Where e_s [L] is the evapo-transpiration rate, e_p [L] is the potential evaporation rate and s_s^* [L] is the intermediate soil moisture deficit given by

$$s_s^* = s_s^{t-1} - r + e_p \quad \text{Equation A4}$$

Where r [L] is the rainfall at the current time step and s_s^{t-1} [L] is the soil moisture deficit calculated at the previous time step.

The new soil moisture deficit is then calculated from:

$$s_s = s_s^{t-1} - r + e_s \quad \text{Equation A5}$$

Griffiths et al. (2006) proposed that the recharge and overland flow are only generated when the calculated soil moisture deficit becomes zero. The remaining volume of water, the excess water, is then split into recharge and overland flow using a runoff coefficient. In Aquimod a baseflow coefficient is used to reflect the fact that a groundwater discharge is calculated rather than overland water. In this application, the baseflow coefficient is one minus the runoff coefficient.

The unsaturated zone module

The Aquimod version used in this study to simulate the movement of groundwater flow within the unsaturated zone is based on a statistical approach rather than a process-based approach. This method distributes the amount of rainfall recharge over several time steps where the soil drainage for each time step is calculated using a two-parameter Weibull probability density function. The Weibull function can represent exponentially increasing, exponentially decreasing, and positively and negatively skewed distributions. This can be used to focus the soil drainage over earlier or later time steps or to spread it over a number of time steps after the infiltration occurs. The shape of the Weibull function is controlled by two parameters, k and λ as shown in Equation A6.

$$f(t, k, \lambda) = \begin{cases} \frac{k}{\lambda} \left(\frac{t}{\lambda}\right)^{k-1} e^{-(t/\lambda)^k} & t > 0 \\ 0 & t \leq 0 \end{cases} \quad \text{Equation A6}$$

Where k and λ are two parameters the values of which are calculated during the calibration of the model and t is the time step.

The saturated zone module

Aquimod considers the saturated zone as a rectangular block of porous medium with dimensions L and B as its length and width [L] respectively. This block is divided into a number of layers, each has a defined hydraulic conductivity value, a storage coefficient value, and a discharging feature. The number of layers define the structure of the saturated module used in the study.

The mass balance equation that gives the variation of hydraulic head with time is given by:

$$SLB \frac{dh}{dt} = RLB - Q - A \quad \text{Equation A7}$$

Where:

S is the storage coefficient of the porous medium [-]

h is the groundwater head [L]

t is the time [T]

R is the infiltration recharge [L T⁻¹]



Q is the discharge out of the aquifer [$L T^{-1}$]
 A is the abstraction rate [$L T^{-1}$]

It must be noted that in a multi-layered groundwater system as shown in Figure A2, we calculate one groundwater head (h) for the whole system. The discharges (Q) from Outlet 1, 2, etc. are calculated using the Darcy law. The total discharges can be summarised using the following equation:

$$Q = \sum_{i=1}^m \frac{T_i B}{0.5 L} \Delta h_i \quad \text{Equation A8}$$

Where:

m is the number of layers in the groundwater system [-]

T_i is the transmissivity of the layer i [$L T^{-2}$]

Δh_i is the difference between the groundwater head h and z_i , the elevation of the base of layer i

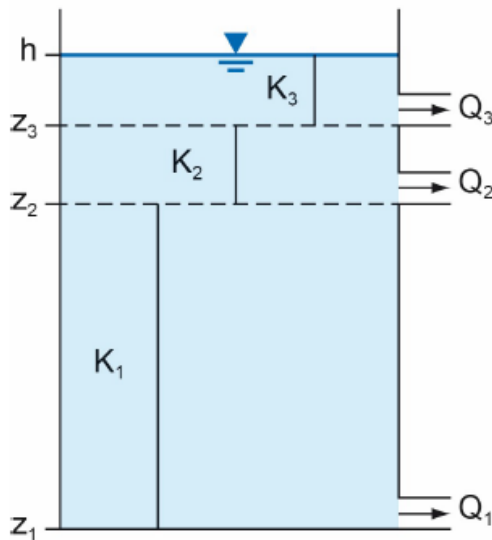


Figure A2 Representation of the saturated zone using a multi-layered groundwater system

Substituting Equation A8 into Equation A7 yields a numerical equation in the form:

$$S \frac{(h-h^*)}{\Delta t} = R - \sum_{i=1}^m \frac{T_i}{0.5 L^2} \Delta h_i - \frac{A}{LB} \quad \text{Equation A9}$$

Equation A9 is an explicit numerical equation that allows the calculation of the groundwater head h [L] at any time and using time steps of Δt [T]. In this equation h^* [L] is the groundwater head calculated at the previous time step and the term Δh_i [L] is calculated as $(h^* - z_i)$.

The terms S , T_i , and L are optimised during the calibration of the model. A groundwater system can be specified with one storage coefficient as shown in the equations above or with different storage coefficient values for the different layers. Several saturated modules are included in Aquimod to provide this flexibility and the model user can select the model structure that represent the conceptual understanding best.



Limitations of the model

AquiMod is a lumped groundwater model that aims at reproducing the behaviour of the observed groundwater levels. It tries to encapsulate the conceptual understanding of a groundwater system in a simple numerical representation. The model results have to be therefore discussed, taking this into consideration. For example, the model represents the groundwater system as a closed homogeneous medium, with no impact from any outer boundary or feature, whether physical or hydrological, such as the presence of rising and falling river stage.

Vertical heterogeneity can be accounted for by using multi-layered groundwater module structure. However, this model setting does not provide any information about the vertical connections between the layers as the discharge from all the layers is calculated using one representative groundwater head value. In other words, it is assumed that all layers are in perfect hydraulic connection.

As mentioned before, the model is designed to simulate the groundwater levels. However, it produces the recharge values and groundwater discharges as by products. In this application we use the calibrated model to calculate recharge. The mass balance equation (Equation A7) shows that recharge is a function of transmissivity and storage coefficient values, which are estimated during the calibration process of the model, i.e. they are not parameters with fixed values provided by the user. The inter-connections between these parameters leads to uncertainties in the estimated recharge values as a high storage coefficient value can produce a high recharge estimate and vice versa. To overcome this problem, it is suggested that the recharge values estimated by AquiMod are always presented as a range of possibilities rather than an absolute value. This can be achieved by estimating the recharge values from all the models that have a performance measure above than a threshold that is deemed acceptable by the user. The recharge estimates can then be presented as an average of all estimates and values corresponding to selected percentiles.

Model input and output

AquiMod includes a number of methods that calculates rainfall recharge as well as a number of model structure from which the user can select what better suits the case study.

Model input consists time series of forcing data including rainfall and potential evaporation, time series of anthropogenic impact mainly groundwater abstraction and time series of groundwater levels that will be used to calibrate the model. These time series must be complete, i.e. a value is available at every time step except the groundwater level time series, which can include missing data. The time step can be one day or multiple of days, and the model automatically calculate the size of the time step based on the input data time series.

The model is run first in calibration mode where a range of parameter values are specified for the different parameters included in the three model modules. A Monte Carlo approach is used to select the best parameter values. The performance of the model is measured by comparing the simulated groundwater levels to the observed ones using the Nash Sutcliffe Efficient (NSE) or

the Root Mean Squared Error (RMSE) performance measures. The parameter set that produces the best model performance is selected to run the model in evaluation mode.

When the model is run in evaluation mode, it produces output files that give recharge values, groundwater levels and groundwater discharges time series with time as specified in the input file. The number of output files is equal to the number of acceptable models set by the user.

Appendix B: Metran methodology

Metran applies transfer function noise modelling of (groundwater head) time series with usually daily precipitation and evaporation as input (Zaadnoordijk et al., 2019). The setup is shown in the Figure B1. If time series of other influences on the groundwater head are available, these contributions can be added to the deterministic part of the model. The stochastic part is the difference between the total deterministic part and the observations (the residuals). The corresponding input of the noise model should have the character of white noise.

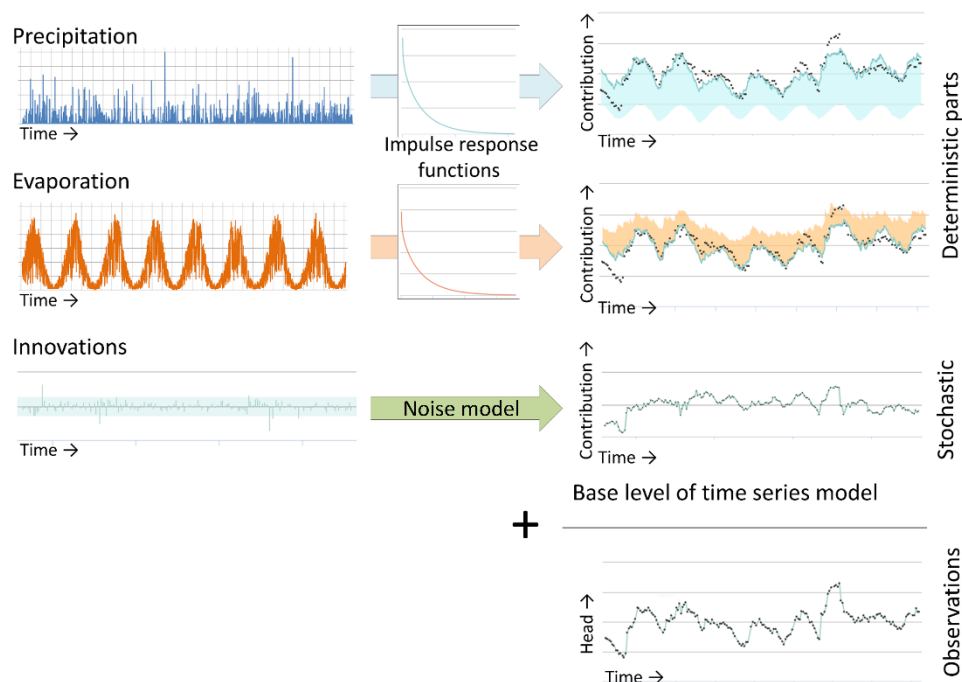


Figure B1 Illustration of METRAN setup

The stochastic part is needed because of the time correlation of the residuals, which does not allow a regular regression to obtain the parameter values of the transfer functions.

The incomplete gamma function is used as transfer function. This is a uni-modal function with only three parameters that has a quite flexible shape and has some physical background (Besbes & de Marsily, 1984). The evaporation response is set equal to the precipitation response except for a factor (f_c). The noise model has one parameter that determines an exponential decay. Thus, for the standard setup with precipitation and evaporation, there are five parameters that have to be determined from the comparison with the observations. Three parameters regarding the precipitation response, the evaporation factor, and the noise model parameter (actually, the time series model has a fifth parameter, the base level, but this is determined from the assumption that the average of the calculated heads is equal to the average of the observations). There are three extra parameters for each additional input series, such as pumping.



Limitations

Metran's time series model is linear. So, the model creation breaks down when the system is strongly nonlinear. This can occur e.g. when drainage occurs for high groundwater levels, when the ratio between the actual evapotranspiration and the inputted reference evaporation varies strongly, or when the groundwater system changed during the simulated period.

Metran is not able to find a decent time series model when the response function is not appropriate for the groundwater system. An example of this is a system with a separate fast and slow response as was found for a French piezometer in the Avre region, as is illustrated in Figure B2.

Finally, the parameter optimization of Metran uses a gradient search method in the parameter space, so it can be sensitive to initial parameter values in finding an optimal solution.

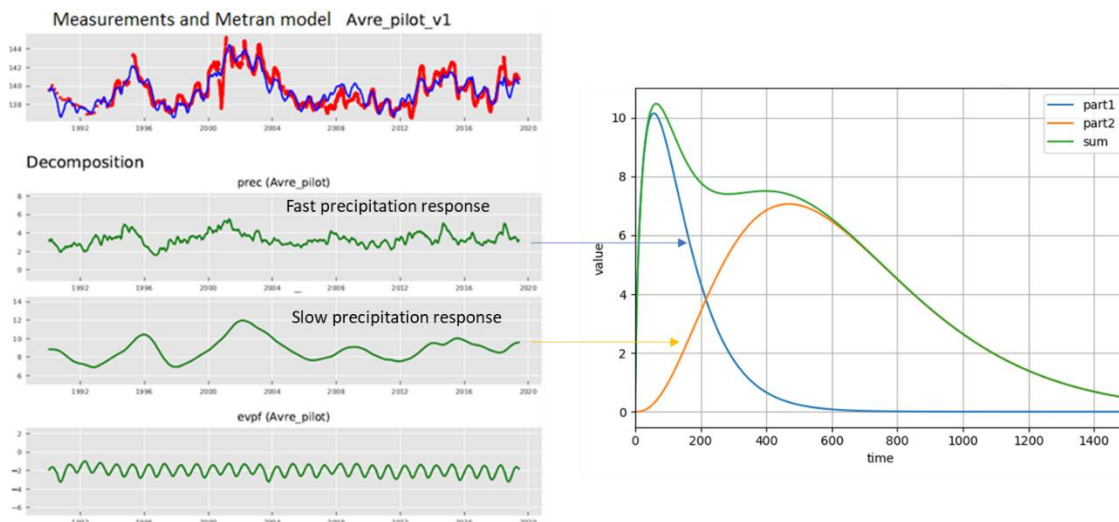


Figure B2. An example where the response function implemented in METRAN is not suitable for the groundwater system

Time step

Metran has been designed to work with explanatory series that have a daily time step. However, it has been adapted so that other time step lengths can be applied; although Metran still has the limitation that the explanatory variables have a constant frequency. For the TACTIC simulations of series with monthly or decadal meteorological input series, the time step has been set to 30 and 10 days, respectively. This time step has been applied from the end date backward.

Note that the heads may be irregular in time as long as the frequency is not greater than the frequency of the explanatory series.

Model output

The evaporation factor f_c gives the importance of evapotranspiration compared to precipitation. The parameter M_0 gives the total precipitation response, which is equal to the area below the impulse response function and the final value of the step response function.



The average response time is another characteristic of the precipitation response. The influence is illustrated in Figure B3 with the impulse response functions and head time series for two models with very different response times for time series of SGU in Sweden.

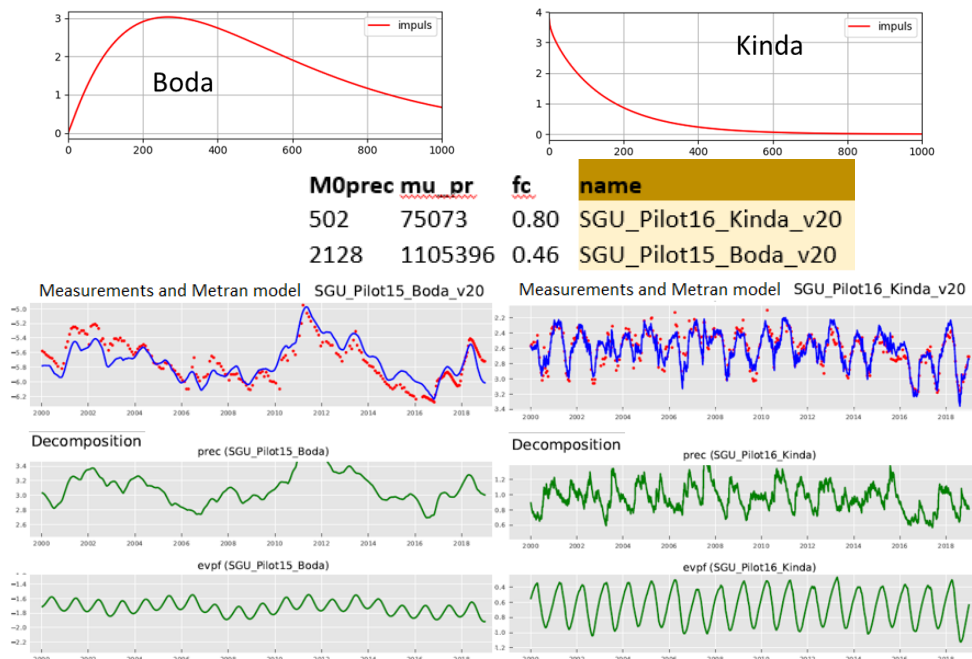


Figure B3 Illustration of Metran output for two case studies in Sweden with different response times.

Model quality

Metran judges a resulting time series model according to a number of criteria and summarizes the quality using two binary parameters Regimeok, Modok (see Zaadnoordijk et al., 2019):

- Regimeok = 1 : highest quality
- Modok = 1 (and Regimeok = 0) : ok
- Both zero = model quality insufficient

More detailed information on the model quality is given in the form of scores for two information criteria (AIC and BIC), a log likelihood, R2, RMSE, and the standard deviations and correlations of the parameters.

Recharge

Although the transfer-noise modelling of Metran determines statistical relations between groundwater heads and explanatory variables, we like to think of the results in physical terms. It is tempting to interpret the evaporation factor, as the factor translating the reference into the actual evapotranspiration. Then, we can calculate a recharge as



$$R = P - fE$$

Equation B1

where R is recharge, P precipitation, E evapotranspiration, and f the evaporation factor.

Following the definitions used in the TACTIC project, this recharge R actually is the effective precipitation. It is equal to the potential recharge when the surface runoff is negligible. This in turn is equal to the actual recharge at the groundwater table if there also is no storage change or interflow. In such cases it may be expected that this formula indeed corresponds to the meteorological forcing of the groundwater head in a piezometer, so that it gives a reasonable estimate of the recharge. Obergfell et al. (2019) showed this for an area on an ice pushed ridge in the Netherlands. However, this assumes that all precipitation recharges the groundwater, which cannot be done in many places.

In Dutch polders with shallow water tables and intense drainage networks, it is reasonable to assume that the actual evapotranspiration is equal to the reference value. In that case, the factor f becomes larger than 1 because 1 mm of evaporation has less effect than 1 mm of precipitation (because part of the evaporation does not enter the ground but is immediately drained to the surface water system). In that case, we can calculate recharge as:

$$\begin{aligned} R &= P - fE & f &\leq 1 \\ R &= P/f - E & f &> 1 \end{aligned}$$

Equation B2

These simple formulas can be applied easily for the situations currently modelled in Metran and for the simulations that are driven by future climate data using the delta-change climate factors. However, it is noted that it is a crude estimate using assumptions that are easily violated. Because of this, the equations should be applied only to long term averages using only models of the highest quality.



Deliverable 4.2

PILOT DESCRIPTION AND ASSESSMENT

Recharge map (Finland)

Authors and affiliation:

Olli Sallasmaa, Nina Hendriksson

Geological Survey of Finland (GTK)

This report is part of a project that has received funding by the European Union's Horizon 2020 research and innovation programme under grant agreement number 731166.



Deliverable Data	
Deliverable number	D4.2
Dissemination level	Public
Deliverable name	Pilots description and assessment report for recharge and groundwater vulnerability
Work package	WP4
Lead WP	BRGM, BGS
Deliverable status	
Version	Version 3
Date	17/03/2021

[This page has intentionally been left blank]

LIST OF ABBREVIATIONS & ACRONYMS

CC Climate change

EPIR Effective Precipitation Infiltration Ratio

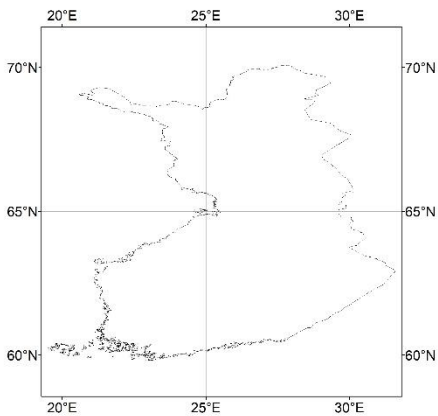
GSOs The Geological Survey Organisations

GTK Geologian Tutkimuskeskus (Geological Survey of Finland)

TABLE OF CONTENTS

LIST OF ABBREVIATIONS & ACRONYMS	5
1 EXECUTIVE SUMMARY	5
2 INTRODUCTION	7
3 PILOT AREA	8
3.1 Location and topography	8
3.2 Land use	9
3.3 Hydrogeology of the pilot area	9
3.4 Climate	12
3.5 Climate change challenge	13
3.5.1 Climatic control of groundwater recharge	13
3.5.2 Future climate and challenges	14
4 METHODOLOGY	15
4.1 Climate data	15
4.1.1 Meteorological data	15
4.2 Effective precipitation calculation	17
4.3 Effective Precipitation Infiltration Ratio	19
4.4 Model calibration	20
4.4.1 Observation data	20
4.4.2 Uncertainty	22
5 RESULTS AND CONCLUSIONS	23
5.1 Climate data	23
5.1.1 Performance to historical data	24
5.2 Potential groundwater recharge map of Finland	25
6 REFERENCES	26

1 EXECUTIVE SUMMARY

Pilot name	Recharge map	
Country	Finland	
EU-region	Northern Europe	
Area (km ²)	336 805	
Aquifer geology and type classification	Porous glacial sand and gravel deposits. To lesser extent fractures, faults and fissures in crystalline bedrock	
Primary water usage	Drinking water / Industry	
Main climate change issues	Risk of high precipitation causing groundwater flooding. Risk of drought.	
Models and methods used	Recharge map following methods used by GSI	
Key stakeholders	Government. Research institutes. Water companies.	
Contact person	Geological Survey of Finland. Olli Sallasmaa	

Geological Survey of Finland (GTK) took part in GeoERA TACTIC project WP4 by making an estimation of potential groundwater recharge in Finland.

Most of the groundwater is in shallow aquifers, which are typically sand and gravel formations on top of the bedrock. 150 largest Finnish water utilities provide water for 90% of households and 75% of that is groundwater or it is from managed aquifer recharge. Finland has crystalline bedrock, which has only relative small fractures enabling groundwater forming. Groundwater is extracted from bedrock, as well, but to a lesser extent than from shallow aquifers. Changes in climate are rapidly reflected in shallow groundwater formations.

In order to estimate potential groundwater recharge, statistical climate/weather data (daily weather data from years 1981-2010, FMI) and geological data (Surficial geology map, GTK) was collected. Daily temperature, precipitation and snow cover data was used to calculate effective precipitation. Geological surficial map by GTK was used to estimate effective precipitation infiltration ration (EPIR). Estimated effective precipitation and effective precipitation infiltration ratio were multiplied to calculate potential amount of precipitation to infiltrate to the ground.



In TACTIC project two climatic scenarios were chosen to represent conditions of low/high precipitation of 1 and 3 °C global change estimates.

In Finland the given scenarios suggest warmer winters with increased precipitation, which results in diminishing seasonal snow cover. In these scenarios the summers are warmer and drier. The potential groundwater recharge was calculated with the estimated temperature and precipitation values of both 1 and 3 °C scenarios. Resulting maps didn't show changes in the overall amount of potential groundwater recharge in Finland.

This study was a simplified first step to estimate potential groundwater recharge in Finland and it was only carried out using a set of existing data. Local studies and measurements are still needed to verify and clarify the actual groundwater recharge.

2 INTRODUCTION

Climate change (CC) already have widespread and significant impacts in Europe, which is expected to increase in the future. Groundwater plays a vital role for the land phase of the freshwater cycle and have the capability of buffering or enhancing the impact from extreme climate events causing droughts or floods, depending on the subsurface properties and the status of the system (dry/wet) prior to the climate event. Understanding and taking the hydrogeology into account is therefore essential in the assessment of climate change impacts. Providing harmonised results and products across Europe is further vital for supporting stakeholders, decision makers and EU policies makers.

The Geological Survey Organisations (GSOs) in Europe compile the necessary data and knowledge of the groundwater systems across Europe. In order to enhance the utilisation of these data and knowledge of the subsurface system in CC impact assessments the GSOs, in the framework of GeoERA, has established the project “Tools for Assessment of Climate change Impact on Groundwater and Adaptation Strategies – TACTIC”. By collaboration among the involved partners, TACTIC aims to enhance and harmonise CC impact assessments and identification and analyses of potential adaptation strategies.

TACTIC is centred around 40 pilot studies covering a variety of CC challenges as well as different hydrogeological settings and different management systems found in Europe. Knowledge and experiences from the pilots will be synthesised and provide a basis for the development of an infrastructure on CC impact assessments and adaptation strategies. The final projects results will be made available through the common GeoERA Information Platform (<http://www.europe-geology.eu>).

The report describes the work undertaken by the Geological Survey of Finland (GTK) as a part of TACTIC WP4 to create a Potential recharge map of Finland. The whole land area of Finland was chosen as a pilot area because of the need to have an estimation of the potential of groundwater recharge in the area.

Geological Survey of Finland is a national research centre and it has been studying groundwater formations for both groundwater and aggregate extraction aspects. Tactic project involved geologists Olli Sallasmaa and Nina Hendriksson.

3 PILOT AREA

3.1 Location and topography

The pilot area covers land area of Finland. It is located between the 60th and 70th northern parallels in the Eurasian continent's coastal zone. Length of the coastline against the Baltic Sea is 1250 km. (Statistics Finland 2019). In total, Finnish region covers 336 805 km² excluding the sea water area (52 456 km²). Lakes cover 34 533 km² of Finnish land area. There are estimated 168 000 lakes with the size larger than 500 m². (Statistics Finland 2019). Most of Finland is plain area with the elevation no higher than 200 m (Figure 1). Coastal area is characterized with lowlands, less than 50 m above sea level. In the middle of Finland, at the main water divide uplands, hilly landscape may reach the elevation level of 300 m above sea level. This is also the case in the hilly eastern Finland. Majority of Lapland (North Finland), except river and lake valleys, is hill and fell area in altitude of 200 – 600 m. The highest point, up to 1324 m a.s.l., located in the northwestern most branch of Finland.

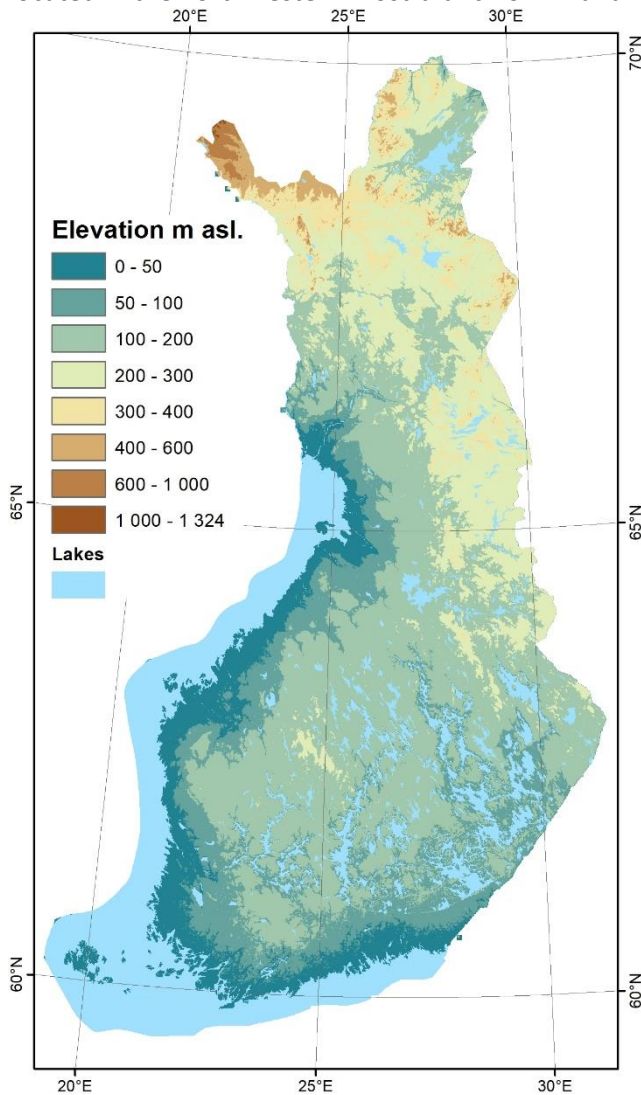


Figure 1 Topography of Finland © National Land Survey of Finland



3.2 Land use

Finland is a sparsely populated country with only metropolitan area of Helsinki exceeding population of one million. Only 1.4% of the land area is covered by artificial surfaces, this including cities and villages. 74.4% of the land area is forests and semi-natural areas (Figure 2). Water bodies cover 10% and agricultural areas 8,3%. (Finnish Environment Institute 2018)

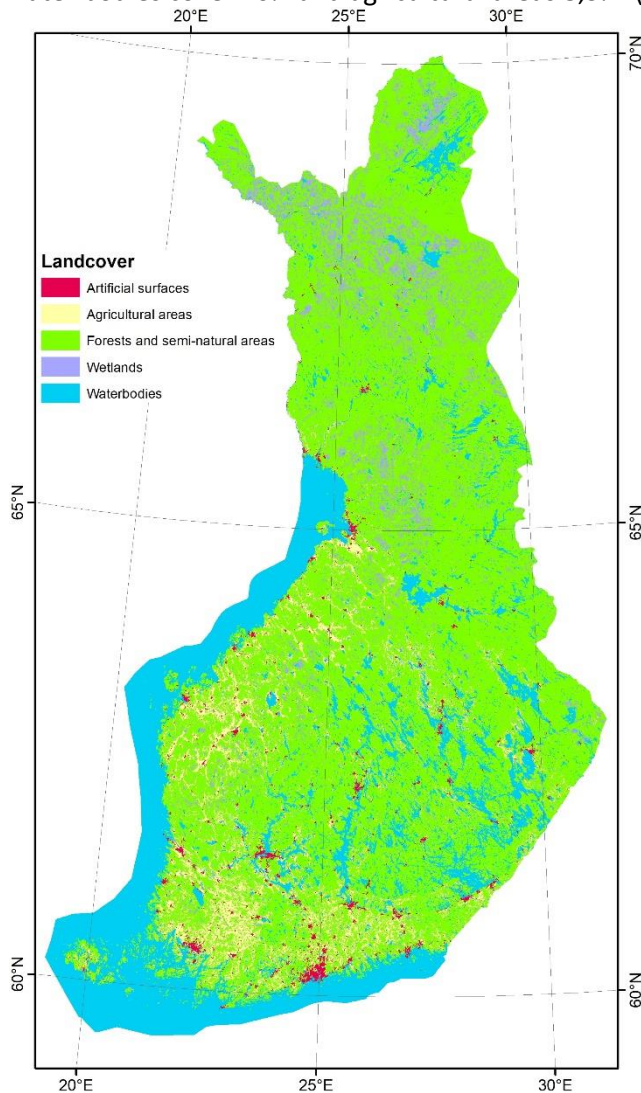


Figure 2 Land use according Corine land cover of Finland (Finnish Environment Institute 2018)

3.3 Hydrogeology of the pilot area

Geological media holding groundwater in Finland contains predominantly unconsolidated Quaternary till and glaciofluvial deposits and as a minor role the underlying crystalline basement with igneous and metamorphic rocks (Tarvainen et al. 2001). Due to repeated glaciations the surficial deposits are composed only of deposits such as till, sand and gravel, glacial and postglacial clay and silt. Hydrogeological properties of the soil deposits, especially porosity and



grain size and shape, dominate the groundwater recharge rate. Highest hydraulic conductivity is attained in coarse grained glacial sorted sand and gravel deposits such as eskers and ice-marginal formations (Salpausselkä). Where, approximately 30 – 60 % of local precipitation is infiltrated to form groundwater (Hatva et al. 2008). These formations are the economically most important Finnish groundwater reserves, despite the fact that they represent only 3 – 4 % area in Finland (Tarvainen et al. 2001). Most common soil sediment type in Finland is till and various moraine deposits (Figure 3). Till is characterized by non-sorted texture of varying grain sizes from very fine to very coarse grained material. Generally only 10 – 30 % of precipitation is infiltrated to coarse grained moraine deposits and even less in fine-grained sediments, such as silt and clay (Hatva et al. 2008). Heterogeneity of the soil material and discontinuity of the sedimentary units within a groundwater formation is common in Finland and this affects both the recharge rates and the groundwater velocities in the system. Groundwater table exists commonly in the depth of 2 – 4 m in Finland. However, in the topographically elevated esker and ice-marginal formations the groundwater table may reach a depth of 30 - 50 meters from the ground surface (Hatva et al. 2008).

Crystalline basement in Finland is characterized by rock types with very low porosity and hydraulic conductivity. In bedrock, groundwater recharge and flow are mainly controlled by the fractures, faults and fissures of the basement and the groundwater flow takes place in the depths of tens to hundreds (even thousands) of meters. Despite of typically smaller volumes of exploitable bedrock groundwater, it has a significant role both in potable water and geothermal energy purposes in Finland.

Aquifer types vary regionally depending on the dominating topographical and Quaternary geological features. Thereby, Finland may be divided into four hydrogeological provinces to characterize the groundwater formation types of certain region: 1. Coastal and archipelago regions in South and Southwest Finland; 2. West coast; 3. Central Finland; and 4. Northeast and North Finland (Figure 3) (Lahermo et al. 2002).

1. The southern coastal belt of Finland is characterized by wide variation of different aquifer types from clay covered, confined aquifers to bedrock, till and glaciofluvial aquifers. Unique to the coastal belt are low-lying areas with numerous river basins and bedrock outcrops (Alalammi, 1986; Karlsson, 1986). The southern Finland coastal belt stretches up to the northern border of the Salpausselkä ice-marginal formations with scattered esker deposits.
2. Western coastal belt areas reach to the northern end of the Bothnian and in East stretches to the water divide where terrain is higher and where relative height differences are larger. The broad coastal plain, cut by numerous rivers, is dominated by clay and silt deposits and bounteous peat lands while till deposits are more common eastward.
3. The central Finland encompasses the main part of the large lake basin characterized by variable topography with structurally controlled valleys (Alalammi, 1986). Numerous lakes, overburden till and small peat lands, lesser deposits are the typical features of the area. The area includes three major river basins and the surface coverage of lakes and

- rivers generally ranges from 10% to 20%. The most frequent aquifer types in this area are till deposits (ca. 50%).
4. Northeast and North Finland is the most hilly and mountainous area in Finland. It is characterized by till-covered, broad elevated areas with locally comparatively steep slopes (Alalammi, 1986). Here the till-covered hills are often peaked by broken bedrock and rock fields and separated from each other by large flat peat lands. Large rivers flow in broad and flat river valleys flanked frequently by extensive sand deposits.

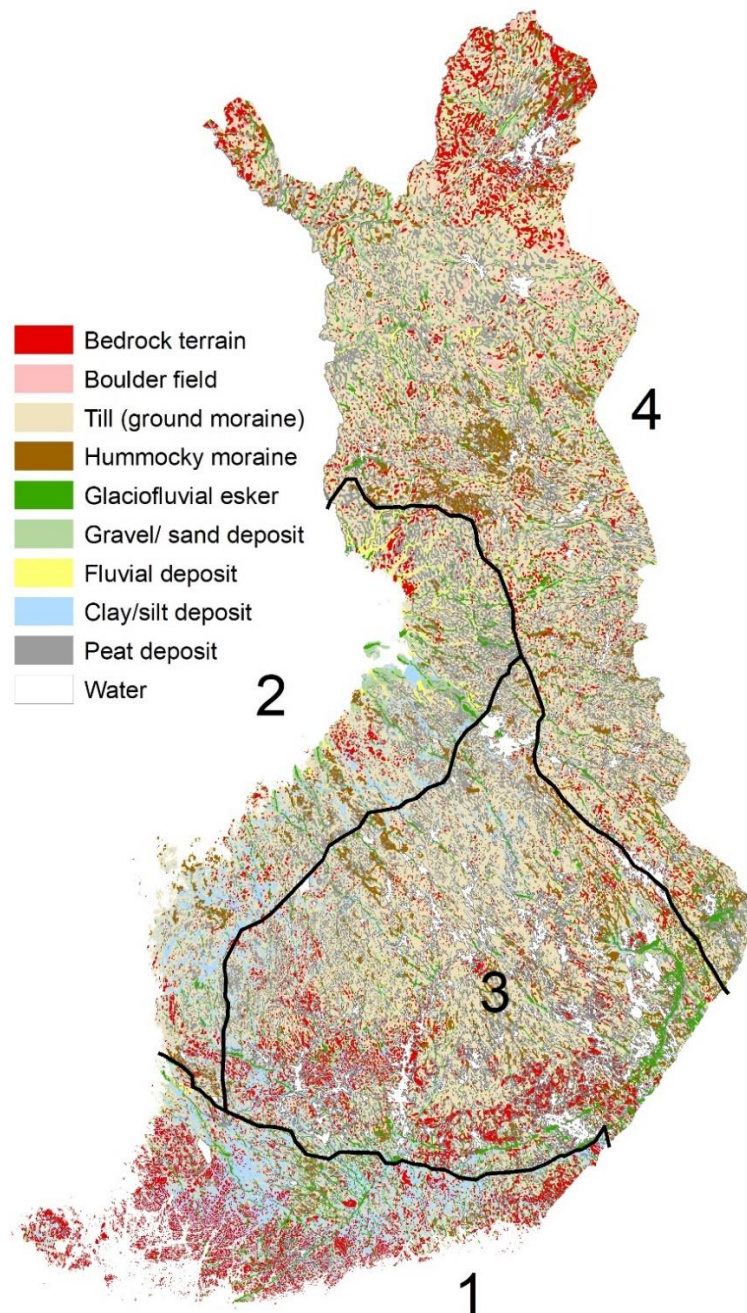


Figure 3 Hydrogeological provinces in Finland by Lahermo et al. (2002): 1. Coastal and archipelago regions in South and Southwest Finland; 2. West coast; 3. Central Finland; 4. Northeast and North Finland. Background: Quaternary deposits of Finland 1:1 000 000 (Kujansuu & Niemelä 1984). Picture modified from Lahermo et al. (2002).

3.4 Climate

Finland belongs mainly in cold (D) climate on the basis of the Köppen-Geiger climate classification (Peel et al. 2007). Predominant climate type in Finland is subarctic (Dfc). Only in the southernmost coast, warm-summer humid continental climate (Dfb) prevails.

The mean annual temperature during the latest long term monitoring period of 1981 – 2010 varies from +5.9 °C (Helsinki) in the south to -0.4 °C (Sodankylä) in the north (Figure 4; FMI 2019). Airflows from the Atlantic Ocean warmed by the Gulf Stream produce a climate that is more temperate compared to other areas at similar latitudes. The precipitation is mainly derived from one vapor source in the North Atlantic Ocean (Alalammi, 1987). Also the vapor from the Baltic Sea serves as an additional moisture source causing increasing precipitation in coastal areas in early winter. The proximity of the Barents Sea in the North has a similar effect in northern Finland. Regionally, the mean annual precipitation varies from 655 mm (Helsinki, 1981 – 2010) to 520 mm (Sodankylä, 1981 – 2010) (Figure 4; FMI 2019). Highest precipitation rates are found in southern and eastern Finland and in the water divide area of central Finland. The lowest precipitation rates are recorded along the north western coast and in northern Finland due to the proximity of the Caledonian mountain range.

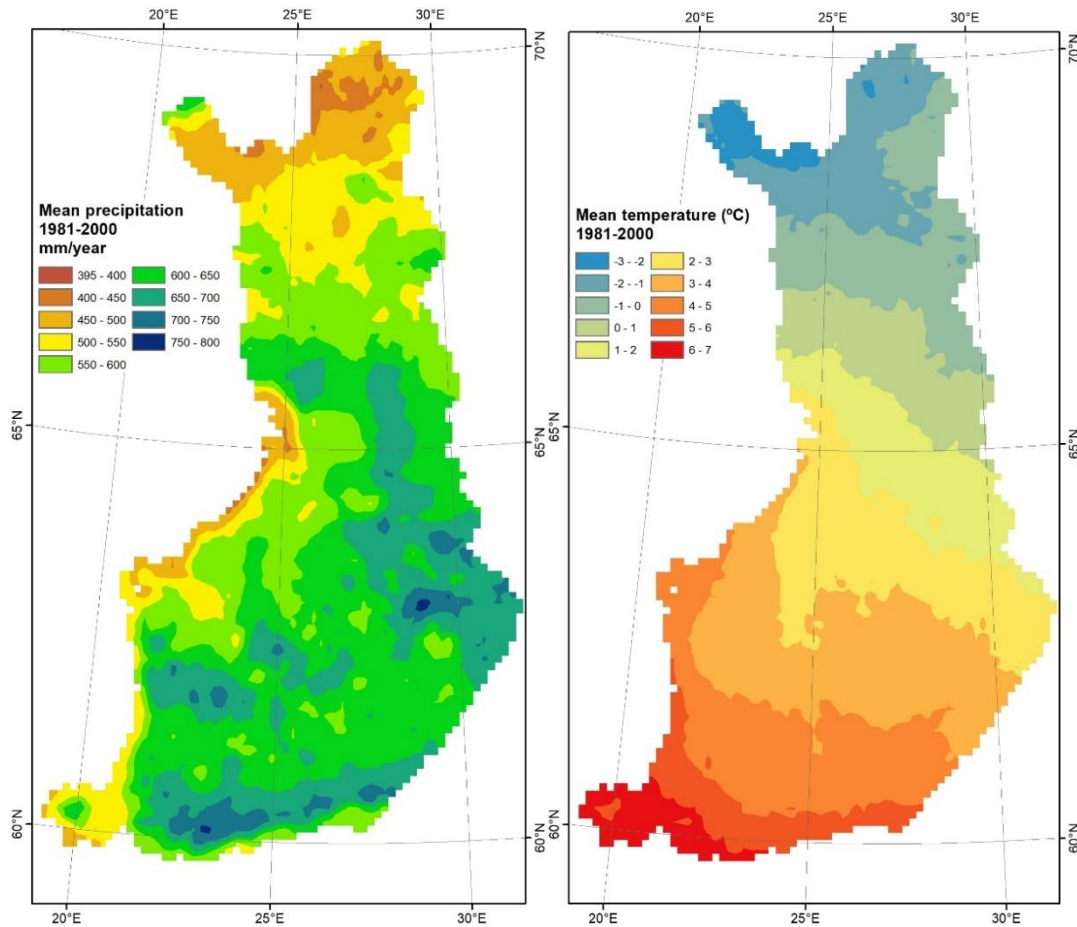


Figure 4 Mean annual precipitation and temperature 1981-2010.

3.5 Climate change challenge

3.5.1 Climatic control of groundwater recharge

In the northern latitudes, the infiltration of precipitation to form groundwater is controlled by the variation between the hydrological processes dominating during four distinct seasons. In Finland, the main two periods of the groundwater recharge are: 1) after snow melt in spring and 2) autumn before developing soil frost. In the winter time, the precipitation is received as snow and infiltration largely ceases in frozen soil. In the South it is known that most of snowmelt is lost by surface flow and evaporation, and in the North by surface flow but less by evaporation. In southern Finland, 10 – 20% of the precipitation is in the form of snow, but in northern and eastern Finland the proportion of snow reaches 20 – 35% (Karlsson, 1986). In the East shallow and discontinuous frost during winter may cause higher rates of recharge in spring time (Karlsson, 1986). As a consequence of evolving climatic conditions, oscillation of the autumn-winter-spring boundaries may also extend the period of groundwater recharge throughout the winter if soil frost is not properly developed. This is recorded especially from the southern and western coastal areas in Finland. The land area of Finland is covered by vegetation and forests, and therefore transpiration by plants is significant during the growing season in summer.



Groundwater recharge by summer precipitation has been considered to be of minor importance for the formation of groundwater in Finland (Karlsson, 1986).

3.5.2 Future climate and challenges

Higher evapotranspiration during summer season, declined groundwater table and local droughts are expected in changing climate. Moreover, extreme weather events may cause e.g. flooding of seawater on coastal areas and surface runoff floods on made grounds as referred in Figure 5.

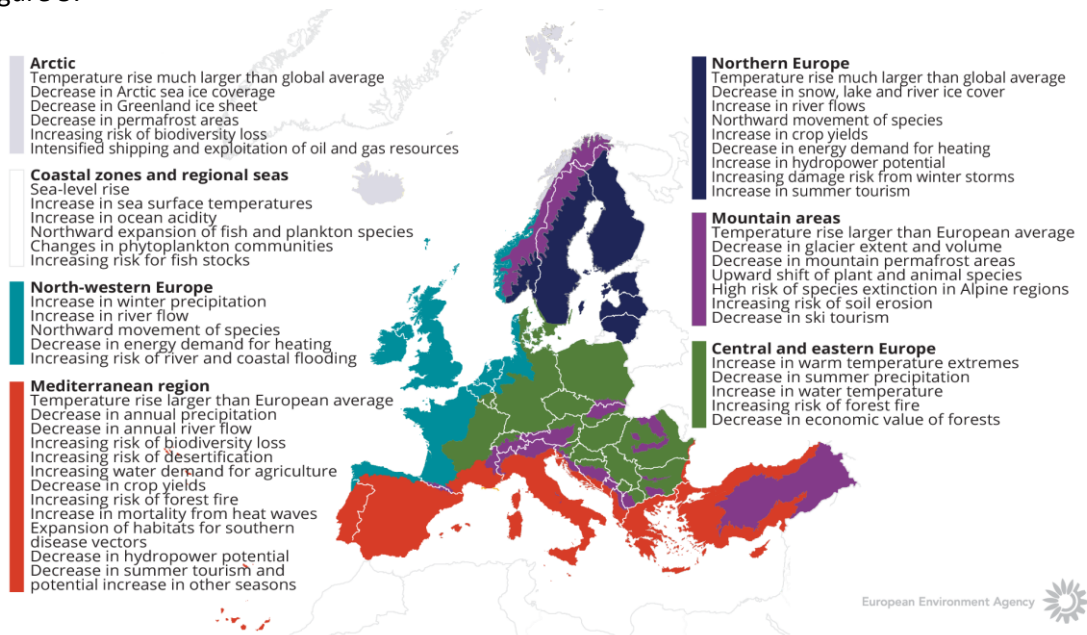


Figure 5 How is climate expected to change in Europe. The European Environment Agency map

4 METHODOLOGY

The methodology applied to assess the potential groundwater recharge is:

$$\text{Recharge} = \text{EPIR} * \text{Effective Precipitation},$$

where EPIR = Effective Precipitation Infiltration Ratio as discussed below in Section 4.3. This approach is applied to evaluate both present and future groundwater recharge.

4.1 Climate data

4.1.1 Meteorological data

The applied meteorological data from years 1981-2010 was all publicly available open data from Finnish Meteorological Institute (FMI 2019). Data consisted of daily precipitation, mean temperature and thickness of snow cover. Data was interpolated to raster format of grid cell size of 10×10 km.

4.1.2 TACTIC standard Climate Change scenarios

The TACTIC standard scenarios were developed based on the ISIMIP (Inter Sectoral Impact Model Intercomparison Project, see www.isimip.org) datasets. The resolution of the data is 0.5°x0.5° global grid and at daily time steps. As part of ISIMIP, much effort has been made to standardise the climate data (a.o. bias correction). Data selection and preparation included the following steps:

1. Fifteen combinations of RCPs and GCMs from the ISIMIP data set were selected. RCPs are the Representative Concentration Pathways determining the development in greenhouse gas concentrations, while GCMs are the Global Circulation Models used to simulate the future climate at the global scale. Three RCPs (RCP4.5, RCP6.0, RCP8.5) were combined with five GCMs (noresm1-m, miroc-esm-chem, ipsl-cm5a-lr, hadgem2-es, gfdl-esm2m).
2. A reference period was selected as 1981 – 2010 and an annual mean temperature was calculated for the reference period.
3. For each combination of RCP-GCM, 30-years moving average of the annual mean temperature were calculated and two time slices identified in which the global annual mean temperature had increased by +1 and +3 °C compared to the reference period, respectively. Hence, the selection of the future periods was made to honour a specific temperature increase instead of using a fixed time-slice. This means that the temperature changes are the same for all scenarios, while the period in which this occurs varies between the scenarios.
4. To represent conditions of low/high precipitation, the RCP-GCM combinations with the second lowest and second highest precipitation were selected among the 15 combinations for the +1 and +3 °C scenarios. This selection was made on a pilot-by-pilot basis to accommodate that the different scenarios have different impact in the various parts of Europe. The scenarios showing the lowest/highest precipitation were avoided, as these endmembers often reflect outliers.
5. Delta change values were calculated on a monthly basis for the four selected scenarios, based on the climate data from the reference period and the selected future period. The delta change values express the changes between the current and future climates, either as a relative factor (precipitation and evapotranspiration) or by an additive factor (temperature).

6. Delta change factors were applied to local climate data by which the local particularities are reflected also for future conditions.

Figure 6 shows all the monthly delta change factors for Finland from TACTIC standard Climate Change scenarios. Monthly precipitation multiplication factors are shown in left side of the figure 6 and same data in numbers in table 2. Both 1 and 3 °C scenarios had minimum and maximum calculations from which average values were used in calculations by GTK. Monthly temperature additive factors are shown in the right side of the figure 6 and same data in numbers in table 1. Average values were used in calculations by GTK.

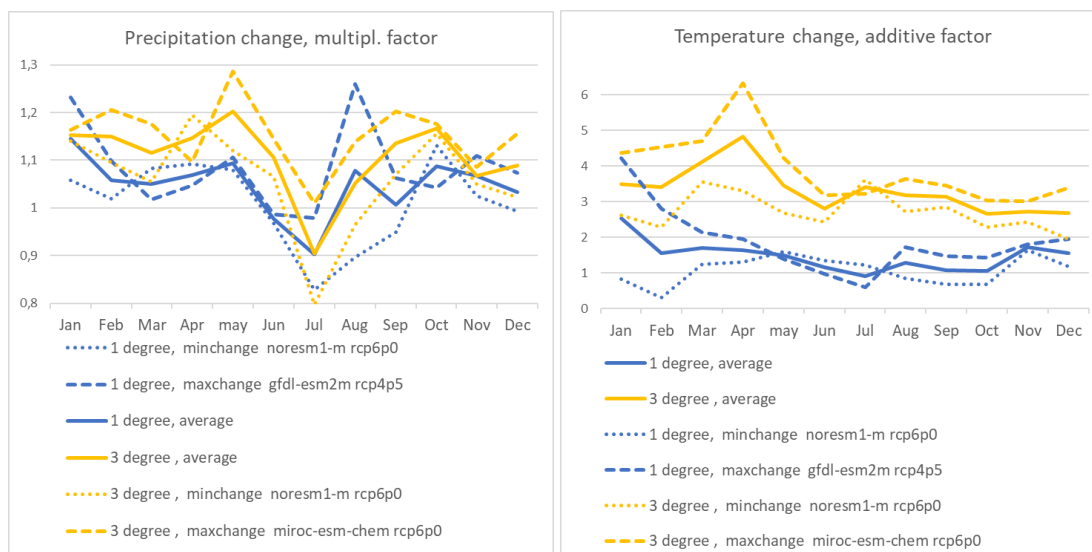


Figure 6 Monthly delta change factors for Finland from TACTIC standard Climate Change scenarios.

Table 1 Monthly temperature delta change additive factors for Finland from TACTIC standard Climate Change scenarios.

3 degree			Jan	Feb	Mar	Apr	May	Jun	Jul	Aug	Sep	Oct	Nov	Dec
minchange	noresm1-m	rcp6p0	2,62	2,28	3,55	3,3	2,67	2,42	3,61	2,72	2,84	2,28	2,42	1,96
maxchange	miroc-esm-chem	rcp6p0	4,36	4,53	4,7	6,33	4,21	3,18	3,21	3,63	3,45	3,03	3,02	3,39
average			3,49	3,405	4,125	4,815	3,44	2,8	3,41	3,175	3,145	2,655	2,72	2,675
1 degree			Jan	Feb	Mar	Apr	May	Jun	Jul	Aug	Sep	Oct	Nov	Dec
minchange	noresm1-m	rcp6p0	0,82	0,31	1,25	1,31	1,6	1,35	1,22	0,84	0,67	0,69	1,63	1,18
maxchange	gfdl-esm2m	rcp4p5	4,23	2,8	2,13	1,95	1,38	0,98	0,6	1,72	1,47	1,42	1,81	1,94
average			2,525	1,555	1,69	1,63	1,49	1,165	0,91	1,28	1,07	1,055	1,72	1,56



Table 2 Monthly precipitation delta change multiplication factors for Finland from TACTIC standard Climate Change scenarios.

3 degree			Jan	Feb	Mar	Apr	may	Jun	Jul	Aug	Sep	Oct	Nov	Dec
minchange	noresm1-m	rcp6p0	1,1405	1,0952	1,0550	1,1954	1,1200	1,0654	0,7970	0,9653	1,0701	1,1563	1,0500	1,0226
maxchange	miroc-esm-chem	rcp6p0	1,1639	1,2056	1,1765	1,0968	1,2857	1,1457	1,0106	1,1383	1,2023	1,1761	1,0854	1,1563
average			1,1522	1,1504	1,1158	1,1461	1,2029	1,1055	0,9038	1,0518	1,1362	1,1662	1,0677	1,0894
1 degree			Jan	Feb	Mar	Apr	may	Jun	Jul	Aug	Sep	Oct	Nov	Dec
minchange	noresm1-m	rcp6p0	1,0579	1,0190	1,0826	1,0920	1,0800	0,9673	0,8274	0,8960	0,9490	1,1312	1,0250	0,9925
maxchange	gfdl-esm2m	rcp4p5	1,2328	1,0980	1,0179	1,0465	1,1064	0,9863	0,9794	1,2597	1,0633	1,0424	1,1098	1,0741
average			1,1453	1,0585	1,0502	1,0692	1,0932	0,9768	0,9034	1,0779	1,0062	1,0868	1,0674	1,0333

4.2 Effective precipitation calculation

Daily evaporation was estimated using daily mean temperature as was described in Swedish work of Groundwater formation in Swedish type soil, "Grundvattenbildning i svenska typjordar - översiktlig beräkning med en vattenbalansmodell." (Rodhe et al 2006).

$$E_{pot} = B(t) \cdot T \text{ for } T > 0^{\circ}C$$

$$E_{pot} = 0 \text{ for } T \leq 0^{\circ}C$$

$$B(t) = (1 + A \cdot \sin(2\pi \frac{t+\psi}{365} - \frac{\pi}{2})) \cdot C_E$$

t = number of the day in a year

A = amplitude

E_{pot} = potential evaporation

Ψ = phase shift (days)

C_E = evaporation parameter ($\text{mm d}^{-1}^{\circ}\text{C}^{-1}$)

The resulting map of effective precipitation calculations by GTK were compared with the provisional calculations made for TACTIC WP4 by Grith Martinsen and Simon Stisen from GEUS. Figure 7 shows the three different effective precipitation calculation maps Peff RRe(GTK), Peff NetRR(GTK) and Peff (TACTIC). The map Peff NetRR(GTK) shows high effective precipitation in south-east Finland and lowest in the north. Peff NetRR(GTK) has the assumption, that effective precipitation does not occur while snow cover is present and that melting snow goes totally as a surface run-off. This seems to be significantly different from the estimations by Martinsen and Stisen. In the map Peff RRe (GTK) there is a sum of Peff for every day, including wintertime with



snow-cover. In Figure 8 there are cell by cell comparison between Peff RRe(GTK) and Peff NetRR(GTK) with Peff (TACTIC).

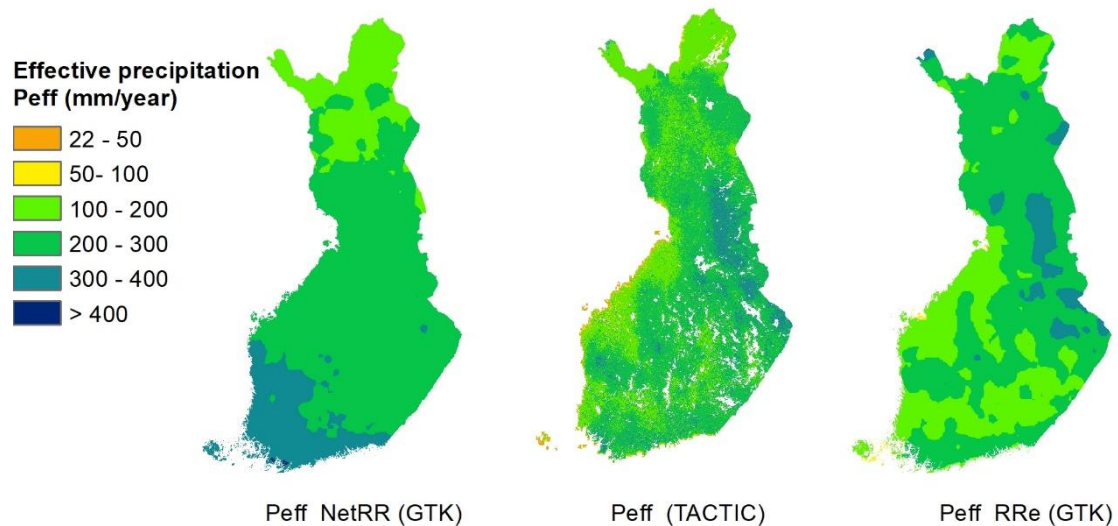


Figure 7 Three different effective precipitation estimation maps Peff RRe(GTK), Peff NetRR(GTK) and Peff (TACTIC).

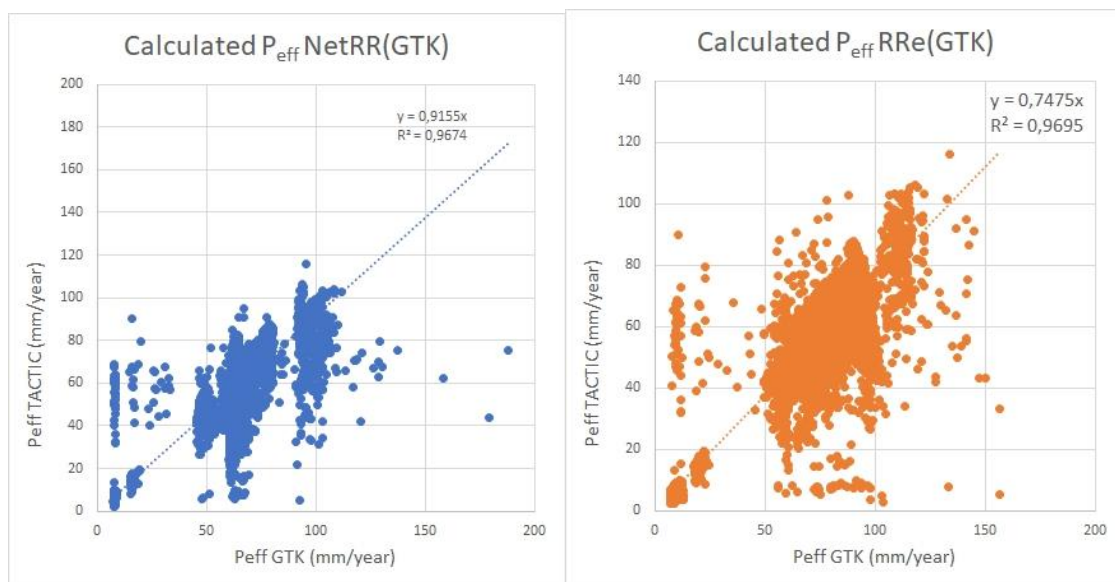


Figure 8 Cell by cell comparison with calculated values (GTK) to calculations of pan-european Peff (TACTIC).



4.3 Effective Precipitation Infiltration Ratio

Effective Precipitation Infiltration Ratio (EPIR) was estimated using the soil type of the Superficial deposits of Finland 1:200 000 (sediment polygons, GTK). It included soil type at depths from 0 to 1 m. The Superficial deposits of Finland 1:1 000 000 (GTK) was also used to distinguish different types of till in various parts of Finland. EPIR for respective soil types was estimated using K-values from literature.

The effective precipitation infiltration ratios for different soil types are shown in Figure 9. Value means how much of the effective precipitation could infiltrate in the ground. This calculation doesn't take into account transpiration through vegetation. Its purpose is to give general view of the groundwater potential and what happens under changing climate.

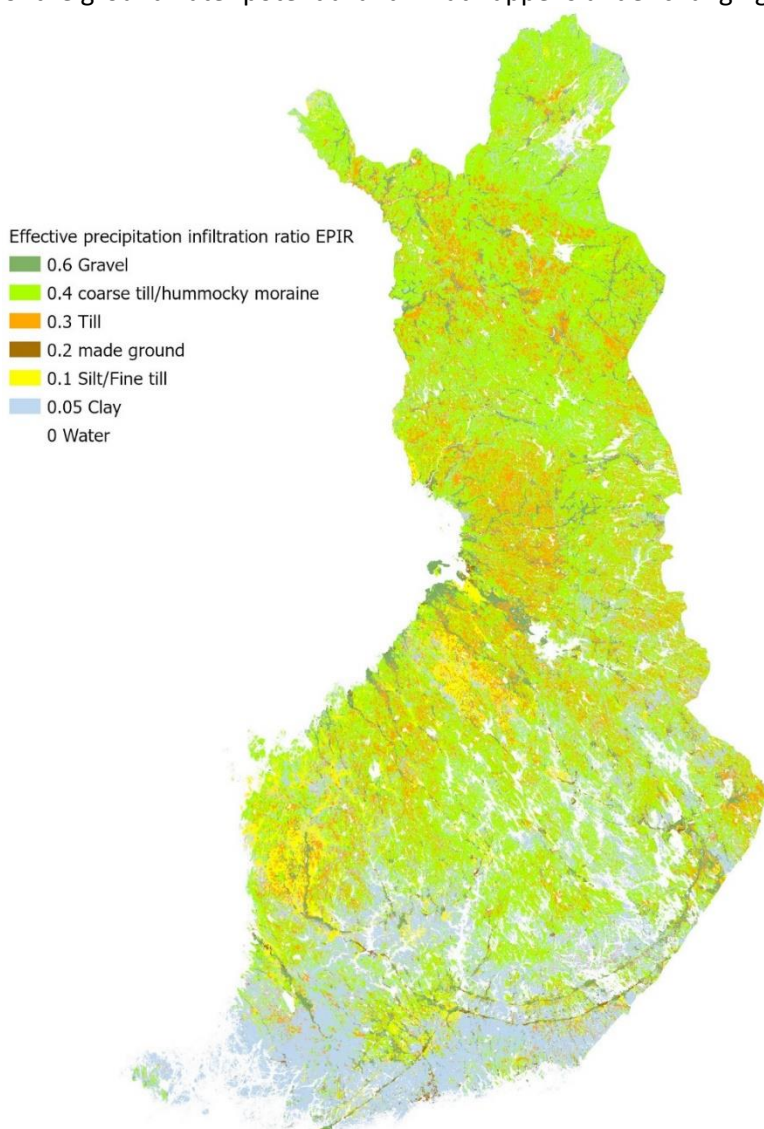


Figure 9 Effective precipitation infiltration ratio and major soil types



4.4 Model calibration

4.4.1 Observation data

Calculated values were compared with estimated values of groundwater formation in groundwater area database provided by (SYKE 2020). Figure 10 shows comparison charts and linear regression estimation. Calculation was done in ArcGIS Pro program with zonal statistics function.

Linear regression was calculated for the entire Finland and also within areas of 13 ELY-centers separately. Finland is divided in ELY-centers, which are “The Centers for Economic Development, Transport and the Environment” and they are responsible for the regional implementation and development tasks of the central government. ELY-Centres are shown in in figure 11. Figure 10 shows linear regression chart for both NetRR and RRe calculations for entire country. Slope of line (Y) shows the relationship between the calculated values and the values in the database by SYKE. Calculated recharge values are in average 60 % of the values that were estimated by SYKE. Different ELY-centers show variation between 53.8 % in 90.6%, as shown in Table 3. Slope-values for each ELY-center are also shown in column Y in Table 3. Potential recharge map for Finland was decided to be calculated using Peff NetRR (GTK) recharge values as they have better correlation with the estimated recharge values of groundwater areas by SYKE.

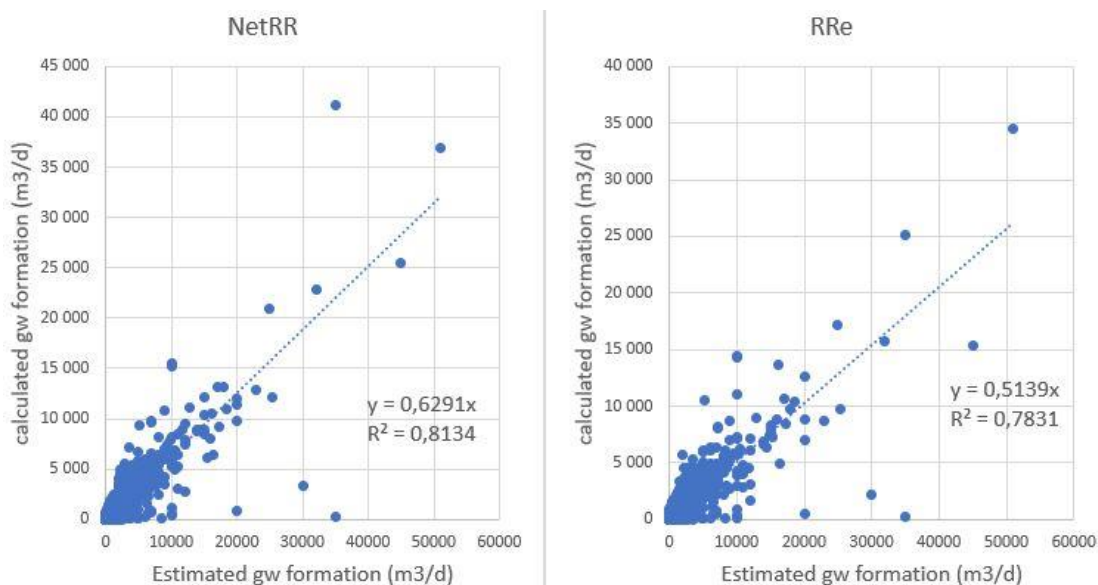


Figure 10 Comparison between calculated and previously estimated groundwater formation values

Table 3 Slope values of the linear regression analysis for each ELY Centres

ID	Area	Count	Calculated/Estimated(SYKE) Y	R ²
EPO	Etelä-Pohjanmaa, Keski-Pohjanmaa and Pohjanmaa	319	0,7615	0,7472
ESA	Etelä-Savo	184	0,6408	0,9327
HAM	Kanta-Häme	297	0,5385	0,6828
KAI	Kainuu	231	0,562	0,9178
KAS	Kymenlaakso and Etelä-Karjala	293	0,6497	0,9461
KES	Keski-Suomi	1,6462	0,7655	0,5575
LAP	Lappi	1744	0,608	0,7059
PIR	Pirkanmaa	144	0,6371	0,8791
POK	Pohjois-Karjala	1,6156	0,8389	0,6171
POP	Pohjois- Pohjanmaa	350	0,6946	0,8774
POS	Pohjois-Savo	1,3114	0,906	0,4836
UUD	Uusimaa	302	0,6419	0,6273
VAR	Varsinais-Suomi and Satakunta	245	0,876	0,895
Sum all		4856	0,6034	0,7188

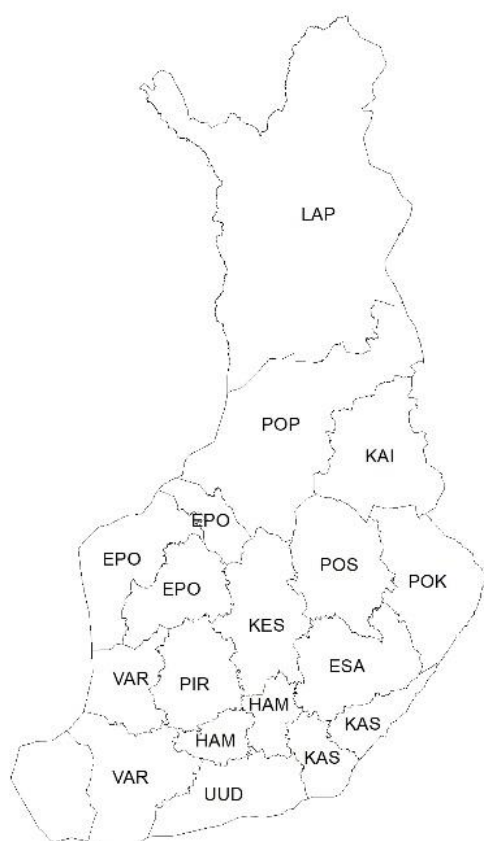


Figure 11 ELY -Centres in Finland



4.4.2 *Uncertainty*

Estimating groundwater recharge in the whole country is certainly challenging. In general estimating evaporation and thus effective precipitation leaves room to errors. Snow cover has appeared in all over Finland every winter in years 1981-2010, nearly half a year in the north and perhaps only a few days in the southwest Finland. Future climate change scenarios predict shorter periods with snow cover. Thick snow cover can keep ground unfrozen and allow infiltration during the snow melting period. On the other hand, absence of snow could lead the ground to freeze, which prevents the water infiltration. These questions remain unanswered in a nation scale approach.

5 RESULTS AND CONCLUSIONS

5.1 Climate data

Monthly temperature delta change additive factors (Table 1) were added to meteorological temperature data and monthly precipitation delta change multiplication factors (table2) were multiplied to monthly precipitation data. Meteorological data and simulated prediction are shown in Figure and Figure 13. Temperature and precipitation are changing according the given delta change factors, as showed in Figure 6 and Table 1 and Table 2 (Chapter 4.1.1). Warm winters and increasing precipitation can change the periods when the groundwater infiltration can take place. Potential groundwater recharge estimations for present and 1 °C scenario and 3 °C scenarios are shown in Figure 14.

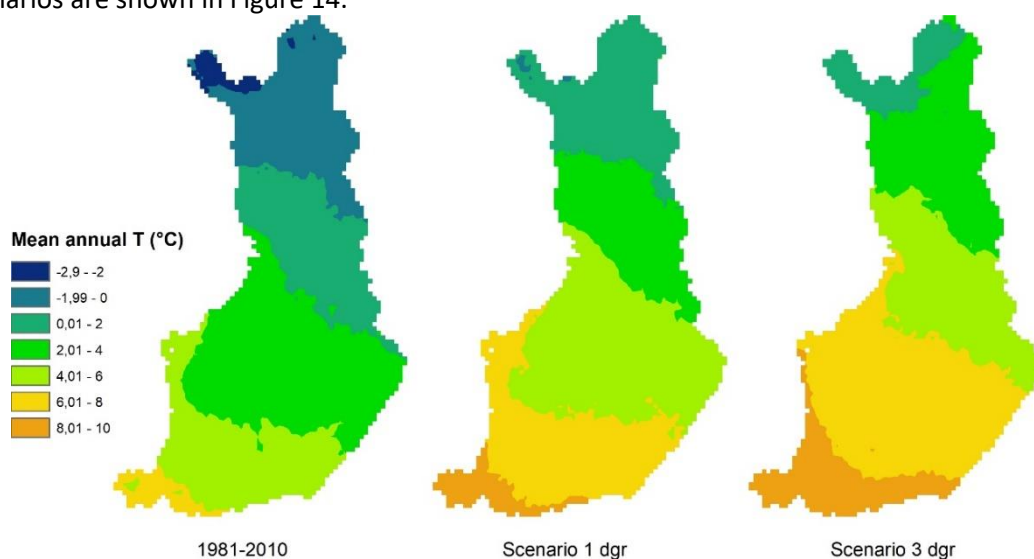


Figure 12 Observed present and predicted temperature values according given scenarios.

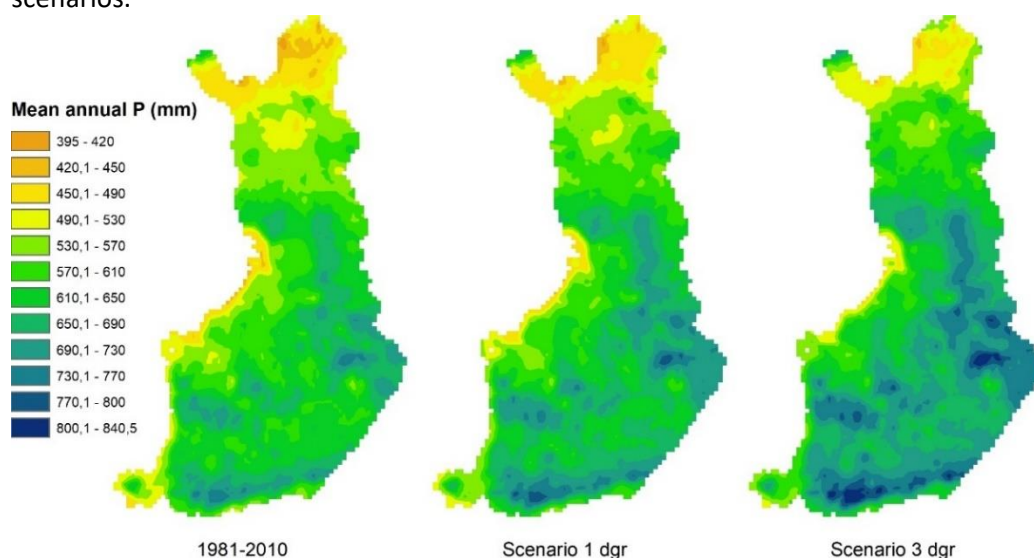


Figure 13 Observed present and predicted precipitation values according given scenarios.



This robust and simplified approach doesn't show major changes in calculated potential groundwater recharge. However, detailed local studies are needed to understand properly the water infiltration dynamics under snow cover and frozen ground.

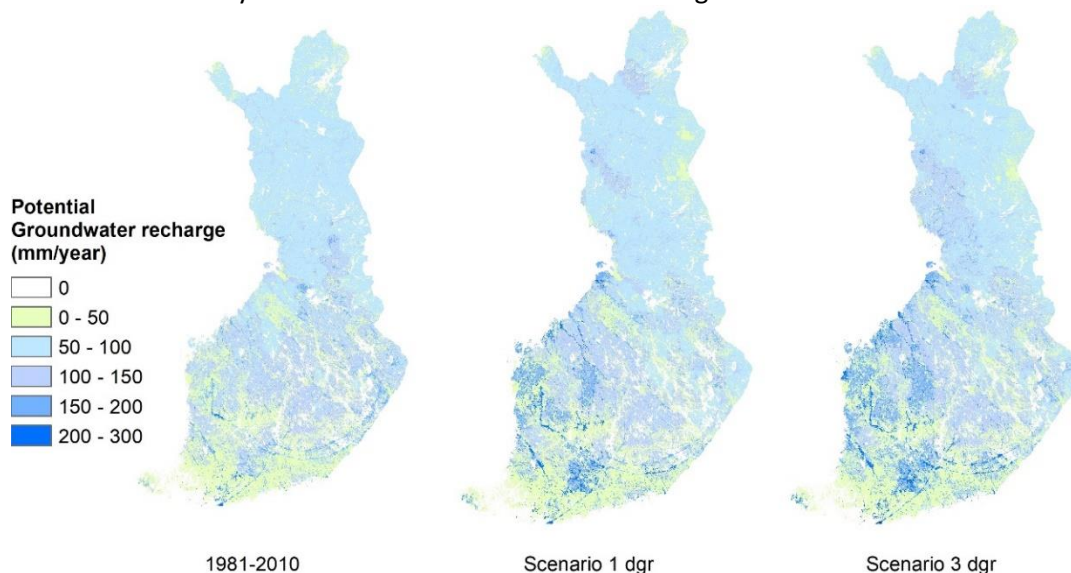


Figure 14 Calculated potential groundwater recharge for present (1981-2010) and for the two future scenarios.

5.1.1 Performance to historical data

This model shows potential groundwater recharge decreasing in eastern Finland in both 1 °C scenario and 3 °C scenario. Small increase is calculated in western part of middle Finland (Figure 155).

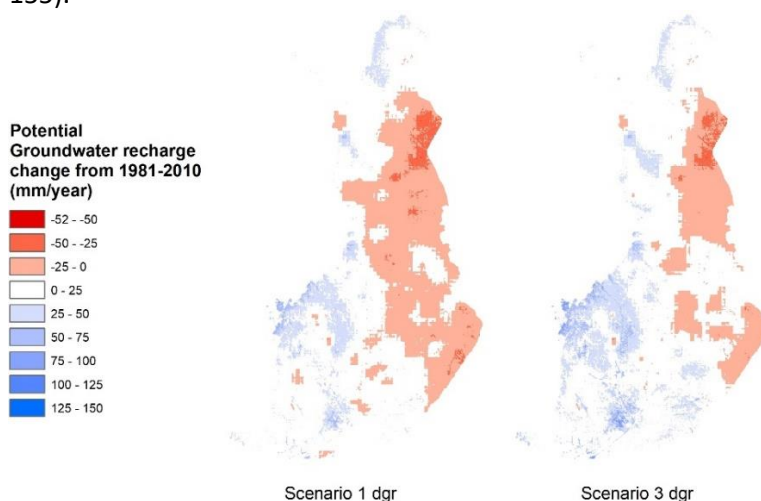


Figure 15 Difference between present values and predicted values of potential groundwater recharge for Climate change scenarios 1 and 3 °C.



5.2 Potential groundwater recharge map of Finland

Potential groundwater recharge was obtained by multiplying EPIR values by effective precipitation. In lakes the potential groundwater recharge was estimated as zero. Resulting map is shown in Figure 116 and chart of the results in Figure 127. Mean recharge value is 68 mm/year.

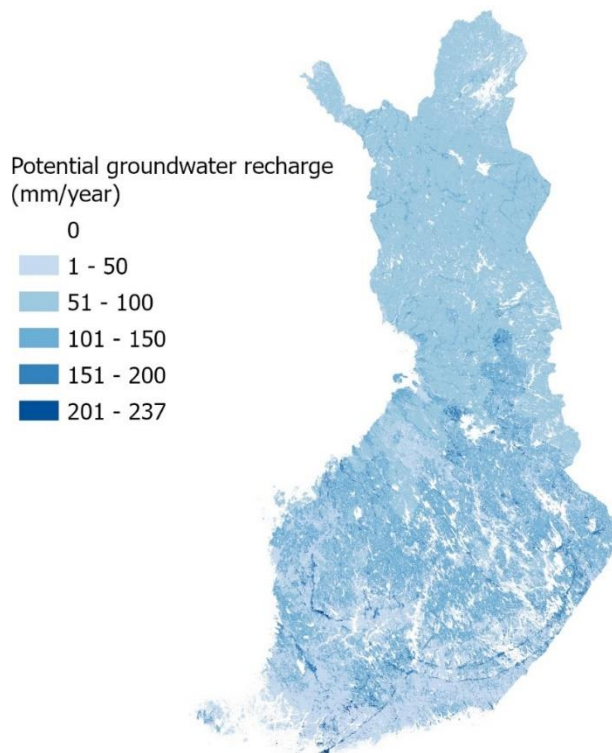


Figure 116 Potential groundwater recharge in Finland as estimated during years 1981-2010.

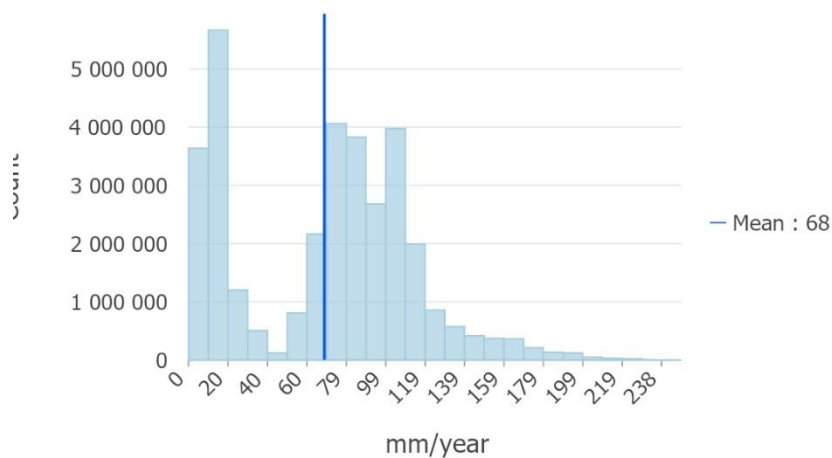


Figure 127 Potential groundwater recharge in Finland as estimated during years 1981-2010.



6 REFERENCES

Alalammi, P. (ed.), 1987. Atlas of Finland, Folio 131, Climate. Helsinki, National Board of Survey and Geographical Society of Finland, 31 p.

Alalammi, P. (ed.), 1986. Atlas of Finland, Folio 121-122, Relief and landforms. Helsinki, National Board of Survey and Geographical Society of Finland, 19 p.

FMI (2019). Climate statistics. Accessible in: <https://en.ilmatieteenlaitos.fi/statistics-from-1961-onwards>

Hatva, T., Lapinlampi, T. & Vienonen, S. (2008). Kaivon paikka – Selvitykset ja tutkimukset kiinteistön kaivon paikan määrittämiseksi. Ympäristöopas 2008. Suomen ympäristökeskus ja Edita. ISBN 978-952-11-3199-8 (PDF). 150 s.

Karlsson, K.-P. (ed.) (1986). Atlas of Finland, Folio 132, Water, National Board of Survey and Geographical Society of Finland, Helsinki, 12 pp.

Kujansuu, R. & Niemelä, J. (eds.) (1984). Suomen maaperä, 1:1 000 000. Espoo: Geologian tutkimuskeskus. [Quaternary geological deposit of Finland]. Geological Survey of Finland, Espoo, Finland.

Lahermo, P., Tarvainen, T., Hatakka, T., Backman, B., Juntunen, R., Kortelainen, N., Lakomaa, T., Nikkarinen, M., Vesterbacka, P., Väisänen, U. & Suomela, P. (2002). Tuhat kaivoa - Suomen kaivovesien fysikaalis-kemiallinen laatu vuonna 1999. Summary: One thousand wells – the physical-chemical quality of Finnish well waters in 1999. Geologian tutkimuskeskus, Tutkimusraportti – Geological Survey of Finland, Report of Investigation 155. 92 pp. ISBN 951-690-842-X.

Peel, M.C., Finlayson, B.L. & McMahon, T. A. (2007). "[http= 1027-5606 Updated world map of the Köppen-Geiger climate classification]". Hydrol. Earth Syst. Sci. 11: 1633-1644.

Rodhe, A., Lindström, G., Rosberg, J., & Pers, C. 2006. Grundvattenbildning i svenska typjordar - översiktlig beräkning med en vattenbalansmodell. Uppsala University, Department of Earth Sciences, Hydrology. Report Series A No. 66

Statistics Finland (2019). http://www.stat.fi/tup/suoluk/suoluk_alue.html

SYKE Suomen ympäristökeskus (2020), Open data, Accessible in: <https://ckan.ymparisto.fi/dataset/%7B8F45F7BF-669F-4434-A8DB-8E686933F6FF%7D>

Tarvainen, T., Lahermo, P., Hatakka, T., Huikuri, P., Ilmasti, M., Juntunen, R., Karhu, J., Kortelainen, N., Nikkarinen, M. & Väisänen, U. (2001). Chemical composition of well water in Finland - main results of the "one thousand wells" project. In: Autio, S. (ed.) Geological Survey of Finland, Current Research 1999-2000. Geological Survey of Finland. Special Paper 31, 57-76.



Establishing the European Geological
Surveys Research Area to deliver a
Geological Service for Europe

Deliverable 4.2

PILOT DESCRIPTION AND ASSESSMENT

France

Authors and affiliation:

**Baulon lisa, Sandra Lanini, H  l  ne
Bess  re and Cl  ment Lattelais**



This report is part of a project that has received funding by the European Union's Horizon 2020 research and innovation programme under grant agreement number 731166.



Deliverable Data	
Deliverable number	D4.2
Dissemination level	Public
Deliverable name	Pilot description and assessment
Work package	WP4, Assessing groundwater recharge and vulnerability to climate change
Lead WP/Deliverable beneficiary	BRGM, BGS
Deliverable status	
Version	Version 2
Date	2021/03/23

LIST OF ABBREVIATIONS & ACRONYMS

TACTIC	Tools for Assessment of Climate change Impact on Groundwater
EGDI	European Geological Data Infrastructure
GSOs	Geological Survey Organisations of Europe
BRGM	Bureau de Recherche Géologique et Minière – French geological survey
IGN	Institut national de l'information géographique et forestière
ONEMA - OFB	Office français pour la biodiversité
CC	Climate Change
GW	Groundwater
EP	Effective Precipitation
IDPR	Indice de Développement et de Persistance des Réseaux
BFI	Baseflow Index
EPIR	Effective Precipitation Infiltration Ratio
EMD	Empirical Mode Decomposition
EEMD	Ensemble Empirical Mode Decomposition
IMF	Intrinsic Mode Functions
WLF	Water Level Fluctuation
AMO	Atlantic Multidecadal Oscillation

TABLE OF CONTENTS

LIST OF ABBREVIATIONS & ACRONYMS	3
1 EXECUTIVE SUMMARY	9
2 INTRODUCTION	12
3 PILOT AREA	14
3.1 Site description and data	15
3.1.1 Location of pilot area and data available.	15
3.1.2 Climate	17
3.1.3 Topography	23
3.1.4 Land use	24
3.1.5 Soil types	25
3.1.6 Geology/Aquifer type	27
3.1.7 Abstractions/irrigation	33
3.2 Climate change challenge	36
3.2.1 How is the climate expected to change in the area	37
3.2.2 What are the challenges related to the expected climate change?	39
4 FUTURE RECHARGE CALCULATION	41
4.1 Methodology	41
4.1.1 Effective precipitation calculation	41
4.1.2 EPIR evaluation	41
4.1.3 Climate data	42
4.2 Results and conclusions	44
4.2.1 Climate data	44
4.2.2 Effective precipitation	47
4.2.3 Groundwater potential recharge	50
5 VULNERABILITY TO CLIMATE CHANGE	52
5.1 Methodology	52
5.1.1 Groundwater and effective precipitation monotonic trend detection	52
5.1.2 Non-linear trend estimation and linkage with effective precipitation	53
5.2 Results and conclusions	55

5.2.1	Groundwater and effective precipitation monotonic trends in metropolitan France	55
5.2.2	Conclusions on the sensitivity of groundwater trends to low-frequency variability (Baulon et al., submitted)	63
5.2.3	Evolution of the filtered groundwater levels and effective precipitation of large-scale atmospheric circulation induced low-frequency variability	64
6	REFERENCES	90

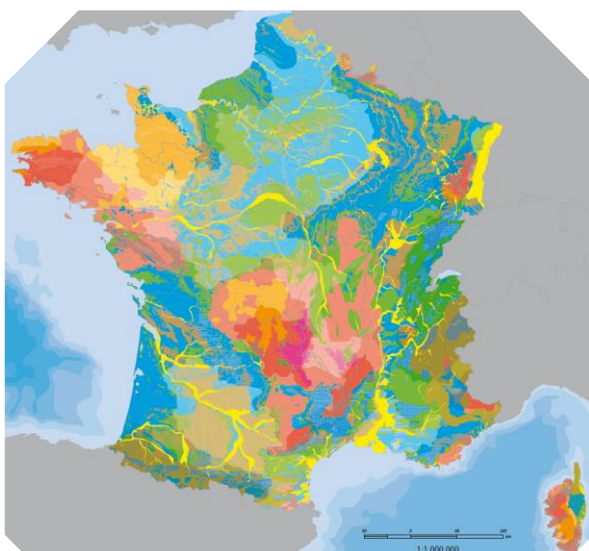
TABLE OF FIGURES

Figure 1: Spatial distribution of sparsely or non-influenced groundwater boreholes through metropolitan France.....	15
Figure 2: Average annual temperature (°C, 1981 – 2010 normal).....	18
Figure 3: The five main climates in France.....	19
Figure 4: Average seasonal temperature (°C, 1981 – 2010 normal).....	20
Figure 5: Cumulative annual rainfall (mm, 1981 – 2010 normal).	21
Figure 6: Cumulative seasonal rainfall (mm, 1981 – 2010 normal).	21
Figure 7: Average annual number of days with rainfall superior to 1 mm (1981 – 2010 normal).	22
Figure 8: Average annual insolation in hours (1991 – 2010 normal).....	23
Figure 9: Map of the land use in France (from the Atlas Régional, SOeS, 2016).	25
Figure 10: Map of the main different soils at the whole metropolitan scale.	27
Figure 11: Geological map of France.....	28
Figure 12: Alluvial aquifers map France.....	29
Figure 13: Location of the three main sedimentary basins (Paris, Aquitaine and South-East).	30
Figure 14: Map of crystalline rocks (red: granite, brown: schist).	32
Figure 15: Map of karstifiable carbonate rocks (blue), modified from Chen et al. 2017.....	33
Figure 16: Evolution of water abstraction for drinking water supply.	34
Figure 17: Observed and projected climate change and impacts for the main biogeographical regions in Europe (European Environmental Agency).....	36
Figure 18: Soil map of Europe, from the EGD interactive maps	37
Figure 19: Deviation from the average annual temperature difference between current and predicted.....	38
Figure 20: Average cumulative annual rainfall difference between current and predicted.	39
Figure 21: Average estimated recharge per year at present time	40
Figure 22: Difference between present day recharge and predicted recharge for the year 2070 (percent for minima projection, mean projection and maxima projection).	40
Figure 23: Sketch of the methodology applied to compute effective precipitation.	42
Figure 24: Monthly precipitation change factors (3°C warming).....	45
Figure 25: Mean annual change factors (3°C warming).....	46
Figure 26: 30-years period interannual mean precipitation (3°C warming)	47
Figure 27: 30-years period interannual mean temperature (3°C warming)	47
Figure 28: 30-years period interannual mean PET (3°C warming).....	47

Figure 29: 30-years period interannual mean effective precipitation	48
Figure 30: Effective precipitation anomalies.....	49
Figure 31: Comparison of effective precipitation anomalies maps.	50
Figure 32: France map of EPIR (SAFRAN cells projection).....	51
Figure 33: France map of present and future groundwater potential recharge	51
Figure 34: Trends magnitude normalised by the maximum water level fluctuation and their statistical significance (threshold of 5%) of monthly groundwater levels averages over the 1976-2019 and 1996-2019 periods.....	56
Figure 35: Comparison between Sen's slope of groundwater levels and effective precipitation over the 1996-2019 period. The statistical significance of trends is tested at a threshold of 5%.	60
Figure 36: Comparison between Sen's slope of groundwater levels and effective precipitation over the 1976-2019 period. The statistical significance of trends is tested at a threshold of 5%.	61
Figure 37: Trends magnitude normalised by the maximum water level fluctuation and their statistical significance (threshold of 5%) of filtered monthly groundwater levels (EEMD residue) over the 1976-2019 and 1996-2019 periods.	65
Figure 38: Comparison between Sen's slope of filtered groundwater levels and effective precipitation over the 1996-2019 period. The statistical significance of trends is tested at a threshold of 5%.	69
Figure 39: Comparison between Sen's slope of filtered groundwater levels and effective precipitation over the 1976-2019 period. The statistical significance of trends is tested at a threshold of 5%.	70
Figure 40: Standardised EEMD residues (i.e. non-linear trends) of groundwater levels (GW) for the borehole of Congerville-Thionville monitoring the limestones of Beauce and effective precipitation (EP) for (a) the selected SAFRAN mesh with the methodology presented in 5.1. to conduct the present study and (b) another SAFRAN mesh within the catchment and a 50 km radius around the well. Sen's slopes estimated on non-standardised EEMD residues of GW and EP are indicated on the right side.	73
Figure 41: Standardised EEMD residues (i.e. non-linear trends) of effective precipitation (EP) and groundwater levels (GW) for the boreholes of (a) Cardonnette monitoring the Seno-Turonian chalk of Artois-Picardy, (b) Cintheaux monitoring the Jurassic limestones from Sarthe to Bessin, (c) Buhuy monitoring the Seno-Turonian chalk of Normandy/Picardy. Sen's slopes estimated on non-standardised EEMD residues of GW and EP are indicated on the right side.	74
Figure 42: K-medoids clustering on non-linear trends (i.e. standardised EEMD residues) over the 1996-2019 period for (a) groundwater levels and (b) effective precipitation. Grey lines are all non-linear trends belonging to the cluster and color lines are cluster medoids (i.e. the most representative non-linear trend within each cluster).....	77
Figure 43: Spatial distribution of clustered non-linear trends over the 1996-2019 period for (a) groundwater levels and (b) effective precipitation.	78
Figure 44: K-medoids clustering on non-linear trends (i.e. standardised EEMD residues) over the 1976-2019 period for (a) groundwater levels and (b) effective precipitation. Grey lines are all non-linear trends belonging to the cluster and color lines are cluster medoids (i.e. the most representative non-linear trend within each cluster).....	81

Figure 45: Spatial distribution of clustered non-linear trends over the 1976-2019 period for (a) groundwater levels and (b) effective precipitation.	82
Figure 46: Examples of non-linear trends showing discrepancies in their cluster membership between effective precipitation and groundwater levels.....	84
Figure 47: Boreholes chosen to determine if non-linear trends are “trends” or low-frequency variability. This figure displays groundwater non-linear trends (black) on the two reference period and the non-linear trend of their corresponding effective precipitation timeseries (red).	86
Figure 48: EEMD residues (solid green) extracted on shorter periods superimposed to the last IMFs (dashed blue) extracted on a longer period.	87

1 EXECUTIVE SUMMARY

Pilot name	France	
Country	France	
EU-region	North Western Europe, Central and Eastern Europe and Mediterranean region	
Area (km²)	543 940 km²	
Aquifer geology and type classification	Multiple	
Primary water usage	Drinking water, irrigation, industry	
Main climate change issues	Groundwater ressource management Drought and groundwater flooding risk prevention	
Models and methods used	Effective precipitation and potential recharge map: Water budget approach, Effective Precipitation Infiltration Ratio Vulnerability analysis: analysis of long-term piezometric time series, trends analysis (monotonic and non-linear), low-frequency variability	
Key stakeholders	Water Agency, French environmental ministry, Biodiversity French Agency	
Contact person	Hélène Bessière, BRGM French Geological survey, h.bessiere@brgm.fr	

This report describes the work undertaken by the French Geological Survey (BRGM) as part of TACTIC WP4 to calculate historical and future potential recharge in the metropolitan France territory and to analyse groundwater vulnerability to climate change with time series analysis.

Five main climates can be observed in the territory, which will evolve differently: oceanic, altered oceanic, semi-continental, mountain and mediterranean. The evolution of those climates will mostly have impacts on temperature and evapotranspiration, thus on effective rainfall available for

groundwater recharge. Aquifers can be grouped in five main themes (terminology used in the French hydrogeological referential BDLISA): alluvial, sedimentary (the most important), bedrock, intensively folded rocks and volcanism (very few). Groundwater recharge is also depending on soils types and land use. Pilot area's land use is mostly agricultural (near 60%).

Historical and future effective precipitation and potential recharge map

The methodology applied to assess the potential groundwater recharge at the country scale combines a water budget approach and the use of an Effective Precipitation Infiltration Ratio. It is applied to evaluate both present and future groundwater recharge. The change factors were applied to the SAFRAN (Meteo France climate model) daily data for the period 01/01/1981 – 31/12/2010, to produce climate data that can be used to simulate future effective precipitation.

At the annual time scale, the “highest” impact scenario predicts a light decrease of precipitation around the Mediterranean sea, but a high increase (up to 10%) in the North-East and North-West parts of France. Temperature increase are particularly important in the South-West part where they reach 2.7°C. PET increase everywhere, between 4 and 10%. The distribution of effective precipitation anomalies computed with the highest impact scenario shows an unexpected pattern, with a decrease of effective precipitation in the middle part of France (between 2.5 and 15%) and an increase elsewhere (up to 17% in Alsace). These results are strongly linked to the precipitation change factor maps.

The “lowest” impact scenario actually shows also marked changes. Precipitation strongly decrease, especially in summer, with annual reduction showing a gradient pattern from 20% in South-West to 4% in North-East. Temperature increases remain under 2.5°C all over France (between 1.2°C in Bretagne to 2.16°C in Centre-East). Effective precipitation anomalies are negative everywhere except along the North border where they are slightly positive. The effective precipitation reduction reaches 33% in the South-West, and gradually decreases northwards.

The “highest” impact scenario results are unexpected and far from other published results. On the other side, the “lowest” impact scenario results are in the same range and show comparable patterns as previous results obtained by BRGM with the same methodology but with different climate data (ensemble simulation with 4 GCM and 2 downscaling methods). The main differences concern the Paris basin and the North part of France. The important decrease of effective precipitation in the South-West region is of the same order of magnitude of the TACTIC results (-30 - -40%) as in the EXPLORE 2070 exercise but higher than in BRGM 2019 results (-20% - -30%).

Vulnerability analysis

The assessment of long-term evolution of groundwater levels is conducted with a non-influenced boreholes database through metropolitan France (Baulon et al., 2020): 215 boreholes with more than 24 years of data. The selected wells span over multiple hydrogeological contexts: alluvial aquifers, sedimentary aquifers, volcanic and bedrock aquifers. Most of selected wells are situated into sedimentary aquifers, mainly in the Parisian Basin, and sporadically in the Aquitaine Basin.

The vulnerability of aquifers to climate change is assessed via monotonic and non-linear trend analyses. The monthly groundwater levels averages and monthly cumulative effective precipitation are used to conduct it. Analyses is performed on two reference periods (1996-2019 and 1976-2019) providing the best compromise between the length of groundwater time series and their spatial distribution through metropolitan France and northern France, respectively.

For each groundwater time series, an effective precipitation time series is assigned to it via the development of an indicator (Manceau et al., 2020). The indicator time series (expressing the effective precipitation) allowing the maximization of the correlation coefficient with monthly groundwater levels is selected as it is the most representative mesh of the groundwater level behaviour.

The study of filtered groundwater levels and effective precipitation has been done via several approaches: (i) the estimation of monotonic trends on these filtered data (*i.e.* EEMD residues or non-linear trends), (ii) the clustering of these non-linear trends, (iii) the questioning of if these non-linear trends are “trends” or only segments of lower frequency variabilities.

The monotonic trends detected on filtered data reveal few differences with monotonic trends estimated on raw data (*i.e.* unfiltered data) on the longest reference period (1976-2019), particularly for groundwater levels. However on shorter period (1996-2019), greater discrepancies appear with monotonic trends estimated on raw data: magnitudes of trends are very often accentuated and even trend direction can be impacted.

Sometimes, we can observe opposite detected monotonic trends between filtered groundwater levels and effective precipitation that may be related to several phenomena: (i) a wrong selection of effective precipitation mesh at the beginning of the analysis leading to a non-linear trend in effective precipitation that does not represent the non-linear trend in groundwater levels, (ii) a long-term anthropogenic influence on aquifers (*e.g.* long-term pumping) and the non-linear trend of groundwater levels no longer represents the one of effective precipitation, (iii) a dephasing between the non-linear trend of groundwater levels and effective precipitation due to the response time of aquifers, (iv) a distortion or modulation of oscillation amplitude induced by catchment and aquifers properties, (v) asymmetry discrepancies between non-linear trends of groundwater levels and effective precipitation also induced by catchment and aquifer properties.

In summary, multiple interpretations of groundwater level trends can be made. These trends may be linked to (i) anthropogenic impacts (*e.g.* groundwater pumping, changes in land cover that may generate a decrease in groundwater recharge), (ii) climate change that may result in a decrease in groundwater recharge, (iii) a segment of low-frequency oscillations which could appear as a trend on the short-term. Without taking into account the anthropogenic impacts (which data are often poorly referenced), the most limiting factor to make the distinction between points (ii) and (iii) remains the availability of groundwater levels data. Therefore, it highlights the complexity to define whether trends in hydroclimate variables can be related to climate change or simply being part of a lower-frequency oscillation originating from large-scale atmospheric or oceanic circulation. In addition, anthropogenic forcing may also impact these large-scale patterns (*e.g.* Dong et al., 2011; Caesar et al., 2018).

2

INTRODUCTION

Climate change (CC) already have widespread and significant impacts in Europe, which is expected to increase in the future. Groundwater plays a vital role for the land phase of the freshwater cycle and have the capability of buffering or enhancing the impact from extreme climate events causing droughts or floods, depending on the subsurface properties and the status of the system (dry/wet) prior to the climate event. Understanding and taking the hydrogeology into account is therefore essential in the assessment of climate change impacts. Providing harmonised results and products across Europe is further vital for supporting stakeholders, decision makers and EU policies makers.

The Geological Survey Organisations (GSOs) in Europe compile the necessary data and knowledge of the groundwater systems across Europe. In order to enhance the utilisation of these data and knowledge of the subsurface system in CC impact assessments the GSOs, in the framework of GeoERA, has established the project “Tools for Assessment of Climate change Impact on Groundwater and Adaptation Strategies – TACTIC”. By collaboration among the involved partners, TACTIC aims to enhance and harmonise CC impact assessments and identification and analyses of potential adaptation strategies.

TACTIC is centred around 40 pilot studies covering a variety of CC challenges as well as different hydrogeological settings and different management systems found in Europe. Knowledge and experiences from the pilots will be synthesised and provide a basis for the development of an infrastructure on CC impact assessments and adaptation strategies. The final projects results will be made available through the common GeoERA Information Platform (<http://www.europe-geology.eu>).

The specific TACTIC activities focus on the following research questions:

- What are the challenges related to groundwater- surface water interaction under future climate projections (TACTIC WP3)?
- Estimation of renewable resources (groundwater recharge) and the assessment of their vulnerability to future climate variations (TACTIC WP4).
- Study the impact of overexploitation of the groundwater resources and the risks of saline intrusion under current and future climates (TACTIC WP5).
- Analyse the effectiveness of selected adaptation strategies to mitigate the impacts of climate change (TACTIC WP6).

The present document reports the TACTIC activities in the pilot France undertaken by the French Geological Survey (BRGM) as part of WP4. WP4 is divided into seven tasks that cover the following activities: Review of tools and methods and identification of data requirements (Task 4.1), identification of principal aquifers and their characteristics aided by satellite data (Task 4.2), recharge estimation and its evolution under climate change scenarios in the principal aquifers (Task 4.3), analysis of long-term piezometric time series to evaluate aquifer vulnerability to climate change (Task 4.4), assessment of subsidence in aquifer systems using DInSAR satellite data (Task 4.5), development of a satellite based net precipitation and recharge map at the pan-European scale (Task 4.6), and tool descriptions and guidelines (Task 4.7).

Two different works are presented in this report and they are related to Task 4.3 and Task 4.4.



The first part of the work aims at the estimation of recharge under current and future climate. This is undertaken using a water budget approach to estimate effective precipitation and the use of an Effective Precipitation Infiltration Ratio to deduce potential recharge.

The second part of the work aims to assess aquifer vulnerability to climate change thanks to the analysis of long-term piezometric time series. The main challenges of this study is the great diversity of aquifer systems in France (confined/unconfined, porous/fissured, alluvial/sedimentary/volcanic, etc) and the lack of very long term time series of groundwater levels and information on abstraction data.

3

PILOT AREA

The pilot area is the whole metropolitan France territory. This area is characterized by several types of climate, aquifers, soils and landscape, and thus will not be affected by climate change the same way depending on the region.

Five main climates can be observed in the territory, which will evolve differently: oceanic, altered oceanic, semi-continental, mountain and mediterranean. The evolution of those climates will mostly have impacts on temperature and evapotranspiration, thus on effective rainfall available for groundwater recharge.

Groundwater recharge is also depending on soils types and land use. Pilot area's land use is mostly agricultural (near 60%), and at this scale, soils represents mostly the high influence of the mineral material nature where the soils have been formed and are still evolving. Those characteristics influence infiltration and transport of rainfall from the surface to the water table. Storage and groundwater transport is then depending on the aquifers characteristics. On the pilot area, aquifers can be clustered in five main themes (terminology used in the French hydrogeological referential BDLISA): alluvial, sedimentary (the most important), bedrock, intensively folded rocks and volcanism (very few). Those formations are bound with multiple landscape characterizing the area, mostly influenced by formations of basins (Paris, Aquitan, and South-East), and several massifs and mountains (the Alps, the Pyrenees, the Massif Central, The Jura, the Vosges and the Armorican Massif).

In a previous study (Explore 2070), climate models projection results predict a virtually systematic decline from 10 to 25% in water table recharge, due to temperature rise and effective rainfall decrease.

These characteristics of the pilot area are developed below to describe the area. They will most likely be used to explain the different results of the study.

3.1 Site description and data

3.1.1 Location of pilot area and data available.

The assessment of long-term evolution of groundwater levels will be conducted with a non-influenced boreholes database through metropolitan France (Baulon et al., 2020). In this report, 215 boreholes among the 254 boreholes constituting this dataset will be used because their length is upper than 24 years and their spatial distribution through metropolitan France is correct. Originally, groundwater level time series are provided by BRGM via the database ADES (<https://ades.eaufrance.fr/>).

The selected wells for this study answer to few criteria:

- The length of groundwater time series must be higher than 24 years.
- A minimum amount of data in a month. This minimum amount is divided in two parts. The date of sampling frequency change is identified in each time series. The minimum sampling frequency is at least one monthly data before this date, and three data per month after this date (which appeared as the best compromise).
- The length of consecutive gaps must be lower than 3 years for time series starting after 1950; and lower than 10 years for time series starting before 1950. It allows time series in the new database to preserve the low-frequency in data.
- A minimum influence of pumping on groundwater levels.

The spatial distribution of the selected boreholes is presented in Figure 1.

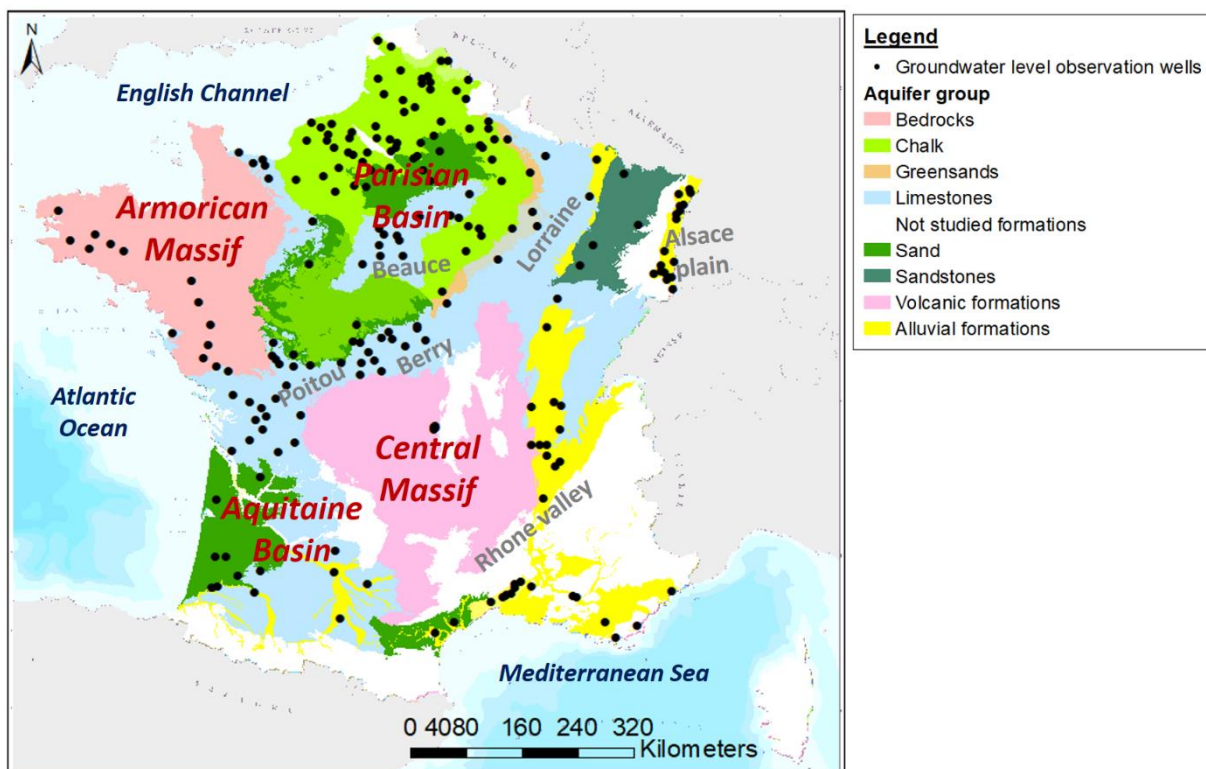


Figure 1: Spatial distribution of sparsely or non-influenced groundwater boreholes through metropolitan France.



The selected wells span over multiple hydrogeological contexts: alluvial aquifers, sedimentary aquifers, volcanic and bedrock aquifers. Most of selected wells are situated into sedimentary aquifers, mainly in the Parisian Basin, and sporadically in the Aquitaine Basin. Each well has been attached to a hydrogeological area based on groundwater bodies and its dynamic.

Concerning the aquifers captured by the selection of wells, the Seno-Turonian chalk aquifer of the Parisian Basin is the most represented, followed by Jurassic limestone aquifers (Lorraine, Berry, Poitou) on the edge of the Parisian Basin, and the Eocene limestones of Beauce aquifer. Wells located in the Aquitaine Basin mainly capture the Jurassic limestone aquifer of the northern Aquitaine Basin, and the multiple sedimentary hydrogeological formations in the southern part (sands, limestones). Finally, most of wells selected in the Rhone valley monitor alluvial and fluvio-glacial formations.

Alluvial aquifers are also well represented in the dataset, especially the Rhine/Vosges recent or ancient alluvium in Alsace region, Garonne alluvium in Toulouse region, and recent alluvium in the Mediterranean region.

Some wells are located in Central Massif volcanic aquifers in various formations with different dynamism. Finally, bedrocks aquifers are monitored by few selected wells in Armorican Massif.

Table 1 synthesizes the number of wells by major hydrogeological entity.

Table 1 *Number of wells by major hydrogeological entity/area.*

Hydrogeological entities	Number of boreholes
Seno-Turonian chalk of Artois-Picardy	18
Seno-Turonian chalk of Normandy/Picardy	30
Seno-Turonian chalk of Champagne	8
Jurassic limestones from Sarthe to Bessin	5
Lutetian and Ypresian sands of Paris Basin	3
Jurassic limestones of Lorraine and Côte-des-Bars	4
Triassic sandstones of Lorraine	2
Upper Eocene limestones of Paris Basin	4
Alluvial formations of Alsace	18
Limestones of Beauce	8
Chalk of Bourgogne and Gâtinais	4
Triassic limestones of Lorraine	1
Bedrocks of Britain	10
Jurassic limestones of Berry	9
Jurassic limestones of Poitou	6
Fractured Jurassic limestones of northern Aquitaine Basin	7
Alluvial and fluvio-glacial formations of Rhone valley	11
Volcanic formations of Central Massif	5
Various calcareous formations of Aquitaine Basin	3



Plio-Quaternary sands of Aquitaine Basin	3
Alluvial formations of Mediterranean region	11
Alluvial formations of Garonne	3
Other (smaller) hydrogeological entities	42

Before the data analysis, a visual check of groundwater level time series was achieved in order to remove or correct erroneous data. As we wanted to qualify groundwater dynamism considering also the annual timescale, we decided to work on monthly averages. Then, missing months in these time series were filled by linear interpolation to perform spectral analyses.

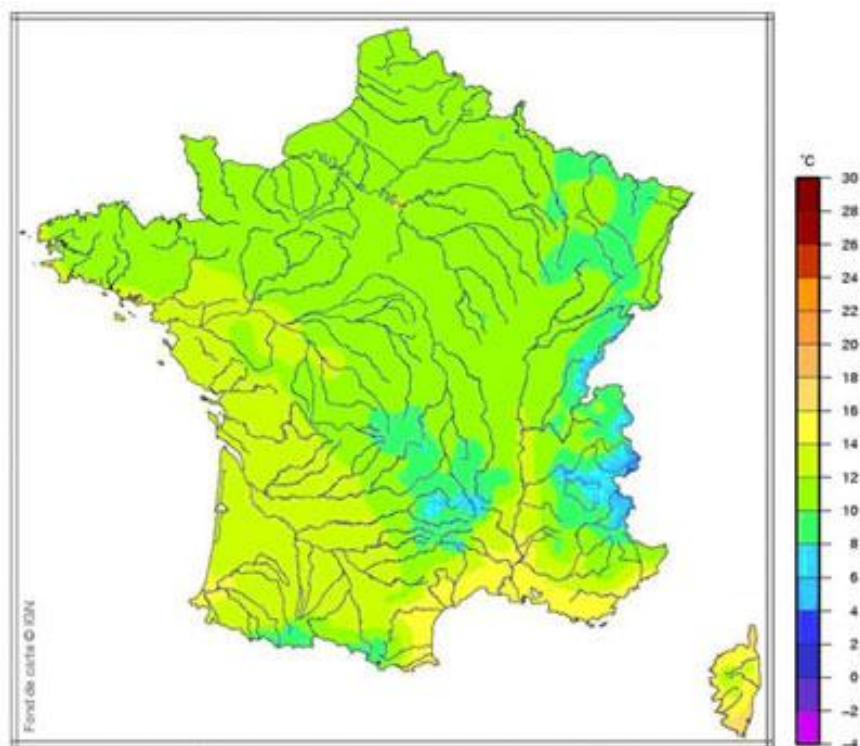
3.1.2 Climate

This part is based on Meteo-France description of the metropolitan France climate.

(www.meteofrance.fr)

3.1.2.1 Climate type

On a global scale, metropolitan France benefits from a temperate climate. Rainfall are distributed throughout the year, and relatively mild temperatures (Figure 2). These characteristics are due to the latitude and the dominance of winds coming from the Atlantic.



*Figure 2: Average annual temperature (°C, 1981 – 2010 normal).
(Meteo-France, map background IGN)*

However, regions experience climates variations, according to their latitude, their altitude and the distance from the sea, reinforced by their position compared to the three important mountains (Pyrenees, Massif Central, Alps).

3.1.2.2 Five main types of climates

At first glance, there are five main climates types in metropolitan France: oceanic, altered oceanic, semi-continental, mountain and mediterranean (Figure 3).



Figure 3: The five main climates in France.
(Meteo-France) Shadow areas correspond to transition zones.

- Oceanic climate is characterized by mild temperatures and relatively abundant rainfall (in connection with Atlantic disturbances), distributed throughout the year with a slight maximum from October to February. The oceanic climate is typical of the Brittany coasts and Lower Normandy. Further north, to the Belgian border, winters are colder. Further south, the lower Loire Valley, Vendée and Charentes have lower rainfall. In Aquitaine, the proximity of the Pyrenees increases rainfall in winter and spring.
- Altered oceanic climate is a transition zone between the oceanic climate, mountain climates and the semi-continental climate. Temperature differences between winter and summer increase with the remoteness of the sea, and rainfall is lower than at seaside (except near reliefs). This climate is located in the Massif Central western and northern foothills, in the Paris Basin, Champagne, eastern Picardy and Nord-Pas-de-Calais.
- Semi-continental climates are characterised by hot summers and rough winters, with many days of snow and frost. Annual rainfall is relatively high, except in Alsace, because of the protective effect of the Vosges. The rains, often stormy, are more important in summer. This climate is typical of the north-eastern quarter of France (Alsace, Lorraine, Ardennes, Argonne, Franche-Comté and part of Burgundy) and some steep sided plains sheltered from the west winds, from the Massif Central and the Alps.
- Mountain climate temperatures decrease quickly with altitude. Cloudiness is minimal in winter and maximum in summer, and there are significant variations in winds and precipitations from a location to another.

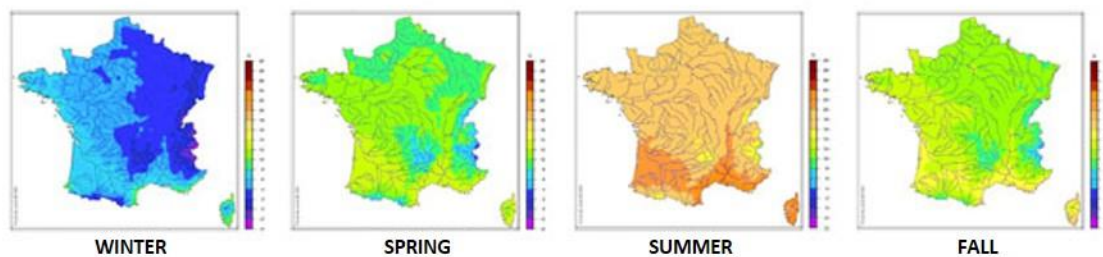


- Mediterranean climate is characterized by mild winters and hot summers, sunshine and frequent high winds. The few rainy days are irregularly distributed over the year. Dry winters and summers are followed by very wet springs and autumns, often as stormy rain (40% of the annual total rainfall in 3 months). This precipitation can bring 4 times more water than the monthly average in a given place in a few hours, especially near the relief (episode Cevennes). The regions concerned by the Mediterranean climate are located in the South East between sea and mountains.

3.1.2.3 Metropolitan France scale

Average temperatures

Autumn and winter average temperature varies with the "continentality" of the area. The further the place is from the Atlantic Ocean or the Mediterranean, the lower the temperature: took apart mountain regions, the temperature is the lowest on the north-east of France (Figure 4). During spring and summer, temperatures vary with the latitude of the area. It depends mainly on the presence or absence of clouds, hence this increase from north-west to south-east, (effect tempered by the mountain massifs).



*Figure 4: Average seasonal temperature (°C, 1981 – 2010 normal).
(Meteo-France, map background IGN)*

Average annual rainfall

Average annual rainfall amounts vary from 500 mm for the drier regions (Mediterranean coasts, Anjou, Paris Basin) to more than 1500 mm for mountain regions (Figure 5Figure 7). Rainfall depends both on the altitude of the place and the ocean proximity. Thus, Atlantic and Channel coasts are rainier than Anjou and Paris Basin, and certain valleys (Alsace, Allier Valley, Upper Loire Valley) are protected from rainfall by their bordering reliefs. In Brittany and on Atlantic coasts, precipitation is due to Atlantic disturbances.



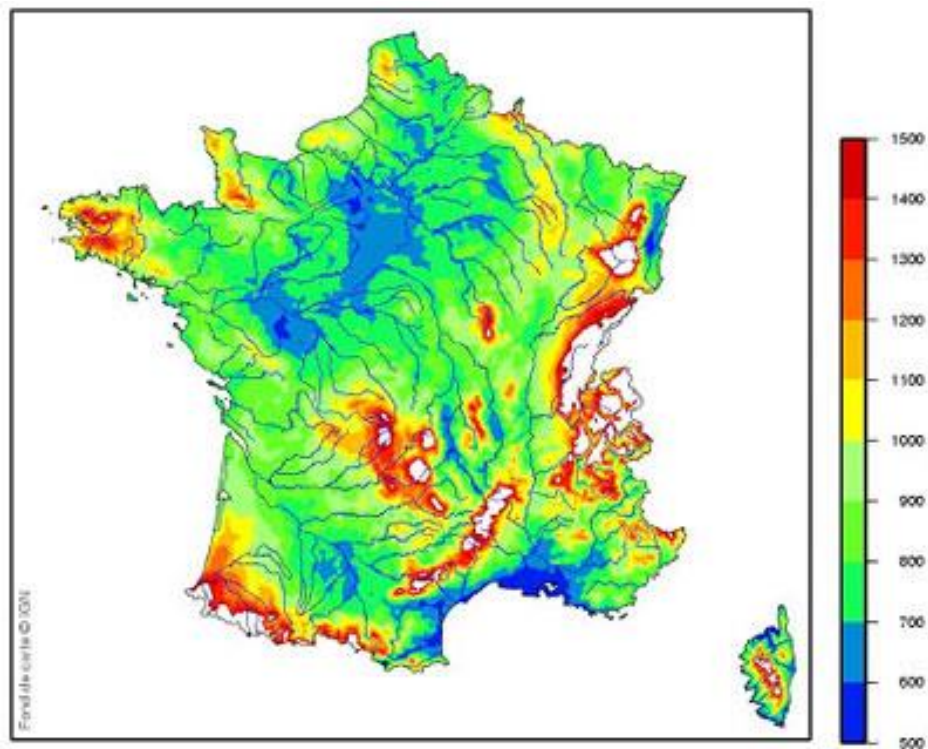


Figure 5: Cumulative annual rainfall (mm, 1981 – 2010 normal).
(Meteo-France, map background IGN)

The winter months are the rainiest. On the other hand, in the northeast, the summer months are wetter than the winter months because of the predominance of thunderstorms. Around the Mediterranean, especially on the Cevennes and the Black Mountain, precipitation occurs mainly in the form of intense rainstorms during autumn or spring (Figure 6).

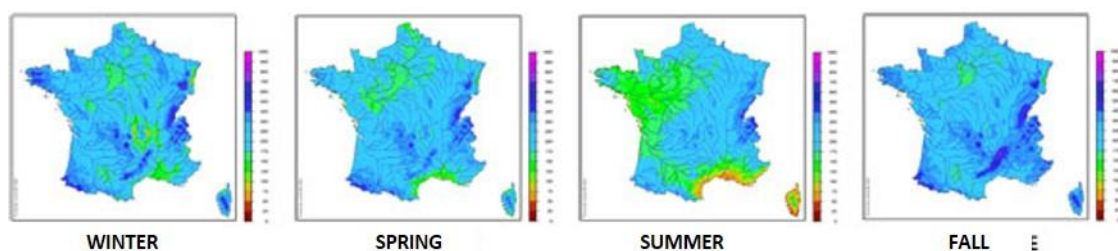


Figure 6: Cumulative seasonal rainfall (mm, 1981 – 2010 normal).
(Meteo-France, map background IGN)

Average annual number of rainy days

The number of days per year with rain (precipitation of the day greater than 1 mm, Figure 7) varies from 40 (Mediterranean coasts) to 180 (Armorican Massif, Vosges). Comparison between the annual precipitation map and the average number of rainy days map, it occurs that with equal amounts of



precipitation, south of France experiences fewer rainy days than north, but because of thunderstorms the rains are less frequent but more intense.

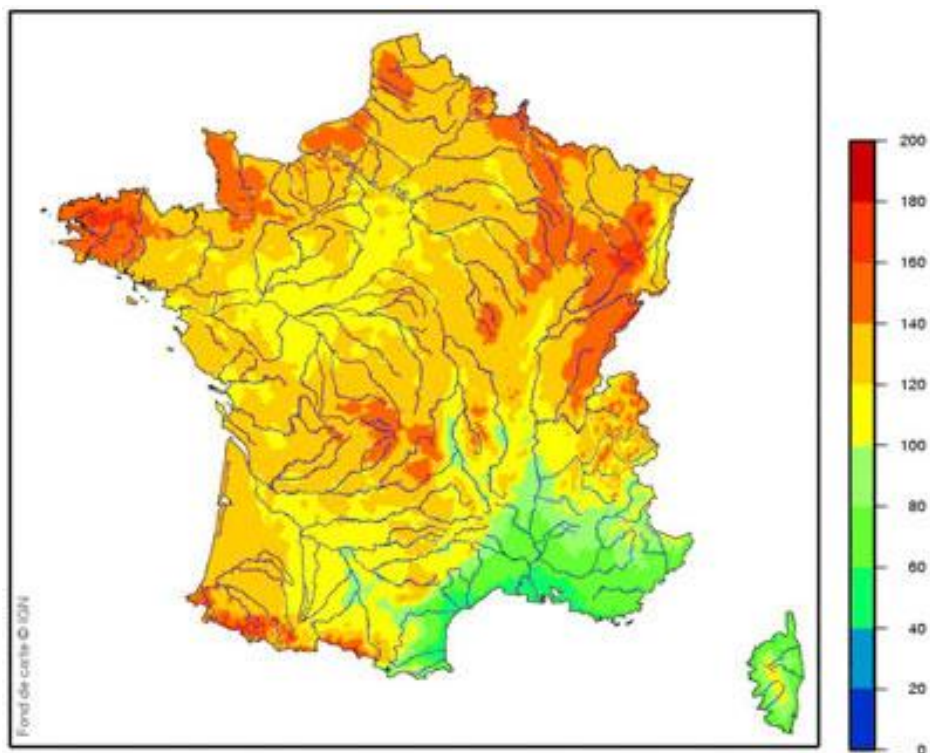
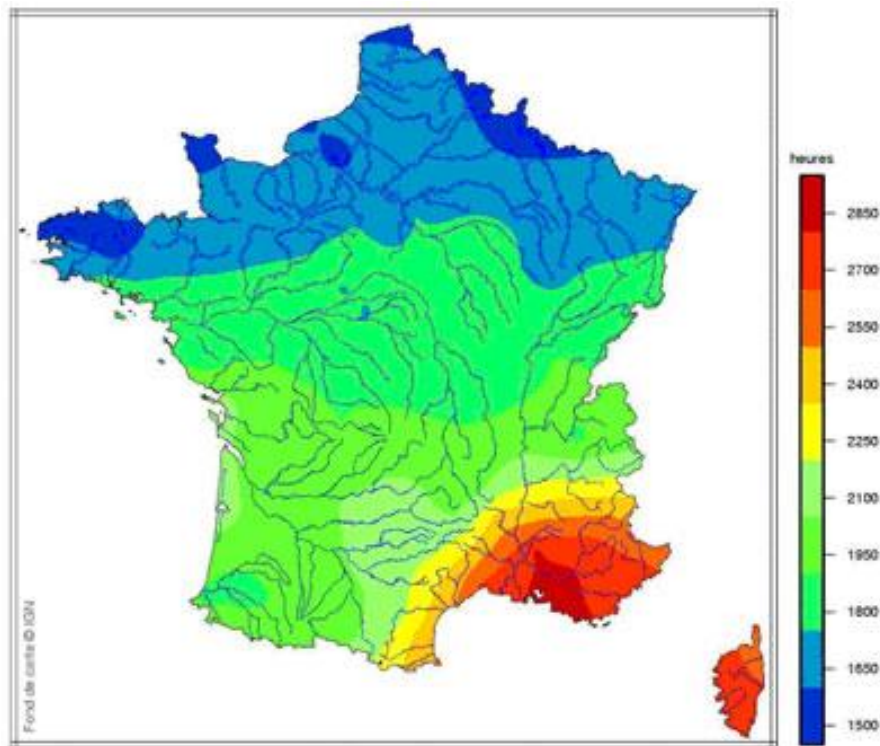


Figure 7: Average annual number of days with rainfall superior to 1 mm (1981 – 2010 normal).
(Meteo-France, map background IGN)

Average annual insolation

The average annual hours of sunshine increase from 1500 hours in northern France to 2800 hours in the south (figure 8).



*Figure 8: Average annual insolation in hours (1991 – 2010 normal).
(Meteo-France, map background IGN)*

Precipitation and evapotranspiration

In metropolitan France latitudes, the actual evapotranspiration is very low between November and March, more or less strong the rest of the year according to the soil water reserve (UK). The effective rainfall will therefore be positive during this period, and none the rest of the year. Nevertheless, an important rainy sequence can still prevail over the evapotranspiration and generate an infiltration towards the aquifer. On the opposite, rainfall deficits occurring in winter can result in low effective rainfall.

3.1.3 Topography

The metropolitan France covers an area of 551 695 km². Its summit is le Mont Blanc, which is at 4810m above the sea levels.

Landscape is composed of six massifs (the Alps, the Pyrenees, the Massif Central, The Jura, the Vosges and the Armorican Massif), and three basins (Paris, Aquitaine and South-East basins).

The area is surrounded by both land frontier and seas. The height land frontiers are common with Belgium, Luxembourg, Germany, Switzerland, Italy, Monaco, Spain and Andorra.

Groundwater in France is almost entirely drained away to four seas: the North Sea, the Channel, the Atlantic Ocean and the Mediterranean, via five principal rivers, which are the Seine, The Loire, The Garonne, The Rhone and the Rhine.



Most of the watercourses in the southern two-thirds of France drain into the Atlantic, through the basins of the Loire, the Garonne and the Adour. The eastern watershed for this area is along the eastern edge of the Massif Central, reaching to within 25 miles of Lyon.

Watercourses in south-eastern and central eastern France mostly flow out to the Mediterranean, via the Rhone. Only the extreme south and southeast of the Massif Central, i.e. the southern edge of the Cévennes mountains, drains into the Mediterranean. Water from areas between the Morvan and the Vosges, notably the Saône Basin, flows south to the Rhone (the two rivers meet at Lyon), and thence down to the Mediterranean.

The extreme east of France, Alsace to the east of the Vosges and Lorraine to the north and northwest of the Vosges, have rivers that drain into the North Sea, directly or indirectly via the Rhine.

A small northwest quarter of France has rivers, notably the Seine and the Somme, that flow into the Channel.

3.1.4 Land use

This part is based on the “Atlas regional 2016” (Regional Atlas 2016) edited by “Le service de l’observation et des statistiques (SOeS)” (statistics and observation service).

Artificialized areas are mostly localised in large agglomerations areas and grow with demographic and economic development. They evolve near the large urban centers (notably in the West of the territory), along main existing and future axes of communication. Artificialization increases at the level of agricultural land and natural habitats, in particular by separating from natural environment.

The land use framework in France metropolitan evolve slowly. National territory remains mostly agricultural (near 60% of the surface area, figure 9). However, from 2006 to 2012, artificialization continues to grow, mainly to the extent of agricultural land (for 87% of areas newly artificialized). Despite the artificialisation grows slower between the period running from 2006 to 2012 than from 2000 to 2006, the agricultural land decrease remains as important through these two periods.

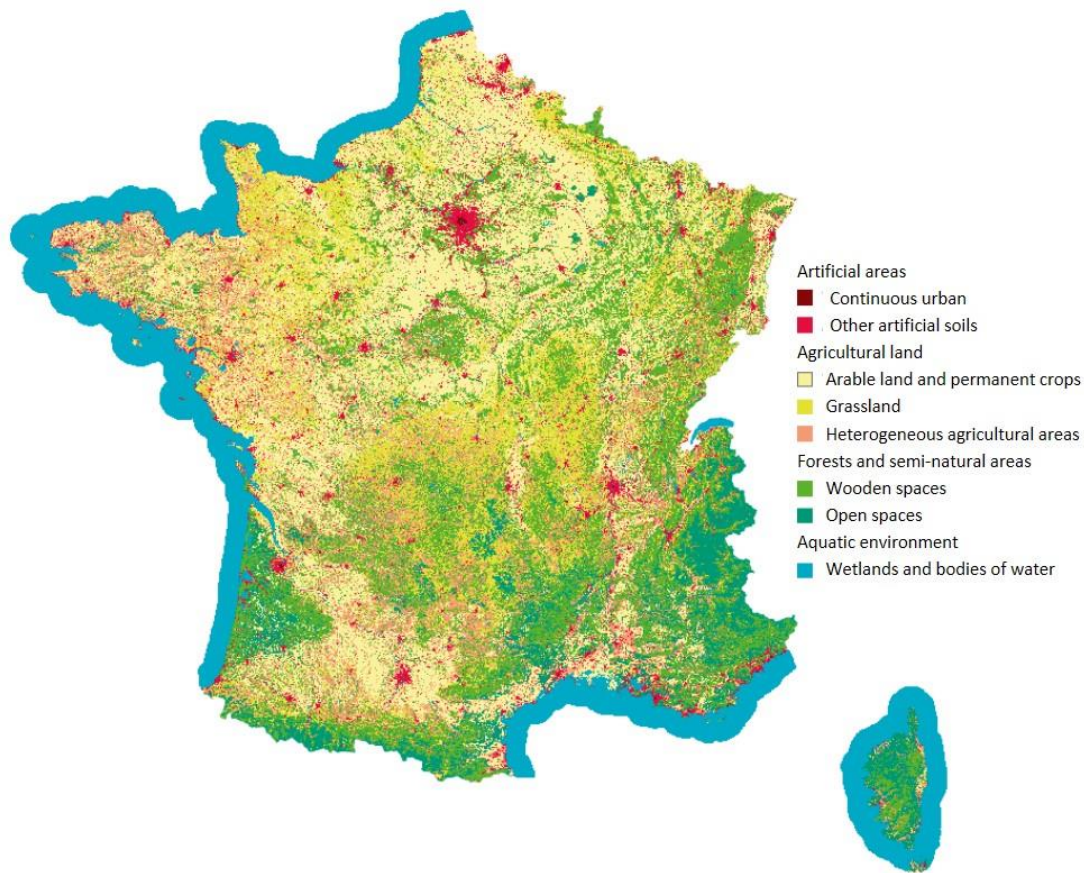


Figure 9: Map of the land use in France (from the Atlas Régional, SOeS, 2016).

3.1.5 Soil types

This part is based on report “L’état des sols de France” (State of the soils of France), the “Référentiel pédologique 2008” (pedologic referential 2008) and the World reference base for soils resources 2006.

Soils mapping is the way to define soil units geographic extension, for a given scale. As a synthesis, it determines the soils spatial framework, based on their formation forcings (geology, climate, topography, vegetation).

It allows to perform spatialized inventories of soils for a given area, and consequently to constitute a supporting tool for public policies. However, according to the scale of the map and its objectives, a distinction can be made on the soil units only, or on groups of soil units.

Thus, small scales with national or continental vocation, such as 1/1 000 000 are used for wide representations, for scientific or didactic purposes. Their also used for decision helping at national or European scales. Units are here groups of soil units. For example, the soils map of France (Figure 10) represents mostly the high influence of the mineral material nature where the soils have been formed and are still evolving.



The distribution of soil types is strongly marked by the great diversity of rocks that are encountered in France:

- The Landes and Sologne's sandy rocks;
- Brittany and Vosges' granites;
- Alps, Brittany and Massif Central's schists;
- Paris and Midi basins hard limestones;
- Champagne's chalks;
- marls within the east and in Limagne;
- Massif Central's basalts;
- Aquitaine, Paris Basins and Alsace's eolian limes;
- Camargue's fluvial and fluviomarine alluviums;
- marshes of the West.
- On a third of the territory, limes deposits from the Quaternary era (between -50,000 and -10,000 years) mark the soils of Beauce, Ile-de-France and Picardy. Also present in Brittany, Brie or in the Garonne valley, their composition varies according to their origin (wind, fluvial or colluvial).



Figure 10: Map of the main different soils at the whole metropolitan scale.

Map from: Inra, Base de données Géographique des Sols de France à 1/1 000 000 (GISSol).

Legend using the French « Référentiel Pédologique 2008 (RP2008) » terminology.

A correspondence table between the RP2008 and the World Reference Base 2006 (WRB) is available in the 5th annex of the Référentiel pédologique (2008).

3.1.6 Geology/Aquifer type

This part is based on the work of Jean-Christophe Maréchal and Josselin Rouillard (BRGM)



3.1.6.1 Geology

French geology consists of a large spectrum of various rocks (Figure 11), leading to very different types of aquifers located in sedimentary basins (depicted in orange to yellow), alluvial plains (light yellow), limestone rocks (blue and dark green) and crystalline rocks (red and brown).



Figure 11: Geological map of France.

3.1.6.2 Aquifer types

Alluvial aquifers

These aquifers (Figure 12) are the main providers (about 45%) of groundwater use in France. They have a very important role in the satisfaction of human needs of the country being favourably located in alluvial plains where the most fertile agricultural lands are located and most cities established. With their high yields of wells for low costs (shallow water table) and their natural ecological role at the origin of wetlands. Besides the diffuse recharge from rainfall, the water balance of alluvial aquifers is highly dependent on groundwater flow from neighbouring aquifers and interaction with surface water. The depletion induced by pumping in the alluvial aquifer increase these inflows. This contributes to improve the well yields but threatens water quality due to the intrusion of poor quality surface water.

At the alluvial aquifers scale, the largest abstraction rates are pumped from the Alsace alluvial aquifer, the Lyon plain and Isere river valley.

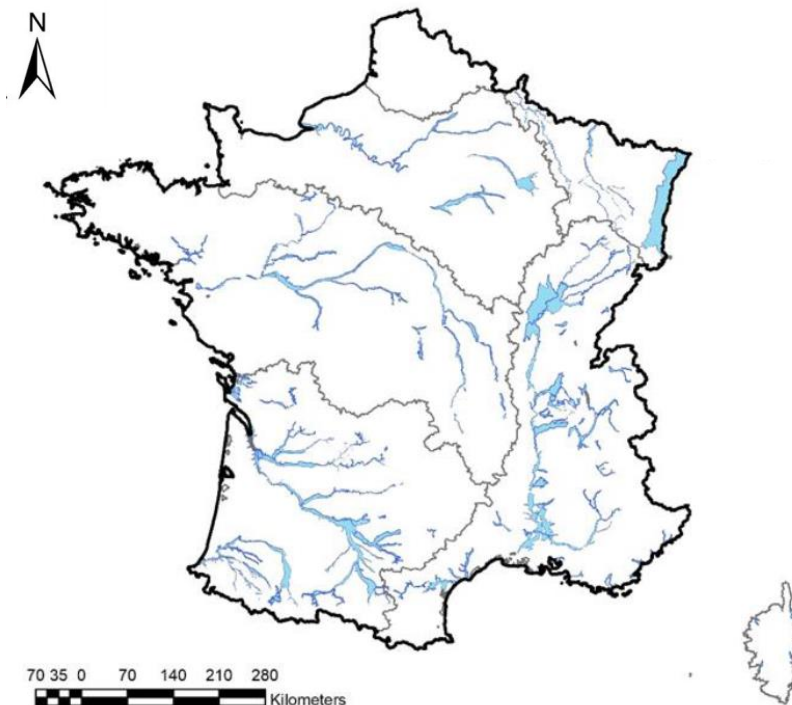


Figure 12: Alluvial aquifers map France.

Sedimentary aquifers

There are three main large sedimentary basins in France: Paris, Aquitaine and southeast basins (Figure 13). According to their structure and flow regimes, these aquifers can be classified according to three types:

- Large single-layer unconfined aquifers, mainly constituted by chalk and limestone rocks. The main aquifers in this category are the chalk aquifer in northern France and a large part of Paris basin, Beauce aquifer, and Landes sandy aquifer.
- Multi-layers aquifers constituted by heterogeneous tertiary sediments located in the centre of Aquitaine (Figure 13) and Paris basins. They are constituted by a shallow unconfined aquifer and several deep confined aquifers.
- Large deep confined aquifers mainly constituted by sands or sandstones (Albien aquifer in the Paris basin) or limestone (Carboniferous rocks in the north). Initially artesian, these aquifers are now highly exploited (Inferior Trias sandstones, inframollasic aquifer in Aquitaine basin), and artesianism has mostly disappeared.

Paris and Aquitaine are the main basins constituted by sedimentary aquifers, with high yields in permeable layers. Chalk aquifers from northern France provide $\sim 360 \text{ Mm}^3/\text{yr}$, multi-layers Aquitaine basin ~ 350 to $450 \text{ Mm}^3/\text{yr}$.

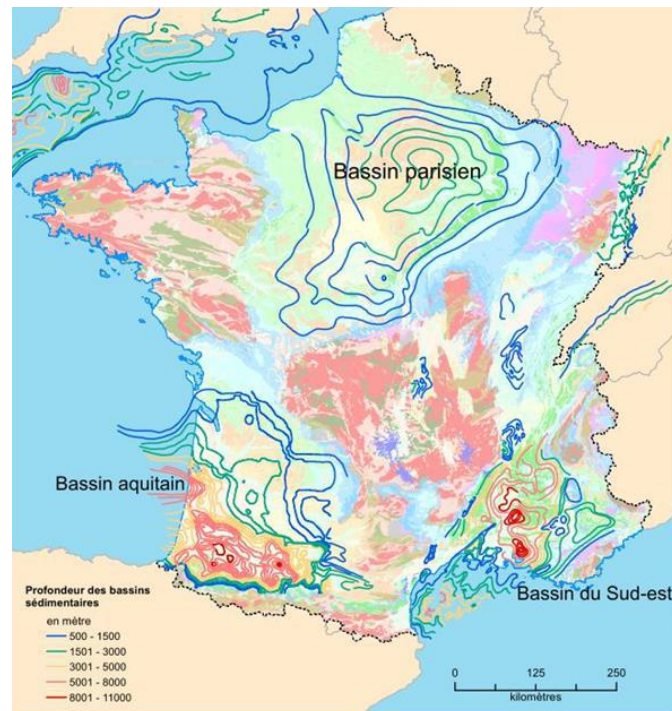


Figure 13: Location of the three main sedimentary basins (Paris, Aquitain and South-East).

The calcareous Beauce aquifer, located north of Orleans (centre of France), is one of the largest aquifers in the country. The aquifer contains an average water volume of 20 billion m³, which extends over 9000 km². This area is one of the big-gest producers of cereals in Europe. Agricultural land represents 6000 km², i.e. more than 70% of the total area, 50% of which (3000 km²) is irrigated (Lejars et al. 2012). The irrigated area in the Beauce increased by 50 percent between 1988 and 2000, mainly driven by cash-crops in the summer (Lejars et al. 2012). The groundwater abstraction has increased also. The conservation of the Beauce aquifer is now reached thanks to an agreement called 'Beauce Aquifer Charter' ('charte nappe de Beauce') which allowed to limit the abstracted volumes for irrigation.

The Paris Basin is the largest sedimentary basin in France. It starts with Permian and Triassic and ends with Tertiary deposits. Vertically, at least seven aquifer layers can be found, the deeper of which are brackish. The main aquifers are the chalk aquifer from Upper Cretaceous (light green on Figure 13), the Albien green sands (dark green), the Lower Jurassic limestone (light and medium blue) and the Vosges Lower Trias sandstones (magenta). Large Tertiary aquifers (Beauce, Brie, yellow) stand above the basin.

Crystalline and volcanic rock aquifers

Crystalline rocks are mainly located in two large mountain ranges: the Armorican Massif range in the west and Central Massif range at the centre of the country (Figure 14). Vosges, Pyrenees and Alps mountains constitute other outcrops. These fractured rocks also mainly constitute Corsica Island.

The typical geological profile in weathered crystalline aquifers follows the lithological description by Dewandel et al. (2006) which, from top to bottom, consists of:

- Red soil from the first decimeteres to the first meter.
- Sandy regolith of a few meters thickness: yellowish colour, sandy-clay composition, sandy texture with many quartz grains.
- Saprolite from about 3 meters to 13 – 24 meters deep, derived from in situ weathering of crystalline rock: yellowish to brownish colour, coarse sand-size clasts texture and laminated structure. This horizon exhibits preserved fractures.
- Granite or gneiss rocks. The upper part of the hard rock is highly weathered and fractured but the fracture frequency decreases rapidly with depth.

In flat areas (Brittany), these aquifers are exploited through shallow (50-100 m deep) boreholes while in mountainous areas (Pyrenees, Alps, Central Massif), water is drained from natural springs. Water abstraction rates are generally low: a few m³/hour.

Volcanic rocks are mainly located in the Massif Central. The total amount of groundwater supplied by Massif Central volcanic rock aquifers is ~40 Mm³/yr. These aquifers provide low yields but they often represent the sole source of supply for small villages or small agriculture farms.

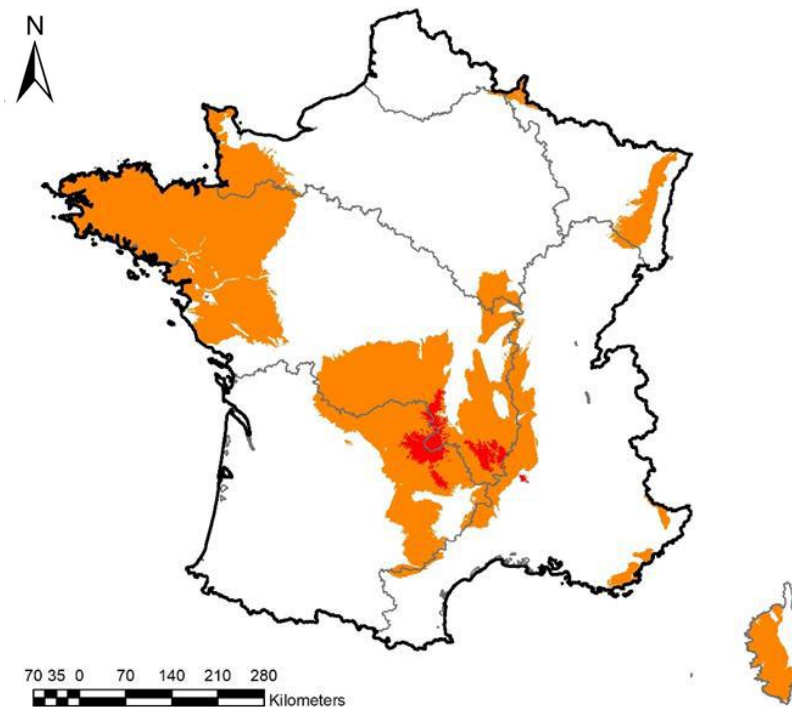


Figure 14: Map of crystalline rocks (red: granite, brown: schist).

Karst aquifers

Karst aquifers are widespread in France with a higher presence in the southern part of the country (Figure 15). Their main advantage is the high permeability of the karst drainage network that drains the whole system and can supply very large amounts of water. They are replenished very quickly through diffuse and localized recharge. Karst aquifers supply 40 % of drinking water supply in France.

Close to the Mediterranean coast, the limestone massifs have been affected by the Messinian salinity crisis (6 M years ago) which consists in a lowering of the Mediterranean sea due to the closing of the Strait of Gibraltar. This eustatic and tectonic phenomenon has increased the erosion and karstification potential of rivers and groundwater in the associated region, creating deep karst cavities and karst drainage networks. An example is the well-known Fontaine de Vaucluse karst spring which has been explored at a depth of 315 meters. This deep development of karstification leads to high volume of stored groundwater which can be pumped under an active management scheme like the Lez aquifer at high rates from a single pumping station. Thanks to this Messinian crisis, deeper karst systems are located under low permeability rock cover (Arc karst aquifer close to Marseille for example).

Apart from the Mediterranean coast, other productive karst aquifers include: La Rochefoucauld aquifer and la Touvre spring supplying Angoulême city, la Chartreux spring supplying Cahors city, and the Arcier spring in Jura mountains supplying Besançon city.

Due to fast groundwater flows in the karst conduits and direct infiltration of water in sinkholes, karst aquifers are highly vulnerable to surface pollution.



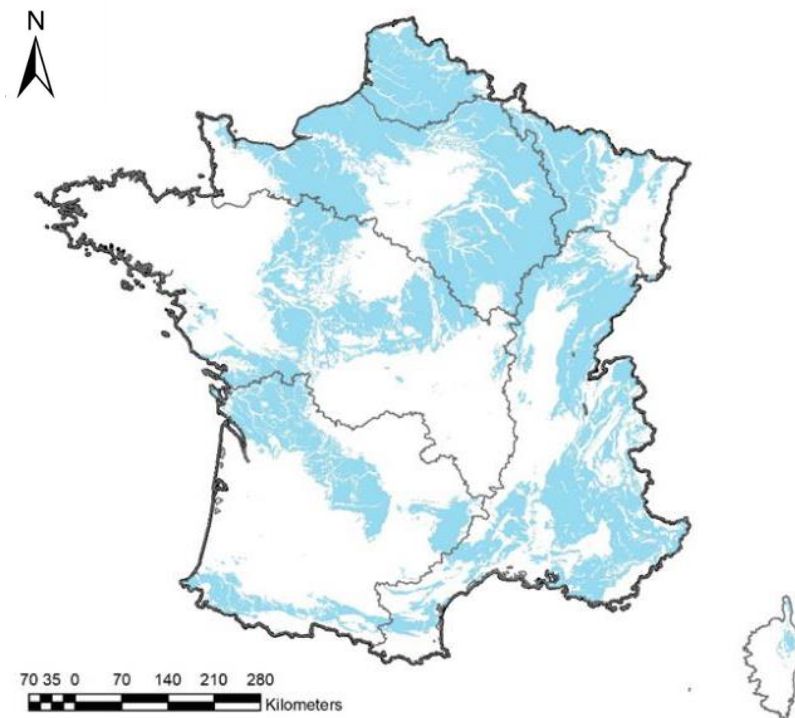


Figure 15: Map of karstifiable carbonate rocks (blue), modified from Chen et al. 2017.

3.1.7 Abstractions/irrigation

Total water abstraction in France is about 38.5 billion m³ in 2013, with the vast majority is (70%) abstracted from surface water to serve as cooling water for electricity production (21.6 billion m³) and to supply navigation canals (5.5 billion m³) (AFB, 2017). Other uses (drinking water, agriculture, industry) use a total of 11.4 billion m³, of which about 50% is from groundwater origin.

About 66% of abstracted water for drinking water is from groundwater (3.7 billion m³ compared to 1.866 billion m³ from surface water). Groundwater is a strategic resource for drinking water supply given its higher quality compared to surface water, and thus the lower treatment costs. Groundwater represent about 36% of water abstracted for agriculture (1.035 billion m³ compared to 1.766 billion m³ from surface water). About 31% of abstraction for industrial use, which includes factories, commercial firms and various public buildings, is based on groundwater (930 M m³ compared to 2,700 M m³ from surface water).

Overall, total water abstraction for drinking water has been reducing since 2003 (- 15% between 2003 and 2013) (Figure 16); for industrial water abstraction, a reduction can be observed since 1998 (-27% between 1998 and 2013). No significant evolution in overall water abstraction in agriculture can be seen since 2008 when monitoring and reporting became more consistent nation-wide.

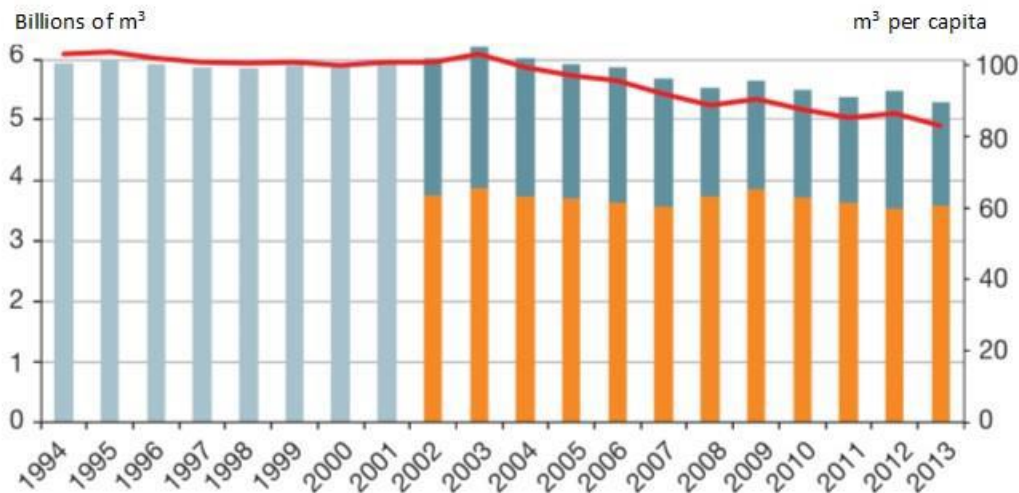


Figure 16: Evolution of water abstraction for drinking water supply.

In light blue: total abstraction. In dark blue: surface water abstraction. In orange: groundwater abstraction. Red line: abstraction water per capita. Source: modified from Banque nationale des prélèvements quantitatifs en eau, ONEMA-SOeS on 2013 data (CGDD, 2017).

3.1.7.1 Groundwater use in agriculture

80% of water use in agriculture in France serves to irrigate crops, while the remaining 20% is used for livestock water supply and cleaning. Figures on irrigation are however difficult to obtain accurately as water meters are not systematically installed on individual water pump and reporting of abstracted volumes is not systematic.

From 500,000 ha in 1970, the surface of irrigated land has steadily increased until 2000 when it reached a maximum of 1.57 million ha or 6% of total used agricultural area. In 2010, the area of irrigated land has not changed significantly while the area of used agricultural land has reduced (-900,000 ha or -3.5% from 26.16 million ha) as well as the area of agricultural area equipped for irrigation (-312,000 ha or -12% from 2.6 million ha). Overall, irrigation appears to be maintained where it is regularly used, and may help to maintain small unit agricultural holdings economically viable in a context of general consolidation of agricultural units and abandonment of agricultural land (Loubier et al., 2013).

The internal irrigation rate of agricultural holdings practicing irrigation in 2010 was 32%, a number that has slightly increased since 2000 and indicating that irrigation is becoming a more important part of some agricultural units. However, apart from specific situations, irrigation in France is not essential for agricultural production as it can be in arid countries; rather, it is used to:

- secure yields against climate risks
- increase average yields
- improve product quality.

On average, irrigation is responsible for about 2,000 m³ of water abstracted per ha.

Most agricultural land equipped for irrigation is situated in the southwest, centre, northeast, southwest of France. The main irrigated crops are maize and cereal production, as well as potatoes,



vegetable cropping and fruit production. Maize represented 41% of all irrigated land in 2010, down from 50% in 2000. This evolution is partly related to the reduction in European subsidies for this crop, as well as stricter restriction on water use and higher prices for other cereal crops, in particular wheat.

Both collective and individual irrigation increased steadily until 2000. Traditionally, collective irrigation from surface water was developed in the Southern regions while individual irrigation from groundwater was developed in the northern regions (Figure 11). Of the 2.6 million ha equipped for irrigation, only represent 4% is equipped for surface irrigation, 4% for micro-irrigation and 92% for overhead irrigation (CGAER, 2017).

In 2010, a sharp reduction in area equipped through collective irrigation systems can be observed, while areas equipped with individual irrigation systems has continued its rise (Loubier et al., 2013). The same trend occurs in the Mediterranean rim where most irrigation is traditional carried out through collective systems. At the time, a reduction of 50% in surface water irrigation is observed in these regions. These trends suggest a move towards more water efficient systems, although it also poses local challenges for groundwater recharge via the distribution canals and surface irrigation practices.

The development of irrigation has led to increasing societal conflicts across France, especially in the agricultural productive regions of the west and southwest of France which underwent a significant increase in irrigation for maize and cereal production in the 1980s and 1990s. Assuring minimum ecological flows is a significant challenge as a result of cumulative pumping in rivers and through individual boreholes in alluvial and sedimentary aquifers (CGEDD-CGAAER, 2015).

3.1.7.2 Groundwater and drinking water supply

Drinking water supply network provides water to domestic users as well as all buildings equipped with sanitary infrastructure (e.g. schools, hospitals, hotels, sports, etc) and small businesses and industries. Water consumption per capita is estimated at 165 litre per day (ONEMA, 2015).

Water use is mainly dependent on residential population; however some basins are characterised by large seasonal population variations due to tourism. This can pose supply challenges in Mediterranean basins during the low flow season similar to those faced by irrigation. Drinking water supply is given the highest priority use during crisis. No restriction to drinking water use due to water shortage has been recorded in France yet; restrictions to water gardening are nevertheless regular.

The vast majority of the population use water delivered to their homes by public water suppliers (98%); however, an increasing number of households in detached or semidetached housing units have drilled private bore-wells since the 1990s for various economic, political and ethical reasons (Rinaudo et al., 2015). Typically, household use alternative water supplies for gardening and other non-consumptive uses in order to reduce their water bills. According to Montginoul and Rinaudo (2011), the presence of domestic tube wells and shallow wells is reported in a majority of French counties both in southern and northern France and is expected to significantly increase in the coming decade, as a result of increased water scarcity, higher tariffs from public water supplies, and the decreasing cost of alternative supply technologies. Furthermore, there is yet little regulation on private domestic drilling.

Overall the main challenge regarding groundwater abstraction for drinking water supply relates to water quality and the risks that pollution emission, mainly from agricultural activities.

3.2 Climate change challenge

This part is based on the BRGM report 61483-FR, Explore 2070 project (2012).

Climate change will not affect the water resources in the whole Europe the same way, depending on various factors, which are mostly related to climate, geology, pedology and land use (Figure 17 and Figure 18).

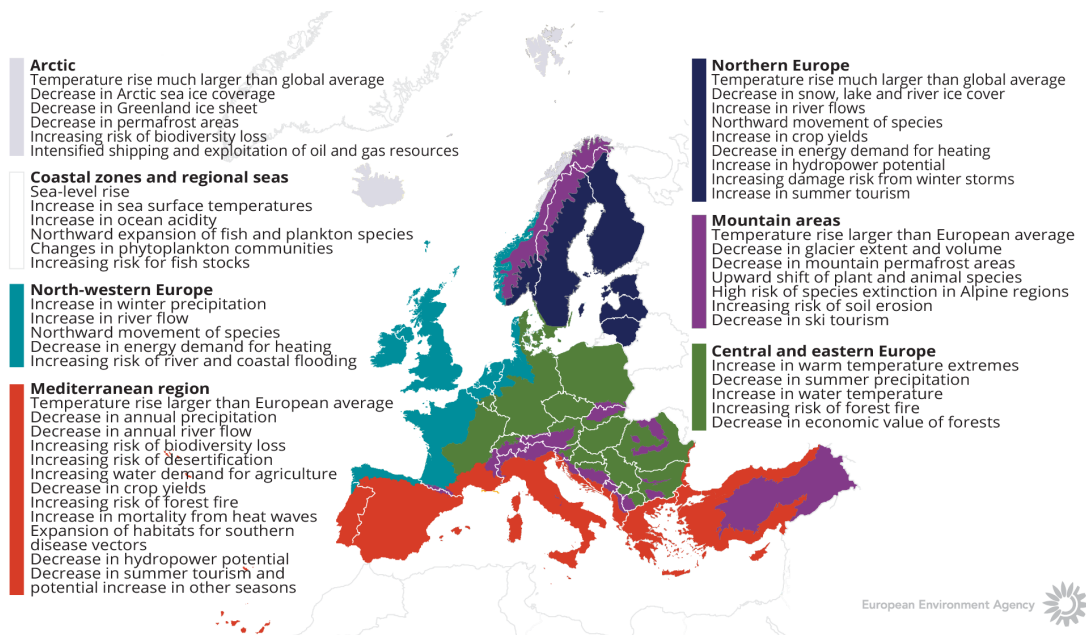


Figure 17: Observed and projected climate change and impacts for the main biogeographical regions in Europe (European Environmental Agency).



Figure 18: Soil map of Europe, from the EGD interactive maps
(map available at: <http://www.europe-geology.eu/soil/soil-map/>; legend available at:
<https://services.bgr.de/wms/boden/eusr5000/?request=GetLegendGraphic%26version=1.3.0%26format=image/png%26layer=2&lang=en>)

3.2.1 ***How is the climate expected to change in the area***

The effect of climate change on the water supply has already been the subject of a previous study, with quantifications of groundwater amounts estimations at present time and at the year 2070.

The method generally used in this type of project is:



- Greenhouse gas and aerosol emission scenario
- global climate model
- disaggregation (regionalization)
- regional hydro(geo)logical model
- impact analysis and uncertainty analysis.

Seven climate models from the IPCC Fourth Assessment Report (2007) have been used for every analysis (ARPEGE V3+, GISS-MODEL-ER, MRI-CGCM2.3.2, ECHAM5/MPI, GFDL-CM2.1, GFDL-CM2.0, CCCMA-CGCM3). The greenhouse-gas and aerosols emissions scenario used in the analysis is the median scenario proposed by the IPCC AR4 (scenario A1B). Abstraction and irrigation are assumed to be stable.

Regarding the general data, Figure 19 and Figure 20 show the main variations in annual thermometry and rainfall of the different models over the period (2045/2065), compared to their reference values (1961-1990). These graphs show that if the average value of temperatures is increasing (about 2 to 2.5 C) and the average rainfall is decreasing (about 6 to 8%), these values are very variable. From one climate model to another and extreme values can be very different. The variability of these results, obtained for all the climate models makes it possible to assess the uncertainties on the climate projections.

The temperature will have a significant influence on the potential evapotranspiration (PET). These few degrees of increase will thus generate an increase in PET of 10 to 15% or more depending on the regions and seasons. This increase in PET will directly increase actual evapotranspiration (AET) since the models used do not incorporate a possible adaptation of natural vegetation to climate change. This increase in AET associated with a decrease in rainfall, relatively low in percentage but significant in quantity, will thus lead to a significant reduction of effective rainfalls. This reduction is very variable depending on the regions and climate models, but it is rarely less than 20%.

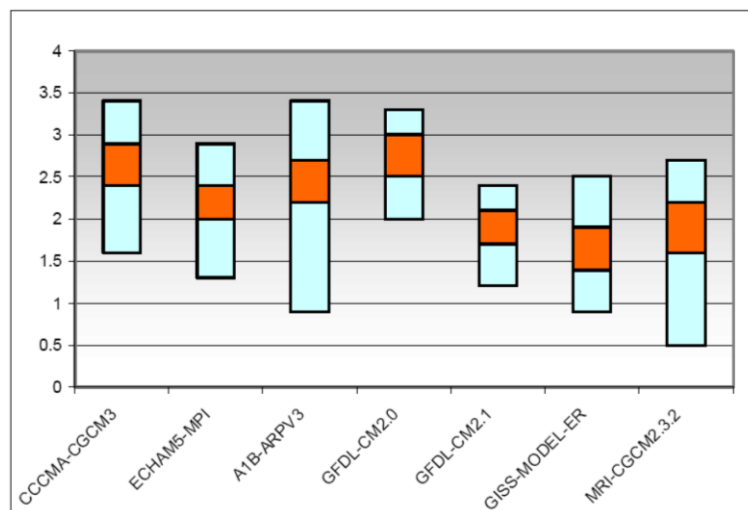


Figure 19: Deviation from the average annual temperature difference between current and predicted. Current: reference period (1961-1990); predicted: (2046-2065). Values presented in Celsius degrees, with confidence intervals (orange) and extremes values. Performed for the 7 climate models on scenario A1B (from Explore 2070, Lot3).

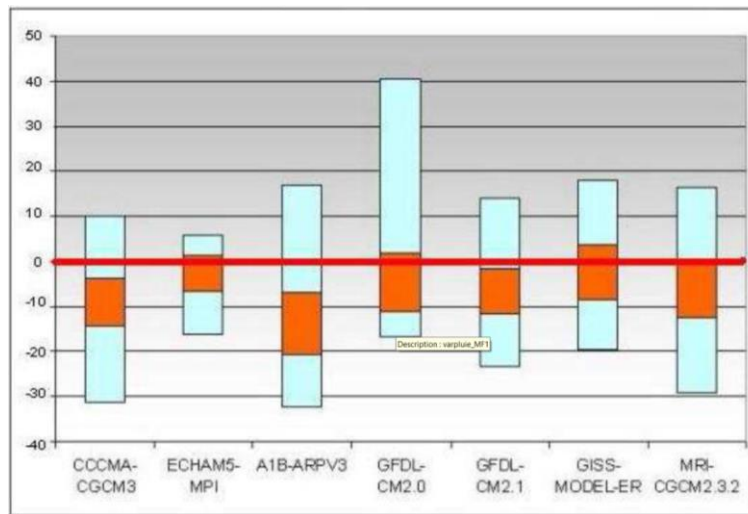


Figure 20: Average cumulative annual rainfall difference between current and predicted. Current: reference period (1961-1990); predicted: (2046-2065). Values presented in percentage of reference periods values, with confidence intervals (orange) and extremes values. Performed for the 7 climate models on scenario A1B (from Explore 2070, Lot3).

3.2.2 What are the challenges related to the expected climate change?

3.2.2.1 Almost universal decline in water recharge

The simulations performed with the seven climate models have produced three maps (minima, mean and maxima projections) indicating a virtually systematic 10 to 25% decline in water table recharge, with two areas more severely affected :

- the Loire basin with a 25 to 30% decline across half of the catchment area,
- and the south-west of France with a 30 to 50% decline.

In each modelling exercise, all of the piezometers show a decline in average monthly water table levels due to lower recharge. The optimistic scenarios show a slight 0.5 to 1.5 m drop in levels and even a possible slight rise in some zones (Aquitaine, Poitou), while the pessimistic scenarios show a very limited drop in piezometric levels beneath alluvial plains in particular, but levels dropping by as much as 10 m in lowland and foothill areas lying above sedimentary basins.

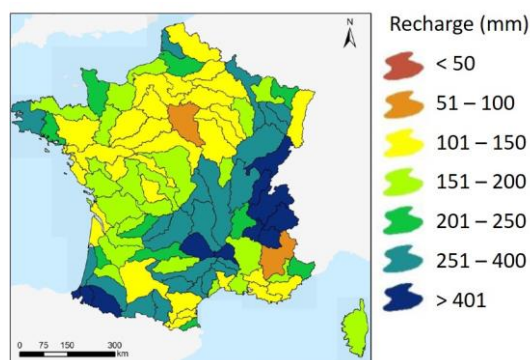


Figure 21: Average estimated recharge per year at present time

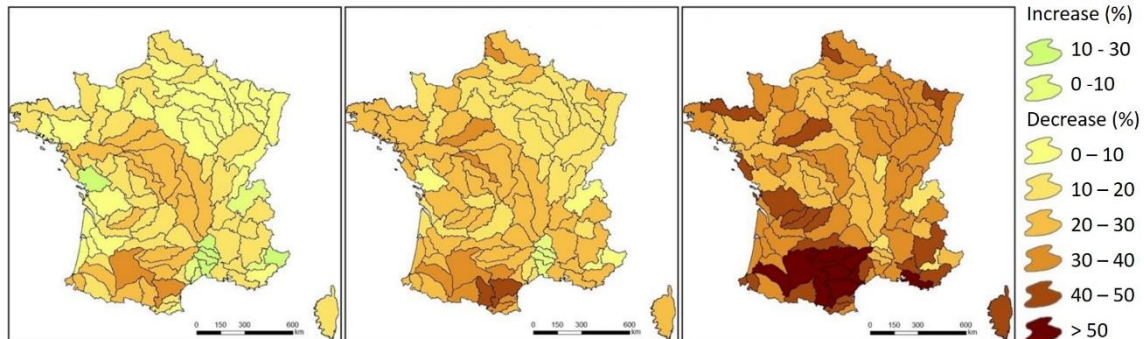


Figure 22: Difference between present day recharge and predicted recharge for the year 2070 (percent for minima projection, mean projection and maxima projection).

3.2.2.2 Decline in average river flow

All of the scenarios also show a decline in average river flow by 2065, which varies from 10 to 40% in the northern half of the country and from 30 to 50% in the southern half, with local extremes of up to 70%. Despite this relative decline in river flow, some models show that very high water levels are nevertheless possible during the winter in some catchment basins (e.g. Somme and Rhine), confirming the likelihood of lengthy periods of flooding.

3.2.2.3 30% potential loss of groundwater resources by 2070

Groundwater resources are therefore likely to decline significantly overall by 2070, with predicted variations of +10 to -30% in the optimistic scenarios and -20 to -55% in the pessimistic scenarios. This would cause a decline of similar proportions in low-water levels.

FUTURE RECHARGE CALCULATION

4.1 Methodology

The methodology applied to assess the potential groundwater recharge at the country scale combines a water budget approach and the use of an Effective Precipitation Infiltration Ratio (EPIR):

$$\text{Recharge} = \text{EPIR} * \text{Effective Precipitation.}$$

It is applied to evaluate both present and future groundwater recharge.

4.1.1 *Effective precipitation calculation*

A gridded water budget model was developed (with Matlab©) to compute the effective precipitation with a resolution of 8 km at a daily time step (see Figure 23). It relies on the water budget method proposed by Edijatno & Michel (1989). This method is implemented in several rainfall-runoff models (e.g. GR4J from Perrin et al., 2003).

4.1.2 *EPIR evaluation*

Assuming that the EPIR is constant over time, the France map of EPIR has been constructed taking advantage of the relationship established between two indices related to infiltration. These are the Indice de Développement et de Persistance des Réseaux (IDPR) and the baseflow index (BFI).

The IDPR is a GIS-built parameter that gives a qualitative indication on the infiltration coefficient. It has been developed by BRGM since 2004 (Mardhel et al., 2004). IDPR is constructed by comparing the theoretical river network computed from Digital Elevation Model to the real one. IDPR is available all over France with a 25 m spatial resolution (Mardhel et al. 2021). The IDPR values are comprised between 0 (only infiltration) and 2000 (only runoff), with a fixed value of 1000 along rivers.

The baseflow is defined as the delayed water contribution to river flow that is not related to direct runoff. It can be calculated from rivers discharge data by applying hydrograph separation algorithms, such as those proposed by the Wallingford Institute (see e.g. Gustard, 2008) or Lyne and Hollick (1979). The baseflow index (BFI) is the long-term ratio of the baseflow to the total stream flow. For undisturbed hydrogeological basins, with no inter-basins lateral exchanges nor vertical leakage and at an annual scale (negligible storage), the BFI appears to be a fair proxy of the EPIR. Obviously, the BFI is only available on gauged watersheds.

A survey was conducted over 357 gauged river basins distributed over France, for which discharges data are known to be undisturbed by pumping or dams. The mean inter-annual BFI values over the 1981 – 2010 period were computed with the Lyne and Hollick method. In parallel, the spatial average of the IDPR over the watersheds was calculated. Correlation between the two datasets were found after sorting the basins according to their lithology. These relationships allowed converting the IDPR map into an EPIR map, with a resolution equal to the hydrogeological unit scale.

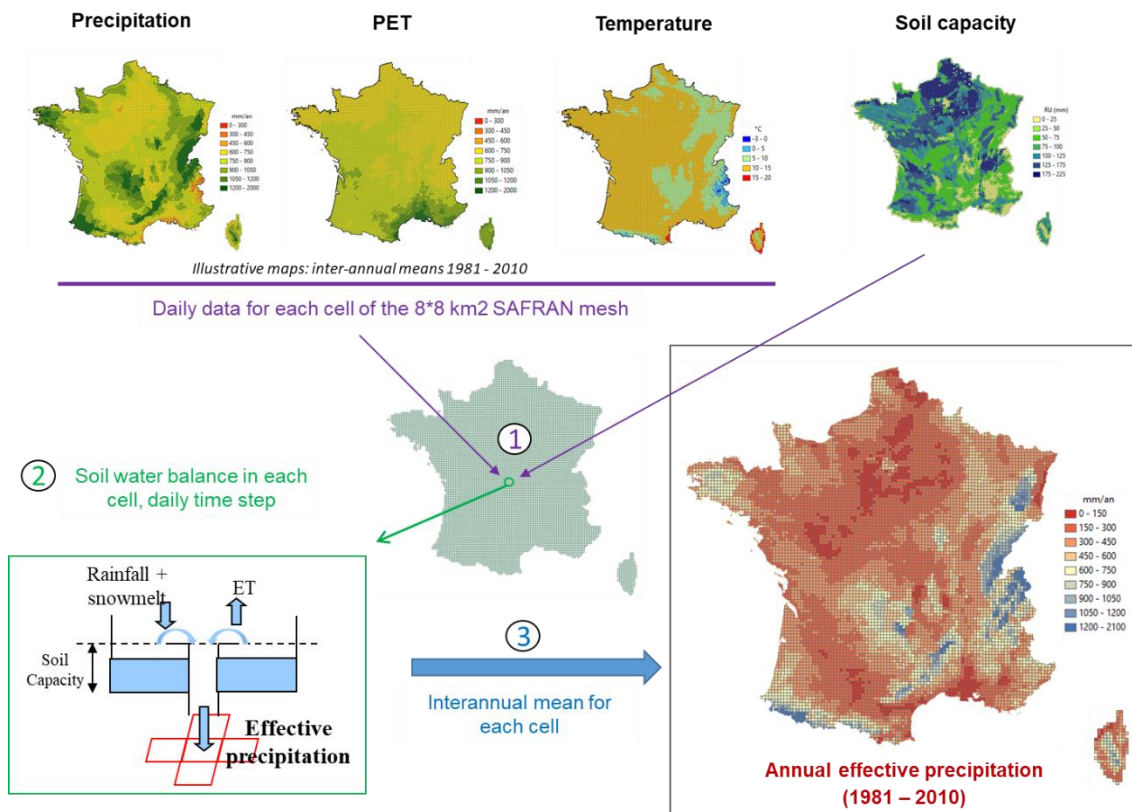


Figure 23: Sketch of the methodology applied to compute effective precipitation.

4.1.3 Climate data

4.1.3.1 Meteorological data

Meteorological data that are used to calculate effective recharge for the France pilot site are the SAFRAN reanalysis data (Vidal et al., 2010). They are available on a 8×8 km² mesh covering France, from 1958 to present day. For the modelling purpose, daily time-step rainfall, snow, temperature and Penman-Monteith PET are used. The chosen reference period, common to all pilot site, is the 30-years 1981-2010 period.

4.1.3.2 TACTIC standard Climate Change scenarios

The TACTIC standard scenarios are developed based on the ISIMIP (Inter Sectoral Impact Model Intercomparison Project, see www.isimip.org) datasets. The resolution of the data is 0.5°x0.5° global grid and at daily time steps. As part of ISIMIP, much effort has been made to standardise the climate data (a.o. bias correction). Data selection and preparation included the following steps:

1. Fifteen combinations of RCPs and GCMs from the ISIMIP data set were selected. RCPs are the Representative Concentration Pathways determining the development in greenhouse gas concentrations, while GCMs are the Global Circulation Models used to simulate the future

climate at the global scale. Three RCPs (RCP4.5, RCP6.0, RCP8.5) were combined with five GCMs (noresm1-m, miroc-esm-chem, ipsl-cm5a-lr, hadgem2-es, gfdl-esm2m).

2. A reference period was selected as 1981 – 2010 and an annual mean temperature was calculated for the reference period.

3. For each combination of RCP-GCM, 30-years moving average of the annual mean temperature were calculated and two time slices identified in which the global annual mean temperature had increased by +1 and +3 degree compared to the reference period, respectively. Hence, the selection of the future periods was made to honour a specific temperature increase instead of using a fixed time-slice. This means that the temperature changes are the same for all scenarios, while the period in which this occur varies between the scenarios.

4. To represent conditions of low/high precipitation, the RCP-GCM combinations with the second lowest and second highest precipitation were selected among the 15 combinations for the +1 and +3 degree scenario. This selection was made on a pilot-by-pilot basis to accommodate that the different scenarios have different impact in the various parts of Europe. The scenarios showing the lowest/highest precipitation were avoided, as these endmembers often reflects outliers.

5. Delta change values were calculated on a monthly basis for the four selected scenarios, based on the climate data from the reference period and the selected future period. The delta change values express the changes between the current and future climates, either as a relative factor (precipitation and evapotranspiration) or by an additive factor (temperature).

6. Delta change factors were applied to local climate data by which the local particularities are reflected also for future conditions.

Only the case of 3°C global warming is considered here (Table 2).

For the France pilot site, the change factors are calculated from the simulations RCP8.5 with the gfdl-esm2m GCM and RCP6.0 with the miroc-esm-chem GCM. The first one forecasts that 3°C warming will be reached (at a global scale) in 2057, and simulates a decrease of inter-annual precipitation for the 30-years period (2057-2086) of 9% (“lowest” impact on precipitation scenario). The second one forecasts that 3°C warming will be reached in 2042, and simulates an increase of inter-annual precipitation for the 30-years period (2042-2071) of 5% (“highest” impact on precipitation scenario).

Table 2 Combinations of RCPs-GCMs used to assess future climate

		RCP	GCM
3-degree	“Dry”	RCP8.5	gfdl-esm2m
	“Wet”	RCP6.0	miroc-esm-chem

Climate data are generated by applying these change factors to historical data used to run the hydrological model. The same reference period, 1981 – 2010, is used. Monthly change factors, which are provided on a 0.25° mesh, are first projected on the grid of reference data. Then temperature

change factors are added to reference time series, whereas precipitation and potential evaporation change factors are multiplied to reference time series.

4.1.3.3 Alternative climate change scenarios

Future effective precipitation and anomalies were calculated at the French national scale by BRGM in 2019. The methodology relies on ensemble simulations. For two contrasted emission scenario (RCP2.6 and RCP8.5), outputs of four General Circulation Model (BCC_CSM1-1-m, CanESM2, IPSL, NorESM1) combined with two statistical downscaling methods (DSCLIM described by Pagé et al. 2009, and the method proposed by Dayon, 2015) were used to run three different water budget models.

4.2 Results and conclusions

4.2.1 Climate data

Monthly change factors (given on a 0.5° grid) were projected on the SAFRAN mesh (8×8km cells). For illustration purpose, the monthly precipitation change factors corresponding to the ensemble simulation members that forecast the “lowest” impact on precipitation (i.e. 9% decrease) and the “highest” impact (i.e. 5% increase) are presented in Figure 24.

The annual mean change factors for precipitation, temperature, and potential evapo-transpiration maps are shown in Figure 25.

At the annual time scale, the “highest” impact scenario predicts a light decrease of precipitation around the Mediterranean sea, but a high increase (up to 10%) in the North-East and North-West parts of France (Figure 25a). Temperature increase are particularly important in the South-West part where they reach 2.7°C (Figure 25b). PET increase everywhere, between 4 and 10% (Figure 25c).

The “lowest” impact scenario actually shows also marked changes. Precipitation strongly decrease, especially in summer, with annual reduction showing a gradient pattern from 20% in South-West to 4% in North-East. Temperature increases remain under 2.5°C all over France (between 1.2°C in Bretagne to 2.16°C in Centre-East).

These change factors were applied to the SAFRAN daily data for the period 01/01/1981 – 31/12/2010, to produce climate data that can be used to simulate future effective precipitation. The resulting inter-annual means of meteorological data are presented in Figure 26, Figure 27 and Figure 28.

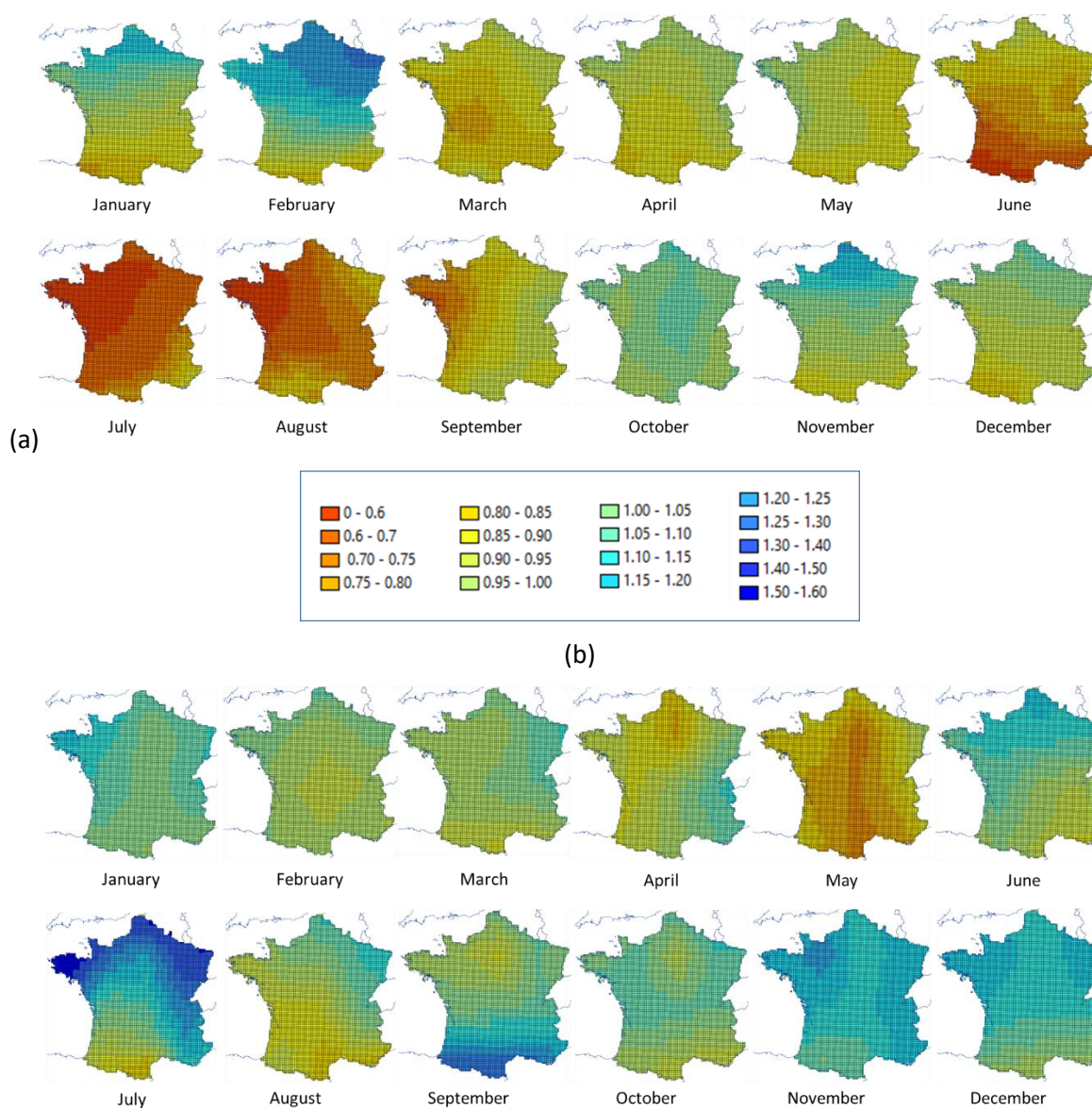


Figure 24: Monthly precipitation change factors (3°C warming)

Legend: (a) =Scenario with lowest impact on precipitation (change factors given by gfdl-esm2m + RCP8.5 simulation, 2057-2086), values range from 0.428 to 1.269. (b)=Scenario with highest impact on precipitation (change factors given by miroc-esm-chem + RCP6.0 simulation, 2042-2071), values range from 0.729 to 1.6

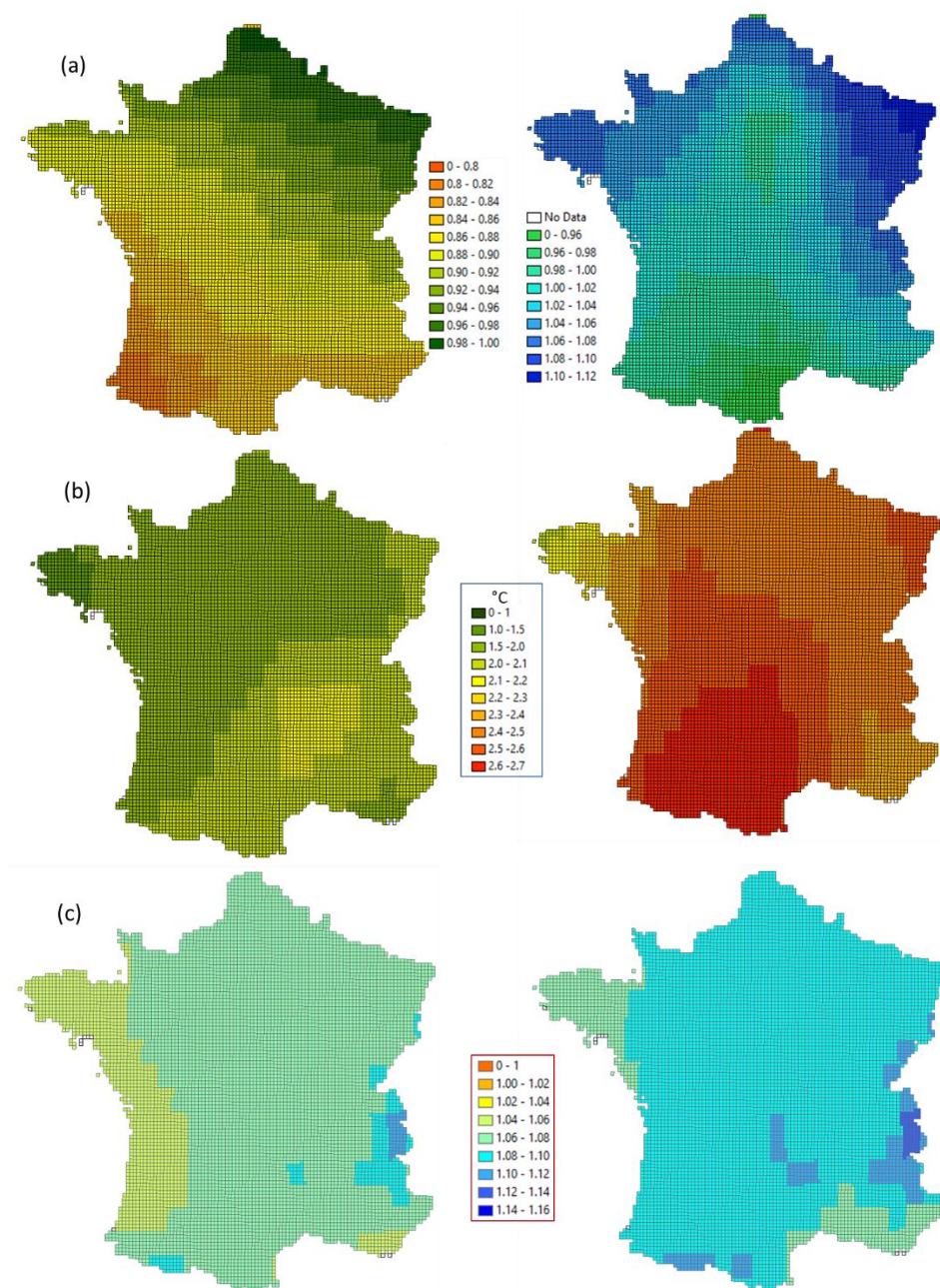


Figure 25: Mean annual change factors (3°C warming).

Legend: (a) Precipitation (b) Temperature (c) Potential evapotranspiration,

left= Scenario with lowest impact on precipitation (change factors given by gfdl-esm2m + RCP8.5 simulation, 2057-2086), Right= Scenario with highest impact on precipitation (change factors given by miroc-esm-chem + RCP6.0 simulation, 2042-2071)



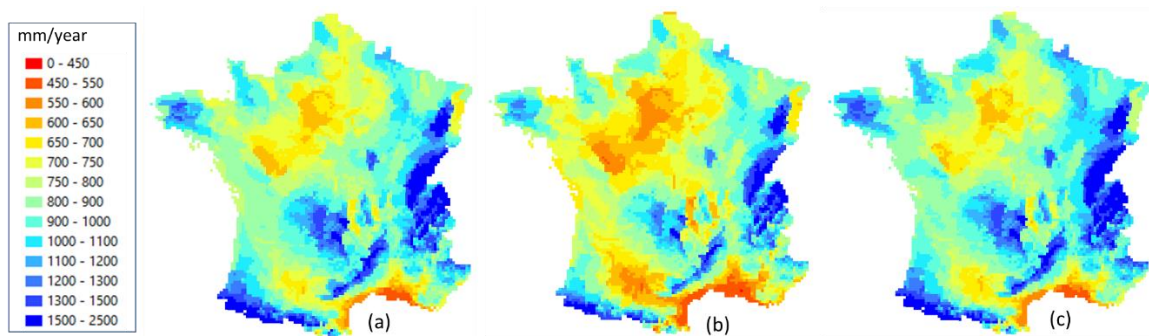


Figure 26: 30-years period interannual mean precipitation (3°C warming)

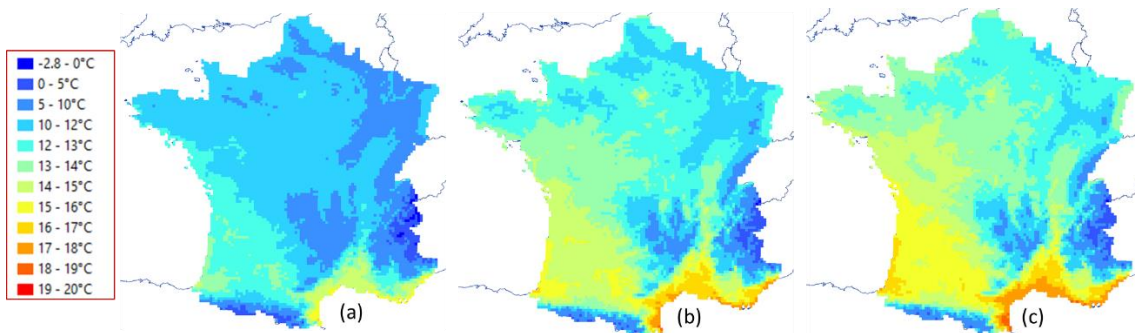


Figure 27: 30-years period interannual mean temperature (3°C warming)

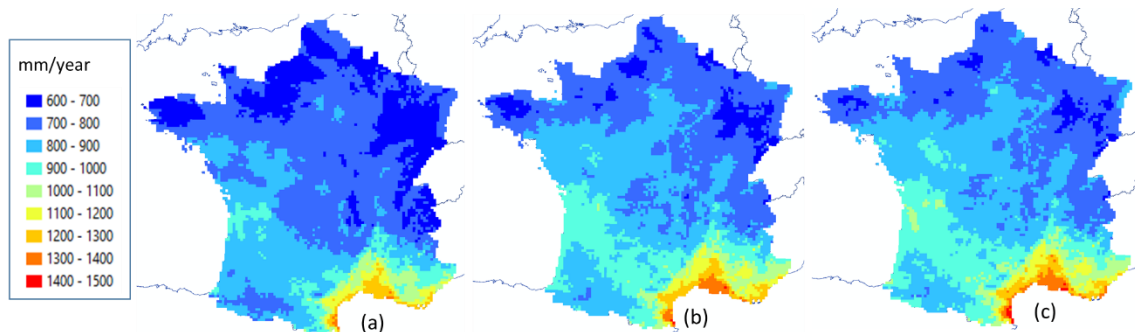


Figure 28: 30-years period interannual mean PET (3°C warming)

Legend: (a) reference, SAFRAN daily data, 1981-2010 (b) Scenario with lowest impact on precipitation (change factors given by gfdl-esm2m + RCP8.5), 2057-2086 (c) scenario with highest impact on precipitation (change factors given by miroc-esm-chem + RCP6.0), 2042-2071

4.2.2 Effective precipitation

Daily effective precipitation for each 64km² cell were computed over the 30-years period by feeding the Matlab© model two SAFRAN datasets. The first consists of the historical climate data and the



second consists of the same data but altered with the change factors to represent future conditions. Maps of mean inter-annual effective precipitation over the 30 years-periods for each cases are shown in Figure 29. As it is difficult to compare these raw results, maps of anomalies are also produced (Figure 30). The anomalies are defined as the ratio, expressed in percentage, of the future effective precipitation minus the present ones related to present ones.

In the case of “lowest” impact scenario, effective precipitation anomalies are negative everywhere except along the North border where they are slightly positive. The effective precipitation reduction reaches 33% in the South-West, and gradually decreases northwards. The distribution of anomalies computed with the highest impact scenario shows an unexpected pattern, with a decrease of effective precipitation in the middle part of France (between 2.5 and 15%) and an increase elsewhere (up to 17% in Alsace). These results are strongly linked to the precipitation change factor maps.

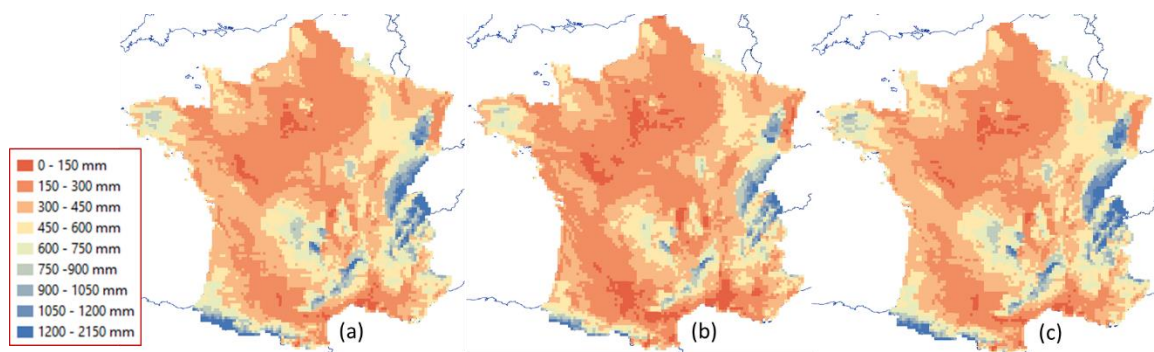


Figure 29: 30-years period interannual mean effective precipitation

Legend: (a) reference, SAFRAN daily data, 1981-2010 (b) Scenario with lowest impact on precipitation (change factors given by gfdl-esm2m + RCP8.5), 2057-2086 (c) scenario with highest impact on precipitation (change factors given by miroc-esm-chem + RCP6.0), 2042-2071

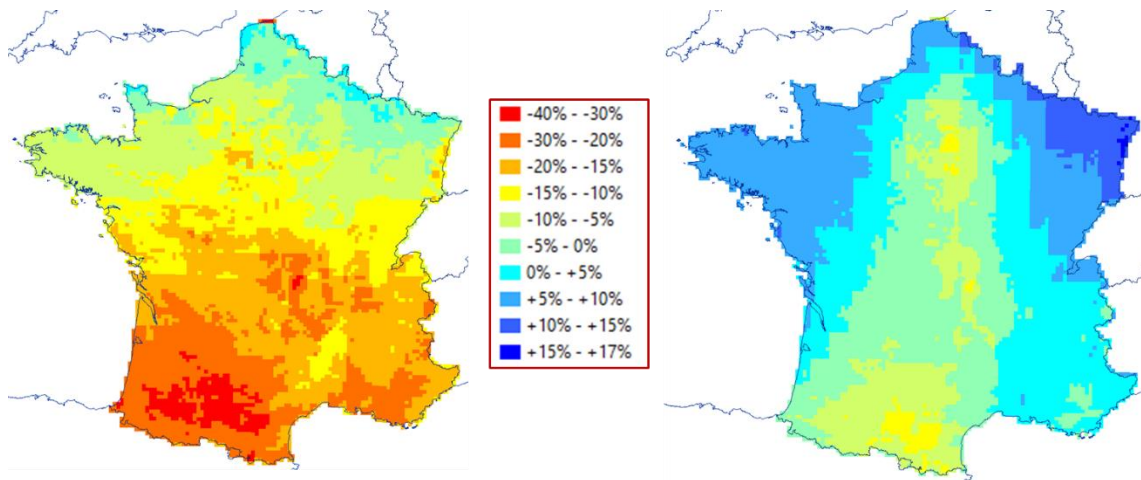


Figure 30: Effective precipitation anomalies

Legend: left=scenario with lowest impact on precipitation (change factors given by gfdl-esm2m + RCP8.5), 2057-2086; right=scenario with highest impact on precipitation (change factors given by miroc-esm-chem + RCP6.0), 2042-2071

The “highest” impact scenario results are unexpected and far from other published results. On the other side, the “lowest” impact scenario results are in the same range and show comparable patterns as previous results obtained by BRGM with the same methodology but with different climate data (ensemble simulation with 4 GCM and 2 downscaling methods). The main differences concern the Paris basin and the North part of France (Figure 31). The important decrease of effective precipitation in the South-West region is of the same order of magnitude of the TACTIC results (-30 - -40%) as in the EXPLORE 2070 exercise¹ (Figure 22) but higher than in BRGM 2019 results (-20% - -30%).

¹ Assuming that the EPIR does not vary in the future, effective precipitation anomalies are equal to potential groundwater recharge anomalies.

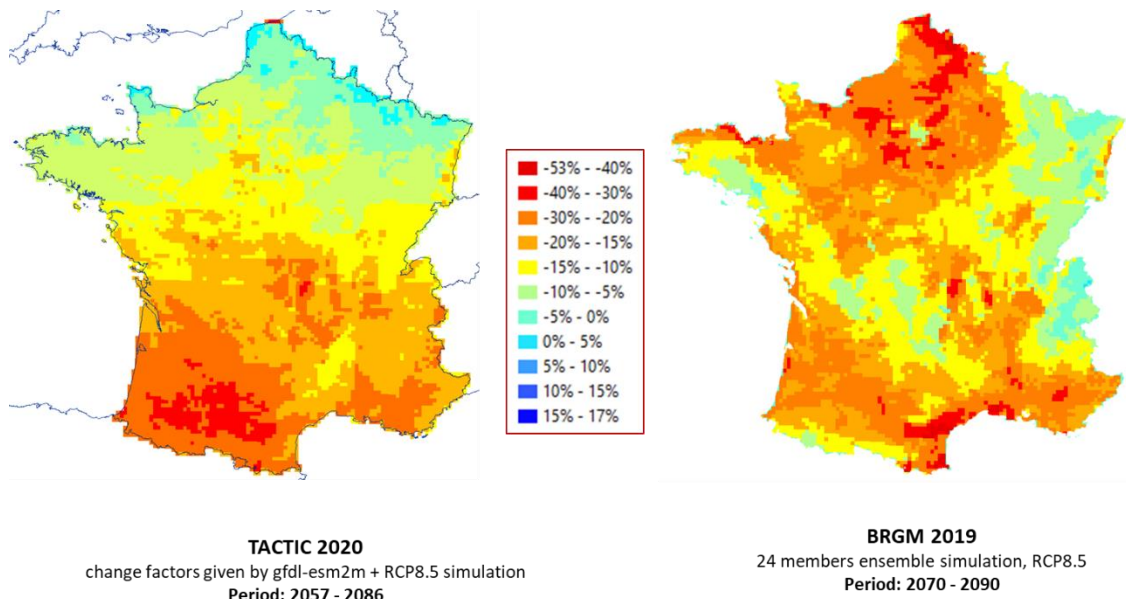


Figure 31: Comparison of effective precipitation anomalies maps.

Legend: left =scenario with lowest impact on precipitation (change factors given by gfdl-esm2m + RCP8.5), 2057-2086 ; right = results of 24 members ensemble simulation, RCP8.5, 2070-2090

4.2.3 Groundwater potential recharge

According to the results of the analysis of IDPR and BFI on 357 gauged basins, the following relationships were applied to convert the France IDPR map into an EPIR map (Figure 32) taking into account the lithology of hydrogeological units (Caballero et al., 2020):

- Alluvial, sedimentary, volcanic formations:

$$\text{EPIR} = 0.9 \text{ if IDPR} < 100 \text{ and } \text{EPIR} = -0.0004 * \text{IDPR} + 0.9517 \text{ if } 100 \leq \text{IDPR} \leq 2000.$$

- Karstic formations:

$$\text{EPIR} = 0.9 \text{ if IDPR} < 100, \text{EPIR} = -0.0004 * \text{IDPR} + 0.9517 \text{ if } 100 \leq \text{IDPR} < 1200, \text{EPIR} = 0.5 \text{ if IDPR} \geq 1200$$

- Bedrock: EPIR = 0.55
- Folded formations: EPIR = 0.65

Finally, recharge maps are obtained multiplying EPIR map by effective precipitation maps (Figure 33).

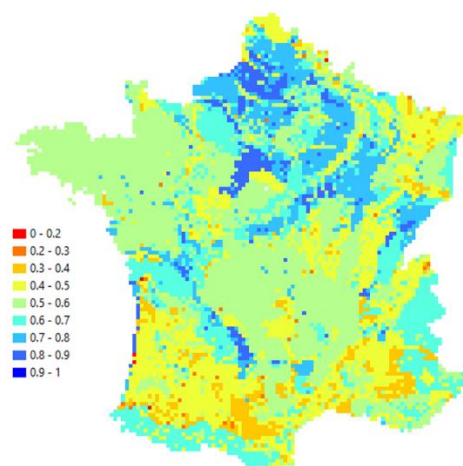


Figure 32: France map of EPIR (SAFRAN cells projection)

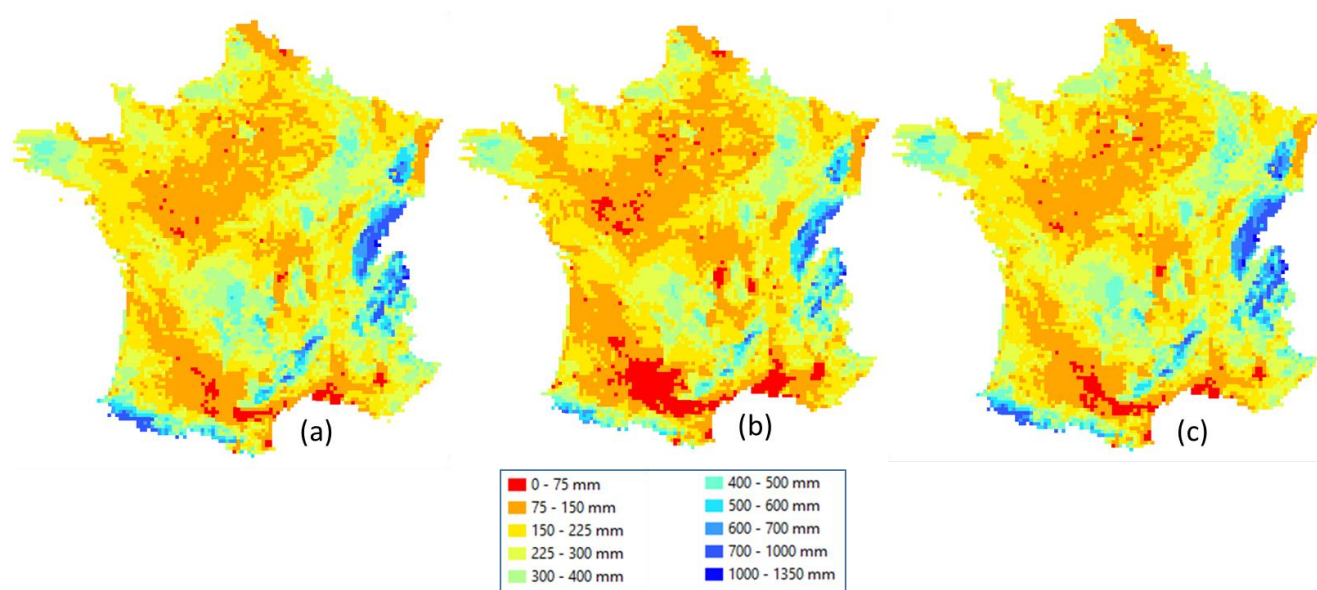


Figure 33: France map of present and future groundwater potential recharge

Legend: (a) reference, SAFRAN daily data, 1981-2010 (b) Scenario with lowest impact on precipitation (change factors given by gfdl-esm2m + RCP8.5), 2057-2086 (c) scenario with highest impact on precipitation (change factors given by miroc-esm-chem + RCP6.0), 2042-2071

5 VULNERABILITY TO CLIMATE CHANGE

5.1 Methodology

The vulnerability of aquifers to climate change will be assessed via monotonic and non-linear trend analyses. The monthly groundwater levels averages and monthly cumulative effective precipitation will be used to conduct it. Analyses will be performed on two reference periods (1996-2019 and 1976-2019) providing the best compromise between the length of groundwater time series and their spatial distribution through metropolitan France and northern France, respectively.

An effective precipitation time series is assigned to each groundwater time series via the development of an indicator (Manceau et al., 2020). Before using this indicator, we preselected all SAFRAN meshes within the catchment and a 50 km radius around each well. This limited area has been chosen to keep a reasonable computing time. These effective precipitation time series are then converted as a statistical indicator of groundwater recharge or discharge modulated by a time lag representing the memory effect of aquifers. The indicator time series (expressing the effective precipitation) allowing the maximization of the correlation coefficient with monthly groundwater levels is selected because considered as the most representative mesh of the groundwater level behaviour.

The following sections describe methodologies applied for trend detection and assessment of the influence of groundwater low-frequency variability on trends.

5.1.1 Groundwater and effective precipitation monotonic trend detection

The trend detection on monthly groundwater levels and cumulative precipitation is achieved on the two reference periods (1996-2019 and 1976-2019). The significance of detected monotonic trends was determined with a modified Mann-Kendall trend test for autocorrelated data (Hamed and Ramachandra Rao, 1998). Comparatively to the well-known Mann-Kendall trend test (Mann, 1945; Kendall et al., 1987), the modified Mann-Kendall trend test considers autocorrelation by correcting probability values (pvalues) after accounting for autocorrelation. The statistical significance threshold was set at 5%. Simultaneously, we assessed the magnitude of trends by estimating Sen's slope (Sen, 1968). This method is emphasized because it is less influenced by extreme values than a linear regression. Indeed, the slope is defined as the median of the set of slopes calculated between each pair of points.

In addition, we aimed to quantify groundwater level trends in relation to aquifer dynamic. For this purpose, we developed an indicator where Sen's slopes are normalised by the maximum water level fluctuation (WLF) with the following expression:

$$\text{Percentage of maximum WLF} = \left(\frac{\text{Sen's slope} * \text{duration}}{\text{Maximum WLF}} \right) * 100$$

The maximum water level fluctuation for each groundwater time series was determined using a boxplot that displays the scope of groundwater levels and avoids taking into account outliers.

Percentages of groundwater level loss/gain against maximum water level fluctuation were split into 5 classes according their magnitude:



- Negligible trend between -1% and +1% of maximum water level fluctuation.
- Moderate upward or downward trend between +1% and +10% or -1% and -10% of maximum water level fluctuation, respectively.
- Strong upward or downward trend between +10% and +100% or -10% and -100% of maximum water level fluctuation, respectively.

5.1.2 *Non-linear trend estimation and linkage with effective precipitation*

5.1.2.1 The Ensemble Empirical Mode Decomposition (EEMD)

To overcome the low-frequency variability induced by large-scale atmospheric/oceanic circulation and to extract the real and non-linear trends of monthly groundwater levels and effective precipitations, we applied an EEMD filtering (Wu and Huang, 2009). This method is widely applied to extract multi time-scale variability and/or get the not parametrically defined trend in environmental variables (e.g. Massei and Fournier, 2012; Bonnet *et al.*, 2020; Song *et al.*, 2020). Basically, it consists to extract the orthogonal intrinsic oscillatory modes (called IMFs: Intrinsic Mode Functions) constituting the signal $x(t)$ to analyse and a residue $r(t)$. Each IMF must satisfy two conditions: (i) numbers of extrema and zero crossings in the signal must equal or differ at most by one; (ii) the mean value of the envelope defined by local maxima and the envelope defined by local minima must be equal to zero at any point. The residue $r(t)$ represents the real trend existing in the signal and is not parametrically defined.

Compared to the Empirical Mode Decomposition (EMD) implemented by Huang *et al.* (1998), the EEMD has the benefit to be a noise-assisted data analysis method. It avoids intermittency problem in the decomposition by the EMD filter bank. In our analysis, the ensemble members was set to 100, and the added-noise was set to 10% of standard deviation for groundwater levels and 20% of standard deviation for precipitation.

The purpose being to get trends on large-scale climatic fluctuations filtered groundwater levels and effective precipitation, the following study was achieved on the EEMD residues $r(t)$ extracted on the 1976-2019 and 1996-2019 periods.

5.1.2.2 Estimation of monotonic trends on both groundwater and effective precipitation EEMD residues

From these EEMD residues, the same analysis of detecting monotonic trends will be repeated.

Firstly, modified Mann-Kendall and Sen's slope are recalculated on groundwater levels and effective precipitation EEMD residues. The purpose is to observe whether the filtering of low-frequency variability allows us to obtain similar trend directions between groundwater levels and effective precipitation. In this case, it would mean that effective precipitation trends explain groundwater levels trends.

Secondly, Sen's slopes calculated on groundwater EEMD residues will be normalised by the maximum WLF of unfiltered signal, to be compared to monotonic trends estimated on raw groundwater levels (section 5.1.1.). The aim is to check whether the filtering of quasi-periodic variabilities (especially low frequencies) in groundwater levels leads to similar or opposite trends (in magnitude and direction).

In order to better understand why detected opposite monotonic trends between filtered groundwater levels and filtered effective precipitation can be obtained, a visual check of non-linear trends (*i.e.* EEMD residues) is conducted simultaneously.

5.1.2.3 Clustering of groundwater and effective precipitation non-linear trends

One of the interests of EEMD method being to get the non-linear trends of signals, a clustering of groundwater and effective precipitation standardised EEMD residues is realised to identify their typical profiles and their geographical distribution. A partitioning using the k-medoids algorithm was preferred to conduct this analysis (Kaufman and Rousseeuw, 1990). Compared to the k-means algorithm, the k-medoids algorithm is stronger towards outliers. Briefly, it consists to search for k medoids among all time series of the dataset. These medoids represent the structure of data (*i.e.* time series). After finding the set of k medoids, k clusters are constructed by assigning each time series to the nearest medoid. The aim is to find k representative objects minimizing the sum of the dissimilarities of the observations to their closest representative object. The medoid of each cluster is the most central time series in the cluster, and therefore is the most representative of a given cluster. Nevertheless, the choice of number of clusters remains arbitrary. Therefore, an internal validation index is used to determine the optimal number of clusters. In our case, the Davies-Bouldin index is used (Davies and Bouldin, 1979). The clustering with a number of clusters minimizing the Davies-Bouldin index is considered as optimal. We also conducted a visual check between several clusterings minimizing the Davies-Bouldin index to select the one providing the best visual agreement.

By means of this clustering, typical profiles of non-linear trends (*i.e.* EEMD residues) are highlighted. Although shapes of non-linear trends within a cluster can be more or less various, the medoid represents their general shape within the cluster. However, medoids do not represent a mean or a median magnitude of change within clusters, they just describe the shape of non-linear trends.

5.1.2.4 Real non-linear trends or part of lower frequency variability?

The last issue remains to identify if the detected non-linear trends of groundwater levels and effective precipitation can be a part of a lower frequency variability. To answer this question, we compared the covariability of standardised non-linear trends (*i.e.* EEMD residues) extracted on a relatively short period with the standardised empirical modes (*i.e.* IMFs) extracted on a longer period. If non-linear trends display clear covariabilities (*i.e.* similar shapes) with the empirical modes extracted on longer periods, we can suggest that these non-linear trends are part of a lower frequency variability.

5.2 Results and conclusions

5.2.1 *Groundwater and effective precipitation monotonic trends in metropolitan France*

5.2.1.1 Groundwater trends in relation to water level fluctuation

Figure 34 displays the detected monotonic trends of groundwater levels (estimated with Sen's slope) normalised by their water level fluctuation over the 1976-2019 and 1996-2019 periods. The statistical significance of trends at the threshold of 5% are also indicated on these maps. For your information, ranges of normalised trends by hydrogeological entities are presented in Table 3 and Table 4.

Trends on groundwater monthly averages display heterogeneous behaviour through metropolitan France from an aquifer to another over the 1996-2019 period (Figure 34b). In similar hydrogeological entities, trends direction are rather consistent, while large discrepancies in the trend magnitude can appear (Figure 34b; Table 3). The Seno-Turonian chalk in the middle and northern part of Artois-Picardy basin is an example of this phenomenon. Groundwater levels in this entity are homogeneously upward, while their magnitude locally differ (Figure 34b). The Beauce calcareous aquifer (excepting northern part) also displays upward groundwater levels, as well as eastern part of Jurassic limestones from Sarthe to Bessin. Although these upward trends appear to be significant in relation to the water level fluctuation, there are very often not statistically significant.

Inversely, other aquifers exhibit consistent downward trends such as fluvio-glacial formations of Rhone valley (mainly statistically significant), the Jurassic limestones of Berry and Poitou (mainly statistically significant), the western bedrocks formations of Britain, the Upper Cretaceous chalk of Bourgogne, the Seno-Turonian chalk of Champagne, and northern part of volcanic formations of Central Massif. While the Seno-Turonian chalk of Normandy/Picardy mainly present downward trends in the western part, discrepancies appear in the eastern part with upward and downward trends. Other entities also display a heterogeneous trend behaviour such as alluvial formations of the Alsace plain, alluvial formations of mediterranean region, or southern bedrocks of Armorican Massif. These trends are very often statistically significant in the two firsts entities, even if they present opposite directions.

Finally, one of the studied entities exhibits rather homogeneous negligible trends on this short period, the fissured Jurassic limestone of northern Aquitaine Basin.

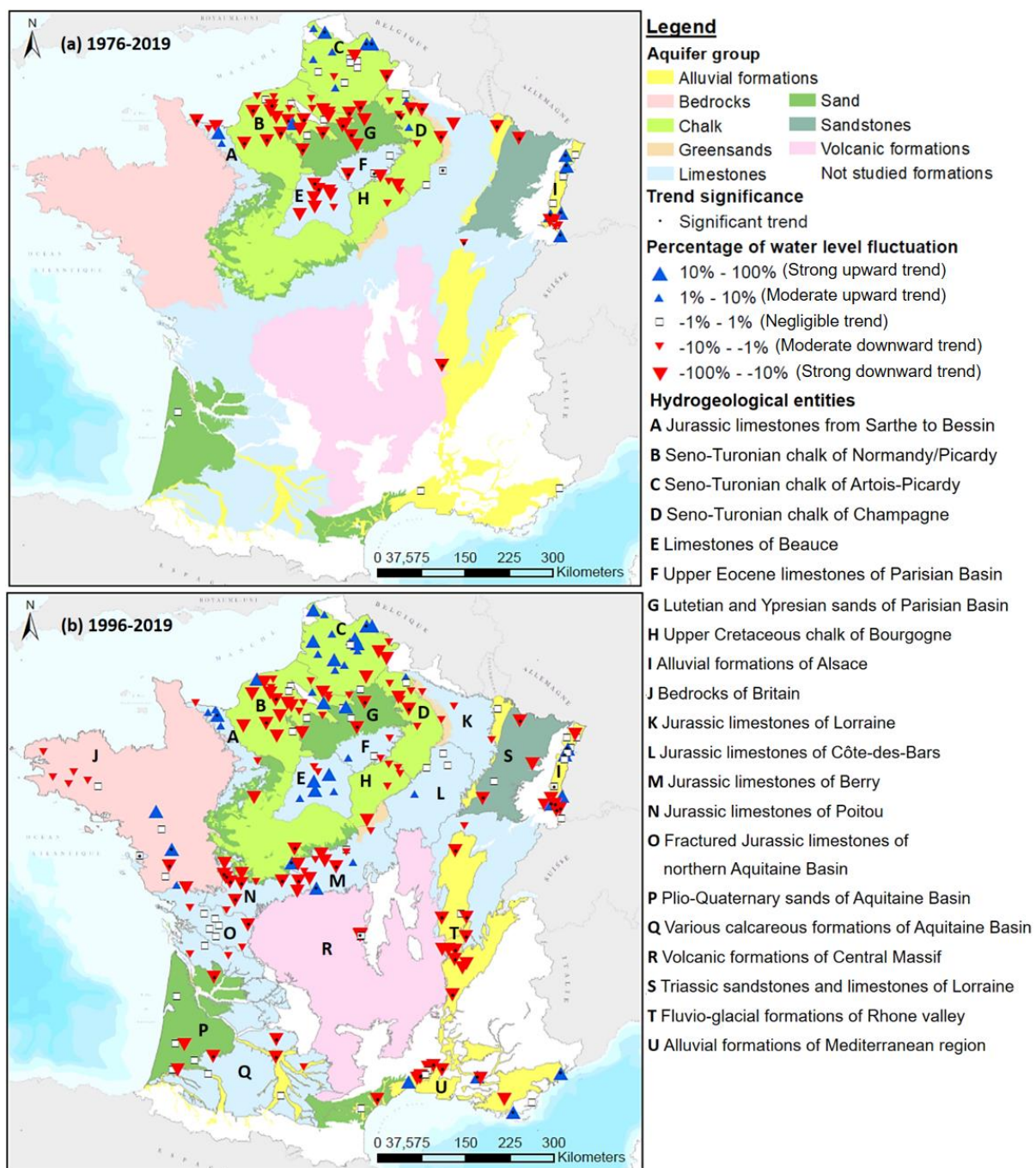


Figure 34: Trends magnitude normalised by the maximum water level fluctuation and their statistical significance (threshold of 5%) of monthly groundwater levels averages over the 1976-2019 and 1996-2019 periods.

Table 3 *Normalised groundwater trends ranges for the main hydrogeological entities over the 1996-2019 period.*

Hydrogeological entities	Lower bound - Slope (% of WLF)	Upper bound - Slope (% of WLF)	Number of boreholes
Seno-Turonian chalk of Artois-Picardy	-22	25	18
Seno-Turonian chalk of Normandy/Picardy	-52	16	30
Seno-Turonian chalk of Champagne	-13	3	8
Jurassic limestones from Sarthe to Bessin	-6	26	5
Lutetian and Ypresian sands of Paris Basin	-57	0	3
Jurassic limestones of Lorraine and Côte-des-Bars	-7	3	4
Triassic sandstones of Lorraine	-76	-16	2
Upper Eocene limestones of Paris Basin	-5	9	4
Alluvial formations of Alsace	-34	40	18
Limestones of Beauce	-8	35	8
Chalk of Bourgogne and Gâtinais	-12	-1	4
Triassic limestones of Lorraine	0	0	1
Bedrocks of Britain	-19	42	10
Jurassic limestones of Berry	-13	0	9
Jurassic limestones of Poitou	-32	-13	6
Fractured Jurassic limestones of northern Aquitaine Basin	-9	0	7
Alluvial and fluvio-glacial formations of Rhone valley	-47	0	11
Volcanic formations of Central Massif	-21	0	5
Various calcareous formations of Aquitaine Basin	-39	-14	3
Plio-Quaternary sands of Aquitaine Basin	-10	0	3
Alluvial formations of Mediterranean region	-35	31	12

Table 4 *Normalised groundwater trends ranges for the main hydrogeological entities over the 1976-2019 period.*

Hydrogeological entities	Lower bound - Slope (% of WLF)	Upper bound - Slope (% of WLF)	Number of boreholes
Seno-Turonian chalk of Artois-Picardy	-31	34	15
Seno-Turonian chalk of Normandy/Picardy	-48	12	29
Seno-Turonian and Turonian chalk of Champagne	-30	5	8
Jurassic limestones from Sarthe to Bessin	-21	13	4
Lutetian and Ypresian sands of Paris Basin	-30	-17	3
Upper Eocene limestones of Paris Basin	-53	0	4
Alluvial formations of Alsace	-11	47	13
Limestones of Beauce	-55	-9	8
Upper Cretaceous chalk of Bourgogne	-13	-3	3

Trends on groundwater levels monthly averages on the 1976-2019 period, become spatially more homogeneous with mostly downward trends in the northern part of metropolitan France (Fig. 4a). Groundwater levels in the limestones of Beauce are homogeneously downward with mostly strong magnitudes (Tab. 2). These downward trends are also noticeable in the Seno-Turonian chalk of Picardy and Normandy with various magnitudes, whether in this last region, some wells do not display trends, and one of them an upward trend. In this hydrogeological entity, strong downward trends are very often statistically significant. In the southern and middle part of Seno-Turonian chalk of Artois-Picardy, groundwater levels do not exhibit homogenous trend direction; while the extreme northern part of Seno-Turonian chalk (near to North sea) is submitted to the increase of its monthly groundwater levels with statistically significant strong upward trends. On smaller hydrogeological entities, many of them display various trend directions: the Seno-Turonian chalk of Champagne exhibits various moderate upward and downward trends, and the Alsace plain alluvial formations exhibit all types of trends. Downward trends in the Seno-Turonian chalk of Champagne are very often statistically significant, while upward trends in alluvial formations of Alsace are all statistically significant. The chalk of Bourgogne still displays downward groundwater levels. Finally, groundwater levels in southern part of Jurassic limestones from Sarthe to Bessin are upward, while they are declining in the border of the English Channel.

5.2.1.2 Comparison between groundwater and effective precipitation detected monotonic trends

A comparison between groundwater (red) and effective precipitation (blue) trends magnitude and direction is established in Figure 35 and Figure 36 by means of Sen's slope over the 1996-2019 and 1976-2019, respectively. A downward stick indicates a negative Sen's slope, and an upward stick indicates a positive Sen's slope, while the stick length indicates the magnitude of trends. The statistical significance at a threshold of 5% is indicated with hatchings.

First of all, we observe on the entire territory consistent downward trends in effective precipitation, even if not statistically significant, over the 1996-2019 period (Figure 35). Very few statistical significant trends in effective precipitation are observed at the scale of metropolitan France. Only the eastern part of France (near the Alsace region) and the Central Massif exhibit consistent statistically significant downward trends. Locally, specific sectors show upward trends but they present very often weak magnitudes and are not statistically significant (e.g. southern Jurassic limestones from Sarthe to Bessin, southern Seno-Turonian chalk of Normandy/Picardy, southern part of fractured Jurassic limestones of northern Aquitaine Basin).

When comparing trends direction of groundwater levels and effective precipitation, major discrepancies appear in the Seno-Turonian chalk of Artois-Picardy (upward groundwater levels vs downward effective precipitation), or in the southern Seno-Turonian chalk of Normandy/Picardy (downward groundwater levels vs upward effective precipitation). In these cases, trends in effective precipitation cannot explain trends in groundwater levels. Many reasons could explain these opposite trends between effective precipitation and groundwater levels such as: a possible anthropogenic influence, a strong influence of low-frequency variability in groundwater levels that could modify the trend, a delay in the long-term evolution of groundwater levels compared to effective precipitation due to memory effects, an error in the choice of effective precipitation SAFRAN mesh.

Otherwise, we observe generally downward trends or stable trends in groundwater levels when effective precipitation exhibit downward trends.

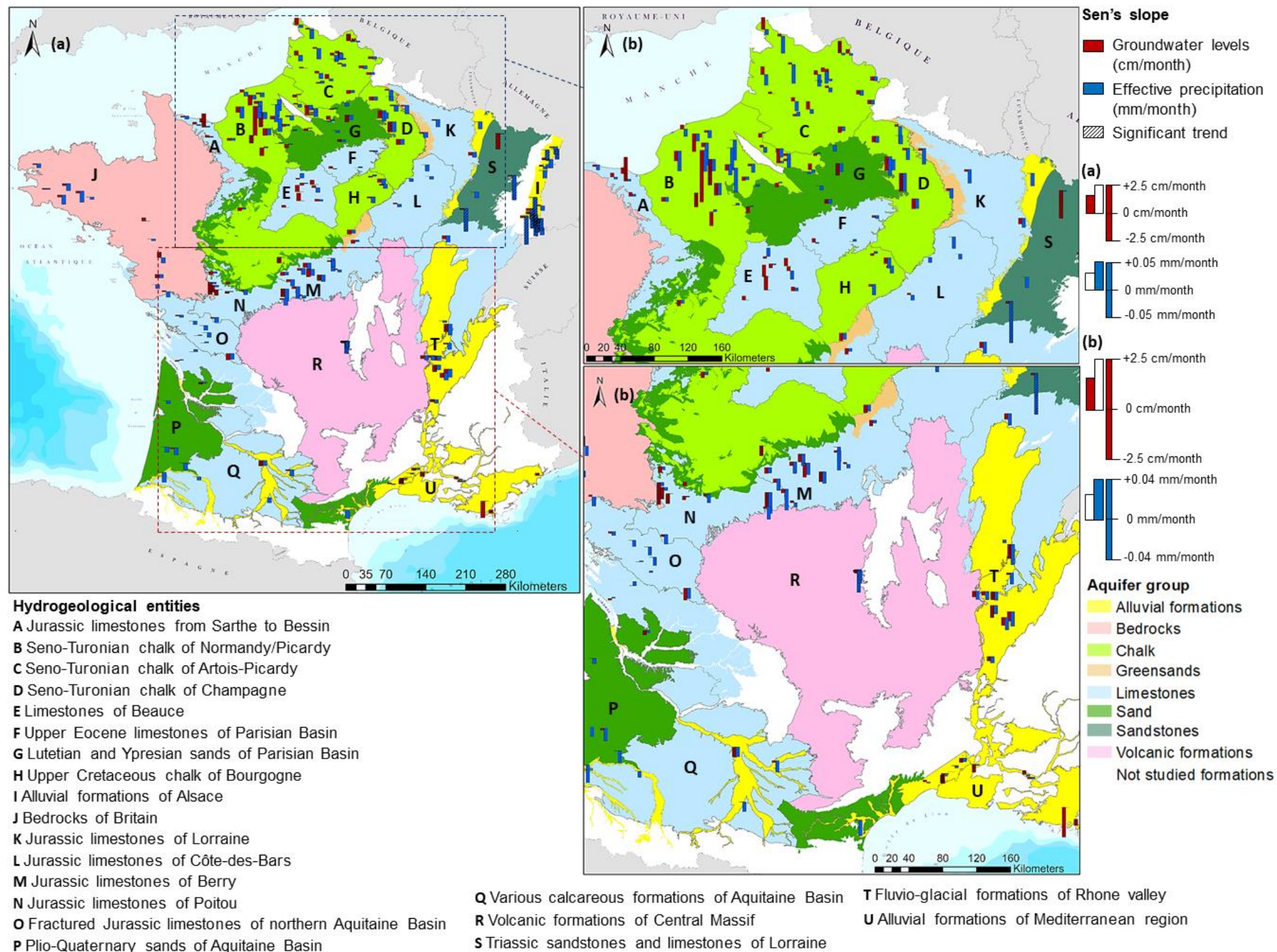


Figure 35: Comparison between Sen's slope of groundwater levels and effective precipitation over the 1996-2019 period. The statistical significance of trends is tested at a threshold of 5%.



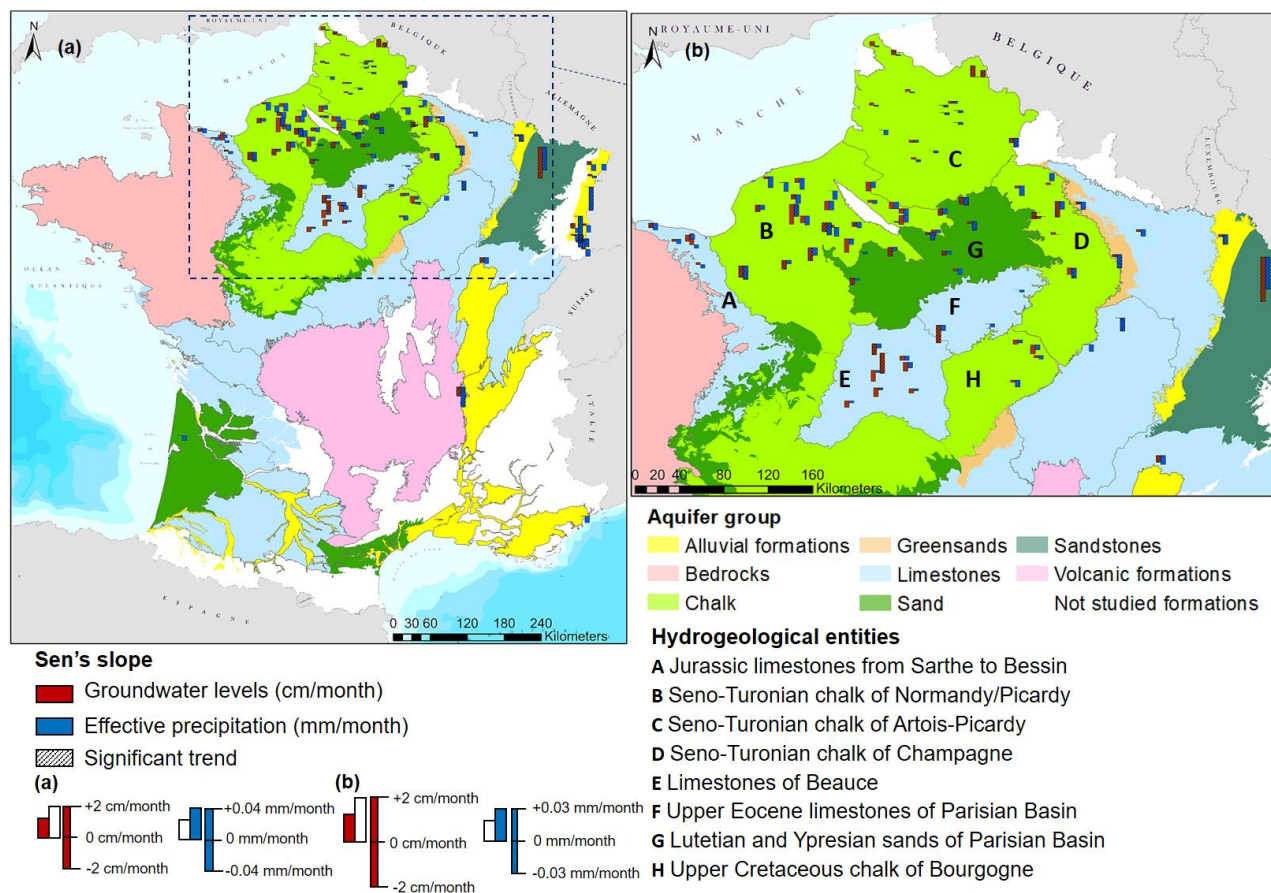


Figure 36: Comparison between Sen's slope of groundwater levels and effective precipitation over the 1976-2019 period. The statistical significance of trends is tested at a threshold of 5%.



Over the 1976-2019 period, trends exhibited by effective precipitation are consistently downward (Figure 36). In contrast, their statistical significance is rather sporadic and not homogeneous at the scale of northern metropolitan France. We still observe on this longer period opposite trends between effective precipitation and groundwater levels in the Seno-Turonian chalk of Artois-Picardy but trends magnitude appear rather weak (upward groundwater levels and downward effective precipitation). On this period, the same phenomenon of opposite trends appears this time for southern Jurassic limestones from Sarthe to Bessin and remains for specific sectors of alluvial formations of Alsace. As explained in the previous paragraph, multiple causes may lead to opposite trends. Inversely, opposite trends between effective precipitation and groundwater levels that appeared over the 1996-2019 period in the southern Seno-Turonian chalk are in the same direction this time (downward) (Figure 35 and Figure 36). In other cases, when effective precipitation display downward trends, groundwater levels also display downward trends or at least no trends, meaning that trends in effective precipitation may explain trends in groundwater levels.

5.2.1.3 Conclusion on the evolution of groundwater levels and effective precipitation in metropolitan France

In metropolitan France, we mainly observe downward groundwater levels on the two studied periods. This pattern is also observed in effective precipitation. Nevertheless, some hydrogeological entities display consistent upward trends in groundwater levels such as the limestones of Beauce (but only on the 1996-2019 period), the Seno-Turonian chalk of Artois-Picardy and the southern Jurassic limestones from Sarthe to Bessin. More locally, we also observe these upward trends in alluvial formations of Alsace (both periods), or in alluvial formations of Mediterranean region (1996-2019 period). Overall, we notice a decrease of the number of upward trends in groundwater levels on the 1976-2019 period compared to the 1996-2019 period.

In hydrogeological entities displaying homogeneous upward trends in groundwater levels, particularly in the Seno-Turonian chalk of Artois-Picardy, effective precipitation exhibit very often downward trends apart from Beauce region. It means that the decrease of groundwater recharge is not reflected in groundwater levels. One of the most probable hypothesis to explain this phenomenon would be relative to the influence of low-frequency variability on trends. Indeed, catchment and aquifers have the ability to smooth out rapid fluctuations from precipitation, and even to exacerbate the large-scale atmospheric/oceanic circulation induced low-frequency variabilities, due to their memory effect. Many researches addressed the influence of low-frequency variability on trends in surface hydrology and concluded to its heavy impact on streamflow or rainfall trends (*e.g.* Hannaford et al., 2013; Peña-Angulo et al., 2020). Therefore, the groundwater low-frequency variability could easily mask real trends induced by the decrease of recharge.

Secondly, the hydrogeological response to trends or to low-frequency variabilities is delayed in comparison to precipitation and effective precipitation, particularly when the characteristic time of aquifers is long. Therefore, this delayed response time could easily lead to opposite trends between effective precipitation and groundwater levels on similar periods.

In view of the influence of low-frequency variability on streamflow or rainfall trends, the investigation of the potential influence of groundwater low-frequency variability on trends was realised and a publication about this subject in our study area has been submitted to the Journal of Hydrology (Baulon et al., submitted). Conclusions about this study are provided in the following section.



5.2.2 Conclusions on the sensitivity of groundwater trends to low-frequency variability (Baulon et al., submitted)

Results of this study highlight the heavy influence of groundwater low-frequency variability (from multiannual to decadal) on trends estimation. The multi-temporal analysis of trends proves that upward trends displayed in the Seno-Turonian chalk of Artois-Picardy, the limestones of Beauce, and the Jurassic limestones from Sarthe to Bessin, either on one reference period or both, are not stable over time meaning that downward trends are detected on other time periods. Therefore, these upward trends are not necessarily indicative of the real evolution of groundwater levels.

Generally, aquifers displaying inertial (i.e. a predominant low-frequency variability) or combined behaviours (i.e. a well-pronounced low-frequency variability superimposed by annual variability) display unstable trends (i.e. regular changes of direction according study period). These alternative trend directions on decreasing periods (e.g. from 1976-2019 to 2000-2019) arise because the trend estimation can be started during either a multiannual high-level or a multiannual low-level, which highly influence trend direction.

Sometimes, in such contexts, stable trends can be detected (i.e. no changes of direction according study period) when an underlying trend is present. These underlying trends are very often segments of slower fluctuations that cannot be highlighted by the length of the study window. Then, the weakening of low-frequency variability observed over last decades is the second factor to get stable trends in some hydrogeological entities.

This study also indicates that multiannual (~7-yr) and decadal (~17-yr) variabilities affect the general trend in groundwater levels by driving upward or downward levels. Indeed, the multiannual variability drives upward groundwater levels in northern inertial aquifers with accentuated upward trends and attenuated downward trends; while in southern aquifers it drives downward groundwater levels with attenuated upward trends and accentuated downward trends. This north/south discrepancy may be directly related to ETP and/or aquifer properties of northern hydrogeological inertial system to interfere and reverse the influence of multiannual variability on trends (from a downward influence in precipitation to an upward influence in groundwater). Finally, the decadal variability drives downward groundwater levels in northern aquifers with attenuated upward trends and accentuated downward trends. No conclusion have been attained for southern aquifers due to the lack of data.

The degree of influence of multiannual and decadal variabilities on trends appears to be related to (i) the proportion of variance that they explain in groundwater levels, (ii) the length of the study period. Thus, the more they explain a large proportion of variance, the greater their influence on trend, and the shorter the study duration, the greater their influence on trend.

Hence, the main issues of trend studies in surface hydrology due to low-frequency variability are also perfectly highlighted in groundwater levels. Therefore, groundwater trend studies must be consider with caution to avoid misleading interpretation, including ours in the section 5.2.1., especially because the low-frequency variability can be exacerbated in aquifers compared to precipitation. It ensues that estimated monotonic trends cannot be extrapolated on other periods, nor used to predict future evolutions.

To overcome issues of the influence of low-frequency variability on trends and detect “real” trends in groundwater levels, we need to remove these variabilities from groundwater levels and effective

precipitation. Therefore, in the next section, we will use the EEMD filtering technique to identify “real” and non-linear trends in groundwater levels.

5.2.3 Evolution of the filtered groundwater levels and effective precipitation of large-scale atmospheric circulation induced low-frequency variability

5.2.3.1 Monotonic trend detection of filtered groundwater levels (EEMD residue) in relation to water level fluctuation

Figure 37 displays the detected monotonic trends of filtered groundwater levels (estimated with Sen’s slope) normalised by their water level fluctuation over the 1976-2019 and 1996-2019 periods. The statistical significance of trends at the threshold of 5% are also indicated on these maps. For your information, ranges of normalised trends by hydrogeological entities are presented in Table 5 and Table 6.

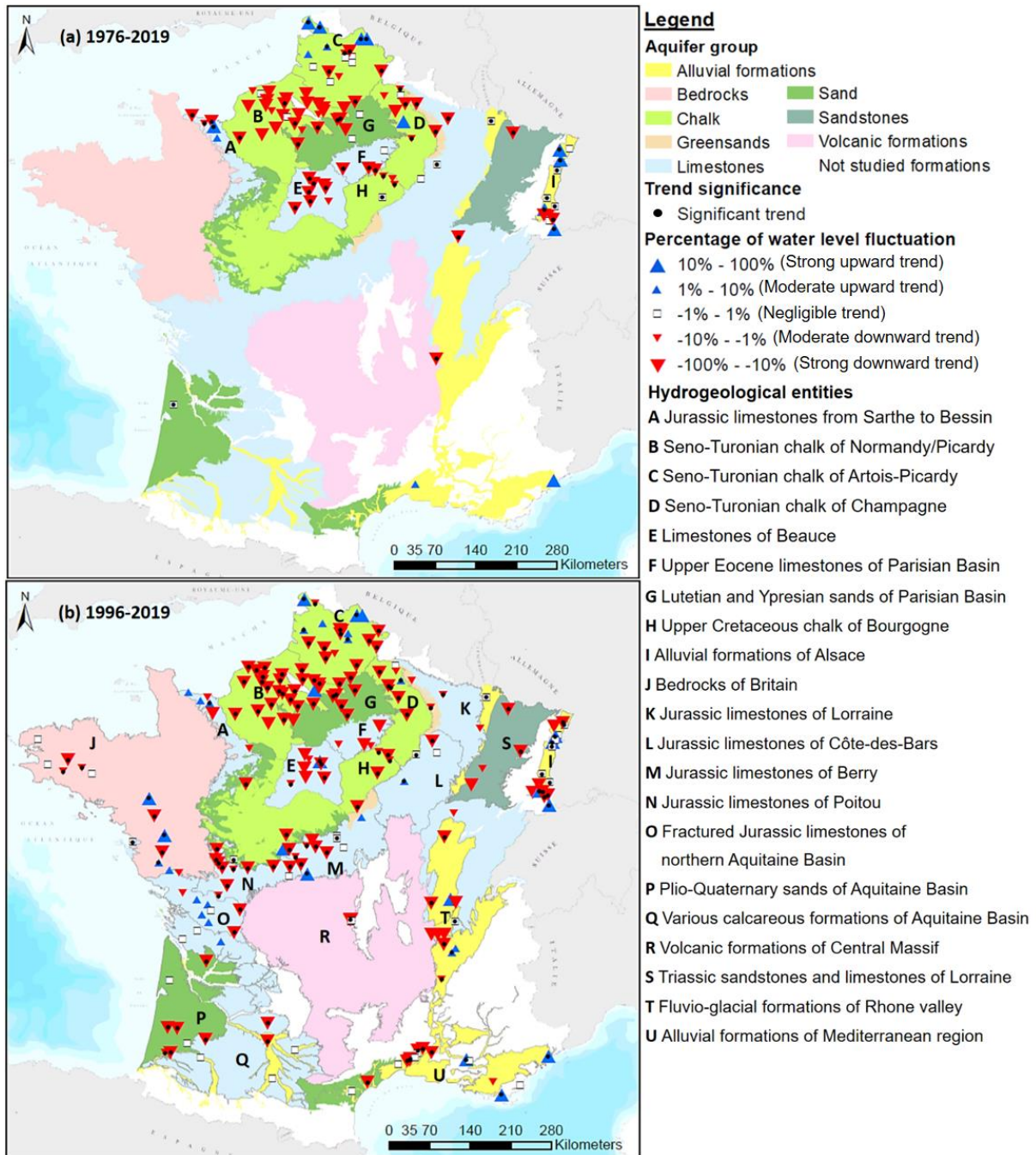


Figure 37: Trends magnitude normalised by the maximum water level fluctuation and their statistical significance (threshold of 5%) of filtered monthly groundwater levels (EEMD residue) over the 1976-2019 and 1996-2019 periods.

The overall picture of filtered groundwater levels trends at the scale of northern metropolitan France over the 1976-2019 period mainly shows downward trends (Figure 37a). Consistent statistically significant downward trends are observed in the northern part of Jurassic limestones from Sarthe to Bessin, the limestones of Beauce and the Upper Cretaceous chalk of Bourgogne. Downward trends are

also displayed in the Seno-Turonian chalk of Normandy/Picardy but they are not statistically significant excepting in the southern part of the entity. The chalk of Champagne also presents downward trends, even if there is a borehole displaying an upward trend not statistically significant. Hydrogeological entities that exhibited upward trends of raw groundwater levels also display such trends in their filtered groundwater levels as the southern Jurassic limestones from Bessin to Sarthe and the northern Seno-Turonian chalk of Artois-Picardy. Lastly, alluvial formations of Alsace still display various trends (from upward to downward).

Monotonic trends detected on the filtered groundwater levels are heavily similar in direction than those exhibited in raw groundwater levels (unfiltered) on the 1976-2019 period (Figure 37a and Figure 34a). Magnitudes of filtered groundwater trends ranges in relation to water level fluctuation remain rather similar than those of raw groundwater levels, excepting in three entities: the Lutetian and Ypresian sands of Paris Basin (reduction), the alluvial formations of Alsace (accentuation), the limestones of Beauce (reduction) (Table 5 and Table 6).

Table 5 *Normalised groundwater trends ranges on EEMD residue for the main hydrogeological entities over the 1976-2019 period.*

Hydrogeological entities	Lower bound - Slope (% of WLF)	Upper bound - Slope (% of WLF)	Number of boreholes
Seno-Turonian chalk of Artois-Picardy	-31	34	15
Seno-Turonian chalk of Normandy/Picardy	-48	0	29
Seno-Turonian and Turonian chalk of Champagne	-34	12	8
Jurassic limestones from Sarthe to Bessin	-21	16	4
Lutetian and Ypresian sands of ParisBasin	-15	0	3
Upper Eocene limestones of Paris Basin	-59	0	4
Alluvial formations of Alsace	-19	70	13
Limestones of Beauce	-37	-4	8
Upper Cretaceous chalk of Bourgogne	-7	-3	3

More discrepancies in trend direction between raw groundwater levels and filtered groundwater levels appear on the 1996-2019 period at the scale of metropolitan France (Figure 37b and Figure 34b). In the Seno-Turonian chalk of Artois-Picardy, the southern Jurassic limestones from Sarthe to Bessin or the fluvio-glacial formations of Rhone valley, filtering the low-frequency variability from groundwater levels leads to a heterogeneity of trend direction while homogeneous trends were observed on raw groundwater levels. Inversely, a consistency in trend direction is reached in the Seno-Turonian chalk of Normandy/Picardy with homogeneous statistically significant downward trends in filtered groundwater levels. A major switch of trend direction is observed in the limestones of Beauce exhibiting downward trends of filtered groundwater levels instead of upward trends in raw groundwater levels. This change of direction is also noticeable in the fractured Jurassic limestones of northern Aquitaine Basin with filtered groundwater levels displaying upward trends while insignificant trends in relation to water level fluctuation were identified in raw groundwater levels.

Filtering the groundwater low-frequency variabilities highlights a homogeneity of statistically significant downward trends in entities of Parisian Basin (the Seno-Turian chalk of Normandy/Picardy and southern Artois-Picardy Basin, the Lutetian and Ypresian sands, the chalk of Champagne and Bourgogne), the Jurassic limestones of Berry and Poitou, and even in western alluvial formations of Mediterranean region (Figure 37b).

Compared to the trend analysis on raw groundwater levels, we can observe a large number of statistically significant trends on filtered groundwater levels (Figure 34b and Figure 37b). This is certainly due to the absence of variability in groundwater EEMD residue. Indeed, a large variability in groundwater levels often leads to non-significant trends, even if their magnitude is considerable.

Filtering the low-frequency variabilities of groundwater levels can have various effects on magnitude of trends in relation to water level fluctuation: accentuation (*e.g.* the Seno-Turonian chalk of Normandy/Picardy), reduction (*e.g.* alluvial and fluvio-glacial formations of Rhone valley), little impact (*e.g.* volcanic formations of Central Massif) (Table 6 and Table 3).

Table 6 *Normalised groundwater trends ranges on EEMD residue for the main hydrogeological entities over the 1996-2019 period.*

Hydrogeological entities	Lower bound - Slope (% of WLF)	Upper bound - Slope (% of WLF)	Number of boreholes
Seno-Turonian chalk of Artois-Picardy	-44	22	18
Seno-Turonian chalk of Normandy/Picardy	-99	11	30
Seno-Turonian and Turonian chalk of Champagne	-19	7	8
Jurassic limestones from Sarthe to Bessin	-13	9	5
Lutetian and Ypresian sands of Paris Basin	-71	-47	3
Jurassic limestones of Lorraine and Côte-des-Bars	-7	10	4
Triassic sandstones of Lorraine	-81	-16	2
Upper Eocene limestones of Paris Basin	-22	-5	4
Alluvial formations of Alsace	-37	40	18
Limestones of Beauce	-24	44	8
Chalk of Bourgogne and Gâtinais	-15	-3	4
Triassic limestones of Lorraine	-2	-2	1
Bedrocks of Britain	-19	34	10
Jurassic limestones of Berry	-17	2	9
Jurassic limestones of Poitou	-40	-7	6
Fractured Jurassic limestones of northern Aquitaine Basin	-9	5	7
Alluvial and fluvio-glacial formations of Rhone valley	-24	16	11
Volcanic formations of Central Massif	-21	0	5
Various calcareous formations of Aquitaine Basin	-39	-14	3
Plio-Quaternary sands of Aquitaine Basin	-13	0	3
Alluvial formations of Mediterranean region	-35	41	12

5.2.3.2 Comparison between the detected monotonic trends of filtered groundwater levels and effective precipitation

A comparison between filtered groundwater levels (red) and effective precipitation (blue) trends magnitude and direction is established in Figure 38 and Figure 39 by means of Sen's slope over the 1996-2019 and 1976-2019, respectively. A downward stick indicates a negative Sen's slope, and an upward stick indicates a positive Sen's slope, while the stick length indicates the magnitude of trends. The statistical significance at a threshold of 5% is indicated with hatchings.

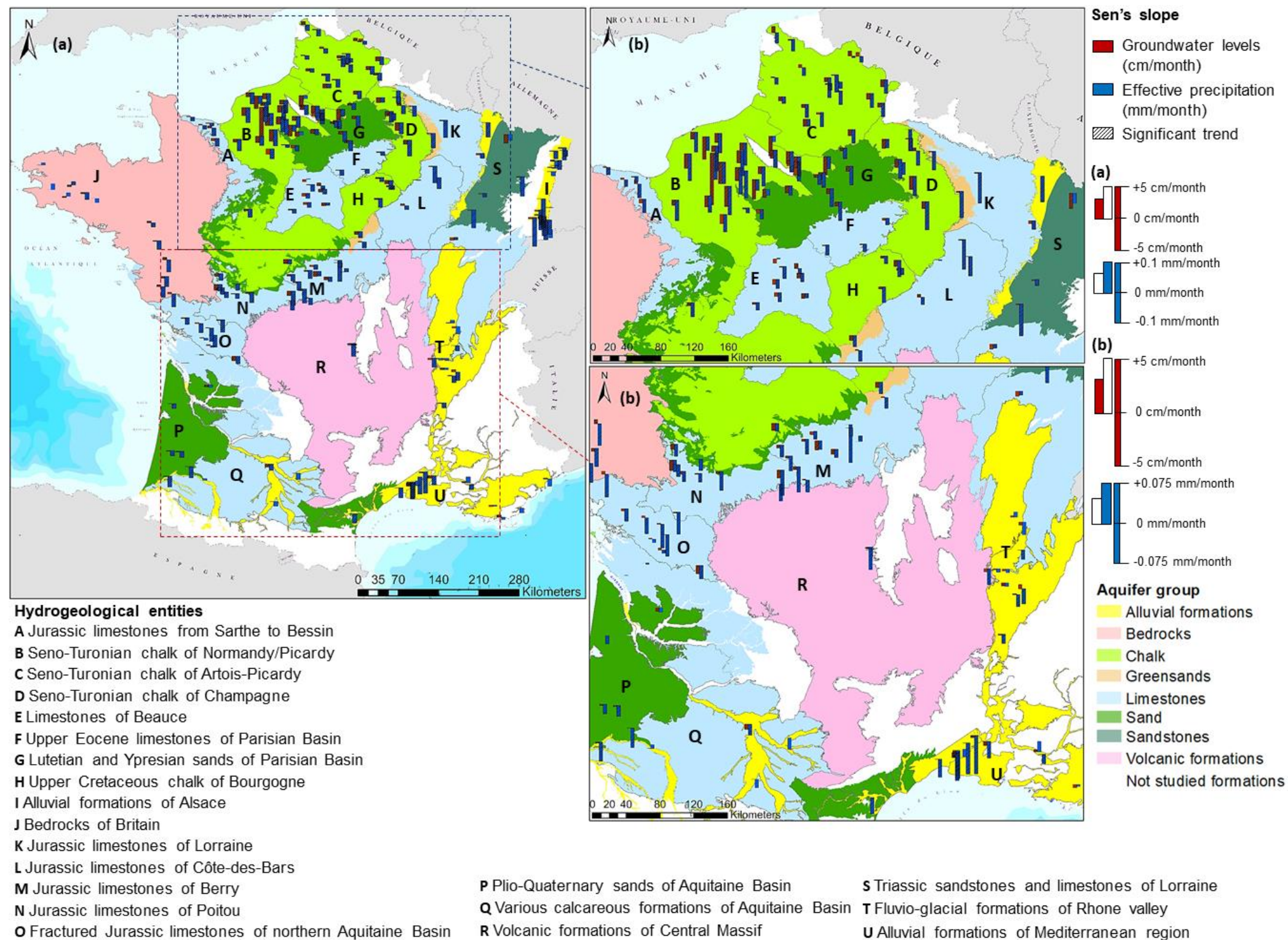


Figure 38: Comparison between Sen's slope of filtered groundwater levels and effective precipitation over the 1996-2019 period. The statistical significance of trends is tested at a threshold of 5%.



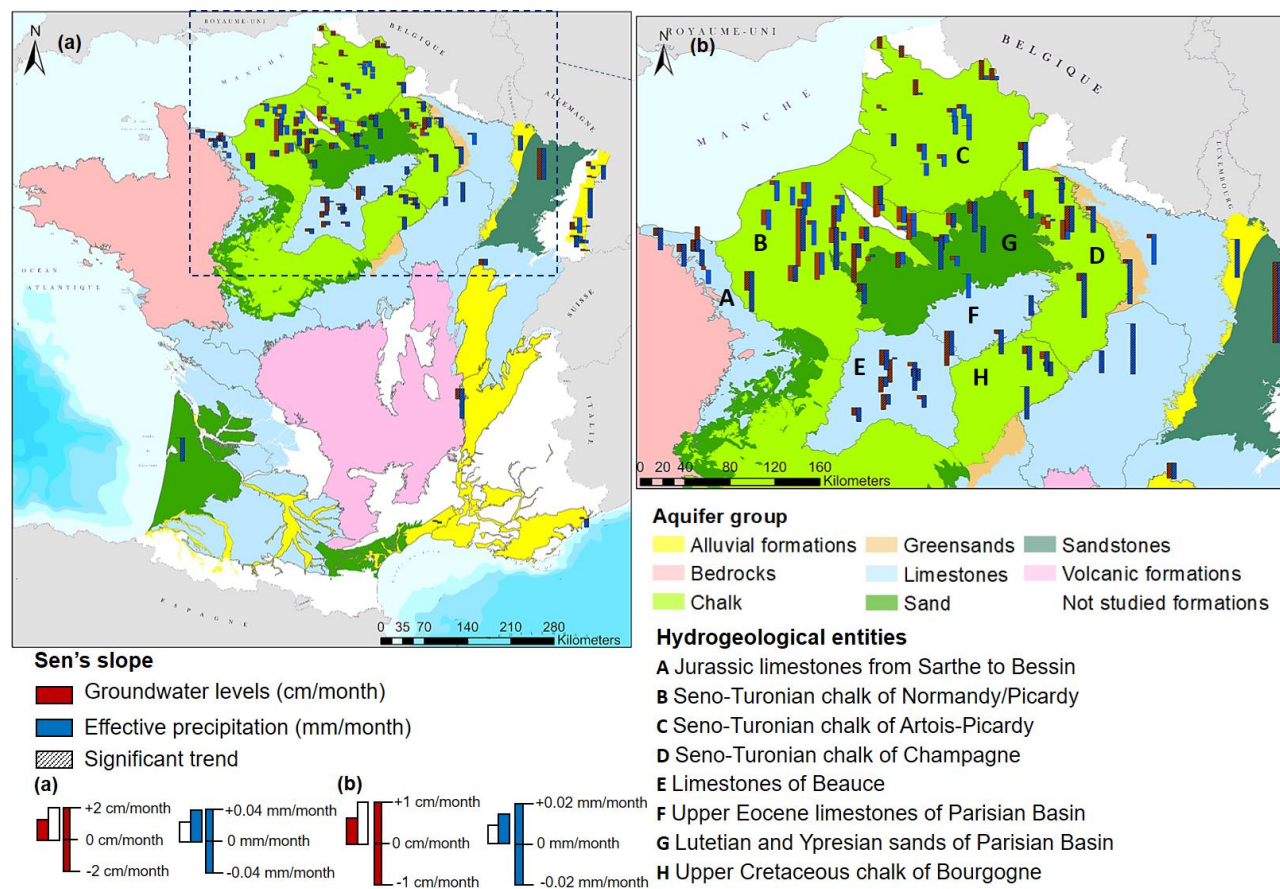


Figure 39: Comparison between Sen's slope of filtered groundwater levels and effective precipitation over the 1976-2019 period. The statistical significance of trends is tested at a threshold of 5%.



As was the case for raw effective precipitation, the filtered effective precipitation exhibit predominantly downward trends at the scale of metropolitan France over 1996-2019, which are this time widely statistically significant (Figure 38). Locally, upward trends can be displayed by filtered effective precipitation particularly in Britain.

Discrepancies that appeared when comparing trends direction of raw groundwater levels and effective precipitation remain for filtered data in northern Seno-Turonian chalk of Artois-Picardy, especially because in this part of the entity, filtered groundwater levels are still upward. Other opposite trends between filtered groundwater levels and effective precipitation appear in the fractured Jurassic limestones of northern Aquitaine Basin (upward filtered groundwater levels and downward filtered effective precipitation), some boreholes of fluvio-glacial formations of Rhone valley (upward filtered groundwater levels and downward filtered effective precipitation), bedrocks of Britain (both sides) and a few boreholes in other hydrogeological entities locally. Inversely in the southern Seno-Turonian chalk of Normandy/Picardy, the filtering of low-frequency variability in effective precipitation allows for highlighting downward trends that matches with the exhibited trends of filtered groundwater levels.

Otherwise, downward trends in filtered effective precipitation lead to downward trends in filtered groundwater levels in most cases (*e.g.* Jurassic limestones of Poitou and Berry, Plio-Quaternary sands of Aquitaine Basin, chalk of Champagne and Bourgogne).

On the longer period (1976-2019), filtered effective precipitation exhibit mainly downward trends through northern metropolitan France (Figure 39). In the northern part of the study area (*i.e.* Seno-Turonian chalk of Normandy/Picardy and southern part of Artois-Picardy basin), there are less downward trends which are statistically significant than in southern-eastern part of the study area. Locally, a few upward trends can be observed but they are marginal.

While opposite trends were exhibited on the shorter period (1996-2019) between filtered effective precipitation and groundwater levels in the northern Seno-Turonian chalk of Artois-Picardy, similar upward trends (or no trend in filtered effective precipitation) are displayed this time, which is more consistent. Opposite trends, with upward filtered groundwater levels and downward filtered effective precipitation, are noticeable sporadically in southern Jurassic limestones from Sarthe to Bessin, the alluvial formations of Alsace or the Seno-Turonian chalk of Artois-Picardy. Inversely, downward filtered groundwater levels and upward filtered effective precipitation are noticeable sporadically in the limestones of Beauce, the Seno-Turonian chalk of Champagne and Normandy/Picardy.

Overall, these opposite trends remain on this period very local meaning the good adequacy between trends in filtered groundwater levels and effective precipitation.

To better understand why such discrepancies and opposite trends are displayed between filtered groundwater levels and effective precipitation; next section will aim to describe the non-linear trends exhibited by EEMD residues of groundwater levels and effective precipitation.

5.2.3.3 Understanding the detected opposite monotonic trends between filtered effective precipitation and groundwater levels

To understand why discrepancies are observed in the detected monotonic trend direction of filtered groundwater levels and their respective filtered effective precipitation time series, a visual analysis of EEMD residues is realised (Figure 40 and Figure 41).

Thanks to this viewing, several phenomena explaining the detected opposite monotonic trends are highlighted. Firstly, we observe cases where the non-linear trend in effective precipitation does not explain the non-linear trend in groundwater levels (*i.e.* the EEMD residues display divergent shapes). In this case, several explanations may be raised:

- a wrong selection of effective precipitation mesh, and the non-linear trend in the selected effective precipitation does not explain the non-linear trend in groundwater levels.
- a long term pumping of groundwater, which may explain why the non-linear trend in groundwater levels does not reflect the non-linear trend observed in effective precipitation, the long term groundwater trend being influenced by anthropogenic activities. However, it may be a complicated task to identify boreholes and aquifers submitted to such phenomenon in view of scarcity of database describing long-term pumpings.
- a distortion of non-linear trend by the physical properties of catchment, vadose zone and aquifers. However, the use of a numerical model should be interesting to test and approve such hypothesis.

Figure 40 displays an example of the first case with detected opposite monotonic trends related to a wrong selection of effective precipitation time series for a borehole monitoring the limestones of Beauce. In this case, the shape of effective precipitation non-linear trend differs than the one exhibited in groundwater levels, meaning that the trend in effective precipitation does not explain the trend in groundwater levels (Figure 40a). Looking at other meshes and effective precipitation time series within the catchment and a 50 km radius around the well allows for identifying effective precipitation time series displaying the same type of non-linear trend than groundwater levels (Figure 40b). Therefore, it means that the indicator allowing us to select the best effective precipitation time series in relation to groundwater recharge/discharge, does not always reflect a good accordance between non-linear trends of effective precipitation and groundwater levels. Further investigations should be conducted to assign to each borehole a mesh of effective precipitation describing the best the dynamic of groundwater levels but also displaying the best agreement between long-term non-linear trends.

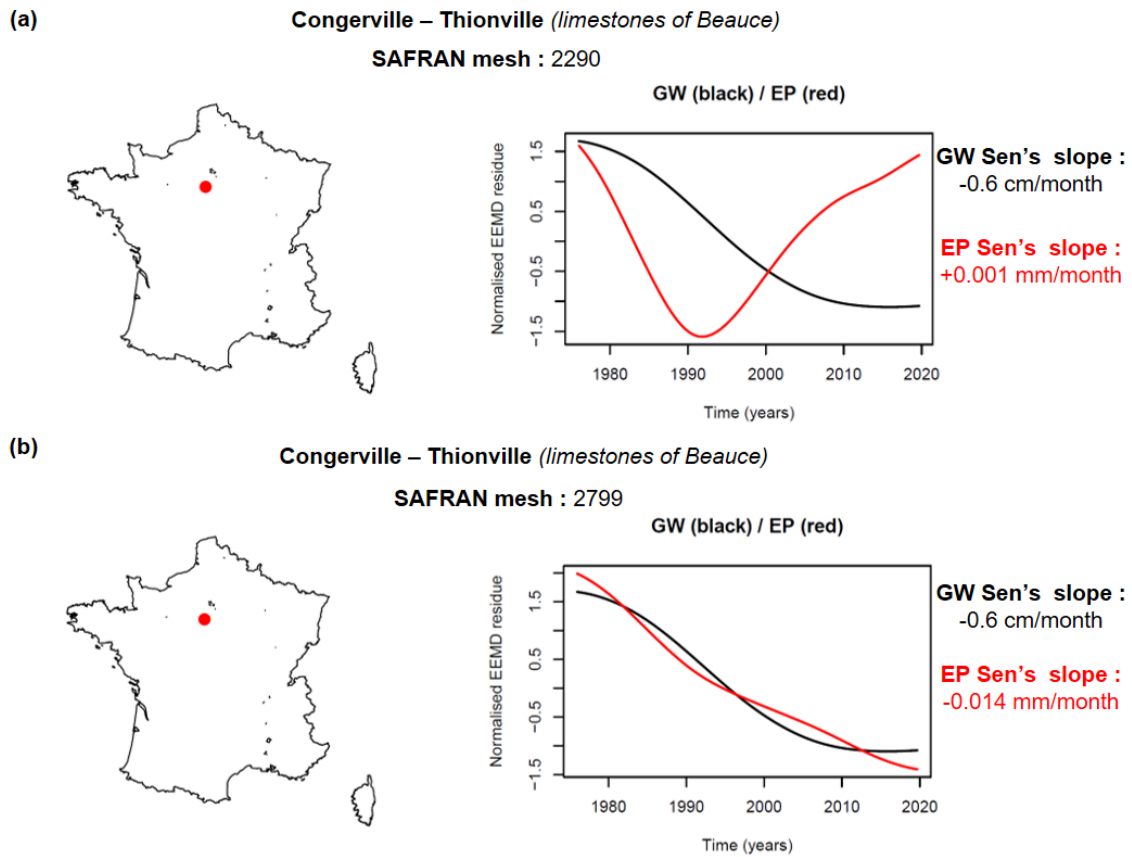


Figure 40: Standardised EEMD residues (i.e. non-linear trends) of groundwater levels (GW) for the borehole of Congerville-Thionville monitoring the limestones of Beauce and effective precipitation (EP) for (a) the selected SAFRAN mesh with the methodology presented in 5.1. to conduct the present study and (b) another SAFRAN mesh within the catchment and a 50 km radius around the well. Sen's slopes estimated on non-standardised EEMD residues of GW and EP are indicated on the right side.

Secondly, we observe cases where the non-linear trend in effective precipitation explains the non-linear trend in groundwater levels (i.e. the EEMD residues display similar shapes) (Figure 41). In this case, several explanations may be raised to justify the detected opposite monotonic trends:

- a dephasing between the two non-linear trends that may be related to the response time of aquifers to effective precipitation input.
- an amplitude modification of the non-linear trend "oscillation" by the intrinsic properties of aquifers and vadose zone.
- a discrepancy in skewness of non-linear trends that may be also related to a modification of signal by aquifers and vadose zone.

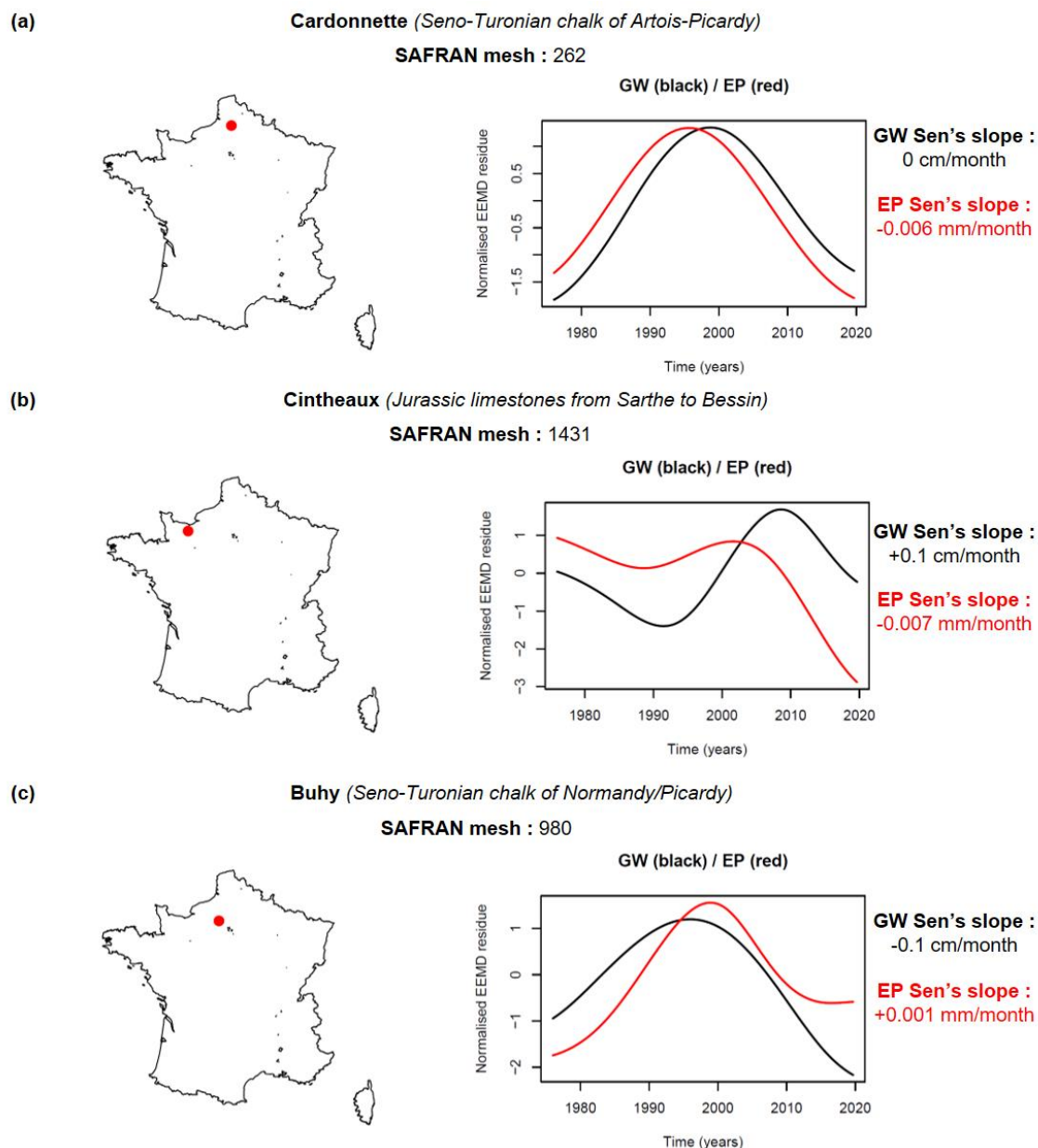


Figure 41: Standardised EEMD residues (i.e. non-linear trends) of effective precipitation (EP) and groundwater levels (GW) for the boreholes of (a) Cardonnette monitoring the Seno-Turonian chalk of Artois-Picardy, (b) Cintheaux monitoring the Jurassic limestones from Sarthe to Bessin, (c) Buhy monitoring the Seno-Turonian chalk of Normandy/Picardy. Sen's slopes estimated on non-standardised EEMD residues of GW and EP are indicated on the right side.

For instance, Figure 41 displays these three phenomena through three boreholes monitoring different hydrogeological entities. The borehole of Cardonnelle in the Seno-Turonian chalk of Artois-Picardy exhibits a typical dephasing between non-linear trends of effective precipitation and groundwater levels (Figure 41a). While the effective precipitation display a downward detected monotonic trend, the groundwater levels does not display trend due to this dephasing. In the same way, groundwater levels of Cintheaux in the Jurassic limestones from Sarthe to Bessin also display a dephasing of its non-linear trend compared to effective precipitation (Figure 41b). In addition, oscillations in groundwater levels are exacerbated compared to effective precipitation, which may be related to the physical properties of aquifers and vadose zone modulating the variance of such oscillation. These two combined phenomena explain why opposite monotonic trends are detected between groundwater levels and effective precipitation. Finally, groundwater levels of Buhy in the Seno-Turonian chalk of Normandy/Picardy and effective precipitation non-linear trends display a quite similar shape (Figure 41c). However, the discrepancy of skewness (probably related to the modulation by system properties) of EEMD residues may affect the detected monotonic trend direction and generate opposite trends.

5.2.3.4 Typical patterns of non-linear trends in groundwater levels and effective precipitation through metropolitan France

1996-2019 period

To identify typical patterns of non-linear trends of groundwater levels and effective precipitation through metropolitan France, a k-medoids clustering is conducted on EEMD residues for the two reference periods (Figure 42Figure 43Figure 44Figure 45). Figure 42 displays for each cluster all non-linear trends belonging to the cluster and the cluster medoid (*i.e.* the most representative non-linear trend within each cluster) on the 1996-2019 period. Figure 43 displays the cluster distribution through metropolitan France on the same period.

Groundwater levels can be clustered in 4 classes (medoids displaying the most central behaviour within the cluster) (Figure 42a):

- a parabolic decrease (cluster 1)
- a steady increase (cluster 2)
- a steady decrease (cluster 3)
- a serpentine shape with a decreasing trend (cluster 4)

The first cluster with non-linear trends showing parabolic decreases appears rather locally but is well represented in the limestones of Beauce, the alluvial formations of Alsace, the Triassic limestones of Lorraine, the Jurassic limestones of Berry, the bedrocks of Britain, or the Jurassic limestones from Sarthe to Bessin (Figure 43a). The second cluster with steady increases is particularly present in northern Seno-Turonian chalk of Artois-Picardy, and more locally in other hydrogeological entities such as the bedrocks of Britain, the Jurassic limestones from Sarthe to Bessin, the alluvial formations of Alsace. The third cluster with steady decreases is largely predominant in the Seno-Turonian chalk of Normandy/Picardy, the southern Seno-Turonian chalk of Artois-Picardy, the chalk of Bourgogne and Champagne, the Lutetian and Ypresian sands of the Paris Basin, the Jurassic limestones of Berry and Poitou, the Plio-Quaternary sands of



Aquitaine Basin, the Triassic sandstones of Lorraine. This pattern is present more locally in the fluvio-glacial formations of Rhone valley, the alluvial formations of Mediterranean region and Alsace, or in the bedrocks of Britain. Finally, the fourth cluster showing non-linear trends with a serpentine shape is predominant in the fractured Jurassic limestones of northern Aquitaine Basin, the Upper Eocene limestones of Paris Basin, specific sectors of fluvio-glacial formations of Rhone valley, and locally present in alluvial formations of mediterranean region.

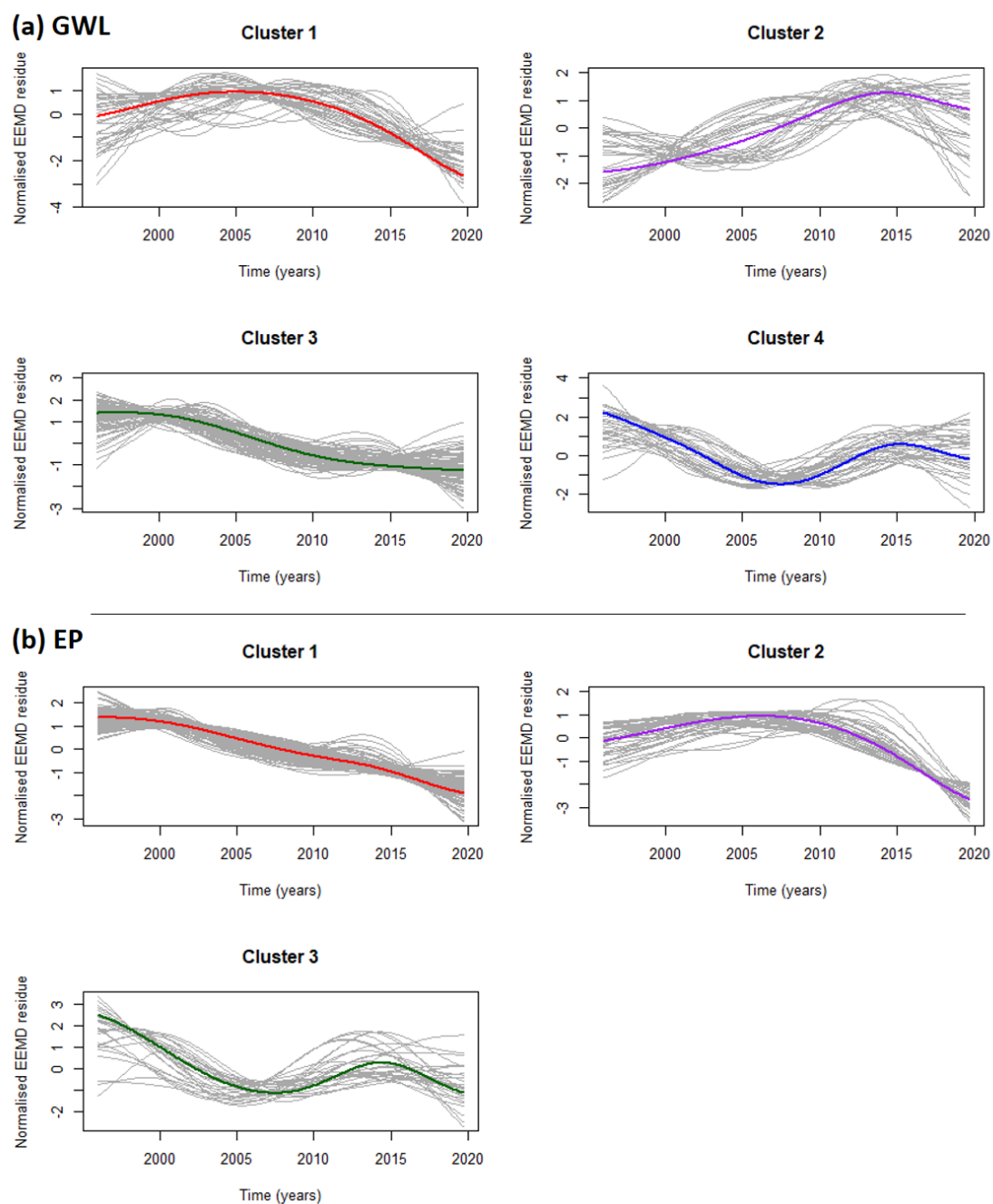


Figure 42: K-medoids clustering on non-linear trends (i.e. standardised EEMD residues) over the 1996-2019 period for (a) groundwater levels and (b) effective precipitation. Grey lines are all non-linear trends belonging to the cluster and color lines are cluster medoids (i.e. the most representative non-linear trend within each cluster).

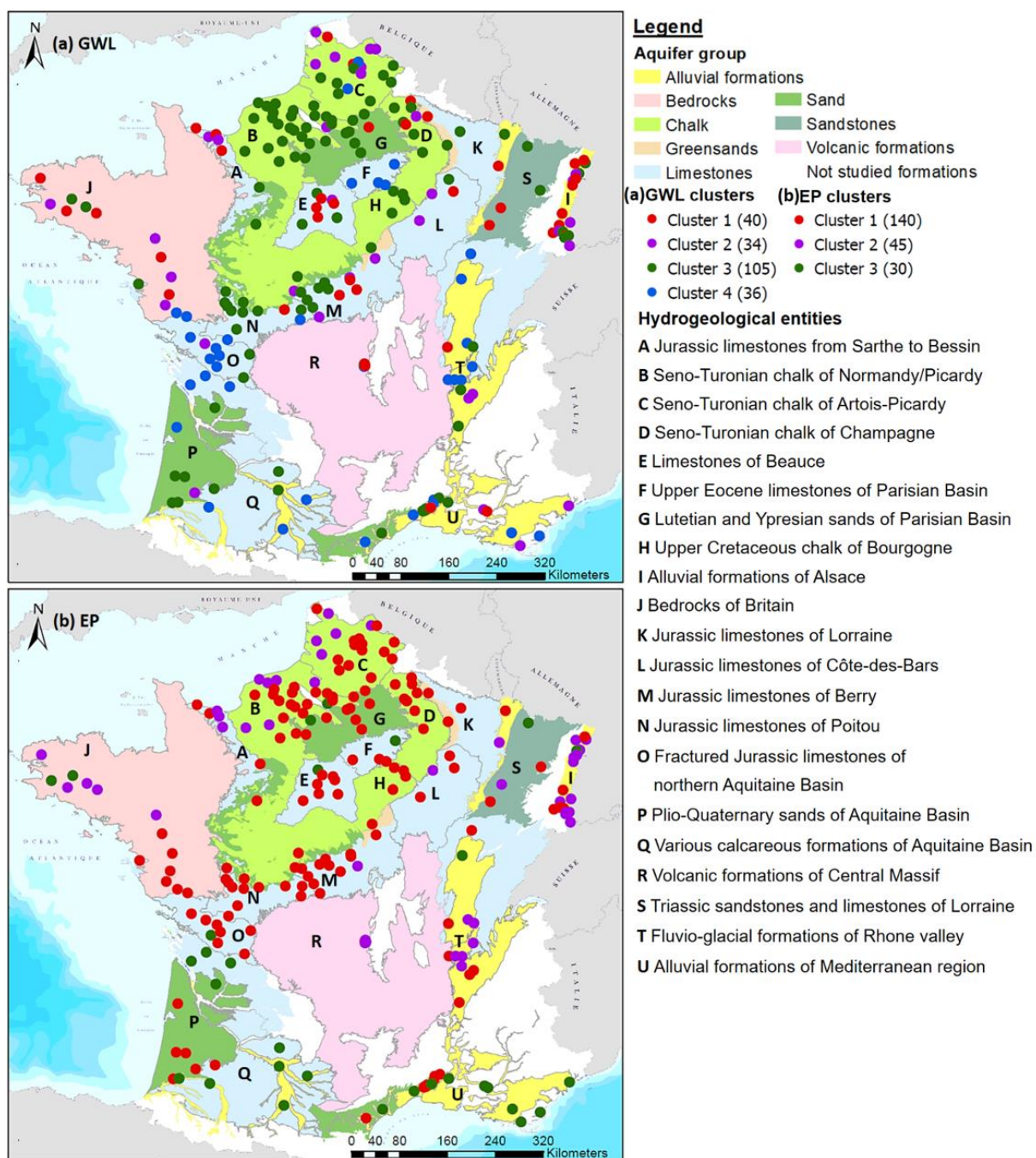


Figure 43: Spatial distribution of clustered non-linear trends over the 1996-2019 period for (a) groundwater levels and (b) effective precipitation.

Simultaneously, effective precipitation can be clustered in 3 classes (medoids displaying the most central behaviour within the cluster) (Figure 42b):

- a steady decrease (cluster 1)
- a parabolic decrease (cluster 2)
- a serpentine shape with a decreasing tendency (cluster 3)

The steady increase displaying by groundwater levels, particularly in northern Seno-Turonian chalk of Artois-Picardy, does not exist in the dataset of effective precipitation.

The first cluster displaying steady decreases of non-linear trends of effective precipitation is largely predominant in hydrogeological entities of Parisian Basin and its borders from the Jurassic limestones of Lorraine to the northern Jurassic limestones of Aquitaine Basin (Figure 43b). This type of non-linear trends are also detected importantly in southern bedrocks of Britain, the Plio-Quaternary sands of Aquitaine Basin, and specific sectors of fluvio-glacial formations of Rhone valley, alluvial formations of Alsace and Mediterranean region, and in the northern part of Jurassic limestones from Sarthe to Bessin. The second cluster with parabolic decreases is predominant in coastal watershed of Seno-Turonian chalk from Normandy to Artois-Picardy, southern Jurassic limestones from Sarthe to Bessin, northern-western bedrocks of Britain, alluvial formations of Alsace and a specific sector of fluvio-glacial formations of Rhone valley. Finally, the third cluster with non-linear trends displaying serpentine shapes is mainly present for southern hydrogeological entities such as the various calcareous formations of Aquitaine Basin, or the alluvial formations of Mediterranean region.

1976-2019 period

The same analysis is conducted on the 1976-2019 period for northern metropolitan France (Figure 44 and Figure 45). Groundwater levels non-linear trends were clustered into 3 classes (Figure 44a):

- a steady increase (cluster 1)
- a parabolic decrease (cluster 2)
- a steady decrease (cluster 3)

The first cluster with non-linear trends displaying steady increase is largely predominant in northern Seno-Turonian chalk of Artois-Picardy, southern Jurassic limestones from Sarthe to Bessin, and alluvial formations of Alsace (Figure 45a). The second cluster showing parabolic decrease of non-linear trends is largely predominant in the Seno-Turonian chalk of Normandy/Picardy, southern Seno-Turonian chalk of Artois-Picardy, the Lutetian and Ypresian sands of Paris Basin and the Seno-Turonian chalk of Champagne. This pattern of non-linear trends is also well represented in the chalk of Bourgogne. Finally, the third cluster displaying steady decrease of non-linear trends is predominant in the limestones of Beauce, the northern Jurassic limestones from Sarthe to Bessin, the eastern Seno-Turonian chalk of Artois-Picardy. This pattern is also well represented in southern Seno-Turonian chalk of Normandy/Picardy, the chalk of Bourgogne and in the various formations of Lorraine region.



Simultaneously, effective precipitation non-linear trends were clustered into 3 classes as well (Figure 44b):

- a parabolic trend (cluster 1)
- a weak increase followed by a significant decrease (cluster 2)
- a steady decrease (cluster 3)

The pattern of the first cluster with a parabolic trend is largely predominant in the Seno-Turonian chalk of Artois-Picardy or the southern alluvial formations of Alsace (Figure 45b). Locally, it appears in southern Seno-Turonian chalk of Normandy/Picardy and the chalk of Champagne. The second cluster, with non-linear trends displaying a weak increase followed by a significant decrease, is predominant in the Jurassic limestones from Sarthe to Bessin, the Seno-Turonian chalk of Normandy/Picardy, the Lutetian and Ypresian sands of Paris Basin. This pattern is also well represented in the chalk of Champagne and locally in the alluvial formations of Alsace. Finally, the third cluster with non-linear trends displaying steady decreases is predominant for southern hydrogeological entities such as the limestones of Beauce, the Upper Eocene limestones of Parisian Basin, the chalk of Bourgogne.

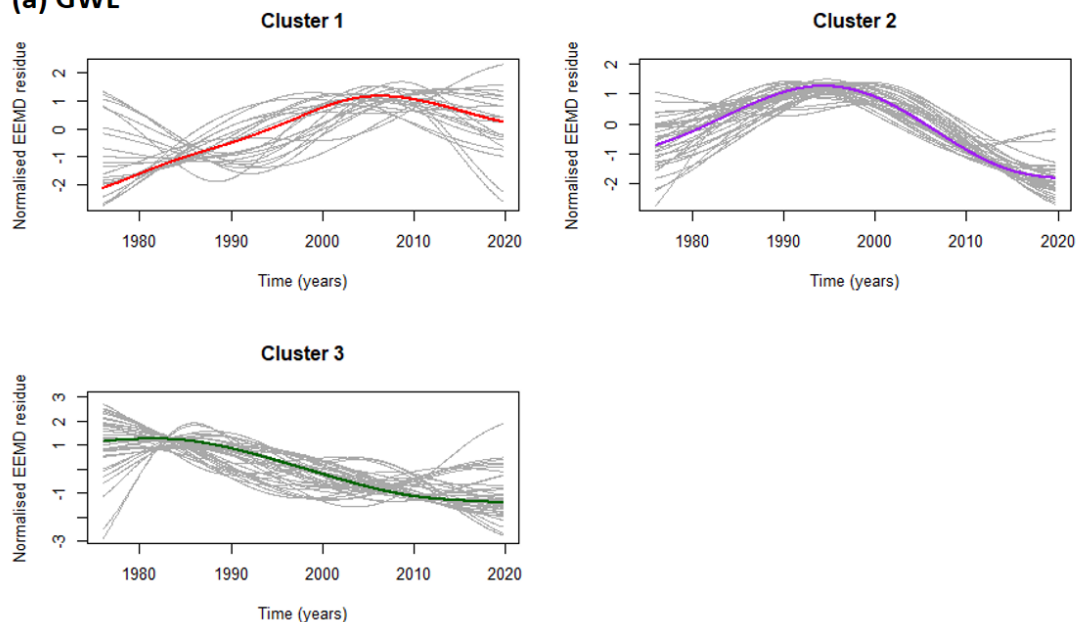
Without considering the Alsace region, the spatial distribution of effective precipitation non-linear trends clusters is rather spread according a north-south axis, with cluster 1 farthest north, cluster 2 at the middle, and cluster 3 farthest south.

Overall, this analysis highlights two different types of spatial distribution of clusters through metropolitan France and northern France between non-linear trends of groundwater levels and effective precipitation. Clusters of effective precipitation non-linear trends are spread rather according the geographical situation indicating the probable climatological influence on the detected trends (Figure 43b and Figure 45b). This is the case for the 1976-2019 period with the north-south spreading of clusters through northern France, but also on the 1996-2019 period through metropolitan France:

- the cluster 1 is predominantly spread rather on northern and western France,
- the cluster 2 is predominantly spread on coastal catchments at the border of English Channel but also on eastern France,
- the cluster 3 is predominantly spread on southern France.

For clusters of groundwater non-linear trends, their spatial distribution seems to be function of hydrogeological entities and their physical properties, even if it can differ locally due to the local variability of them (Figure 43a and Figure 45a).

(a) GWL



(b) EP

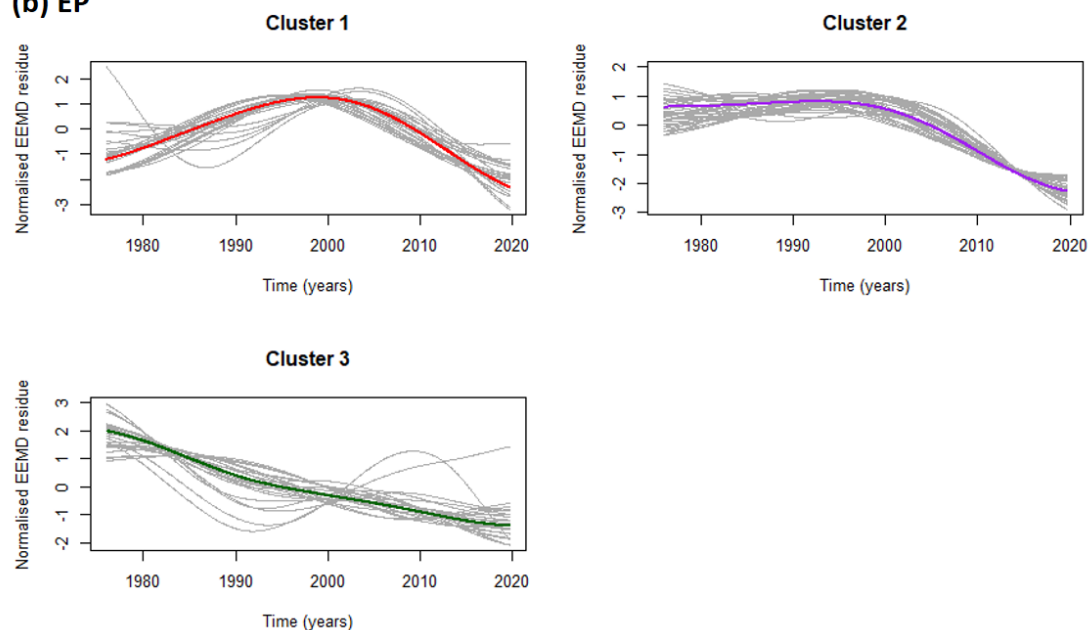


Figure 44: K-medoids clustering on non-linear trends (i.e. standardised EEMD residues) over the 1976-2019 period for (a) groundwater levels and (b) effective precipitation. Grey lines are all non-linear trends belonging to the cluster and color lines are cluster medoids (i.e. the most representative non-linear trend within each cluster).

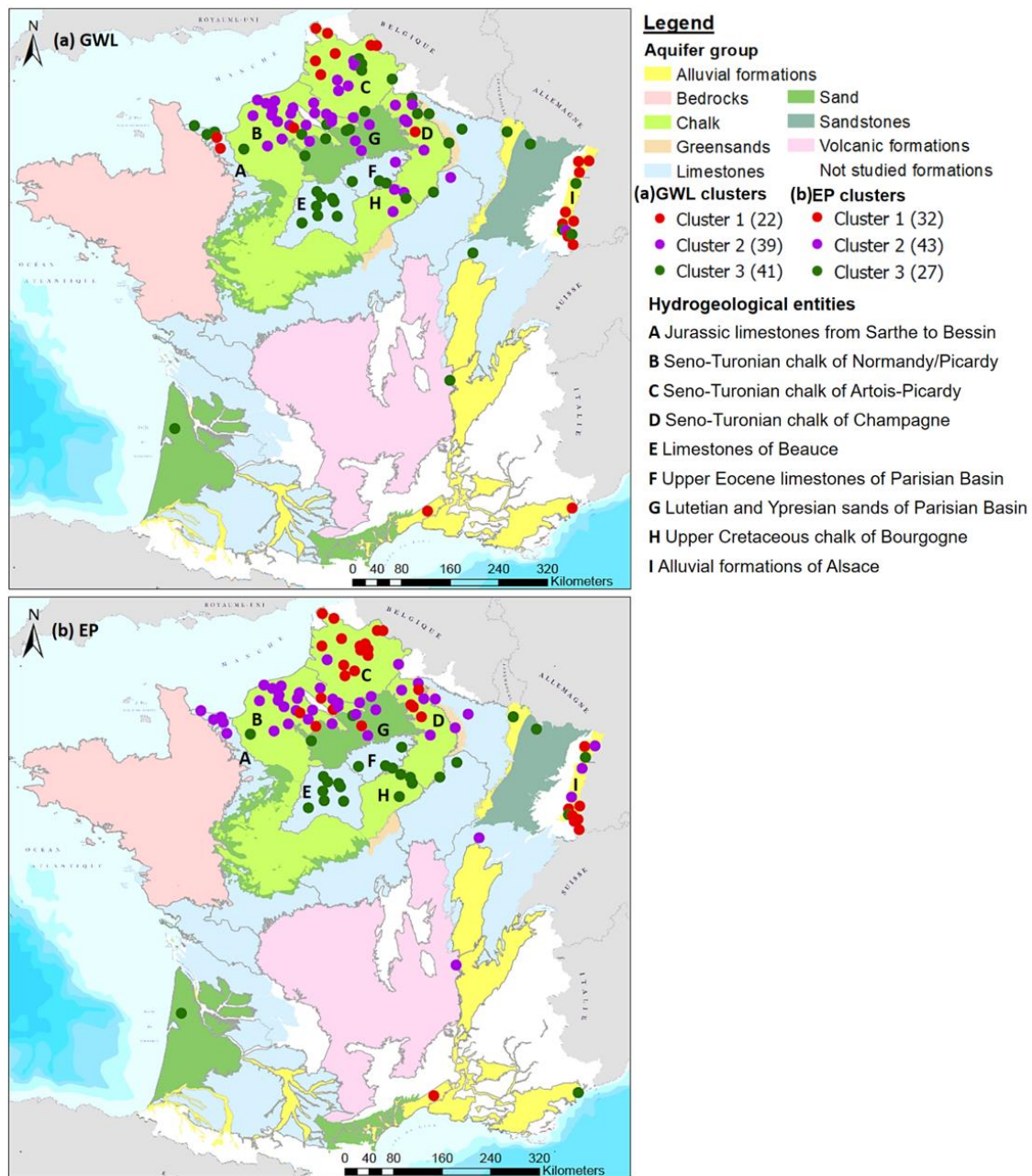


Figure 45: Spatial distribution of clustered non-linear trends over the 1976-2019 period for (a) groundwater levels and (b) effective precipitation.

Findings over the two periods

It can arise discrepancies in the accordance of non-linear trends clusters of groundwater levels and effective precipitation (Figure 42Figure 43Figure 44 Figure 45). Indeed for the 1996-2019 period, cluster 1 of groundwater levels should correspond to cluster 2 of effective precipitation, cluster 3 of groundwater levels to cluster 1 of effective precipitation, and cluster 4 of groundwater levels to cluster 3 of effective precipitation (Figure 42). However, for specific points, there is a discrepancy in this theoretical accordance. This is the case for numerous boreholes monitoring the limestones of Beauce for instance (Figure 43). While their non-linear trends display parabolic decreases (cluster 1), the non-linear trends of their corresponding effective precipitation time series display steady decreases (cluster 1). In this case, this discrepancy may be related to the dephasing between non-linear trends of effective precipitation and groundwater levels (Figure 46a). The capability of aquifers and catchment to dampen or accentuate oscillation amplitude may be also a factor to get non-corresponding clusters between groundwater levels and effective precipitation. This is what happening in the fractured Jurassic limestones of northern Aquitaine Basin, with an accentuated oscillation in groundwater levels providing a serpentine shape with a decreasing tendency to the non-linear trend (cluster 4) (Figure 46b). These oscillations are less pronounced in the non-linear trends of effective precipitation and consequently the non-linear trend belongs to the cluster with a steady decrease (cluster 1). Moreover within a cluster, it may be possible to get a large diversity of non-linear trends shape. Therefore, non-linear trends of a given borehole and its corresponding effective precipitation mesh with quite similar shape, but a bit different due to a dephasing or oscillation modulation by catchment and aquifers, can be spread in different clusters depicting by medoids with quite different shape. For instance, this is the case for the borehole of Nort-Leulinghem in the Seno-Turonian chalk of Artois-Picardy (Figure 46c). The non-linear trends of groundwater levels and its corresponding effective precipitation mesh are quite similar in terms of shape on the 1976-2019 period, but signals are lagged with an opposite asymmetry. Consequently, the groundwater levels non-linear trend is classified into the cluster for which the medoid displays steady increase (cluster 1), while effective precipitation non-linear trend is classified into the cluster for which the medoid displays a parabolic shape (cluster 1).

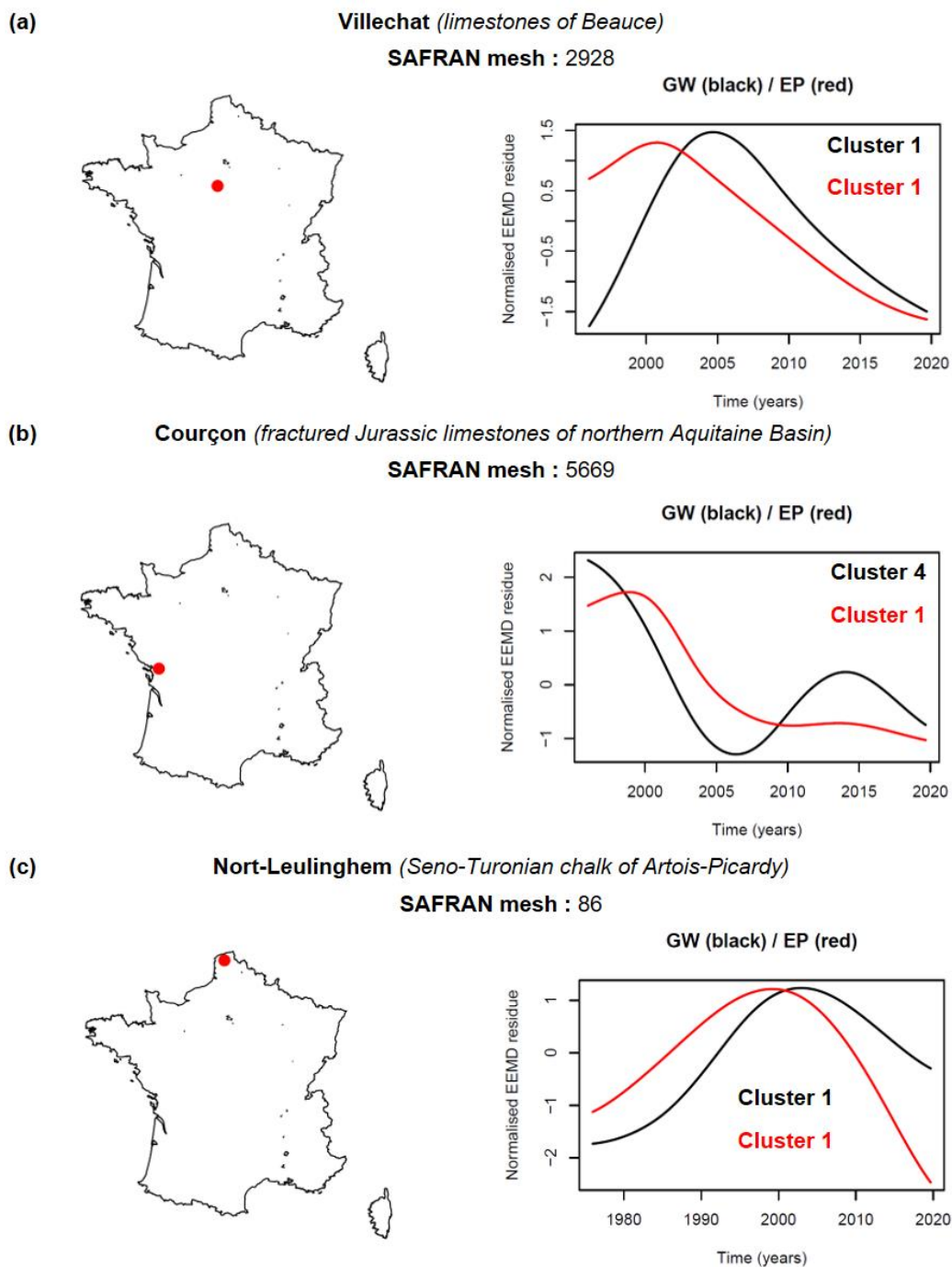


Figure 46: Examples of non-linear trends showing discrepancies in their cluster membership between effective precipitation and groundwater levels.

5.2.3.5 Non-linear trends or low-frequency variability?

The non-linear trends exhibited by groundwater levels or effective precipitation display different patterns and some of them could remind us of long-term oscillation (*i.e.* to a low-frequency variability). To determine if these non-linear trends are “trends” or a low-frequency variability that the study window does not allow us to identify as such, the non-linear trends (*i.e.* the EEMD residues) can be compared to the intrinsic oscillatory modes (*i.e.* IMF’s) extracted on a longer period. This work is realised for 3 boreholes (one per cluster). The chosen groundwater time series to achieve this work display non-linear trends that are quite explained by the non-linear trends of effective precipitation (Figure 47).

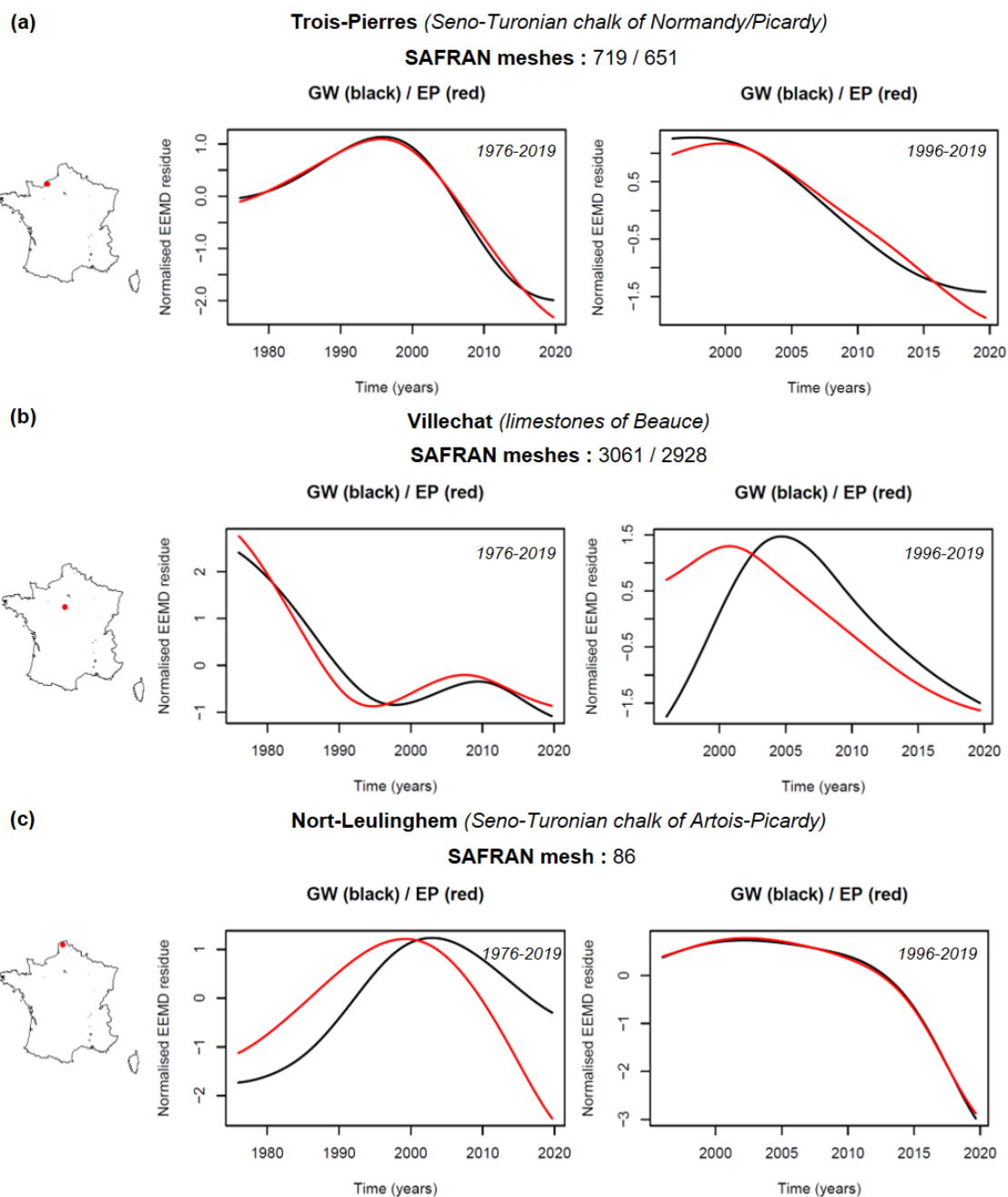


Figure 47: Boreholes chosen to determine if non-linear trends are “trends” or low-frequency variability. This figure displays groundwater non-linear trends (black) on the two reference period and the non-linear trend of their corresponding effective precipitation timeseries (red).

The comparison between EEMD residues extracted on “short periods” and IMFs (*i.e.* empirical modes) extracted on longer periods highlights the similarity between the non-linear trends and low-frequency variabilities (Figure 48). In these three cases, each non-linear trend appears to be a segment of a lower-frequency fluctuation. This is particularly striking for the borehole of Villechat in the limestones of Beauce with a non-linear trend over the 1996-2019 period exhibiting a similar behaviour than the ~24 years empirical mode over the 1976-2019 period (Figure 48b). Although the covariability of non-linear trends and the last empirical modes (IMF) extracted on longer periods is less pronounced for boreholes of Trois-Pierres and Nort-Leulinghem in the Seno-Turonian chalk of Normandy and Artois-Picardy, respectively, than the borehole of Villechat, they still display quite similar shape (Figure 48a and Figure 48c). This result means that although EEMD methods may be a good approach to filter redundant oscillations, they do not have the capacity to filter oscillations at a larger scale than the study window. Therefore in our case, the detected non-linear trends are still trends generated by low-frequency variability, but over our short study periods they are not considered as low-frequency variabilities. Such conclusions are reached also on other variables such as streamflows by Massei and Fournier (2012) or Palmer Drought Severity Index by Song et al. (2020), with non-linear trends that may be related to large-scale atmospheric and oceanic circulation low-frequency variabilities or well-known climate indices meaning the potential reversibility of such trends.

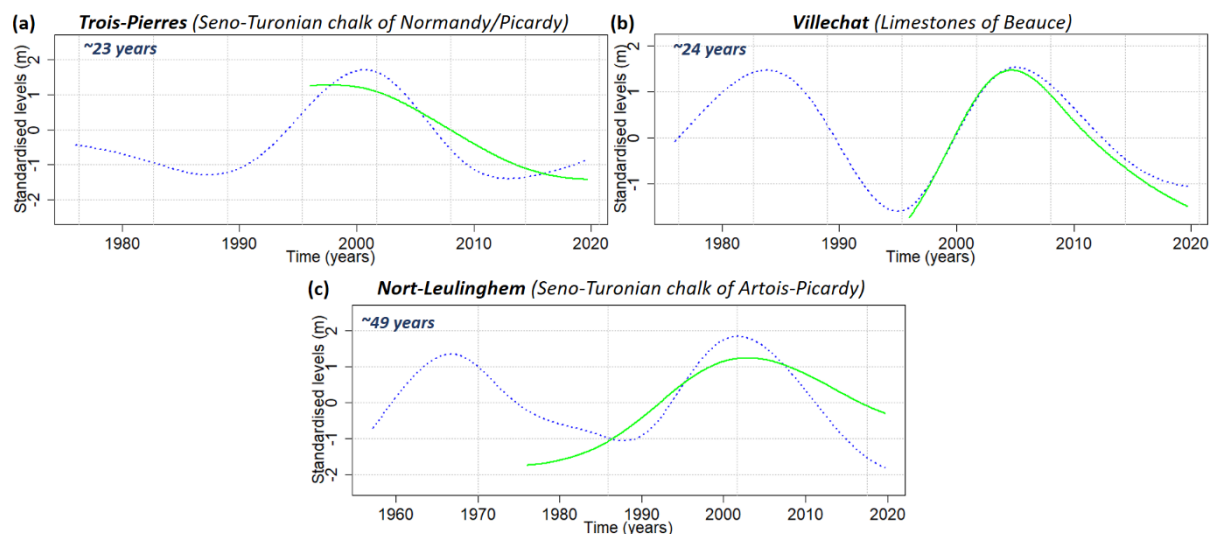


Figure 48: EEMD residues (solid green) extracted on shorter periods superimposed to the last IMFs (dashed blue) extracted on a longer period.

5.2.3.6 Conclusion on the evolution of the filtered groundwater levels and effective precipitation

The study of filtered groundwater levels and effective precipitation has been done via several approaches: (i) the estimation of monotonic trends on these filtered data (*i.e.* EEMD residues or



non-linear trends), (ii) the clustering of these non-linear trends, (iii) the questioning of if these non-linear trends are “trends” or only segments of lower frequency variabilities.

The monotonic trends detected on filtered data reveal few differences with monotonic trends estimated on raw data (*i.e.* unfiltered data) on the longest reference period (1976-2019), particularly for groundwater levels. However on shorter period (1996-2019), greater discrepancies appear with monotonic trends estimated on raw data: magnitudes of trends are very often accentuated and even trend direction can be impacted. The filtering of low-frequency variability widely impacts the significance of trends, with lots of non-significant trend on raw data becoming significant on filtered data. This phenomenon may be related to data variability that is considerably reduced in filtered data and consequently no longer affects the significance of trends. Therefore, filtering low-frequency variability or not from data can lead to different results in terms of trend magnitude, direction and significance inducing different interpretations.

The opposite detected monotonic trends between filtered groundwater levels and effective precipitation may be related to several phenomena: (i) a wrong selection of effective precipitation mesh at the beginning of the analysis leading to a non-linear trend in effective precipitation that does not represent the non-linear trend in groundwater levels, (ii) a long-term anthropogenic influence on aquifers (*e.g.* long-term pumping) and the non-linear trend of groundwater levels no longer represents the one of effective precipitation, (iii) a dephasing between the non-linear trend of groundwater levels and effective precipitation due to the response time of aquifers, (iv) a distortion or modulation of oscillation amplitude induced by catchment and aquifers properties, (v) asymmetry discrepancies between non-linear trends of groundwater levels and effective precipitation also induced by catchment and aquifer properties.

The clustering of groundwater and effective precipitation non-linear trends exhibits a heavy predominance of decreasing patterns for both variables. Increasing patterns of non-linear trends are only displayed by groundwater levels, particularly in the Seno-Turonian chalk of Artois-Picardy, and more locally in other hydrogeological entities. Overall, spatial distribution maps of effective precipitation non-linear trends patterns reveals a spread according to geographical location, with a good spatial homogeneity of clusters. For groundwater levels non-linear trends, the spread of clusters seems to be more as a function of hydrogeological entities, and their physical properties at local or regional scale.

Generally, we expect a well accordance between groundwater levels and effective precipitation clusters for a given borehole and its corresponding precipitation mesh, because non-linear trends are quite similar. In many cases, this assumption is true, but sometimes this is not the case and several explanations can be arised involving the capability of catchment, vadose zone and aquifers to modulate and delay oscillations from effective precipitation.

Finally, the non-linear trends detected in groundwater levels appear to be part of lower frequency variabilities. Although EEMD method is a usefulness tool to filter the low-frequency variability, and therefore to limit its influence on the trend estimation, it does not have the capacity to filter an oscillation at a larger scale than the study window. Therefore, monotonic trends that were estimated on EEMD residues are still impacted by low-frequency variability and



underline it. Since large-scale atmospheric and oceanic oscillations are expressed over a wide range of timescales, any groundwater trend could be the result of a slower fluctuation (Rossi et al., 2011). For instance, the Atlantic Multidecadal Oscillation (AMO) oscillates on ~60 years timescales (Kerr, 2000; Enfield et al., 2001). Thus, the youth of French piezometric networks does not, in most cases, allow us to grasp such low-frequency timescale as a fluctuation, but it can grasp it as a trend. Therefore, it highlights the complexity to define whether trends in hydroclimate variables can be related to climate change or simply being part of a lower-frequency oscillation originating from large-scale atmospheric or oceanic circulation. It can be even more complicated when working on groundwater levels that are also subjected to significant long-term anthropogenic pressures (*e.g.* pumping) not necessarily well referenced.

In summary, multiple interpretations of groundwater level trends can be made. These trends may be linked to (i) anthropogenic impacts (*e.g.* groundwater pumping, changes in land cover that may generate a decrease in groundwater recharge), (ii) climate change that may result in a decrease in groundwater recharge, (iii) a segment of low-frequency oscillations which could appear as a trend on the short-term. Without taking into account the anthropogenic impacts (which data are often poorly referenced), the most limiting factor to make the distinction between points (ii) and (iii) remains the availability of groundwater levels data and the length of time series. Works on groundwater levels reconstruction might overcome this constraint via, for instance, deep learning approaches or tree-ring-based reconstruction (Vu et al., 2020; Tegel et al., 2020). However, differentiate between climate change or variability associated to large-scale atmospheric or oceanic circulation could remain difficult, even with longer timeseries, because anthropogenic forcing may also impact these large-scale patterns (*e.g.* Dong et al., 2011; Caesar et al., 2018).

6 REFERENCES

AFB (Agence Française pour la Biodiversité) (2017) Bulletin n°2 : prélèvements quantitatifs sur la ressource en eau. Edition Mars 2017, données 2013.

Baize, Denis, and Michel-Claude Girard. 2008. *Savoir Faire Référentiel Pédologique*.

Baulon, L., Allier, D., Massei, N., Bessière, H., Fournier, M., Bault, V., 2020. Influence de la variabilité basse-fréquence sur l'occurrence et l'amplitude des extrêmes piézométriques. *Revue Géologues* n°207, décembre 2020.

Baulon, L., Allier, D., Massei, N., Bessière, H., Fournier, M., Bault, V., 2021. Influence of low-frequency variability on trends in groundwater levels. *Journal of Hydrology*, submitted.

Bonnet, R., Boé, J., Habets, F., 2020. Influence of multidecadal variability on high and low flows: the case of the Seine basin. *Hydrology and Earth System Sciences* 24, 1611-1631.

<https://doi.org/10.5194/hess-24-1611-2020>

Caballero Y., Lanini S., Lechevalier J., (2020), Caractérisation de la recharge des aquifères et évolution future en contexte de changement climatique - Application au bassin Rhône Méditerranée Corse - Phase 2. Rapport final. BRGM/RP-69217-FR, 135 p., 83 ill., 9 ann.,

Caesar, L., Rahmstorf, S., Robinson, A., Feulner, G., Saba, V., 2018. Observed fingerprint of a weakening Atlantic Ocean overturning circulation. *Nature* 556, 191-196.
<https://doi.org/10.1038/s41586-018-0006-5>

Davies, D.L., Bouldin, D.W., 1979. A Cluster Separation Measure. *IEEE Transactions on Pattern Analysis and Machine Intelligence* PAMI-1, 224-227.
<https://doi.org/10.1109/TPAMI.1979.4766909>

CGAER (Conseil Général de l'Alimentation, de l'Agriculture et des Espaces Ruraux) 2017 Eau, agriculture et changement climatique Statu quo ou anticipation ? Un état de l'art. Available at : agriculture.gouv.fr

CGDD (Commissariat Général au Développement Durable) (2017). Les prélèvements d'eau douce en France : les grands usages en 2013 et leur évolution depuis 20 ans. Service de l'observation et des statistiques, MEEM, France, 26pp.

CGEDD-CGAAER 2015 Evaluation de la mise en oeuvre des protocoles Etat-pro-fession agricole conclus en 2011 dans le bassin Adour-Garonne pour la gestion quantitative de l'eau. CGEDD-CGAAER, Paris, France, 171 pp.

Dayon G. (2015) Evolution du cycle hydrologique continental en France au cours des prochaines décennies. Thèse de doctorat de l'Université Toulouse 3 Paul Sabatier.

Dewandel B, Lachassagne P, Wyns R, Maréchal JC, Krishnamurthy NS (2006) A generalized 3-D geological and hydrogeological conceptual model of granite aquifers controlled by single or multiphase weathering. *Journal of Hydrology* 330 (1-2): 260-284.



- Dingman S. L. (2008), Physical Hydrology, pp. 575, Waveland Press, 2nd edition, ISBN: 978-1-57766-561-8
- Dong, B., Sutton, R.T., Woollings, T., 2011. Changes of interannual NAO variability in response to greenhouse gases forcing. *Climate Dynamics* 37, 1621-1641. <https://doi.org/10.1007/s00382-010-0936-6>
- Edijatno et Michel C. (1989). Un modèle pluie-débit journalier à trois paramètres. *La Houille Blanche*, n°2, pp 113-122. doi:10.1051/lhb/1989007
- Enfield, D.B., Mestas-Nuñez, A.M., Trimble, P.J., 2001. The Atlantic Multidecadal Oscillation and its relation to rainfall and river flows in the continental U.S. *Geophysical Research Letters* 28, 2077–2080. <https://doi.org/10.1029/2000GL012745>
- Gis Sol. 2011. L'état des sols de France. Groupement d'intérêt scientifique sur les sols, 188 p.
- Gustard A. & Demuth S. Editors, Manual on Low-Flow Estimation and Prediction, Operational Hydrology Report n°50 - WMO n°1029, 2008
- Hamed, K.H., Ramachandra Rao, A., 1998. A modified Mann-Kendall trend test for autocorrelated data. *Journal of Hydrology* 204, 182–196. [https://doi.org/10.1016/S0022-1694\(97\)00125-X](https://doi.org/10.1016/S0022-1694(97)00125-X)
- Hannaford, J., Buys, G., Stahl, K., Tallaksen, L.M., 2013. The influence of decadal-scale variability on trends in long European streamflow records. *Hydrology and Earth System Sciences* 17, 2717–2733. <https://doi.org/10.5194/hess-17-2717-2013>
- Huang, N.E., Shen, Z., Long, S.R., Wu, M.C., Shih, H.H., Zheng, Q., Yen, N.-C., Tung, C.C., Liu, H.H., 1998. The empirical mode decomposition and the Hilbert spectrum for nonlinear and non-stationary time series analysis. *Proceedings of the Royal Society of London. Series A: Mathematical, Physical and Engineering Sciences* 454, 903-995. <https://doi.org/10.1098/rspa.1998.0193>
- IUSS Working Group WRB. 2006. World reference base for soil resources 2006. World Soil Resources Reports No. 103. FAO, Rome.
- Janvier, Frédérique, Marlène Kraszewski, Michael Levi-Valensin, and Stéphane Trainel. 2016. "Atlas Régional 2016." : 200.
- Kaufman, L., Rousseeuw, P.J., 1990. Finding Groups in Data – Chapter 2: Partitioning Around Medoids (Program PAM). John Wiley & Sons, Ltd. pp 68-125. <https://doi.org/10.1002/9780470316801.ch2>
- Kendall, M.G., Stuart, A., Ord, J.K., 1987. Kendall's advanced theory of statistics. Oxford University Press, Inc., USA.
- Kerr, R.A., 2000. A North Atlantic Climate Pacemaker for the Centuries. *Science* 288, 1984–1985. <https://doi.org/10.1126/science.288.5473.1984>
- Lejars, C., Fusilier, J.L., Bouarfa, S., Coutant, C., Brunel, L., and G. Rucheton 2012 Limitation of agricultural groundwater uses in Beauce (France): what are the impacts on farms and on the food-processing sector, *Irrigation and Drainage*, 61(S1), 54-64.



- Loubier, S., Campardon, M., & Morardet, S. (2013). L'irrigation diminue-t-elle en France? Premiers enseignements du recensement agricole de 2010. *Sciences Eaux & Territoires*, (2), 12-19.
- Lyne V., and Hollick M. (1979) Stochastic time-variable rainfall-runoff modelling, I.E. Aust. Natl. Conf. Publ. 79/10, pp. 89-93, Inst. of Eng. Aust., Canberra, ACT, 1979.
- Manceau JC, Allier D, Buscarlet E (2020) – Analyse de la sécheresse hydrogéologique dans la région Grand Est – Phase 2 : amélioration des indicateurs de gestion. Rapport final. BRGM/RP-69867-FR, 336p., 29 ill., 3 tabl., 5 ann., 1 CD.
- Mann, H.B., 1945. Nonparametric Tests Against Trend. *Econometrica* 13, 245–259. <https://doi.org/10.2307/1907187>
- Mardhel, V., Frantar P., Uhan J. and Miso A. (2004). Index of development and persistence of the river networks as a component of regional groundwater vulnerability assessment in Slovenia. International conference on groundwater vulnerability assessment and mapping, Ustron, Poland, 15-18 June 2004
- Mardhel V., Pinson S., Allier D. (2021) Description of an indirect method (IDPR) to determine spatial distribution of infiltration and runoff and its hydrogeological applications to the french territory. *Journal of Hydrology*, 592:125609, 2021.
- Massei, N., Fournier, M., 2012. Assessing the expression of large-scale climatic fluctuations in the hydrological variability of daily Seine river flow (France) between 1950 and 2008 using Hilbert–Huang Transform. *Journal of Hydrology* 448–449, 119–128. <https://doi.org/10.1016/j.jhydrol.2012.04.052>
- Montginoul, M., & Rinaudo, J. D. (2011). Controlling households' drilling fever in France: An economic modeling approach. *Ecological Economics*, 71, 140-150.
- ONEMA 2015 Observatoire des services publics d'eau et d'assainissement - Pano-rama des services et de leur performance en 2012. Les rapports, juillet 2015, p. 4 <http://www.services.eaufrance.fr/panorama/rapports>
- Pagé, C., L. Terray et J. Boé, (2009) Dsclim: A software package to downscale climate scenarios at regional scale using a weather-typing based statistical methodology. Technical Report TR/CMGC/09/21, SUC au CERFACS, URA CERFACS/CNRS No1875, Toulouse, France
- Peña-Angulo, D., Vicente-Serrano, S.M., Domínguez-Castro, F., Murphy, C., Reig, F., Trambly, Y., Trigo, R.M., Luna, M.Y., Turco, M., Noguera, I., Aznárez-Balta, M., García-Herrera, R., Tomas-Burguera, M., Kenawy, A.E., 2020. Long-term precipitation in Southwestern Europe reveals no clear trend attributable to anthropogenic forcing. *Environ. Res. Lett.* 15, 094070. <https://doi.org/10.1088/1748-9326/ab9c4f>
- Perrin, C., Michel, C. and Andreassian, V. 2003. Improvement of a parsimonious model for streamflow simulation. *Journal of hydrology*, 279(1-4), 275-289. doi:10.1016/s0022-1694(03)00225-7. Nimmo, J.R., Horowitz, C. and Mitchell, L. 2015. Discrete-Storm Water-Table Fluctuation Method to Estimate Episodic Recharge. *Groundwater*, 53: 282-292. doi:10.1111/gwat.12177



- Rinaudo, J. D., Montginoul, M., & Desprats, J. F. (2015). The development of private bore-wells as independent water supplies: challenges for water utilities in France and Australia. In *Understanding and managing urban water in transition* (pp. 155-174). Springer, Dordrecht.
- Rossi, A., Massei, N., Laignel, B., 2011. A synthesis of the time-scale variability of commonly used climate indices using continuous wavelet transform. *Global and Planetary Change* 78, 1–13. <https://doi.org/10.1016/j.gloplacha.2011.04.008>
- Sen, P.K., 1968. Estimates of the Regression Coefficient Based on Kendall's Tau. *Biometrika* 63, 1379–1389. <https://doi.org/10.1080/01621459.1968.10480934>
- Song, X., Song, Y., Chen, Y., 2020. Secular trend of global drought since 1950. *Environ. Res. Lett.* 15, 094073. <https://doi.org/10.1088/1748-9326/aba20d>
- Stollsteiner, Philippe (Bureau de recherches géologiques et minières BRGM). 2012. "BRGM/RP-61483-FR Projet Explore 2070 - Evaluation de l'impact Du Changement Climatique."
- Tegel, W., Seim, A., Skiadaresis, G., Ljungqvist, F.C., Kahle, H.-P., Land, A., Muigg, B., Nicolussi, K., Büntgen, U., 2020. Higher groundwater levels in western Europe characterize warm periods in the Common Era. *Scientific Reports* 10, 16284. <https://doi.org/10.1038/s41598-020-73383-8>
- Thorntwaite, C. W. (1948), An approach toward a rational classification of climate, *Geograph. Rev.*, 38, 55-94,
- Vidal, J. P., E. Martin, L. Franchistéguy, M. Baillon and J. M. Soubeyroux, (2010). A 50-year high-resolution atmospheric reanalysis over France with the Safran system, *Int.J.Climatol.*, 30(11), 1627-1644.
- Vu, M.T., Jardani, A., Massei, N., Fournier, M., 2020. Reconstruction of missing groundwater level data by using Long Short-Term Memory (LSTM) deep neural network. *Journal of Hydrology* 125776. <https://doi.org/10.1016/j.jhydrol.2020.125776>
- Wu, Z., Huang, N.E., 2009. Ensemble empirical mode decomposition: a noise-assisted data analysis method. *Advances in Adaptive Data Analysis* 1, 1-41. <https://doi.org/10.1142/S1793536909000047>



Deliverable **4.2**

PILOT DESCRIPTION AND ASSESSMENT

**North East Po Plain
(Veneto Plain)
Italy**

Authors and affiliation

**Barbara Dessì
Lucio Martarelli**

ISPRA – Geological Survey of Italy

This report is part of a project that has received funding by the European Union's Horizon 2020 research and innovation programme under grant agreement number 731166.



Deliverable Data	
Deliverable number	D4.2
Dissemination level	Public
Deliverable name	Pilots description and assessment report for recharge and groundwater vulnerability
Work package	WP4
Lead WP	BRGM, BGS
Deliverable status	
Version	Version 04
Date	16/03/2021

[This page has intentionally been left blank]

LIST OF ABBREVIATIONS & ACRONYMS

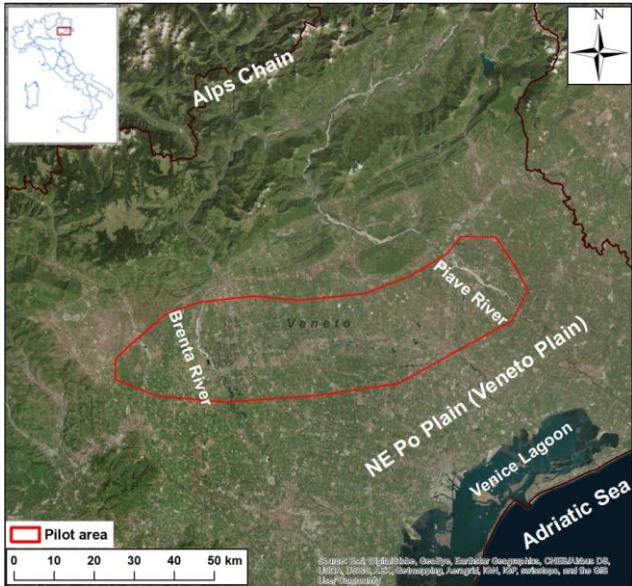
ARPAV	Agenzia Regionale per la Protezione Ambientale del Veneto (Veneto Regional Environment Protection Agency)
CC	Climate Change
EU	European Union
FAO	Food and Agriculture Organization
GCM	Global Circulation Models
GSO	Geological Survey Organization
ISIMIP	Inter Sectoral Impact Model Intercomparison Project
ISPRA	Istituto Superiore per la Protezione e la Ricerca Ambientale (Italian Environment Protection and Research Institute)
NSE	Nash-Sutcliffe Efficiency
PET	Potential EvapoTranspiration
R	Regression coefficient error
RCP	Representative Concentration Pathways
WP	Work Package

TABLE OF CONTENTS

LIST OF ABBREVIATIONS & ACRONYMS	5
1 EXECUTIVE SUMMARY	5
2 INTRODUCTION	7
3 PILOT AREA	9
3.1 Site description and data	9
3.1.1 Location of pilot area	9
3.1.2 Topography	10
3.1.3 Land use and Climate	10
3.1.4 Soil types	10
3.1.5 Geology/Aquifer type	10
3.1.6 Surface water bodies	12
3.1.7 Abstractions/irrigation	12
3.2 Climate change challenge	12
3.2.1 Expected climate changes	12
3.2.2 Challenges	12
4 METHODOLOGY	14
4.1 Methodology and climate data	14
4.1.1 AquiMod	14
4.1.2 Gardènia	14
4.1.3 Metran	15
4.1.4 Climate data	16
4.2 Model set-up	17
4.2.1 AquiMod	18
4.2.2 Gardènia	19
4.2.3 Metran	20
4.3 Model calibration	21
4.3.1 Calibration of AquiMod models	21
4.3.2 Calibration of Gardènia models	23
4.3.3 Calibration of Metran models	24
5 RESULTS AND CONCLUSIONS	26
5.1 Historical recharge values	26
5.2 Projected recharge values	28
6 REFERENCES	31
7 APPENDICES	32
7.1 Appendix A: AquiMod methodology	32
The soil moisture module	33
The unsaturated zone module	33
The saturated zone module	34
Limitations of the model	35
Model input and output	36
7.2 Appendix B: Metran methodology	36
Limitations	37
Time step	38
Model output	38
Model quality	39
Recharge	39
7.3 Appendix C: Gardènia methodology	40
Introduction	40
Methodology	41

"Production" function and "transfer" function	42
Model data and parameters	42
The required data are:	42
Hydro(geo)logical parameters	43
Initialization	43
Model calibration.....	43
Limitation and specific difficulties in the simulation of piezometric levels.....	44

1 EXECUTIVE SUMMARY

Pilot name	North East Po Plain (Veneto Plain)	
Country	Italy	
EU-region	Mediterranean region	
Area (km ²)	1150 km ² (only pilot area)	
Aquifer geology and type classification	Fluvial deposits of major streams. Porous unconfined aquifer	
Primary water usage	Irrigation, drinking water, industry	
Main climate change issues	Due to climate change impacts, in the last years, sustainable water supply has been a major issue for the area	
Models and methods used	Integrated Hydrogeological models: (i) lumped groundwater model AquiMOD; (ii) lumped groundwater model Gardènia; (iii) transfer function-noise model Metran	
Key stakeholders	Veneto Region. Water supply and utility companies. Regional Environmental Protection Agencies. ISPRA – Geological Survey of Italy	
Contact person	Barbara Dessì, ISPRA, barbara.dessi@isprambiente.it; Lucio Martarelli, ISPRA, lucio.martarelli@isprambiente.it	

The selected Italian pilot area is within the North East Po Plain (Veneto Plain; elevation 20÷80 m a.s.l.). This area consists of fluvial deposits of major streams (mixed clay-silt-sand-gravel alluvial sediments; Pleistocene-Holocene). The porous, monolayered and unconfined local aquifer has a depth to top of 10÷15 m below ground surface and a thickness of some hundreds meter. A number of springs occurring along the *Line of Resurgence* crop out in the area.

The collected meteorological data consist of time series of rainfall, air temperature and groundwater heads. The Castelfranco Veneto and the Cittadella boreholes were selected within the pilot area. The local complex hydrogeological situation caused difficulties for AquiMod model to produce an acceptable simulation using the whole 1997-2018 data. In any case, a successful calibration was produced using the period 2011-2018 (NSE value over 0.7). Comparison of the obtained models at the two selected boreholes by a second method (Gardènia) produced similar calibration results. These simulations were used for the evaluation stage by both AquiMod and Gardènia models. A similar recharge estimation of about 0.5÷0.6 mm/day was obtained by both models.

Evaluation of recharge at selected boreholes using climate change scenario data was also performed by AquiMod. It was evidenced, as expected in comparison with the historical



scenario, a reduction (by 17%) in recharge when both the 1°C Min and 3°C Min data are used and, on the contrary, an increasing (by 9%) for both the values of 1°C Max and 3°C Max.

2 INTRODUCTION

Climate change (CC) already has widespread and significant impacts on Europe's hydrological systems including groundwater bodies, which is expected to intensify in the future. Groundwater plays a vital role for the land phase of the freshwater cycle and has the capability of buffering or enhancing the impact from extreme climate events causing droughts or floods, depending on the subsurface properties and the status of the system (dry/wet) prior to the climate event. Understanding and taking the hydrogeology into account is therefore essential in the assessment of climate change impacts. Providing harmonised results and products across Europe is further vital for supporting stakeholders, decision makers and EU policies makers.

The Geological Survey Organisations (GSOs) in Europe compile the necessary data and knowledge of the groundwater systems across Europe. To enhance the utilisation of these data and knowledge of the subsurface system in CC impact assessments, the GSOs, in the framework of GeoERA, has established the project "Tools for Assessment of Climate change Impact on Groundwater and Adaptation Strategies – TACTIC". By collaboration among the involved partners, TACTIC aims to enhance and harmonise CC impact assessments and identification and analyses of potential adaptation strategies.

TACTIC is centred around 40 pilot studies covering a variety of CC challenges as well as different hydrogeological settings and different management systems found in Europe. Knowledge and experiences from the pilots will be synthesised and provide a basis for the development of an infrastructure on CC impact assessments and adaptation strategies. The final projects results will be made available through the common GeoERA Information Platform (<http://www.europe-geology.eu>).

The specific TACTIC activities focus on the following research questions:

- What are the challenges related to groundwater- surface water interaction under future climate projections (TACTIC WP3).
- Estimation of renewable resources (groundwater recharge) and the assessment of their vulnerability to future climate variations (TACTIC WP4).
- Study the impact of overexploitation of the groundwater resources and the risks of saline intrusion under current and future climates (TACTIC WP5).
- Analyse the effectiveness of selected adaptation strategies to mitigate the impacts of climate change (TACTIC WP6).

This report describes the work undertaken by the ISPRA – Geological Survey of Italy as a part of TACTIC WP4 to calculate groundwater recharge at two selected boreholes within the NE Po Plain (Veneto Plain) aquifer.

WP4 is divided into seven tasks that cover the following activities: Review of tools and methods and identification of data requirements (Task 4.1), identification of principal aquifers and their characteristics aided by satellite data (Task 4.2), recharge estimation and its evolution under climate change scenarios in the principal aquifers (Task 4.3), analysis of long-term piezometric time series to evaluate aquifer vulnerability to climate change (Task 4.4), assessment of subsidence in aquifer systems using DInSAR satellite data (Task 4.5),

development of a satellite based net precipitation and recharge map at the pan-European scale (Task 4.6), and tool descriptions and guidelines (Task 4.7).

The work presented here is related to Task 4.3 and Task 4.4 that aim at the estimation of recharge under current and future climates. This is undertaken using multiple tools selected from the TACTIC toolbox that is developed under WP2 of the TACTIC project. The toolbox is a collection of hydrogeological models, scripts, spreadsheets that serves all the activities identified in TACTIC workpackages. Here we use the lumped groundwater model *AquiMod* (Mackay et al., 2014a and 2014b), *Gardénia* (Thiéry, 2013, 2014 and 2015) and the Transfer Function-Noise Model *Metran* (Zaadnoordijk et al., 2019) with main challenge to calibrate these models to reproduce the behaviour of the observed groundwater level time series. The calibrated models are then used to calculate historical and future recharge values.

3 PILOT AREA

3.1 Site description and data

The North East part of the Po plain (Veneto Plain) is characterized by a high exploitation rate for several water uses; due to climate change impacts, in the last years water supply has been a major issue for the area. The aim of our research is to assess the capability of the groundwater body to sustain water demand assessing recharge processes of the aquifer.

3.1.1 Location of pilot area

Location of pilot area is shown in Figure 1. The area is situated in the middle plain of the NE Po Plain (Veneto Plain), interposed between the Adriatic Sea basin and the Alps Chain. The WGS84 coordinates of centroid of pilot area are 45°43'30"N 12°07'30"E.

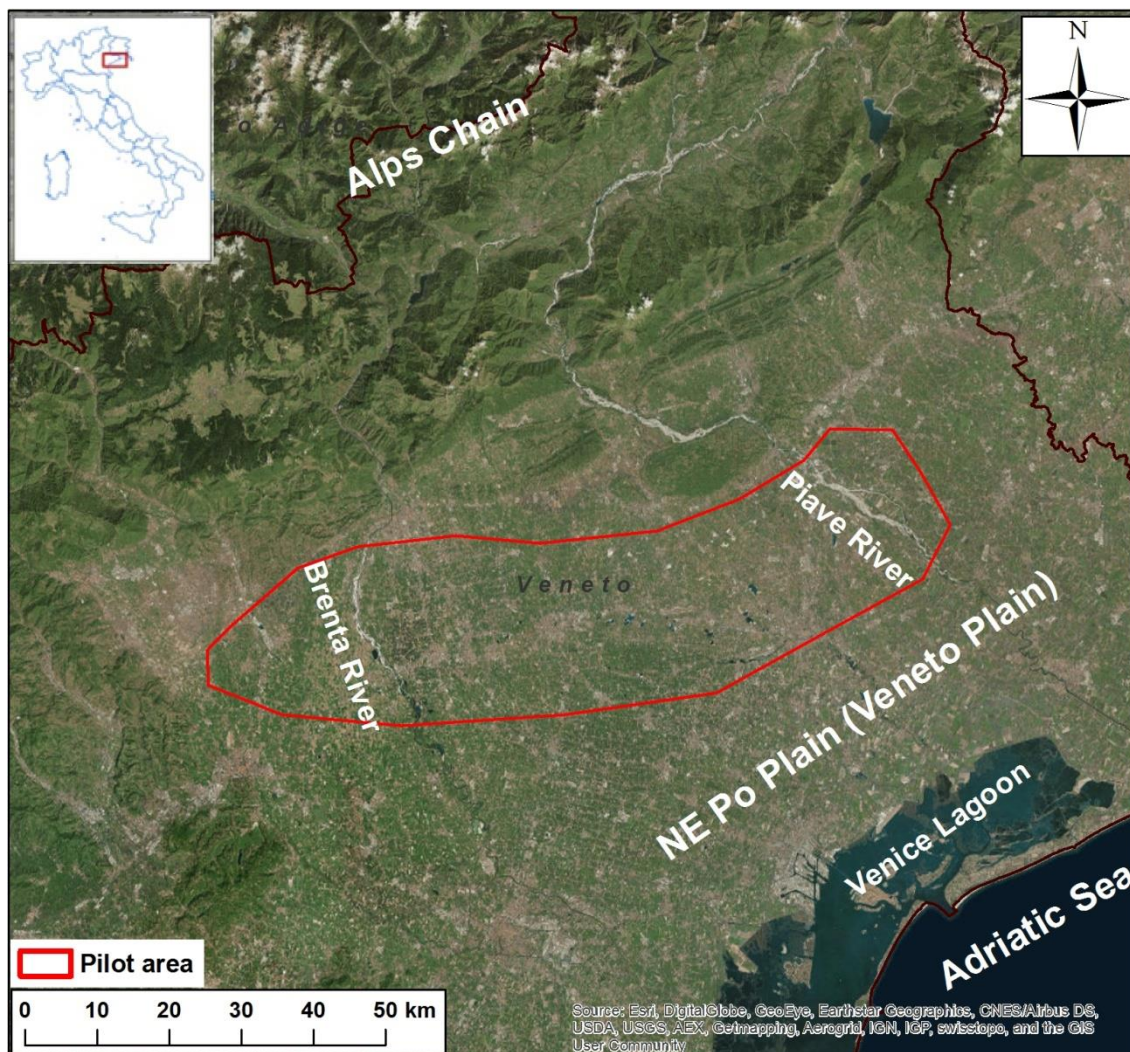


Figure 1: Location of pilot area.

3.1.2 Topography

The pilot area is featured by plain morphology and is comprised in an elevation range from about 20 to 80 m a.s.l. The Brenta and Piave river courses are partially included and cross approximately from NW to SE the pilot area (at the W and E borders, respectively).

3.1.3 Land use and Climate

The widespread land use in the pilot area is related to the diffuse presence of arable land (mainly corn and soy) (ARPAV and Regione del Veneto, 2015).

The climate type of the pilot area is sub-continental, with a mitigating effect of the Adriatic Sea that, along with the contrasting effect of the Alps Chain in the backside, leads to a general temperate climate, with relatively cold and wet winters and hot and sweltering summers.

Average precipitation is about 1200-1300 mm/year. Average potential evapotranspiration is about within the same value range. Furthermore, average real evapotranspiration is about 450-550 mm/year (meteo-climatic data provided by Veneto Environmental Protection Agency and calculated by ISPRA with Turc method). Precipitation is distributed between spring and autumn. Annual mean air temperature is 13-14 °C. The number of days below freezing point is 4-5 days/year on average.

Available meteoroclimatic data collected by Veneto Region Environmental Protection Agency consist of time series of daily rainfall and air temperature (> 30 years worth of data for both) with recorded gaps infrequent and random.

3.1.4 Soil types

The pilot area consists of fine-grained deposits in asset of sandy bumps, plains and troughs (Pleistocene-Holocene). Soil differentiation is from moderate (Cambisols) to high (Calcisols) (ARPAV and Regione del Veneto, 2015).

3.1.5 Geology/Aquifer type

Fluvatile deposits of major streams occur in the pilot area. From a lithological point of view, these deposits consist in mixed clay-silt-sand-gravel alluvial sediments, sporadically associated to calcareous and volcanic rocks (limestone and mafic lavas) and rarely to calcareous-arenaceous sediments (Amanti et al., 2007). The geological framework of the pilot area is shown in Figure 2.

Accordingly, groundwater resources in the pilot area are hosted within unconfined porous aquifers. The transmissivity and storage coefficient values are estimated to be in the range between 10^{-2} - 10^{-4} m²/s and 10^{-2} - 10^{-1} , respectively.

The aquifer recharge in the whole Veneto Plain is mainly due to dispersion from rivers (e.g. Piave and Brenta) in their high valley courses (over 20-30 m³/s) and rainfall infiltration (about 600 mm/year). The outflow occurs in a number of resurgence spring and towards a confined aquifer system in the middle-low plain (Zangheri, 2000). The pilot area including the selected

boreholes is on the contrary 10-15 km far from major streams (minor streams with moderate surface runoff are 200 to 300 m away from the boreholes).

Figure 2 also shows the distribution of the observation boreholes and the location of the selected boreholes across the pilot area, while Table 1 reports the main features of these latter. Lumped groundwater models are built to estimate the recharge values.

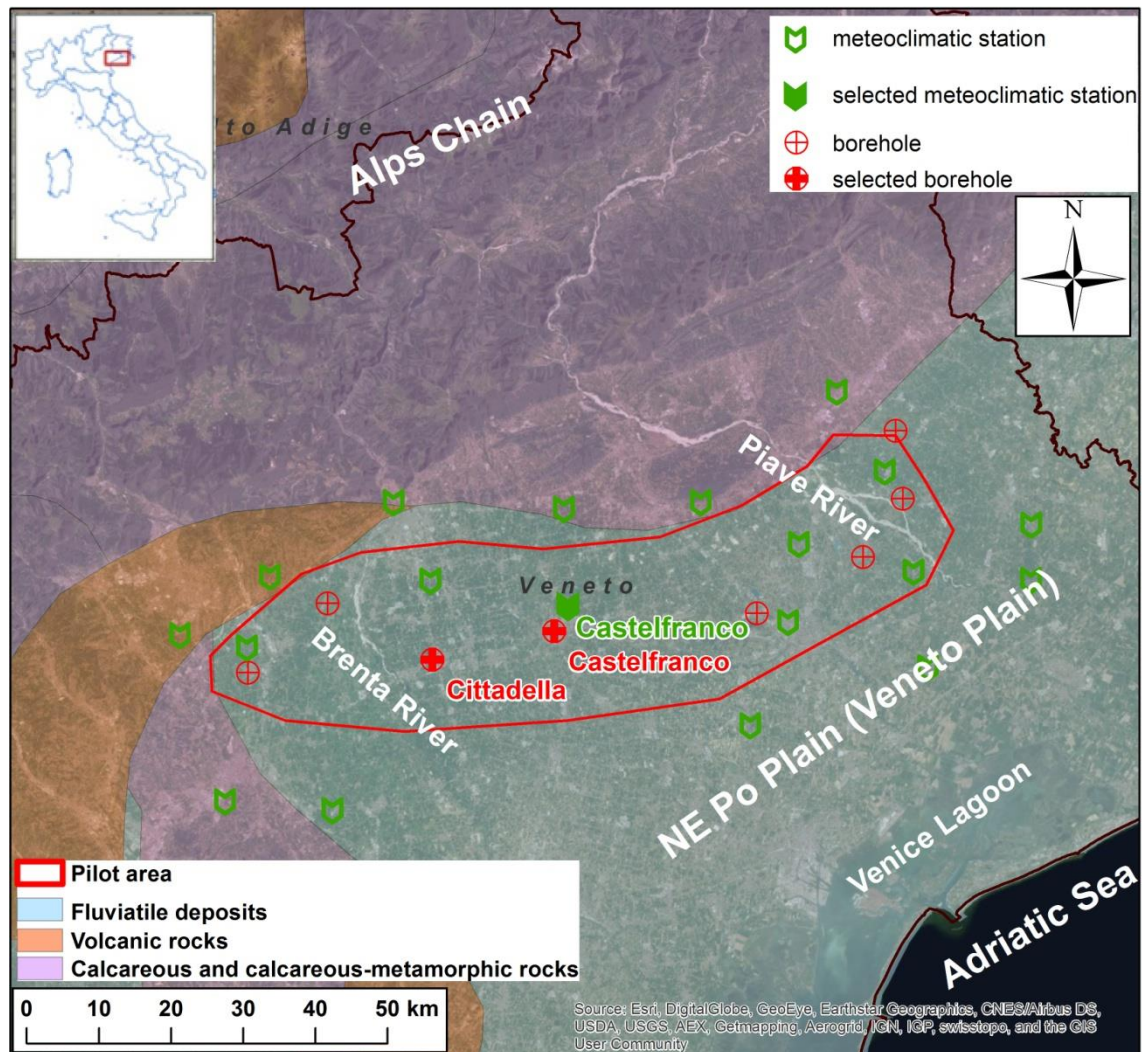


Figure 2: Geological framework of the pilot area (modified from Amanti et al., 2007) and borehole locations.

Table 1: Description of selected observation boreholes.

Borehole name	Elevation (m a.s.l.)	GWs record	Data time step
Castelfranco Veneto	42	1997-current	twice-weekly
Cittadella	47	1997-current	twice-weekly

3.1.6 Surface water bodies

The multilayer aquifer system of the NE Po Plain (Veneto Plain) includes a complex aquifer system consisting of different unconfined or semi-confined aquifers that are hydraulically connected to some different degrees. Their depth is about 90 m from the ground surface.

In any case, the depth to top of aquifer within the pilot area including the selected boreholes is 10-15 m below terrain surface and locally represents a monolayered aquifer characterized by some hundreds meter depth.

3.1.7 Abstractions/irrigation

The groundwater abstractions by wells from the pilot area are mainly related to irrigation (about 35%), industry and productive activity (about 20%), drinking water (15%) and domestic (25%) purposes. In any case, the groundwater resource of the study area did not suffer from major exploitation actions in the recent years, due to the progressive abandoning of intensive agricultural and industrial activities. This has led to the reactivation of a large number of springs along the *Line of Resurgences* occurring in the area.

A number of observation boreholes in alluvial plain geological settings are available (time series of groundwater head data > 15 years; mostly twice-weekly data). They are managed by Veneto Region Environmental Protection Agency (ARPAV).

3.2 Climate change challenge

3.2.1 Expected climate changes

The expected climate changes in the pilot area but also at a larger regional scale included in the Mediterranean region (Figure 3), regard the temperature rise, which is occurring from the last years, and the precipitation distribution with time, characterized during the last years by high (flood) and low (drought) rain events, often having also a spatially random distribution.

3.2.2 Challenges

Due to the previously described climate change impacts, in the last years, sustainable management and supply of (ground)water resources have been major issues for the pilot area and the host district.

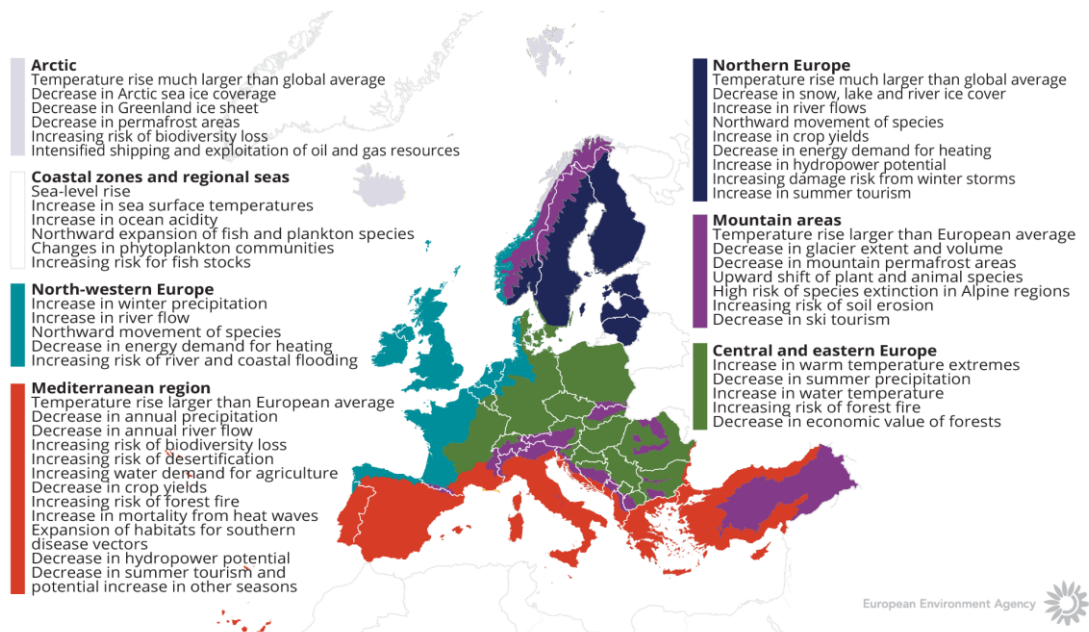


Figure 3: How climate is expected to change in Europe. The European Environment Agency map.

4 METHODOLOGY

The assessment of climate change impacts on recharge in the Italian pilot area of NE Po Plain (Veneto Plain) is performed using the TACTIC standard climate change scenarios and the lumped models AQUIMOD and GARDÉNIA, and the transfer noise model METRAN.

4.1 Methodology and climate data

4.1.1 *AquiMod*

AquiMod is a lumped parameter computer model that has been developed to simulate groundwater level time series at observational boreholes (Mackay et al., 2014a). It is based on hydrological algorithms that simulate the movement of groundwater within the soil zone, the unsaturated zone, and the saturated zone. The lumped models neglect complexities included in distributed groundwater models but maintain some of the fundamental physical principles that can be related to the conceptual understanding of the groundwater system (Mackay et al., 2014b).

The primary aim of AquiMod is to capture the behaviour of a groundwater system through the analysis of the available groundwater level time series. Once calibrated the model can be run in predictive mode and be used to fill in gaps in historical groundwater level time series and to calculate future groundwater levels. In addition to groundwater levels, it also provides predictions of historical and future recharge values and groundwater discharges.

The mathematical equations that are used to simulate the movement of groundwater flows within the three modules are detailed in Appendix A. The model uses rainfall and potential evaporation time series as forcing data. These are interpreted by the soil module representing the soil zone. The soil module calculates the rainfall infiltration and pass it to the unsaturated zone module. This module delays the arrival of the infiltrating water to the saturated zone module. The latter calculates the variations of groundwater heads and flows accordingly.

The model is calibrated using a Monte Carlo approach. It compares the simulated and observed groundwater level fluctuations and calculates a goodness of fit. The AquiMod version used in this work employs the Root Square Mean Error (RMSE) or the Nash Sutcliffe (NSE) performance measures to assess the performance of the model. The user sets a threshold value to accept all the models that perform better than the specified threshold. The possibility of producing many models that are all equally acceptable, allows the user to interpret the results from all these models and calculate uncertainty.

The recharge values calculated for AquiMod are those that reach the aquifer system and drive the groundwater levels. Thus, it is assumed that these are the actual recharge values as defined for TACTIC Project.

4.1.2 *Gardènia*

Gardenia is a lumped hydrological model for the simulation of relationships between series of stream or spring flow data at the outlet of a watershed, and/or groundwater level data at an observation well situated in the underlying aquifer and the rainfall received over the

corresponding watershed. Withdrawals by pumping groundwater can be considered if necessary. Further information about the model is given in Appendix C.

Gardenia estimates the different components of the hydrological balance for a given basin including: actual evapotranspiration, runoff, infiltration, and recharge. The hydrological balance can be used for the evaluation of the renewable resources mainly the groundwater recharge of aquifers. GARDENIA produces time series of river flows, groundwater levels or recharge data over a long period for which precipitation and potential evaporation data are known. These river flows and/or groundwater level time series can then be used to:

- forecast river flows or groundwater levels for civil engineering applications
- study particular events such as groundwater flooding or the occurrence of droughts
- quantify the water balance components of a catchment at a pre-defined time-step (varying from one day to one month) for water resource evaluation or as input for a distributed groundwater model
- study the impact of climate change.

The climate data required for the model are:

- a continuous series of rainfall data,
- a continuous series of potential evapotranspiration data (PET). PET values can be either calculated from information related to sunshine duration, air temperature and relative humidity data, or it can be obtained directly from Meteorological offices.

One or two series of observations can be considered: river flows at the basin outlet and/or representative groundwater levels at an observation borehole located in the basin. The model can take into account impact of groundwater or river abstraction.

These different series of data must be at a regular time step: daily, 5 days, 10 days, or monthly. All the series should refer to the same period. The time step of each series is not necessarily identical (e.g. daily rainfall and monthly PET).

The modelling of the relationships between rainfall and river flows and/or rainfall and groundwater levels includes a minimum of 4 to 6 lumped parameters (soil capacity, recession times, etc.) representative for a basin or a homogeneous unit within the basin.

The software is executed in calibration phase first where model parameters are optimized automatically. The user has to select an objective function to evaluate model efficiency. This is usually dependent on the type of the investigated problem.

4.1.3 Metran

Metran applies a transfer function-noise model to simulate the fluctuation of groundwater heads with precipitation and evaporation as independent variables (Zaadnoordijk et al., 2019). The modelling approach consists mainly of two impulse functions and a noise model. The first impulse function is used for convolution with the precipitation to yield the precipitation contribution to the piezometric head. The second is for evaporation which is either a separately estimated function, or a factor times the function used for precipitation. The noise model is a stochastic noise process described by a first-order autoregressive model with one

parameter and zero mean white noise. Further information about the model is given in Appendix B with the model setup shown in Figure 15.

Metran allows the addition of other processes affecting the behaviour of the groundwater heads, for example pumping or the presence of surface features such as rivers. The contributions from these processes are added to the deterministic part of the model. Metran has been designed to work with explanatory series that have a daily time step. However, it has been adapted so that other time step lengths can be applied. However, the explanatory variables must still have a constant frequency.

The model is calibrated automatically; however, the model uses two binary parameters, Regimeok and Modok, to judge a resulting time series model. Regimeok cross-examines the explained variance R^2 (> 0.3), the absolute correlation between deterministic component and residuals (< 0.2), and the null hypothesis of non-correlated innovations (p value > 0.01). If all these criteria are satisfied, Regimeok returns a value of 1 indicating highest quality. Modok also cross-examines the explained variance R^2 (> 0.1) and the absolute correlation between deterministic component and residuals (< 0.3) as well as the decay rate parameter (> 0.002) and if all these criteria are satisfied, it is given a value of 1. If Modok = 1 and Regimeok = 0, the model is still considered acceptable. If both these parameters are 0, the model quality is insufficient and the model is rejected.

Metran's time series model is linear and the model creation fails when the system is strongly nonlinear. It is also limited to the response function being appropriate for the simulated groundwater system. Metran uses a gradient search method in the parameter space, so it can be sensitive to initial parameter values in finding an optimal solution.

The model calculates an evaporation factor f that gives the importance of evapotranspiration compared to precipitation. It is possible to use this factor to calculate the recharge values as shown by Equation B2 in appendix B. However, it must be noted that the use of Equation B2 is based on too many assumptions that are easily violated. Because of this, the equations should be applied only to long-term averages using only models of the highest quality.

Following the definitions used in the TACTIC project, this recharge quantity corresponds to the effective precipitation. It is equal to the potential recharge when the surface runoff is negligible. This in turn is equal to the actual recharge at the groundwater table if there is also no storage change or interflow.

4.1.4 Climate data

The TACTIC standard scenarios are developed based on the ISIMIP (Inter Sectoral Impact Model Intercomparison Project, see www.isimip.org) datasets. The resolution of the data is $0.5^\circ \times 0.5^\circ \text{C}$ global grid and at daily time steps. As part of ISIMIP, much effort has been made to standardise the climate data (e.g. bias correction). Data selection and preparation included the following steps:

1. Fifteen combinations of RCPs and GCMs from the ISIMIP data set were selected. RCPs are the Representative Concentration Pathways determining the development in greenhouse gas concentrations, while GCMs are the Global Circulation Models used to



- simulate the future climate at the global scale. Three RCPs (RCP4.5, RCP6.0, RCP8.5) were combined with five GCMs (noresm1-m, miroc-esm-chem, ipsl-cm5a-lr, hadgem2-es, gfdl-esm2m).
2. A reference period was selected between 1981 – 2010 and an annual mean temperature was calculated for the reference period.
 3. For each combination of RCP-GCM, 30-years moving average of the annual mean temperature were calculated and two time slices identified in which the global annual mean temperature had increased by +1 and +3 degree compared to the reference period, respectively. Hence, the selection of the future periods was made to honour a specific temperature increase instead of using a fixed time-slice. This means that the temperature changes are the same for all scenarios, while the period in which this occurs varies between the scenarios.
 4. To represent conditions of low/high precipitation, the RCP-GCM combinations with the second lowest and second highest precipitation were selected among the 15 combinations for the +1 and +3 degree scenario. This selection was made on a pilot-by-pilot basis to accommodate that the different scenarios have different impact on the various parts of Europe. The scenarios showing the lowest/highest precipitation were avoided, as these endmembers often reflects outliers.
 5. Delta change values were calculated on a monthly basis for the four selected scenarios, based on the climate data from the reference period and the selected future period. The delta change values express the changes between the current and future climates, either as a relative factor (precipitation and evapotranspiration) or by an additive factor (temperature).
 6. Delta change factors were applied to local climate data by which the local particularities are reflected also for future conditions.

For the analysis in the present pilot the RCP-GCM combinations shown in the next table were employed.

Table 2: Combinations of RCPs-GCMs used to assess future climate.

		RCP	GCM
1-degree	"Dry"	rcp6p0	noresm1-m
	"Wet"	rcp4p5	miroc-esm-chem
3-degree	"Dry"	rcp4p5	hadgem2-es
	"Wet"	rcp8p5	miroc-esm-chem

4.2 Model set-up

The two selected boreholes within the NE PO Plain (Veneto Plain) pilot area addressed in this study are listed in paragraph 3.1.5. These two boreholes (Castelfranco Veneto and Cittadella) were preferred since they have available and continuous groundwater level time series (1997-2018).

Enough information on rainfall and air temperature in the same time span was also available for allowing recharge calculation. Potential evapotranspiration was calculated from air temperature.

Stream discharge and abstraction were not included since they are not significant in the boreholes area.

The complex hydrogeological situation (e.g. wideness of recharge area, thickness of unsaturated zone) and the variation of hydraulic conditions of some local elements (e.g. hydraulic contribution from adjacent areas, presence of many active ponds and canals and of diffuse resurgence areas) likely contribute to cause the relatively low NSE values during simulation model processing.

4.2.1 *AquiMod*

Aquimod model setup relies mainly on two input files. The first input file “Input.txt” is a control file where the module types and model structure are defined. AquiMod is executed first under a calibration mode where a range of parameter values of the different selected modules are given in corresponding text files and a Monte Carlo approach is used to select the parameter values that yield best model performance. “Input.txt” also controls the mode under which AquiMod is executed, the number of Monte Carlo runs to perform, the number of models to keep with an acceptable performance, and the number of runs to execute in evaluation mode.

The second file AquiMod uses is called “observations.dat”. This file holds the forcing data mainly the potential evaporation and rainfall. However, it is also possible to include the anthropogenic impact on groundwater levels by including a time series of pumping data in this file. The boreholes studied here not include pumping data. The observed groundwater levels that are used for model calibration are also given in this file. The data are provided to the model on a daily basis, and this forces AquiMod to run using a time step length of one day. Figure 4 shows daily time series of rainfall and potential evaporation values (mm/month) as well as the fluctuations of water table at the two selected boreholes.

All AquiMod models built for the boreholes in Table 1 use the FAO Drainage and Irrigation Paper 56 (Allen et al., 1998) method in the soil module, and employ the two-parameter Weibull probability density function to control the movement of infiltrated water in the unsaturated zone (Appendix A1). However, the groundwater module structures vary between the different boreholes. The best groundwater module structure is found by trial and error during the calibration process. The simplest structure, one layer with one discharge feature, is selected first and then the complexity of the module structure is increased gradually to see if the model performance improves. The structure with best model performance is selected to undertake the recharge calculations. The structure selected for the two selected boreholes is of one layer layered systems.

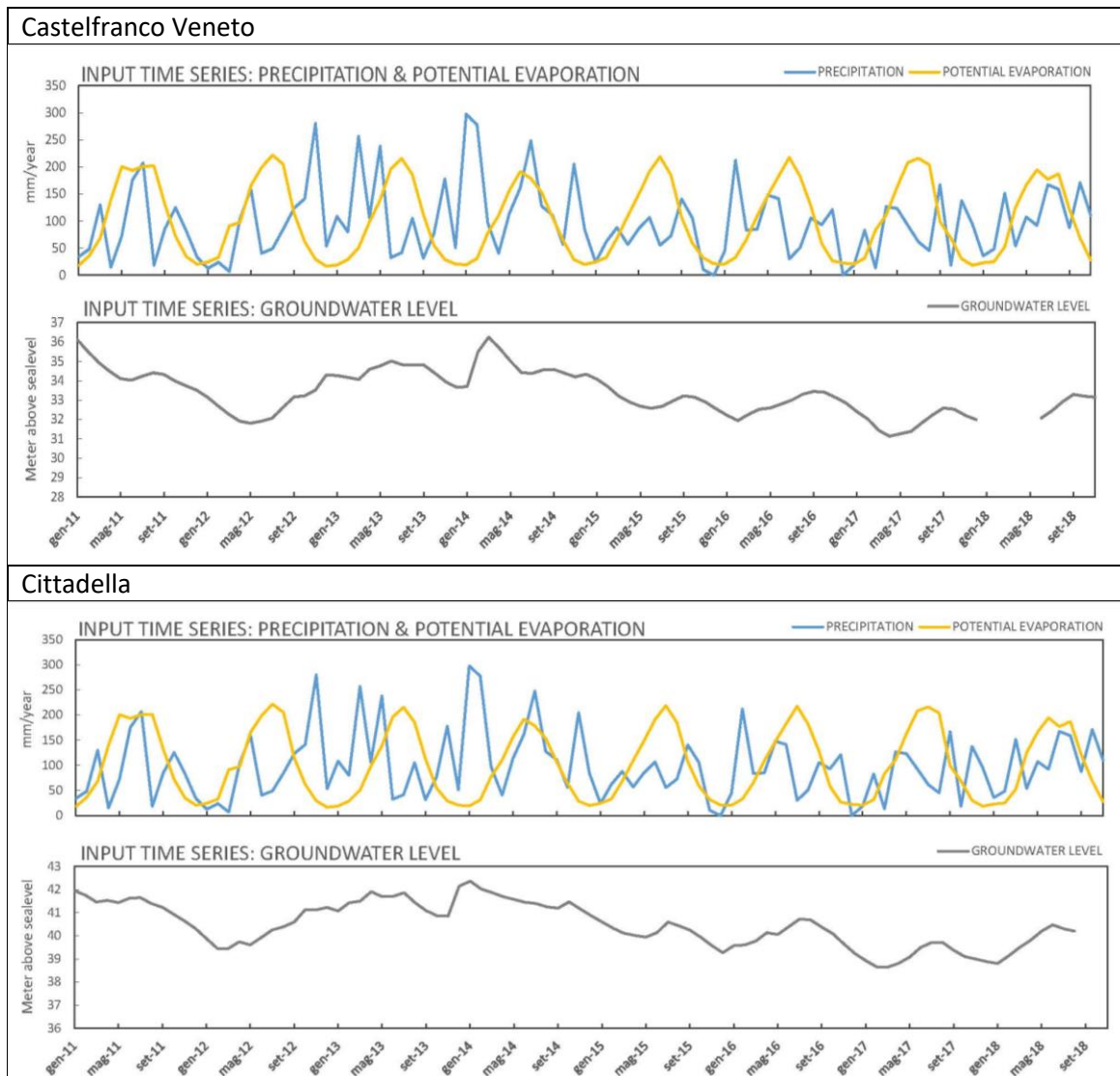


Figure 4: Time series of daily rainfall and potential evaporation values (mm/month) and fluctuations of water table at the two selected boreholes.

4.2.2 Gardènia

Gardènia model setup relies on separated files for different parameter time series. In the present modelling study, we define groundwater levels, precipitation and potential evapotranspiration time series. However, it is also possible to include files for water abstraction and river discharge data. These are not included here because in the last decades intensive groundwater exploitation activities were abandoned and the major river are quite far from the selected boreholes. Furthermore, the Gardènia model was mainly applied in order to get a confirmation of the results from Aquimod, which were obtained without inclusion of pumping and river data. The data provided to the model, like those applied for Aquimod model, are on a daily basis.

The module types and model structure are directly defined within the Gardènia application by input parameter control windows. Gardènia is consequently executed first under a calibration mode followed by an evaluation mode to select the parameter values that yield best model performance.

Gardènia models built for the boreholes in Table 1 were performed with the same one layer with one discharge hydrostratigraphical feature and input data used for AquiMod (Figure 4), to allow for a direct comparison between the two model results.

4.2.3 Metran

Metran applies transfer function noise modelling with daily precipitation and evaporation as input and of groundwater levels as output (Zaadnoordijk et al., 2019). The setup is shown in Figure 5. If time series of other influences on the groundwater head are available, these contributions can be added to the deterministic part of the model. An input file that holds the daily information of precipitation, potential evaporation and groundwater levels is prepared for each borehole in Table 1. Plots of these data are shown in Figure 4. It must be noted that, while the groundwater levels used in AquiMod and Gardènia shown in Figure 4 have missing values, these have to be provided as complete time series to Metran. To achieve this, a linear interpolation procedure is used to fill in the missing values in the groundwater level time series. Once executed, it calculates the characteristics of the impulse functions and the corresponding parameters automatically.

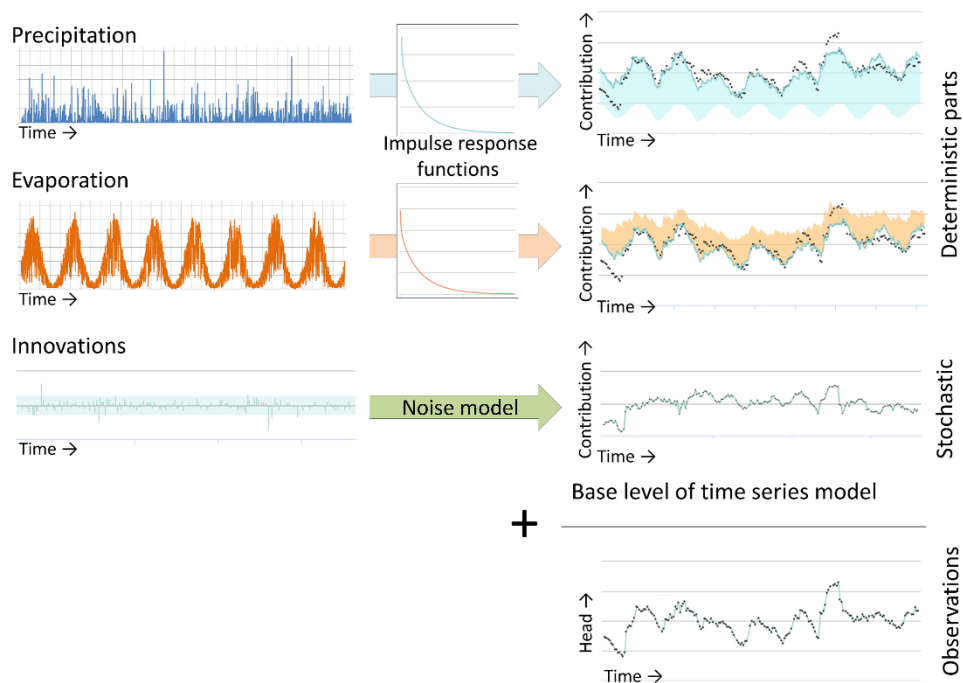


Figure 5: Illustration of METRAN setup.

4.3 Model calibration

Many attempts have been undertaken to calibrate the Aquimod model. However, it was not possible to produce a simulation with an acceptable performance measure, using the rainfall, potential evapotranspiration and groundwater level time series from 1997 to recent time at the selected boreholes (maximum Nash-Sutcliffe Efficiency value produced was approximately 0.3).

The complex hydrogeological situation (e.g. wideness of recharge area, thickness of unsaturated zone) and the variation of hydraulic conditions of some local elements (e.g. hydraulic contribution from adjacent areas, presence of many active ponds and canals and of diffuse resurgence areas) likely contribute to the relatively low NSE values during simulation model processing.

The analysis of time series using the Metran model with the help of TNO (model owner) identified three different periods of the used time series that are having diverse, but internally homogeneous suitable trend features (1998-2002; 2003-2010, 2011-2018). The use of the most recent period to calibrate the Aquimod model yielded a simulation with an NSE value over 0.7. This simulation was selected with the evaluation stage by Aquimod model.

The factors that may have induced different trends in the three former periods are not still clear. Among the major possibilities there are: (i) the thickness of the unsaturated zone (10-15 m); (ii) the non-linearity features within the groundwater system; (iii) the temporal variation in ratio between actual and potential evapotranspiration (some runs gave a precipitation response that explains a reasonable part of the head variation but no contribution of potential evapotranspiration); (iv) the occurring of land use changes (actually with no real evidence in the area).

At the end, the two (out of eight) selected boreholes were successfully improved and calibrated ($NSE > 0.7$) by Aquimod on 8 years span data (2011-2018). On the contrary, the other two former periods (1998-2002; 2003-2010) provided not suitable calibration results. Comparison of the obtained models at the two selected boreholes by a second method (Gardenia model by BRGM) with the same input data produced similar calibration results.

4.3.1 Calibration of Aquimod models

The calibration of Aquimod is performed automatically using the Monte Carlo approach. The user populates the files of the selected modules with minimum and maximum parameter values and then the model randomly selects a value from the specified range for any given run. The selection of the minimum and maximum values is physically based depending on the characteristics of the study area. The storage coefficients bounds of a groundwater module are set to much lower values in a confined aquifer compared to those used for an aquifer under unconfined conditions.

A conceptual hydrogeological understanding must be available before the use of Aquimod, since this is necessary to set the limits of the parameter values for the calibration process. In some cases, it is not possible to obtain a good performing model with the selected values and that necessitates the relaxation of these parameters beyond the limits informed by the



conceptual understanding. In such cases, the parameter values must feed back into the conceptual understanding if better performing models are obtained.

AquiMod execution time is relatively small, which allows the calibration of the model using hundreds of thousands of runs in couple of hours. The performance measure used to assess the quality of the simulation is the Nash Sutcliffe Error (Appendix A) that takes a maximum value of unity for a perfect match between the simulated and observed data. The threshold at which models are accepted is set to a value of 0.6. All the models that achieve an NSE higher than 0.6 are included in the analysis but a maximum number of 1000 runs are used if the number of acceptable models is greater than 1000.

Next table shows the best NSE values obtained for the models calibrated at the two selected boreholes listed in Table 1. It is evident that a relatively low but sufficient match was achieved only for the 2011-2018 period between the simulated and observed groundwater levels, as illustrated in the plots shown in Figure 6. This happened since the whole time series 1997-2018 displayed different trends among the 1997-2002, 2002-2009, 2009-2011 and 2011-2018 periods and only the last one reached the sufficient NSE values reported in the nex table. The distinction among the different periods was confirmed by the values of the “residuals” featured by Metran model.

Table 3: Nash-Sutcliff Error at the two selected observation boreholes obtained by AquiMod.

Borehole name	NSE
Castelfranco Veneto	0.72
Cittadella	0.73

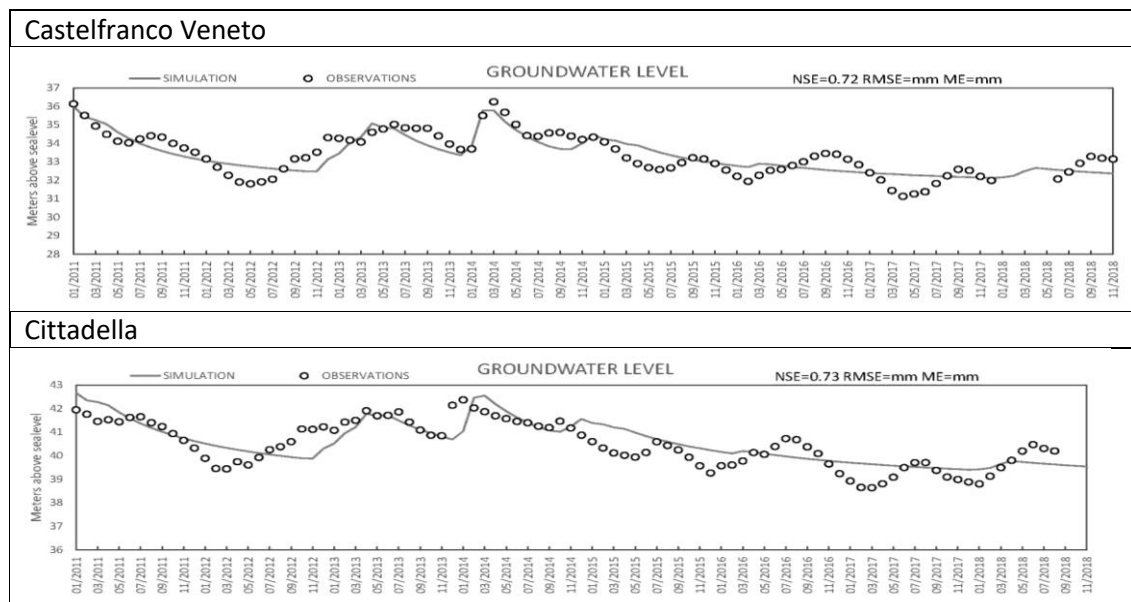


Figure 6: Comparison between the simulated and observed groundwater levels obtained by Aquimod at the two selected observation boreholes.

4.3.2 Calibration of Gardènia models

The data used for Gardènia model calibration at the two selected boreholes are: (i) model "input" continuous series of rainfall and evapotranspiration; (ii) model "output" observed series (levels) not necessarily continuous, but covering a concomitant period with the input series. Calibration was done in a semi-automatic way on the initial set of observed groundwater levels, also indicating which other involved parameters should be optimised.

The model uses a non-linear optimisation algorithm, makes the chosen parameters vary (within a range of values defined by the user) and searches for a set which gives the best fit between observed and simulated series has been found.

The model produces: (i) for each time-step a water balance of the different components of the hydrological cycle (runoff, actual evaporation, groundwater flow, etc.); (ii) a graphical representation of observed and simulated values for a visual evaluation of the calibration; (iii) numerical criteria for the evaluation of the quality of calibration.

Taking into account this information, the user then estimates whether to attempt a new optimization from another set of parameters. When both the numerical fitting criteria and the graphs for visual comparison are satisfactory, the user may consider if the obtained values are realistic.

Next table shows the best NSE and R coefficient values obtained for the models calibrated at the two selected boreholes listed in Table 1. It is evident that the calibration results of Aquimod have been substantially confirmed. The comparison between the simulated and observed groundwater levels are illustrated in the plots shown in Figure 7.

Table 4: NSE and R coefficients at the two selected observation boreholes obtained by Gardènia.

Borehole name	NSE	R
Castelfranco Veneto	0.69	0.83
Cittadella	0.65	0.81

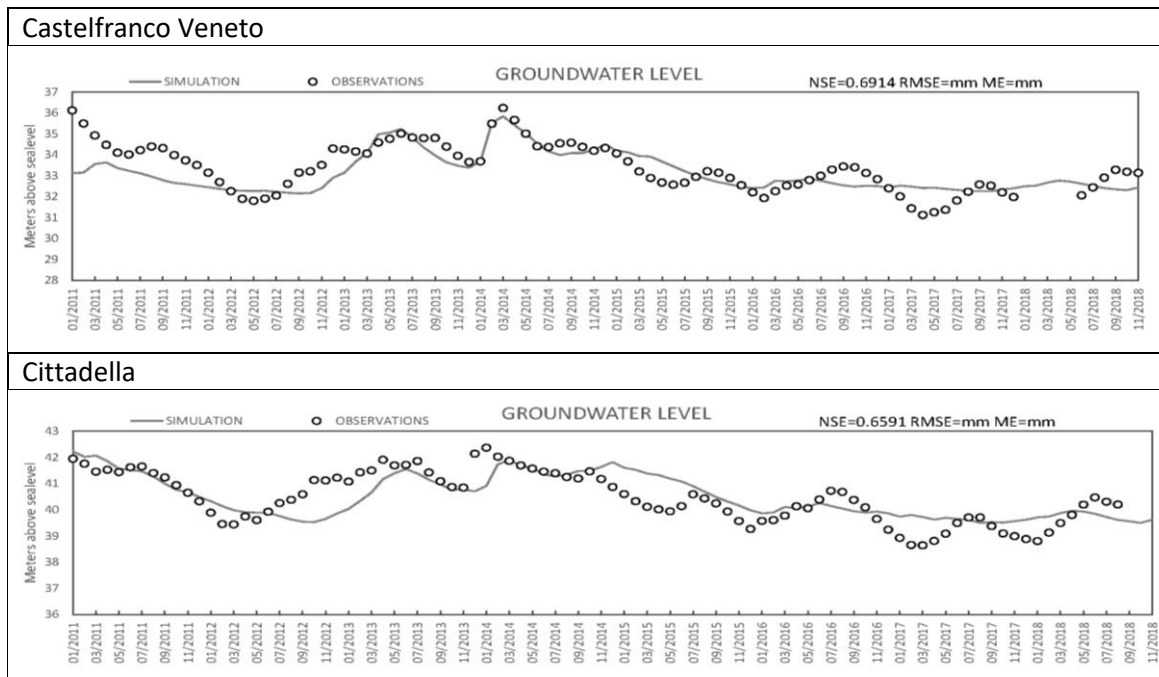


Figure 7: Comparison between the simulated and observed groundwater levels obtained by Gardènia at the two selected observation boreholes.

4.3.3 Calibration of Metran models

For the standard setup with precipitation and evaporation, there are five parameters that have to be determined: three are related to the precipitation response, the evaporation factor and the noise model parameter (Appendix B). There are three extra parameters for each additional input series, such as pumping. The parameter optimization of Metran uses a gradient search method in the parameter space to reach a global minimum. As explained in Appendix B, two parameters indicate if Metran succeeded with producing a match between the simulated and observed data. These are called the Regimeok and Modok. When Regimeok is equal to one, the calibration is of highest quality. If Modok is equal to one and Regimeok is equal to zero, the calibration is of acceptable quality. Finally, if both parameters are equal to zero, the calibration quality is insufficient.

Next table shows the performance of Metran for the Castelfranco Veneto selected borehole. It is clear that according to criteria set above, Metran succeeds to produce an acceptable model at Castelfranco borehole with the model output showing a 0.69 value of R^2 . The reasons that may have induced the not reaching of a highest quality acceptance of the model are still not clear.

Table 5: Performance of Metran across the Castelfranco Veneto selected borehole.

Borehole name	Metran performance parameter Regimeok	Metran performance parameter Modok	Overall quality	R ²	RMSE
Castelfranco Veneto	1	0	Acceptable	0.69	0.67

5 RESULTS AND CONCLUSIONS

As shown in Section 1.4, two simulations with NSE greater than 0.7 were produced at the two selected boreholes using rainfall and precipitation data recorded from 2011 to 2018. Using the parameter values of these two simulations and running the model in evaluation mode, AquiMod produced an estimation of recharge (about 0.5-0.6 mm/day). AquiMod results have been compared with those produced by Gardènia to investigate the uncertainty in the estimated recharge values associated to model methodology.

Evaluation of recharge at selected boreholes using climate change scenario data was also performed.

5.1 Historical recharge values

Figure 8 shows the time series of the historical recharge values calculated using the AquiMod model at the two selected boreholes of the NE Po Plain (Veneto Plain) pilot area. The plots in this table also show the 10th percentile, the mean, and the 90th percentile of recharge values calculated from the time series. The 10th percentile values are not visible in the histograms since they are approximately equal to zero.

As mentioned in Appendix B, the formulas used by Metran are based on assumptions that it is better to use only models of the highest quality to calculate long-term average values of recharge with the long-term average values of rainfall and potential evaporation. Therefore, since the performance of Metran for the Castelfranco Veneto selected borehole was acceptable but not of highest quality, it was not possible to produce suitable time series of recharge values using Metran.

One of the benefits of running AquiMod in Monte Carlo mode is the possibility of producing many models with acceptable performance. Consequently, the recharge values estimated from these models are all equally likely. This provides us with a range of recharge values at each borehole that reflects the uncertainty of the optimised hydraulic parameter values. In the current study, the long-term average recharge values are calculated from up to 1000 acceptable models if they exist at each borehole; otherwise, all the acceptable models are used. The mean, 10th and 90th percentiles are then calculated from these long-term recharge values and displayed in Figure 9. It is clear that the differences between the 10th and 90th percentile values are quite significant at the selected boreholes indicating a high degree of uncertainty associated with these values. It is noteworthy that AquiMod calculates actual recharge.

Figure 10 shows historical time series of recharge calculated using Gardènia model at these boreholes. The pattern of the recharge values calculated using Gardènia match that of the recharge values calculated by the other model at the two selected observation boreholes. While the agreement between these two models increases the confidence in the calculated recharge values, it should be noted that the large differences between the 90th and 10th percentiles shown by both models are a clear indication about the high uncertainty associated with the estimated recharge values.

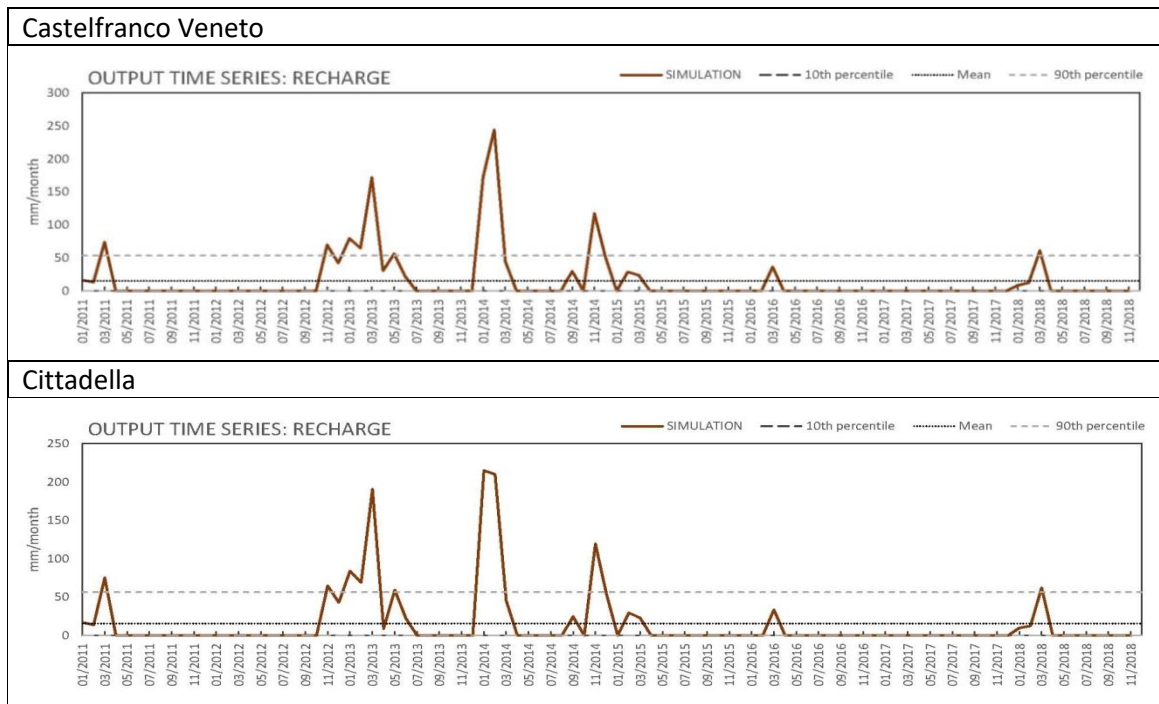


Figure 8: Time series of recharge values obtained from the best performing AquiMod models at the two selected observation boreholes.

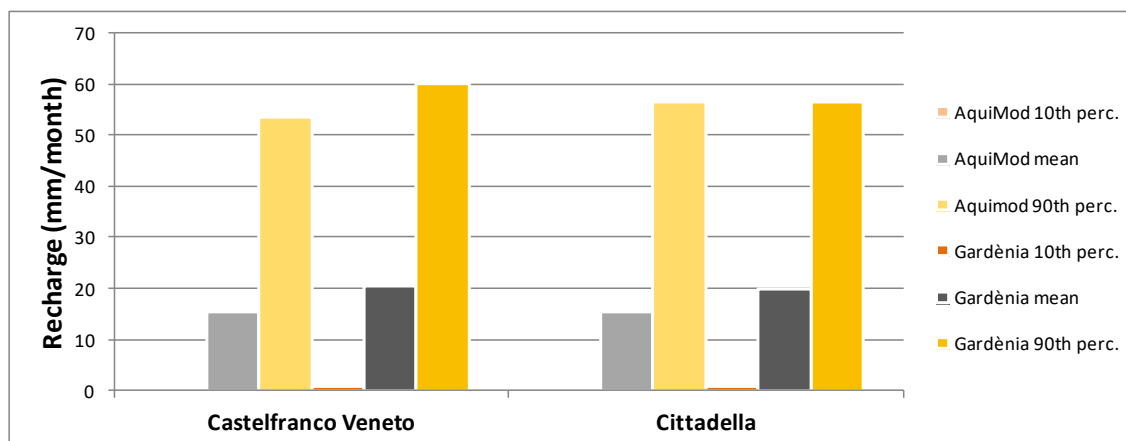


Figure 9: Historical recharge values calculated by AquiMod and Gardènia models at the two selected boreholes. The 10th percentile values are not visible since they are approximatively equal to zero.

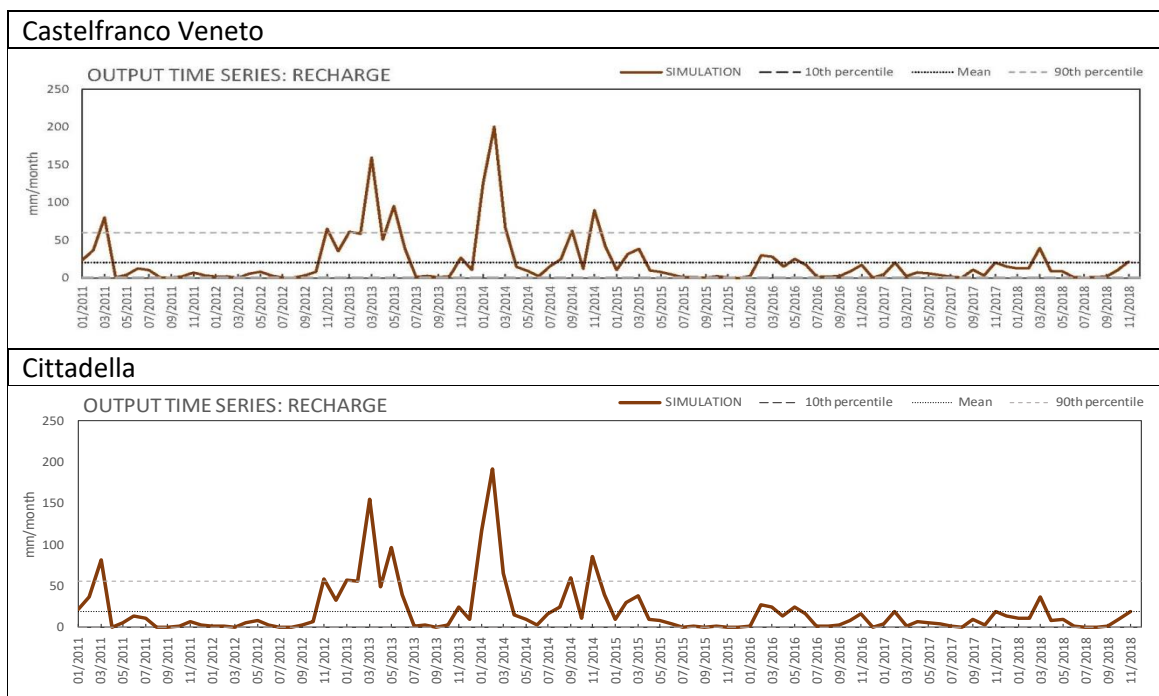


Figure 10: Time series of recharge values obtained from the best performing Gardènia models at the two selected observation boreholes.

5.2 Projected recharge values

The forcing data, rainfall and potential evaporation, are altered using the change factors of the climate models (see Section 4.1.4). For the NE Po Plain (Veneto Plain) area, the set of monthly change factors used with the data driving Aquimod are shown in Table 6: Monthly change factors as multipliers used for the two selected borehole data.. These change factors are used as multipliers to both the historical rainfall and potential evaporation values.

For the application involving Aquimod, these factors are used to alter the time series of historical rainfall and potential evaporation values used to drive the model.

According to the ISIMIP (Inter Sectoral Impact Model Intercomparison Project), these change factors have been used to modify the historical gridded rainfall and potential evaporation data before using them as input to calculate the recharge. In this case, and for any simulation date, the rainfall and potential evaporation change factors for the month corresponding to the date, are used to modify all the spatially distributed historical rainfall and potential evaporation values, respectively.

Table 6: Monthly change factors as multipliers used for the two selected borehole data.

	Scenario	Jan	Feb	Mar	Apr	May	Jun	Jul	Aug	Sep	Oct	Nov	Dec
Rainfall	1°C Min	0.790	0.978	0.983	1.081	1.039	1.015	0.997	0.976	0.956	1.064	0.850	0.987
	1°C Max	1.099	0.979	1.100	1.069	1.025	1.002	1.117	0.961	1.091	1.091	1.097	1.023
	3°C Min	1.093	1.062	1.031	1.294	1.005	0.860	0.659	0.634	0.783	0.896	0.895	0.976
	3°C Max	1.250	1.089	1.177	1.052	1.268	0.781	0.986	0.956	0.989	1.085	1.063	1.214
PE	1°C Min	1.079	1.010	1.005	1.013	1.016	1.016	1.022	1.032	1.030	1.029	1.007	0.994
	1°C Max	1.140	1.127	1.065	1.069	1.078	1.080	1.074	1.075	1.082	1.083	1.083	1.100
	3°C Min	1.173	1.152	1.082	1.065	1.053	1.080	1.133	1.118	1.116	1.105	1.044	1.191
	3°C Max	1.171	1.145	1.084	1.098	1.051	1.066	1.073	1.079	1.097	1.094	1.085	1.109

Figure 11 shows the historical and future long-term average recharge values calculated using the best performing AquiMod model. The results between the two selected boreholes are very similar. It is clear that the highest reduction in recharge values are observed when the 3°C Min rainfall and evaporation data are used (even if they are very similar to 1°C Min values), while the highest increase in recharge values are observed when the 3° Max rainfall and potential evaporation data are used.

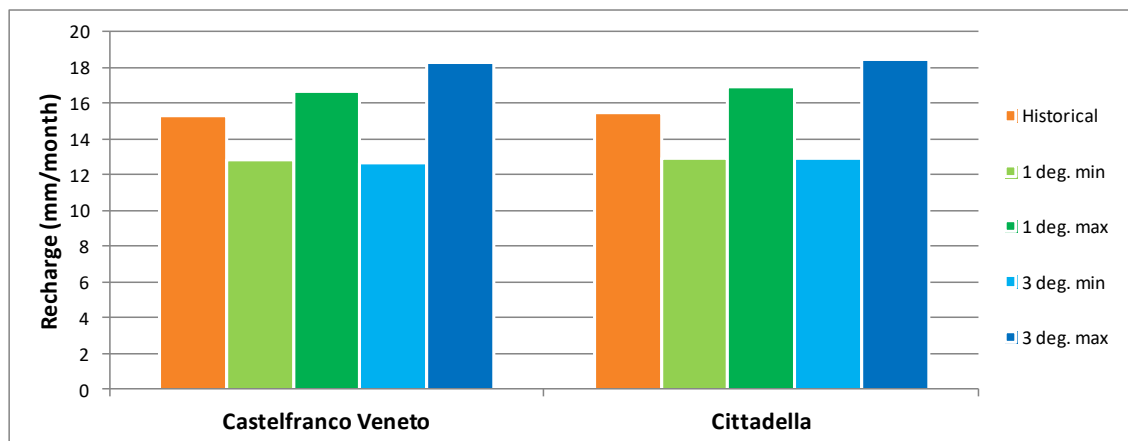


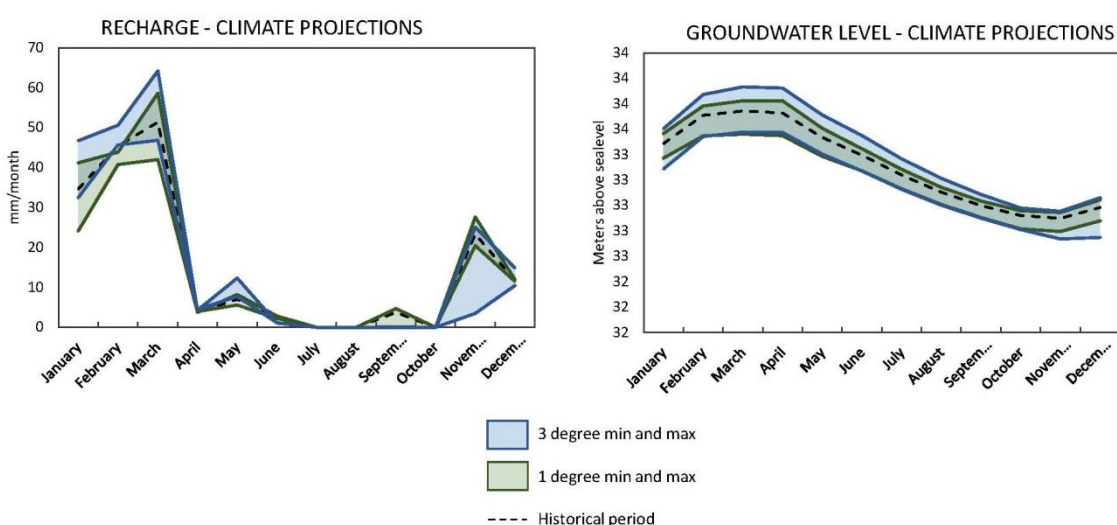
Figure 11: Historical (orange) and future average recharge values (blue and green) as produced by the best performing AquiMod model.

Next table shows, as mean values (mm/day) of the two selected boreholes, the average and maximum estimate of the climate projection recharge data (Figure 12; mm/month). Looking at both the average and maximum recharge values, it is clear that there is a similar reduction (about 17%) in recharge when the 1°C Min and 3°C Min data are used compared to the historical scenario, as expected. On the contrary, the average and maximum recharge values for 1°C Max and 3°C Max projections are higher (about 9%) than those from the historical scenario, as also expected.

Table 7: Statistical information of the climate projection recharge data shown in Figure 12, as mean values of the two selected boreholes.

Recharge scenario	Average recharge (mm/day)	Maximum recharge (mm/day)
Historical scenario	0.513	1.712
CC scenario: 1 degree min	0.429	1.399
CC scenario: 1 degree max	0.559	1.954
CC scenario: 3 degrees min	0.426	1.561
CC scenario: 3 degrees max	0.612	2.139

Castelfranco Veneto



Cittadella

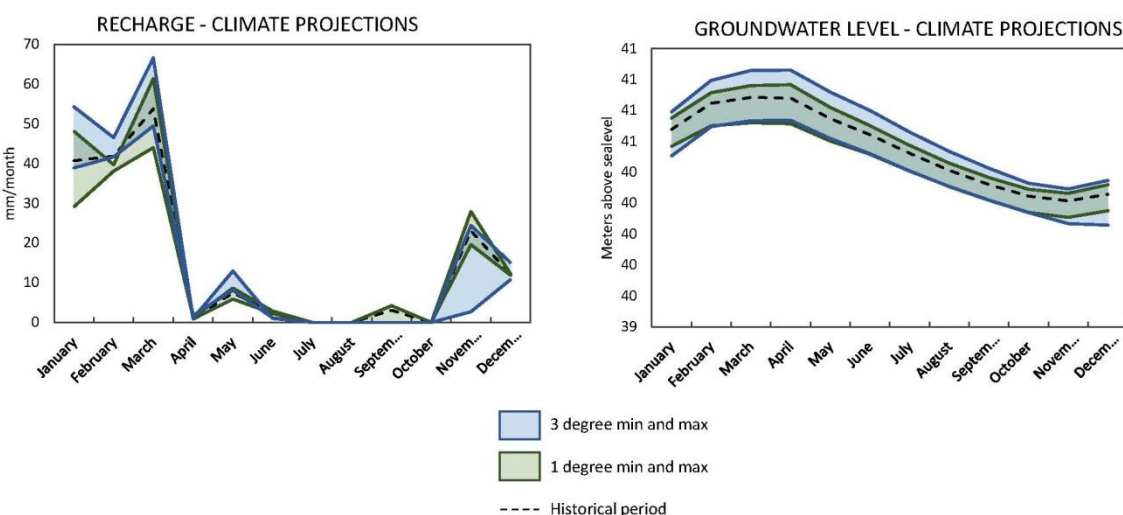


Figure 12: Monthly recharge and groundwater level values estimated by Aquimod using the historical and the projected forcing data.

6 REFERENCES

Allen, R. G., Pereira, L. S., Raes, D. & Smith, M. (1998) Crop evapotranspiration - Guidelines for computing crop water requirements - FAO Irrigation and drainage paper 56. Food and Agriculture Organization of the United Nations.

Amanti, M., Battaglini, L., Campo, V., Cipolloni, C., Congi, M.P., Conte, G., Delogu, D., Ventura, R. & Zonetti, C. (2007) La Carta Litologica d'Italia alla scala 1:100.000 (The Lithological Map of Italy at the 1:100,000 scale). Proceedings of the 11th ASITA Conference, Turin (Italy).

ARPAV & Regione del Veneto (2015) Carta dei suoli del Veneto in scala 1:250.000 (Soil Map of Veneto Region). Versione (version) 2015.

Besbes, M. & de Marsily, G. (1984) From infiltration to recharge: use of a parametric transfer function. *Journal of Hydrology*, 74, p. 271-293.

Griffiths, J., Keller, V., Morris, D. & Young, A. R. (2006) Continuous Estimation of River Flows (CERF) - Technical Report: Task 1.3: Model scheme for representing rainfall interception and soil moisture. Environment Agency R & D Project W6-101. Centre for Ecology and Hydrology, Wallingford, UK.

Mackay, J. D., Jackson, C. R. & Wang, L. (2014a) A lumped conceptual model to simulate groundwater level time-series. *Environmental Modelling and Software*, 61. 229-245. <https://doi.org/10.1016/j.envsoft.2014.06.003>

Mackay, J. D., Jackson, C. R. & Wang, L. (2014b) *AquiMod user manual (v1.0)*. Nottingham, UK, British Geological Survey, 34pp. (OR/14/007) (Unpublished)

Thi  ry, D. (2015) Validation du code de calcul GARD  NIA par mod  lisations physiques comparatives. Rapport BRGM/RP-64500-FR, 48 p., 28 fig. (Mise    jour v8.6). <http://infoterre.brgm.fr/rapports/RP-64500-FR.pdf>. (Accessed July 2018).

Thi  ry, D. (2014) Logiciel GARD  NIA, version 8.2. Guide d'utilisation. Rapport BRGM/RP-62797-FR, 126 p., 65 fig., 2 ann. (Mise    jour v8.6). <http://infoterre.brgm.fr/rapports/RP-62797-FR.pdf>. (Accessed July 2018).

Thi  ry, D. (2013) Didacticiel du code de calcul Gard  nia v8.1. Vos premi  res mod  lisations. Rapport BRGM/RP-61720-FR, 130 p., 93 fig. (Mise    jour v8.6) <http://infoterre.brgm.fr/rapports/RP-61720-FR.pdf>. (Accessed July 2018).

Zaadnoordijk, W.J., Bus, S.A.R., Lourens, A. & Berendrecht, W.L. (2019) Automated Time Series Modeling for Piezometers in the National Database of the Netherlands. *Groundwater*, 57, no. 6, p. 834-843. <https://onlinelibrary.wiley.com/doi/epdf/10.1111/gwat.12819>

Zangheri, P. (2000) L'acqua sotterranea: una risorsa nascosta. Pozzi, acquiferi e falde nella provincia di Venezia (Groundwater: a hidden resource. Wells, aquifers and water bodies in the Venice Province). Assessorato alle Politiche Ambientali della Provincia di Venezia.



7 APPENDICES

7.1 Appendix A: AquiMod methodology

AquiMod is a lumped parameter computer model that has been developed to simulate groundwater level time series at observational boreholes (Mackay et al., 2014a). It is based on hydrological algorithms that simulates the movement of groundwater within the soil zone, the unsaturated zone, and the saturated zone. The lumped models neglect complexities included in distributed groundwater models but maintains some of the fundamental physical principles that can be related to the conceptual understanding of the groundwater system (Mackay et al., 2014b).

While AquiMod was originally designed to capture the behaviour of a groundwater system through the analysis of groundwater level time series, it can produce the infiltration recharge values and groundwater discharges from the aquifer as a by-product. AquiMod is driven by complete time series of forcing data for either historical or predicted future conditions. Running AquiMod in predictive mode can be used to fill in gaps in historical groundwater level time series, or calculate future groundwater levels. In addition to groundwater levels, it also provides predictions of historical and future recharge values and groundwater discharges. In the current application we use calibrated AquiMod models to estimate the recharge values at selected boreholes.

AquiMod consists of three modules (Figure 13). The first is a soil water balance module that calculates the amount of water that infiltrates the soil as well as the soil storage. The second module controls the movement of water in the unsaturated zone, mainly it delays the arrival of infiltrating water to the saturated zone. The third module calculates the variations in groundwater levels and discharges. The model executes the modules separately following the order listed above.

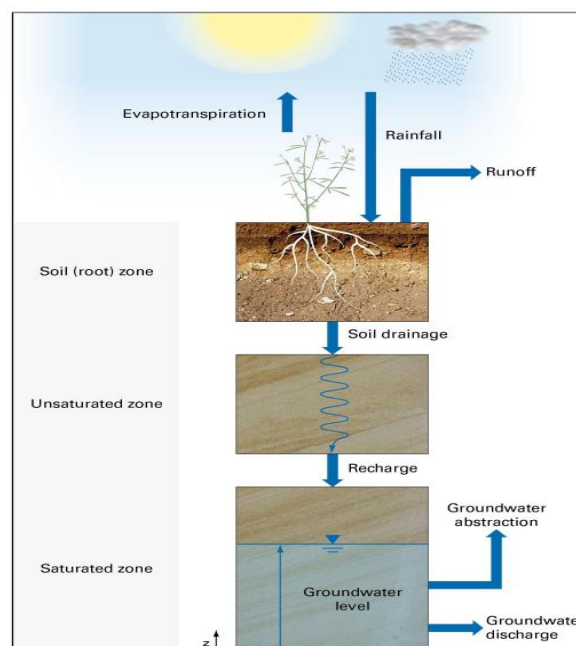


Figure 13: Generalised structure of AquiMod (after Mackay et al., 2014a).

The soil moisture module

There are several methods available in Aquimod that can be used to calculate the rainfall infiltration into the soil zone. In this study we use the FAO Drainage and Irrigation Paper 56 (Allen et al., 1998) approach. In this method, the capacity of the soil zone, from which plants draw water to evapotranspire, is calculated first using the plants and soil characteristics. Evapotranspiration is calculated according to the soil moisture deficit level compared to two parameters: Readily Available Water (RAW) and Total Available Water (TAW). These are a function of the root depth and the depletion factor of the plant in addition to the soil moisture content at field capacity and wilting point as shown in Equations A1 and A2.

$$TAW = Z_r(\theta_{fc} - \theta_{wp}) \quad \text{Equation A1}$$

$$RAW = p \cdot TAW \quad \text{Equation A2}$$

Where Z_r [L] and p [-] are the root depth and depletion factor of a plant respectively, θ_{fc} [L³ L⁻³] and θ_{wp} [L³ L⁻³] are the moisture content at field capacity and wilting point respectively.

The FAO method is simplified by Griffiths et al. (2006) who developed a modified EA-FAO method. In this method the evapotranspiration rates are calculated as a function of the potential evaporation and an intermediate soil moisture deficit as:

$$\begin{aligned} e_s &= e_p \left[\frac{s_s^*}{TAW - RAW} \right]^{0.2} & s_s^* > RAW \\ e_s &= e_p & s_s^* \leq RAW \\ e_s &= 0 & s_s^* \geq TAW \end{aligned} \quad \text{Equation A3}$$

Where e_s [L] is the evpo-transpiration rate, e_p [L] is the potential evaporation rate and s_s^* [L] is the intermediate soil moisture deficit given by

$$s_s^* = s_s^{t-1} - r + e_p \quad \text{Equation A4}$$

Where r [L] is the rainfall at the current time step and s_s^{t-1} [L] is the soil moisture deficit calculated at the previous time step.

The new soil moisture deficit is then calculated from:

$$s_s = s_s^{t-1} - r + e_s \quad \text{Equation A5}$$

Griffiths et al. (2006) proposed that the recharge and overland flow are only generated when the calculated soil moisture deficit becomes zero. The remaining volume of water, the excess water, is then split into recharge and overland flow using a runoff coefficient. In Aquimod a baseflow coefficient is used to reflect the fact that a groundwater discharge is calculated rather than overland water. In this application, the baseflow coefficient is one minus the runoff coefficient.

The unsaturated zone module

The Aquimod version used in this study to simulate the movement of groundwater flow within the unsaturated zone is based on a statistical approach rather than a process-based approach. This method distributes the amount of rainfall recharge over several time steps where the soil drainage for each time step is calculated using a two-parameter Weibull probability density function. The Weibull function can represent exponentially increasing, exponentially decreasing, and positively and negatively skewed distributions. This can be used to focus the soil drainage over earlier or later time steps or to spread it over a number of time steps after the infiltration occurs. The shape of the Weibull function is controlled by two parameters, k and λ as shown in Equation A6.

$$f(t, k, \lambda) = \begin{cases} \frac{k}{\lambda} \left(\frac{t}{\lambda}\right)^{k-1} e^{-(t/\lambda)^k} & t > 0 \\ 0 & t \leq 0 \end{cases} \quad \text{Equation A6}$$

Where k and λ are two parameters the values of which are calculated during the calibration of the model and t is the time step.

The saturated zone module

AquiMod considers the saturated zone as a rectangular block of porous medium with dimensions L and B as its length and width [L] respectively. This block is divided into a number of layers, each has a defined hydraulic conductivity value, a storage coefficient value, and a discharging feature. The number of layers define the structure of the saturated module used in the study.

The mass balance equation that gives the variation of hydraulic head with time is given by:

$$SLB \frac{dh}{dt} = RLB - Q - A \quad \text{Equation A7}$$

Where:

S is the storage coefficient of the porous medium [-]

h is the groundwater head [L]

t is the time [T]

R is the infiltration recharge [L T⁻¹]

Q is the discharge out of the aquifer [L T⁻¹]

A is the abstraction rate [L T⁻¹]

It must be noted that in a multi-layered groundwater system as shown in Figure 14, we calculate one groundwater head (h) for the whole system. The discharges (Q) from Outlet 1, 2, etc. are calculated using the Darcy law. The total discharges can be summarised using the following equation:

$$Q = \sum_{i=1}^m \frac{T_i B}{0.5 L} \Delta h_i \quad \text{Equation A8}$$

Where:

m is the number of layers in the groundwater system [-]

T_i is the transmissivity of the layer i [L T⁻²]

Δh_i is the difference between the groundwater head h and z_i , the elevation of the base of layer i

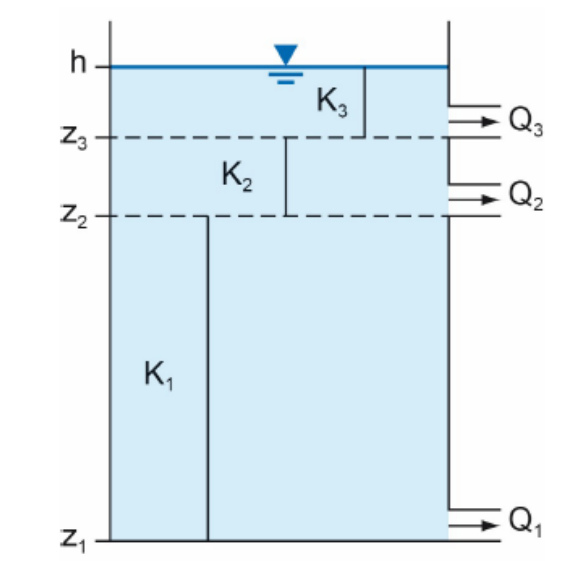


Figure 14: Representation of the saturated zone using a multi-layered groundwater system).

Substituting Equation A8 into Equation A7 yields a numerical equation in the form:

$$S \frac{(h-h^*)}{\Delta t} = R - \sum_{i=1}^m \frac{T_i}{0.5 L^2} \Delta h_i - \frac{A}{LB} \quad \text{Equation A9}$$

Equation A9 is an explicit numerical equation that allows the calculation of the groundwater head h [L] at any time and using time steps of Δt [T]. In this equation h^* [L] is the groundwater head calculated at the previous time step and the term Δh_i [L] is calculated as $(h^* - z_i)$.

The terms S , T_i , and L are optimised during the calibration of the model. A groundwater system can be specified with one storage coefficient as shown in the equations above or with different storage coefficient values for the different layers. Several saturated modules are included in Aquimod to provide this flexibility and the model user can select the model structure that represent the conceptual understanding best.

Limitations of the model

Aquimod is a lumped groundwater model that aims at reproducing the behaviour of the observed groundwater levels. It tries to encapsulate the conceptual understanding of a groundwater system in a simple numerical representation. The model results have to be therefore discussed, taking this into consideration. For example, the model represents the groundwater system as a closed homogeneous medium, with no impact from any outer boundary or feature, whether physical or hydrological, such as the presence of rising and falling river stage.

Vertical heterogeneity can be accounted for by using multi-layered groundwater module structure. However, this model setting does not provide any information about the vertical connections between the layers as the discharge from all the layers is calculated using one representative groundwater head value. In other words, it is assumed that all layers are in perfect hydraulic connection.

As mentioned before, the model is designed to simulate the groundwater levels. However, it produces the recharge values and groundwater discharges as by products. In this application we use the calibrated model to calculate recharge. The mass balance equation (Equation A7) shows that recharge is a function of transmissivity and storage coefficient values, which are



estimated during the calibration process of the model, i.e. they are not parameters with fixed values provided by the user. The inter-connections between these parameters leads to uncertainties in the estimated recharge values as a high storage coefficient value can produce a high recharge estimate and vice versa. To overcome this problem, it is suggested that the recharge values estimated by AquiMod are always presented as a range of possibilities rather than an absolute value. This can be achieved by estimating the recharge values from all the models that have a performance measure above than a threshold that is deemed acceptable by the user. The recharge estimates can then be presented as an average of all estimates and values corresponding to selected percentiles.

Model input and output

AquiMod includes a number of methods that calculates rainfall recharge as well as a number of model structure from which the user can select what better suits the case study.

Model input consists time series of forcing data including rainfall and potential evaporation, time series of anthropogenic impact mainly groundwater abstraction and time series of groundwater levels that will be used to calibrate the model. These time series must be complete, i.e. a value is available at every time step except the groundwater level time series, which can include missing data. The time step can be one day or multiple of days, and the model automatically calculate the size of the time step based on the input data time series.

The model is run first in calibration mode where a range of parameter values are specified for the different parameters included in the three model modules. A Monte Carlo approach is used to select the best parameter values. The performance of the model is measured by comparing the simulated groundwater levels to the observed ones using the Nash Sutcliffe Efficient (NSE) or the Root Mean Squared Error (RMSE) performance measures. The parameter set that produces the best model performance is selected to run the model in evaluation mode.

When the model is run in evaluation mode, it produces output files that give recharge values, groundwater levels and groundwater discharges time series with time as specified in the input file. The number of output files is equal to the number of acceptable models set by the user.

7.2 Appendix B: Metran methodology

Metran applies transfer function noise modelling of (groundwater head) time series with usually daily precipitation and evaporation as input (Zaadnoordijk et al., 2019). The setup is shown in the Figure 15. If time series of other influences on the groundwater head are available, these contributions can be added to the deterministic part of the model. The stochastic part is the difference between the total deterministic part and the observations (the residuals). The corresponding input of the noise model should have the character of white noise.

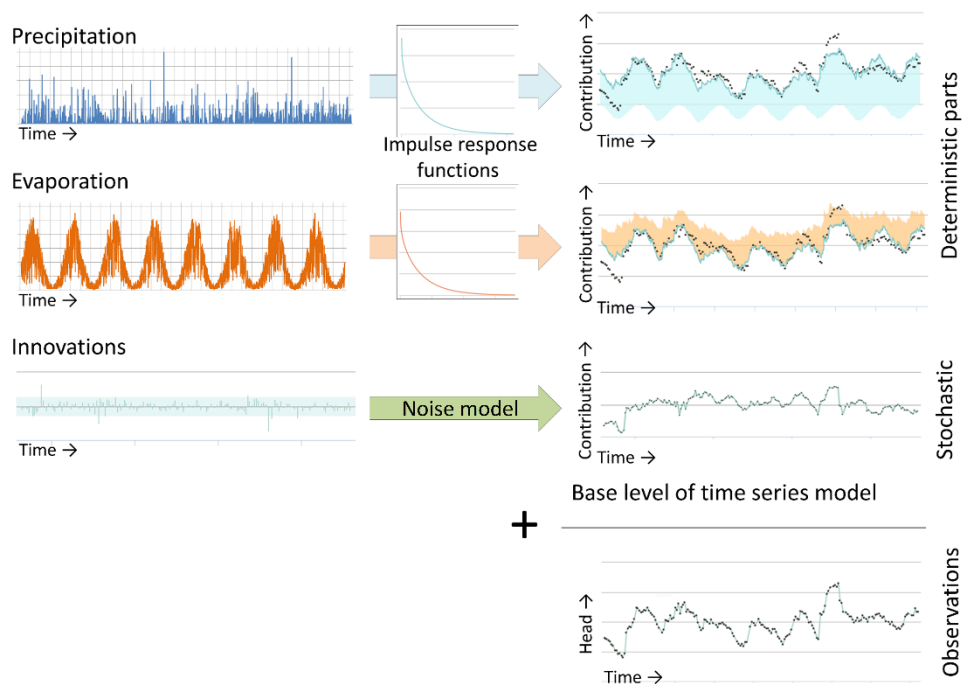


Figure 15: Illustration of METRAN setup

The stochastic part is needed because of the time correlation of the residuals, which does not allow a regular regression to obtain the parameter values of the transfer functions.

The incomplete gamma function is used as transfer function. This is a uni-modal function with only three parameters that has a quite flexible shape and has some physical background (Besbes & de Marsily, 1984). The evaporation response is set equal to the precipitation response except for a factor (f_c). The noise model has one parameter that determines an exponential decay. Thus, for the standard setup with precipitation and evaporation, there are five parameters that have to be determined from the comparison with the observations. Three parameters regarding the precipitation response, the evaporation factor, and the noise model parameter (actually, the time series model has a fifth parameter, the base level, but this is determined from the assumption that the average of the calculated heads is equal to the average of the observations). There are three extra parameters for each additional input series, such as pumping.

Limitations

Metran's time series model is linear. So, the model creation breaks down when the system is strongly nonlinear. This can occur e.g. when drainage occurs for high groundwater levels, when the ratio between the actual evapotranspiration and the inputted reference evaporation varies strongly, or when the groundwater system changed during the simulated period.

Metran is not able to find a decent time series model when the response function is not appropriate for the groundwater system. An example of this is a system with a separate fast and slow response as was found for a French piezometer in the Avre region, as is illustrated in Figure 16.

Finally, the parameter optimization of Metran uses a gradient search method in the parameter space, so it can be sensitive to initial parameter values in finding an optimal solution.

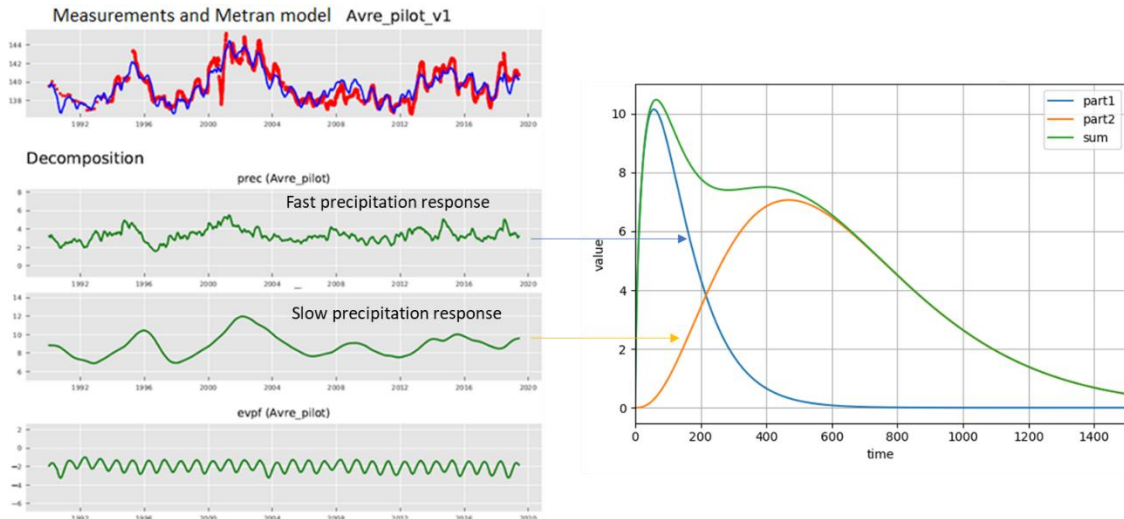


Figure 16: An example where the response function implemented in METRAN is not suitable for the groundwater system

Time step

Metran has been designed to work with explanatory series that have a daily time step. However, it has been adapted so that other time step lengths can be applied; although Metran still has the limitation that the explanatory variables have a constant frequency. For the TACTIC simulations of series with monthly or decadal meteorological input series, the time step has been set to 30 and 10 days, respectively. This time step has been applied from the end date backward.

Note that the heads may be irregular in time as long as the frequency is not greater than the frequency of the explanatory series.

Model output

The evaporation factor fc gives the importance of evapotranspiration compared to precipitation.

The parameter M_0 gives the total precipitation response, which is equal to the area below the impulse response function and the final value of the step response function.

The average response time is another characteristic of the precipitation response. The influence is illustrated in Figure 17 with the impulse response functions and head time series for two models with very different response times for time series of SGU in Sweden.

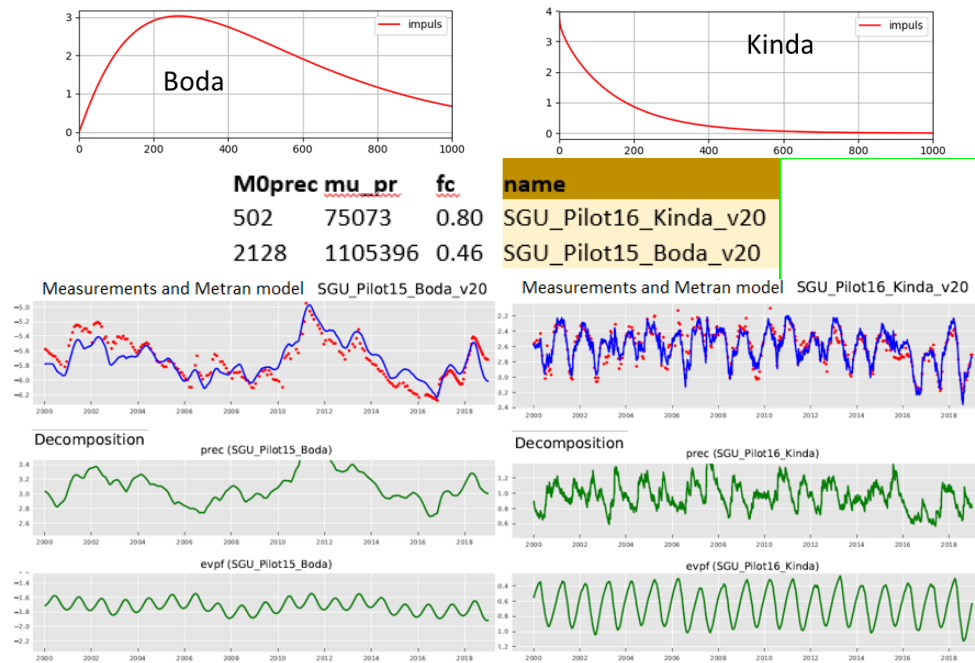


Figure 17: Illustration of Metran output for two case studies in Sweden with different response times.

Model quality

Metran judges a resulting time series model according to a number of criteria and summarizes the quality using two binary parameters Regimeok, Modok (see Zaadnoordijk et al., 2019):

- Regimeok = 1 : highest quality
- Modok = 1 (and Regimeok = 0) : ok
- Both zero = model quality insufficient

More detailed information on the model quality is given in the form of scores for two information criteria (AIC and BIC), a log likelihood, R2, RMSE, and the standard deviations and correlations of the parameters.

Recharge

Although the transfer-noise modelling of Metran determines statistical relations between groundwater heads and explanatory variables, we like to think of the results in physical terms. It is tempting to interpret the evaporation factor, as the factor translating the reference into the actual evapotranspiration. Then, we can calculate a recharge as

$$R = P - fE$$

Equation B1

where R is recharge, P precipitation, E evapotranspiration, and f the evaporation factor.

Following the definitions used in the TACTIC project, this recharge R actually is the effective precipitation. It is equal to the potential recharge when the surface runoff is negligible. This in turn is equal to the actual recharge at the groundwater table if there also is no storage change or interflow. In such cases it may be expected that this formula indeed corresponds to the meteorological forcing of the groundwater head in a piezometer, so that it gives a reasonable estimate of the recharge. Obergfell et al. (2019) showed this for an area on an ice pushed ridge



in the Netherlands. However, this assumes that all precipitation recharges the groundwater, which cannot be done in many places.

In Dutch polders with shallow water tables and intense drainage networks, it is reasonable to assume that the actual evapotranspiration is equal to the reference value. In that case, the factor f becomes larger than 1 because 1 mm of evaporation has less effect than 1 mm of precipitation (because part of the evaporation does not enter the ground but is immediately drained to the surface water system). In that case, we can calculate recharge as:

$$\begin{aligned} R &= P - fE & f &\leq 1 \\ R &= P/f - E & f &> 1 \end{aligned} \quad \text{Equation B2}$$

These simple formulas can be applied easily for the situations currently modelled in Metran and for the simulations that are driven by future climate data using the delta-change climate factors. However, it is noted that it is a crude estimate using assumptions that are easily violated. Because of this, the equations should be applied only to long term averages using only models of the highest quality.

7.3 Appendix C: Gardènia methodology

Introduction

The computer code GARDÉNIA (modèle Global A Réservoirs pour la simulation des Débits et des Niveaux Aquifères) is a lumped hydrological model for watersheds. It uses time series of meteorological data (rainfall, potential evapo-transpiration) recorded or calculated at a catchment to calculate:

- the river flows at the outlet of a river (or source) basin;
and / or
- the groundwater levels at a borehole drilled in the underlying aquifer.

The effects of pumping or of a pumping group all located in the watershed can be taken into account.

Calculations can be performed at a daily time step, decadal (ten days) or monthly. It is possible to take into account the snow melting process.

The modelling of the relationships between the rainfall and river flows and/or rainfall and groundwater levels includes 4 to 6 lumped parameters (soil capacity, recession times, etc...) representative for a basin or a homogeneous unit within the basin. These parameters are optimized using rainfall and river flow (and/or groundwater level) data over same observation period. The software under control of the user does this calibration phase of the model automatically.

After completion of the calibration, GARDENIA enables:

- The calculation of a hydrological water balance for the basin including actual evapotranspiration, runoff, infiltration, recharge (some terms can be used as input data in a discretized groundwater model). The hydrological water balance can be used for the evaluation of the renewable groundwater resources, mainly the groundwater recharge, of aquifers;
- the prediction of river flows, groundwater levels or recharge estimates over a historical or a future period for which precipitation and potential evaporation data are



known. These projected river flow and/or groundwater level series can then be used for:

- the forecasting of river flows or groundwater levels for the design of structures;
- the study of particular events such as the rise of groundwater levels (flooding) or the occurrence of droughts;
- the study of the impact of climate change.

In addition to the possibility of estimating the different elements of the hydrological cycle (infiltration, evapotranspiration, runoff), GARDENIA allows the characterization of the hydraulic characteristics of the catchment through the calculation of the different runoff components (fast, slow and very slow components).

Methodology

The GARDENIA model represents the water cycle in a basin from rainfall received by the soil surface till the river flow at the outlet, and/or the aquifer level at a given point. GARDENIA is a lumped model because it considers a lumped input (rainfall and potential evaporation representative for the basin) averaged over a catchment area and a single output (river flow at the outlet and/or groundwater level in the aquifer).

A lumped hydrological model simulates, through a series of reservoirs, the main mechanisms of the water cycle in a catchment (rainfall, evapotranspiration, infiltration, and runoff). Indeed, the exponential form of the recession of river flows or aquifer levels looks like the emptying of a reservoir (or tank). Therefore, the behavior of an aquifer system can be represented by a series of inter-connected tanks. Non-linear transfer functions improve the capability of this schematic representation to simulate a complex system.

GARDENIA simulates the water cycle through a series of 3 or 4 connected tanks that represent respectively (Figure 18):

- the few decimeters of the soil that are subjected to the influence of evapotranspiration (root zone of the present vegetation);
- an intermediate zone generating rapid flow;
- one or two aquifer zones generating delayed slow flow.

The outflow from one reservoir to another is controlled by simple laws, specific to each reservoir; these laws are governed by the model parameters (active storage, duration of outflow, overflow threshold, etc.).

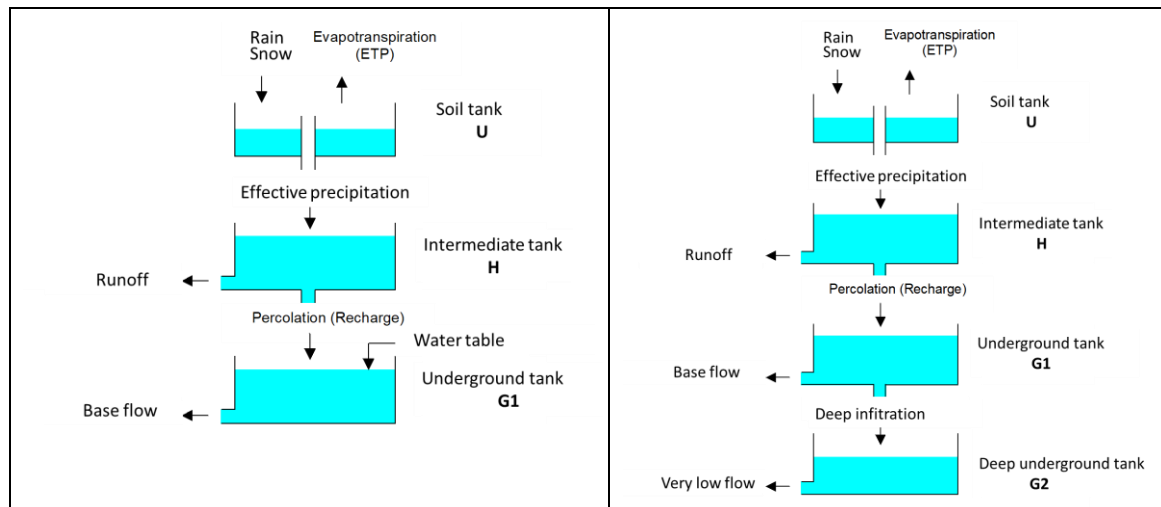


Figure 18: Schematic representation of GARDÉNIA with one underground reservoir (left) or two underground reservoirs (right).

"Production" function and "transfer" function

The calculation consists of two parts, traditionally called: "production" function and "transfer" function.

The "production" function determines the amount of water reaching the system, and the amount that will evaporate or that will infiltrate into the lower horizons to emerge "later". The "transfer" function determines at what time the water, which has not evaporated, leaves the outlet of the basin or will reach the aquifer below. The transfer is represented as the passing of water through the 2 or 3 lower reservoirs of the model.

Due to the lumped nature of the model and the complexity of the hydrological system in reality, the different parameters of the tanks cannot be determined a priori from the local physiographical characteristics of the catchment (geology, vegetation cover, etc.).

Model data and parameters

The required data are:

- a continuous time series of rainfall data,
- a continuous time series of potential evapotranspiration data (PET). PET values can be either calculated from sunshine duration, air temperature and relative humidity data, or can be obtained directly at Meteorological offices;
- one or two series of observations, which may include gaps, of:
 - o river flows at the basin outlet; and / or representative groundwater levels at an observation well located in the basin.
- possibly a series of water withdrawals (pumping)

These different series of data must at a regular time step: daily, 5 days, 10 days, or monthly. It is also possible to use any regular time step (5 minutes, 1 hour, 60 days etc.).

All the series should refer to the same period. The time step of each series is not necessarily identical (e.g. daily rainfall and monthly PET).



Hydro(geo)logical parameters

In general a number of 4 to 6 parameters (maximum 8 parameters) is required by the model (15 parameters in case precipitation in form of snowfall are to be taken into account). The dimensional parameters characteristics of the different reservoirs are:

- RUMAX (mm): capacity of reservoir RU, or the storage available for evapotranspiration
- THG (months): time of half-filling of reservoir G
- RUIPER (mm): level in reservoir H for which there is an equal distribution between fast runoff and percolation.
- TG1 (months): time of half-recession of reservoir G1
- TG12 (*) (months): time of half-filling or reservoir G2 (time of half-transfer from G1 to G2)
- TG2 (months): time of half-recession of reservoir G2 (time of half- slow recession)

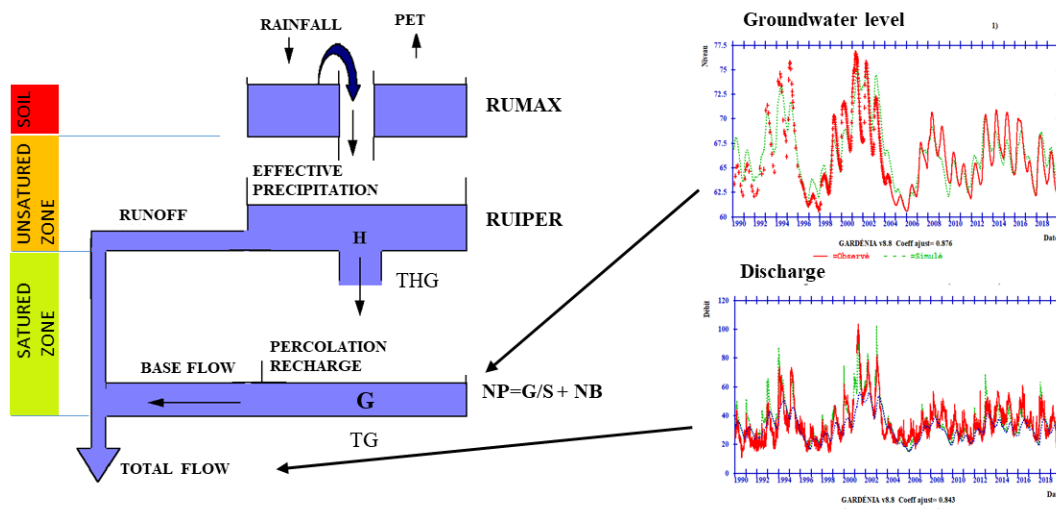


Figure 19: Principle of GARDÉNIA global hydrological model for simulating the flow of a watercourse and/or a groundwater level.

Initialization

It is evident that due to the sometimes considerable hydrological inertia of the system, the calculation of the first values depends a lot on the conditions of the previous years.

To avoid the difficulties that could result from the above, the possibility has been introduced in the model to take into consideration a few years, prior to the first hydrological observations.

However, since it often takes very long for the flow regime to establish, the model is placed in hydrological equilibrium at the beginning of calculations, this means that the out coming flow (or piezometric level) corresponds to incoming effective rainfall.

Model calibration

Model calibration consists of adjusting model parameters, within given limits, with the aim of producing simulated river flows and/or groundwater level series that match the observed ones as precisely as possible.

The data required for calibration are:

- model "input" continuous series: rainfall and evapotranspiration (and air temperature if snowmelt is taken into consideration);
- model "output" observed series (flows or levels) not necessarily continuous. but covering a concomitant period with the input series.

Calibration is done in a semi-automatic way. The user provides an initial set of parameters and indicates which parameters should be optimised. The model uses a non-linear optimisation algorithm adopted from the Rosenbrock method. The model makes the chosen parameters vary (within a range of values defined by the user) and searches for a set which gives the best fit between observed and simulated series has been found.

The model produces the following results:

- for each time-step a water balance of the different components of the hydrological cycle (runoff, actual evaporation, groundwater flow, ...) ;
- a graphical representation of observed and simulated values for a visual evaluation of the calibration ;
- numerical criteria for the evaluation of the quality of calibration.

Taking into account this information, the user then estimates whether to attempt a new optimization from another set of parameters. When both the numerical fitting criteria and the graphs for visual comparison are satisfactory, the user may consider which set of parameters are representative of the catchment as far as the obtained values are realistic. He may then test different values of the parameters around this solution, in order to determine the family of parameter values that are representative, i.e. acceptable from his point of view, of the water cycle (sensitivity study).

Limitation and specific difficulties in the simulation of piezometric levels

The model GARDENIA has been developed to simulate flows as well as piezometric levels indifferently: in fact, the hydrological scheme is the same; the level in the underground reservoir can be thought of as being linked to the piezometric level by a linear relationship irrespective of the type of the aquifer considered.

The storage coefficient then plays the role of an amplitude factor, like the surface area of the catchment in the case of the calculation of flows. Nevertheless, the simulations of levels involve very specific problems.

The storage coefficient is not known, not even in order of magnitude, whereas the surface area of catchment is generally known. In fact, it represents a coefficient of global influence of the fluctuations of a reserve on a particular piezometric level.

This coefficient of influence will only be equal to the average storage coefficient of the aquifer if the point of observation is located far away from any watercourse.

This coefficient cannot be linked easily to interpretations of pumping tests (whose validity remains local) and which are often carried out over short periods and can give a confined aquifer storage coefficient. The storage coefficient in GARDENIA corresponds more to level variations over periods that are much longer and the type of storage coefficient to be taken into consideration is that of an unconfined aquifer. Moreover, the storage coefficient in its traditional meaning is most frequently defined only with a precision far below 20 %, while deviations of 20 percent in the balance equation are difficult to accept.

In case of simulations of levels, the balance established should be interpreted as an analysis of the flux only with extreme care. Although this method of analysis may be a bit dangerous for



effective input estimations, it is often the only method available and it should thus not be rejected in advance.



Deliverable 4.2

PILOT DESCRIPTION AND ASSESSMENT

Posavina (Serbia)

Authors and affiliation:

Katarina Atanasković Samolov
Tanja Petrović Pantić
Milan Tomić
Saša Todorović

Geological Survey of Serbia (GSS)



This report is part of a project that has received funding by the European Union's Horizon 2020 research and innovation programme under grant agreement number 731166.



Deliverable Data	
Deliverable number	D4.2
Dissemination level	Public
Deliverable name	<i>Pilot description and assessment</i>
Work package	WP4 and WP6
Lead WP/Deliverable beneficiary	BRGM (WP4), IGME (WP6)
Deliverable status	
Version	Version 2
Date	17/3/2021

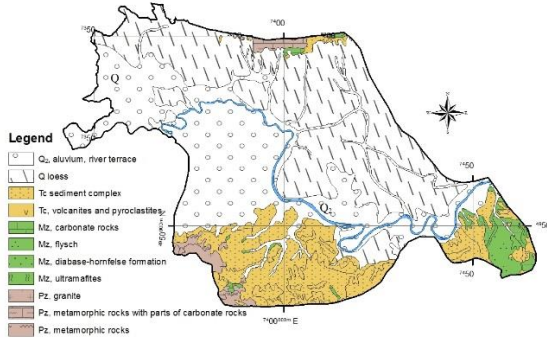
[This page has intentionally been left blank]

LIST OF ABBREVIATIONS & ACRONYMS

TABLE OF CONTENTS

LIST OF ABBREVIATIONS & ACRONYMS	5
1 EXECUTIVE SUMMARY	5
2 INTRODUCTION	7
3 PILOT AREA	8
3.1 Site description and data	8
3.2 Climate	9
3.2.1 Climate type	9
3.2.2 Precipitation and evapotranspiration	9
3.3 Topography	9
3.4 Land use	10
3.5 Geology/Aquifer type	11
3.6 Surface water bodies	13
3.7 Abstractions/irrigation	13
3.8 Climate change challenge	14
4 METHODOLOGY	15
4.1 Methodology and climate data	15
4.1.1 AquMod	15
4.1.2 Metran	15
4.1.3 Climate data	16
4.2 Tool(s) / Model set-up	18
4.2.1 AquMod	18
4.2.2 METRAN	20
4.3 Tools/ Model calibration/ test	21
4.3.1 Calibration of AquMod models	21
4.3.2 Calibration of Metran models	23
4.4 Uncertainty	23
5 RESULTS AND CONCLUSIONS	25
5.1 Performance to historical data	25
5.2 Future projections	25
REFERENCES	28
Appendix A: AquMod methodology	29
The soil moisture module	30
The unsaturated zone module	30
The saturated zone module	31
Limitations of the model	32
Model input and output	33
Appendix B: Metran methodology	34
Limitations	35
Time step	35
Model output	35
Model quality	36
Recharge	36

1 EXECUTIVE SUMMARY

Pilot name	Posavina (Sava River Basin)	
Country	Serbia	
EU-region	Central and Eastern Europe	
Area (km ²)	5250 km ²	
Aquifer geology and type classification	Sand and gravel. Porous aquifer	
Primary water usage	Irrigation/ Drinking/ Industry	
Main climate change issues	The catchment of Sava River has a history of high and low groundwater and surface water levels due to increase of temperature, extreme weather conditions, floods (due to heavy rainfall) and even droughts (in some years). Therefore, the three main potential impacts of climate change on water resources in the area are related to the problems of water availability, water quality and frequency of floods and droughts. Changes in the water regime with these three aspects would inevitably influence water management.	
Models and methods used	AquiMod, METRAN	
Key stakeholders	Ministry of Mining and Energy of the Republic of Serbia, Ministry of Agriculture, Forestry and Water Management, Ministry of Environmental Protection, water supply and utility companies	
Contact person	K. Atanasković Samolov, T. Petrović Pantić, M. Tomić, S. Todorović, (GSS) k.samolov@gmail.com , tanjapetrovic.hg@gmail.com , milantomichg@gmail.com , sasa.todorovic@gzs.gov.rs	

Posavina Pilot area is situated in the area of the Sava River Basin in Serbia. From the border with Croatia on the West, to Belgrade in the East, Fruška Gora Mountain to the North and Cer Mountain in the South. The area includes part of Vojvodina (Pannonian Basin) - Srem, then Macva and parts around Belgrade, the capital city.

Besides capital city, groundwater is the only source of water supply in this area. Recharge is mainly from the Sava River, and infiltration from precipitation and surface waters from irrigation canals. In addition, there is a small infiltration of groundwater from the terrace sediments into the aquifer. Groundwater discharges into the Sava riverbed at low water levels. In the area of the alluvial plain in the semi-permeable layer, an accumulation of groundwater was formed, which is in direct hydraulic connection with the shallow aquifer. Depth to groundwater table is 2-6 m. Groundwater level fluctuations are driven by infiltration recharge and by evapotranspiration (Josipović and Soro, 2012).



The impact of climate change is focused on the shallow aquifer, which is the most important in terms of drinking water supply in this area. For research purposes Aquimod and Metran time series models were applied. However, the Aquimod models were tested at the five boreholes and could not obtain the satisfactory results, mostly because of the great influence of Sava River water levels. Metran, on the other hand, succeeded in groundwater simulations and recharge estimation only when the river water levels were added as an additional input signal. A Metran model applied at one borehole was used to estimate the long term average historical recharge value as well as the projected recharge values using four standard climate change scenarios developed for the TACTIC project. The TACTIC standard scenarios were developed based on the ISIMIP (Inter Sectoral Impact Model Inter-comparison Project) dataset.

Geological Survey of Serbia has groundwater monitoring net only for the purposes of creating the Basic Hydrogeological Maps, and therefore monitoring is conducted for a hydrologic year. Hence for the purposes of the time series analyses the groundwater data, precipitation, evapotranspiration, and temperature for the Posavina area are taken from the Republic Hydrometeorological Service of Serbia (RHMS).

2 INTRODUCTION

Climate change (CC) already have widespread and significant impacts on Europe's hydrological systems including groundwater bodies, which is expected to intensify in the future. Groundwater plays a vital role for the land phase of the freshwater cycle and has the capability of buffering or enhancing the impact from extreme climate events causing droughts or floods, depending on the subsurface properties and the status of the system (dry/wet) prior to the climate event. Understanding and taking the hydrogeology into account is therefore essential in the assessment of climate change impacts. Providing harmonised results and products across Europe is further vital for supporting stakeholders, decision makers and EU policies makers.

The Geological Survey Organisations (GSOs) in Europe compile the necessary data and knowledge of the groundwater systems across Europe. To enhance the utilisation of these data and knowledge of the subsurface system in CC impact assessments, the GSOs, in the framework of GeoERA, has established the project "Tools for Assessment of Climate change Impact on Groundwater and Adaptation Strategies – TACTIC". By collaboration among the involved partners, TACTIC aims to enhance and harmonise CC impact assessments and identification and analyses of potential adaptation strategies.

TACTIC is centred around 40 pilot studies covering a variety of CC challenges as well as different hydrogeological settings and different management systems found in Europe. Knowledge and experiences from the pilots will be synthesised and provide a basis for the development of an infrastructure on CC impact assessments and adaptation strategies. The final projects results will be made available through the common GeoERA Information Platform (<http://www.europe-geology.eu>).

3 PILOT AREA

The major groundwater reserves in Serbia are accumulated in thick Quaternary and Neogene aquifers. Alluvial aquifers of large rivers are particularly important and widely used for drinking water supply. This study focuses on groundwater resources in the area of the Sava River Basin. The main purpose of investigating this area is to define general water balance (surface water, precipitation, and groundwater). General water balance is of utmost importance for understanding hydrogeological and agricultural features of the terrain. Assessing the impact of climate characteristics and surface water to the shallow aquifer, will allow efficient planning of measures for sustainable use and protection of shallow groundwater.

Significant climate change observations on the territory of Serbia in the past 20 years, especially in the area of Sava River Basin, have led to conclusion that the major floods (for example in 2014), winter and summer droughts (in 2000, 2012) had great impact to the groundwater table and arable land in this area.

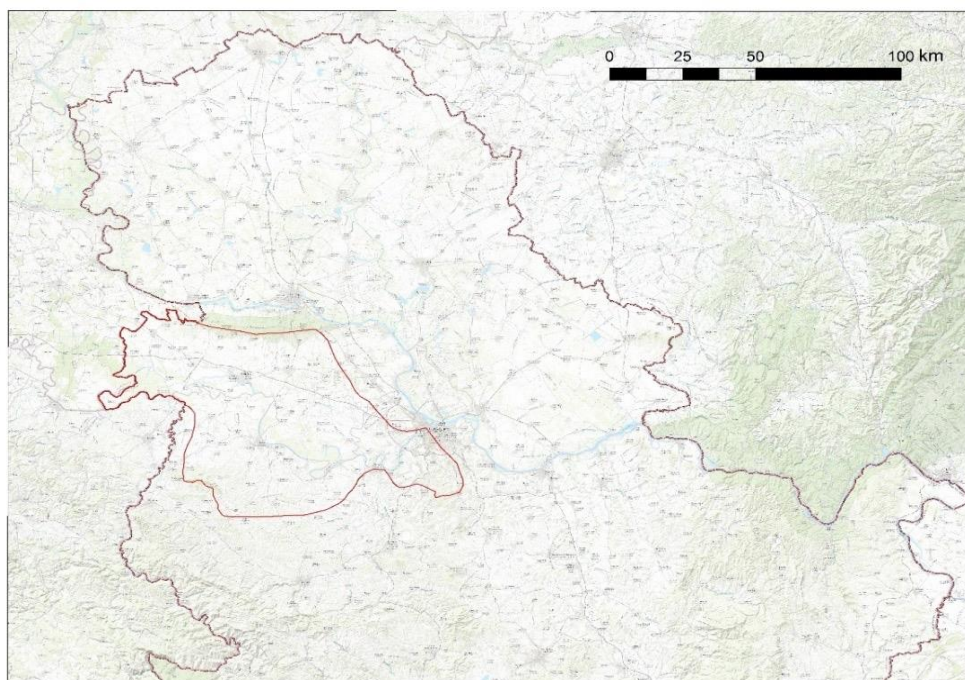


Figure 1. Pilot area

3.1 Site description and data

The area of research covers the Sava River Basin in Serbia. This area stretches from the border with Croatia on the West to Belgrade in the East, and from Fruška Gora Mountain to the North to Cer Mountain in the South (Figure 1). The area includes a significant part of Srem, Macva and parts around Belgrade, the capital city. The territory covers an area of about 5250 km², and Sava River catchment size in Serbia is 9057,29 km². Posavina includes a large part of Srem (Vojvodina, Pannonian Basin) and a large part of the Macva (except the part along River Drina).



3.2 Climate

3.2.1 Climate type

The climate in the area is continental, with cold winters, and hot, humid summers with well-distributed rainfall patterns.

The climate data of the Republic Hydrometeorological Service of Serbia were used. The climate elements, air temperature, precipitation, and PET for the period 1997-2016 at the meteorological stations Sremska Mitrovica, Sabac, and Belgrade were analysed.

A comparative analysis of air temperature for meteorological stations Sremska Mitrovica, Sabac and Belgrade (for the period 1997-2016) was performed in order to examine the elements of climate (air temperature) of the terrain and environment. Based on data obtained from RHMSS, which were monitored between 1997 and 2016 the average air temperature at meteorological stations is: 11.2 °C for Sremska Mitrovica; 11.3°C for Sabac; and 12.7 °C for Belgrade.

3.2.2 Precipitation and evapotranspiration

In order to assess the amount of precipitation in the pilot site, a comparative analysis of the amount of precipitation for meteorological stations Sremska Mitrovica, Sabac and Belgrade was performed.

Based on the data obtained from the RHMSS, which were monitored between 1997 and 2016 the sum of rainfall at meteorological stations are: 624 mm for Sremska Mitrovica, 681 mm for Sabac, 706 mm for Belgrade.

By comparison, the mean values of precipitation for the period between 1997 and 2016 on these three stations and significant deviation of differences in precipitation quantities were observed. Notable amount of precipitation in the area is registered, especially for 2014 (sum 1095 mm).

Evapotranspiration is very low between November and March, more or less strong the rest of the year according to the RHMSS. The PET for these three locations is calculated using the Penman- Monteith method.

3.3 Topography



Posavina is a spacious floodplain of Srem and Mačva and parts of the terrain are peripheral parts of Fruška Gora and Cer mountains. The orographic peculiarities of the terrain are a direct consequence of its creation and, the slopes of the mountain hills in the south and north are part of the Pannonian basin filled with young lacustrine deposits.

The largest hydrographic potential is Sava River and its tributaries, as a very important waterway and strategic traffic direction in this part of Europe. The Sava River flows through Serbia in a length of 206 km, mostly through Srem, and its entire length is navigable. Bosut River is the significant watercourse in the area, and there are several artificial reservoirs and irrigation canals.

Neotectonic movements formed tectonic trenches and depressions in which the accumulation process during Neogene was intense. Thickness of the deposits reaches up to two and three thousand meters. Lower non-structural blocks and intensive accumulations continues throughout the Quaternary. Horst of Fruška Gora rises at a rate of 2 mm per year.

In the zone of the Sava River, there are also the most important urban and industrial centres, thus in the same area are the most important sources of water supply.

3.4 Land use

The area is in state ownership managed by Public Enterprise Vojvodina sume, predominantly covered by the forests (95%, see Figure 3). Public Enterprise Vode Vojvodine manages some land in state ownership. Serbian Armed Forces manages the area for hunting and fishing tourism - VU Morović. The rest is private agricultural land (Zingstra, et al. 2010).

A dyke along the Sava protects the largest part of the site but the water regime of the area is managed through a dam in the River Bosut. Flooding of the site is not regular, but managed depending mostly upon needs of agriculture and flooding protection of settlements and towns in the vicinity and downstream. Due to high level of ground water in spring, significant part of the forest area protected by the dyke is regularly waterlogged. Oldest natural forest remnants cover only 1% of the site and are under protection in form of six separated Strict Nature Reserves. Dominant land use is forestry (Zingstra, et al. 2010).

Most of the Pilot area was under influence of frequent inundations from the Sava and Bosut rivers until the dyke was built in the 1930s. Thanks to low altitude and strategic importance of oak forest present in the area, the site remained in close-to-natural state, with gradually, but not obvious changes in land cover and land use. During 20th century, most of area around the site was converted from forests into arable land. Nowadays, during dry summer season, the forests and wetlands suffer from insufficient groundwater. Water management is not adjusted to forest needs, even though it would not cause damage to arable land. Modification of water management is necessary in order to maintain good forest health and biodiversity of the area. Extensive grazing is necessary for maintaining open wetland areas, which used to be present before the changes in natural processes (flooding) and traditional land use activities (Zingstra, et al. 2010).

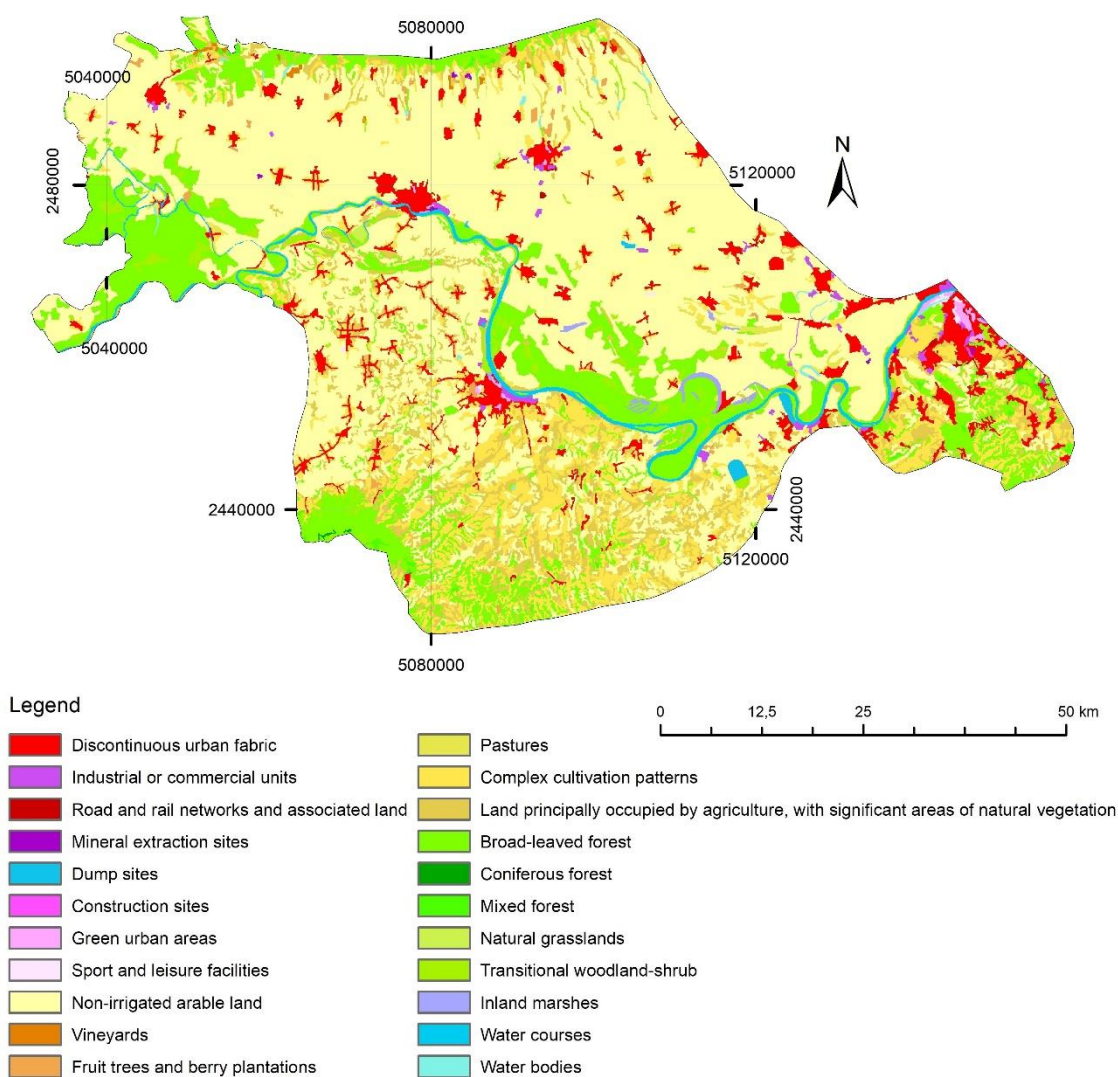


Figure 3. Corine land use map of Pilot area

3.5 Geology/Aquifer type

Pilot area is mostly covered with Quaternary sediments (Figure 4). On the territory of Republic of Serbia, the Sava River makes an extensive alluvial plain. Such an extensive plain enabled the



formation of an abundant aquifer. According to hydrogeological researches, alluvial formations of this aquifer are made of gravel-sand and sand sediments that represent the basic groundwater collector, while fine-grained and slurry sands and clays make upper layer. The depth of the water-bearing layer varies between 12 m and 20 m, in some cases even 25 m (Stojadinović, et al. 2005)

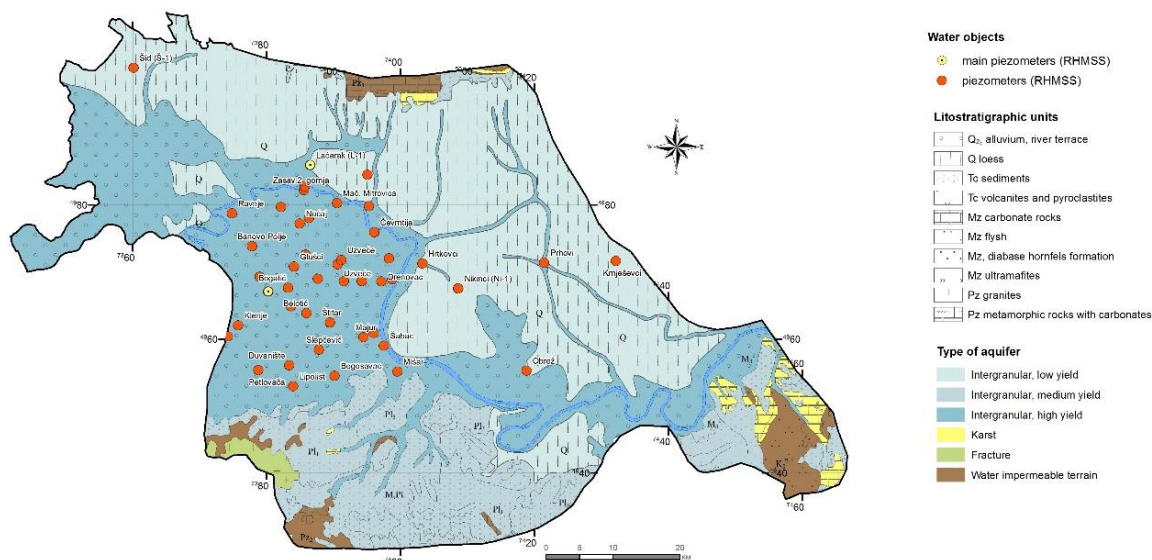


Figure 4. Hydrogeological map of the Pilot area with observation boreholes

Gravel-sand sediments, as a water-bearing environment, have good filtration properties with the infiltration rate of 10—4 m/s. Groundwater recharge is mainly from precipitation and groundwater inflow. To some extent, irrigation also recharge the aquifer. However, main inflows of the water to this aquifer are from the surface water of the Sava River. The analysis of the groundwater regime points out that groundwater table weakens with the distance from Sava. Generally, groundwater table is 3 m below the ground, while in the zone of exploitation wells dynamic level is between 3.5—4.0 m below the surface. Significant depth of alluvial formations, favorable filtration characteristics of the water-bearing layer and the way of its recharge enable the occurrence of an abundant aquifer that is thoroughly in use (Stojadinović, et al. 2005). Figure 5 shows the average groundwater levels interpolation using groundwater levels observed over the period from 1997 to 2016.

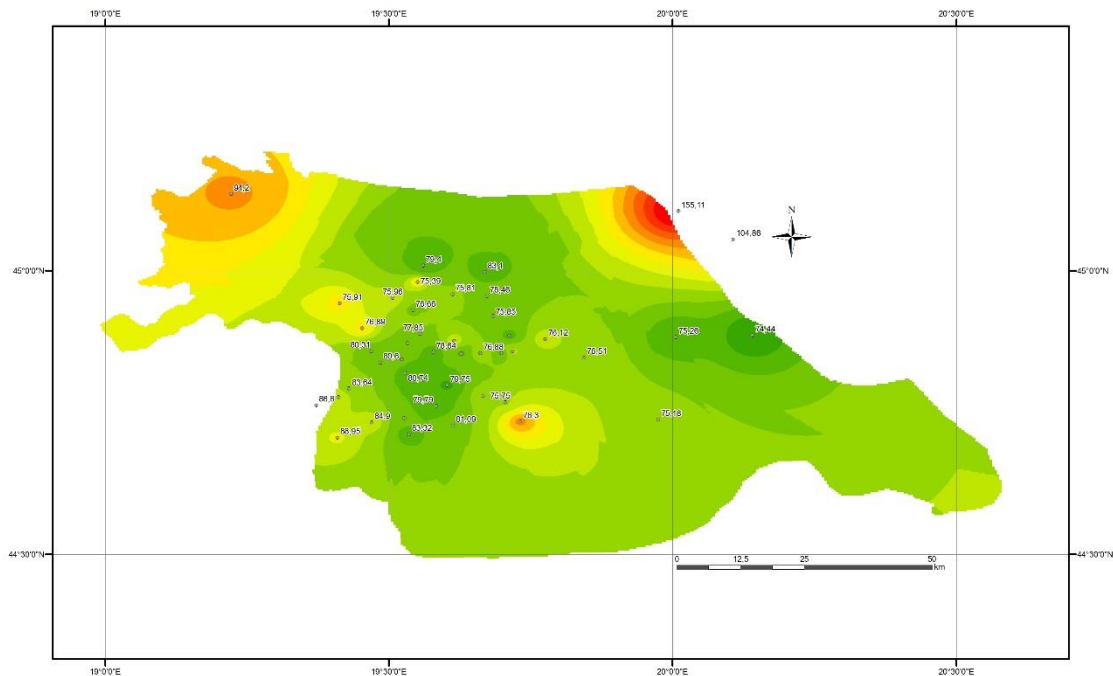


Figure 5. Interpolation of average groundwater levels for the 1997-2016 period

3.6 Surface water bodies

The Sava River is one of the most complex as well as interesting rivers in Europe. The river attracted international attention due to a historic flood in 2014. It originates in the Slovenian mountains and flows into the Danube in Belgrade. Sava River basin is 926 km long – together with tributaries and it is the best preserved and most diverse river systems in Europe: from narrow gorges, to areas with extensive gravel banks, to huge alluvial forests with oxbows and species-rich alluvial meadows (Schwarz, 2016).

3.7 Abstractions/irrigation

Water from aquifers that are formed in alluvial deposits is one of the main sources of water supply worldwide. Basic characteristic of river- bank infiltration type of water source is depending on hydraulic connection between surface water and groundwater. Intensity of this connection has a direct influence on quality of water. River always carry a load of suspended material that has been deposited on the contact between river and riverbed and riverbanks. Infiltration rate of surface water could decrease and initial capacity of water source can be depleted because of the clogging process.



Alluvial aquifer is a major potential source of water supply (of population and industry) in Serbia. However, the shallow aquifer is highly dependable on amount of infiltrated water from precipitation and river water and thus susceptible to negative effects of climate change.

3.8 Climate change challenge

Obvious effect of climate change is an increase of mean annual air temperature and decrease of precipitation. Decrease of annual quantity of precipitation will be followed by its irregular distribution during the year. Decreased precipitation, along with the temperature rising, will negatively affect groundwater balance due to reduced infiltration of surface water and intensified evapotranspiration. Recharge of aquifers will be reduced and groundwater reserves will be endangered.

The most affected aquifers are shallow (alluvial). During analysis of possible climate changes and their effect, the two possible scenarios must be taken into consideration such as long drought period and flood occurrence.

Figure 6 describes the expected climate change across the different areas in Europe as prepared by the European Environment Agency.

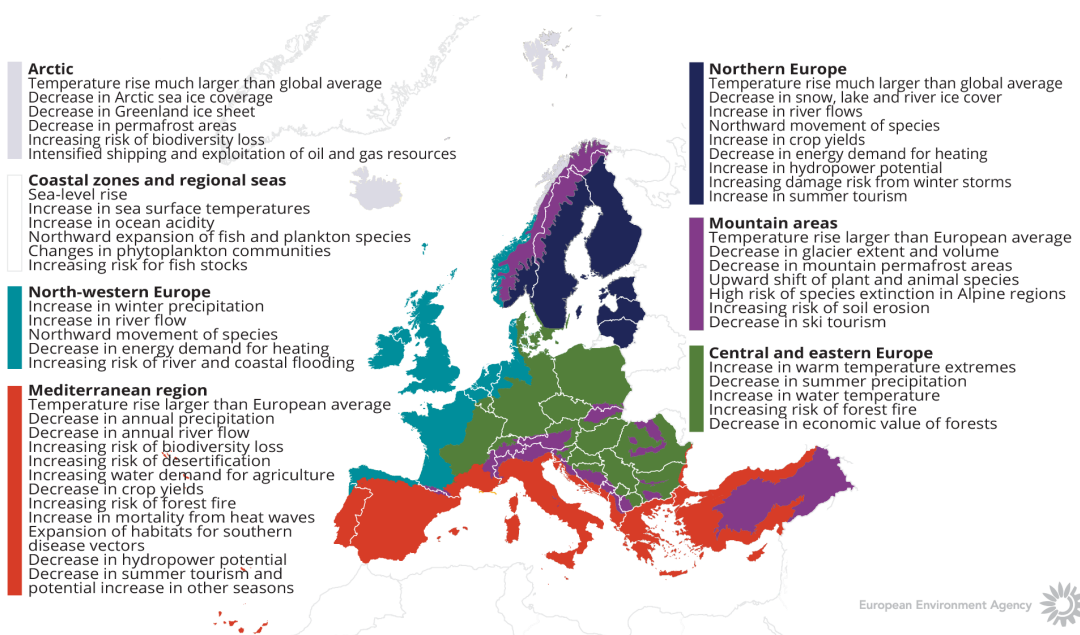


Figure 6. How is climate expected to change in Europe. The European Environment Agency map

4 METHODOLOGY

4.1 Methodology and climate data

4.1.1 *AquiMod*

AquiMod is a lumped parameter computer model that has been developed to simulate groundwater level time series at observational boreholes (Mackay et al., 2014a). It is based on hydrological algorithms that simulate the movement of groundwater within the soil zone, the unsaturated zone, and the saturated zone. The lumped models neglect complexities included in distributed groundwater models but maintain some of the fundamental physical principles that can be related to the conceptual understanding of the groundwater system (Mackay et al., 2014b).

The primary aim of AquiMod is to capture the behaviour of a groundwater system through the analysis of the available groundwater level time series. Once calibrated the model can be run in predictive mode and be used to fill in gaps in historical groundwater level time series and to calculate future groundwater levels. In addition to groundwater levels, it also provides predictions of historical and future recharge values and groundwater discharges.

The mathematical equations that are used to simulate the movement of groundwater flows within the three modules are detailed in Appendix A. The model uses rainfall and potential evaporation time series as forcing data. These are interpreted by the soil module representing the soil zone. The soil module calculates the rainfall infiltration and pass it to the unsaturated zone module. This module delays the arrival of the infiltrating water to the saturated zone module. The latter calculates the variations of groundwater heads and flows accordingly.

The model is calibrated using a Monte Carlo approach. It compares the simulated and observed groundwater level fluctuations and calculates a goodness of fit. The AquiMod version used in this work employs the Root Square Mean Error (RMSE) or the Nash Sutcliffe (NSE) performance measures to assess the performance of the model. The user sets a threshold value to accept all the models that perform better than the specified threshold. The possibility of producing many models that are all equally acceptable, allows the user to interpret the results from all these models and calculate uncertainty.

The recharge values calculated from AquiMod are those that reach the aquifer system and drive the groundwater levels. However, the recharge was not calculated using Aquimod for this Pilot area since the NSE results were unsatisfactory.

4.1.2 *Metran*

Metran applies a transfer function-noise model to simulate the fluctuation of groundwater heads with precipitation and evaporation as independent variables (Zaadnoordijk et al., 2019). The modelling approach consists mainly of two impulse functions and a noise model. The first impulse function is used for convolution with the precipitation to yield the precipitation contribution to the piezometric head. The second is for evaporation which is either a separately estimated function, or a factor times the function used for precipitation. The noise model is a stochastic noise process described by a first-order autoregressive model with one parameter



and zero mean white noise. Further information about the model is given in Appendix B with the model setup shown in the Figure B1.

Metran allows the addition of other processes affecting the behaviour of the groundwater heads, for example pumping or the presence of surface features such as rivers. The contributions from these processes are added to the deterministic part of the model.

Metran has been designed to work with explanatory series that have a daily time step. However, it has been adapted so that other time step lengths can be applied. However, the explanatory variables must still have a constant frequency.

The model is calibrated automatically; however, the model uses two binary parameters, Regimeok and Modok, to judge a resulting time series model. Regimeok cross-examines the explained variance R^2 (> 0.3), the absolute correlation between deterministic component and residuals (< 0.2), and the null hypothesis of non-correlated innovations (p value > 0.01). If all these criteria are satisfied, Regimeok returns a value of 1 indicating highest quality. Modok also cross-examines the explained variance R^2 (> 0.1) and the absolute correlation between deterministic component and residuals (< 0.3) as well as the decay rate parameter (> 0.002) and if all these criteria are satisfied, it is given a value of 1. If Modok = 1 and Regimeok = 0, the model is still considered acceptable. If both these parameters are 0, the model quality is insufficient and the model is rejected.

Metran's time series model is linear and the model creation fails when the system is strongly nonlinear. It is also limited to the response function being appropriate for the simulated groundwater system. Metran uses a gradient search method in the parameter space, so it can be sensitive to initial parameter values in finding an optimal solution.

The model calculates an evaporation factor f that gives the importance of evapotranspiration compared to precipitation. It is possible to use this factor to calculate the recharge values as shown by Equation B2 in appendix B. However, it must be noted that the use of Equation B2 is based on too many assumptions that are easily violated. Because of this, the equations should be applied only to long-term averages using only models of the highest quality.

Following the definitions used in the TACTIC project the recharge quantity corresponds to the effective precipitation. It is equal to the potential recharge when the surface runoff is negligible. This in turn is equal to the actual recharge at the groundwater table if there is also no storage change or interflow.

4.1.3 Climate data

The TACTIC standard scenarios are developed based on the ISIMIP (Inter Sectoral Impact Model Intercomparison Project, see www.isimip.org) datasets. The resolution of the data is $0.5^\circ \times 0.5^\circ$ global grid and at daily time steps. As part of ISIMIP, much effort has been made to standardise the climate data (e.g. bias correction). Data selection and preparation included the following steps:



1. Fifteen combinations of RCPs and GCMs from the ISIMIP data set were selected. RCPs are the Representative Concentration Pathways determining the development in greenhouse gas concentrations, while GCMs are the Global Circulation Models used to simulate the future climate at the global scale. Three RCPs (RCP4.5, RCP6.0, RCP8.5) were combined with five GCMs (noresm1-m, miroc-esm-chem, ipsl-cm5a-lr, hadgem2-es, gfdl-esm2m).
2. A reference period was selected between 1981 – 2010 and an annual mean temperature was calculated for the reference period.
3. For each combination of RCP-GCM, 30-years moving average of the annual mean temperature were calculated and two time slices identified in which the global annual mean temperature had increased by +1 and +3 degree compared to the reference period, respectively. Hence, the selection of the future periods was made to honour a specific temperature increase instead of using a fixed time-slice. This means that the temperature changes are the same for all scenarios, while the period in which this occur varies between the scenarios.
4. To represent conditions of low/high precipitation, the RCP-GCM combinations with the second lowest and second highest precipitation were selected among the 15 combinations for the +1 and +3 degree scenario. This selection was made on a pilot-by-pilot basis to accommodate that the different scenarios have different impact on the various parts of Europe. The scenarios showing the lowest/highest precipitation were avoided, as these endmembers often reflects outliers.
5. Delta change values were calculated on a monthly basis for the four selected scenarios, based on the climate data from the reference period and the selected future period. The delta change values express the changes between the current and future climates, either as a relative factor (precipitation and evapotranspiration) or by an additive factor (temperature).
6. Delta change factors were applied to local climate data by which the local particularities are reflected also for future conditions.

For the analysis in the present pilot the following RCP-GCM combinations were employed:

Table 1. Combinations of RCPs-GCMs used to assess future climate

		RCP	GCM
1-degree	"Dry"	rcp6p0	ipsl-cm5a-lr
	"Wet"	rcp4p5	miroc-esm-chem
3-degree	"Dry"	rcp4p5	hadgem2-es
	"Wet"	rcp8p5	miroc-esm-chem

4.2 Tool(s) / Model set-up

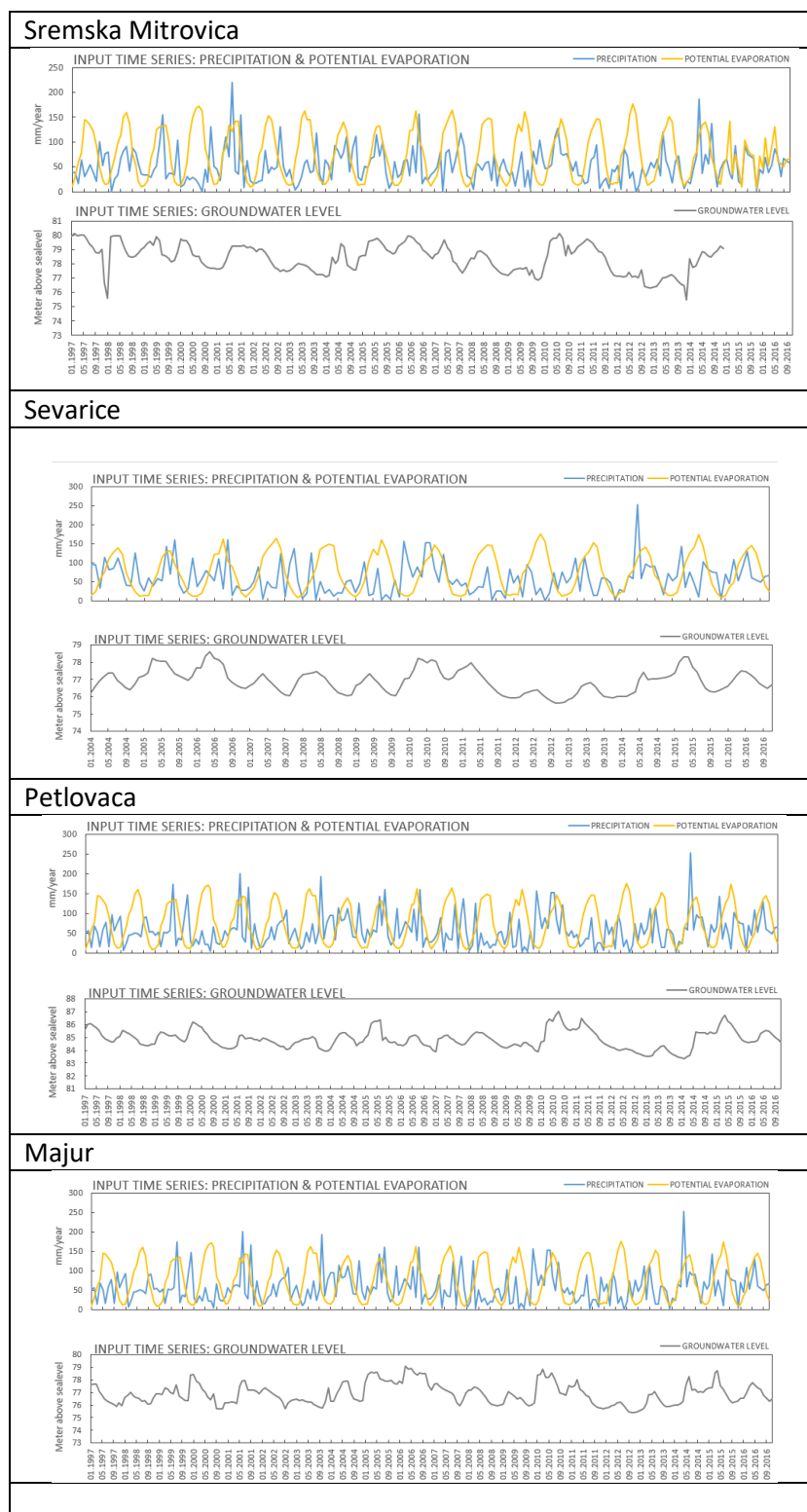
4.2.1 *AquiMod*

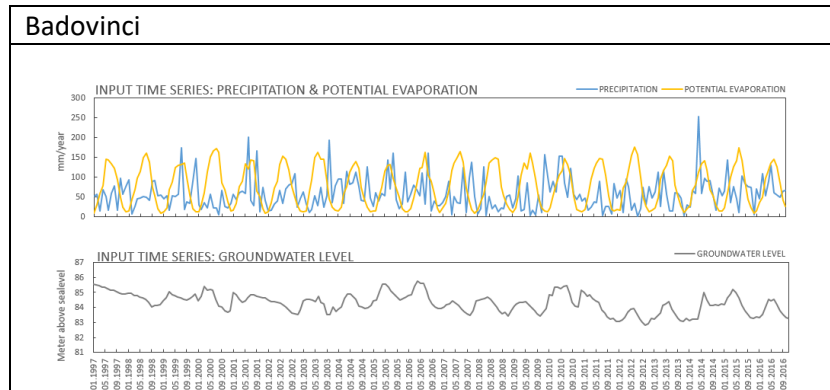
Aquimod model setup relies mainly on two input files. The first input file “Input.txt” is a control file where the module types and model structure are defined. AquiMod is executed first under a calibration mode where a range of parameter values of the different selected modules are given in corresponding text files and a Monte Carlo approach is used to select the parameter values that yield best model performance. “Input.txt” also controls the mode under which AquiMod is executed, the number of Monte Carlo runs to perform, the number of models to keep with an acceptable performance, and the number of runs to execute in evaluation mode.

The second file AquiMod uses is called “observations.dat”. This file holds the forcing data mainly the potential evaporation and rainfall. However, it is also possible to include the anthropogenic impact on groundwater levels by including a time series of pumping data in this file. None of the boreholes studied here includes pumping data. The observed groundwater levels that are used for model calibration are also given in this file. The data are provided to the model on a monthly basis, and this forces AquiMod to run using a time step length of one month. The table 2 shows daily time series of rainfall and potential evaporation values (mm/month) as well as the fluctuations of water table at the different boreholes.

All AquiMod models built for the boreholes in Table 2 use the FAO Drainage and Irrigation Paper 56 (FAO, 1988) method in the soil module, and employ the two-parameter Weibull probability density function to control the movement of infiltrated water in the unsaturated zone (Appendix A1). The groundwater module structures vary between the different boreholes. The best groundwater module structure is found by trial and error during the calibration process. The simplest structure, one layer with one discharge feature, is selected first and then the complexity of the module structure is increased gradually to see if the model performance improves. The structure with best model performance should be selected to undertake the recharge calculations. However, in Posavina the structures that gave the best performance at the selected boreholes are mainly of one layer except at the Badovinci borehole..

Table 2. Figures showing time series of daily rainfall and potential evaporation values (mm/month) as well as the fluctuations of water table at the different boreholes.





4.2.2 METRAN

Metran applies transfer function noise modelling with daily precipitation and evaporation as input and of groundwater levels as output (Zaadnoordijk et al., 2019). The setup is shown in [Figure 1](#)[Figure 7](#). If time series of other influences on the groundwater head are available, these contributions can be added to the deterministic part of the model. An input file that holds the monthly information of precipitation, potential evaporation and groundwater levels is prepared for each borehole. Plots of these data are shown in Table 2. Metran calculates the characteristics of the impulse functions and the corresponding parameters automatically.

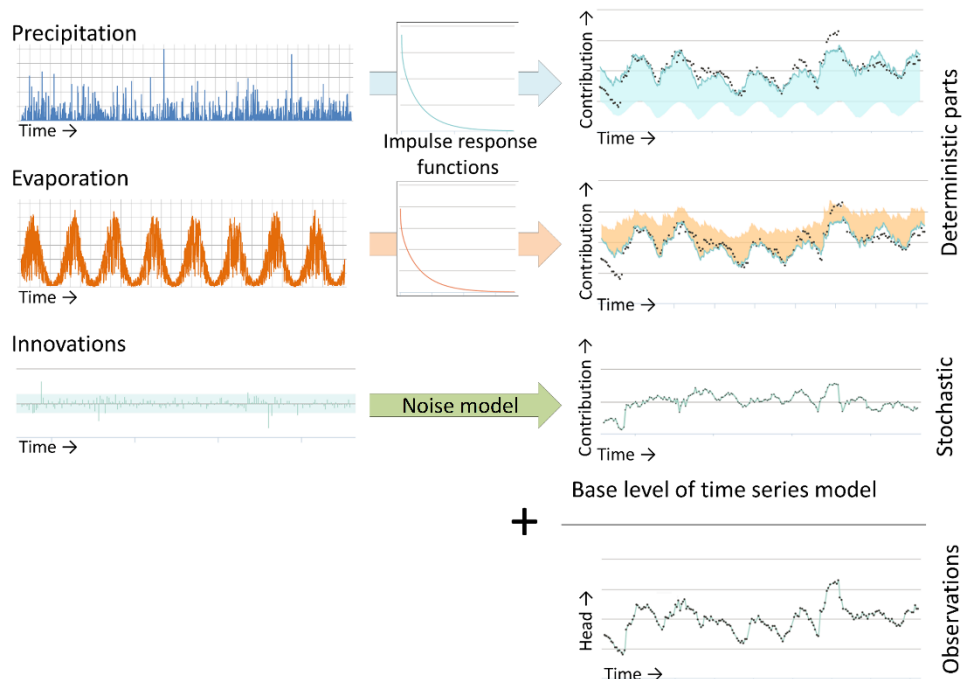


Figure 17. Illustration of METRAN setup

4.3 Tools/ Model calibration/ test

4.3.1 Calibration of *AquiMod* models

The calibration of *AquiMod* is performed automatically using the Monte Carlo approach. The user populates the files of the selected modules with minimum and maximum parameter values and then the model randomly selects a value from the specified range for any given run. The selection of the minimum and maximum values is physically based depending on the characteristics of the study area. For example, the minimum and maximum values of the root depth in the soil module are set to 15 cm and 60 cm respectively for a study area covered with grass, while these values are set to 120 cm and 200 cm for a woodland area. The storage coefficients bound of a groundwater module are set to much lower values in a confined aquifer compared to those used for an aquifer under unconfined conditions.

A conceptual hydrogeological understanding must be available before the use of *AquiMod*, since this is necessary to set the limits of the parameter values for the calibration process. In some cases, it is not possible to obtain a good performing model with the selected values and that necessitates the relaxation of these parameters beyond the limits informed by the conceptual understanding. In such cases, the parameter values must feed back into the conceptual understanding if better performing models are obtained.

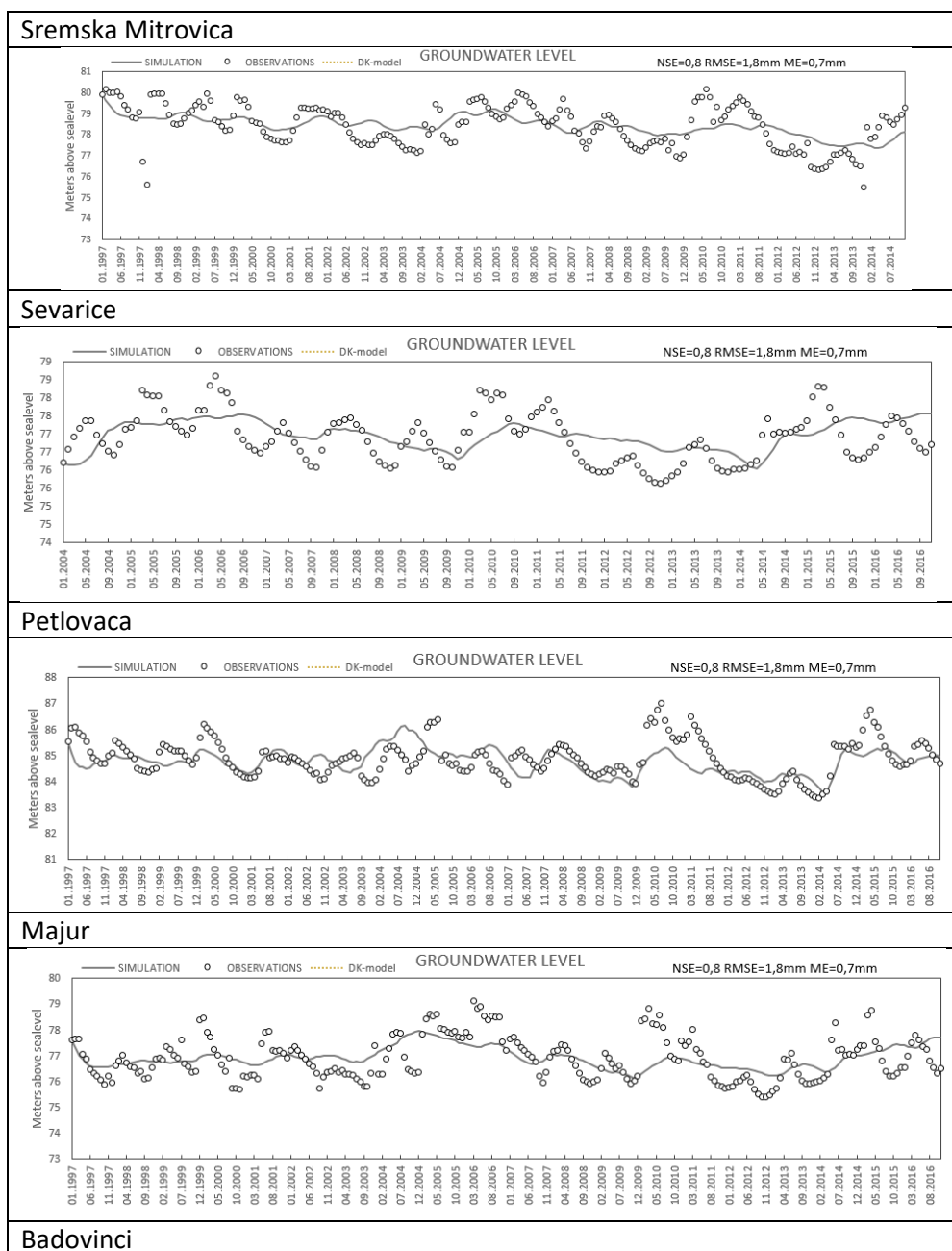
AquiMod execution time is relatively small, which allows the calibration of the model using hundreds of thousands of runs in couple of hours. The performance measure used to assess the quality of the simulation is the Nash Sutcliffe Error (Appendix A) that takes a maximum value of unity for a perfect match between the simulated and observed data. The threshold at which models are accepted is set to a value of 0.6. However, in Pilot area none of the models achieved the NSE higher than 0.6.

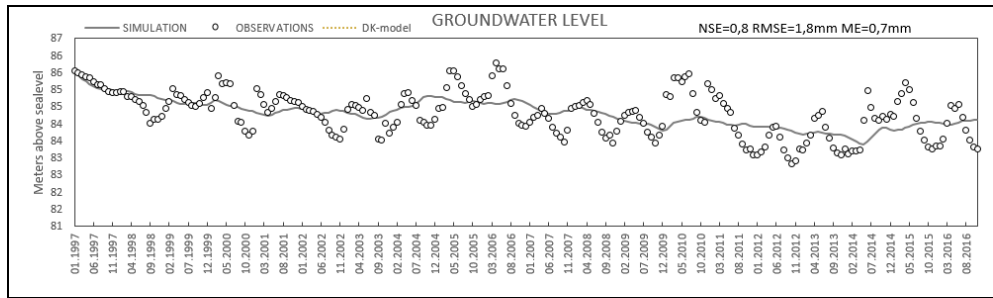
Table 3 shows the best Nash Sutcliffe Efficiency (NSE) measures attained at the selected boreholes using the *AquiMod* model. According to these values, it is clear that the match between the simulated and observed groundwater levels have not been achieved. The plots in table 4 show the comparison between observed groundwater levels and those simulated using *AquiMod*. In this case, the best NSE value of 0.32 is obtained at Sremska Mitrovica borehole. The structures selected for these boreholes are of one layer (Sremska Mitrovica, Sevarice, Petlovaca, Majur) or two layered systems (Badovinci). Because of these low NSE values, these models were not selected to undertake the recharge calculations.

Table 3. Nash Sutcliffe Error measure at Posavina boreholes

Borehole name	NSE
Sremska Mitrovica	0.32
Sevarice	0.17
Petlovaca	0.20
Majur	0.22
Badovinci	0.255

Table 4. Comparison between the simulated and observed groundwater levels at Posavina boreholes





4.3.2 Calibration of Metran models

For the standard setup with precipitation and evaporation, five parameters have to be determined during the calibration of the model. Three parameters are related to the precipitation response, the evaporation factor, and the noise model parameter (Appendix B). There are three extra parameters for each additional input series, such as Sava River levels in this case. The parameter optimization of Metran uses a gradient search method in the parameter space to reach a global minimum. As explained in Appendix B, two parameters indicate if Metran succeeded with producing a match between the simulated and observed data. These are called the Regimeok and Modok. When Regimeok is equal to one, the calibration is of highest quality. If Modok is equal to one and Regimeok is equal to zero, the calibration is of acceptable quality. Finally, if both parameters are equal to zero, the calibration quality is insufficient.

Metran also failed to produce an acceptable model at the selected boreholes. However, the inclusion of the fluctuations of the nearby river stage with time as an input signal to Metran, has led to significant improvement to the match between the simulated and observed groundwater levels. The inclusion of river stage time series was trialled at Sremska Mitrovica only. Metran output showed highest quality (Medok 1, Regimeok 1, RMSE 0.6 and R^2 0.6) and the model was used for recharge calculations at this borehole. However, due to the limited availability of time and resources, it was not possible to check the performance of Metran with this third river stage included at the remaining boreholes.

4.4 Uncertainty

Aquimod is designed to simulate the groundwater levels as described in Appendix A. The model represents the groundwater system as a closed homogeneous medium, with no impact from any outer boundary or feature, whether physical or hydrological, such as the presence of rising and falling river stage. However, the Pilot area there is a great impact on groundwater recharge from Sava River, because of their hydraulic connection. Therefore, the good models with application of Aquimod with only groundwater levels could not be obtained.

In the beginning, the same happened with the application of Metran. Firstly, we used the input files with groundwater levels and precipitation only for the same five boreholes Sremska Mitrovica, Sevarice, Petlovaca, Majur, and Badovinci). Afterward we added data of PE, however, we could not obtain the good fit. The fit of high quality was obtained only after adding the data



of surface water levels. Therefore, recharge and future simulations were taken into consideration for Sremska Mitrovica borehole where we have achieved the satisfactory model.

5 RESULTS AND CONCLUSIONS

5.1 Performance to historical data

As mentioned previously, the Aquimod failed to reproduce the behaviour of the groundwater level time series at all the selected boreholes. The model was not used for recharge calculation. Throughout the calibration, all parameters and model structure combinations that were trialled could not meet the NSE-criteria. The reason for Aquimod failure is anticipated to the fact that river stage fluctuations have significant influence on the fluctuations of groundwater levels. This is clearly demonstrated by Metran, which also failed to produce an acceptable model at all the boreholes but was successful when river stage fluctuations are included as an additional input signal.

Metran uses formulas that are based on assumptions that can be violated (Appendix B). It is better to use the infiltration coefficient f_c with the long-term average values of rainfall and potential evaporation to calculate long-term average values of recharge and using only model of the highest quality. Time series of recharge values, from the analysis undertaken using Metran are not produced. However, the long-term average recharge values were calculated using Metran as shown in table 5.

As the infiltration coefficient is less than unity, the recharge was calculated using the following equation (Appendix B):

$$R = P - fE$$

where R is recharge, P precipitation, E evapotranspiration, and f the evaporation factor.

Table 5 Recharge values calculated using the recharge factors estimated by Metran

Borehole name	Average precipitation (mm/day)	Average potential evaporation (mm/day)	Recharge factor	Recharge (mm/day)
Sremska Mitrovica	1.72	2.47	0.29 ± 0.67	1.15

Metran estimates an upper and a lower value for the infiltration coefficient f_c as shown in Table 5. This can be used as an indication of uncertainty associated with the calculated f_c value. Unfortunately the upper and lower bounds are significantly large compared to the initial value of f_c . Therefore, it is impossible to calculate an upper and lower recharge bounds in this case. In addition, these bounds indicate that the estimated recharge value should be treated with care.

5.2 Future projections

The forcing data, rainfall and potential evaporation, are altered using the change factors of the climate models (see Section 4.1.3.). For the Posavina area, there is set of monthly change factors, used with the data driving Metran. These change factors are used as multipliers to both the historical rainfall and potential evaporation values (Table 6).



The historical time series are altered using these factors first and then the long-term average rainfall and potential evaporation values are calculated using Metran. The recharge coefficient f_c values are calculated from the calibration of Metran model using the historical data, then applied to calculate the projected long-term average recharge values.

Table 6. Monthly change factors as multipliers used for the borehole data

	Scenario	Jan	Feb	Mar	Apr	May	Jun	Jul	Aug	Sep	Oct	Nov	Dec
Rainfall	1° Min	0.76	0.98	1.12	1.08	0.98	0.97	0.85	0.91	1.04	1.04	0.90	0.99
	1° Max	1.02	0.95	0.89	1.16	1.18	1.20	1.01	1.09	0.92	1.08	1.34	1.10
	3° Min	1.28	1.03	1.13	1.26	0.96	0.89	0.46	0.66	0.72	0.78	1.14	0.93
	3° Max	0.95	1.07	1.15	1.00	1.04	1.15	0.98	0.90	0.88	1.17	0.85	1.19
PE	1° Min	1.10	1.09	1.03	1.04	1.05	1.06	1.05	1.05	1.06	1.04	1.07	1.04
	1° Max	1.16	1.12	1.11	1.09	1.04	1.06	1.07	1.07	1.09	1.09	1.07	1.16
	3° Min	1.19	1.17	1.21	1.15	1.09	1.07	1.10	1.08	1.10	1.09	1.13	1.13
	3° Max	1.33	1.35	1.29	1.29	1.14	1.09	1.09	1.11	1.12	1.13	1.16	1.22

Table 7. Long-term average recharge values calculated for the period 1997-2016

name	calibration	1min	1max	3min	3max
6_SREMSKA-MITROVICA-GWLcleaned_v10	1,15	1,07	1,26	0,94	1,11

Table 7 shows the historical and future long-term average recharge values calculated using the best performing Metran model and using the data observed at Sremska Mitrovica borehole. It is clear that the highest reduction in recharge values are observed when the 3° Min rainfall and evaporation data are used, while the highest increase in recharge values are observed when the 1° Max rainfall and potential evaporation data are used.

Figure 8 shows the data listed in Table 7. It is clear that in almost all the cases, the recharge values become lower than the historical values when the 1° Min, 3° Min, and 3° Max data are used and they become higher than the historical values when the 1° Max is used. While the reduction in recharge values are expected with the use of the 3° Min and 1° Min change factors as these scenarios represent drier scenarios, the reduction of recharge when the 3° Max comes as a surprise as this is expected to be the wettest scenario. This behaviour could be related to the complex effect of the use of the change factors, which may reduce both the rainfall and potential evaporation at the same period but at different rates. However, additional investigations are required to confirm this behaviour.

The same applies for the groundwater head simulations produced by Metran. Figure 9 shows historical and future long-term groundwater head simulations for Sremska Mitrovica with climate change projections. Here, groundwater levels simulated using the 3° Max change factors fluctuates at a lower levels than those simulated using the 1° Max change factors. This is counter intuitive as the 3° Max scenario is expected to be a wetter scenario than the 1° Max scenario. These results must be treated with care until they are verified by future research work.



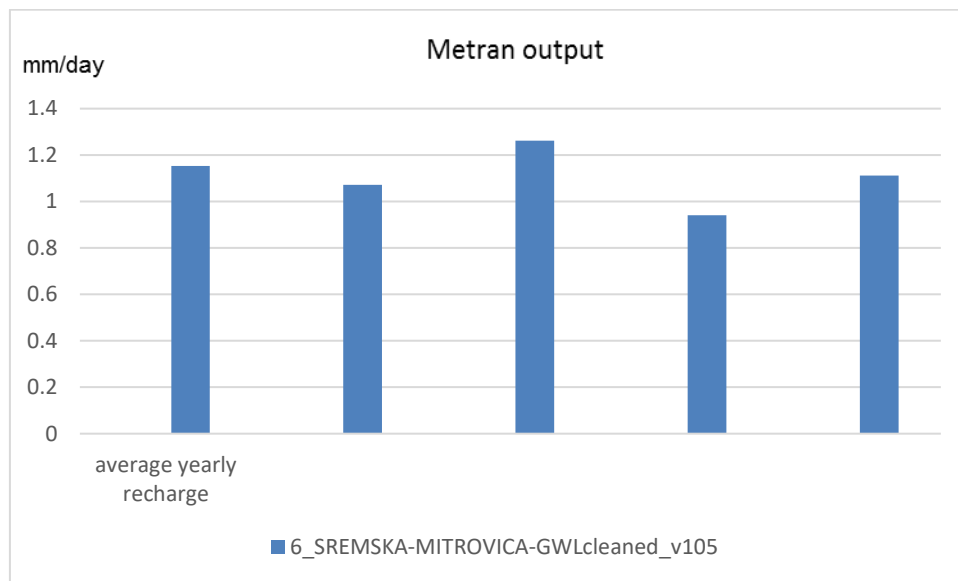


Figure 8. Historical and future recharge projections produced by Metran

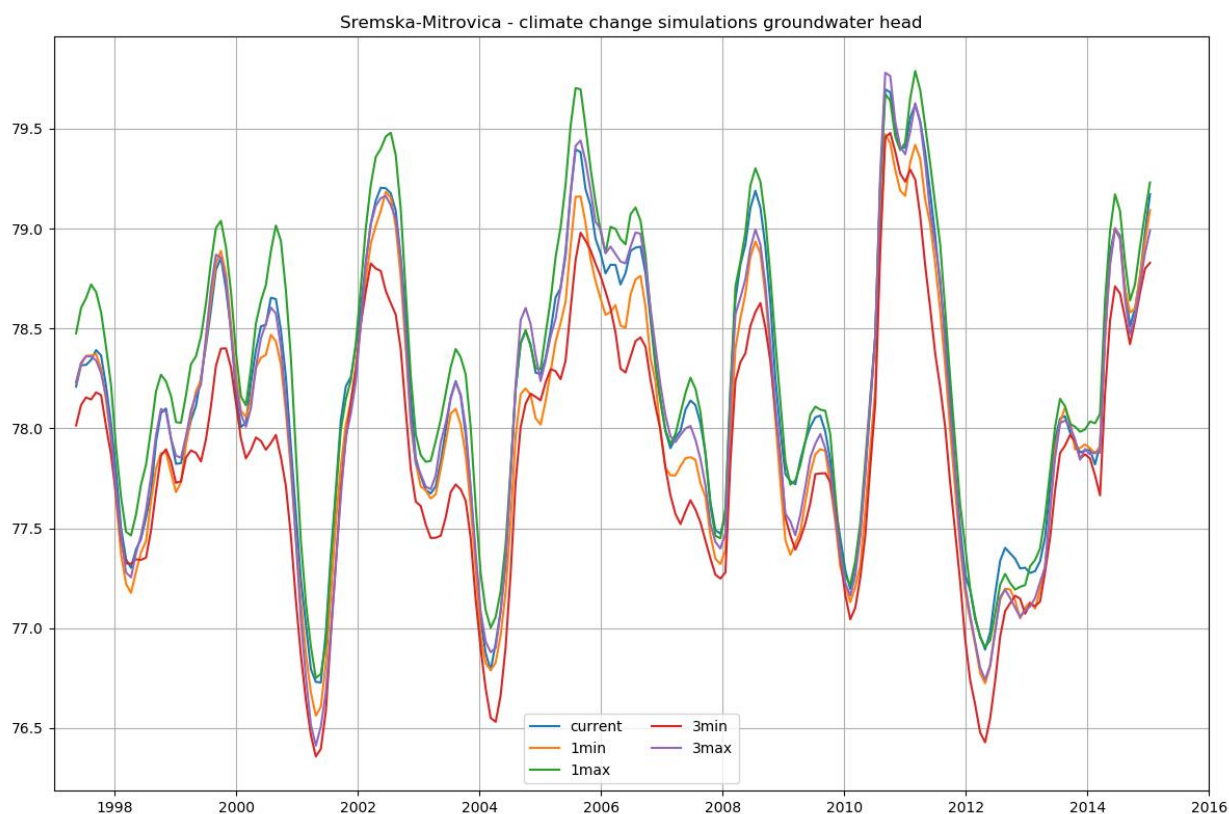


Figure 9. The results of groundwater head time series at Sremska Mitrovica with climate change simulations produced by Metran

REFERENCES

Mackay, J. D., Jackson, C. R., Wang, L. 2014. A lumped conceptual model to simulate groundwater level time-series. *Environmental Modelling and Software*, 61. 229-245. <https://doi.org/10.1016/j.envsoft.2014.06.003>

Mackay, J. D., Jackson, C. R., Wang, L. 2014. *AquiMod user manual (v1.0)*. Nottingham, UK, British Geological Survey, 34pp. (OR/14/007) (Unpublished)

Josipović, J., Soro, A., 2012. *Podzemne vode Vojvodine. Monografija. Institut za vodoprivredu "Jaroslav Černi", Beograd [Groundwater of Vojvodina– in Serbian]*.

Schwartz, U. 2016. *Sava White Book. 'The River Sava: Threats and Restoration Potential.'* Radolfzell/Wien: EuroNatur/Riverwatch

Stojadinović, D., Nikić, Z., Isaković, D., 2005. 'Hydro-geological properties of Sava in the county Obrenovac'. *Proc. Nat. Sci., Matica Srpska Novi Sad*, No. 109, 39-44 UDC 556.33 (497.11 Obrenovac)

Zaadnoordijk, W.J., Bus, S.A.R., Lourens, A., Berendrecht, W.L. (2019) Automated Time Series Modeling for Piezometers in the National Database of the Netherlands. *Groundwater*, 57, no. 6, p. 834-843. <https://onlinelibrary.wiley.com/doi/epdf/10.1111/gwat.12819>

Zingstra, H., Kiš, A., Ribarić A., Ilijaš, I., Jeremić, J., Predić, T. 2010. 'Protection of Biodiversity of the Sava River Basin Floodplains; The relevance of farming and farmland for maintaining the landscape and biodiversity of the Sava floodplains' – Project Report; Wageningen UR Center for Development and Innovation.

Appendix A: AquiMod methodology

AquiMod is a lumped parameter computer model that has been developed to simulate groundwater level time series at observational boreholes (Mackay et al., 2014a). It is based on hydrological algorithms that simulates the movement of groundwater within the soil zone, the unsaturated zone, and the saturated zone. The lumped models neglect complexities included in distributed groundwater models but maintains some of the fundamental physical principles that can be related to the conceptual understanding of the groundwater system (Mackay et al., 2014b).

While AquiMod was originally designed to capture the behaviour of a groundwater system through the analysis of groundwater level time series, it can produce the infiltration recharge values and groundwater discharges from the aquifer as a by-product. AquiMod is driven by complete time series of forcing data for either historical or predicted future conditions. Running AquiMod in predictive mode can be used to fill in gaps in historical groundwater level time series, or calculate future groundwater levels. In addition to groundwater levels, it also provides predictions of historical and future recharge values and groundwater discharges. In the current application we use calibrated AquiMod models to estimate the recharge values at selected boreholes.

AquiMod consists of three modules (Figure A1). The first is a soil water balance module that calculates the amount of water that infiltrates the soil as well as the soil storage. The second module controls the movement of water in the unsaturated zone, mainly it delays the arrival of infiltrating water to the saturated zone. The third module calculates the variations in groundwater levels and discharges. The model executes the modules separately following the order listed above.

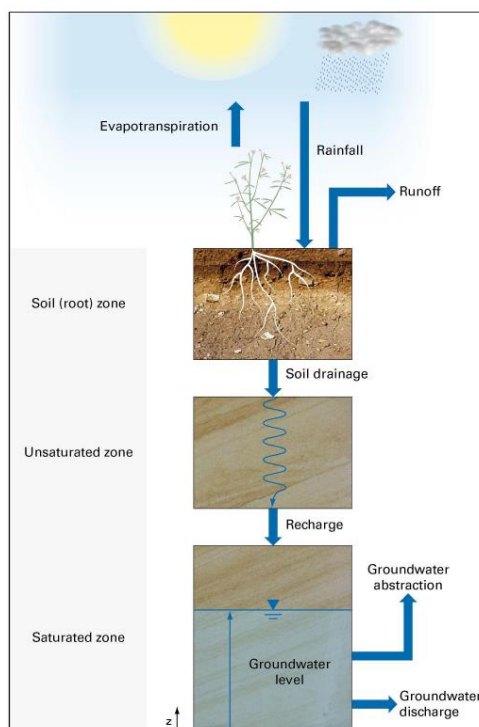


Figure A1 Generalised structure of Aquimod (after Mackay et al., 2014a)

The soil moisture module

There are several methods available in Aquimod that can be used to calculate the rainfall infiltration into the soil zone. In this study we use the FAO Drainage and Irrigation Paper 56 (FAO, 1988) approach. In this method, the capacity of the soil zone, from which plants draw water to evapo-transpire, is calculated first using the plants and soil characteristics. Evapo-transpiration is calculated according to the soil moisture deficit level compared to two parameters: Readily Available Water (RAW) and Total Available Water (TAW). These are a function of the root depth and the depletion factor of the plant in addition to the soil moisture content at field capacity and wilting point as shown in Equations A1 and A2.

$$TAW = Z_r(\theta_{fc} - \theta_{wp}) \quad \text{Equation A1}$$

$$RAW = p \cdot TAW \quad \text{Equation A2}$$

Where Z_r [L] and p [-] are the root depth and depletion factor of a plant respectively, θ_{fc} [L³ L⁻³] and θ_{wp} [L³ L⁻³] are the moisture content at field capacity and wilting point respectively.

The FAO method is simplified by Griffiths et al. (2006) who developed a modified EA-FAO method. In this method the evapotranspiration rates are calculated as a function of the potential evaporation and an intermediate soil moisture deficit as:

$$\begin{aligned} e_s &= e_p \left[\frac{s_s^*}{TAW - RAW} \right]^{0.2} & s_s^* > RAW \\ e_s &= e_p & s_s^* \leq RAW \\ e_s &= 0 & s_s^* \geq TAW \end{aligned} \quad \text{Equation A3}$$

Where e_s [L] is the evapo-transpiration rate, e_p [L] is the potential evaporation rate and s_s^* [L] is the intermediate soil moisture deficit given by

$$s_s^* = s_s^{t-1} - r + e_p \quad \text{Equation A4}$$

Where r [L] is the rainfall at the current time step and s_s^{t-1} [L] is the soil moisture deficit calculated at the previous time step.

The new soil moisture deficit is then calculated from:

$$s_s = s_s^{t-1} - r + e_s \quad \text{Equation A5}$$

Griffiths et al. (2006) proposed that the recharge and overland flow are only generated when the calculated soil moisture deficit becomes zero. The remaining volume of water, the excess water, is then split into recharge and overland flow using a runoff coefficient. In Aquimod a baseflow coefficient is used to reflect the fact that a groundwater discharge is calculated rather than overland water. In this application, the baseflow coefficient is one minus the runoff coefficient.

The unsaturated zone module

The Aquimod version used in this study to simulate the movement of groundwater flow within the unsaturated zone is based on a statistical approach rather than a process-based approach. This method distributes the amount of rainfall recharge over several time steps where the soil drainage for each time step is calculated using a two-parameter Weibull probability density



function. The Weibull function can represent exponentially increasing, exponentially decreasing, and positively and negatively skewed distributions. This can be used to focus the soil drainage over earlier or later time steps or to spread it over a number of time steps after the infiltration occurs. The shape of the Weibull function is controlled by two parameters, k and λ as shown in Equation A6.

$$f(t, k, \lambda) = \begin{cases} \frac{k}{\lambda} \left(\frac{t}{\lambda}\right)^{k-1} e^{-(t/\lambda)^k} & t > 0 \\ 0 & t \leq 0 \end{cases} \quad \text{Equation A6}$$

Where k and λ are two parameters the values of which are calculated during the calibration of the model and t is the time step.

The saturated zone module

AquiMod considers the saturated zone as a rectangular block of porous medium with dimensions L and B as its length and width [L] respectively. This block is divided into a number of layers, each has a defined hydraulic conductivity value, a storage coefficient value, and a discharging feature. The number of layers define the structure of the saturated module used in the study.

The mass balance equation that gives the variation of hydraulic head with time is given by:

$$SLB \frac{dh}{dt} = RLB - Q - A \quad \text{Equation A7}$$

Where:

S is the storage coefficient of the porous medium [-]

h is the groundwater head [L]

t is the time [T]

R is the infiltration recharge [L T⁻¹]

Q is the discharge out of the aquifer [L T⁻¹]

A is the abstraction rate [L T⁻¹]

It must be noted that in a multi-layered groundwater system as shown in Figure A2, we calculate one groundwater head (h) for the whole system. The discharges (Q) from Outlet 1, 2, etc. are calculated using the Darcy law. The total discharges can be summarised using the following equation:

$$Q = \sum_{i=1}^m \frac{T_i B}{0.5 L} \Delta h_i \quad \text{Equation A8}$$

Where:

m is the number of layers in the groundwater system [-]

T_i is the transmissivity of the layer i [L T⁻²]

Δh_i is the difference between the groundwater head h and z_i , the elevation of the base of layer i

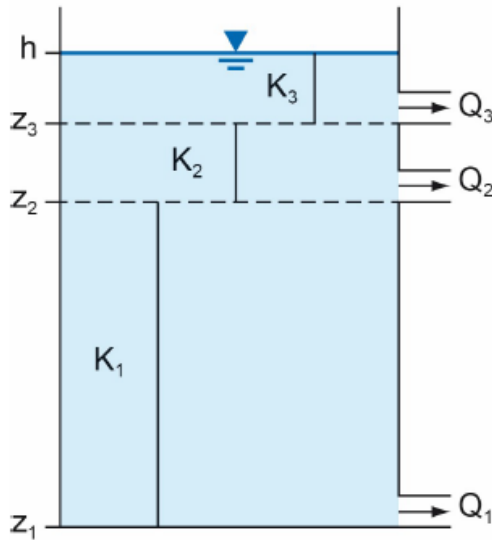


Figure A2 Representation of the saturated zone using a multi-layered groundwater system

Substituting Equation A8 into Equation A7 yields a numerical equation in the form:

$$S \frac{(h-h^*)}{\Delta t} = R - \sum_{i=1}^m \frac{T_i}{0.5 L^2} \Delta h_i - \frac{A}{LB} \quad \text{Equation A9}$$

Equation A9 is an explicit numerical equation that allows the calculation of the groundwater head h [L] at any time and using time steps of Δt [T]. In this equation h^* [L] is the groundwater head calculated at the previous time step and the term Δh_i [L] is calculated as $(h^* - z_i)$.

The terms S , T_i , and L are optimised during the calibration of the model. A groundwater system can be specified with one storage coefficient as shown in the equations above or with different storage coefficient values for the different layers. Several saturated modules are included in AquiMod to provide this flexibility and the model user can select the model structure that represent the conceptual understanding best.

Limitations of the model

AquiMod is a lumped groundwater model that aims at reproducing the behaviour of the observed groundwater levels. It tries to encapsulate the conceptual understanding of a groundwater system in a simple numerical representation. The model results have to be therefore discussed, taking this into consideration. For example, the model represents the groundwater system as a closed homogeneous medium, with no impact from any outer boundary or feature, whether physical or hydrological, such as the presence of rising and falling river stage.

Vertical heterogeneity can be accounted for by using multi-layered groundwater module structure. However, this model setting does not provide any information about the vertical connections between the layers as the discharge from all the layers is calculated using one representative groundwater head value. In other words, it is assumed that all layers are in perfect hydraulic connection.

As mentioned before, the model is designed to simulate the groundwater levels. However, it produces the recharge values and groundwater discharges as by products. In this application we use the calibrated model to calculate recharge. The mass balance equation (Equation A7) shows that recharge is a function of transmissivity and storage coefficient values, which are estimated during the calibration process of the model, i.e. they are not parameters with fixed values provided by the user. The inter-connections between these parameters leads to uncertainties in the estimated recharge values as a high storage coefficient value can produce a high recharge estimate and vice versa. To overcome this problem, it is suggested that the recharge values estimated by Aquimod are always presented as a range of possibilities rather than an absolute value. This can be achieved by estimating the recharge values from all the models that have a performance measure above than a threshold that is deemed acceptable by the user. The recharge estimates can then be presented as an average of all estimates and values corresponding to selected percentiles.

Model input and output

Aquimod includes a number of methods that calculates rainfall recharge as well as a number of model structure from which the user can select what better suits the case study.

Model input consists time series of forcing data including rainfall and potential evaporation, time series of anthropogenic impact mainly groundwater abstraction and time series of groundwater levels that will be used to calibrate the model. These time series must be complete, i.e. a value is available at every time step except the groundwater level time series, which can include missing data. The time step can be one day or multiple of days, and the model automatically calculate the size of the time step based on the input data time series.

The model is run first in calibration mode where a range of parameter values are specified for the different parameters included in the three model modules. A Monte Carlo approach is used to select the best parameter values. The performance of the model is measured by comparing the simulated groundwater levels to the observed ones using the Nash Sutcliff Efficient (NSE) or the Root Mean Squared Error (RMSE) performance measures. The parameter set that produces the best model performance is selected to run the model in evaluation mode.

When the model is run in evaluation mode, it produces output files that give recharge values, groundwater levels and groundwater discharges time series with time as specified in the input file. The number of output files is equal to the number of acceptable models set by the user.

Appendix B: Metran methodology

Metran applies transfer function noise modelling of (groundwater head) time series with usually daily precipitation and evaporation as input (Zaadnoordijk et al., 2019). The setup is shown in the Figure B1. If time series of other influences on the groundwater head are available, these contributions can be added to the deterministic part of the model. The stochastic part is the difference between the total deterministic part and the observations (the residuals). The corresponding input of the noise model should have the character of white noise.

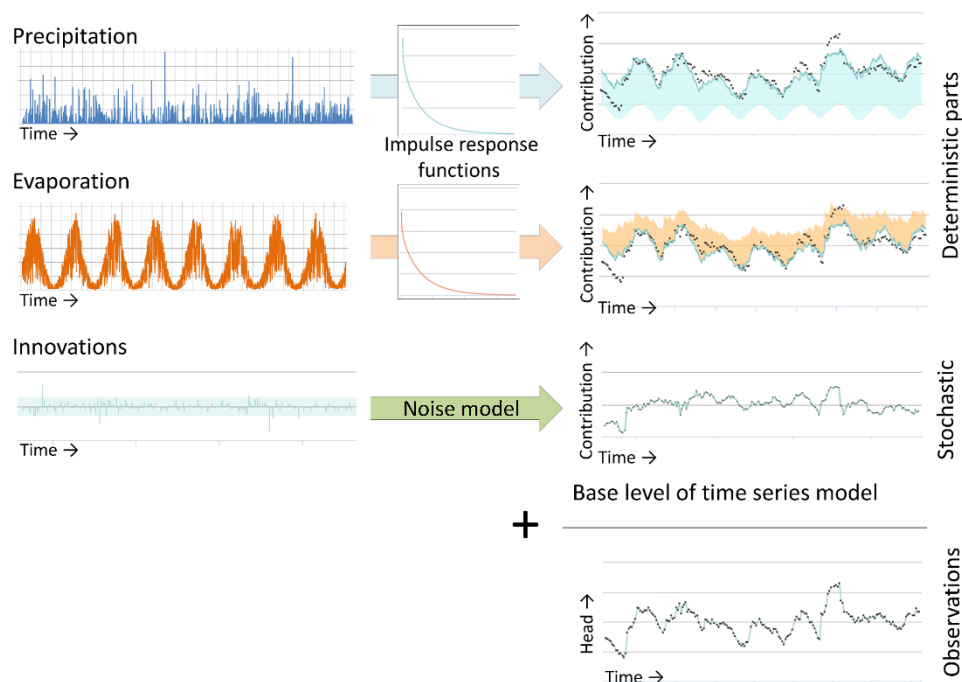


Figure B1 Illustration of METRAN setup

The stochastic part is needed because of the time correlation of the residuals, which does not allow a regular regression to obtain the parameter values of the transfer functions.

The incomplete gamma function is used as transfer function. This is a uni-modal function with only three parameters that has a quite flexible shape and has some physical background (Besbes & de Marsily, 1984). The evaporation response is set equal to the precipitation response except for a factor (f_c). The noise model has one parameter that determines an exponential decay. Thus, for the standard setup with precipitation and evaporation, there are five parameters that have to be determined from the comparison with the observations. Three parameters regarding the precipitation response, the evaporation factor, and the noise model parameter (actually, the time series model has a fifth parameter, the base level, but this is determined from the assumption that the average of the calculated heads is equal to the average of the observations). There are three extra parameters for each additional input series, such as pumping.



Limitations

Metran's time series model is linear. So, the model creation breaks down when the system is strongly nonlinear. This can occur e.g. when drainage occurs for high groundwater levels, when the ratio between the actual evapotranspiration and the inputted reference evaporation varies strongly, or when the groundwater system changed during the simulated period.

Metran is not able to find a decent time series model when the response function is not appropriate for the groundwater system. An example of this is a system with a separate fast and slow response as was found for a French piezometer in the Avre region, as is illustrated in Figure B2.

Finally, the parameter optimization of Metran uses a gradient search method in the parameter space, so it can be sensitive to initial parameter values in finding an optimal solution.

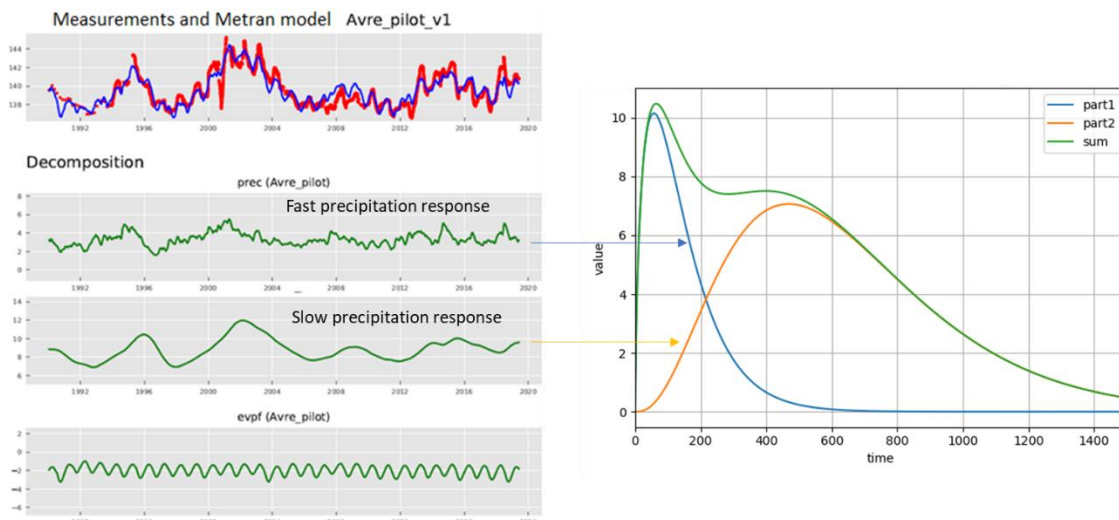


Figure B2. An example where the response function implemented in METRAN is not suitable for the groundwater system

Time step

Metran has been designed to work with explanatory series that have a daily time step. However, it has been adapted so that other time step lengths can be applied; although Metran still has the limitation that the explanatory variables have a constant frequency. For the TACTIC simulations of series with monthly or decadal meteorological input series, the time step has been set to 30 and 10 days, respectively. This time step has been applied from the end date backward.

Note that the heads may be irregular in time as long as the frequency is not greater than the frequency of the explanatory series.

Model output

The evaporation factor f_c gives the importance of evapotranspiration compared to precipitation. The parameter M_0 gives the total precipitation response, which is equal to the area below the impulse response function and the final value of the step response function.



The average response time is another characteristic of the precipitation response. The influence is illustrated in Figure B3 with the impulse response functions and head time series for two models with very different response times for time series of SGU in Sweden.

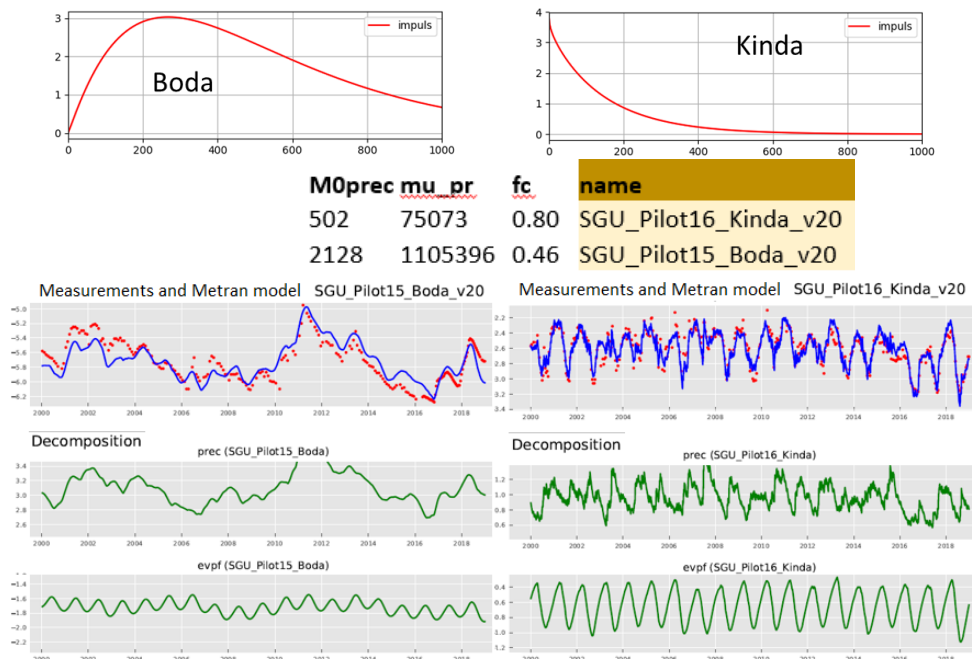


Figure B3 Illustration of Metran output for two case studies in Sweden with different response times.

Model quality

Metran judges a resulting time series model according to a number of criteria and summarizes the quality using two binary parameters Regimeok, Modok (see Zaadnoordijk et al., 2019):

- Regimeok =1 : highest quality
- Modok = 1 (and Regimeok = 0) : ok
- Both zero = model quality insufficient

More detailed information on the model quality is given in the form of scores for two information criteria (AIC and BIC), a log likelihood, R2, RMSE, and the standard deviations and correlations of the parameters.

Recharge

Although the transfer-noise modelling of Metran determines statistical relations between groundwater heads and explanatory variables, we like to think of the results in physical terms. It is tempting to interpret the evaporation factor, as the factor translating the reference into the actual evapotranspiration. Then, we can calculate a recharge as

$$R = P - fE$$

Equation B1



where R is recharge, P precipitation, E evapotranspiration, and f the evaporation factor.

Following the definitions used in the TACTIC project, this recharge R actually is the effective precipitation. It is equal to the potential recharge when the surface runoff is negligible. This in turn is equal to the actual recharge at the groundwater table if there also is no storage change or interflow. In such cases it may be expected that this formula indeed corresponds to the meteorological forcing of the groundwater head in a piezometer, so that it gives a reasonable estimate of the recharge. Obergfell et al. (2019) showed this for an area on an ice pushed ridge in the Netherlands. However, this assumes that all precipitation recharges the groundwater, which cannot be done in many places.

In Dutch polders with shallow water tables and intense drainage networks, it is reasonable to assume that the actual evapotranspiration is equal to the reference value. In that case, the factor f becomes larger than 1 because 1 mm of evaporation has less effect than 1 mm of precipitation (because part of the evaporation does not enter the ground but is immediately drained to the surface water system). In that case, we can calculate recharge as:

$$\begin{aligned} R &= P - fE & f &\leq 1 \\ R &= P/f - E & f &> 1 \end{aligned} \quad \text{Equation B2}$$

These simple formulas can be applied easily for the situations currently modelled in Metran and for the simulations that are driven by future climate data using the delta-change climate factors. However, it is noted that it is a crude estimate using assumptions that are easily violated. Because of this, the equations should be applied only to long term averages using only models of the highest quality.



Deliverable 4.2

PILOT DESCRIPTION AND ASSESSMENT

Sierra de las Nieves aquifer (Spain)

Authors and affiliation:

AJ. Collados-Lara, E. Pardo-Igúzquiza, D. Pulido-Velazquez, L. Baena-Ruiz.

Geological Survey of Spain (IGME)



This report is part of a project that has received funding by the European Union's Horizon 2020 research and innovation programme under grant agreement number 731166.



Deliverable Data	
Deliverable number	D4.2
Dissemination level	Public
Deliverable name	Pilots description and assessment report for Groundwater Recharge and vulnerability
Work package	WP4
Lead WP	BRGM & BGS (WP4)
Deliverable status	
Version	Version 1
Date	14/01/2019

[This page has intentionally been left blank]

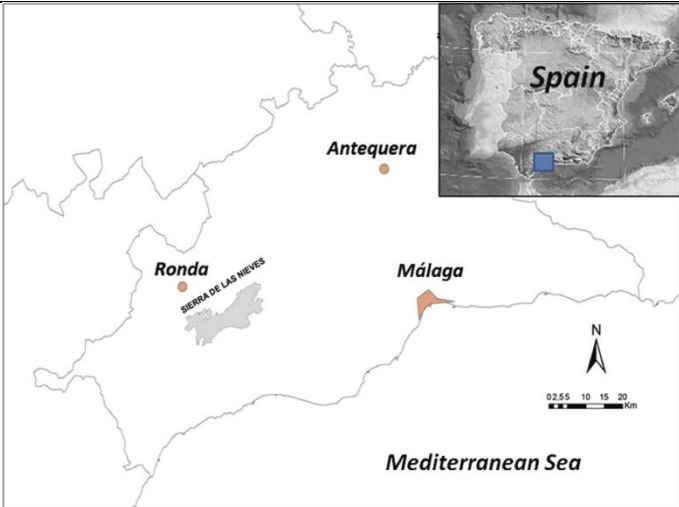
LIST OF ABBREVIATIONS & ACRONYMS

SN	Sierra de las Nieves
----	----------------------

TABLE OF CONTENTS

	LIST OF ABBREVIATIONS & ACRONYMS	5
1	EXECUTIVE SUMMARY	5
2	INTRODUCTION	7
3	PILOT AREA	9
	3.1 Site description and data	9
	3.1.1 Location and extension of the pilot area	9
	3.1.2 Geology/Aquifer type	10
	3.1.3 Topography and soil types	10
	3.1.4 Surface water bodies	12
	3.1.5 Hydraulic head distribution	12
	3.1.6 Climate	13
	3.1.7 Land use	13
	3.1.8 Abstractions/irrigation	14
	3.1.9 Flow balance components	14
	3.2 Climate change challenge	15
4	METHODOLOGY	16
	4.1 Methodology and climate data	16
	4.1.1 Climate data	16
	4.1.2 Generation of local climate scenarios	16
	4.1.3 Recharge model	17
	4.2 Tool(s) / Model set-up /calibration	17
	4.2.1 Generation of local climate scenarios	17
	4.2.2 Recharge model	18
	4.3 Uncertainty	19
5	RESULTS AND CONCLUSIONS	20
	5.1 Impacts of climate change on precipitation and temperature	20
	5.1 Impacts of climate change on recharge	21
6	REFERENCES	23

1 EXECUTIVE SUMMARY

Pilot name	SIERRA DE LAS NIEVES AQUIFER	 <p>Modified from Pardo-Igúzquiza et al., 2015</p>
Country	Spain	
EU-region	Mediterranean region	
Area (km ²)	110	
Aquifer geology and type classification	karstic	
Primary water usage	Nature	
Main climate change issues	The SN high relief karst aquifer is located inside the Natural Park and UNESCO Biosphere Reserve with the same name. This zone is a terrain of great relevance by its geological, geomorphological, hydrogeological and ecological value. It is under near natural hydrological conditions, being the climatic characterized by relatively high rainfall and moderate temperatures. The aquifer contains important water resources and the three main karst springs are the starting points of three important regional rivers: Río Grande, Río Verde and Río Genal. The SN aquifer is located in a Mediterranean high elevation region where the latest studies on climate change forecast important increases in temperature and decreases in precipitation. These changes can provoke important perturbations on the hydrological and hydrogeological cycle in the future which will cause important impacts on the environmental values of the SN aquifer.	
Models and methods used	Generation of local future climate change scenarios following the method proposed in the framework of this project (Collados-Lara et al., 2018) and analysis and discussion of the impact that the changes suggested by the temperature and precipitation future projections can have in the aquifer using recharge models.	
Key stakeholders	Natural Park of SN, UNESCO Biosphere Reserve of SN, Environmental Conservation Groups, visitors of the park	
Contact person	Aj Collados-Lara, E. Pardo -Igurquiza, L. Baena, D. Pulido. IGME (Spain), aj.collados@igme.es.; e. pardo@igme.es; d.pulido@igme.es; l.baena@igme.es;	

The SN aquifer is located in the Mediterranean region of EU, inside the province of Málaga (south Spain). The karst aquifer has an extension of around 110 km². It is a high-relief karst aquifer, which is located in the natural park and UNESCO biosphere reserve of the same name, is an area of great interest due to its geological, geomorphological (both at the surface and underground), hydrogeological and ecological value. The aquifer is not influenced by pumping and is considered to be a natural laboratory for karst research because of how well developed the main karst characteristics are at both the surface (karst depressions and karst springs) and underground (with a large network of caves). The hydrological cycle is sustained by relatively high precipitation (annual mean precipitation of approximately 1000 mm) and moderate temperatures (annual mean temperature of approximately 16 °C). However, these climate parameters are susceptible to significant disruption due to climate change. Note that the mediterranean area, where is located the SN aquifer, is very vulnerable to climate change.

In the SN aquifer we generated local future climate change scenarios of precipitation and temperature and analysed the impact that these changes can have in the aquifer using recharge models. Different climate models have been corrected using several techniques based on two hypotheses, bias correction and delta change approaches. We have focus on the future assessment for the horizon 2071-2100 under the most pessimistic emission scenario (RCP 8.5) contemplated within the last published IPCC report (AR5, 2014). It is expected that there will be, on average, a 27% reduction in precipitation and a 19% increase in temperature. This is a dangerous combination that will dramatically decrease recharge. The mean reductions of recharge vary from 34 % to 63 % for the bias correction approach depending on the RCM considered. In the case of delta change approach the mean reduction vary from 41 % to 59 %. These dramatic decreases expected in recharge will require new strategies for adapting to and mitigating climate change.

2 INTRODUCTION

Climate change (CC) already have widespread and significant impacts on Europe's hydrological systems including groundwater bodies, which is expected to intensify in the future. Groundwater plays a vital role for the land phase of the freshwater cycle and has the capability of buffering or enhancing the impact from extreme climate events causing droughts or floods, depending on the subsurface properties and the status of the system (dry/wet) prior to the climate event. Understanding and taking the hydrogeology into account is therefore essential in the assessment of climate change impacts. Providing harmonised results and products across Europe is further vital for supporting stakeholders, decision makers and EU policies makers.

The Geological Survey Organisations (GSOs) in Europe compile the necessary data and knowledge of the groundwater systems across Europe. To enhance the utilisation of these data and knowledge of the subsurface system in CC impact assessments, the GSOs, in the framework of GeoERA, has established the project "Tools for Assessment of Climate change Impact on Groundwater and Adaptation Strategies – TACTIC". By collaboration among the involved partners, TACTIC aims to enhance and harmonise CC impact assessments and identification and analyses of potential adaptation strategies.

TACTIC is centred around 40 pilot studies covering a variety of CC challenges as well as different hydrogeological settings and different management systems found in Europe. Knowledge and experiences from the pilots will be synthesised and provide a basis for the development of an infrastructure on CC impact assessments and adaptation strategies. The final projects results will be made available through the common GeoERA Information Platform (<http://www.europe-geology.eu>).

The specific TACTIC activities focus on the following research questions:

- What are the challenges related to groundwater- surface water interaction under future climate projections (TACTIC WP3).
- Estimation of renewable resources (groundwater recharge) and the assessment of their vulnerability to future climate variations (TACTIC WP4).
- Study the impact of overexploitation of the groundwater resources and the risks of saline intrusion under current and future climates (TACTIC WP5).
- Analyse the effectiveness of selected adaptation strategies to mitigate the impacts of climate change (TACTIC WP6).

This report describes the work undertaken by the Spanish Geological Survey (IGME) as a part of TACTIC WP4 to assess impacts of climate change on groundwater recharge at the Sierra de las Nieves (SN) karst aquifer (south Spain). WP4 is divided into seven tasks that cover the following activities: Review of tools and methods and identification of data requirements (Task 4.1), identification of principal aquifers and their characteristics aided by satellite data (Task 4.2), recharge estimation and its evolution under climate change scenarios in the principal aquifers (Task 4.3), analysis of long-term piezometric time series to evaluate aquifer vulnerability to climate change (Task 4.4), assessment of subsidence in aquifer systems using



DInSAR satellite data (Task 4.5), development of a satellite based net precipitation and recharge map at the pan-European scale (Task 4.6), and tool descriptions and guidelines (Task 4.7).

The work presented here is related to Task 4.1 and 4.3 and aims to analyze the sensitivity of the potential impacts of climate change on precipitation, temperature, and recharge to different regional climate models (RCMs) and conceptual approaches to generate local scenarios. We used the bias correction and delta change approaches to generate future local scenarios of precipitation and temperature for the lumped area of the Sierra de las Nieves karst aquifer. The time series were generated by using nine RCMs nested to different global climate models (GCMs). These projections were used to assess the impacts of CC on recharge by using a recharge model for diffuse recharge and by employing the changes of precipitation for concentrated recharge.

3 PILOT AREA

The SN is a high relief karst aquifer, which is located in the Natural Park and UNESCO Biosphere Reserve with the same name. This place has great relevance by its geological, geomorphological (both at the surface and underground), hydrogeological and ecological values. The botanical variety inside the Park is impressive (around 1500 types of plants, 19 of them exclusive of the Ronda area. The main protagonist is the pinsapo, a Mediterranean fir which is a botanical relic with the last specimens in these mountains. The Natural Park ecosystem is very dependent of the availability of water which can be reduced in the future due to climate change impacts. Different ensemble and downscaling techniques will be employed to define potential future global change scenarios for the study area based on the data coming from simulations with different Regional Circulation Models (RCMs). For this pilot area we intent to assess future potential impacts of global change scenarios in aquifer recharge.

3.1 Site description and data

3.1.1 Location and extension of the pilot area

The SN aquifer is located in the Mediterranean region of EU, inside the province of Málaga (south Spain) (see Fig.1). The karst aquifer has an extension of around 110 km². The aquifer operates in natural regime and it is considered a natural laboratory for karst research due to the spectacular development of the main karst characteristics as karst depressions, karst springs or caves.

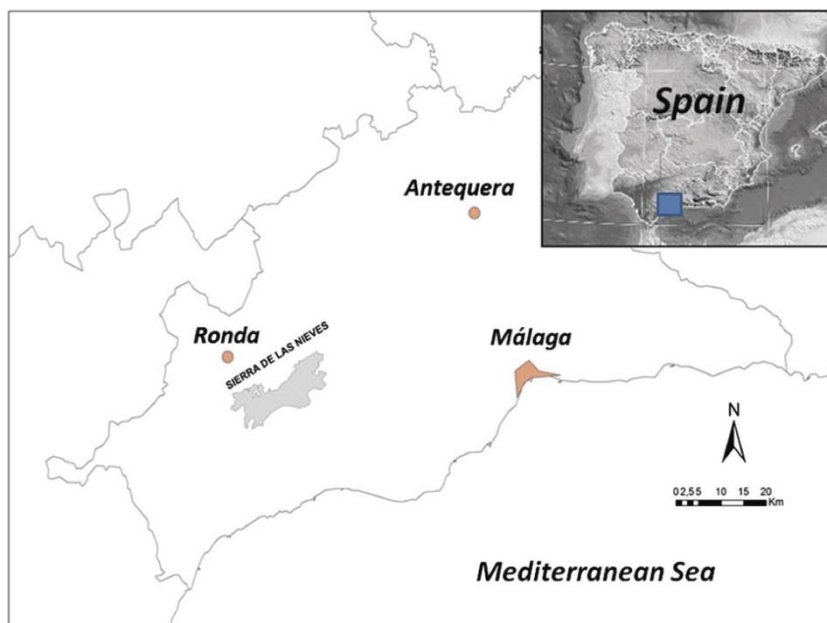


Fig. 1. Location of the pilot area (Modified from Pardo-Igúzquiza et al., 2015)



3.1.2 Geology/Aquifer type

The aquifer is formed mainly by a succession of carbonate rocks: Triassic marbles and dolostones, Jurassic limestones and a Tertiary carbonatic breccia (Fig. 2). The Mesozoic sequence is folded by a NE-SW trending overturned syncline plunging towards the NW (Liñán-Baena, 2005). The carbonatic breccia unconformably overlies the Mesozoic succession but is also deformed by the fold. In this sequence of rocks there is a important Mediterranean high relief karst which forms the aquifer. The conceptual model of the karstified massif can be defined by the existence of two main tectonic blocks: the Nava block in the west and the Torrecilla block in the east. The Torrecilla block has been uplifted (around 500 m) with respect to the Nava block with the Turquillas fault zone separating the two blocks (Fig. 2). In geomorphic terms, the Nava block is the zone of karst depressions and the Torrecilla block is the zone of super-caves.

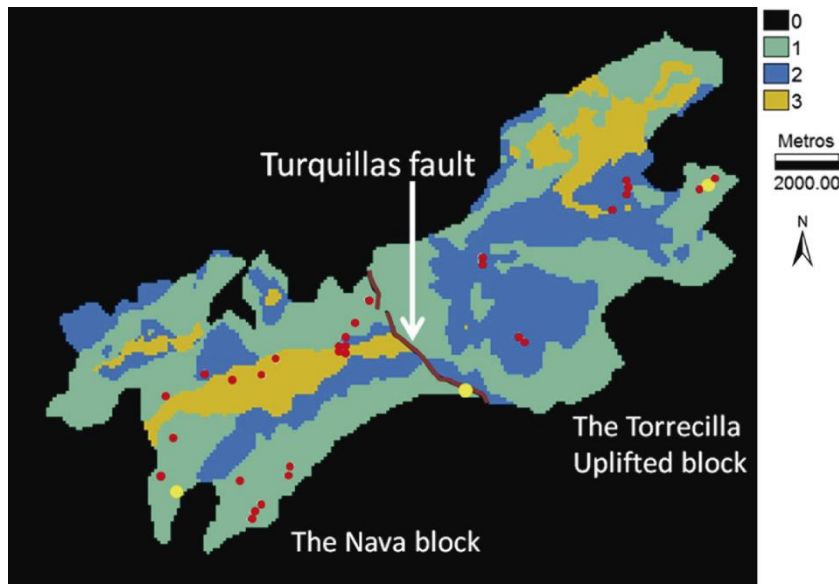


Fig. 2. Geological map of the SN aquifer with the main lithologies: dolostone (1) limestone (2) carbonatic breccia (3). Sampling locations for rock matrix porosity measurement are marked with red dots. Yellow dots show the three main karst springs that discharge the aquifer: Genal, Verde and Grande springs, W–E respectively. (From Pardo-Igúzquiza et al., 2015).

3.1.3 Topography and soil types

The SN aquifer is located in a high elevation zone where the elevation varies from 400 to 1900 m.a.s.l. (see Fig. 3) and the terrain is very rugged. The soils in the aquifer surface are mainly Lithosols, Chromic Luvisols and Rendisins with Calcium Cambisols but other kind of soils can be found around the aquifer (see Fig. 4).



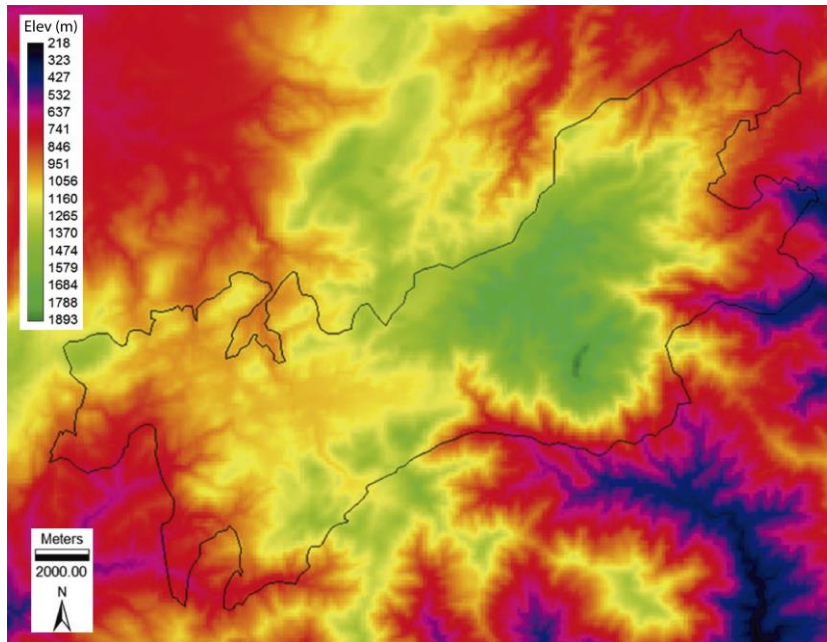


Fig. 3. Topography (Digital Elevation Model map) of the SN aquifer (modified from Pardo-Igúzquiza et al., 2015).

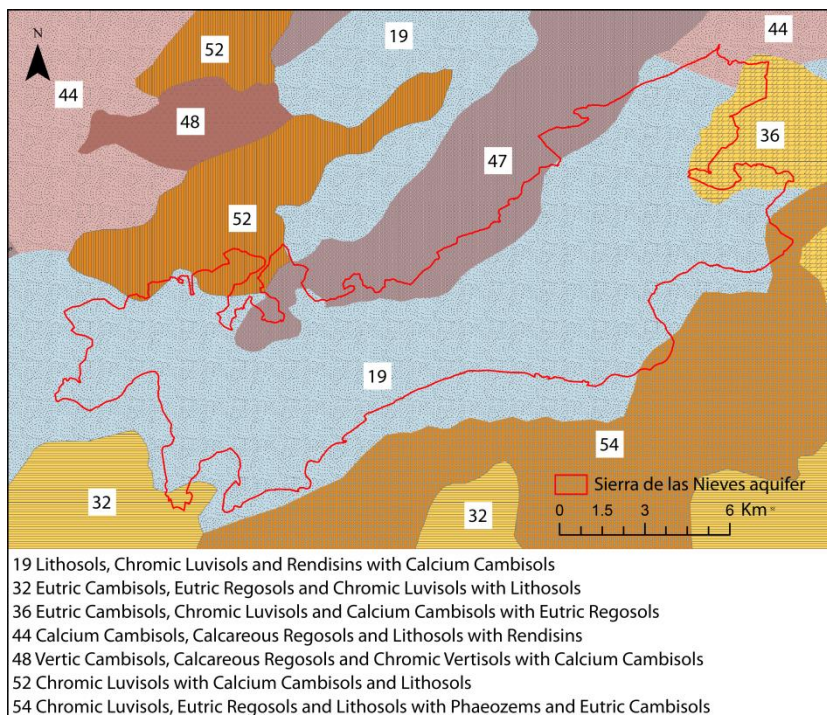


Fig. 4. Soil map of the SN aquifer (Elaborated with data from the Map of Soils of Andalusia at scale 1: 400000 (REDIAM)).

3.1.4 Surface water bodies

The SN Mountain is essential for the water availability in many rivers of the region. In particular, the SN aquifer water contributes to the headwaters of some rivers. The river system related to the SN aquifer is showed in Fig. 5. The aquifer has a great importance for the rivers Grande, Verde and Genal because its springs are associated directly to the SN aquifer.

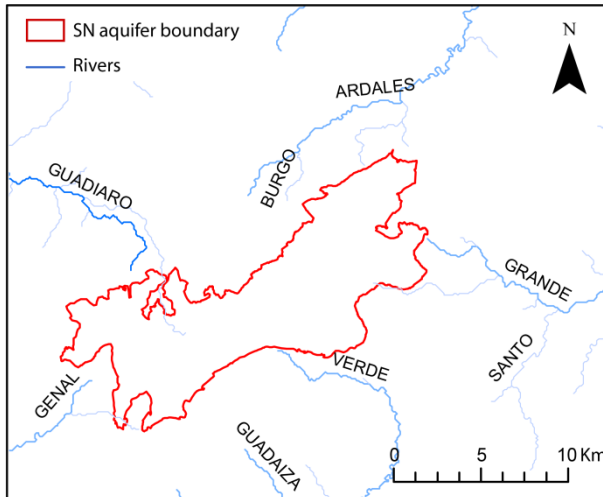


Fig. 5. River system in the SN aquifer region.

3.1.5 Hydraulic head distribution

The piezometric levels in the SN karstic aquifer are monitored in four points (see location in Fig. 6). The three springs of the rivers (Grande, Verde and Genal) and a pothole that reaches water-saturated siphons which is deepest pothole in south Spain, with a vertical variation of minus 1100 m relative to the land surface. The estimated hydraulic head obtained from these data is showed in Fig. 6.

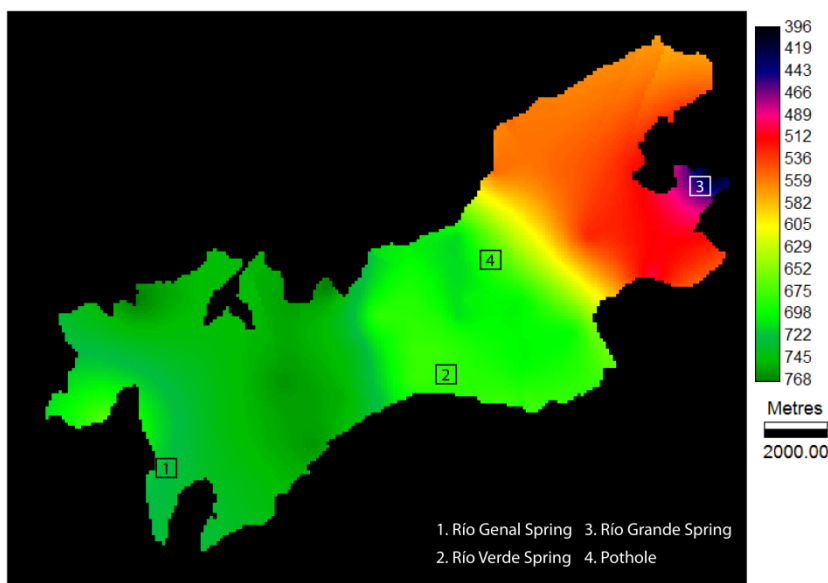


Fig. 6. Estimated hydraulic head map and monitoring points for the SN aquifer (from the research project CGL2015-CGL2015-71510-R from the Ministerio de Economía y Competitividad of Spain).

3.1.6 Climate

The whole Natural Park of SN is located within the zone of Mediterranean climate. Nevertheless, the presence of three essential factors as latitude, influence of the Mediterranean Sea and Atlantic Ocean and the strong variation of elevation provoke many variations in the climate, particularly with respect to the temperatures during the whole year and the abundance of the rainfall. The E-W alignment of the mountains favours the entry of precipitation fronts from the Atlantic Ocean that discharge in the SN due to the high elevation. Most of the rainfall concentrated between November to January. The coldest months are December and January while the hottest months are July and August. The annual mean temperature and precipitation for the period 1971-2000 in the SN aquifer are respectively 15.6 °C and 993 mm/year. The mean values of temperature and precipitation for the different months are showed in Fig. 7.

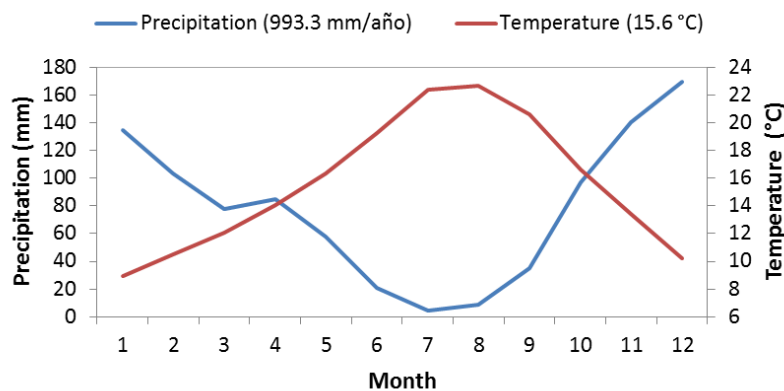


Fig. 7. Mean temperature and precipitation for the SN aquifer in the period 1971-2000 (from Collados-Lara et al., 2017; Data from Spain02 v4 project (Herrera et al., 2016)).

3.1.7 Land use

The SN aquifer is located inside a protected area (Natural Park and UNESCO Biosphere Reserve) where the human influence in the land uses is limited. The main land uses in the aquifer surface are dense trees formations, scrub and grassland formations with trees and open areas with shrubbery or scarce vegetation (see Fig. 8).

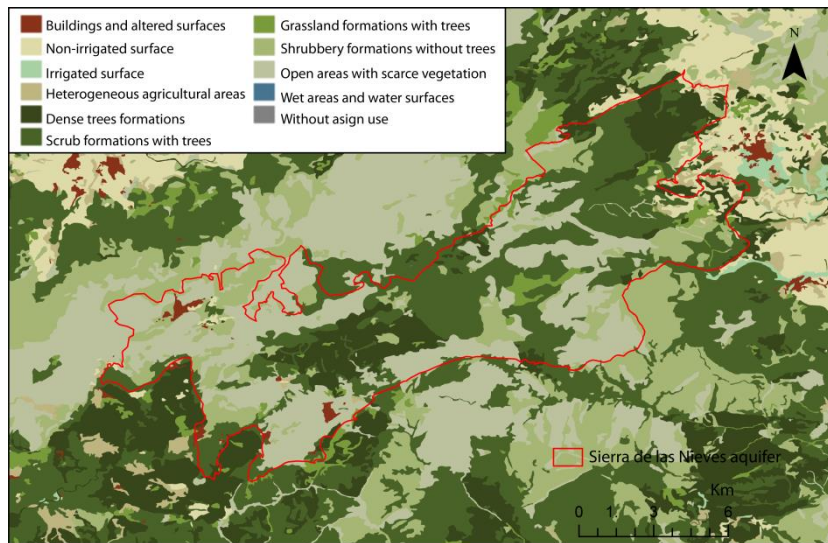


Fig. 8. Land use of the SN aquifer (Elaborated with data from the land use and vegetation cover map of Andalusia in 2007 at a scale of 1:25000 (REDIAM)).

3.1.8 Abstractions/irrigation

As commented previously, the SN aquifer is located in a Natural Park and UNESCO Biosphere Reserve where there is no pumping. The main outputs of the aquifer are the natural discharges to the springs thus the main water usage of the aquifer is the maintenance of natural ecosystems.

3.1.9 Flow balance components

The aquifer which operates in natural regime has as main input the precipitation recharge and the main outputs are the discharges to the springs (Rio Grande, Rio Verde and Rio Genal). Table 1 shows the water balance in the SN aquifer for the hydrological years 1995-1996, 1996-1997 and 1997-1998.

Table 1. Global water balance for the SN karst aquifer for three hydrological years. 1 hm³ is 1 Million Cubic Meters (MCM) (modified from Pardo-Igúzquiza et al., 2012)

	Year 1995-1996	Year 1996-1997	Year 1997-1998
Discharged volume Rio Grande spring (hm ³)	73	55	50
Discharged volume Rio Verde spring (hm ³)	30	24	21
Discharged volume Rio Genal spring (hm ³)	24	17	16
Total discharged volume of the three springs (hm ³)	127	96	87
Discharged volume of other springs (hm ³)	21	16	14
Total discharged volume of all springs (hm ³)	148	112	101
Total volume of rainfall (hm ³)	175	167	148
Annual rainfall (mm)	1710	1638	1452
Modelled recharge volume (hm ³)	146	112	111
Recharge as % of rainfall (%)	66	52	58

3.2 Climate change challenge

In accordance with the EEA map the main expected issues due to climate change in this case study are those described in Fig. 9 for the Mediterranean regions. Existing national estimates show also a significant reduction (around a 19% for the RCP8.5 emission scenario in the horizon 2071-2100) of the aquifer recharge in the area (see Pulido-Velazquez et al., 2017).

The main challenge is to find adaptation measures to reduce the impacts of future climate change scenarios in the aquifer recharge in order to maintain a good status in the Natural Park of SN to conserve the geological, geomorphological, hydrogeological and ecological values of the zone.

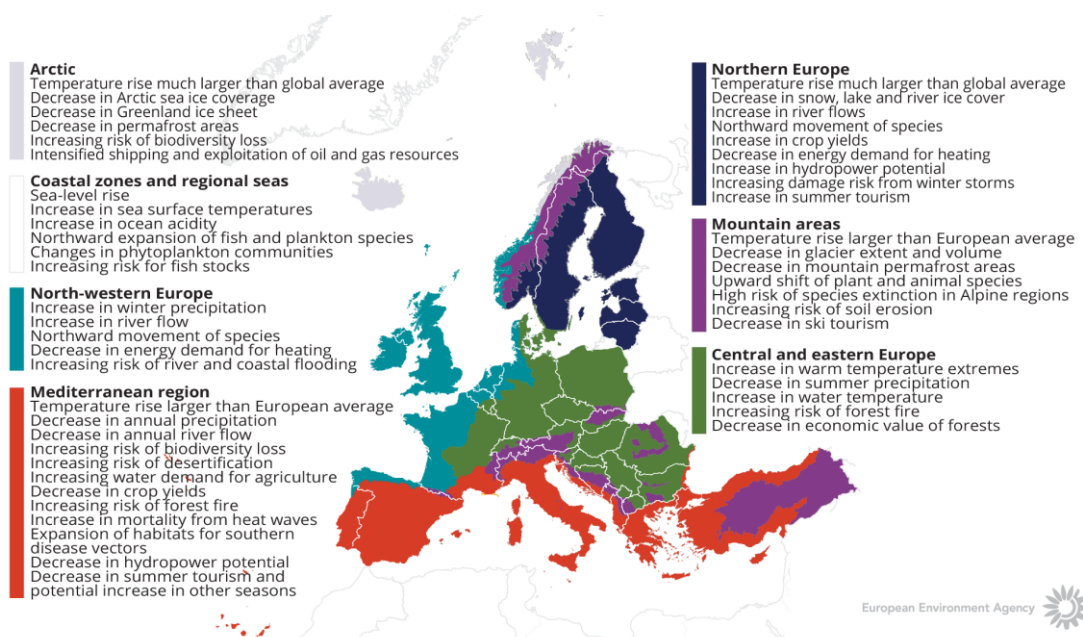


Fig. 9. How is climate expected to change in Europe. The European Environment Agency map

4 METHODOLOGY

The assessment of climate change impacts on recharge in SN aquifer is performed using climate change scenarios generated by using the GROUNDSD tool (Collados-Lara et al., 2020) and the R package qmap (Gudmundsson et al., 2012). To quantify the changes in recharge, the concentrated and diffuse recharge within the karst aquifers has been taken into account.

4.1 Methodology and climate data

4.1.1 Climate data

The historical precipitation and temperature data have been taken from the project Spain02 v4 (Herrera et al. 2016) for the period 1971–2000. Periods of 30 years are frequently employed in climate change impact studies. The Spain02 project provides an estimation of precipitation and temperature obtained using the original data from the Agencia Estatal de Meteorología (State Meteorological Agency—AEMET). The spatial resolution of the data is around 12.5 km and the spatial support is the same than the Euro-CORDEX project, from which the different RCMs were obtained. We used nine RCMs (see Table 2) nested to different GCMs under the most pessimistic scenario of the AR5 of the IPCC, the RCP 8.5, for the period 2071-2100.

Table 2. RCMs and GCMs considered.

RCM \ GCM	CNRM-CM5	EC-EARTH	MPI-ESM-LR	IPSL-CM5A-MR
CCLM4-8-17	X	X	X	
RCA4	X	X	X	
HIRHAM5		X		
RACMO22E		X		
WRF331F				X

4.1.2 Generation of local climate scenarios

For the SN aquifer pilot area two tools were explored. The GROUNDSD tool (Collados-Lara et al., 2020) allows to generate local potential scenarios climatic variables. The tool uses two approaches under different statistical correction techniques (first moment correction, first and second moment correction, and regression) to generate individual local projections and ensembles of them. The qmap tool (Gudmundsson et al., 2012) includes several empirical adjustments of variables originating from climate model simulations using quantile mapping. For both tools, the correction techniques can be used under two approaches, bias correction and delta change. The first applies a transformation function to the control simulation series to force some of its statistics or quantile distribution to get closer to the historical ones. This transformation function is also applied to the future simulation series to obtain the corrected future scenarios. It assumes that the bias between the statistics of historical data and the control simulation will remain invariant in the future. On the other hand, the delta change approach assumes that the relative changes between future simulation and control simulation from regional climate models are accurate and applies these changes to the historical series to obtain the corrected future series.

4.1.3 Recharge model

Recharge in most karst aquifers can be divided into concentrated and diffuse recharge. Concentrated recharge enters the aquifer along preferential flow paths related to underground karst conduits connected to potholes, sinkholes and the epikarst at the surface. Variation in this part of the recharge is due solely to precipitation and thus any modifications to it simply equal the modification in precipitation:

$$\Delta CR = \Delta P. \quad (1)$$

On the other hand, diffuse recharge must go through a soil-epikarst layer and represents a balance between precipitation and actual evapotranspiration which can be written as:

$$R = C(P - AET), \quad (2)$$

where P is precipitation, AET is actual evapotranspiration and C is a coefficient of infiltration that is considered to be constant during the historic and future periods. AET has been calculated at yearly scale by the empirical method proposed by Turc (1954):

$$AET = \frac{P}{\sqrt{0.9 + \frac{P^2}{L^2}}}. \quad (3)$$

Where the factor L is expressed as:

$$L = 300 + 25T + 0.05T^3, \quad (4)$$

where T is the mean annual temperature.

Historical annual recharge is provided by:

$$R_h = C_h(P_h - AET_h), \quad (5)$$

Future recharge is provided by:

$$R_f = C_f(P_f - AET_f), \quad (6)$$

where equation (5) is equal to equation (6) but with the subscript f denoting final or projected values.

The variation in diffuse recharge (ΔDR) is provided by:

$$\Delta DR = \frac{R_f - R_h}{R_h}. \quad (7)$$

Thus, taking into account the previous equations, one has:

$$\Delta DR = \frac{C_f(P_f - AET_f) - C_h(P_h - AET_h)}{C_h(P_h - AET_h)}. \quad (8)$$

Taking into account the hypothesis that the recharge coefficient C does not vary over time, so $C_f = C_h$, finally:

$$\Delta DR = \frac{(P_f - AET_f)}{(P_h - AET_h)} - 1. \quad (9)$$

4.2 Tool(s) / Model set-up /calibration

4.2.1 Generation of local climate scenarios

We used the historical information and regional climate models (see section 4.1.1) to generate local scenarios for the SN aquifer (Fig. 10). In the case of temperature we used a first and second moment correction (GROUNDS tool) and in the case of precipitation an empirical quantile mapping (qmap tool). Both techniques were applied under the bias correction and delta changes approaches. We obtained nine projections (from nine RCMs) for each approach.



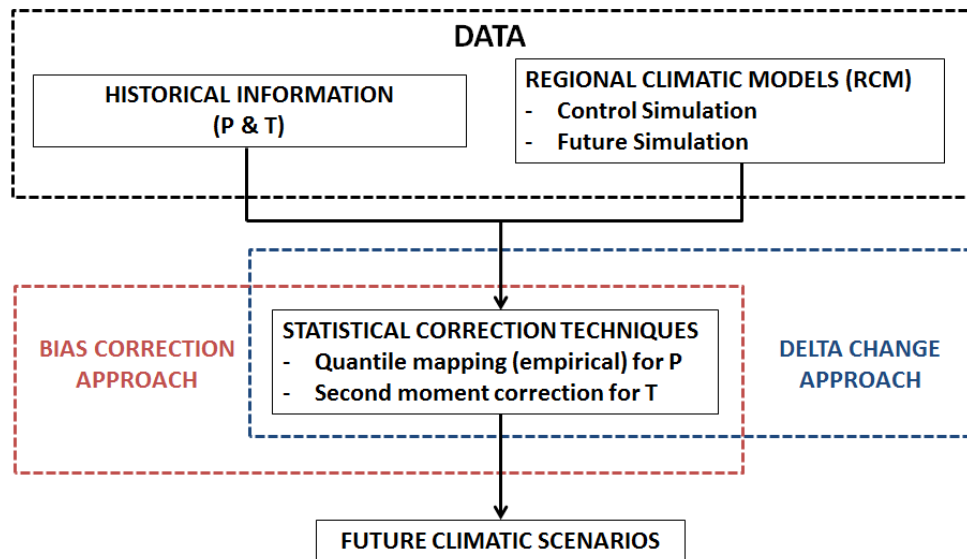


Fig. 10. Flowchart of the methodology used to generate potential future local climate scenarios in SN aquifer (from Pardo-Igúzquiza et al., 2019).

4.2.2 Recharge model

The historical and future climatic variables were used to calculate the changes in concentrated and diffuse recharge by using Equations 1 and 9 respectively (see Fig. 11). The final variation in recharge is a weighted average between the percentage of concentrated and diffuse recharge that takes place in the particular aquifer:

$$\Delta R = \alpha \Delta DR + (1 - \alpha) \Delta CR, \quad (10)$$

where ΔR is the variation in recharge, α is the ratio of diffuse recharge, ΔDR is the variation in diffuse recharge, $(1 - \alpha)$ is the ratio of concentrated recharge and ΔCR is the variation in concentrated recharge.

In the SN karst aquifer α is 0.7. The 30% of the recharge is concentrated and the remaining 70% is diffuse (Pardo-Igúzquiza et al. 2012). It has been assumed that this ratio will remain constant over time.

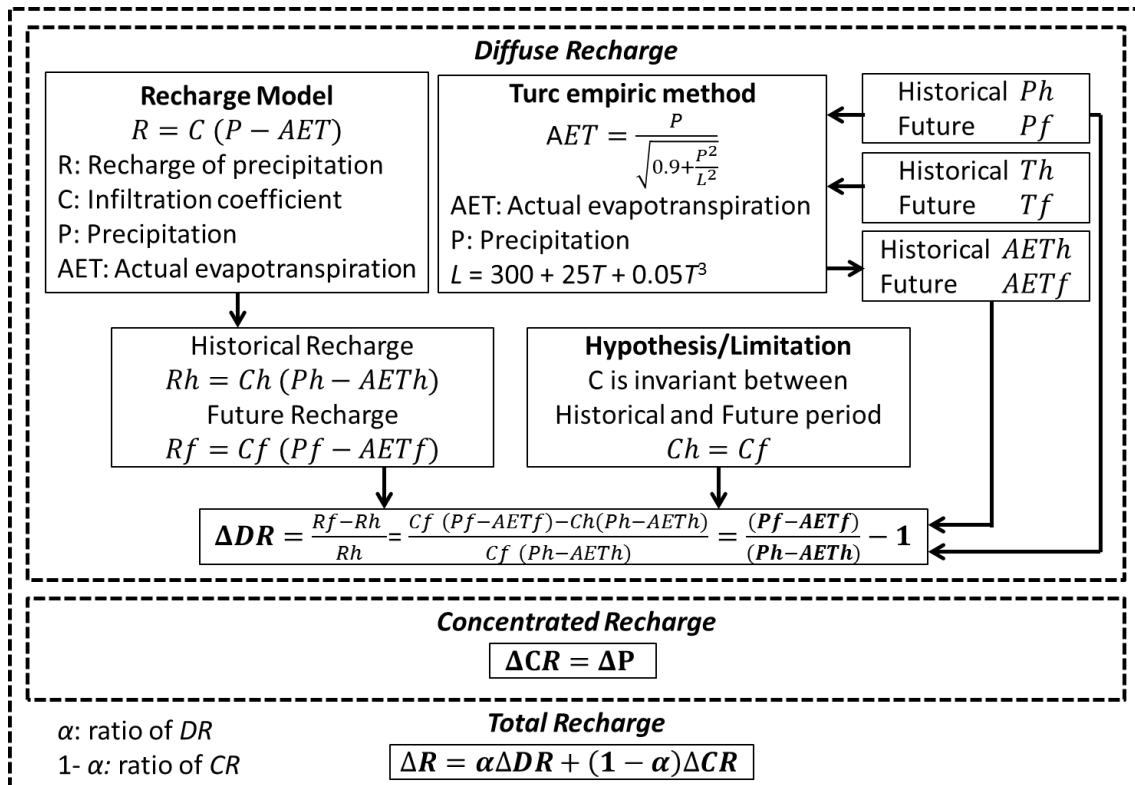


Fig. 11. Flowchart for assessing future changes in aquifer recharge (from Pardo-Igúzquiza et al., 2019).

4.3 Uncertainty

In this study the dominating source of uncertainty is related to RCMs. In general, there is a large degree of uncertainty in climate change impacts assessments. There are different climate models (both RCMs and GCMs) that can be used to make future climate projections. Every climate model includes its own model for the atmosphere, the ocean, the Earth's surface, and ice sheets as well, as different parameterizations of the physical processes that must be considered within each of these models. The correction approaches are another source of uncertainty but its importance in climate change impacts assessments is lower (Collados-Lara et al., 2018).

In this study we considered different RCMs (nine) and two correction approaches to take into account uncertainty. Note that the impacts on recharge was assessed by considering 18 future projections. It allows us to calculate mean changes and the ranges of variability of these changes.

5 RESULTS AND CONCLUSIONS

5.1 Impacts of climate change on precipitation and temperature

The statistics for the future time series generated using the bias correction and delta change approaches are shown in Figs. 12 and 13 respectively. The mean reduction in precipitation is 27.2% and the mean increase in temperature is 19.4%. However, the time series are different depending on the RCM used. Each RCM predicts different future climate changes. The correction technique used also has an influence on these time series. With the first and second moment approach (used for temperature), the same mean values are obtained for the mean and standard deviation in both correction approaches (bias correction and delta change). Note that the monthly time series generated are different for the two approaches. However, the quantile mapping technique generates times series with different mean and standard deviations with the two correction approaches in the case of precipitation. The differences range from 1.3 to 6.7%, which is also not that large. These values increase when sensitivity is measured with respect to the RCM used; in this case, the maximum differences are 0.68% for temperature and 21.0% and 18.2% for precipitation using the bias correction and delta change approaches, respectively. This implies that uncertainty related to the correction approach is low compared to the uncertainty associated to the RCMs.

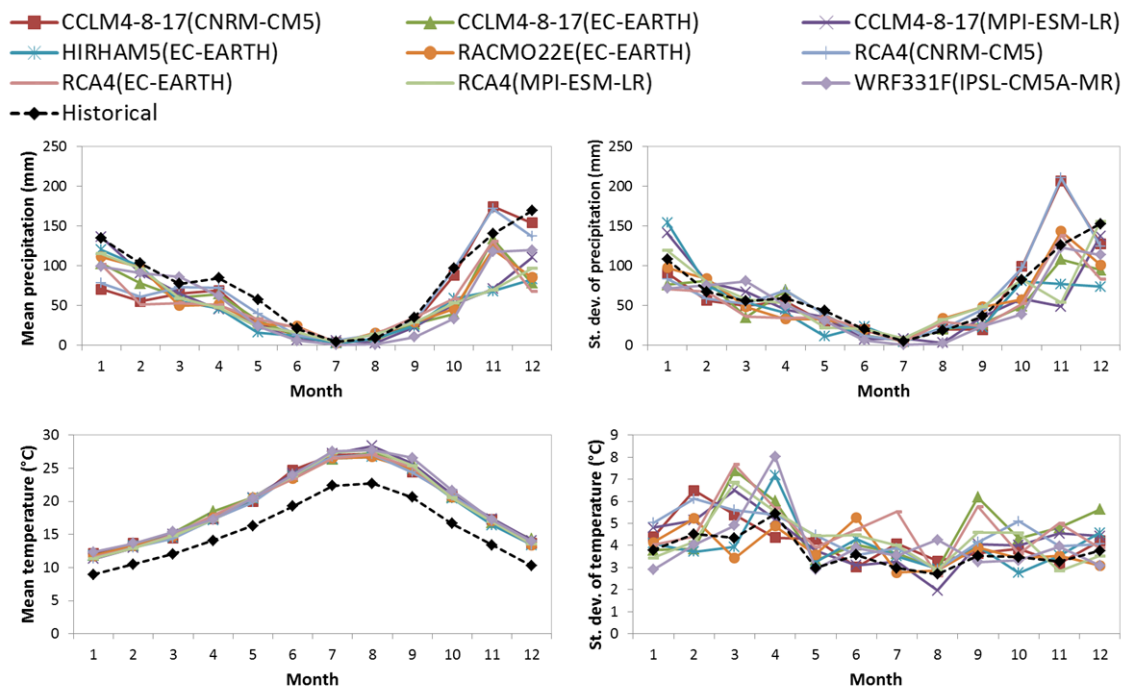


Fig. 12. Mean and standard deviation of the historical and generated future precipitation and temperature time series (bias correction approach) (from Pardo-Igúzquiza et al., 2019).



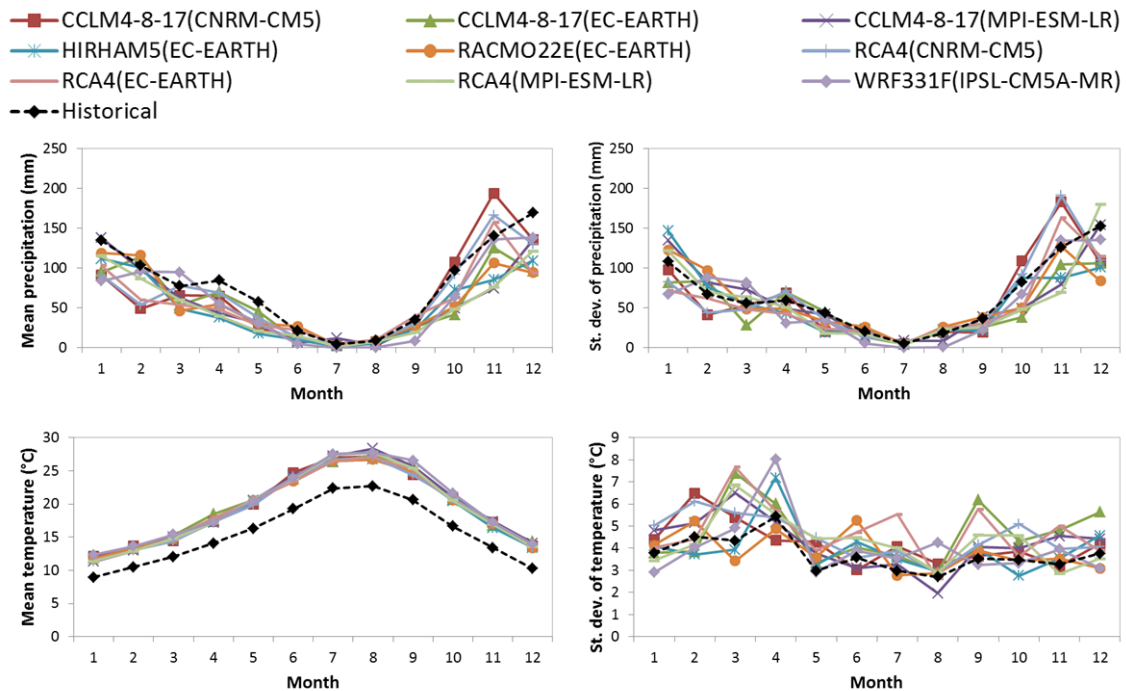


Fig. 13. Mean and standard deviation of the historical and generated future precipitation and temperature time series (delta change approach) (from Pardo-Igúzquiza et al., 2019).

5.1 Impacts of climate change on recharge

The changes of the climatic variables were used to propagate the impacts of climate change to recharge. Table 3 shows the relative changes in precipitation, temperature, and recharge forecasted for the period 2071–2100 as compared to the historical period 1971–2000. The mean reductions of recharge vary from 34 % to 63 % for the bias correction approach depending on the RCM considered. In the case of delta change approach the mean reduction vary from 41 % to 59 %. These dramatic decreases expected in recharge will require new strategies for adapting to and mitigating climate change. Park managers should take the results as a warning sign, and the issue of climate change should be included on their agenda.

Table 3. Relative change (in percentage) of future precipitation (P) and temperature (T) for the bias correction and delta change approaches and the different RCMs employed. The relative change in diffuse recharge (DR) and total recharge (R) has also been calculated (from Pardo-Igúzquiza et al., 2019).

RCM (GCM)	Bias correction				Delta change			
	ΔP (%)	ΔT (%)	ΔDR (%)	ΔR (%)	ΔP (%)	ΔT (%)	ΔDR (%)	ΔR (%)
CCLM4-8-17(CNRM-CM5)	-18.84	19.36	-48.51	-39.61	-16.17	19.36	-51.96	-41.22
CCLM4-8-17(EC-EARTH)	-31.74	19.52	-70.89	-59.15	-26.33	19.52	-66.18	-54.23
CCLM4-8-17(MPI-ESM-LR)	-31.88	19.60	-69.28	-58.06	-26.93	19.60	-62.28	-51.68
HIRHAM5(EC-EARTH)	-36.22	19.13	-74.37	-62.93	-33.08	19.13	-68.65	-57.98
RACMO22E(EC-EARTH)	-29.06	19.20	-69.17	-57.14	-26.50	19.20	-63.68	-52.53
RCA4(CNRM-CM5)	-15.18	19.12	-42.04	-33.98	-17.09	19.12	-53.06	-42.27
RCA4(EC-EARTH)	-33.24	19.26	-72.49	-60.72	-26.54	19.26	-65.39	-53.74



RCA4(MPI-ESM-LR)	-33.04	19.35	-70.43	-59.21	-34.32	19.35	-70.02	-59.31
WRF331F(IPSL-CM5A-MR)	-30.14	19.81	-68.82	-57.22	-23.63	19.81	-64.34	-52.13

6 REFERENCES

Collados-Lara, A.J.; Pulido-Velazquez, D.; Pardo-Igúzquiza, E. (2018). An Integrated Statistical Method to Generate Potential Future Climate Scenarios to Analyse Droughts. *Water*, 10, 1224. doi:10.3390/w10091224.

Collados-Lara, A.J.; Pulido-Velazquez, D.; Pardo-Igúzquiza, E. (2017). Escenarios futuros del cambio climático en el acuífero kárstico de la Sierra de las Nieves (Málaga) a partir de proyecciones de temperatura y precipitación generadas por modelos climáticos regionales. In Calvache, M.L., Duque, C., Pulido-Velazquez, D. (eds) *Impacts of global change on western mediterranean aquifers*. pp. 181 - 187. Universidad de Granada. ISBN 978-84-338-6152-8.

Collados-Lara, A. J., Pulido-Velazquez, D., & Pardo-Iguzquiza, E. (2020). A Statistical Tool to Generate Potential Future Climate Scenarios for Hydrology Applications. *Scientific Programming*. <https://doi.org/10.1155/2020/8847571>

Gudmundsson, L., Bremnes, J. B., Haugen, J. E., & Engen-Skaugen, T. (2012). Technical Note: Downscaling RCM precipitation to the station scale using statistical transformations – A comparison of methods. *Hydrology and Earth System Sciences*. <https://doi.org/10.5194/hess-16-3383-2012>

Herrera, S., Fernández, J., & Gutiérrez, J. M. (2016). Update of the Spain02 gridded observational dataset for EURO-CORDEX evaluation: Assessing the effect of the interpolation methodology. *International Journal of Climatology*. <https://doi.org/10.1002/joc.4391>

Liñan-Baena, C. (2005). Hidrogeología de acuíferos carbonatados en la unidad Yunquera-Nieves (Málaga). In: *Publicaciones del Instituto Geológico y Minero de España. Serie: Hidrogeología y Aguas Subterráneas*, vol 16. Instituto Geológico y Minero de España, Madrid.

Pardo-Igúzquiza, E.; Durán-Valsero, J.J.; Dowd P.A.; Guardiola-Albert, C.; Liñan-Baena, C.; Robledo-Ardila, P.A. (2012). Estimation of spatiotemporal recharge of aquifers in mountainous karst terrains: application to Sierra de las Nieves (Spain). *Journal of Hydrology*, 470–471:124–137. doi: 10.1016/j.jhydrol.2012.08.042.

Pardo-Igúzquiza, E.; Durán, J.J.; Luque-Espinar, J.A.; Robledo-Ardila, P.A.; Martos-Rosillo, S.; Guardiola-Albert, C.; Pedrera, A. (2015). Karst massif susceptibility from rock matrix, fracture and conduit porosities: a case study of the Sierra de las Nieves (Málaga, Spain). *Environmental Earth Sciences*, 74, 7583–7592. doi: 0.1007/s12665-015-4545-x.

Pardo-Igúzquiza, E., Collados-Lara, A. J., & Pulido-Velazquez, D. (2019). Potential future impact of climate change on recharge in the Sierra de las Nieves (southern Spain) high-relief karst aquifer using regional climate models and statistical corrections. *Environmental Earth Sciences*. <https://doi.org/10.1007/s12665-019-8594-4>

Pulido-Velazquez, D.; Collados-Lara, A.-J.; Alcalá, F.J. (2017). Assessing impacts of future potential climate change scenarios on aquifer recharge in continental Spain. J. Hydrol. doi:10.1016/j.jhydrol.2017.10.077.

Turc, L. (1955). Le bilan d'eau des sols : relations entre les précipitations, l'évaporation et l'écoulement. Journées de l'hydraulique.



Deliverable 4.2

PILOT DESCRIPTION AND ASSESSMENT

South East Midlands aquifers (Ireland)

Authors and affiliation:

Taly Hunter Williams, Harrison Bishop, Ross Mowbray, Katie Tedd

Geological Survey Ireland (GSI)

This report is part of a project that has received funding by the European Union's Horizon 2020 research and innovation programme under grant agreement number 731166.



Deliverable Data	
Deliverable number	D4.2
Dissemination level	Public
Deliverable name	Pilots description and assessment report for recharge and groundwater vulnerability
Work package	WP4
Lead WP	BRGM, BGS (NERC)
Deliverable status	
Version	Version 2
Date	28/04/2021

[This page has intentionally been left blank]

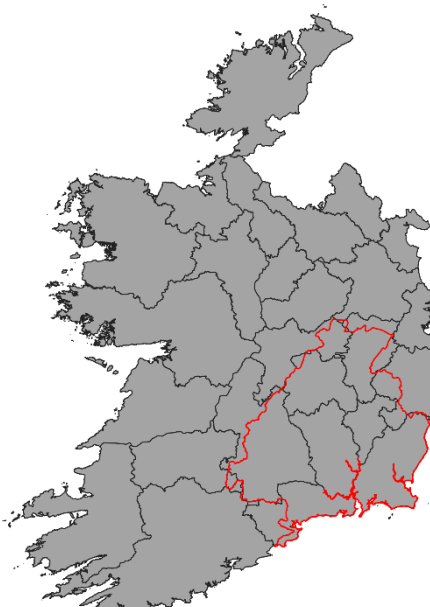
LIST OF ABBREVIATIONS & ACRONYMS

AE or ET_a	Actual Evapotranspiration
DECC	Department of Environment, Climate and Communications
ECMWF	European Centre for Medium-Range Weather Forecast
EPA	Environment Protection Agency
ER	Effective Rainfall
E	evaporation
ET_0 or PE	Reference Evapotranspiration/ Potential Evapotranspiration
f	evaporation factor (for Metran models)
FAO	Food and Agriculture Organisation of the United Nations
GSI	Geological Survey Ireland
ICHEC	Irish Centre for High End Computing
INRM	Irish National Recharge Model
m aOD	meters above Ordnance Datum
m bgl	metres below ground level
MÉRA	Met Éireann ReAnalysis
NWP	Numerical weather prediction
P	precipitation (for Metran models)
R	Rainfall
R	Recharge (for Metran models)
SMD	Soil Moisture Deficit

TABLE OF CONTENTS

LIST OF ABBREVIATIONS & ACRONYMS	5
1 EXECUTIVE SUMMARY	1
2 INTRODUCTION	4
3 PILOT AREA	6
3.1 Site description and data	6
3.1.1 Index boreholes in the pilot area	7
3.1.2 Topography	10
3.1.3 Landuse and Climate	10
3.1.4 Geology	13
3.1.5 Hydrology	14
3.1.6 Hydrogeology	14
3.1.7 Groundwater levels	15
3.2 Climate change challenge	16
4 METHODOLOGY	18
4.1 Methodology and climate data	18
4.1.1 AquiMod	18
4.1.2 GARDENIA	18
4.1.3 Metran	20
4.1.4 Irish Groundwater Recharge Method	21
4.1.5 Climate data	22
4.1.6 Tool(s) / Model set-up	25
4.2 Initialization	33
4.3 Tool(s)/ Model calibration/ test	33
4.3.1 Observation data	33
4.3.2 Calibration of AquiMod models	38
4.3.3 Calibration of GARDENIA models	38
4.3.4 Calibration of Metran models	40
4.3.5 Calibration of Irish Groundwater Recharge model	42
4.4 Uncertainty	43
5 RESULTS AND CONCLUSIONS	45
5.1 Historical recharge values	45
5.2 Projected recharge values	52
6 REFERENCES	62
7 ACKNOWLEDGEMENTS	65
APPENDICES	66

1 EXECUTIVE SUMMARY

Pilot name	SE Midlands aquifer	
Country	Ireland	
EU-region	North-western Europe	
Area (km ²)	13,188	
Aquifer geology and type classification	<p>The principal aquifers of interest are</p> <p>(i) pure, bedded limestones: secondary porosity diffusely karstified bedrock aquifers. Groundwater flows within a network of solutionally enlarged fractures and occasional conduits. Some areas are dolomitised giving secondary intergranular porosity. Yields are typically of the order of 5-20 l/sec.</p> <p>(ii) sand/gravel aquifers, where flow and storage is primary intergranular. Yields range from 2.5-15 l/sec.</p> <p>For context: other regionally important aquifers are fissured volcanic rocks with secondary permeability only, and sand/gravel aquifers, where flow and storage is primary intergranular. Minor aquifers are all secondary porosity/permeability fissured bedrock. Over much of the karst limestone, subsoil cover is medium permeability. In parts of the SE of the study area, subsoils are thick and low permeability.</p>	
Primary water usage	Drinking water / Agri-Industry.	
Main climate change issues	Increase in water abstraction over time – irrigation, livestock. Risk of drought. Other issues = water table rebound after mines closures.	
Models and methods used	Conceptual model, Time series analysis (local), satellite (exploratory)	
Key stakeholders	Government. Water companies. Research institutes. Industry. Farming.	
Contact person	Geological Survey Ireland. Taly Hunter Williams .	

This report describes the work undertaken by Geological Survey Ireland (GSI) as a part of TACTIC WP4 to calculate historical and future groundwater recharge in the catchment to selected observation boreholes in the south-east of Ireland. Multiple tools, selected from the TACTIC toolbox that is developed under WP2 of the TACTIC project, have been used for this purpose.

The south-east region encompasses four Regionally-important aquifer types, two of which are assessed in this study, as well as minor aquifers:

(1) karst aquifers are significant in south-east Ireland. These aquifers comprise pure, bedded limestones with zero primary porosity and permeability, but with well-developed and interconnected fracture networks and solution enhancement fractures. In some areas, these aquifers are bedded and massive limestones that have been dolomitised, resulting in patchy secondary intergranular porosity development. The karstified limestones occupy low-lying areas between non-karst hills, and are characterised by an extensive, well-drained rolling landscape. In parts of the area, depending on the orientation of the 'grain' and the river network, karst limestones can occur in relatively narrow river valleys. Much of the aquifer is overlain by glacial deposits of the late Quaternary. These are typically well-drained, and groundwater within the aquifer is mostly unconfined or part-confined. Some areas are overlain by thick low permeability tills (diamicts) or post-glacial peats, and are confined.

(2) large glacio-fluvial sands and gravels form significant groundwater resources in the pilot area. These primary porosity and intergranular permeability sand and gravel aquifers overlie the bedrock. Grain size distribution can be broad, with complex internal sedimentary architecture, but the deposits are characterised by high permeabilities and porosities. The majority of the aquifers are found along major rivers, although large glacial outwash fans also occur.

Land use over the karst aquifers is primarily dairying within enclosed fields, lesser tillage (crops), limited woodland, harvested peat, and relatively small built-up areas. Over the less productive aquifers, tillage dominates, with forestry in upland areas.

Groundwater from the Regionally important aquifers provides up to 90% of the public water supply in some counties within the region, and is important for agricultural and other private uses. These aquifers tend to occur in the lowlands, whereas the Locally important fissured aquifers tend to underlie higher ground. One groundwater level monitoring station from the poorer aquifers has been assessed as part of this study.

Four tools have been used to estimate the recharge values. These are the lumped parameter computer model Aquimod (Mackay *et al.*, 2014a), the transfer function-noise model Metran (Zaadnoordijk *et al.*, 2019), GARDENIA (Thiéry, 2013), and the spatially-distributed groundwater recharge model map (Hunter Williams *et al.*, 2013). Future climate scenarios are developed based on the ISIMIP (Inter Sectoral Impact Model Inter-comparison Project (www.isimip.org) datasets. The resolution of the data is 0.5° x 0.5° global grid and at daily time steps. As part of ISIMIP, much effort has been made to standardise the climate data (e.g. bias correction).

The long term average (LTA) historical recharge calculated for each borehole shows little correlation between AquiMod, GARDENIA and Metran. One observation station (Freshford) showed an order of magnitude difference between estimates. The smallest variation is a factor of two (Borrismore Creek). AquiMod and the Irish Groundwater Recharge model were consistent most frequently, although there wasn't a consistency of similarity/difference between models across all of the groundwater monitoring stations. The model which consistently calculates the highest recharge value is Metran which, in most cases, is roughly 10-20 mm/month greater than the next highest model. Most of the LTA recharge values calculated from GARDENIA boreholes are lower than those calculated from AquiMod, with two exceptions (Freshford and Vickerstown) which are both much higher than the recharge values from AquiMod.

These differences are perhaps not surprising, due to the different approaches and different catchment sizes modelled by AquiMod and GARDENIA, as well as the differences in how the models operate and how they calculate recharge. In the case of GARDENIA, it was difficult to find river flow data appropriate for the groundwater monitoring points used, and it might be that Irish catchments are heterogeneous on a scale that is too fine relative to the density of hydrometric data. Furthermore, due to time constraints within the study, the simplest model structures were used for AquiMod (1 layer) and GARDENIA (1 groundwater reservoir).

The difference between recharge estimates does pose a difficulty in deciding which is the 'right' value but, on the other hand, highlights the uncertainty in deriving recharge estimates and may also indicate where improvements in model set-up and hydrogeological representation are required.

Future recharge values were calculated using AquiMod, GARDENIA and Metran.

All three models show the greatest increase in recharge values observed across all boreholes when the 3°C max scenario data are used (excluding the anomalous projected values for Borrismore Creek, BMC), with the exception of Freshford (Metran) which shows a 10.4% decrease in recharge.

The greatest reduction in recharge values are observed in:

- AquiMod: the 3°C min scenario, with the exception of Freshford which displays a 5.3% increase in recharge. s.
- GARDENIA: the 3°C min scenario
- Metran: the 3°C min scenario, with values ranging from -4.0% to -22.7%.

Future estimates are discussed in this report using long term average recharge values. It is recommended to carry out further analyses of these outputs in order to understand the temporal changes in recharge values in future, especially over the different seasons. In addition, it is recommended that the values and conclusion produced from this work should be compared to those obtained from different studies that apply future climate data obtained from different climate models. Future climate change scenarios will be applied to the Irish Groundwater Recharge model.

2 INTRODUCTION

Climate change (CC) has already had widespread and significant impacts in Europe, which is expected to increase in the future. Groundwater plays a vital role for the land phase of the freshwater cycle and have the capability of buffering or enhancing the impact from extreme climate events causing droughts or floods, depending on the subsurface properties and the status of the system (dry/wet) prior to the climate event. Understanding and taking the hydrogeology into account is therefore essential in the assessment of climate change impacts. Providing harmonised results and products across Europe is further vital for supporting stakeholders, decision makers and EU policies makers.

The Geological Survey Organisations (GSOs) in Europe compile the necessary data and knowledge of the groundwater systems across Europe. In order to enhance the utilisation of these data and knowledge of the subsurface system in CC impact assessments the GSOs, in the framework of GeoERA, has established the project “Tools for Assessment of Climate change Impact on Groundwater and Adaptation Strategies – TACTIC”. By collaboration among the involved partners, TACTIC aims to enhance and harmonise CC impact assessments and identification and analyses of potential adaptation strategies.

TACTIC is centred around 40 pilot studies covering a variety of CC challenges as well as different hydrogeological settings and different management systems found in Europe. Knowledge and experiences from the pilots will be synthesised and provide a basis for the development of an infra structure on CC impact assessments and adaptation strategies. The final projects results will be made available through the common GeoERA Information Platform (<http://www.europe-geology.eu>).

The specific TACTIC activities focus on the following research questions:

- What are the challenges related to groundwater- surface water interaction under future climate projections (TACTIC WP3)?
- Estimation of renewable resources (groundwater recharge) and the assessment of their vulnerability to future climate variations (TACTIC WP4).
- Study the impact of overexploitation of the groundwater resources and the risks of saline intrusion under current and future climates (TACTIC WP5).
- Analyse the effectiveness of selected adaptation strategies to mitigate the impacts of climate change (TACTIC WP6).

The present document reports the TACTIC activities in the Irish midlands and South-east pilot area undertaken by Geological Survey Ireland (GSI) as part of WP4.

WP4 is divided into seven tasks that cover the following activities: Review of tools and methods and identification of data requirements (Task 4.1), identification of principal aquifers and their characteristics aided by satellite data (Task 4.2), recharge estimation and its evolution under climate change scenarios in the principal aquifers (Task 4.3), analysis of long-term piezometric time series to evaluate aquifer vulnerability to climate change (Task 4.4), assessment of subsidence in aquifer systems using DInSAR satellite data (Task 4.5),

development of a satellite based net precipitation and recharge map at the pan-European scale (Task 4.6), and tool descriptions and guidelines (Task 4.7).

Two different works are presented in this report and they are related to Task 4.3 and Task 4.4.

The pilot area is in the SE part of Ireland, and comprises the river basins of the Suir, Nore, Barrow and Slaney rivers, as well as a number of smaller coastal rivers. It also incorporates small parts of other river catchments where certain aquifers extend over catchment boundaries.

The main aquifers of interest within the pilot area are (1) the diffusely karstified limestone aquifer and (2) the extensive sands and gravels aquifers. The karst aquifers occupy the valleys and lowlands and are used for several major public drinking water abstractions, for agriculture, and for industrial abstractions. There are also two lead-zinc mines in the aquifer that have been closed, and groundwater levels are now rebounding. Sands and gravels are mainly found along the major rivers, but also occur as extensive 'domes'. They are used for public drinking water supplies and for private abstractions. Groundwater from these principal aquifers supports river flows to a significant extent.

Other aquifers, both major and minor, are however also of interest for representativity for the rest of Ireland. The other major aquifers in the area include a fissured volcanic rock aquifer and a productive dual porosity sandstone aquifer. The remainder of the area is underlain by poor and locally important fissured aquifers. In general, the karst limestone aquifers are coincident with the valleys, and the glacio-fluvial sand and gravel aquifers lie along the principal rivers. The higher ground is formed by more resistant bedrock that typically comprise poor or only locally important aquifers.

The southeast of Ireland is a relatively dry and warm region within the Irish cool temperate climatic zone. Annual mean rainfall is 800–1000 mm in the lowlands, which is the area occupied by the main aquifers of interest in the study area. The annual potential evapotranspiration varies spatially between 450 mm and in excess of 500 mm. Therefore, effective rainfall is (for Ireland) low, at approximately 250-400 mm/yr.

The area is, therefore, one for which concerns currently exist about water resources availability, and it anticipated that this area will become progressively water stressed under future climate change scenarios (e.g. Hunter Williams and Lee, 2007; Ball, 2010).

The work undertaken in the pilot area will build on the study by Tedd *et al.* (2012), which examined groundwater level variations to ascertain aquifer response to rainfall, and tried to determine whether there was evidence of climate change impacts. It is hoped that analysis of data and inferences and results from the pilot area will be used to improve the current Irish national groundwater recharge map (Hunter Williams *et al.*, 2013). As part of the study, an updated 30 year average groundwater recharge map using current recharge coefficients was produced, which will be used for climate change scenarios in the future.

3 PILOT AREA

3.1 Site description and data

The pilot area is in the SE part of Ireland, and comprises the river basins of the Suir, Nore, Barrow and Slaney rivers, as well as a number of smaller coastal rivers (**Figure 1**). It also takes in a small area of the adjacent river catchments in some places where limestone aquifer units cross catchment boundaries in the north of the area. The Suir, Nore and Barrow rivers converge into Waterford estuary; the Slaney river flows into Wexford estuary.

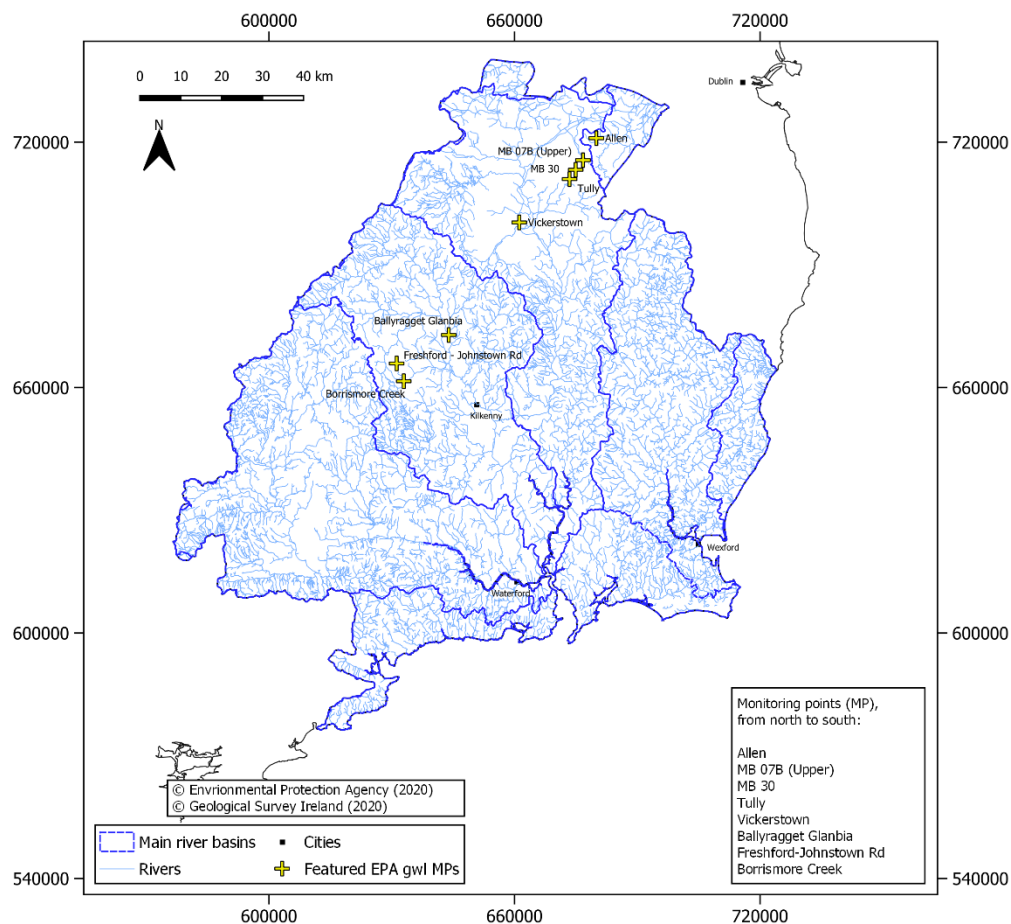


Figure 1. Pilot area in the SE of Ireland

The study area is bounded to the NE, NW and SW by mountain ranges (elevation up to 920 m aOD (metres above Ordnance Datum)), and to the E, SE and S by the coast. Within the study area the Castlecomer Plateau and the Slieveardagh Hills (up to 600 m aOD) separate two NE–SW-trending lowlands areas, which are occupied by karst limestone and glacio-fluvial gravel aquifers.



Within the pilot area as a whole, the principal aquifers of interest are the karstified (and sometimes dolomitised) limestones that occupy the lowland areas, and the extensive sands and gravels that follow the main rivers, and also occur as topographic domes (**Figure 2**).

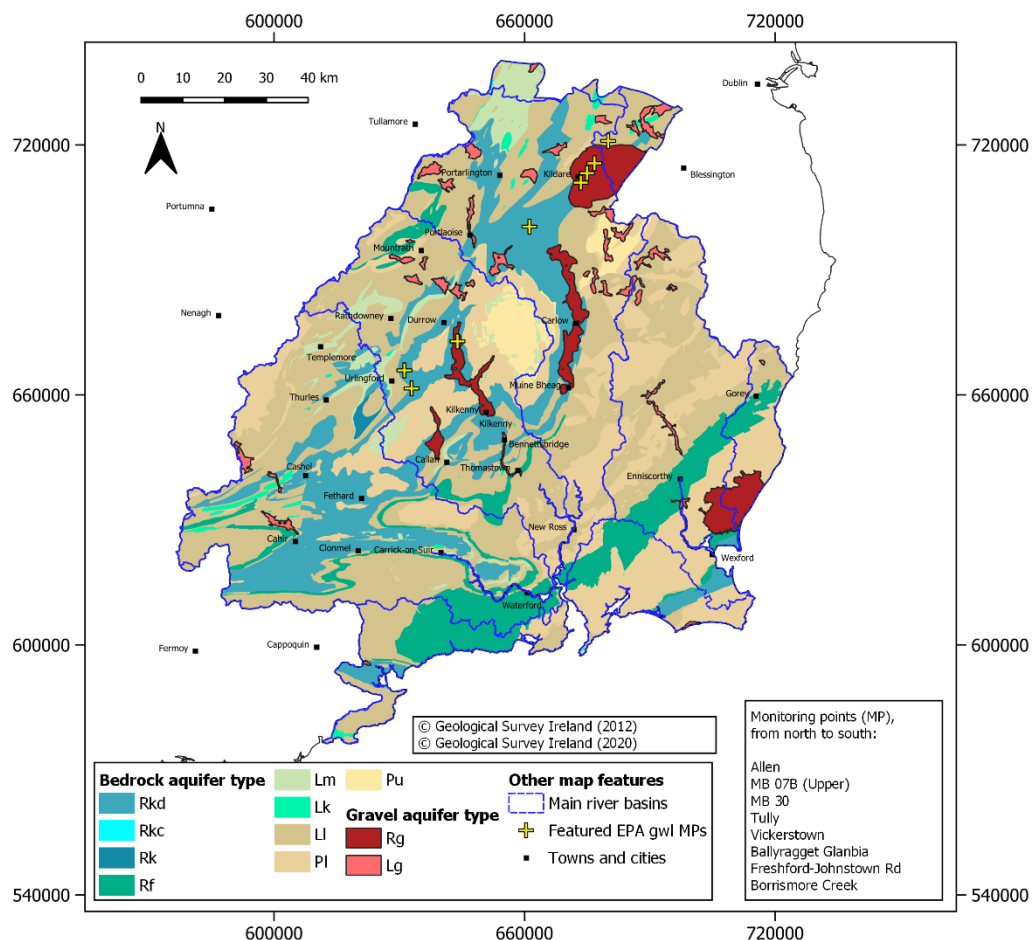


Figure 2. Aquifers in the pilot area and locations of selected observation boreholes. The main aquifers of interest are the karst (Rk, Rkc, Rkd) and extensive sand and gravel (Rg) aquifers.

3.1.1 Index boreholes in the pilot area

Diffusely karstified limestone aquifers are important in the midlands and SE, and supply the whole of Co. Laois public water supply network. They are also important for the neighbouring counties of Kilkenny and Carlow. The aquifer comprises pure, bedded limestones that have been folded and fractured. These fissures have been enlarged through the solution of limestone by percolating recharge and flowing groundwaters. Whilst some conduits have developed and caves are known, the area is considered to be 'diffusely' karstified, such that groundwater flow pathways are well-distributed through the rock mass. Some of the limestones have also been dolomitised, which has further increased permeability and porosity.



The fissured limestones have only secondary, fissure porosity and permeability. Dolomitisation has introduced spatially limited secondary intergranular porosity and permeability. This aquifer extends from the north of the pilot area southwards and southwestwards. The subcrop of the aquifer splits around the higher ground of the Castlecomer plateau. However, it is thought that the aquifer is continuous through the syncline below the younger rocks of the plateau.

In contrast to bedrock aquifers, Quaternary glacio-fluvial sand and gravel aquifers provide an opportunity for intergranular groundwater flow. There are five regionally important sand and gravel aquifers in the study area, including the c. 200 km² Mid-Kildare Sand and Gravel Aquifer, which extends into the north-east of the study area and is one of the most extensive sand/gravel bodies in Ireland, and the c. 55 km² Nore River sands and gravels. Aquifer thickness varies from 20-40 m, but the mid-Kildare gravel can be significantly thicker. The Nore Gravels can be variable in thickness, with bedrock 'towers' poking through. The sediments vary considerably over short distances but are dominated by gravel and sand. Sorting can be poor or good, and there can also be clay horizons.

The SE region has been relatively well-studied over the years, including by E. Daly (1978, 1980, 1981, 1982, 1990, 1993, 1994), Cawley (1990) and Tedd *et al.* (2012, 2013). Studies included data collection, groundwater system conceptualisation, interpretation of groundwater levels, hydrometeorological studies, and preliminary inferences about climate change impacts. There are also almost 100 source-specific studies for groundwater-fed drinking water supplies (public schemes and group schemes).

The study area has a number of observed groundwater level data obtained from some of the number of boreholes that have been drilled in the area. In addition to the important role these groundwater level data can play in calibration of numerical models, they can be also used to undertake statistical analysis and apply lumped models. This allows better understanding of the hydrogeological behaviour of the aquifer, the reconstruction of past groundwater levels to study past drought and flooding events, making short-term groundwater level predictions, and studying the impact of climate change. The groundwater level observation boreholes analysed in this study are summarised in **Table 1** and are shown on **Figure 1** and subsequent maps. The objectives of the analyses are to improve understanding of groundwater recharge mechanisms and timing, and to begin to make predictions about the variation of groundwater recharge under the future climate conditions.

The actively monitored boreholes are part of the Environmental Protection Agency (EPA) groundwater monitoring network. The historic borehole data are from previous Geological Survey Ireland studies, some of which were incorporated into the active EPA network.

Table 1: Details of Groundwater Level Monitoring point, meteorological stations and surface flow gauging stations, and other catchment details

Groundwater level Monitoring Point						Land Use (CORINE 2018)	Precipitation			Potential Evapotranspiration			Evaporation (Metran only)		River Discharge/Flow		
Name	Record Length	Bore- hole depth (m bgl)	Depth to groundw ater (m bgl)	Aquifer Type	Aquifer Vulnera- bility		Station Name	Distance to 1 st Station (km)	Record Length	Station Name	Distance to Station (km)	Record Length	Station Name	Record Length	Station Name	Distance to Station (km)	Record Length
Allen	Jan 1997 – Jul 2020	37.4	1.55 - 3.055	Poorly productive fissured	Moderate & Low	Discontin- uous urban fabric	Naas (Osberstown)	7.2	May 2008 – Jul 2020	Casement	25.6	Jan 1967 – Jan 2021	Casement	May 2008 – Jul 2020	Osberstown House	7.6	May 2009 – Dec 2020
Ballyragget Glanbia	Mar 2008 – Oct 2020	18	2.2 - 5.61	Sand & Gravel and karst	High & Extreme	Pastures	Parknahown Cullahill, Durrow, Ballyroan	9.8	Nov 1981 – Aug 2020 (all same)	Oak Park	30.1	Jan 2008 – Sep 2020	Oak Park	Mar 2008 – Dec 2020	John's Bridge	18.1	Oct 1971 – Dec 2017
Borrismore Creek	Apr 1975 – Aug 2020	36	9.02 - 18.86	Regionally important karst	Extreme & High	Complex cultivation patterns	Parknahown Cullahill, Drangan	12.5	Apr 1975 – Aug 2020 (all same)	Kilkenny, Oak Park	44.4	Jan 1970 – Jan 2019	Kilkenny, Oak Park	May 1975 – Aug 2020	Ballinfrase	12.1	Jul 2001 – Mar 2021
Freshford – Johnstown Rd	Apr 2008 – Aug 2020	13.5 (sump at 12.3 m)	10.60 - 12.31	Regionally important karst	Moderate, High & Extreme	Pastures	Parknahown Cullahill	8.6	Apr 2008 – Aug 2020	Oak Park	44.3	Jan 2008 – Sep 2020	Oak Park	Apr 2008 – Aug 2020	Durrow Ft Bridge	14.9	Jan 1972 – Oct 2018
MB 07B Upper	May 2008 – Jul 2020	Un- known (<48)	17.95 - 19.38	Sand & Gravel	High	Pastures	Naas (Osberstown)	11.5	May 2008 – Jul 2020	Casement	30.7	Jan 1967 – Jan 2021	Casement	May 2008 – Jul 2020	Rathangan	10.3	Jan 1999 – Jun 2020
MB 30	Apr 2008 – Jul 2020	24	5.53 - 9.67	Sand & Gravel	High	Natural grasslands	Naas (Osberstown)	14.1	Apr 2008 – Jul 2020	Oak Park	34.3	Jan 2008 – Sep 2020	Oak Park	Apr 2008 – Jul 2020	Japanese Gardens	2.9	Jan 1982 – Sep 2020
Tully	Jun 2008 – Jul 2020	9	0.27 - 1.17	Sand & Gravel	High	Pastures	Naas (Osberstown), Casement	16.6	Jun 2008 – Jul 2020 (all same)	Casement	32.1	Jan 2008 – Sep 2020	Casement	Jun 2008 – Jul 2020	Japanese Gardens	0.2	Jan 1982 – Sep 2020
Vickerstown	Oct 1995 – Sep 2020	25	2.35 - 6.4	Regionally important karst	High & Moderate	Pastures	Athy (Chanterlands) , Castledermot Kilkea House	10.4	Jul 1993 – Sep 2020, Jan 1990 – Dec 2020	Kilkenny, Oak Park	24.7	Jan 1970 – Jan 2019	Kilkenny, Oak Park	Jan 1990 – Dec 2020	Derrybrock	1.3	Feb 1980 – Oct 2020



3.1.2 Topography

The study area is bounded to the NE, NW and SW by mountain ranges (elevation up to 927 m aOD (metres above Ordnance Datum)), and to the SE by the coast. Within the study area the Castlecomer Plateau and the Slieveardagh Hills (up to 600 m aOD) separate two NE–SW-trending lowlands areas. The main lowlands of the study area are:

- to the west of the Castlecomer Plateau and Slieveardagh Hills, which lie typically between 130 and 100 m aOD;
- to the east of the Castlecomer Plateau and the Slieveardagh Hills, which lie typically between 90 and 30 m aOD; and
- coastal (to the east of the Blackstairs Mountains), which lie typically between 60 m aOD and sea level.

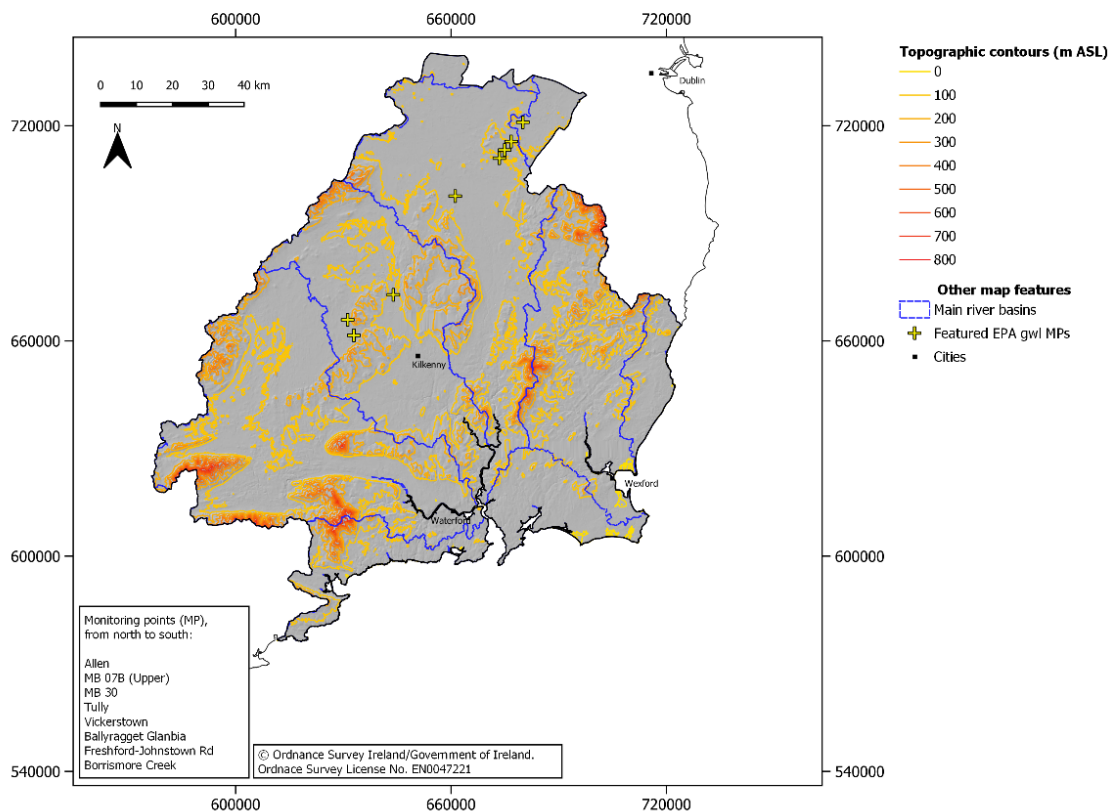


Figure 3. Topography over the pilot area

3.1.3 Landuse and Climate

Landuse

Land use includes enclosed fields, woodland, open land, and built-up areas. There are also two closed lead-zinc mines (one of which is planning to re-open). Much of the land over the diffusely karstified limestones is in agricultural use, while there are smaller areas of



urbanisation, including residential or commercial developments. There are also one-off houses, with their own septic systems, either on scattered farms or as ribbon developments. Farming activities above the limestone aquifers are dominated by intensive dairying, with lesser amounts of tillage. Over sands and gravels, sheep grazing is common, or drystock. In non-limestone areas, farming includes tillage, dairying and drystock.

Landuse data can be extracted from the Corine map (CLC2018, EPA 2018) specify the model parameters that control evapotranspiration.

Rainfall

On a national scale, the pilot area is a relatively dry region. The Agroclimate Atlas of Ireland (Collins and Cummins, 1996) shows the annual mean rainfall to be between 800 and 1,000 mm in the lowlands of the SE Region, 1,000 and 1,250 mm in upland areas (200– 600 m), and in excess of 2,000 mm in mountainous areas (greater than 600 m). Precipitation values in excess of 1,200 mm are typical over most of the rest of the country.

Rainfall is measured by Met Éireann at 61 rainfall stations throughout the pilot area. There are two synoptic stations within the SE region: Oak Park (which replaced Kilkenny in March 2008) and Johnstown Castle (which replaced Rosslare in March 2008). At synoptic stations, meteorological elements, such as air temperature, rainfall, humidity, vapour pressure, wind speed, wind direction and atmospheric pressure, are recorded on an hourly basis. Daily evaporation, potential evapotranspiration (PE) and soil moisture deficits (SMDs) are calculated for these stations (<http://www.met.ie>). Spatially distributed rainfall data are available at daily time steps starting from 1961 to 2018 (Met Éireann). These are on a 5 x 5 km grid. While the size of this time step is too coarse to represent storm events for hydrological analysis, it is fine enough to calculate recharge values to drive groundwater models.

Projected (future) values of rainfall data and PE and AE are also available through the work of Met Éireann and ICHEC (Irish Centre for High End Computing), e.g. Nolan (2015). These data will be available for use for the estimation of projected (future) recharge values. It was not possible to incorporate them within this study for various reasons.

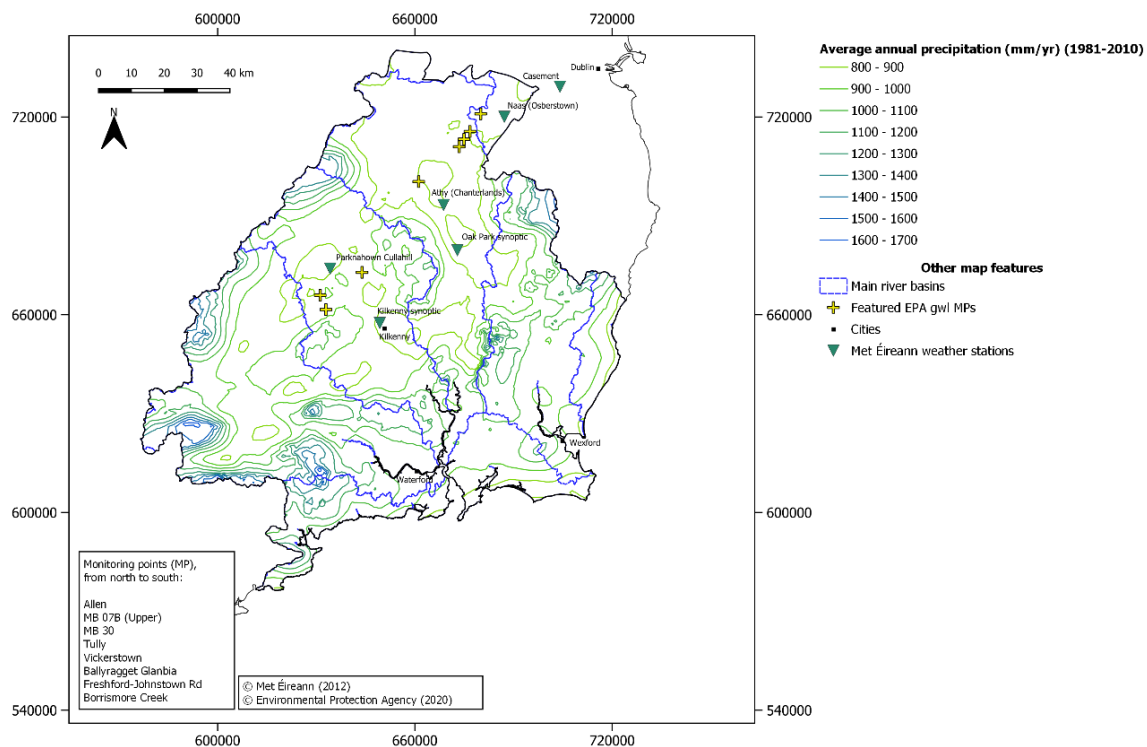


Figure 4. Spatial distribution of rainfall in the SE region

Potential evaporation

The Agroclimate Atlas of Ireland (Collins and Cummins, 1996) shows the annual PE in the SE region varies spatially between 450 mm and in excess of 500 mm. Potential evapotranspiration is relatively stable throughout the country, increasing with proximity to the coast. Calculated PE is available for the synoptic weather stations at Kilkenny and Oakpark. PE is minimum in winter, increasing during the spring to a maximum in the summer, before declining in the autumn. Grass growth typically starts around the start of March, and can continue into October, although annual variations in climate will impact this.

Average monthly PE values calculated and reported by Tedd *et al.* (2012) for the Kilkenny synoptic station range from approximately 5-10 mm in December and January, to 75-85 mm in June and July. Estimated average monthly AE ranges from 5-10 mm (December and January) to 60-75 mm in summer. The corresponding annual average PE ranges from 448 – 535 mm/yr, and AE from 421 – 491 mm/yr. Note that these are ranges due to different sources of information, estimation methods, and reference time periods.

Daily potential (reference) evapotranspiration and Actual evapotranspiration are available on a km-scale grid for the period 1981 onwards (Werner, Nolan and Naughton, 2019). These are available for a reference crop and for different soil classes.



Similar to rainfall data, potential and actual evaporation data from Met Éireann and ICHEC will be available in the future to be used to run simulations to calculate future recharge values.

3.1.4 Geology

The study area is underlain by extremely heterogeneous strata, principally of Lower Palaeozoic, Devonian and Carboniferous age (**Figure 5**), with extensive, and spatially variable, overlying subsoil deposits. The majority of bedrock geological information comes from the GSI reports accompanying the GSI's 1:100,000 geological map sheets covering the area (Tietzsch-Tyler et al., 1994; Archer et al., 1996) and from the hydrostratigraphic units map (GSI, 2005a).

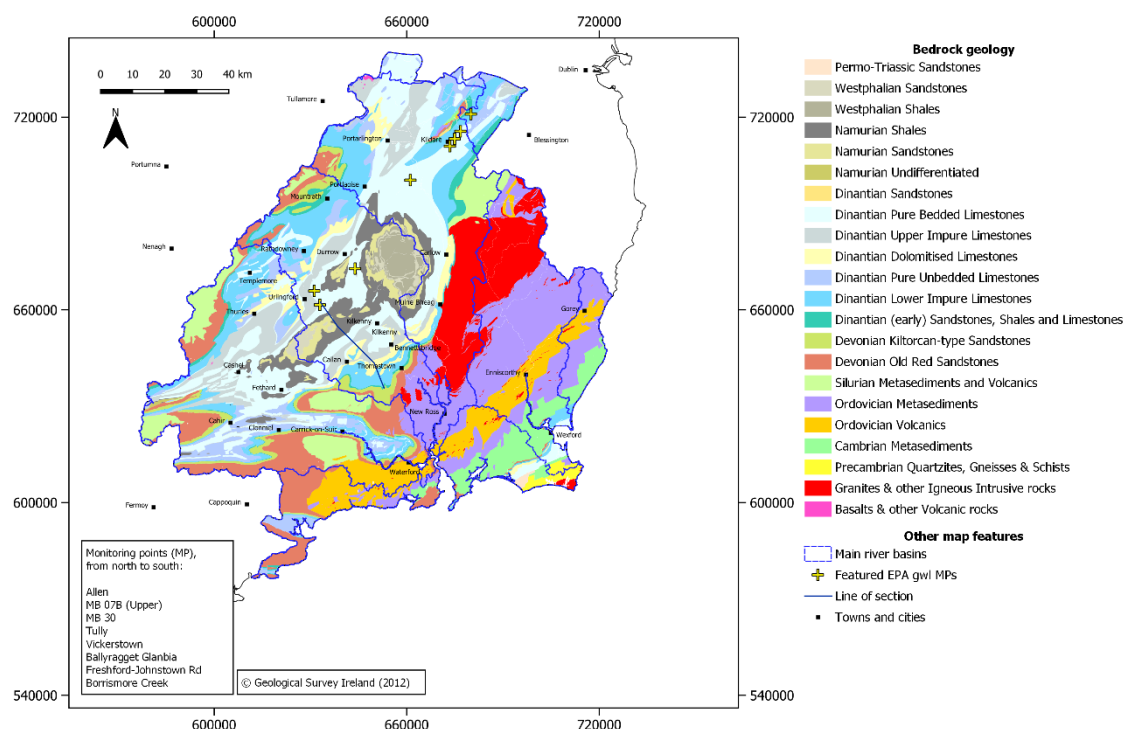


Figure 5. Generalised bedrock geology (hydrostratigraphic units) of the South Eastern region. Cross-section shown in line of section on this map (blue) is in Figure 6.

Lower Palaeozoic strata outcrop in the east of the study area and underlie the majority of Counties Wexford, Waterford and Wicklow and the east of Counties Carlow, Kilkenny and Kildare. They are also exposed via inliers in the Galtee, Slieve Bloom and Slievenamon Mountains. The deposits comprise metasedimentary and volcanic rocks associated with the evolution of the Iapetus Ocean. They are folded with a north-east to south-west trend and are extensively faulted; therefore, they are typically steeply dipping and include overturned beds (Archer et al., 1996). The Ordovician volcanics are well-fractured and form a major aquifer. Late Devonian-early Carboniferous dual porosity sandstones skirt the higher ground. They have a relatively limited outcrop area, but extend below overlying strata as confined systems. The remainder of the Lower Palaeozoic rocks are categorised as locally important or poor aquifers.



Lower Carboniferous strata comprise:

- impure and shaley limestones (the early Sandstones, Shales and Limestones; Lower Impure Limestones and Upper Impure Limestones rock unit groups (see **Figure 5**), which form poorly productive aquifers in general, and;
- pure limestones (Pure Unbedded Limestones rock unit group, also known as the Waulsortian, Pure Bedded Limestones rock unit group, and Dolomitised Limestones rock unit group), which generally form karstified regionally important aquifers.

There are a few exceptions, including: Waulsortian limestones don't always karstify significantly, and can be poorly productive aquifers; the early Carboniferous strata in some areas are dominated by calcareous sandstone, which does form a principal aquifer; impure limestones can be dolomitised and become more porous and permeable.

Upper Carboniferous strata form the core of a syncline and underlie the high ground in the centre of the study area.

3.1.5 Hydrology

The Rivers Suir, Barrow and Nore rise in the Slieve Bloom to Silvermines Mountains. The three rivers – known as the 'Three Sisters' – take different courses before converging in the Waterford Estuary. The River Slaney rises in the Wicklow Mountains and flows south-east into the Wexford Estuary (see **Figure 1**). The EPA and other organisations monitor the flow of rivers at 134 hydrometric stations within the river catchments. Only a subset of these is for flow as well as level, however. Baseflows are high where rivers have crossed the major karst limestone aquifers or the extensive glacio-fluvial sand and gravel aquifers.

3.1.6 Hydrogeology

The solid geology underlying the SERBD is heterogeneous. In general, alteration, cementation and intensive structural deformation means that groundwater flow is through secondary porosity and dominated by fracture flow. In a typical fractured hydrogeological system, the occurrence of open water-bearing fractures is greatest at shallow depths. Typically, hydraulic conductivity declines with depth as fractures become tighter and less common. Therefore, groundwater flow paths are likely to be shallow, predominantly in the upper layer of the aquifer with enhanced weathering and open fractures (Robins and Misstear, 2000). These types of aquifers typically have limited yields, transmissivities and storage, and are classified as Locally important and poor aquifers (LL, PL and Pu).

The karstified and dolomitised limestones have permeable zones at greater depths, relating to earlier periods of alteration. This is in addition to solutionally-enlarged fissures and development of cavities from recrystallization. Consequently, they are classified as regionally important aquifers (**Figure 2**). The regionally important aquifers in the study area are (GSI, 2006):

- Ordovician volcanics (Rf);
- Devonian to Early-Carboniferous Kiltorcan Sandstone Aquifer (including sandstones of the overlying Porter's Gate Formation) (Rf)



- Dinantian Dolomitised Limestones (Waulsortian, Butlersgrove and Milford Formations and equivalent horizons) (Rkd);
- Dinantian Karstified Limestones (Ballyadams and Clogrennan Formations) (Rkd); and
- Quaternary Sand and Gravel aquifers (Rg and Lg).

The aquifers of principal interest in the pilot area comprise:

(1) a north-south/NE-SW oriented band of limestone that occupies the valleys either side of the upland Castlecomer Plateau, whose younger rocks form the core of a syncline.

The pure limestones form a highly transmissive but low storativity aquifer. Fractures are solutionally-enhanced, leading to a distributed network of enlarged fissures. Conduits and caves are known, but are not thought to dominate groundwater flow. Well yields range from 30 – 3,000 m³/d, and are typically 250-1,000 m³/d. Transmissivities are on the order of 20-2,000 m²/d, generally 200-250 m²/d. Specific yields are very low, ranging from 0.005 to 0.05. Where dolomitised, porosity and storage is at the upper end of this range.

The karstified/dolomitised limestones are typically overlain by medium permeability glacial tills or sands and gravels. Groundwater within the outcrop part of the limestone is mostly under unconfined conditions. Where the aquifer is overlain by Namurian and Westphalian bedrock, it is confined. The nature of this part of the aquifer is not well-known, and it is not clear to what extent porosity and permeability are developed compared to the unconfined portions.

(2) extensive glacio-fluvial sands and gravels that form highly transmissive and high storativity aquifers. Well yields are in the range 250-1,000 m³/d. Transmissivities are on the order of 200–2,000 m²/d, typically 250–450 m²/d depending on the sorting and thickness of the aquifer. Specific yields are typically 0.12–0.19. There are five large sand and gravel aquifers in the study area. The two aquifers containing groundwater level monitoring boreholes assessed in this study are the mid-Kildare (Curragh) and Nore River gravels. The mid-Kildare aquifer can reach thicknesses of >100 m, but is mostly 20-40 m thick. It is generally unconfined, although very localised confined conditions exist under fen peats. The Nore River gravels are typically 10-30 m thick and are unconfined. The other three gravel bodies are typically unconfined, although where the aquifer is overlain by very thick Irish Sea tills, it is confined.

3.1.7 Groundwater levels

Groundwater level variation is influenced by the level of subsoil cover and the position of the monitoring point relative to the catchment (i.e. in elevated or interfluvial areas, or adjacent to rivers). Within the pilot area, in elevated areas with little subsoil, recharge can reach the saturated zone very rapidly through fractures and solutionally-enlarged fissures. Groundwater levels in fractured and karstified bedrock aquifers can vary by up to 40 m seasonally, although this is exceptional, and annual variations are more typically 10-15 m in these settings. Where there is subsoil covering the aquifer, this process is attenuated and slowed down. Groundwater level variation adjacent to rivers shows annual variations of around 2-3 m, typically (**Figure 6**), and are also much shallower. Groundwater level ranges in the sand and gravel aquifers are on the order of 2-3 m seasonally.



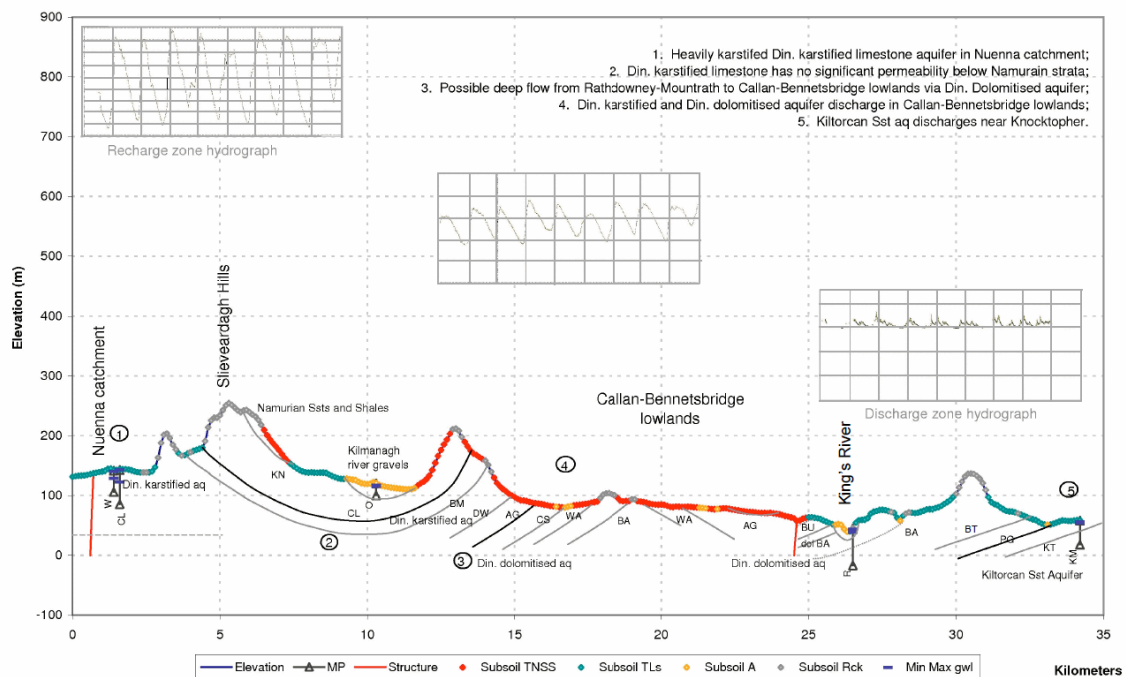


Figure 6. Schematic conceptual model cross-section through the southeastern region. From Tedd *et al.* (2011). Cross-section is oriented from NW to SE and line is shown on Figure 5.

3.2 Climate change challenge

The European Environment Agency map describes the expected climate change across the different areas in Europe as shown in **Figure 7**. This indicates that a shortening of recharge season, potentially resulting in aquifers becoming more vulnerable to droughts if rainfall fails in one or two months rather than a prolonged dry winter as can occur now.

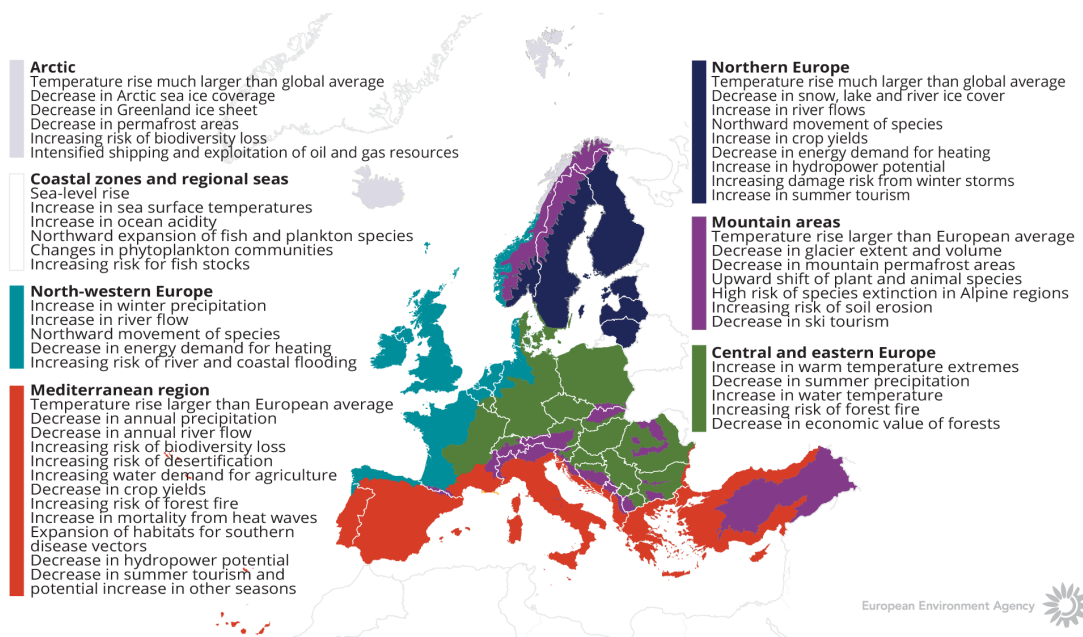
The main climate challenge for water resources managers and stakeholders is to assess the risk of future drought events. This requires detailed assessment of the variation of resources at regional and local scales rather than national or continental scales.

Higher winter rainfalls and groundwater recharge will result in higher groundwater levels, if overlying subsoils are sufficiently permeable to allow the recharge through. This will, in turn, lead to higher discharges of groundwater in winter and spring. The problems that will arise relate to the capacity of the combined groundwater surface water system downgradient of the recharge area. If the down gradient system is not able to take the higher groundwater flow rates, then there will be flooding. In the Southeast region, this is not expected to be extensive. However, increased magnitude and length of groundwater fluxes will lead to greater baseflow, which may exacerbate river flooding extents and durations. Conversely, drier than usual



summers will adversely impact summer river flows where they cross poorly productive aquifers, and baseflows are generally lower.

High groundwater flow rates through karstified aquifers may result in an increase in turbidity and contamination. This may occur in spring waters used as a water supply, and also in inadequately constructed boreholes.



**Figure 7. How climate is expected to change in Europe.
The European Environment Agency map**

4 METHODOLOGY

4.1 Methodology and climate data

4.1.1 *AquiMod*

AquiMod is a lumped parameter computer model that has been developed to simulate groundwater level time series at observational boreholes (Mackay et al., 2014a). It is based on hydrological algorithms that simulate the movement of groundwater within the soil zone, the unsaturated zone, and the saturated zone. The lumped models neglect complexities included in distributed groundwater models but maintain some of the fundamental physical principles that can be related to the conceptual understanding of the groundwater system (Mackay et al., 2014b).

The primary aim of AquiMod is to capture the behaviour of a groundwater system through the analysis of the available groundwater level time series. Once calibrated, the model can be run in predictive mode and be used to fill in gaps in historical groundwater level time series and to calculate future groundwater levels. In addition to groundwater levels, it also provides predictions of historical and future recharge values and groundwater discharges.

The mathematical equations that are used to simulate the movement of groundwater flows within the three modules are detailed in **Appendix C**. The model uses rainfall and potential evaporation time series as forcing data. These are interpreted by the soil module representing the soil zone. The soil module calculates the rainfall infiltration and passes it to the unsaturated zone module. This module delays the arrival of the infiltrating water to the saturated zone module. The latter calculates the variations of groundwater heads and flows accordingly.

AquiMod is calibrated using a Monte Carlo approach. It compares the simulated and observed groundwater level fluctuations and calculates a goodness of fit. The AquiMod version used in this work employs the Nash Sutcliffe (NSE) to assess the performance of the model. The user sets a threshold value to accept all the models that perform better than the specified threshold. The possibility of producing many models that are all equally acceptable, allows the user to interpret the results from all these models and calculate uncertainty.

The recharge values calculated from AquiMod are those that reach the aquifer system and drive the groundwater levels. Thus, it is assumed that these are the actual recharge values as defined in Karlsson et al. (2020).

4.1.2 *GARDENIA*

GARDENIA is a lumped hydrological model for the simulation of relationships between series of stream or spring flow data at the outlet of a watershed, and/or groundwater level data at an observation well situated in the underlying aquifer and the rainfall received over the corresponding watershed. Withdrawals by pumping groundwater can be considered if necessary.

GARDENIA enables the user to set a hydrological balance for the basin: actual evapotranspiration, runoff, infiltration, and recharge. The hydrological balance can be used for the evaluation of natural groundwater recharge of aquifers. GARDENIA gives the extension of river flow, groundwater level or recharge data over a long period for which precipitation and potential evaporation data are known. These long river flows and/or groundwater level series can then be used to:

- forecast river flows or groundwater levels for civil engineering applications;
- study particular events such as groundwater flooding or the occurrence of droughts;
- quantify the water balance components of a catchment at a pre-defined time-step (varying from one day to one month) for water resource evaluation or as input for a distributed groundwater model; and
- study the impact of climate change.

The climate data required for the model are:

- A continuous series of rainfall data.
- A continuous series of potential evapotranspiration data (PET). PET values can be either calculated from information related to sunshine duration, air temperature and relative humidity data, or it can be obtained directly from Meteorological offices.

One or two series of observations can be considered: river flows at the basin outlet and/or representative groundwater levels at an observation well located in the basin. The model can take into account impact of groundwater or river abstraction.

These different series of data must at a regular time step: daily, 5 days, 10 days, or monthly. All the series should refer to the same period. The time step of each series is not necessarily identical (e.g. daily rainfall and monthly PET).

The modelling of the relationships between rainfall and river flows and/or rainfall and groundwater levels includes a minimum of 4 to 6 lumped parameters (soil capacity, recession times, etc.) representative for a basin or a homogeneous unit within the basin. The software is executed in calibration phase first where model parameters are optimized automatically. The user has to select an objective function to evaluate model efficiency. This is usually dependent on the type of the investigated problem.

The computer code GARDÉNIA (modèle Global A Réservoirs pour la simulation des Débits et des Niveaux Aquifères) is a lumped hydrological model for watersheds. It uses time series of meteorological data (rainfall, potential evapotranspiration) recorded or calculated at a catchment to calculate:

- the river flows at the outlet of a river (or source) basin; and / or
- the groundwater levels at a borehole drilled in the underlying aquifer.

The effects of pumping or of a pumping group all located in the watershed can be taken into account. Calculations can be performed at a daily time step, decadal (ten days) or monthly. It is possible to take into account the snow melting process.

The modelling of the relationships between the rainfall and river flows and/or rainfall and groundwater levels includes 4 to 6 lumped parameters (soil capacity, recession times, etc.) representative for a basin or a homogeneous unit within the basin. These parameters are optimized using rainfall and river flow (and/or groundwater level) data over same observation period. The software under control of the user does this calibration phase of the model automatically.

After completion of the calibration, GARDENIA enables:

- The calculation of a hydrological water balance for the basin including actual evapotranspiration, runoff, infiltration, recharge (some terms can be used as input data in a discretized groundwater model). The hydrological water balance can be used for the evaluation of the renewable groundwater resources, mainly the groundwater recharge, of aquifers.
- The prediction of river flows, groundwater levels or recharge estimates over a historical or a future period for which precipitation and potential evaporation data are known. These projected river flow and/or groundwater level series can then be used for:
 - the forecasting of river flows or groundwater levels for the design of structures;
 - the study of particular events such as the rise of groundwater levels (flooding) or the occurrence of droughts; and
 - the study of the impact of climate change.

In addition to the possibility of estimating the different elements of the hydrological cycle (infiltration, evapotranspiration, runoff), GARDENIA allows the characterization of the hydraulic characteristics of the catchment through the calculation of the different runoff components (fast, slow and very slow components).

4.1.3 Metran

Metran applies a transfer function-noise model to simulate the fluctuation of groundwater heads with precipitation and evaporation as independent variables (Zaadnoordijk et al., 2019). The modelling approach consists mainly of two impulse functions and a noise model. The first impulse function is used for convolution with the precipitation to yield the precipitation contribution to the piezometric head. The second is for evaporation which is either a separately estimated function, or a factor times the function used for precipitation. The noise model is a stochastic noise process described by a first-order autoregressive model with one parameter and zero mean white noise. Further information about the model is given in **Appendix B** with the model setup shown in the Figure D1.

Metran allows the addition of other processes affecting the behaviour of the groundwater heads, for example pumping or the presence of surface features such as rivers. The contributions from these processes are added to the deterministic part of the model.

Metran has been designed to work with explanatory series that have a daily time step. However, it has been adapted so that other time step lengths can be applied. However, the explanatory variables must still have a constant frequency.

The model is calibrated automatically. However, the model uses two binary parameters, Regimeok and Modok, to judge a resulting time series model. Regimeok cross-examines the explained variance R^2 (> 0.3), the absolute correlation between deterministic component and residuals (< 0.2), and the null hypothesis of non-correlated innovations (p value > 0.01). If all these criteria are satisfied, Regimeok returns a value of 1 indicating highest quality. Modok also cross-examines the explained variance R^2 (> 0.1) and the absolute correlation between deterministic component and residuals (< 0.3) as well as the decay rate parameter (> 0.002) and if all these criteria are satisfied, it is given a value of 1. If Modok = 1 and Regimeok = 0, the model is still considered acceptable. If both these parameters are 0, the model quality is insufficient, and the model is rejected.

Metran's time series model is linear and the model creation fails when the system is strongly nonlinear. It is also limited to the response function being appropriate for the simulated groundwater system. Metran uses a gradient search method in the parameter space, so it can be sensitive to initial parameter values in finding an optimal solution.

The model calculates an evaporation factor, f , that gives the importance of evapotranspiration compared to precipitation. It is possible to use this factor to calculate the recharge values as shown by Equation D2 in appendix D. However, it must be noted that the use of Equation D2 is based on too many assumptions that are easily violated. Because of this, the equations should be applied only to long-term averages using only models of the highest quality.

Following the definitions used in the TACTIC project (Karlsson et al., 2020), this recharge quantity corresponds to the effective precipitation. It is equal to the potential recharge when the surface runoff is negligible. This in turn is equal to the actual recharge at the groundwater table if there is also no storage change or interflow.

4.1.4 Irish Groundwater Recharge Method

The Irish Groundwater Recharge Map is a spatially-distributed lumped hydrogeological model of average annual recharge to the deep groundwater system. The 'deep groundwater' is conceptualised as the resource that can be tapped steadily year-round and where yields aren't significantly influenced by seasonal changes in water table or extended dry periods. In addition to the 'deep groundwater' recharge, 'potential recharge' is also estimated. Conceptually, this is the water that percolates into the subsurface below the rooting zone, but may move sideways as interflow, or may have a relatively short residence time in the aquifer and not become part of the sustainable groundwater resource.

The recharge amount is shown in units of millimetres per year (mm/yr). It was calculated on a daily time-step over the period 1981–2010 and then averaged to give a yearly amount.

For WP4, the map is derived from two elements:

- (1) existing and new hydrogeological data layers that are combined to give recharge coefficients, and;
- (2) new agri-meteorological data layers.

Geological and hydrogeological map inputs include: soil drainage, subsoil permeability, groundwater vulnerability, peat, sand/gravel aquifer, and bedrock aquifer class.

The geological and hydrogeological maps are combined to generate 24 groundwater recharge coefficients using a ‘geological engine’ outlined in Hunter Williams et al. (2013). These are summarised in Hunter Williams et al. (in press) and in the Table in **Appendix E**. They are a slight update from Hunter Williams et al. (2013). The key improvements are summarised in a table in **Appendix E**.

The recharge coefficient polygons multiply agri-meteorological input data (Effective Rainfall, ER), as shown in the flow diagram in **Appendix E**. The ERI is on a 2.5 x 2.5 km grid and was produced by Irish Centre for High-End Computing (ICHEC) from downscaled numerical weather prediction (NWP) models (MÉRA, produced by Met Éireann). The FAO Penman Monteith Method was applied to dataset variables to produce reference evapotranspiration (ET_0), and the Soil Moisture Deficit Model (Schulte et al. 2005) was used to produce ET_a , SMD and ER variables used for this study.

4.1.5 Climate data

The TACTIC standard scenarios are developed based on the ISIMIP (Inter Sectoral Impact Model Intercomparison Project, see www.isimip.org) datasets. The resolution of the data is 0.5°x0.5° global grid and at daily time steps. As part of ISIMIP, much effort has been made to standardise the climate data (e.g. bias correction). Data selection and preparation included the following steps:

1. Fifteen combinations of RCPs and GCMs from the ISIMIP data set were selected. RCPs are the Representative Concentration Pathways determining the development in greenhouse gas concentrations, while GCMs are the Global Circulation Models used to simulate the future climate at the global scale. Three RCPs (RCP4.5, RCP6.0, RCP8.5) were combined with five GCMs (noresm1-m, miroc-esm-chem, ipsl-cm5a-lr, hadgem2-es, gfdl-esm2m).
2. A reference period was selected between 1981–2010 and an annual mean temperature was calculated for the reference period.
3. For each combination of RCP-GCM, 30-years moving average of the annual mean temperature were calculated and two time slices identified in which the global annual mean temperature had increased by +1 and +3 degree compared to the reference period, respectively. Hence, the selection of the future periods was made to honour a specific temperature increase instead of using a fixed time-slice. This means



- that the temperature changes are the same for all scenarios, while the period in which this occur varies between the scenarios.
4. To represent conditions of low/high precipitation, the RCP-GCM combinations with the second lowest and second highest precipitation were selected among the 15 combinations for the +1 and +3 degree scenario. This selection was made on a pilot-by-pilot basis to accommodate that the different scenarios have different impact on the various parts of Europe. The scenarios showing the lowest/highest precipitation were avoided, as these end-members often reflects outliers.
 5. Delta change values were calculated on a monthly basis for the four selected scenarios, based on the climate data from the reference period and the selected future period. The delta change values express the changes between the current and future climates, either as a relative factor (precipitation and evapotranspiration) or by an additive factor (temperature).
 6. Delta change factors were applied to local climate data by which the local particularities are reflected also for future conditions.

For the analysis in the present pilot the following RCP-GCM combinations were employed (**Table 2**):

Table 2: Combinations of RCPs-GCMs used to assess future climate

		RCP	GCM
1-degree	"Dry"	rcp6p0	hadgem2-es
	"Wet"	rcp4p5	gfdl-esm2m
3-degree	"Dry"	rcp4p5	hadgem2-es
	"Wet"	rcp4p5	miroc-esm-chem

Table 3: Yearly average delta change factors per climate change scenario for the Ireland Midlands & SE Region pilot area

	1C Min	1C Max	3C Min	3C Max
Precipitation	0.990	1.035	0.973	1.078
PET	1.006	1.053	1.060	1.062

The yearly average delta change factors shown in **Table 3** above do not show any major variation in nether PET nor precipitation rates. In contrast, the monthly delta change (non-averaged) factors shown in **Figure 8** below highlight a greater range of values, more so in PET variation across the midlands & SE region of Ireland.



Figure 8. Comparison of monthly precipitation and PET delta change factors for the Ireland Midlands & SE region pilot area



4.1.6 Tool(s) / Model set-up

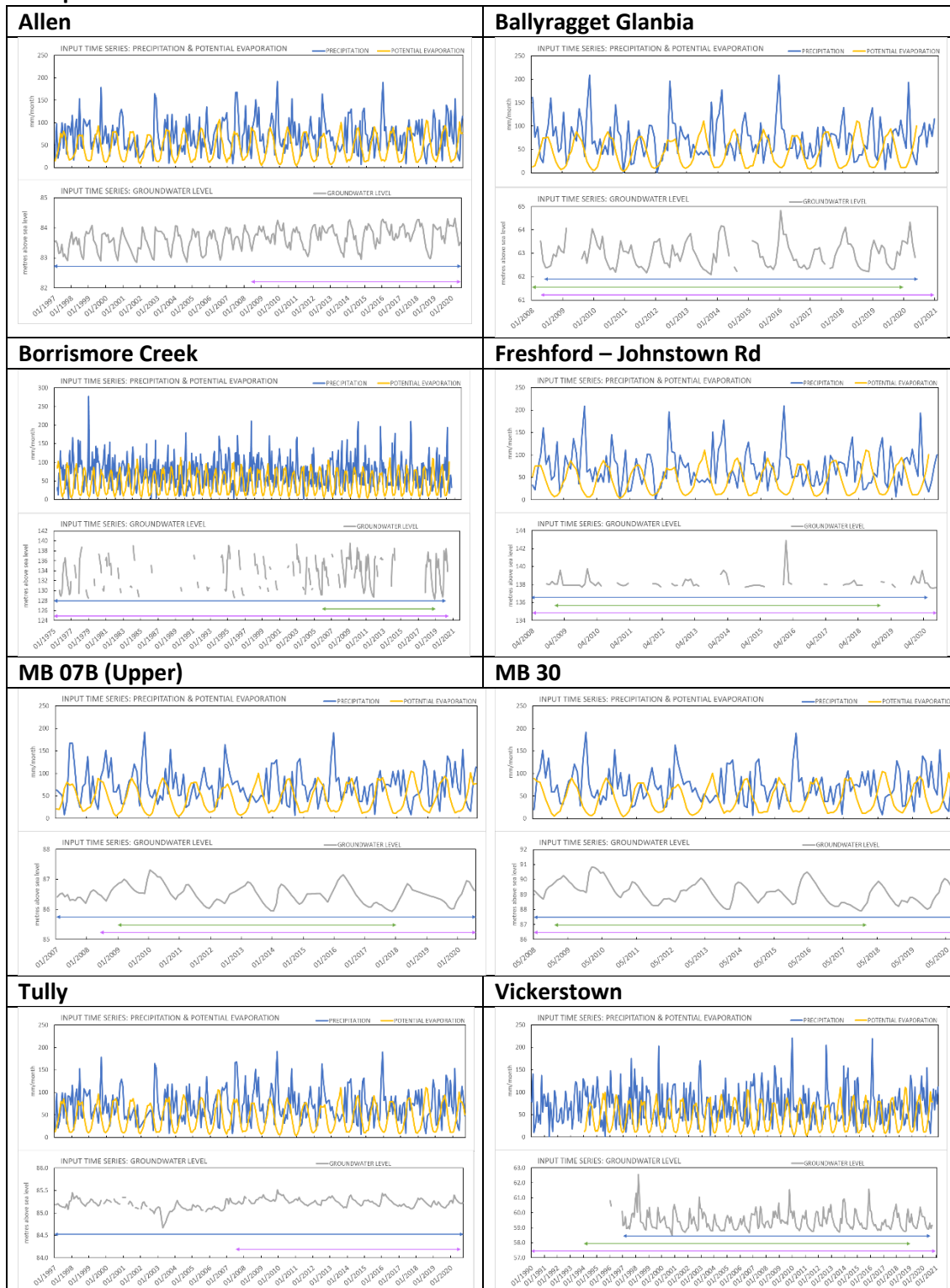
AquiMod

AquiMod model setup relies primarily on two input files. The first, “Input.txt”, is a control file where the module types and model structures are defined. AquiMod is executed first under a calibration mode where a range of parameter values of the different selected modules are given in corresponding text files, and a Monte Carlo approach is used to select the parameter values that yield the best model performance. “Input.txt” also controls the mode under which AquiMod is executed, the number of Monte Carlo runs to perform, the number of models to keep with an acceptable performance, and the number of runs to execute in an evaluation mode.

The second file AquiMod uses is called “Observations.txt”. This file contains the groundwater level observations and the forcing data, mainly the potential evapotranspiration (PET) and rainfall. However, it is also possible to include the anthropogenic impact on groundwater levels by including a time series of abstraction data in this file. None of the boreholes in this study include abstraction data, as part of the selection criteria for a borehole was to have no known influences from abstraction. The data are provided to the model on a monthly basis, and this forces AquiMod to run using a time step length of one month. However, PET and rainfall values are recorded in “Observations.txt” in mm/day which were calculated by dividing the monthly sum of PET and rainfall by the average number of days per month. **Table 4** shows observed monthly time series data of rainfall and PET as well as water level fluctuations at the different boreholes.

All AquiMod models built for the boreholes in **Table 1** use the FAO Drainage and Irrigation Paper 56 (Allen et al./ FAO, 1988) method in the soil module, and employ the two-parameter Weibull probability density function to control the movement of infiltrated water in the unsaturated zone (**Appendix C**). For the groundwater module structure, the simplest structure with one layer and one discharge feature, was selected. Due to limited resources, it was not possible to test more complex structures on each of the boreholes. The model that yielded the best NSE score was selected to undertake the recharge calculations.

Table 4: Rainfall, Potential Evapotranspiration and Groundwater level time series and modelling periods for each model type. Blue arrow = AquiMod; green arrow = GARDENIA; and pink arrow = Metran



GARDENIA

The GARDENIA model represents the water cycle in a basin from rainfall received by the soil surface until the river flow at the outlet, and/or the aquifer level at a given point. GARDÉNIA is a lumped model because it considers a lumped input (rainfall and potential evaporation representative for the basin) averaged over a catchment area and a single output (river flow at the outlet and/or groundwater level in the aquifer).

A lumped hydrological model simulates, through a series of reservoirs, the main mechanisms of the water cycle in a catchment (rainfall, evapotranspiration, infiltration, and runoff). Indeed, the exponential form of the recession of river flows or aquifer levels looks like the emptying of a reservoir (or tank). Therefore, the behaviour of an aquifer system can be represented by a series of inter-connected tanks. Non-linear transfer functions improve the capability of this schematic representation to simulate a complex system.

GARDENIA simulates the water cycle through a series of 3 or 4 connected tanks that represent respectively (**Figure 9**):

- the few decimetres of the soil that are subjected to the influence of evapotranspiration (root zone of the present vegetation).
- an intermediate zone generating rapid flow.
- one or two aquifer zones generating delayed slow flow.

The outflow from one reservoir to another is controlled by simple laws, specific to each reservoir; these laws are governed by the model parameters (active storage, duration of outflow, overflow threshold, etc.).

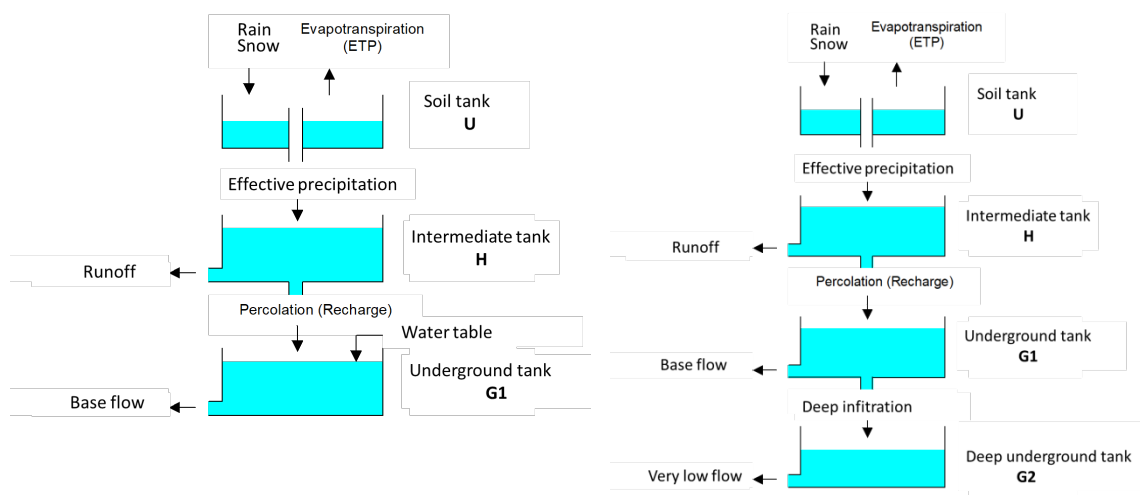


Figure 9 : Schematic representation of GARDÉNIA with one underground reservoir (left) or two underground reservoirs (right)



Production function and transfer function

The calculation consists of two parts, traditionally called: "production" function and "transfer" function.

The "production" function determines the amount of water reaching the system, and the amount that will evaporate or that will infiltrate into the lower horizons to emerge "later". The "transfer" function determines at what time the water, which has not evaporated, leaves the outlet of the basin or will reach the aquifer below. The transfer is represented as the passing of water through the 2 or 3 lower reservoirs of the model.

Due to the lumped nature of the model and the complexity of the hydrological system in reality, the different parameters of the tanks cannot be determined a priori from the local physiographical characteristics of the catchment (geology, vegetation cover, etc.).

Model data and parameters

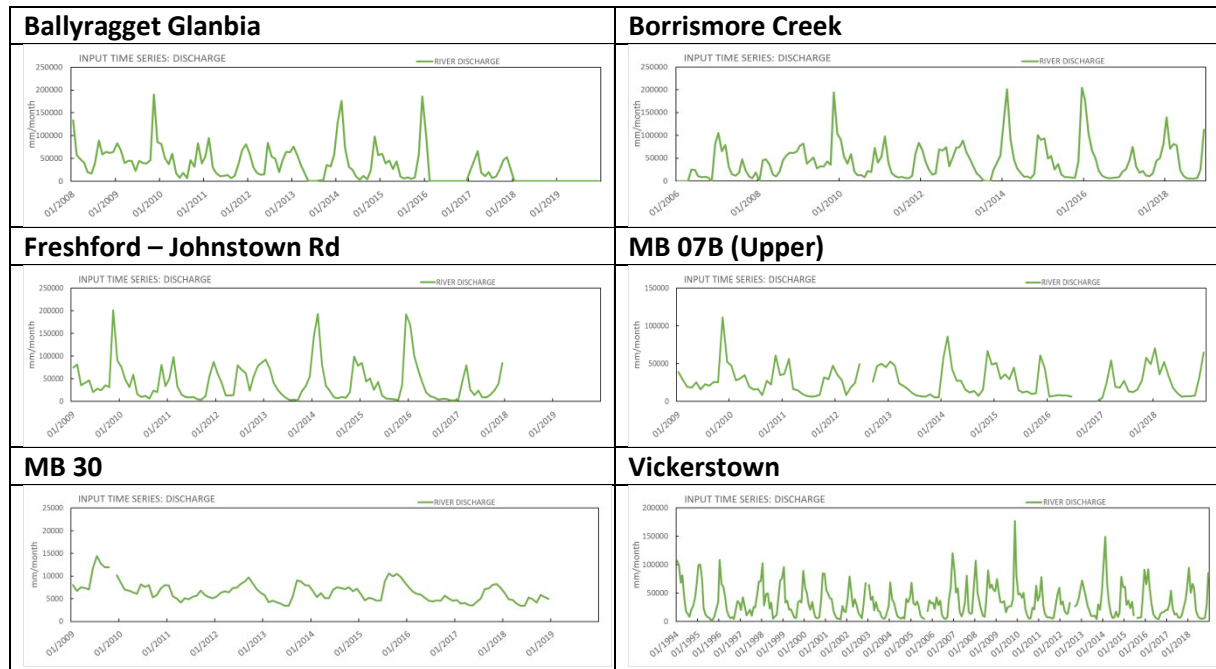
The required data are:

- a continuous time series of rainfall data.
- a continuous time series of potential evapotranspiration data (PET). PET values can be either calculated from sunshine duration, air temperature and relative humidity data, or can be obtained directly at Meteorological offices.
- one or two series of observations, which may include gaps, of:
 - river flows at the basin outlet (table x below observed discharge data used in GARDENIA); and / or representative groundwater levels at an observation well located in the basin.
- possibly a series of water withdrawals (pumping).

These different series of data must at a regular time step: daily, 5 days, 10 days, or monthly. It is also possible to use any regular time step (5 minutes, 1 hour, 60 days etc.). All the series should refer to the same period. The time step of each series is not necessarily identical (e.g. daily rainfall and monthly PET).

Input groundwater level and meteorological data are shown in **Table 4**, and river flow data are shown in **Table 5**.

Table 5: Input time series of river flow (discharge) associated with the borehole groundwater levels modelled in GARDENIA



Hydro(geo)logical parameters

In general, a number of 4 to 6 parameters (maximum 8 parameters) is required by the model (15 parameters in case precipitation in form of snowfall are to be taken into account). The dimensional parameters characteristics of the different reservoirs are (**Figure 10**):

- RUMAX (mm): capacity of reservoir RU, or the storage available for evapotranspiration.
- THG (months): time of half-filling of reservoir G.
- RUIPER (mm): level in reservoir H for which there is an equal distribution between fast runoff and percolation.
- TG1 (months): time of half-recession of reservoir G1.
- TG12 (*) (months): time of half-filling or reservoir G2 (time of half-transfer from G1 to G2).
- TG2 (months): time of half-recession of reservoir G2 (time of half- slow recession).

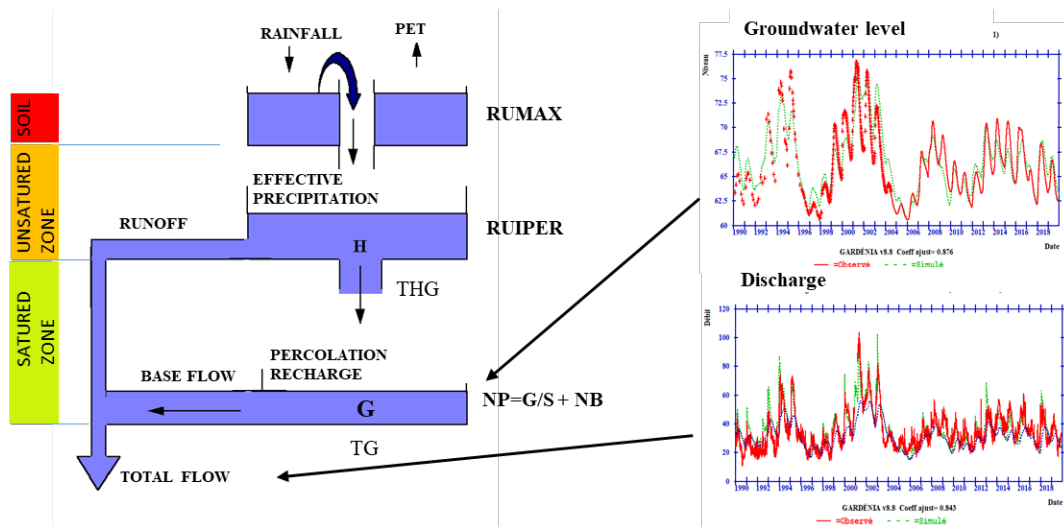


Figure 10 : Principle of GARDÉNIA global hydrological model for simulating the flow of a watercourse and/or a groundwater level.

Metran

Metran applies transfer function noise modelling with daily precipitation and evaporation as input and of groundwater levels as output (Zaadnoordijk *et al.*, 2019). The setup is shown in **Figure 11**. If time series of other influences on the groundwater head are available, these contributions can be added to the deterministic part of the model. An input file that holds the daily information of precipitation, potential evaporation and groundwater levels is prepared for each borehole in **Table 1**. Plots of these data are shown in **Table 4** above. It must be noted that, while Freshford–Johnstown Rd and Borrismore Creek groundwater levels used in Aquimod and GARDENIA and shown in **Table 4** have missing values, these have to be provided as complete time series to Metran. To achieve this, a linear interpolation procedure is used to fill in the missing values in the groundwater level time series. Once executed, it calculates the characteristics of the impulse functions and the corresponding parameters automatically.

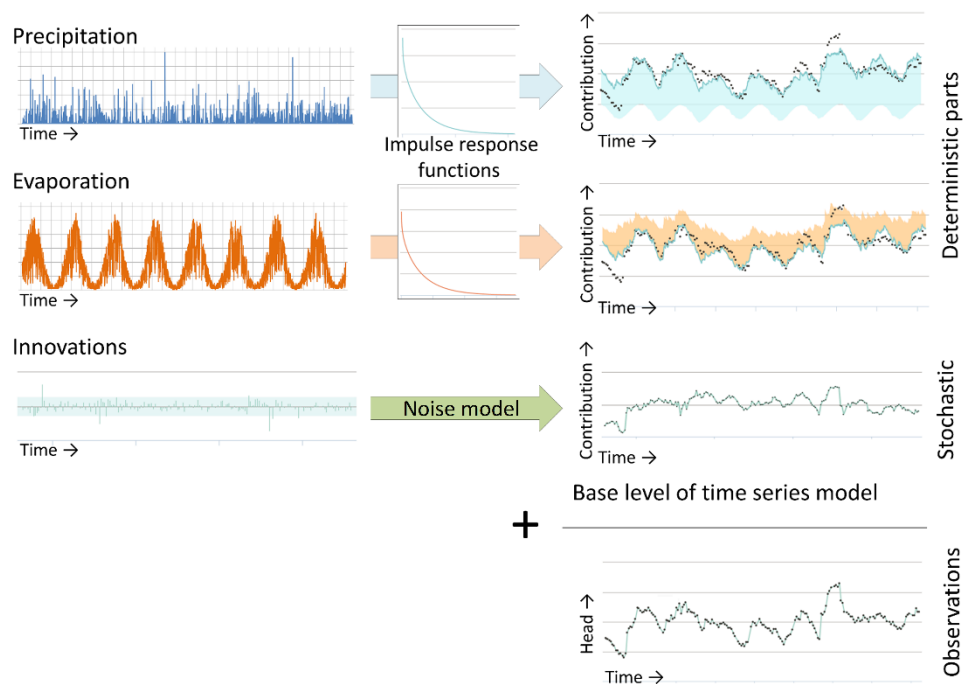


Figure 11 : Principle of Metran for simulating the groundwater level over time at a location.

Irish Groundwater Recharge method

The output from the Irish Groundwater Recharge method is a spatially-distributed estimate of average annual groundwater recharge. The method uses a lumped approach to model:

- (1) 'potential recharge' – this is the water that percolates into the subsurface below the rooting zone, but may move sideways as interflow, or may have a relatively short residence time in the aquifer and not become part of the sustainable groundwater resource;
- (2) 'deep groundwater' resource – this is conceptualised as the resource that can be tapped steadily year-round and where yields aren't significantly influenced by seasonal changes in water table or extended dry periods

Model inputs are:

- 1) The geological and hydrogeological data layers that represent the controls on infiltration and percolation, and on recharge acceptance: soil drainage and modified soil drainage; subsoil permeability; groundwater vulnerability and (indirectly) subsoil thickness; subsoil type (for peat, sand and gravel); aquifer type and class (for sand/gravel aquifers and the poorest three bedrock aquifer classes);
- 2) The meteorological and agronomic data layers that produce the effective rainfall.

The geological and hydrogeological maps are combined to generate 24 groundwater hydrogeological scenarios and associated recharge coefficients as outlined in **Table E.2, Appendix E**. The hydrogeological scenarios and recharge coefficients are a slight update from



Hunter Williams et al. (2013) (see **Table E.1** for summary of improvements). The hydrogeological scenarios give a minimum, maximum and inner range of expected recharge coefficient. For the national map, the mid-point of the inner recharge coefficient range is used. (For site-specific studies, other recharge coefficient values within the outer range can be chosen.)

To derive an estimate of potential or long-term (deep) recharge, the recharge coefficient polygons multiply agri-meteorological input data (Effective Rainfall, ER), as shown in the flow diagram in **Figure 12**. This gives the Potential recharge value. If the bedrock aquifer is poorly productive (in Ireland: LI, PI and Pu aquifer categories), a maximum recharge capacity is applied to simulate the limited recharge acceptance of poorly fractured, low storage aquifers.

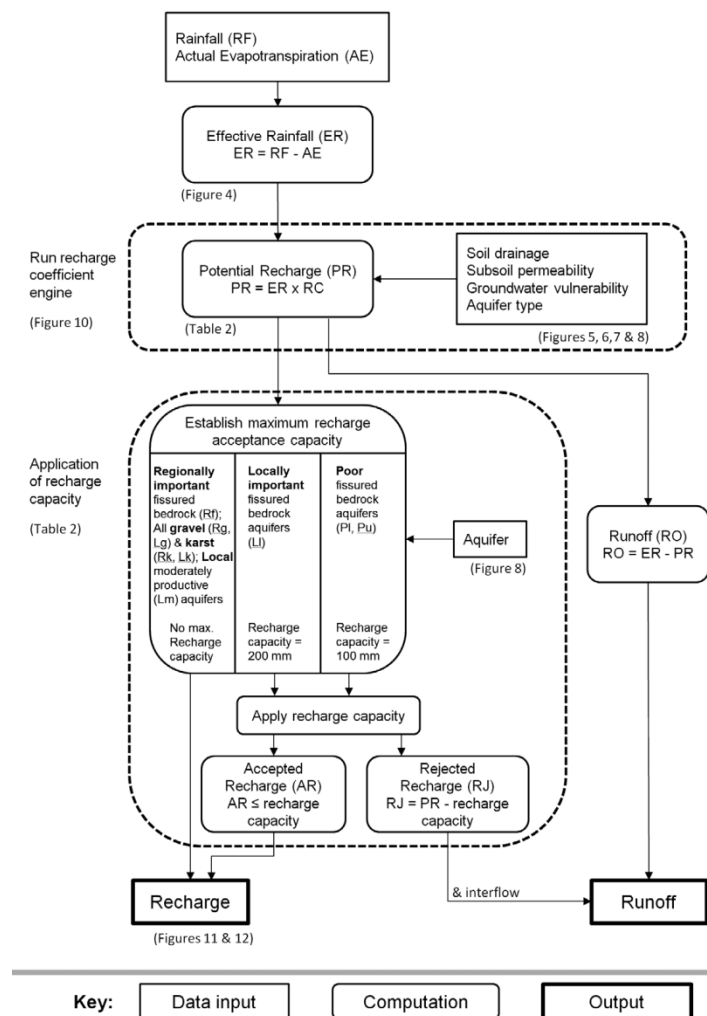


Figure 12. Indicative structure and method of GIS-based tool for estimating recharge (from Hunter Williams et al., 2013). RF, total rainfall; AE, actual evapotranspiration; ER, effective rainfall; PR, potential recharge; RC, recharge coefficient; RO, runoff.

The input ER is on a 2.5 x 2.5 km grid and was produced by Irish Centre for High-End Computing (ICHEC; Werner et al., 2019) from downscaled numerical weather prediction (NWP) models. To derive the ER, three climate models were evaluated, and MÉRA, produced by Met Éireann, was chosen as it had the highest overall skill. The FAO Penman Monteith Method was applied to dataset variables to produce reference evapotranspiration (ET_0), and the Soil Moisture Deficit Model (Schulte et al. 2005) was used to produce ET_a , SMD and ER variables used for this study.

The groundwater recharge amount is presented in units of millimetres per year (mm/yr). It was calculated on a daily time-step over the period 1981-2010 and then averaged to give a yearly amount. It is therefore temporally one-dimensional, but spatially two-dimensional. Annual recharge

4.2 Initialization

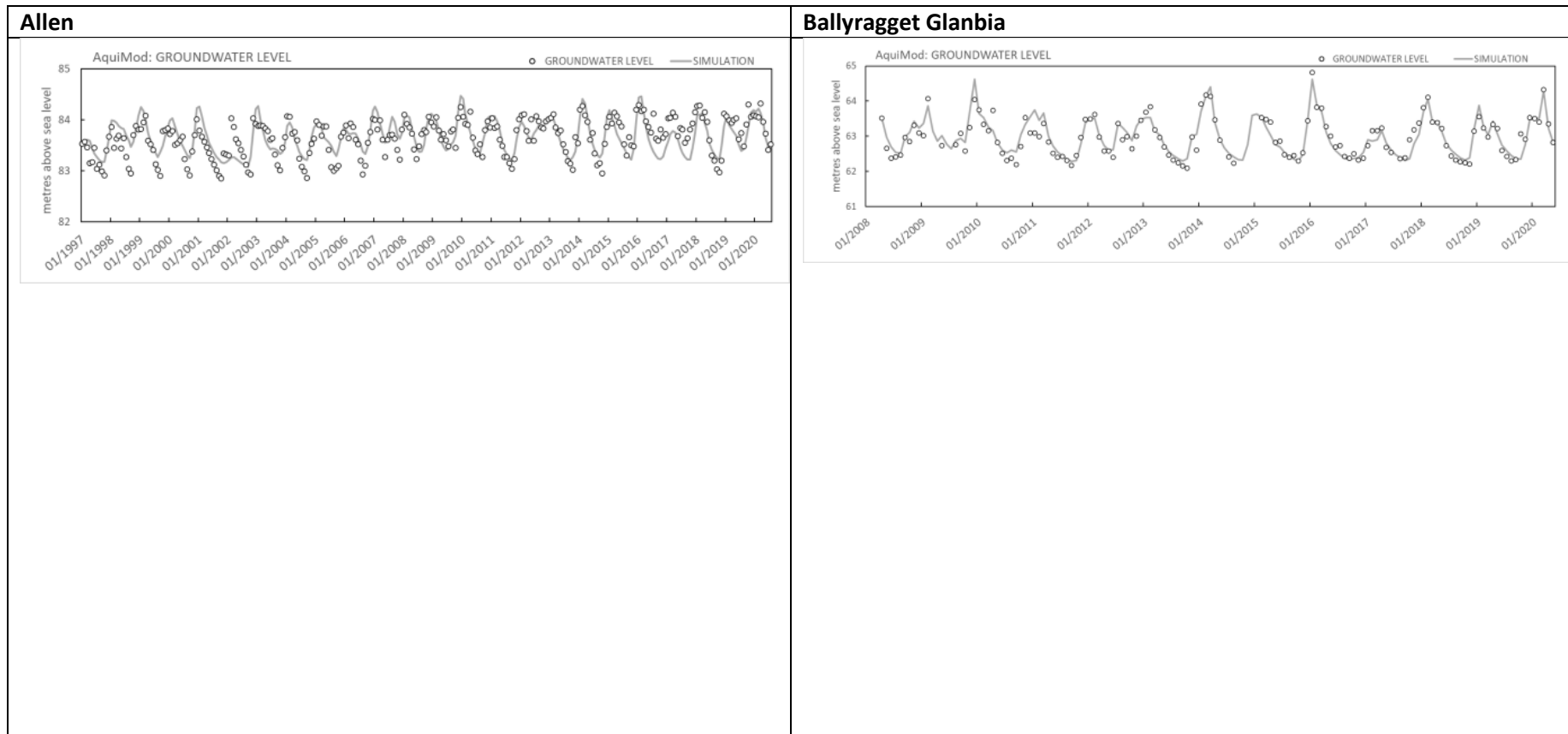
It is evident that due to the sometimes considerable hydrological inertia of the system, the calculation of the first values depends a lot on the conditions of the previous years. To avoid the difficulties that could result from the above, the possibility has been introduced in the Aquimod, GARDENIA and Metran models to take into consideration a few years, prior to the first hydrological observations. However, since it often takes very long for the flow regime to establish, the model is placed in hydrological equilibrium at the beginning of calculations, this means that the outcoming flow (or piezometric level) corresponds to incoming effective rainfall.

4.3 Tool(s)/ Model calibration/ test

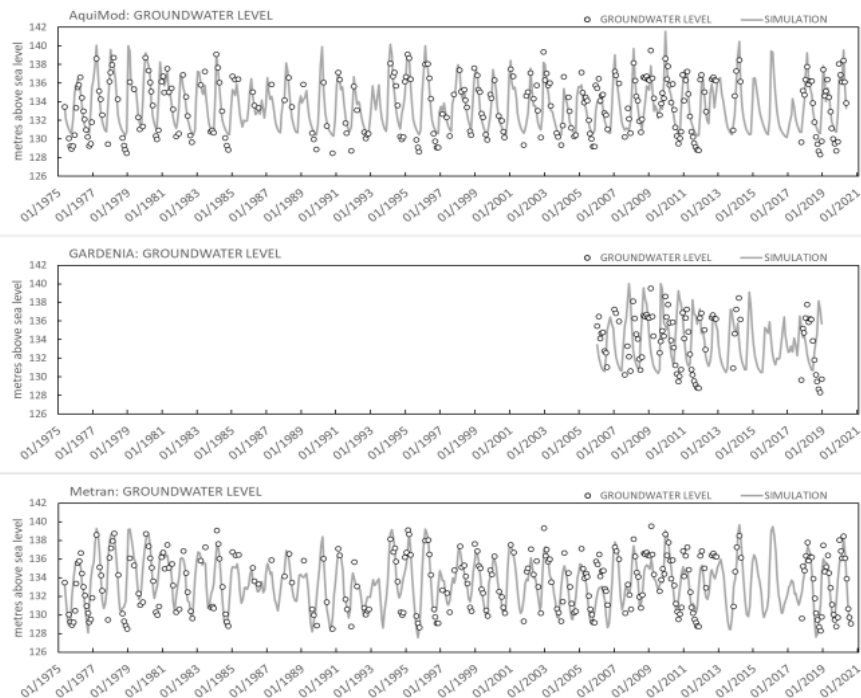
4.3.1 Observation data

Graphs of groundwater levels at all monitoring stations are shown in **Table 4**, river flows associated with groundwater monitoring stations are shown graphically in **Table 5**. Observed vs simulated groundwater levels and river flows (for Gardenia models) are shown in **Table 6**. Data for models which failed calibration tests have not been included.

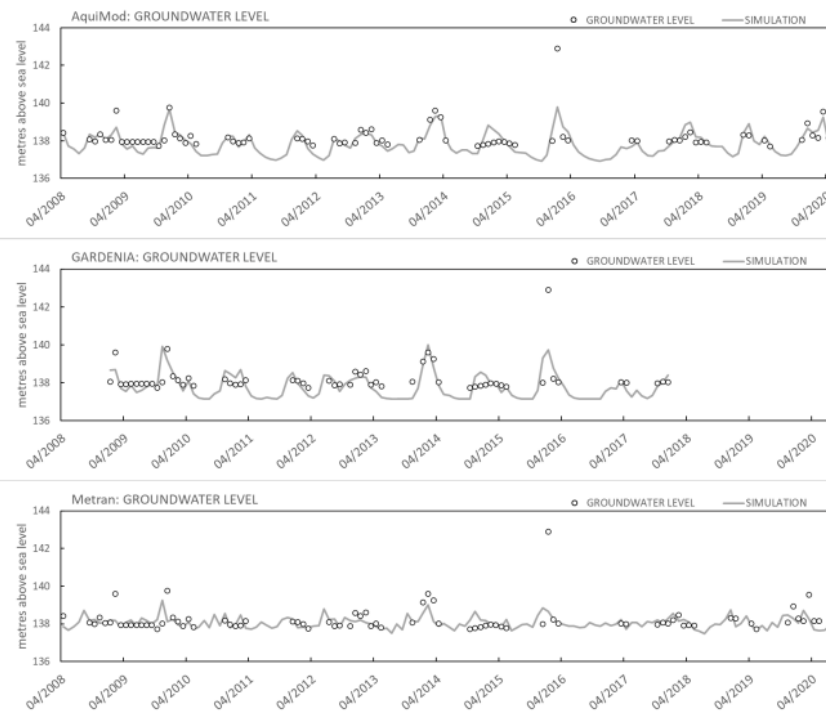
Table 6: Observed vs. simulated groundwater levels for each model type and reference period. Modelling periods vary due to the data requirements of each model. For example, both Metran and GARDENIA can operate without groundwater level data at the start of the modelling period. However, Aqumod must start with an observed groundwater level. Models which failed calibration tests have not been included.



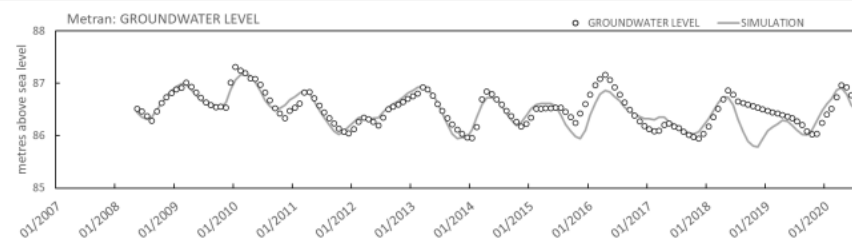
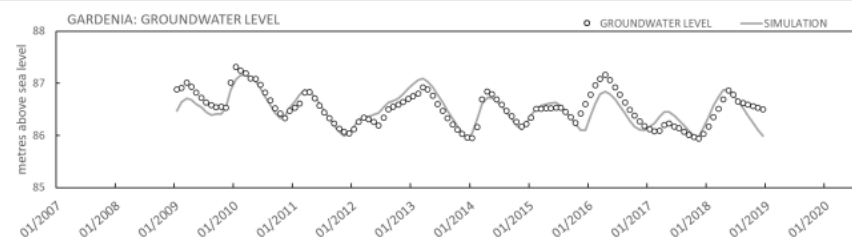
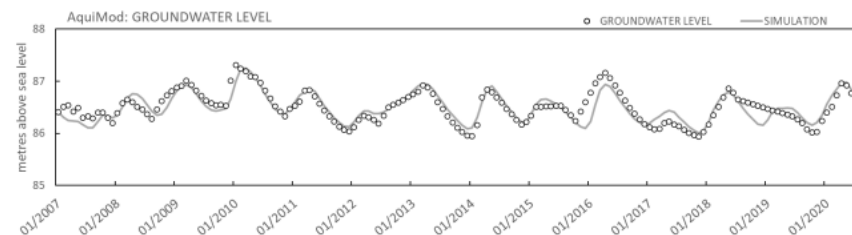
Borrismore Creek



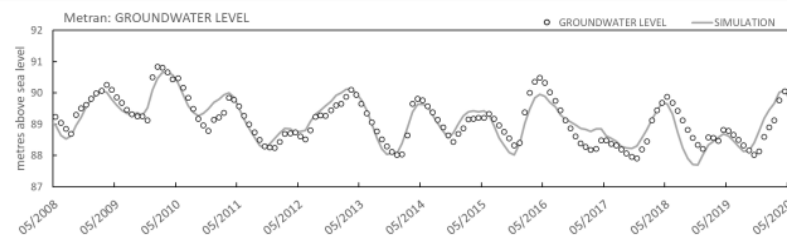
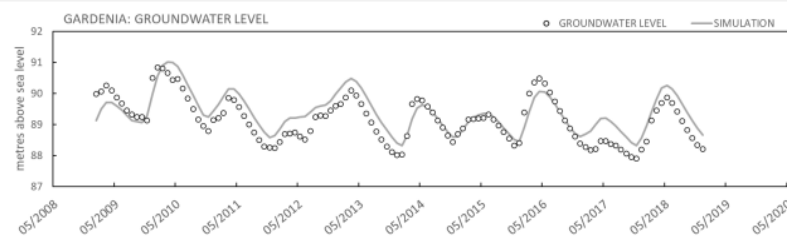
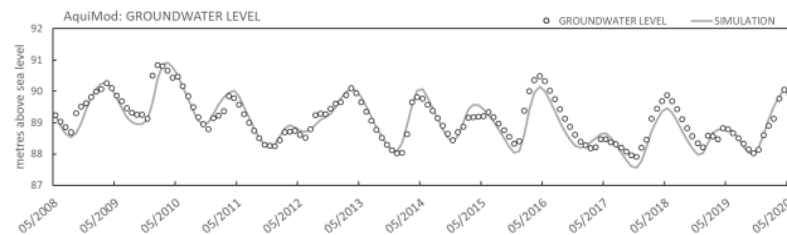
Freshford – Johnstown Rd



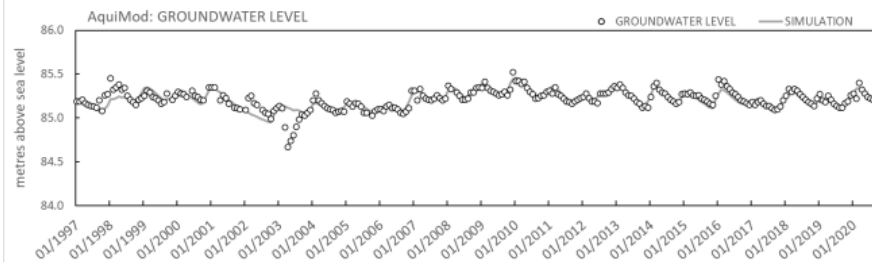
MB 07B (Upper)



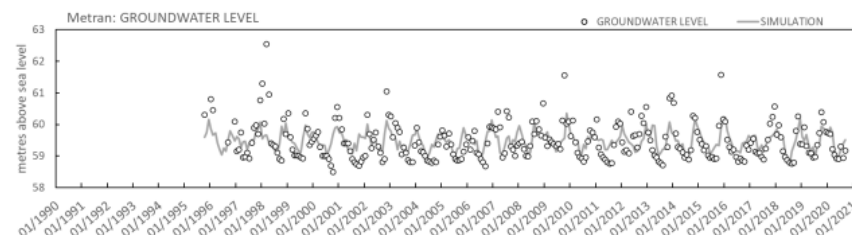
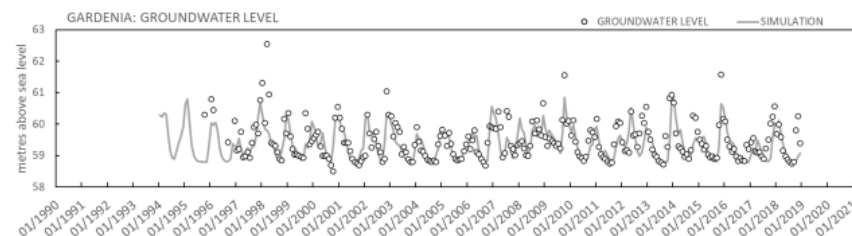
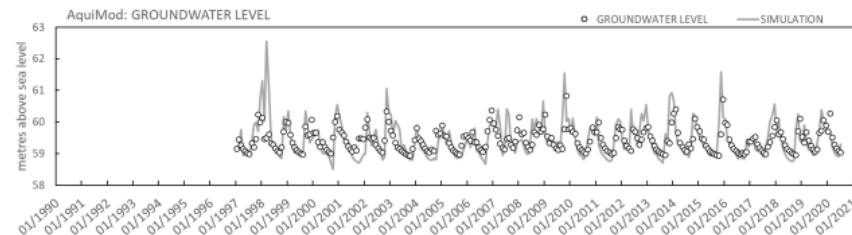
MB 30



Tully



Vickerstown



4.3.2 Calibration of *AquiMod* models

The calibration of *AquiMod* is performed automatically using the Monte Carlo approach. The user populates the files of the selected modules with minimum and maximum parameter values and then the model randomly selects a value from the specified range for any given run. The selection of the minimum and maximum values is physically based depending on the characteristics of the study area. For example, the minimum and maximum values of the storage coefficient in the saturated zone module are set to lower values in a fractured karst limestone aquifer compared to those used for a gravel aquifer.

A conceptual understanding of the hydrogeological system must be available before the use of *AquiMod*, since this is necessary to set the limits of the parameter values for the calibration process. In some cases, it is not possible to obtain a good performing model with the selected values and that necessitates the relaxation of these parameters beyond the limits informed by the conceptual understanding. In such cases, the parameter values must feed back into the conceptual understanding if better performing models are obtained.

AquiMod execution time is relatively small, which allows the calibration of the model using hundreds of thousands of runs in couple of minutes. The performance measure used to assess the quality of the simulation is the Nash Sutcliffe efficiency (**Appendix C**) that takes a maximum value of unity for a perfect match between the simulated and observed data. The threshold at which models are accepted is set to a value of 0.1. All the models that achieve an NSE higher than 0.1 are included in the analysis but a maximum number of 100000 runs are used if the number of acceptable models is greater than 100,000.

Table 7 shows the best NSE values obtained for the models calibrated at the boreholes listed in **Table 1**. It is clear that a good match was achieved between the simulated and observed groundwater levels as illustrated in the plots shown **Table 6**. The best performing model is produced from MB 30 data with an NSE value of 0.86 and is closely followed by Ballyragget Glanbia with an NSE of 0.85. The worst performing *AquiMod* model is produced with the Vickerstown borehole with an NSE value of 0.36.

4.3.3 Calibration of *GARDENIA* models

Model calibration in *GARDENIA* consists of adjusting model parameters, within given limits, with the aim of producing simulated river flows and/or groundwater level series that match the observed ones as precisely as possible.

The data required for calibration are:

- model "input" continuous series: rainfall and evapotranspiration (and air temperature if snowmelt is taken into consideration);
- model "output" observed series (flows or levels) not necessarily continuous, but covering a concomitant period with the input series.

Calibration is done in a semi-automatic way. The user provides an initial set of parameters and indicates which parameters should be optimised. The model uses a non-linear optimisation algorithm adopted from the Rosenbrock method. The model makes the chosen parameters



vary (within a range of values defined by the user) and searches for a set which gives the best fit between observed and simulated series has been found.

The model produces the following results:

- For each time-step a water balance of the different components of the hydrological cycle (runoff, actual evaporation, groundwater flow, etc.).
- A graphical representation of observed and simulated values for a visual evaluation of the calibration.
- Numerical criteria for the evaluation of the quality of calibration.

Taking into account this information, the user then estimates whether to attempt a new optimization from another set of parameters. When both the numerical fitting criteria and the graphs for visual comparison are satisfactory, the user may consider which set of parameters are representative of the catchment as far as the obtained values are realistic. The user may then test different values of the parameters around this solution, in order to determine the family of parameter values that are representative, i.e., acceptable from point of view, of the water cycle (sensitivity study).

Table 7 summarises the best model efficiency scores for the models calibrated by GARDENIA for the boreholes listed in **Table 1** and shown in **Table 6**. The majority of models achieved a good match between the simulated and observed groundwater levels, with five out of six boreholes producing positive groundwater level NSE values, ranging from 0.33 (Vickerstown) to 0.80 (MB 07B). Four of these five models also achieved good river flow NSE values, with the exception of MB 30 which produced a river flow NSE of -102.55. We acknowledge that this is not an ideal NSE score. However, given that the quality of AquMod models are based on its groundwater level NSE score, we deemed this a passable result. Ballyragget Glanbia did not pass model efficiency tests, scoring negative NSE values for both the groundwater level (-0.24) and river flow (-0.26) time series. Therefore, this borehole has not been used for climate projections.

Limitations and specific difficulties in the simulation of piezometric levels

The GARDENIA model has been developed to simulate river flows as well as piezometric levels indifferently: in fact, the hydrological scheme is the same; the level in the underground reservoir can be thought of as being linked to the piezometric level by a linear relationship irrespective of the type of the aquifer considered.

The storage coefficient then plays the role of an amplitude factor, like the surface area of the catchment in the case of the calculation of flows. Nevertheless, the simulations of levels involve very specific problems.

The storage coefficient is not known, not even in order of magnitude, whereas the surface area of catchment is generally known. In fact, it represents a coefficient of global influence of the fluctuations of a reserve on a particular piezometric level. This coefficient of influence will only be equal to the average storage coefficient of the aquifer if the point of observation is located far away from any watercourse. This coefficient cannot be linked easily to interpretations of pumping tests (whose validity remains local) and which are often carried out



over short periods and can give a confined aquifer storage coefficient. The storage coefficient in GARDENIA corresponds more to level variations over periods that are much longer and the type of storage coefficient to be taken into consideration is that of an unconfined aquifer. Moreover, the storage coefficient in its traditional meaning is most frequently defined only with a precision far below 20 %, while deviation of 20 percent in the balance equation is difficult to accept.

In case of simulations of groundwater levels only (and not conditioned to river flows), the water balance established should be interpreted as an analysis of the flux only with extreme care. Although this method of analysis may be a bit dangerous for effective input estimations, it is often the only method available, and it should thus not be rejected in advance.

4.3.4 Calibration of Metran models

For the standard setup with precipitation and evaporation, there are five parameters that have to be determined during the calibration of the model. Three parameters are related to the precipitation response, the evaporation factor, and the noise model parameter (**Appendix D**). There are three extra parameters for each additional input series, such as pumping. The parameter optimization of Metran uses a gradient search method in the parameter space to reach a global minimum. As explained in **Appendix D**, two parameters indicate if Metran succeeded in producing a match between the simulated and observed data. These are called the *Regimeok* and *Modok*. When *Regimeok* is equal to one, the calibration is of highest quality. If *Modok* is equal to one and *Regimeok* is equal to zero, the calibration is of acceptable quality. Finally, if both parameters are equal to zero, the calibration quality is insufficient.

Table 7 shows the performance of Metran across the Irish boreholes considered in this study. It is clear that according to criteria set above, Metran fails to produce a model at three boreholes but succeeds at the five other boreholes with the model output showing highest quality at four of these boreholes (with highest value of R^2). Models which failed the calibration tests have been excluded from historical and future recharge calculations.

Table 7: Modelling periods used per model type and performance parameter scores. AquiMod and GARDENIA assess the groundwater level model efficiency using Nash Sutcliffe Efficiency (NSE) and Metran summarizes the quality using two binary parameters, Regimeok and Modok, with more detailed model quality information given with R2 and RMSE.

Monitoring point name	Models used	Observation period	NSE (GWL)	NSE (river flow)	regimeok	modok	Overall quality	R2	RMSE
Allen	AquiMod	01/1997 – 07/2020	0.54						
	Metran	05/2008 – 07/2020			0	0	Insufficient	0.14	0.3
Ballyragget Glanbia	AquiMod	04/2008 – 05/2020	0.85						
	GARDENIA	01/2008 – 12/2019	-0.24	-0.26					
	Metran	03/2008 – 12/2020			0	0	Insufficient	-0.7	0.69
Borrismore Creek	AquiMod	05/1975 – 05/2020	0.78						
	GARDENIA	01/2006 – 12/2018	0.65	0.83					
	Metran	05/1975 – 08/2020			1	1	Highest	0.75	1.49
Freshford – Johnstown Rd	AquiMod	04/2008 – 05/2020	0.48						
	GARDENIA	01-2009 – 12/2019	0.69	0.8					
	Metran	04/2008 – 08/2020			1	1	Highest	0.48	0.51
MB 07B (Upper)	AquiMod	01/2007 – 07/2020	0.77						
	GARDENIA	01/2009 – 12/2018	0.8	0.14					
	Metran	05/2008 – 07/2020			1	1	Highest	0.87	0.12
MB 30	AquiMod	05/2008 – 07/2020	0.86						
	GARDENIA	01/2009 – 12/2018	0.58	-102.55					
	Metran	04/2008 – 07/2020			1	1	Highest	0.81	0.3
Tully	AquiMod	01/1997 – 09/2020	0.64						
	Metran	06/2008 – 07/2020			0	0	Insufficient	0.56	0.05
Vickerstown	AquiMod	01/1997 – 07/2020	0.36						
	GARDENIA	01/1994 – 12/2018	0.33	0.35					
	Metran	01/1990 – 31/2020			0	1	Acceptable	0.42	0.44

4.3.5 Calibration of Irish Groundwater Recharge model

There is no structured calibration process for the Irish Groundwater Recharge Model. For the national map, the mid-point of the inner recharge coefficient range is used and is considered *a priori* to be appropriate. The map in **Figure 13** shows the long-term sustainable average annual groundwater recharge estimated using the Irish Groundwater Recharge method.

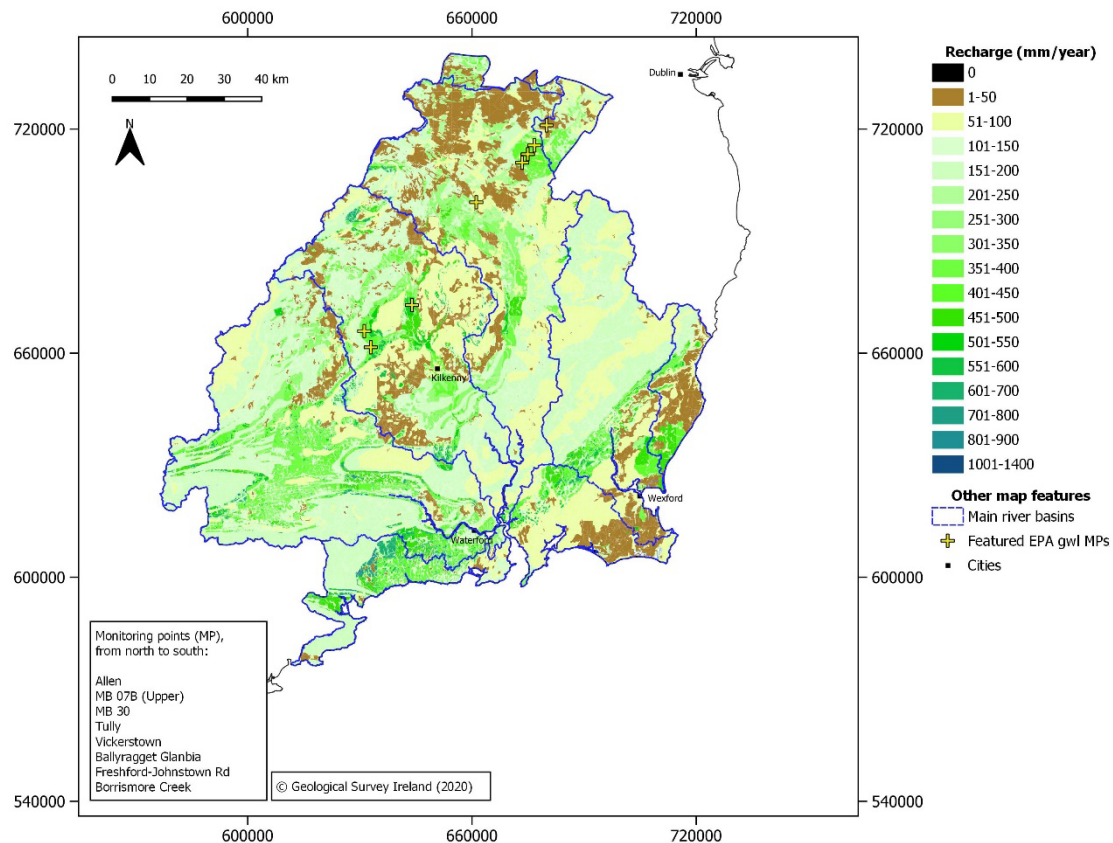


Figure 13. Long-term sustainable average annual groundwater recharge estimated using the Irish Groundwater Recharge method.

Whilst the recharge coefficients are assigned *a priori*, and groundwater recharge is forward modelled, the recharge coefficients summarised in **Table E.2 (Appendix E)** were based on a set of detailed studies summarised in Hunter Williams et al. (2013) and then extrapolated using expert judgement to cover the 24 scenarios.

Catchment-scale (10's – 100's km²) area-summed groundwater recharge from the national (average) map has been compared to catchment outflows and baseflow separations from gauging stations in two studies (Hunter Williams et al., 2011 and Mullarkey et al, 2021) and has been found to have good correspondence. For site-specific studies, other recharge coefficient



values within the outer range can be chosen on the basis of observed geological conditions, or to match observational data or recharge estimates derived from other methods.

4.4 Uncertainty

The selection of groundwater level monitoring points used in this study is based on research by Tedd *et al.* (2011). In the report, the authors analysed groundwater level data from a network of monitoring points in the southeast of Ireland and provide insights on the hydrogeological situation: grouping boreholes by catchment positioning; aquifer confinement; and influences on the groundwater levels such as abstraction, nearby rivers or discharge-dominated areas. These interpretations influenced our selection of monitoring points for the study, avoiding boreholes that were identified as being confined aquifers, abstraction- or river-influenced. However, it is possible the hydrogeological situation surrounding each borehole has changed since 2011.

The precipitation and potential evapotranspiration time series data were collected from rainfall and synoptic weather stations operated by Met Éireann. The Met Éireann database contains 353 rainfall stations in the pilot area, including historical records from weather stations which are no longer in use. **Figure 4** shows weather stations used in the study, and **Table 1** displays summary information relating to these stations. As precipitation data can vary over a relatively short distance, it was necessary to choose a station close to the borehole. However, the nearest stations did not always have data that ran the full length of the groundwater level monitoring period. Therefore, the next most appropriate station was selected. In some cases, the station used for rainfall can be up to approximately 17 km from the borehole (Tully). Potential evaporation data were also selected based on proximity and topographical suitability to the monitoring points, and came from three synoptic stations: Casement, Kilkenny, and Oakpark (**Table 1**). It is worth noting that the relatively short distance between some of the monitoring points meant the same rainfall and PET data are applicable for more than one borehole.

Suitable values for permeability and specific yield were assigned to the aquifers based on values derived from a bulk analysis of Irish aquifer types (Kelly *et al.*, 2015), as local pumping test and field data was not available for the boreholes at the time of this study. Therefore, these bulk values may not be accurate due to localised heterogeneity of aquifers resulting in hydrogeological properties.

Groundwater level data from Borrismore Creek and Freshford–Johnstown Rd (Freshford) are more inconsistent and, therefore, less reliable than the other boreholes in this study. The Borrismore Creek time series has a number of consecutive months of data missing; most notable is a large gap in recorded data from 2013 to 2017. The Freshford borehole is 13.5 m deep, and the bottom 1.2 m of the borehole consists of a sump. Consequently, the water level in the borehole does not drop below 12.3 m. During periods when the water level data is recorded as 12.3 m below ground level, this may not accurately reflect the actual groundwater level in the surrounding aquifer (Environmental Protection Agency, 2021) and, therefore, values below 12.3 m were removed from the time series before modelling. The missing

groundwater level data from both of these boreholes could impact the result of the model efficiency tests.

When comparing model results, it is worth emphasising the differences between each of the models' input parameters. For example, as well as using groundwater level, rainfall and potential evaporation data, GARDENIA also requires the input of: a catchment area, effective rainfall estimates for the catchment, and discharge data from an appropriate river flow station which acts as a proxy for the monitoring borehole. AquiMod requires a different suite of parameters for each module type which must be constrained during the calibration process (**Appendix C**). AquiMod also models the catchment size based on the linear distance to the nearest discharge zone, whereas GARDENIA requires a catchment area for the river flow station which is often much larger. Like AquiMod and GARDENIA, Metran also requires groundwater level and precipitation data, but uses an evaporation time series instead of a potential evaporation. Finally, both GARDENIA and Metran use daily timesteps for input observational data and also output time series on a daily timestep. AquiMod can run with daily timesteps. However, it produces much better model efficiency scores when monthly timesteps are used. The Irish Groundwater Recharge Model does not simulate groundwater levels; potential groundwater recharge is calculated at a daily timestep over the whole study area, but is summed and average over the reference period (1981-2010).

There are also variations between the modelling period for each model type. One of the benefits of Metran is that it can produce results with discontinuous groundwater level data and without any groundwater level data at the start of the modelling period. Therefore, if the groundwater level time series is relatively short and there are precipitation data which precedes it, you are able to execute Metran and produce results. Similarly, GARDENIA is able to function without groundwater level time series at the start of the modelling period, as long as a discharge time series are available. AquiMod, however, must have groundwater level data input for the start of the modelling period. Most of the boreholes modelled in Metran and AquiMod share similar modelling periods, with the exception of Allen, Tully, and Vickerstown. Generally, the time series lengths for each monitoring borehole in GARDENIA are shorter than in AquiMod and Metran. This is due to the fact that there must be direct coherence between the groundwater level data lengths and discharge data. With shorter river discharge data time series available, the groundwater level time series had to be clipped to the length of the discharge series.

5 RESULTS AND CONCLUSIONS

5.1 Historical recharge values

Long-term average (LTA) recharge estimated using the different models is shown in **Figure 14**.

- LTA recharge for AquiMod and GARDENIA was calculated using the recharge time series output by the best models.
- A recharge time series is not produced directly from Metran. Instead, LTA recharge is calculated using the formula $R = P - fE$ (**Appendix D**), where R recharge, P precipitation, f evaporation factor, and E evaporation. As mentioned in Appendix D, the formulas used to calculate recharge from Metran results are based on assumptions that can be easily violated. Therefore, the equations should only be applied to LTA rainfall and evaporation data and using only models of the highest quality.
- To derive an estimate of (a) Potential Recharge, the agri-meteorological input data (Effective Rainfall, ER) are multiplied by the recharge coefficient polygons (**Figure 12**). (b) long-term (deep) recharge is restricted if the bedrock aquifer is poorly productive (in Ireland: LI, PI and Pu aquifer categories), so a maximum recharge capacity is applied to simulate the limited recharge acceptance of poorly fractured, low storage aquifers.

Table 8 displays the historical recharge time series simulations from AquiMod and GARDENIA. Clear differences are observed between the mean and range of recharge values produced by the two models. Borrismore Creek, MB 07B and MB 30 show a higher mean value and wider distribution of recharge values from AquiMod than GARDENIA. Whereas, with Freshford and Vickerstown, the opposite is true.

The LTA recharge calculated for each borehole show little correlation between AquiMod, GARDENIA and Metran. This is perhaps not surprising, due to the different approaches and different catchment sizes modelled by AquiMod and GARDENIA, as well as the differences in how the models operate and calculate recharge. Freshford displays a high degree of variation between average recharge values calculated by the four models, with the lowest value of 6.4 mm/month (AquiMod) and 63.0 mm/month (Metran). Borrismore Creek displays the smallest range in recharge values between the four models, with the lowest value of 15.7 mm/month (GARDENIA) and 32.9 mm/month (Metran).

There is some agreement between AquiMod and the INRM at three boreholes: at MB 30, AquiMod calculates an average recharge of 28.6 mm/month with a recharge value of 28.0 mm/month for the INRM (non-capped and capped estimate); at Borrismore Creek, AquiMod slightly underestimates average recharge at 23.7 mm/month, with a value of 24.5 mm/month for the non-capped INRM; and at Vickerstown, there is an average recharge of 10.9 mm/month for AquiMod and 7.8 mm/month for the INRM (capped and non-capped). Similarly, two of the boreholes modelled by GARDENIA also show similar average recharge values when compared with the INRM: at MB 30, GARDENIA calculates an average recharge of 24.4 mm/month which is approximately 4 mm/month less than the INRM value of 28.3 mm/month (capped and non-capped); and at Borrismore Creek, the average recharge from GARDENIA is 15.4 mm/month compared with 16.8 mm/month for the INRM (capped).



The model which consistently calculates the highest recharge value is Metran which, in most cases, is roughly 10-20 mm/month greater than the next highest model. Most of the LTA recharge values calculated from GARDENIA boreholes are lower than those calculated from AquiMod, with the exception of Freshford (45.7 mm/month) and Vickerstown (35.0 mm/month) which are both much higher than the recharge values from AquiMod (6.4 and 10.9 mm/month, respectively).

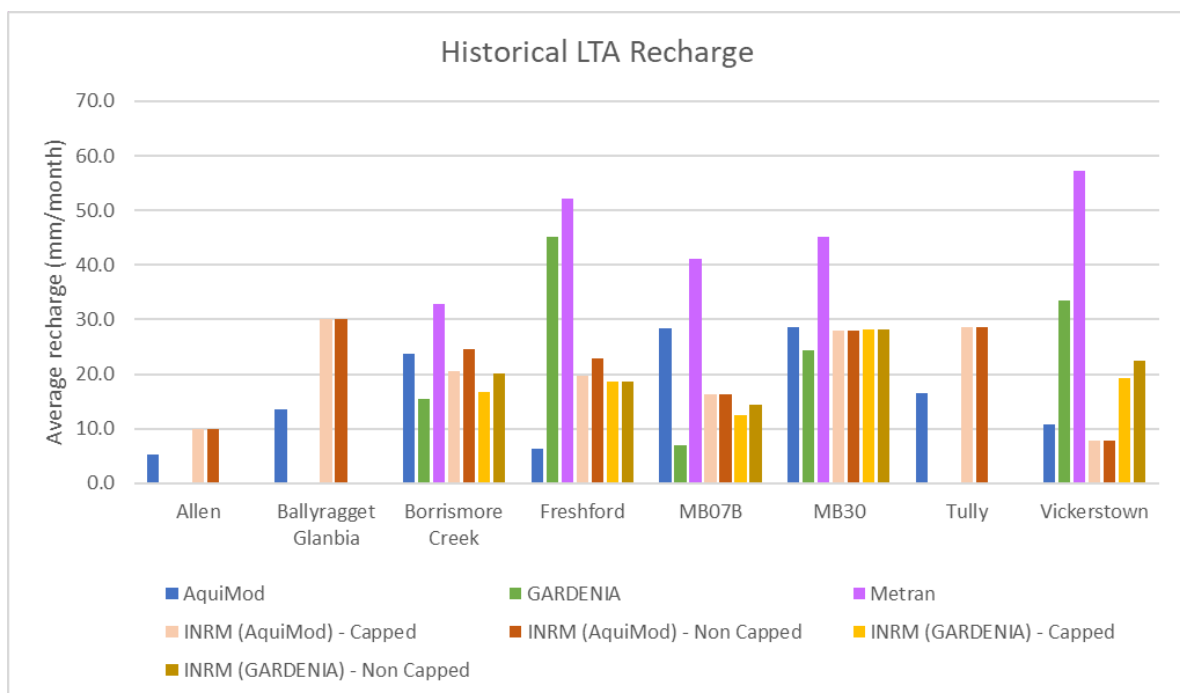


Figure 14 : Comparison of historical Long Term Average (LTA) recharge values for each site per model. Comparing AquiMod, GARDENIA, the Irish National Recharge Model (INRM) & Metran models. Different estimations of recharge from the INRM were calculated to accommodate the different catchment sizes modelled in AquiMod and GARDENIA. Ballyragget Glanbia (GARDENIA) was removed due to poor NSE scores.

Table 8: Simulated historical recharge time series produced by AquiMod (top) and GARDENIA (bottom). Note the differing y-axis scales between the AquiMod and GARDENIA graphs for Borrismore Creek, Freshford–Johnstown Rd, MB 07B (Upper). Models which failed calibration tests have not been displayed.

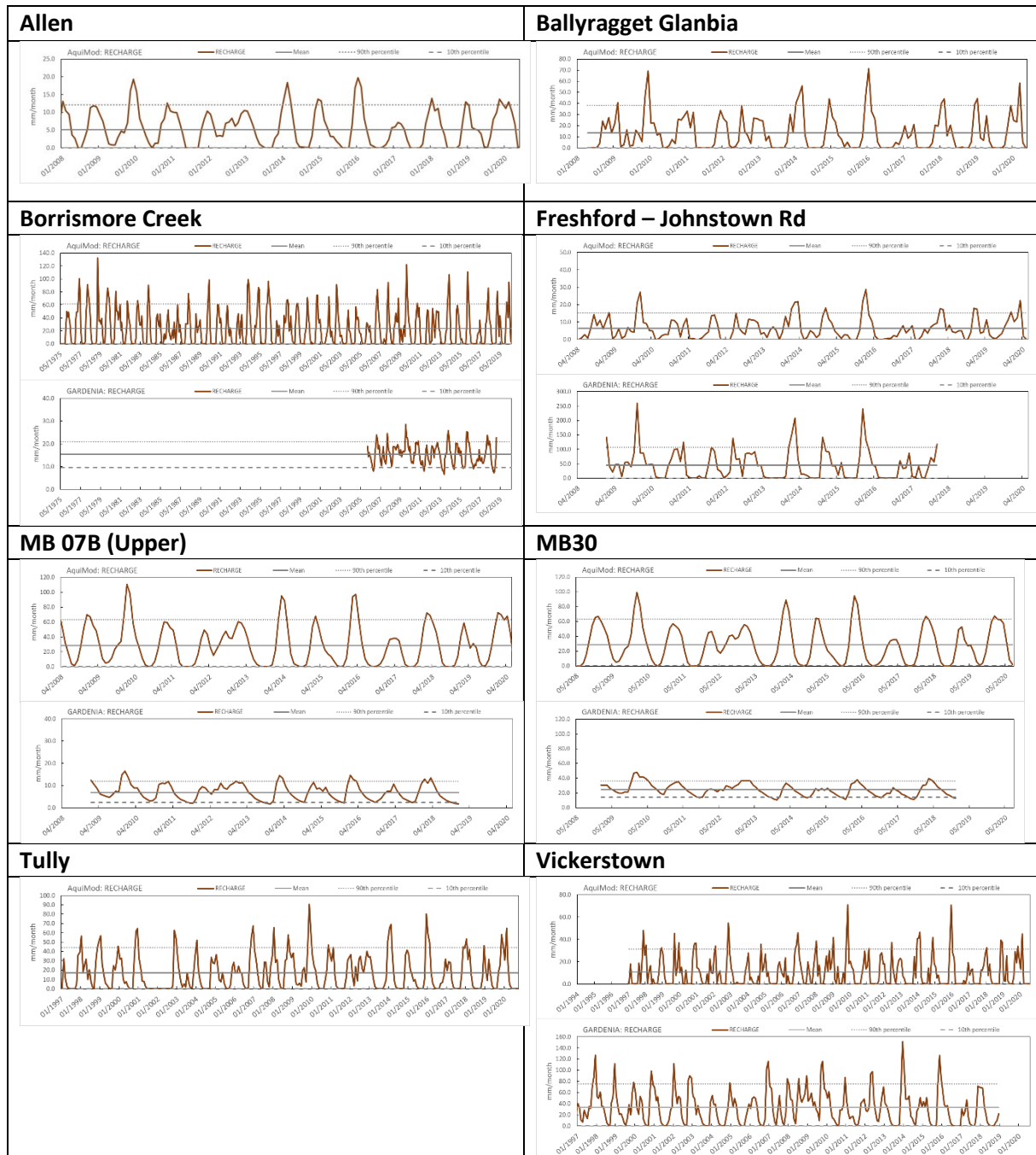
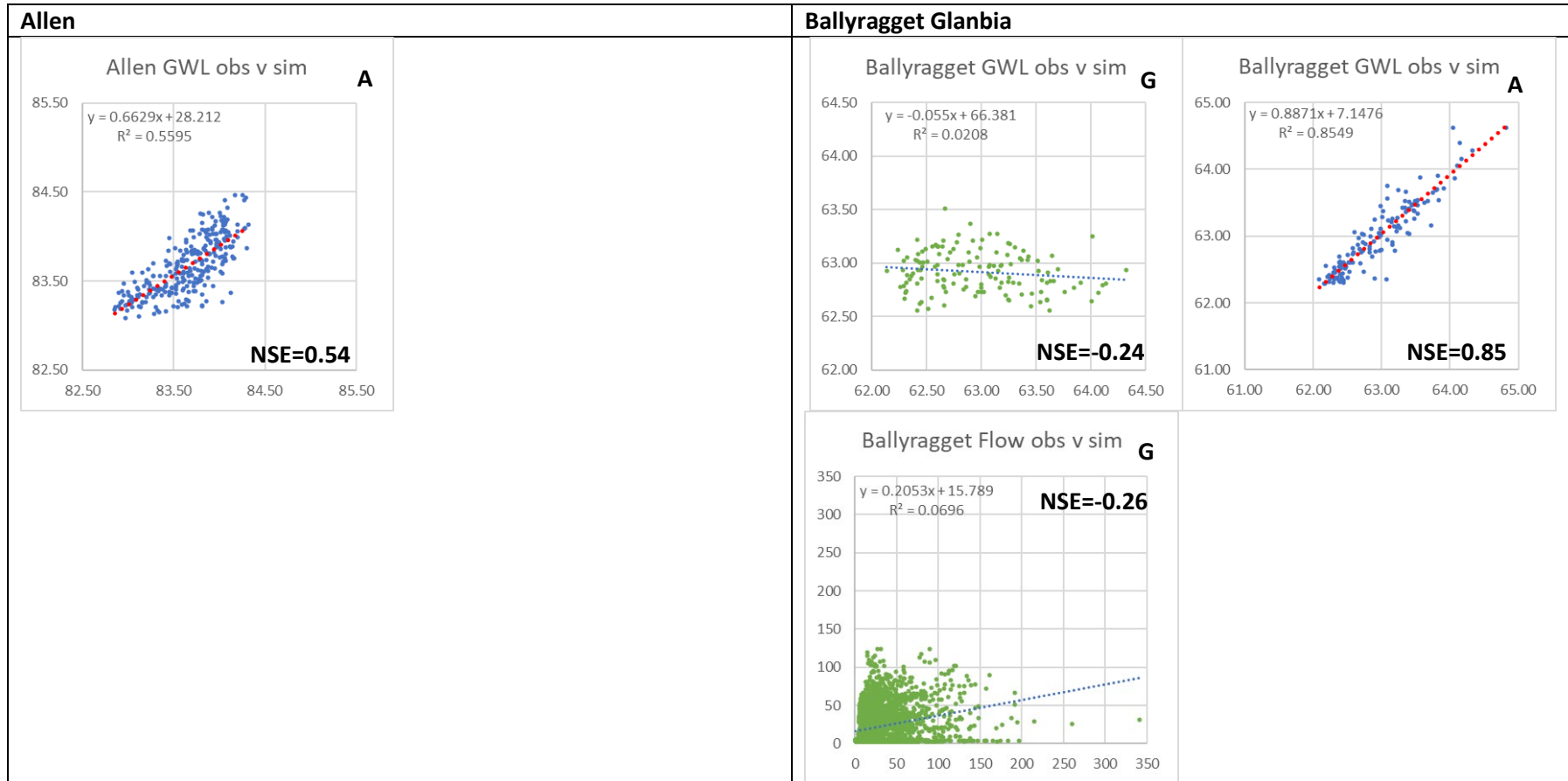
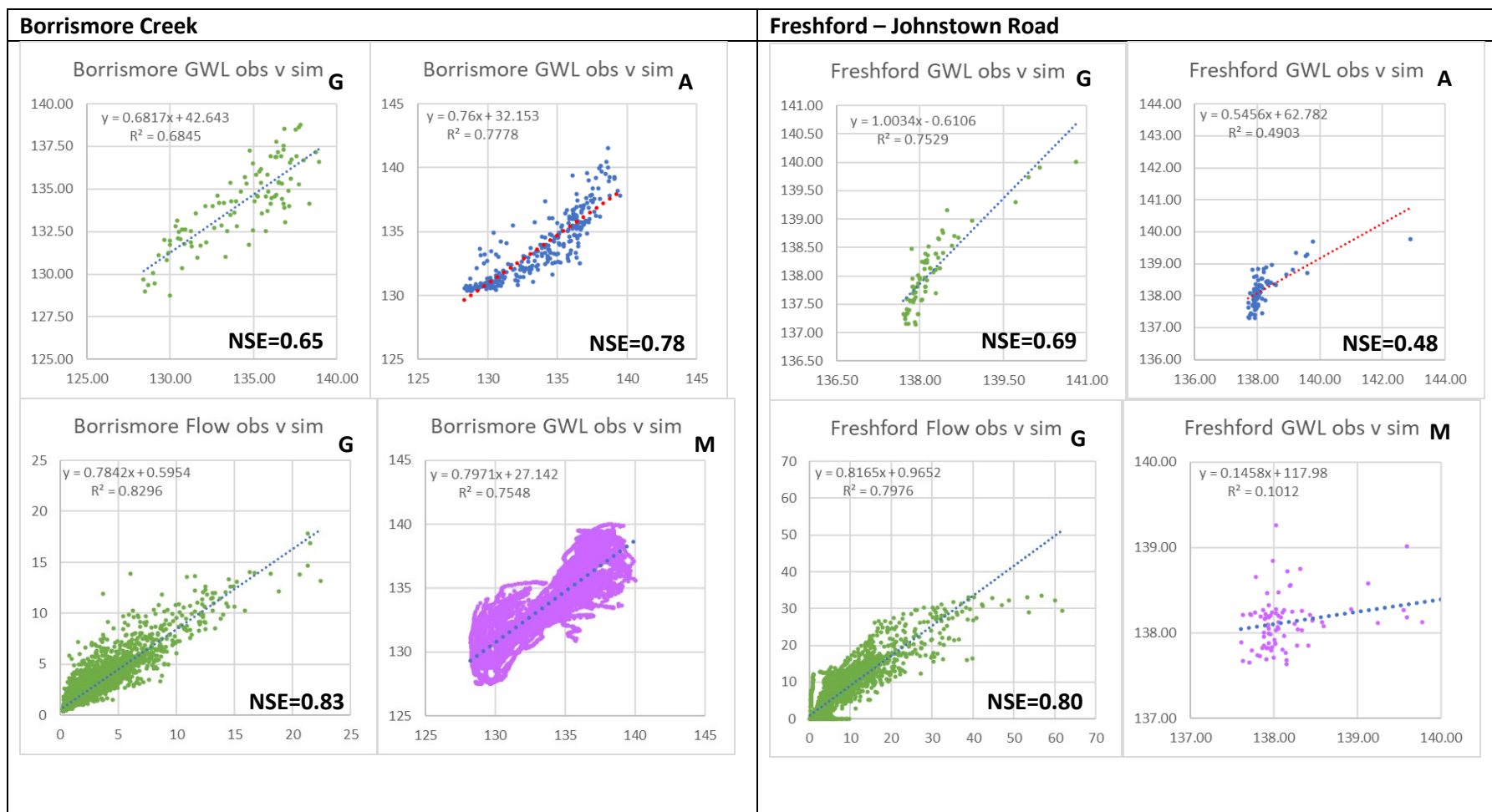
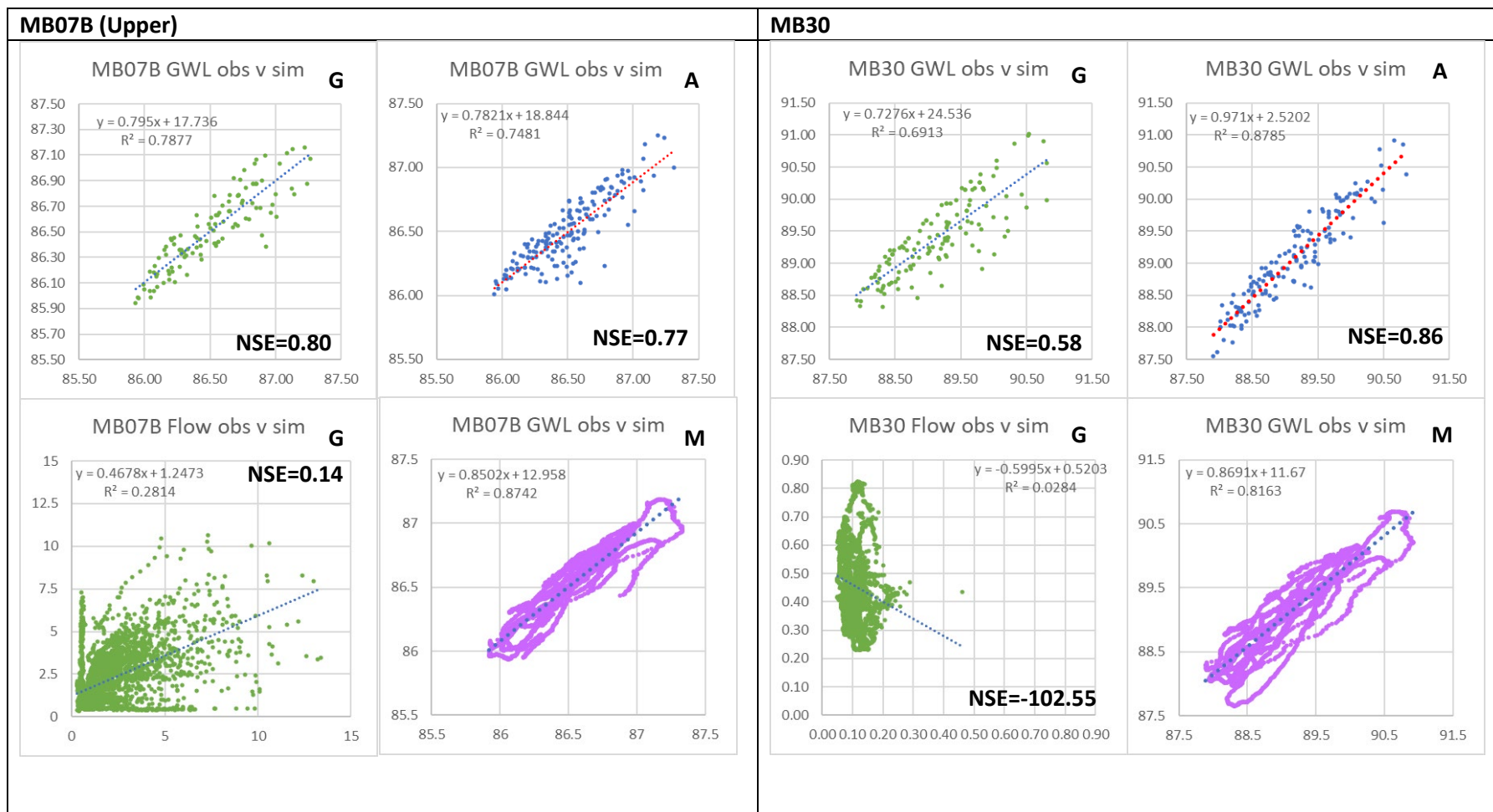
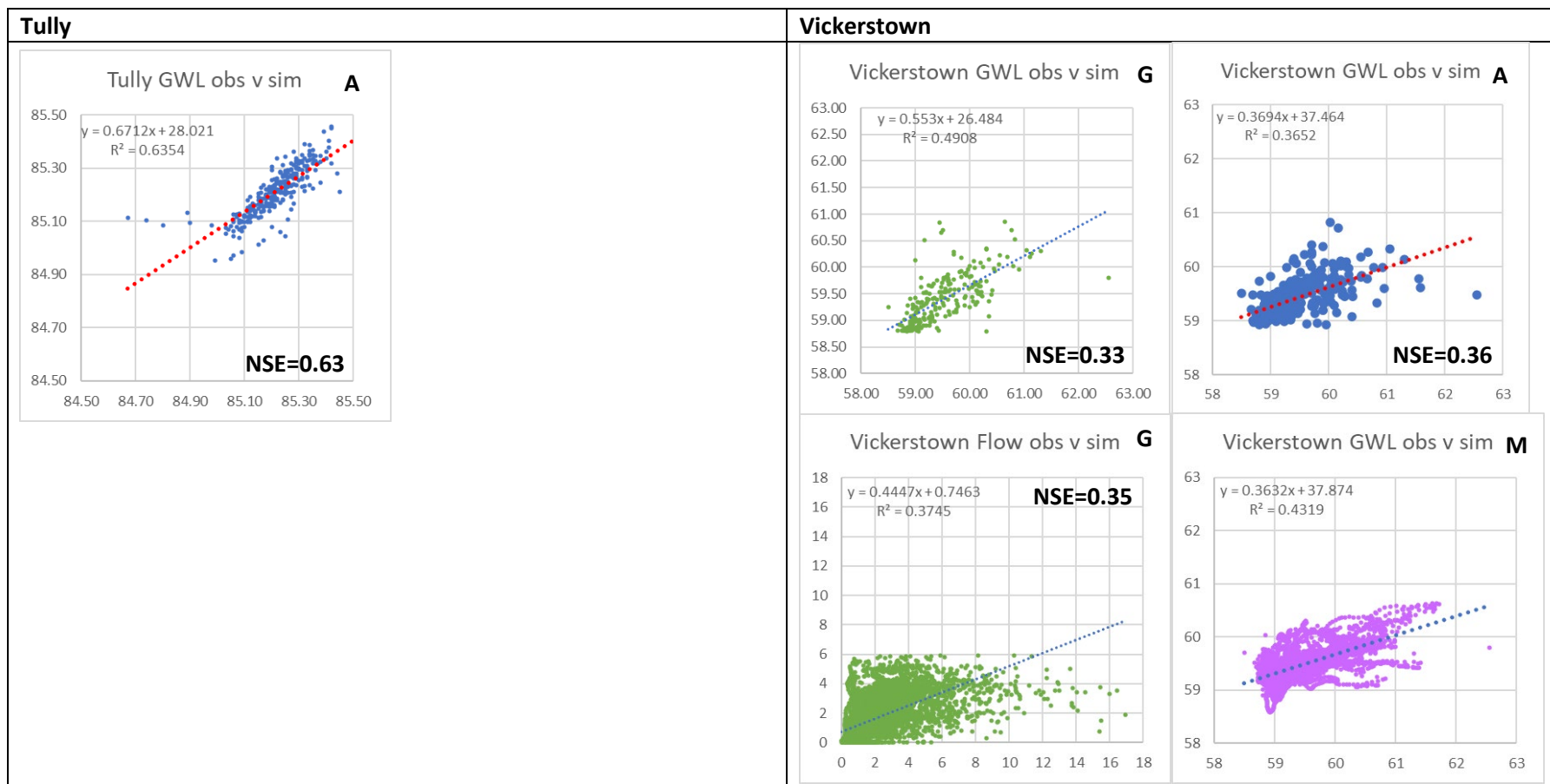


Figure 15: Scatterplots of observed groundwater levels (GWL) and river discharges (Flow, GARDENIA only) compared to the simulated results in AquiMod, GARDENIA and Metran. Blue points ("A"): AquiMod; green points ("G"): GARDENIA; pink points ("M") are Metran.









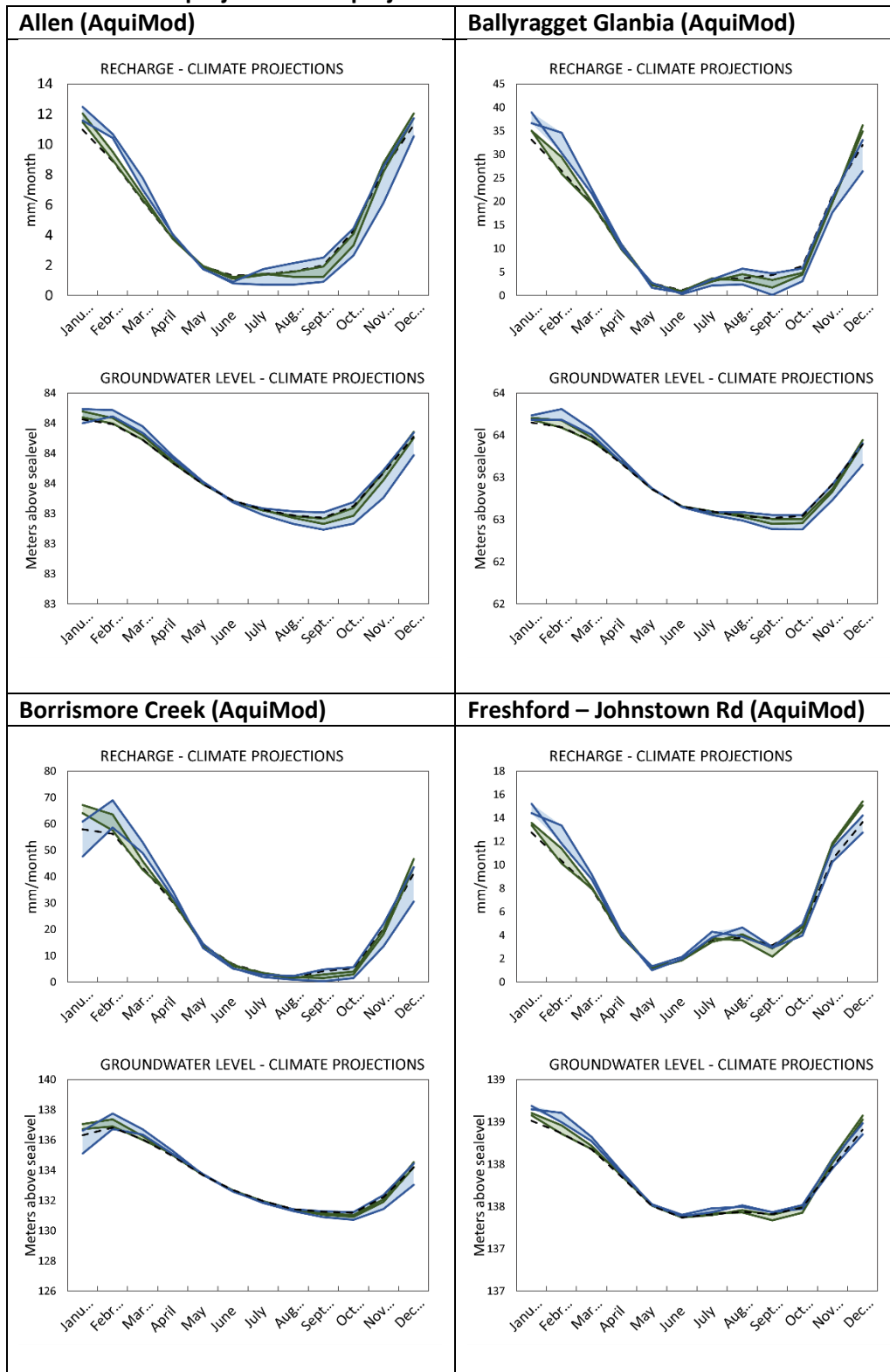
5.2 Projected recharge values

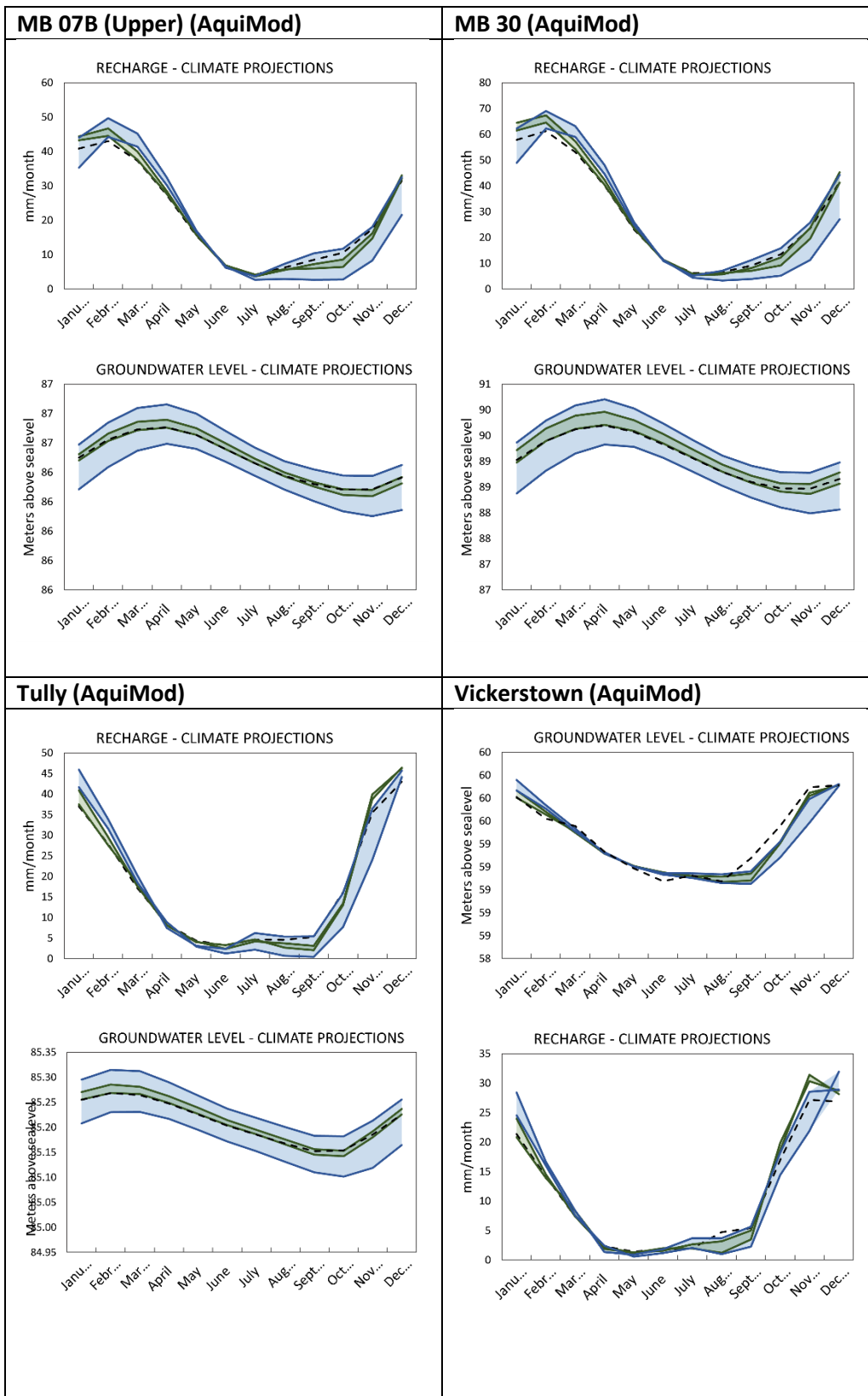
The forcing data, rainfall and potential evaporation, are altered using the change factors of the climate models (see **Table 3**). These change factors are used as multipliers to both the historical rainfall, potential evaporation and, in the case of Metran, evaporation values.

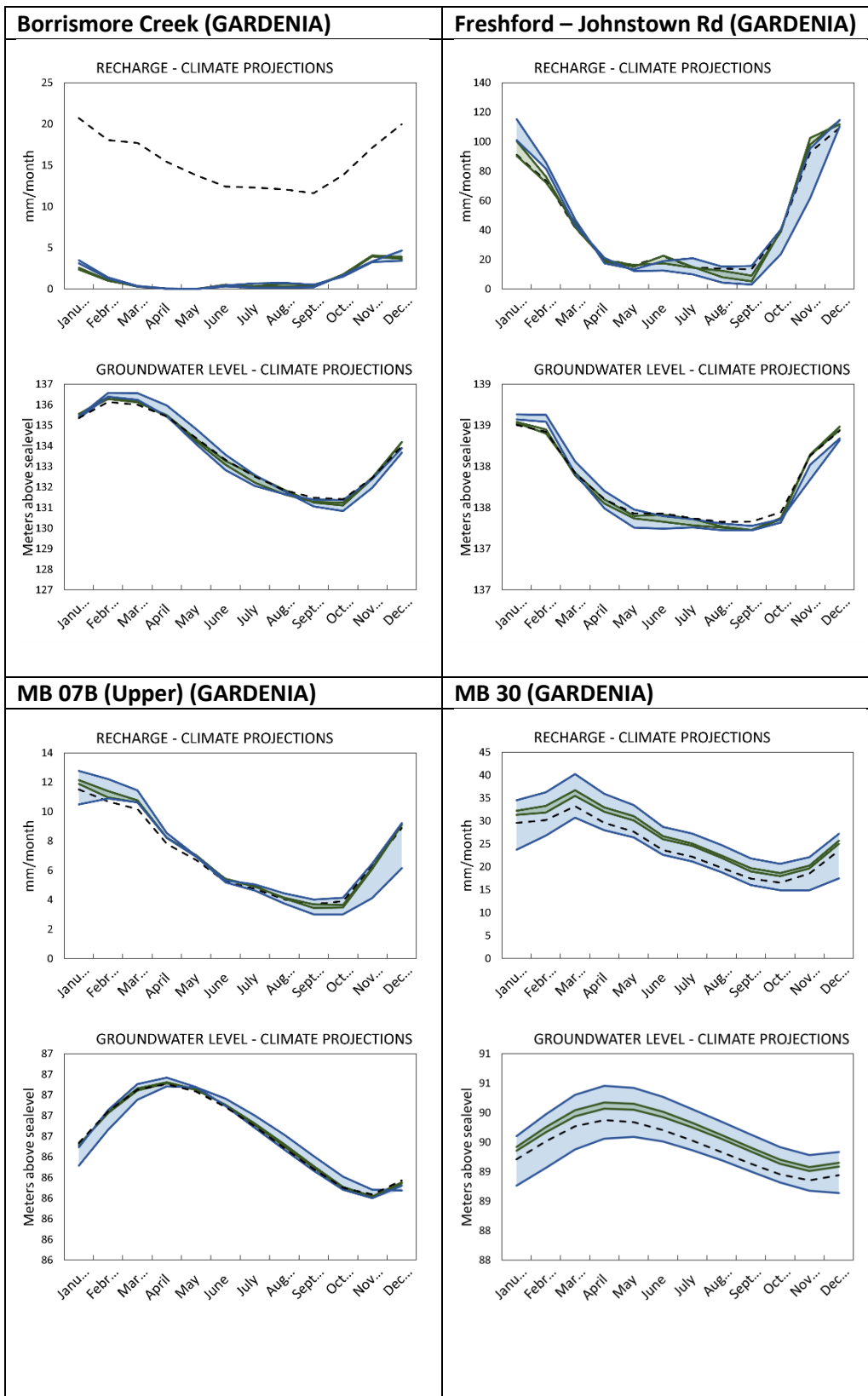
For the application involving Aquimod and GARDENIA, these factors are used to alter the time series of historical rainfall and potential evaporation values used to drive the model. When using Metran, the historical time series are altered using these factors first, and then the long-term average rainfall and evaporation values are calculated. The recharge coefficient f_c (**Appendix B**) values of the different boreholes, as calculated from the calibration of Metran model using the historical data, are then applied to calculate the projected long-term average recharge values.

Table 9 (below) shows the results of applying climate projections within Aquimod and GARDENIA. Typically, the range of projected recharge observed at each borehole is much smaller from April to June/July. During this time of the year, potential evaporation increases as temperature increases, and begins to exceed precipitation. A soil moisture deficit occurs as a result and precipitation is, therefore, taken up by this deficit which results in less precipitation entering the groundwater system as recharge. Conversely, as potential evaporation begins to drop in the mid-to-late summer, precipitation increases and exceeds potential evaporation with an eventual peak around December-January. It is during these months that we see the range in projected recharge across the different warming scenarios increase. Therefore, in Ireland, this period of the year is responsible for providing the greatest potential change to recharge.

Table 9: Predicted average monthly recharge and groundwater levels using AquiMod and GARDENIA and project climate projections







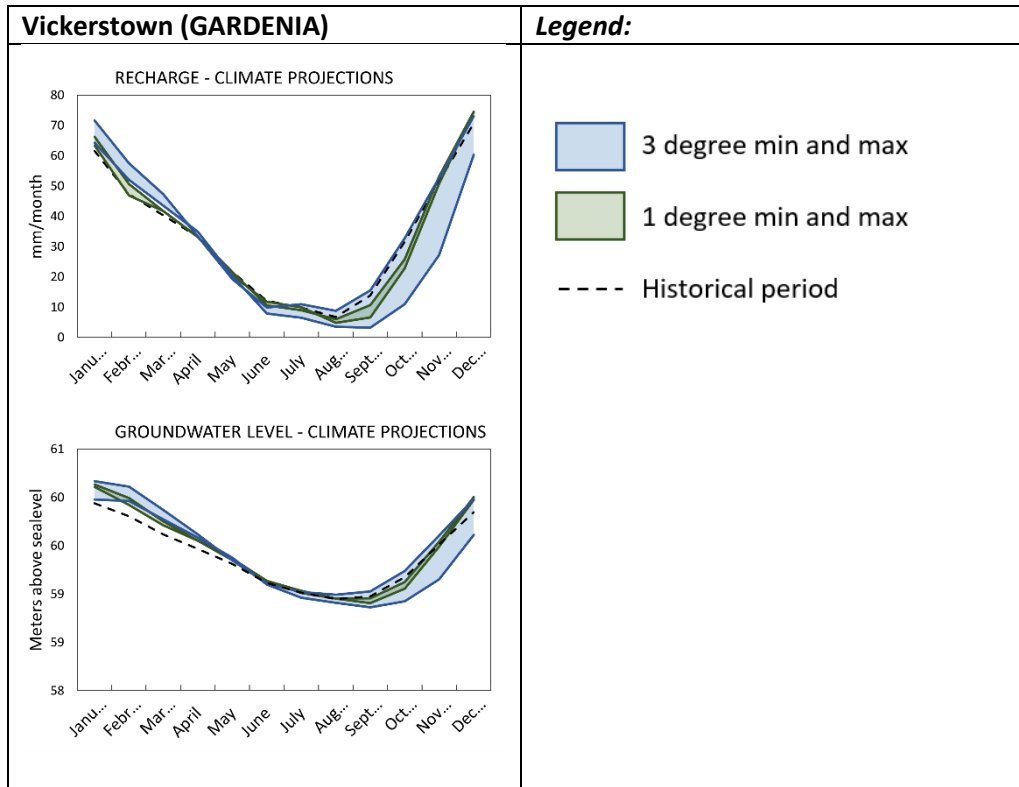


Table 10 shows the historical and projected long-term average recharge values calculated using the best performing AquiMod, GARDENIA, and Metran models and the 1°C and 3°C minimum and maximum warming scenarios outlined previously.

Figure 16 shows the historical and future long-term average recharges values calculated using the best performing AquiMod model. The greatest increase in recharge values is consistently observed when the 3°C maximum rainfall and potential evaporation data are used. The greatest reduction in recharge values is observed when the 3°C minimum rainfall and potential evaporation data are used, with the exception of Freshford which displays a 5.3% increase in recharge.

The 1°C minimum scenario shows the smallest magnitude of change to recharge, but the most variation with regards to positive or negative changes. The boreholes in the north of the study area (see **Figure 1**) show a reduction in recharge values. This includes all the boreholes situated in the Curragh gravel aquifer (MB 07B -1.3%, MB 30 -0.6%, and Tully -0.4%), a poorly productive fractured limestone aquifer (Allen -1.7%), and a karst limestone aquifer (Ballyragget Glanbia 1.0%). Contrastingly, the boreholes located in the central part of the study area, within karst limestone aquifers (Borrismore Creek +1.1%, Freshford +2.6%, and Vickerstown +1.6%) all show an increase in recharge values.

When the 1°C maximum rainfall and potential evaporation data are used, seven of eight AquiMod models display an increase in recharge, with the greatest increase observed at



Borrismore Creek (7.2%) and the smallest increase at Tully (2.9%). The exception to this increase in recharge is observed at MB 07B, which exhibits a -24.2% reduction.

Simulated historic and climate projection recharge values calculated by GARDENIA are displayed in **Figure 17**. Similar to the Aquimod results, the highest increase in recharge values is observed across all boreholes when using the 3°C maximum rainfall and potential evaporation data (excluding the anomalous projected values for Borrismore Creek). Conversely, the greatest reduction in recharge values is observed when the 3°C minimum climate scenario data was used (**Table 10**). (Excluding Borrismore Creek, as an error seems to have occurred here. No changes have been made to the input parameters, so it is unusual why the future recharge predictions are so low.)

The 1°C minimum scenario also results in the most variation with positive or negative changes to recharge values. However, when compared to Aquimod, the pattern of the percentage increase or decrease at boreholes is reversed, with the gravel aquifers in the north of the pilot area showing an increase in recharge and the karst aquifers in the middle of the pilot area showing a decrease in recharge. The highest increase in recharge is observed at MB 30 (+7.9%) and the smallest increase is observed at MB 07B (+1.8%). The greatest reduction in recharge is observed at Vickerstown (-2.5%), with the smallest reduction in recharge value observed at Freshford (-0.6%).

The 1°C maximum climate scenario results in consistent increases to recharge values for all boreholes modelled in GARDENIA, with most of the boreholes showing a ~1-4% increase in recharge and MB 30 yielding an +11.2% increase.

Similar patterns are observed with the simulated and climate projection recharge values calculated from Metran data (**Figure 18**). The use of the 3°C maximum climate scenario data results in the highest increase in recharge values across most of the boreholes, with an increase of 8.4-11.6% observed. Freshford observes a reduction of -10.4%. All boreholes modelled in Metran with the 3°C minimum climate scenario show a reduction in recharge, with values ranging from -4.0% to -22.7% (Vickerstown and Freshford, respectively).

The Metran data modelled with the 1°C minimum climate scenario data mostly follows a trend like that of GARDENIA which opposes the positive/negative changes to recharge values observed by Aquimod, with the exception of MB 07B which shows the same 1.3% decrease in recharge as Aquimod. The highest reduction is observed at Freshford (-18.5%) and the smallest reduction is observed at Vickerstown (-0.5%).

Like Aquimod and all but one of the GARDENIA models, most boreholes modelled in Metran using the 1°C maximum climate scenario data showed an increase in recharge values, with the highest increase observed at MB 30 (+5.4%) and the smallest increase at Borrismore Creek (+1.6%). Freshford displayed a -15% reduction in recharge.

Table 10: Simulated LTA historical recharge compared with simulated LTA projected recharge for the different climate change scenarios.

		Historical mm/month	1deg min mm/month	% change	1 deg max mm/month	% change	3 deg min mm/month	% change	3 deg max mm/month	% change
Allen	AquiMod	5.16	5.07	-1.7	5.38	4.3	4.50	-12.7	5.41	4.7
Ballyragget Glanbia	AquiMod	13.54	13.40	-1.0	13.99	3.3	12.89	-4.8	14.92	10.2
BMC	AquiMod	23.72	23.99	1.1	25.44	7.2	21.32	-10.1	26.38	11.2
	GARDENIA	15.66	1.29	-91.8	1.31	-91.6	1.34	-91.4	1.34	-91.5
	Metran	32.89	32.35	-1.7	33.42	1.6	28.82	-12.4	36.06	9.6
Freshford	AquiMod	6.38	6.55	2.6	6.81	6.6	6.73	5.3	7.20	12.8
	GARDENIA	45.65	45.39	-0.6	46.72	2.3	40.37	-11.6	50.01	9.5
	Metran	63.04	51.37	-18.5	53.59	-15.0	48.72	-22.7	56.46	-10.4
MB 07B (Upper)	AquiMod	28.44	28.07	-1.3	21.57	-24.2	24.98	-12.2	31.66	11.3
	GARDENIA	6.98	7.11	1.8	7.23	3.6	6.42	-8.0	7.56	8.3
	Metran	41.08	40.52	-1.3	42.18	2.7	36.71	-10.6	44.89	9.3
MB 30	AquiMod	28.59	28.40	-0.6	30.16	5.5	25.25	-11.7	32.00	11.9
	GARDENIA	24.32	26.23	7.9	27.06	11.2	21.78	-10.4	29.39	20.8
	Metran	45.13	45.60	1.0	47.55	5.4	42.15	-6.6	50.26	11.4
Tully	AquiMod	17.11	17.04	-0.4	17.60	2.9	15.21	-11.1	18.86	10.2
Vickerstown	AquiMod	10.88	11.06	1.6	11.56	6.2	10.43	-4.2	12.11	11.2
	GARDENIA	34.98	34.11	-2.5	35.61	1.8	30.25	-13.5	38.18	9.2
	Metran	57.31	57.03	-0.5	59.48	3.8	54.99	-4.0	62.15	8.4



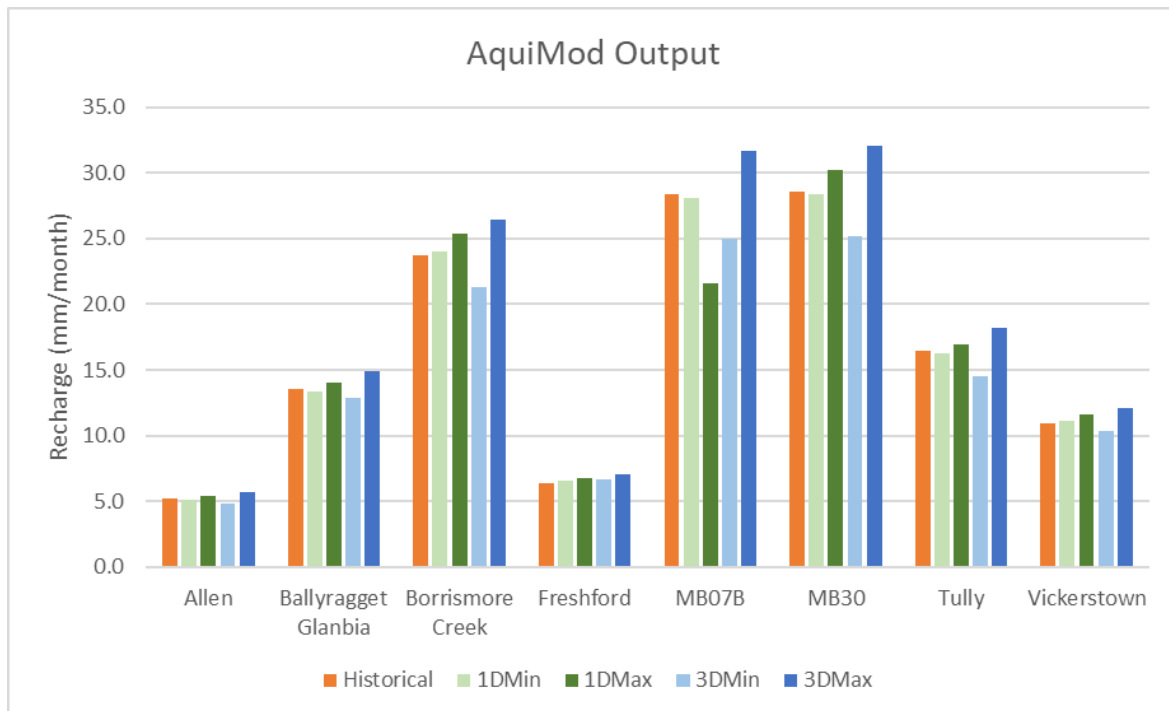


Figure 16: Historical/simulated and future recharge values as produced by the best performing AquiMod model

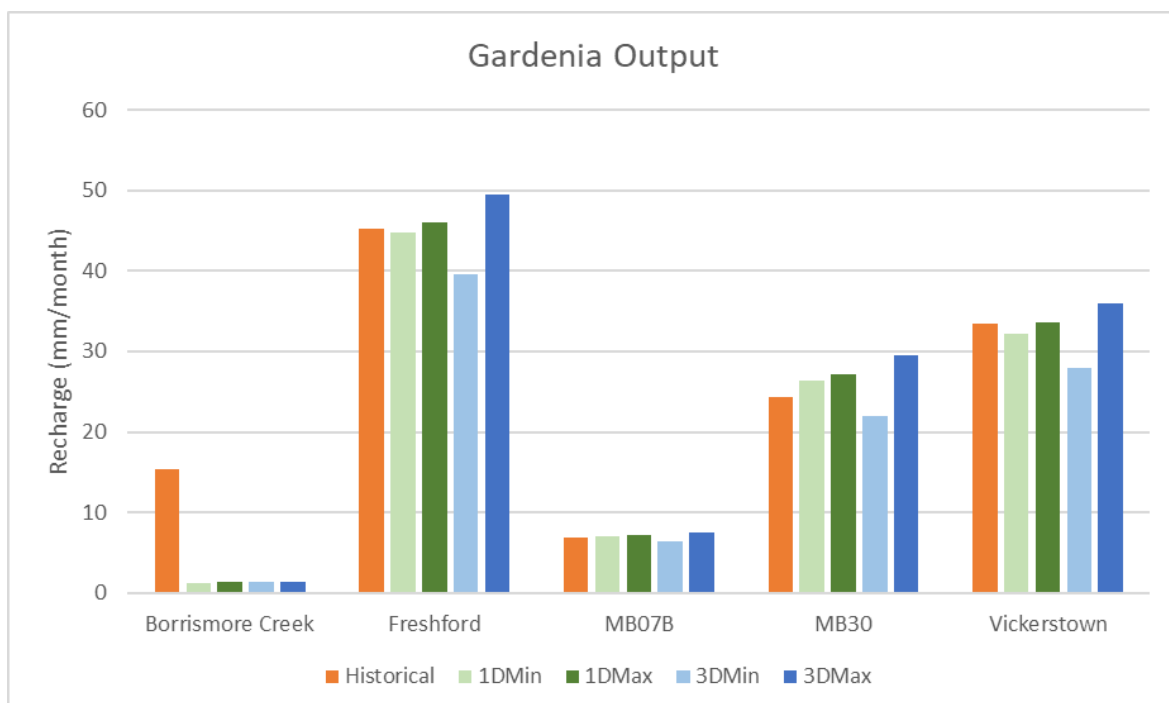


Figure 17: Historical/simulated and future recharge values as produced by the best performing GARDENIA model. Note that no future predictions were modelled for Ballyragget Glanbia due to poor NSE scores.



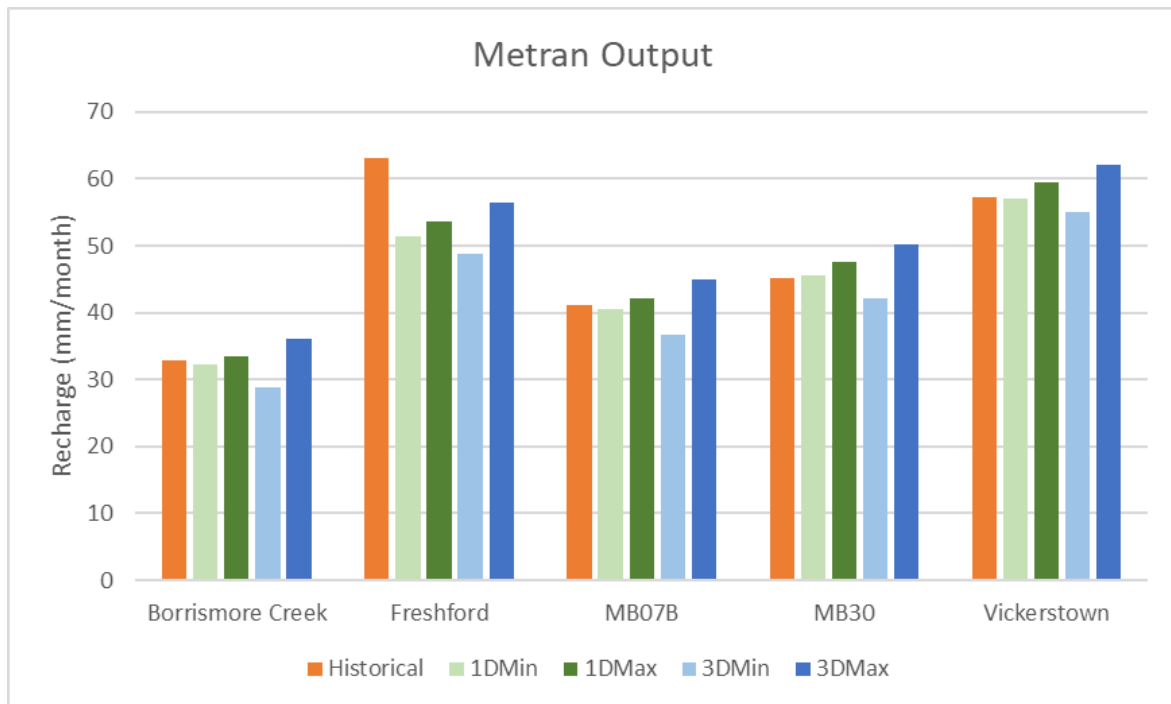


Figure 18: Historical/simulated and future recharge values as produced by the best performing Metran model.

It is evident that trends are observed with regards to relative increases or decrease to recharge values observed for most of the climate scenarios. The greatest consistent reduction in recharge across all models is observed when the 3°C minimum rainfall and potential evaporation data are used, with the exception of Freshford (AquiMod) which displays a 5.3% increase in recharge.

The greatest increase in recharge values across all models is observed when the 3°C maximum rainfall and potential evaporation data are used, with the exception of Freshford (Metran) which shows a 10.4% decrease in recharge. Similarly, when the 1°C maximum rainfall and potential evaporation data are used, the GARDENIA models, Metran models (excluding Freshford), and AquiMod models (excluding MB 07B) all show an increase in recharge values.

When the 1°C minimum climate scenario data are used, there are no clear trends observed when comparing results from the three models.

It is also evident that there are few similarities between the amounts of calculated LTA recharge across all climate scenarios from each model. For example, recharge calculated from Metran is, roughly 10-20 mm/month greater than that of the next highest recharge value from another model.

Excluding the modelling of Borrismore Creek in GARDENIA which has yielded anomalously low results, the Freshford data displays the most variation across the models and climate



scenarios, with some calculated recharge values contradicting otherwise relatively consistent results from other boreholes in the same climate scenario. For example, Freshford (Metran) is the only model which shows a reduction in recharge in the 3°C max scenario, with Freshford (AquiMod) being the only model which predicts a recharge increase in the 3°C min scenario. This may have been a result of sparse groundwater level observations due to a sump in the bottom 1.2 m of the Freshford borehole which caused inaccurate groundwater level readings, and model assumptions not representing the groundwater system sufficiently well.

As previously mentioned, there appears to be an issue with the GARDENIA – Borrismore Creek 'Recharge – Climate Projections' graph shown above. This anomaly is unusual as no parameters have been changed from the historical simulated recharge predictions to the future projections scenarios. All delta change functions calculations have been double checked and there does not appear to be any errors in the daily to monthly recharge conversions. As such, we can suggest that this result is due to some sort of scaling error in the graphs, as the 1C and 3C projections follow a similar trend to that of the historical period, albeit at a reduced scale.

6 REFERENCES

Archer, J.B., Sleeman, A.G. and Smith, D.C., 1996. *A Geological Description of Tipperary and Adjoining Parts of Laois, Kilkenny, Offaly, Clare and Limerick – to accompany the Bedrock Geology 1:100,000 Scale Map Series; Sheet 18, Tipperary*, with contributions by K. Claringbold, G. Staley (Mineral Resources) and G. Wright (Groundwater Resources). Geological Survey of Ireland, Dublin, Ireland. 76 pp.

Ball, D., 2010. What will the Impacts of Climate Change be for Groundwater Systems in Ireland? Proceedings of the 30th Annual Conference of the IAH (Irish Group), Groundwater in the Hydrological Cycle – Pressures and Protection. Tullamore, Ireland, 20-21 April, 2010.

Cawley, A., 1990. The Hydrological Analysis of a Karst Aquifer System. Unpublished M.Eng. Thesis. Department of Engineering Hydrology, University College Galway, Galway, Ireland.

Collins, J.F., and Cummins, T., 1996. *Agroclimatic Atlas of Ireland*. AGMET. Joint Working Group on Applied Agricultural Meteorology, AGMET, Dublin, Ireland.

Daly, E.P., 1978. Groundwater Investigations in County Laois in 1976. Groundwater Division, Geological Survey of Ireland. Internal Report Number 4. Geological Survey of Ireland, Dublin, Ireland.

Daly, E.P., 1980. The Drilling and Testing of Two Boreholes and Groundwater Development in the Westphalian Sandstones of the Slieveardagh Hills, Co Tipperary. Groundwater Division, Geological Survey of Ireland. Internal Report Number 7. Geological Survey of Ireland, Dublin, Ireland.

Daly, E.P., 1981. Case Study: The Kilmanagh River Gravels. Groundwater Division, Geological Survey of Ireland. Geological Survey of Ireland, Dublin, Ireland.

Daly, E.P., 1982. The Groundwater Resources of the Southeast Industrial Development Region. Unpublished draft report of the Geological Survey of Ireland, Dublin, Ireland.

Daly, E.P., 1990. The Likely Effects of Significant Climatic Changes on the Flow Regime in the Principal Irish Aquifers. Proceedings of 10th Annual Seminar, International Association of Hydrogeologists (Irish Group), Portlaoise, Ireland.

Daly, E.P., 1993. Hydrogeology of the Dolomite Aquifer in the Southeast of Ireland. Proceedings of 13th Annual Seminar, International Association of Hydrogeologists (Irish Group), Portlaoise, Ireland.

Daly, E.P., 1994. Groundwater Resources of the Nore River Basin. Geological Survey of Ireland Report Series RS 94/1 (Groundwater). Geological Survey of Ireland, Dublin, Ireland.

Environmental Protection Agency, 2018. Corine Landcover 2018. Available from <https://data.gov.ie/dataset/corine-landcover-2018>

Environmental Protection Agency, 2016. *EPA HydroNet*. Viewed 26 March 2021. Available from: http://www.epa.ie/hydronet/#IE_SE_G_0156_1500_0009

Allen, R.G., Pereira, L.S., Raes, D. and Smith, M. (1988) Crop evapotranspiration - Guidelines for computing crop water requirements - FAO Irrigation and drainage paper 56. Food and Agriculture Organisation of the United Nations, Rome.

Flanagan, J., Nolan, P., McGrath, R. and Werner, C., 2019. Towards a definitive historical high-resolution climate dataset for Ireland – promoting climate research in Ireland. *Advances in Science and Research*, 15, pp.263-276.

GSI (Geological Survey of Ireland), 2005a. *Grouped Rock Units*. Scale 1:100,000. Geological Survey of Ireland, Dublin, Ireland.

Hunter Williams, N.H. and Lee, M., 2007. Ireland at risk - Possible implications for groundwater resources of climate change. Irish Academy of Engineering. <http://iae.ie/publications/?years=2007>

Hunter Williams, N.H., Misstear, B.D.R., Daly, D., Johnston, P.M., Lee, M., Cooney, P. and Hickey, C. (2011) A National Groundwater Recharge Map for Ireland. Proceedings of the *National Hydrology Conference 2011*. 15 November 2011, Athlone, Co. Westmeath, Ireland.

Hunter Williams, N.H., Misstear, B.D.R., Daly, D. and Lee, M., 2013. Development of a national groundwater recharge map for the Republic of Ireland. *Quarterly Journal of Engineering Geology and Hydrogeology*, **46**, 2013, pp. 493–506.

Hunter Williams, N.H., Carey, S., Werner, C. and Nolan, P. (in press) Updated National Groundwater Recharge Map, *Irish Groundwater Newsletter*.

Karlsson, I. B., Eisenbruchner, L. T., Kidmose, J., and Højberg, A. L.: National scale climate change impact assessment – investigating long-term variations in the climate change signal for groundwater levels across geologies and aquifers, *EGU General Assembly 2020*, Online, 4–8 May 2020, EGU2020-4741, <https://doi.org/10.5194/egusphere-egu2020-4741>

Kelly, C., Hunter Williams, N.H. and Misstear, B.D.R., 2015. *Irish Aquifer Properties – A reference manual and guide*. Version 1. March 2015. Geological Survey Ireland, Dublin, Ireland.

Mullarkey, E., Tedd, K., Meehan, R., Kelly, C., Pilmer, A., Doherty, D., Greene, J., O’Keeffe, M., Kabza, M., Duncan, N. and Schuler, P. (2021) Using hydrograph separation methods for catchment water balances: an output from GSI's GW3D project. Poster presented at *41st Annual IAHR Irish Group Groundwater Conference: “Catchment Science and Management – The Role of Geoscience and Groundwater”*, 26-27 April, 2021.

Nolan, P., 2015. Ensemble of regional climate model projections for Ireland. Report 2008-FS-CC-m. Prepared for the Environmental Protection Agency, Wexford, Ireland.

Robins, N.S. and Missteart, B.D.R., 2000. *Groundwater in the Celtic Regions: Studies in Hard Rock and Quaternary Hydrogeology*. Geological Society, Special Publication No. 182. pp. 5–17. The Geological Society, London, UK.

Schulte, R.P.O., Diamond, J., Finkle, K., Holden, N.M. and Brereton, A.J., 2005. Predicting the soil moisture conditions of Irish grasslands. *Irish Journal of Agricultural and Food Research* 44: 95–110.

Tedd, K., Missteart, B., Coxon, C., Daly, D., Hunter Williams, N.H., Craig, M. and Mannix, M. 2011. *Review of groundwater level data in the South Eastern River Basin District*. EPA STRIVE Programme 2007–2013. Environmental Protection Agency, Dublin.

Tedd, K., Missteart, B., Coxon, C., Daly, D., and Hunter Williams, N.H., 2012. Hydrogeological insights from groundwater level hydrographs in SE Ireland. *Quarterly Journal of Engineering Geology and Hydrogeology*, **45**, 19 –30. DOI: 10.1144/1470-9236/10-026.

Thi  ry D., 1988. Forecast of changes in piezometric levels by a lumped hydrological model. *Journal of Hydrology* 97 (1988), pp. 129-148.

Thi  ry, D., 2010. Reservoir Models in Hydrogeology. in “Mathematical Models Volume 2, chapter 13, pp. 409-418 Environmental Hydraulics Series”. Tanguy J.M. (Ed.) –   ditions Wiley/ISTE London. ISBN: 978-1-84821-154-4.

Thi  ry, D., 2013. Didacticiel du code de calcul Gard  nia v8.1. Vos premi  res mod  lisations. Rapport BRGM/RP-61720-FR, 130 p., 93 fig. (Updated v8.6)

Thi  ry, D., 2014. Logiciel GARD  NIA, version 8.2. Guide d’usage. Rapport BRGM/RP-62797-FR, 126 p., 65 fig., 2 ann. (Updated v8.6).

Thi  ry, D., 2015. Validation du code de calcul GARD  NIA par mod  lisations physiques comparatives. Rapport BRGM/RP-64500-FR, 48 p., 28 fig. (Updated v8.6).

Tietzsch-Tyler, D., Sleeman, A.G., McConnell, B.J., Daly, E.P., Flegg, A.M., O’Connor, P.J. and Warren, W.P., 1994. *Geology of Carlow–Wexford. A geological description to accompany the Bedrock Geology 1:100,000 Scale Map Series; Sheet 19, Carlow – Wexford*. Geological Survey of Ireland, Dublin, Ireland, 58 pp.

Werner, C., Nolan, P. and Naughton, O., 2019. *High-Resolution Gridded Datasets of Hydro-Climate Indices for Ireland*. EPA/GSI funded research project. 2016-W-DS-29 EPA, Wexford, Ireland.

Zaadnoordijk, W.J., Bus, S.A.R., Lourens, A., Berendrecht, W.L. (2019) Automated Time Series Modeling for Piezometers in the National Database of the Netherlands. *Groundwater*, 57, no. 6, p. 834-843. <https://onlinelibrary.wiley.com/doi/epdf/10.1111/gwat.12819>

7 ACKNOWLEDGEMENTS

Willem Zaadnoordijk from TNO kindly ran all of the Metran models (historic and future climate scenarios) for the Irish groundwater level observations used in this study.

Majdi Mansoor from BGS was very generous with his time in helping us to start using AquiMod and to develop successful model runs.

Hélène Bessiere from BRGM was very generous with her time in helping us to get going with GARDENIA and to better understand the model parameters and set up.

APPENDICES

APPENDIX A – groundwater monitoring points in SE region pilot area

From Tedd *et al.*, 2011.

Table 1. Historic groundwater level monitoring points (MPs).

Name	GSI (EPA) MP code	County	X	Y	Geology	Aquifer type ²	Subsoils	Subsoil permeability	Vulnerability	Operator	Type of MP	Type of monitoring	Start date	End date	Depth (mbgl)	Datum (maOD)
Oldtown	Kny 18/92 (10_013)	Kilkenny	238700	154400	Sand and gravel	Rg	18 m sand & gravel	H	E	GSI/OPW	BH	Chart recorder to Mar-08, then logger	Oct-80	Ongoing	20	118.45
Kilmeague		Kildare	278900	223700	Sand and gravel	Lm	Sand & gravel	H	H	GSI	BH	Manual dips	Jun-70	Jul-88	27.4	~107
Rahilla		Kildare	271420	271420	Till with gravel	Rg	Till with gravel	H	H	GSI	DW	Manual dips	Nov-68	Oct-87	35.4	~124
Ballincurry	Tip 55/65	Tipperary	227800	148500	Westphalian Sst	Lm	6 m clay; down-gradient of Rck	L	HL	GSI	BH	Chart recorder	Oct-77	Oct-82	60	170.35
Woodsgrift/Borrismore Creek	Kny 12/8 (10_005)	Kilkenny	233000	161500	Karstified Imst	Rkd	0–3 m TLs	M	E	GSI/OPW	BH	Chart recorder to Oct-07; then logger	Apr-75	Ongoing	36	147.34
Tubrid Lower	Kny 12/34	Kilkenny	23423	16192	Karstified Imst	Rkd	0–3 m TLs	M	E	GSI		Chart recorder	Aug-71	Dec-91	12.7	128.12
Clomantagh Lower	Kny 13/42	Kilkenny	234600	163800	Karstified Imst	Rkd	3–10 m TLs; close to KaRck	M	H	GSI		Chart recorder	Jul-74	Oct-94	57	149.39
Cullahill	Kny 35/39	Laois	237400	175700	Karstified Imst	LI	3–10 m TLs; alluvium	M	H	GSI/OPW			Sep-76	Jun-09	–	~85
Masterson		Laois	261600	193100	Karstified Imst	Rkd	3–10 m TLs; alluvium	M	H	GSI	DW	Manual dips	Nov-70	Oct-90	14	~105
Land Commission 2		Laois	259300	193100	Karstified Imst	Rkd	0–3 m TLs; close to KaRck	M	E	GSI	BH	Manual dips	Jul-71	Jan-81	–	~159
Rathduff	Kny 27/58 (10_017)	Kilkenny	250500	143300	Dolomitised Imst	Rkd	18 m TLs	M	H	GSI/OPW	BH	Chart recorder to Mar-08, then logger	Aug-81	Ongoing	62	46.75
Boston Co. Co.		Kildare	271900	220400	Dolomitised Imst	LI	Rck	–	X	GSI	DW	Manual dips	Apr-70	Aug-85	15.9	~119
Granston Manor	Ls 28/168	Laois	234100 ¹	178600	Crosspatrick Fm	LI	6.8 m clay; 1.4 m sand	M	H	GSI/Arcon	BH	Chart recorder	Sep-78	Jul-96	30	84.57
Ardscull DW		Kildare	272200	198700	Ballysteen Fm	LI	0–3 m TLs; close to Rck	–	E	GSI	DW	Manual dips	Jul-69	Oct-90	18.9	~89
Knocktopher Manor	Kny 31/72 (10_012)	Kilkenny	253140	135930	Kiltorcan Sst	Rf	5 m TLs	L	E	GSI/OPW	BH	Chart recorder to May-08; then logger	Aug-80	Ongoing	40	61.67

¹The co-ordinates of the Granston Manor fall within a lake, the actual location of the boreholes is likely to be close to this lake; ~, approximate elevations were taken from the appropriate Ordnance Survey Ireland Discovery Series (1:50,000) map.

²For aquifer type codes, please refer to Box 5.1.

Sst, sandstone; Imst, limestone; FM, Formation; Rck, bedrock outcrop and subcrop; TLs, tills derived chiefly from limestone; KaRck, karstified limestone bedrock outcrop or subcrop; H, High; M, Moderate; L, Low; E, Extreme; HL, High to Low (only interim data available); GSI, Geological Survey of Ireland; OPW, Office of Public Works; EPA, Environmental Protection Agency; BH, borehole; DW, drinking water; mbgl, metres below ground level; maOD, metres above Ordnance Datum.

Table 1 Environmental Protection Agency (EPA) Water Framework Directive monitoring programme monitoring points (MPs).

Name	EPA (GSI) MP code	County	X	Y	Start date	End date	Type of MP	Type of monitoring	Geology	Depth of borehole (mbgl)	Datum (maOD)	Operator
Oldtown	10_013 (Kny 18/92)	Kilkenny	238700	154400	Oct-80	Ongoing	BH	Chart recorder to Mar-08, then logger	Sand and gravel	20.00	118.45	GSI/OPW
Ballyragget Glanbia Factory	10_002	Kilkenny	244002	172803	Mar-08	Ongoing	BH	Logger	Sand and gravel	18.00		EPA/LA
Ballysax	09_002	Kildare	280278	210832	Jun-08	Ongoing	BH	Logger	Sand and gravel	18.00		EPA/LA
Brownstown	09_004	Kildare	278639	210092	Jun-08	Ongoing	BH	Logger	Sand and gravel	13.00		EPA/LA
Landfill Site	01_004	Carlow	270647	170052	Mar-08	Ongoing	BH	Logger	Sand and gravel	69.00		EPA/LA
PF – MB29	09_011	Kildare	275043	213065	Apr-08	Ongoing	BH	Logger	Sand and gravel	13.30		EPA/LA
PF – MB30	09_012	Kildare	275042	213190	Apr-08	Ongoing	BH	Logger	Sand and gravel	24.00		EPA/LA
PF – MB37	09_013	Kildare	277433	217126	Jun-08	Ongoing	BH	Logger	Sand and gravel	18.20		EPA/LA
PF – S10	09_017	Kildare	276426	215904	No data	No data	BH		Sand and gravel	–		EPA/LA
PF – SB31	09_018	Kildare	276423	215894	No data	No data	BH		Sand and gravel	9.00		EPA/LA
PF – MB7 (Lower)	09_016	Kildare	276810	215540	May-08	Ongoing	BH	Logger	Sand and gravel			EPA/LA
PF – MB7 (Middle)	09_015	Kildare	276810	215540	May-08	Ongoing	BH	Logger	Sand and gravel			EPA/LA
PF – MB7 (Upper)	09_014	Kildare	276810	215540	May-08	Ongoing	BH	Logger	Sand and gravel			EPA/LA
PF – Hangedman's Arch	09_010	Kildare	275916	217539	No data	No data	Spring		Sand and gravel			EPA/LA
Kyle Public Water Supply	11_008	Laois	255501	192243	Jan-77	Ongoing	Spring		Sand and gravel			EPA/LA
Tully (BH1)	09_019	Kildare	273313	210923	Jun-08	Ongoing	BH	Logger	Sand and gravel	9.00		EPA/LA
Borrismore Creek	10_005 (Kny 12/8)	Kilkenny	233000	161500	Apr-75	Ongoing	BH	Chart recorder to Oct-07, then logger	Dinantian karstified limestone	36.00	147.34	GSI/OPW
Freshford to Johnstown Rd BH	10_009	Kilkenny	231261	167072	Oct-07	Ongoing	BH	Logger	Dinantian pure bedded limestone	13.50		EPA/LA
Laffansbridge	22_005	Tipperary	219100	146620	Oct-07	Ongoing	BH	Logger	Dinantian pure bedded limestone	10.00		EPA/LA
Mayglass	26_008	Wexford	300134	112570	Mar-08	Ongoing	BH	Logger	Dinantian pure bedded limestone	60.00		EPA/LA
San Antone House (B&B)	26_011	Wexford	305307	114357	Mar-09	Ongoing	BH	Logger	Dinantian pure bedded limestone	100.00		EPA/LA
Vickerstown	11_014	Laois	261234	200342	Jan-08	Ongoing	BH	Logger	Dinantian pure bedded limestone	25.00		EPA/LA
Paulstown	10_014	Kilkenny	266048	157294	No data	No data	Spring		Dinantian pure bedded limestone			EPA/LA
Rathduff	10_017 (Kny 27/58)	Kilkenny	250500	143300	Aug-81	Ongoing	BH	Chart recorder to Mar-08, then logger	Dinantian dolomitised limestone	62.00	46.75	GSI/OPW
Pub in Pike	10_016	Kilkenny	254859	156017	Oct-07	Ongoing	BH	Logger	Dinantian upper impure limestone	20.00		EPA/LA
Kilmaganny	10_011	Kilkenny	245805	137446	May-08	Ongoing	BH	Logger	Dinantian lower impure limestone	15.00		EPA/LA
Knocktopher	10_012 (Kny 31/72)	Kilkenny	253140	135930	Aug-80	Ongoing	BH	Chart recorder to May-08, then logger	Kiltorcan Sandstone	40.00	61.67	GSI/OPW
Adamstown (BH2 – Deer Farm)	26_001	Wexford	285900	126000	Mar-08	Ongoing	BH	Logger	Ordovician Volcanics	44.00		EPA/LA
Slieveroe (BH1)	10_018	Kilkenny	263315	113960	Mar-08	Ongoing	BH	Logger	Ordovician Volcanics	100.00		EPA/LA
Bord na Móna – Allen	09_003	Kildare	280086	220996	No data	No data	BH	Logger				EPA/LA
Duffy's Crossroads	09_007	Kildare	266614	238096	Jun-08	Ongoing	BH	Logger				EPA/LA

PF, Pollardstown Fen; BH, borehole; GSI, Geological Survey of Ireland; OPW, Office of Public Works; LA, local authority; mbgl, metres below ground level; maOD, metres above Ordnance Datum.

APPENDIX B – typical hydrogeological parameters for aquifers in SE region pilot area

From Tedd *et al.*, 2011.

Geological age	Group	Aquifer name	Hydrogeologically significant formations	Aquifer category	Thickness (m)	Well yield ³ (m ³ /day)		Specific capacity ³ (m ³ /day/m)		Transmissivity ³ (m ² /day)		Hydraulic conductivity ⁵ (m/day)	Specific yield ⁶ (–)		
						Typical	Range ⁴	Typical	Range	Typical	Range				
Carboniferous	Westphalian		Sand and gravel ¹	Lg		500	200–1,000	200	50–1,000	400	100–2,000	1–250	0.05–0.15		
		Deltaic cycles of coals and thick sandstones	Westphalian Sandstones ¹	Lickfinn Coal Fm/ Clay Gall Sandstone Fm	Lm	<350/250–320	200–500	100–1,100	10–50	5–50	5–15	1–500	0.001–50	0.01	
		Sandstones, shales and limestones	Namurian Sandstones and Shales ^{1,7}	Bregau Flagstone Fm	PI	390–460	20–50	10–200	1–5	0–15				0.005–0.01	
	Dinantian			Killeslin Siltstone Fm	PI										
				Luggacurran Shale Fm	Pu										
				Clogrennan Fm	Rkd/Lk										
		Visean Limestones	Karstified Limestones ^{1,7}	Ballyadams Fm	Rkd/Lk	225–400	20–500	10–2,000	5–100	1–3,000	200	5–3,000	0.1–100	0.005–0.05	
				Durrow Fm	LI										
				Aghmacart Fm	LI	125–160									
			Crosspatrick Fm ¹	Crosspatrick Fm	Lm	<60	250–400	100–500	10–20	10–50	20–40	10–100	0.1–10	0.01–0.02	
		Waulsortian Mudbank Complex		Waulsortian Limestones	Rkd, Lf (LI)	50–220	1,000	300–3,000	100	10–350	250	20–800	0.1–20	0.02–0.04	
		Sub-Waulsortian Limestones	Dolomitised Limestones ^{1,7}	Ballysteen Fm	Rkd, Rf (LI)	300–500	(20–40)	(10–150)	(2–10)	(0–100)				(0.01–0.03)	
				Ballymartin Fm	Rf, Lm (LI)										
					Ballyvergin Fm		3–5								
			Lower Carboniferous Sandstones and Shales		Porter's Gate Fm	Rf	30–80								
			Old Red Sandstone		Kiltorcan Sandstone ¹	Rf	20–230	500	50–1,300	40	2–270	60	10–500	0.1–10	0.01–0.02
		Devonian													
		Lower Palaeozoic	Tullow and Blackstairs Granites		Granites	PI/LI									
Metasedimentary and volcanics strata	Ordovician Volcanics ²		Campile Fm	Rf	400–1,500	200–2,000		5–200		15 to >500			0.01		

¹After Daly (1994).

²After Daly (1982).

³Derived from pumping tests on wells that are mainly partially penetrating.

⁴Tests are not practical where the yield is less than 10 m³/day.

⁵An average value over the productive section of pumped wells.

⁶Obtained from pumping tests, core measurement or hydrograph analysis.



⁷Boreholes failing to provide a minimum domestic supply (10 m³/day) are not uncommon in these formations.












APPENDIX 3 – additional hydrogeological maps and catchment areas for each of the 8 monitoring points studied.

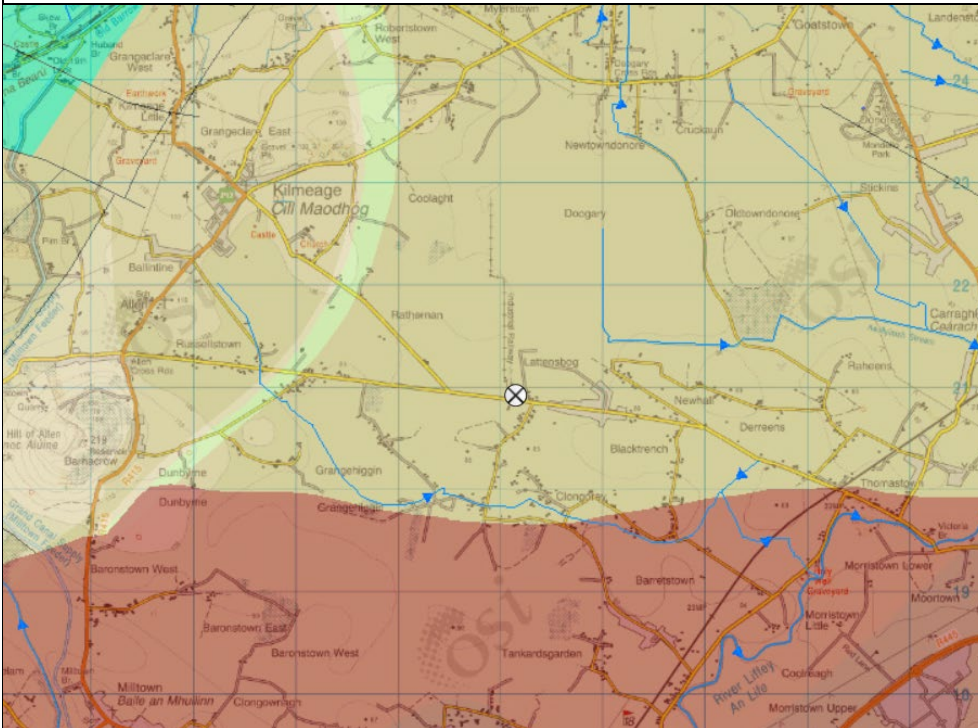
Aquifer map legend

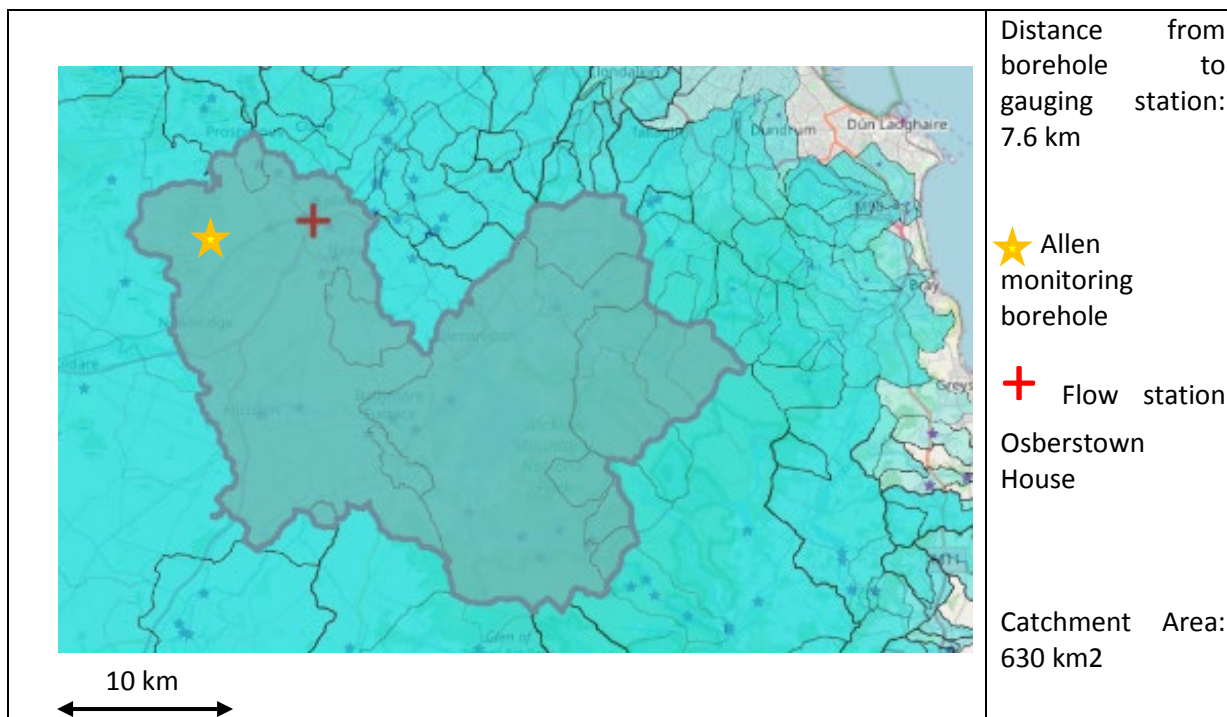
Gravel Aquifer

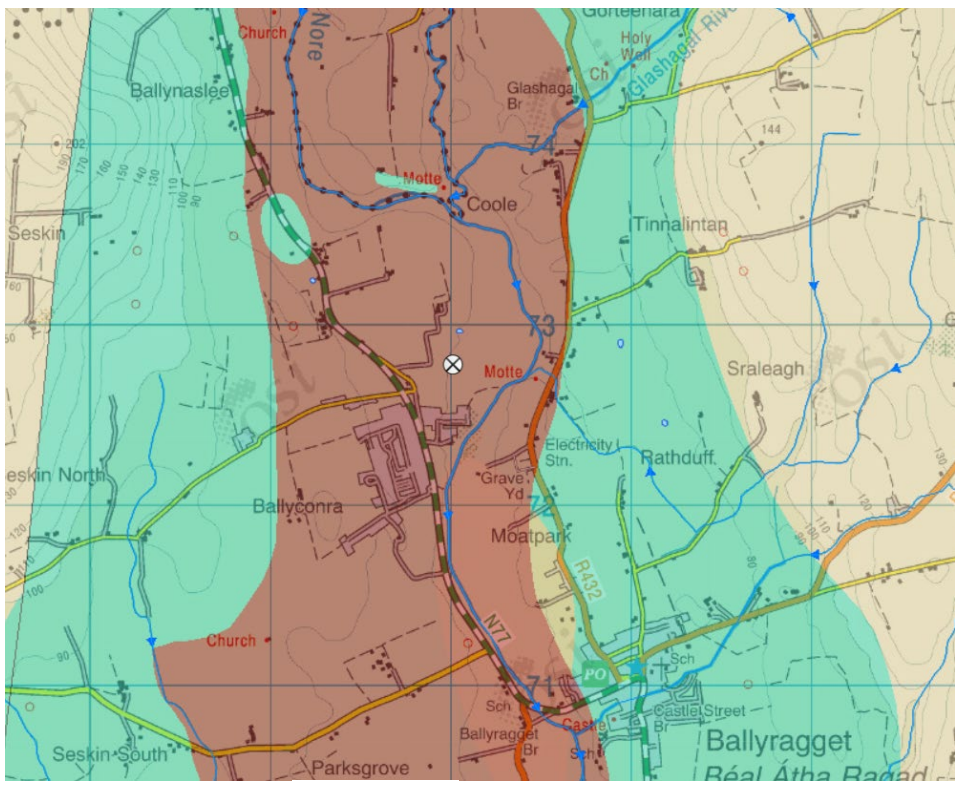


-  Locally important gravel aquifer
-  Regionally important gravel aquifer

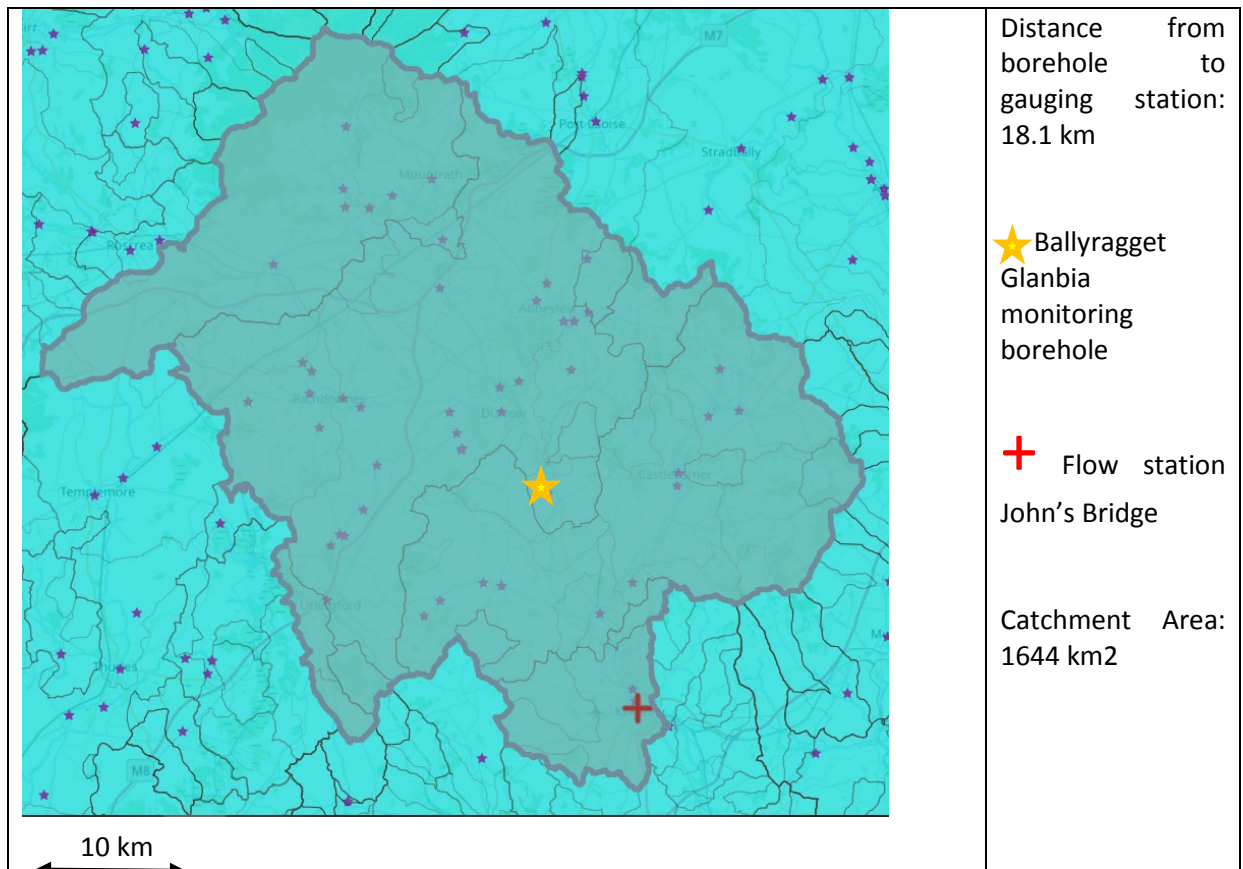
Bedrock Aquifer

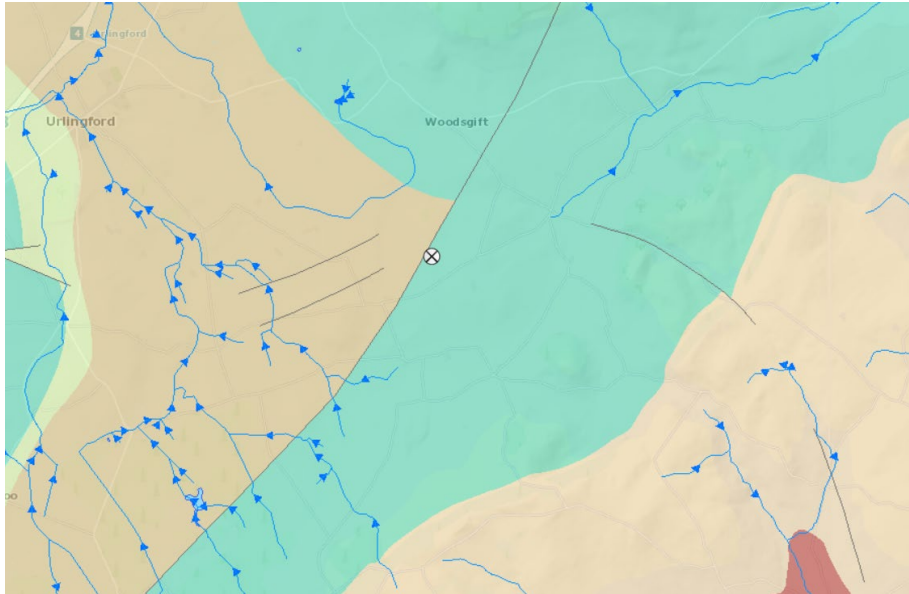
-  Rkc - Regionally Important Aquifer - Karstified (conduit)
-  Rkd - Regionally Important Aquifer - Karstified (diffuse)
-  RK - Regionally Important Aquifer - Karstified
-  Rf - Regionally Important Aquifer - Fissured bedrock
-  Lm - Locally Important Aquifer - Bedrock which is Generally Moderately Productive
-  Lk - Locally Important Aquifer - Karstified
-  LI - Locally Important Aquifer - Bedrock which is Moderately Productive only in Local Zones
-  PI - Poor Aquifer - Bedrock which is Generally Unproductive except for Local Zones
-  Pu - Poor Aquifer - Bedrock which is Generally Unproductive

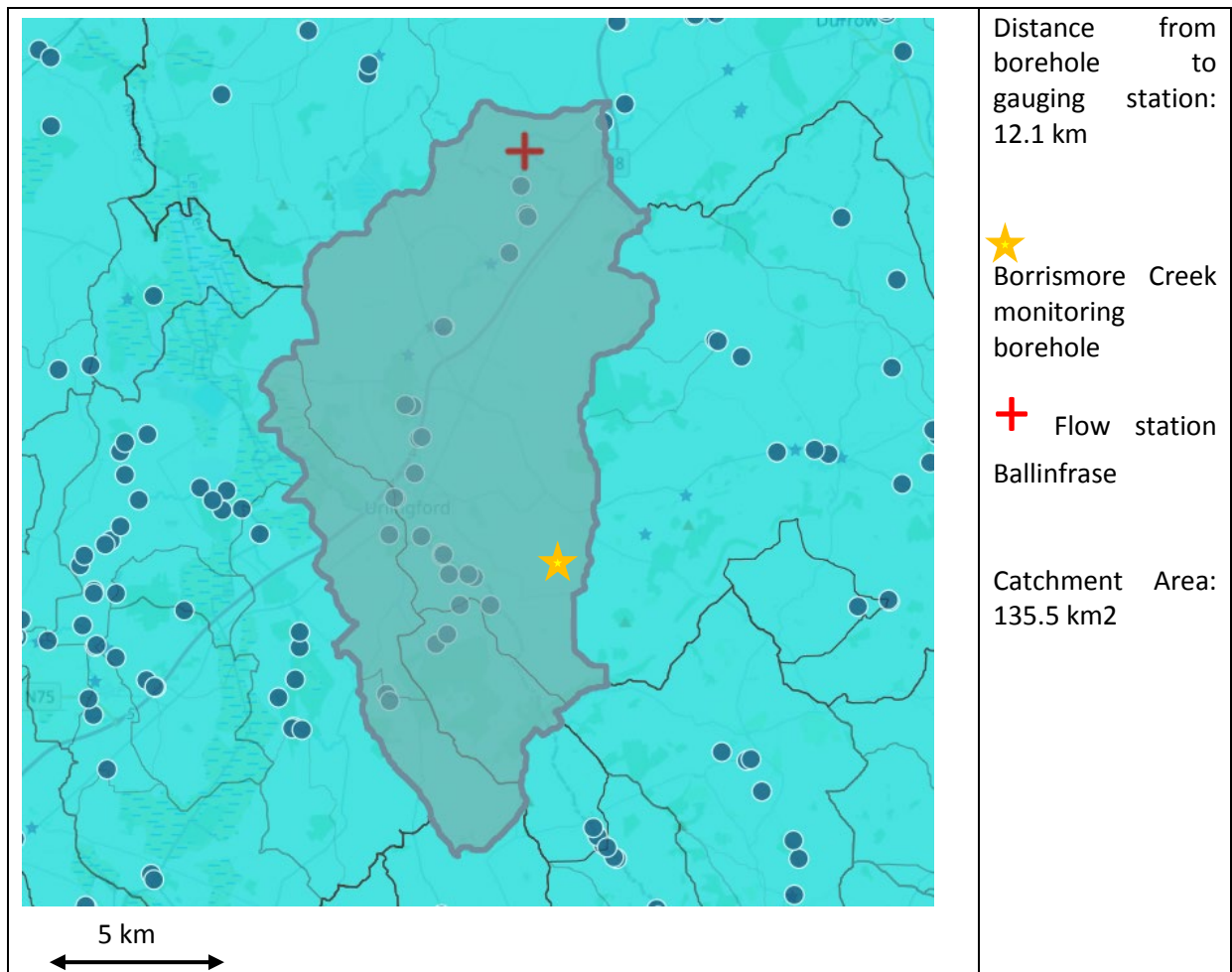
Groundwater monitoring station name	Grid refs (Irish National Grid)
ALLEN (IE_EA_G_0008_1400_0003)	E 280087.00 , N 220935.00
Depth of borehole(m)	Elevation/dipping reference (mAOD, Malin)
37.4 m	86 mAOD
Subsoil thickness (m)	Groundwater level range (max/min) (m)
5-10 m (depth to top of aquifer, m below surface)	82.85 – 84.32 m
Record length (from/to)	
Jan 1997 – Jul 2020	
Surface water monitoring station	Grid refs (Irish National Grid)
Osberstown House	E 287669.00 , N 221566.00
Elevation (mAOD, Malin)	Flow range (max/min) (m3/s)
72.5 m	0.041 – 0.461 m3/s
Record length (from/to)	
May 2009 – Dec 2020	LIMESTONE KARST AQUIFER
 <p>Distance from borehole to river: 900 - 1200 m</p> <p>⊗ Allen monitoring borehole</p> <p>→ Surface water features</p> <p>1 km</p>	

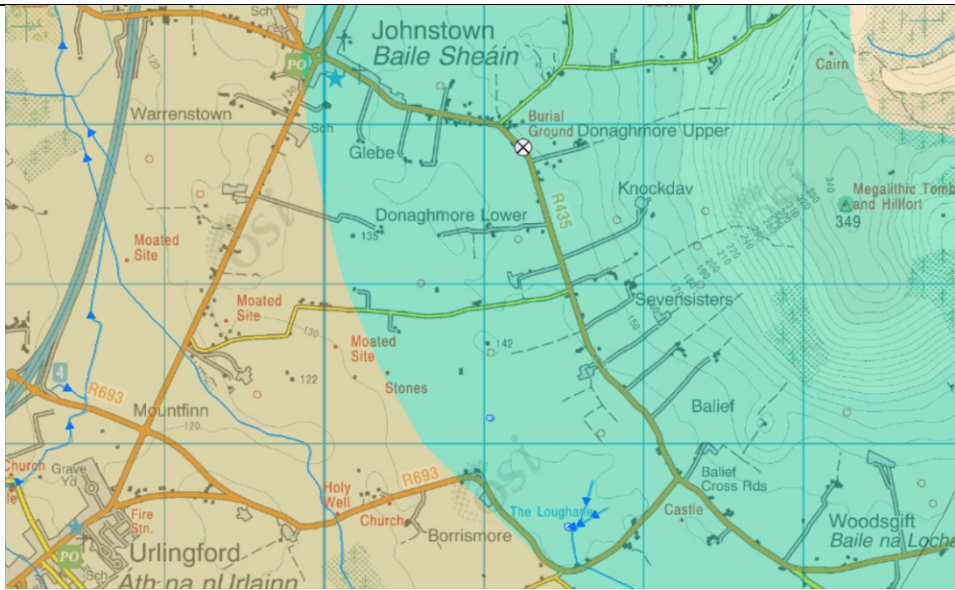



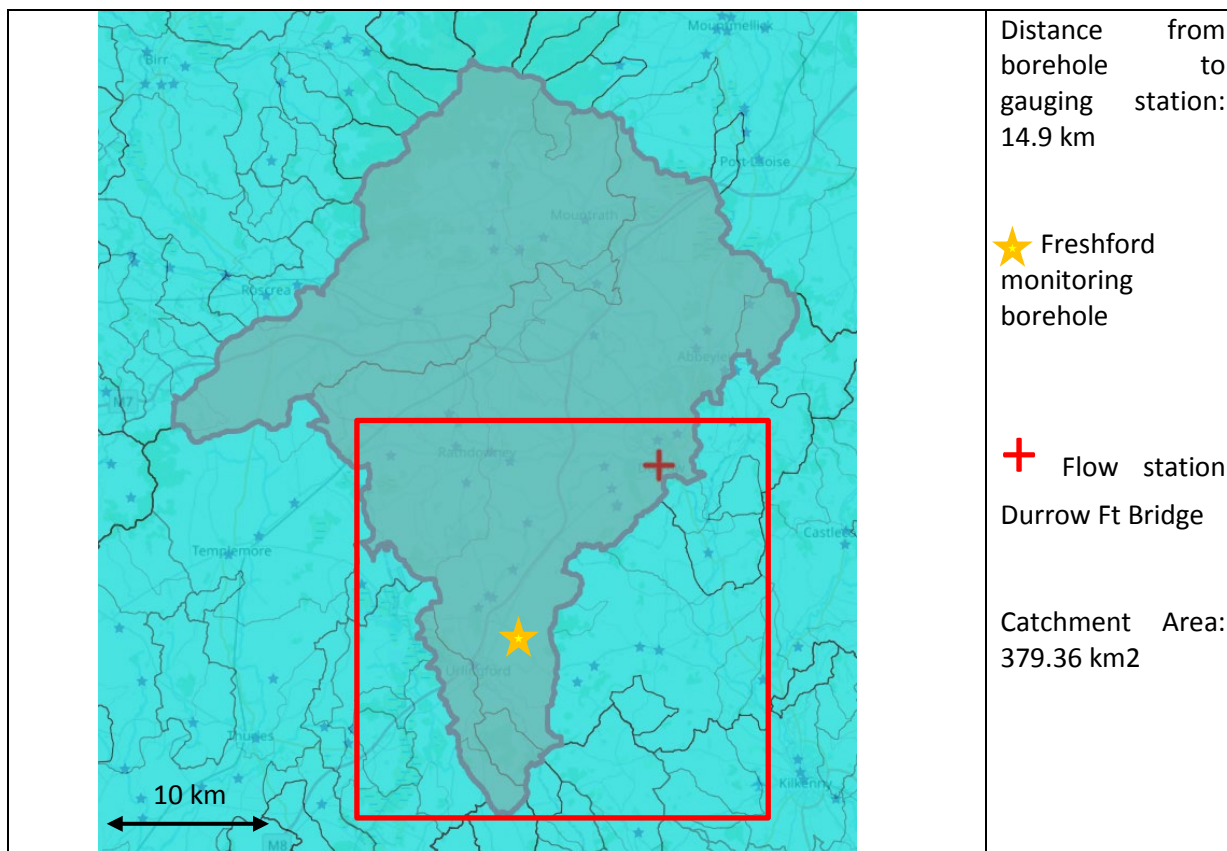
Groundwater monitoring station name		Grid refs (Irish National Grid)
BALLYRAGGET (IE_SE_G_0163_1500_0002)	GLANBIA	E 244002.00 , N 172802.00
Depth of borehole(m)		Top borehole/dipping reference (mAOD, Malin)
18 m		67 mAOD Malin
Subsoil thickness (m)		Groundwater level range (max/min) (m)
5-12.2 m (depth to top of aquifer, m below surface)		64.819 m to 62.097 m
Record length (from/to)		
Mar 2008 – Oct 2020		
Surface water monitoring station		Grid refs (Irish National Grid)
John's Bridge (15002)		E 250777.00 , N 156020.00
Elevation (mAOD, Malin)		Flow range (max/min) (m3/s)
44.17 m		0.524 – 341.142 m3/s
Record length (from/to)		
Oct 1971 – Dec 2017		SAND & GRAVEL AQUIFER
		Distance from borehole to river: 250 - 450 m (River Nore)
		 Ballyragget Glanbia monitoring borehole  Surface water features

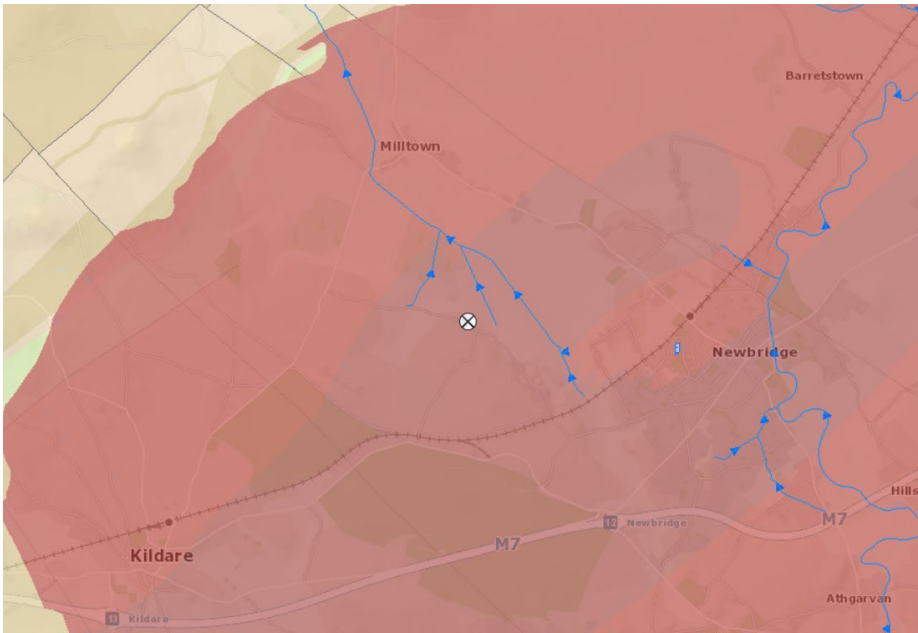


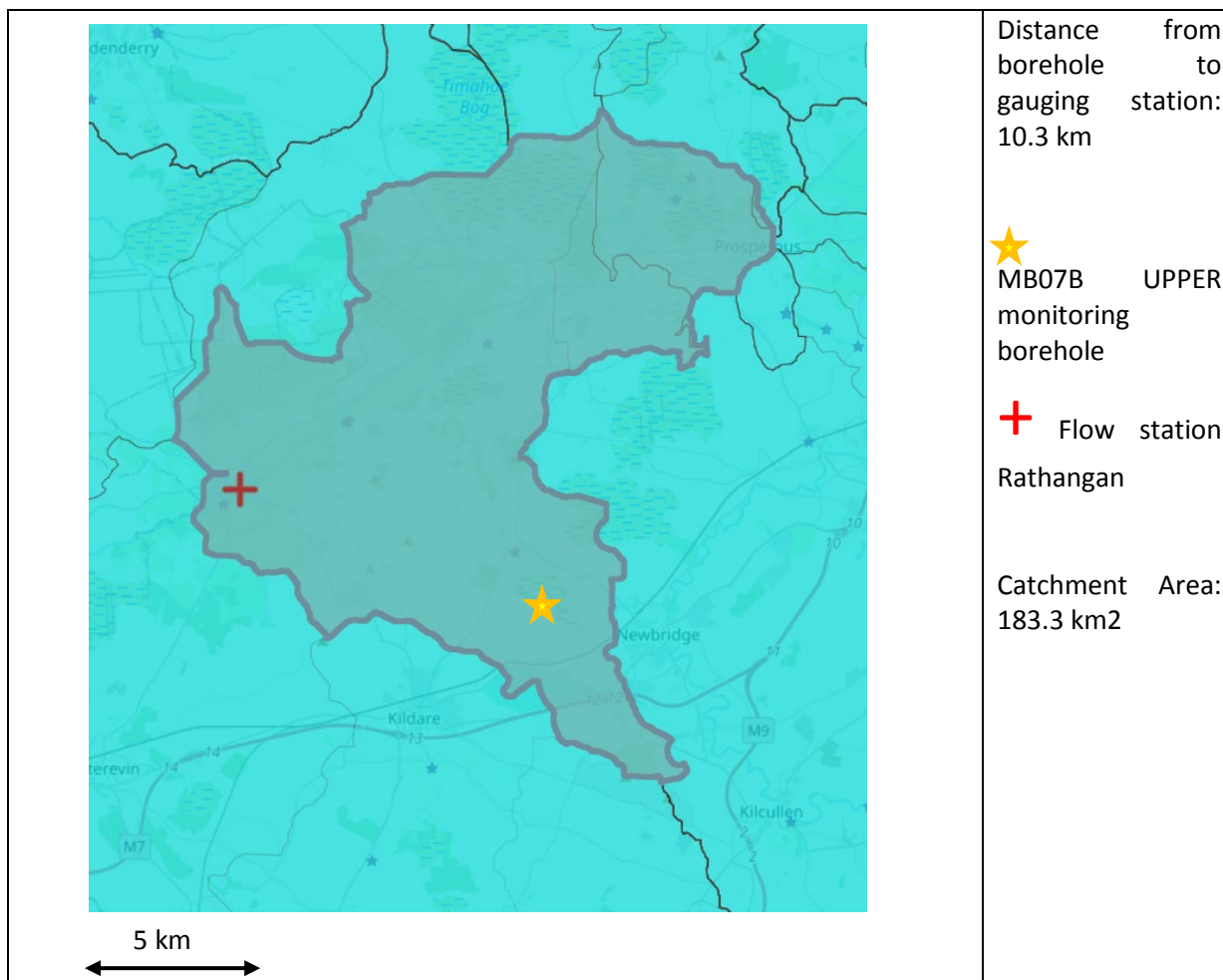
Groundwater monitoring station name		Grid refs (Irish National Grid)
BORRISMORE CREEK (IE_SE_G_0156_1500_0005)		E 233000.00 , N 161499.00
Depth of borehole(m)		Elevation/dipping reference (mAOD, Malin)
36 m		141 mAOD
Subsoil thickness (m)		Groundwater level range (max/min) (m)
6.1 m (depth to top of aquifer, m below surface)		128.22 – 140.04 m
Record length (from/to)		
Apr 1975 – Aug 2020		
Surface water monitoring station		Grid refs (Irish National Grid)
BALLINFRASE		E 231570.00 , N 173535.00
Elevation (mAOD, Malin)		Flow range (max/min) (m ³ /s)
102.237 m		0.214 – 22.4 m ³ /s
Record length (from/to)		
Jul 2001 – Mar 2021		KARST AQUIFER
 <p>1 km</p>		Distance from borehole to river: 1150 – 1350 m
		<p>⊗ Borrismore Creek monitoring borehole</p> <p>→ Surface water features</p>

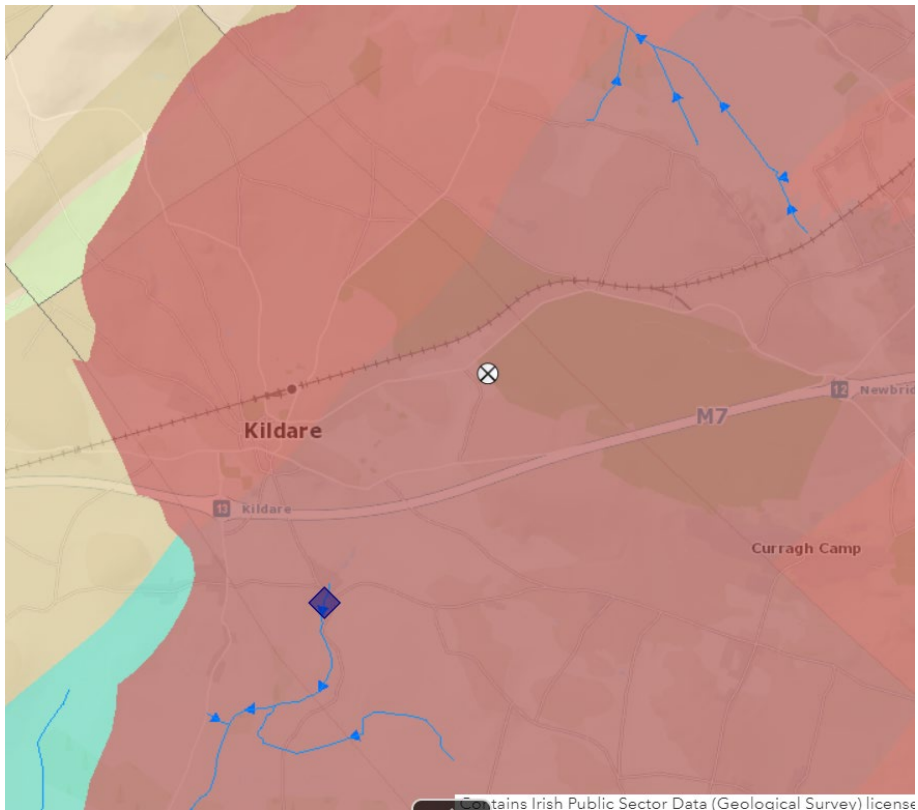


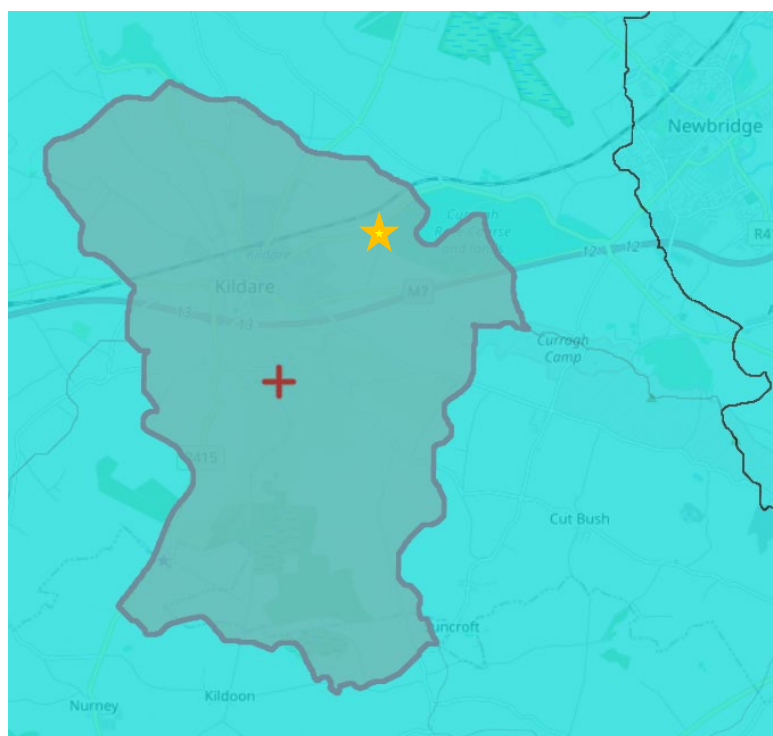
Groundwater monitoring station name			Grid refs (Irish National Grid)
FRESHFORD	–	JOHNSTOWN RD	E 231211.90 , N 165880.24
(IE_SE_G_0156_1500_0009)			
Depth of borehole(m)			Elevation/dipping reference (mAOD, Malin)
13.5 m (sump at 12.3 m)			151 mAOD Malin
Subsoil thickness (m)			Groundwater level range (max/min) (m)
13.7 m			143.09 m to 137.6 mAOD
Record length (from/to)			
Apr 2008 – Aug 2020			
Surface water monitoring station			Grid refs (Irish National Grid)
DURROW FR BRIDGE			E 240611.00 , N 177479.00
Elevation (mAOD, Malin)			Flow range (max/min) (m3/s)
83 mAOD			61.761 m3/s to 0.038 m3/s
Record length (from/to)			
Jan 1972 – Oct 2018			KARSTIC AQUIFER
			
			Distance from borehole to river: 2400 - 2600 m (River Goul)
			 Freshford monitoring borehole



Groundwater monitoring station name	Grid refs (Irish National Grid)
MB07B UPPER (IE_SE_G_0106_1400_0014)	E 276820.00 , N 215562.00
Depth of borehole(m)	Elevation/dipping reference (mAOD, Malin)
48.04 (depth of continuous borehole MB 07A Middle)	105 mAOD
Subsoil thickness (m)	Groundwater level range (max/min) (m)
3-5 m (depth to top of aquifer, m below surface)	85.92 – 87.33 m
Record length (from/to)	
May 2008 – Jul 2020	
Surface water monitoring station	Grid refs (Irish National Grid)
Rathangan	E 267336.00 , N 219356.00
Elevation (mAOD, Malin)	Flow range (max/min) (m3/s)
72 m	0.134 – 13.367 m3/s
Record length (from/to)	
Jan 1999 – Jun 2020	SAND & GRAVEL AQUIFER
<div>  <div> <p>Distance from borehole to river: 250 – 450 m</p> <p>⊗ MB07B UPPER monitoring borehole</p> <p>➔ Surface water features</p> </div> </div>	



Groundwater monitoring station name	Grid refs (Irish National Grid)
MB30 (IE_SE_G_0106_1400_0012)	E 275029.00 , N 213206.00
Depth of borehole(m)	Elevation/dipping reference (mAOD, Malin)
24 m	108 mAOD
Subsoil thickness (m)	Groundwater level range (max/min) (m)
3-5 m (depth to top of aquifer, m below surface)	87.89 – 90.92 m
Record length (from/to)	
Apr 2008 – Jul 2020	
Surface water monitoring station	Grid refs (Irish National Grid)
Japanese Gardens	E 273420.00 , N 210801.00
Elevation (mAOD, Malin)	Flow range (max/min) (m3/s)
87 m	0.025 – 0.461 m3/s
Record length (from/to)	
Jan 1982 – Sep 2020	SAND & GRAVEL AQUIFER
<div>  <div> <p>Distance from borehole to river: 2800 – 3100 m</p> <p>⊗ MB30 monitoring borehole</p> <p>→ Surface water features</p> <p>◆ Japanese Gardens flow station</p> </div> </div>	



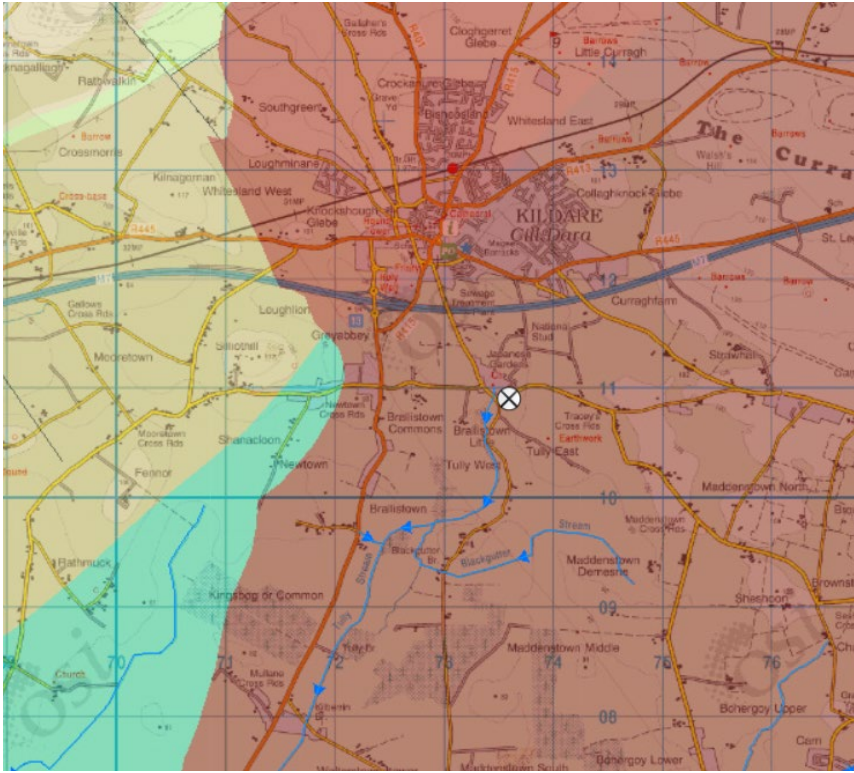
Distance from
borehole to
gauging station:
2.9 km

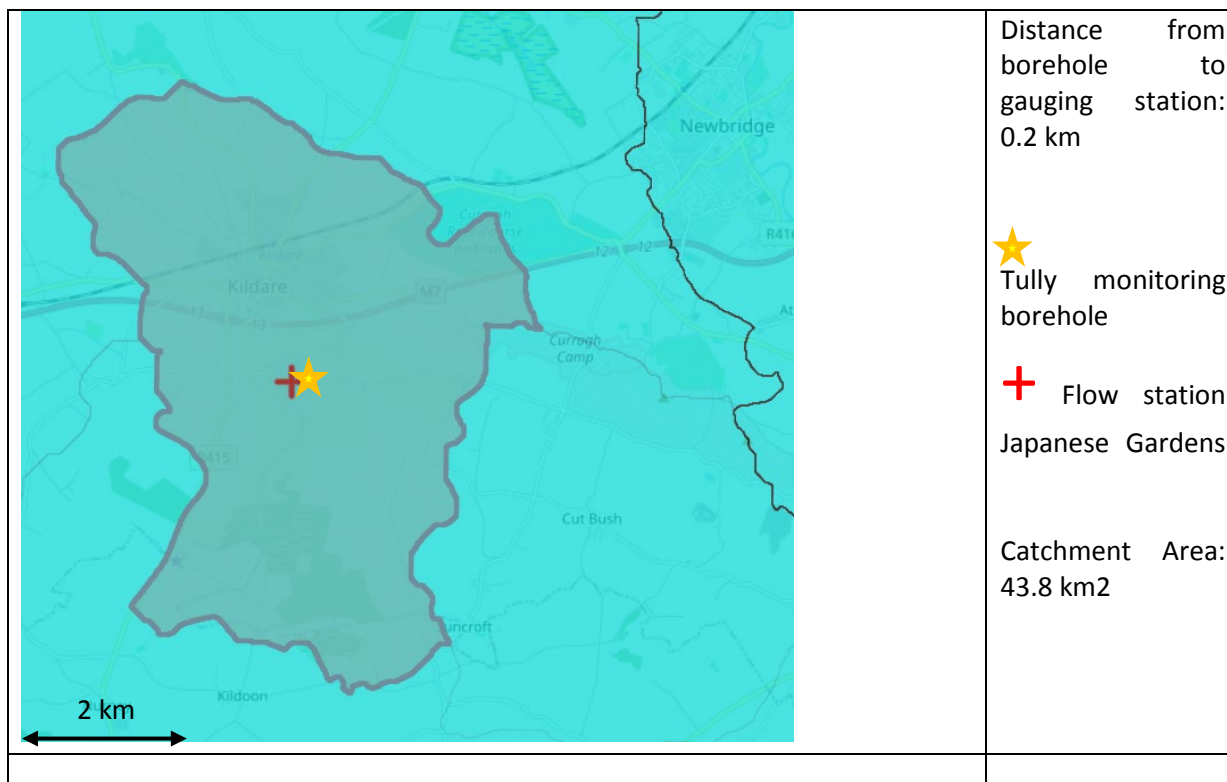
★
MB30 monitoring
borehole

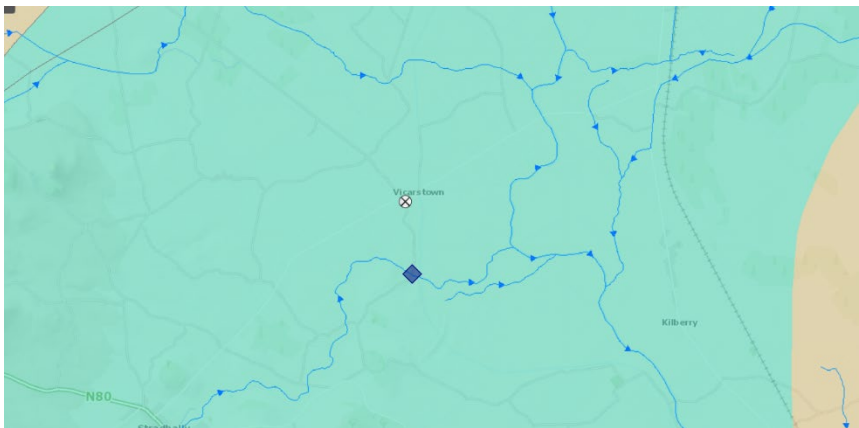
✚ Flow station
Japanese Gardens

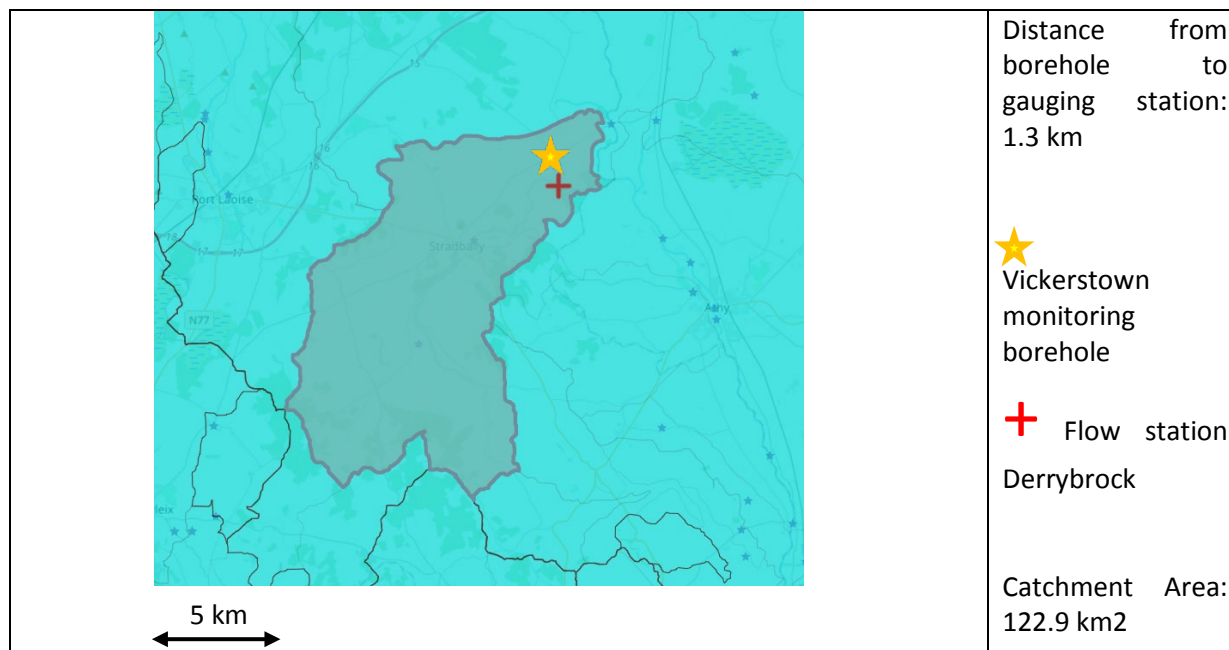
Catchment Area:
43.8 km²

Groundwater monitoring station name	Grid refs (Irish National Grid)
TULLY (IE_SE_G_0133_1400_0019)	E 273531.00 , N 210922.00
Depth of borehole(m)	Elevation/dipping reference (mAOD, Malin)
9 m	87 mAOD
Subsoil thickness (m)	Groundwater level range (max/min) (m)
3-5 m (depth to top of aquifer, m below surface)	84.67 – 85.52 m
Record length (from/to)	
Jan 2008 – Sep 2020	
Surface water monitoring station	Grid refs (Irish National Grid)
Japanese Gardens	E 273420.00 , N 210801.00
Elevation (mAOD, Malin)	Flow range (max/min) (m3/s)
87 m	0.025 – 0.461 m3/s
Record length (from/to)	
Jan 1982 – Sep 2020	SAND & GRAVEL AQUIFER

 <p>1 km</p>	<p>Distance from borehole to river: 150 – 250 m</p> <p>⊗ Tully monitoring borehole</p> <p>➔ Surface water features</p>
---	--



Groundwater monitoring station name	Grid refs (Irish National Grid)
VICKERSTOWN (IE_SE_G_0153_1600_0014)	E 261234.00 , N 200341.00
Depth of borehole(m)	Elevation/dipping reference (mAOD, Malin)
25 m	65 mAOD
Subsoil thickness (m)	Groundwater level range (max/min) (m)
13.7 m (depth to top of aquifer, m below surface)	58.50 – 62.55 m
Record length (from/to)	
Oct 1995 – Sep 2020	
Surface water monitoring station	Grid refs (Irish National Grid)
Derrybrock	E 261424.00 , N 199067.00
Elevation (mAOD, Malin)	Flow range (max/min) (m3/s)
58 m	0 – 16.917 m3/s
Record length (from/to)	
Feb 1980 – Oct 2020	KARST AQUIFER
<div>  <p>1 km</p> </div> <div> <p>Distance from borehole to river: m</p> <p>⊗ Vickerstown monitoring borehole</p> <p>→ Surface water features</p> <p>◆ Derrybrock flow station</p> </div>	



APPENDIX C – AquiMod methodology

AquiMod is a lumped parameter computer model that has been developed to simulate groundwater level time series at observational boreholes (Mackay et al., 2014a). It is based on hydrological algorithms that simulates the movement of groundwater within the soil zone, the unsaturated zone, and the saturated zone. The lumped models neglect complexities included in distributed groundwater models but maintains some of the fundamental physical principles that can be related to the conceptual understanding of the groundwater system (Mackay et al., 2014b).

While AquiMod was originally designed to capture the behaviour of a groundwater system through the analysis of groundwater level time series, it can produce the infiltration recharge values and groundwater discharges from the aquifer as a by-product. AquiMod is driven by complete time series of forcing data for either historical or predicted future conditions. Running AquiMod in predictive mode can be used to fill in gaps in historical groundwater level time series, or calculate future groundwater levels. In addition to groundwater levels, it also provides predictions of historical and future recharge values and groundwater discharges. In the current application we use calibrated AquiMod models to estimate the recharge values at selected boreholes.

AquiMod consists of three modules (Figure C1). The first is a soil water balance module that calculates the amount of water that infiltrates the soil as well as the soil storage. The second module controls the movement of water in the unsaturated zone, mainly it delays the arrival of infiltrating water to the saturated zone. The third module calculates the variations in groundwater levels and discharges. The model executes the modules separately following the order listed above.

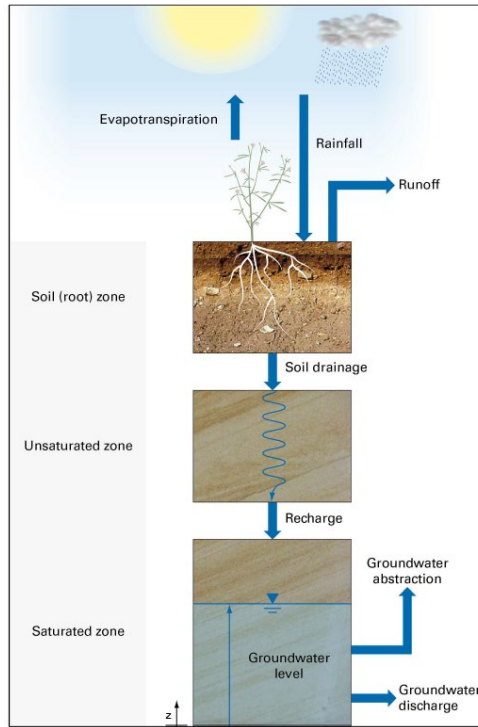


Figure C1 Generalised structure of AquMod (after Mackay et al., 2014a)

The soil moisture module

There are several methods available in AquMod that can be used to calculate the rainfall infiltration into the soil zone. In this study we use the FAO Drainage and Irrigation Paper 56 (FAO, 1988) approach. In this method, the capacity of the soil zone, from which plants draw water to evapotranspire, is calculated first using the plants and soil characteristics. Evapotranspiration is calculated according to the soil moisture deficit level compared to two parameters: Readily Available Water (RAW) and Total Available Water (TAW). These are a function of the root depth and the depletion factor of the plant in addition to the soil moisture content at field capacity and wilting point as shown in Equations C1 and C2.

$$TAW = Z_r(\theta_{fc} - \theta_{wp})$$

Equation C1

$$RAW = p \cdot TAW$$

Equation C2

Where Z_r [L] and p [-] are the root depth and depletion factor of a plant respectively, θ_{fc} [$L^3 L^{-3}$] and θ_{wp} [$L^3 L^{-3}$] are the moisture content at field capacity and wilting point respectively.

The FAO method is simplified by Griffiths et al. (2006) who developed a modified EA-FAO method. In this method the evapotranspiration rates are calculated as a function of the potential evaporation and an intermediate soil moisture deficit as:

$$\begin{aligned} e_s &= e_p \left[\frac{s_s^*}{TAW - RAW} \right]^{0.2} & s_s^* > RAW \\ e_s &= e_p & s_s^* \leq RAW \\ e_s &= 0 & s_s^* \geq TAW \end{aligned}$$

Equation C3



Where e_s [L] is the evpo-transpiration rate, e_p [L] is the potential evaporation rate and s_s^* [L] is the intermediate soil moisture deficit given by

$$s_s^* = s_s^{t-1} - r + e_p \quad \text{Equation C4}$$

Where r [L] is the rainfall at the current time step and s_s^{t-1} [L] is the soil moisture deficit calculated at the previous time step.

The new soil moisture deficit is then calculated from:

$$s_s = s_s^{t-1} - r + e_s \quad \text{Equation C5}$$

Griffiths et al. (2006) proposed that the recharge and overland flow are only generated when the calculated soil moisture deficit becomes zero. The remaining volume of water, the excess water, is then split into recharge and overland flow using a runoff coefficient. In Aquimod a baseflow coefficient is used to reflect the fact that a groundwater discharge is calculated rather than overland water. In this application, the baseflow coefficient is one minus the runoff coefficient.

The unsaturated zone module

The Aquimod version used in this study to simulate the movement of groundwater flow within the unsaturated zone is based on a statistical approach rather than a process-based approach. This method distributes the amount of rainfall recharge over several time steps where the soil drainage for each time step is calculated using a two-parameter Weibull probability density function. The Weibull function can represent exponentially increasing, exponentially decreasing, and positively and negatively skewed distributions. This can be used to focus the soil drainage over earlier or later time steps or to spread it over a number of time steps after the infiltration occurs. The shape of the Weibull function is controlled by two parameters, k and λ as shown in Equation A6.

$$f(t, k, \lambda) = \begin{cases} \frac{k}{\lambda} \left(\frac{t}{\lambda}\right)^{k-1} e^{-(t/\lambda)^k} & t > 0 \\ 0 & t \leq 0 \end{cases} \quad \text{Equation C6}$$

Where k and λ are two parameters the values of which are calculated during the calibration of the model and t is the time step.

The saturated zone module

Aquimod considers the saturated zone as a rectangular block of porous medium with dimensions L and B as its length and width [L] respectively. This block is divided into a number of layers, each has a defined hydraulic conductivity value, a storage coefficient value, and a discharging feature. The number of layers define the structure of the saturated module used in the study.

The mass balance equation that gives the variation of hydraulic head with time is given by:

$$SLB \frac{dh}{dt} = RLB - Q - A \quad \text{Equation C7}$$

Where:



S is the storage coefficient of the porous medium [-]

h is the groundwater head [L]

t is the time [T]

R is the infiltration recharge [$L T^{-1}$]

Q is the discharge out of the aquifer [$L T^{-1}$]

A is the abstraction rate [$L T^{-1}$]

It must be noted that in a multi-layered groundwater system as shown in Figure C2, we calculate one groundwater head (h) for the whole system. The discharges (Q) from Outlet 1, 2, etc. are calculated using the Darcy law. The total discharges can be summarised using the following equation:

$$Q = \sum_{i=1}^m \frac{T_i B}{0.5 L} \Delta h_i \quad \text{Equation C8}$$

Where:

m is the number of layers in the groundwater system [-]

T_i is the transmissivity of the layer i [$L T^{-2}$]

Δh_i is the difference between the groundwater head h and z_i , the elevation of the base of layer i

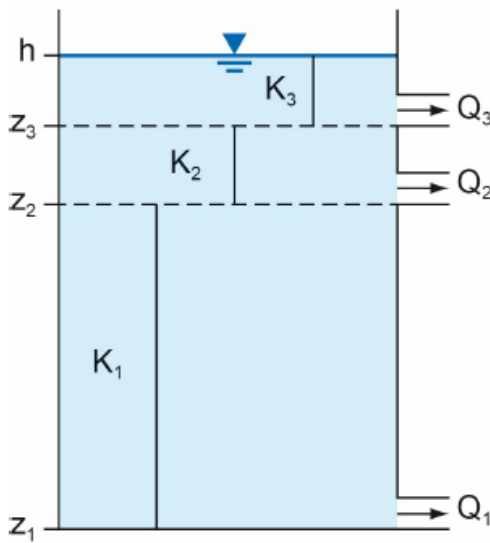


Figure C2 Representation of the saturated zone using a multi-layered groundwater system

Substituting Equation C8 into Equation C7 yields a numerical equation in the form:

$$S \frac{(h-h^*)}{\Delta t} = R - \sum_{i=1}^m \frac{T_i}{0.5 L^2} \Delta h_i - \frac{A}{LB} \quad \text{Equation A9}$$

Equation C9 is an explicit numerical equation that allows the calculation of the groundwater head h [L] at any time and using time steps of Δt [T]. In this equation h^* [L] is the groundwater head calculated at the previous time step and the term Δh_i [L] is calculated as $(h^* - z_i)$.



The terms S , T_i , and L are optimised during the calibration of the model. A groundwater system can be specified with one storage coefficient as shown in the equations above or with different storage coefficient values for the different layers. Several saturated modules are included in AquiMod to provide this flexibility and the model user can select the model structure that represent the conceptual understanding best.

Limitations of the model

AquiMod is a lumped groundwater model that aims at reproducing the behaviour of the observed groundwater levels. It tries to encapsulate the conceptual understanding of a groundwater system in a simple numerical representation. The model results have to be therefore discussed, taking this into consideration. For example, the model represents the groundwater system as a closed homogeneous medium, with no impact from any outer boundary or feature, whether physical or hydrological, such as the presence of rising and falling river stage.

Vertical heterogeneity can be accounted for by using multi-layered groundwater module structure. However, this model setting does not provide any information about the vertical connections between the layers as the discharge from all the layers is calculated using one representative groundwater head value. In other words, it is assumed that all layers are in perfect hydraulic connection.

As mentioned before, the model is designed to simulate the groundwater levels. However, it produces the recharge values and groundwater discharges as by products. In this application we use the calibrated model to calculate recharge. The mass balance equation (Equation C7) shows that recharge is a function of transmissivity and storage coefficient values, which are estimated during the calibration process of the model, i.e. they are not parameters with fixed values provided by the user. The inter-connections between these parameters leads to uncertainties in the estimated recharge values as a high storage coefficient value can produce a high recharge estimate and vice versa. To overcome this problem, it is suggested that the recharge values estimated by AquiMod are always presented as a range of possibilities rather than an absolute value. This can be achieved by estimating the recharge values from all the models that have a performance measure above than a threshold that is deemed acceptable by the user. The recharge estimates can then be presented as an average of all estimates and values corresponding to selected percentiles.

Model input and output

AquiMod includes a number of methods that calculates rainfall recharge as well as a number of model structure from which the user can select what better suits the case study.

Model input consists time series of forcing data including rainfall and potential evaporation, time series of anthropogenic impact mainly groundwater abstraction and time series of groundwater levels that will be used to calibrate the model. These time series must be complete, i.e. a value is available at every time step except the groundwater level time series, which can include missing data. The time step can be one day or multiple of days, and the model automatically calculate the size of the time step based on the input data time series.



The model is run first in calibration mode where a range of parameter values are specified for the different parameters included in the three model modules. A Monte Carlo approach is used to select the best parameter values. The performance of the model is measured by comparing the simulated groundwater levels to the observed ones using the Nash Sutcliff Efficient (NSE) or the Root Mean Squared Error (RMSE) performance measures. The parameter set that produces the best model performance is selected to run the model in evaluation mode.

When the model is run in evaluation mode, it produces output files that give recharge values, groundwater levels and groundwater discharges time series with time as specified in the input file. The number of output files is equal to the number of acceptable models set by the user.

APPENDIX D – Metran methodology

Metran applies transfer function noise modelling of (groundwater head) time series with usually daily precipitation and evaporation as input (Zaadnoordijk et al., 2019). The setup is shown in the Figure D1. If time series of other influences on the groundwater head are available, these contributions can be added to the deterministic part of the model. The stochastic part is the difference between the total deterministic part and the observations (the residuals). The corresponding input of the noise model should have the character of white noise.

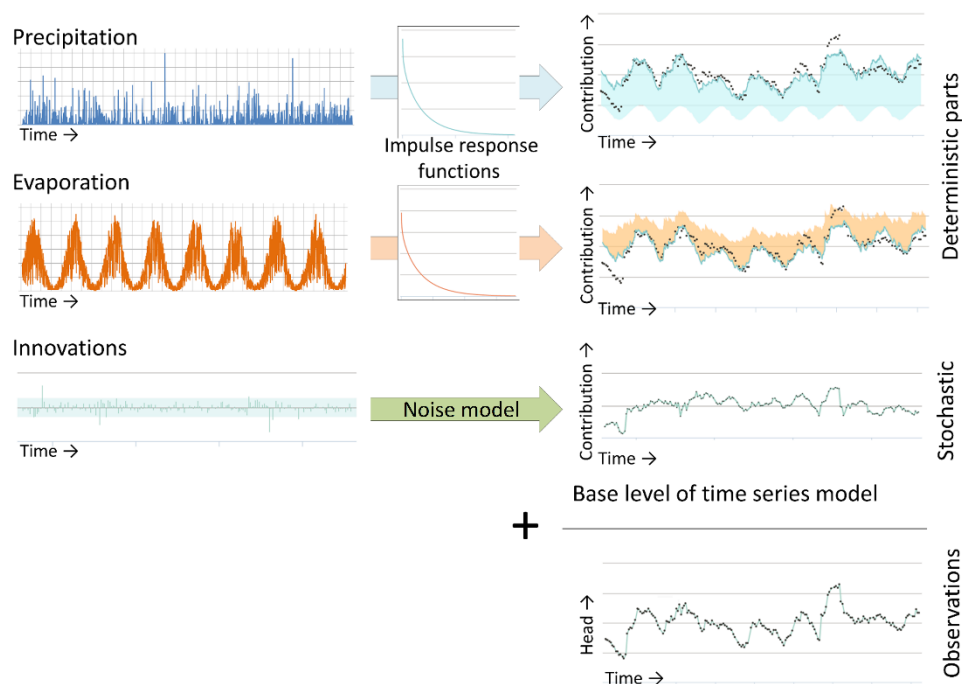


Figure D1 Illustration of METRAN setup

The stochastic part is needed because of the time correlation of the residuals, which does not allow a regular regression to obtain the parameter values of the transfer functions.

The incomplete gamma function is used as transfer function. This is a unimodal function with only three parameters that has a quite flexible shape and has some physical background (Besbes & de Marsily, 1984). The evaporation response is set equal to the precipitation response except for a factor (f_c). The noise model has one parameter that determines an exponential decay. Thus, for the standard setup with precipitation and evaporation, there are five parameters that have to be determined from the comparison with the observations. Three parameters regarding the precipitation response, the evaporation factor, and the noise model parameter (actually, the time series model has a fifth parameter, the base level, but this is



determined from the assumption that the average of the calculated heads is equal to the average of the observations). There are three extra parameters for each additional input series, such as pumping.

Limitations

Metran's time series model is linear. So, the model creation breaks down when the system is strongly nonlinear. This can occur e.g. when drainage occurs for high groundwater levels, when the ratio between the actual evapotranspiration and the inputted reference evaporation varies strongly, or when the groundwater system changed during the simulated period.

Metran is not able to find a decent time series model when the response function is not appropriate for the groundwater system. An example of this is a system with a separate fast and slow response as was found for a French piezometer in the Avre region, as is illustrated in Figure D2.

Finally, the parameter optimization of Metran uses a gradient search method in the parameter space, so it can be sensitive to initial parameter values in finding an optimal solution.

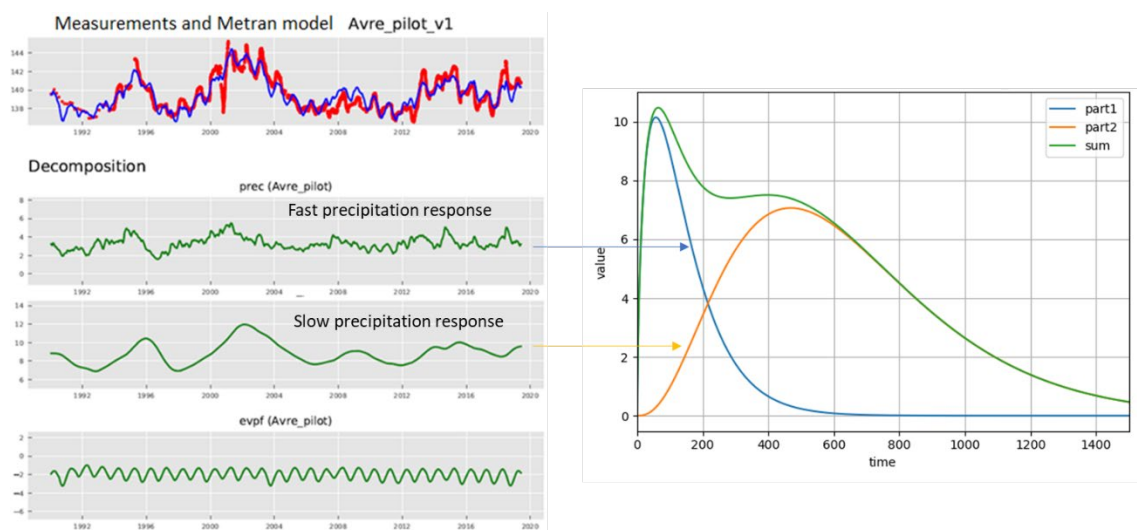


Figure D2. An example where the response function implemented in METRAN is not suitable for the groundwater system

Time step

Metran has been designed to work with explanatory series that have a daily time step. However, it has been adapted so that other time step lengths can be applied; although Metran still has the limitation that the explanatory variables have a constant frequency. For the TACTIC simulations of series with monthly or decadal meteorological input series, the time step has been set to 30 and 10 days, respectively. This time step has been applied from the end date backward.



Note that the heads may be irregular in time as long as the frequency is not greater than the frequency of the explanatory series.

Model output

The evaporation factor fc gives the importance of evapotranspiration compared to precipitation.

The parameter M_0 gives the total precipitation response, which is equal to the area below the impulse response function and the final value of the step response function.

The average response time is another characteristic of the precipitation response. The influence is illustrated in Figure D3 with the impulse response functions and head time series for two models with very different response times for time series of SGU in Sweden.

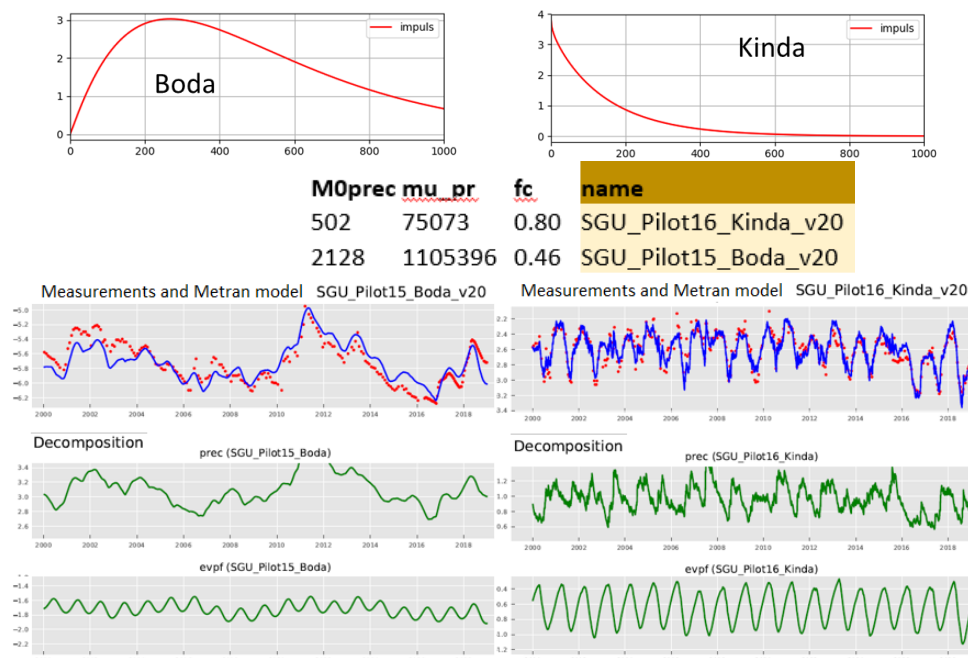


Figure D3 Illustration of Metran output for two case studies in Sweden with different response times.

Model quality

Metran judges a resulting time series model according to a number of criteria and summarizes the quality using two binary parameters Regimeok, Modok (see Zaadnoordijk et al., 2019):

- Regimeok = 1 : highest quality
- Modok = 1 (and Regimeok = 0) : ok
- Both zero = model quality insufficient



More detailed information on the model quality is given in the form of scores for two information criteria (AIC and BIC), a log likelihood, R², RMSE, and the standard deviations and correlations of the parameters.

Recharge

Although the transfer-noise modelling of Metran determines statistical relations between groundwater heads and explanatory variables, we like to think of the results in physical terms. It is tempting to interpret the evaporation factor, as the factor translating the reference into the actual evapotranspiration. Then, we can calculate a recharge as

$$R = P - fE \quad \text{Equation D1}$$

where R is recharge, P precipitation, E evapotranspiration, and f the evaporation factor.

Following the definitions used in the TACTIC project, this recharge R actually is the effective precipitation. It is equal to the potential recharge when the surface runoff is negligible. This in turn is equal to the actual recharge at the groundwater table if there also is no storage change or interflow. In such cases it may be expected that this formula indeed corresponds to the meteorological forcing of the groundwater head in a piezometer, so that it gives a reasonable estimate of the recharge. Obergfell et al. (2019) showed this for an area on an ice pushed ridge in the Netherlands. However, this assumes that all precipitation recharges the groundwater, which cannot be done in many places.

In Dutch polders with shallow water tables and intense drainage networks, it is reasonable to assume that the actual evapotranspiration is equal to the reference value. In that case, the factor f becomes larger than 1 because 1 mm of evaporation has less effect than 1 mm of precipitation (because part of the evaporation does not enter the ground but is immediately drained to the surface water system). In that case, we can calculate recharge as:

$$\begin{aligned} R &= P - fE & f &\leq 1 \\ R &= P/f - E & f &> 1 \end{aligned} \quad \text{Equation D2}$$

These simple formulas can be applied easily for the situations currently modelled in Metran and for the simulations that are driven by future climate data using the delta-change climate factors. However, it is noted that it is a crude estimate using assumptions that are easily violated. Because of this, the equations should be applied only to long term averages using only models of the highest quality.

APPENDIX E – Irish National Groundwater Recharge methodology

The groundwater recharge map shows estimated average annual recharge to the deep groundwater system. The ‘deep groundwater’ can be tapped steadily year-round and yields aren’t significantly influenced by seasonal changes. The recharge amount is shown in units of millimetres per year (mm/yr). The amount of recharge was calculated on daily timesteps over the period 1981-2010 and then averaged to give a yearly amount. The map has been updated as part of this project. The table below summarises the updates made to the Irish Groundwater Recharge map as part of this project (Hunter Williams et al, in press).

Table E.1: summary of main improvements in the Irish National Groundwater Recharge methodology and input data.

Dataset	2011 map	2020 map
Rainfall	30 year average annual rainfall 1971-2000. Data source Met Éireann.	MÉRA Daily rainfall in the period 1981-2010. Data source Met Éireann.
Actual Evapotranspiration	30 year average annual AE. Data source Met Éireann. One soil and reference crop type.	Daily AE in the period 1981-2010. Three soil drainage classes. One reference crop type. Data source Werner et al. (2019). Modified by GSI for areas underlain by peat (AE = ?? x PE)
Effective Rainfall	Average Annual Effective Rainfall = (30 year average annual Rainfall – 30 year average annual AE)	Average Annual Effective Rainfall = $\sum_{1981}^{2000} \frac{(\text{daily rainfall} - \text{daily AE})}{30 \text{ years}}$
Grid cell size	5 km x 5 km	2.5 km
Soil drainage	Teagasc soils map 1:40,000 (Fealy, 2007), re-categorised by GSI to Wet, Dry, Peat, Made	Teagasc soils map 1:40,000 (Fealy, 2007), re-categorised by GSI to Wet, Dry, Peat, Made Teagasc Indicative Soil Drainage map 1:250,000 (Creamer <i>et al.</i> , 2016), recategorised to well-drained, moderately-drained and poorly-drained soils Hybrid map created by mapping indicative soil drainage categories onto 1:40,000 soils map
Subsoil permeability and Groundwater vulnerability	GSI mapping available in 2011	GSI mapping available in 2020
Sand and gravel aquifers	GSI sand and gravel aquifer map (2008)	GSI sand and gravel aquifer map (2019)
Hydrogeological Scenarios	21 hydrogeological scenarios (excluding High-Low vulnerability areas)	24 hydrogeological scenarios (see table below. Better representation and improved recharge coefficients for peats; better representation of scree; additional scenarios for sand and gravel.

The main geological controls on groundwater recharge include soil drainage, subsoil type, subsoil permeability, subsoil thickness, and the ability of the underlying aquifer to accept percolating waters.

The amount of rain falling on the land minus how much of that rain is taken up by plants is also a factor that determines how much groundwater recharge there is at a particular location. This is known as the 'effective rainfall'.

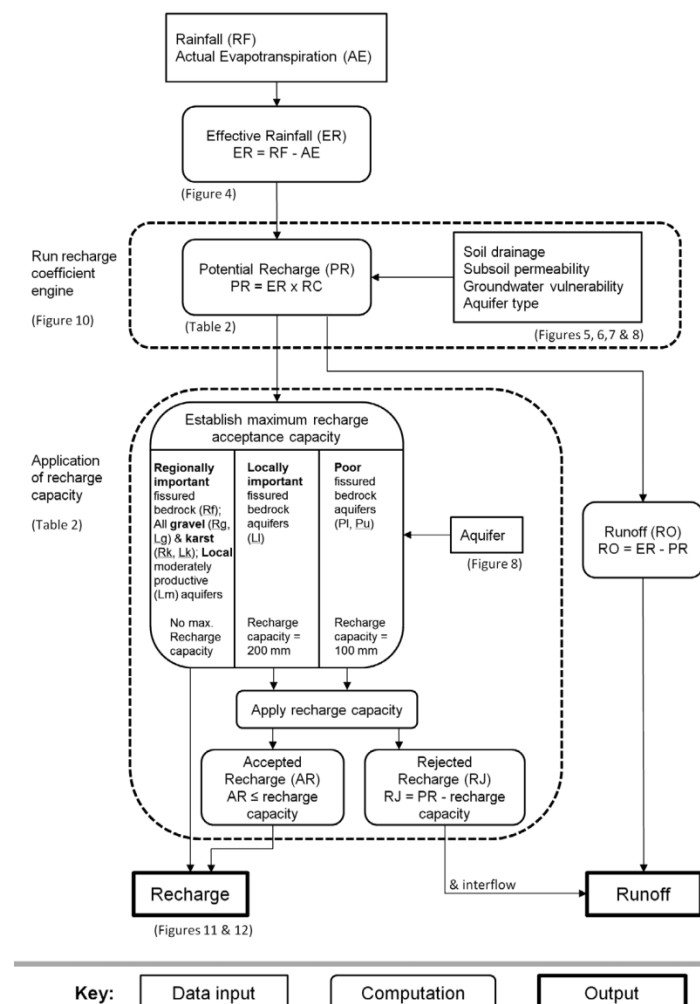
Different combinations of the geological factors give 24 hydrogeological scenarios. There is a 'recharge coefficient' for each scenario, which is the percentage of the 'effective rainfall' that may become groundwater recharge. The hydrogeological scenarios are summarised in Hunter Williams et al (in press) and are an update from Hunter Williams et al (2013). They are given in the Table below.

Table E.2: Hydrogeological scenarios and lower, mid and upper recharge coefficients (%)

Hydrogeological		Recharge coefficients (%)		
		Lower	Mid	Upper
1.i	E Vul: Areas where rock is at ground surface or karst feature	30	80-90	100
1.ii	E Vul: Sand & gravel overlain by well-drained soil	50	80-90	100
1.iii	E Vul: Sand & gravel overlain by poorly-drained (gley) soil	15	35-50	70
1.iv	E Vul: Till overlain by well-drained soil	45	50-70	80
1.v	E Vul: Till overlain by poorly-drained (gley) soil	5	15-30	50
1.vi	E Vul: Sand & gravel aquifer where the water table is ≤ 3 m below surface and overlain by well-drained soil	50	80-90	100
1.vii	E Vul: Sand & gravel aquifer where the water table is ≤ 3 m below surface and overlain by poorly-drained soil or peat	1	3-5	10
1.viii	E Vul: Blanket peat and Cut peat	1	15-30	50
1.ix	E Vul: Fen peat	1	3-5	10
2.i	H Vul: Sand & gravel aquifer, overlain by well-drained soil	50	80-90	100
2.ii	H Vul: High permeability subsoil (sand & gravel) overlain by well-drained soil	50	80-90	100
2.iii	H Vul: High permeability subsoil (sand & gravel) overlain by poorly-drained soil or peat	15	35-50	70
2.iv	H Vul: Sand & gravel aquifer, overlain by poorly-drained soil or peat	15	35-50	70
2.v	H Vul: Moderate permeability subsoil overlain by well-drained soil	35	50-70	80
2.vi	H Vul: Moderate permeability subsoil overlain by poorly-drained (gley) soil	10	15-30	50
2.vii	H Vul: Low permeability subsoil	1	20-30	40
2.viii	H Vul: Peat	1	5-15	20
2.ix	H Vul: Fen peat	1	3-5	10
3.i	M Vul: Moderate permeability subsoil overlain by well-drained soil	35	50-70	80
3.ii	M Vul: Moderate permeability subsoil overlain by poorly-drained (gley) soil	10	15-30	50
3.iii	M Vul: Low permeability subsoil	1	10-20	30
3.iv	M Vul: Peat	1	3-5	10
4.i	L Vul: Low permeability subsoil	1	5-10	20
4.ii	L Vul: Basin peat	1	3-5	10



The recharge coefficient polygons multiply agri-meteorological input data on a 2.5 x 2.5 km grid. The agri-meteorological data are produced by the Irish Centre for High-End Computing (ICHEC) from downscaled numerical weather prediction (NWP) models. The NWP models analysed in Werner et al. (2019) downscaled the European Centre for Medium-Range Weather Forecasts (ECMWF) ERAInterim global reanalyses dataset, and required significant computational hours on Ireland's national supercomputer to produce variables such as temperature, humidity, solar radiation wind-speed, etc. Two datasets (WRF v3.7.1, COSMO-CLM5) were downscaled by Dr. Paul Nolan (ICHEC) (Flanagan et al. 2019), and the third (MÉRA) was produced by Met Éireann. The FAO Penman Monteith Method was applied to dataset variables to produce reference evapotranspiration (ET_0), and the Soil Moisture Deficit Model (Schulte et al. 2005) was used to produce ET_a , SMD and ER variables used for this study. From the validations performed by Werner et al. 2019, the MÉRA dataset was chosen as having the highest overall skill. The figure below shows the process.



Indicative structure and method of GIS-based tool for estimating recharge
(from Hunter Williams et al 2013)





Deliverable 4.2

PILOT DESCRIPTION AND ASSESSMENT

Permo-Triassic aquifer (United Kingdom)

Authors and affiliation:

**Majdi Mansour, Vasileios
Christelis**

British Geological Survey (BGS)

This report is part of a project that has received funding by the European Union's Horizon 2020 research and innovation programme under grant agreement number 731166.



Deliverable Data	
Deliverable number	D4.2
Dissemination level	Public
Deliverable name	Pilots description and assessment report for recharge and groundwater vulnerability
Work package	WP4
Lead WP	BRGM, BGS
Deliverable status	
Version	Version 3
Date	23/3/2021

[This page has intentionally been left blank]

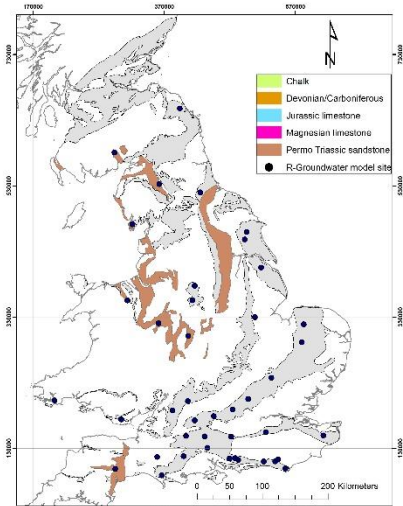
LIST OF ABBREVIATIONS & ACRONYMS

BGS	British Geological Survey
CC	Climate Change
EU	European Union
FAO	Food and Agriculture Organization
GCM	Global Circulation Models
GSO	Geological Survey Organization
ISIMIP	Inter Sectoral Impact Model Inter-comparison Project
NSE	Nash-Sutcliffe Efficiency
PET	Potential Evapo-Transpiration
R	Regression coefficient error
WP	Work Package

TABLE OF CONTENTS

LIST OF ABBREVIATIONS & ACRONYMS	5
1 EXECUTIVE SUMMARY	5
2 INTRODUCTION	7
3 PILOT AREA	9
3.1 Site description and data	9
3.1.1 Index boreholes in the Permo-Triassic aquifer in the UK	9
3.1.2 Topography	11
3.1.3 Land use	12
3.1.4 Rainfall	13
3.1.5 Potential evaporation	14
3.1.6 Hydrogeology	16
3.1.7 Groundwater levels	17
3.2 Climate change challenge	17
4 METHODOLOGY	19
4.1 Methodology and climate data	19
4.1.1 AquiMod	19
4.1.2 Metran	19
4.1.3 The distributed recharge model ZOODRM applied at the UK scale	20
Climate data	21
4.2 Model set-up	22
4.2.1 AquiMod	22
4.2.2 Metran	25
4.2.3 National scale model (ZOODRM)	25
4.3 Model calibration	27
4.3.1 Calibration of AquiMod models	27
4.3.2 Calibration of Metran models	29
4.3.3 Calibration of the UK national scale model using ZOODRM	30
5 RESULTS AND CONCLUSIONS	32
5.1 Historical recharge values	32
5.2 Projected recharge values	34
REFERENCES	42
APPENDICES	44
Appendix A: AquiMod methodology	44
The soil moisture module	45
The unsaturated zone module	46
The saturated zone module	46
Limitations of the model	48
Model input and output	48
Appendix B: Metran methodology	50
Limitations	51
Time step	51
Model output	51
Model quality	52
Recharge	52

1 EXECUTIVE SUMMARY

Pilot name	Boreholes in the Permo-Triassic sandstone aquifer	
Country	United Kingdom	
EU-region	North-western Europe	
Area (km ²)	NA	
Aquifer geology and type classification	Consists of Monitoring boreholes for water resources management up to 600 m thick. A possible yield up to 125 l/sec of good quality hard to moderately hard water from the upper parts of the aquifer.	
Primary water usage	Irrigation / Drinking water / Industry	
Main climate change issues	Risk of high precipitation causing increased river flows and flooding. Risk of drought.	
Models and methods used	Lumped groundwater modelling (AquiMOD)	
Key stakeholders	Government. Research institutes. Water companies.	
Contact person	British Geological Survey. Andrew McKenzie	

This report describes the work undertaken by the British Geological Survey (BGS/UKRI) as a part of TACTIC WP4 to calculate historical and future groundwater recharge across the outcrop of the Permo-Triassic sandstone aquifer and at selected observation boreholes within the aquifer. Groundwater levels and weather data at seven boreholes are examined in this study. Multiple tools, selected from the TACTIC toolbox that is developed under WP2 of the TACTIC project, have been used for this purpose.

The Permo-Triassic sandstone aquifer is the second major aquifer after the Chalk in the UK. These sandstone formations are mainly red sandstones that originated in a desert environment. Much of the sandstone is a soft, compact rock that is only weakly cemented. Groundwater flows through the matrix but the permeability of the aquifer is also considerably enhanced by the presence of fractures. The topography of the Permo-Triassic aquifer outcrop varies significantly nationally with a dominant landuse over the aquifer outcrop being mainly arable and improved



grassland. the groundwater in the Permo-Triassic aquifer can be under confined or unconfined conditions or alternating between these conditions.

Three tools have been used to estimate the recharge values. These are the lumped parameter computer model *AquiMod* (Mackay et al., 2014a), the transfer function-noise model *Metran* (Zaadnoordijk et al., 2019), and the distributed recharge model *ZOODRM* (Mansour and Hughes, 2004). Future climate scenarios are developed based on the ISIMIP (Inter Sectoral Impact Model Inter-comparison Project (www.isimip.org) datasets. The resolution of the data is 0.5°x0.5° global grid and at daily time steps. As part of ISIMIP, much effort has been made to standardise the climate data (e.g. undertake bias correction).

The estimation of the recharge model using the lumped model *AquiMod* is achieved by running the model in Monte Carlo mode. This produces many runs that are equally acceptable and consequently the uncertainty in the estimated recharge values can be assessed. The application of additional tools provides an additional mean to assess this uncertainty. Generally speaking, the differences between the 75th and 25th percentile recharge values are not significant when compared to the absolute recharge values calculated at the selected boreholes. In this study, the recharge values estimated using the distributed recharge model at these boreholes are different from those obtained from the lumped model. It is worth noting that the national recharge model calculates potential recharge, while the lumped model calculates actual recharge. In all cases the potential recharge values calculated by the national recharge model are higher than those calculated by the lumped model. The absolute recharge values calculated by the transfer function-noise model *Metran* are different from those calculated by the lumped model, but the pattern of spatial distribution is maintained.

Future recharge values have been calculated using the projected rainfall and potential evaporation values are 5 to 15% different from historical values on average. The 3° Max scenario, the wettest used in this work, produces values that are very different from the historical ones. This is observed in the output of both the lumped and the distributed models. Finally, future estimates are discussed in this report using long term average recharge values. It is recommended that further analysis being carried out to extract additional information from the produced output to understand the temporal implications of the recharge values in future, especially over the different seasons. In addition, it is recommended that the values and conclusion produced from this work should be compared to those obtained from different studies that applies future climate data obtained from different climate models.

2 INTRODUCTION

Climate change (CC) already has widespread and significant impacts on Europe's hydrological systems including groundwater bodies, which is expected to intensify in the future. Groundwater plays a vital role for the land phase of the freshwater cycle and has the capability of buffering or enhancing the impact from extreme climate events causing droughts or floods, depending on the subsurface properties and the status of the system (dry/wet) prior to the climate event. Understanding the hydrogeology is therefore essential in the assessment of climate change impacts. Providing harmonised results and products across Europe is further vital for supporting stakeholders, decision makers and EU policies makers.

The Geological Survey Organisations (GSOs) in Europe compile the necessary data and knowledge of the groundwater systems across Europe. To enhance the utilisation of these data and knowledge of the subsurface system in CC impact assessments, the GSOs, in the framework of GeoERA, has established the project "Tools for Assessment of Climate change Impact on Groundwater and Adaptation Strategies – TACTIC". By collaboration among the involved partners, TACTIC aims to enhance and harmonise CC impact assessments and identification and analyses of potential adaptation strategies.

TACTIC is centred around 40 pilot studies covering a variety of CC challenges as well as different hydrogeological settings and different management systems found in Europe. Knowledge and experiences from the pilots will be synthesised and provide a basis for the development of an infrastructure on CC impact assessments and adaptation strategies. The final projects results will be made available through the common GeoERA Information Platform (<http://www.europe-geology.eu>).

The specific TACTIC activities focus on the following research questions:

- What are the challenges related to groundwater- surface water interaction under future climate projections (TACTIC WP3)?
- Estimation of renewable resources (groundwater recharge) and the assessment of their vulnerability to future climate variations (TACTIC WP4).
- Study the impact of overexploitation of the groundwater resources and the risks of saline intrusion under current and future climates (TACTIC WP5).
- Analyse the effectiveness of selected adaptation strategies to mitigate the impacts of climate change (TACTIC WP6).

This report describes the work undertaken by the British Geological Survey (BGS/UKRI) as a part of TACTIC WP4 to calculate groundwater recharge at selected locations within the Permo-Triassic sandstone aquifer. WP4 is divided into seven tasks that cover the following activities: Review of tools and methods and identification of data requirements (Task 4.1), identification of principal aquifers and their characteristics aided by satellite data (Task 4.2), recharge estimation and its evolution under climate change scenarios in the principal aquifers (Task 4.3), analysis of long-term piezometric time series to evaluate aquifer vulnerability to climate change (Task 4.4), assessment of subsidence in aquifer systems using DInSAR satellite data (Task 4.5),

development of a satellite based net precipitation and recharge map at the pan-European scale (Task 4.6), and tool descriptions and guidelines (Task 4.7).

The work presented here is related to Task 4.3 that aims at the estimation of recharge under current and future climates. This is undertaken using multiple tools selected from the TACTIC toolbox that has been developed under WP2 of the TACTIC project. The toolbox is a collection of groundwater models, scripts, spreadsheets that serves all the activities identified in TACTIC workpackages. Here we use the lumped groundwater model *AquiMod* (Mackay et al., 2014a and Mackay et al., 2014b) and the Transfer Function-Noise Model *Metran* (Zaadnoordijk et al., 2019) with main challenge to calibrate these models to reproduce the behaviour of the observed groundwater level time series. The calibrated models are then used to calculate historical and future recharge values. In addition to these two models, we apply the UK national scale recharge model (Mansour et al., 2018) to validate the calculated recharge values and also to address the uncertainty associated with the calculation of these values.

3 PILOT AREA

3.1 Site description and data

3.1.1 *Index boreholes in the Permo-Triassic aquifer in the UK*

The Permo-Triassic sandstones forms the second major aquifer after the Chalk in the UK. These sandstones are mainly red sandstones that originated in a desert environment. They are found in a series of deep sedimentary basins in western England and on the eastern and western flanks of the Pennines. The packing of the quartz grains in the sandstones gives a porosity of 30% and the specific yield can be as high as 20 to 25%. Much of the sandstone is a soft, compact rock that is only weakly cemented. Groundwater flows through the matrix but the permeability of the aquifer is also considerably enhanced by the presence of fractures. The sandstones are very permeable and high yielding with large boreholes producing as much as 5 to 10 Ml/d (Source: UK Groundwater forum).

The Permo-Triassic aquifer provides important groundwater resources, especially in northern and central England, where the Sherwood Sandstone Group forms the most important aquifer (Figure 1). The sandstones have substantial thicknesses with the Sherwood Sandstone Group being up to 600 m thick and around the northern edge of the Cheshire Basin, the Permo-Triassic sandstones approach 1000 m in thickness. In the south-west and north-east of England, the sandstones dip to the east and become confined down dip by the Mercia Mudstone Group. In the west Midlands the aquifer occurs in a number of basins and in the north west, dip beneath the Irish Sea. The aquifer properties of the sandstones are greatly affected by their sedimentary structure and by post-depositional diagenesis (Allen, 1996).

There are a number of industrial estates over the aquifer outcrop, one of the largest being Trafford Park where historical over abstraction has resulted in high salinity. In addition, water companies, significant groundwater users in the study area include breweries, golf courses and plant nurseries.

Table 1 shows the locations of the observation boreholes across the Permo-Triassic sandstones. Lumped groundwater models are built to estimate the recharge values at these boreholes.

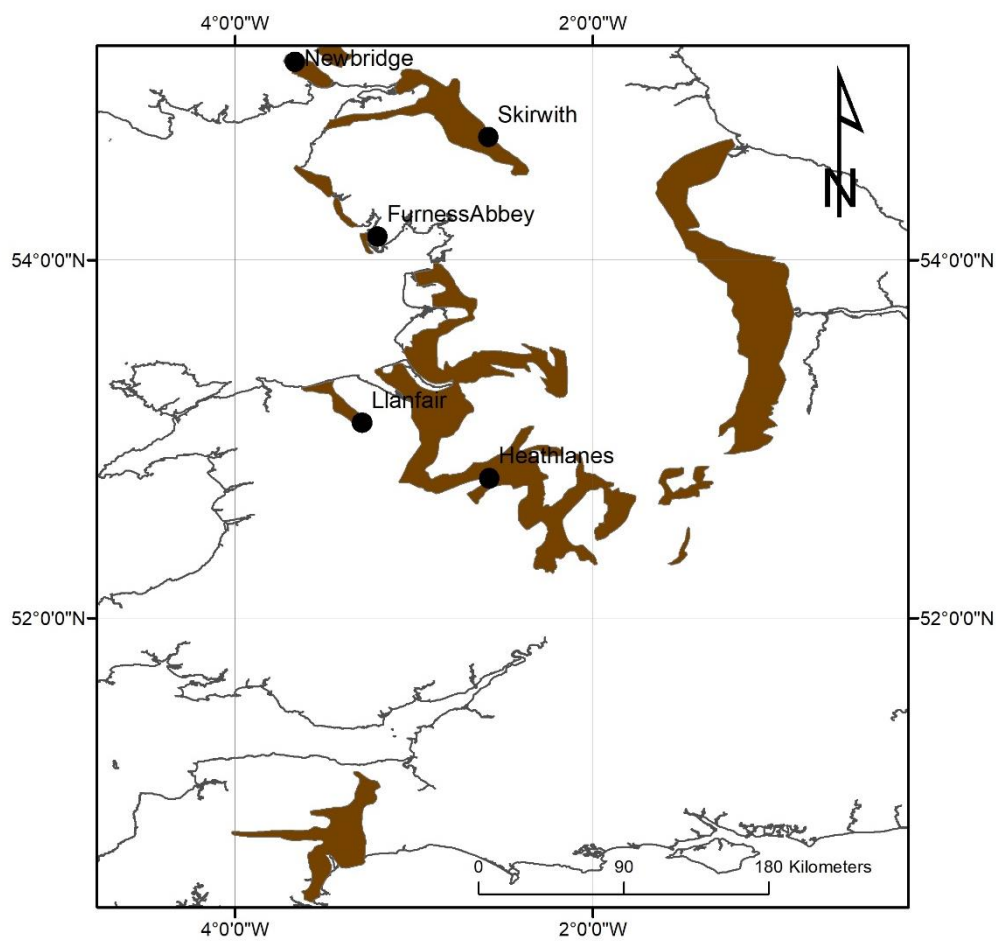


Figure 1. Extent of the Permo-Triassic aquifer and borehole locations.

Table 1. Description of observation boreholes

Borehole name	Location	GWls record	Hydrogeological response
Furness Abbey	Northwest of England	1971-2008	The hydrograph has an annual sinusoidal, but spiky, appearance.
Heathlanes	West of England	1978-current	Hydrograph indicates that the groundwater system is responsive to both seasonal recharge (fluctuations are normally less than 0.5 m) and longer term aquifer scale fluctuations (around 3 m amplitude).
Llanfair Dyffryn Clwyd	North of Wales	1836-current	The hydrograph shows a spiky annual sinusoidal pattern, within a relatively restricted range, with fluctuations generally less than 1 metre per annum.
Newbridge	South of Scotland	1996-current	The hydrograph exhibits an annual sinusoidal, but somewhat spiky response. The minimum water level appears to be controlled, possibly by the river level.
Skirwith	North of England	1889-current	The hydrograph has an annual sinusoidal pattern.

3.1.2 Topography

The topography of the Permo-Triassic aquifer outcrop varies significantly nationally. Raised ground surfaces in the outcrop in the Midlands reach elevations above 550 metres while to the northeast and northwest of England the ground surface is low lying. However, the ground surface of the outcrop of the aquifer in the Eden Valley occurs at relatively high elevations (Figure 2).

The sandstones are very permeable and yield significant part of the water that they store. Pumping from large boreholes reach rates as high as 10 Ml/d. The aquifer also provides an essential source of baseflow to maintain river flow. However, in some areas, river flows are artificially influenced by reservoirs and sewage work discharges. For example, much of Manchester's drinking water comes from the Lake District and therefore sewage discharges represent an additional input to the catchment.

Topographical data can be extracted at the selected boreholes to study the occurrences flooding events under future climate conditions.

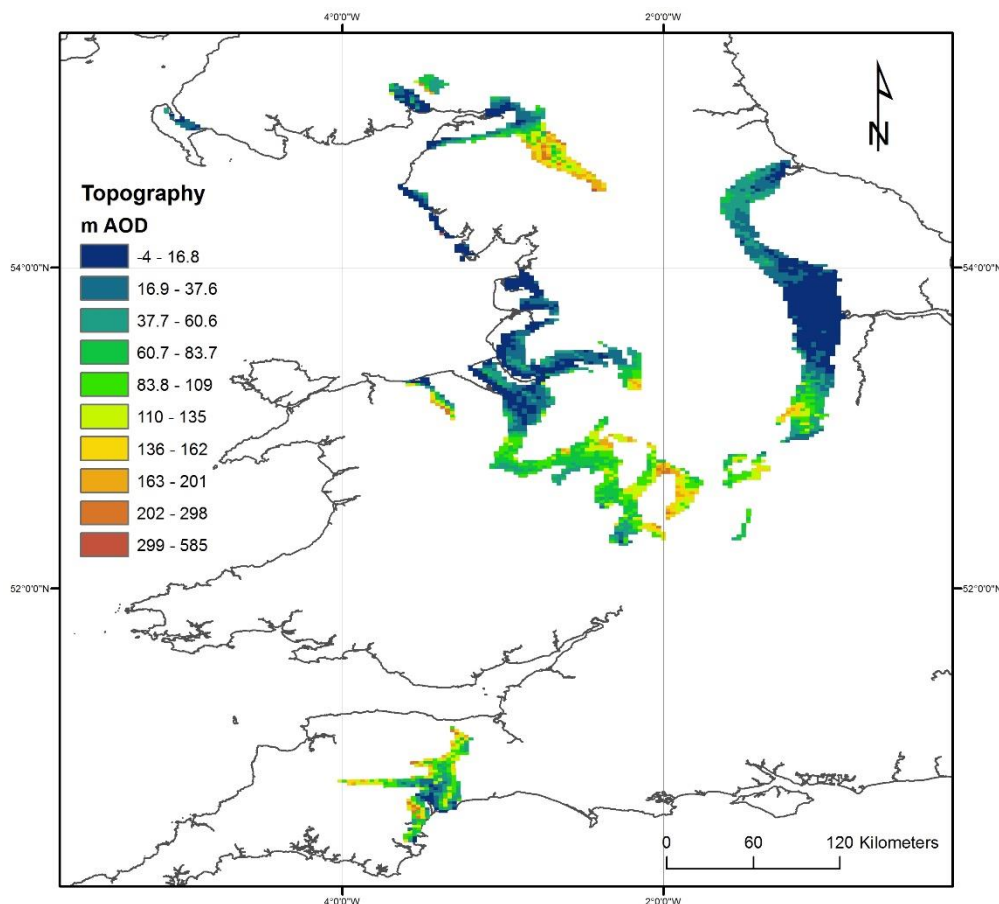


Figure 2. Topography map over the Permo-Triassic formation

3.1.3 Land use

The dominant landuse over the aquifer outcrop is mainly arable and improved grassland except in the Eden Valley where the dominant land use becomes improved grassland. The outcrop incorporates a number of urban and industrial areas including most of Greater Manchester and Stockport (Figure 3). Figure 3 shows the spatial distribution of landuse classes over the Permo-Triassic outcrop (Bibby, 2009). In some areas the main landuse is rural, which includes dairy farming and agriculture.

Landuse data can be extracted from this map at the selected boreholes to specify the model parameters that control evapo-transpiration, which is an important component of the total water balance produced by the applied models. Specific information about the landuse types at the selected boreholes are listed in Table 2.

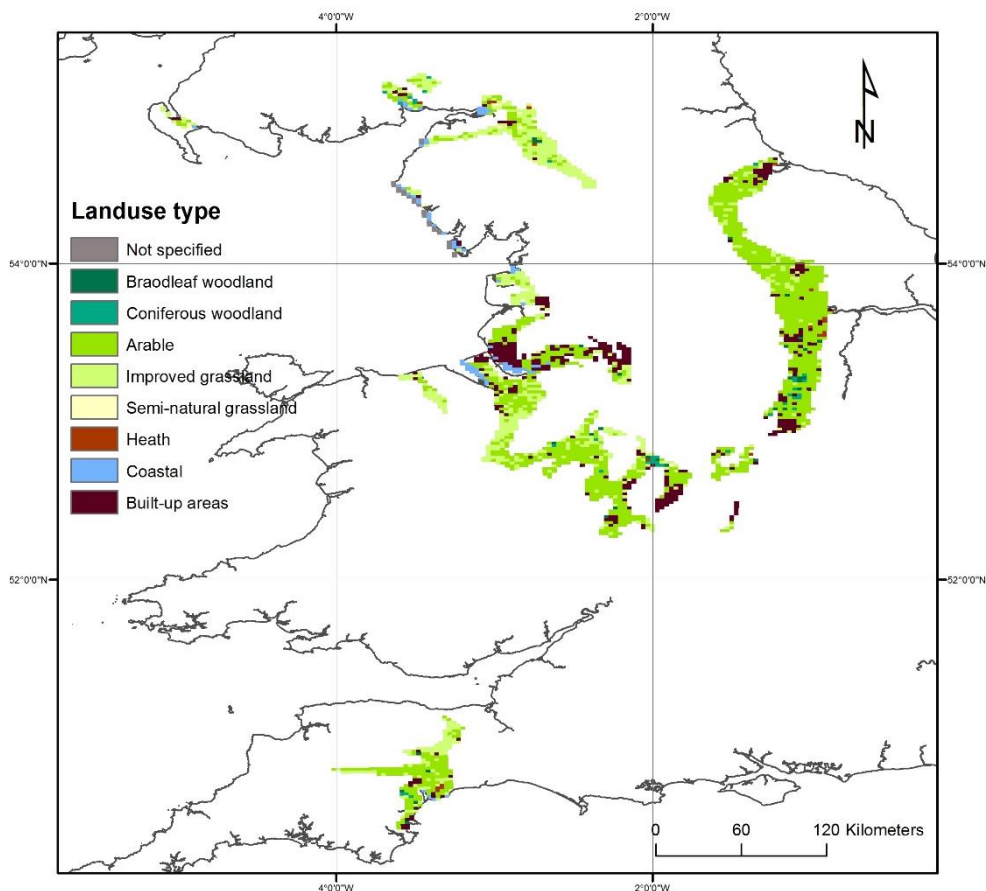


Figure 3. Map of land use over the Permo-Triassic formation

3.1.4 Rainfall

Daily rainfall raster data (1×1 km) were obtained from the Centre for Ecology and Hydrology (CEH) and were used to retrieve the daily rainfall values at the grid nodes pertain to the Permo-Triassic aquifer. The long-term average (LTA) rainfall across the outcrop is approximately 751 mm year^{-1} (2.06 mm day^{-1}); however, very high rainfall values above $2500 \text{ mm year}^{-1}$ (7 mm day^{-1}) are observed to the northwest of the aquifer outcrop (Figure 4).

Spatially distributed rainfall data are available at daily time steps starting from 1961 to 2016 (CEH). While the size of this time step is coarse to represent storm events for hydrological analysis, it is fine enough to calculate recharge values to drive groundwater models. These data are, therefore, used to drive the lumped models. Table 2 presents specific information about the rainfall values at the selected Permo-Triassic boreholes.

Projected (future) values of rainfall data are also available by the work of UKCP09 (Prudhomme et al., 2012; Murphy et al, 2007; Jenkins et al., 2009; Murphy et al, 2009), which provides projections of climate change in the UK. The probabilistic climate projections provided by



UKCP09 are not fully spatially coherent; however, (IPCC, 2000) produced 11 physically plausible simulations, generated under the medium emissions scenario known as A1B SRES emission scenario, that overcome this problem. These data can be used for the estimation of projected (future) recharge values.

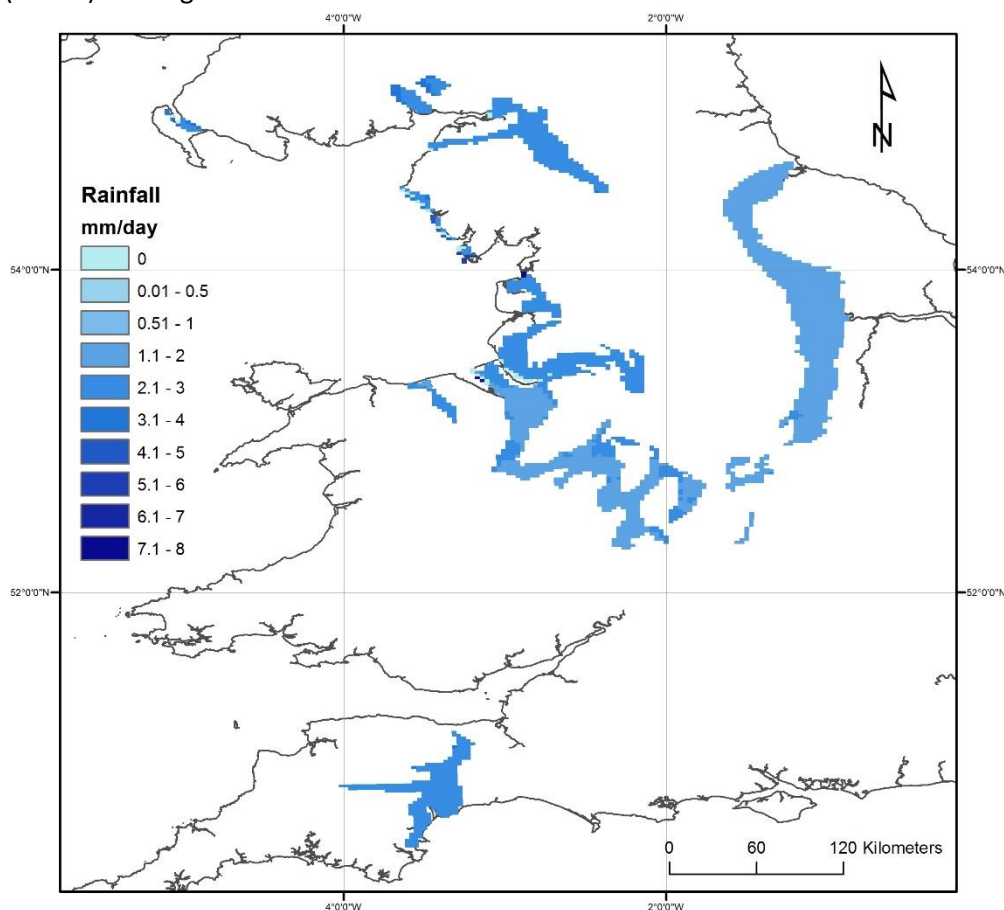


Figure 4. Spatial distribution of rainfall in the Permo-Triassic

3.1.5 Potential evaporation

The monthly potential evapotranspiration (PE) raster datasets (40×40 km) were gathered from a Met Office Rainfall and Evaporation Calculation System (MORECS) in the Met Office of the UK (Hough and Jones 1997). Figure 5 shows the distributed long-term average potential evaporation data. Highest potential evaporation rates of approximately 650 mm year^{-1} (1.78 mm day^{-1}) are observed to the west of the aquifer outcrop. Lowest potential evaporation rates of approximately 470 mm year^{-1} (1.28 mm day^{-1}) are observed to the north of the aquifer outcrop and the Eden Valley (Figure 5). The average potential evaporation rates over the whole of the Permo-Triassic aquifer is approximately 580 mm year^{-1} (1.59 mm day^{-1}). Table 2 presents specific information about the PE records at the selected boreholes in the Permo-Triassic aquifer.

Similar to rainfall data, UKCP09 potential evaporation data can be used to run simulations to calculate future recharge values.



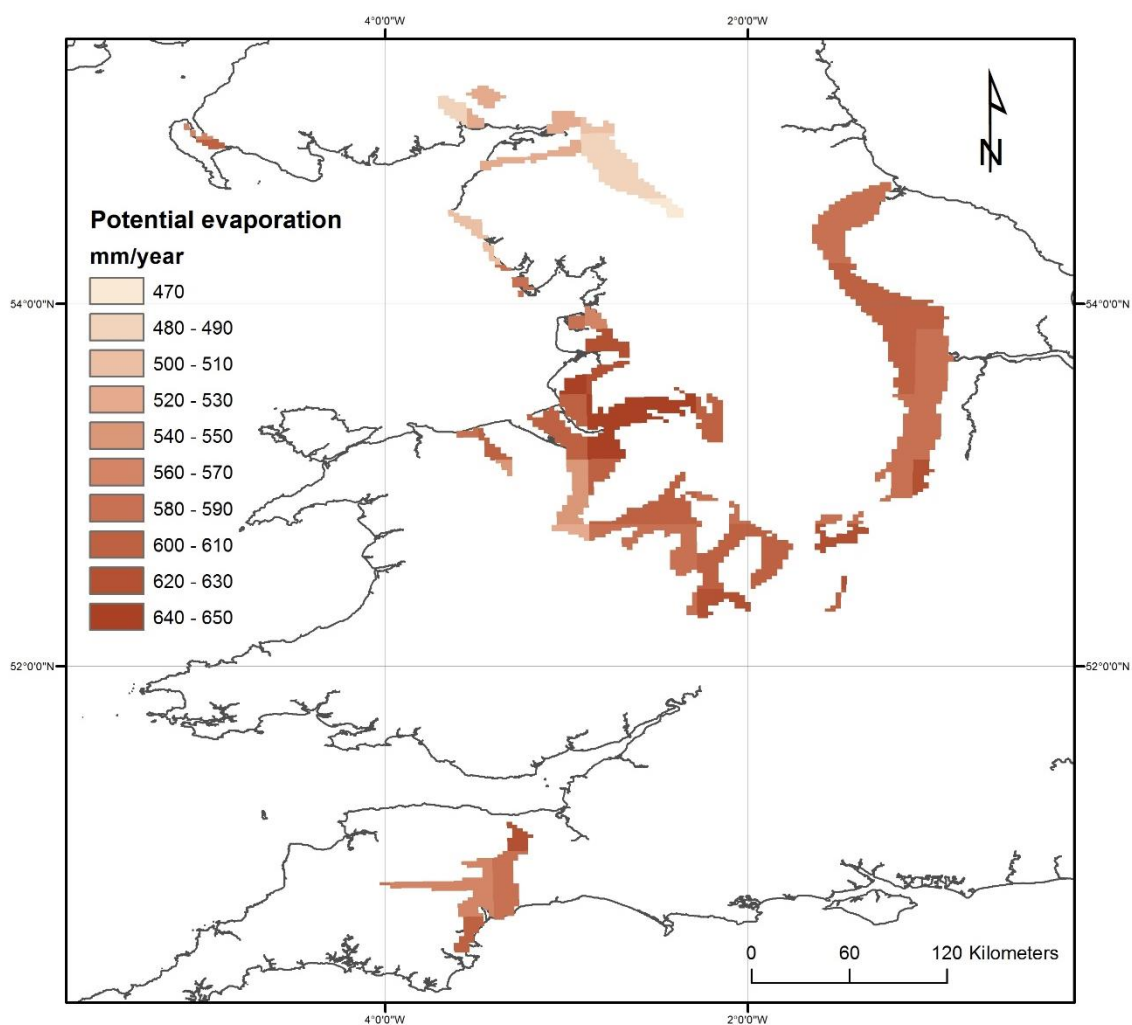


Figure 5. Spatial distribution of potential evaporation in the Permo-Triassic chalk

Table 2. Landuse, rainfall and evapotranspiration information for the Permo-Triassic

Borehole name	Dominant landuse	Av. Rainfall (mm/day)	Rainfall record	Av. PE (mm/day)	PE record
Furness Abbey	Improved grassland	2.77	1961-current	1.60	1961-current
Heathlanes	Arable	1.8	1961-current	1.59	1961-current
Llanfair Dyffryn Clwyd	Improved grassland	2.26	1961-current	1.45	1961-current
Newbridge	Arable	3.0	1961-current	1.33	1961-current
Skirwith	Improved grassland	2.2	1961-current	1.33	1961-current
Bussels	Arable	2.23	1961-current	1.56	1961-current
Nuttalls Farm	Urban	2.01	1961-current	1.67	1961-current

3.1.6 Hydrogeology

The Permo-Triassic sandstones consist of the Permian sandstones and the Triassic Sherwood Sandstone Group. The Permian marls, where present, form an aquitard and separate the Permian sandstones from the overlying Triassic sandstones. The Mercia Mudstone Group is an aquitard that overlies and confines the Sherwood Sandstones (Allen et al., 1996).

The hydraulic conductivity within the Permo-Triassic sandstones may be directional, higher in one direction, due to the channel nature of the deposits. Fine-grained layers within the Permo-Triassic sandstone have lower permeabilities, and can act as confining layers. In addition, the lateral facies changes can cause deposits to change from being aquifers to aquitards and the content of fine-grained sediments also varies vertically, often increasing towards the top of the aquifer.

Discontinuities including bedding-plane fractures, inclined joints of either tectonic or due to dissolution of vein infills, and solution-enlarged fractures play a significant role in saturated groundwater flow through the Permo-Triassic sandstones. They can provide preferential flow paths and have a significant effect on the physical properties of the aquifer. The hydraulic effects of faults in the Permo-Triassic sandstones vary widely, ranging from impermeable features which form barriers to groundwater flow, to highly transmissive structures which may act as recharge boundaries.

3.1.7 Groundwater levels

Depending on the investigated location, the groundwater in the Permo-Triassic aquifer can be under confined or unconfined conditions or alternating between these conditions. For example, the aquifer is confined at Llanfair and Skirwith observation boreholes but is under unconfined conditions at Heathlanes and New Bridge boreholes. The aquifer conditions vary between confined and unconfined at Furness Abbey observation borehole. Information available at the observation boreholes included in the analysis, it is clear that the unsaturated zone is not very thick ranging between 3 and 5 metres at New Bridge and Heathlanes respectively and that when the aquifer is confined, the piezometric surface is relatively close to the ground surface at approximately two metres away from the ground surface.

These time series are used in this study to characterise the aquifer properties and to estimate the infiltration recharge values for water resources management.

While the boreholes are selected so that they are not significantly impacted by the presence of nearby surface features, the records show that some boreholes are affected by nearby pumping. Pumping data are available on a daily basis and these can be included in the simulations if necessary.

3.2 Climate change challenge

The British Geological Survey (BGS) with the support of the Environment Agency (EA) have undertaken a study to investigate the impact of climate change on groundwater resources using the distributed recharge model ZOODRM (Mansour and Hughes, 2018). Potential recharge values for Great Britain (England, Scotland and Wales) are produced using rainfall and potential evaporation data from the Future Flows Climate datasets (11 ensembles of the HadCM3 Regional Climate Model or RCM). This study has shown that generally the recharge season appears to be forecast to become shorter, but with greater amount of recharge “squeezed” into fewer months. This conclusion is aligned with the European Environment Agency map that describes the expected climate change across the different areas in Europe as shown in Figure 6.

The shortening of recharge season indicates that aquifers may become more vulnerable to droughts if rainfall fails in one or two months rather than a prolonged dry winter as can occur now. At the very least, water management measures have to be put in place to account for periods when recharge volumes reduce. On the other hand, the increased recharge signal could result in flashier groundwater level response and potentially leading to more flooding.

The main climate challenge for water resources managers and stakeholders is to assess the risk of future flooding and drought events. This requires detailed assessment of the variation of resources at regional and local scales rather than national or continental scales.

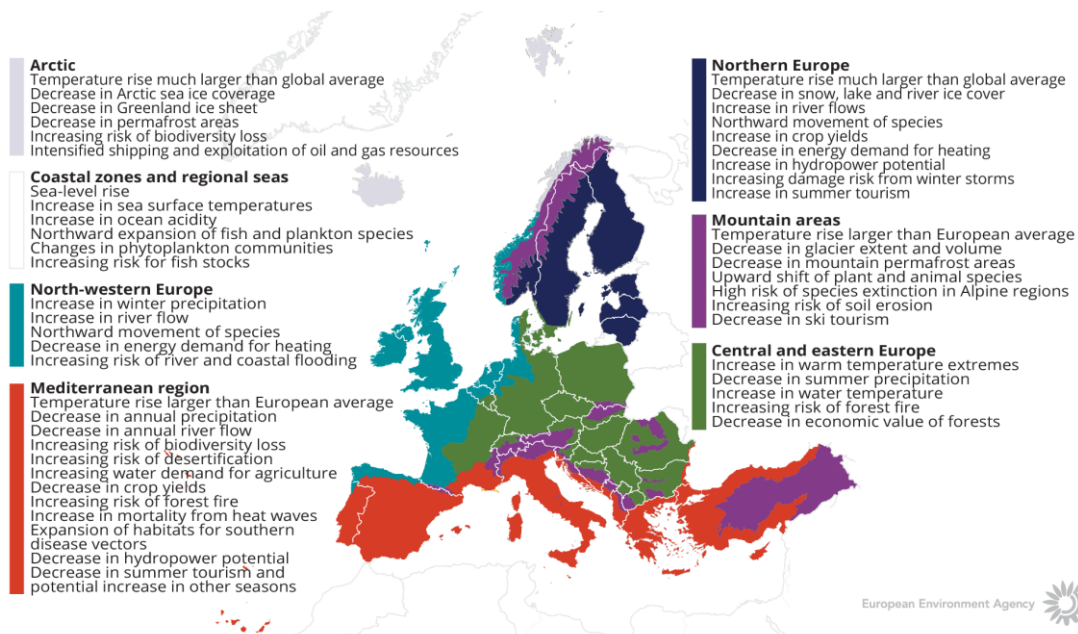


Figure 6. How is climate expected to change in Europe. The European Environment Agency map

4 METHODOLOGY

4.1 Methodology and climate data

4.1.1 *AquiMod*

AquiMod is a lumped parameter computer model that has been developed to simulate groundwater level time series at observational boreholes (Mackay et al., 2014a). It is based on hydrological algorithms that simulate the movement of groundwater within the soil zone, the unsaturated zone, and the saturated zone. The lumped models neglect complexities included in distributed groundwater models but maintain some of the fundamental physical principles that can be related to the conceptual understanding of the groundwater system (Mackay et al., 2014b).

The primary aim of AquiMod is to capture the behaviour of a groundwater system through the analysis of the available groundwater level time series. Once calibrated the model can be run in predictive mode and be used to fill in gaps in historical groundwater level time series and to calculate future groundwater levels. In addition to groundwater levels, it also provides predictions of historical and future recharge values and groundwater discharges.

The mathematical equations that are used to simulate the movement of groundwater flows within the three modules are detailed in Appendix A. The model uses rainfall and potential evaporation time series as forcing data. These are interpreted by the soil module representing the soil zone. The soil module calculates the rainfall infiltration and pass it to the unsaturated zone module. This module delays the arrival of the infiltrating water to the saturated zone module. The latter calculates the variations of groundwater heads and flows accordingly.

The model is calibrated using a Monte Carlo approach. It compares the simulated and observed groundwater level fluctuations and calculates a goodness of fit. The AquiMod version used in this work employs the Root Square Mean Error (RMSE) or the Nash Sutcliffe (NSE) performance measures to assess the performance of the model. The user sets a threshold value to accept all the models that perform better than the specified threshold. The possibility of producing many models that are all equally acceptable, allows the user to interpret the results from all these models and calculate uncertainty.

The recharge values calculated from AquiMod are those that reach the aquifer system and drive the groundwater levels. Thus, it is assumed that these are the actual recharge values as defined in the guidance report prepared by TACTIC project.

4.1.2 *Metran*

Metran applies a transfer function-noise model to simulate the fluctuation of groundwater heads with precipitation and evaporation as independent variables (Zaadnoordijk et al., 2019). The modelling approach consists mainly of two impulse functions and a noise model. The first impulse function is used for convolution with the precipitation to yield the precipitation contribution to the piezometric head. The second is for evaporation which is either a separately estimated function, or a factor times the function used for precipitation. The noise model is a

stochastic noise process described by a first-order autoregressive model with one parameter and zero mean white noise. Further information about the model is given in Appendix B with the model setup shown in the Figure B1.

Metran allows the addition of other processes affecting the behaviour of the groundwater heads, for example pumping or the presence of surface features such as rivers. The contributions from these processes are added to the deterministic part of the model.

Metran has been designed to work with explanatory series that have a daily time step. However, it has been adapted so that other time step lengths can be applied. However, the explanatory variables must still have a constant frequency.

The model is calibrated automatically; however, the model uses two binary parameters, Regimeok and Modok, to judge a resulting time series model. Regimeok cross-examines the explained variance R^2 (> 0.3), the absolute correlation between deterministic component and residuals (< 0.2), and the null hypothesis of non-correlated innovations (p value > 0.01). If all these criteria are satisfied, Regimeok returns a value of 1 indicating highest quality. Modok also cross-examines the explained variance R^2 (> 0.1) and the absolute correlation between deterministic component and residuals (< 0.3) as well as the decay rate parameter (> 0.002) and if all these criteria are satisfied, it is given a value of 1. If Modok = 1 and Regimeok = 0, the model is still considered acceptable. If both these parameters are 0, the model quality is insufficient and the model is rejected.

Metran's time series model is linear and the model creation fails when the system is strongly nonlinear. It is also limited to the response function being appropriate for the simulated groundwater system. Metran uses a gradient search method in the parameter space, so it can be sensitive to initial parameter values in finding an optimal solution.

The model calculates an evaporation factor f that gives the importance of evapotranspiration compared to precipitation. It is possible to use this factor to calculate the recharge values as shown by Equation B2 in appendix B. However, it must be noted that the use of Equation B2 is based on too many assumptions that are easily violated. Because of this, the equations should be applied only to long-term averages using only models of the highest quality.

Following the definitions used in the TACTIC project (See the guidance report), this recharge quantity corresponds to the effective precipitation. It is equal to the potential recharge when the surface runoff is negligible. This in turn is equal to the actual recharge at the groundwater table if there is also no storage change or interflow.

4.1.3 The distributed recharge model ZOODRM applied at the UK scale

A distributed recharge model, ZOODRM, has been developed by the British Geological Survey to calculate recharge values required to drive groundwater flow simulators. This recharge model allows grid nesting to increase the resolution over selected area and is called therefore the zooming object-oriented distributed recharge model (ZOODRM) (Mansour and Hughes, 2004). The model can implement a number of recharge calculation methods that are suitable for



temperate climates, semi-arid climates, or for urban areas. One of the methods that is implemented is the recharge calculation method used by Aquimod and detailed in Appendix A1.

ZOODRM uses a Cartesian grid to discretise the study area. It reads daily rainfall and potential evaporation data in time series or gridded format and calculates the recharge and overland flow at a grid node using a runoff coefficient as detailed in appendix A1. However, since this is a spatially distributed model, it reads a digital terrain model and calculates the topographical gradients between the grid nodes. It then uses the steepest gradient to route the calculated surface water downstream until a surface feature, such as a river or a pond, is reached. While the connections between the grid nodes based on the topographical gradients define the water paths along which surface water moves, major rivers are also user-defined in the model. This allows the simulation of river water accretion on a daily basis and the production of surface flow hydrograph. The model is then calibrated by matching the simulated river flows at selected gauging stations to the observed flows, by varying the values of the runoff coefficients.

The procedure used to calibrate the model involves dividing the study area into a number of zones and then to specify runoff values for each one. It is possible to vary the runoff coefficient values on a seasonal basis by using different runoff values for the different months of the year.

The recharge model ZOODRM calculates rainfall infiltration after accounting for evapotranspiration and soil storage. The simulated infiltration may not reach the aquifer system as it may travel laterally within the soil and discharge into surface water features away from the infiltration location. The simulated infiltration is therefore considered, as potential recharge according to the definitions of recharge processes provided the guidance report prepared by TACTIC project.

Climate data

The TACTIC standard scenarios are developed based on the ISIMIP (Inter Sectoral Impact Model Intercomparison Project, see www.isimip.org) datasets. The resolution of the data is 0.5°x0.5° global grid and at daily time steps. As part of ISIMIP, much effort has been made to standardise the climate data (e.g. bias correction). Data selection and preparation included the following steps:

1. Fifteen combinations of RCPs and GCMs from the ISIMIP data set were selected. RCPs are the Representative Concentration Pathways determining the development in greenhouse gas concentrations, while GCMs are the Global Circulation Models used to simulate the future climate at the global scale. Three RCPs (RCP4.5, RCP6.0, RCP8.5) were combined with five GCMs (noresm1-m, miroc-esm-chem, ipsl-cm5a-lr, hadgem2-es, gfdl-esm2m).
2. A reference period was selected between 1981 – 2010 and an annual mean temperature was calculated for the reference period.
3. For each combination of RCP-GCM, 30-years moving average of the annual mean temperature were calculated and two time slices identified in which the global annual mean temperature had increased by +1 and +3 degree compared to the reference period, respectively. Hence, the selection of the future periods was made to honour a



- specific temperature increase instead of using a fixed time-slice. This means that the temperature changes are the same for all scenarios, while the period in which this occurs varies between the scenarios.
4. To represent conditions of low/high precipitation, the RCP-GCM combinations with the second lowest and second highest precipitation were selected among the 15 combinations for the +1 and +3 degree scenario. This selection was made on a pilot-by-pilot basis to accommodate that the different scenarios have different impact on the various parts of Europe. The scenarios showing the lowest/highest precipitation were avoided, as these endmembers often reflect outliers.
 5. Delta change values were calculated on a monthly basis for the four selected scenarios, based on the climate data from the reference period and the selected future period. The delta change values express the changes between the current and future climates, either as a relative factor (precipitation and evapotranspiration) or by an additive factor (temperature).
 6. Delta change factors were applied to local climate data by which the local particularities are reflected also for future conditions. These monthly values (one set of rainfall and PE for each warming scenario) are used to drive the groundwater models presented in this report.

For the analysis in the present pilot the following RCP-GCM combinations were employed:

Table 3. Combinations of RCPs-GCMs used to assess future climate

		RCP	GCM
1-degree	"Dry"	rcp6p0	noresm1-m
	"Wet"	rcp4p5	miroc-esm-chem
3-degree	"Dry"	rcp4p5	hadm2-es
	"Wet"	rcp8p5	miroc-esm-chem

4.2 Model set-up

4.2.1 *AquiMod*

The boreholes located in the Permo-Triassic sandstone aquifer are listed in Table 1. *AquiMod* model setup relies mainly on two input files. The first input file "Input.txt" is a control file where the module types and model structure are defined. *AquiMod* is executed first under a calibration mode where a range of parameter values of the different selected modules are given in corresponding text files and a Monte Carlo approach is used to select the parameter values that yield best model performance. "Input.txt" also controls the mode under which *AquiMod* is executed, the number of Monte Carlo runs to perform, the number of models to keep with an acceptable performance, and the number of runs to execute in evaluation mode.

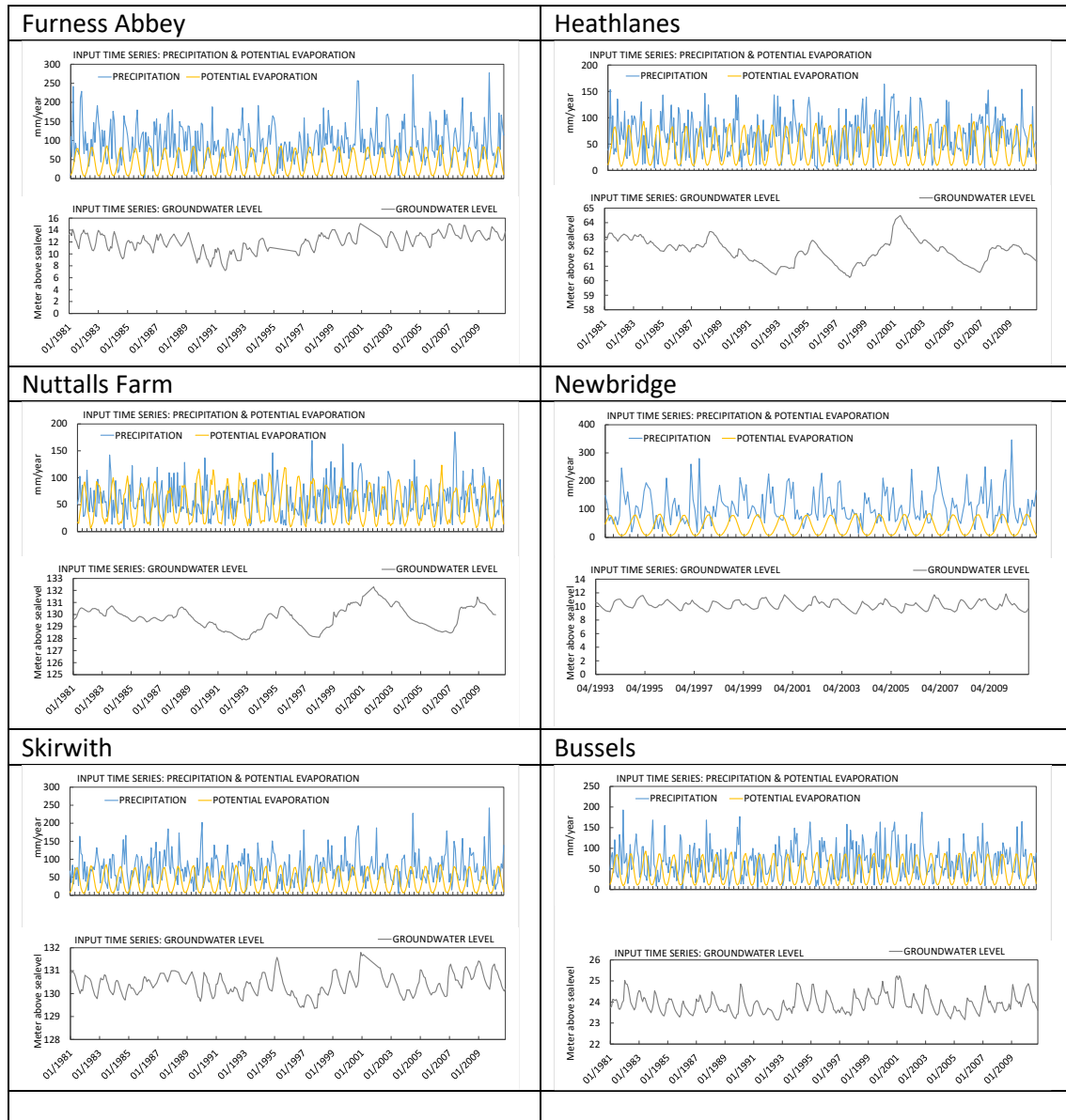
The second file *AquiMod* uses is called "observations.dat". This file holds the forcing data mainly the potential evaporation and rainfall. However, it is also possible to include the anthropogenic impact on groundwater levels by including a time series of pumping data in this file. None of the boreholes studied here includes pumping data. The observed groundwater levels that are used



for model calibration are also given in this file. The data are provided to the model on a daily basis, and this forces AquiMod to run using a time step length of one day. Table 4 shows daily time series of rainfall and potential evaporation values (mm/month) as well as the fluctuations of water table at the different boreholes.

All AquiMod models built for the boreholes in Table 1 use the FAO Drainage and Irrigation Paper 56 (FAO, 1988) method in the soil module, and employ the two-parameter Weibull probability density function to control the movement of infiltrated water in the unsaturated zone (Appendix A1). However, the groundwater module structures vary between the different boreholes. The best groundwater module structure is found by trial and error during the calibration process. The simplest structure, one layer with one discharge feature, is selected first and then the complexity of the module structure is increased gradually to see if the model performance improves. The structure with best model performance is selected to undertake the recharge calculations. The structures selected for these boreholes are mainly of one layer or three layered systems.

Table 4 Figures showing time series of daily rainfall and potential evaporation values (mm/month) as well as the fluctuations of water table at the different boreholes.



4.2.2 Metran

Metran applies transfer function noise modelling with daily precipitation and evaporation as input and of groundwater levels as output (Zaadnoordijk et al., 2019). The setup is shown in Figure 7. If time series of other influences on the groundwater head are available, these contributions can be added to the deterministic part of the model. An input file that holds the daily information of precipitation, potential evaporation and groundwater levels is prepared for each borehole in Table 1. Plots of these data are shown in Table 4. It must be noted that, while the groundwater levels used in AquiMod and shown in Table 4 have missing values, these have to be provided as complete time series to Metran. To achieve this, a linear interpolation procedure is used to fill in the missing values in the groundwater level time series.. Once executed, it calculates the characteristics of the impulse functions and the corresponding parameters automatically.

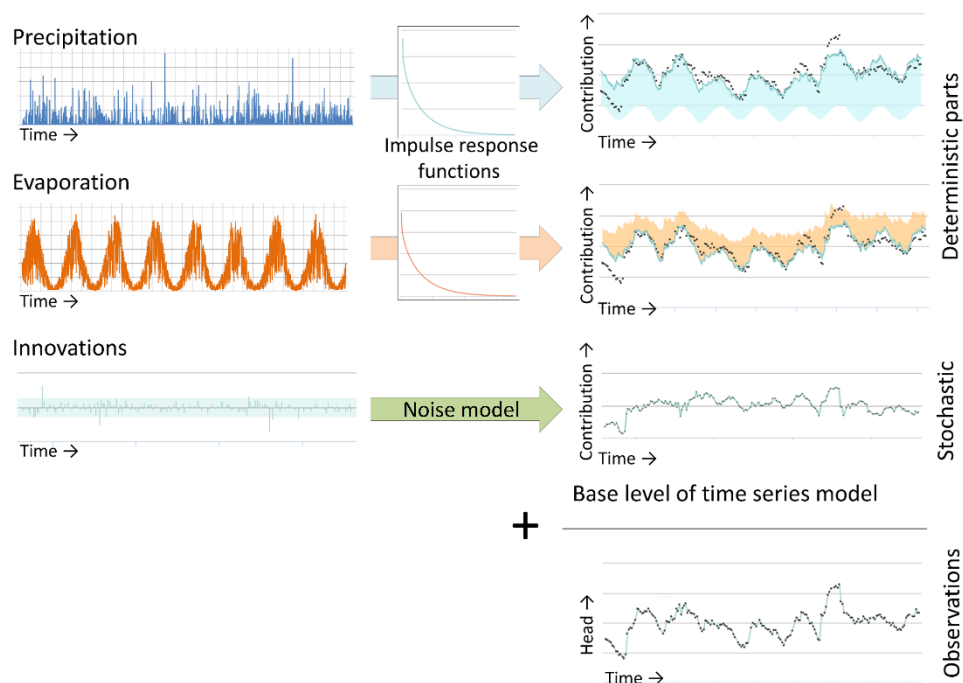


Figure 7 Illustration of METRAN setup

4.2.3 National scale model (ZOODRM)

The distributed recharge model (ZOODRM) is applied at national over the British Mainland (England, Scotland, and Wales) (Figure 8) using a Cartesian grid with 2 km square cells. The model reads a text file that defines the locations of the grid nodes as well as the connections between the nodes. This text file is prepared using a specific tool, called ZETUP (Jackson, 2004), where the extent of the study area is defined using the coordinates of the lower left and upper right corners of a rectangle that covers the modelled area. The spacing between the nodes and the information that dictate the boundary of the irregular shape of the area are also given in this



file. This tool also uses a file that contains the locations of the nodes as obtained from a geographical information system tool (GIS) and converts this information into a text file that describes the river extents and characteristics.

The map defining the runoff zones is based on the hydrogeology of the study area. It is produced in gridded ascii format using the hydrogeological map available for Great Britain. Additional text files, one for each runoff zone, are also prepared to define the monthly runoff values.

The topographical information is also provided in a gridded ascii format for the model to calculate the topographical gradients between the nodes. While a surface water routing procedure that accounts for indirect recharge and surface water storage is available in the model, this is not used in the current application. It is assumed that all the water originated at one grid nodes travel downstream and reaches a discharging feature in one day, which is equal to the length of the time step used.

Landuse data (Section **Error! Reference source not found.**) and soil data that are required to calculate the water capacity at every grid node are also provided to the model using maps in gridded ascii format. A set of landuse gridded maps, a total of ten, are used to give the percentage of landuse type at any given location. The gridded soil map gives the soil type at a selected location. The landuse type and soil type ids are linked to text files that hold the corresponding information such as the soil moisture at saturation, the soil moisture at wilting and the root constants can be obtained.

The driving data are provided to the model as daily gridded rainfall data (Sections **Error! Reference source not found.**) and time series of monthly potential evaporation values as described in (Section **Error! Reference source not found.**). Mansour et al. (2018) provide a full description of the construction of this model together with a more detailed description of the data used. The calculated recharge values are also provided in the published work; however, it must be noted that the historical recharge values shown in this work are simulated over the period from 1981 to 2010 in order to be consistent and comparable with the recharge values calculated by AquiMod and Metran. In addition, in this study, the model is rerun using the climate change data specifically provided by the TACTIC project to calculate the projected distributed recharge values.

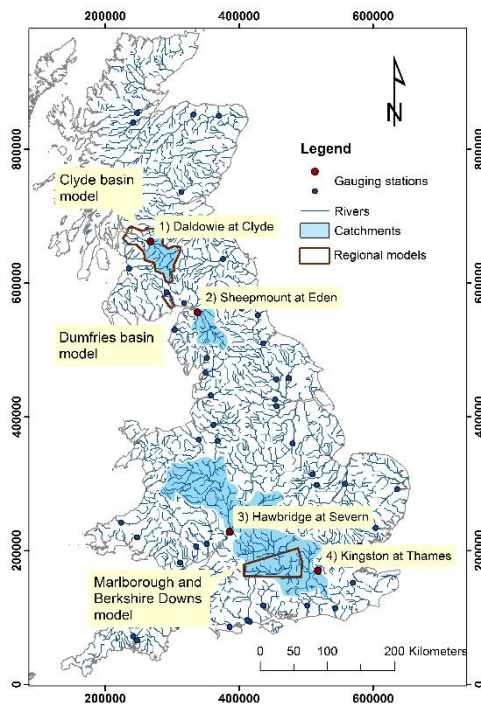


Figure 8. Extent of the UK national scale recharge model in UK national grid reference after Mansour et al. (2018). Figure also shows the locations of the gauging stations downstream of the major rivers used for model calibration.

4.3 Model calibration

4.3.1 Calibration of AquiMod models

The calibration of AquiMod is performed automatically using the Monte Carlo approach. The user populates the files of the selected modules with minimum and maximum parameter values and then the model randomly selects a value from the specified range for any given run. The selection of the minimum and maximum values is physically based depending on the characteristics of the study area. For example, the minimum and maximum values of the root depth in the soil module are set to 15 cm and 60 cm respectively for a study area covered with grass, while these values are set to 120 cm and 200 cm for a woodland area. The storage coefficients bounds of a groundwater module are set to much lower values in a confined aquifer compared to those used for an aquifer under unconfined conditions.

A conceptual hydrogeological understanding must be available before the use of AquiMod, since this is necessary to set the limits of the parameter values for the calibration process. In some cases, it is not possible to obtain a good performing model with the selected values and that necessitates the relaxation of these parameters beyond the limits informed by the conceptual



understanding. In such cases, the parameter values must feed back into the conceptual understanding if better performing models are obtained.

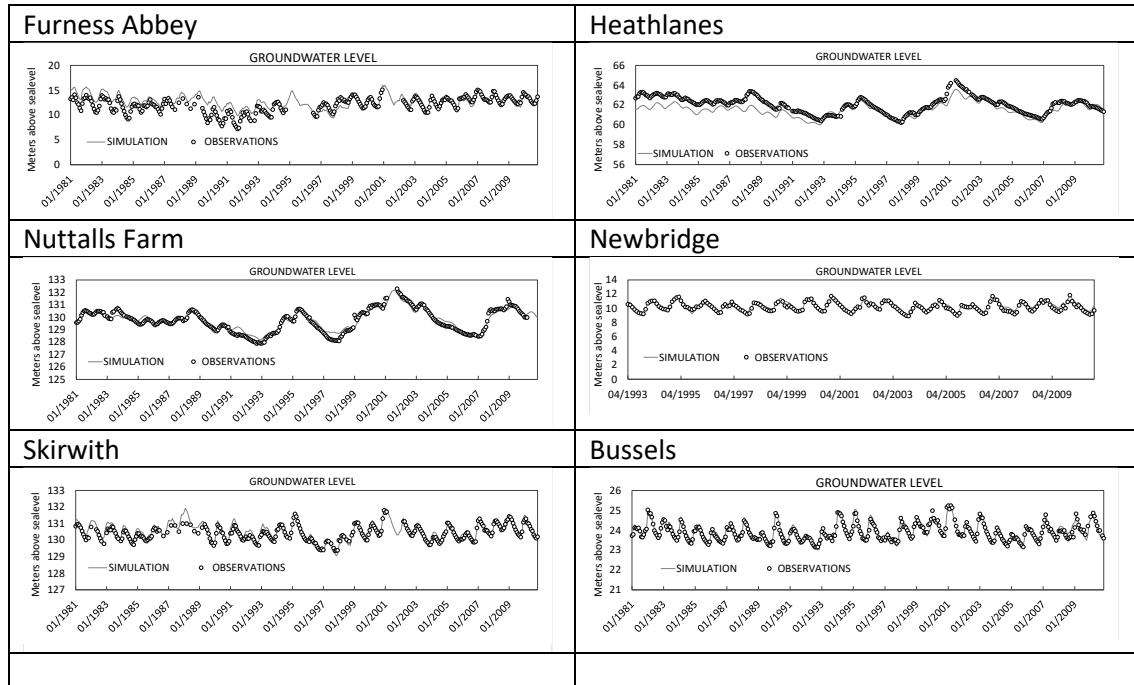
AquiMod execution time is relatively small, which allows the calibration of the model using hundreds of thousands of runs in couple of hours. The performance measure used to assess the quality of the simulation is the Nash Sutcliffe Error (Appendix A) that takes a maximum value of unity for a perfect match between the simulated and observed data. The threshold at which models are accepted is set to a value of 0.6. All the models that achieve an NSE higher than 0.6 are included in the analysis but a maximum number of 1000 runs are used if the number of acceptable models is greater than 1000.

Table 5 shows the best NSE values obtained for the models calibrated at the Permo-Triassic sandstone boreholes listed in Table 1. It is clear that a good match was achieved between the simulated and observed groundwater levels as illustrated in the plots shown in Table 6. The best performing model is the AquiMod model built at Bussels borehole with an NSE value of 0.95. The least performing AquiMod model is that built for Furness Abbey borehole with an NSE value of 0.75.

Table 5 Nash Sutcliff Error measure at the Permo-Triassic boreholes

Borehole name	NSE
Furness Abbey	0.75
Heathlanes	0.81
Llanfair	0.92
Newbridge	0.8
Skirwith	0.93
Bussels	0.95
Nuttalls Farm	0.91

Table 6 Comparison between the simulated and observed groundwater levels at the Permo-Triassic observation boreholes.



4.3.2 Calibration of Metran models

For the standard setup with precipitation and evaporation, there are five parameters that have to be determined during the calibration of the model. Three parameters are related to the precipitation response, the evaporation factor, and the noise model parameter (Appendix B). There are three extra parameters for each additional input series, such as pumping. The parameter optimization of Metran uses a gradient search method in the parameter space to reach a global minimum. As explained in Appendix B, two parameters indicate if Metran succeeded with producing a match between the simulated and observed data. These are called the Regimeok and Modok. When Regimeok is equal to one, the calibration is of highest quality. If Modok is equal to one and Regimeok is equal to zero, the calibration is of acceptable quality. Finally, if both parameters are equal to zero, the calibration quality is insufficient.

Time series of rainfall, potential evaporation and groundwater levels are provided to Metran on a monthly basis. Metran input data must be complete dataset, i.e. without missing data. To overcome this problem that may exist in the groundwater level time series, these data are aggregated to monthly values first and then missing values were filled using linear interpolation. Table 7 shows the performance of Metran across the Permo-Triassic boreholes considered in this study. It is clear that according to criteria set above, Metran fails to produce a model at four boreholes but succeeds at the seven other boreholes with the model output showing highest quality at four of these boreholes (with highest value of R^2).

Table 7 Performance of Metran across the selected Permo-Triassic boreholes.

Borehole name	Metran performance parameter Modok	Metran performance parameter Regimeok	Overall quality	R2	RMSE
Furness Abbey	1	0	Acceptable	0.44	1.15
Heathlanes	1	0	Acceptable	0.61	0.53
Llanfair	1	0	Acceptable	0.37	0.37
Newbridge	1	1	Highest	0.81	0.28
Skirwith	1	0	Acceptable	0.72	0.25
Bussels	1	0	Acceptable	0.76	0.21

4.3.3 Calibration of the UK national scale model using ZOODRM

Model calibration of the national scale recharge model was based on the comparison of the simulated long-term average overland flows to the observed ones (Mansour et al., 2018) recorded at gauging stations of selected major rivers (Figure 8). However, additional checks were also undertaken to assess the performance of the model. These include checking the match between the seasonal overland flow volumes at four boreholes, shown in red in Figure 8, checking the calculated recharge volumes with those calculated by other tools over selected catchment areas, and checking the temporal fluctuations of soil moisture deficit with those calculated by other tools. Figure 9 shows a Q plot for the simulated vs observed long term average runoff values at the 56 gauging stations shown in Figure 8. The solid line shows the one to one match and the dotted line shows the linear relationship between the two datasets.

It must be noted that while this model uses the same recharge calculation methods used by Aquimod, these two models are calibrated using different datasets, with Aquimod using the groundwater levels and the distributed recharge model using the overland flows.

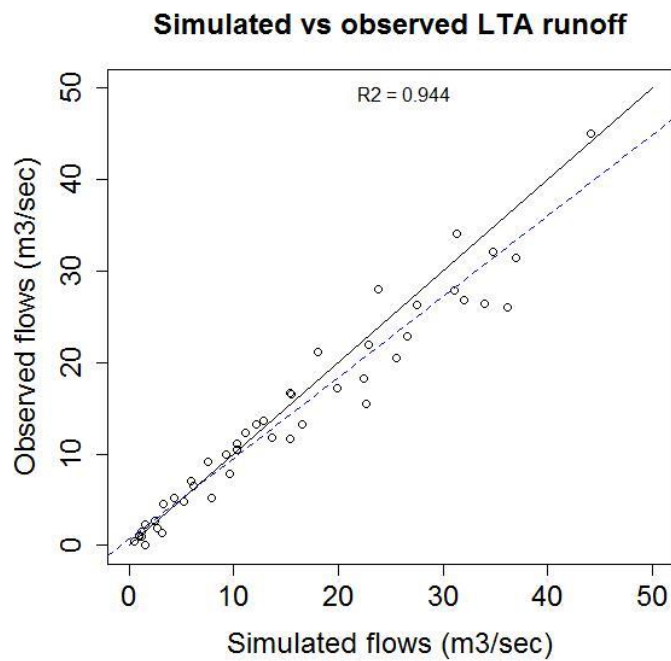


Figure 9 Q plot for the simulated vs observed long term average runoff values at the 56 gauging stations shown in Figure 8 after Mansour et al. (2018)

5 RESULTS AND CONCLUSIONS

5.1 Historical recharge values

Table 8 shows the time series of the historical recharge values calculated using the Aquimod model at the Permo-Triassic boreholes listed in Table 1. The plots in this table also show the 10th percentile, the mean, and the 90th percentile of recharge values calculated from the time series.

As mentioned Appendix B, the formulas used by Metran are based on assumptions that can be violated and it is better to use the infiltration coefficient f_c with the long-term average values of rainfall and potential evaporation to calculate long-term average values of recharge and using only models of the highest quality. Time series of recharge values are not therefore produced from the analysis undertaken using Metran. The long-term average recharge values calculated using Metran are shown in Table 9.

One of the benefits of running Aquimod in Monte Carlo mode is the possibility of producing many models with acceptable performance. Consequently, the recharge values estimated from these models are all equally likely. This provides us with a range of recharge values at each borehole that reflects the uncertainty of the optimised hydraulic parameter values. In the current study, the long-term average recharge values are calculated from up to 1000 acceptable models if they exist at each borehole; otherwise, all the acceptable models are used. The mean, 25th and 75th percentiles are then calculated from these long-term recharge values and displayed in Figure 10. It is clear that the differences between the 75th and 25th percentile values is negligible at almost all the boreholes; however, the most noticeable difference can be seen at the Nuttalls Farm borehole with approximately a 3.9 mm/month between the 25th (16.4 mm/month) and 75th (20.3 mm/month) percentile values yielding.

In addition to the recharge values calculated using Aquimod, Figure 10 shows the recharge values calculated using Metran and the distributed national scale model at these boreholes. It is clear that there is a good agreement between the Aquimod calculated recharge values and those calculated using the distributed national scale model at Nuttalls Farm and Newbridge boreholes. However, the values estimated from these boreholes vary significantly at the other four boreholes with Aquimod producing higher recharge values at Furness Abbey and Heathlanes boreholes and lower recharge values at Bussels and Skirwith. It must be noted that the recharge values calculated by these two models are of different types. The distributed recharge model calculates potential recharge and Aquimod calculates actual recharge. However, the inconsistency between the national scale model producing higher recharge values as expected, indicates that there are complex surface process heterogeneity that needs further investigations.

The pattern of the recharge values calculated using Metran at the selected boreholes match that of the recharge values calculated by the other two models. However, Metran produces higher recharge values at all the boreholes. Note that Metran failed to produce a model at Nuttalls Farm borehole. Metran estimates an upper and a lower value for the infiltration coefficient f_c . This can be used as an indication of uncertainty associated with the calculated f_c value. These

bounds are also shown in Table 9. The upper and lower bound values at all the boreholes are greater than the estimated f_c value. It is not possible to use these bound values to correct the recharge estimated by Metran and highlights that the recharge values estimated by Metran and shown in Figure 10 are highly uncertain.

Table 8 Time series of recharge values obtained from the best performing AquiMod models at the Permo-Triassic boreholes

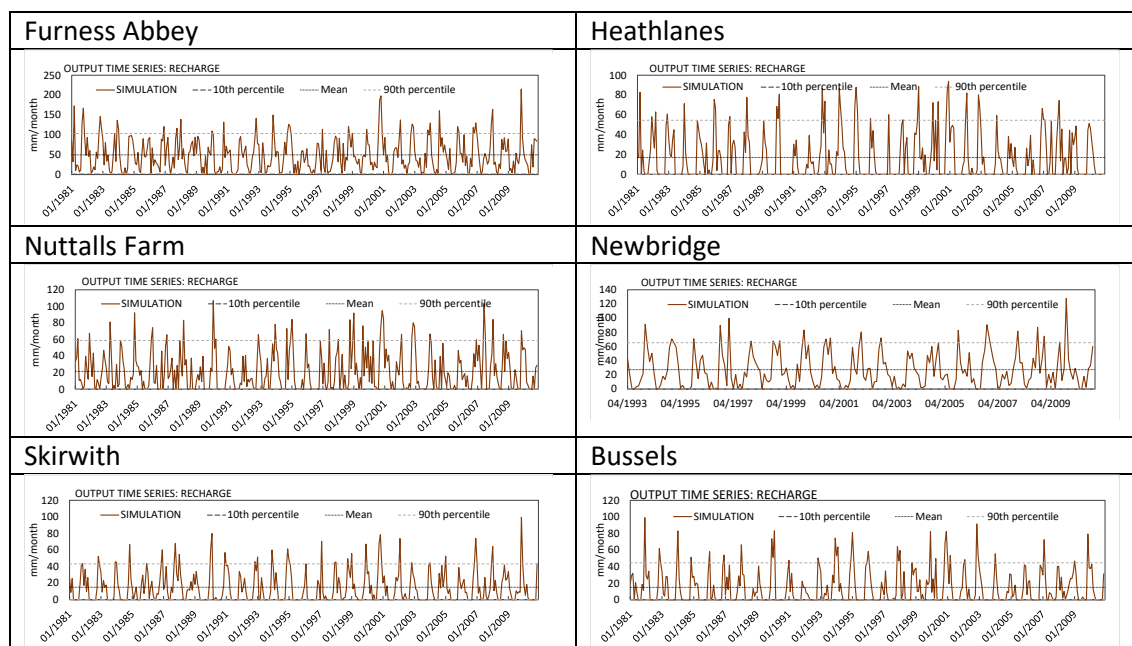


Table 9 Recharge values calculated using the recharge factors estimated by Metran

Borehole name	Average precipitation (mm/month)	Average potential evaporation (mm/month)	Recharge factor	Recharge (mm/month)
Furness Abbey	95.00	40.91	1.02 +- 2.13	52.13
Heathlanes	66.13	43.44	0.56 +- 6.94	41.63
Newbridge	108.03	39.33	0.6 +- 3.31	84.51
Skirwith	74.06	38.99	0.83 +- 5.35	41.70
Bussels	68.08	45.12	0.835 +- 4.56	30.45

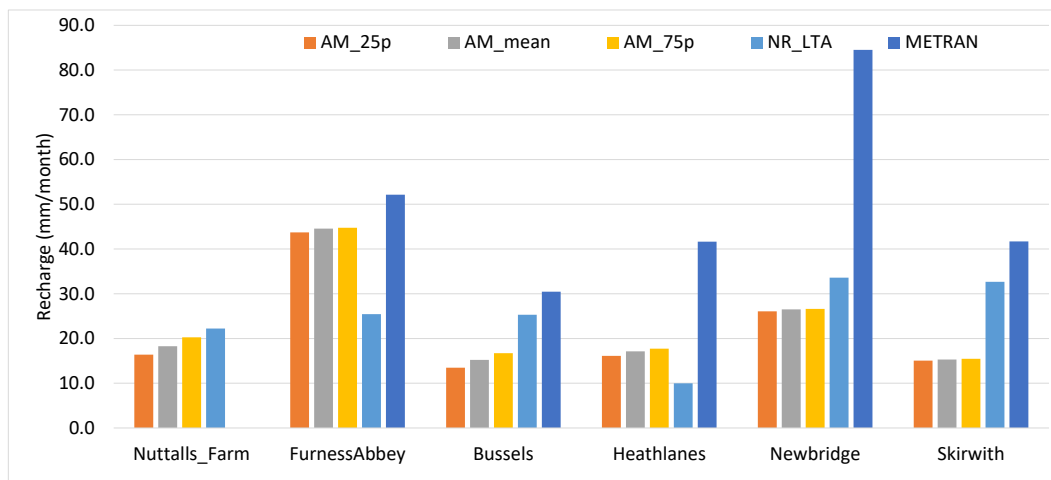


Figure 10 Historical recharge values calculated by AquiMod, Metran, and the national scale recharge model.

5.2 Projected recharge values

The forcing data, rainfall and potential evaporation, are altered using the change factors of the climate models (see Section **Error! Reference source not found.**). For the United Kingdom, there are two sets of monthly change factors, one used with the data driving AquiMod and Metran (Table 10), and the other used to calculate the spatially distributed recharge (Table 11). These change factors are used as multipliers to both the historical rainfall and potential evaporation values.

For the application involving AquiMod, these factors are used to alter the time series of historical rainfall and potential evaporation values used to drive the model.

When using Metran, the historical time series are altered using these factors first and then the long-term average rainfall and potential evaporation values are calculated. The recharge coefficient f_c values of the different boreholes, as calculated from the calibration of Metran model using the historical data, are then applied to calculate the projected long-term average recharge values.

The distributed recharge model ZOODRM includes the functionality of using these change factors to modify the historical gridded rainfall and potential evaporation data before using them as input to calculate the recharge. In this case, and for any simulation date, the rainfall and potential evaporation change factors for the month corresponding to the date, are used to modify all the spatially distributed historical rainfall and potential evaporation values respectively.

Table 10 Monthly change factors as multipliers used for the borehole data

	Scenario	Jan	Feb	Mar	Apr	May	Jun	Jul	Aug	Sep	Oct	Nov	Dec
Rainfall	1° Min	1.087	0.956	0.994	1.072	0.888	0.909	0.836	0.988	1.017	1.106	0.962	1.031
	1° Max	1.140	1.012	1.033	1.045	1.022	0.863	1.086	0.953	0.995	1.067	1.148	1.053
	3° Min	0.936	1.056	0.994	1.153	1.063	0.900	0.846	0.721	0.854	0.970	1.047	1.116
	3° Max	1.191	1.177	0.989	1.014	0.949	0.986	1.473	1.145	1.173	1.074	1.152	1.112
PE	1° Min	1.082	1.082	1.062	1.089	1.091	1.061	1.078	1.083	1.082	1.063	1.049	1.076
	1° Max	1.049	0.993	1.014	1.007	1.019	1.013	1.021	1.015	1.029	1.028	1.020	1.026
	3° Min	1.034	1.057	1.039	1.056	1.060	1.086	1.085	1.091	1.109	1.097	1.064	1.066
	3° Max	1.072	1.070	1.055	1.071	1.105	1.106	1.072	1.083	1.082	1.076	1.072	1.060

Table 11 Monthly change factors as multipliers used for the distributed recharge model

	Scenario	Jan	Feb	Mar	Apr	May	Jun	Jul	Aug	Sep	Oct	Nov	Dec
Rainfall	1° Min	1.086	0.953	0.975	1.064	0.918	0.914	0.856	0.973	1.008	1.103	0.976	1.038
	1° Max	1.132	1.090	1.008	0.899	1.034	1.087	1.310	0.983	1.020	1.006	1.012	1.025
	3° Min	1.156	1.118	1.033	1.011	0.914	0.821	0.908	0.656	0.821	0.986	0.980	1.181
	3° Max	1.192	1.131	0.960	0.990	0.899	0.957	1.437	1.109	1.134	1.068	1.139	1.106
PE	1° Min	1.081	1.081	1.059	1.089	1.091	1.061	1.078	1.083	1.085	1.063	1.049	1.076
	1° Max	1.051	1.036	1.020	1.039	1.051	1.049	1.031	1.043	1.054	1.039	1.044	1.034
	3° Min	1.016	1.031	1.021	1.029	1.038	1.029	1.047	1.057	1.059	1.059	1.040	1.045
	3° Max	1.070	1.066	1.051	1.071	1.105	1.106	1.072	1.083	1.083	1.076	1.072	1.060

Figure 11 shows the historical and future long-term average recharge values calculated using the best performing AquiMod model. It is clear that the highest reduction in recharge values are observed when the 3° Min rainfall and evaporation data are used, while the highest increase in recharge values are observed when the 3° Max rainfall and potential evaporation data are used.

When the 1° Min scenario data are used, all the boreholes show reduction in recharge values with the highest reduction observed at both Heathlanes and Skirwith boreholes (-9.9%) and the smallest reduction observed at Newbridge borehole (-1.8%). When the 1° Max scenario data are used, all the boreholes show increase in recharge values with the smallest increase observed at Skirwith borehole (5.9%) and the highest increase observed at Bussels borehole (9.3%).

When the 3° Min scenario data are used, all the boreholes show reduction in recharge values with the smallest reduction observed at Newbridge borehole (-4.7%) and the highest reduction observed at Skirwith borehole (-15.2%). When the 3° Max scenario data are used, all the boreholes show increase in recharge values with the smallest increase observed at Newbridge borehole (14.65%) and the highest increase observed at Heathlanes borehole (17.5%). Recharge values calculated by Metran and using the future climate data are shown in Figure 12.

Table 12 shows the monthly historical and future recharge values calculated at the different boreholes. It is clear that in almost all the cases, the recharge values become lower than the



historical values when the 1° Min and 3° Min data are used and they become higher than the historical values when the 1° Max and 3° Max are used. The exceptions of this observation are due to the complex effect of the use of the change factors, which may reduce both the rainfall and potential evaporation at the same period but at different rates. The reduction in potential evaporation volume in one month may yield increased recharge volume even if the rainfall volume is reduced for that month.

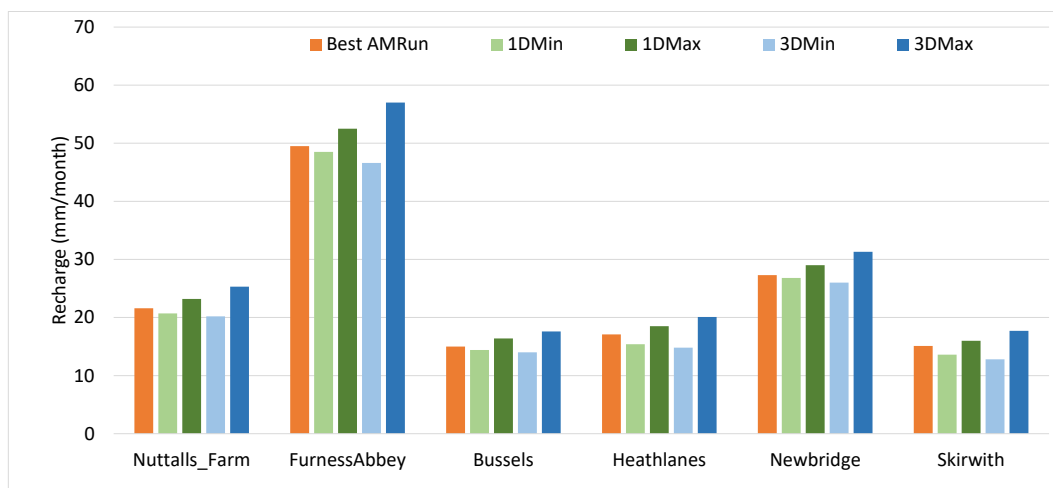


Figure 11 Historical (orange) and future recharge values (blue and green) as produced by the best performing AquiMod model.

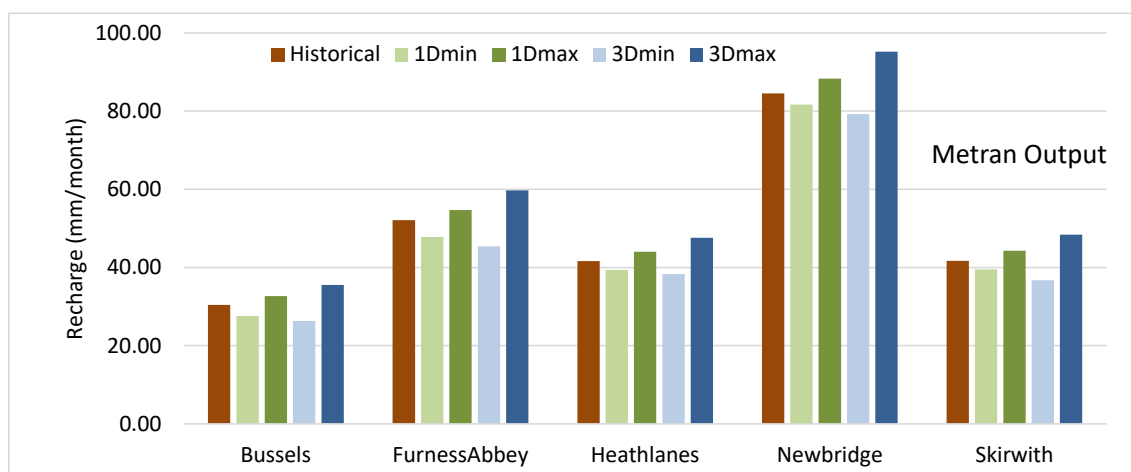


Figure 12 Historical (orange) and future recharge values (blue and green) produced by Metran.

Table 12 Monthly recharge values estimated using the historical and the projected forcing data. Dotted line is the monthly historical recharge values. Green shaded area shows the 1° Min and Max monthly recharge values and the blue shaded area shows the 3° Min and Max monthly recharge values

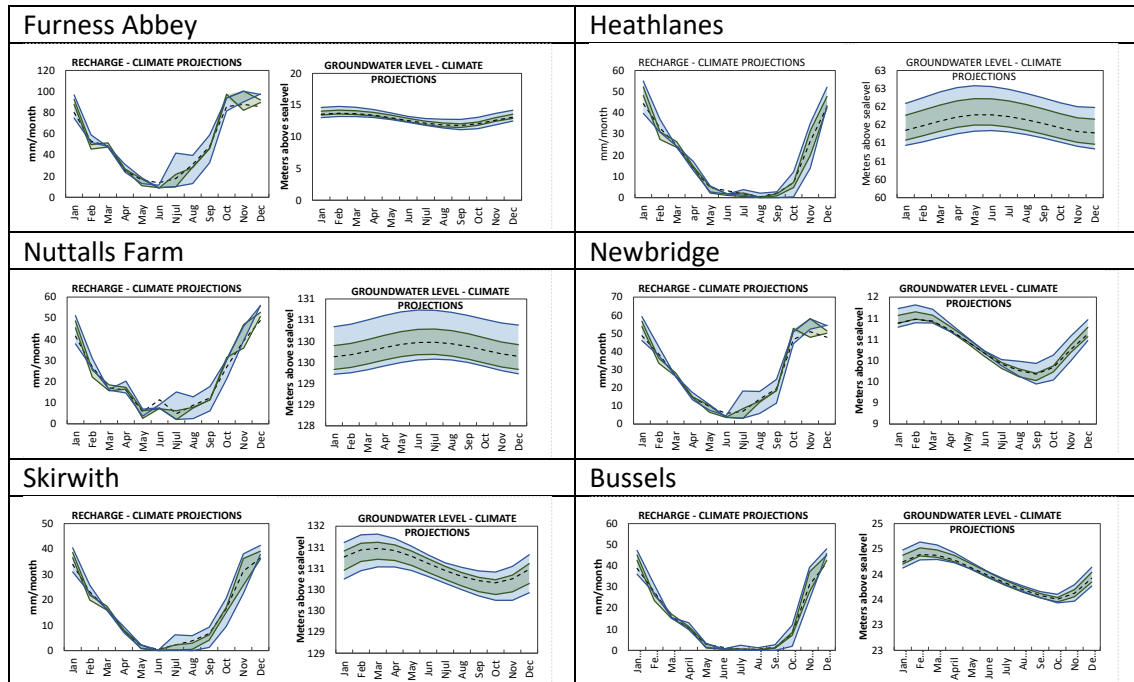


Table 13 shows maps of the spatially distributed recharge values calculated over the Permo-Triassic aquifer. The plots are for the historical potential recharge values as well as those calculated using the distributed recharge model but with rainfall potential evaporation data altered using the 1° Min, 1° Max, 3° Min, and 3° Max UK change factors. The differences in the maps are not clear, however, the 1° Min and 3° Min data produce drier recharge maps and the 1° Max and 3° Max data produce wetter recharge maps as confirmed with the difference maps listed in Table 14.

The differences between the simulated future recharge values and the historical ones are shown in the plots in Table 14. While the differences between the future and historical recharge values is mainly between -3.5% and 5.3%, when the rainfall and potential evaporation data are altered using the 1° Min, 1° Max, and 3° Min change factors, the differences are much more noticeable when the 3° Max change factors are used. In the latter case, the recharge increase is greater than 15% indicating that this is a very wet scenario.

Table 15 shows the average, maximum, and the standard deviation values calculated using the pixel values of the maps shown in Table 13. Looking at the average values, it is clear that there is reduction in recharge when the 1° Min or the 3° Min data are used compared to the historical recharge. However, it must be noted that the average recharge value estimated using the 3° Min data used is higher than that estimated using the 1° Min data and this is opposite to what was

expected. The maximum of the pixel values of the 1° Min map is higher than the maximum of the pixel values of the 3° Min map as expected. The average recharge values of the pixel values of the 1° Max and 3° Max maps are both higher than the average from the historical map as expected. The maximum value from these two maps are also higher than the maximum obtained from the historical. Finally, there is little difference in the standard deviation values shown in Table 15 indicating that the spatial distribution of recharge values is not notably different between the different scenarios.

Table 13 Spatially distributed historical and projected recharge values

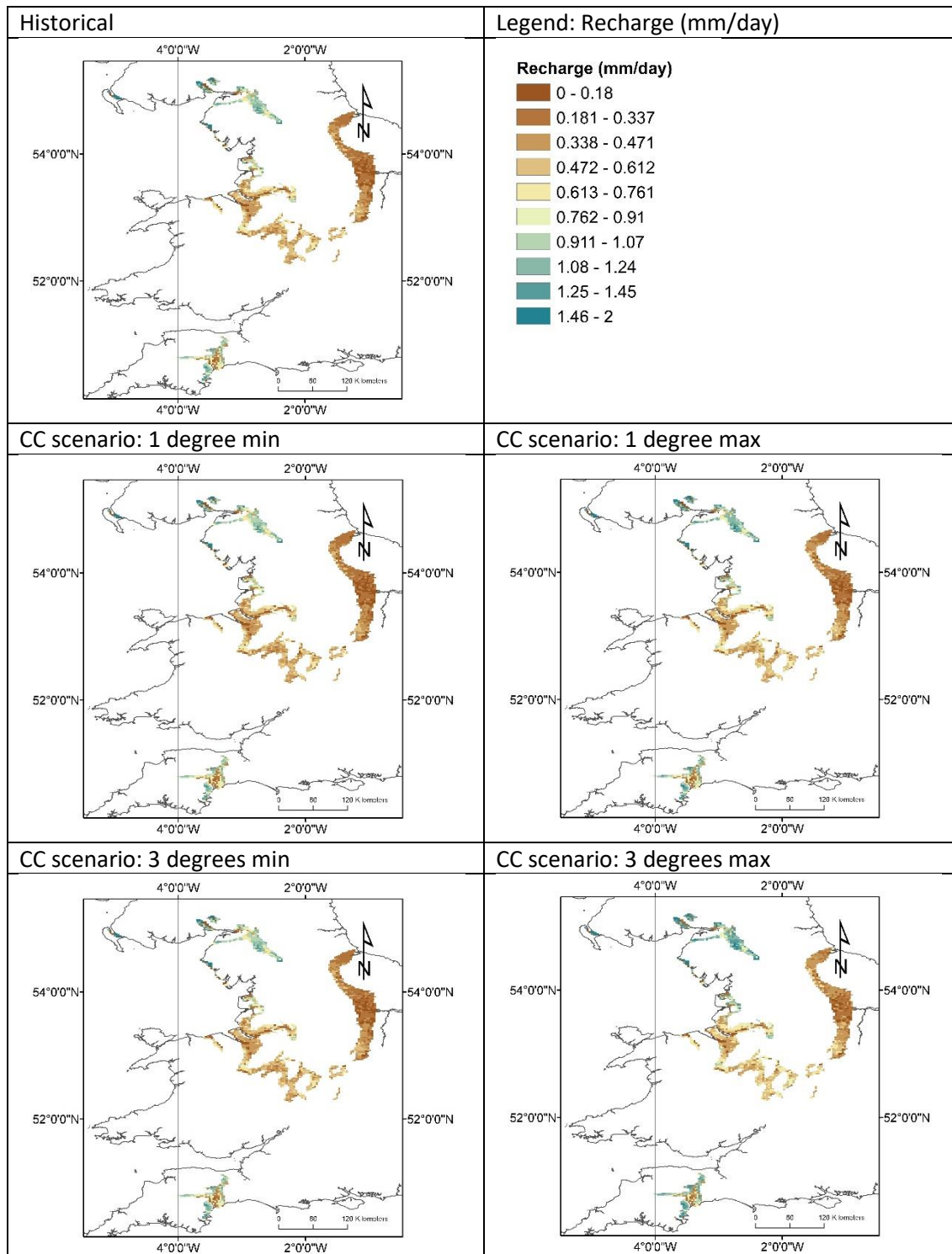


Table 14 Differences between the projected and historical recharge values calculated as projected values minus historical values

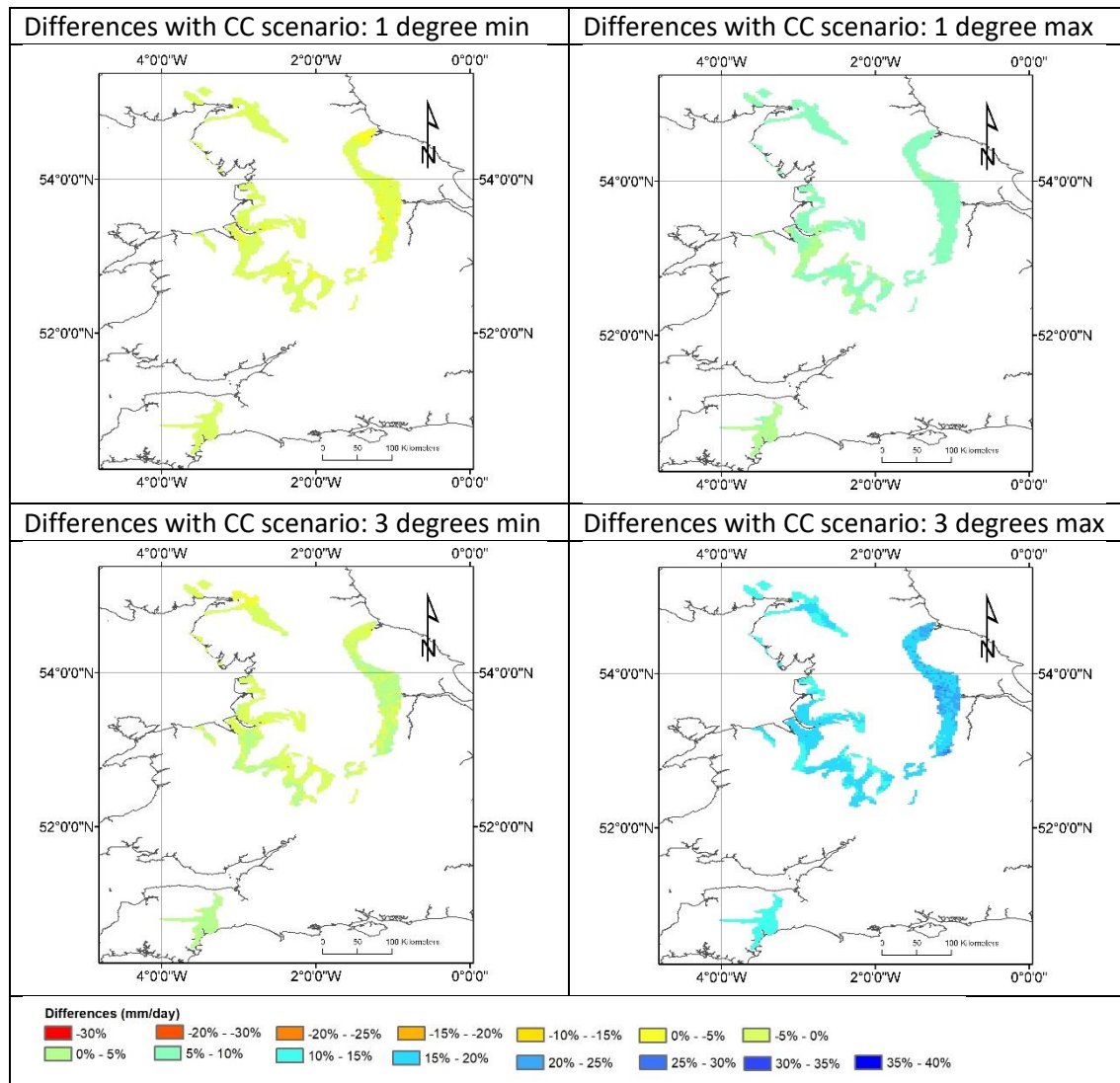


Table 15 Statistical information about the maps shown in Table 13

Map	Average recharge (mm/day)	Maximum recharge (mm/day)	Standard deviation (mm/day)
Historical	0.545	2.108	0.342
CC scenario: 1 degree min	0.526	2.06	0.335
CC scenario: 1 degree max	0.574	2.218	0.361
CC scenario: 3 degrees min	0.536	2.03	0.334
CC scenario: 3 degrees max	0.627	2.36	0.385

REFERENCES

- Allen, D. J., L. J. Brewerton, L. M. Coleby, B. R. Gibbs, M. A. Lewis, A. M. MacDonald, S. J. Wagstaff, A. T. Williams. 1997. 'The Physical Properties of Major Aquifers in England and Wales'.
- Besbes, M. & de Marsily, G. (1984) From infiltration to recharge: use of a parametric transfer function. *Journal of Hydrology*, 74, p. 271-293.
- Hough, M. N. & Jones, R. J. A. 1997. The United Kingdom Meteorological Office rainfall and evaporation calculation system: MORECS version 2.0 – an overview. *Hydrology and Earth System Sciences*, 1, 227–239.
- IPCC: 2000, Special report on emissions scenarios (SRES): A special report of Working Group III of the Intergovernmental Panel on Climate Change, Cambridge University Press, Cambridge, p. 599
- Jenkins, G.J., Murphy, J.M., Sexton, D.S., Lowe, J.A., Jones, P. and Kilsby, C.G. 2009, UK Climate Projections: Briefing report, Met Office Hadley Centre, Exeter, UK.
- Mackay, J. D., Jackson, C. R., Wang, L. 2014. A lumped conceptual model to simulate groundwater level time-series. *Environmental Modelling and Software*, 61. 229-245. <https://doi.org/10.1016/j.envsoft.2014.06.003>
- Mackay, J. D., Jackson, C. R., Wang, L. 2014. *AquiMod user manual (v1.0)*. Nottingham, UK, British Geological Survey, 34pp. (OR/14/007) (Unpublished)
- Mansour, M. M. and Hughes, A. G. 2018. Summary of results for national scale recharge modelling under conditions of predicted climate change. British Geological Survey Internal report. Commissioned Report OR/17/026.
- Mansour, M. M., Wang, L., Whiteman, Mark, Hughes, A. G. 2018. Estimation of spatially distributed groundwater potential recharge for the United Kingdom. *Quarterly Journal of Engineering Geology and Hydrogeology*, 51 (2). 247-263. <https://doi.org/10.1144/qjegh2017-051>
- Murphy, J.M., Booth, B.B.B., Collins, M., Harris, G.R., Sexton, D.M.H., and Webb, M.J. 2007. A methodology for probabilistic predictions of regional climate change from perturbed physics ensembles. *Phil. Trans. R. Soc. A* 365, 1993–2028.
- Murphy, J.M., Sexton, D.M.H., Jenkins, G.J., Boorman, P.M., Booth, B.B.B., Brown, C.C., Clark, R.T., Collins, M., Harris, G.R., Kendon, E.J., Betts, R.A., Brown, S.J., Howard, T. P., Humphrey, K. A., McCarthy, M. P., McDonald, R. E., Stephens, A., Wallace, C., Warren, R., Wilby, R., and Wood, R. A. 2009, 'UK Climate Projections' Science Report: Climate change projections. Met Office Hadley Centre, Exeter.

Obergfell, C., Bakker, M., & Maas, K. (2019). Estimation of average diffuse aquifer recharge using time series modeling of groundwater heads. *Water Resources Research*, 55. <https://doi.org/10.1029/2018WR024235>

Prudhomme, C., Dadson, S., Morris, D., Williamson, J., Goodsell, G., Crooks, S., Boelee, L., Davies, H., Buys, G., Lafon, T. and Watts, G., 2012. Future Flows Climate: an ensemble of 1-km climate change projections for hydrological application in Great Britain. *Earth System Science Data*, 4(1), pp.143-148.

Zaadnoordijk, W.J., Bus, S.A.R., Lourens, A., Berendrecht, W.L. (2019) Automated Time Series Modeling for Piezometers in the National Database of the Netherlands. *Groundwater*, 57, no. 6, p. 834-843. <https://onlinelibrary.wiley.com/doi/epdf/10.1111/gwat.12819>

APPENDICES

Appendix A: AquiMod methodology

AquiMod is a lumped parameter computer model that has been developed to simulate groundwater level time series at observational boreholes (Mackay et al., 2014a). It is based on hydrological algorithms that simulates the movement of groundwater within the soil zone, the unsaturated zone, and the saturated zone. The lumped models neglect complexities included in distributed groundwater models but maintains some of the fundamental physical principles that can be related to the conceptual understanding of the groundwater system (Mackay et al., 2014b).

While AquiMod was originally designed to capture the behaviour of a groundwater system through the analysis of groundwater level time series, it can produce the infiltration recharge values and groundwater discharges from the aquifer as a by-product. AquiMod is driven by complete time series of forcing data for either historical or predicted future conditions. Running AquiMod in predictive mode can be used to fill in gaps in historical groundwater level time series, or calculate future groundwater levels. In addition to groundwater levels, it also provides predictions of historical and future recharge values and groundwater discharges. In the current application we use calibrated AquiMod models to estimate the recharge values at selected boreholes.

AquiMod consists of three modules (Figure A1). The first is a soil water balance module that calculates the amount of water that infiltrates the soil as well as the soil storage. The second module controls the movement of water in the unsaturated zone, mainly it delays the arrival of infiltrating water to the saturated zone. The third module calculates the variations in groundwater levels and discharges. The model executes the modules separately following the order listed above.

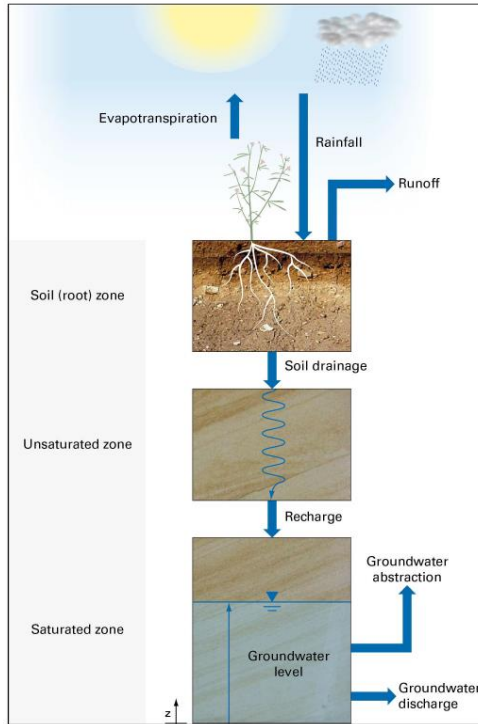


Figure A1 Generalised structure of Aquimod (after Mackay et al., 2014a)

The soil moisture module

There are several methods available in Aquimod that can be used to calculate the rainfall infiltration into the soil zone. In this study we use the FAO Drainage and Irrigation Paper 56 (FAO, 1988) approach. In this method, the capacity of the soil zone, from which plants draw water to evapo-transpire, is calculated first using the plants and soil characteristics. Evapo-transpiration is calculated according to the soil moisture deficit level compared to two parameters: Readily Available Water (RAW) and Total Available Water (TAW). These are a function of the root depth and the depletion factor of the plant in addition to the soil moisture content at field capacity and wilting point as shown in Equations A1 and A2.

$$TAW = Z_r(\theta_{fc} - \theta_{wp})$$

Equation A1

$$RAW = p \cdot TAW$$

Equation A2

Where Z_r [L] and p [-] are the root depth and depletion factor of a plant respectively, θ_{fc} [$L^3 L^{-3}$] and θ_{wp} [$L^3 L^{-3}$] are the moisture content at field capacity and wilting point respectively.

The FAO method is simplified by Griffiths et al. (2006) who developed a modified EA-FAO method. In this method the evapotranspiration rates are calculated as a function of the potential evaporation and an intermediate soil moisture deficit as:

$$\begin{aligned} e_s &= e_p \left[\frac{s_s^*}{TAW - RAW} \right]^{0.2} & s_s^* > RAW \\ e_s &= e_p & s_s^* \leq RAW \\ e_s &= 0 & s_s^* \geq TAW \end{aligned}$$

Equation A3



Where e_s [L] is the evpo-transpiration rate, e_p [L] is the potential evaporation rate and s_s^* [L] is the intermediate soil moisture deficit given by

$$s_s^* = s_s^{t-1} - r + e_p \quad \text{Equation A4}$$

Where r [L] is the rainfall at the current time step and s_s^{t-1} [L] is the soil moisture deficit calculated at the previous time step.

The new soil moisture deficit is then calculated from:

$$s_s = s_s^{t-1} - r + e_s \quad \text{Equation A5}$$

Griffiths et al. (2006) proposed that the recharge and overland flow are only generated when the calculated soil moisture deficit becomes zero. The remaining volume of water, the excess water, is then split into recharge and overland flow using a runoff coefficient. In Aquimod a baseflow coefficient is used to reflect the fact that a groundwater discharge is calculated rather than overland water. In this application, the baseflow coefficient is one minus the runoff coefficient.

The unsaturated zone module

The Aquimod version used in this study to simulate the movement of groundwater flow within the unsaturated zone is based on a statistical approach rather than a process-based approach. This method distributes the amount of rainfall recharge over several time steps where the soil drainage for each time step is calculated using a two-parameter Weibull probability density function. The Weibull function can represent exponentially increasing, exponentially decreasing, and positively and negatively skewed distributions. This can be used to focus the soil drainage over earlier or later time steps or to spread it over a number of time steps after the infiltration occurs. The shape of the Weibull function is controlled by two parameters, k and λ as shown in Equation A6.

$$f(t, k, \lambda) = \begin{cases} \frac{k}{\lambda} \left(\frac{t}{\lambda}\right)^{k-1} e^{-(t/\lambda)^k} & t > 0 \\ 0 & t \leq 0 \end{cases} \quad \text{Equation A6}$$

Where k and λ are two parameters the values of which are calculated during the calibration of the model and t is the time step.

The saturated zone module

Aquimod considers the saturated zone as a rectangular block of porous medium with dimensions L and B as its length and width [L] respectively. This block is divided into a number of layers, each has a defined hydraulic conductivity value, a storage coefficient value, and a discharging feature. The number of layers define the structure of the saturated module used in the study.

The mass balance equation that gives the variation of hydraulic head with time is given by:

$$SLB \frac{dh}{dt} = RLB - Q - A \quad \text{Equation A7}$$

Where:

S is the storage coefficient of the porous medium [-]

h is the groundwater head [L]

t is the time [T]

R is the infiltration recharge [L T⁻¹]



Q is the discharge out of the aquifer [$L T^{-1}$]
 A is the abstraction rate [$L T^{-1}$]

It must be noted that in a multi-layered groundwater system as shown in Figure A2, we calculate one groundwater head (h) for the whole system. The discharges (Q) from Outlet 1, 2, etc. are calculated using the Darcy law. The total discharges can be summarised using the following equation:

$$Q = \sum_{i=1}^m \frac{T_i B}{0.5 L} \Delta h_i \quad \text{Equation A8}$$

Where:

m is the number of layers in the groundwater system [-]

T_i is the transmissivity of the layer i [$L T^{-2}$]

Δh_i is the difference between the groundwater head h and z_i , the elevation of the base of layer i

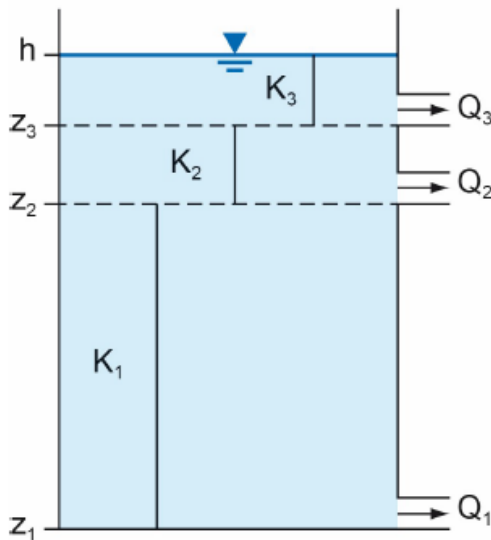


Figure A2 Representation of the saturated zone using a multi-layered groundwater system

Substituting Equation A8 into Equation A7 yields a numerical equation in the form:

$$S \frac{(h-h^*)}{\Delta t} = R - \sum_{i=1}^m \frac{T_i}{0.5 L^2} \Delta h_i - \frac{A}{LB} \quad \text{Equation A9}$$

Equation A9 is an explicit numerical equation that allows the calculation of the groundwater head h [L] at any time and using time steps of Δt [T]. In this equation h^* [L] is the groundwater head calculated at the previous time step and the term Δh_i [L] is calculated as $(h^* - z_i)$.

The terms S , T_i , and L are optimised during the calibration of the model. A groundwater system can be specified with one storage coefficient as shown in the equations above or with different storage coefficient values for the different layers. Several saturated modules are included in Aquimod to provide this flexibility and the model user can select the model structure that represent the conceptual understanding best.



Limitations of the model

AquiMod is a lumped groundwater model that aims at reproducing the behaviour of the observed groundwater levels. It tries to encapsulate the conceptual understanding of a groundwater system in a simple numerical representation. The model results have to be therefore discussed, taking this into consideration. For example, the model represents the groundwater system as a closed homogeneous medium, with no impact from any outer boundary or feature, whether physical or hydrological, such as the presence of rising and falling river stage.

Vertical heterogeneity can be accounted for by using multi-layered groundwater module structure. However, this model setting does not provide any information about the vertical connections between the layers as the discharge from all the layers is calculated using one representative groundwater head value. In other words, it is assumed that all layers are in perfect hydraulic connection.

As mentioned before, the model is designed to simulate the groundwater levels. However, it produces the recharge values and groundwater discharges as by products. In this application we use the calibrated model to calculate recharge. The mass balance equation (Equation A7) shows that recharge is a function of transmissivity and storage coefficient values, which are estimated during the calibration process of the model, i.e. they are not parameters with fixed values provided by the user. The inter-connections between these parameters leads to uncertainties in the estimated recharge values as a high storage coefficient value can produce a high recharge estimate and vice versa. To overcome this problem, it is suggested that the recharge values estimated by AquiMod are always presented as a range of possibilities rather than an absolute value. This can be achieved by estimating the recharge values from all the models that have a performance measure above than a threshold that is deemed acceptable by the user. The recharge estimates can then be presented as an average of all estimates and values corresponding to selected percentiles.

Model input and output

AquiMod includes a number of methods that calculates rainfall recharge as well as a number of model structure from which the user can select what better suits the case study.

Model input consists time series of forcing data including rainfall and potential evaporation, time series of anthropogenic impact mainly groundwater abstraction and time series of groundwater levels that will be used to calibrate the model. These time series must be complete, i.e. a value is available at every time step except the groundwater level time series, which can include missing data. The time step can be one day or multiple of days, and the model automatically calculate the size of the time step based on the input data time series.

The model is run first in calibration mode where a range of parameter values are specified for the different parameters included in the three model modules. A Monte Carlo approach is used to select the best parameter values. The performance of the model is measured by comparing the simulated groundwater levels to the observed ones using the Nash Sutcliffe Efficient (NSE) or



the Root Mean Squared Error (RMSE) performance measures. The parameter set that produces the best model performance is selected to run the model in evaluation mode.

When the model is run in evaluation mode, it produces output files that give recharge values, groundwater levels and groundwater discharges time series with time as specified in the input file. The number of output files is equal to the number of acceptable models set by the user.

Appendix B: Metran methodology

Metran applies transfer function noise modelling of (groundwater head) time series with usually daily precipitation and evaporation as input (Zaadnoordijk et al., 2019). The setup is shown in the Figure B1. If time series of other influences on the groundwater head are available, these contributions can be added to the deterministic part of the model. The stochastic part is the difference between the total deterministic part and the observations (the residuals). The corresponding input of the noise model should have the character of white noise.

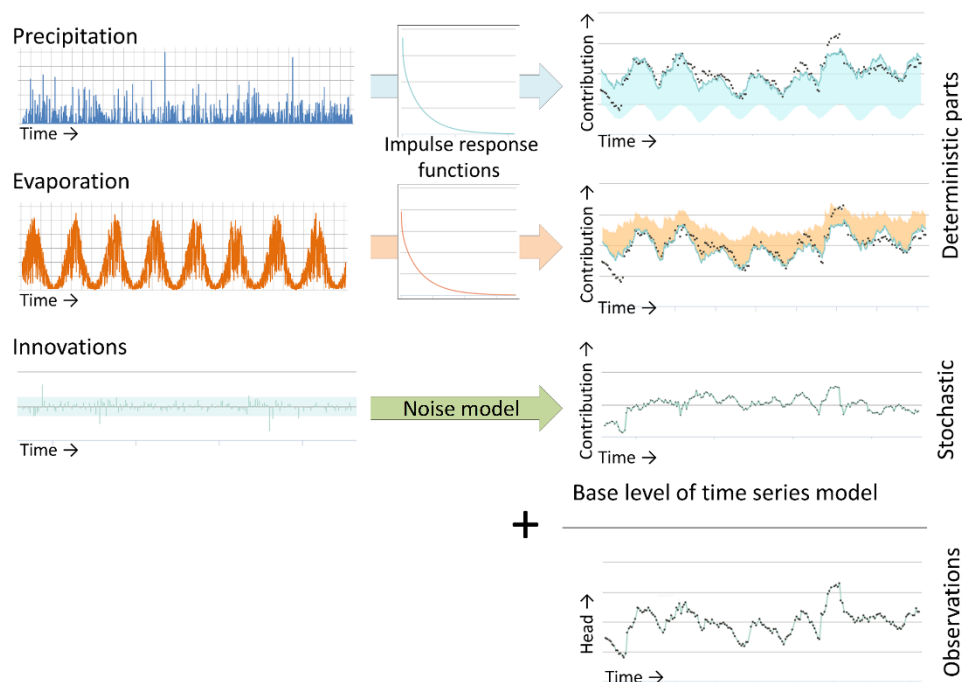


Figure B1 Illustration of METRAN setup

The stochastic part is needed because of the time correlation of the residuals, which does not allow a regular regression to obtain the parameter values of the transfer functions.

The incomplete gamma function is used as transfer function. This is a uni-modal function with only three parameters that has a quite flexible shape and has some physical background (Besbes & de Marsily, 1984). The evaporation response is set equal to the precipitation response except for a factor (f_c). The noise model has one parameter that determines an exponential decay. Thus, for the standard setup with precipitation and evaporation, there are five parameters that have to be determined from the comparison with the observations. Three parameters regarding the precipitation response, the evaporation factor, and the noise model parameter (actually, the time series model has a fifth parameter, the base level, but this is determined from the assumption that the average of the calculated heads is equal to the average of the observations). There are three extra parameters for each additional input series, such as pumping.



Limitations

Metran's time series model is linear. So, the model creation breaks down when the system is strongly nonlinear. This can occur e.g. when drainage occurs for high groundwater levels, when the ratio between the actual evapotranspiration and the inputted reference evaporation varies strongly, or when the groundwater system changed during the simulated period.

Metran is not able to find a decent time series model when the response function is not appropriate for the groundwater system. An example of this is a system with a separate fast and slow response as was found for a French piezometer in the Avre region, as is illustrated in Figure B2.

Finally, the parameter optimization of Metran uses a gradient search method in the parameter space, so it can be sensitive to initial parameter values in finding an optimal solution.

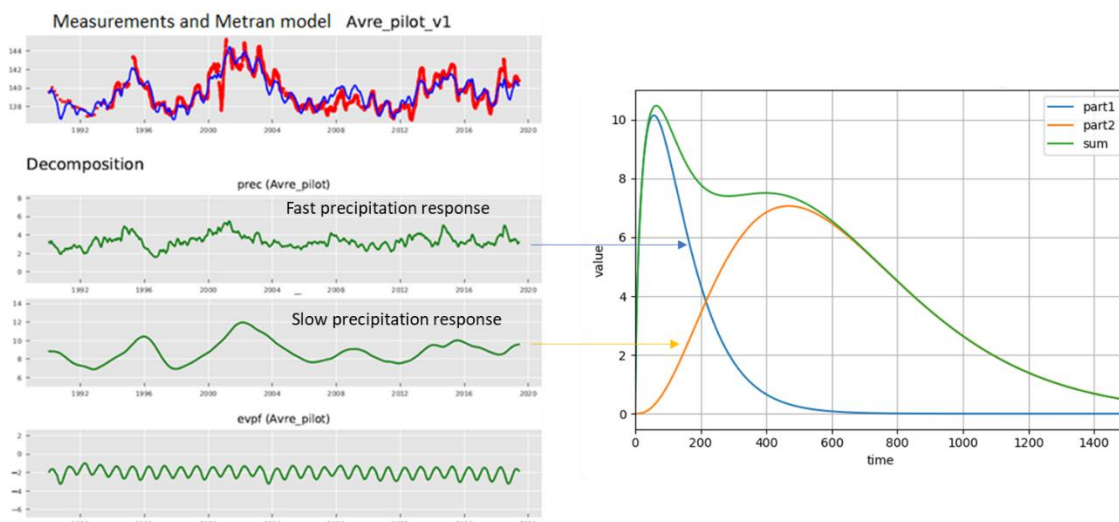


Figure B2. An example where the response function implemented in METRAN is not suitable for the groundwater system

Time step

Metran has been designed to work with explanatory series that have a daily time step. However, it has been adapted so that other time step lengths can be applied; although Metran still has the limitation that the explanatory variables have a constant frequency. For the TACTIC simulations of series with monthly or decadal meteorological input series, the time step has been set to 30 and 10 days, respectively. This time step has been applied from the end date backward.

Note that the heads may be irregular in time as long as the frequency is not greater than the frequency of the explanatory series.

Model output

The evaporation factor f_c gives the importance of evapotranspiration compared to precipitation. The parameter M_0 gives the total precipitation response, which is equal to the area below the impulse response function and the final value of the step response function.



The average response time is another characteristic of the precipitation response. The influence is illustrated in Figure B3 with the impulse response functions and head time series for two models with very different response times for time series of SGU in Sweden.

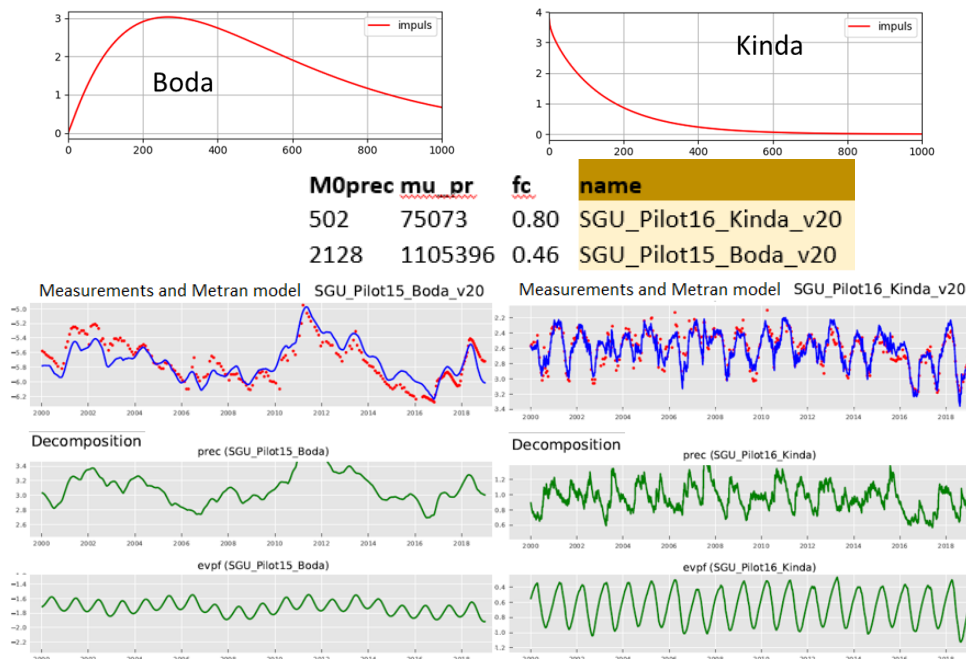


Figure B3 Illustration of Metran output for two case studies in Sweden with different response times.

Model quality

Metran judges a resulting time series model according to a number of criteria and summarizes the quality using two binary parameters Regimeok, Modok (see Zaadnoordijk et al., 2019):

- Regimeok = 1 : highest quality
- Modok = 1 (and Regimeok = 0) : ok
- Both zero = model quality insufficient

More detailed information on the model quality is given in the form of scores for two information criteria (AIC and BIC), a log likelihood, R², RMSE, and the standard deviations and correlations of the parameters.

Recharge

Although the transfer-noise modelling of Metran determines statistical relations between groundwater heads and explanatory variables, we like to think of the results in physical terms. It is tempting to interpret the evaporation factor, as the factor translating the reference into the actual evapotranspiration. Then, we can calculate a recharge as



$$R = P - fE$$

Equation B1

where R is recharge, P precipitation, E evapotranspiration, and f the evaporation factor.

Following the definitions used in the TACTIC project, this recharge R actually is the effective precipitation. It is equal to the potential recharge when the surface runoff is negligible. This in turn is equal to the actual recharge at the groundwater table if there also is no storage change or interflow. In such cases it may be expected that this formula indeed corresponds to the meteorological forcing of the groundwater head in a piezometer, so that it gives a reasonable estimate of the recharge. Obergfell et al. (2019) showed this for an area on an ice pushed ridge in the Netherlands. However, this assumes that all precipitation recharges the groundwater, which cannot be done in many places.

In Dutch polders with shallow water tables and intense drainage networks, it is reasonable to assume that the actual evapotranspiration is equal to the reference value. In that case, the factor f becomes larger than 1 because 1 mm of evaporation has less effect than 1 mm of precipitation (because part of the evaporation does not enter the ground but is immediately drained to the surface water system). In that case, we can calculate recharge as:

$$\begin{aligned} R &= P - fE & f &\leq 1 \\ R &= P/f - E & f &> 1 \end{aligned}$$

Equation B2

These simple formulas can be applied easily for the situations currently modelled in Metran and for the simulations that are driven by future climate data using the delta-change climate factors. However, it is noted that it is a crude estimate using assumptions that are easily violated. Because of this, the equations should be applied only to long term averages using only models of the highest quality.